

SYNTHESIS AND APPLICATIONS OF TERPENOID  
NATURAL PRODUCTS: TOTAL SYNTHESIS OF  
SCABROLIDE A AND HAVELLOCKATE, AND  
SYNTHESIS OF PINENE OXIDATION PRODUCTS  
FOR ATMOSPHERIC INVESTIGATIONS

Thesis by  
Nicholas Joseph Hafeman

In Partial Fulfillment of the Requirements for  
the degree of  
Doctor of Philosophy

CALIFORNIA INSTITUTE OF TECHNOLOGY  
Pasadena, California

2022  
(Defended May 24, 2022)

© 2022

Nicholas Joseph Hafeman  
ORCID: 0000-0001-7525-7597

*For Elana*

*“Nothing I see can be taken from me”*

*–Anastasio/Marshall*

## ACKNOWLEDGEMENTS

During my time at Caltech I have been very fortunate to meet and work with many incredibly talented and kind people. The relationships I have forged during my graduate career are some of the strongest and most cherished of my life so far. People often say that Caltech is a special place, and I believe it is the people here that make it so special.

First of all, I have to thank Brian for having me in his group and continuing to facilitate my research over the last five years. Brian is an incredible advisor. The amount of freedom he provides his students is unparalleled and represents a remarkable level of trust in us. I know I have benefitted greatly from being allowed to pursue my own ideas (good and bad), and I think we as students are all better off for it. Additionally, Brian's love for the craft of organic synthesis is infectious, and has many times reinvigorated me when the going was rough. Finally, Brian is the kindest and most understanding advisor one could ask for. People have said that they rarely don't feel better after a talk with Brian, and I have found this to be true for myself as well.

I must thank Sarah Reisman for acting as chair of my committee as well as being like a second advisor to our group. Throughout the years it has been a privilege to benefit from her feedback and suggestions on my chemistry and proposals. I have enjoyed the discussions we have had during my committee meetings and exams and have especially appreciated Sarah's skill in chairing these meetings. I also need to thank the rest of my committee, Profs. Paul Wennberg and Hosea Nelson for agreeing to join on when they did, and for their great input during the last few years of my graduate studies.

I have to thank Dr. Scott Virgil for all of his help throughout the years. I have to say that working with Scott at the end of the scabrolide synthesis was one of the best months of my graduate career. The many hours spent “belly up” to the prep HPLC offered a lot of time for good stories and conversation. Also, in that month I probably learned the most information in the shortest period of time that I ever have in my life.

I also must thank Dr. Dave Vander Velde for maintaining the incredible NMR facility that we have at Caltech, and for his helpful suggestions with difficult NMR problems. Also, thanks to Dr. Mike Takase and Larry Henling for assistance with X-ray diffraction, and for getting such great structures from my often terrible crystals. Many thanks to Dr. Mona Shahgholi for maintaining the mass spec. facility and for help getting HRMS data for publications. Finally, thanks to Joe Drew, as well as Greg Rolette and Armando Villasenor for working so hard to keep everything running smoothly. I will fondly remember the orange cart rides with Armando to Central Shipping to pick up solvents when they had accidentally been delivered there.

During my early years at Caltech I was lucky enough to be mentored by Steven Loskot, who brought me on to his project and showed me the ropes of being in the group, and for this I am very grateful. I also thank him and Fu lab alum Carson Matier for allowing me (and Elana) to join their fantasy hockey league, which was a lot of fun for both of us. Also influential in my early days in the group were Chris Reimann, Austin Wright, and my hoodmate, Dr. Eric “E-dubs” Welin. Austin and I worked alongside one another for many years, and our long conversations about chemistry as well as music and movies made each day far more enjoyable. Eric and I had a lot of fun working together at the bench, and the advice he gave me in my first couple of years was truly invaluable.

Joining the lab as a class of one, I was extremely lucky to be taken in by the older students who quickly treated me like one of their own. Close friendships that I made early on with Eric Alexy, Tyler Fulton, Chris Reimann and Fa Ngamnithiporn made my transition to grad school very enjoyable. Feeling included in such a tightly knit group so quickly was really important to me, and I will be forever grateful to these people for being so welcoming. Specifically, lunches at Ernie's, "Fun Lunches" off-campus, watching Game of Thrones, afternoon ping pong, and weekend trips to restaurants and Dave and Busters will always be some of my fondest memories of graduate school.

I must especially thank Tyler Fulton, who has since essentially become like a classmate to me, and also one of my closest friends. As we transitioned into being the senior students in the group, having Tyler to talk to and joke with really helped to ease the stress of stepping into that role. It was also a pleasure to have him join on the havellockate synthesis, as he is an incredibly talented chemist whose contributions to that project were invaluable. Finally, I have to thank Tyler for all of the invaluable help he has provided with the writing of this thesis, including proofreading and providing templates and help with formatting.

I must also thank the G4 class, Alexia Kim, Alex Cusumano, Zack Sercel, and Tyler "TC" Casselman for being good friends and colleagues throughout my time at Caltech. As some of the people that I overlapped with the longest, it was a pleasure working along side each of them and watching them pass the major milestones of the PhD. As I leave, I am confident that the lab is left in good hands.

I need to thank Melinda Chan, who was brave enough to start on the havellockate project in its infancy, and allow me to serve as her mentor in the group. The experience of first mentoring, and then working alongside Melinda has been wonderful. Seeing her develop

into an independent and skilled chemist over the past three years has been one of the greatest joys of graduate school for me. I am also extremely thankful for her sticking around on the project, despite all of the difficulty it has presented. I am excited to see where the rest of her PhD takes her.

I also need recognize the younger students in the group. During my last two years in the Stoltz lab we have taken two back-to-back classes of seven. At a time when the group was smaller, these two classes have completely changed the dynamic in the lab. The enthusiasm and excitement that each one of these incredibly talented people bring to the lab on a daily basis is amazing, and I am grateful to have been around to see it.

I specifically want to thank Samir Rezgui, my last hoodmate, for some great times in the last couple of years. Whether it was working at the bench or taking trips to Home Depot to buy 20L drums of acetone, I am glad to have had the opportunity to get to know Samir and am excited to see what he accomplishes during the rest of his graduate career. Likewise, I'd like to thank Elliot Hicks for being a great friend, especially during the 306 Church days (both while doing chemistry and while writing props). Kevin Gonzolez has also become a close friend, both in the lab as well as our many trips bagging peaks in the area. I have to thank Farbod Moghadam for some really good times, especially joking around in the office, as well as Adrian Samkian for great conversations (about chemistry and beyond). I'd also like to thank Jay Barbor for putting up with me in the office, and Kali Flesch, who was also around for the early 306 Church days. Finally, I'd like to thank all of the first years for making the lab such a fun place to be. You are all extremely talented and I can't wait to see where you all take the group in the future.



I also must thank the Robb lab for being so welcoming when we were relocated to the third floor of Church during the COVID-19 pandemic. In particular, reconnecting with my classmate Molly McFadden was one of the highlights of this time for me. As I was starting the last year of my graduate studies, it was good to have someone else to talk to who was also going through the same process. Likewise, I'd like to thank my classmates in the Reisman lab: Mike Maser, Travis DeLano, Karli Holman, and Alex Shimozono. It has been a pleasure getting to know all of you over the last five years and I hope our paths cross sometime in the future. Finally, I must thank Chris Kenseth, with whom I had the pleasure of collaborating with on the atmospheric project for several years, for some truly good times both inside the lab as well as at the ping pong table.

None of this would have been possible without the incredible mentorship I received during my undergraduate years. Starting at Oakton Community College, Dr. Chad Landrie and Dr. Gary Mines really deserve credit for my interest in chemistry. My advisor at UIC, Dr. Duncan Wardrop, was instrumental in teaching me the fundamentals of the craft of organic chemistry, as well as piquing my interest in the field of natural product total synthesis. Much like Brian, I believe that the freedom he afforded me was instrumental in making me into the scientist that I am today. Additionally, I have to thank Dr. J. T. Mohr, a Stoltz lab alum, for convincing me to apply to Caltech, and for all of his advice and assistance during the graduate school application process.

Of course I have to thank my family, my parents in particular, without whom none of this would have been possible. Their constant and unwavering support, both during and before graduate school has been critical in getting me to where I am today. I also must thank my sister, Leigh, my brother-in-law Justin, and their three kids Aiden, Maya, and Evan.

Every year our trips home to Chicago to see them was a highlight, and I am very much looking forward to returning to the area and spending more time with the family.

Finally, I have to thank my partner Elana. In many ways, this PhD is as much hers as it is mine. I thank her for the sacrifices she has made that allowed me to complete my graduate studies. To most people, moving across the country so that your significant other can go work in a lab for six days out of the week doesn't sound like much fun. But she was up for it, and for that I will be forever grateful. I am incredibly lucky to have had her constant love and support throughout this process, which has occasionally been tough on both of us. Together, we have been fortunate to have two incredible dogs during this time, the late pug Winston, who made the journey to California with us, and our newest four-legged addition, Agnes. I am extremely grateful for both of them, for being (at times, much-needed) sources of comfort and happiness. Finally, I have to thank Elana for her patience. If being a graduate student is hard, I can imagine that being *with* a graduate student is even harder, so I am thankful for her understanding throughout my time in graduate school. I am very excited for us to relocate back to Chicago and start the next chapter together and can't wait to see what adventures come next.

## ABSTRACT

The total synthesis of complex natural products remains one of the enduring challenges in organic chemistry. Whether motivated by the biological activity of the target, or its structural complexity, total synthesis continues to serve as a proving ground for synthetic methodology as well as strategic planning. Herein is described the first total synthesis of the polycyclic furanobutenolide-derived (nor)cembranoid diterpenoids scabrolide A and havellockate. Our total synthesis of scabrolide A involves an intramolecular [4+2] cycloaddition, which forges a fused [5–5–6] tricycle possessing two of the three carbocycles that characterize the natural product. Next, a photocycloaddition/fragmentation sequence is employed to forge the final seven-membered ring and complete the total synthesis. Using a similar strategy, we could forge the [5–5–6] tricyclic core of the related diterpenoid havellockate with an intramolecular [4+2] cycloaddition. This is followed by a challenging enone allylation which installs the final carbon atoms of the target. Finally, elaboration of the allyl group, followed by a Cu/TEMPO-catalyzed oxidative lactonization furnishes havellockate. The final chapter of this thesis describes the synthesis and characterization of several pinene oxidation products and their dimers, which have been observed in pinene-derived secondary organic aerosol samples, as standards for atmospheric studies. This research uses the power of chemical synthesis to confirm (and in some cases reassign) the structures of naturally occurring, yet difficult to characterize chemical species found in the atmosphere.

## PUBLISHED CONTENT AND CONTRIBUTIONS

1. Kenseth, C. M.; Hafeman, N. J.; Huang, Y.; Dalleska, N. F.; Stoltz, B. M.; Seinfeld, J. H. “Synthesis of Carboxylic Acid and Dimer Ester Surrogates to Constrain the Abundance and Distribution of Molecular Products in  $\alpha$ -Pinene and  $\beta$ -Pinene Secondary Organic Aerosol.” *Environ. Sci. Technol.* **2020**, *54*, 12829–12938. DOI: 10.1021/acs.est.0c01566.

N. J. H. participated in project design, experimental work (synthesis), data acquisition and analysis, and manuscript preparation.

2. Hafeman, N. J.<sup>†</sup>; Loskot, S. A.<sup>†</sup>; Reimann, C. E.; Pritchett, B. P.; Virgil, S. C.; Stoltz, B. M. “The Total Synthesis of (–)-Scabrolide A.” *J. Am. Chem. Soc.* **2020**, *142*, 8585–8590. DOI: 10.1021/jacs.0c02513. <sup>†</sup>Denotes equal contribution.

N. J. H. participated in project design, experimental work, data acquisition and analysis, and manuscript preparation.

3. Inanaga, K.; Wollenburg, M.; Bachman, S.; Hafeman, N. J.; Stoltz, B. M. “Catalytic Enantioselective Synthesis of Carbocyclic and Heterocyclic Spiranes via a Decarboxylative Aldol Cyclization.” *Chem. Sci.* **2020**, *11*, 7390–7395. DOI: 10.1039/D0SC02366C. <sup>†</sup>Denotes equal contribution.

N. J. H. participated in manuscript preparation.

**TABLE OF CONTENTS**

Dedication.....	iii
Acknowledgements .....	v
Abstract .....	xi
Published Content and Contributions .....	xii
Table of Contents.....	xiii
List of Figures.....	xvii
List of Schemes .....	xxxv
List of Tables.....	xxxix
List of Abbreviations .....	l
<b>CHAPTER 1</b>	<b>1</b>
<i>The Total Synthesis of (-)-Scabrolide A</i>	
1.1 Introduction.....	1
1.2 Initial Retrosynthetic Analysis of Scabrolide A.....	4
1.3 Synthesis of Coupling Partners and Esterification .....	5
1.4 Failed Macrocyclization and Diels–Alder .....	6
1.5 Second-Generation Approach .....	8
1.6 Ring-Expansion Strategy: Simplified System.....	12
1.7 Ring Expansion Strategy: Complete System.....	18

1.8	Failed [2+2] Photocycloaddition .....	21
1.9	Isopropenyl Protecting Group Strategy .....	23
1.10	Ring Expansion and Failed Dehydration .....	25
1.11	Completion of the Total Synthesis.....	28
1.12	Conclusion .....	30
1.13	Experimental Section .....	31
1.13.1	Materials and Methods .....	31
1.13.2	Experimental Procedures .....	32
1.13.3	Comparison of Synthetic (–)-Scabrolide A to Published Data.....	87
1.13.4	Comparison of Synthetic (–)-Yonarolide to Published Data .....	91
1.14	Notes and References .....	92
<b>APPENDIX 1</b>		<b>101</b>
<i>Synthetic Summary for Chapter 1</i>		
<b>APPENDIX 2</b>		<b>104</b>
<i>Spectra Relevant to Chapter 1</i>		
<b>APPENDIX 3</b>		<b>217</b>
<i>X-Ray Crystallography Reports Relevant to Chapter 1</i>		
<b>APPENDIX 4</b>		<b>384</b>
<i>Synthesis of a Tricyclic Model System</i>		
<b>APPENDIX 5</b>		<b>392</b>
<i>Spectra Relevant to Appendix 4</i>		

<b>CHAPTER 2</b>	<b>401</b>
<i>Asymmetric Total Synthesis of Havellockate</i>	
2.1 Introduction .....	401
2.2 Retrosynthetic Analysis of Havellockate .....	402
2.3 Synthesis of Olefination Building Blocks .....	403
2.4 Julia–Kocienski Olefination and Diels–Alder .....	405
2.5 Synthesis of the Enone .....	407
2.6 Allylation .....	408
2.8 Transesterification, Allylation, and Completion of the Synthesis .....	412
2.9 Conclusion .....	415
2.10 Experimental Section .....	416
2.10.1 Materials and Methods .....	416
2.10.2 Experimental Procedures .....	417
2.10.3 Comparison of Synthetic Havellockate A to Published Data.....	438
2.11 Notes and References .....	92
 <b>APPENDIX 6</b>	 <b>445</b>
<i>Synthetic Summary for Chapter 2</i>	
 <b>APPENDIX 7</b>	 <b>448</b>
<i>Spectra Relevant to Chapter 2</i>	
 <b>APPENDIX 8</b>	 <b>485</b>
<i>X-Ray Crystallography Reports Relevant to Chapter 2</i>	

<b>CHAPTER 3</b>	<b>549</b>
<i>Synthesis of Carboxylic Acids and Dimer Esters from Pinene-Derived Secondary Organic Aerosol</i>	
3.1	Introduction..... 549
3.2	Synthesis and Characterization of Monomers <b>145, 146, and 152, and Dimer Ester Homologues 153–155</b> ..... 551
3.3	Synthesis and Characterization of Dimer Esters <b>156–158</b> ..... 554
3.4	Synthesis and Characterization of Isomeric Dimer Esters <b>168–170</b> ..... 557
3.5	Conclusion ..... 560
3.6	Experimental Section ..... 561
3.6.1	Materials and Methods..... 561
3.6.2	Synthetic Procedures ..... 562
3.7	Notes and References ..... 583



## LIST OF FIGURES

**CHAPTER 1***The Total Synthesis of (-)-Scabrolide A*

<b>Figure 1.1.1</b>	Polycyclic Furanobutenolide-derived norcembranoids .....	2
<b>Figure 1.2.1</b>	Initial retrosynthetic analysis of scabrolide A ( <b>1</b> ) .....	4
<b>Figure 1.5.1</b>	Second-generation retrosynthetic analysis of scabrolide A ( <b>1</b> ) .....	8
<b>Figure 1.6.1</b>	Third-generation retrosynthetic analysis of scabrolide A ( <b>1</b> ) .....	12
<b>Figure 1.8.1</b>	Mechanistic rationale for the photocycloaddition .....	23
<b>Figure 1.10.1</b>	Rationale for failure of dehydration attempts of Enone <b>91</b> and switching to a different substrate ( <b>90</b> ) .....	25
<b>Figure 1.13.1</b>	Overlaid <sup>1</sup> H NMR spectra of natural ( <i>Sheu, 2002</i> ) and synthetic scabrolide A ( <b>1</b> ) .....	88
<b>Figure 1.13.2</b>	Overlaid <sup>13</sup> C NMR spectra of natural ( <i>Sheu, 2002</i> ) and synthetic scabrolide A ( <b>1</b> ) .....	90

**APPENDIX 2***Spectra Relevant to Chapter 1*

<b>Figure A2.1</b>	<sup>1</sup> H NMR (500 MHz, CDCl <sub>3</sub> ) of compound <b>ent-25</b> .....	105
<b>Figure A2.2</b>	Infrared spectrum NMR (thin film, NaCl) of compound <b>ent-25</b> .....	106
<b>Figure A2.3</b>	<sup>13</sup> C NMR (100 MHz, CDCl <sub>3</sub> ) of compound <b>ent-25</b> .....	106
<b>Figure A2.4</b>	<sup>1</sup> H NMR (500 MHz, CDCl <sub>3</sub> ) of compound <b>26</b> .....	107
<b>Figure A2.5</b>	Infrared spectrum NMR (thin film, NaCl) of compound <b>26</b> .....	108
<b>Figure A2.6</b>	<sup>13</sup> C NMR (100 MHz, CDCl <sub>3</sub> ) of compound <b>26</b> .....	108
<b>Figure A2.7</b>	<sup>1</sup> H NMR (400 MHz, CDCl <sub>3</sub> ) of compound <b>27</b> .....	109

<b>Figure A2.8</b>	Infrared spectrum NMR (thin film, NaCl) of compound <b>27</b> .....	110
<b>Figure A2.9</b>	$^{13}\text{C}$ NMR (100 MHz, $\text{CDCl}_3$ ) of compound <b>27</b> .....	110
<b>Figure A2.10</b>	$^1\text{H}$ NMR (400 MHz, $\text{CDCl}_3$ ) of compound <b>28</b> .....	111
<b>Figure A2.11</b>	Infrared spectrum NMR (thin film, NaCl) of compound <b>28</b> .....	112
<b>Figure A2.12</b>	$^{13}\text{C}$ NMR (100 MHz, $\text{CDCl}_3$ ) of compound <b>28</b> .....	112
<b>Figure A2.13</b>	$^1\text{H}$ NMR (400 MHz, $\text{CDCl}_3$ ) of compound <b>29</b> .....	113
<b>Figure A2.14</b>	Infrared spectrum NMR (thin film, NaCl) of compound <b>29</b> .....	114
<b>Figure A2.15</b>	$^{13}\text{C}$ NMR (100 MHz, $\text{CDCl}_3$ ) of compound <b>29</b> .....	114
<b>Figure A2.16</b>	$^1\text{H}$ NMR (400 MHz, $\text{CDCl}_3$ ) of compound <b>31</b> .....	115
<b>Figure A2.17</b>	Infrared spectrum NMR (thin film, NaCl) of compound <b>31</b> .....	116
<b>Figure A2.18</b>	$^{13}\text{C}$ NMR (100 MHz, $\text{CDCl}_3$ ) of compound <b>31</b> .....	116
<b>Figure A2.19</b>	$^1\text{H}$ NMR (400 MHz, $\text{CDCl}_3$ ) of compound <b>38</b> .....	117
<b>Figure A2.20</b>	Infrared spectrum NMR (thin film, NaCl) of compound <b>38</b> .....	118
<b>Figure A2.21</b>	$^{13}\text{C}$ NMR (100 MHz, $\text{CDCl}_3$ ) of compound <b>38</b> .....	118
<b>Figure A2.22</b>	$^1\text{H}$ NMR (400 MHz, $\text{CDCl}_3$ ) of compound <b>39</b> .....	119
<b>Figure A2.23</b>	Infrared spectrum NMR (thin film, NaCl) of compound <b>39</b> .....	120
<b>Figure A2.24</b>	$^{13}\text{C}$ NMR (100 MHz, $\text{CDCl}_3$ ) of compound <b>39</b> .....	120
<b>Figure A2.25</b>	$^1\text{H}$ NMR (400 MHz, $\text{CDCl}_3$ ) of compound <b>40</b> .....	121
<b>Figure A2.26</b>	Infrared spectrum NMR (thin film, NaCl) of compound <b>40</b> .....	122
<b>Figure A2.27</b>	$^{13}\text{C}$ NMR (100 MHz, $\text{CDCl}_3$ ) of compound <b>40</b> .....	122
<b>Figure A2.28</b>	$^1\text{H}$ NMR (400 MHz, $\text{CDCl}_3$ ) of compound <b>41</b> .....	123
<b>Figure A2.29</b>	Infrared spectrum NMR (thin film, NaCl) of compound <b>41</b> .....	124

<b>Figure A2.30</b>	$^{13}\text{C}$ NMR (100 MHz, $\text{CDCl}_3$ ) of compound <b>41</b> .....	124
<b>Figure A2.31</b>	$^1\text{H}$ NMR (400 MHz, $\text{CDCl}_3$ ) of compound <b>42</b> .....	125
<b>Figure A2.32</b>	Infrared spectrum NMR (thin film, NaCl) of compound <b>42</b> .....	126
<b>Figure A2.33</b>	$^{13}\text{C}$ NMR (100 MHz, $\text{CDCl}_3$ ) of compound <b>42</b> .....	126
<b>Figure A2.34</b>	$^1\text{H}$ NMR (400 MHz, $\text{CDCl}_3$ ) of compound <b>43</b> .....	127
<b>Figure A2.35</b>	Infrared spectrum NMR (thin film, NaCl) of compound <b>43</b> .....	128
<b>Figure A2.36</b>	$^{13}\text{C}$ NMR (100 MHz, $\text{CDCl}_3$ ) of compound <b>43</b> .....	128
<b>Figure A2.37</b>	$^1\text{H}$ NMR (400 MHz, $\text{CDCl}_3$ ) of compound <b>44</b> .....	129
<b>Figure A2.38</b>	Infrared spectrum NMR (thin film, NaCl) of compound <b>44</b> .....	130
<b>Figure A2.39</b>	$^{13}\text{C}$ NMR (100 MHz, $\text{CDCl}_3$ ) of compound <b>44</b> .....	130
<b>Figure A2.40</b>	$^1\text{H}$ NMR (400 MHz, $\text{CDCl}_3$ ) of compound <b>45</b> .....	131
<b>Figure A2.41</b>	Infrared spectrum NMR (thin film, NaCl) of compound <b>45</b> .....	132
<b>Figure A2.42</b>	$^{13}\text{C}$ NMR (100 MHz, $\text{CDCl}_3$ ) of compound <b>45</b> .....	132
<b>Figure A2.43</b>	$^1\text{H}$ NMR (400 MHz, $\text{CDCl}_3$ ) of compound <b>47</b> .....	133
<b>Figure A2.44</b>	Infrared spectrum NMR (thin film, NaCl) of compound <b>47</b> .....	134
<b>Figure A2.45</b>	$^{13}\text{C}$ NMR (100 MHz, $\text{CDCl}_3$ ) of compound <b>47</b> .....	134
<b>Figure A2.46</b>	$^1\text{H}$ NMR (400 MHz, $\text{CDCl}_3$ ) of compound <b><i>epi-47</i></b> .....	135
<b>Figure A2.47</b>	Infrared spectrum NMR (thin film, NaCl) of compound <b><i>epi-47</i></b> .....	136
<b>Figure A2.48</b>	$^{13}\text{C}$ NMR (100 MHz, $\text{CDCl}_3$ ) of compound <b><i>epi-47</i></b> .....	136
<b>Figure A2.49</b>	$^1\text{H}$ NMR (400 MHz, $\text{CDCl}_3$ ) of compound <b>48</b> .....	137
<b>Figure A2.50</b>	Infrared spectrum NMR (thin film, NaCl) of compound <b>48</b> .....	138
<b>Figure A2.51</b>	$^{13}\text{C}$ NMR (100 MHz, $\text{CDCl}_3$ ) of compound <b>48</b> .....	138

<b>Figure A2.52</b>	$^1\text{H}$ NMR (400 MHz, $\text{CDCl}_3$ ) of compound <b>49</b> .....	139
<b>Figure A2.53</b>	Infrared spectrum NMR (thin film, NaCl) of compound <b>49</b> .....	140
<b>Figure A2.54</b>	$^{13}\text{C}$ NMR (100 MHz, $\text{CDCl}_3$ ) of compound <b>49</b> .....	140
<b>Figure A2.55</b>	$^1\text{H}$ NMR (400 MHz, $\text{CDCl}_3$ ) of compound <b>50</b> .....	141
<b>Figure A2.56</b>	Infrared spectrum NMR (thin film, NaCl) of compound <b>50</b> .....	142
<b>Figure A2.57</b>	$^{13}\text{C}$ NMR (100 MHz, $\text{CDCl}_3$ ) of compound <b>50</b> .....	142
<b>Figure A2.58</b>	$^1\text{H}$ NMR (400 MHz, $\text{CDCl}_3$ ) of compound <b>51</b> .....	143
<b>Figure A2.59</b>	Infrared spectrum NMR (thin film, NaCl) of compound <b>51</b> .....	144
<b>Figure A2.60</b>	$^{13}\text{C}$ NMR (100 MHz, $\text{CDCl}_3$ ) of compound <b>51</b> .....	144
<b>Figure A2.61</b>	$^1\text{H}$ NMR (400 MHz, $\text{CDCl}_3$ ) of compound <b>59</b> .....	145
<b>Figure A2.62</b>	Infrared spectrum NMR (thin film, NaCl) of compound <b>59</b> .....	146
<b>Figure A2.63</b>	$^{13}\text{C}$ NMR (100 MHz, $\text{CDCl}_3$ ) of compound <b>59</b> .....	146
<b>Figure A2.64</b>	$^1\text{H}$ NMR (400 MHz, $\text{CDCl}_3$ ) of compound <b>100</b> .....	147
<b>Figure A2.65</b>	Infrared spectrum NMR (thin film, NaCl) of compound <b>100</b> ....	148
<b>Figure A2.66</b>	$^{13}\text{C}$ NMR (100 MHz, $\text{CDCl}_3$ ) of compound <b>100</b> .....	148
<b>Figure A2.67</b>	$^1\text{H}$ NMR (400 MHz, $\text{CDCl}_3$ ) of compound <b>101</b> .....	149
<b>Figure A2.68</b>	Infrared spectrum NMR (thin film, NaCl) of compound <b>101</b> ....	150
<b>Figure A2.69</b>	$^{13}\text{C}$ NMR (100 MHz, $\text{CDCl}_3$ ) of compound <b>101</b> .....	150
<b>Figure A2.70</b>	$^1\text{H}$ NMR (400 MHz, $\text{CDCl}_3$ ) of compound <b>60</b> .....	151
<b>Figure A2.71</b>	Infrared spectrum NMR (thin film, NaCl) of compound <b>60</b> .....	152
<b>Figure A2.72</b>	$^{13}\text{C}$ NMR (100 MHz, $\text{CDCl}_3$ ) of compound <b>60</b> .....	152
<b>Figure A2.73</b>	$^1\text{H}$ NMR (400 MHz, $\text{CDCl}_3$ ) of compound <b>61</b> .....	153

<b>Figure A2.74</b>	Infrared spectrum NMR (thin film, NaCl) of compound <b>61</b> .....	154
<b>Figure A2.75</b>	$^{13}\text{C}$ NMR (100 MHz, $\text{CDCl}_3$ ) of compound <b>61</b> .....	154
<b>Figure A2.76</b>	$^1\text{H}$ NMR (400 MHz, $\text{CDCl}_3$ ) of compound <b>62</b> .....	155
<b>Figure A2.77</b>	Infrared spectrum NMR (thin film, NaCl) of compound <b>62</b> .....	156
<b>Figure A2.78</b>	$^{13}\text{C}$ NMR (100 MHz, $\text{CDCl}_3$ ) of compound <b>62</b> .....	156
<b>Figure A2.79</b>	$^1\text{H}$ NMR (400 MHz, $\text{CDCl}_3$ ) of compound <b>63</b> .....	157
<b>Figure A2.80</b>	Infrared spectrum NMR (thin film, NaCl) of compound <b>63</b> .....	158
<b>Figure A2.81</b>	$^{13}\text{C}$ NMR (100 MHz, $\text{CDCl}_3$ ) of compound <b>63</b> .....	158
<b>Figure A2.82</b>	$^1\text{H}$ NMR (400 MHz, $\text{CDCl}_3$ ) of compound <b>64</b> .....	159
<b>Figure A2.83</b>	Infrared spectrum NMR (thin film, NaCl) of compound <b>64</b> .....	160
<b>Figure A2.84</b>	$^{13}\text{C}$ NMR (100 MHz, $\text{CDCl}_3$ ) of compound <b>64</b> .....	160
<b>Figure A2.85</b>	$^1\text{H}$ NMR (400 MHz, $\text{CDCl}_3$ ) of compound <b>67</b> .....	161
<b>Figure A2.86</b>	Infrared spectrum NMR (thin film, NaCl) of compound <b>67</b> .....	162
<b>Figure A2.87</b>	$^{13}\text{C}$ NMR (100 MHz, $\text{CDCl}_3$ ) of compound <b>67</b> .....	162
<b>Figure A2.88</b>	$^1\text{H}$ NMR (400 MHz, $\text{CDCl}_3$ ) of compound <b>72</b> .....	163
<b>Figure A2.89</b>	Infrared spectrum NMR (thin film, NaCl) of compound <b>72</b> .....	164
<b>Figure A2.90</b>	$^{13}\text{C}$ NMR (100 MHz, $\text{CDCl}_3$ ) of compound <b>72</b> .....	164
<b>Figure A2.91</b>	$^1\text{H}$ NMR (400 MHz, $\text{CDCl}_3$ ) of compound <b>74</b> .....	165
<b>Figure A2.92</b>	Infrared spectrum NMR (thin film, NaCl) of compound <b>74</b> .....	166
<b>Figure A2.93</b>	$^{13}\text{C}$ NMR (100 MHz, $\text{CDCl}_3$ ) of compound <b>74</b> .....	166
<b>Figure A2.91</b>	$^1\text{H}$ NMR (400 MHz, $\text{CDCl}_3$ ) of compound <b>74</b> .....	165
<b>Figure A2.92</b>	Infrared spectrum NMR (thin film, NaCl) of compound <b>74</b> .....	166

<b>Figure A2.93</b>	$^{13}\text{C}$ NMR (100 MHz, $\text{CDCl}_3$ ) of compound <b>74</b> .....	166
<b>Figure A2.94</b>	$^1\text{H}$ NMR (400 MHz, $\text{CDCl}_3$ ) of compound <b>75</b> .....	167
<b>Figure A2.95</b>	Infrared spectrum NMR (thin film, NaCl) of compound <b>75</b> .....	168
<b>Figure A2.96</b>	$^{13}\text{C}$ NMR (100 MHz, $\text{CDCl}_3$ ) of compound <b>75</b> .....	168
<b>Figure A2.97</b>	$^1\text{H}$ NMR (400 MHz, $\text{CDCl}_3$ ) of compound <b>76</b> .....	169
<b>Figure A2.98</b>	Infrared spectrum NMR (thin film, NaCl) of compound <b>76</b> .....	170
<b>Figure A2.99</b>	$^{13}\text{C}$ NMR (100 MHz, $\text{CDCl}_3$ ) of compound <b>76</b> .....	170
<b>Figure A2.100</b>	$^1\text{H}$ NMR (400 MHz, $\text{CDCl}_3$ ) of compound <b>57</b> .....	171
<b>Figure A2.101</b>	Infrared spectrum NMR (thin film, NaCl) of compound <b>57</b> .....	172
<b>Figure A2.102</b>	$^{13}\text{C}$ NMR (100 MHz, $\text{CDCl}_3$ ) of compound <b>57</b> .....	172
<b>Figure A2.103</b>	$^1\text{H}$ NMR (400 MHz, $\text{CDCl}_3$ ) of compound <b>77</b> .....	173
<b>Figure A2.104</b>	Infrared spectrum NMR (thin film, NaCl) of compound <b>77</b> .....	174
<b>Figure A2.105</b>	$^{13}\text{C}$ NMR (100 MHz, $\text{CDCl}_3$ ) of compound <b>77</b> .....	174
<b>Figure A2.106</b>	$^1\text{H}$ NMR (400 MHz, $\text{CDCl}_3$ ) of compound <b>78</b> .....	175
<b>Figure A2.107</b>	Infrared spectrum NMR (thin film, NaCl) of compound <b>78</b> .....	176
<b>Figure A2.108</b>	$^{13}\text{C}$ NMR (100 MHz, $\text{CDCl}_3$ ) of compound <b>78</b> .....	176
<b>Figure A2.109</b>	$^1\text{H}$ NMR (400 MHz, $\text{CDCl}_3$ ) of compound <b>79</b> .....	177
<b>Figure A2.110</b>	Infrared spectrum NMR (thin film, NaCl) of compound <b>79</b> .....	178
<b>Figure A2.111</b>	$^{13}\text{C}$ NMR (100 MHz, $\text{CDCl}_3$ ) of compound <b>79</b> .....	178
<b>Figure A2.112</b>	$^1\text{H}$ NMR (400 MHz, $\text{CDCl}_3$ ) of compound <b>80</b> .....	179
<b>Figure A2.113</b>	Infrared spectrum NMR (thin film, NaCl) of compound <b>80</b> .....	180
<b>Figure A2.114</b>	$^{13}\text{C}$ NMR (100 MHz, $\text{CDCl}_3$ ) of compound <b>80</b> .....	180

<b>Figure A2.115</b>	$^1\text{H}$ NMR (400 MHz, $\text{CDCl}_3$ ) of compound <b>56</b> .....	181
<b>Figure A2.116</b>	Infrared spectrum NMR (thin film, NaCl) of compound <b>56</b> .....	182
<b>Figure A2.117</b>	$^{13}\text{C}$ NMR (100 MHz, $\text{CDCl}_3$ ) of compound <b>56</b> .....	182
<b>Figure A2.118</b>	$^1\text{H}$ NMR (400 MHz, $\text{CDCl}_3$ ) of compound <b>55</b> .....	183
<b>Figure A2.119</b>	Infrared spectrum NMR (thin film, NaCl) of compound <b>55</b> .....	184
<b>Figure A2.120</b>	$^{13}\text{C}$ NMR (100 MHz, $\text{CDCl}_3$ ) of compound <b>55</b> .....	184
<b>Figure A2.121</b>	$^1\text{H}$ NMR (400 MHz, $\text{CDCl}_3$ ) of compound <b>83</b> .....	185
<b>Figure A2.122</b>	Infrared spectrum NMR (thin film, NaCl) of compound <b>83</b> .....	186
<b>Figure A2.123</b>	$^{13}\text{C}$ NMR (100 MHz, $\text{CDCl}_3$ ) of compound <b>83</b> .....	186
<b>Figure A2.124</b>	$^1\text{H}$ NMR (400 MHz, $\text{CDCl}_3$ ) of compound <b>85</b> (diastereomer 1) .....	187
<b>Figure A2.125</b>	Infrared spectrum NMR (thin film, NaCl) of compound <b>85</b> (diastereomer 1) .....	188
<b>Figure A2.126</b>	$^{13}\text{C}$ NMR (100 MHz, $\text{CDCl}_3$ ) of compound <b>85</b> (diastereomer 1) .....	188
<b>Figure A2.127</b>	$^1\text{H}$ NMR (400 MHz, $\text{CDCl}_3$ ) of compound <b>85</b> (diastereomer 2) .....	189
<b>Figure A2.128</b>	Infrared spectrum NMR (thin film, NaCl) of compound <b>85</b> (diastereomer 2) .....	190
<b>Figure A2.129</b>	$^{13}\text{C}$ NMR (100 MHz, $\text{CDCl}_3$ ) of compound <b>85</b> (diastereomer 2) .....	190

<b>Figure A2.130</b>	$^1\text{H}$ NMR (400 MHz, $\text{CDCl}_3$ ) of compound <b>86</b> (diastereomer 1) .....	191
<b>Figure A2.131</b>	Infrared spectrum NMR (thin film, NaCl) of compound <b>86</b> (diastereomer 1).....	192
<b>Figure A2.132</b>	$^{13}\text{C}$ NMR (100 MHz, $\text{CDCl}_3$ ) of compound <b>86</b> (diastereomer 1) .....	192
<b>Figure A2.133</b>	$^1\text{H}$ NMR (400 MHz, $\text{CDCl}_3$ ) of compound <b>86</b> (diastereomer 2) .....	193
<b>Figure A2.134</b>	Infrared spectrum NMR (thin film, NaCl) of compound <b>86</b> (diastereomer 2).....	194
<b>Figure A2.135</b>	$^{13}\text{C}$ NMR (100 MHz, $\text{CDCl}_3$ ) of compound <b>86</b> (diastereomer 2) .....	194
<b>Figure A2.136</b>	$^1\text{H}$ NMR (400 MHz, $\text{CDCl}_3$ ) of compound <b>87</b> (diastereomer 1) .....	195
<b>Figure A2.137</b>	Infrared spectrum NMR (thin film, NaCl) of compound <b>87</b> (diastereomer 1).....	196
<b>Figure A2.138</b>	$^{13}\text{C}$ NMR (100 MHz, $\text{CDCl}_3$ ) of compound <b>87</b> (diastereomer 1) .....	196
<b>Figure A2.139</b>	$^1\text{H}$ NMR (400 MHz, $\text{CDCl}_3$ ) of compound <b>87</b> (diastereomer 2) .....	197
<b>Figure A2.140</b>	Infrared spectrum NMR (thin film, NaCl) of compound <b>87</b> (diastereomer 2).....	198



<b>Figure A2.141</b>	$^{13}\text{C}$ NMR (100 MHz, $\text{CDCl}_3$ ) of compound <b>87</b> (diastereomer 2) .....	198
<b>Figure A2.142</b>	$^1\text{H}$ NMR (400 MHz, $\text{CD}_3\text{OD}$ ) of compound <b>89</b> .....	199
<b>Figure A2.143</b>	Infrared spectrum NMR (thin film, NaCl) of compound <b>89</b> .....	200
<b>Figure A2.144</b>	$^{13}\text{C}$ NMR (100 MHz, $\text{CD}_3\text{OD}$ ) of compound <b>89</b> .....	200
<b>Figure A2.145</b>	$^1\text{H}$ NMR (400 MHz, $\text{CD}_3\text{OD}$ ) of compound <b><i>epi-89</i></b> .....	201
<b>Figure A2.146</b>	Infrared spectrum NMR (thin film, NaCl) of compound <b><i>epi-89</i></b> .....	202
<b>Figure A2.147</b>	$^{13}\text{C}$ NMR (100 MHz, $\text{CD}_3\text{OD}$ ) of compound <b><i>epi-89</i></b> .....	202
<b>Figure A2.148</b>	$^1\text{H}$ NMR (400 MHz, $\text{CD}_3\text{OD}$ ) of compound <b>90</b> .....	203
<b>Figure A2.149</b>	Infrared spectrum NMR (thin film, NaCl) of compound <b>90</b> .....	204
<b>Figure A2.150</b>	$^{13}\text{C}$ NMR (100 MHz, $\text{CD}_3\text{OD}$ ) of compound <b>90</b> .....	204
<b>Figure A2.151</b>	$^1\text{H}$ NMR (400 MHz, $\text{CD}_3\text{OD}$ ) of compound <b><i>epi-90</i></b> .....	205
<b>Figure A2.152</b>	Infrared spectrum NMR (thin film, NaCl) of compound <b><i>epi-90</i></b> .....	206
<b>Figure A2.153</b>	$^{13}\text{C}$ NMR (100 MHz, $\text{CD}_3\text{OD}$ ) of compound <b><i>epi-90</i></b> .....	206
<b>Figure A2.154</b>	$^1\text{H}$ NMR (400 MHz, $\text{CDCl}_3$ ) of compound <b>91</b> .....	207
<b>Figure A2.155</b>	Infrared spectrum NMR (thin film, NaCl) of compound <b>91</b> .....	208
<b>Figure A2.156</b>	$^{13}\text{C}$ NMR (100 MHz, $\text{CDCl}_3$ ) of compound <b>91</b> .....	208
<b>Figure A2.157</b>	$^1\text{H}$ NMR (400 MHz, $\text{CDCl}_3$ ) of compound <b>94</b> .....	209
<b>Figure A2.158</b>	Infrared spectrum NMR (thin film, NaCl) of compound <b>94</b> .....	210
<b>Figure A2.159</b>	$^{13}\text{C}$ NMR (100 MHz, $\text{CDCl}_3$ ) of compound <b>94</b> .....	210
<b>Figure A2.160</b>	$^1\text{H}$ NMR (400 MHz, $\text{CDCl}_3$ ) of compound <b>53</b> .....	211

<b>Figure A2.161</b>	Infrared spectrum NMR (thin film, NaCl) of compound <b>53</b> .....	212
<b>Figure A2.162</b>	<sup>13</sup> C NMR (100 MHz, CDCl <sub>3</sub> ) of compound <b>53</b> .....	212
<b>Figure A2.163</b>	<sup>1</sup> H NMR (400 MHz, CDCl <sub>3</sub> ) of compound <b>1</b> .....	213
<b>Figure A2.164</b>	Infrared spectrum NMR (thin film, NaCl) of compound <b>1</b> .....	214
<b>Figure A2.165</b>	<sup>13</sup> C NMR (100 MHz, CDCl <sub>3</sub> ) of compound <b>1</b> .....	214
<b>Figure A2.166</b>	<sup>1</sup> H NMR (400 MHz, CDCl <sub>3</sub> ) of compound <b>4</b> .....	215
<b>Figure A2.167</b>	Infrared spectrum NMR (thin film, NaCl) of compound <b>4</b> .....	216
<b>Figure A2.168</b>	<sup>13</sup> C NMR (100 MHz, CDCl <sub>3</sub> ) of compound <b>4</b> .....	216

### **APPENDIX 3**

#### *X-Ray Crystallography Reports Relevant to Chapter 1*

<b>Figure A3.1.1</b>	X-ray Crystal Structure of Tetracycle <b>47</b> .....	218
<b>Figure A3.2.1</b>	X-ray Crystal Structure of Cyclobutane <b>63</b> .....	238
<b>Figure A3.3.1</b>	X-ray Crystal Structure of Cyclobutane <b>64</b> .....	256
<b>Figure A3.4.1</b>	X-ray Crystal Structure of Cycloheptane <b>72</b> .....	277
<b>Figure A3.5.1</b>	X-ray Crystal Structure of Cyclobutane <b>83</b> .....	302
<b>Figure A3.6.1</b>	X-ray Crystal Structure of Cyclobutanol <b>90</b> .....	322
<b>Figure A3.7.1</b>	X-ray Crystal Structure of Cyclobutanol <b>epi-90</b> .....	337
<b>Figure A3.8.1</b>	X-ray Crystal Structure of Nitrile <b>94</b> .....	355
<b>Figure A3.9.1</b>	X-ray Crystal Structure of Scabrolide A ( <b>1</b> ) .....	370

### **APPENDIX 5**

#### *Spectra Relevant to Appendix 5*

<b>Figure A5.1</b>	<sup>1</sup> H NMR (400 MHz, C <sub>6</sub> D <sub>6</sub> ) of compound <b>104</b> .....	393
<b>Figure A5.2</b>	Infrared spectrum NMR (thin film, NaCl) of compound <b>104</b> .....	394

<b>Figure A5.3</b>	$^{13}\text{C}$ NMR (100 MHz, $\text{C}_6\text{D}_6$ ) of compound <b>104</b> .....	394
<b>Figure A5.4</b>	$^1\text{H}$ NMR (500 MHz, $(\text{CD})_3\text{CO}$ ) of compound <b>105</b> .....	395
<b>Figure A5.5</b>	Infrared spectrum NMR (thin film, NaCl) of compound <b>105</b> .....	396
<b>Figure A5.6</b>	$^{13}\text{C}$ NMR (100 MHz, $\text{C}_6\text{D}_6$ ) of compound <b>105</b> .....	396
<b>Figure A5.7</b>	$^1\text{H}$ NMR (500 MHz, $\text{CDCl}_3$ ) of compound <b>81</b> .....	397
<b>Figure A5.8</b>	Infrared spectrum NMR (thin film, NaCl) of compound <b>81</b> .....	398
<b>Figure A5.9</b>	$^{13}\text{C}$ NMR (100 MHz, $\text{CDCl}_3$ ) of compound <b>81</b> .....	398
<b>Figure A5.10</b>	$^1\text{H}$ NMR (500 MHz, $\text{CDCl}_3$ ) of compound <b>82</b> .....	399
<b>Figure A5.11</b>	Infrared spectrum NMR (thin film, NaCl) of compound <b>82</b> .....	400
<b>Figure A5.12</b>	$^{13}\text{C}$ NMR (100 MHz, $\text{CDCl}_3$ ) of compound <b>82</b> .....	400

## **CHAPTER 2**

### *Asymmetric Synthesis of Havellockate*

<b>Figure 2.1.1</b>	Examples of the polycyclic furanobutenolide-derived cembranoids .....	401
<b>Figure 2.1.2</b>	Havellockate ( <b>106</b> ) in two- and three- dimensions.....	402
<b>Figure 2.2.1</b>	Retrosynthetic analysis of havellockate ( <b>106</b> ).....	402

## **APPENDIX 7**

### *Spectra Relevant to Chapter 2*

<b>Figure A7.1</b>	$^1\text{H}$ NMR (400 MHz, $\text{CDCl}_3$ ) of compound <b>115</b> .....	449
<b>Figure A7.2</b>	Infrared spectrum NMR (thin film, NaCl) of compound <b>115</b> .....	450
<b>Figure A7.3</b>	$^{13}\text{C}$ NMR (100 MHz, $\text{CDCl}_3$ ) of compound <b>115</b> .....	450
<b>Figure A7.4</b>	$^1\text{H}$ NMR (400 MHz, $\text{CDCl}_3$ ) of compound <b>116</b> .....	451
<b>Figure A7.5</b>	Infrared spectrum NMR (thin film, NaCl) of compound <b>116</b> .....	452

<b>Figure A7.6</b>	$^{13}\text{C}$ NMR (100 MHz, $\text{CDCl}_3$ ) of compound <b>116</b> .....	452
<b>Figure A7.7</b>	$^1\text{H}$ NMR (400 MHz, $\text{CDCl}_3$ ) of compound <b>117</b> .....	453
<b>Figure A7.8</b>	Infrared spectrum NMR (thin film, NaCl) of compound <b>117</b> .....	454
<b>Figure A7.9</b>	$^{13}\text{C}$ NMR (100 MHz, $\text{CDCl}_3$ ) of compound <b>117</b> .....	454
<b>Figure A7.10</b>	$^1\text{H}$ NMR (400 MHz, $\text{CDCl}_3$ ) of compound <b>118</b> .....	455
<b>Figure A7.11</b>	Infrared spectrum NMR (thin film, NaCl) of compound <b>118</b> .....	456
<b>Figure A7.12</b>	$^{13}\text{C}$ NMR (100 MHz, $\text{CDCl}_3$ ) of compound <b>118</b> .....	456
<b>Figure A7.13</b>	$^1\text{H}$ NMR (400 MHz, $\text{CDCl}_3$ ) of compound <b>113</b> .....	457
<b>Figure A7.14</b>	Infrared spectrum NMR (thin film, NaCl) of compound <b>113</b> .....	458
<b>Figure A7.15</b>	$^{13}\text{C}$ NMR (100 MHz, $\text{CDCl}_3$ ) of compound <b>113</b> .....	458
<b>Figure A7.16</b>	$^1\text{H}$ NMR (400 MHz, $\text{CDCl}_3$ ) of compound <b>122</b> .....	459
<b>Figure A7.17</b>	Infrared spectrum NMR (thin film, NaCl) of compound <b>122</b> .....	460
<b>Figure A7.18</b>	$^{13}\text{C}$ NMR (100 MHz, $\text{CDCl}_3$ ) of compound <b>122</b> .....	460
<b>Figure A7.19</b>	$^1\text{H}$ NMR (500 MHz, $\text{CDCl}_3$ ) of compound <b>114</b> .....	461
<b>Figure A7.20</b>	Infrared spectrum NMR (thin film, NaCl) of compound <b>114</b> .....	462
<b>Figure A7.21</b>	$^{13}\text{C}$ NMR (100 MHz, $\text{CDCl}_3$ ) of compound <b>114</b> .....	462
<b>Figure A7.22</b>	$^1\text{H}$ NMR (400 MHz, $\text{CDCl}_3$ ) of compound <b>126</b> .....	463
<b>Figure A7.23</b>	Infrared spectrum NMR (thin film, NaCl) of compound <b>126</b> .....	464
<b>Figure A7.24</b>	$^{13}\text{C}$ NMR (100 MHz, $\text{CDCl}_3$ ) of compound <b>126</b> .....	464
<b>Figure A7.25</b>	$^1\text{H}$ NMR (400 MHz, $\text{CDCl}_3$ ) of compound <b>111</b> .....	465
<b>Figure A7.26</b>	Infrared spectrum NMR (thin film, NaCl) of compound <b>111</b> .....	466
<b>Figure A7.27</b>	$^{13}\text{C}$ NMR (100 MHz, $\text{CDCl}_3$ ) of compound <b>111</b> .....	466

<b>Figure A7.28</b>	$^1\text{H}$ NMR (400 MHz, $\text{CDCl}_3$ ) of compound <b>127</b> .....	467
<b>Figure A7.29</b>	Infrared spectrum NMR (thin film, NaCl) of compound <b>127</b> .....	468
<b>Figure A7.30</b>	$^{13}\text{C}$ NMR (100 MHz, $\text{CDCl}_3$ ) of compound <b>127</b> .....	468
<b>Figure A7.31</b>	$^1\text{H}$ NMR (400 MHz, $\text{CDCl}_3$ ) of compound <b>128</b> .....	469
<b>Figure A7.32</b>	Infrared spectrum NMR (thin film, NaCl) of compound <b>128</b> .....	470
<b>Figure A7.33</b>	$^{13}\text{C}$ NMR (100 MHz, $\text{CDCl}_3$ ) of compound <b>128</b> .....	470
<b>Figure A7.34</b>	$^1\text{H}$ NMR (400 MHz, $\text{CDCl}_3$ ) of compound <b>110</b> .....	471
<b>Figure A7.35</b>	Infrared spectrum NMR (thin film, NaCl) of compound <b>110</b> .....	472
<b>Figure A7.36</b>	$^{13}\text{C}$ NMR (100 MHz, $\text{CDCl}_3$ ) of compound <b>110</b> .....	472
<b>Figure A7.37</b>	$^1\text{H}$ NMR (400 MHz, $\text{C}_6\text{D}_6$ ) of compound <b>131</b> .....	473
<b>Figure A7.38</b>	Infrared spectrum NMR (thin film, NaCl) of compound <b>131</b> .....	474
<b>Figure A7.39</b>	$^{13}\text{C}$ NMR (100 MHz, $\text{C}_6\text{D}_6$ ) of compound <b>131</b> .....	474
<b>Figure A7.40</b>	$^1\text{H}$ NMR (400 MHz, $\text{CDCl}_3$ ) of compound <b>133</b> .....	475
<b>Figure A7.41</b>	Infrared spectrum NMR (thin film, NaCl) of compound <b>133</b> .....	476
<b>Figure A7.42</b>	$^{13}\text{C}$ NMR (100 MHz, $\text{CDCl}_3$ ) of compound <b>133</b> .....	476
<b>Figure A7.43</b>	$^1\text{H}$ NMR (400 MHz, $\text{CDCl}_3$ ) of compound <b>138</b> .....	477
<b>Figure A7.44</b>	Infrared spectrum NMR (thin film, NaCl) of compound <b>138</b> .....	478
<b>Figure A7.45</b>	$^{13}\text{C}$ NMR (100 MHz, $\text{CDCl}_3$ ) of compound <b>138</b> .....	478
<b>Figure A7.46</b>	$^1\text{H}$ NMR (400 MHz, $\text{CDCl}_3$ ) of compound <b>140</b> .....	479
<b>Figure A7.47</b>	Infrared spectrum NMR (thin film, NaCl) of compound <b>140</b> .....	480
<b>Figure A7.48</b>	$^{13}\text{C}$ NMR (100 MHz, $\text{CDCl}_3$ ) of compound <b>140</b> .....	480
<b>Figure A7.49</b>	$^1\text{H}$ NMR (400 MHz, $\text{CDCl}_3$ ) of compound <b>141</b> .....	481

<b>Figure A7.50</b>	Infrared spectrum NMR (thin film, NaCl) of compound <b>141</b> .....	482
<b>Figure A7.51</b>	$^{13}\text{C}$ NMR (100 MHz, $\text{CDCl}_3$ ) of compound <b>141</b> .....	482
<b>Figure A7.52</b>	$^1\text{H}$ NMR (600 MHz, pyridine- $d_5$ ) of compound <b>141</b> .....	481
<b>Figure A7.53</b>	Infrared spectrum NMR (thin film, NaCl) of compound <b>141</b> .....	482
<b>Figure A7.54</b>	$^{13}\text{C}$ NMR (100 MHz, pyridine- $d_5$ ) of compound <b>141</b> .....	482

## **APPENDIX 8**

### *X-Ray Crystallography Reports Relevant to Chapter 2*

<b>Figure A8.1.1</b>	X-Ray Coordinate of Compound <b>111</b> .....	486
<b>Figure A8.2.1</b>	X-Ray Coordinate of Allylation Product <b>133</b> .....	503
<b>Figure A8.3.1</b>	X-Ray Coordinate of Havellockate ( <b>106</b> ) .....	503

## **CHAPTER 3**

### *Synthesis of Carboxylic Acids and Dimer Esters from*

#### *Pinene-Derived Secondary Organic Aerosol*

<b>Figure 3.1.1</b>	Examples of SOA components derived from $\alpha$ -pinene ( <b>144</b> ) ....	549
<b>Figure 3.1.2</b>	Examples of pinene-derived dimer esters detected in SOA mixtures .....	550

- Figure 3.2.1** UPLC/(-)ESI-Q-TOF-MS BPI chromatogram of an equimolar (1.00  $\mu\text{M}$ ) aqueous solution of carboxylic acids **145**, **146**, and **152** and dimer esters **153–155**. (-)ESI efficiencies, normalized to that of cis-pinonic acid (**145**), are given in parentheses. (Inset) Weighted (1/X), linear ( $R^2 > 0.998$ ) calibration curves, generated from triplicate measurements (1s) of equimolar aqueous solutions of carboxylic acids **145**, **146**, and **152** and dimer esters **153–155** spanning a concentration range from 0.200 to 5.00  $\mu\text{M}$ .....554
- Figure 3.3.1** Pinic acid dimer ester targets **156–158**.....555
- Figure 3.4.1** Extracted ion chromatograms (EIC) and MS/MS spectra of synthesized secondary (red) and primary (blue) dimer esters of *cis*-pinic acid and (A)  $\beta$ -pinene diol, (B)  $\alpha$ -pinene diol, and (C) 6-hydroxyhexanoic acid, as well as of dimer esters identified in SOA (black diamonds, dashed lines).....555

## APPENDIX 9

### *Spectra Relevant to Chapter 3*

- Figure A8.1**  $^1\text{H}$  NMR (500 MHz,  $\text{CDCl}_3$ ) of compound **171**..... 588
- Figure A8.2** Infrared spectrum NMR (thin film, NaCl) of compound **171**..... 589
- Figure A8.3**  $^{13}\text{C}$  NMR (125 MHz,  $\text{CDCl}_3$ ) of compound **171**..... 589

<b>Figure A8.4</b>	$^1\text{H}$ NMR (500 MHz, $\text{CDCl}_3$ ) of compound <b>151</b> .....	590
<b>Figure A8.5</b>	Infrared spectrum NMR (thin film, NaCl) of compound <b>151</b> .....	591
<b>Figure A8.6</b>	$^{13}\text{C}$ NMR (125 MHz, $\text{CDCl}_3$ ) of compound <b>151</b> .....	591
<b>Figure A8.7</b>	$^1\text{H}$ NMR (500 MHz, $\text{CDCl}_3$ ) of compound <b>152</b> .....	592
<b>Figure A8.9</b>	Infrared spectrum NMR (thin film, NaCl) of compound <b>152</b> .....	593
<b>Figure A8.9</b>	$^{13}\text{C}$ NMR (125 MHz, $\text{CDCl}_3$ ) of compound <b>152</b> .....	593
<b>Figure A8.10</b>	$^1\text{H}$ NMR (500 MHz, $\text{CDCl}_3$ ) of compound <b>172</b> .....	594
<b>Figure A8.11</b>	Infrared spectrum NMR (thin film, NaCl) of compound <b>172</b> .....	595
<b>Figure A8.12</b>	$^{13}\text{C}$ NMR (125 MHz, $\text{CDCl}_3$ ) of compound <b>172</b> .....	595
<b>Figure A8.13</b>	$^1\text{H}$ NMR (500 MHz, $\text{CDCl}_3$ ) of compound <b>153</b> .....	596
<b>Figure A8.14</b>	Infrared spectrum NMR (thin film, NaCl) of compound <b>153</b> .....	597
<b>Figure A8.15</b>	$^{13}\text{C}$ NMR (125 MHz, $\text{CDCl}_3$ ) of compound <b>153</b> .....	597
<b>Figure A8.16</b>	$^1\text{H}$ NMR (500 MHz, $\text{CDCl}_3$ ) of compound <b>173</b> .....	598
<b>Figure A8.17</b>	Infrared spectrum NMR (thin film, NaCl) of compound <b>173</b> .....	599
<b>Figure A8.18</b>	$^{13}\text{C}$ NMR (125 MHz, $\text{CDCl}_3$ ) of compound <b>173</b> .....	599
<b>Figure A8.19</b>	$^1\text{H}$ NMR (500 MHz, $\text{CDCl}_3$ ) of compound <b>154</b> .....	600
<b>Figure A8.20</b>	Infrared spectrum NMR (thin film, NaCl) of compound <b>154</b> .....	601
<b>Figure A8.21</b>	$^{13}\text{C}$ NMR (125 MHz, $\text{CDCl}_3$ ) of compound <b>154</b> .....	601
<b>Figure A8.22</b>	$^1\text{H}$ NMR (500 MHz, $\text{CDCl}_3$ ) of compound <b>174</b> .....	602
<b>Figure A8.23</b>	Infrared spectrum NMR (thin film, NaCl) of compound <b>174</b> .....	603
<b>Figure A8.24</b>	$^{13}\text{C}$ NMR (125 MHz, $\text{CDCl}_3$ ) of compound <b>174</b> .....	603
<b>Figure A8.25</b>	$^1\text{H}$ NMR (500 MHz, $\text{CDCl}_3$ ) of compound <b>155</b> .....	604



<b>Figure A8.26</b>	Infrared spectrum NMR (thin film, NaCl) of compound <b>155</b> .....	605
<b>Figure A8.27</b>	$^{13}\text{C}$ NMR (125 MHz, $\text{CDCl}_3$ ) of compound <b>155</b> .....	605
<b>Figure A8.28</b>	$^1\text{H}$ NMR (500 MHz, $\text{CDCl}_3$ ) of compound <b>160</b> .....	606
<b>Figure A8.29</b>	Infrared spectrum NMR (thin film, NaCl) of compound <b>160</b> .....	607
<b>Figure A8.30</b>	$^{13}\text{C}$ NMR (100 MHz, $\text{CDCl}_3$ ) of compound <b>160</b> .....	607
<b>Figure A8.31</b>	$^1\text{H}$ NMR (400 MHz, $\text{CDCl}_3$ ) of compound <b>161</b> .....	608
<b>Figure A8.32</b>	Infrared spectrum NMR (thin film, NaCl) of compound <b>161</b> .....	609
<b>Figure A8.33</b>	$^{13}\text{C}$ NMR (100 MHz, $\text{CDCl}_3$ ) of compound <b>161</b> .....	609
<b>Figure A8.34</b>	$^1\text{H}$ NMR (400 MHz, $\text{CDCl}_3$ ) of compound <b>162</b> .....	610
<b>Figure A8.35</b>	Infrared spectrum NMR (thin film, NaCl) of compound <b>162</b> .....	611
<b>Figure A8.36</b>	$^{13}\text{C}$ NMR (100 MHz, $\text{CDCl}_3$ ) of compound <b>162</b> .....	611
<b>Figure A8.37</b>	$^1\text{H}$ NMR (400 MHz, $\text{CDCl}_3$ ) of compound <b>163</b> .....	612
<b>Figure A8.38</b>	Infrared spectrum NMR (thin film, NaCl) of compound <b>163</b> .....	613
<b>Figure A8.39</b>	$^{13}\text{C}$ NMR (100 MHz, $\text{CDCl}_3$ ) of compound <b>163</b> .....	613
<b>Figure A8.40</b>	$^1\text{H}$ NMR (400 MHz, $\text{CDCl}_3$ ) of compound <b>164</b> .....	614
<b>Figure A8.41</b>	Infrared spectrum NMR (thin film, NaCl) of compound <b>164</b> .....	615
<b>Figure A8.42</b>	$^{13}\text{C}$ NMR (100 MHz, $\text{CDCl}_3$ ) of compound <b>164</b> .....	615
<b>Figure A8.43</b>	$^1\text{H}$ NMR (400 MHz, $\text{CDCl}_3$ ) of compound <b>156</b> .....	616
<b>Figure A8.44</b>	Infrared spectrum NMR (thin film, NaCl) of compound <b>156</b> .....	617
<b>Figure A8.45</b>	$^{13}\text{C}$ NMR (100 MHz, $\text{CDCl}_3$ ) of compound <b>156</b> .....	617
<b>Figure A8.46</b>	$^1\text{H}$ NMR (400 MHz, $\text{CDCl}_3$ ) of compound <b>157</b> .....	618
<b>Figure A8.47</b>	Infrared spectrum NMR (thin film, NaCl) of compound <b>157</b> .....	619

<b>Figure A8.48</b>	$^{13}\text{C}$ NMR (100 MHz, $\text{CDCl}_3$ ) of compound <b>157</b> .....	619
<b>Figure A8.49</b>	$^1\text{H}$ NMR (400 MHz, $\text{CDCl}_3$ ) of compound <b>158</b> .....	620
<b>Figure A8.50</b>	Infrared spectrum NMR (thin film, NaCl) of compound <b>158</b> .....	621
<b>Figure A8.51</b>	$^{13}\text{C}$ NMR (100 MHz, $\text{CDCl}_3$ ) of compound <b>158</b> .....	621
<b>Figure A8.52</b>	$^1\text{H}$ NMR (400 MHz, $\text{CDCl}_3$ ) of compound <b>168</b> .....	622
<b>Figure A8.53</b>	Infrared spectrum NMR (thin film, NaCl) of compound <b>168</b> .....	623
<b>Figure A8.54</b>	$^{13}\text{C}$ NMR (100 MHz, $\text{CDCl}_3$ ) of compound <b>168</b> .....	623
<b>Figure A8.55</b>	$^1\text{H}$ NMR (400 MHz, $\text{CDCl}_3$ ) of compound <b>169</b> .....	624
<b>Figure A8.56</b>	Infrared spectrum NMR (thin film, NaCl) of compound <b>169</b> .....	625
<b>Figure A8.57</b>	$^{13}\text{C}$ NMR (100 MHz, $\text{CDCl}_3$ ) of compound <b>169</b> .....	625
<b>Figure A8.58</b>	$^1\text{H}$ NMR (400 MHz, $\text{CDCl}_3$ ) of compound <b>170</b> .....	626
<b>Figure A8.59</b>	Infrared spectrum NMR (thin film, NaCl) of compound <b>170</b> .....	627
<b>Figure A8.60</b>	$^{13}\text{C}$ NMR (100 MHz, $\text{CDCl}_3$ ) of compound <b>170</b> .....	627

## LIST OF SCHEMES

### CHAPTER 1

#### *The Total Synthesis of (–)-Scabrolide A*

<b>Scheme 1.1.1</b>	Proposed biosynthesis of scabrolides A ( <b>1</b> ) and B ( <b>12</b> ), sinulochmodin C ( <b>3</b> ), and ineleganolide ( <b>6</b> ) .....	3
<b>Scheme 1.3.1</b>	First-generation synthesis of vinylcyclopentenone <i>ent</i> - <b>15</b> .....	5
<b>Scheme 1.3.2</b>	Synthesis of RCM substrate <b>28</b> .....	6
<b>Scheme 1.4.1</b>	A. Failed RCM macrocyclization. B. Diels–Alder of ester <b>28</b> .....	7
<b>Scheme 1.5.1</b>	Second-generation synthesis of vinylcyclopentenone <b>15</b> .....	9
<b>Scheme 1.5.2</b>	Synthesis of ester <b>44</b> , Diels–Alder cycloaddition, and undesired aldol cyclization .....	10
<b>Scheme 1.5.3</b>	Diels–Alder reaction of <b>48</b> , directed epoxidation reductive epoxide opening and failed oxidation of alcohol <b>51</b> .....	11
<b>Scheme 1.6.2</b>	Synthesis of simplified [2+2] substrate <b>62</b> .....	13
<b>Scheme 1.6.3</b>	[2+2] photocycloaddition of enone <b>62</b> .....	15
<b>Scheme 1.6.4</b>	Tamao–Fleming oxidation of <b>63</b> and failed Tamao–Fleming oxidation of <b>64</b> .....	17
<b>Scheme 1.6.5</b>	Oxidative ring expansion of cyclobutanol <b>67</b> to <b>72</b> .....	18
<b>Scheme 1.7.1</b>	Synthesis of isopropenyl-bearing ynoic acid <b>57</b> .....	19
<b>Scheme 1.7.2</b>	Esterification of ynoic acid <b>57</b> and Diels–Alder/oxidation sequence .....	20

<b>Scheme 1.8.1</b>	Photocyclization of fully elaborated substrate 55 to form undesired product <b>83</b> .....	22
<b>Scheme 1.9.1</b>	Epoxidation of 56 and successful [2+2] of protected substrate <b>86</b> .....	24
<b>Scheme 1.9.2</b>	Failed Tamao–Fleming oxidation of epoxide <b>87</b> , reductive opening of epoxide <b>87</b> , and successful Tamao–Fleming oxidation of <b>89</b> .....	25
<b>Scheme 1.10.1</b>	Oxidative ring-expansion of cyclobutanol <b>90</b> and unexpected cyclization to <b>91</b> during Grieco dehydration ...	26
<b>Scheme 1.10.1</b>	Failed dehydration attempts of alcohol <b>91</b> .....	27
<b>Scheme 1.11.1</b>	Successful Grieco dehydration of triol <b>90</b> , NIS-mediated ring expansion of cyclobutanol <b>53</b> to Complete the total synthesis of scabrolide A ( <b>1</b> ), And dehydration of scabrolide A ( <b>1</b> ) to yonarolide ( <b>4</b> ).....	29

## **APPENDIX 1**

### *Synthetic Summary for Chapter 1*

<b>Scheme A1.1</b>	Synthesis of vinyl cyclopentenone <b>15</b> .....	102
<b>Scheme A1.2</b>	Synthesis of ynoic acid <b>57</b> .....	102
<b>Scheme A1.3</b>	Synthesis of (–)-scabrolide A ( <b>1</b> ) .....	102

## **APPENDIX 4**

### *Synthesis of a Tricyclic Model System*

<b>Scheme A4.2.1</b>	Synthesis of tricyclic enone <b>82</b> .....	102
----------------------	----------------------------------------------	-----

**CHAPTER 2***Asymmetric Total Synthesis of Havellockate*

<b>Scheme 2.3.1</b>	Synthesis of aldehyde <b>113</b> .....	404
<b>Scheme 2.3.2</b>	Synthesis of sulfone <b>114</b> .....	405
<b>Scheme 2.4.1</b>	Synthesis of tricycle <b>111</b> .....	406
<b>Scheme 2.5.1</b>	Synthesis of enone <b>110</b> , and failed Grignard addition.....	407
<b>Scheme 2.6.1</b>	Allylation of enone <b>110</b> with acetoxyallylzinc reagent.....	410
<b>Scheme 2.7.1</b>	A. Planned cross-metathesis of triol <b>133</b> B. Unexpected oxidative cleavage. ....	411
<b>Scheme 2.7.2</b>	Failed removal of the <i>t</i> -Bu ester from enone <b>133</b> .....	412
<b>Scheme 2.8.1</b>	Successful transesterification of enone <b>110</b> and allylation to generate triol <b>140</b> .....	413
<b>Scheme 2.8.2</b>	Completion of the total synthesis of havellockate ( <b>106</b> ) .....	414

**APPENDIX 6***Synthetic Summary for Chapter 2*

<b>Scheme A6.1</b>	Synthesis of aldehyde <b>113</b> .....	446
<b>Scheme A6.2</b>	Synthesis of sulfone <b>114</b> .....	446
<b>Scheme A6.3</b>	Completion of the synthesis of havellockate ( <b>106</b> ) .....	446

**CHAPTER 3***Synthesis of Carboxylic Acids and Dimer Esters from**Pinene-Derived Secondary Organic Aerosol*

<b>Scheme 3.2.1</b>	Synthesis of pinonic acid ( <b>145</b> ), pinic acid ( <b>146</b> ), and pinolic acid ( <b>148</b> ) and dimers <b>153–155</b> .....	552
---------------------	-----------------------------------------------------------------------------------------------------------------------------------------	-----

<b>Scheme 3.3.1</b>	Synthesis of pinic acid monobenzyl ester ( <b>164</b> ) .....	555
<b>Scheme 3.3.2</b>	Synthesis of pinic acid dimer esters <b>156–158</b> .....	556
<b>Scheme 3.4.1</b>	Synthesis of isomeric dimer esters <b>168–170</b> .....	558

## LIST OF TABLES

**CHAPTER 1***The Total Synthesis of (-)-Scabrolide A*

<b>Table 1.7.1</b>	Optimization of the C(6) oxidation .....	21
<b>Table 1.13.1</b>	Comparison of <sup>1</sup> H NMR shifts of synthetic and natural scabrolide A ( <b>1</b> ).....	87
<b>Table 1.13.2</b>	Comparison of <sup>13</sup> C NMR shifts of synthetic and natural scabrolide A ( <b>1</b> ).....	89
<b>Table 1.13.3</b>	Comparison of <sup>1</sup> H and <sup>13</sup> C NMR shifts of synthetic and natural yonarolide ( <b>4</b> ).....	91

**APPENDIX 8***X-Ray Crystallography Reports Relevant to Chapter 1*

<b>Table A3.1.1</b>	Experimental Details for X-Ray Structure Determination of Tetracycle <b>47</b> .....	219
<b>Table A3.1.2</b>	Crystal Data and Structure Refinement for Tetracycle <b>47</b> .....	220
<b>Table A3.1.3</b>	Atomic Coordinates (x 10 <sup>4</sup> ) and Equivalent Isotropic Displacement Parameters (Å <sup>2</sup> x 10 <sup>3</sup> ) for Tetracycle <b>47</b> . U(eq) is Defined as One Third of the Orthogonalized U <sup>ij</sup> Tensor. ....	221
<b>Table A3.1.4</b>	Bond Lengths [Å] and angles [°] for Tetracycle <b>47</b> .....	223

<b>Table A3.1.5</b>	Anisotropic Displacement Parameters ( $\text{\AA}^2 \times 10^3$ ) for Tetracycline <b>47</b> . The Anisotropic Displacement Factor Exponent Takes the Form: $-2p^2[h^2a^*2U^{11} + \dots + 2hka^*b^*U^{12}]$ . ....	230
<b>Table A3.1.6</b>	Hydrogen Coordinates ( $\times 10^4$ ) and Isotropic Displacement Parameters ( $\text{\AA}^2 \times 10^3$ ) for Tetracycline <b>47</b> .....	232
<b>Table A3.1.7</b>	Torsion Angles [ $^\circ$ ] for Tetracycline <b>47</b> .....	234
<b>Table A3.1.8</b>	Hydrogen Bonds for Tetracycline <b>47</b> [ $\text{\AA}$ and $^\circ$ ] .....	237
<b>Table A3.2.1</b>	Experimental Details for X-Ray Structure Determination of Cyclobutane <b>63</b> .....	239
<b>Table A3.2.2</b>	Crystal Data and Structure Refinement for Cyclobutane <b>63</b> .....	240
<b>Table A3.2.3</b>	Atomic Coordinates ( $\times 10^4$ ) and Equivalent Isotropic Displacement Parameters ( $\text{\AA}^2 \times 10^3$ ) for Cyclobutane <b>63</b> . $U(\text{eq})$ is Defined as One Third of the Orthogonalized $U^{ij}$ Tensor .....	241
<b>Table A3.2.4</b>	Bond Lengths [ $\text{\AA}$ ] and angles [ $^\circ$ ] for Cyclobutane <b>63</b> .....	243
<b>Table A3.2.5</b>	Anisotropic Displacement Parameters ( $\text{\AA}^2 \times 10^3$ ) for Cyclobutane <b>63</b> . The Anisotropic Displacement Factor Exponent Takes the Form: $-2p^2[h^2a^*2U^{11} + \dots + 2hka^*b^*U^{12}]$ .....	249



<b>Table A3.2.6</b>	Hydrogen Coordinates ( $\times 10^4$ ) and Isotropic Displacement Parameters ( $\text{\AA}^2 \times 10^3$ ) for Cyclobutane <b>63</b> .....	250
<b>Table A3.2.7</b>	Torsion Angles [ $^\circ$ ] for Cyclobutane <b>63</b> .....	252
<b>Table A3.2.8</b>	Hydrogen Bonds for Cyclobutane <b>63</b> [ $\text{\AA}$ and $^\circ$ ] .....	255
<b>Table A3.3.1</b>	Experimental Details for X-Ray Structure Determination of Cyclobutane <b>64</b> .....	257
<b>Table A3.3.2</b>	Crystal Data and Structure Refinement for Cyclobutane <b>64</b> .....	258
<b>Table A3.3.3</b>	Atomic Coordinates ( $\times 10^4$ ) and Equivalent Isotropic Displacement Parameters ( $\text{\AA}^2 \times 10^3$ ) for Cyclobutane <b>64</b> . $U(\text{eq})$ is Defined as One Third of the Orthogonalized $U^{ij}$ Tensor .....	259
<b>Table A3.3.4</b>	Bond Lengths [ $\text{\AA}$ ] and angles [ $^\circ$ ] for Cyclobutane <b>64</b> .....	261
<b>Table A3.3.5</b>	Anisotropic Displacement Parameters ( $\text{\AA}^2 \times 10^3$ ) for Cyclobutane <b>64</b> . The Anisotropic Displacement Factor Exponent Takes the Form: $-2p^2[h^2a^*2U^{11} + \dots + 2hka^*b^*U^{12}]$ .....	267
<b>Table A3.3.6</b>	Hydrogen Coordinates ( $\times 10^4$ ) and Isotropic Displacement Parameters ( $\text{\AA}^2 \times 10^3$ ) for Cyclobutane <b>64</b> .....	269
<b>Table A3.3.7</b>	Torsion Angles [ $^\circ$ ] for Cyclobutane <b>64</b> .....	271
<b>Table A3.3.8</b>	Hydrogen Bonds for Cyclobutane <b>64</b> [ $\text{\AA}$ and $^\circ$ ] .....	275

<b>Table A3.4.1</b>	Experimental Details for X-Ray Structure Determination of Cycloheptane <b>72</b> .....	277
<b>Table A3.4.2</b>	Crystal Data and Structure Refinement for Cycloheptane <b>72</b> .....	279
<b>Table A3.4.3</b>	Atomic Coordinates ( $\times 10^4$ ) and Equivalent Isotropic Displacement Parameters ( $\text{\AA}^2 \times 10^3$ ) for Cycloheptane <b>72</b> . $U(\text{eq})$ is Defined as One Third of the Orthogonalized $U^{ij}$ Tensor .....	280
<b>Table A3.4.4</b>	Bond Lengths [ $\text{\AA}$ ] and angles [ $^\circ$ ] for Cycloheptane <b>72</b> .....	282
<b>Table A3.4.5</b>	Anisotropic Displacement Parameters ( $\text{\AA}^2 \times 10^3$ ) for Cycloheptane <b>72</b> . The Anisotropic Displacement Factor Exponent Takes the Form: $-2p^2[h^2a^*2U^{11} + \dots + 2hka^*b^*U^{12}]$ .....	292
<b>Table A3.4.6</b>	Hydrogen Coordinates ( $\times 10^4$ ) and Isotropic Displacement Parameters ( $\text{\AA}^2 \times 10^3$ ) for Cycloheptane <b>72</b> .....	294
<b>Table A3.4.7</b>	Torsion Angles [ $^\circ$ ] for Cycloheptane <b>72</b> .....	296
<b>Table A3.4.8</b>	Hydrogen Bonds for Cycloheptane <b>72</b> [ $\text{\AA}$ and $^\circ$ ] .....	301
<b>Table A3.5.1</b>	Experimental Details for X-Ray Structure Determination of Cyclobutane <b>83</b> .....	303
<b>Table A3.5.2</b>	Crystal Data and Structure Refinement for Cyclobutane <b>83</b> .....	304

<b>Table A3.5.3</b>	Atomic coordinates ( $\times 10^5$ ) and equivalent isotropic displacement parameters ( $\text{\AA}^2 10^{-2}$ ) for cyclobutane <b>83</b> . $U(\text{eq})$ is defined as one third of the trace of the orthogonalized $U^{ij}$ tensor. ....	305
<b>Table A3.5.4</b>	Bond Lengths [ $\text{\AA}$ ] and angles [ $^\circ$ ] for Cyclobutane <b>83</b> .....	307
<b>Table A3.5.5</b>	Anisotropic displacement parameters ( $\text{\AA}^2 \times 10^4$ ) for cyclobutane <b>83</b> . The anisotropic displacement factor exponent takes the form: $-2\pi^2 [h^2 a^{*2} U^{11} + \dots + 2 h k a^* b^* U^{12}]$ .....	314
<b>Table A3.5.6</b>	Hydrogen Coordinates ( $\times 10^2$ ) and Isotropic Displacement Parameters ( $\text{\AA}^2 \times 10^2$ ) for Cyclobutane <b>83</b> .....	316
<b>Table A3.5.7</b>	Torsion Angles [ $^\circ$ ] for Cyclobutane <b>83</b> .....	318
<b>Table A3.5.8</b>	Hydrogen Bonds for Cyclobutane <b>83</b> [ $\text{\AA}$ and $^\circ$ ] .....	321
<b>Table A3.6.1</b>	Experimental Details for X-Ray Structure Determination of Cyclobutanol <b>90</b> .....	323
<b>Table A3.6.2</b>	Crystal Data and Structure Refinement for Cyclobutanol <b>90</b> .....	324
<b>Table A3.6.3</b>	Atomic coordinates ( $\times 10^5$ ) and equivalent isotropic displacement parameters ( $\text{\AA}^2 10^{-3}$ ) for cyclobutanol <b>90</b> . $U(\text{eq})$ is defined as one third of the trace of the orthogonalized $U^{ij}$ tensor. ....	325

<b>Table A3.6.4</b>	Bond Lengths [ $\text{\AA}$ ] and angles [ $^\circ$ ] for Cyclobutanol <b>90</b> .....	326
<b>Table A3.6.5</b>	Anisotropic displacement parameters ( $\text{\AA}^2 \times 10^4$ ) for cyclobutanol <b>90</b> . The anisotropic displacement factor exponent takes the form: $-2\pi^2 [ h^2 a^{*2} U^{11} + \dots + 2 h k a^* b^* U^{12} ]$ .....	331
<b>Table A3.6.6</b>	Hydrogen Coordinates ( $\times 10^4$ ) and Isotropic Displacement Parameters ( $\text{\AA}^2 \times 10^2$ ) for Cyclobutanol <b>90</b> .....	332
<b>Table A3.6.7</b>	Torsion Angles [ $^\circ$ ] for Cyclobutanol <b>90</b> .....	333
<b>Table A3.6.8</b>	Hydrogen Bonds for Cyclobutanol <b>90</b> [ $\text{\AA}$ and $^\circ$ ].....	336
<b>Table A3.7.1</b>	Experimental Details for X-Ray Structure Determination of Cyclobutanol <b>epi-90</b> .....	338
<b>Table A3.7.2</b>	Crystal Data and Structure Refinement for Cyclobutanol <b>epi-90</b>	339
<b>Table A3.7.3</b>	Atomic coordinates ( $\times 10^4$ ) and equivalent isotropic displacement parameters ( $\text{\AA}^2 \times 10^2$ ) for cyclobutanol <b>epi-90</b> . $U(\text{eq})$ is defined as one third of the trace of the orthogonalized $U^{ij}$ tensor. ....	340
<b>Table A3.7.4</b>	Bond Lengths [ $\text{\AA}$ ] and angles [ $^\circ$ ] for Cyclobutanol <b>epi-90</b> .....	342
<b>Table A3.7.5</b>	Anisotropic displacement parameters ( $\text{\AA}^2 \times 10^3$ ) for cyclobutanol <b>epi-90</b> . The anisotropic displacement factor exponent takes the form: $-2\pi^2 [ h^2 a^{*2} U^{11} + \dots + 2 h k a^* b^* U^{12} ]$ .....	348

<b>Table A3.7.6</b>	Hydrogen Coordinates ( $\times 10^4$ ) and Isotropic Displacement Parameters ( $\text{\AA}^2 \times 10^3$ ) for Cyclobutanol <b>epi-90</b> .....	349
<b>Table A3.7.7</b>	Torsion Angles [ $^\circ$ ] for Cyclobutanol <b>epi-90</b> .....	351
<b>Table A3.7.8</b>	Hydrogen Bonds for Cyclobutanol <b>epi-90</b> [ $\text{\AA}$ and $^\circ$ ] .....	354
<b>Table A3.8.1</b>	Experimental Details for X-Ray Structure Determination of Nitrile <b>94</b> .....	356
<b>Table A3.8.2</b>	Crystal Data and Structure Refinement for Nitrile <b>94</b> .....	357
<b>Table A3.8.3</b>	Atomic coordinates ( $\times 10^4$ ) and equivalent isotropic displacement parameters ( $\text{\AA}^2 \times 10^2$ ) for nitrile <b>94</b> . $U(\text{eq})$ is defined as one third of the trace of the orthogonalized $U^{ij}$ tensor. ....	358
<b>Table A3.8.4</b>	Bond Lengths [ $\text{\AA}$ ] and angles [ $^\circ$ ] for nitrile <b>94</b> .....	359
<b>Table A3.8.5</b>	Anisotropic displacement parameters ( $\text{\AA}^2 \times 10^3$ ) for nitrile <b>94</b> . The anisotropic displacement factor exponent takes the form: $-2\pi^2 [h^2 a^{*2} U^{11} + \dots + 2 h k a^* b^* U^{12}]$ .....	364
<b>Table A3.8.6</b>	Hydrogen Coordinates ( $\times 10^4$ ) and Isotropic Displacement Parameters ( $\text{\AA}^2 \times 10^3$ ) for Nitrile <b>94</b> .....	365
<b>Table A3.8.7</b>	Torsion Angles [ $^\circ$ ] for Nitrile <b>94</b> .....	366

<b>Table A3.8.8</b>	Hydrogen Bonds for nitrile <b>94</b> [Å and °] .....	369
<b>Table A3.9.1</b>	Experimental Details for X-Ray Structure Determination of scabrolide A ( <b>1</b> ) .....	371
<b>Table A3.9.2</b>	Crystal Data and Structure Refinement for scabrolide A ( <b>1</b> ) .....	372
<b>Table A3.9.3</b>	Atomic coordinates ( $\times 10^4$ ) and equivalent isotropic displacement parameters ( $\text{Å}^2 10^3$ ) for scabrolide A ( <b>1</b> ). $U(\text{eq})$ is defined as one third of the trace of the orthogonalized $U^{ij}$ tensor. ....	373
<b>Table A3.9.4</b>	Bond Lengths [Å] and angles [°] for scabrolide A ( <b>1</b> ) .....	374
<b>Table A3.9.5</b>	Anisotropic displacement parameters ( $\text{Å}^2 \times 10^3$ ) for compound <b>1</b> . The anisotropic displacement factor exponent takes the form: - $2\pi^2 [ h^2 a^{*2} U^{11} + \dots + 2 h k a^* b^* U^{12} ]$ .....	379
<b>Table A3.9.6</b>	Hydrogen Coordinates ( $\times 10^4$ ) and Isotropic Displacement Parameters ( $\text{Å}^2 \times 10^3$ ) for compound <b>1</b> .....	380
<b>Table A3.8.7</b>	Torsion Angles [°] for compound <b>1</b> .....	381
<b>Table A3.8.8</b>	Hydrogen Bonds for compound <b>1</b> [Å and °] .....	383
<b>CHAPTER 2</b>		
<i>Asymmetric Total Synthesis of Havellockate</i>		
<b>Table 2.6.1</b>	Initial investigation of the 1,2-addition to enone <b>110</b> .....	409

<b>Table 2.10.1</b>	Comparison of $^1\text{H}$ NMR shifts of synthetic and Natural havellockate ( <b>106</b> ) .....	438
<b>Table 2.10.2</b>	Comparison of $^{13}\text{C}$ NMR shifts of synthetic and Natural havellockate ( <b>106</b> ) .....	439
<b>Table A8.1.1</b>	Experimental Details for X-Ray Structure Determination of Tetracycle <b>111</b> .....	487
<b>Table A8.1.2</b>	Crystal Data and Structure Refinement for compound <b>111</b> .....	488
<b>Table A8.1.3</b>	Atomic coordinates ( $\times 10^4$ ) and equivalent isotropic displacement parameters ( $\text{\AA}^2 10^3$ ) for compound <b>111</b> . $U(\text{eq})$ is defined as one third of the trace of the orthogonalized $U^{ij}$ tensor. ....	489
<b>Table A8.1.4</b>	Bond Lengths [ $\text{\AA}$ ] and angles [ $^\circ$ ] for compound <b>111</b> .....	491
<b>Table A8.1.5</b>	Anisotropic displacement parameters ( $\text{\AA}^2 \times 10^3$ ) for compound <b>111</b> . The anisotropic displacement factor exponent takes the form: $-2\pi^2 [ h^2 a^{*2} U^{11} + \dots + 2 h k a^* b^* U^{12} ]$ .....	497
<b>Table A8.1.6</b>	Hydrogen Coordinates ( $\times 10^4$ ) and Isotropic Displacement Parameters ( $\text{\AA}^2 \times 10^3$ ) for compound <b>111</b> .....	498
<b>Table A8.1.7</b>	Torsion Angles [ $^\circ$ ] for compound <b>111</b> .....	500
<b>Table A8.1.8</b>	Hydrogen Bonds for compound <b>111</b> [ $\text{\AA}$ and $^\circ$ ].....	502
<b>Table A8.2.1</b>	Experimental Details for X-Ray Structure Determination of compound <b>133</b> .....	504

<b>Table A8.2.2</b>	Crystal Data and Structure Refinement for compound <b>133</b> .505	
<b>Table A8.2.3</b>	Atomic coordinates ( $\times 10^4$ ) and equivalent isotropic displacement parameters ( $\text{\AA}^2 10^3$ ) for compound <b>133</b> . $U(\text{eq})$ is defined as one third of the trace of the orthogonalized $U^{ij}$ tensor. ....506	
<b>Table A8.2.4</b>	Bond Lengths [ $\text{\AA}$ ] and angles [ $^\circ$ ] for compound <b>133</b> .....508	
<b>Table A8.2.5</b>	Anisotropic displacement parameters ( $\text{\AA}^2 \times 10^3$ ) for compound <b>133</b> . The anisotropic displacement factor exponent takes the form: $-2\pi^2 [ h^2 a^{*2} U^{11} + \dots + 2 h k a^* b^* U^{12} ]$ .....520	
<b>Table A8.2.6</b>	Hydrogen Coordinates ( $\times 10^4$ ) and Isotropic Displacement Parameters ( $\text{\AA}^2 \times 10^3$ ) for compound <b>133</b> .....523	
<b>Table A8.2.7</b>	Torsion Angles [ $^\circ$ ] for compound <b>133</b> .....526	
<b>Table A8.2.8</b>	Hydrogen Bonds for compound <b>111</b> [ $\text{\AA}$ and $^\circ$ ].....531	
<b>Table A8.3.1</b>	Experimental Details for X-Ray Structure Determination of Havellockate ( <b>106</b> ) .....533	
<b>Table A8.3.2</b>	Crystal Data and Structure Refinement for c .....534	
<b>Table A8.3.3</b>	Atomic coordinates ( $\times 10^4$ ) and equivalent isotropic displacement parameters ( $\text{\AA}^2 10^3$ ) havellockate ( <b>106</b> ). $U(\text{eq})$ is defined as one third of the trace of the orthogonalized $U^{ij}$ tensor. ....535	



<b>Table A8.3.4</b>	Bond Lengths [Å] and angles [°] for havellockate ( <b>106</b> ). ....	537
<b>Table A8.3.5</b>	Anisotropic displacement parameters (Å <sup>2</sup> × 10 <sup>3</sup> ) for havellockate ( <b>106</b> ). The anisotropic displacement factor exponent takes the form: $-2\pi^2 [ h^2 a^{*2} U^{11} + \dots + 2 h k a^* b^* U^{12} ]$ .....	543
<b>Table A8.3.6</b>	Hydrogen Coordinates (×10 <sup>4</sup> ) and Isotropic Displacement Parameters (Å <sup>2</sup> × 10 <sup>3</sup> ) for havellockate ( <b>106</b> ). ....	544
<b>Table A8.3.7</b>	Torsion Angles [°] for havellockate ( <b>106</b> ). ....	545
<b>Table A8.3.8</b>	Hydrogen Bonds for havellockate ( <b>106</b> ) [Å and °] .....	548

## LIST OF ABBREVIATIONS

$[\alpha]_D$	specific rotation at wavelength of sodium D line
$^{\circ}\text{C}$	degrees Celcius
Å	Ångstrom
app	apparent
aq	aqueous
Ar	aryl
atm	atmosphere
Bn	benzyl
bp	boiling point
br	broad
<i>c</i>	concentration for specific rotation measurements
calc'd	calculated
$\text{cm}^{-1}$	wavenumber(s)
d	doublet
D	deuterium
DIC	N,N'-diisopropylcarbodiimide

DDQ	2,3-dichloro-5,6-dicyano- <i>p</i> -benzoquinone
DMAP	4-dimethylaminopyridine
DMF	dimethylformamide
DMS	dimethylsulfide
dr	diastereomeric ratio
EDC	<i>N</i> -(3-dimethylaminopropyl)- <i>N</i> '-ethylcarbodiimide
ee	enantiomeric excess
EI+	electron impact
equiv	equivalent(s)
ESI	electrospray ionization
Et	ethyl
EtOAc	ethyl acetate
FAB	fast atom bombardment
g	gram(s)
h	hour(s)
HG-II	Hoveyda–Grubbs catalyst 2 <sup>nd</sup> generation
HPLC	high-performance liquid chromatography

HRMS	high-resolution mass spectrometry
Hz	hertz
<i>i</i> -Bu	<i>iso</i> -butyl
IR	infrared (spectroscopy)
<i>J</i>	coupling constant
K	Kelvin (absolute temperature)
kcal	kilocalorie
KHMDS	potassium hexamethyldisilazide
L	liter; ligand
LDA	lithium diisopropylamide
m	multiplet, milli
<i>m</i>	meta
<i>m/z</i>	mass to charge ratio
Me	methyl
mg	milligram(s)
MHz	megahertz
min	minute(s)

mol	mole(s)
mp	melting point
n	nano
<i>n</i> -Bu	<i>n</i> -butyl
NBS	<i>N</i> -bromosuccimide
NMR	nuclear magnetic resonance
NPhth	phthalimide
Nu	nucleophile
<i>o</i>	ortho
<i>p</i>	para
Pd/C	palladium on carbon
Ph	phenyl
pH	hydrogen ion concentration in aqueous solution
PHOX	phosphinooxazoline
ppm	parts per million
Pr	propyl

q	quartet
R	generic for any atom or functional group
Ref.	reference
$R_f$	retention factor
s	singlet
sat.	saturated
t	triplet
<i>t</i> -Bu	<i>tert</i> -butyl
TBAF	tetrabutylammonium fluoride
TBS	<i>tert</i> -butyldimethylsilyl
TES	triethylsilyl
THF	tetrahydrofuran
TLC	thin-layer chromatography
TMS	trimethylsilyl
$t_R$	retention time
UV	ultraviolet
<i>v/v</i>	volume to volume

w/v weight to volume

$\lambda$  wavelength

$\mu$  micro

# CHAPTER 1

## The Total Synthesis of (–)-Scabrolide A<sup>†</sup>

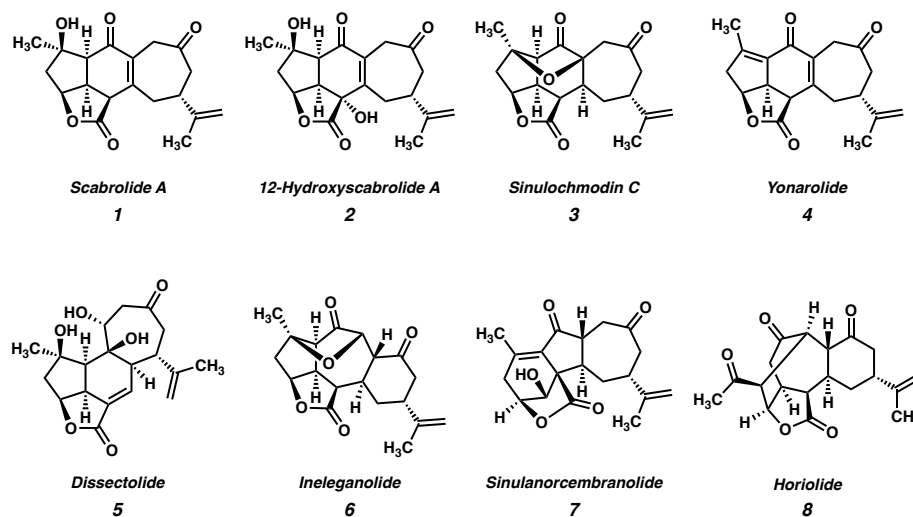
### 1.1 INTRODUCTION

The polycyclic furanobutenolide-derived norcembranoids are a small family of structurally diverse, highly oxygenated C<sub>19</sub> norditerpenoids which are isolated exclusively from soft corals of the genus *Sinularia* (Figure 1.1.1).<sup>1</sup> Since the first reports of their isolation over two decades ago, these molecules have captivated synthetic chemists owing to their unique and synthetically challenging structural features, as well as the range of biological effects they have been shown to elicit. Consequently, the polycyclic furanobutenolide-derived norcembranoids have garnered considerable attention from the synthetic community, and several attempted total syntheses have been reported to date.<sup>2,3</sup>

All known polycyclic furanobutenolide-derived norcembranoids are believed to originate from the macrocyclic norcembranoids sinuleptolide and 5–episinuleptolide (**9**, Scheme 1.1.1), which are thought to be in equilibrium in vivo. Through a series of divergent, transannular reaction cascades, these two progenitors give rise to the diverse set of carbocyclic skeletons that make up the furanobutenolide-derived polycyclic norcembranoid family. For example, scabrolide A (**1**) is proposed to arise from

<sup>†</sup>This research was performed in collaboration Dr. Steven A. Loskot, Dr. Christopher E. Reimann, Dr. Beau P. Pritchett, and Dr. Scott C. Virgil. Portions of this chapter have been adapted from Hafeman, N. J.; Loskot, S. A.; Reimann, C. E.; Pritchett, B. P. Virgil, S. C. *J. Am. Chem. Soc.* **2020**, *19*, 8585–8590. © American Chemical Society.

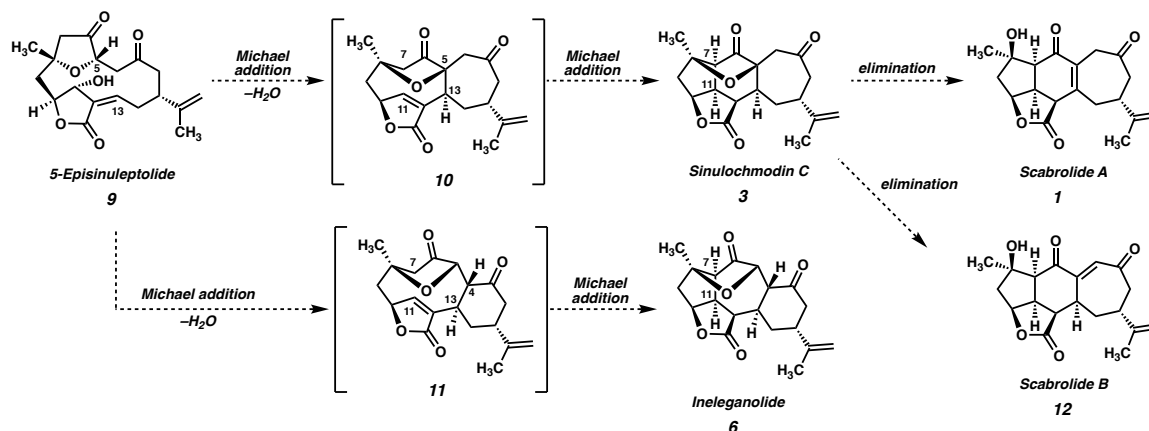


**Figure 1.1.1** Polycyclic furanobutenolide-derived norcembranoids.

5-episinulectolide (**9**) following a series of two transannular Michael additions: a 7-*exo-trig* cyclization between C(5) and C(13), and a 5-*exo-trig* cyclization between C(7) and C(11), which produce isomeric sinulochmodin C (**3**).  $\beta$ -elimination of the C(5) tertiary ether and olefin isomerization then generates scabrolide A (**1**). This biosynthetic hypothesis is supported by the fact that these natural products are often isolated together, and alongside their macrocyclic counterparts.<sup>1</sup> Furthermore, Pattenden's groundbreaking biomimetic semisyntheses of sinulochmodin C (**3**) and ineleganolide (**6**) from the same naturally-derived precursor (**9**) beautifully demonstrated the feasibility of this type of chemistry.<sup>4</sup>

Many efforts have been reported toward the total synthesis of several of the polycyclic furanobutenolide-derived norcembranoid diterpenoids. Ineleganolide (**6**) has a long history of thwarted attempted syntheses. Most recently, disclosures by Vanderwal<sup>2d</sup> as well as our group<sup>2e</sup> detailed the syntheses of highly advanced intermediates en route to this target, which could not be carried forward to the natural product itself. With regard to the [5–6–7] fused carbocyclic core of the yonarane-type norcembranoids (scabrolide A,

**Scheme 1.1.1** Proposed biosynthesis of scabrolides A (**1**) and B (**12**), sinulochmodin C (**3**), and ineleganolide (**6**).



yonarolide, sinulochmodin C), two recent publications<sup>5</sup> demonstrated strategies for the synthesis of the fused [5–6] portion of this framework. However, these reports did not detail the formation of the 7-membered carbocycle. Additionally, pioneering research by Barriault,<sup>6</sup> Ito,<sup>7</sup> and Mehta<sup>8</sup> detailed approaches to this ring system, but again without further advancement to any natural product targets. Very recently, after our initial disclosure of the following synthesis, Fürstner published an elegant total synthesis of both scabrolide A (**1**) and the reported structure of the isomeric scabrolide B (**12**).<sup>9</sup> The physical data of the synthetic sample of nominal scabrolide B (**12**) did not, however, match that of the isolated natural sample,<sup>10</sup> thus calling into question the actual structure of this natural product.

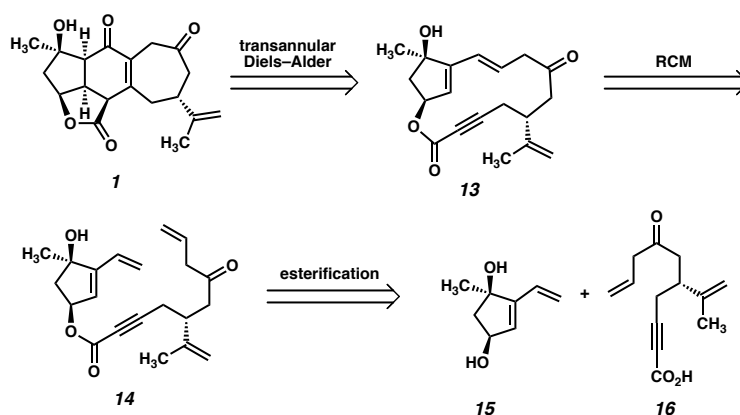
Given our laboratory's interest in the total synthesis of structurally complex natural products, we have had a longstanding fascination with the polycyclic furanobutenolide-derived norcembranoid diterpenoids. Beginning with our efforts toward ineleganolide (**6**), which culminated in the enantioselective synthesis of several isomeric “ineleganoloids”,<sup>2c</sup> we have continued our pursuit of this family of natural products, shifting our focus to (–)-

scabrolide A (**1**). Our efforts resulted in the first total syntheses of (–)-scabrolide A (**1**),<sup>11</sup> as well as the related natural product yonarolide (**4**) and also represented the first successful total synthesis of any member of the polycyclic furanobutenolide-derived norcembranoid class. This chapter contains a complete account of this research.

## 1.2 INITIAL RETROSYNTHETIC ANALYSIS OF SCABROLIDE A

At the outset, we planned to exploit a bioinspired approach to scabrolide A (**1**), in which the core ring system would be assembled via a transannular Diels–Alder reaction, which retrosynthetically delivers macrolactone **13** (Figure 1.2.1). Given the fact that the central six-membered ring of the natural product is believed to arise from a transannular double-Michael cascade (i.e., a formal Diels–Alder) in vivo, we hypothesized that this approach might be feasible provided we could access macrocycle **13**. We anticipated that a ring-closing metathesis (RCM) of an intermediate such as ester **14** might deliver the requisite macrocycle, given the longstanding precedent for the use of this reaction for the formation of large and medium-sized rings.<sup>12</sup> Ester **14**, in turn, would be formed by a convergent esterification of two enantioenriched fragments: dihydroxyvinylcyclopentene **15** and ynoic acid **16**.

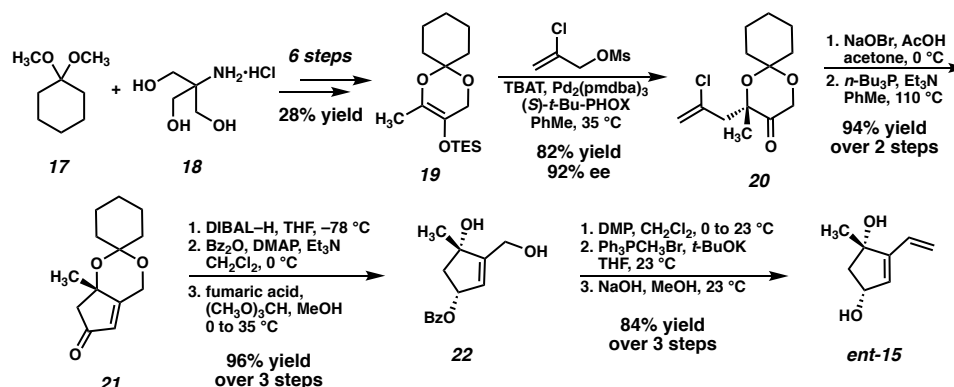
**Figure 1.2.1** Initial retrosynthetic analysis of scabrolide A (**1**).



### 1.3 SYNTHESIS OF COUPLING PARTNERS AND ESTERIFICATION

The synthesis of dihydroxyvinylcyclopentene *ent*-**15** had been previously reported by our laboratory during our efforts toward ineleganolide (**6**).<sup>13,2e</sup> It should be noted that, at the outset of that study, the absolute stereochemistry of ineleganolide (**6**)<sup>11,14</sup> and of several of the other polycyclic furanobutenolide-derived norcembranoids<sup>15</sup> was not known (and had been erroneously reported as the *ent*-series). It was later shown that these molecules possess the opposite absolute stereochemistry, shown correctly in Figure 1.1.1.<sup>16</sup> Thus, unbeknownst to us at the time, our initial efforts targeted the *ent*-series of these natural products.

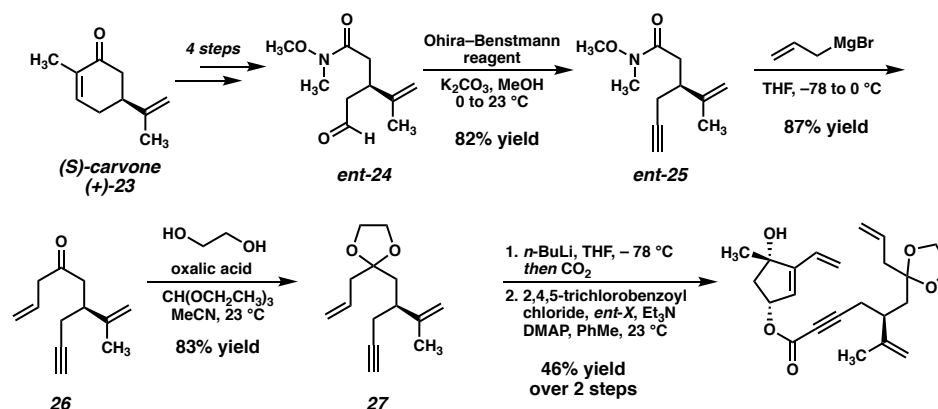
**Scheme 1.3.1** First-generation synthesis of vinylcyclopentenone *ent*-**15**.



Our original synthesis of dihydroxyvinylcyclopentene *ent*-**15**, outlined in Scheme 1.3.1, commences with the advancement of 1,1-dimethoxycyclohexane (**17**) and TRIS•HCl (**18**) to TES enol ether **19**, achieved in 6 steps and 28% overall yield. Enol ether **19** then serves as a substrate for a Pd-catalyzed asymmetric allylic alkylation, delivering enantioenriched tertiary ether **20** in 82% yield and 92% ee. Following an oxidative bromination/Wittig-type cyclization, enone **21** is obtained. A diastereoselective reduction followed by protecting group manipulations results in the formation of monoprotected triol

**22**, which may then undergo oxidation, Wittig methenylation, and deprotection to deliver the key fragment **ent-15**.

**Scheme 1.3.2** Synthesis of RCM substrate **28**.



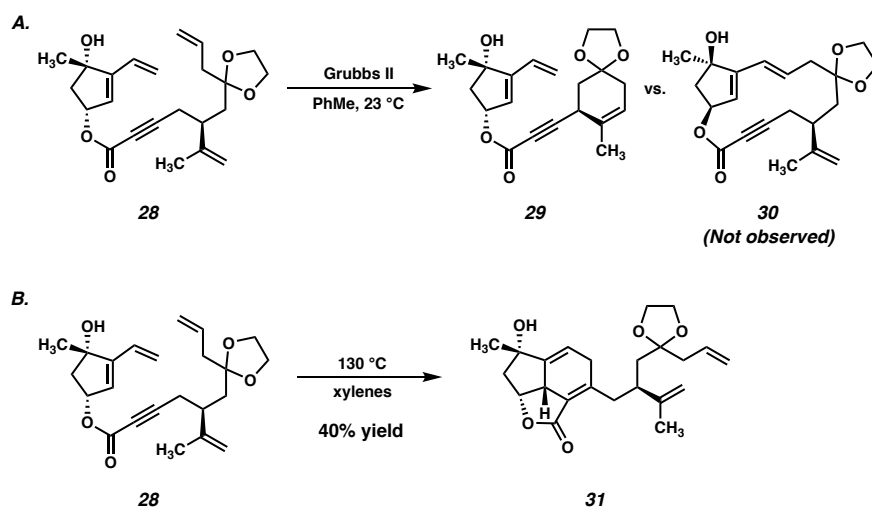
The second coupling partner is accessed from (*S*)-carvone (**23**) beginning with a known sequence<sup>17</sup> which delivers Weinreb amide **ent-24** in 4 steps (Scheme 1.3.2). Seyferth–Gilbert homologation<sup>18</sup> affords terminal alkyne **ent-25**, and subsequent monoaddition of allyl magnesium bromide furnishes ketone **26**, which is then protected as the corresponding dioxolane (**27**). Deprotonation of **27** with *n*-BuLi and quenching with CO<sub>2</sub> delivers the desired ynoic acid, which is carried forward crude to the convergent esterification. Gratifyingly, we found that the two fragments are smoothly coupled under Yamaguchi conditions,<sup>19</sup> delivering ester **28** in 44% yield over the two steps, setting the stage for the key macrocyclization reaction.

#### 1.4 FAILED MACROCYCLIZATION AND DIELS–ALDER

Despite the ample precedent for RCM-mediated macrocyclization, ester **28** failed to undergo the desired RCM, instead delivering undesired cyclohexene **29** as the predominant product (Scheme 1.4.1A). Despite examining a variety of known RCM

catalysts, macrocycle **30** was never observed, thus thwarting this synthetic plan. Although substrate **28** possesses two monosubstituted olefins (the vinyl group and the allyl group), it is likely that the electronic deactivation of the conjugated vinyl group causes the allyl olefin to be the preferential site of initial reactivity.<sup>20</sup> The resulting Ru-carbenoid is then poised to undergo a facile 6-membered ring closure, resulting in undesired RCM product **29**.

**Scheme 1.4.1** A. Failed RCM macrocyclization. B. Diels–Alder of ester **28**.



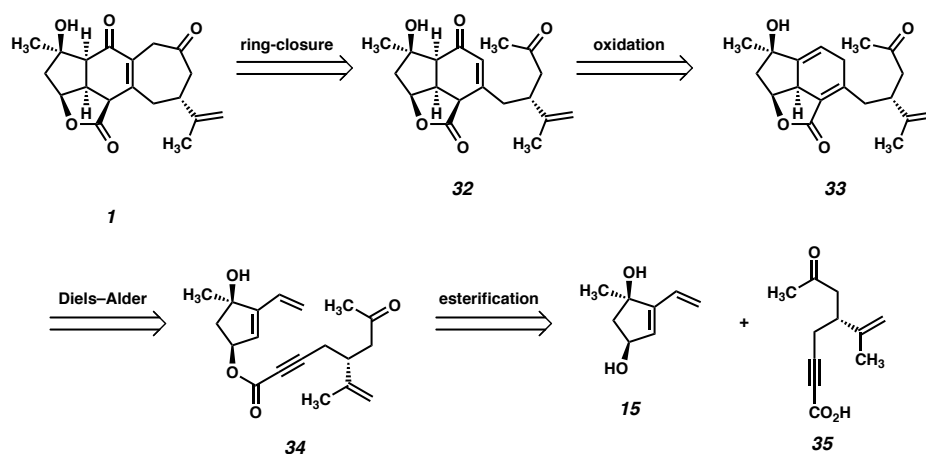
Although disappointed in the failure of our key macrocyclization, we recognized that access to **28** still represented an important milestone in the synthesis, and we proceeded to probe its reactivity further. Specifically, we viewed this as an opportunity to test whether an intramolecular Diels–Alder reaction of a compound such as **28** would be feasible. To that end, heating of ester **28** to 130 °C in xylenes resulted in a facile Diels–Alder cycloaddition, delivering tricyclic **31** in 40% yield as a single diastereomer (Scheme 1.4.1B). Although adduct **31** would not serve as a viable intermediate in our total synthesis given the incorrect substitution on the carvone-derived tether, the success of this reaction

served to validate our hypothesis that the central six-membered ring of scabrolide A (**1**) could be formed by an intramolecular Diels–Alder reaction. Thus, we opted to revise our retrosynthetic strategy around this significant result.

## 1.5 SECOND-GENERATION APPROACH

Our second-generation retrosynthetic analysis (Scheme 1.5.1) relies upon a late-stage annulation of the eastern seven-membered carbocycle of scabrolide A (**1**) from a precursor such as enone **32**. We envisioned access to **32** from Diels–Alder adduct **33**, which, in turn, could be furnished from ester **34**. Ester **34** would be prepared by a similar convergent esterification of dihydroxyvinylcyclopentene **15** and a new ynolic acid, **35**, appended with a methyl ketone.

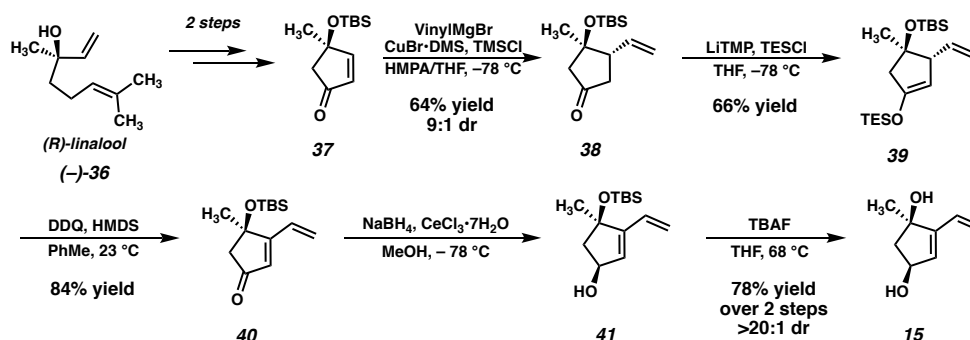
**Figure 1.5.1** Second-generation retrosynthetic analysis of scabrolide A (**1**).



At this point, we also became interested in a more expedient route to dihydroxyvinylcyclopentene **15**. Inspired by a report from Maimone and coworkers detailing the synthesis of enone **37** (Scheme 1.5.1) in two steps from (*R*)-linalool (**36**),<sup>21</sup> we hypothesized that we could exploit this building block for the preparation of **15**. Our second-generation synthesis of this fragment commences with a conjugate addition of vinyl

cuprate to enone **37**, and, following a dehydrogenation protocol, vinyl enone **40** is furnished in good yield. A diastereoselective Luche reduction then establishes the final stereocenter, delivering a TBS-protected variant of the desired fragment (**41**). Treatment with TBAF at elevated temperature then delivers dihydroxyvinylcyclopentene **15** in 20% yield over 7 steps (vs. 15), and in the correct enantiomeric series.

**Scheme 1.5.1** Second-generation synthesis of vinylcyclopentenone **15**.

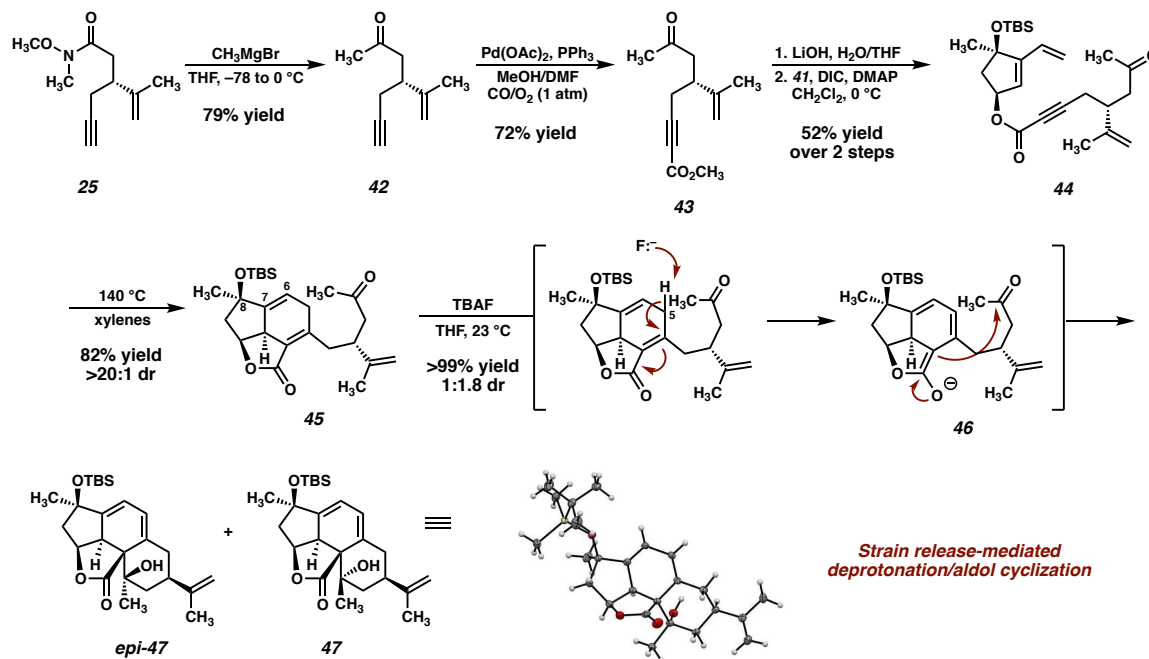


The new ynoic acid coupling partner (**35**) is prepared from alkyne **25** (Scheme 1.5.2), intercepted from the route to the ynoic acid used previously (now starting from (*R*)-carvone to match the enantiomer of dihydroxyvinylcyclopentene **15**). Monoaddition of methyl magnesium bromide installs the requisite methyl ketone in the form of intermediate **42**. Pd-catalyzed oxidative carboxylation<sup>22</sup> then affords methyl ester **43**, which, following saponification, is coupled with TBS-protected dihydroxyvinylcyclopentene **41** under Steglich conditions<sup>23</sup> to afford Diels–Alder precursor **44**.

As before, heating ester **44** to 140 °C in xylenes smoothly triggers the desired [4+2] cycloaddition, delivering tricycle **45** in good yield as a single diastereomer. At this stage, oxidation of the  $\Delta^{6,7}$  olefin is required in order to install the C(6) ketone present in the natural product. Initially, we planned to accomplish this via a directed epoxidation and



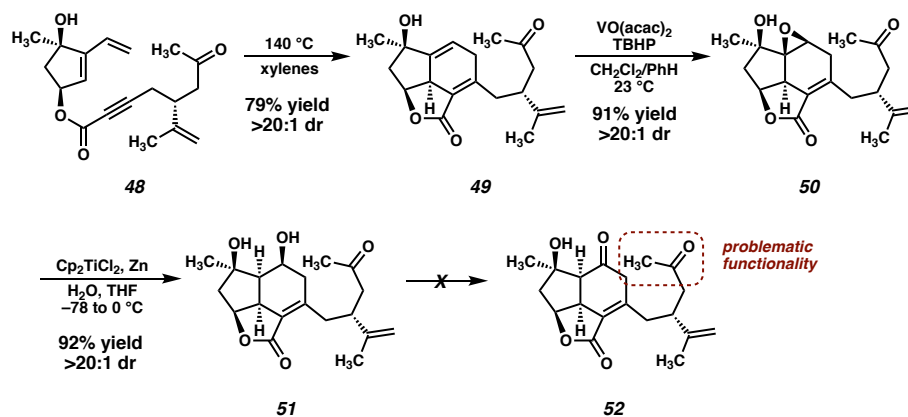
**Scheme 1.5.2** Synthesis of ester **44**, Diels–Alder cycloaddition, and undesired aldol cyclization.



subsequent Mienwald rearrangement. To this end, we attempted the deprotection of the C(8) alcohol by treatment of **42** with TBAF, however, we were surprised to isolate tetracycles **47** and *epi*-**47** instead of the anticipated deprotected alcohol. We hypothesize that these unexpected products are the result of an aldol cyclization between an extended enolate (**46**) generated by deprotonation of **45** at C(5) with TBAF. Although TBAF is typically far too weak of a base to deprotonate  $\gamma$ -protons of an  $\alpha,\beta$ -unsaturated lactone, we reason that the strain imparted on tricycle **45** significantly reduces the  $\text{pK}_a$  of these protons, thus facilitating deprotonation and subsequent cyclization. Interestingly, a compound possessing a ring system very similar to **47** was recently observed by Gaich and coworkers during their total synthesis of Norcembrene 5 (a macrocyclic norcembranoid) resulting from an unexpected [4+2] cycloaddition.<sup>24</sup> The authors propose that this ring system may

correspond to a yet-undiscovered subclass of the polycyclic norcembranoid natural products.

**Scheme 1.5.3** Diels–Alder reaction of **48**, directed epoxidation, reductive epoxide-opening and failed oxidation of alcohol **51**.



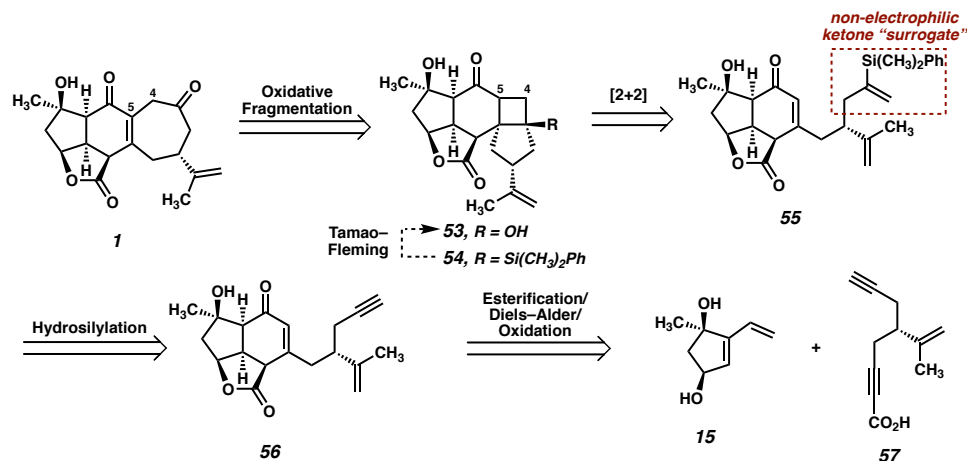
In light of this undesired reactivity, we simply opted to utilize dihydroxyvinylcyclopentene **15** instead of its TBS-protected congener (Scheme 1.5.3). Not surprisingly, the Diels–Alder reaction of ester **48** proceeds smoothly, delivering tricycle **49** in good yield as a single diastereomer. The now free hydroxyl group can then direct a VO(acac)<sub>2</sub>-catalyzed epoxidation, which furnishes epoxide **50** in excellent yield. Unfortunately, the planned Meinwald rearrangement failed under a variety of Lewis acid-mediated conditions forcing us to settle on a two-step approach to enone **32**.<sup>25</sup> To this end, a Ti-mediated reductive opening<sup>26</sup> of epoxide **50** furnishes diol **51**. However, despite surveying a wide variety of oxidation conditions, ketone **52** (or enone **32**) was never isolated. Instead, decomposition through the aforementioned aldol pathway was observed under several oxidation conditions (i.e., Swern, DMP, Cr(VI)), while other conditions (i.e., TPAP/NMO, CuOTf/ABNO/O<sub>2</sub>)<sup>27,28</sup> failed to induce any reactivity whatsoever. The

failure of this oxidation ultimately thwarted the advancement of intermediate **51** to enone **32**.

## 1.6 RING-EXPANSION STRATEGY: SIMPLIFIED SYSTEM

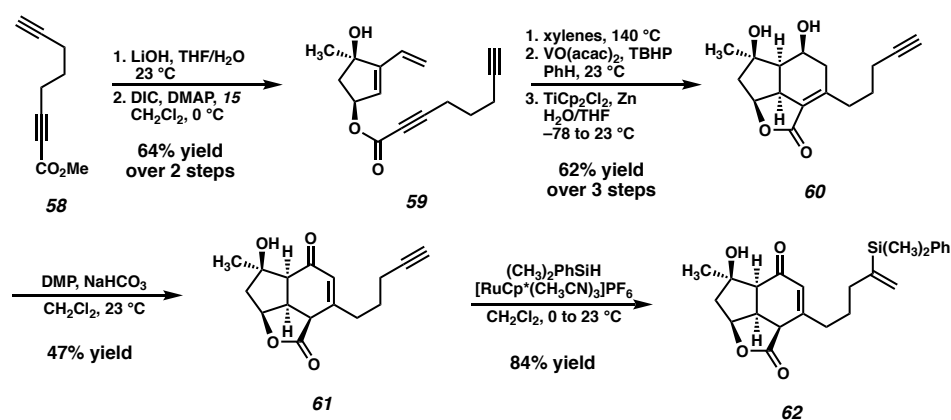
Although surprised by the difficulty of this transformation, we immediately identified the pendant ketone as the problematic functionality in diol **51**, which was hampering the advancement of this intermediate further in the synthesis. As such, we wondered whether the replacement of the ketone with a non-electrophilic surrogate might mitigate the undesired reactivity and facilitate the completion of the synthesis. Identifying a vinyl silane as a suitable choice, which would be converted to the ketone via a Tamao–Fleming<sup>29</sup> oxidation at a later point in the synthesis, we redesigned our route once again. When considering the proposed intermediate (i.e., **55**) we identified the vinyl silane/enone system as a well suited substrate for a [2+2] photocycloaddition,<sup>30</sup> which might prove successful in forging the final C–C bond (C(4)–C(5)) of the natural product. With these facts in mind, we ultimately developed the retrosynthetic plan outlined in Figure 1.6.1 as a suitable path forward.

**Figure 1.6.1** Third-generation retrosynthetic analysis of scabrolide A (**1**)

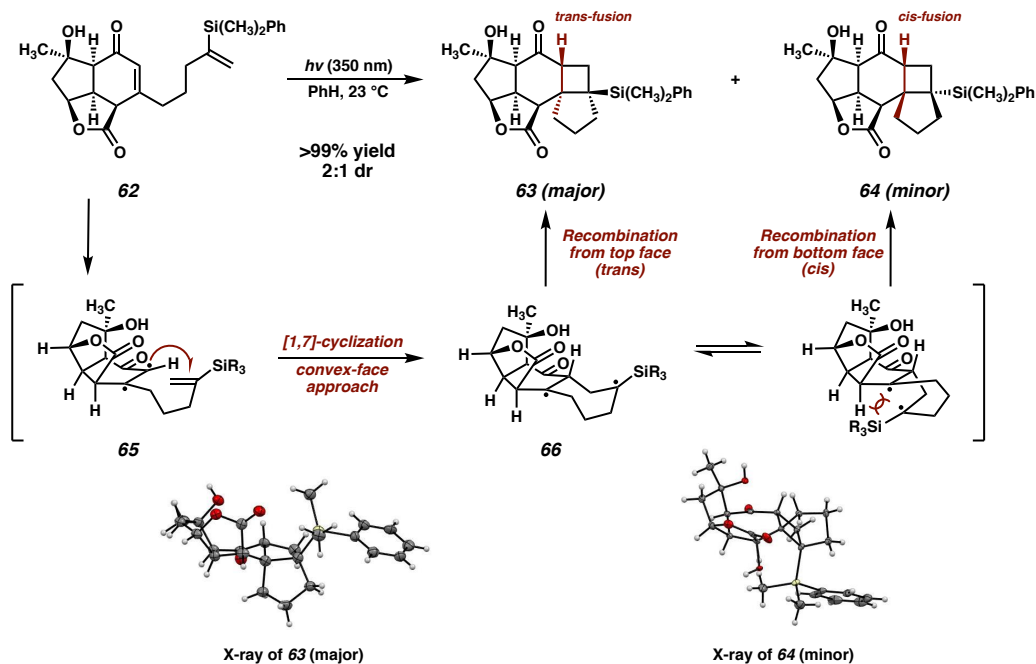


In this approach the seven-membered carbocycle would be introduced at a late stage via an oxidative fragmentation<sup>31</sup> of a fused [4–5] ring system such as **53**, which would be accessed by Tamao–Fleming oxidation of tertiary silane **54**. Pentacycle **54** was envisioned as the product of an intramolecular enone–olefin photocycloaddition, retrosynthetically delivering vinyl silane **55**, which would be accessed via a hydrosilylation of alkyne **56**. Notably, we hoped that replacement of the pendant methyl ketone present in prior intermediates with a relatively inert alkyne might allow access to the previously intractable enone (in this case **56**) by suppression of problematic decomposition pathways (i.e., aldol). In order to first test this new strategy, we opted to utilize a simplified system which omits the isopropenyl group. Removal of this distal stereocenter obviates the need for an enantiospecific synthesis of the carboxylic acid coupling partner in the esterification reaction, which allows expedient access to this fragment. We reasoned that, once a route to the core of the natural product was established, we would then go back and modify the route to include the isopropenyl group from an early stage.

**Scheme 1.6.2** Synthesis of simplified [2+2] substrate **62**.



In the event, known ester **58**,<sup>32</sup> available in one step from commercially available 1,6-heptadiyne, is saponified and coupled with dihydroxyvinylcyclopentene **15** (Scheme 1.6.2). The previously established Diels–Alder/epoxidation/reductive epoxide opening sequence then delivers diol **60**. With the problematic ketone now replaced with a relatively inert terminal alkyne, the oxidation of diol **60** proceeds under the action of DMP, delivering enone **61** after migration of the olefin into conjugation with the newly formed ketone. However, the outcome of this transformation proved to be highly variable, with a maximum yield of 47%, although yields as low as 20% were also observed. Specifically, this oxidation tended to proceed very slowly, and often completely stalled despite addition of excess DMP and heating. In spite of this irreproducibility, we were still able to access sufficient quantities of crucial intermediate **61** to explore the feasibility of the remainder of our new strategy. To this end, a Ru-catalyzed hydrosilylation<sup>33</sup> delivers vinyl silane **62**, setting the stage for the exploration of the crucial [2+2] photocycloaddition.

**Scheme 1.6.3** [2+2] photocycloaddition of simplified enone **62**.

To our delight, irradiation of vinyl silane **62** at 350 nm in benzene smoothly initiates the enone–olefin cycloaddition, delivering cyclobutanes **63** and **64** as a separable, 2:1 mixture of diastereomers (both of which were characterized unambiguously by X-ray diffraction). Notably, diastereomer **63**, the major product of this reaction displays *trans*-fusion at the [6–4] ring juncture, which is an uncommon stereochemical outcome of [2+2] photocycloadditions.<sup>34</sup> This observation can be rationalized as outlined in Scheme 1.6.3.<sup>35</sup> The photoexcited, triplet-state enone (**65**) first undergoes a highly diastereoselective [1,7]-cycloaddition with the terminal carbon of the vinyl silane, with the olefin approaching from the convex face of the molecule. The resulting 1,4-diradical (**66**) then can recombine either from the top face, leading to the (major) *trans*-fused product (**63**), or from the bottom face leading to the *cis*-fused product (**64**). Closer examination of the latter reveals a severe steric

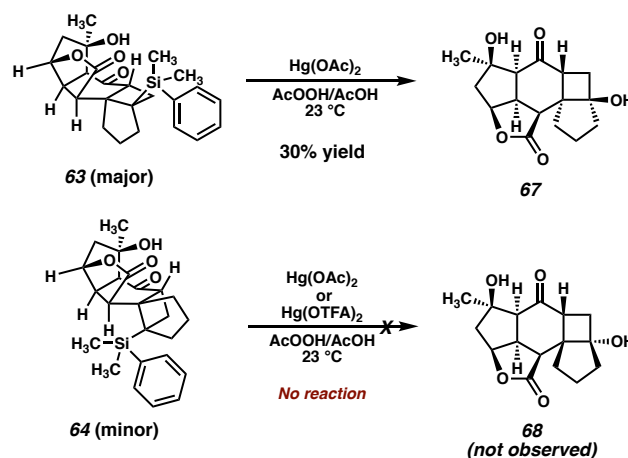
interaction between the bulky  $\text{Ph}(\text{CH}_3)_2\text{Si}$  group and the 6-membered ring, which we hypothesize is the driver for this unusual preference in diastereoselectivity.

Although it is typically understood in intramolecular enone-olefin photocycloadditions that triplet-state enones preferentially form 5-membered rings when possible,<sup>36</sup> exceptions to this tendency do exist, and the prevailing mechanism in each case is believed to be highly substrate-dependent. Specifically, cases in which the reacting ground-state olefin is substituted at the internal position (e.g., 1,1-disubstituted olefins) this type of reactivity is often observed.<sup>37</sup> This is presumably due to steric repulsion between the enone and the fully substituted olefinic carbon, and in the case of a bulky  $\text{Ph}(\text{CH}_3)_2\text{Si}$  substituent, it would be expected that this steric effect would be even more pronounced. Evidence for this type of mechanism operating in our cycloaddition includes the preferential formation of the *trans*-fused cyclobutane, as well as the conservation of stereochemistry at C(5) between both the *trans*- and *cis*- fused cyclobutane products. Thus, we believe that the initial [1,7]-cyclization occurs with high facial selectivity, and the subsequent radical recombination occurs with lower diastereoselectivity.

Gratified that our simplified system successfully undergoes the key [2+2] photocycloaddition, we set out to explore the remainder of our new strategy to access the carbocyclic core of scabrolide A. The next task would be the Tamao–Fleming oxidation, which would convert the tertiary silane to the oxygen atom which would eventually become the C(3) ketone of the natural product. To our delight, *trans*-fused silyl cyclobutane **63** readily undergoes Hg-mediated Tamao–Fleming oxidation, affording tertiary alcohol **67** in 30% yield (Scheme 1.6.4). Interestingly, the *cis*-fused diastereomer **64** fails to engage in the same reaction either in the presence of  $\text{Hg}(\text{OAc})_2$  or more reactive  $\text{Hg}(\text{OTFA})_2$ ,<sup>38</sup>

returning only starting material. This may be due to the inaccessibility of the tertiary silane in **64**, which is shielded by the bulk of the molecule, preventing access to activation/nucleophilic attack. Efforts to perform this reaction at elevated temperatures simply result in the nonspecific decomposition of silane **64**. Fortuitously, the reactive diastereomer happens to be the major product of the photocycloaddition, and thus material throughput is not significantly hampered by this unexpected divergence in reactivity.

**Scheme 1.6.4** Tamao–Fleming oxidation of **63** and failed Tamao–Fleming oxidation of **64**.

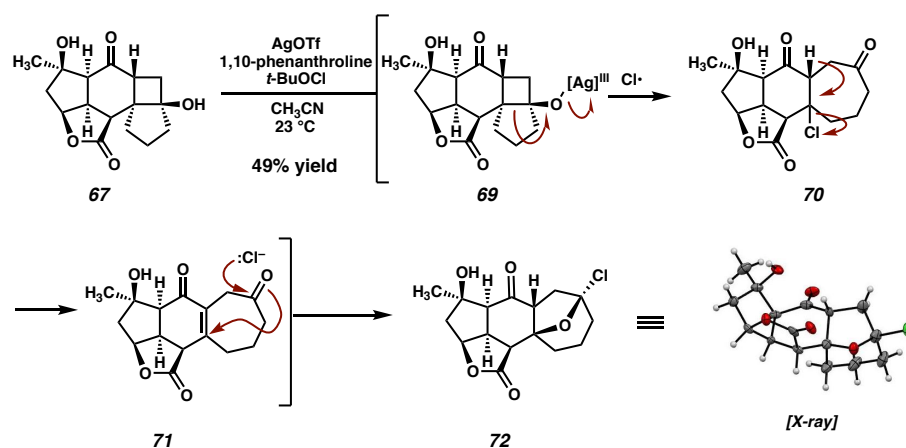


With cyclobutanone **67** in hand, we were presented with the opportunity to examine the final phase of our strategy on this model system. Specifically, an oxidative fragmentation of the cyclobutanone moiety present in intermediate **67** to generate the cycloheptenone was all that remained for the synthesis of the carbocyclic framework of scabrolide A (**1**). To this end, we were intrigued by a report from Qi and Zhang<sup>39</sup> which details the Ag-catalyzed oxidative fragmentation of a variety of cyclobutanone substrates to the corresponding  $\gamma$ -chloroketones. When we subjected model cyclobutanone **67** to these conditions, we were initially pleased to observe signs of selective reactivity. Upon



purification, however, we were surprised to isolate pentacycle **72** as the predominant product of this reaction (Scheme 1.6.5), rather than the expected  $\gamma$ -chloroketone or enone. We believe that **72**, the structure of which was determined unambiguously by X-ray diffraction, arises from chlorohydrin formation/*oxa*-Michael addition of enone **71**, after initial oxidative cyclobutanol fragmentation and chloride elimination. Although not the expected product, we were delighted to note that **72** is adorned with the requisite 7-membered carbocycle, and thus possesses the full carbocyclic framework of scabrolide A (1).

**Scheme 1.6.5** Oxidative ring expansion of cyclobutanol **67** to ether **72**.

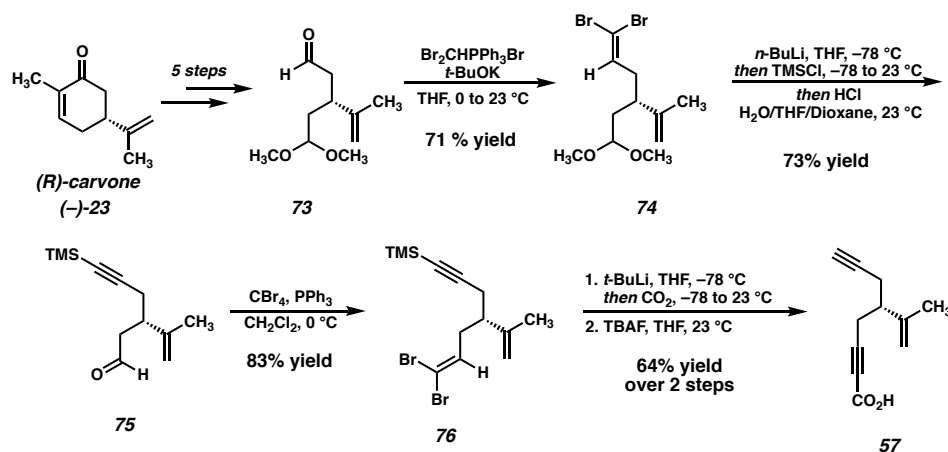


## 1.7 RING-EXPANSION STRATEGY: COMPLETE SYSTEM

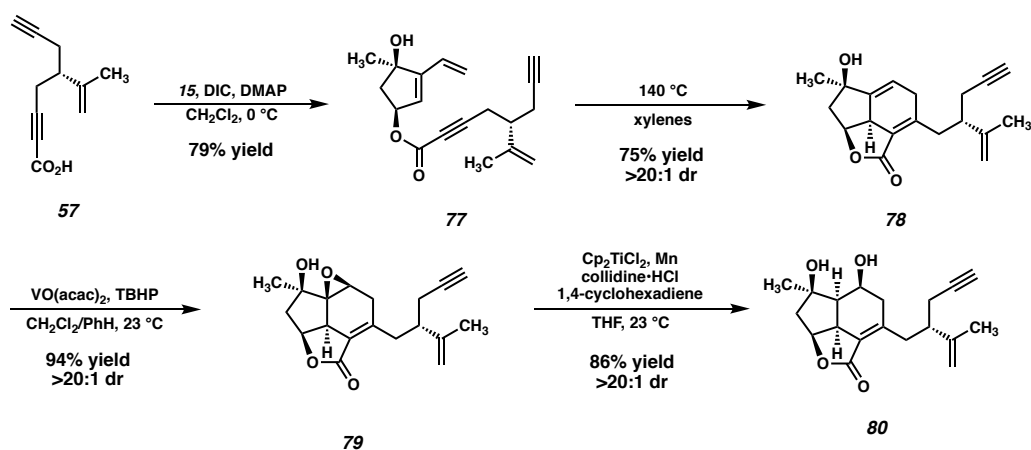
Given these results, we were confident that our newly designed strategy would be successful in delivering the natural product if we introduced the isopropenyl group at an early stage, and carried it through the remainder of the synthesis. To this end, we targeted ynoic acid **57** (Scheme 1.7.1) as a coupling partner for the convergent esterification. Returning to (*R*)-carvone ((-)-**23**) as our chiral-pool starting material, we designed a synthesis of the requisite fragment (**57**) starting from known monoprotected dialdehyde

**73.**<sup>40</sup> A series of two Corey–Fuchs homologations<sup>41</sup> enables the sequential installation of both alkynyl fragments while maintaining the stereochemical fidelity of the isopropenyl stereogenic center.

**Scheme 1.7.1** Synthesis of isopropenyl-bearing ynoic acid **57**.

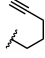
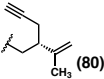


With acid **57** in hand, the convergent esterification is performed between diol **15** and ynoic acid **57**, and, following the intramolecular Diels–Alder reaction, tricycle **78** is obtained. This adduct is then carried through the same epoxidation/reductive opening sequence, this time utilizing a catalytic quantity of Ti.<sup>42</sup> At this stage, we recognized the need to address the challenging oxidation of diol **80**, and turned our attention toward a model system for this optimization (Table 1.7.1).

**Scheme 1.7.2** Esterification of ynoic acid **57** and Diels–Alder/oxidation sequence.

As noted earlier, buffered DMP could be employed for this oxidation in previous systems, however, these results were highly irreproducible. Specifically, the degree of conversion varied widely between batches both on the same and different scales. Initial experiments with Cr(VI) oxidants proved somewhat promising, inducing the desired reactivity, however large amounts of nonspecific decomposition were observed, and the yield was never optimized past 35% (Entry 2). Interestingly, TPAP/NMO, Cu(OTf)/ABNO/O<sub>2</sub>, and TEMPO systems failed to produce any meaningful levels of reactivity, returning only starting material (entries 3–5). We were pleased to see oxidation when utilizing IBX in DMSO, however, in this solvent the formation of several unidentified byproducts was observed (entry 6). Gratifyingly, switching the solvent to MeCN and elevating the temperature suppressed the undesired side reactivity, delivering model enone **82** in 71% yield (entry 7). To our delight, after slight modification, this IBX/MeCN system proved effective on the full system, delivering enone **56** in 72% yield (entry 8).

**Table 1.7.1** Optimization of the C(6) oxidation.

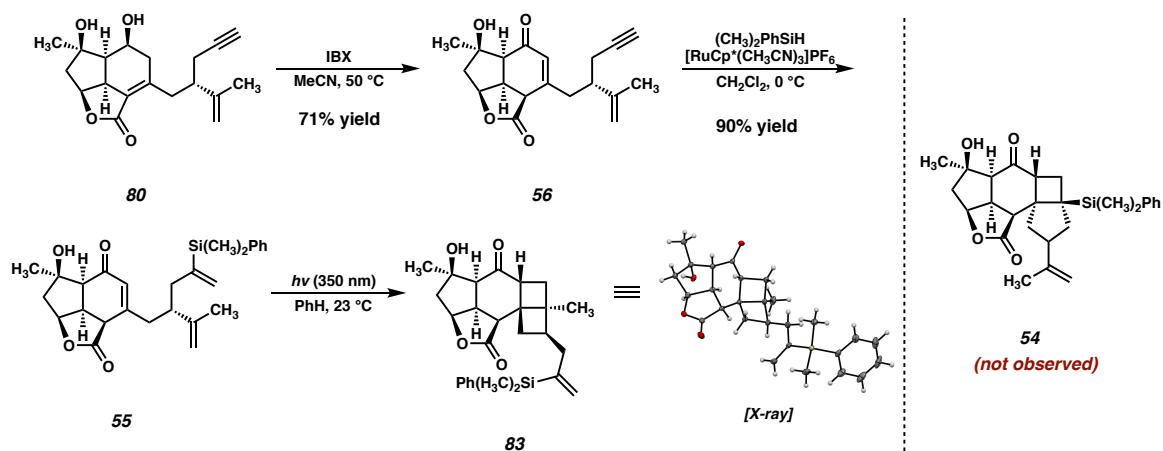
Entry	Conditions	R	Result
1	DMP, CH <sub>2</sub> Cl <sub>2</sub> , 23 °C	H,  (60)	Inconsistent yield/ incomplete conversion
2	PCC, CH <sub>2</sub> Cl <sub>2</sub> , 23 °C	H	35% yield
3	TPAP, NMO, 3ÅMS CH <sub>2</sub> Cl <sub>2</sub> , 23 °C	H	No reaction
4	Cu(CH <sub>3</sub> CN) <sub>3</sub> OTf, MeOPpy ABNO, NMI, CH <sub>3</sub> CN, O <sub>2</sub> , 23 °C	H	No reaction
5	TEMPO, PIDA, CH <sub>2</sub> Cl <sub>2</sub> , 23 °C	H	No reaction
6	IBX, DMSO, 23 °C	H	43% yield, decomposition
7	IBX, CH <sub>3</sub> CN, 80 °C	H	71% yield
8	IBX, CH <sub>3</sub> CN, 50 °C	 (80)	72% yield

## 1.8 FAILED [2+2] PHOTOCYCLOADDITION

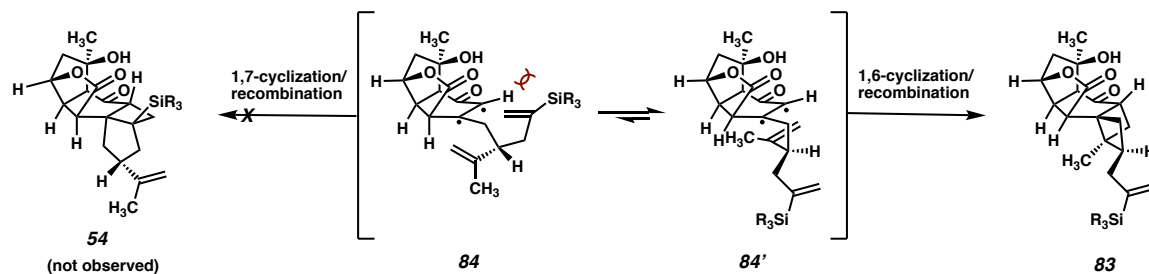
With a robust route to enone **56** now established, we were poised to examine the key [2+2] photocycloaddition with the now fully elaborated system (Scheme 1.8.1). To this end, hydrosilylation of enone **56** delivers vinyl silane **55** in good yield, setting the stage for the key [2+2] photocycloaddition, this time on the fully elaborated system. To our dismay, however, upon irradiation of **55** at 350 nm in benzene, the expected fused [6–4–5] product (i.e., **54**) was not observed. Instead, we isolated fused [6–4–4] product **83**, the major product of this photocycloaddition, which arises from the undesired reaction between the enone and the isopropenyl olefin rather than the vinyl silane. While the presence of two olefins on our [2+2] substrate was always a concern, we reasoned that, due to the highly strained nature of **83**, that the desired product **54** would likely be formed with at least some degree of selectivity. Consequently, we were astonished to discover that this transformation

was exquisitely selective for the [6–4–4] fused system, with no signs of the isopropenyl vinyl proton signals observed in the crude  $^1\text{H}$  NMR.

**Scheme 1.8.1** Photocyclization of fully elaborated substrate **55** to form undesired product **83**.

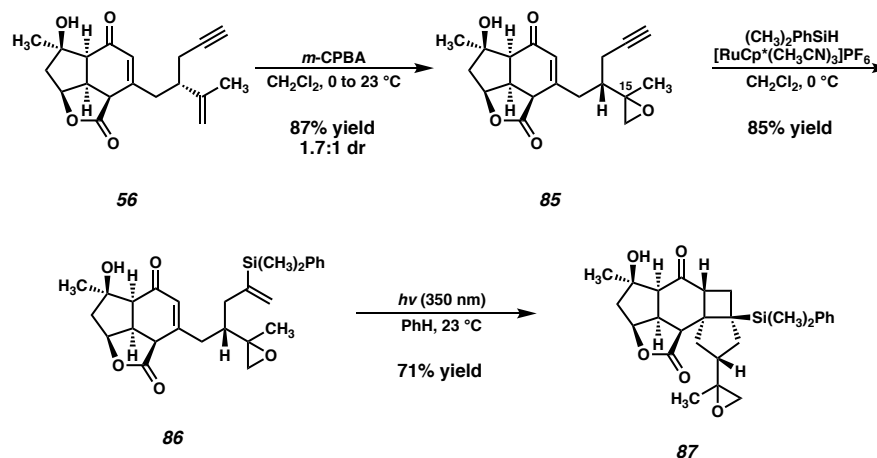


As outlined in Figure 1.8.1, we believe that the observed regioselectivity arises from steric interactions imposed by the bulky  $\text{Ph}(\text{CH}_3)_2\text{Si}$  group. In the desired reactive conformation of photoexcited enone **84** (i.e., for 1,7-cyclization leading ultimately to **54**), the large silyl group is required to come into close proximity with tricyclic core of the intermediate (Figure 1.8.1, left). We believe that this causes the favorability of a conformation such as **84'**, where the silyl group is held at a distance, thus bringing the isopropenyl olefin into closer proximity to the triplet-state enone. Subsequent 1,6-cyclization<sup>43</sup> results in the formation of a 1,4-diradical, which then undergoes radical recombination to the observed [6–4–4] product (**83**).

**Figure 1.8.1** Mechanistic rationale for the photocycloaddition.

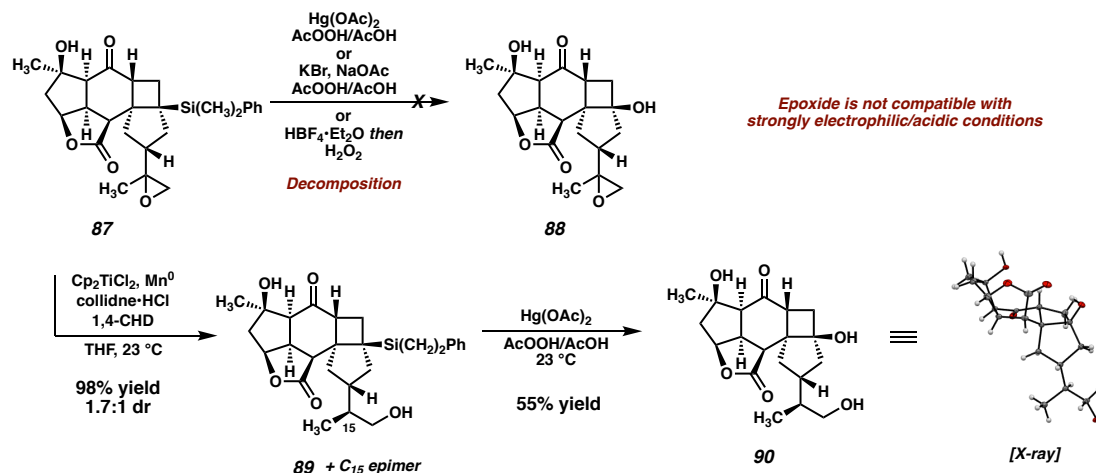
## 1.9 ISOPROPENYL PROTECTING GROUP STRATEGY

Given the overwhelming preference for the formation of **83** in the photocycloaddition, we reasoned that it would likely prove fruitless to attempt overturning selectivity for the desired product. We instead opted to utilize a protecting group strategy to overcome this undesired reactivity, where temporary “masking” of the isopropenyl olefin could allow for the correct regioselectivity in the [2+2]. In practice, this would require a functional group which could be easily installed on the olefin in question, and more importantly, could be removed at a later stage in the synthesis. After surveying several options, we decided that an epoxide could meet both of these criteria. To this end, treatment of enone **56** with *m*-CPBA delivers epoxide **85** as an inseparable mixture of epimers at C(15), which can then undergo hydrosilylation to furnish vinyl silane **86**. To our delight, with the reactive isopropenyl group now suitably protected as the corresponding epoxide, this intermediate smoothly undergoes the [2+2] cycloaddition at the intended olefin, delivering the desired *trans*-fused [6–4–5] product **87** in 71% yield.

**Scheme 1.9.1** Epoxidation of **56** and successful [2+2] of protected substrate **86**.

Initial attempts at performing the Tamao–Fleming oxidation on silane **87** proved unsuccessful. Treatment with  $\text{Hg}(\text{OAc})_2/\text{AcOOH}$ ,  $\text{KBr}/\text{AcOOH}$ , and  $\text{HBF}_4/\text{H}_2\text{O}_2$  all result in rapid decomposition, presumably due to the instability of the reactive epoxide under these strongly acidic conditions. Indeed, control experiments revealed that, even in the absence of activating agents, **87** quickly decomposes in solution with  $\text{AcOOH}/\text{AcOH}$ , rendering the desired Tamao–Fleming oxidation infeasible. This being the case, we chose to circumvent this issue by converting the problematic epoxide to the corresponding primary alcohol via a second Ti-catalyzed epoxide opening, which also serves as the first of two steps for the removal of the olefin protecting group. Silane **89** and its C(15) epimer are obtained excellent yield from this reaction, and are readily separable by column chromatography at this stage. Gratifyingly, we found that, in the absence of the epoxide, silane **89** smoothly undergoes a Tamao–Fleming oxidation to deliver cyclobutanol **90** (*epi-89* is also competent in this transformation, and can thus be carried through the remainder of the synthesis in an analogous to produce *epi-90*).

**Scheme 1.9.2** Failed Tamao–Fleming oxidation of epoxide **87**, reductive opening of epoxide **87** and successful Tamao–Fleming oxidation of **89**.

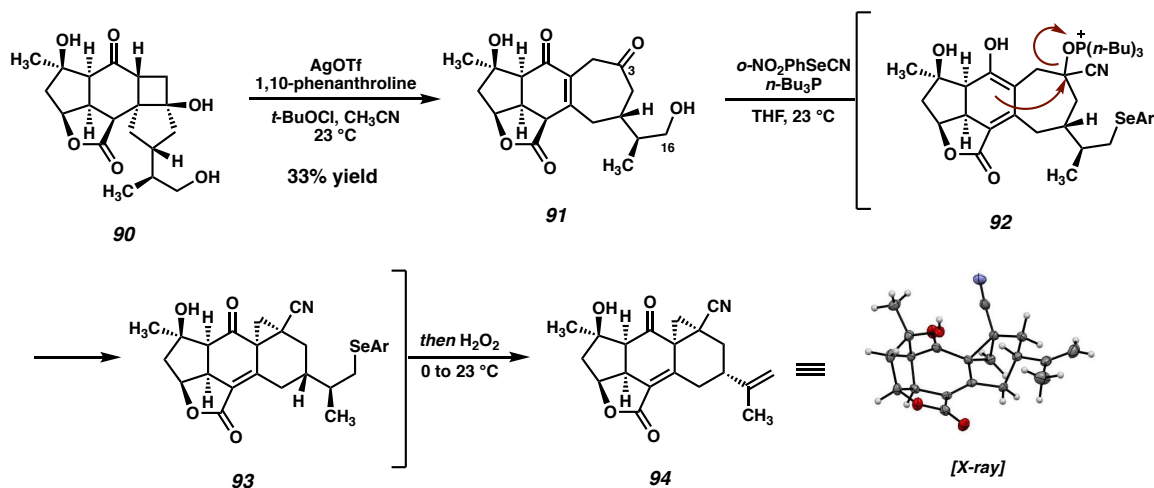


### 1.10 RING EXPANSION AND FAILED DEHYDRATION

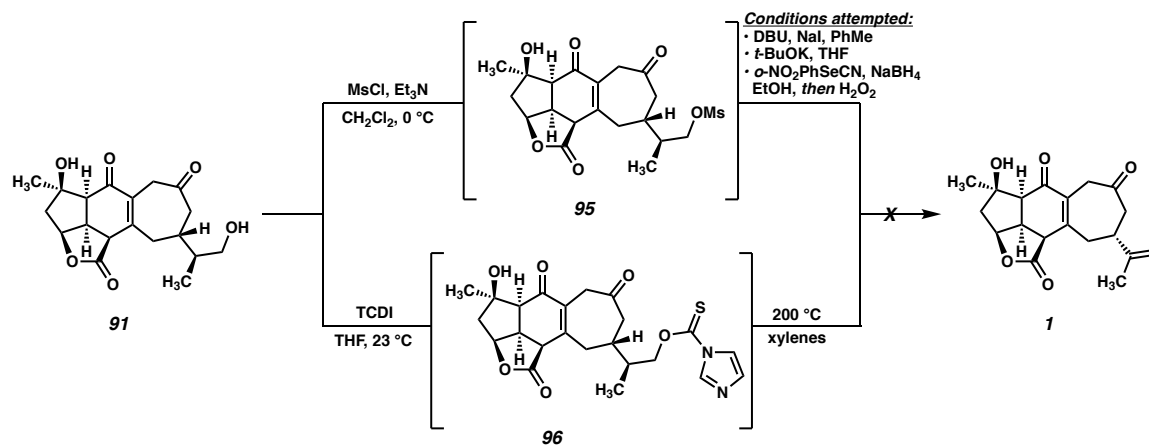
With cyclobutanol **90** in hand, we were poised to investigate the critical fragmentation reaction. To our delight, under our previously employed Ag-catalyzed conditions, cyclobutanol **90** undergoes fragmentation to cycloheptenone **91** (Scheme 1.11.1). Presumably the formation of **91** proceeds through the intermediacy of the corresponding  $\gamma$ -chloroketone (or a THF-bridged species analogous to **72**), however, the chloride is conveniently eliminated during purification by preparatory TLC (or stirring in a suspension of TLC  $\text{SiO}_2$  in  $\text{MeOH}$ ) to deliver the desired enone directly. With this key transformation complete and the carbocyclic core of the natural product now established on a fully elaborated system, the final remaining task was the elimination of the C(16) alcohol to regenerate the isopropenyl group and complete the total synthesis.



**Scheme 1.10.1** Oxidative ring-expansion of cyclobutanol **90** and unexpected cyclization of **91** during Grieco dehydration.



Given its frequent use in total synthesis, particularly in late-stage, complex settings, we turned to the venerable Grieco elimination<sup>44</sup> for this critical step (Scheme 1.11.1). To our surprise, however, exposure of alcohol **91** to the canonical Grieco conditions did not afford any trace of scabrolide A (**1**). After several attempts, we were able to isolate and characterize pentacycle **94** as the primary product of this reaction. While initially puzzling, we recognized that this product might arise if, under the reaction conditions, a cyanohydrin is formed at the C(3) ketone by HCN generated during the Grieco reaction. Activation of the cyanohydrin hydroxyl group by adventitious phosphonium (an intermediate in the Grieco reaction) could preclude cyclization either via a cationic intermediate or by direct displacement to close the three-membered ring. Following the usual oxidation/elimination of the selenide at C(16), pentacycle **94** would be formed. Upon closer analysis (LCMS) no trace of the diketone-selenide is detected during the course of the reaction, suggesting that cyanohydrin formation is faster than alcohol displacement under these conditions, and thus that this undesired cyclization would be difficult to suppress.

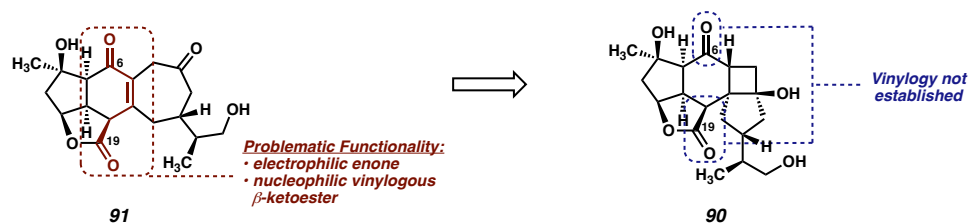
**Scheme 1.10.2** Failed dehydration attempts of alcohol **91**.

In light of this unexpected result, we turned our attention to alternative alcohol elimination protocols (Scheme 1.11.2). The mesylate **95** is readily formed using standard conditions, however, all attempts at performing the final elimination proved fruitless. Instead, nonspecific decomposition was observed in all cases, presumably a consequence of the base sensitivity of the substrate. Alternatively, thiocarbamate **96** could be prepared, which has been shown to undergo Chugaev-type eliminations at elevated temperatures.<sup>45</sup> In our hands, however, this intermediate failed to undergo the required elimination, instead decomposing when heated to high temperatures.

Upon examining intermediate **91**, the presence of the relatively reactive vinylogous  $\beta$ -ketoester is evident (Figure 1.11.1, red), which we hypothesize may be responsible for the undesired reactivity observed in this system. Indeed, armed with the knowledge that, under the Grieco conditions, this system does have the capability of undergoing transannular enolate chemistry across the 7-membered ring, we reasoned that the presence of this reactive functional group might be hindering our efforts toward elimination of the primary alcohol at C(16). With this in mind, we concluded that an intermediate in which the vinylogous relationship between the C(6) and C(19) carbonyls had not yet been

established might be better suited for this elimination reaction. As such, we identified triol **90** as a suitable substrate for the key dehydration.

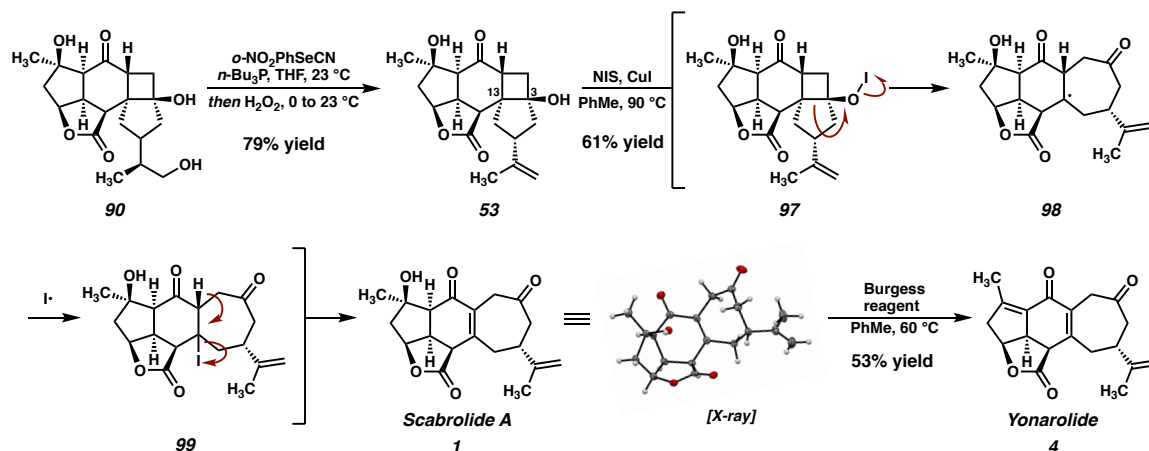
**Figure 1.10.1** Rationale for failure of dehydration attempts of enone **91**, and switching to a different substrate (**90**).



## 1.11 COMPLETION OF THE TOTAL SYNTHESIS

To our delight, both **90** and its C(18) epimer smoothly undergo dehydration under Grieco conditions to deliver cyclobutanol **53** in good yield, converging these two diastereomeric intermediates to a single product. With the isopropenyl group effectively deprotected, all that remained at this stage was the oxidative fragmentation of the cyclobutanol to generate the cycloheptenone and complete the synthesis. However, with the isopropenyl olefin now fully unmasked, this transformation was complicated by the potential for undesired oxidation of the newly revealed olefin. Indeed, exposure of cyclobutanol **53** to the Ag- catalyzed conditions previously established for this ring expansion generated a complex mixture of polychlorinated products (detected by LCMS). This can be attributed to the strongly oxidizing *t*-BuOCl, which is known to chlorinate both olefins and allylic systems in many cases.<sup>46</sup>

**Scheme 1.11.1** Successful Grieco dehydration of triol **90**, NIS-mediated ring expansion of cyclobutanol **53** to complete the total synthesis of scabrolide A (**1**), and dehydration of scabrolide A (**1**) to yonarolide (**4**).



In search of milder conditions for our oxidative ring expansion, we turned our attention to previously reported protocols for this type of transformation that employ weaker oxidants. To our delight, we found that the NIS/CuI-mediated protocol reported by Takasu and Ihara<sup>47</sup> proved to be selective for the desired transformation, furnishing scabrolide A (**1**) in 61% yield after oxidative ring-expansion of the cyclobutanol. Under these conditions, it is proposed that reaction between the tertiary cyclobutanol (**53**) and NIS generates a hypiodite (**97**), which then undergoes thermal homolysis to generate an *O*-centered radical. This high-energy intermediate then undergoes a  $\beta$ -scission of the C(3)–C(13) bond with subsequent recombination of the resultant tertiary *C*-centered radical (**98**) with iodine. The resultant iodide (**99**), situated at the  $\beta$ -position of both the C(6) ketone and the C(19) lactone, then undergoes facile elimination spontaneously under the reaction conditions to deliver scabrolide A (**1**). We were also able to convert scabrolide A (**1**) to a

closely related natural product, yonarolide (**4**), after dehydration with Burgess reagent. This research represents the first total synthesis of either of these two natural products.

## 1.12 CONCLUSION

Disclosed herein is the full account of our total synthesis of (–)-scabrolide A (**1**). An initial bioinspired macrocyclization/transannular cycloaddition strategy was thwarted by a failed RCM, but revealed a possible sequential ring-forming strategy which ultimately proved successful. As such, an approach consisting of convergent esterification of two chiral pool-derived fragments followed by West-to-East ring formation was designed. This involved an intramolecular [4+2] cycloaddition for the construction of the central 6-membered ring of the natural product, followed by a [2+2] cycloaddition/cyclobutane fragmentation sequence to generate the 7-membered ring. This strategy was initially realized in a *des*-isopropenyl model system. Translation to the full system revealed an unexpected regioselectivity issue in the [2+2] step, which was overcome using an unconventional olefin-protection strategy (i.e., masking of the olefin as an epoxide). Finally, efforts to perform a late-stage elimination of a primary alcohol revealed unexpected and unprecedented reactivity, which was overcome by a slight modification in the synthetic sequence. Our route provided access to both scabrolide A (**1**) as well as closely related yonarolide (**4**), neither of which had been previously prepared by total synthesis.

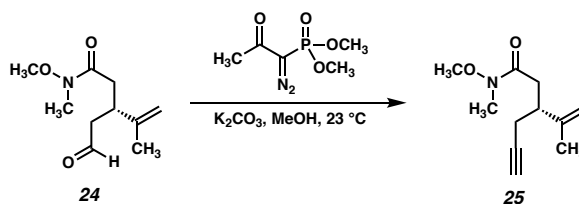
## 1.13 EXPERIMENTAL SECTION

### 1.13.1 MATERIALS AND METHODS

Unless otherwise stated, reactions were performed in flame-dried glassware under a nitrogen atmosphere using dry, deoxygenated solvents. Solvents were dried by passage through an activated alumina column under argon.<sup>48</sup> Reaction progress was monitored by thin-layer chromatography (TLC). TLC was performed using E. Merck silica gel 60 F254 precoated glass plates (0.25 mm) and visualized by UV fluorescence quenching, *p*-anisaldehyde, or KMnO<sub>4</sub> staining. Silicycle SiliaFlash® P60 Academic Silica gel (particle size 40–63 μm) was used for flash chromatography. <sup>1</sup>H NMR spectra were recorded on Varian Inova 500 MHz and 600 MHz and Bruker 400 MHz spectrometers and are reported relative to residual CHCl<sub>3</sub> (δ 7.26 ppm), C<sub>6</sub>D<sub>6</sub> (δ 7.16 ppm) or CD<sub>3</sub>OD (δ 3.31 ppm). <sup>13</sup>C NMR spectra were recorded on a Varian Inova 500 MHz spectrometer (125 MHz) and Bruker 400 MHz spectrometers (100 MHz) and are reported relative to CHCl<sub>3</sub> (δ 77.16 ppm), C<sub>6</sub>D<sub>6</sub> (δ 128.06 ppm) or CD<sub>3</sub>OD (δ 49.01 ppm). Data for <sup>1</sup>H NMR are reported as follows: chemical shift (δ ppm) (multiplicity, coupling constant (Hz), integration). Multiplicities are reported as follows: s = singlet, d = doublet, t = triplet, q = quartet, p = pentet, sept = septuplet, m = multiplet, br s = broad singlet, br d = broad doublet. Data for <sup>13</sup>C NMR are reported in terms of chemical shifts (δ ppm). IR spectra were obtained by use of a Perkin Elmer Spectrum BXII spectrometer or Nicolet 6700 FTIR spectrometer using thin films deposited on NaCl plates and reported in frequency of absorption (cm<sup>-1</sup>). Optical rotations were measured with a Jasco P-2000 polarimeter operating on the sodium D-line (589 nm), using a 100 mm path-length cell. High resolution mass spectra (HRMS) were obtained from the Caltech Mass Spectral Facility using a JEOL JMS-600H High

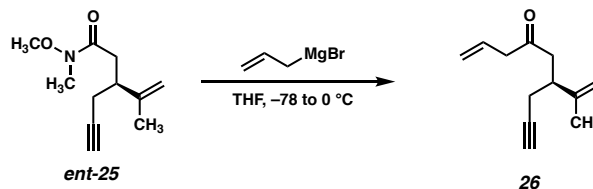
Resolution Mass Spectrometer in fast atom bombardment (FAB+) or electron ionization (EI+) mode, or using an Agilent 6200 Series TOF with an Agilent G1978A Multimode source in electrospray ionization (ESI+), atmospheric pressure chemical ionization (APCI+), or mixed ionization mode (MM: ESI-APCI+).

### 1.14.2 EXPERIMENTAL PROCEDURES



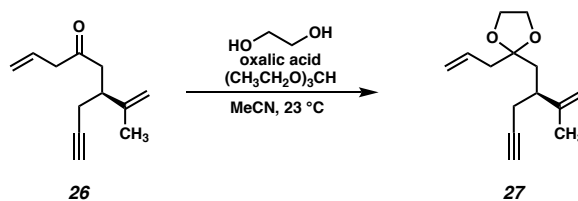
**Alkyne 25:** In a round-bottom flask, aldehyde **24**<sup>17</sup> (6.27 g, 31.5 mmol, 1.0 equiv) and  $\text{K}_2\text{CO}_3$  (8.7 g, 62.9 mmol, 2.0 equiv) was diluted with dry methanol (52.5 mL, 0.6 M) and cooled to 0 °C (ice/water bath). Ohira–Bestmann reagent (7.25 g, 37.8 mmol, 1.2 equiv) was added dropwise via syringe and the resultant suspension was allowed to stir for 12 h while gradually warming to 23 °C. Upon complete consumption of starting material (determined by TLC analysis), the reaction was diluted with  $\text{Et}_2\text{O}$  and washed with a saturated solution of  $\text{NaHCO}_3$ . The organic layer was dried over  $\text{Na}_2\text{SO}_4$ , filtered, and concentrated in vacuo. The crude product was purified by flash chromatography ( $\text{SiO}_2$ , 10%  $\text{EtOAc}/\text{CH}_2\text{Cl}_2$ ) to generate alkyne **25** (5.0 g, 82% yield) as a pale yellow oil;  $^1\text{H}$  NMR (500 MHz,  $\text{CDCl}_3$ )  $\delta$  4.85 (p,  $J = 1.5$  Hz, 1H), 4.82 (dp,  $J = 1.7, 0.9$  Hz, 1H), 3.70 (s, 3H), 3.17 (s, 3H), 2.92–2.82 (m, 1H), 2.76–2.60 (m, 2H), 2.38 (ddd,  $J = 6.4, 3.5, 2.7$  Hz, 2H), 1.99 (t,  $J = 2.7$  Hz, 1H), 1.77 (dd,  $J = 1.6, 0.8$  Hz, 3H);  $^{13}\text{C}$  NMR (125 MHz,  $\text{CDCl}_3$ )  $\delta$  173.0, 146.2, 111.6, 82.4, 69.9, 61.3, 40.8, 34.8, 32.2, 23.0, 20.7; IR (thin film, NaCl) 3293, 3250, 3076, 2967, 2938, 2820, 2116, 1661, 1430, 1384, 1334, 1175, 1175,

1108, 1002, 936, 894  $\text{cm}^{-1}$ ; HRMS (ES/APCI)  $m/z$  calc'd  $\text{C}_{11}\text{H}_{18}\text{O}_2\text{N}$   $[\text{M}+\text{H}]^+$ : 196.1332, found: 196.1336.  $[\alpha]_{\text{D}}^{25.0} + 22.8^\circ$  ( $c$  1.0,  $\text{CHCl}_3$ ).

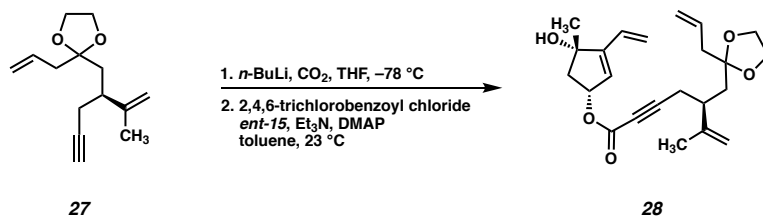


**Ketone 26:** In a flame dried round bottom flask, amide *ent-25* (50 mg, 0.26 mmol, 1.0 equiv) was dissolved in THF (0.8 mL, 0.3 M) and cooled to  $-78^\circ\text{C}$ . Allyl magnesium bromide (0.52 mL, 0.52 mmol, 1.0 M, 2.0 equiv) was added dropwise to the reaction solution. The reaction was allowed to stir for 15 min at  $-78^\circ\text{C}$  and then warmed to  $0^\circ\text{C}$  and stirred for 16 h. Upon complete consumption of starting material (determined by TLC analysis, 10%  $\text{Et}_2\text{O}$ /hexanes), the reaction was quenched with a saturated solution of  $\text{NH}_4\text{Cl}$  and the product was extracted from the biphasic mixture with  $\text{Et}_2\text{O}$  (3x). The combined organic layers were washed with brine, dried over  $\text{MgSO}_4$ , filtered, and concentrated in vacuo. The crude product was purified by flash chromatography ( $\text{SiO}_2$ , 10%  $\text{Et}_2\text{O}$ /hexanes) to generate alkyne **26** (39 mg, 87% yield) as a pale yellow oil;  $^1\text{H}$  NMR (500 MHz,  $\text{CDCl}_3$ )  $\delta$  5.91 (ddt,  $J = 17.2, 10.2, 7.0$  Hz, 1H), 5.18 (dq,  $J = 10.2, 1.3$  Hz, 1H), 5.14 (dq,  $J = 17.1, 1.5$  Hz, 1H), 4.82 (p,  $J = 1.5$  Hz, 1H), 4.78 (dt,  $J = 1.5, 0.8$  Hz, 1H), 3.18 (dt,  $J = 6.9, 1.4$  Hz, 2H), 2.86–2.77 (m, 1H), 2.74 (dd,  $J = 16.7, 6.6$  Hz, 1H), 2.62 (dd,  $J = 16.7, 7.4$  Hz, 1H), 2.32 (ddd,  $J = 14.5, 6.5, 2.7$  Hz, 2H), 1.99 (t,  $J = 2.7$  Hz, 1H), 1.73 (dd,  $J = 1.5, 0.8$  Hz, 3H);  $^{13}\text{C}$  NMR (125 MHz,  $\text{CDCl}_3$ )  $\delta$  207.3, 145.9, 130.52, 119.1, 111.8, 82.2, 70.3, 48.2, 45.1, 40.2, 23.0, 20.7; IR (thin film, NaCl) 3297, 3078, 2969, 2917, 2117, 1715, 1646, 1430, 1376, 993, 920, 895  $\text{cm}^{-1}$ ; HRMS (ESI)  $m/z$  calc'd  $\text{C}_{12}\text{H}_{16}\text{O}$   $[\text{M}]^+$ : 176.1201, found: 176.1191;  $[\alpha]_{\text{D}}^{25} - 24.90^\circ$  ( $c$  3.7,  $\text{CDCl}_3$ ).





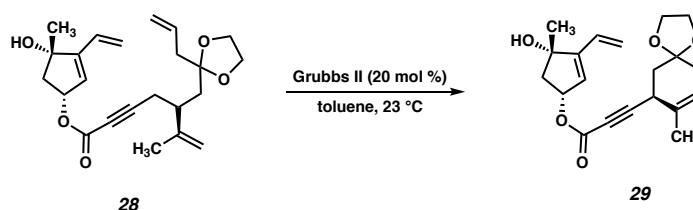
**Dioxolane 27:** Dried oxalic acid (109 mg, 1.2 mmol, 8.5 equiv) was dissolved in a solution of ethylene glycol (0.27 mL, 4.69 mmol, 33 equiv), triethyl orthoformate (0.14 mL, 0.85 mmol, 6 equiv), and MeCN (1.95 mL, 0.073 M). After complete dissolution of the oxalic acid, ketone **26** (25 mg, 0.14 mmol, 1 equiv) was added. The reaction was sealed and allowed to stir at ambient temperature (23 °C) for 36 h. Upon complete consumption of starting material (as determined by TLC analysis), the reaction was diluted with H<sub>2</sub>O and the product was extracted with Et<sub>2</sub>O (3 x 5 mL). The combined organic layers were washed with brine, dried with MgSO<sub>4</sub>, filtered, and concentrated in vacuo. The crude product was purified by flash chromatography (SiO<sub>2</sub>, 25% Et<sub>2</sub>O/hexanes) to afford dioxolane **27** (26 mg, 83% yield) as a pale yellow oil; <sup>1</sup>H NMR (400 MHz, CDCl<sub>3</sub>) δ = 5.81 (ddt, *J* = 16.9, 10.5, 7.2 Hz, 1H), 5.12 (ddt, *J* = 8.2, 2.2, 1.3 Hz, 1H), 5.08 (t, *J* = 1.3 Hz, 1H), 4.79 (q, *J* = 1.3 Hz, 2H), 3.94 (q, *J* = 1.3 Hz, 4H), 2.52 (dq, *J* = 8.2, 6.3 Hz, 1H), 2.43–2.34 (m, 3H), 2.26 (ddd, *J* = 16.7, 8.1, 2.7 Hz, 1H), 1.97 (t, *J* = 2.6 Hz, 1H), 1.83 (d, *J* = 6.5 Hz, 2H), 1.70 (t, *J* = 1.2 Hz, 3H); <sup>13</sup>C NMR (100 MHz, CDCl<sub>3</sub>) δ = 147.5, 133.3, 118.4, 111.4, 110.8, 83.3, 69.4, 65.0, 65.0, 42.5, 41.3, 39.2, 24.1, 19.2; IR (thin film, NaCl) 3302, 3075, 2949, 2888, 2117, 1643, 1433, 1374, 1311, 1124, 1100, 996, 918, 890, 862, 837, 635 cm<sup>-1</sup>; HRMS (FAB<sup>+</sup>) *m/z* calc'd C<sub>14</sub>H<sub>21</sub>O<sub>2</sub> [M+H]<sup>+</sup>: 221.1536, found: 221.1531; [α]<sub>23</sub><sup>D</sup> = - 2.45 (c = 0.79, CHCl<sub>3</sub>).



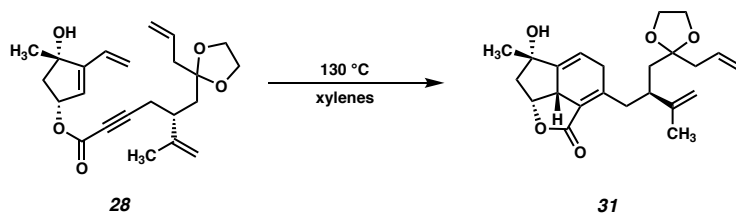
**Ester 28:** Dioxolane **27** (95 mg, 0.43 mmol, 1 equiv) was dissolved in THF (4.3 mL, 0.1 M) and cooled  $-78\text{ }^\circ\text{C}$ . *n*-BuLi (2.17 M in hexanes, 395  $\mu\text{L}$ , 0.863 mmol, 2 equiv) was then added dropwise. The solution was allowed to stir for 5 min followed by the addition powdered dry ice (0.56 g, 1.3 g/mmol of **27**). After 10 min, the reaction was quenched with a saturated solution of  $\text{NH}_4\text{Cl}$  and was allowed to warm to ambient temperature ( $23\text{ }^\circ\text{C}$ ). The solution was acidified with a 5% solution of citric acid (5 mL) and the product was extracted with EtOAc (5 x 15 mL). The combined organic layers were dried over  $\text{MgSO}_4$ , filtered, and concentrated in vacuo leaving an acid (103 mg, 93%) was used crude in the following reaction.

To a solution of the crude acid (58 mg, 0.22 mmol, 1.1 equiv) in THF (2 mL, 0.1 M),  $\text{Et}_3\text{N}$  (92  $\mu\text{L}$ , 0.66 mmol, 3.3 equiv) and 2,4,6-trichlorobenzoyl chloride (34  $\mu\text{L}$ , 0.22 mmol, 1.1 equiv) was added. The reaction was allowed to stir for 1 h followed by the addition of a THF solution (2 mL, 0.1 M) of diol *ent*-**15** (28 mg, 0.2 M, 1 equiv) and DMAP (24 mg, 0.2 mmol, 1 equiv). The reaction was allowed to stir at  $23\text{ }^\circ\text{C}$  until complete. Upon complete consumption of diol *ent*-**15** (as determined by TLC analysis) the reaction was directly purified by column chromatography ( $\text{SiO}_2$ , 100% hexanes then 50% EtOAc/hexanes) to afford ester **28** (43 mg, 50%) as a yellow oil;  $^1\text{H}$  NMR (400 MHz,  $\text{CDCl}_3$ )  $\delta$  6.31 (dd,  $J = 17.8, 11.3$  Hz, 1H), 5.87–5.73 (m, 3H), 5.53 (ddd,  $J = 7.1, 4.5, 2.3$  Hz, 1H), 5.32 (dd,  $J = 11.3, 1.6$  Hz, 1H), 5.16–5.10 (m, 1H), 5.08 (t,  $J = 1.3$  Hz, 1H), 4.80 (d,  $J = 1.2$  Hz, 2H), 3.94 (s, 4H), 2.65–2.53 (m, 3H), 2.45–2.39 (m, 1H), 2.36 (dq,  $J = 6.1,$

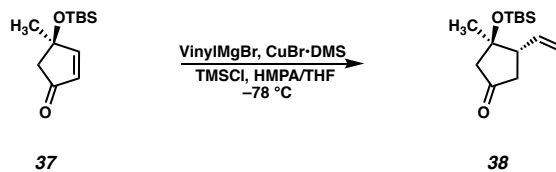
1.2 Hz, 2H), 2.08–2.01 (m, 1H), 1.92 (s, 1H), 1.85 (dd,  $J = 14.7, 6.1$  Hz, 1H), 1.77 (dd,  $J = 14.7, 6.2$  Hz, 1H), 1.69 (t,  $J = 1.2$  Hz, 3H), 1.43 (s, 3H);  $^{13}\text{C}$  NMR (101 MHz,  $\text{CDCl}_3$ )  $\delta$  153.6, 151.7, 146.6, 133.2, 129.0, 126.2, 119.5, 118.6, 112.1, 110.7, 88.9, 81.0, 77.0, 74.2, 65.1, 65.0, 49.0, 42.5, 40.6, 39.4, 26.7, 24.2, 19.4; IR (thin film, NaCl) 3369, 2956, 2918, 2847, 2232, 1705, 1633, 1460, 1418, 1372, 1258, 1063, 801  $\text{cm}^{-1}$ ; HRMS (FAB $^+$ )  $m/z$  calc'd  $\text{C}_{23}\text{H}_{31}\text{O}_5$   $[\text{M}+\text{H}]^+$ : 387.2171, found: 387.2158;  $[\alpha]_{25}^{\text{D}} = +26.7$  ( $c = 0.045$ ,  $\text{CHCl}_3$ ).



**Cyclohexene 29:** To a stirred, Ar-sparged solution of ester **28** (6 mg, 0.016 mmol, 1.0 equiv) in toluene (1 mL, 0.016 M) was added Grubbs 2<sup>nd</sup>-generation catalyst (2.6 mg, 3.1  $\mu\text{mol}$ , 0.2 equiv) in one portion. The reaction was allowed to stir for 2 h followed by direct purification by column chromatography ( $\text{SiO}_2$ , 100% hexanes to 20% EtOAc/hexanes) to afford cyclohexene **29** (1.7 mg, 31 %) as a pale yellow oil;  $^1\text{H}$  NMR (400 MHz,  $\text{CDCl}_3$ )  $\delta$  6.26 (ddt,  $J = 17.8, 11.3, 0.7$  Hz, 1H), 5.76 (d,  $J = 2.4$  Hz, 1H), 5.75–5.68 (m, 1H), 5.52–5.45 (m, 1H), 5.35 (ddt,  $J = 4.6, 3.2, 1.5$  Hz, 1H), 5.27 (dd,  $J = 11.3, 1.6$  Hz, 1H), 3.94–3.87 (m, 4H), 2.58 (dd,  $J = 14.3, 7.3$  Hz, 1H), 2.50 (d,  $J = 1.9$  Hz, 3H), 2.26–2.11 (m, 2H), 2.00 (dd,  $J = 14.2, 4.4$  Hz, 1H), 1.90–1.76 (m, 2H), 1.64 (q,  $J = 2.0$  Hz, 3H), 1.38 (s, 3H);  $^{13}\text{C}$  NMR (100 MHz,  $\text{CDCl}_3$ )  $\delta$  153.6, 151.8, 133.9, 128.9, 126.1, 121.8, 119.6, 108.0, 88.5, 81.1, 77.1, 74.4, 64.7, 64.5, 49.0, 38.1, 36.2, 36.1, 26.8, 22.6, 21.1; IR (thin film, NaCl) 3447, 2926, 2233, 1734, 1701, 1559, 1540, 1420, 1372, 1248, 1122, 1072, 988, 948, 874, 810, 753, 731; HRMS (ESI)  $m/z$  calc'd  $\text{C}_{21}\text{H}_{27}\text{O}_5$   $[\text{M}+\text{H}]^+$ : 358.1853, found: 358.1833;  $[\alpha]_{\text{D}}^{23} = +125.4$  ( $c = 0.75$ ,  $\text{CHCl}_3$ ).

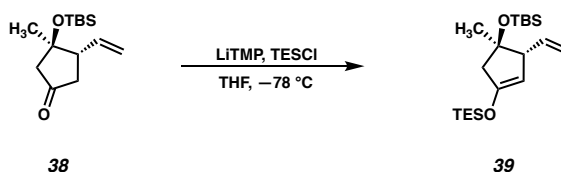


**Cyclohexadiene 31:** Ester **28** (5.3 mg, 13.7  $\mu\text{mol}$ , 1 equiv) was dissolved in xylenes (0.5 mL), sparged with Ar, sealed, and heated to 130 °C for 1 h. Upon complete consumption of starting material (as determined by TLC analysis), the reaction was loaded directly onto a flash column (SiO<sub>2</sub>, 100% hexanes to 50% EtOAc/Hexanes) to afford cyclohexadiene **31** (2.1 mg, 40% yield) as an amorphous solid; <sup>1</sup>H NMR (400 MHz, CDCl<sub>3</sub>)  $\delta$  5.91–5.72 (m, 2H), 5.16–5.03 (m, 2H), 4.96 (ddd,  $J = 9.1, 8.0, 7.0$  Hz, 1H), 4.64 (dq,  $J = 2.9, 1.5$  Hz, 1H), 4.57 (dd,  $J = 2.3, 1.0$  Hz, 1H), 4.01–3.86 (m, 4H), 3.30 (t,  $J = 9.7$  Hz, 1H), 3.10–2.90 (m, 2H), 2.75–2.59 (m, 3H), 2.50 (ddd,  $J = 12.7, 7.0, 0.9$  Hz, 1H), 2.39 (dq,  $J = 7.2, 1.5$  Hz, 2H), 1.90 (dd,  $J = 14.8, 7.9$  Hz, 1H), 1.72–1.64 (m, 4H), 1.64–1.60 (m, 1H), 1.40 (d,  $J = 1.0$  Hz, 3H); <sup>13</sup>C NMR (101 MHz, CDCl<sub>3</sub>)  $\delta$  168.3, 156.7, 152.0, 148.6, 133.5, 124.9, 118.4, 116.6, 111.3, 110.9, 80.0, 75.2, 65.1, 65.0, 49.8, 45.7, 42.5, 41.9, 39.4, 36.8, 35.3, 26.6, 18.3; IR (thin film, NaCl) 3458, 2924, 1749, 1642, 1432, 1210, 1093, 1044, 823 cm<sup>-1</sup>; HRMS (FAB<sup>+</sup>)  $m/z$  calc'd C<sub>23</sub>H<sub>31</sub>O<sub>5</sub> [M+H]<sup>+</sup>: 387.2171, found: 387.2188;  $[\alpha]_D^{23} + 37.5$  ( $c$  0.12, CHCl<sub>3</sub>).



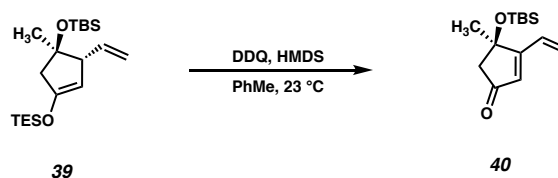
**Vinylcyclopentanone 38:** To a 500 mL three-necked flask was added CuBr • DMS (543 mg, 2.65 mmol, 0.12 equiv). The flask was evacuated and back-filled three times with argon, and charged with THF (110 mL). The solution was cooled to  $-78\text{ }^{\circ}\text{C}$  and vinylmagnesium bromide in THF (1.0 M, 26.5 mL, 1.2 equiv) was added. The flask was equipped with an addition funnel and stirred at  $-78\text{ }^{\circ}\text{C}$  for 30 minutes, during which time the solution turned from dark to red-brown. In a separate 100 mL flask, enone **37** (5.0 g, 22.1 mmol, 1 equiv) was dissolved in THF (22.1 mL). HMPA (10.97 mL, 66.1 mmol, 3.0 equiv) and TMSCl (6.94 mL, 55.2 mmol, 2.5 equiv) were added at room temperature, and stirred for 5 minutes. This solution was transferred to the addition funnel and slowly added to the flask over 1 hour; an internal temperature no greater than  $-70\text{ }^{\circ}\text{C}$  was maintained and the solution turned orange to yellow to dark brown. Upon complete addition, the reaction was stirred at  $-78\text{ }^{\circ}\text{C}$  for an additional hour, and then warmed to  $0\text{ }^{\circ}\text{C}$ . Saturated aqueous  $\text{NH}_4\text{Cl}$  (125 mL) was added before stirring at  $0\text{ }^{\circ}\text{C}$  for 1 hour. The layers were separated and the aqueous layer was extracted with  $\text{Et}_2\text{O}$  (3x). The combined organics were washed with brine, dried with  $\text{MgSO}_4$  and concentrated under reduced pressure. Flash column chromatography (10-20%  $\text{Et}_2\text{O}$ /Hexanes) afforded cyclopentanone **38** (3.59 g, 64% yield, 9:1 mixture of diastereomers) as a yellow oil; *Major Diastereomer*:  $^1\text{H}$  NMR (400 MHz,  $\text{CDCl}_3$ )  $\delta$  5.81 (ddd,  $J = 17.1, 10.4, 7.4$  Hz, 1H), 5.26 – 4.92 (m, 2H), 2.89 (dtd,  $J = 8.1, 6.7, 1.2$  Hz, 1H), 2.64 (ddd,  $J = 18.7, 8.2, 1.1$  Hz, 1H), 2.39 (d,  $J = 17.8$  Hz, 1H), 2.32 (dd,  $J = 17.6, 1.1$  Hz, 1H), 2.17 (dd,  $J = 18.7, 6.6, 1.1$  Hz, 1H), 1.27 (s, 3H), 0.85 (s,

6H), 0.10 (d,  $J = 8.0$  Hz, 6H);  $^{13}\text{C}$  NMR (100 MHz,  $\text{CDCl}_3$ )  $\delta$  216.2, 136.9, 116.6, 79.7, 53.5, 52.8, 42.2, 25.7, 24.2, 18.0, -2.2, -2.4; IR (Neat film, NaCl) 2956, 2930, 2857, 1750, 1471, 1462, 1402, 1378, 1257, 1162, 1114, 1025, 997, 918, 836, 774, 617  $\text{cm}^{-1}$ ; HRMS (FAB+)  $m/z$  calc'd for  $\text{C}_{14}\text{H}_{27}\text{O}_2\text{Si}$   $[\text{M}+\text{H}]^+$ : 255.1780, found 255.1784;  $[\alpha]_{\text{D}}^{25.0} -30.0^\circ$  ( $c$  1.0,  $\text{CHCl}_3$ ).



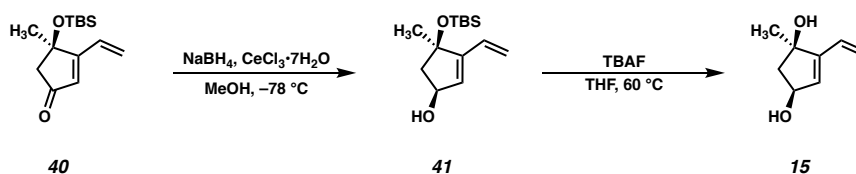
**Silyl Enol Ether 39:** A 500 mL round-bottom flask was soaked in a base bath overnight, then washed, flame-dried, and placed under nitrogen atmosphere. The flask was charged with 2,2,6,6-tetramethylpiperidine (4.01 mL, 23.63 mmol, 1.2 equiv) and THF (108 mL) before being cooled to  $-78^\circ\text{C}$ .  $n\text{-BuLi}$  (9.30 mL of 2.33 M, 1.1 equiv) was added to the flask, then stirred at  $0^\circ\text{C}$  for 1 hr. The flask was cooled to  $-78^\circ\text{C}$  and charged with TESCl (3.96 mL, 23.6 1.2 equiv), then stirred for 5 minutes. Using a syringe pump, vinylcyclopentanone **38** (5.00 g, 19.69 mmol, 1.0 equiv) in THF (20 mL) was added dropwise over 1 hour. Upon complete addition, the reaction was stirred until complete by TLC (15 minutes.) Triethylamine (5 mL) was then added and the reaction was quenched with a saturated aqueous sodium bicarbonate solution, and gradually warmed to  $23^\circ\text{C}$ . The layers were separated and the aqueous layer was extracted with hexanes (5x). The combined organics were washed with water and 0.1 M citric acid solution, dried with sodium sulfate, and concentrated under reduced pressure. Flash column chromatography (2.5%  $\text{Et}_2\text{O}$ /Hexanes) afforded silyl enol ether **39** (4.78 g, 12.96 mmol, 66% yield, 9:1 mixture of diastereomers) as a colorless oil; *Major diastereomer*:  $^1\text{H}$  NMR (400 MHz,

$C_6D_6$ )  $\delta$  5.81 (ddd,  $J = 17.1, 10.1, 7.9$  Hz, 1H), 5.16 (ddd,  $J = 17.1, 2.2, 1.2$  Hz, 1H), 5.05 (ddd,  $J = 10.1, 2.2, 0.9$  Hz, 1H), 4.66 (q,  $J = 1.8$  Hz, 1H), 3.42 (ddq,  $J = 6.6, 2.3, 1.2$  Hz, 1H), 2.68 (dt,  $J = 15.7, 1.6$  Hz, 1H), 2.41 (dt,  $J = 15.7, 1.4$  Hz, 1H), 1.27 (s, 3H), 1.04 – 0.99 (m, 18H), 0.73 – 0.61 (m, 6H), 0.15 (s, 3H), 0.14 (s, 3H);  $^{13}C$  NMR (100 MHz,  $C_6D_6$ )  $\delta$  153.9, 139.3, 115.2, 103.2, 81.9, 59.9, 50.7, 26.8, 26.3, 18.5, 7.2, 5.5, –2.0, –1.9. IR (Neat film, NaCl) 3078, 2955, 2933, 2477, 2856, 1647, 1459, 1360, 1334, 1250, 1226, 1135, 1091, 1018 1004, 918, 834, 799, 774, 746  $cm^{-1}$ ; HRMS (FAB+)  $m/z$  calc'd for  $C_{20}H_{39}O_2Si_2$   $[M-H]^+$ : 367.2489, found 367.2489;  $[\alpha]_D^{25.0}$  –66.8° ( $c$  1.0,  $CHCl_3$ ).



**Dienone 40:** A 1 L round-bottomed flask was charged with silyl enol ether **39** (5.80 g, 15.76 mmol, 1.0 equiv) in benzene (310 mL). HMDS was then added dropwise via syringe and the resulting solution was stirred for 5 minutes. DDQ (7.87 g, 34.67 mmol, 2.2 equiv) was added in a single portion, and the reaction was stirred for 45 minutes, during which time it turned from black to bright red. Celite® (30 g) was added to the reaction, then the solvent was removed by rotary evaporation, and the remaining solid dried on high vacuum for 1 h. Flash column chromatography (1%-10%  $Et_2O$ /Hexanes) afforded enone **40** (3.35 g, 13.27 mmol, 84% yield) as a gold oil, along with triethylsilanol as a coeluted impurity (1.16 g as determined by  $^1H$  NMR). A pure sample for characterization was obtained by preparative TLC (30%  $Et_2O$ /Hexane);  $^1H$  NMR (400 MHz,  $CDCl_3$ )  $\delta$  6.56 (ddd,  $J = 17.8, 11.1, 0.8$  Hz, 1H), 6.14 – 5.99 (m, 2H), 5.70 (dd,  $J = 11.1, 1.5$  Hz, 1H), 2.70 (dd,  $J = 17.9, 0.7$  Hz, 1H), 2.57 (d,  $J = 17.8$  Hz, 1H), 1.53 (d,  $J = 0.6$  Hz, 3H), 0.86 (s, 9H), 0.13 (s, 3H),

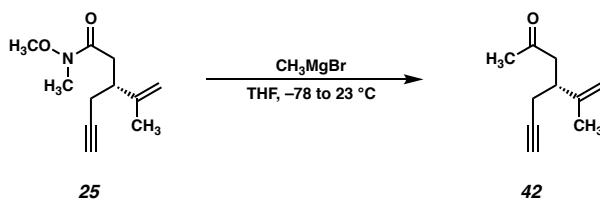
0.07 (s, 3H).  $^{13}\text{C}$  NMR (100 MHz,  $\text{CDCl}_3$ )  $\delta$  205.0, 175.9, 129.0, 126.5, 125.5, 78.8, 53.2, 29.2, 25.8, 18.1, -2.3, -2.7; IR (Neat film, NaCl) 2955, 2930, 2857, 1709, 1603, 1473, 1361, 1336, 1253, 1232, 1206, 1159, 1074, 1004, 938, 862, 834, 776  $\text{cm}^{-1}$ ; HRMS (FAB+)  $m/z$  calc'd for  $\text{C}_{14}\text{H}_{25}\text{O}_2\text{Si}$   $[\text{M}+\text{H}]^+$ : 253.1624, found 253.1622;  $[\alpha]_{\text{D}}^{25.0}$   $-92.1^\circ$  ( $c$  0.2,  $\text{CHCl}_3$ ).



**Diol 15:** A 500-mL round-bottom flask was charged with dienone **40** (2.69 g, 10.67 mmol, 1.0 equiv) in MeOH (110 mL) and cooled to  $-78^\circ\text{C}$ .  $\text{CeCl}_3 \cdot 7 \text{H}_2\text{O}$  (5.17 g, 13.87 mmol, 1.3 equiv) was added, and the solution stirred for 5 minutes before  $\text{NaBH}_4$  (534 mg, 13.87 mmol, 1.3 equiv) was added in a single portion. The reaction was stirred at  $-78^\circ\text{C}$  for 1 hour, warmed to room temperature, and quenched with saturated, aqueous  $\text{NH}_4\text{Cl}$ . The mixture was partially concentrated on a rotary evaporator to remove methanol, transferred to a separatory funnel, and extracted with diethyl ether (3x). The combined organics were then washed with brine, dried with  $\text{MgSO}_4$ , and concentrated to afford an orange oil which was used directly in the next step without further purification. A pure sample for characterization was obtained by flash chromatography ( $\text{SiO}_2$ , 25% EtOAc/hexanes);  $^1\text{H}$  NMR (400 MHz,  $\text{CDCl}_3$ )  $\delta$  6.32–6.22 (m, 1H), 5.75–5.67 (m, 2H), 5.25–5.19 (m, 1H), 4.64–4.55 (m, 1H), 2.53 (dd,  $J = 12.7, 6.9$  Hz, 1H), 1.93 (ddd,  $J = 12.7, 6.0, 0.8$  Hz, 1H), 1.59 (s, 1H), 1.36 (d,  $J = 0.9$  Hz, 3H), 0.86 (s, 9H), 0.12 (s, 3H), 0.10 (s, 3H);  $^{13}\text{C}$  NMR (100 MHz,  $\text{CDCl}_3$ )  $\delta$  150.6, 129.8, 129.1, 118.1, 82.5, 73.5, 53.2, 28.7, 25.9, 18.2, -2.0, -2.4; IR (thin film, NaCl) 3324, 2957, 2929, 2886, 2857, 1590, 1472, 1462, 1370, 1254,

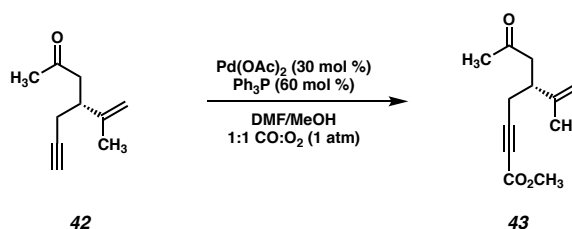


1204, 1170, 1134, 1042, 1017, 835, 774, 679  $\text{cm}^{-1}$ ; HRMS (FAB+)  $m/z$  calc'd  $\text{C}_{14}\text{H}_{30}\text{NO}_2\text{Si}$   $[\text{M}+\text{NH}_4]^+$ : 272.204, found 272.2027;  $[\alpha]_D^{23} + 25.4$  ( $c$  0.19,  $\text{CHCl}_3$ ). To a 500 mL round-bottom flask was added the crude reduction product in THF (150 mL). 1M TBAF in THF (15.0 mL equiv, 15.0 mmol, 1.4 equiv) was added dropwise by syringe. The flask was then equipped with a reflux condenser and heated to reflux for 8 h. After completion as judged by TLC, the reaction was cooled to 23 °C and quenched with brine. The mixture was then extracted with EtOAc (5x) before the combined organic layers were washed with brine, dried with  $\text{Na}_2\text{SO}_4$ , and concentrated under reduced pressure onto silica gel. The mixture was purified by flash column chromatography to afford diol **15** (1.17 g, 8.35 mmol, 78% yield over two steps) as an amorphous white solid. All spectral data for **15** was found to be in good accordance with literature values previously reported by our group.<sup>2e</sup>



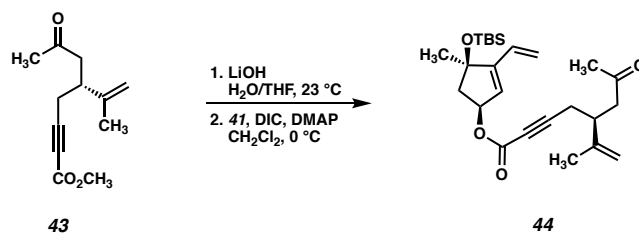
**Ketone 42:** Amide **25** (2.0 g, 10.2 mmol, 1 equiv) in THF (51 mL, 0.2 M) was cooled to –78 °C. A solution of  $\text{MeMgBr}$  in  $\text{Et}_2\text{O}$  (7.1 mL, 21.5 mmol, 3 M, 2.1 equiv) was added dropwise. The reaction was allowed to stir for 12 h while gradually warming to 23 °C. Upon complete consumption of starting material (as determined by TLC analysis), the reaction was quenched with a saturated solution of  $\text{NH}_4\text{Cl}$  (50 mL) and diluted with  $\text{Et}_2\text{O}$  (25 mL). The organics were separated, and the aqueous layer was extracted with  $\text{Et}_2\text{O}$  (3 x 40 mL) and the combined organic extracts were washed with brine, dried over  $\text{MgSO}_4$ ,

filtered, and concentrated in vacuo. The crude product was purified by column chromatography (SiO<sub>2</sub>, 20% Et<sub>2</sub>O/hexanes) to afford ketone **42** (1.2 g, 79%) as a pale yellow oil; <sup>1</sup>H NMR (400 MHz, CDCl<sub>3</sub>) δ = 4.83 (p, *J* = 1.5 Hz, 1H), 4.78 (dt, *J* = 1.6, 0.8 Hz, 1H), 2.81 (p, *J* = 6.7 Hz, 1H), 2.73 (dd, *J* = 16.5, 6.6 Hz, 1H), 2.59 (dd, *J* = 16.5, 7.5 Hz, 1H), 2.36 (ddd, *J* = 16.9, 6.3, 2.7 Hz, 1H), 2.29 (ddd, *J* = 16.9, 6.6, 2.7 Hz, 1H), 2.15 (s, 3H), 1.99 (t, *J* = 2.6 Hz, 1H), 1.73 (dd, *J* = 1.5, 0.8 Hz, 3H); <sup>13</sup>C NMR (100 MHz, CDCl<sub>3</sub>) δ = 207.6, 145.9, 111.9, 82.2, 70.2, 46.5, 40.5, 30.5, 23.1, 20.6; IR (thin film, NaCl) 3294, 3078, 2970, 2918, 2117, 1715, 1648, 1433, 1360, 1233, 1160, 1059, 997, 896, 641; HRMS (ESI) *m/z* calc'd C<sub>10</sub>H<sub>15</sub>O [M+H]<sup>+</sup>: 151.1197, found: 151.1115; [α]<sub>D</sub><sup>23</sup> + 22.2 (*c* 0.59, CHCl<sub>3</sub>).



**Methyl Ester 43:** Palladium acetate (112 mg, 0.5 mmol, 0.3 equiv) and triphenylphosphine (260 mg, 1.0 mmol, 0.6 equiv) were dissolved in dimethylformamide (17 mL, 0.1 M) in a round-bottomed flask under N<sub>2</sub> and allowed to stir for 5 min. Methanol (1.7 mL, 41.5 mmol, 25 equiv) and ketone **42** (250 mg, 1.66 mmol, 1 equiv) were added, followed by attachment of 2 rubber balloons, one filled with O<sub>2</sub> and the other CO, to the flask. The reaction was sparged with both CO and O<sub>2</sub> balloons for 5 min and allowed to stir at ambient temperature (23 °C) for 16 h. Upon complete consumption of starting material (as determined by TLC), the mixture was diluted with Et<sub>2</sub>O and a saturated solution of LiCl and the aqueous layer was extracted with Et<sub>2</sub>O. The combined organic extracts were dried over MgSO<sub>4</sub>, filtered,

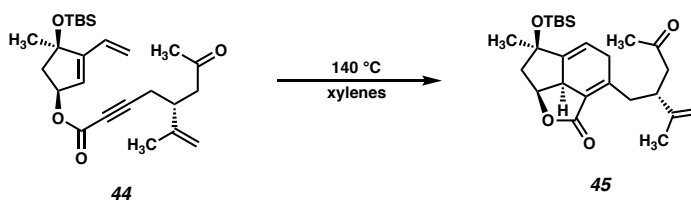
and concentrated in vacuo. The crude product was purified by column chromatography (SiO<sub>2</sub>, 20% EtOAc/hexanes) to afford ester **43** (249 mg, 86%) as a colorless oil; <sup>1</sup>H NMR (400 MHz, CDCl<sub>3</sub>) δ = 4.86 (t, *J* = 1.4 Hz, 1H), 4.81 (q, *J* = 0.9 Hz, 1H), 3.75 (s, 3H), 2.85 (p, *J* = 6.7 Hz, 1H), 2.66 (dd, *J* = 9.4, 7.1 Hz, 2H), 2.48 (dd, *J* = 6.5, 4.9 Hz, 2H), 2.16 (s, 3H), 1.73 (dd, *J* = 1.4, 0.8 Hz, 3H); <sup>13</sup>C NMR (100 MHz, CDCl<sub>3</sub>) δ = 207.0, 154.2, 145.2, 112.5, 87.3, 74.6, 52.8, 46.3, 39.7, 30.6, 23.1, 20.7; IR (thin film, NaCl) 2923, 2236, 1714, 1647, 1434, 1361, 1259, 1158, 1074, 942, 901, 752, 679 cm<sup>-1</sup>, HRMS (FAB<sup>+</sup>) *m/z* calc'd C<sub>12</sub>H<sub>17</sub>O<sub>3</sub> [M+H]<sup>+</sup>: 209.1172; found 209.1164; [α]<sub>D</sub><sup>23</sup> + 46.5 (*c* 0.18, CHCl<sub>3</sub>).



**Ester 44:** A solution of methyl ester **43** (1.5 g, 5.7 mmol, 1 equiv) in THF (28 mL, 0.2M), was added to a solution of LiOH (205 mg, 8.6 mmol, 1.5 equiv) in H<sub>2</sub>O (28 mL, 0.2M). The reaction was stirred vigorously for 4 h at 23 °C when complete consumption of starting material was observed (as determined by TLC). The reaction was washed with EtOAc (1 X) and the aqueous layer was subsequently acidified to a pH of 1 with 1 N HCl. The acidic aqueous layer was then extracted with EtOAc (5 x 30 mL) and the combined organic layers were washed with brine, dried over MgSO<sub>4</sub>, filtered, and concentrated in vacuo leaving a crude acid (1.3 g, 81%) which was used without further purification or characterization.

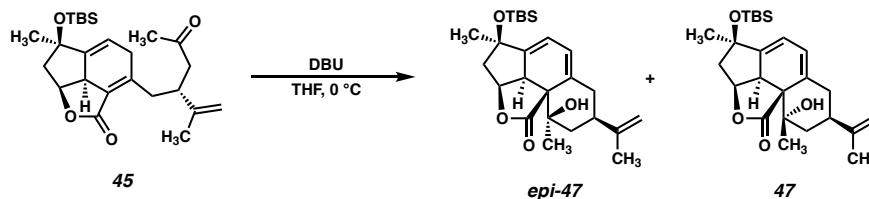
Alcohol **41** (10 mg, 0.039 mmol, 1 equiv), the crude acid (15 mg, 0.079 mmol 2 equiv), and DMAP (16 mg, 0.039 mmol, 1 equiv) were added to CH<sub>2</sub>Cl<sub>2</sub> (0.4 mL, 0.1 M) and cooled to 0 °C. DIC (12 μL, 0.079 mmol, 2 equiv) was added dropwise and the reaction

was allowed to stir for 2 h at 0 °C. Upon complete consumption of starting material (as determined by TLC analysis), the reaction was diluted with H<sub>2</sub>O and extracted with Et<sub>2</sub>O (3x). The combined organic layers were dried over MgSO<sub>4</sub>, filtered, and concentrated in vacuo. The crude product was purified by column chromatography (SiO<sub>2</sub>, 20% EtOAc/hexanes) to afford ester **44** (12 mg, 70%) as a pale yellow oil; <sup>1</sup>H NMR (400 MHz, CDCl<sub>3</sub>) δ = 6.27 (ddd, *J* = 17.8, 11.2, 0.8 Hz, 1H), 5.75–5.69 (m, 2H), 5.53 (dddd, *J* = 7.3, 5.9, 2.3, 0.8 Hz, 1H), 5.27 (dd, *J* = 11.3, 1.9 Hz, 1H), 4.86–4.83 (m, 1H), 4.83–4.77 (m, 1H), 2.93–2.81 (m, 1H), 2.67 (dd, *J* = 13.2, 7.1 Hz, 2H), 2.63–2.56 (m, 1H), 2.48 (dd, *J* = 7.5, 6.4 Hz, 2H), 2.16 (s, 3H), 2.10 (ddd, *J* = 13.1, 5.9, 0.8 Hz, 1H), 1.73 (dd, *J* = 1.5, 0.8 Hz, 3H), 1.38 (d, *J* = 0.8 Hz, 3H), 0.86 (s, 9H), 0.12 (s, 3H), 0.08 (s, 3H); <sup>13</sup>C NMR (100 MHz, CDCl<sub>3</sub>) δ = 207.1, 153.7, 152.7, 145.2, 129.3, 123.9, 119.0, 112.4, 87.2, 82.3, 74.9, 48.9, 46.3, 39.7, 30.5, 29.2, 25.9, 23.2, 20.7, 18.2, -2.2, -2.6; IR (thin film, NaCl) 2956, 2929, 2856, 2234, 1711, 1649, 1472, 1439, 1359, 1250, 1169, 1069, 1022, 837, 774, 752 cm<sup>-1</sup>; HRMS (FAB+) *m/z* calc'd C<sub>25</sub>H<sub>39</sub>O<sub>4</sub>Si [M+H]<sup>+</sup>: 431.2612; found 431.2629; [α]<sub>D</sub><sup>23</sup> – 71.1 (*c* 0.59, CHCl<sub>3</sub>).



**Cyclohexadiene 45:** Ester **44** (65 mg, 0.15 mmol) was transferred to a Schlenk bomb with xylenes (15 mL, 0.01 M). The Schlenk was then degassed by standard freeze-pump-thaw technique, and upon reaching ambient temperature (23 °C) the flask was sealed and heat to 140 °C. The reaction was allowed to stir at this temperature of 2 h at which time complete consumption of starting material was observed (as determined by TLC analysis,). The

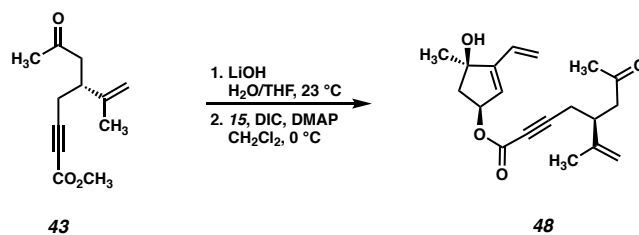
reaction was allowed to cool to room temperature and was directly purified by column chromatography (SiO<sub>2</sub>, 0%–20% EtOAc/hexanes) to furnish cyclohexadiene **45** (53 mg, 82%) as a white amorphous solid; <sup>1</sup>H NMR (400 MHz, CDCl<sub>3</sub>) δ = δ 5.78 (ddd, *J* = 6.4, 2.9, 1.9 Hz, 1H), 4.93 (ddd, *J* = 9.0, 8.1, 7.0 Hz, 1H), 4.68 (p, *J* = 1.5 Hz, 1H), 4.63 (dt, *J* = 1.8, 0.8 Hz, 1H), 3.19 (t, *J* = 9.6 Hz, 1H), 3.13–3.04 (m, 1H), 2.93 (p, *J* = 7.1 Hz, 1H), 2.84 (dddd, *J* = 10.7, 7.1, 2.4, 1.3 Hz, 1H), 2.75 (ddd, *J* = 12.7, 7.7, 1.2 Hz, 1H), 2.66 (ddt, *J* = 18.1, 10.1, 1.6 Hz, 1H), 2.59 (d, *J* = 1.4 Hz, 1H), 2.57 (d, *J* = 1.5 Hz, 1H), 2.42–2.34 (m, 1H), 2.12 (s, 3H), 1.70–1.63 (m, 4H), 1.36 (d, *J* = 1.0 Hz, 3H), 0.86 (s, 9H), 0.10 (s, 3H), 0.03 (s, 3H); <sup>13</sup>C NMR (100 MHz, CDCl<sub>3</sub>) δ = 208.0, 168.7, 156.7, 151.8, 146.4, 125.4, 116.5, 112.3, 81.2, 76.2, 48.8, 47.3, 44.8, 40.9, 35.7, 34.8, 30.8, 28.1, 25.8, 19.5, 18.1, -2.1, -2.3; IR (thin film, NaCl) 2957, 2929, 2857, 1753, 1714, 1645, 1442, 1359, 1327, 1291, 1257, 1209, 1177, 1028, 856, 836, 774, 680 cm<sup>-1</sup>; HRMS (FAB<sup>+</sup>) *m/z* calc'd C<sub>25</sub>H<sub>39</sub>O<sub>4</sub>Si [M+H]<sup>+</sup>: 431.2612, found; 431.2643; [α]<sub>D</sub><sup>23</sup> -64.5 (*c* 0.39, CHCl<sub>3</sub>).



**Aldol Products **47** and *epi-47*:** Tetracycles **47** and *epi-47* were originally isolated after an attempted TBAF-mediated deprotection. Analytical samples were prepared according to the following procedure: Tricyclic **45** (3 mg, 7.2 μmol, 1 equiv) was dissolved in THF (0.2 mL) and cooled to 0 °C. DBU (1.7 μL, 7.2 μmol, 1 equiv) was added. After 5 min, the reaction was concentrated and directly purified by column chromatography (SiO<sub>2</sub>, 20% EtOAc/hexanes) to afford tetracycles **47** and *epi-47* (1.8:1 dr, 3 mg, >99%) as an amorphous film.

**47:**  $^1\text{H}$  NMR (400 MHz,  $\text{CDCl}_3$ )  $\delta$  = 5.99 (dd,  $J$  = 5.7, 2.5 Hz, 1H), 5.83 (ddd,  $J$  = 5.8, 2.8, 1.1 Hz, 1H), 4.89–4.68 (m, 3H), 3.76–3.69 (m, 1H), 2.88–2.76 (m, 1H), 2.47 (dd,  $J$  = 13.7, 7.4 Hz, 1H), 2.39–2.27 (m, 2H), 2.27–2.04 (m, 1H), 1.86 (dd,  $J$  = 13.7, 3.9 Hz, 1H), 1.78 (dd,  $J$  = 1.5, 0.8 Hz, 3H), 1.71 (dt,  $J$  = 13.0, 2.6 Hz, 1H), 1.40 (d,  $J$  = 1.0 Hz, 3H), 1.25 (s, 3H), 0.89 (s, 9H), 0.12 (s, 3H), 0.08 (s, 3H);  $^{13}\text{C}$  NMR (100 MHz,  $\text{CDCl}_3$ )  $\delta$  = 176.6, 148.1, 142.2, 131.1, 123.2, 112.7, 110.2, 80.0, 79.7, 74.4, 56.7, 49.0, 42.0, 40.7, 40.0, 35.7, 29.9, 28.5, 25.9, 24.9, 20.6, 18.2, 14.3, -2.0, -2.2; IR (thin film, NaCl) 3523, 2925, 2856, 2759, 1461, 1372, 1292, 1257, 1153, 1065, 964, 833, 771, 732, 705, 655  $\text{cm}^{-1}$ ; HRMS (FAB+)  $m/z$  calc'd  $\text{C}_{25}\text{H}_{42}\text{O}_4\text{SiN}$   $[\text{M}+\text{NH}_4]^+$  448.2878, found: 448.2889;  $[\alpha]_{\text{D}}^{23}$  +4.12 ( $c$  0.235,  $\text{CHCl}_3$ ).

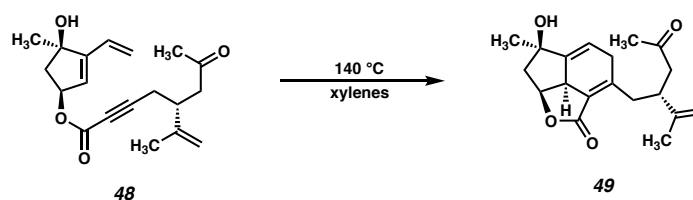
**epi-47:**  $^1\text{H}$  NMR (400 MHz,  $\text{CDCl}_3$ )  $\delta$  = 5.86 (dd,  $J$  = 5.7, 2.6 Hz, 1H), 5.82 (ddd,  $J$  = 5.8, 2.7, 1.0 Hz, 1H), 4.89 (td,  $J$  = 7.2, 3.2 Hz, 1H), 4.80 (dq,  $J$  = 1.8, 0.9 Hz, 1H), 4.78 (q,  $J$  = 1.5 Hz, 1H), 3.47 (d,  $J$  = 7.4 Hz, 1H), 2.86–2.73 (m, 1H), 2.48–2.36 (m, 2H), 2.31 (ddd,  $J$  = 15.0, 4.4, 1.9 Hz, 1H), 2.20 (tt,  $J$  = 12.8, 3.8 Hz, 1H), 1.94 (dd,  $J$  = 14.0, 3.1 Hz, 1H), 1.78 (s, 3H), 1.66 (ddd,  $J$  = 12.0, 3.4, 1.9 Hz, 1H), 1.39 (d,  $J$  = 1.1 Hz, 3H), 1.29 (d,  $J$  = 0.8 Hz, 3H), 0.88 (d,  $J$  = 1.1 Hz, 9H), 0.12 (s, 3H), 0.08 (s, 3H);  $^{13}\text{C}$  NMR (100 MHz,  $\text{CDCl}_3$ )  $\delta$  = 177.3, 148.1, 142.1, 132.2, 121.3, 113.4, 110.1, 80.1, 80.0, 76.2, 57.8, 48.7, 42.7, 42.3, 41.3, 35.5, 29.2, 26.7, 25.9, 20.5, 18.2, -2.0, -2.3; IR (thin film, NaCl) 3462, 2956, 2928, 2856, 1739, 1643, 1450, 1375, 1293, 1257, 1163, 1132, 1018, 837, 809, 773  $\text{cm}^{-1}$ ; HRMS (FAB+)  $m/z$  calc'd  $\text{C}_{25}\text{H}_{42}\text{O}_4\text{SiN}$   $[\text{M}+\text{NH}_4]^+$  448.2878, found: 448.2890;  $[\alpha]_{\text{D}}^{23}$  -33.7 ( $c$  0.1,  $\text{CHCl}_3$ ).



**Ester 48:** A solution of methyl ester **43** (1.5 g, 5.7 mmol, 1 equiv) in THF (28 mL, 0.2M), was added to a solution of LiOH (205 mg, 8.6 mmol, 1.5 equiv) in H<sub>2</sub>O (28 mL, 0.2M). The reaction was stirred vigorously for 4 h at 23 °C when complete consumption of starting material was observed (as determined by TLC). The reaction was washed with EtOAc (1 X) and the aqueous layer was subsequently acidified to a pH of 1 with 1 N HCl. The acidic aqueous layer was then extracted with EtOAc (5 x 30 mL) and the combined organic layers were washed with brine, dried over MgSO<sub>4</sub>, filtered, and concentrated in vacuo leaving a crude acid (1.3 g, 81%) which was used without further purification or characterization.

Diol **15** (18 mg, 0.13 mmol, 1 equiv), the crude acid (56 mg, 0.28 mmol 2.2 equiv), and DMAP (17 mg, 0.17 mmol, 1.1 equiv) were added to a solution of CH<sub>2</sub>Cl<sub>2</sub> (1.4 mL, 0.09 M) and cooled to 0 °C. DIC (44 μL, 0.28 mmol, 2.2 equiv) was added dropwise and the reaction was allowed to stir for 1 h. Upon complete consumption of starting material (as determined by TLC analysis) the reaction was diluted with H<sub>2</sub>O (5 mL) and extracted with Et<sub>2</sub>O (3 x 5 mL). The combined organic layers were dried over MgSO<sub>4</sub>, filtered, and concentrated in vacuo. The crude product was purified by column chromatography (SiO<sub>2</sub>, 50% EtOAc/hexanes) to afford ester **48** (30 mg, 73%) as a colorless oil; <sup>1</sup>H NMR (400 MHz, CDCl<sub>3</sub>) δ = 6.32 (ddt, *J* = 17.8, 11.3, 0.8 Hz, 1H), 5.85–5.75 (m, 2H), 5.54 (ddd, *J* = 7.1, 4.7, 2.5 Hz, 1H), 5.33 (dd, *J* = 11.3, 1.6 Hz, 1H), 4.90–4.82 (m, 1H), 4.80 (q, *J* = 0.9 Hz, 1H), 2.86 (p, *J* = 6.6 Hz, 1H), 2.74–2.59 (m, 3H), 2.55–2.41 (m, 2H), 2.16 (s, 3H), 2.06

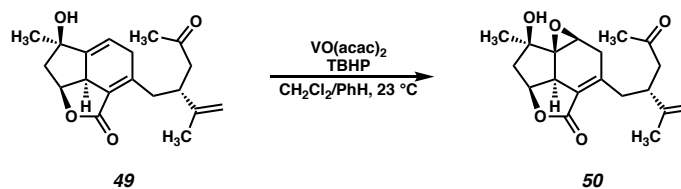
(dd,  $J = 14.3, 4.4$  Hz, 1H), 1.73 (dd,  $J = 1.4, 0.8$  Hz, 3H), 1.44 (s, 3H);  $^{13}\text{C}$  NMR (100 MHz,  $\text{CDCl}_3$ )  $\delta = 207.1, 153.5, 151.9, 145.2, 129.0, 126.1, 119.6, 112.5, 87.5, 81.1, 77.4, 74.8, 48.9, 46.4, 39.7, 30.6, 26.8, 23.2, 20.7$ ; IR (thin film, NaCl) 3462, 2969, 2926, 2233, 1704, 1422, 1249, 1163, 1071, 944, 751  $\text{cm}^{-1}$ ; HRMS (ESI)  $m/z$  calc'd  $\text{C}_{19}\text{H}_{26}\text{O}_5$   $[\text{M}+\text{H}_2\text{O}]^+$ : 334.1775, found: 334.1785;  $[\alpha]_{\text{D}}^{23} -65.9$  ( $c$  0.18,  $\text{CHCl}_3$ ).



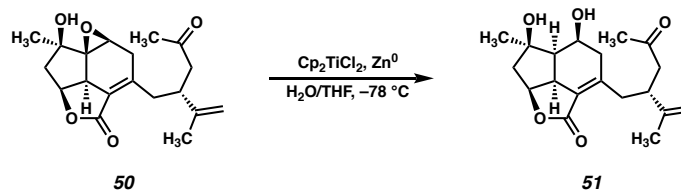
**Cyclohexadiene 49:** Ester **48** (100 mg, 0.32 mmol) was transferred to a Schlenk bomb with xylenes (32 mL, 0.01 M). The Schlenk was rigorously degassed by standard freeze-pump-thaw technique and upon reaching ambient temperature (23 °C) the flask was sealed and heat to 140 °C. The reaction was allowed to stir at this temperature of 2 h at which time complete consumption of starting material was observed (as determined by TLC analysis). The reaction was allowed to cool to room temperature and was directly purified by column chromatography ( $\text{SiO}_2, 0\%–50\%$  EtOAc/hexanes) to furnish tricycle **49** (79 mg, 79%) as a white amorphous solid;  $^1\text{H}$  NMR (400 MHz,  $\text{CDCl}_3$ )  $\delta = 5.84$  (dt,  $J = 6.4, 2.3$  Hz, 1H), 5.02–4.91 (m, 1H), 4.75–4.69 (m, 1H), 4.67 (d,  $J = 1.9$  Hz, 1H), 3.26 (t,  $J = 9.6$  Hz, 1H), 3.12–2.98 (m, 2H), 2.97–2.87 (m, 1H), 2.74 (ddt,  $J = 18.2, 10.1, 1.6$  Hz, 1H), 2.59 (dd,  $J = 6.7, 4.1$  Hz, 2H), 2.57–2.44 (m, 2H), 2.11 (s, 3H), 1.69 (d,  $J = 1.3$  Hz, 3H), 1.64 (dd,  $J = 12.8, 8.0$  Hz, 1H), 1.40 (s, 3H);  $^{13}\text{C}$  NMR (101 MHz,  $\text{CDCl}_3$ )  $\delta = 207.9, 168.4, 156.5, 151.6, 146.9, 125.2, 116.6, 112.0, 80.0, 75.4, 49.7, 47.2, 45.6, 41.1, 36.2, 35.4, 30.7, 26.7, 19.6$ ; IR (thin film, NaCl) 3440, 2968, 1746, 1713, 1644, 1442, 1418,



1359, 1289, 1213, 1117, 1042, 1021, 995, 973, 913, 810, 732; HRMS (ESI)  $m/z$  calc'd  $C_{19}H_{25}O_4$   $[M+H]^+$ : 317.1747, found: 317.1733;  $[\alpha]_D^{23}$   $-99.1$  ( $c$  0.375,  $CHCl_3$ ).



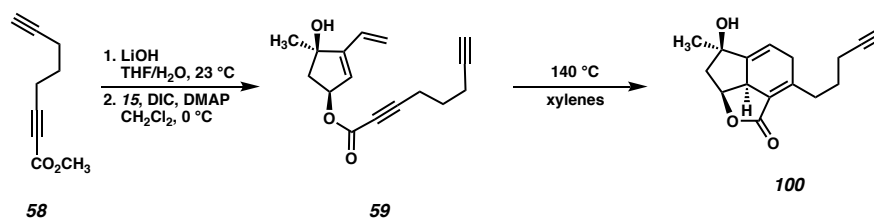
**Epoxide 50:** To a stirred solution of cyclohexadiene **49** (80 mg, 0.25 mmol, 1.0 equiv) in benzene (8.4 mL, 0.044M) and  $CH_2Cl_2$  (0.2 mL, 1 M) was added  $VO(acac)_2$  (6.7 mg, 0.025 mmol, 0.1 equiv). After 15 minutes, *t*-butyl hydroperoxide (TBHP, 76  $\mu$ L, 0.38 mmol, 1.5 equiv, 5 M solution in decane) was added, causing the reaction to immediately become deep red. After 1 hours, the reaction had lost all red color and become pale yellow and complete consumption of starting material was observed (as determined by TLC analysis). The crude reaction was directly purified by column chromatography ( $SiO_2$ , 0%–50% EtOAc/hexanes) to furnish epoxide **50** (76.3 mg, 91%) as a white amorphous solid;  $^1H$  NMR (400 MHz,  $C_6D_6$ )  $\delta$  4.83 (q,  $J = 0.9$  Hz, 1H), 4.75 (t,  $J = 1.6$  Hz, 1H), 4.08 (ddd,  $J = 8.5, 7.4, 6.3$  Hz, 1H), 3.38–3.31 (m, 1H), 3.05 (d,  $J = 3.4$  Hz, 1H), 2.90 (dq,  $J = 9.3, 6.3$  Hz, 1H), 2.41 (dd,  $J = 17.0, 6.8$  Hz, 3H), 2.29–2.20 (m, 3H), 2.11 (ddd,  $J = 12.7, 5.4, 1.9$  Hz, 1H), 2.05 (dd,  $J = 13.5, 7.5$  Hz, 1H), 1.86 (dd,  $J = 16.7, 2.4$  Hz, 1H), 1.82–1.74 (m, 1H), 1.70 (s, 3H), 1.63 (t,  $J = 1.2$  Hz, 3H), 0.99 (s, 3H);  $^{13}C$  NMR (101 MHz,  $C_6D_6$ )  $\delta = 206.0, 168.9, 149.6, 147.7, 120.8, 111.5, 76.3, 73.3, 69.5, 51.6, 50.2, 47.0, 44.5, 41.0, 37.6, 36.0, 30.2, 22.4, 20.0$ ; IR (thin film, NaCl) 3469, 2933, 1746, 1711, 1645, 1360, 1294, 1200, 1114, 1029, 967, 792  $cm^{-1}$ ; HRMS (ESI)  $m/z$  calc'd  $C_{19}H_{25}O_5$   $[M+H]^+$ : 333.1697, found: 333.1703;  $[\alpha]_D^{23}$   $-88.9$  ( $c$  0.375,  $CHCl_3$ ).

**Alcohol 51:**

*Preparation of a 0.50 M Stock Solution: of Titanocene Monochloride (Cp<sub>2</sub>TiCl):* A flame-dried Schlenk tube under an overpressure of argon was charged with zinc dust (647 mg, 9.90 mmol, 3.00 equiv) and titanocene dichloride (Cp<sub>2</sub>TiCl<sub>2</sub>, 822 mg, 3.30 mmol, 1.00 equiv). The flask was then evacuated and back filled with argon (3 x 5 minute cycles). To the reaction vessel was then added THF (6.6 mL) and the resulting red suspension was stirred vigorously. After 1.5 h, the bright red reaction mixture had become dark green and stirring was halted, allowing the zinc dust to settle to the bottom of the tube. After 30 minutes, the green supernatant was used as a 0.50 M stock solution of Cp<sub>2</sub>TiCl.

*Reductive Epoxide Opening:* A stirred solution of epoxide **50** (15 mg, 0.045 mmol, 1.0 equiv) in THF (1.5 mL, 0.03 M) was cooled to  $-78\text{ }^\circ\text{C}$ , followed by the addition of H<sub>2</sub>O (62  $\mu\text{L}$ , 3.46 mmol, 76.9 equiv). After stirring for 5 minutes, Cp<sub>2</sub>TiCl (0.87 mmol, 0.50 M in THF, 19.2 equiv) was added dropwise. After 2 h, the green reaction mixture was allowed to warm to ambient temperature ( $23\text{ }^\circ\text{C}$ ). After an additional 12 h, the complete consumption of starting material was observed (as determined by TLC). The reaction was quenched by the addition of saturated NaH<sub>2</sub>PO<sub>4</sub> (1.0 mL) and brine (1.0 mL), sparged with compressed air for 5 minutes, and allowed to stir for an additional 15 minutes. The resulting orange slurry was then filtered through a Celite<sup>®</sup> plug, washing with H<sub>2</sub>O and EtOAc. The biphasic mixture was separated and the aqueous layer was extracted with EtOAc (3x). The combined organic layers were dried over MgSO<sub>4</sub>, filtered, and concentrated in vacuo. The

crude product was purified by column chromatography (SiO<sub>2</sub>, 75% EtOAc/hexanes), furnishing diol **51** (14 mg, 92% yield) as a white amorphous solid (*R<sub>f</sub>* = 0.22); <sup>1</sup>H NMR (400 MHz, CDCl<sub>3</sub>) δ = 4.90 (ddd, *J* = 8.2, 6.6, 4.1 Hz, 1H), 4.80 (dt, *J* = 1.7, 0.8 Hz, 1H), 4.76 (p, *J* = 1.5 Hz, 1H), 4.69 (dt, *J* = 7.8, 3.2 Hz, 1H), 3.35–3.25 (m, 1H), 3.05 (ddd, *J* = 9.9, 8.0, 2.0 Hz, 1H), 2.94 (dq, *J* = 9.2, 6.5 Hz, 1H), 2.67–2.49 (m, 3H), 2.41–2.29 (m, 2H), 2.14–1.98 (m, 6H), 1.75 (dd, *J* = 1.5, 0.8 Hz, 3H), 1.43 (s, 3H); <sup>13</sup>C NMR (100 MHz, CDCl<sub>3</sub>) δ = 208.3, 169.7, 151.7, 147.8, 124.9, 111.5, 81.7, 79.2, 68.5, 49.6, 48.5, 47.2, 44.4, 41.3, 40.6, 37.7, 30.8, 28.8, 20.1; IR (thin film, NaCl) 3384, 2966, 1738, 1666, 1420, 1359, 1304, 1222, 1200, 1145, 1105, 1040, 1020, 910, 733 cm<sup>-1</sup>; HRMS (ESI) *m/z* calc'd C<sub>19</sub>H<sub>27</sub>O<sub>5</sub> [M+H]<sup>+</sup>: 335.1853, found: 335.1844; [α]<sub>D</sub><sup>23</sup> -15.4 (*c* 0.21, CHCl<sub>3</sub>).

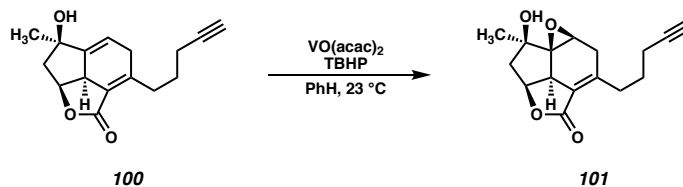


**Ester 59 and Cyclohexadiene 100:** Ester **58** was saponified under the same conditions reported above for ester **43**. A stirred solution of diol **15** (250 mg, 1.8 mmol, 1 equiv), octa-2,7-diynoic acid (435 mg, 3.2 mmol, 1.8 equiv), and DMAP (21.8 mg, 0.18 mmol, 0.1 equiv) in CH<sub>2</sub>Cl<sub>2</sub> (18 mL, 0.1 M) and THF (10 mL, 0.18 M) was cooled to 0 °C. DIC (0.50 mL, 3.2 mmol, 1.8 equiv) was added dropwise via syringe and the resultant solution was allowed to stir for 2 h. Upon complete consumption of starting material (as determined by TLC analysis), the reaction was diluted with H<sub>2</sub>O and extracted with Et<sub>2</sub>O (3x). The combined organic layers were dried over MgSO<sub>4</sub>, filtered, and concentrated in vacuo. The crude product was purified by column chromatography (SiO<sub>2</sub>, 20% EtOAc/Hexanes) to afford a mixture of diisopropyl urea and ester **59** which is used directly in the next reaction.

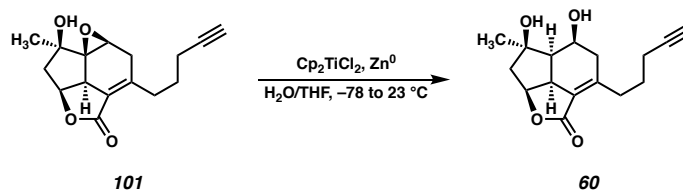
Ester **59** can be further purified by another column of the same eluent to obtain pure ester **59**;  $^1\text{H}$  NMR (400 MHz,  $\text{CDCl}_3$ )  $\delta$  = 6.32 (ddt,  $J$  = 17.8, 11.3, 0.8 Hz, 1H), 5.82 (dd,  $J$  = 2.3, 0.8 Hz, 1H), 5.81–5.75 (m, 1H), 5.55 (dddd,  $J$  = 7.4, 4.4, 2.3, 0.7 Hz, 1H), 5.33 (dd,  $J$  = 11.3, 1.5 Hz, 1H), 2.64 (dd,  $J$  = 14.3, 7.3 Hz, 1H), 2.48 (t,  $J$  = 7.1 Hz, 2H), 2.32 (td,  $J$  = 6.9, 2.7 Hz, 2H), 2.06 (dd,  $J$  = 14.3, 4.4 Hz, 1H), 1.98 (t,  $J$  = 2.6 Hz, 1H), 1.80 (p,  $J$  = 7.0 Hz, 2H), 1.44 (s, 3H);  $^{13}\text{C}$  NMR (100 MHz,  $\text{CDCl}_3$ )  $\delta$  = 153.5, 151.9, 128.9, 126.0, 119.6, 88.7, 82.8, 81.1, 77.1, 73.7, 69.6, 48.9, 26.8, 26.5, 17.8, 17.7; IR (thin film, NaCl) 3295, 2972, 2236, 1703, 1432, 1252, 1073, 990, 950, 872, 752, 641  $\text{cm}^{-1}$ ; HRMS (ESI)  $m/z$  calc'd  $\text{C}_{16}\text{H}_{22}\text{NO}_3$   $[\text{M}+\text{NH}_4]^+$ : 276.1595, found: 276.15811;  $[\alpha]_{\text{D}}^{23}$   $-155.1$  ( $c$  0.57,  $\text{CHCl}_3$ ).

Crude ester **59** (460 mg, 1.78 mmol) was transferred to a Schlenk bomb with xylenes (178 mL, 0.01 M). The Schlenk was degassed by standard freeze-pump-thaw technique and upon reaching ambient temperature (23 °C) the flask was sealed and heat to 140 °C. The reaction was allowed to stir at this temperature of 2 h at which time complete consumption of starting material was observed (as determined by TLC analysis). The reaction was allowed to cool to room temperature and was directly purified by column chromatography ( $\text{SiO}_2$ , 0%–50% EtOAc/Hexanes) to furnish tricycle **100** (560 mg, 84% over 3 steps) as a pale yellow solid;  $^1\text{H}$  NMR (400 MHz,  $\text{CDCl}_3$ )  $\delta$  = 5.85 (ddd,  $J$  = 6.3, 2.9, 1.9 Hz, 1H), 4.97 (ddd,  $J$  = 9.0, 7.9, 7.1 Hz, 1H), 3.30 (ttd,  $J$  = 9.2, 1.9, 1.0 Hz, 1H), 3.11–2.96 (m, 2H), 2.75 (ddt,  $J$  = 18.4, 10.1, 1.5 Hz, 1H), 2.62–2.54 (m, 1H), 2.51 (ddd,  $J$  = 12.8, 7.1, 0.8 Hz, 1H), 2.22 (tt,  $J$  = 7.1, 2.5 Hz, 2H), 1.98 (t,  $J$  = 2.6 Hz, 1H), 1.78 (td,  $J$  = 6.6, 5.5, 3.3 Hz, 1H), 1.76–1.63 (m, 3H), 1.41 (d,  $J$  = 1.1 Hz, 3H);  $^{13}\text{C}$  NMR (100 MHz,  $\text{CDCl}_3$ )  $\delta$  = 168.2, 157.1, 152.1, 124.4, 116.4, 84.0, 80.0, 75.4, 69.1, 49.7, 45.5, 35.2, 31.0, 27.2, 26.8, 18.4; IR (thin film, NaCl) 3425, 3288, 2971, 1738, 1643, 1439, 1326, 1288,

1256, 1218, 1194, 1117, 1041, 996, 967, 817, 742, 638  $\text{cm}^{-1}$ ; HRMS (ESI)  $m/z$  calc'd  $\text{C}_{16}\text{H}_{19}\text{O}_3$   $[\text{M}+\text{H}]^+$ : 259.1329, found: 259.1323;  $[\alpha]_{\text{D}}^{23}$   $-120.3$  ( $c$  0.64,  $\text{CHCl}_3$ ).

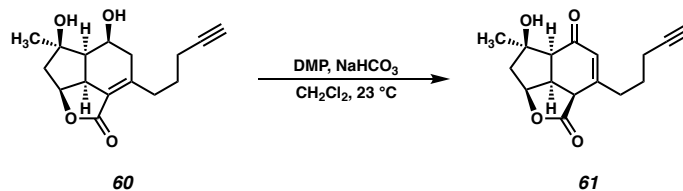


**Epoxide 101:** To a stirred solution of diene **100** (376 mg, 1.5 mmol, 1.0 equiv) in benzene (49 mL, 0.03M) was added  $\text{VO(acac)}_2$  (29 mg, 0.11 mmol, 0.075 equiv). After 15 minutes, *t*-butyl hydroperoxide (TBHP, 0.58 mL, 2.9 mmol, 2.0 equiv, 5 M solution in decane) was added dropwise, causing the reaction to immediately become deep red. After 2 hours, the reaction had lost all red color and become pale yellow and complete consumption of starting material was observed (as determined by TLC analysis). The crude reaction was directly purified by column chromatography ( $\text{SiO}_2$ , 0%–30% EtOAc/Hexanes) to furnish epoxide **101** (307 mg, 77%) as a white amorphous solid;  $^1\text{H}$  NMR (400 MHz,  $\text{CDCl}_3$ )  $\delta$  = 4.83 (ddd,  $J$  = 8.5, 7.4, 6.3 Hz, 1H), 3.81 (dd,  $J$  = 3.3, 0.8 Hz, 1H), 3.28 (d,  $J$  = 8.1 Hz, 1H), 2.88 (dd,  $J$  = 16.7, 3.4 Hz, 1H), 2.84–2.68 (m, 2H), 2.59 (ddd,  $J$  = 13.6, 7.4, 0.6 Hz, 1H), 2.55–2.45 (m, 2H), 2.35–2.12 (m, 2H), 2.08–1.99 (m, 1H), 1.98 (t,  $J$  = 2.6 Hz, 1H), 1.81–1.62 (m, 2H), 1.44 (d,  $J$  = 1.0 Hz, 3H);  $^{13}\text{C}$  NMR (100 MHz,  $\text{CDCl}_3$ )  $\delta$  = 169.1, 150.9, 119.9, 84.1, 76.6, 73.6, 70.0, 69.0, 51.8, 50.1, 44.8, 35.7, 31.6, 26.9, 22.7, 18.3; IR (thin film, NaCl) 3529, 3270, 2976, 2938, 2116, 1742, 1649, 1454, 1422, 1391, 1348, 1324, 1296, 1268, 1195, 1113, 1093, 1030, 964, 923, 899, 795, 756, 733, 678  $\text{cm}^{-1}$ ; HRMS (ESI)  $m/z$  calc'd  $\text{C}_{16}\text{H}_{19}\text{O}_4$   $[\text{M}+\text{H}]^+$ : 275.1278, found: 275.1268;  $[\alpha]_{\text{D}}^{23}$   $-179.9$  ( $c$  0.39,  $\text{CHCl}_3$ ).

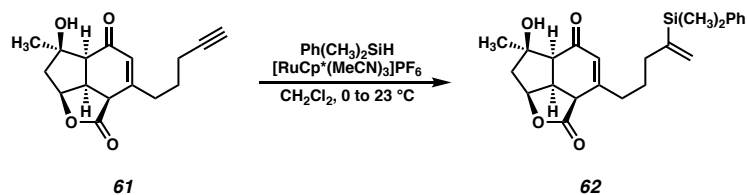


**Alcohol 60:** A stirred solution of epoxide **101** (278 mg, 1.01 mmol, 1.0 equiv) in THF (34 mL, 0.03 M) was cooled to  $-78\text{ }^{\circ}\text{C}$ , followed by the addition of  $\text{H}_2\text{O}$  (0.9 mL, 50.0 mmol, 50 equiv). After stirring for 5 minutes,  $\text{Cp}_2\text{TiCl}$  (11.1 mmol, 0.50 M in THF, 11 equiv) was added dropwise. After 2 h, the reaction was allowed to slowly warm to  $23\text{ }^{\circ}\text{C}$ . After stirring an additional 12 h, the complete consumption of starting material was observed (as determined by TLC). The reaction was quenched by the addition of saturated  $\text{NaH}_2\text{PO}_4$  and brine, sparged with compressed air for 5 minutes, and allowed to stir for an additional 15 minutes. The orange suspension was then filtered through a Celite<sup>®</sup> plug, washing with  $\text{H}_2\text{O}$  and EtOAc. The biphasic mixture was separated and the aqueous layer was extracted with EtOAc (3x). The combined organic layers were dried over  $\text{MgSO}_4$ , filtered, and concentrated in vacuo. The crude product was purified by column chromatography ( $\text{SiO}_2$ , 75% EtOAc/hexanes), furnishing diol **60** (270 mg, 96% yield) as a viscous colorless oil;  $^1\text{H}$  NMR (400 MHz,  $\text{CDCl}_3$ )  $\delta$  = 4.91 (ddd,  $J$  = 8.1, 6.7, 3.1 Hz, 1H), 4.69 (ddd,  $J$  = 8.1, 3.5, 2.8 Hz, 1H), 3.43 (s, 2H), 3.08 (ddd,  $J$  = 9.7, 7.9, 2.0 Hz, 1H), 2.98–2.88 (m, 1H), 2.70 (dtd,  $J$  = 12.6, 7.4, 1.8 Hz, 1H), 2.58 (dd,  $J$  = 14.9, 2.8 Hz, 1H), 2.39 (dd,  $J$  = 9.4, 8.0 Hz, 1H), 2.23 (qd,  $J$  = 7.2, 2.6 Hz, 2H), 2.13 (dd,  $J$  = 14.4, 3.1 Hz, 1H), 2.10–2.03 (m, 1H), 1.99 (dd,  $J$  = 14.3, 6.6 Hz, 1H), 1.95 (t,  $J$  = 2.6 Hz, 1H), 1.72 (p,  $J$  = 7.4 Hz, 2H), 1.44 (s, 3H);  $^{13}\text{C}$  NMR (101 MHz,  $\text{CDCl}_3$ )  $\delta$  = 169.9, 152.5, 124.3, 84.4, 82.0, 79.5, 68.8, 68.3, 49.8, 48.6, 44.6, 41.4, 31.9, 28.6, 26.5, 18.5; IR (thin film) 3302, 2966, 2930, 2251, 1738, 1731, 1668, 1454, 1427, 1358, 1336, 1305, 1278, 1248, 1222, 1198, 1144, 1119, 1104,

1069, 1045, 1018, 989, 926, 912, 874, 853, 768, 737, 650; HRMS (ESI)  $m/z$  calc'd  $C_{16}H_{21}O_4$   $[M+H]^+$ : 277.1434, found: 277.1430;  $[\alpha]_D^{23}$   $-16.0$  ( $c$  0.72,  $CHCl_3$ ).

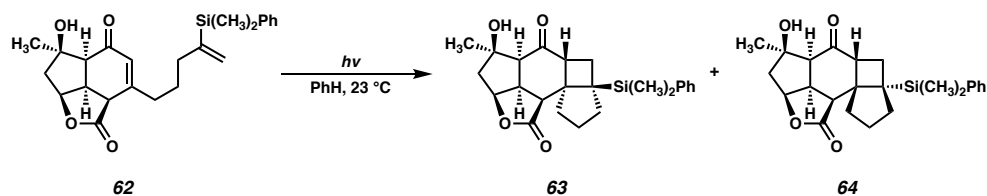


**Enone 61:** To a solution of diol **60** (270 mg, 0.98 mmol, 1.0 equiv) in  $CH_2Cl_2$  (27 mL, 0.036 M) was added  $NaHCO_3$  (330 mg, 3.9 mmol, 4 equiv) followed by DMP (538 mg, 1.3 mmol, 1.3 equiv) at 23 °C with stirring. The reaction vessel was then sealed and stirred for 3 h. Each subsequent hour, more DMP (1 equiv) was added until complete consumption of starting material (as determined by TLC analysis). The reaction was then quenched by the addition of saturated  $NaS_2O_3$  (30 mL) and saturated  $NaHCO_3$  (20 mL). After stirring for 10 minutes, the reaction mixture was extracted with  $CH_2Cl_2$  (3x). The combined organics were then dried over  $MgSO_4$ , filtered, and concentrated in vacuo. The crude product was purified by column chromatography ( $SiO_2$ , 75% EtOAc/hexanes) to afford enone **61** (117 mg, 47%) as a colorless viscous oil;  $^1H$  NMR (400 MHz,  $CDCl_3$ )  $\delta$  = 6.07 (q,  $J$  = 1.5 Hz, 1H), 5.12 (dd,  $J$  = 7.1, 5.4 Hz, 1H), 3.63 (dddd,  $J$  = 10.9, 10.2, 7.1, 0.6 Hz, 1H), 3.51–3.45 (m, 1H), 2.90–2.78 (m, 1H), 2.78–2.66 (m, 1H), 2.53 (d,  $J$  = 10.2 Hz, 1H), 2.33 (d,  $J$  = 15.0 Hz, 1H), 2.27 (tdd,  $J$  = 7.1, 6.1, 2.7 Hz, 2H), 1.99 (t,  $J$  = 2.6 Hz, 1H), 1.91 (dd,  $J$  = 15.0, 5.5 Hz, 1H), 1.87–1.74 (m, 2H), 1.51 (s, 3H);  $^{13}C$  NMR (100 MHz,  $CDCl_3$ )  $\delta$  = 196.0, 173.5, 157.6, 127.5, 83.6, 82.8, 82.5, 69.4, 55.2, 47.4, 42.5, 42.2, 34.7, 26.4, 25.6, 18.2; IR (thin film, NaCl) 3442, 3282, 2966, 1757, 1649, 1375, 1289, 1255, 1214, 1179, 1104, 1033, 1017, 993, 938; HRMS (ESI)  $m/z$  calc'd  $C_{16}H_{19}O_4$   $[M+H]^+$ : 275.1278, found: 275.1269;  $[\alpha]_D^{23}$   $-195$  ( $c$  0.32,  $CHCl_3$ ).



**Vinyl Silane 62:** Enone **61** (28 mg, 0.1 mmol, 1 equiv) and dimethylphenylsilane (18  $\mu\text{L}$ , 0.12 mmol, 1.2 equiv) was dissolved in  $\text{CH}_2\text{Cl}_2$  (0.5 mL, 0.2 M) and sparged with Ar for 5 min. A stock solution of  $[\text{RuCp}^*(\text{MeCN})_3]\text{PF}_6$  (0.5 mg, 1mg/mL, 0.01 equiv) prepared in a nitrogen-filled gloved box and was added to the reaction. The reaction was allowed to stir for 15 min, at which time complete consumption of starting material was observed (as determined by TLC analysis). The solution was then concentrated and directly purified by column chromatography ( $\text{SiO}_2$ , 75% EtOAc/hexanes) to afford vinyl silane **62** (19 mg, 64%) as a colorless amorphous solid;  $^1\text{H}$  NMR (400 MHz,  $\text{CDCl}_3$ )  $\delta$  = 7.60–7.48 (m, 2H), 7.44–7.30 (m, 3H), 5.94 (q,  $J$  = 1.4 Hz, 1H), 5.70 (dt,  $J$  = 2.9, 1.5 Hz, 1H), 5.46 (dt,  $J$  = 2.7, 1.0 Hz, 1H), 5.07 (dd,  $J$  = 7.2, 5.4 Hz, 1H), 3.48 (dddd,  $J$  = 10.9, 10.2, 7.1, 0.6 Hz, 1H), 3.16 (dd,  $J$  = 11.1, 1.5 Hz, 1H), 2.66–2.50 (m, 2H), 2.48 (d,  $J$  = 10.2 Hz, 1H), 2.30 (d,  $J$  = 15.0 Hz, 1H), 2.24–2.08 (m, 2H), 1.89 (dd,  $J$  = 15.0, 5.5 Hz, 1H), 1.67–1.51 (m, 2H), 1.49 (s, 3H), 0.37 (s, 6H);  $^{13}\text{C}$  NMR (100 MHz,  $\text{CDCl}_3$ )  $\delta$  = 196.0, 173.4, 158.7, 149.7, 138.4, 134.1, 129.1, 128.0, 127.3, 126.7, 82.7, 82.4, 55.2, 47.4, 42.2, 41.9, 35.7, 35.4, 26.5, 26.1, -2.8, -2.9; IR (thin film, NaCl) 3450, 2958, 1759, 1650, 1378, 1290, 1248, 1173, 1107, 992, 818  $\text{cm}^{-1}$ ; HRMS (ESI)  $m/z$  calc'd  $\text{C}_{23}\text{H}_{31}\text{O}_4\text{Si}$   $[\text{M}+\text{H}]^+$ : 411.1986, found: 411.1972;  $[\alpha]_{\text{D}}^{23}$  -115.3 ( $c$  0.25,  $\text{CHCl}_3$ ).



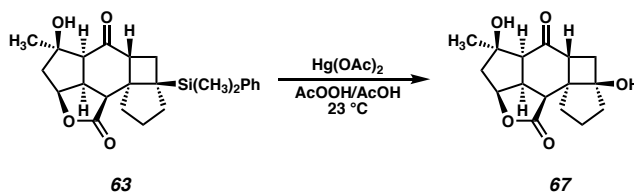


**Cyclobutanes 63 and 64:** Enone **62** (19 mg, 0.0465 mmol, 1 equiv) in a 20 mL vial was dissolved in benzene (4.65 mL, 0.01 M) and was sparged with Ar for 10 min. The reaction vessel was sealed and irradiated at 350 nm. After 2 h complete consumption of starting material was observed (as determined by TLC analysis) and was directly purified by column chromatography (SiO<sub>2</sub>, 0%–50% EtOAc/hexanes) to afford a 2:1 mixture of pentacycles **63** and **64** (19 mg total, >99%) as a colorless amorphous solid which crystallizes in benzene.

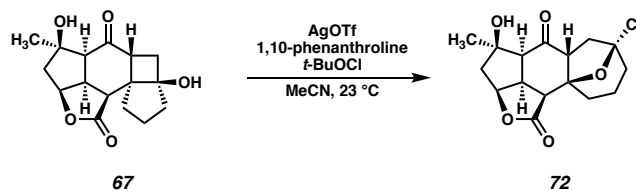
**63 (maj):** <sup>1</sup>H NMR (400 MHz, CDCl<sub>3</sub>) δ = 7.57–7.47 (m, 2H), 7.37–7.28 (m, 3H), 4.91 (dd, *J* = 6.1, 4.5 Hz, 1H), 3.60–3.52 (m, 1H), 3.52–3.48 (m, 1H), 2.94 (dd, *J* = 9.0, 0.7 Hz, 1H), 2.56 (d, *J* = 10.6 Hz, 1H), 2.36 (d, *J* = 15.2 Hz, 1H), 2.21–2.14 (m, 2H), 2.08–2.00 (m, 1H), 1.96–1.88 (m, 2H), 1.88–1.76 (m, 1H), 1.73–1.59 (m, 2H), 1.45 (s, 3H), 1.32 (dd, *J* = 11.9, 6.6 Hz, 1H), 0.55 (s, 3H), 0.52 (s, 3H); <sup>13</sup>C NMR (101 MHz, CDCl<sub>3</sub>) δ = 205.7, 174.8, 141.4, 134.2, 128.5, 127.6, 82.1, 81.4, 60.6, 60.1, 51.3, 50.1, 48.6, 47.7, 43.9, 39.9, 37.1, 27.6, 27.1, 24.5, -2.1, -4.7; IR (thin film, NaCl) 3393, 2949, 1769, 1687, 1373, 1242, 1209, 1147, 1104, 1089, 826, 783, 733; HRMS (ESI) *m/z* calc'd C<sub>23</sub>H<sub>31</sub>O<sub>4</sub>Si [M+H]<sup>+</sup>: 411.1986, found: 411.1972; [α]<sub>D</sub><sup>23</sup> –19.7 (*c* 0.35, CHCl<sub>3</sub>).

**64 (min):** <sup>1</sup>H NMR (400 MHz, CDCl<sub>3</sub>) δ = 7.66–7.53 (m, 2H), 7.45–7.37 (m, 3H), 4.59 (ddd, *J* = 6.6, 5.6, 2.0 Hz, 1H), 3.02 (s, 1H), 2.92 (ddd, *J* = 11.1, 9.8, 6.7 Hz, 1H), 2.74–2.66 (m, 2H), 2.41–2.33 (m, 2H), 2.31–2.21 (m, 1H), 2.17 (s, 1H), 2.13 (dd, *J* = 14.6, 2.0 Hz, 1H), 2.03–1.82 (m, 4H), 1.81–1.72 (m, 1H), 1.66–1.59 (m, 1H), 1.18 (s, 3H), 0.41 (s,

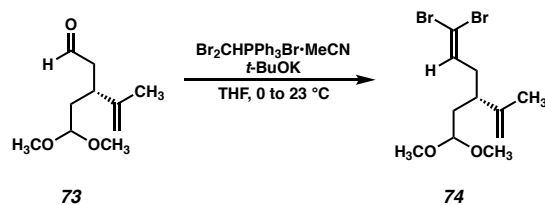
3H), 0.30 (s, 3H);  $^{13}\text{C}$  NMR (101 MHz,  $\text{CDCl}_3$ )  $\delta$  = 215.6, 174.9, 138.3, 134.4, 129.9, 128.5, 80.9, 80.9, 55.4, 53.3, 48.4, 45.8, 44.5, 43.4, 39.7, 39.0, 38.7, 29.0, 28.6, 24.5, -2.9, -3.9; IR (thin film, NaCl) 3416, 2957, 1759, 1673, 1359, 1107, 731  $\text{cm}^{-1}$ ; HRMS (ESI)  $m/z$  calc'd  $\text{C}_{23}\text{H}_{31}\text{O}_4\text{Si}$   $[\text{M}+\text{H}]^+$ : 411.1986, found: 411.1976;  $[\alpha]_{\text{D}}^{23}$  -17.7 ( $c$  0.3,  $\text{CHCl}_3$ ).



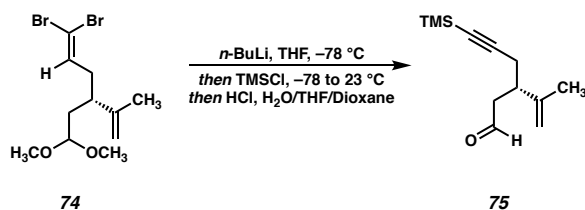
**Cyclobutanol 67:** To a solution of cyclobutane **63** (25 mg, 0.061 mmol) in 35% AcOOH-AcOH (3.05 mL, 0.02 M) at 23 °C was added  $\text{Hg}(\text{OAc})_2$  (92 mg, 0.29 mmol, 4.8 equiv), and the solution was stirred for 1 h, after which complete consumption of starting material was observed (as determined by TLC analysis). The reaction mixture was diluted with  $\text{Et}_2\text{O}$ , washed sequentially with 10% aq  $\text{Na}_2\text{S}_2\text{O}_3$ ,  $\text{H}_2\text{O}$ , saturated solution of  $\text{NaHCO}_3$ , and brine, dried over  $\text{MgSO}_4$ , filtered, and concentrated in vacuo. The crude product was purified by column chromatography ( $\text{SiO}_2$ , 75% EtOAc/hexanes) to afford cyclobutanol **67** (6 mg, 30%) as a white amorphous powder;  $^1\text{H}$  NMR (400 MHz,  $\text{CDCl}_3$ )  $\delta$  = 6.16 (s, 1H), 5.13 (dd,  $J$  = 5.9, 4.6 Hz, 1H), 3.90 (t,  $J$  = 9.5 Hz, 1H), 3.57–3.43 (m, 1H), 3.21 (dd,  $J$  = 9.0, 0.8 Hz, 1H), 2.58 (d,  $J$  = 10.6 Hz, 1H), 2.47–2.34 (m, 2H), 2.07–1.94 (m, 2H), 1.94–1.87 (m, 1H), 1.87–1.78 (m, 1H), 1.78–1.68 (m, 3H), 1.48 (s, 3H), 1.25 (d,  $J$  = 2.5 Hz, 1H);  $^{13}\text{C}$  NMR (101 MHz,  $\text{CDCl}_3$ )  $\delta$  = 205.5, 179.1, 88.5, 86.1, 81.5, 60.8, 55.4, 52.3, 49.4, 47.7, 47.1, 38.1, 36.4, 34.5, 27.8, 23.1; IR (thin film, NaCl) 3421, 2972, 2923, 1741, 1686, 1448, 1400, 1377, 1305, 1276, 1211, 1161, 1112, 1088, 1069, 1010, 921, 850, 813, 777, 733, 719; HRMS (ESI)  $m/z$  calc'd  $\text{C}_{16}\text{H}_{21}\text{O}_5$   $[\text{M}+\text{H}]^+$ : 293.1384, found: 293.1372;  $[\alpha]_{\text{D}}^{23}$  -40.4 ( $c$  0.13,  $\text{CHCl}_3$ ).



**Furan 72:** Cyclobutanol **67** (10 mg, 0.034 mmol, 1 equiv), AgOTf (1.2 mg, 0.012 mmol, 0.4 equiv), and 1,10-phenanthroline (4.8 mg, 0.024 mmol, 0.8 equiv) were placed in a round-bottom flask and dissolved in MeCN (1 mL, 0.034 M) followed by the addition of *t*-BuOCl (7.8  $\mu$ L, 0.068 mmol, 2 equiv). The reaction mixture was stirred at 23 °C for 6 h. The reaction was quenched with saturated solution of Na<sub>2</sub>S<sub>2</sub>O<sub>3</sub> and extracted with EtOAc (3 x 5 mL). The combined organic layers were washed with brine, dried over MgSO<sub>4</sub>, filtered, and concentrated in vacuo. The crude product was purified by column chromatography (SiO<sub>2</sub>, 75% EtOAc/Hexanes) to obtain furan **67** (5.4 mg, 49%) as a white amorphous solid which can be crystallized in CHCl<sub>3</sub>; <sup>1</sup>H NMR (400 MHz, CDCl<sub>3</sub>)  $\delta$  = 5.02 (dd, *J* = 5.9, 4.5 Hz, 1H), 3.79–3.66 (m, 1H), 3.42 (dddd, *J* = 10.3, 9.5, 5.9, 0.6 Hz, 1H), 3.34 (dd, *J* = 9.5, 0.7 Hz, 1H), 2.88 (ddd, *J* = 13.8, 7.4, 0.9 Hz, 1H), 2.71 (d, *J* = 10.4 Hz, 1H), 2.42 (d, *J* = 15.4 Hz, 1H), 2.35 (ddd, *J* = 13.8, 11.6, 1.1 Hz, 1H), 2.29–2.09 (m, 1H), 2.07–1.96 (m, 2H), 1.75–1.64 (m, 3H), 1.49 (s, 3H), 1.46–1.34 (m, 1H); <sup>13</sup>C NMR (101 MHz, CDCl<sub>3</sub>)  $\delta$  = 202.8, 172.0, 101.8, 85.2, 82.7, 82.3, 60.6, 56.4, 48.6, 47.5, 45.9, 40.1, 36.3, 33.1, 27.6, 18.9; IR (thin film, NaCl) 3472, 2921, 1766, 1713, 1359, 1243, 1214, 1171, 1126, 1093, 1000, 953, 905, 845, 759, 731; HRMS (ESI) *m/z* calc'd C<sub>16</sub>H<sub>20</sub>O<sub>5</sub>Cl [M+H]<sup>+</sup>: 327.0994, found: 327.0980; [ $\alpha$ ]<sub>D</sub><sup>23</sup> –43.3 (*c* 0.13, CHCl<sub>3</sub>).

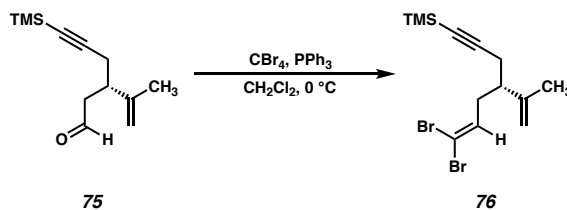


**Dibromide 74:** A 500 mL round-bottom flask was charged with  $\text{Br}_2\text{CHPh}_3\text{Br}\cdot\text{MeCN}$  (55.6 g, 100.0 mmol, 1.4 equiv; prepared according to the method of Schmidt)<sup>49</sup> and THF (238 mL, 0.3 M). The reaction mixture was cooled to 0 °C and *t*-BuOK (9.6 g, 85.7 mmol, 1.2 equiv) was added in one portion. This mixture was stirred 1.5 h at 0 °C and then warmed to 23 °C and stirred an additional 30 min. The mixture was then cooled to 0 °C and aldehyde **73**<sup>40</sup> (13.3 g, 71.4 mmol, 1.0 equiv) was added dropwise via syringe. The dark suspension was stirred for 2 h at 0 °C, until no aldehyde (**12**) is detected by TLC. The mixture was quenched with saturated, aqueous  $\text{NH}_4\text{Cl}$  and partitioned between water and  $\text{Et}_2\text{O}$ . The aqueous phase was extracted with  $\text{Et}_2\text{O}$  (3x). The organic extracts were combined, washed with brine, dried over magnesium sulfate, filtered through a sand/cotton plug and concentrated under reduced pressure. The crude residue was purified by flash chromatography (Dry load crude on Celite;  $\text{SiO}_2$ , 20%  $\text{Et}_2\text{O}$ /Hexanes) to afford dibromide **74** (20.9 g, 61.1 mmol, 86% yield) as a red/orange oil;  $^1\text{H}$  NMR (400 MHz,  $\text{CDCl}_3$ ) 6.30 (t,  $J = 7.0$  Hz, 1H), 4.83 (dt,  $J = 2.9, 1.5$  Hz, 1H), 4.77 (dt,  $J = 1.9, 0.8$  Hz, 1H), 4.36 – 4.28 (m, 1H), 3.32 (s, 3H), 3.30 (s, 3H), 2.43 – 2.30 (m, 1H), 2.24 – 2.07 (m, 2H), 1.72 – 1.62 (m, 5H);  $^{13}\text{C}$  NMR (125 MHz,  $\text{CDCl}_3$ ) 145.7, 137.0, 113.0, 102.9, 89.2, 53.3, 52.7, 42.0, 36.9, 35.7, 18.6; IR (Neat film, NaCl) 3073, 2948, 2829, 1645, 1440, 1377, 1191, 1127, 1060, 896, 787  $\text{cm}^{-1}$ ; HRMS (FAB+)  $m/z$  calc'd for  $\text{C}_{11}\text{H}_{17}\text{O}_2\text{Br}_2$   $[\text{M}-\text{H}]^+$ : 340.9575, found 340.9579;  $[\alpha]_{\text{D}}^{25.0} - 4.5^\circ$  ( $c$  1.0,  $\text{CHCl}_3$ ).

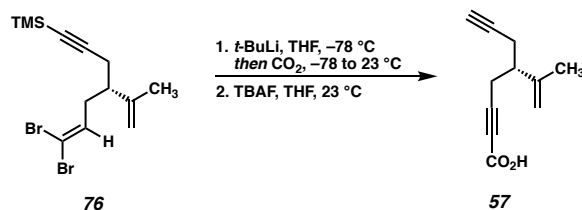


**Aldehyde 75:** A 500 mL round-bottom flask was charged with dibromide **74** (16.6 g, 48.5 mmol, 1.0 equiv) in THF (100 mL, 0.5 M), and cooled to  $-78^\circ\text{C}$ . *n*-BuLi (2.3 M in hexanes; 42.2 mL, 97.1 mmol, 2.0 equiv) was added dropwise over 10 min, and the mixture was allowed to stir for 15 min at  $-78^\circ\text{C}$  after which complete consumption of dibromide **13** was observed by TLC. TMSCl (18.5 mL, 145.5 mmol, 3.0 equiv) was added dropwise to the reaction mixture, which was then allowed to gradually warm to  $23^\circ\text{C}$  over 2 h. The mixture was then cooled to  $0^\circ\text{C}$  and water (100 mL) was added followed by 1,4-dioxane (50 mL). HCl (36% w/w, 40 mL, 10.0 equiv) was added and the reaction mixture warmed to room temperature and allowed to stir for 16 h.  $\text{NaHCO}_3$  (sat. aq.) was added until the pH of the solution was roughly 7. The reaction mixture was partitioned between water and  $\text{Et}_2\text{O}$ , and extracted with  $\text{Et}_2\text{O}$  (3x). The combined organic extracts were washed with brine, dried over sodium sulfate, and concentrated to afford an orange oil which was purified by flash chromatography ( $\text{SiO}_2$ , 10%  $\text{Et}_2\text{O}$ /Hexanes). Aldehyde **75** (7.37 g, 35.4 mmol, 73% yield) was isolated as a pale-yellow oil;  $^1\text{H}$  NMR (400 MHz,  $\text{CDCl}_3$ )  $\delta$  9.70 (dd,  $J = 2.4, 1.6$  Hz, 1H), 4.83 – 4.80 (m, 1H), 4.79 – 4.76 (m, 1H), 2.89 – 2.77 (m, 1H), 2.68 (ddd,  $J = 16.8, 6.1, 1.7$  Hz, 1H), 2.52 (ddd,  $J = 16.7, 8.4, 2.5$  Hz, 1H), 2.40 (dd,  $J = 16.9, 5.8$  Hz, 1H), 2.29 (dd,  $J = 17.0, 7.9$  Hz, 1H), 1.70 (dd,  $J = 1.5, 0.9$  Hz, 3H), 0.11 (s, 9H);  $^{13}\text{C}$  NMR (100 MHz,  $\text{CDCl}_3$ ) 201.6, 145.4, 112.3, 104.5, 87.3, 46.3, 40.2, 24.8, 20.3, 0.1; IR (Neat film, NaCl) 3077, 2959, 2900, 2827, 2720, 1727, 1648, 1430, 1408, 1377,

1250, 1024, 1038, 896, 760, 644  $\text{cm}^{-1}$ ; HRMS (MM: ESI-APCI+)  $m/z$  calc'd for  $\text{C}_{12}\text{H}_{21}\text{OSi}$   $[\text{M}+\text{H}]^+$  209.1356, found 209.1352.;  $[\alpha]_{\text{D}}^{25.0} -13.5^\circ$  ( $c$  1.0,  $\text{CHCl}_3$ ).

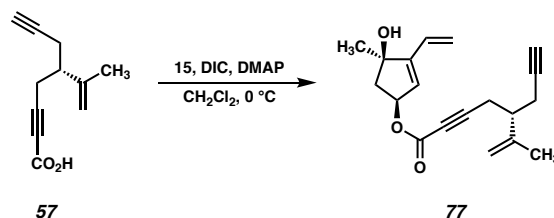


**Dibromide 76:** A 500 mL round-bottom flask was charged with triphenylphosphine (50.4 g, 192.0 mmol, 4.0 equiv) in  $\text{CH}_2\text{Cl}_2$  (96 mL). The solution was cooled to  $0^\circ\text{C}$ , and  $\text{CBr}_4$  (31.8 g, 96.0 mmol, 2.0 equiv) added in one portion. The colorless solution immediately changed to yellow/orange in color. The mixture was allowed to stir for 10 min at  $0^\circ\text{C}$ , after which aldehyde **75** (10.0 g, 48.0 mmol, 1.0 equiv) was added via syringe. The aldehyde was consumed immediately, as judged by TLC. The reaction mixture was then quenched with water, and partitioned between water and  $\text{CH}_2\text{Cl}_2$ . The aqueous phase was extracted with  $\text{CH}_2\text{Cl}_2$  (3x), and the combined organic extracts washed with brine and dried over  $\text{MgSO}_4$ . The crude was concentrated onto  $\text{SiO}_2$ , loaded onto a column, and purified by flash chromatography ( $\text{SiO}_2$ , 5%  $\text{Et}_2\text{O}/\text{Hexanes}$ ) to afford dibromide **76** (14.48 g, 39.8 mmol, 83% yield) as a yellow oil;  $^1\text{H}$  NMR (400 MHz,  $\text{CDCl}_3$ ) 6.34 (t,  $J = 6.9$  Hz, 1H), 4.84 (p,  $J = 1.5$  Hz, 1H), 4.76 (dt,  $J = 1.7, 0.8$  Hz, 1H), 2.47 – 2.16 (m, 5H), 1.69 (dd,  $J = 1.5, 0.8$  Hz, 3H), 0.14 (s, 9H);  $^{13}\text{C}$  NMR (100 MHz,  $\text{CDCl}_3$ - $d$ ) 145.4, 136.9, 112.7, 105.1, 89.5, 86.75, 44.9, 35.8, 24.7, 19.7, 0.3; IR (Neat film, NaCl) 2958, 2922, 2176, 1646, 1441, 1248  $\text{cm}^{-1}$ ; HRMS (EI+)  $m/z$  calc'd for  $\text{C}_{13}\text{H}_{20}\text{SiBr}_2$   $[\text{M}^+]$  363.9681, found 363.9668;  $[\alpha]_{\text{D}}^{25.0} +4.1^\circ$  ( $c$  1.0,  $\text{CHCl}_3$ ).



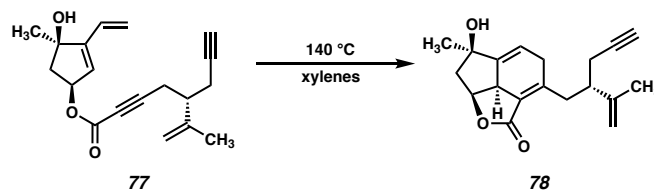
**Ynoic Acid 57:** A 250 mL round bottom flask was charged with dibromide **76** (3.92 g, 10.76 mmol, 1.0 equiv) in THF (143 mL). This solution was cooled to  $-78\text{ }^\circ\text{C}$ , followed by the dropwise addition of *t*-BuLi (1.61 M solution in pentane, 14.0 mL, 22.6 mmol, 2.1 equiv), after which no starting material remained (as judged by TLC). The solution was then sparged with  $\text{CO}_2$  at  $-78\text{ }^\circ\text{C}$  for 10 min, then warmed to  $23\text{ }^\circ\text{C}$  with continuous sparging. The reaction was then quenched with aqueous  $\text{NaHCO}_3$ , and extracted with  $\text{Et}_2\text{O}$  (1x). The aqueous phase was then acidified with conc. HCl to pH  $\sim 2$ . The acidified aqueous phase was then extracted with EtOAc (3x). The EtOAc extracts were combined, washed with brine, dried over  $\text{Na}_2\text{SO}_4$ , filtered, and concentrated to afford an intermediate acid (1.87 g, 7.53 mmol, 70% yield). The intermediate acid (886 mg, 3.57 mmol, 1.0 equiv) was dissolved in THF (36 mL), and TBAF (1.0 M solution in THF, 7.31 mL, 7.31 mmol, 2.0 equiv) was added at  $23\text{ }^\circ\text{C}$ . The solution was stirred for 2 h at  $23\text{ }^\circ\text{C}$ , after which no starting material remained (as judged by LCMS). The reaction mixture was diluted with  $\text{H}_2\text{O}$ , then extracted with EtOAc (3x). The organic extracts were washed with brine, dried over  $\text{Na}_2\text{SO}_4$ , filtered, and concentrated to afford acid **57** (577 mg, 3.27 mmol, 92% yield, 64% yield over the two steps) as an orange oil;  $^1\text{H}$  NMR (400 MHz,  $\text{CDCl}_3$ )  $\delta$  10.98 (s, 1H), 4.92 (p,  $J = 1.4\text{ Hz}$ , 1H), 4.84 (q,  $J = 1.0\text{ Hz}$ , 1H), 2.71 – 2.47 (m, 3H), 2.41 (d,  $J = 2.7\text{ Hz}$ , 1H), 2.40 – 2.39 (m, 1H), 2.01 (t,  $J = 2.6\text{ Hz}$ , 1H), 1.73 (dd,  $J = 1.5, 0.8\text{ Hz}$ , 3H);  $^{13}\text{C}$  NMR (100 MHz,  $\text{CDCl}_3$ )  $\delta$  158.4, 144.1, 113.1, 90.3, 81.6, 74.1, 70.6, 43.7, 22.5, 22.4, 20.2; IR (Neat film, NaCl) 3302, 2928, 2643, 2236, 2119, 1964, 1416, 1244, 1078, 899, 775, 792,

759, 641, 648; HRMS (MM: ESI-APCI+)  $m/z$  calc'd for  $C_{11}H_{13}O_2$   $[M+H]^+$ : 177.0910, found 177.0916;  $[\alpha]_D^{25.0} -1.6^\circ$  ( $c$  1.0,  $CHCl_3$ ).

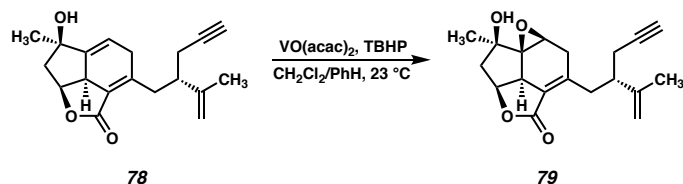


**Ester 77:** A 250 mL round-bottom flask was charged with diol **15** (1.03 g, 7.35 mmol, 1.0 equiv), acid **57** (1.30 g, 7.35 mmol, 1.0) and DMAP (90 mg, 0.735 mmol, 0.10 equiv) in  $CH_2Cl_2$  (74 mL). The solution was cooled to 0 °C, and DIC (1.15 mL, 7.35 mmol, 1.0 equiv) was added dropwise. The reaction was then stirred for 2 h while gradually warming to 23 °C, and then stirred an additional 3 h at 23 °C. The mixture was partitioned between  $CH_2Cl_2$  and  $H_2O$ , and the aqueous phase is extracted with  $CH_2Cl_2$  (3x). The organic extracts were washed with brine, dried over  $Na_2SO_4$ , and concentrated. The crude residue was purified by flash chromatography (0%-5%-10%-15%-20% EtOAc/Hexanes) to afford ester **77** (1.74 g, 5.83 mmol, 79% yield) as a colorless oil;  $^1H$  NMR (400 MHz,  $CDCl_3$ )  $\delta$  6.43 – 6.20 (m, 1H), 5.82 (d,  $J = 2.4$  Hz, 1H), 5.78 (dd,  $J = 17.8, 1.7$  Hz, 1H), 5.64 – 5.49 (m, 1H), 5.33 (dd,  $J = 11.2, 1.6$  Hz, 1H), 4.92 (p,  $J = 1.4$  Hz, 1H), 4.84 (dd,  $J = 1.4, 0.8$  Hz, 1H), 2.77 – 2.46 (m, 4H), 2.44 – 2.39 (m, 2H), 2.05 (dd,  $J = 14.7, 4.4$  Hz, 1H), 2.01 (t,  $J = 2.6$  Hz, 1H), 1.74 (dd,  $J = 1.5, 0.8$  Hz, 3H), 1.44 (s, 3H);  $^{13}C$  NMR (100 MHz,  $CDCl_3$ )  $\delta$  153.5, 151.8, 144.3, 129.0, 126.1, 119.6, 113.0, 87.6, 81.7, 81.1, 77.1, 74.5, 70.5, 49.0, 43.8, 26.8, 22.5, 22.4, 20.3; IR (Neat film, NaCl) 3396, 2938, 2235, 1708, 1252, 1071, 942, 752  $cm^{-1}$ ; HRMS (MM: ESI-APCI+)  $m/z$  calc'd for  $C_{19}H_{23}O_3$   $[M+H]^+$ : 299.1642, found 299.1632;  $[\alpha]_D^{25.0} -130.8^\circ$  ( $c$  1.0,  $CHCl_3$ ).

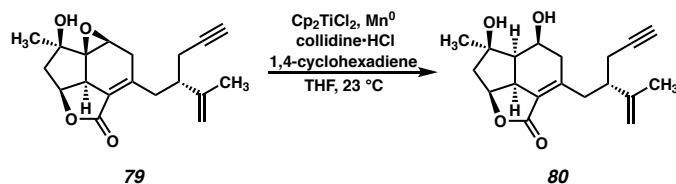




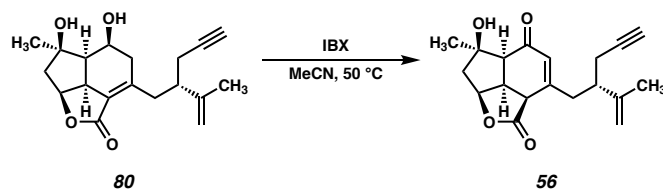
**Cyclohexadiene 78:** Ester **77** (804 mg, 2.69 mmol, 1.0 equiv) was dissolved in xylenes (270 mL). This solution was then divided between two 500 mL Schlenk flasks. Each flask was subjected to three freeze-pump-thaw cycles, and then back-filled with nitrogen. The flasks were sealed, heated to 140 °C, and stirred for 3 h. The flasks were then cooled to ambient temperature and the reaction mixtures were combined in a 2 L round-bottom flask. The solvent was removed under reduced pressure, and the resulting solid purified by flash chromatography (30%-40%-50% EtOAc/Hexanes) to afford cyclohexadiene **78** (604 mg, 2.02 mmol, 75% yield) as a flakey white solid;  $^1\text{H}$  NMR (400 MHz,  $\text{CDCl}_3$ )  $\delta$  5.84 (ddd,  $J = 6.4, 3.0, 1.9$  Hz, 1H), 4.97 (ddd,  $J = 9.1, 8.0, 7.0$  Hz, 1H), 4.77 (t,  $J = 1.7$  Hz, 1H), 4.69 – 4.65 (m, 1H), 3.31 (t,  $J = 9.8$  Hz, 1H), 3.12 – 2.98 (m, 2H), 2.83 – 2.61 (m, 2H), 2.63 – 2.41 (m, 2H), 2.33 (d,  $J = 2.6$  Hz, 1H), 2.32 (dd,  $J = 2.7, 1.4$  Hz, 1H), 2.00 (t,  $J = 2.6$  Hz, 1H), 1.69 (dd,  $J = 1.4, 0.8$  Hz, 3H), 1.67 – 1.60 (m, 1H), 1.41 (d,  $J = 1.1$  Hz, 3H);  $\delta$   $^{13}\text{C}$  NMR (100 MHz,  $\text{CDCl}_3$ )  $\delta$  168.2, 155.9, 152.0, 146.1, 125.5, 116.5, 112.8, 82.9, 80.0, 75.3, 69.7, 49.8, 45.7, 45.7, 35.3, 26.7, 22.9, 18.8; IR (Neat film, NaCl) 3305, 2967, 2920, 2360, 2118, 1730, 1647, 1447, 1374, 1358, 1290, 1219, 1045, 1018, 896, 632  $\text{cm}^{-1}$ ; HRMS (MM: ESI-APCI+)  $m/z$  calc'd for  $\text{C}_{19}\text{H}_{23}\text{O}_3$   $[\text{M}+\text{H}]^+$ : 299.1642, found 299.1631.  $[\alpha]_{\text{D}}^{25.0} -87.4^\circ$  ( $c$  0.5,  $\text{CHCl}_3$ ).



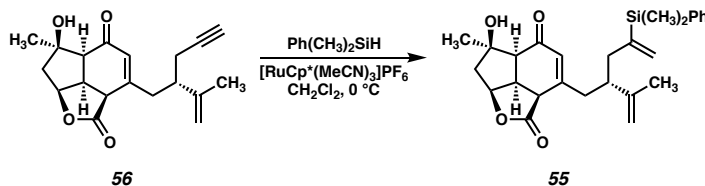
**Epoxide 79:** A 500 mL round-bottom flask was charged with Diels–Alder adduct **78** (1.75 g, 5.87 mmol, 1.0 equiv) in a mixture of CH<sub>2</sub>Cl<sub>2</sub> (59 mL) and benzene (196 mL). VO(acac)<sub>2</sub> was added (117 mg, 0.440 mmol, 0.075 equiv) in one portion, and the mixture was stirred 10 min at 23 °C until pale-green in color. TBHP (5.0 M in decane, 2.30 mL, 11.74 mmol, 2.0 equiv) was added dropwise via syringe, and the mixture became deep-red in color. The mixture was stirred at 23 °C for 1 h, at which point no starting material remained, as judged by TLC. The reaction mixture was poured directly onto a flash column and purified by flash chromatography (0%-50%-70%-80% EtOAc/Hexanes) to afford the epoxide **79** (1.73 g, 5.50 mmol, 94% yield) as a white solid; <sup>1</sup>H NMR (400 MHz, CDCl<sub>3</sub>) δ 4.90 – 4.77 (m, 3H), 3.78 (d, *J* = 3.4 Hz, 1H), 3.40 – 3.18 (m, 2H), 2.87 (dd, *J* = 16.7, 3.4 Hz, 1H), 2.62 – 2.43 (m, 3H), 2.41 – 2.26 (m, 3H), 2.06 – 1.95 (m, 2H), 1.74 (t, *J* = 1.1 Hz, 3H), 1.46 – 1.41 (m, 3H); <sup>13</sup>C NMR (100 MHz, CDCl<sub>3</sub>) δ 168.9, 149.9, 146.1, 120.7, 112.5, 82.9, 76.6, 73.6, 69.8, 69.7, 51.8, 50.1, 45.7, 44.8, 36.7, 36.6, 22.7, 22.7, 19.4; IR (Neat film, NaCl) 3474, 3267, 1735, 1655, 1421, 1358, 1195, 1120, 1030, 901, 793, 674 cm<sup>-1</sup>; HRMS (MM: ESI-APCI+) *m/z* calc'd for C<sub>19</sub>H<sub>23</sub>O<sub>4</sub> [M+H]<sup>+</sup>: 315.1591, found 315.1586; [α]<sub>D</sub><sup>25.0</sup> -69.8° (*c* 0.5, CHCl<sub>3</sub>).



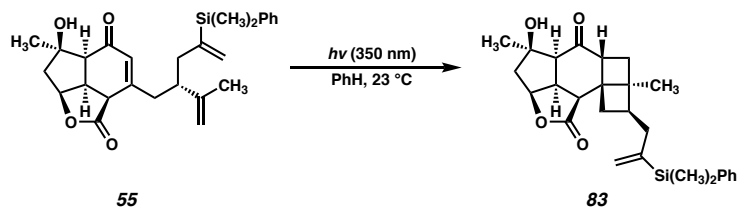
**Diol 80:** A 250 mL round bottom flask was charged with epoxide **79** (1.70 g, 5.41 mmol, 1.0 equiv), Cp<sub>2</sub>TiCl<sub>2</sub> (269 mg, 1.08 mmol, 0.20 equiv), Mn dust (326 mg, 5.95 mmol, 1.10 equiv), and collidine•HCl (1.07 g, 6.76 mmol, 1.25 equiv) in THF (54 mL, 0.10 M). 1,4-cyclohexadiene was then added dropwise to the red suspension, which gradually changed to a blue/grey color. The suspension was stirred vigorously for 2 h at 23 °C, after which the starting material was consumed, as judged by TLC. Celite was added directly to the mixture, and the solvent removed under reduced pressure. The resulting solid was loaded directly on to a flash column and purified by flash chromatography (40%-50%-60% EtOAc/Hexanes) to afford diol **80** (1.47 g, 4.65 mmol, 86% yield) as an off-white solid; <sup>1</sup>H NMR (400 MHz, CDCl<sub>3</sub>) 4.90 (ddd, *J* = 8.1, 6.5, 3.9 Hz, 1H), 4.83 (d, *J* = 1.4 Hz, 2H), 4.67 (td, *J* = 5.4, 2.9 Hz, 1H), 3.40 (d, *J* = 6.0 Hz, 1H), 3.37 – 3.28 (m, 1H), 3.18 (s, 1H), 3.10 (ddd, *J* = 9.9, 7.9, 2.1 Hz, 1H), 2.64 – 2.48 (m, 3H), 2.36 (dd, *J* = 9.5, 7.8 Hz, 1H), 2.32 (dd, *J* = 2.7, 1.1 Hz, 1H), 2.31 – 2.29 (m, 1H), 2.13 – 1.98 (m, 3H), 1.97 (t, *J* = 2.6 Hz, 1H), 1.80 – 1.71 (m, 3H), 1.43 (s, 3H); δ<sup>13</sup>C NMR (100 MHz, CDCl<sub>3</sub>) δ 169.8, 151.3, 146.8, 125.2, 112.4, 83.2, 81.7, 79.4, 69.5, 68.3, 49.6, 48.4, 45.2, 44.6, 41.4, 36.8, 28.6, 22.9, 19.3; IR (Neat film, NaCl) 3296, 3076, 2116, 1738, 1731, 1668, 1424, 1375, 1360, 1306, 1223, 1198, 1105, 896 cm<sup>-1</sup>; HRMS (MM: ESI-APCI+) *m/z* calc'd for C<sub>19</sub>H<sub>25</sub>O<sub>4</sub> [M+H]<sup>+</sup>: 317.1747, found 317.1761; [α]<sub>D</sub><sup>25.0</sup> -11.8° (c 0.5, CHCl<sub>3</sub>).



**Enone 56:** Diol **80** (1.0 g, 3.16 mmol, 1.0 equiv) was divided into 20 scintillation vials (not flame dried, 50 mg, 0.158 mmol per vial) each equipped with a magnetic stir bar and a septum cap. To each vial was added IBX (188 mg, 0.671 mmol, 4.25 equiv) and each vial was evacuated and back-filled with N<sub>2</sub>. MeCN (11 mL) was added to each vial, after which the vials were sealed, heated to 50 °C, and stirred 2 h. The reactions were cooled to 23 °C, combined, and filtered over a plug of SiO<sub>2</sub>, rinsing generously with EtOAc. The filtrate was concentrated under reduced pressure, and the residue obtained was purified by flash chromatography (30%-40%50% EtOAc/Hexanes) to afford enone **56** (716 mg, 2.28 mmol, 72% yield) as a white foam; <sup>1</sup>H NMR (400 MHz, CDCl<sub>3</sub>) δ 6.00 (d, *J* = 1.0 Hz, 1H), 5.11 (dd, *J* = 6.7, 5.4 Hz, 1H), 4.88 – 4.81 (m, 1H), 4.78 (dt, *J* = 1.6, 0.8 Hz, 1H), 3.68 – 3.45 (m, 2H), 3.16 – 3.05 (m, 1H), 2.79 – 2.59 (m, 2H), 2.48 (d, *J* = 9.2 Hz, 1H), 2.39 – 2.28 (m, 3H), 2.03 (t, *J* = 2.6 Hz, 1H), 1.88 (dd, *J* = 15.0, 5.5 Hz, 1H), 1.71 (s, 1H), 1.67 (d, *J* = 0.7 Hz, 3H), 1.49 (s, 3H); δ <sup>13</sup>C NMR (100 MHz, CDCl<sub>3</sub>) δ 196.1, 173.6, 156.3, 145.0, 128.8, 113.6, 82.7, 82.6, 82.2, 70.5, 55.2, 47.4, 44.0, 42.1, 41.4, 38.2, 26.3, 23.9, 18.8; IR (Neat film, NaCl) 3450, 3290, 2970, 2930, 2118, 1758, 1649, 1376, 1290, 1176, 1161, 1107, 912, 735 cm<sup>-1</sup>; HRMS (MM: ESI-APCI+) *m/z* calc'd for C<sub>19</sub>H<sub>23</sub>O<sub>4</sub> [M+H]<sup>+</sup>: 315.1591, found 315.1571; [α]<sub>D</sub><sup>25.0</sup> -150.0° (*c* 0.5, CHCl<sub>3</sub>).

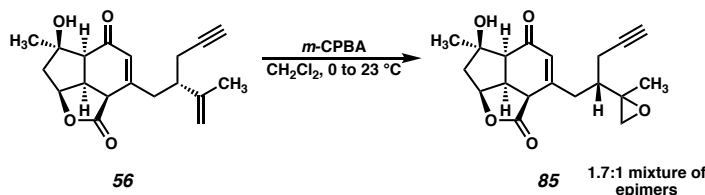


**Vinyl Silane 55:** A 1-dram vial was charged with enone **56** (7.0 mg, 0.0223 mmol, 1.0 equiv) in  $\text{CH}_2\text{Cl}_2$  (400  $\mu\text{L}$ ). Phenyltrimethylsilane (4  $\mu\text{L}$ , 0.0267 mmol, 1.2 equiv) was added, and the mixture is cooled to 0  $^\circ\text{C}$ .  $[\text{RuCp}^*(\text{MeCN})_3]\text{PF}_6$  (10 mg/mL stock solution 56  $\mu\text{L}$ , 0.00112 mmol, 0.05 equiv, prepared in a nitrogen-filled glovebox) was added dropwise. Following the addition, the reaction was stirred 5 min at 0  $^\circ\text{C}$ , after which alkyne **5** was no longer detectable by TLC. The reaction mixture was loaded directly onto a preparatory TLC plate and purified by preparative TLC (80% EtOAc/Hexanes) to afford vinyl silane **55** (9.0 mg, 0.0200 mmol, 90% yield) as a colorless oil;  $^1\text{H}$  NMR (400 MHz,  $\text{CDCl}_3$ )  $\delta$  7.68 – 7.46 (m, 2H), 7.39 – 7.31 (m, 3H), 5.80 (t,  $J = 1.4$  Hz, 1H), 5.70 – 5.64 (m, 1H), 5.54 (d,  $J = 2.8$  Hz, 1H), 5.04 (dd,  $J = 7.1, 5.3$  Hz, 1H), 4.66 – 4.59 (m, 1H), 4.40 – 4.32 (m, 1H), 3.32 (td,  $J = 10.6, 7.1$  Hz, 1H), 2.94 – 2.74 (m, 2H), 2.50 – 2.24 (m, 5H), 2.22 – 2.09 (m, 1H), 1.85 (dd,  $J = 14.9, 5.5$  Hz, 1H), 1.52 (s, 3H), 1.47 (s, 3H), 0.41 (s, 3H), 0.39 (s, 3H);  $^{13}\text{C}$  NMR (100 MHz,  $\text{CDCl}_3$ )  $\delta$  196.0, 173.4, 157.3, 147.7, 146.3, 138.9, 134.2, 129.0, 128.6, 128.6, 128.0, 112.7, 82.6, 82.3, 55.1, 47.3, 43.7, 42.1, 41.9, 40.5, 38.3, 26.5, 18.0, -2.7, -3.2. ; IR (Neat Film NaCl) 3434, 3049, 2962, 1762, 1654, 1427, 1376, 1290, 1250, 1216, 1173, 1160, 1109, 1030, 992, 933, 891, 834, 817, 776, 736, 703  $\text{cm}^{-1}$ ; HRMS (MM: ES+)  $m/z$  calc'd for  $\text{C}_{27}\text{H}_{35}\text{O}_4\text{Si}$   $[\text{M}+\text{H}]^+$ : 451.2305, found 451.2314;  $[\alpha]_{\text{D}}^{25.0} -106.1$  ( $c$  0.60,  $\text{CHCl}_3$ ).



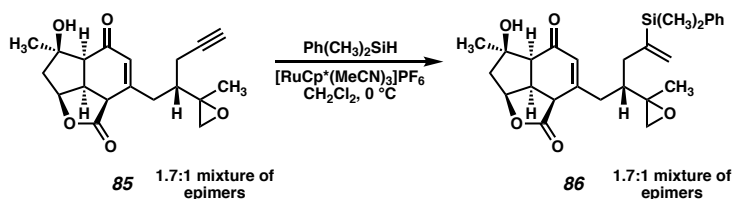
**Cyclobutane 83:** A 1-dram vial was charged with vinyl silane **55** (22 mg, 0.0488 mmol, 1.0 equiv) in PhH (5.0 mL). The solution was sparged with N<sub>2</sub> for 5 min, and placed in a photoreactor equipped with Hitachi UVA bulbs (F8T5-BLB, ~350 nm). The reaction was stirred under 350 nm irradiation for 10 h, after which no starting material remained (as judged by TLC). An <sup>1</sup>H NMR spectrum of the crude product shows a mixture with **83** as the major constituent. The crude white solid was purified by flash chromatography (50% EtOAc/Hexanes), followed by normal-phase (SiO<sub>2</sub>) preparative HPLC (EtOAc/Hexanes, 7.0 mL/min, monitoring wavelength = 254 nm, isocratic–50% EtOAc/Hexanes, 10 min) then reverse-phase (C18) preparative HPLC (MeCN/H<sub>2</sub>O, 9.0 mL/min, monitoring wavelength = 260 nm, isocratic– 70% MeCN/H<sub>2</sub>O, 10 min) to afford pure **83** (5.0 mg, 0.0111 mmol, 23 % yield). X-ray quality crystals were grown by slow cooling from *i*-PrOH; <sup>1</sup>H NMR (400 MHz, CDCl<sub>3</sub>) δ 7.54 – 7.46 (m, 2H), 7.38 – 7.32 (m, 3H), 5.68 – 5.61 (m, 1H), 5.40 (d, *J* = 2.8 Hz, 1H), 4.95 (ddd, *J* = 7.0, 5.6, 1.6 Hz, 1H), 3.46 (td, *J* = 10.2, 6.7 Hz, 1H), 3.09 – 2.93 (m, 1H), 2.89 – 2.78 (m, 2H), 2.77 – 2.61 (m, 2H), 2.33 – 2.14 (m, 4H), 1.98 (dd, *J* = 14.8, 5.6 Hz, 1H), 1.94 – 1.85 (m, 1H), 1.75 (dd, *J* = 13.1, 4.3 Hz, 1H), 1.41 (s, 3H), 1.00 (s, 3H), 0.37 (s, 6H); <sup>13</sup>C NMR (100 MHz, CDCl<sub>3</sub>) δ 215.1, 175.7, 148.1, 138.2, 134.1, 129.2, 127.9, 126.9, 82.0, 81.5, 55.1, 49.2, 46.6, 46.6, 44.5, 43.5, 38.7, 38.6, 36.1, 34.1, 31.0, 27.6, 21.7, -2.8, -2.9; IR (Neat Film NaCl) 3453, 2934, 2858, 1759, 1689, 1428, 1375, 1248, 1206, 1106, 1012, 938, 858, 833, 818, 703 cm<sup>-1</sup>; HRMS (MM:

ES+)  $m/z$  calc'd for  $C_{27}H_{35}O_4Si$   $[M+H]^+$ : 451.2305, found 451.2321;  $[\alpha]_D^{25.0} -113.4^\circ$  ( $c$  0.12,  $CHCl_3$ ).



**Epoxides 85 and *epi*-85:** A 100 mL round-bottom flask was charged with enone **56** (450 mg, 1.43 mmol, 1.0 equiv) in  $CH_2Cl_2$  (48 mL). The solution was cooled to  $0^\circ C$ , and *m*-CPBA (~70% wt/wt; 1.06 g, 4.29 mmol, 3.0 equiv) was added in one portion. The mixture was stirred while gradually warming to  $23^\circ C$  over 2 h, and then stirred an additional 10 h at  $23^\circ C$ , at which point **56** had been completely consumed as judged by TLC. The reaction mixture was poured directly onto a flash column and purified by flash chromatography (50%-60%-70%-80% EtOAc/Hexanes) to afford epoxides **85** and *epi*-**85** (410 mg, 1.24 mmol, 87% yield) as a white foam. The products are isolated as a 1.7:1 mixture of diastereomers (judged by  $^1H$  NMR) which was used in the subsequent reaction. A portion of this mixture was subjected to normal phase ( $SiO_2$ ) preparative HPLC (EtOAc/Hexanes, 7.0 mL/min, monitor wavelength 254 nm, 60% EtOAc/Hexanes) to obtain pure samples of the two products for the purposes of characterization; *Diastereomer 1 (minor)*:  $^1H$  NMR (400 MHz,  $CDCl_3$ )  $\delta$  6.05 (d,  $J = 1.4$  Hz, 1H), 5.12 (dd,  $J = 6.7, 5.4$  Hz, 1H), 3.75 – 3.42 (m, 2H), 2.99 (ddt,  $J = 15.6, 6.2, 1.2$  Hz, 1H), 2.76 – 2.63 (m, 2H), 2.57 (d,  $J = 4.5$  Hz, 1H), 2.54 – 2.44 (m, 2H), 2.44 – 2.27 (m, 2H), 2.05 (t,  $J = 2.7$  Hz, 1H), 1.99 – 1.84 (m, 2H), 1.50 (s, 3H), 1.34 (d,  $J = 0.7$  Hz, 3H);  $^{13}C$  NMR (100 MHz,  $CDCl_3$ )  $\delta$  196.0, 173.6, 156.4, 128.5, 82.9, 82.7, 81.8, 71.2, 58.6, 55.2, 54.2, 47.5, 42.6, 42.3, 42.2, 36.5, 26.4, 21.0, 18.4; IR (Neat film, NaCl) 3436, 3283, 2970, 2926, 1758, 1656, 1378, 1292, 1177, 1109,

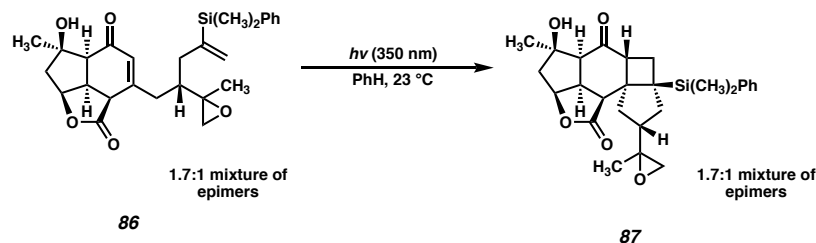
735  $\text{cm}^{-1}$ ; (MM: ESI-APCI+)  $m/z$  calc'd for  $\text{C}_{19}\text{H}_{23}\text{O}_5$   $[\text{M}+\text{H}]^+$ : 331.1545, found 331.1538;  $[\alpha]_{\text{D}}^{25.0} -144.5$  ( $c$  1.0,  $\text{CHCl}_3$ ); *Diastereomer 2 (major)*:  $^1\text{H}$  NMR (400 MHz,  $\text{CDCl}_3$ )  $\delta$  6.10 (t,  $J = 1.6$  Hz, 1H), 5.11 (dd,  $J = 7.1, 5.4$  Hz, 1H), 3.84 (dt,  $J = 10.9, 1.2$  Hz, 1H), 3.76 – 3.57 (m, 1H), 3.35 – 3.16 (m, 1H), 2.70 (dd,  $J = 4.6, 0.8$  Hz, 1H), 2.63 – 2.45 (m, 3H), 2.40 – 2.24 (m, 3H), 2.05 (t,  $J = 2.6$  Hz, 1H), 1.95 – 1.84 (m, 2H), 1.49 (s, 3H), 1.25 (s, 3H);  $^{13}\text{C}$  NMR (100 MHz,  $\text{CDCl}_3$ )  $\delta$  196.4, 174.1, 156.4, 129.3, 82.9, 82.9, 81.3, 71.1, 58.5, 55.5, 54.2, 47.5, 42.8, 42.8, 41.3, 38.5, 26.4, 22.5, 16.0; IR (Neat film, NaCl) 3436, 3283, 2250, 1758, 1657, 1378, 1109, 735  $\text{cm}^{-1}$ ; HRMS (MM: ESI-APCI+)  $m/z$  calc'd for  $\text{C}_{19}\text{H}_{23}\text{O}_5$   $[\text{M}+\text{H}]^+$ : 331.1545, found 331.1540;  $[\alpha]_{\text{D}}^{25.0} -83.5^\circ$  ( $c$  1.0,  $\text{CHCl}_3$ ).



**Vinyl Silanes **86** and *epi-86*:** A 250 mL round-bottom flask was charged with a mixture of **85** and *epi-85* (725 mg, 2.19 mmol, 1.0 equiv) in  $\text{CH}_2\text{Cl}_2$  (22 mL). Phenyltrimethylsilane (400  $\mu\text{L}$ , 2.63 mmol, 1.2 equiv) was added, and the mixture was cooled to 0  $^\circ\text{C}$ .  $[\text{RuCp}^*(\text{MeCN})_3]\text{PF}_6$  (10 mg/mL stock solution, 5.5 mL, 0.110 mmol, 0.05 equiv, prepared in a nitrogen-filled glovebox) was added dropwise. Following the addition, the reaction was stirred 5 min at 0  $^\circ\text{C}$ , after which the starting material was no longer detectable by TLC. The reaction mixture was poured directly onto a flash column and purified by flash chromatography (0%-50% EtOAc/Hexanes) to afford vinyl silanes **86** and *epi-86* (870 mg, 1.86 mmol, 85% yield) as a colorless foam. The products were isolated as a 1.7:1 mixture of diastereomers (judged by  $^1\text{H}$  NMR), which were characterized separately;

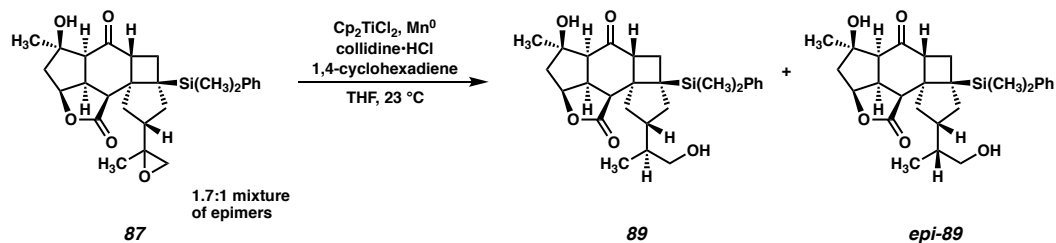


*Diastereomer 1 (minor):*  $^1\text{H}$  NMR (400 MHz,  $\text{CDCl}_3$ )  $\delta$  7.54 (ddd,  $J = 4.9, 2.4, 1.7$  Hz, 2H), 7.37 – 7.29 (m, 3H), 5.83 (d,  $J = 1.2$  Hz, 1H), 5.71 (dd,  $J = 2.3, 1.3$  Hz, 1H), 5.61 (d,  $J = 2.7$  Hz, 1H), 4.99 (dd,  $J = 7.0, 5.3$  Hz, 1H), 3.15 (td,  $J = 10.6, 7.0$  Hz, 1H), 2.84 (ddd,  $J = 14.2, 3.3, 1.6$  Hz, 1H), 2.72 (dt,  $J = 13.6, 2.2$  Hz, 1H), 2.45 (d,  $J = 4.7$  Hz, 1H), 2.39 (d,  $J = 10.4$  Hz, 1H), 2.29 (d,  $J = 15.0$  Hz, 1H), 2.20 – 1.98 (m, 5H), 1.84 (dd,  $J = 15.0, 5.4$  Hz, 1H), 1.47 (s, 3H), 1.20 (s, 3H), 0.46 (s, 3H), 0.38 (s, 3H);  $^{13}\text{C}$  NMR (100 MHz,  $\text{CDCl}_3$ )  $\delta$  195.7, 173.0, 157.2, 147.4, 139.6, 134.4, 129.2, 128.7, 128.7, 127.9, 82.7, 82.0, 58.6, 55.2, 54.9, 47.3, 42.3, 41.9, 40.4, 40.0, 36.3, 26.5, 16.6, -2.7, -3.9; IR (Neat film, NaCl) 3435, 2960, 1762, 1659, 1426, 1376, 1288, 1247, 1217, 1163, 1106, 1034, 992, 938, 838, 818, 753, 703  $\text{cm}^{-1}$ ; HRMS (FAB+)  $m/z$  calc'd for  $\text{C}_{27}\text{H}_{35}\text{O}_5\text{Si}$   $[\text{M}+\text{H}]^+$ : 467.2254, found 467.2265;  $[\alpha]_{\text{D}}^{25.0} -62.0^\circ$  ( $c$  1.0,  $\text{CHCl}_3$ ); *Diastereomer 2 (major):*  $^1\text{H}$  NMR (400 MHz,  $\text{CDCl}_3$ )  $\delta$  7.63 – 7.44 (m, 2H), 7.39 – 7.31 (m, 3H), 6.03 (t,  $J = 1.5$  Hz, 1H), 5.73 (dt,  $J = 2.4, 1.2$  Hz, 1H), 5.58 (d,  $J = 2.6$  Hz, 1H), 5.07 (dd,  $J = 7.1, 5.3$  Hz, 1H), 3.53 (td,  $J = 10.6, 7.1$  Hz, 1H), 3.38 (dt,  $J = 11.0, 1.2$  Hz, 1H), 3.23 – 3.07 (m, 1H), 2.48 (d,  $J = 10.3$  Hz, 1H), 2.43 – 2.19 (m, 5H), 2.17 – 2.06 (m, 2H), 1.89 (dd,  $J = 14.9, 5.5$  Hz, 1H), 1.50 (s, 3H), 1.13 (d,  $J = 0.6$  Hz, 3H), 0.40 (d,  $J = 0.8$  Hz, 6H);  $^{13}\text{C}$  NMR (100 MHz,  $\text{CDCl}_3$ )  $\delta$  196.0, 173.8, 157.8, 147.0, 138.2, 134.2, 129.3, 129.3, 129.0, 128.2, 82.7, 82.5, 59.2, 55.3, 53.6, 47.5, 42.2, 42.1, 40.7, 40.2, 38.3, 26.6, 15.9, -2.8, -2.9; IR (Neat film, NaCl) 3439, 2924, 2854, 2282, 1758, 1656, 1428, 1373, 1291, 1266, 1248, 1214, 1164, 1108, 992, 937, 838, 821, 738  $\text{cm}^{-1}$ ; HRMS (FAB+)  $m/z$  calc'd for  $\text{C}_{27}\text{H}_{35}\text{O}_5\text{Si}$   $[\text{M}+\text{H}]^+$ : 467.2254, found 467.2265;  $[\alpha]_{\text{D}}^{25.0} -17.9^\circ$  ( $c$  0.6,  $\text{CHCl}_3$ ).



**Cyclobutanes 87 and *epi*-87:** A mixture of vinyl silanes **86** and *epi*-**86** (870 mg, 1.86 mmol, 1.0 equiv) was divided into 11 portions (79 mg each). Each portion was added to a 40 mL scintillation vial with PhH (34 mL). Each vial was then sparged with nitrogen for 5 min, and placed in a photoreactor equipped with Hitachi UVA bulbs (F8T5-BLB, ~350 nm). The reactions were stirred under 350 nm irradiation for 5 h, after which no starting material remained (as judged by TLC). The reactions were combined in a 1 L round bottom flask, and concentrated onto Celite<sup>®</sup>. The resulting solid was loaded onto a column, and purified by flash chromatography (30%-40%-50%-60%-70%-80% EtOAc/Hexanes) to afford the cyclobutanes **86** and *epi*-**86** (620 mg, 1.33 mmol, 71% yield) as a white solid. The products are isolated as a 1.7:1 mixture of diastereomers (judged by <sup>1</sup>H NMR), which were characterized separately; *Note: The <sup>1</sup>H NMR spectra of these intermediates show broadened signals which were difficult to assign and integrate properly. Additionally, several signals were found to be missing from the <sup>13</sup>C NMR spectra. We attribute these observations to hindered rotation of the –Si(CH<sub>3</sub>)<sub>2</sub>Ph group about the highly congested cyclobutane ring. The NMR spectra are reported as observed, and the stereochemistry (and identity) of these products is assigned based upon the NMR and X-ray data obtained for **90** and *epi*-**90**. Diastereomer 1 (minor): <sup>1</sup>H NMR (400 MHz, CDCl<sub>3</sub>) δ 7.51 (s, 2H), 7.35 – 7.28 (m, 3H), 4.93 (s, 1H), 3.70 – 3.54 (m, 1H), 3.47 (s, 1H), 3.03 (d, *J* = 9.3 Hz, 1H), 2.70 – 2.30 (m, 4H), 1.93 (dd, *J* = 15.2, 4.8 Hz, 1H), 1.68 (s, 1H), 1.45 (d, *J* = 2.1 Hz, 3H),*

1.34 – 1.17 (m, 4H), 0.56 (d,  $J = 18.1$  Hz, 4H);  $^{13}\text{C}$  NMR (100 MHz,  $\text{CDCl}_3$ )  $\delta$  205.8, 134.3, 128.5, 127.6, 82.1, 81.4, 60.3, 57.6, 52.3, 50.9, 49.0, 47.7, 47.6, 40.1, 38.9, 35.0, 27.5; IR (Neat film, NaCl) 3395, 2958, 1773, 1686, 1369, 1256, 1202, 1089, 1014, 815, 776, 732  $\text{cm}^{-1}$ ; HRMS (ES+)  $m/z$  calc'd for  $\text{C}_{27}\text{H}_{35}\text{O}_5\text{Si}$   $[\text{M}+\text{H}]^+$ : 467.2254, found 467.2280;  $[\alpha]_{\text{D}}^{25.0} -41.1^\circ$  ( $c$  0.19,  $\text{CHCl}_3$ ); *Diastereomer 2 (major)*:  $^1\text{H}$  NMR (400 MHz,  $\text{CDCl}_3$ )  $\delta$  7.59 – 7.45 (m, 2H), 7.34 – 7.28 (m, 3H), 4.92 (s, 1H), 3.60 (td,  $J = 9.8, 6.2$  Hz, 1H), 3.47 (s, 1H), 3.02 (d,  $J = 9.3$  Hz, 1H), 2.56 (dd,  $J = 10.0, 5.3$  Hz, 3H), 2.42 – 2.31 (m, 1H), 1.94 (dd,  $J = 15.1, 4.8$  Hz, 1H), 1.67 (s, 2H), 1.45 (s, 3H), 1.25 (d,  $J = 1.7$  Hz, 3H), 0.53 (s, 5H);  $^{13}\text{C}$  NMR (100 MHz,  $\text{CDCl}_3$ )  $\delta$  205.8, 134.3, 128.5, 127.7, 82.1, 81.5, 60.3, 57.1, 53.9, 50.9, 49.0, 47.7, 40.7, 38.6, 29.8, 27.5; IR (Neat film, NaCl) 3388, 2960, 2929, 1773, 1686, 1552, 1426, 1368, 1248, 1203, 1178, 1107, 1088, 817, 724, 696  $\text{cm}^{-1}$ ; HRMS (ES+)  $m/z$  calc'd for  $\text{C}_{27}\text{H}_{35}\text{O}_5\text{Si}$   $[\text{M}+\text{H}]^+$ : 467.2254, found 467.1853;  $[\alpha]_{\text{D}}^{25.0} -23.1^\circ$  ( $c$  0.19,  $\text{CHCl}_3$ ).

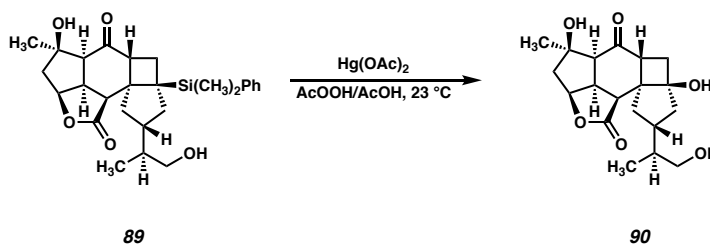


**Diols 89 and epi-89:** A 100 mL round-bottom flask was charged with a mixture of epoxides **87** and *epi-87* (620 mg, 1.33 mmol, 1.0 equiv),  $\text{Cp}_2\text{TiCl}_2$  (66 mg, 0.266 mmol, 0.20 equiv), Mn dust (80 mg, 1.46 mmol, 1.10 equiv) and collidine·HCl (262 mg, 1.66 mmol, 1.25 equiv) in THF (27 mL). To this red suspension was added 1,4-cyclohexadiene (567  $\mu\text{L}$ , 599 mmol, 4.5 equiv) and the suspension gradually changed to a blue/grey color. The mixture was stirred at 23 °C for 1.5 h, after which the starting material was completely

consumed, as judged by TLC. Celite® was then added directly to the reaction mixture and the solvent was removed under reduced pressure. The resulting solid was loaded directly onto a flash column and purified by flash chromatography (60%-65%-70%-75%-80%-90%-100% EtOAc/Hexanes) to afford diols **89** (385 mg, 0.781 mmol, 62% yield) and *epi*-**89** (224 mg, 0.478 mmol, 36% yield) as white solids, which were separable at this point.

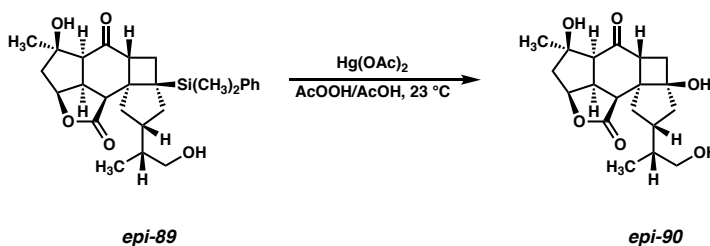
*Note: The <sup>1</sup>H NMR spectra of these intermediates show broadened signals which were difficult to assign and integrate properly. Additionally, several signals were found to be missing from the <sup>13</sup>C NMR spectra. We attribute these observations to hindered rotation of the –Si(CH<sub>3</sub>)<sub>2</sub>Ph group about the highly congested cyclobutane ring. The NMR spectra are reported as observed, and the stereochemistry (and identity) of these products is assigned based upon the NMR and X-ray data obtained for **90** and *epi*-**90**; **89**: <sup>1</sup>H NMR (400 MHz, CD<sub>3</sub>OD) δ 7.57 – 7.48 (m, 2H), 7.30 – 7.22 (m, 3H), 4.95 (s, 1H), 3.98 (s, 1H), 3.74 (tt, *J* = 10.1, 5.1 Hz, 1H), 3.64 (q, *J* = 10.2, 9.2 Hz, 1H), 3.52 – 3.38 (m, 1H), 3.30 – 3.15 (m, 1H), 2.76 – 1.38 (m, 11H), 1.34 (s, 3H), 1.10 – 0.83 (m, 3H), 0.52 (s, 4H); <sup>13</sup>C NMR (100 MHz, CD<sub>3</sub>OD) δ 210.1, 168.5, 151.9, 135.3, 129.2, 128.4, 108.8, 84.4, 81.6, 81.6, 67.3, 65.6, 61.9, 52.5, 45.9, 41.7, 41.5, 27.3, 15.7; IR (Neat film, NaCl) 3380, 2958, 2924, 2869, 1770, 1694, 1360, 1254, 1204, 1090, 1416, 828, 736, 730, 702 cm<sup>-1</sup>; HRMS (ES+) *m/z* calc'd for C<sub>27</sub>H<sub>37</sub>O<sub>5</sub>Si [M+H]<sup>+</sup>: 469.2410, found 469.2437; [α]<sub>D</sub><sup>25.0</sup> –37.0° (*c* 0.24, CHCl<sub>3</sub>); *epi*-**89**: <sup>1</sup>H NMR (400 MHz, CD<sub>3</sub>OD) δ 7.58 – 7.46 (m, 2H), 7.27 (t, *J* = 3.2 Hz, 3H), 4.94 (t, *J* = 5.7 Hz, 1H), 3.81 – 3.69 (m, 1H), 3.69 – 3.58 (m, 1H), 3.48 (q, *J* = 7.1, 4.5 Hz, 1H), 3.33 (d, *J* = 13.8 Hz, 4H), 3.25 – 3.11 (m, 1H), 2.68 – 1.39 (m, 11H), 1.34 (s, 3H), 1.10 – 0.74 (m, 4H), 0.52 (d, *J* = 11.9 Hz, 5H); <sup>13</sup>C NMR (100 MHz, CD<sub>3</sub>OD) δ 210.1, 178.1, 135.3, 129.2, 128.4, 84.3, 81.6, 67.4, 61.9, 52.5, 47.8, 47.1, 47.1, 46.2, 44.1, 42.4, 41.8,*

40.0, 35.9, 27.3, 15.6, -2.1, -4.9; IR (Neat film, NaCl) 3378, 2954, 2937, 2868, 2353, 1771, 1696, 1558, 1364, 1258, 1245, 1086, 827  $\text{cm}^{-1}$ ; HRMS (ES+)  $m/z$  calc'd for  $\text{C}_{27}\text{H}_{37}\text{O}_5\text{Si}$   $[\text{M}+\text{H}]^+$ : 469.2410, found 469.2440;  $[\alpha]_{\text{D}}^{25.0}$   $-39.9^\circ$  ( $c$  0.90,  $\text{CHCl}_3$ ).



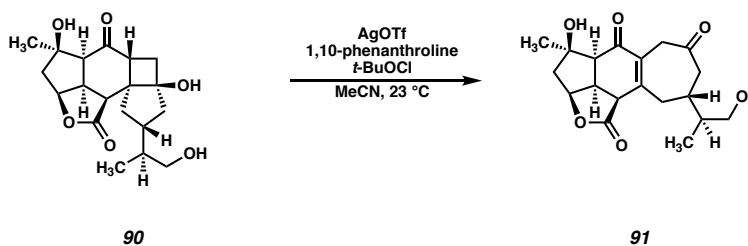
**Triol 90:** A 20 mL scintillation vial was charged with **89** (80 mg, 0.171 mmol, 1.0 equiv) and AcOOH (30% in aqueous AcOH, 3.4 mL). To this solution was added  $\text{Hg}(\text{OAc})_2$  (100 mg, 0.341 mmol, 2.0 equiv) in a single portion. The reaction was stirred 45 min at 23  $^\circ\text{C}$ , after which no **89** remained (as judged by LCMS). The reaction mixture was diluted with EtOAc and pipetted over an ice-cold mixture of sat. aq.  $\text{Na}_2\text{S}_2\text{O}_3$  and saturated, aqueous  $\text{NaHCO}_2$  (1:4). This aqueous solution was then extracted with EtOAc (3x) then  $\text{CHCl}_3/i\text{-PrOH}$  (3:1) (2x). The organic extracts were combined and dried over  $\text{Na}_2\text{SO}_4$ , filtered, and concentrated under reduced pressure to afford a crude solid which was purified by flash chromatography (80%-100% EtOAc/Hexanes) to afford triol **90** (33 mg, 0.942 mmol, 55% yield) as a white solid. X-ray quality crystals were obtained by slow cooling from EtOH/ $\text{CH}_2\text{Cl}_2$ /Hexanes;  $^1\text{H}$  NMR (400 MHz,  $\text{CD}_3\text{OD}$ )  $\delta$  5.16 (dd,  $J = 6.2, 4.7$  Hz, 1H), 3.88 (dd,  $J = 9.8, 7.7$  Hz, 1H), 3.72 (ddd,  $J = 10.6, 9.3, 6.3$  Hz, 1H), 3.55 – 3.47 (m, 2H), 3.37 – 3.32 (m, 1H), 2.58 (d,  $J = 10.6$  Hz, 1H), 2.35 (d,  $J = 15.0$  Hz, 1H), 2.23 (dd,  $J = 11.9, 9.7$  Hz, 1H), 2.19 – 1.98 (m, 3H), 1.95 (dd,  $J = 15.1, 4.9$  Hz, 1H), 1.85 (ddd,  $J = 12.9, 6.1, 2.0$  Hz, 1H), 1.70 (dd,  $J = 13.1, 9.9$  Hz, 1H), 1.54 – 1.41 (m, 2H), 1.35 (s, 3H), 0.93

(d,  $J = 6.8$  Hz, 3H);  $^{13}\text{C}$  NMR (100 MHz,  $\text{CD}_3\text{OD}$ )  $\delta$  209.4, 181.7, 89.3, 88.2, 81.6, 67.1, 62.1, 59.0, 51.8, 51.3, 47.8, 47.3, 45.8, 41.8, 41.3, 41.2, 40.7, 27.3, 15.3; IR (Neat Film NaCl) 3308, 2936, 1694, 1371, 1217, 1184, 1120, 1016  $\text{cm}^{-1}$ ; HRMS (MM: ESI-APCI+)  $m/z$  calc'd for  $\text{C}_{19}\text{H}_{27}\text{O}_6$   $[\text{M}+\text{H}]^+$ : 351.1802, found 315.1790;  $[\alpha]_{\text{D}}^{25.0} -61.1^\circ$  ( $c$  0.5, MeOH).



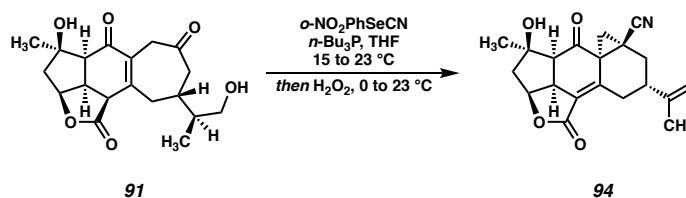
**Triol *epi-90*:** A 20 mL scintillation vial was charged with *epi-89* (80 mg, 0.171 mmol, 1.0 equiv) and AcOOH (30% in aqueous AcOH, 3.4 mL). To this solution was added  $\text{Hg}(\text{OAc})_2$  (100 mg, 0.341 mmol, 2.0 equiv) in a single portion. The reaction was stirred 45 min at 23 °C, after which no *epi-89* remained (as judged by LCMS). The reaction mixture was diluted with EtOAc (10 mL) and pipetted over an ice-cold mixture of sat. aq.  $\text{Na}_2\text{S}_2\text{O}_3$  and saturated, aqueous  $\text{NaHCO}_2$  (1:4). This aqueous solution was then extracted with EtOAc (3x) then  $\text{CHCl}_3/i\text{-PrOH}$  (3:1) (2x). The organic extracts were combined and dried over  $\text{Na}_2\text{SO}_4$ , filtered, and concentrated under reduced pressure to afford a crude solid which was purified by flash chromatography (80%-100% EtOAc/Hexanes) to afford the title compound (37 mg, 0.0106 mmol, 62% yield) as a white solid. X-ray quality crystals were obtained by layer diffusion of hexanes into  $\text{CH}_2\text{Cl}_2/\text{EtOH}$ ;  $^1\text{H}$  NMR (400 MHz,  $\text{CD}_3\text{OD}$ )  $\delta$  5.16 (dd,  $J = 6.2, 4.7$  Hz, 1H), 3.88 (dd,  $J = 9.8, 7.7$  Hz, 1H), 3.79 – 3.64 (m, 1H), 3.57 – 3.45 (m, 2H), 3.40 – 3.34 (m, 1H), 2.57 (d,  $J = 10.6$  Hz, 1H), 2.35 (d,  $J = 15.1$  Hz, 1H), 2.28 – 2.11 (m, 2H), 2.07 (dd,  $J = 11.9, 7.7$  Hz, 1H), 2.02 – 1.90 (m, 2H), 1.87

(ddd,  $J = 13.0, 6.1, 2.1$  Hz, 1H), 1.68 (dd,  $J = 13.1, 10.2$  Hz, 1H), 1.57 – 1.43 (m, 2H), 1.35 (s, 3H), 0.94 (d, 3H);  $^{13}\text{C}$  NMR (100 MHz,  $\text{CD}_3\text{OD}$ )  $\delta$  209.4, 181.7, 89.0, 88.2, 81.6, 66.9, 62.1, 59.3, 51.8, 51.3, 47.8, 47.3, 45.1, 41.7, 41.5, 41.4, 40.7, 27.3, 15.4; IR (Neat Film NaCl) 3464, 3292, 2953, 1720, 1693, 1372, 1190, 1104  $\text{cm}^{-1}$ ; HRMS (MM: ESI-APCI+)  $m/z$  calc'd for  $\text{C}_{19}\text{H}_{27}\text{O}_6$   $[\text{M}+\text{H}]^+$ : 351.1802, found 315.1790;  $[\alpha]_{\text{D}}^{25.0} -42.2^\circ$  ( $c$  0.5, MeOH).



**Diol 91:** To a stirred suspension of triol **90** (21 mg, 0.0599 mmol, 1.0 equiv), AgOTf (6 mg, 0.0240 mmol, 0.40 equiv), and 1,10-phenanthroline (9 mg, 0.0479 mmol, 0.80 equiv) in MeCN (3.2 mL, 0.019 M) was added *t*-BuOCl (14  $\mu\text{L}$ , 0.120 mmol, 2.0 equiv) at 23  $^\circ\text{C}$ . The suspension changed from white to red, and then to dark brown. The reaction mixture was allowed to stir at 23  $^\circ\text{C}$  for 12 h, after which no starting material remained (as judged by TLC and LCMS). The reaction mixture was diluted with EtOAc (5 mL), and quenched with 5 drops of saturated aqueous  $\text{Na}_2\text{S}_2\text{O}_3$ , after which the dark brown color quickly dissipated. The mixture was passed directly over a short plug of  $\text{SiO}_2$ , and the eluent was concentrated onto  $\text{SiO}_2$  and dry loaded onto a column. The crude was purified by flash chromatography (50 – 100% EtOAc/hexanes) to afford an unstable intermediate (presumed to be the  $\gamma$ -chloroketone) which was not characterized further. This product was dissolved in MeOH (5 mL). TLC  $\text{SiO}_2$  (scraped from TLC plates and crushed with a mortar and pestle) was added (c.a. 1 g). The suspension was allowed to stir for 12 h at 23  $^\circ\text{C}$ , after

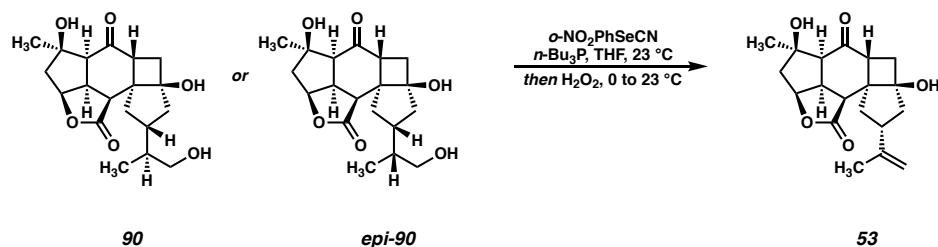
which the abovementioned product had been completely consumed (as judged by TLC). The MeOH was removed under reduced pressure, and then the solids were resuspended in acetone (10 mL) and stirred for 1 h. The suspension was filtered through a plug of Celite® and concentrated to afford diol **91** (10 mg, 40% yield) as a white solid; <sup>1</sup>H NMR (400 MHz, CDCl<sub>3</sub>) δ 5.14 (dd, *J* = 6.9, 5.6 Hz, 1H), 3.91 (d, *J* = 14.7 Hz, 1H), 3.69 – 3.47 (m, 4H), 3.27 (dd, *J* = 14.8, 1.8 Hz, 1H), 2.74 (d, *J* = 12.8 Hz, 1H), 2.67 – 2.52 (m, 5H), 2.31 (d, *J* = 15.0 Hz, 1H), 1.91 (dd, *J* = 15.0, 5.6 Hz, 1H), 1.49 (s, 3H), 0.86 (d, *J* = 7.1 Hz, 3H). <sup>13</sup>C NMR (100 MHz, CDCl<sub>3</sub>) δ 208.0, 192.9, 174.6, 152.3, 132.7, 82.9, 65.1, 54.6, 49.5, 47.4, 45.5, 41.3, 41.1, 39.6, 35.9, 34.5, 26.1, 11.5; IR (Neat Film NaCl) 3778, 3680, 2918, 2848, 1758, 1709, 1657, 1461, 1372, 1167, 1089, 1030, 823 cm<sup>-1</sup>; HRMS (MM: ESI-APCI+) *m/z* calc'd for C<sub>19</sub>H<sub>23</sub>O<sub>6</sub> [M–OH]<sup>+</sup>: 331.1540, found 331.1541; [α]<sub>D</sub><sup>25.0</sup> –60.5° (*c* 0.1, CHCl<sub>3</sub>).



**Nitrile 94:** To a stirred solution of diol **91** (4 mg, 0.0115 mmol, 1.0 equiv) in THF (400 μL, 0.029 M) cooled to 15 °C in a nitrogen-filled glovebox was added *o*-NO<sub>2</sub>PhSeCN (156 mg/mL solution in THF, 25 μL, 0.0173 mmol, 1.5 equiv). To this light-brown solution was added *n*-Bu<sub>3</sub>P (83 mg/mL solution in THF, 42 μL, 0.0173 mmol, 1.5 equiv), at which point the solution rapidly changed to deep red in color. The reaction mixture was stirred 20 min at 15 °C and then warmed to 23 °C and stirred an additional 2 h. At this point, a small amount of starting material was detected by LCMS. An additional portion of *o*-NO<sub>2</sub>PhSeCN (156 mg/mL solution in THF, 8 μL, 0.00775 mmol, 0.5 equiv) was added, followed by *n*-Bu<sub>3</sub>P (83 mg/mL solution in THF, 14 μL, 0.00775 mmol, 0.5 equiv) at 23

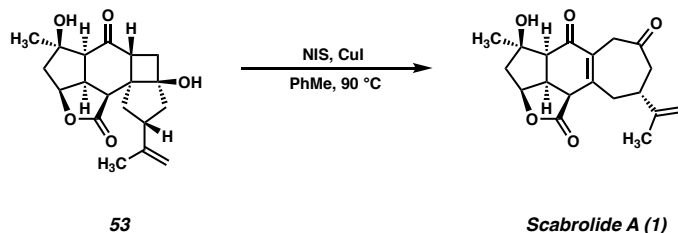


°C, and the reaction was subsequently allowed to stir an additional 2 h. The reaction was removed from the glovebox and cooled to 0 °C. H<sub>2</sub>O<sub>2</sub> (30%, 60 μL) was added dropwise, and the reaction was stirred 1 h at 0 °C. The mixture was allowed to warm to 23 °C, and stirred an additional 12 h. The reaction mixture was purified directly by preparative HPLC to afford nitrile **94** (1.0 mg, 26% yield) as a white solid. X-ray quality crystals were obtained by layer-diffusion of hexanes into a CH<sub>2</sub>Cl<sub>2</sub> solution of **94**. <sup>1</sup>H NMR (400 MHz, CDCl<sub>3</sub>) δ 5.16 (td, *J* = 7.8, 3.1 Hz, 1H), 4.82 (t, *J* = 1.6 Hz, 1H), 4.74 (d, *J* = 0.9 Hz, 1H), 4.07 – 4.00 (m, 1H), 3.83 (td, *J* = 7.9, 4.2 Hz, 1H), 2.88 (dd, *J* = 7.6, 1.1 Hz, 1H), 2.66 (ddd, *J* = 13.9, 4.7, 1.7 Hz, 1H), 2.46 (dd, *J* = 4.8, 0.9 Hz, 1H), 2.35 – 2.25 (m, 2H), 2.23 – 2.14 (m, 1H), 1.90 (dd, *J* = 14.1, 11.9 Hz, 1H), 1.73 (t, *J* = 1.3 Hz, 3H), 1.60 (d, *J* = 5.0 Hz, 1H), 1.54 (s, 3H); *Due to the limited quantity of material obtained, not all expected <sup>13</sup>C signals are visible because of the low concentration of the sample. The shifts are reported as observed:* <sup>13</sup>C NMR (100 MHz, CDCl<sub>3</sub>) δ 198.8, 192.2, 146.8, 146.0, 111.2, 83.9, 80.6, 58.2, 49.2, 45.2, 39.7, 36.3, 31.5, 29.2, 28.5, 24.5, 20.9; IR (Neat Film NaCl) 3603, 2924, 2852, 1738, 1703, 1658, 1547, 1464, 1377, 1295, 1219, 1171, 1054 cm<sup>-1</sup>; HRMS (MM: ESI-APCI+) *m/z* calc'd for C<sub>20</sub>H<sub>22</sub>O<sub>4</sub>N [M+H]<sup>+</sup>: 340.1543, found 340.1553; [α]<sub>D</sub><sup>25.0</sup> -7.0 ° (*c* 0.1, CHCl<sub>3</sub>).



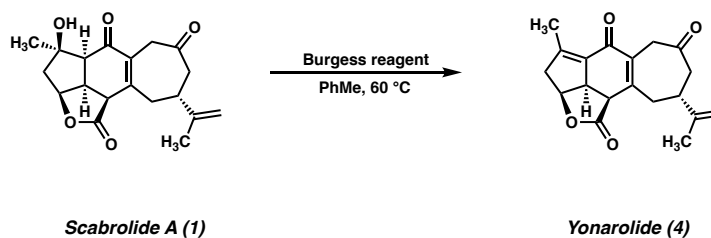
**Cyclobutanol 53:** In a nitrogen filled glovebox a 1-dram vial was charged with triol **90** (8.0 mg, 0.0228 mmol, 1.0 equiv) and  $o\text{-NO}_2\text{PhSeCN}$  (15.5 mg, 0.0685 mmol, 3.0 equiv) in THF (450  $\mu\text{L}$ ). To this orange solution was added  $n\text{-Bu}_3\text{P}$  (17  $\mu\text{L}$ , 0.0685 mmol, 3.0 equiv) dropwise via syringe, at which point the reaction mixture became deep red/brown in color. This solution was allowed to stir in the glovebox at  $23\text{ }^\circ\text{C}$  for 7 h, at which point **25** had been completely consumed, as judged by LCMS. The vial was then removed from the glovebox and cooled to  $0\text{ }^\circ\text{C}$  after which  $\text{H}_2\text{O}_2$  (30% w/w, 80  $\mu\text{L}$ ) was cautiously added dropwise. This orange solution was then stirred while gradually warming to  $23\text{ }^\circ\text{C}$  over c.a. 2 h and then stirred at  $23\text{ }^\circ\text{C}$  an additional 18 h. The reaction was then loaded directly onto a column and purified by flash chromatography (30%-40%-50% EtOAc/Hexanes) to afford cyclobutanol **53** (6.0 mg, 0.0181 mmol, 79% yield) as a white solid:  $^1\text{H}$  NMR (400 MHz,  $\text{CDCl}_3$ )  $\delta$  6.08 (s, 1H), 5.14 (dd,  $J = 6.1, 4.6$  Hz, 1H), 4.75 – 4.71 (m, 1H), 4.71 – 4.68 (m, 1H), 3.83 (dd,  $J = 9.6, 8.0$  Hz, 1H), 3.66 – 3.56 (m, 1H), 3.36 (d,  $J = 9.1$  Hz, 1H), 2.79 (ddd,  $J = 15.9, 13.0, 8.0$  Hz, 1H), 2.60 (d,  $J = 10.7$  Hz, 1H), 2.43 (d,  $J = 15.4$  Hz, 1H), 2.34 (dd,  $J = 12.1, 9.6$  Hz, 1H), 2.24 (dd,  $J = 12.1, 8.0$  Hz, 1H), 2.14 (ddd,  $J = 13.2, 9.8, 2.2$  Hz, 1H), 1.96 (dd,  $J = 15.3, 4.8$  Hz, 1H), 1.90 – 1.78 (m, 2H), 1.74 – 1.67 (m, 5H), 1.48 (s, 3H);  $^{13}\text{C}$  NMR (100 MHz,  $\text{CDCl}_3$ )  $\delta$  205.8, 179.2, 146.1, 109.9, 88.0, 86.0, 81.3, 60.6, 57.8, 50.3, 50.3, 47.7, 46.3, 45.3, 44.7, 40.8, 40.5, 27.6, 21.1; IR (Neat Film NaCl) 3346, 2936, 1726, 1710, 1598, 1366, 1325, 1218, 1194, 1123, 1088, 1011, 850, 822; HRMS

(MM: ESI-APCI+)  $m/z$  calc'd for  $C_{19}H_{25}O_5$   $[M+H]^+$ : 333.1697, found 333.1694;  $[\alpha]_D^{25.0}$   $-31.1^\circ$  ( $c$  0.4,  $CHCl_3$ ).



**Scabrolide A (1):** In a nitrogen-filled glovebox, a 1-dram vial was charged with cyclobutanol **53** (5.0 mg, 0.0151 mmol, 1.0 equiv), CuI (22.0 mg, 0.117 mmol, 7.8 equiv) and NIS (6.7 mg, 0.0300 mmol, 2.0 equiv) in PhMe (1.5 mL). The vial was stirred at 23 °C for 5 min, and then transferred to a preheated, 90 °C aluminum block. The reaction was stirred at 90 °C for 1 h. At this point, starting material remained, so an additional portion of NIS (3.3 mg, 0.0150 mmol, 1.0 equiv) was added, and the reaction stirred an additional 20 min at 90 °C. The mixture was then cooled to 23 °C and filtered through a pad of Celite, washing with EtOAc. This solution was concentrated to a red film, which was directly purified by reverse-phase (C18) preparative HPLC (MeCN/H<sub>2</sub>O, 5.0 mL/min, monitor wavelength = 260 nm, 30% MeCN ramp to 45% MeCN over 6 min) to afford scabrolide A (**1**) (3.0 mg, 0.00909 mmol, 61% yield) as a white solid. X-ray quality crystals were obtained by layer-diffusion of hexanes into a CH<sub>2</sub>Cl<sub>2</sub> solution of **1**; <sup>1</sup>H NMR (400 MHz, CDCl<sub>3</sub>)  $\delta$  5.11 (dd,  $J = 7.1, 5.4$  Hz, 1H), 4.87 – 4.84 (m, 1H), 4.85 – 4.82 (m, 1H), 3.70 (dd,  $J = 45.1, 17.2$  Hz, 1H), 3.61 (ddd,  $J = 11.1, 10.0, 7.2$  Hz, 1H), 3.51 (d,  $J = 11.3$  Hz, 1H), 3.43 (dd,  $J = 17.3, 1.6$  Hz, 1H), 3.18 – 3.03 (m, 1H), 2.97 – 2.80 (m, 2H), 2.68 – 2.55 (m, 2H), 2.60 (d,  $J = 10.1$  Hz, 1H), 2.30 (d,  $J = 15.0$  Hz, 1H), 1.93 (dd,  $J = 15.0, 5.6$  Hz, 1H), 1.83 (t,  $J = 1.0$  Hz, 3H), 1.50 (s, 3H); <sup>13</sup>C NMR (100 MHz, CDCl<sub>3</sub>)  $\delta$  208.2, 193.1, 173.7, 151.8, 147.2, 132.9, 111.0, 83.2, 82.3, 54.6, 47.6, 46.4, 44.8, 41.7, 41.1, 39.7, 37.3,

26.3, 21.5; IR (Neat Film NaCl) 3366, 2965, 2930, 2858, 1765, 1696, 1636, 1445, 1374, 1358, 1275, 1260, 1219, 1182, 1162, 1120, 1090, 1012, 899, 690  $\text{cm}^{-1}$ ; HRMS (MM: ESI-APCI+)  $m/z$  calc'd for  $\text{C}_{19}\text{H}_{23}\text{O}_5$   $[\text{M}+\text{H}]^+$ : 331.1540, found 331. 1539;  $[\alpha]_{\text{D}}^{25.0} -210.7^\circ$  ( $c$  0.39,  $\text{CHCl}_3$ ).



**Yonarolide (4):** In a nitrogen-filled glovebox, a 1-dram vial was charged with scabrolide A (**1**, 1.0 mg, 0.00303 mmol, 1.0 equiv) in PhMe (1.0 mL). Burgess reagent (5.0 mg, 0.0210 mmol, 6.9 equiv) was added, and the vial was capped, sealed with electrical tape, and removed from the glovebox. The vial was then transferred to a preheated, 60 °C aluminum block, and the reaction was stirred for 30 min at 60 °C. The vial was removed from the heating block and cooled to 23 °C. The solvent was then removed under vacuum, and the resulting residue was purified by preparative TLC (70% EtOAc/hexanes) to afford yonarolide (**4**) (0.5 mg, 0.00160 mmol, 53% yield) as a colorless oil;  $^1\text{H}$  NMR (400 MHz,  $\text{CDCl}_3$ )  $\delta$  5.02 (t,  $J = 4.6$  Hz, 1H), 4.87 (d,  $J = 1.2$  Hz, 1H), 4.85 – 4.82 (m, 1H), 4.03 – 3.90 (m, 1H), 3.60 (s, 3H), 3.45 (d,  $J = 8.2$  Hz, 1H), 3.12 – 3.01 (m, 1H), 2.96 (ddt,  $J = 19.2, 4.6, 1.6$  Hz, 1H), 2.87 (dd,  $J = 15.6, 4.3$  Hz, 1H), 2.80 – 2.71 (m, 1H), 2.67 (dd,  $J = 13.3, 9.3$  Hz, 1H), 2.61 (dd,  $J = 13.3, 6.3$  Hz, 1H), 2.11 (td,  $J = 1.6, 0.8$  Hz, 2H), 1.85 – 1.81 (m, 3H).  $^{13}\text{C}$  NMR (100 MHz,  $\text{CDCl}_3$ )  $\delta$  207.9, 183.4, 172.5, 150.8, 149.2, 146.9, 134.2, 126.5, 111.2, 80.9, 50.1, 47.5, 47.2, 45.8, 41.4, 39.6, 38.5, 21.5, 15.8; IR (Neat Film NaCl) 2920, 1763, 1707, 1652, 1633, 1441, 1359, 1302, 1252, 1144, 1053, 1005, 895, 841,

820  $\text{cm}^{-1}$ ; HRMS (MM: ESI-APCI+)  $m/z$  calc'd for  $\text{C}_{19}\text{H}_{21}\text{O}_4$   $[\text{M}+\text{H}]^+$ : 313.1434, found 313.1433;  $[\alpha]_{\text{D}}^{25.0} -63.0^\circ$  ( $c$  0.083,  $\text{CHCl}_3$ ).

## 1.13.3 COMPARISON OF SYNTHETIC (-)-SCABROLIDE A TO PUBLISHED DATA

**Table 1.13.1** Comparison of  $^1\text{H}$  NMR shifts of synthetic and natural scabrolide A (**1**).

Synthetic Scabrolide A	Natural Scabrolide A (Sheu, 2002)	Natural Scabrolide A (Liang, Guo, 2020)
$^1\text{H}$ NMR, 400 MHz, $\text{CDCl}_3$	$^1\text{H}$ NMR, 400 MHz, $\text{CDCl}_3$	$^1\text{H}$ NMR, 400 MHz, $\text{CDCl}_3$
5.11 (dd, $J = 7.1, 5.4, 1\text{H}$ )	5.11 (t, $J = 6.4, 1\text{H}$ )	5.11 (dd, $J = 5.6, 7.0, 1\text{H}$ )
4.86 (m, 1H)	4.85 (s, 1H)	4.85 (s, 1H)
4.84 (m, 1H)	4.83 (s, 1H)	4.83 (s, 1H)
3.70 (d, $J = 17.2, 1\text{H}$ )	3.70 (d, $J = 17.2, 1\text{H}$ )	3.70 (d, $J = 17.2, 1\text{H}$ )
3.61 (ddd, $J = 11.1, 10.0, 7.2, 1\text{H}$ )	3.62 (dd, $J = 11.2, 6.4, 1\text{H}$ )	3.62 (dd, $J = 11.2, 6.4, 1\text{H}$ )
3.51 (d, $J = 11.3, 1\text{H}$ )	3.51 (d, $J = 11.2, 1\text{H}$ )	3.51 (d, $J = 11.2, 1\text{H}$ )
3.43 (dd, $J = 17.3, 1.6, 1\text{H}$ )	3.42 (d, $J = 17.2, 1\text{H}$ )	3.42 (d, $J = 17.2, 1\text{H}$ )
3.09 (m, 1H)	3.07 (q, $J = 6.4, 1\text{H}$ )	3.07 (m, 1H)
2.88 (m, 2H)	2.88 (m, 1H), 2.88 (m, 1H)	2.86 (m, 2H)
2.62 (m, 2H)	2.63 (m, 2H)	2.63 (m, 2H)
2.60 (d, $J = 10.1, 1\text{H}$ )	2.62 (d, $J = 10.0, 1\text{H}$ )	2.62 (d, $J = 10.0, 1\text{H}$ )
2.30 (d, $J = 15.0, 1\text{H}$ )	2.30 (d, $J = 15.2, 1\text{H}$ )	2.30 (d, $J = 15.2, 1\text{H}$ )
1.93 (dd, $J = 15.0, 5.6, 1\text{H}$ )	1.92 (dd, $J = 15.2, 5.6, 1\text{H}$ )	1.92 (dd, $J = 15.2, 5.6, 1\text{H}$ )
1.83 (s, 3H)	1.82 (s, 3H)	1.82 (s, 3H)
1.50 (s, 3H)	1.49 (s, 3H)	1.49 (s, 3H)

**Figure 1.13.1** Overlaid  $^1\text{H}$  NMR spectra of natural (Sheu, 2002) and synthetic scabrolide A (**1**).

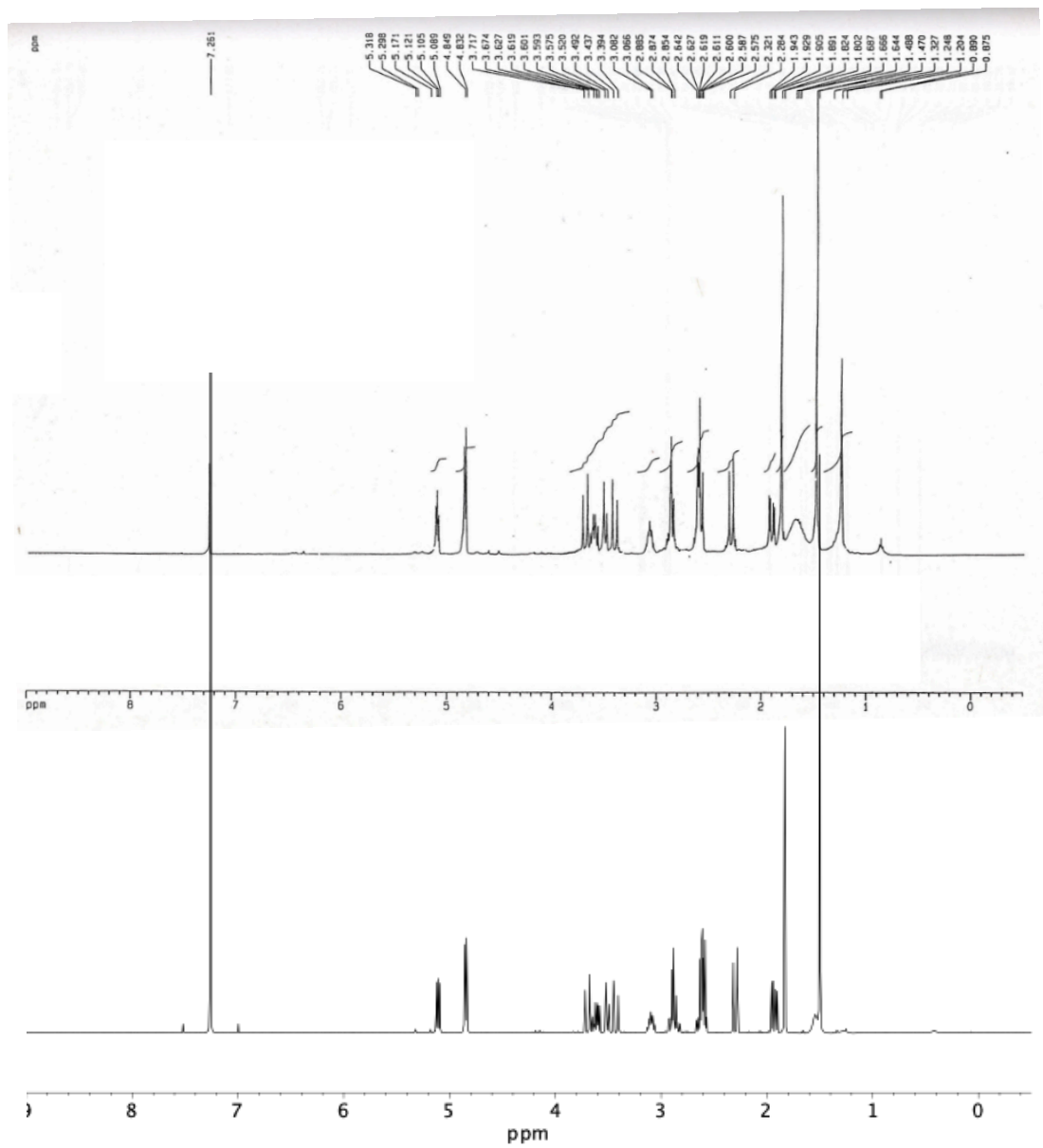
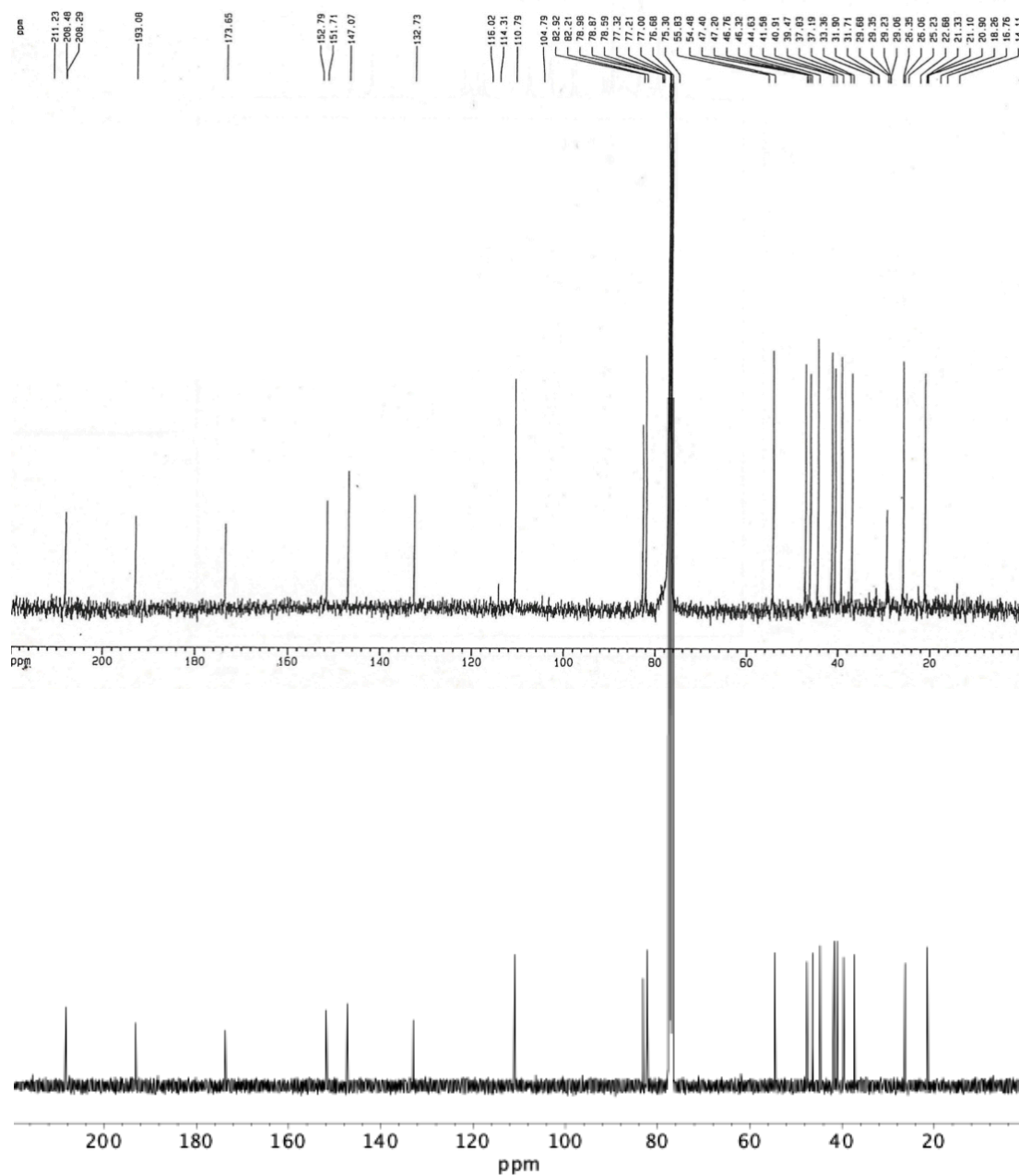


**Table 1.13.2** Comparison of  $^{13}\text{C}$  NMR shifts of synthetic and natural scabrolide A (**1**).

<b>Synthetic Scabrolide A</b>	<b>Natural Scabrolide A (Sheu, 2002)</b>	<b>Natural Scabrolide A (Liang, Guo, 2020)</b>
$^{13}\text{C}$ NMR, 100 MHz, $\text{CDCl}_3$	$^{13}\text{C}$ NMR, 100 MHz, $\text{CDCl}_3$	$^{13}\text{C}$ NMR, 100 MHz, $\text{CDCl}_3$
208.2	208.3	208.2
193.1	193.1	193.2
173.7	173.7	173.7
151.8	151.7	151.8
147.2	147.1	147.3
132.9	132.7	133.0
111.0	110.8	111.0
83.2	82.9	83.1
82.3	82.2	82.3
54.6	54.5	54.6
47.6	47.4	47.6
46.4	46.3	46.5
44.8	44.6	44.8
41.7	41.6	41.7
41.1	40.9	41.1
39.7	38.5	39.7
37.3	37.2	37.4
26.3	26.1	26.3
21.5	21.3	21.5



**Figure 1.13.2** Overlaid  $^{13}\text{C}$  NMR spectra of natural (Sheu, 2002) and synthetic scabrolide A (**1**).



## 1.13.4 COMPARISON OF SYNTHETIC (-)-YONAROLIDE A TO PUBLISHED DATA

**Table 1.13.3** Comparison of  $^1\text{H}$  and  $^{13}\text{C}$  NMR shifts of synthetic and natural yonarolide (**4**).

Synthetic Yonarolide $^1\text{H}$ NMR, 400 MHz, $\text{CDCl}_3$	Natural Yonarolide (Yamada, 1995) $^1\text{H}$ NMR, 400 MHz, $\text{CDCl}_3$
5.02 (t, $J = 4.6$ , 1H)	5.01 (t, $J = 4.6$ , 1H)
4.87 (t, $J = 1.2$ , 1H)	4.86 (t, $J = 1.1$ , 1H)
4.83 (s, 1H)	4.83 (s, 1H)
3.97 (m, 1H)	3.95 (m, 1H)
3.60 (s, 2H)	3.59 (s, 2H)
3.45 (d, $J = 8.2$ , 1H)	3.44 (d, $J = 8.2$ , 1H)
3.06 (m, 1H)	3.05 (m, 1H)
2.96 (ddt, $J = 19.2, 4.6, 1.6$ 1H)	2.96 (br dd, $J = 19.0, 4.6$ , 1H)
2.87 (dd, $J = 15.6, 4.3$ , 1H)	2.87 (dd, $J = 15.5, 4.2$ , 1H)
2.71–2.79 (m, 2H)	2.76 (dd, $J = 7.8, 15.5$ , 1H)
---	2.74 (br d, $J = 19.0$ , 1H)
2.66 (dd, 13.3, 9.3, 1H)	2.66 (dd, 13.3, 9.2, 1H)
2.61 (dd, $J = 13.3, 6.3$ , 1H)	2.62 (dd, 13.3, 6.2, 1H)
2.11 (s, 3H)	2.09 (s, 3H)
1.84 (s, 3H)	1.82 (s, 3H)

Synthetic Yonarolide $^{13}\text{C}$ NMR, 100 MHz, $\text{CDCl}_3$	Natural Yonarolide (Yamada, 1995) $^{13}\text{C}$ NMR, 100 MHz, $\text{CDCl}_3$
207.9	207.8
183.4	183.3
172.5	172.4
150.8	150.7
149.1	149.1
146.9	146.9
134.2	134.1
126.5	126.5
111.1	111.0
80.9	80.9
50.1	50.1
47.5	47.5
47.1	47.1
45.8	45.7
41.4	41.4
39.6	39.5
38.5	38.5
21.5	21.4
15.8	15.7

## 1.14 NOTES AND REFERENCES

<sup>1</sup> To date, there are nine known members of this natural product family. For reviews of the polycyclic norcembranoids see: (a) Li, Y.; Pattenden, G. Novel Macrocyclic and Polycyclic Norcembranoid Diterpenes from *Simularia* Species of Soft Coral: Structural Relationships and Biosynthetic Speculations. *Nat. Prod. Rep.* **2011**, *28*, 429–440. (b) Li, Y.; Pattenden, G. Perspectives on the Structural and Biosynthetic Interrelationships Between Oxygenated Furanocembranoids and Their Polycyclic Congeners Found in Corals. *Nat. Prod. Rep.* **2011**, *28*, 1269–1310. (c) Craig, R. A., II; Stoltz, B. M. Polycyclic Furanobutenolide-Derived Cembranoid and Norcembranoid Natural Products: Biosynthetic Connections and Synthetic Efforts. *Chem. Rev.* **2017**, *117*, 7878–7909.

<sup>2</sup> For synthetic efforts toward ineleganolide see: (a) Tang, F.; Moeller, K. D. Anodic Oxidations and Polarity: Exploring the Chemistry of Olefinic Radical Cations. *Tetrahedron* **2009**, *65*, 10863–10875. (b) Moeller, K. D. Intramolecular Anodic Olefin Coupling Reactions: Using Radical Cation Intermediates to Trigger New Umpolung Reactions. *Synlett* **2009**, *2009*, 1208–1218. (c) Tang, F.; Moeller, K. D. Intramolecular Anodic Olefin Coupling Reactions: The Effect of Polarization on Carbon–Carbon Bond Formation. *J. Am. Chem. Soc.* **2007**, *129*, 12414–12415. (d) Horn, E. J.; Vanderwal, C. D. A Failed Late-Stage Epimerization Thwarts an Approach to Ineleganolide. *J. Org. Chem.* **2016**, *81*, 1819–1838. (e) Craig, R. A., II; Roizen, J. L.; Smith, R. C.; Jones, A. C.; Virgil, S. C.; Stoltz, B. M. Enantioselective, Convergent Synthesis of the Ineleganolide Core by a Tandem Annulation Cascade. *Chem. Sci.* **2017**, *8*, 507–514.

<sup>3</sup> For synthetic efforts toward yonarolide see: Ueda, Y.; Abe, H.; Iguchi, K.; Ito, H. Synthetic Study of Yonarolide: Stereoselective Construction of the Tricyclic Core. *Tetrahedron Lett.* **2011**, *52*, 3379–3381.

<sup>4</sup> Li, Y.; Pattenden, G. Biomimetic Syntheses of Ineleganolide and Sinulochmodin C From 5-episinuleptolide via A Sequence of Transannular Michael Reactions. *Tetrahedron* **2011**, *67*, 10045–10052.

<sup>5</sup> a) Deng, M.; Zhang, X.; Li, Z.; Chen, H.; Zang, S.; Liang, G. Rapid Construction of the Common [5–5–6] Tricyclic Ring Skeleton in Polycyclic Cembranoids and Norcembranoids via Intramolecular 1,3-Dipolar Cycloaddition. *Org. Lett.* **2019**, *21*, 1493–1496. (b) Truax, N. J.; Ayinde, S.; Van, K.; Liu, J. O.; Romo, D. Pharmacophore-Directed Retrosynthesis Applied to Rameswaralide: Synthesis and Bioactivity of Sinularia Natural Product Tricyclic Cores. *Org. Lett.* **2019**, *21*, 7394–7399.

<sup>6</sup> Beingessner, R. L.; Farand, J. A.; Barriault, L. Progress toward the Total Synthesis of (±)-Havellockate. *J. Org. Chem.* **2010**, *75*, 6337–6346.

<sup>7</sup> Ueda, Y.; Abe, H.; Iguchi, K.; Ito, H. Synthetic Study of Yonarolide: Stereoselective Construction of the Tricyclic Core. *Tetrahedron Lett.* **2011**, *52*, 3379–3381.

<sup>8</sup> Mehta, G.; Kumaran, R. S. Studies Towards the Total Synthesis of Novel Marine Diterpene Havellockate. Construction of the Tetracyclic Core. *Tetrahedron Lett.* **2001**, *42*, 8097–8100.

<sup>9</sup> Meng, Z.; Fürstner, A. Total Syntheses of Scabrolide A and Nominal Scabrolide B. *J. Am. Chem. Soc.* **2022**, *144*, 1528–1533.

<sup>10</sup> For the isolation of scabrolides A and B see: (a) Sheu, J.; Ahmed, A. F.; Shiue, R.; Dai, C.; Kuo, Y.; Scabrolides A-D, Four New Norditerpenoids Isolated from the Soft Coral

*Sinularia scabra*. *J. Nat. Prod.* 2002, 65, 1904–1908

<sup>11</sup> Hafeman, N. J.; Loskot, S. A.; Reimann, C. E.; Pritchett, B. P.; Virgil, S. C.; Stoltz, B. M. The Total Synthesis of (–)-Scabrolide A. *J. Am. Chem. Soc.* **2020**, 142, 8585–8590.

<sup>12</sup> For reviews of ring-closing metathesis in the context of macrocyclization see: Gradillas, A.; Pérez-Castells, J. Macrocyclization by Ring-Closing Methathesis in the Total Synthesis of Natural Products: Reaction Conditions and Limitations. *Angew. Chem. Int. Ed.* **2006**, 45, 6086–6101.

<sup>13</sup> Craig, R. A., II; Roizen, J. L.; Smith, R. C.; Jones, A. C.; Stoltz, B. M. Enantioselective Synthesis of a Hydroxymethyl-*cis*-1,3-cyclopentendiol Building Block. *Org. Lett.* **2012**, 14, 5716–5719.

<sup>14</sup> Duh, C.-Y.; Wang, S.-K.; Chia, M.-C.; Chiang, M. Y. A Novel Cytotoxic Norditerpenoid From the Formosan Soft Coral *Sinularia inelegans*. *Tetrahedron Lett.* **1999**, 40, 6033–6035.

<sup>15</sup> For the isolation of yonanolide see: Iguchi, K.; Kajiyama, K.; Yamada, Y. Yonanolide: A New Marine Norditerpenoid Possessing a Novel Tricyclic Skeleton, from the Okinawan Soft Coral of the Genus, *Sinularia*. *Tetrahedron Lett.* **1995**, 36, 8807–8808.

<sup>16</sup> In their report of the isolation of sinulochmodin C, the authors determine the absolute stereochemistry of two macrocyclic norcembranoids coisolated and report the absolute stereochemistry of sinulochmodin C, and the other polycyclic furanobutenolide-derived norcembranoids by analogy; see: (a) Tseng, Y.-J.; Ahmend, A. F.; Dai, C.-F.; Chiang M. Y.; Sheu, J.-H. Sinulochmodins A–C, Three Novel Terpenoids from the Soft Coral *Sinularia lochmodes*, *Org. Lett.* **2005**, 7, 3813–3816. The absolute stereochemistry of ineleganolide was very recently determined unambiguously by X-ray diffraction, and, in

the same study, the absolute stereochemistry of scabrolide A was determined by ECD methods; see: Cui, W.-X.; Yang, M.; Li, H.; Li, S.-W.; Yao, L.-G.; Li, G.; Tang, W.; Wang, C.-H.; Liang, L.-F.; Guo, Y.-W. Polycyclic furanolbutenolide-derived norditerpenoids from the South China Sea soft corals *Sinularia scabra* and *Sinularia polydactyla* with immunosuppressive activity. *Bioorg. Chem.* **2020**, *94*, 103350. Furthermore, this research serves as confirmation of the absolute stereochemistry of scabrolide A.

<sup>17</sup> González, M. A.; Ghosh, S.; Rivas, F.; Fischer, D.; Theodorakis, E. A. Synthesis of (+)- and (–)-isocarvone. *Tetrahedron Lett.* **2004**, *45*, 5039–5041.

<sup>18</sup> (a) Ohira, S. Methanolysis of Dimethyl (1-Diazo-2-oxopropyl) Phosphonate: Generation of Dimethyl (Diazomethyl) Phosphonate and Reaction with Carbonyl Compounds. *Synth. Commun.* **1989**, *19*, 561–564. (b) Müller, S.; Liepold, B.; Roth, G. J.; Bestmann, H. J. An Improved One-pot Procedure for the Synthesis of Alkynes from Aldehydes. *Synlett*, **1996**, 521–522.

<sup>19</sup> Inanaga, J.; Hirata, K.; Hiroko, S.; Tsutomu, K.; Yamaguchi, M. A Rapid Esterification by Means of Mixed Anhydride and Its Application to Large-ring Lactonization. *Bull. Chem. Soc. Jpn.* **1979**, *52*, 1989–1993.

<sup>20</sup> Chatterjee, A. K.; Choi, T.-L.; Sanders, D. P.; Grubbs, R. H. A General Model for Selectivity in Olefin Cross Metathesis. *J. Am. Chem. Soc.* **2003**, *125*, 11360–11370.

<sup>21</sup> (a) Brill, Z. G.; Grover, H. K.; Maimone, T. J. Enantioselective Synthesis of an Ophiobolin Sesterpene via a Programmed Radical Cascade. *Science* **2016**, *352*, 1078–1082. (b) Thach, D. Q.; Brill, Z. G.; Grover, H. K.; Esguerra, K. V.; Thompson, J. K.; Maimone, T. J. Total Synthesis of (+)-6-epi-Ophiobolin A. *Angew. Chem., Int. Ed.* **2020**, *59*, 1532–1536.

<sup>22</sup> Izawa Y.; Shimizu, I.; Yamamoto, A. Palladium-Catalyzed Oxidative Carbonylation of 1-Alkynes into 2-Alkynoates with Molecular Oxygen as Oxidant. *Bull. Chem. Soc. Jpn.* **2004**, *77*, 2033–2045.

<sup>23</sup> Neises, B.; Steglich, W. Simple Method for the Esterification of Carboxylic Acids. *Angew. Chem., Int. Ed. Engl.* **1978**, *17*, 522–524.

<sup>24</sup> Breunig, M.; Yuan, P.; Gaich, T. An Unexpected Transannular [4+2] Cycloaddition during the Total Synthesis of (+)-Norcembrene 5. *Angew. Chem. Int. Ed.* **2020**, *59*, 5521–5525.

<sup>25</sup> A similar epoxidation/Meinwald rearrangement strategy was attempted by our laboratory on the ineleganolide scaffold but also failed, requiring a reductive opening/oxidation sequence to prepare the analogous ketone. See reference 2e for details.

<sup>26</sup> (a) RajanBabu, T. V.; Nugent, W. A.; Beattie, M. S. Free Radical Mediated Reduction and Deoxygenation of Epoxides. *J. Am. Chem. Soc.* **1990**, *112*, 6408–6409. (b) RajanBabu, T. V.; Nugent, W. A. Selective Generation of Free Radicals from Epoxides Using a Transition-Metal Radical. A Powerful New Tool for Organic Synthesis. *J. Am. Chem. Soc.* **1994**, *116*, 986–997.

<sup>27</sup> Griffith, W. P.; Ley, S. V.; Whitcombe, G. P.; White, A. D. Preparation and Use of Tetra-*n*-butylammonium Per-Ruthenate (TBAP reagent) and Tetra-*n*-propylammonium Per-Ruthenate (TPAP) as New Catalytic Oxidants for Alcohols. *J. Chem. Soc., Chem. Commun.* **1987**, *21*, 1625–1627.

<sup>28</sup> Steves, J. E.; Stahl, S. S. Copper(I)/ABNO-Catalyzed Aerobic Alcohol Oxidation: Alleviating Steric and Electronic Constraints of Cu/TEMPO Catalyst Systems. *J. Am. Chem. Soc.* **2013**, *135*, 15742–15745.

<sup>29</sup> (a) Fleming, I.; Henning, R.; Plaut, H. The Phenyltrimethylsilyl Group as a Masked Form of the Hydroxy Group. *J. Chem. Soc., Chem. Commun.* **1984**, 29–31. (b) Fleming, I.; Sanderson, P. E. J. A One-Pot Conversion of the Phenyltrimethylsilyl Group into a Hydroxyl Group. *Tetrahedron Lett.* **1987**, 28, 4229–4232.

<sup>30</sup> For reviews of [2 + 2] photocycloadditions see: (a) Crimmins, M. T. Synthetic Applications of Intramolecular Enone–Olefin Photocycloadditions. *Chem. Rev.* **1988**, 88, 1453–1473. (b) Sarkar, D.; Bera, N.; Ghosh, S. [2 + 2] Photochemical Cycloaddition in Organic Synthesis. *Eur. J. Org. Chem.* **2020**, 2020, 1310–1326. (c) Hoffman, N. Photochemical Reactions as Key Steps in Organic Synthesis. *Chem. Rev.* **2008**, 108, 1052–1103. (d) Kärkäs, M. D.; Porco, J. A., Jr.; Stephenson, C. R. J. Photochemical Approaches to Complex Chemotypes: Applications in Natural Product Synthesis. *Chem. Rev.* **2016**, 116, 9683–9747.

<sup>31</sup> For reviews of cyclobutane fragmentation strategies in synthesis see: (a) Oppolzer, W. Intramolecular [2 + 2] Photoaddition/Cyclobutane-Fragmentation Sequence in Organic Synthesis. *Acc. Chem. Res.* **1982**, 15, 135–141. (b) Winkler, J. D.; Bowen, C. M.; Liotta, F. [2 + 2] Photocycloaddition/Fragmentation Strategies for the Synthesis of Natural and Unnatural Products. *Chem. Rev.* **1995**, 95, 2003–2020.

<sup>32</sup> Piers, E.; Wong, T.; Ellis, K. A. Use of Lithium (Trimethylstannyl)(cyano)cuprate for the Conversion of Alkyl 2-alkynoates into Alkyl (*Z*)- and (*E*)-3-trimethylstannyl-2-alkenoates. *Can. J. Chem.* **1992**, 70, 2058–2064.

<sup>33</sup> Trost, B. M.; Ball, Z. T. Alkyne Hydrosilylation Catalyzed by a Cationic Ruthenium Complex: Efficient and General Trans Addition. *J. Am. Chem. Soc.* **2005**, 127, 17644–17655.



<sup>34</sup> Crimmins, M. T.; Reinhold, T. L. Enone Olefin [2+2] Photochemical Cycloadditions. In *Organic Reactions, Vol 44*; Paquette, L. A.; Wiley: Hoboken, NJ, 1993; 297–599.

<sup>35</sup> For a computational investigation of this mechanism, see: Zhang, T.; Cusumano, A. Q.; Hafeman, N. J.; Loskot, S. A.; Reimann, C. E.; Virgil, S. C.; Goddard, W. A., III; Stoltz, B. M. Investigations of an Unexpected [2+2] Photocycloaddition in the Synthesis of (–)-Scabrolide A: Mechanism and Strategy for Biasing of Chemoselectivity Predicted from Quantum Mechanics Calculations. *Submitted*.

<sup>36</sup> (a) Srinivasan, R.; Carlough, K. H. Mercury (<sup>3</sup>P<sub>1</sub>) Photosensitized Internal Cycloaddition Reactions in 1,4-, 1,5-, and 1,6-Dienes. *J. Am. Chem. Soc.* **1967**, *89*, 4932–4936.

<sup>37</sup> For an example of this type of diastereoselectivity, see: (a) Pirrung, M. C. Total Synthesis of (±)-Isocomenme. *J. Am. Chem. Soc.* **1979**, *101*, 7130–7131. (b) Pirrung, M. C. Total Synthesis of (±)-Isocomene and Related Studies. *J. Am. Chem. Soc.* **1981**, *103*, 82–87.

<sup>38</sup> (a) Kolb, H. C.; Ley, S. V. Chemistry of Insect Antifeedants from *Azadirachta Indica* (Part 10); Synthesis of a Highly Functionalised Decalin Fragment of Azadirachtin. *Tetrahedron Lett.* **1991**, *32*, 6187–6190. (b) Kolb, H. C.; Ley, S. V.; Slawin, A. M. Z.; Williams, D. J. Chemistry of Insect Antifeedants from *Azadirachta indica* (Part 12): Use of Silicon as a Control Element in the Synthesis of a Highly Functionalized Decalin Fragment of Azadirachtin. *J. Chem. Soc. Perkin. Trans.1* **1992**, 2735–2760.

<sup>39</sup> Huang, F.-Q.; Xie, J.; Sun, J.-G.; Wang, Y.-W.; Dong, X.; Qi, L.-W.; Zhang, B. Regioselective Synthesis of Carbonyl-Containing Alkyl Chlorides via Silver-Catalyzed Ring-Opening Chlorination of Cycloalkanols. *Org. Lett.* **2016**, *18*, 684–687.

<sup>40</sup> Weinstabl, H.; Gaich, T.; Mulzer, J. Applications of the Rodriguez–Pattenden Photo-Ring Contraction: Total Synthesis and Configurational Reassignment of 11-Gorgiacerol and 11-Epigorgiacerol. *Org. Lett.* **2012**, *14*, 2834–2837.

<sup>41</sup> Corey, E. J.; Fuchs, P. L. A Synthetic Method for Formyl–Ethyne Conversion (RCHO–>RCCH or RCCR'). *Tetrahedron Lett.* **1972**, *13*, 3769–3772.

<sup>42</sup> Gansäuer, A.; Bluhm, H.; Pierobon, M. Emergence of a Novel Catalytic Radical Reaction: Titanocene-Catalyzed Reductive Opening of Epoxides. *J. Am. Chem. Soc.* **1998**, *120*, 12849–12859.

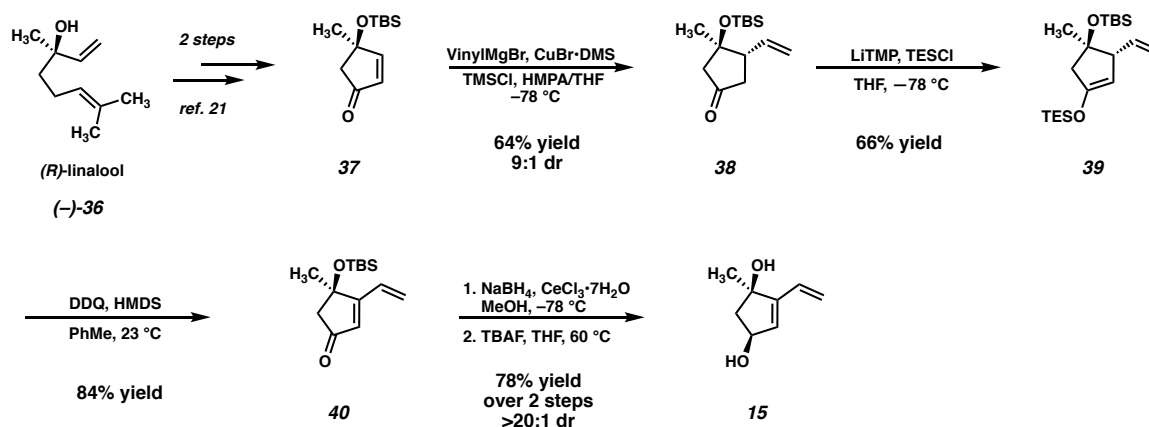
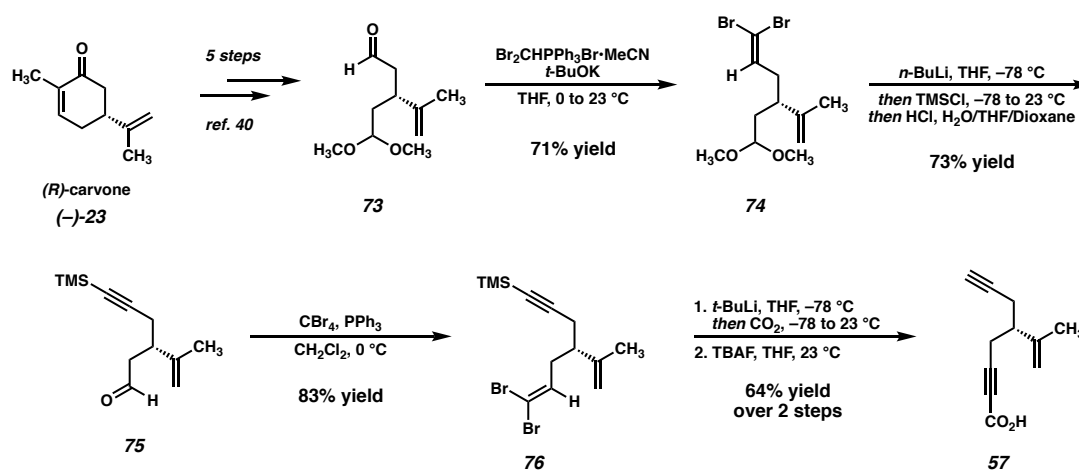
<sup>43</sup> Similar preference for the formation of fused [4–4] systems (as opposed to bridging “crossed adducts” resulting from initial 1,5-cyclization) has been observed in intramolecular [2+2] reactions, particularly in cases in which the internal position of the reacting olefin is substituted. For examples see: (a) Wolff, S.; Agosta, W. C. A Short Synthesis of Tricyclo[4.2.0.01,4]octanes. *J. Org. Chem.* **1981**, *46*, 4821–4825. (b) Wolff, S.; Agosta, W. C. Preparation of Derivatives of Tricyclo[4.2.001,4]octane, Broken Window Compounds. *J. Chem. Soc., Chem. Commun.* **1981**, 118–120. (c) Wolff, S.; Agosta, W. C. Regiochemical Control in Intramolecular Photochemical Reactions of 1,5-Hexadien-3-ones and 1-Acyl-1,5-hexadienes. *J. Am. Chem. Soc.* **1983**, *105*, 1292–1299.

<sup>44</sup> (a) Greico, P. A.; Gilman, S.; Nishizawa, M. Organoselenium Chemistry. A Facile One-Step Synthesis of Alkyl Aryl Selenides from Alcohols. *J. Org. Chem.* **1976**, *41*, 1485–1486. (b) Sharpless, K. B.; Young, M. W. Olefin Synthesis. Rate Enhancement of the Elimination of Alkyl Aryl Selenoxides by Electron-Withdrawing Substituents. *J. Org. Chem.* **1975**, *40*, 947–949.

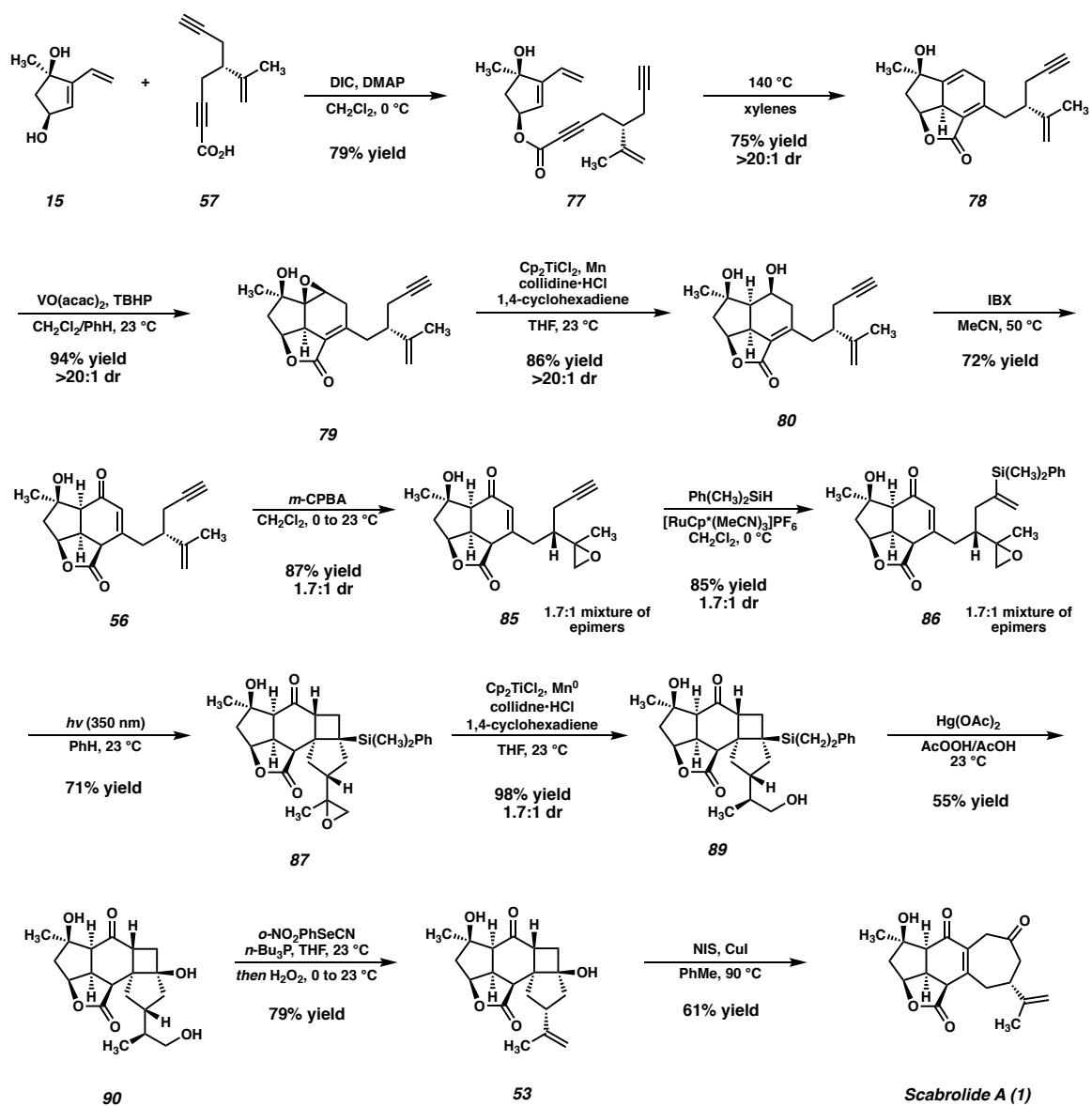
- <sup>45</sup> (a) Ge, Y.; Isoe, S. An Efficient Synthesis of Cerbinal, a 10  $\pi$  Aromatic Iridoid. *Chem Lett.* **1992**, 139–140. (b) Holmbo, S. D.; Pronin, S. V. A Concise Approach to Anthraquinone–Xanthone Heterodimers. *J. Am. Chem. Soc.* **2018**, *140*, 5065–5068.
- <sup>46</sup> Simpkins, N. S.; Cha, J. K. *t*-Butyl Hypochlorite. In *Encyclopedia of Reagents for Organic Synthesis*. Wiley, 2001.
- <sup>47</sup> Takasu, K.; Nagao, S.; Ihara, M. Synthesis of Medium-sized Cyclic  $\gamma$ -Haloketones By Radical Mediated Ring-opening Reaction of Lewis Acid Catalyzed (2 + 2)-Cycloaddition Products. *Tetrahedron Lett.* **2005**, *46*, 1005–1008.
- <sup>48</sup> Safe and Convenient Procedure for Solvent Purification. A. M. Pangborn, M. A. Giardello, R. H. Grubbs, R. K. Rosen, F. J. Timmers, *Organometallics* **1996**, *15*, 1518–1520.
- <sup>49</sup> Schmidt, B.; Audörsch, S. Stereoselective Total Synthesis of Atractylodemayne A, a Conjugated 2(*E*).8(*Z*).10(*E*)-Triene-4.6-diyne. *Org. Lett.* **2016**, *18*, 1162–1165.

## **APPENDIX 1**

*Synthetic Summary for Chapter 1:  
The Total Synthesis of (-)-Scabrolide A*

**Scheme A1.1** Synthesis of vinyl cyclopentenone **15**.**Scheme A1.2** Synthesis of ynoic acid **57**.

## Scheme A1.3 Synthesis of (-)-scabrolide A (1)



## **APPENDIX 2**

*Spectra Relevant to Chapter 1:  
The Total Synthesis of (-)-Scabrolide A*

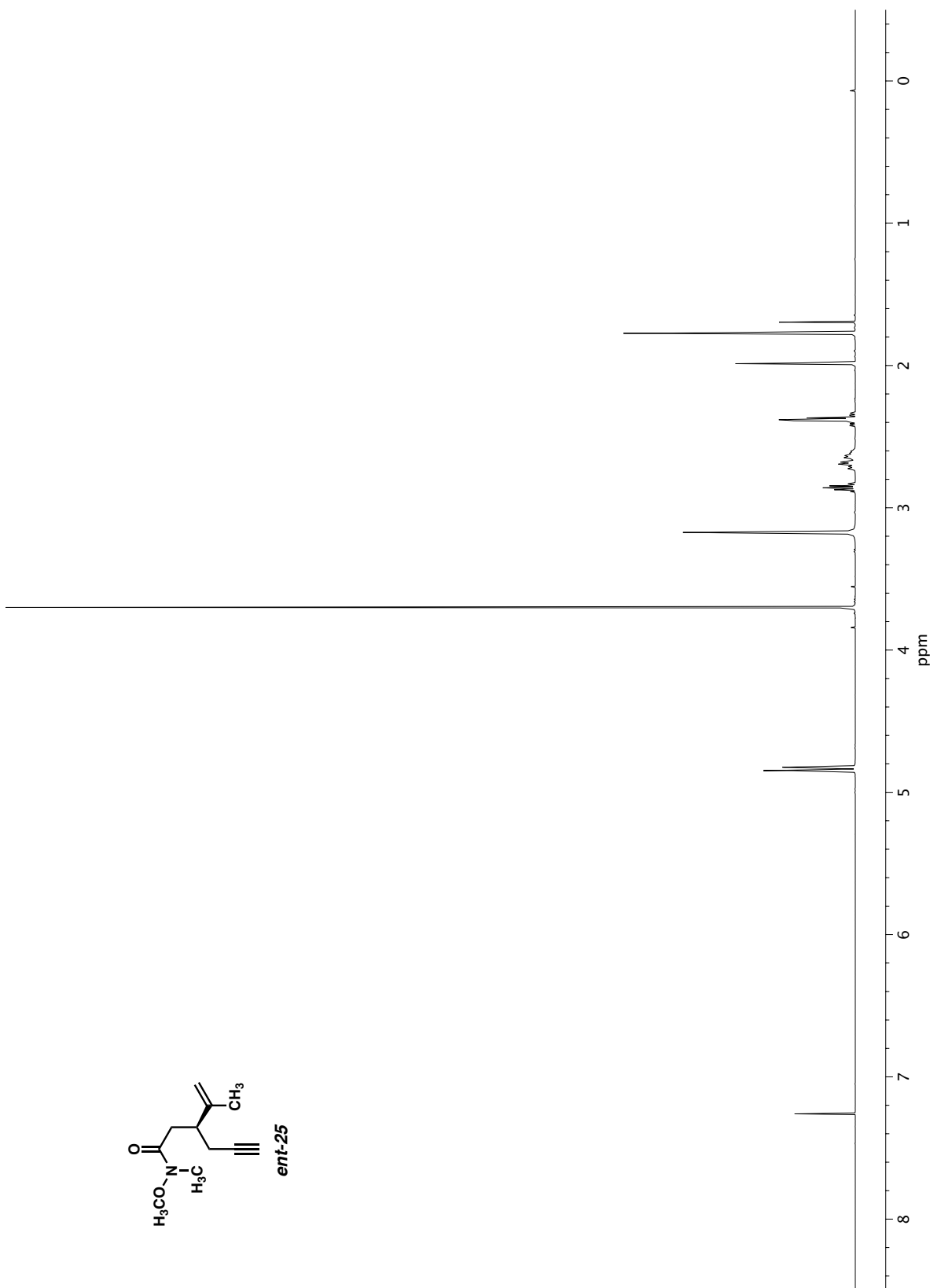
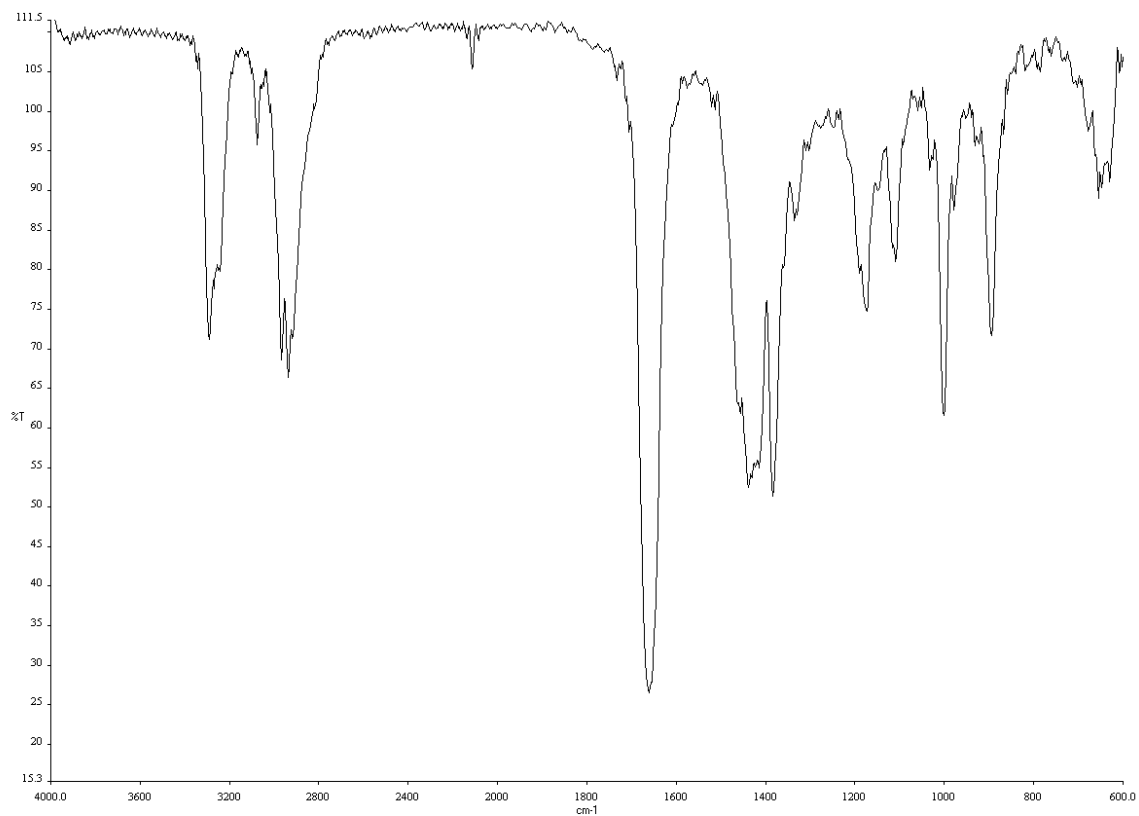
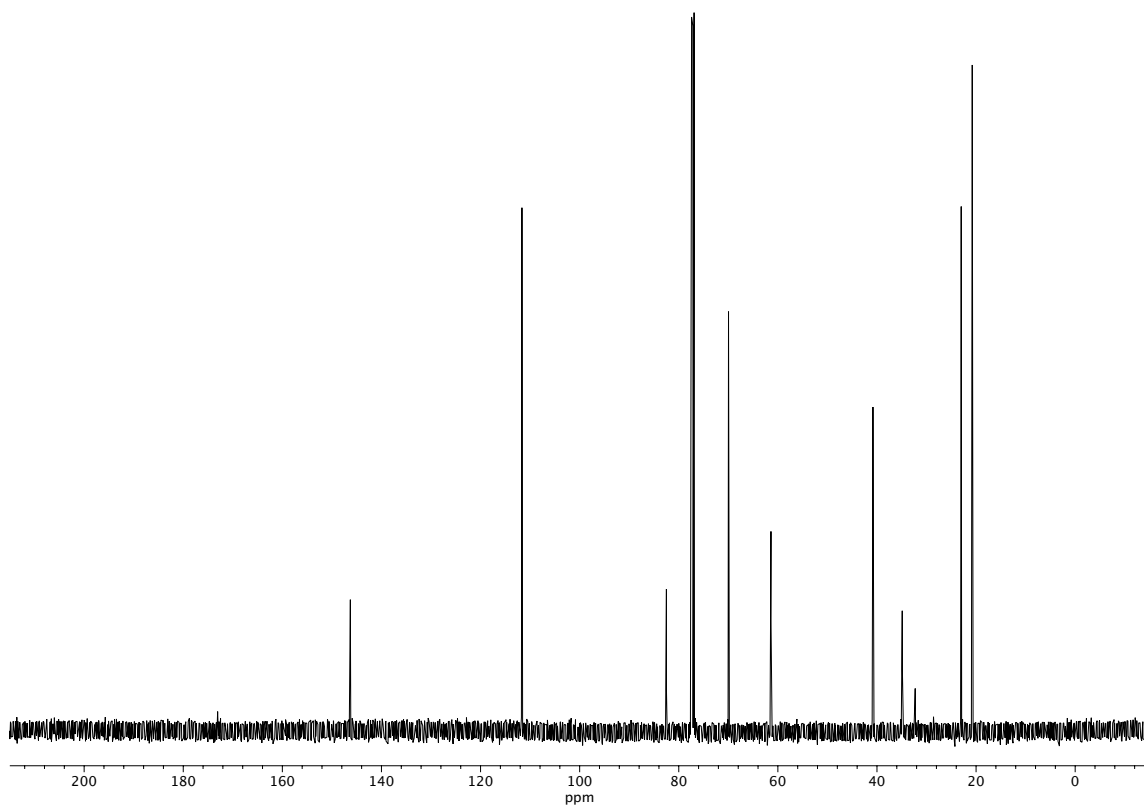


Figure A2.1 <sup>1</sup>H NMR (500 MHz, CDCl<sub>3</sub>) of compound **ent-25**.





**Figure A2.2** Infrared spectrum (Thin Film, NaCl) of compound *ent-25*.



**Figure A2.3**  $^{13}\text{C}$  NMR (125 MHz,  $\text{CDCl}_3$ ) of compound *ent-25*.

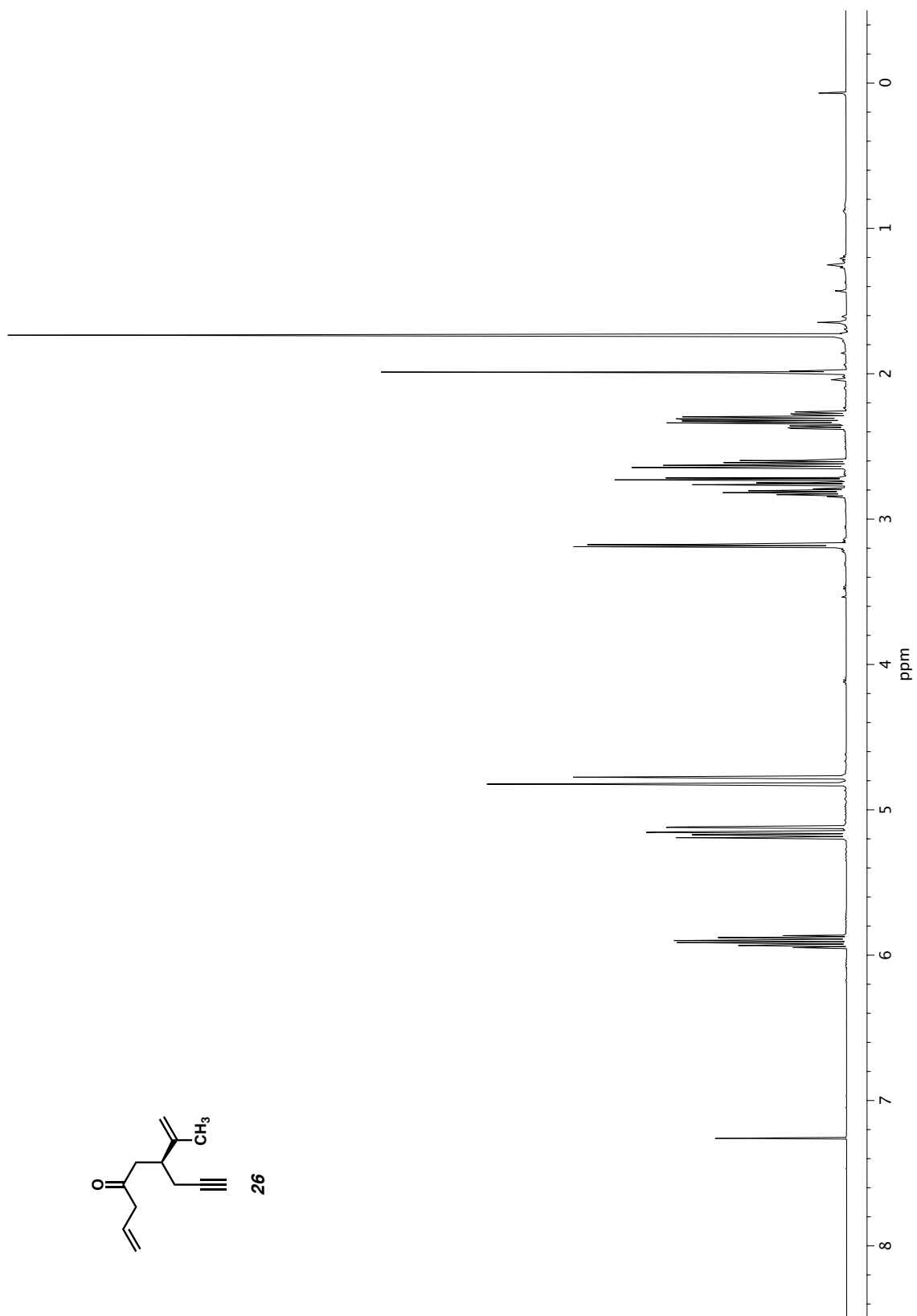
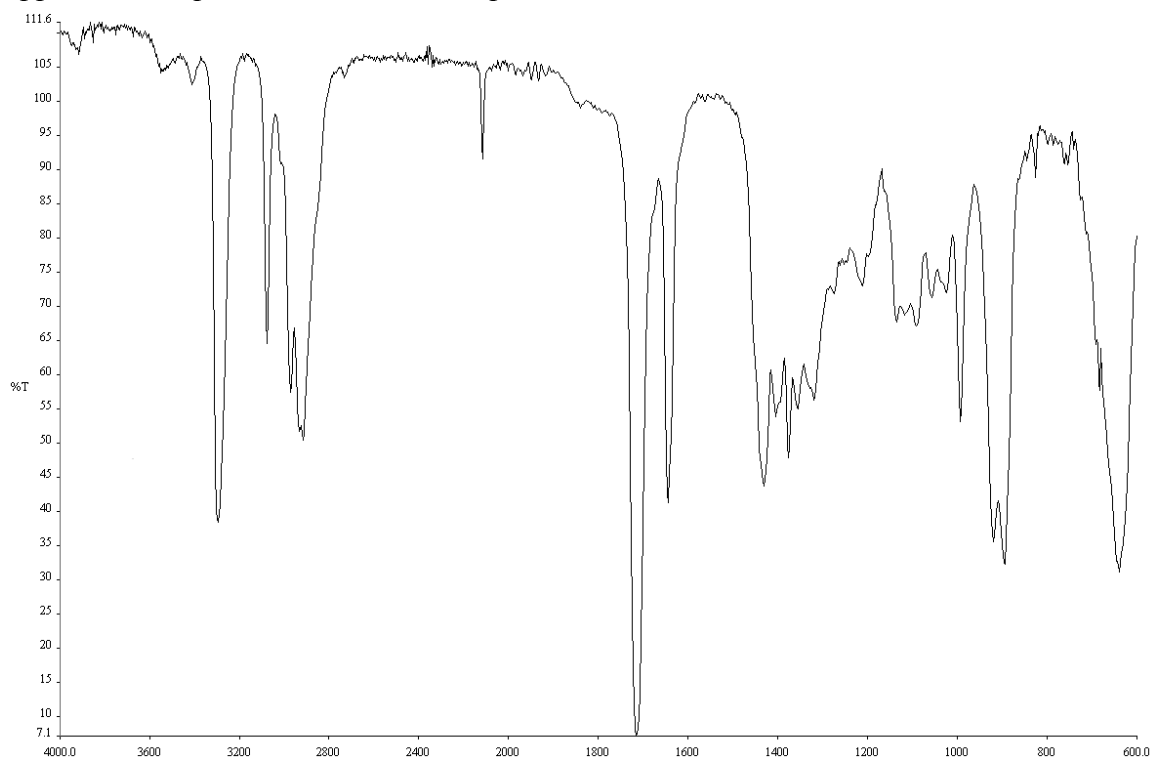
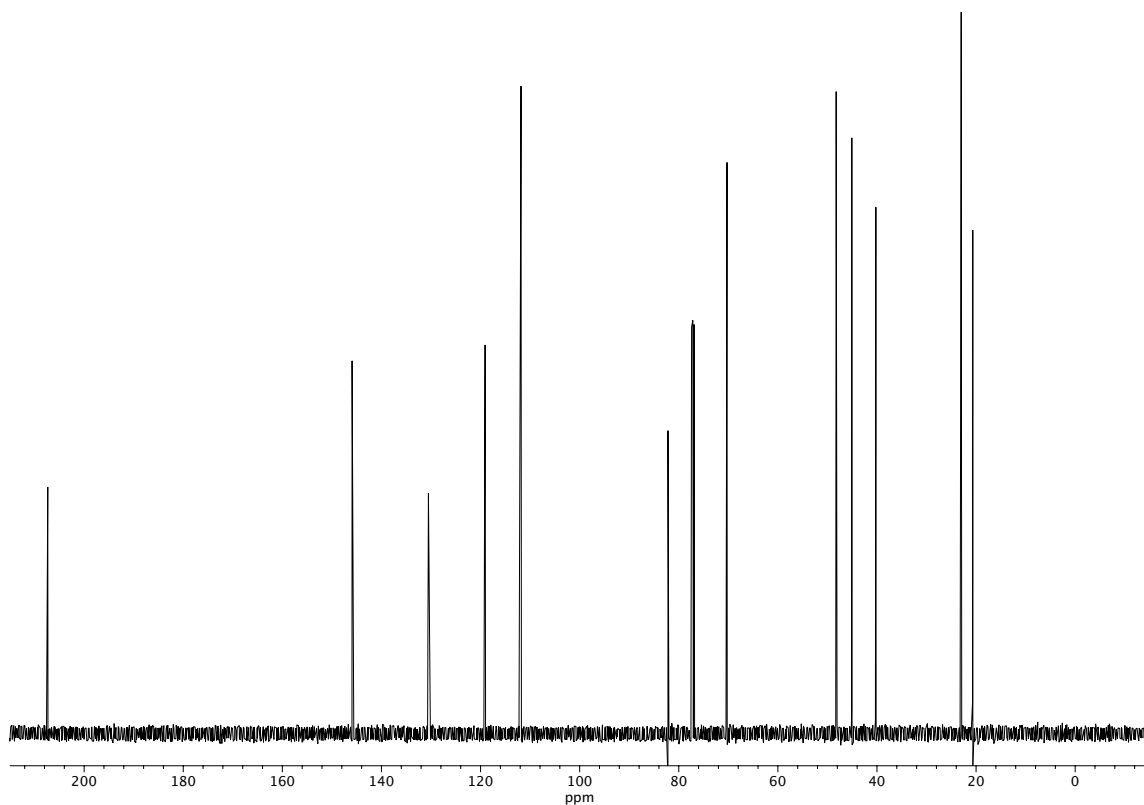


Figure A2.4 <sup>1</sup>H NMR (500 MHz, CDCl<sub>3</sub>) of compound 26.



**Figure A2.5** Infrared spectrum (Thin Film, NaCl) of compound **26**.



**Figure A2.6**  $^{13}\text{C}$  NMR (125 MHz,  $\text{CDCl}_3$ ) of compound **26**.

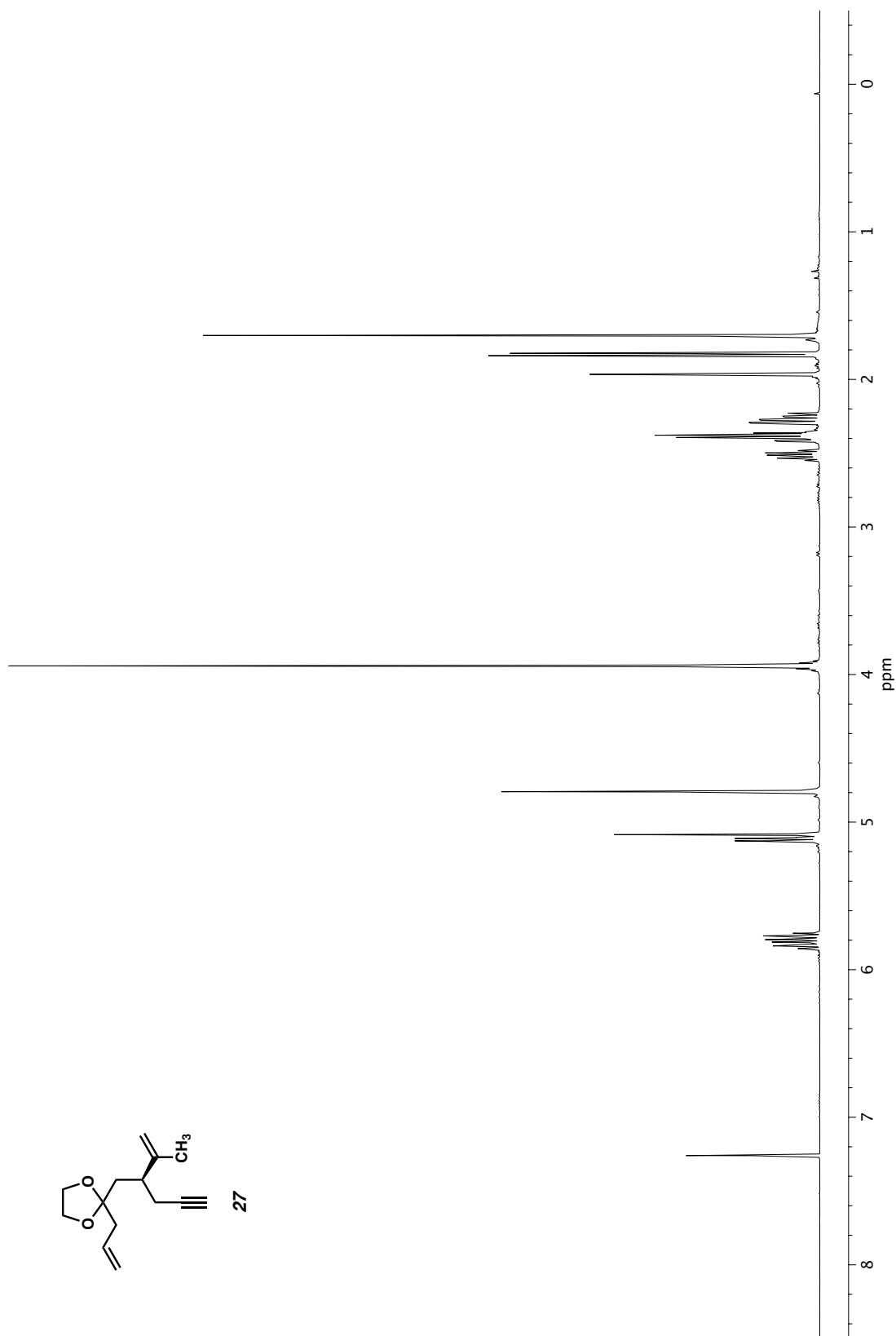
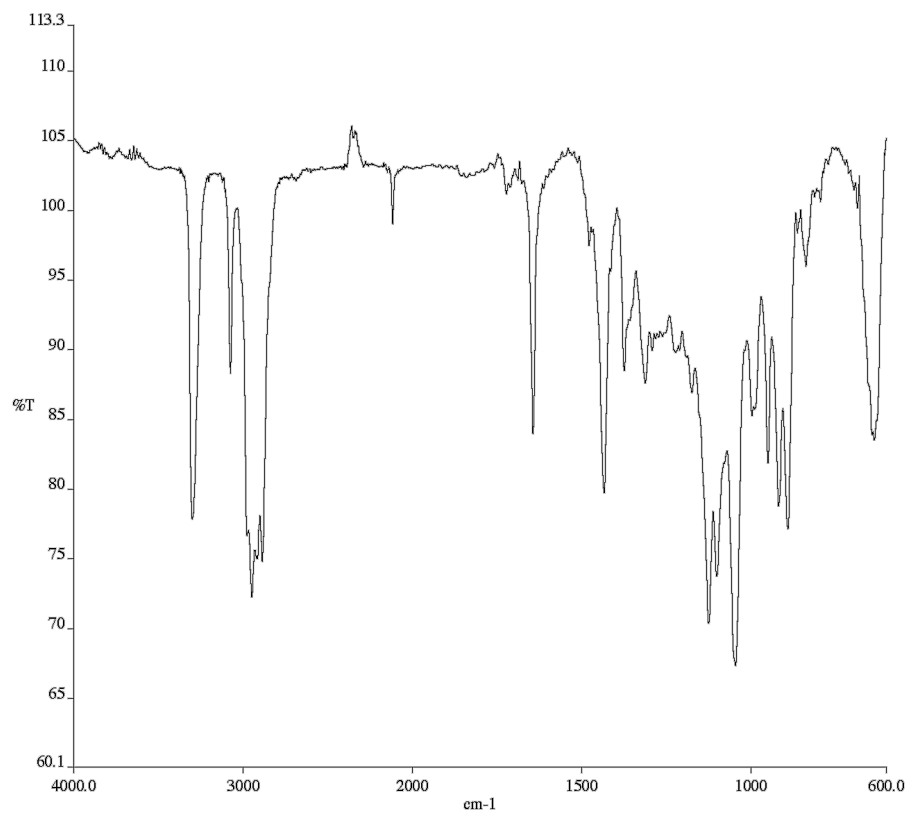
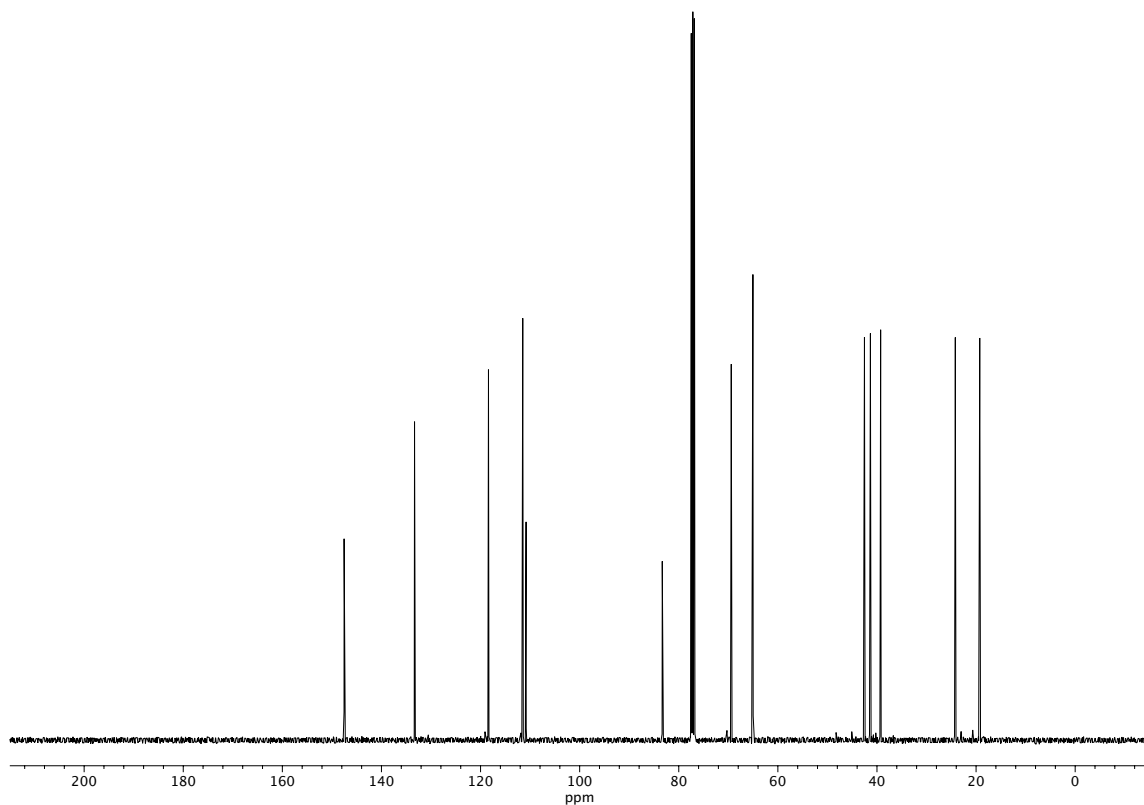


Figure A2.7 <sup>1</sup>H NMR (400 MHz, CDCl<sub>3</sub>) of compound 27.



**Figure A2.8** Infrared spectrum (Thin Film, NaCl) of compound **27**.



**Figure A2.9** <sup>13</sup>C NMR (100 MHz, CDCl<sub>3</sub>) of compound **27**.

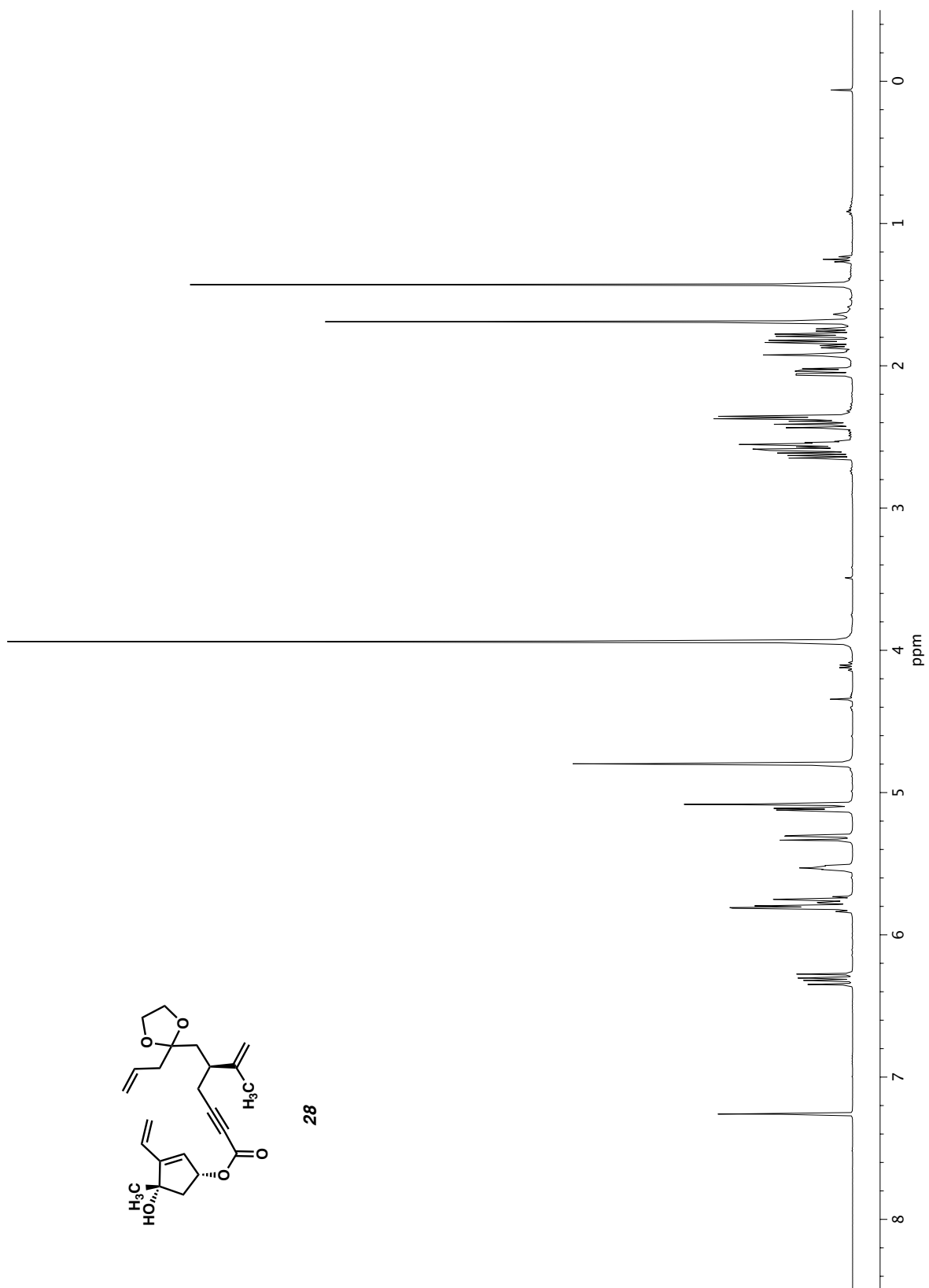
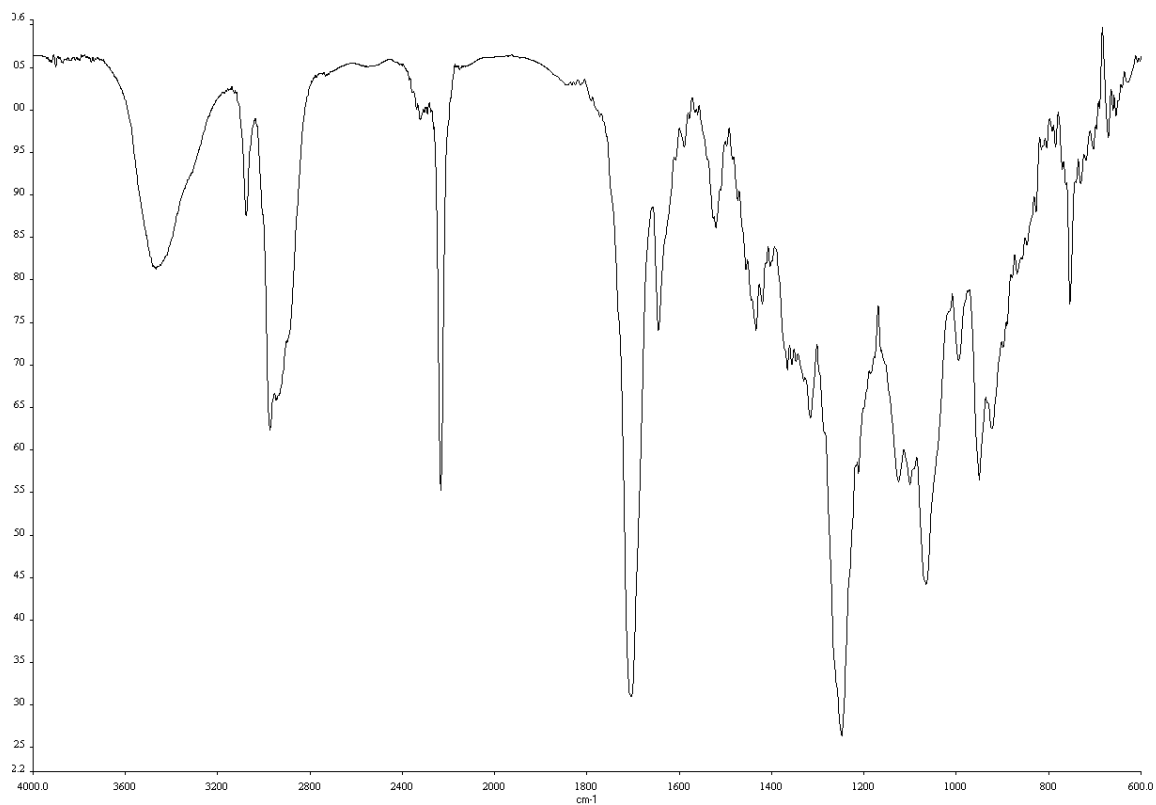
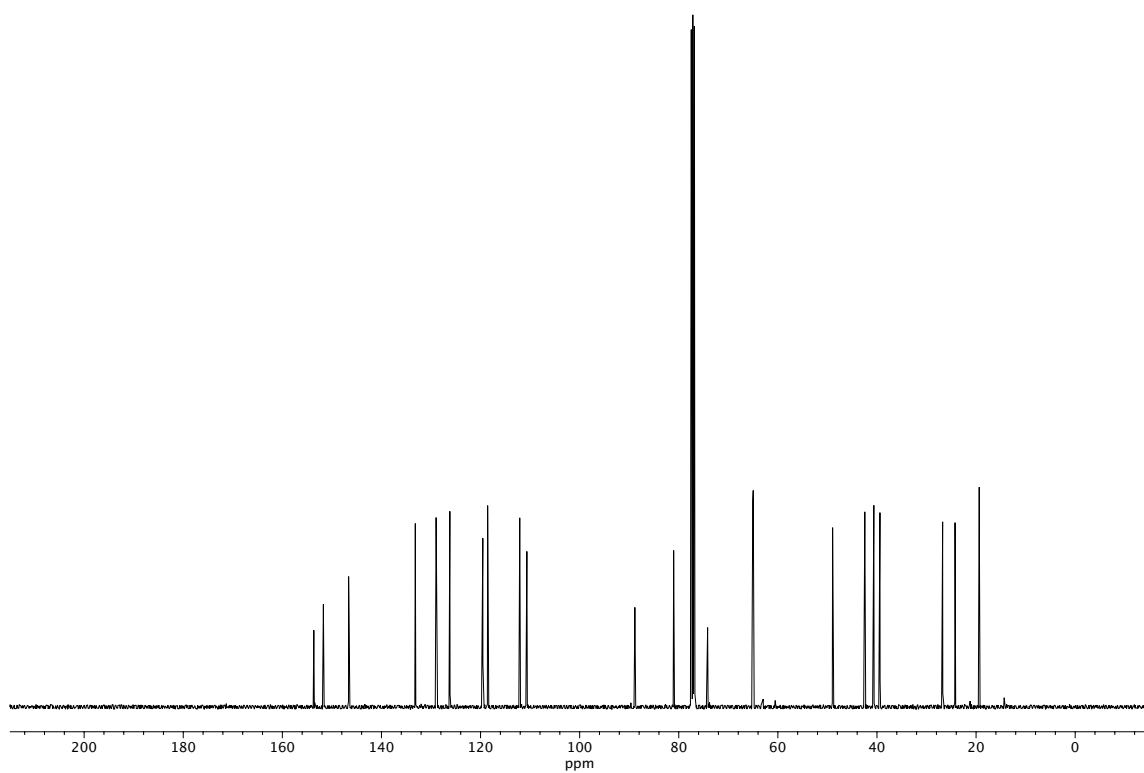


Figure A2.10 <sup>1</sup>H NMR (400 MHz, CDCl<sub>3</sub>) of compound 28.



**Figure A2.11** Infrared spectrum (Thin Film, NaCl) of compound **28**.



**Figure A2.12** <sup>13</sup>C NMR (100 MHz, CDCl<sub>3</sub>) of compound **28**.

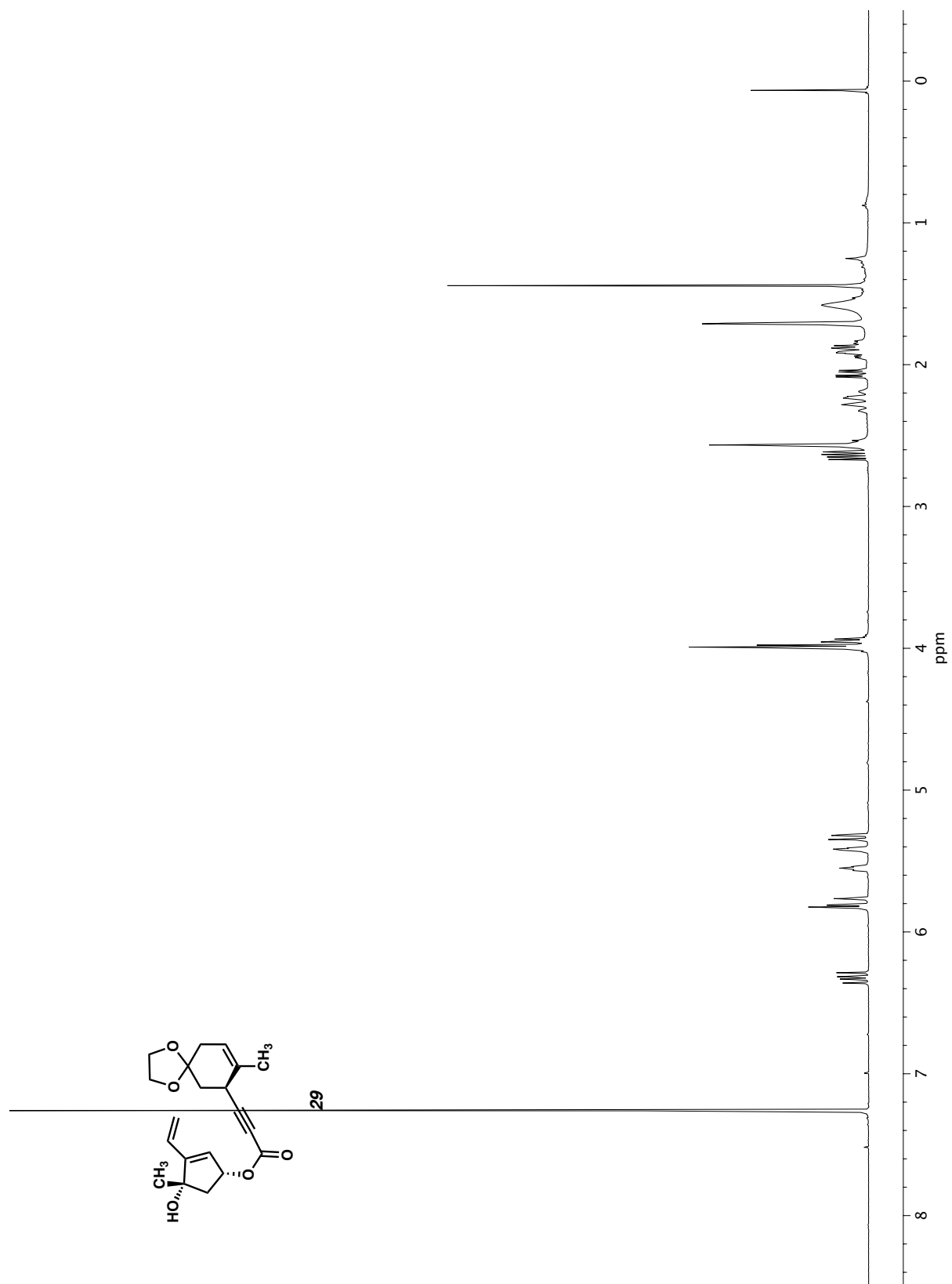
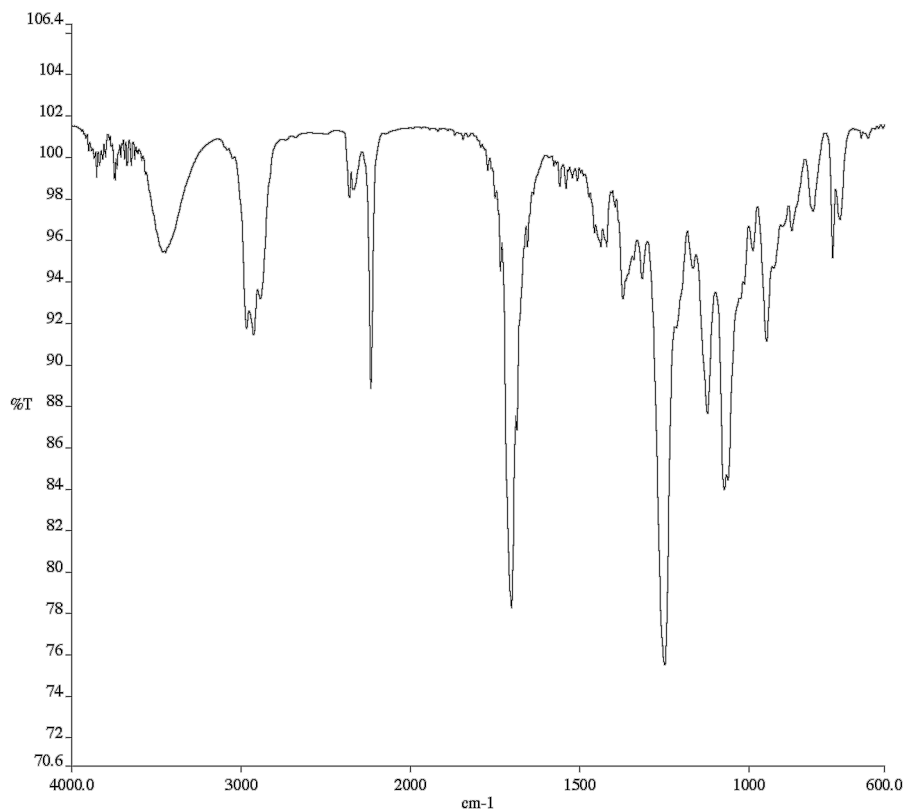
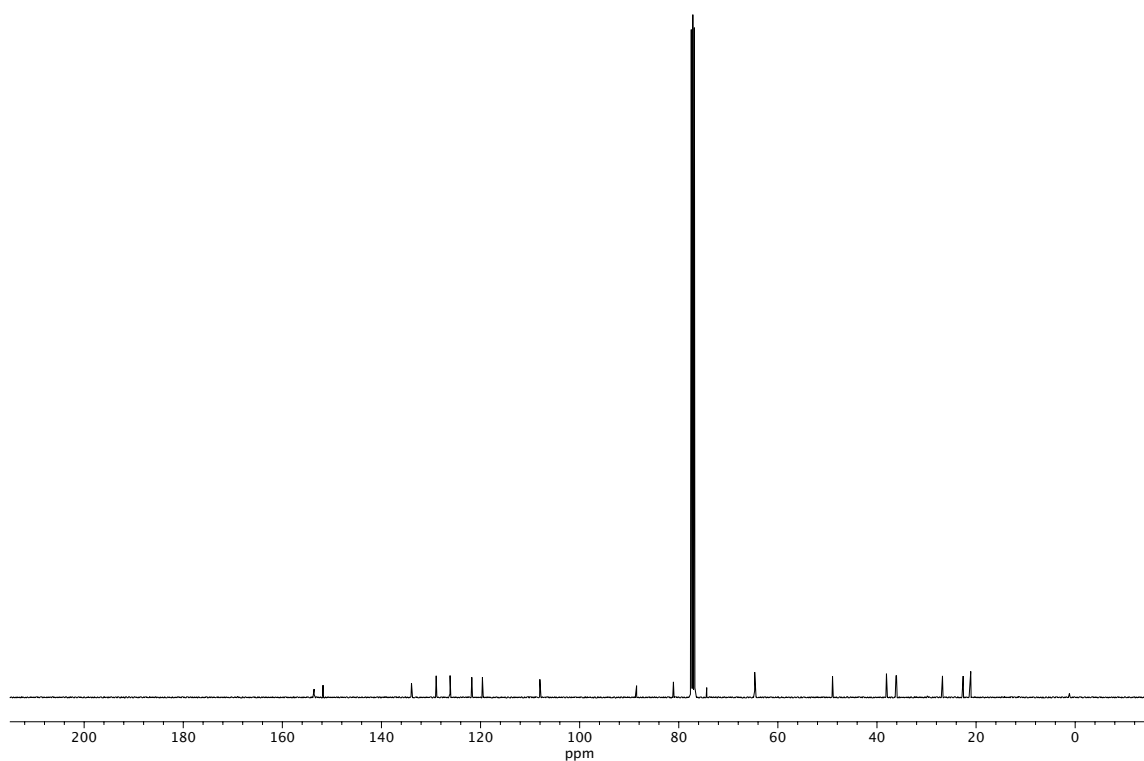


Figure A2.13 <sup>1</sup>H NMR (400 MHz, CDCl<sub>3</sub>) of compound 29.





**Figure A2.14** Infrared spectrum (Thin Film, NaCl) of compound **29**.



**Figure A2.15** <sup>13</sup>C NMR (100 MHz, CDCl<sub>3</sub>) of compound **29**.

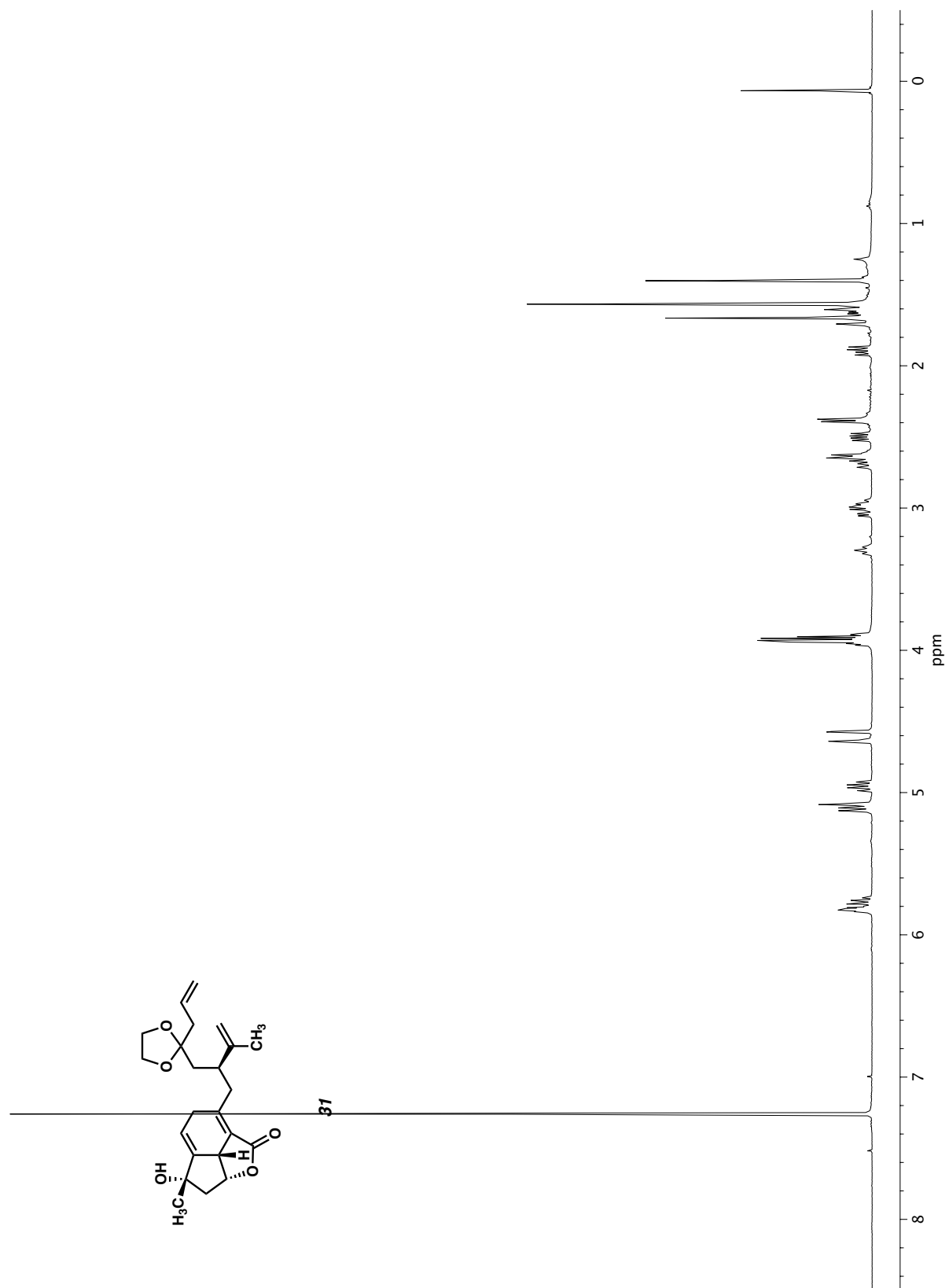


**Figure A2.16** <sup>1</sup>H NMR (400 MHz, CDCl<sub>3</sub>) of compound **31**.

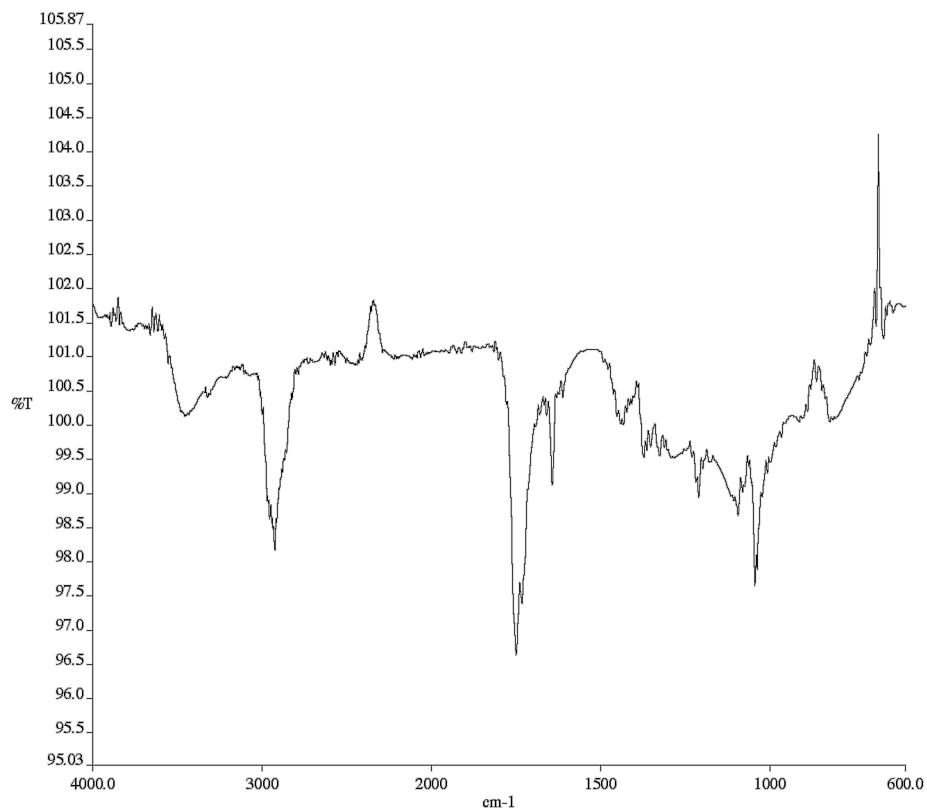


**Figure A2.17** Infrared spectrum (Thin Film, NaCl) of compound **31**.

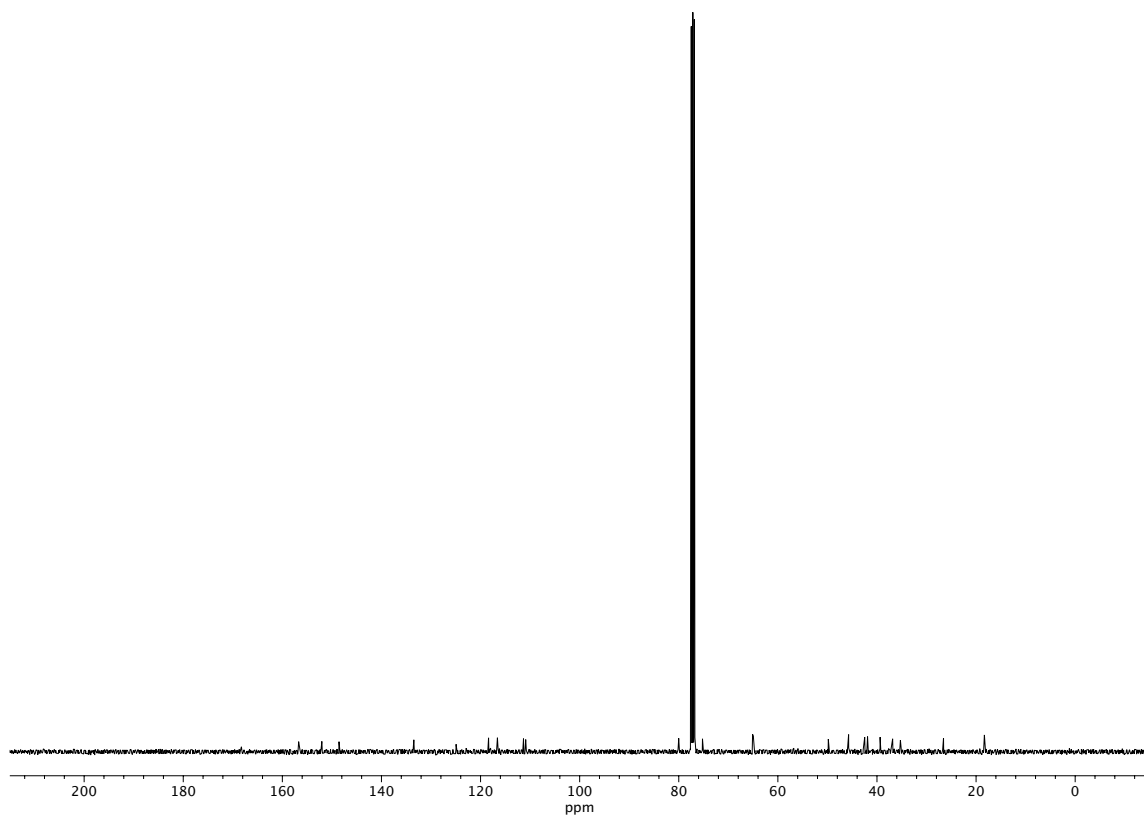


**Figure A2.18** <sup>13</sup>C NMR (100 MHz, CDCl<sub>3</sub>) of compound **31**.

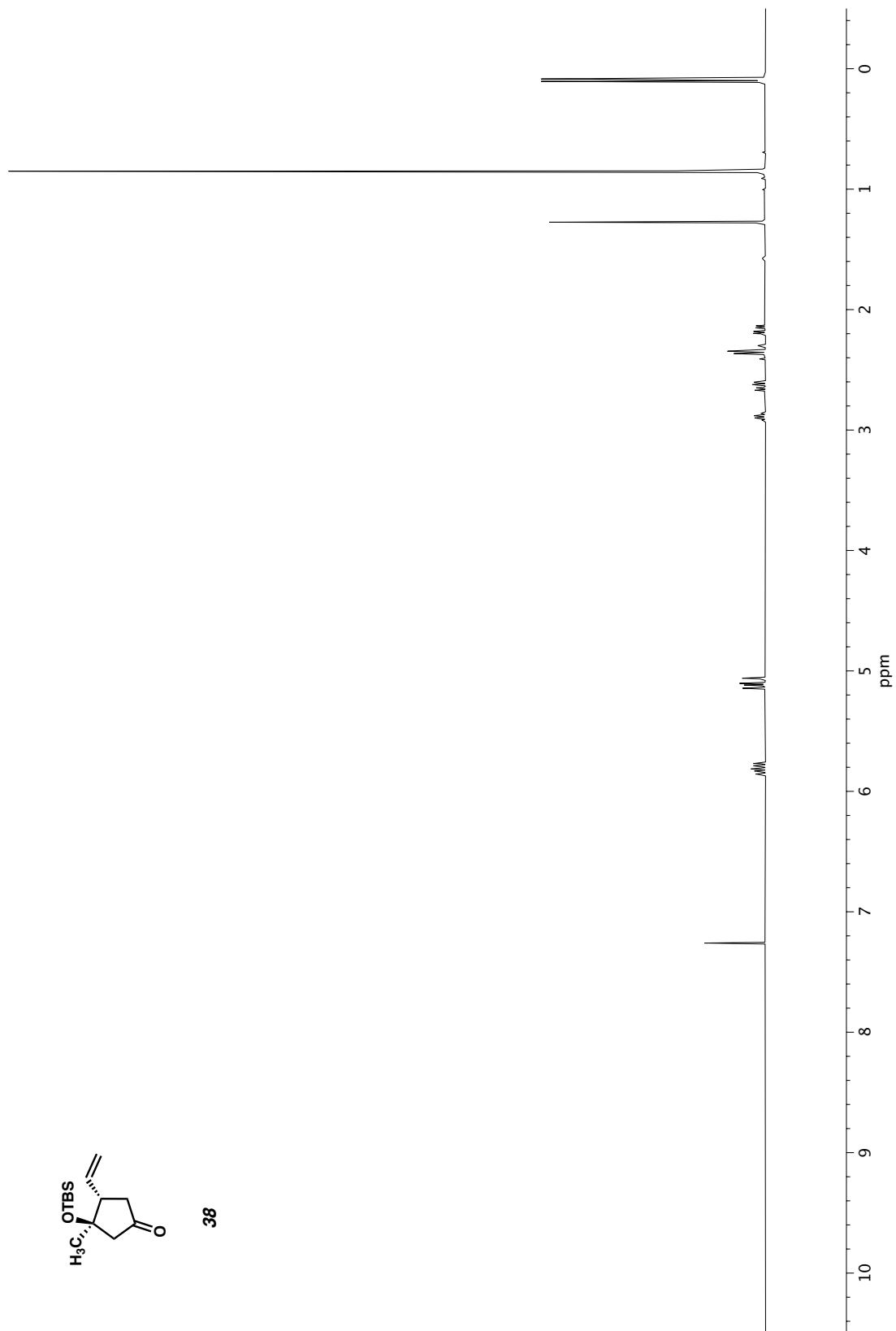
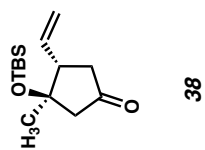


**Figure A2.19** <sup>1</sup>H NMR (400 MHz, CDCl<sub>3</sub>) of compound **38**.

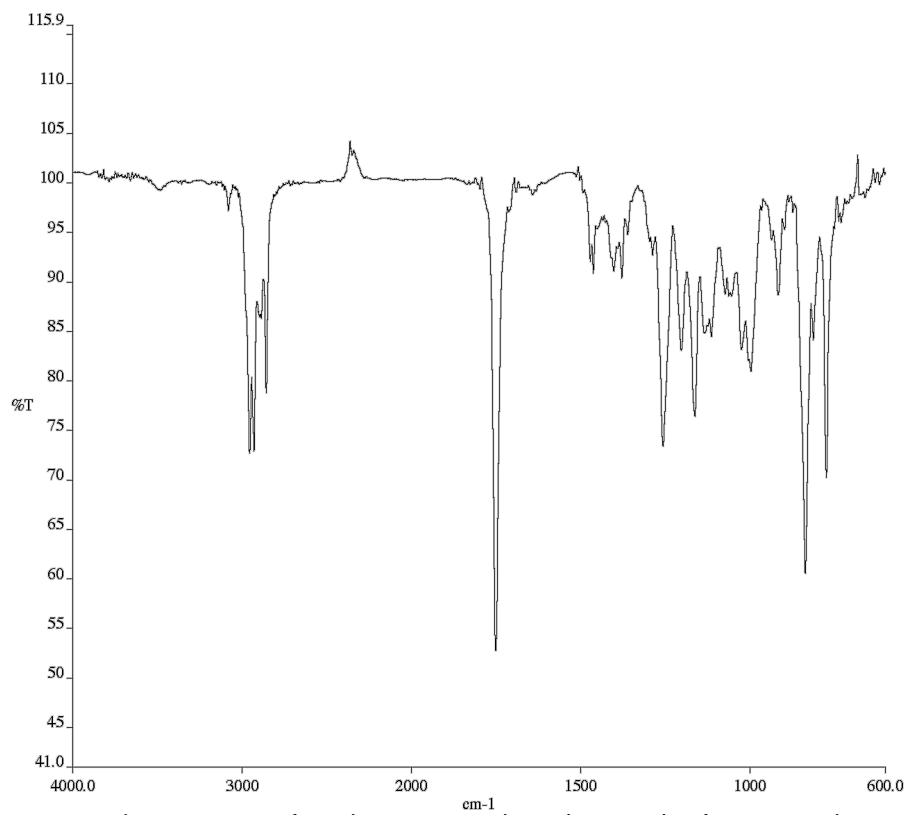


**Figure A2.20** Infrared spectrum (Thin Film, NaCl) of compound **38**.

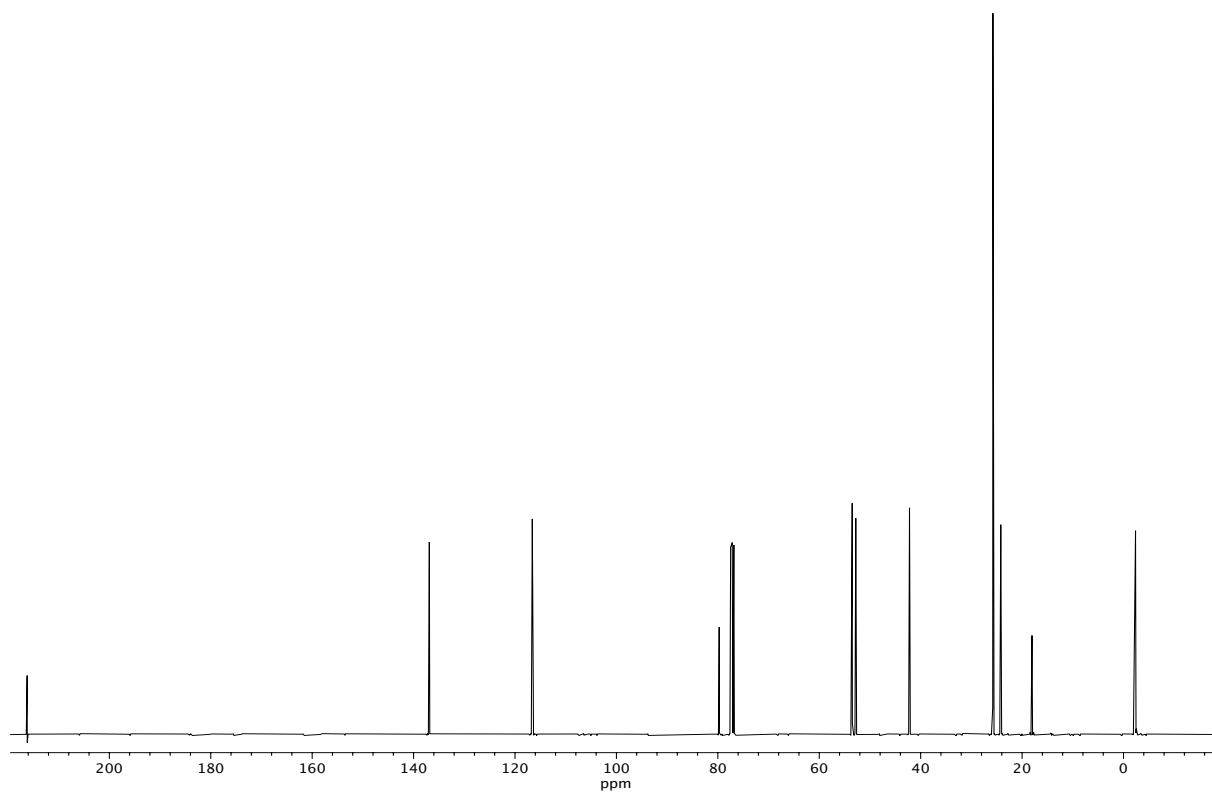


**Figure A2.21** <sup>13</sup>C NMR (100 MHz, CDCl<sub>3</sub>) of compound **38**.

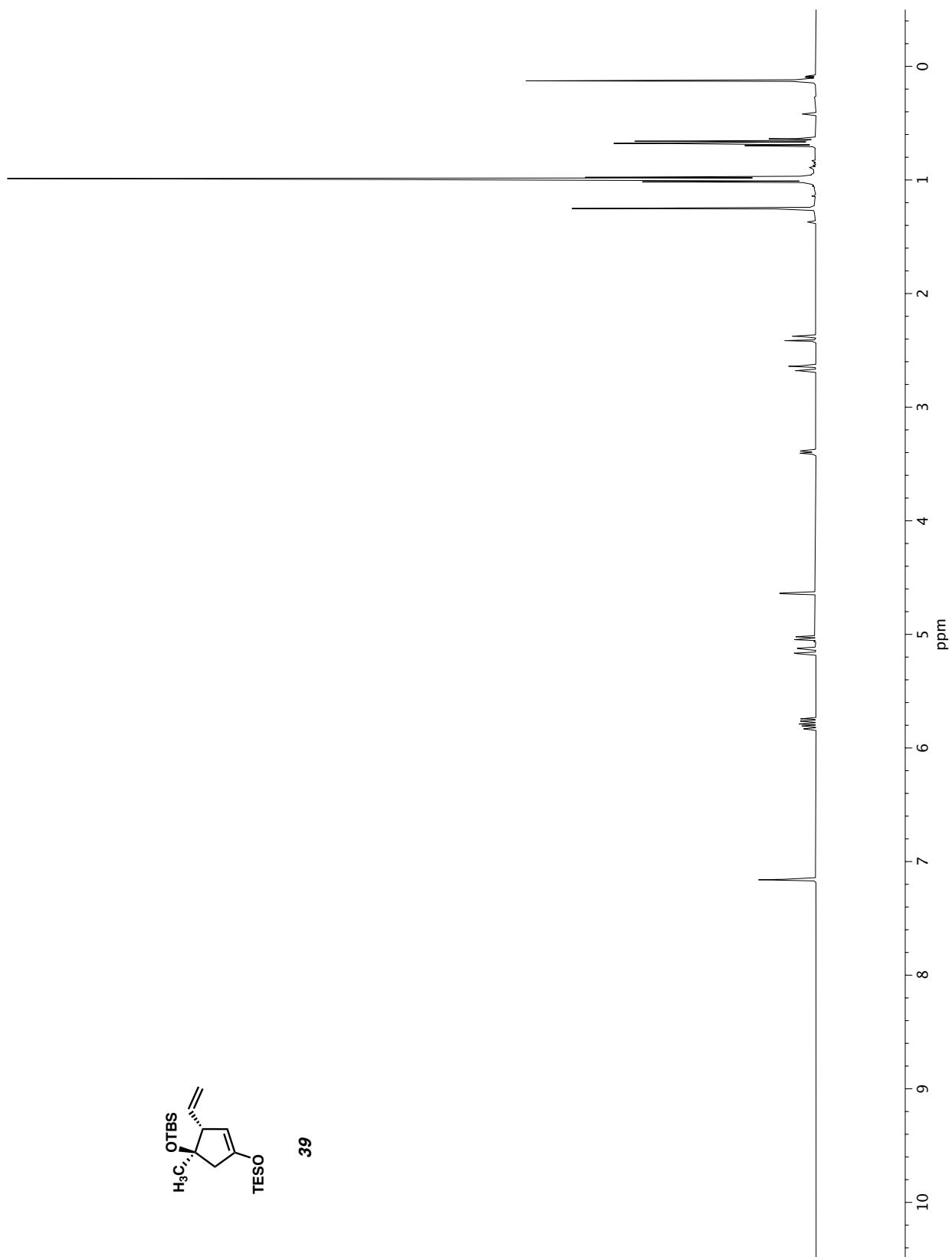
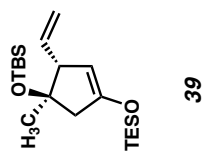
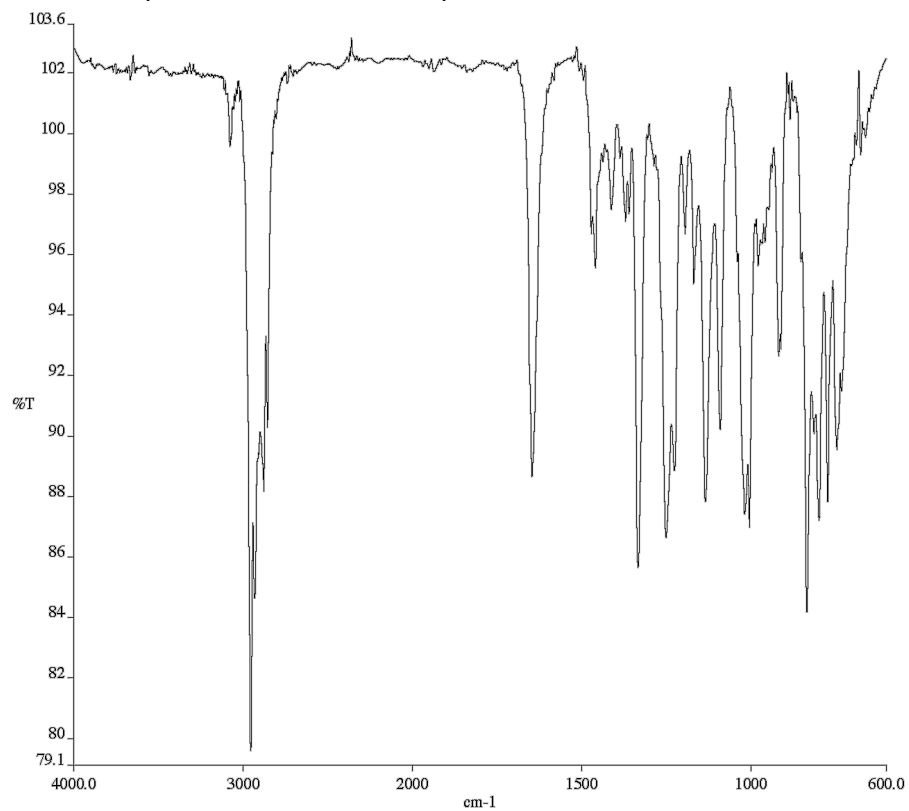
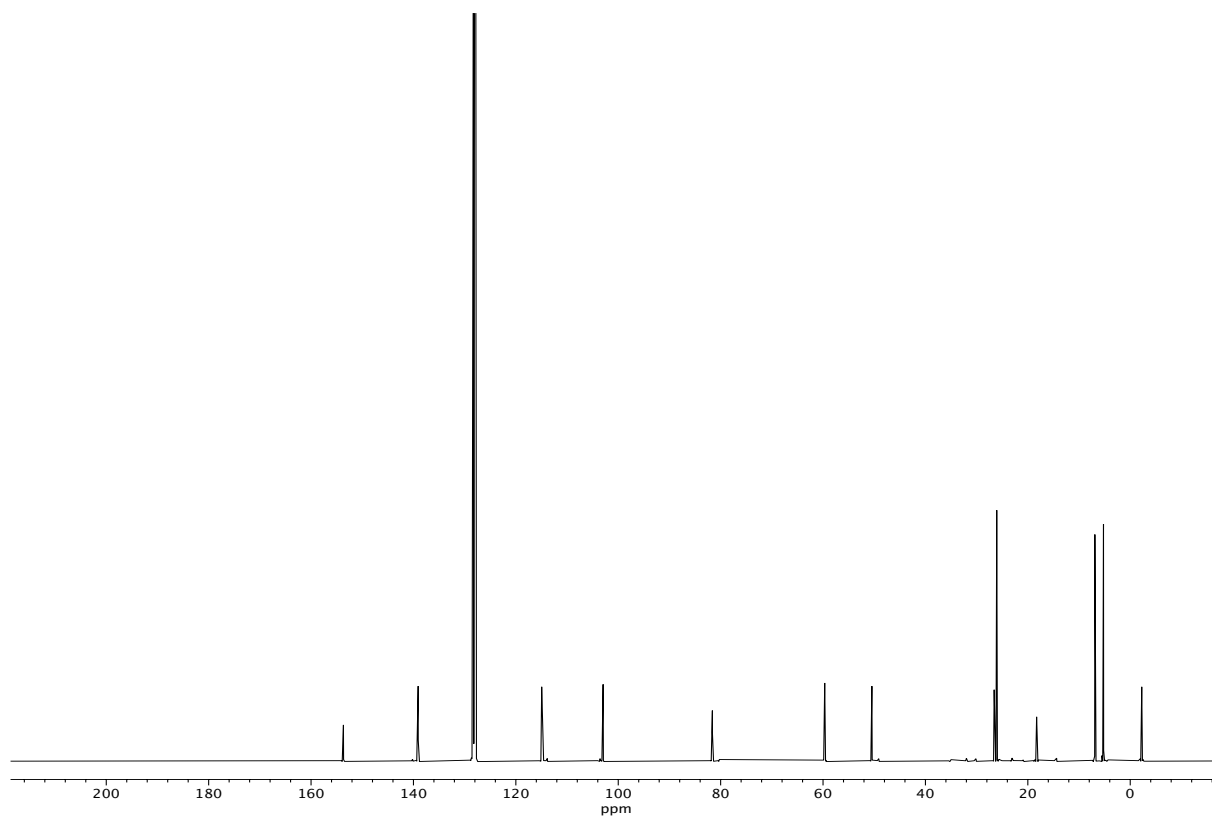


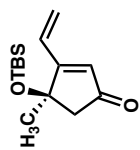
Figure A2.22 <sup>1</sup>H NMR (400 MHz, CDCl<sub>3</sub>) of compound 39.



**Figure A2.23** Infrared spectrum (Thin Film, NaCl) of compound **39**.



**Figure A2.24** <sup>13</sup>C NMR (100 MHz, CDCl<sub>3</sub>) of compound **39**.



40

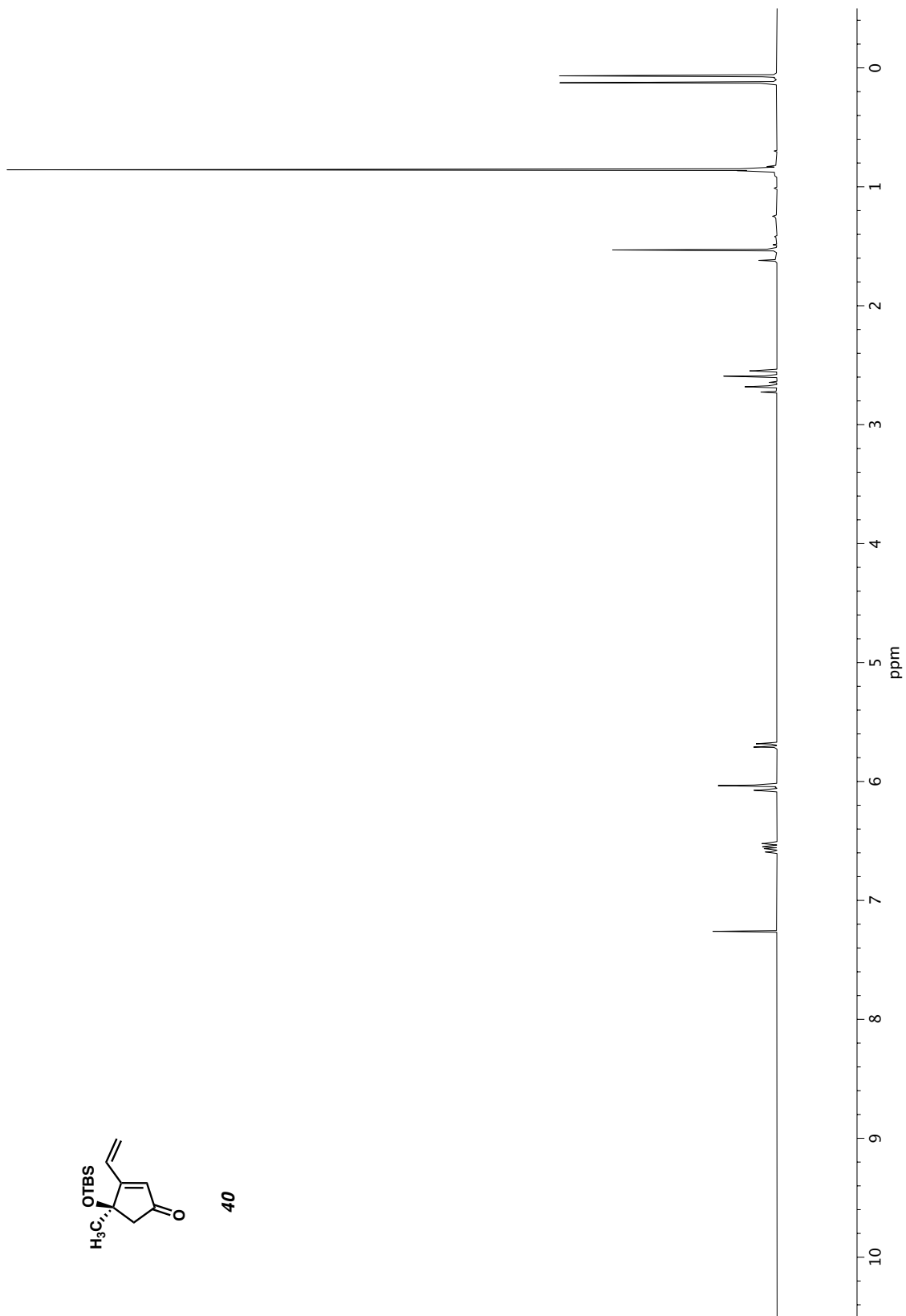
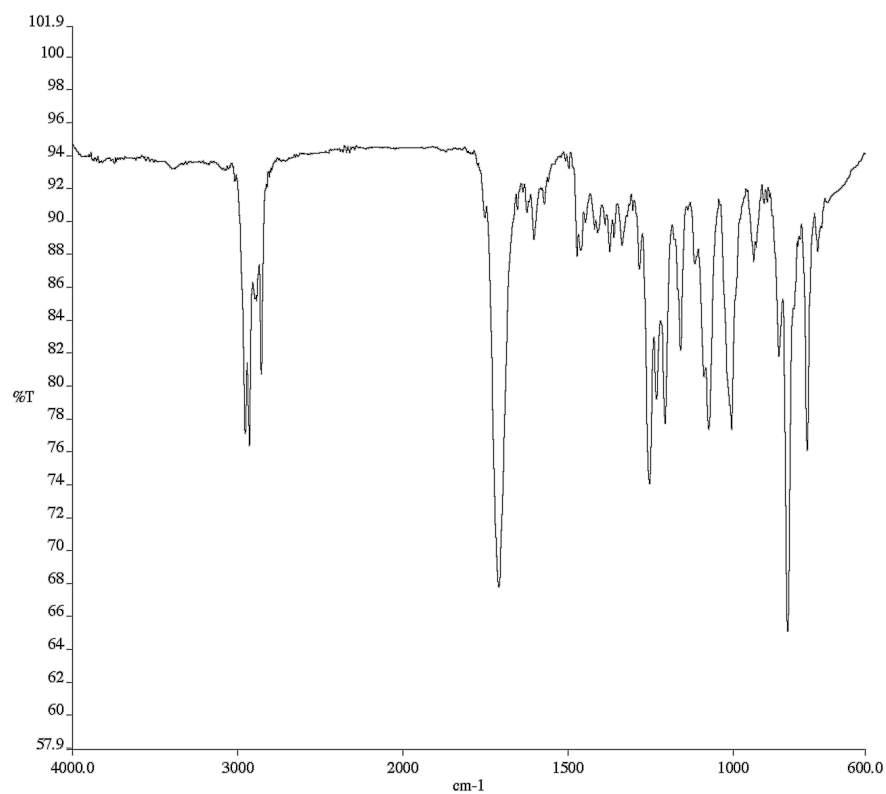
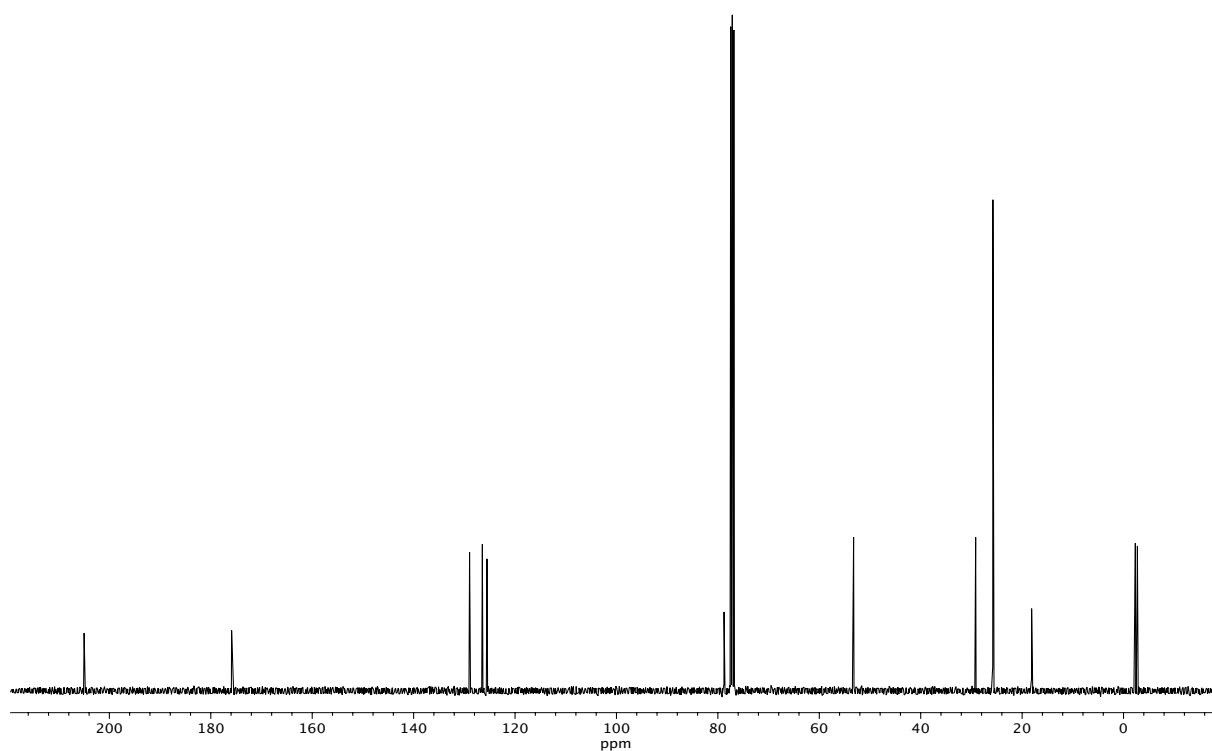


Figure A2.25 <sup>1</sup>H NMR (400 MHz, CDCl<sub>3</sub>) of compound 40.





**Figure A2.26** Infrared spectrum (Thin Film, NaCl) of compound **40**.



**Figure A2.27** <sup>13</sup>C NMR (100 MHz, CDCl<sub>3</sub>) of compound **40**.

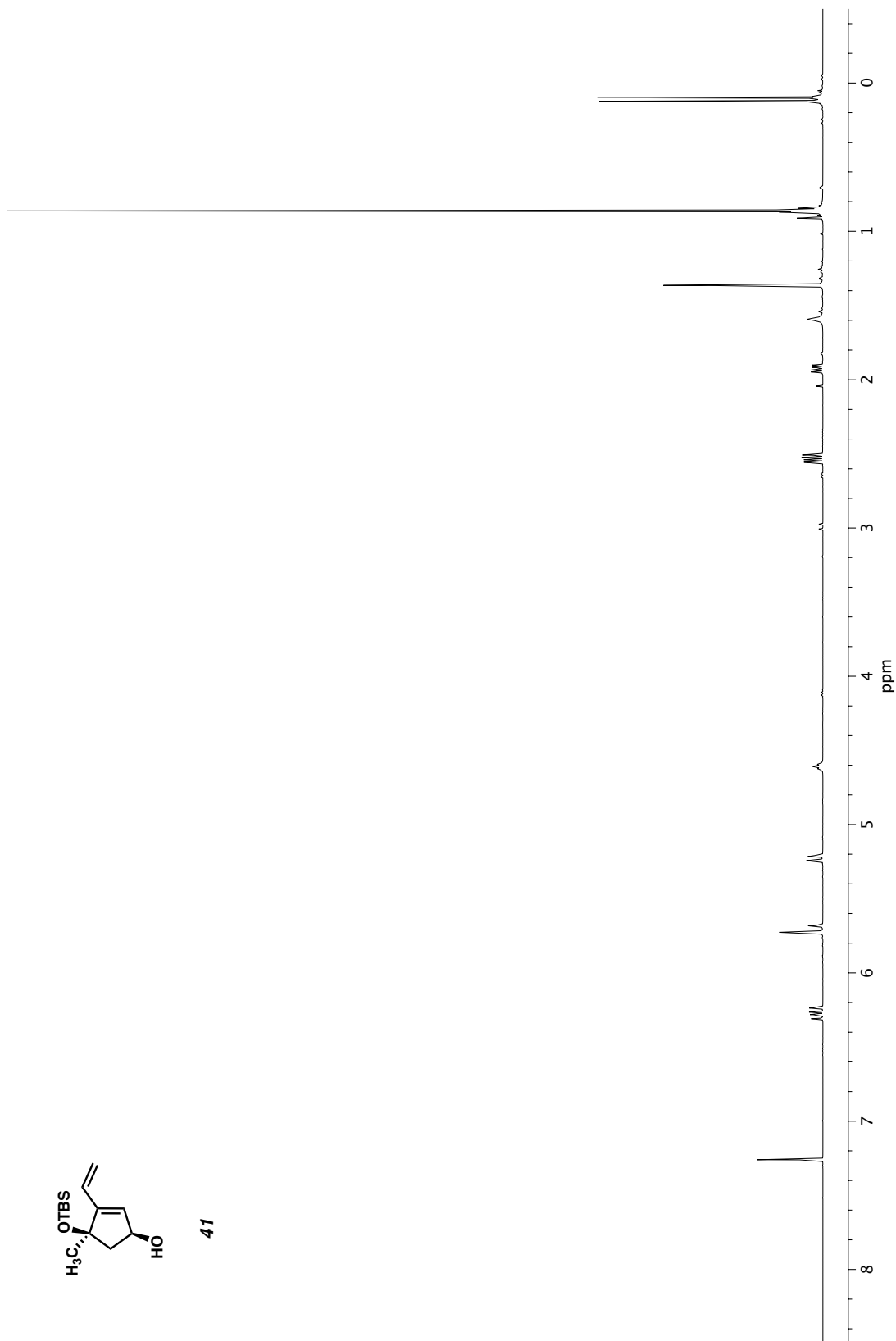
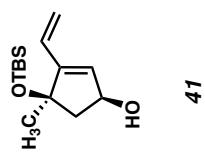
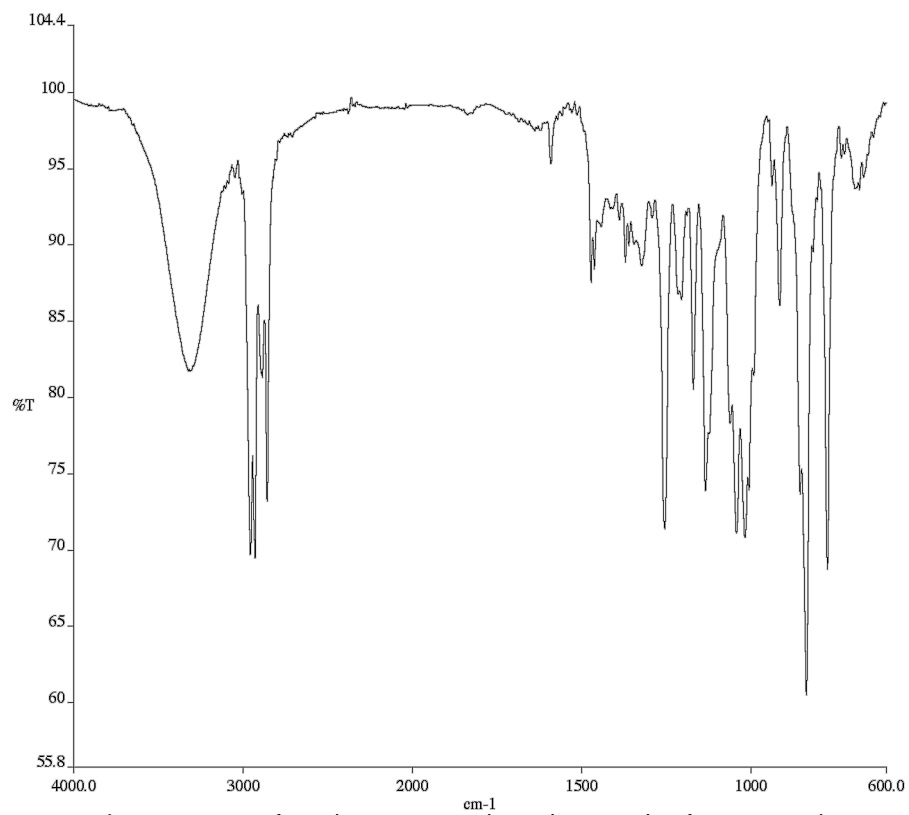
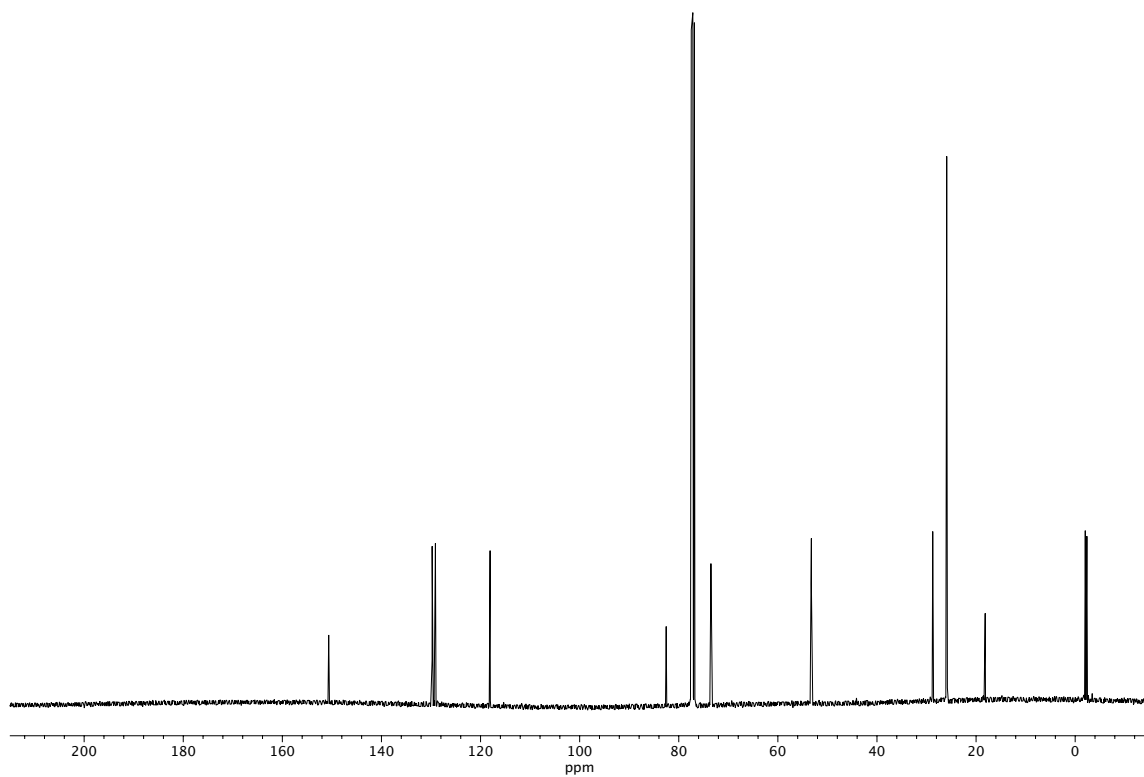


Figure A2.28 <sup>1</sup>H NMR (400 MHz, CDCl<sub>3</sub>) of compound 41.



**Figure A2.29** Infrared spectrum (Thin Film, NaCl) of compound **41**.



**Figure A2.30** <sup>13</sup>C NMR (100 MHz, CDCl<sub>3</sub>) of compound **41**.

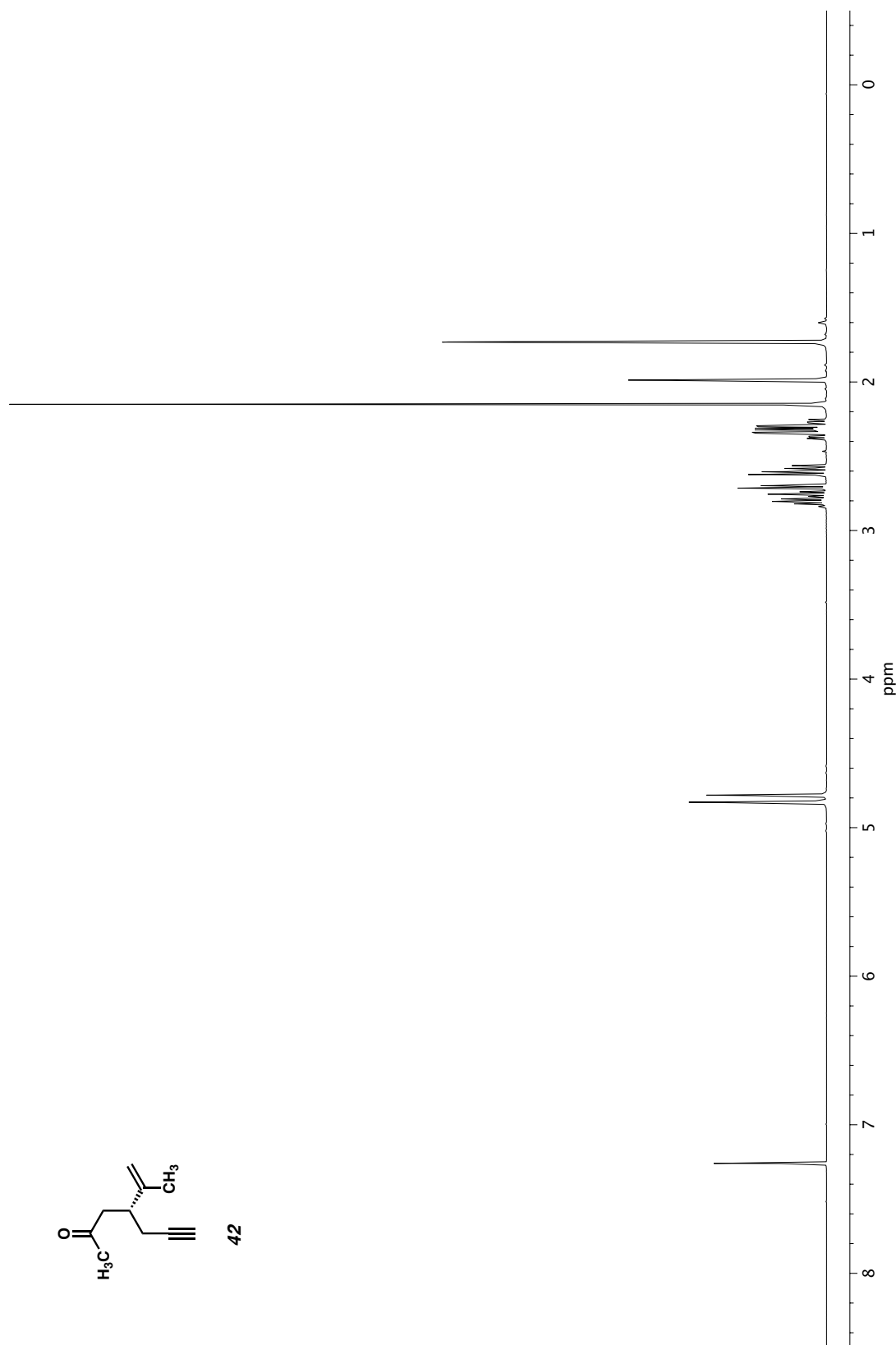
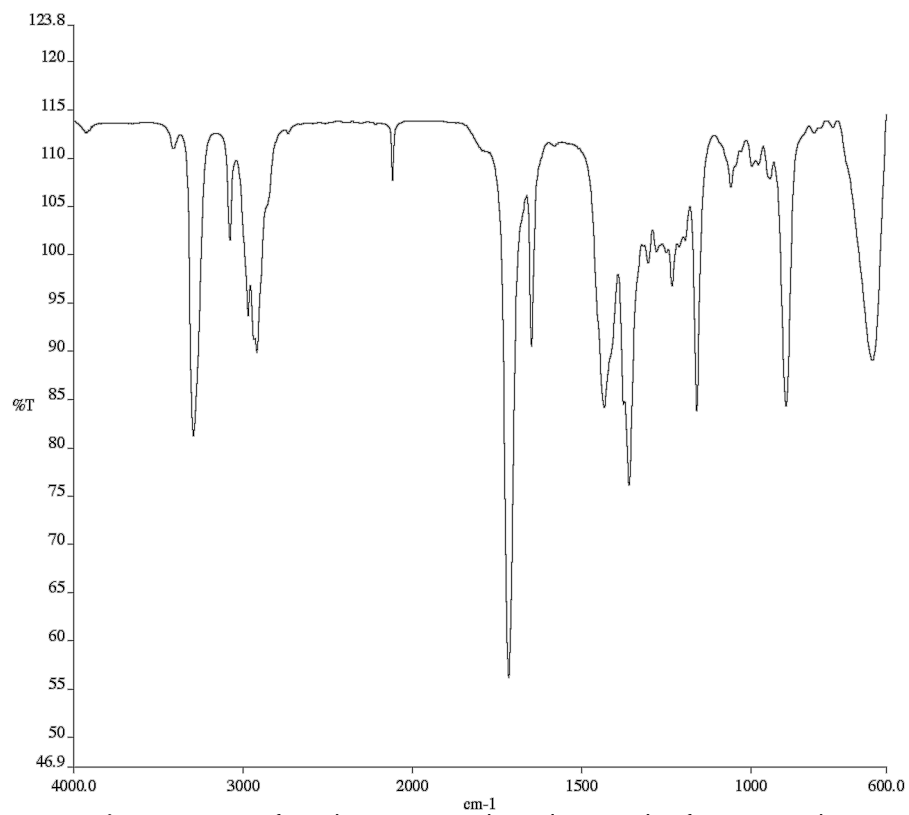
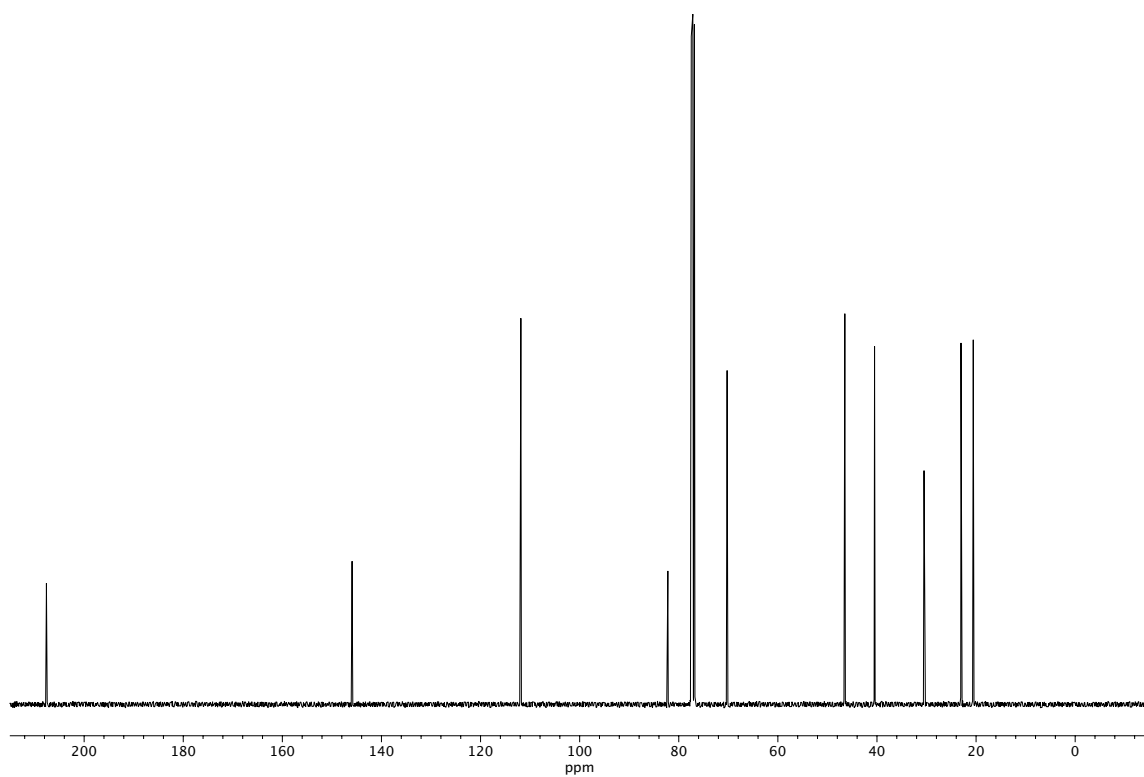


Figure A2.31 <sup>1</sup>H NMR (400 MHz, CDCl<sub>3</sub>) of compound 42.



**Figure A2.32** Infrared spectrum (Thin Film, NaCl) of compound **42**.



**Figure A2.33** <sup>13</sup>C NMR (100 MHz, CDCl<sub>3</sub>) of compound **42**.

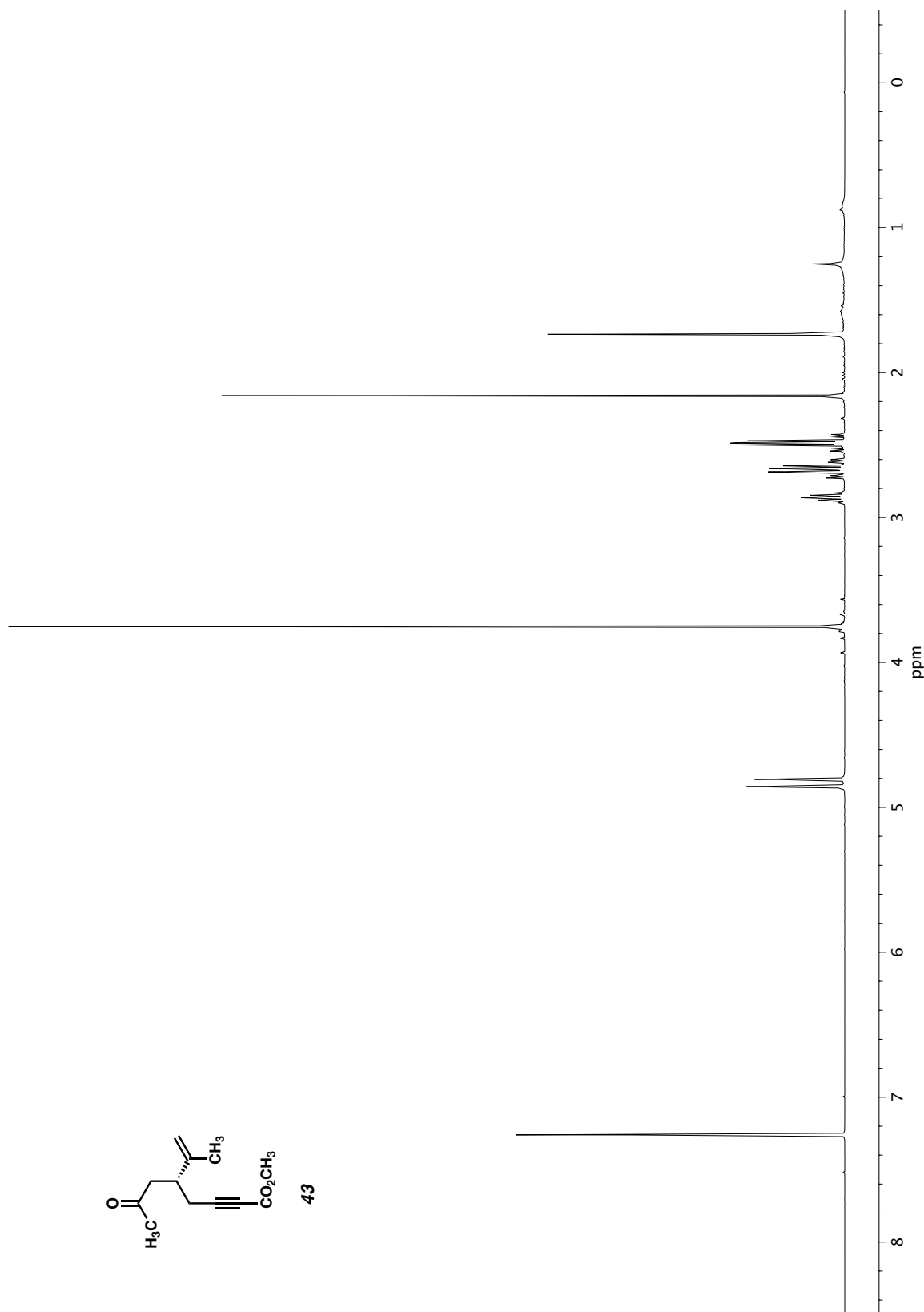
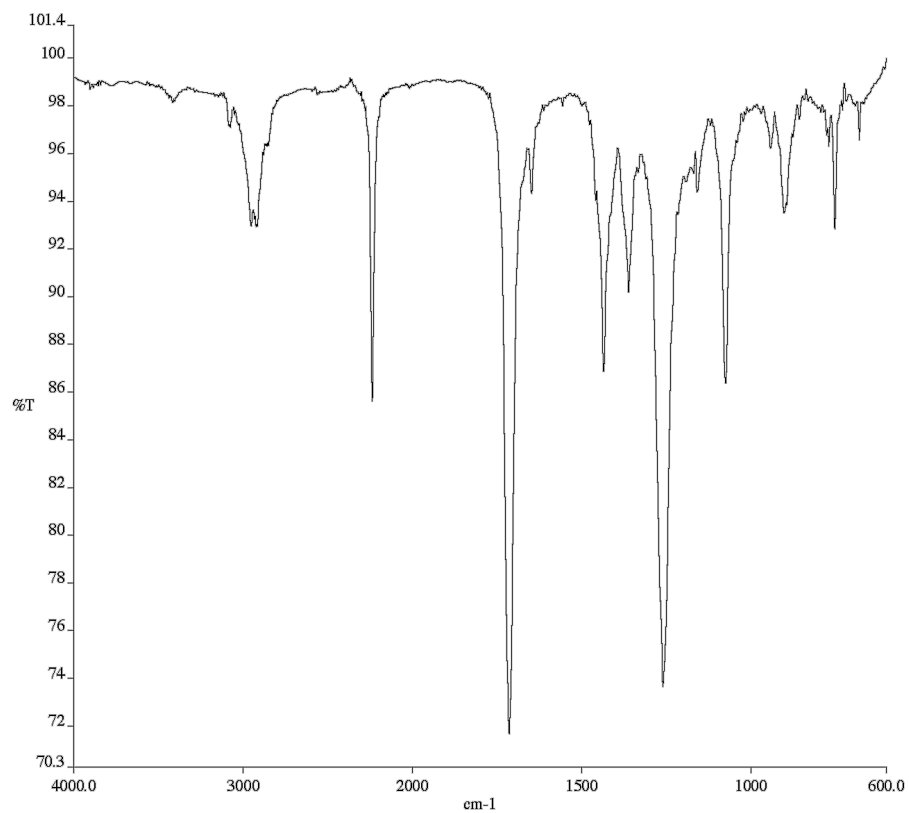
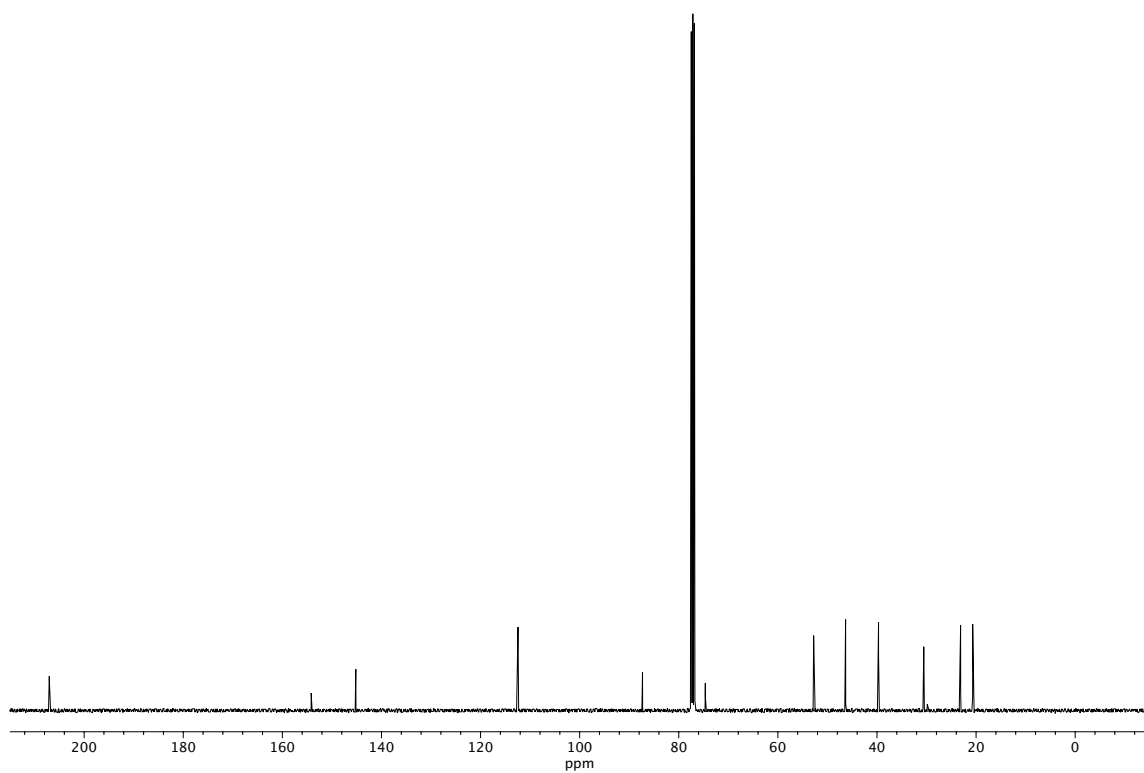


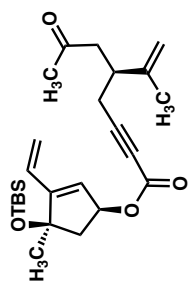
Figure A2.34  $^1\text{H}$  NMR (400 MHz,  $\text{CDCl}_3$ ) of compound 43.



**Figure A2.35** Infrared spectrum (Thin Film, NaCl) of compound **43**.



**Figure A2.36** <sup>13</sup>C NMR (100 MHz, CDCl<sub>3</sub>) of compound **43**.



44

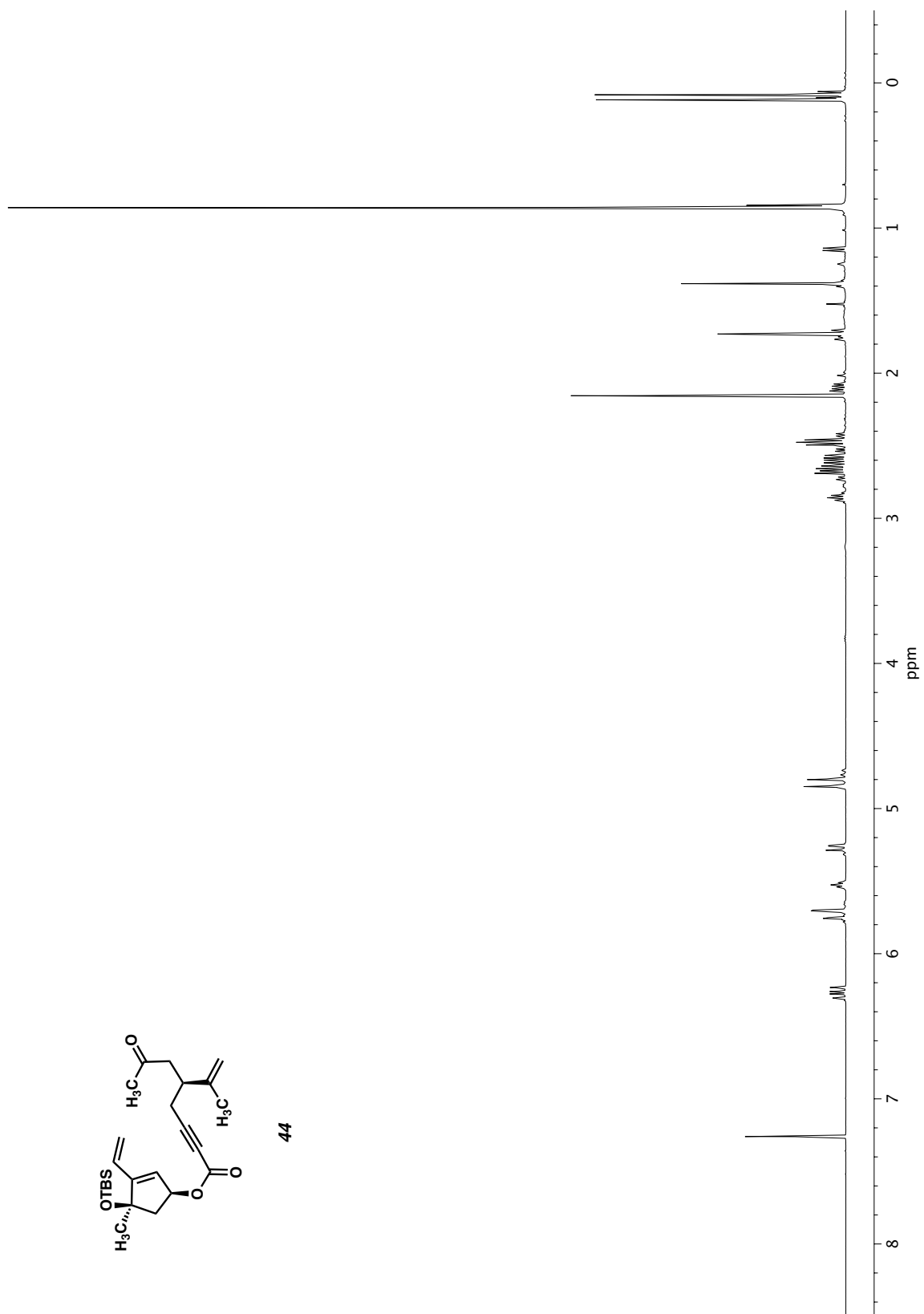
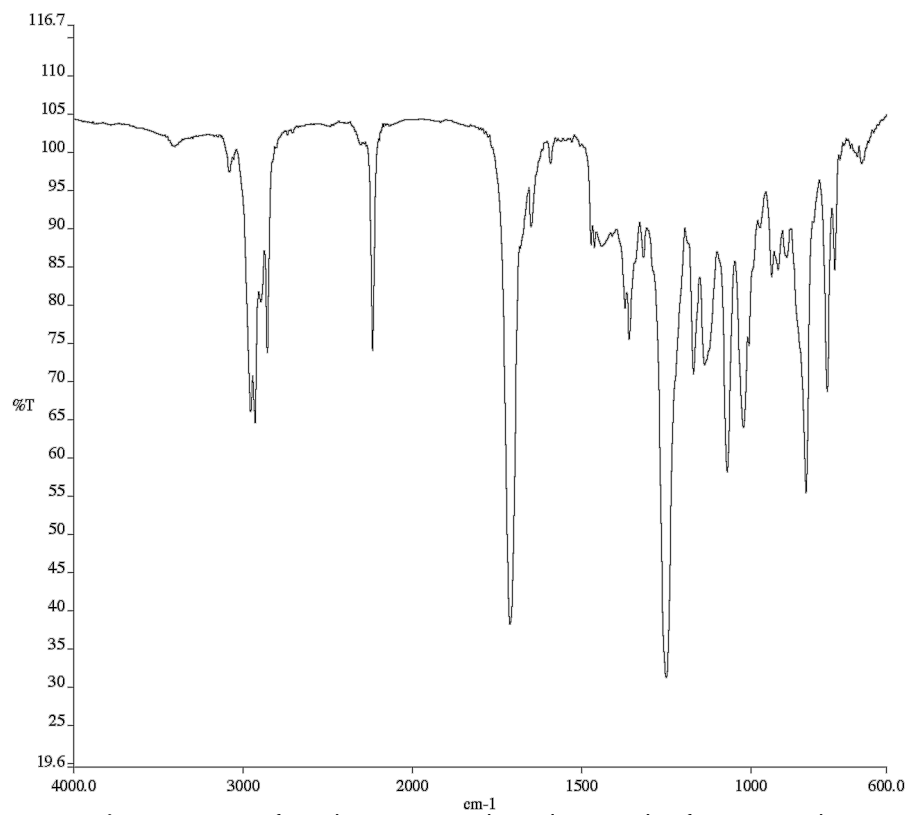
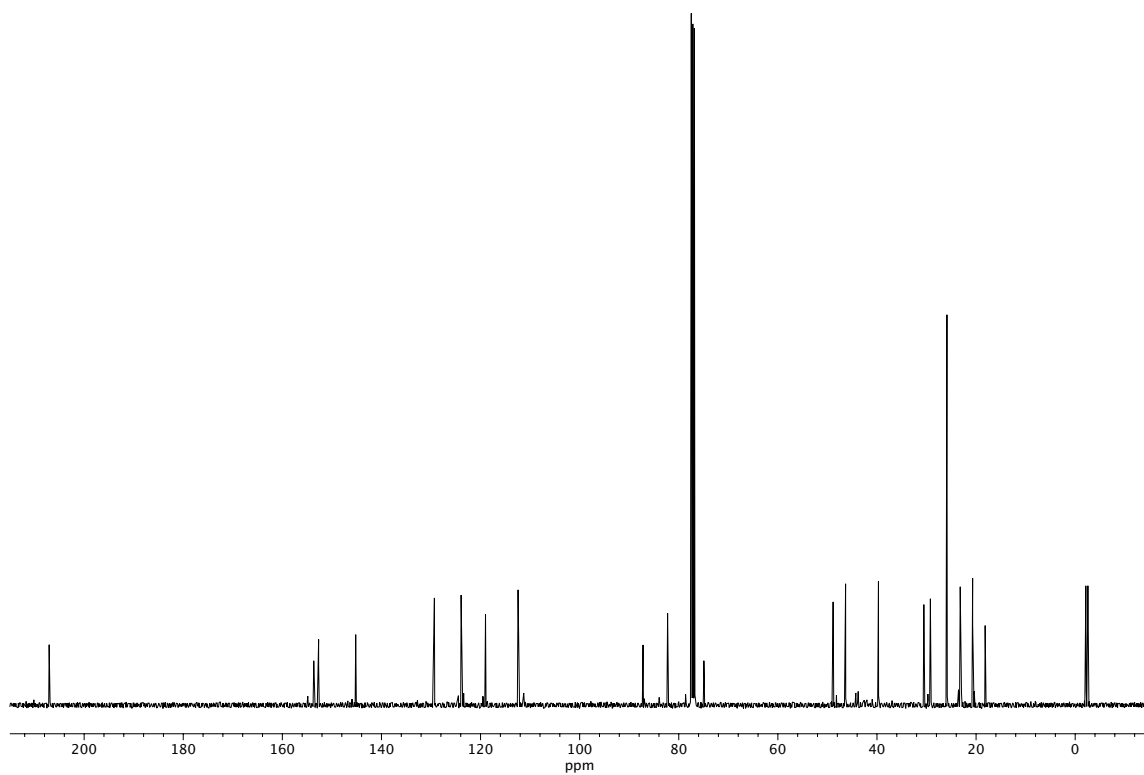


Figure A2.37  $^1\text{H NMR}$  (400 MHz,  $\text{CDCl}_3$ ) of compound 44.





**Figure A2.38** Infrared spectrum (Thin Film, NaCl) of compound **44**.



**Figure A2.39** <sup>13</sup>C NMR (100 MHz, CDCl<sub>3</sub>) of compound **44**.

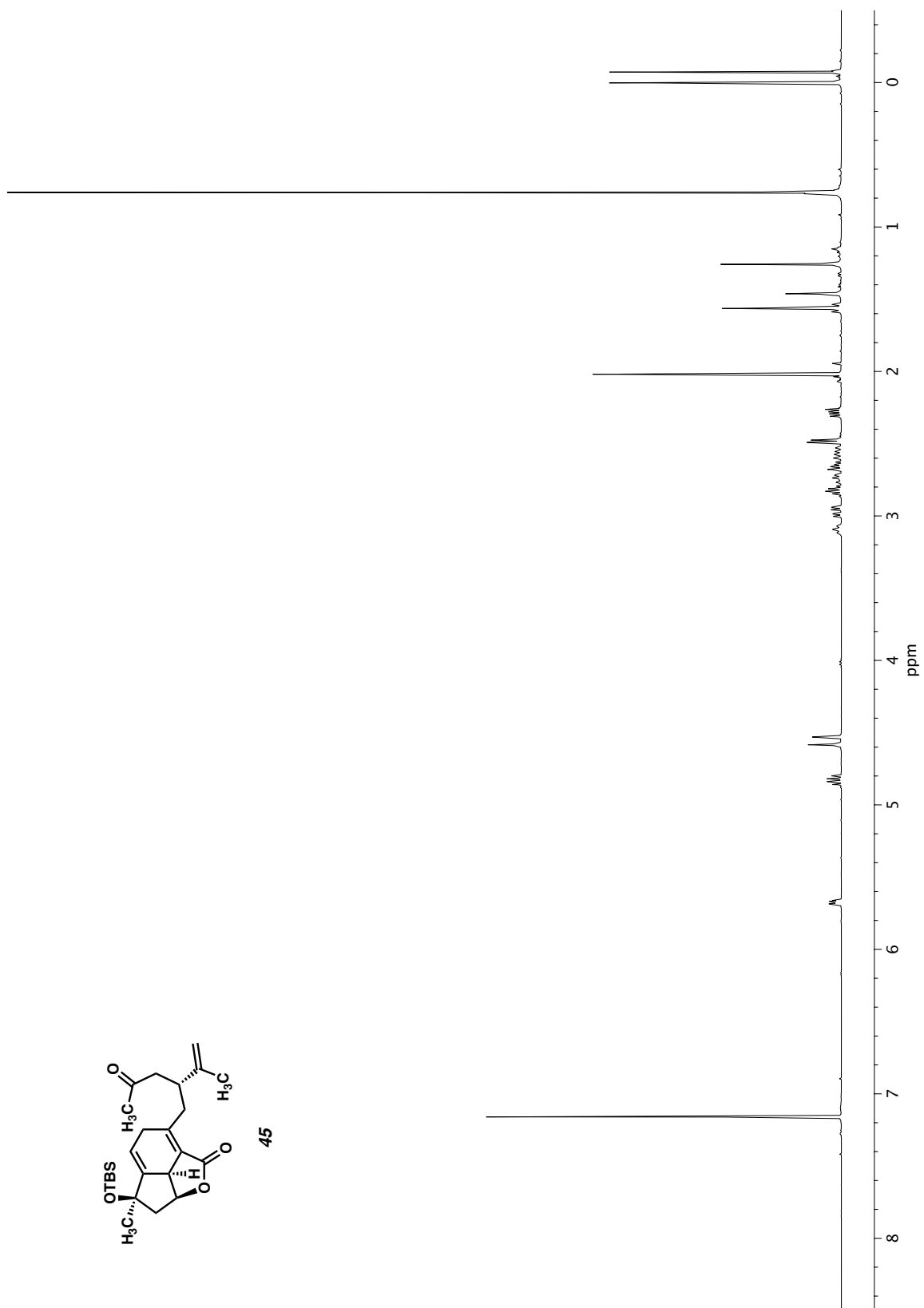
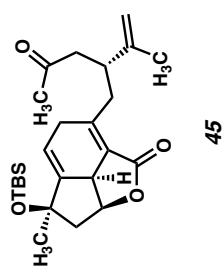
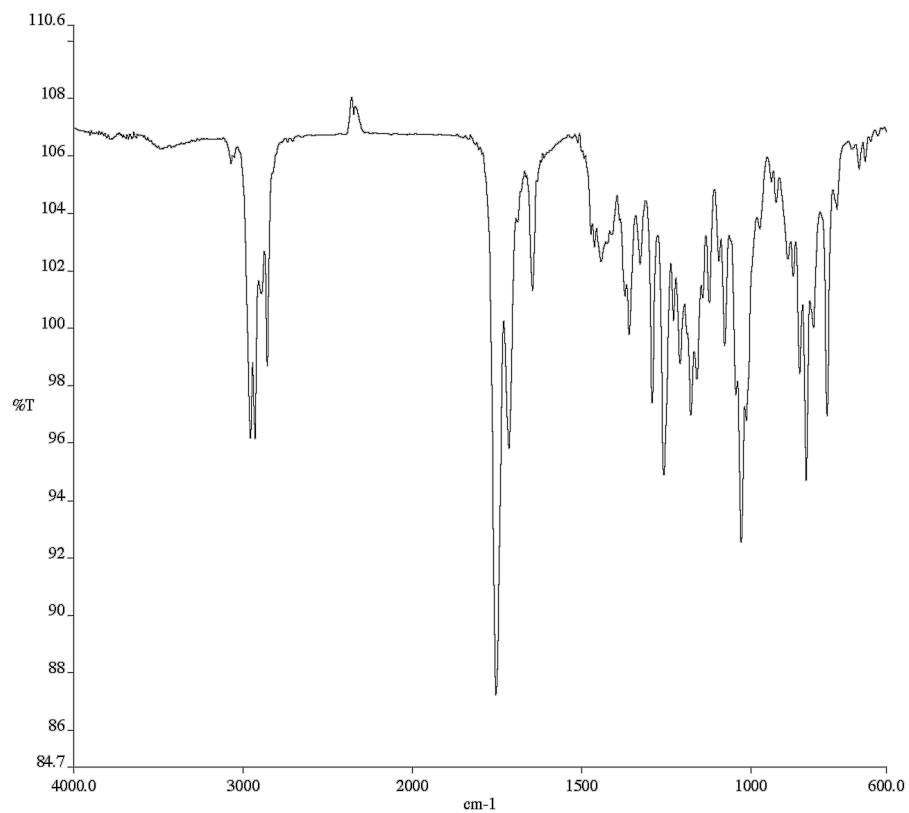
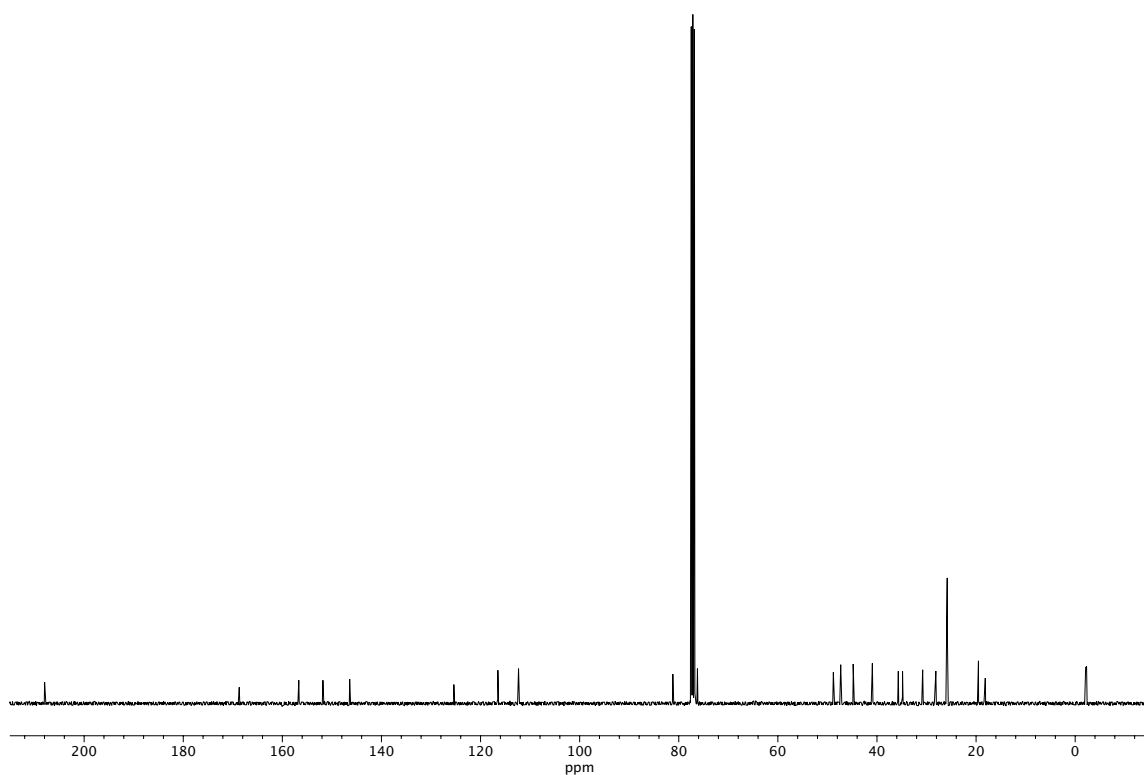


Figure A2.40 <sup>1</sup>H NMR (400 MHz, CDCl<sub>3</sub>) of compound 45.



**Figure A2.41** Infrared spectrum (Thin Film, NaCl) of compound **45**.



**Figure A2.42** <sup>13</sup>C NMR (100 MHz, CDCl<sub>3</sub>) of compound **45**.

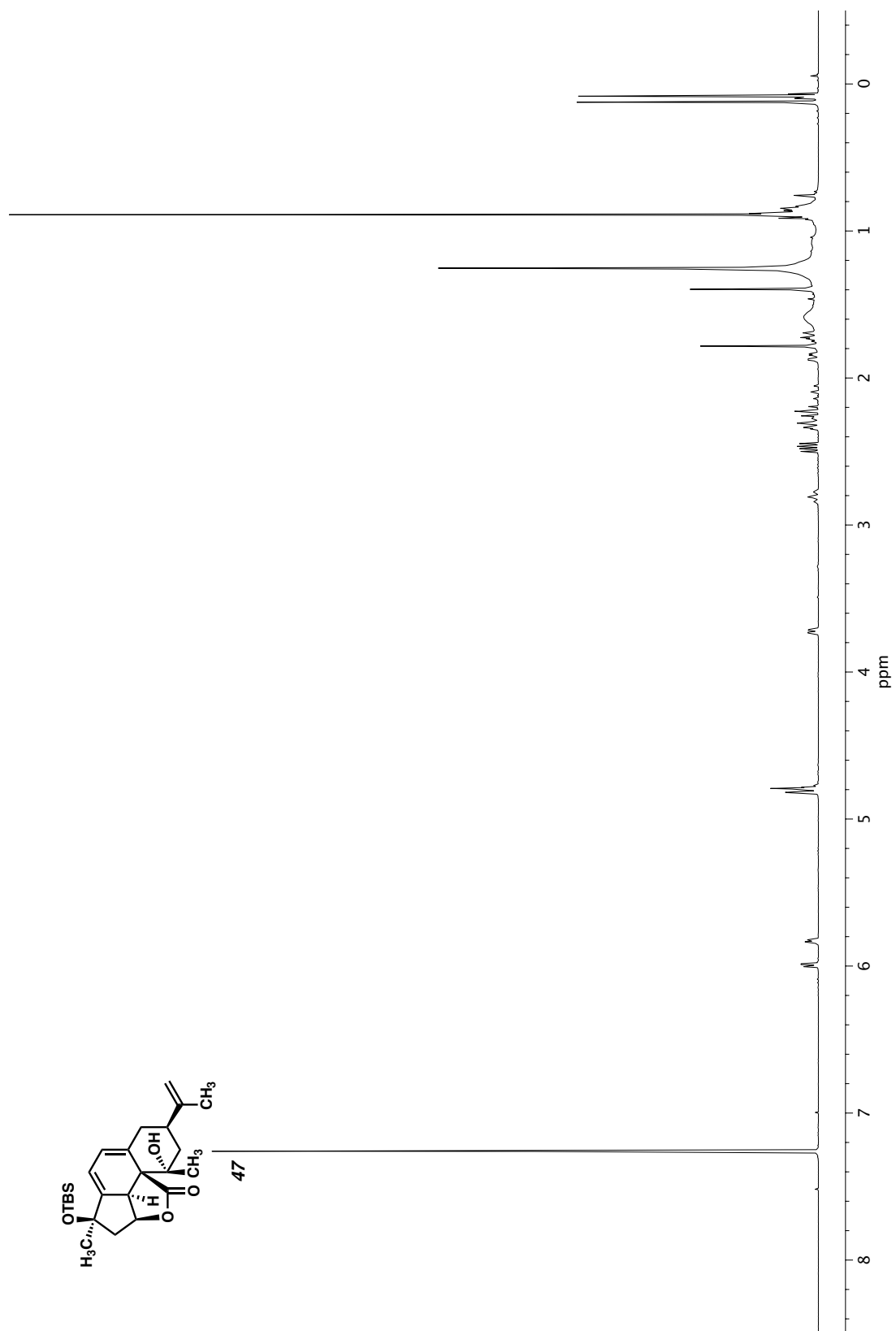
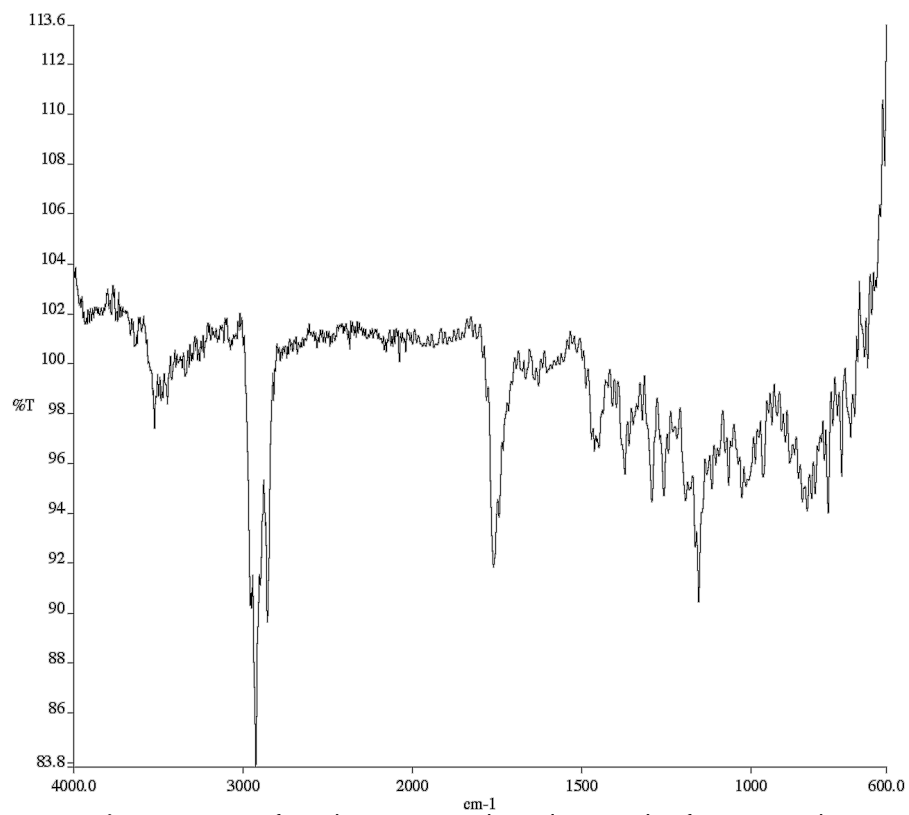
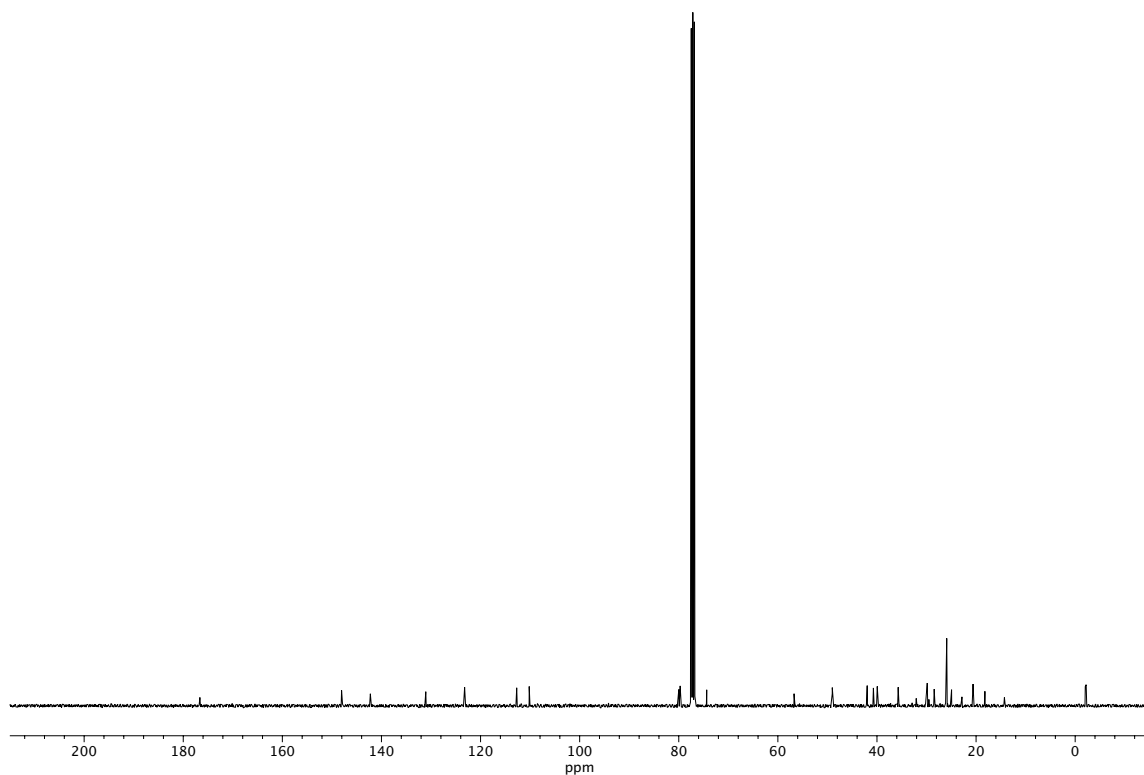


Figure A2.43 <sup>1</sup>H NMR (400 MHz, CDCl<sub>3</sub>) of compound 47.



**Figure A2.44** Infrared spectrum (Thin Film, NaCl) of compound **47**.



**Figure A2.45** <sup>13</sup>C NMR (100 MHz, CDCl<sub>3</sub>) of compound **47**.

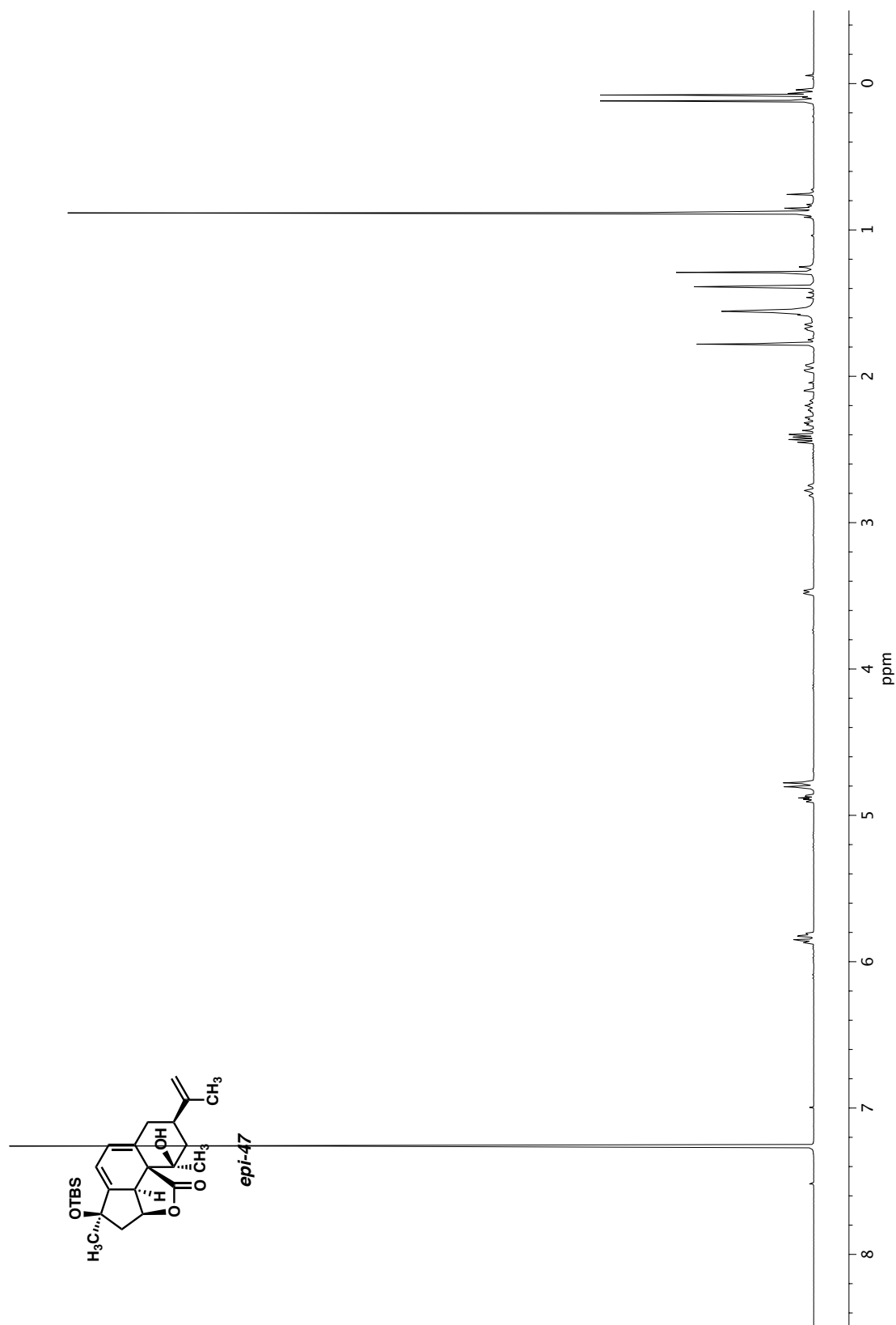
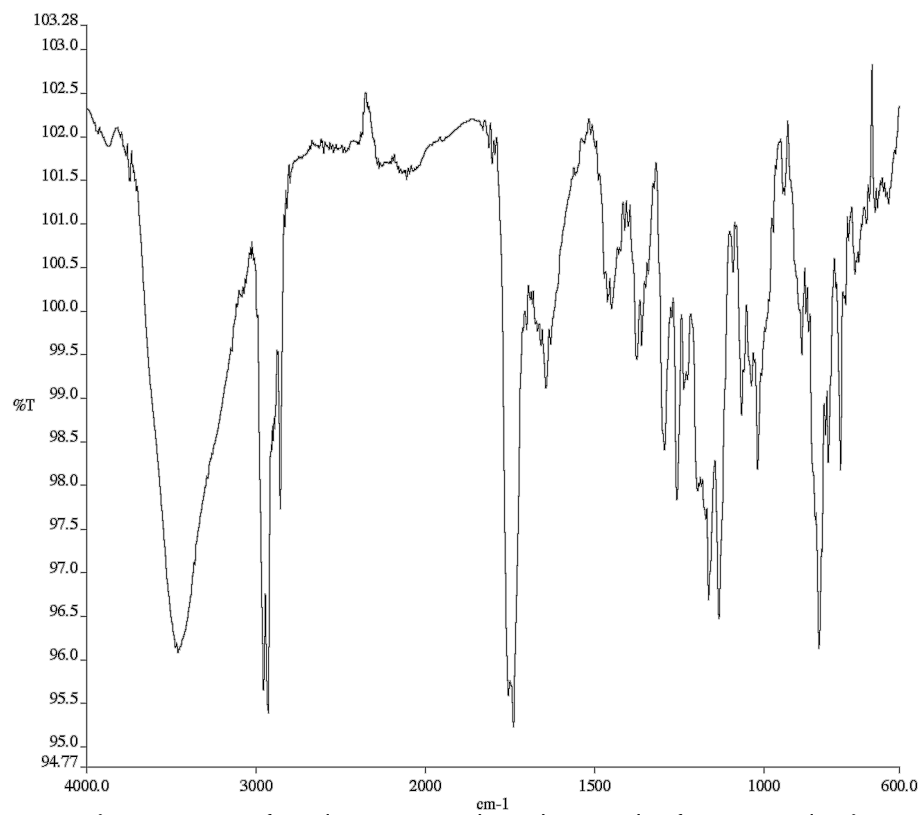
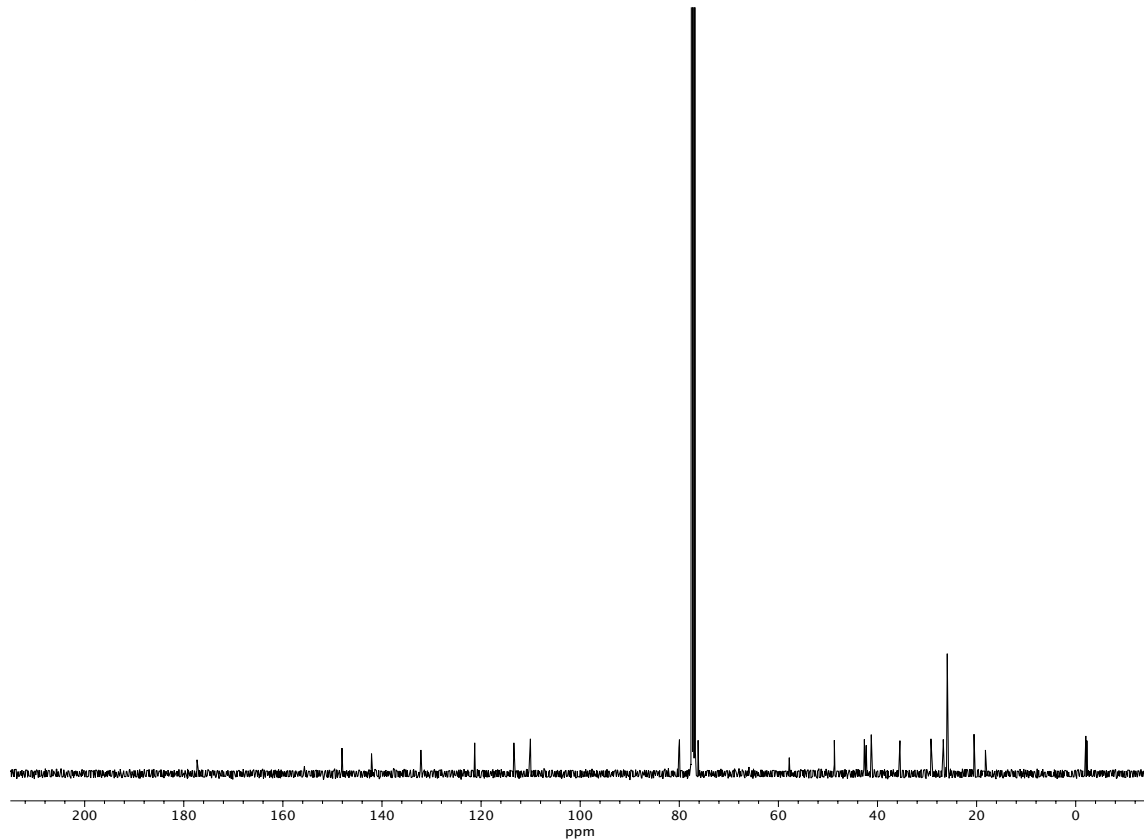


Figure A2.46 <sup>1</sup>H NMR (400 MHz, CDCl<sub>3</sub>) of compound **epi-47**.



**Figure A2.47** Infrared spectrum (Thin Film, NaCl) of compound **epi-47**.



**Figure A2.48** <sup>13</sup>C NMR (100 MHz, CDCl<sub>3</sub>) of compound **epi-47**.

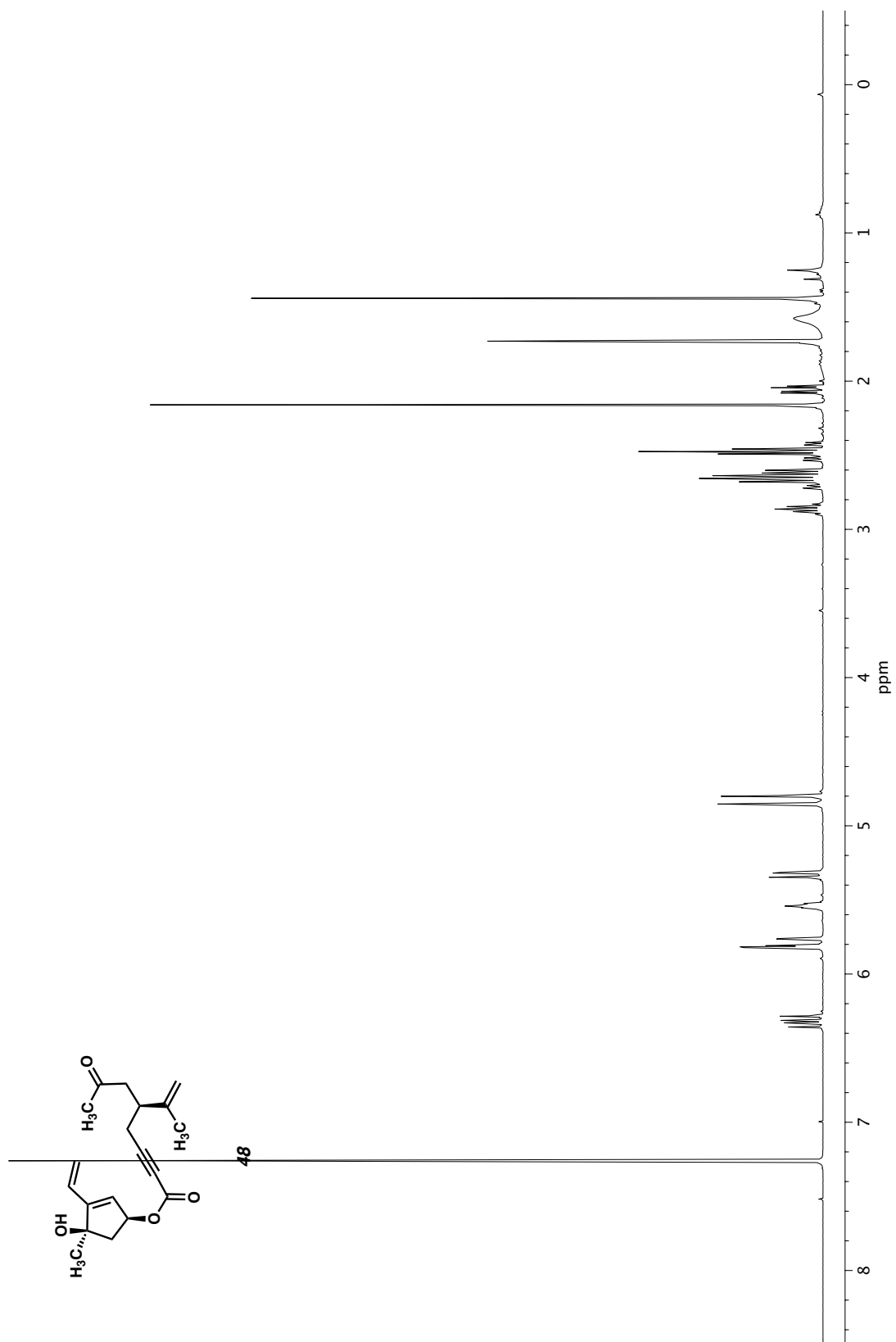
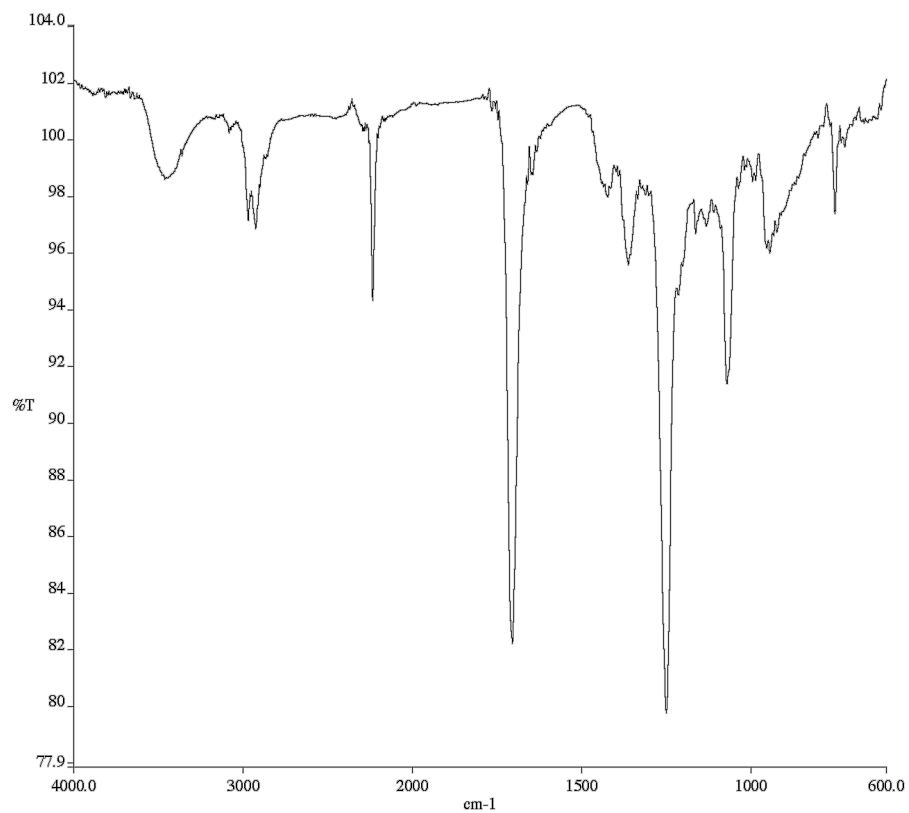
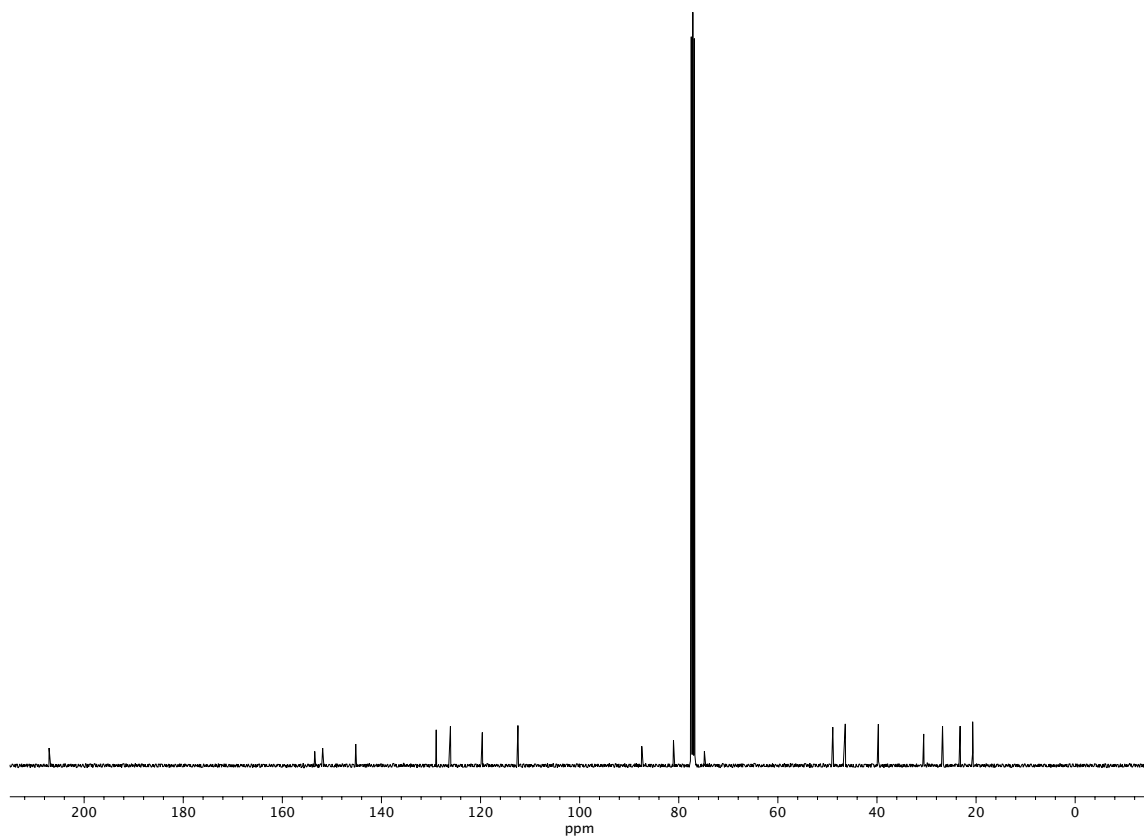


Figure A2.49 <sup>1</sup>H NMR (400 MHz, CDCl<sub>3</sub>) of compound 48.





**Figure A2.50** Infrared spectrum (Thin Film, NaCl) of compound **48**.



**Figure A2.51** <sup>13</sup>C NMR (100 MHz, CDCl<sub>3</sub>) of compound **48**.

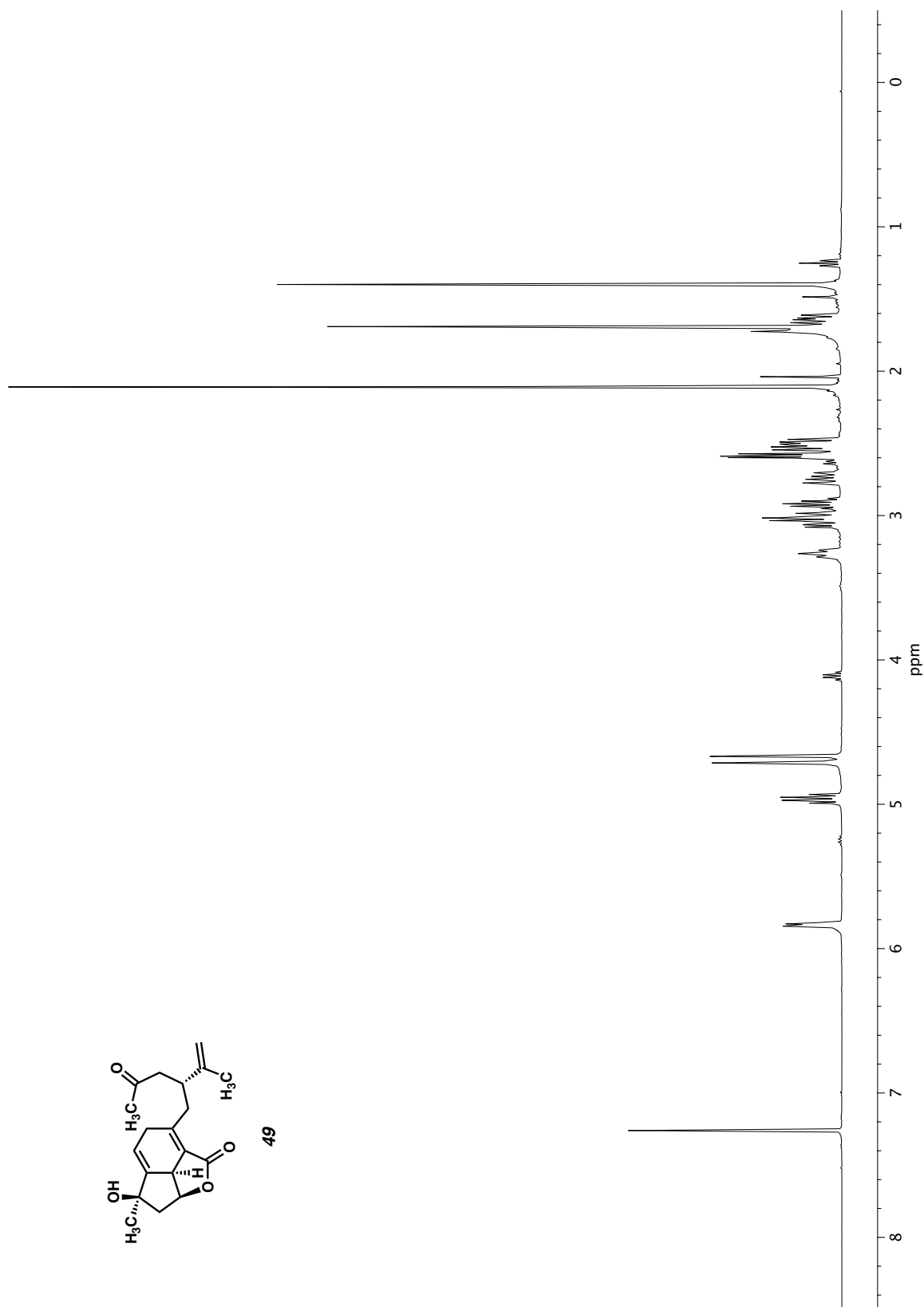
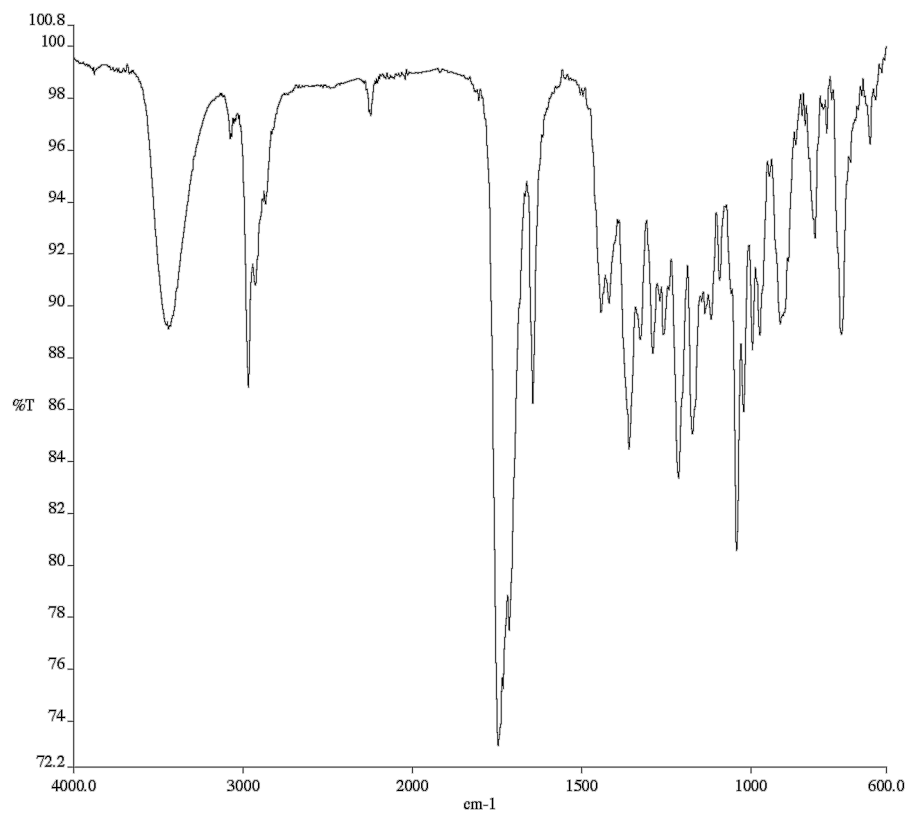
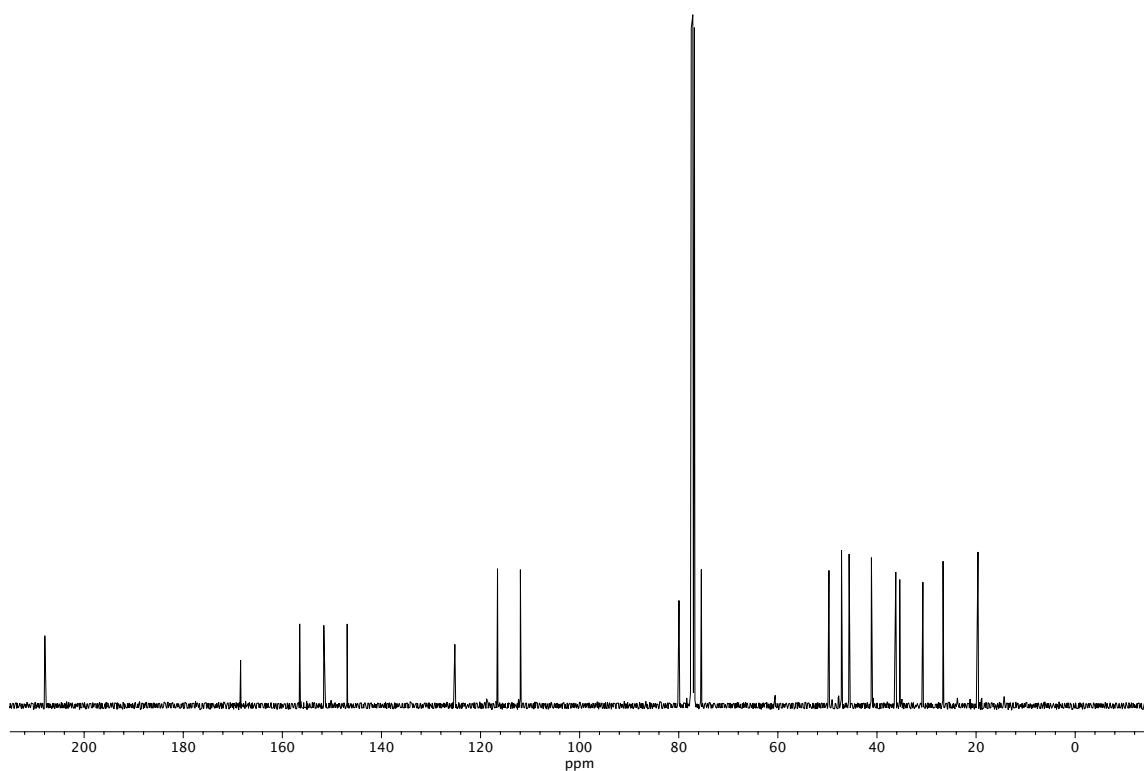


Figure A2.52 <sup>1</sup>H NMR (400 MHz, CDCl<sub>3</sub>) of compound 49.



**Figure A2.53** Infrared spectrum (Thin Film, NaCl) of compound **49**.



**Figure A2.54** <sup>13</sup>C NMR (100 MHz, CDCl<sub>3</sub>) of compound **49**.

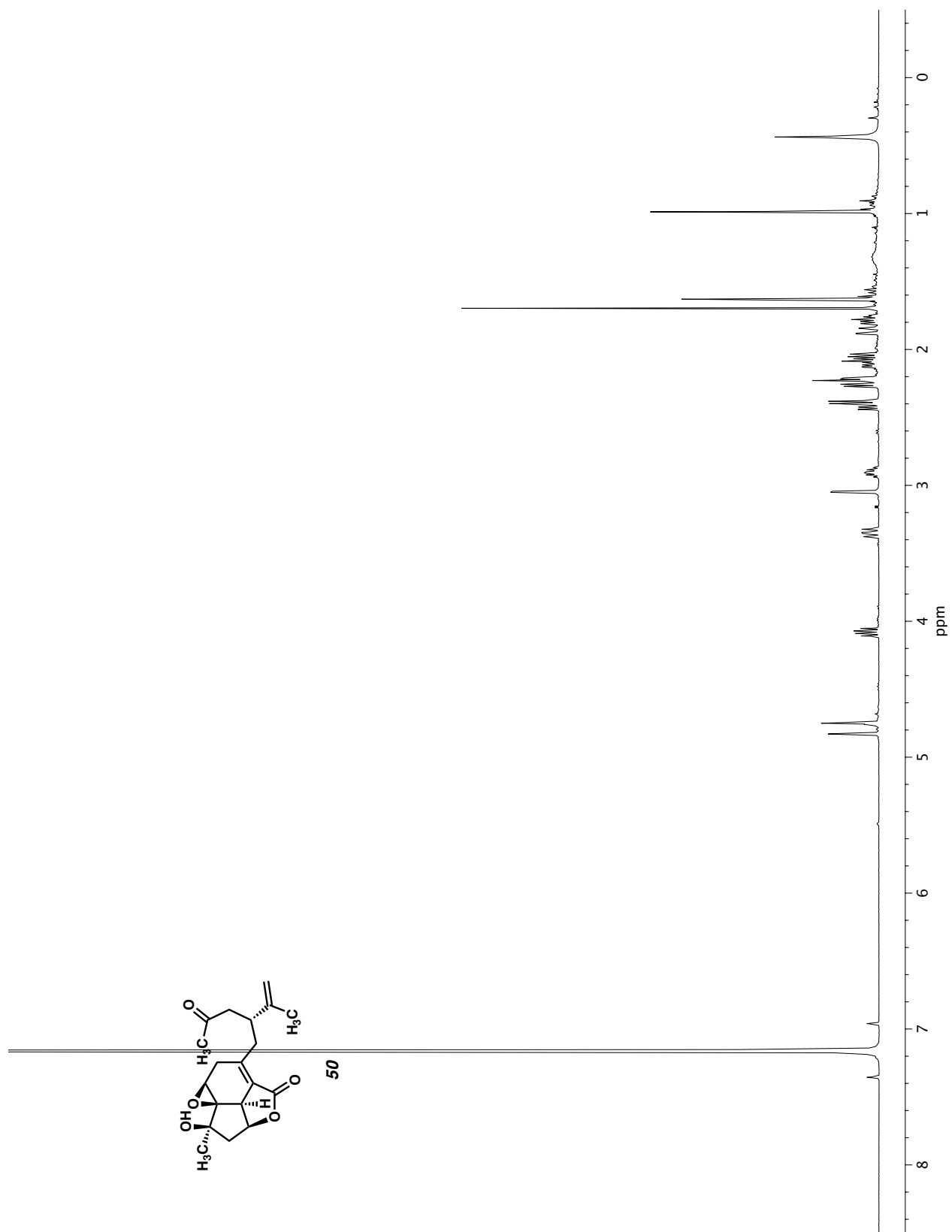
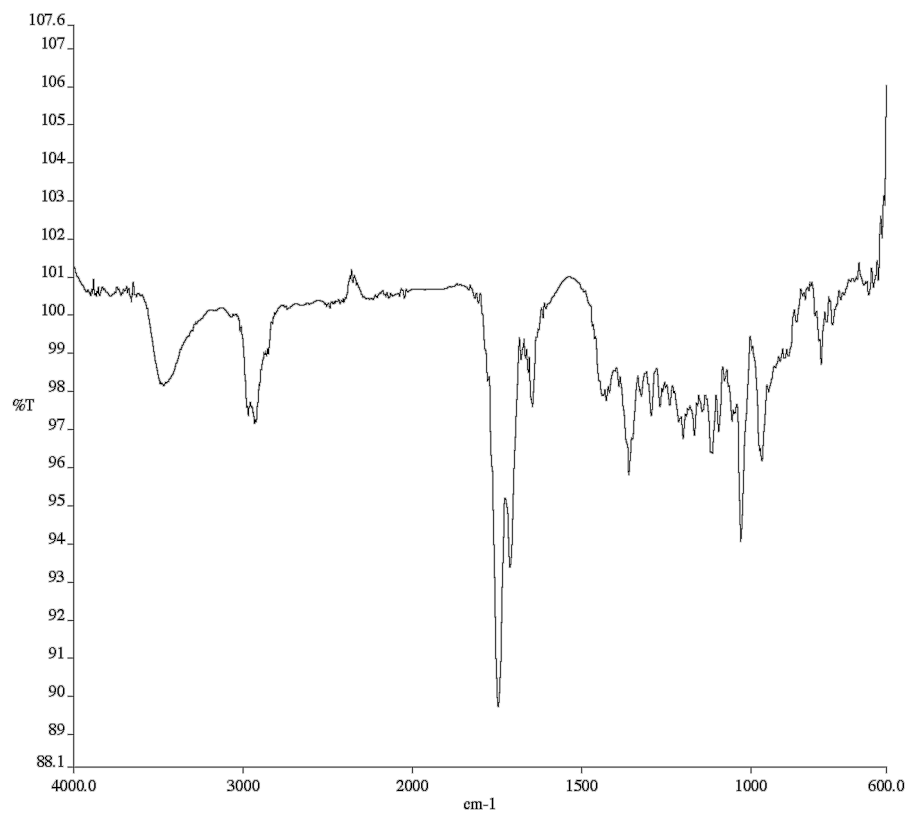
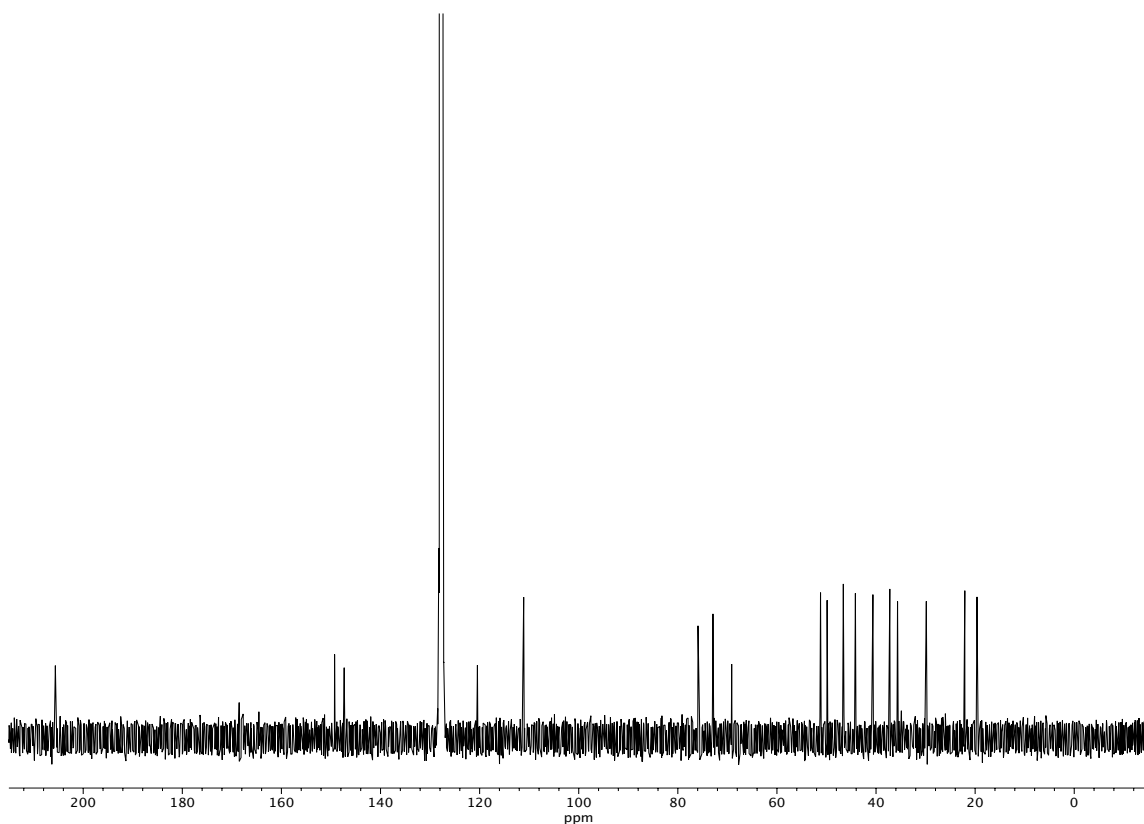


Figure A2.55 <sup>1</sup>H NMR (400 MHz, CDCl<sub>3</sub>) of compound 50.



**Figure A2.56** Infrared spectrum (Thin Film, NaCl) of compound **50**.



**Figure A2.57** <sup>13</sup>C NMR (100 MHz, CDCl<sub>3</sub>) of compound **50**.

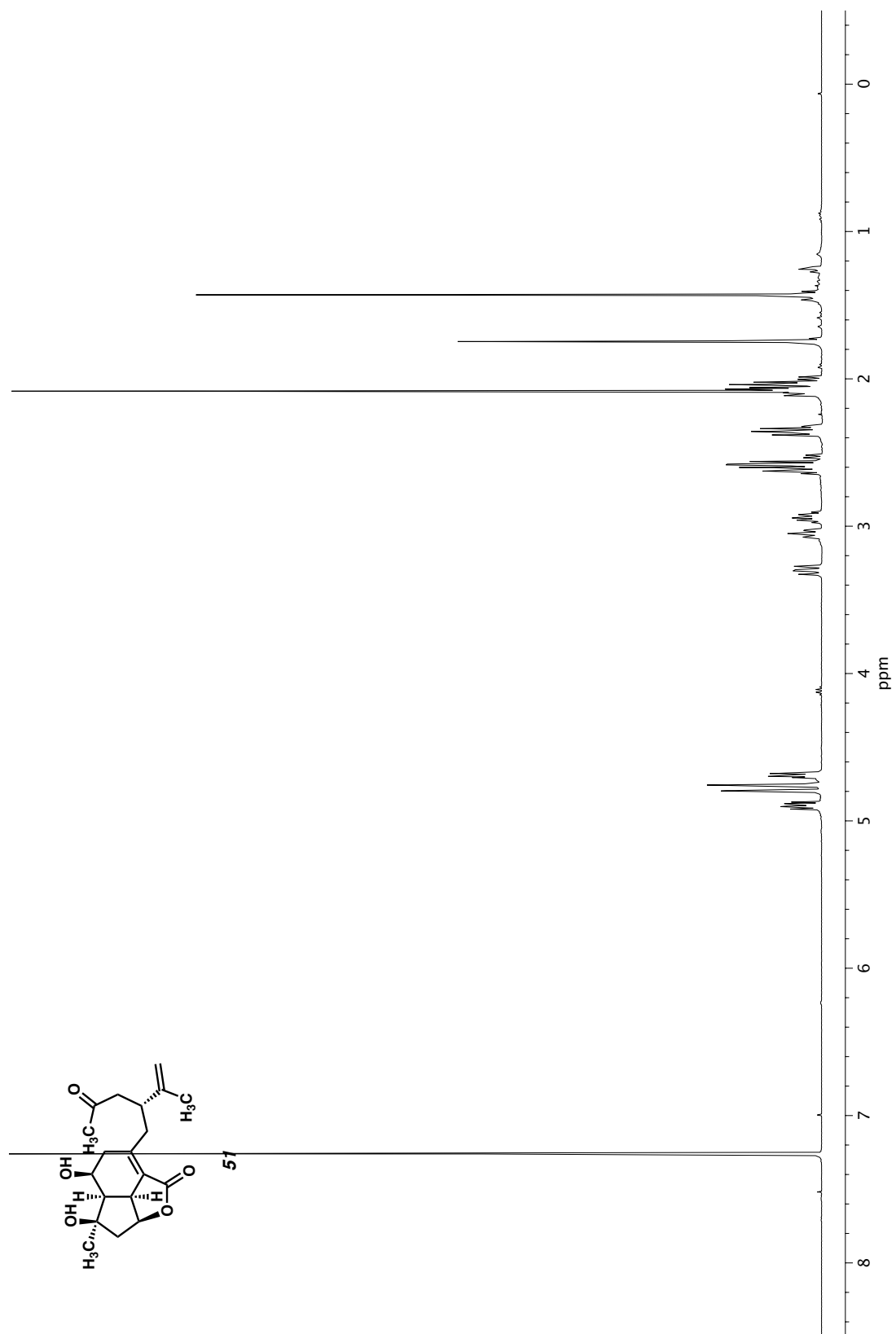
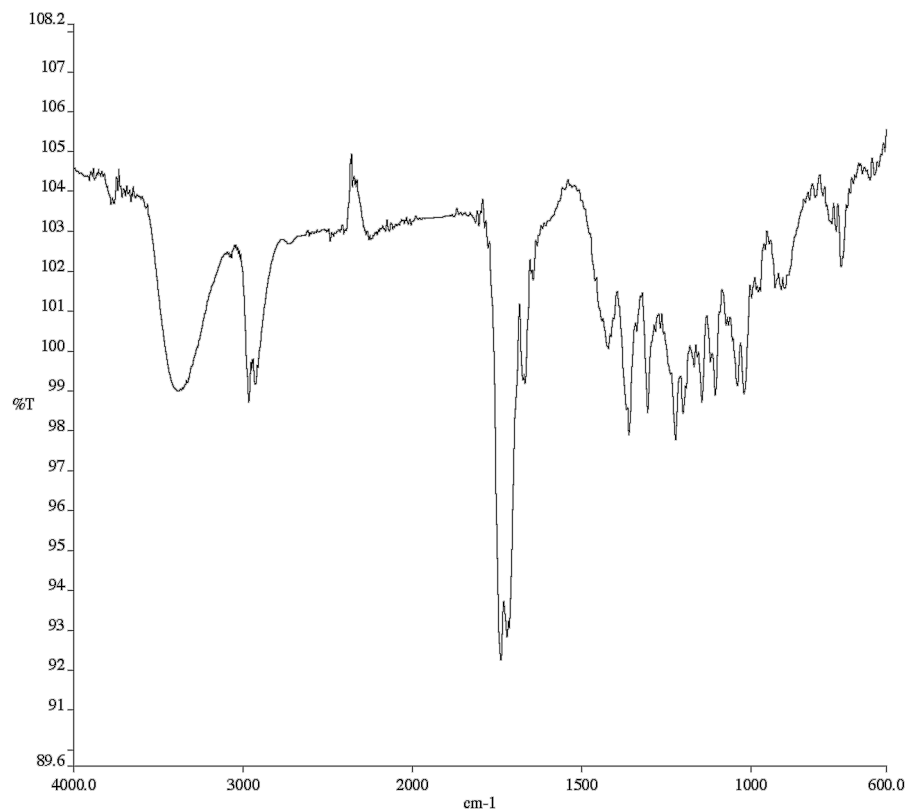
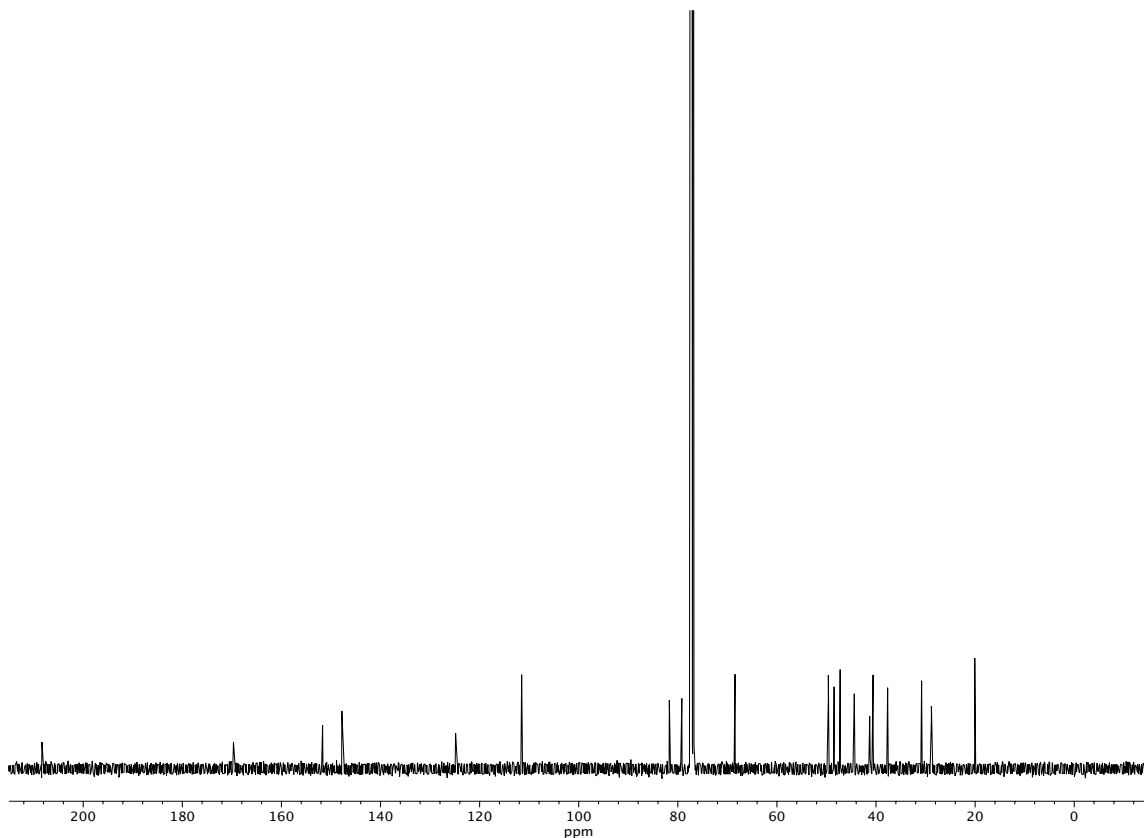


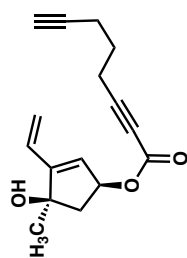
Figure A2.58 <sup>1</sup>H NMR (400 MHz, CDCl<sub>3</sub>) of compound 51.



**Figure A2.59** Infrared spectrum (Thin Film, NaCl) of compound **51**.



**Figure A2.60** <sup>13</sup>C NMR (100 MHz, CDCl<sub>3</sub>) of compound **50**.



59

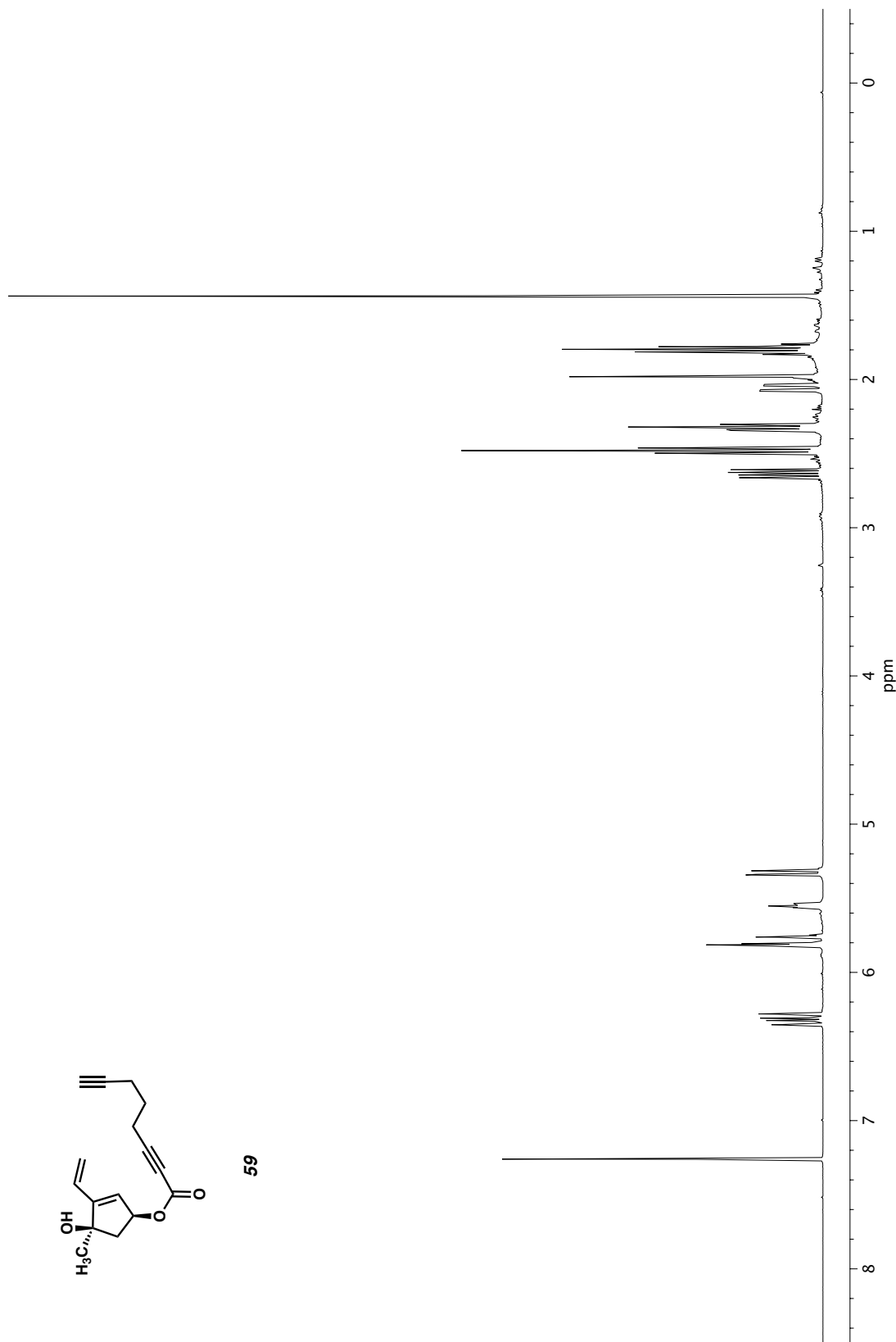
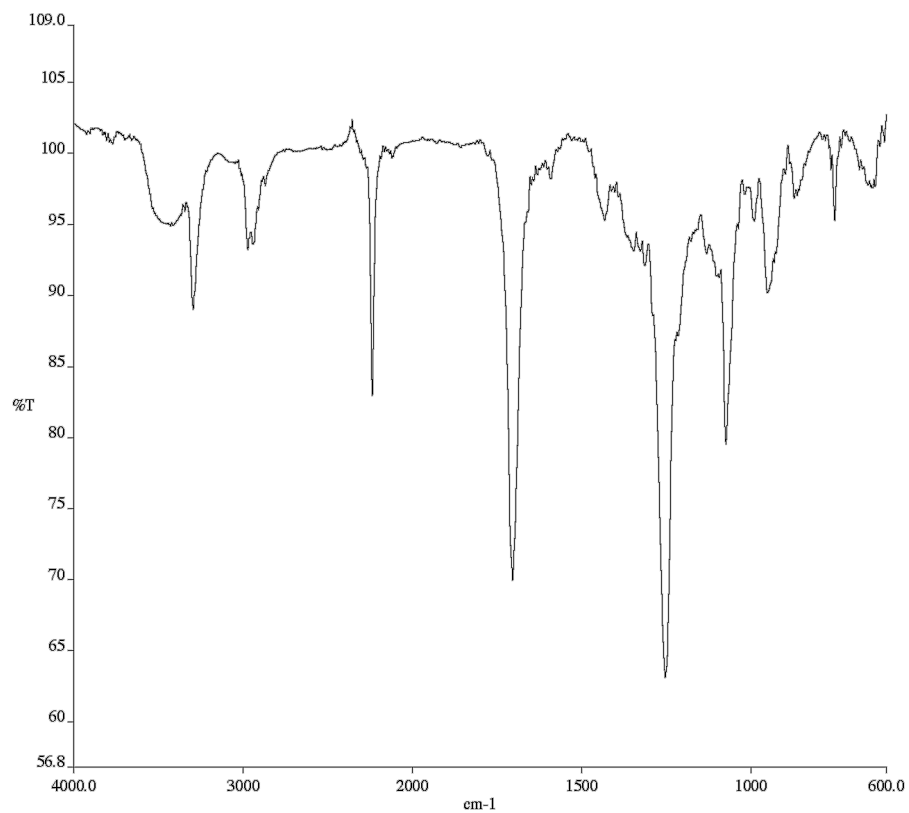
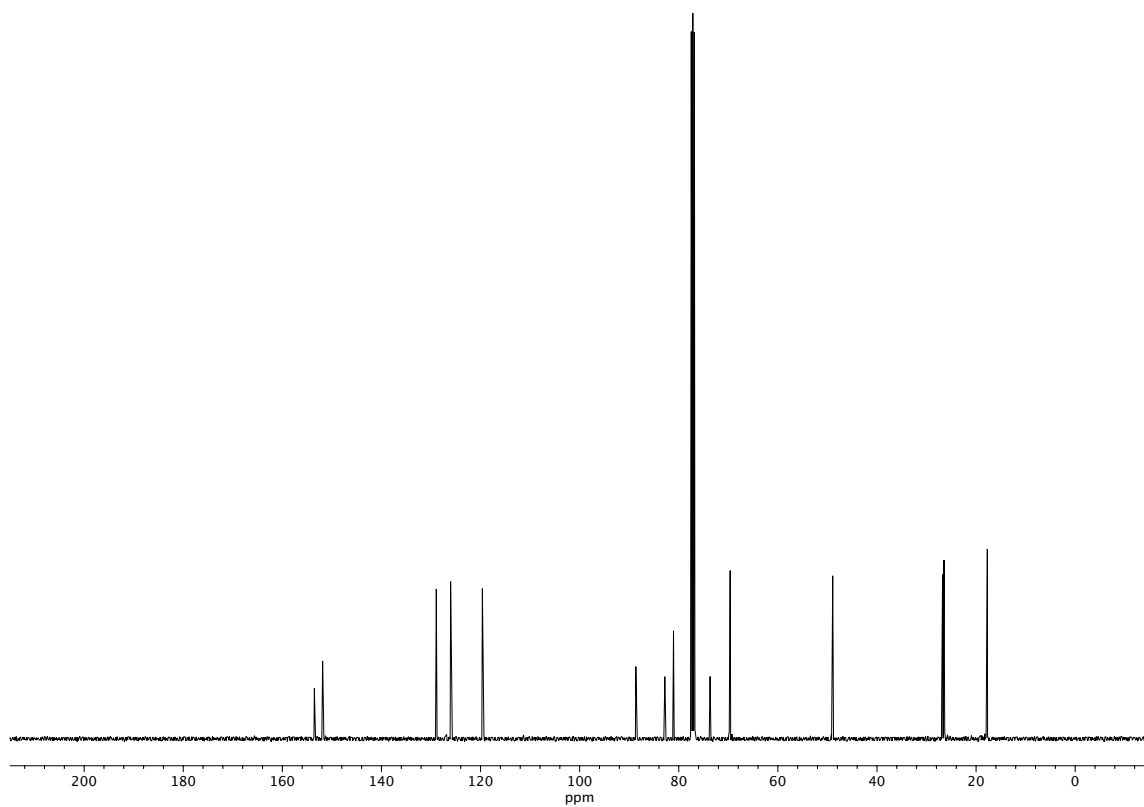


Figure A2.61 <sup>1</sup>H NMR (400 MHz, CDCl<sub>3</sub>) of compound 59.





**Figure A2.62** Infrared spectrum (Thin Film, NaCl) of compound **59**.



**Figure A2.63** <sup>13</sup>C NMR (100 MHz, CDCl<sub>3</sub>) of compound **59**.

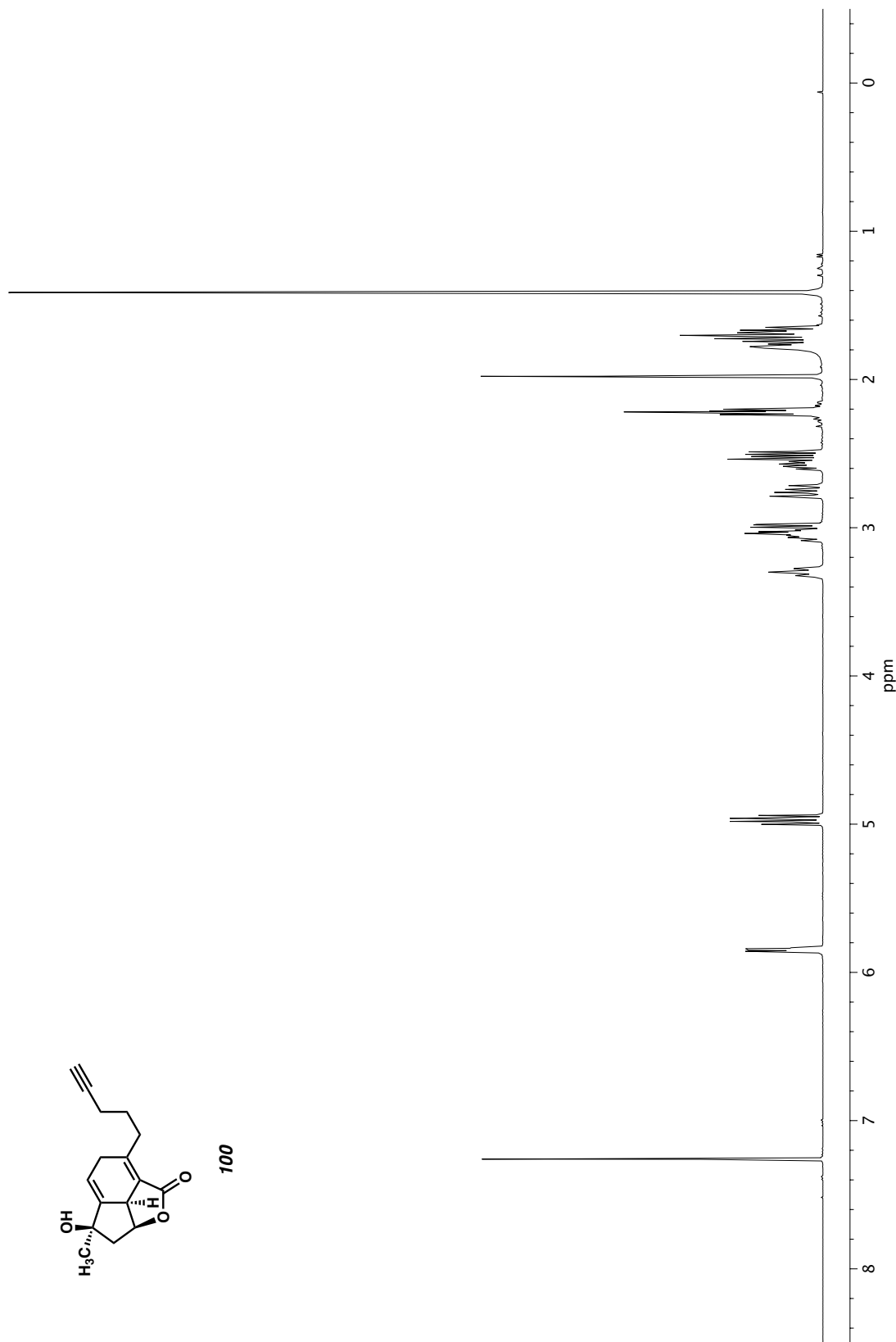
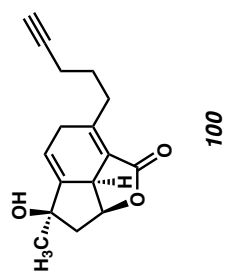
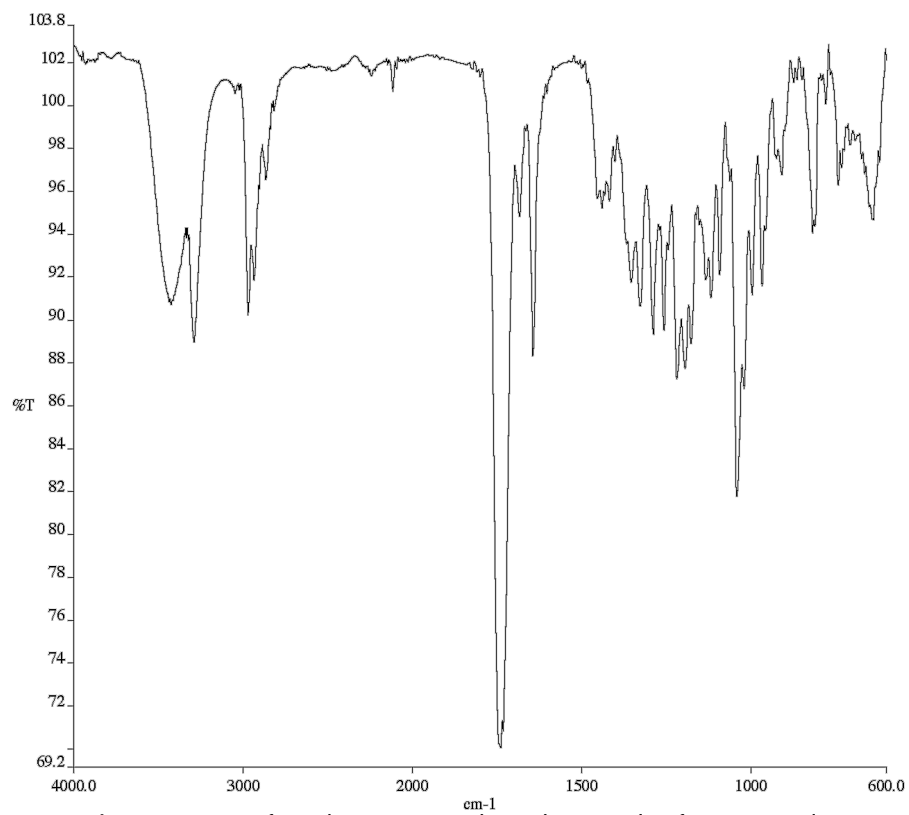
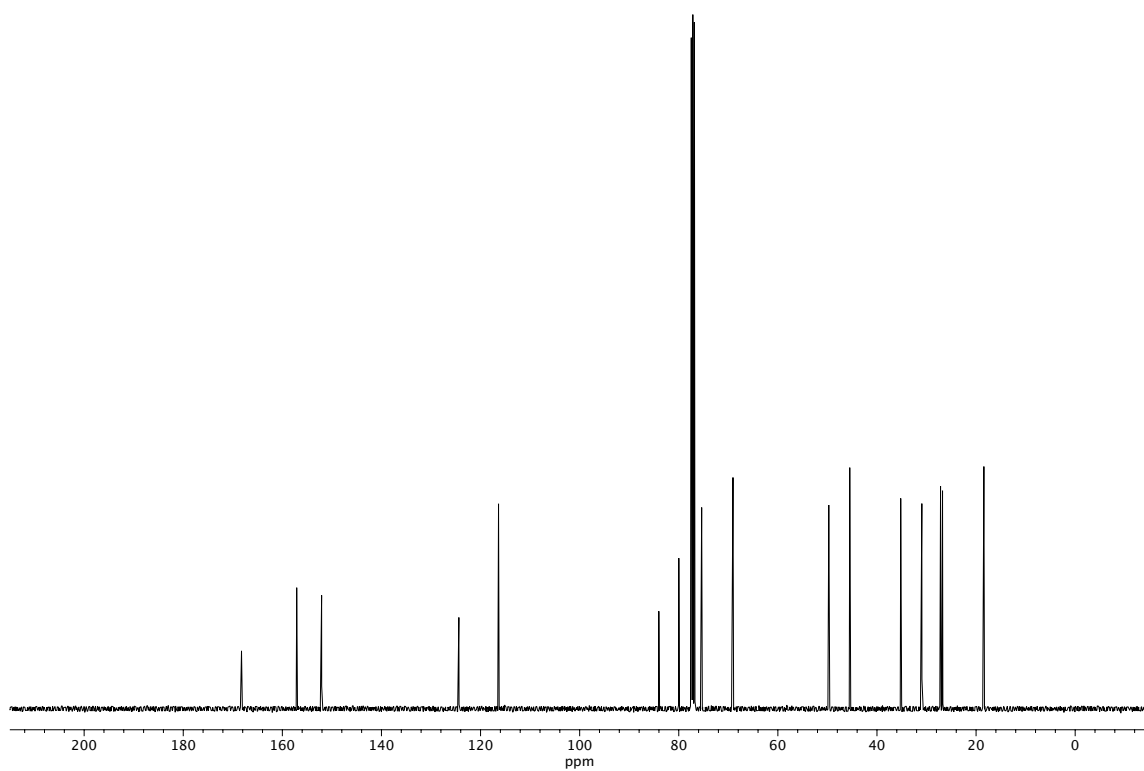


Figure A2.64  $^1\text{H}$  NMR (400 MHz,  $\text{CDCl}_3$ ) of compound **100**.



**Figure A2.65** Infrared spectrum (Thin Film, NaCl) of compound **100**.



**Figure A2.66** <sup>13</sup>C NMR (100 MHz, CDCl<sub>3</sub>) of compound **100**.

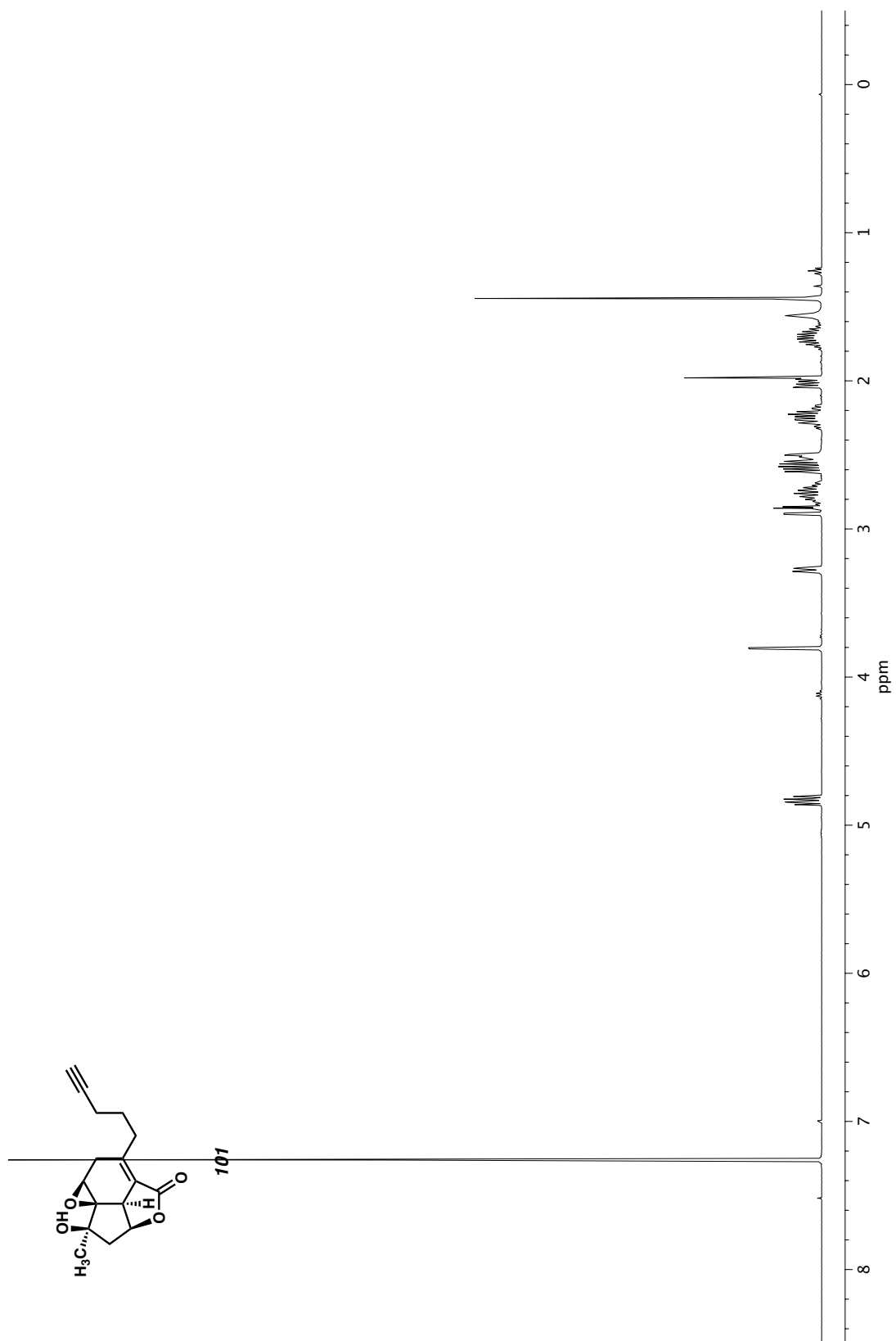
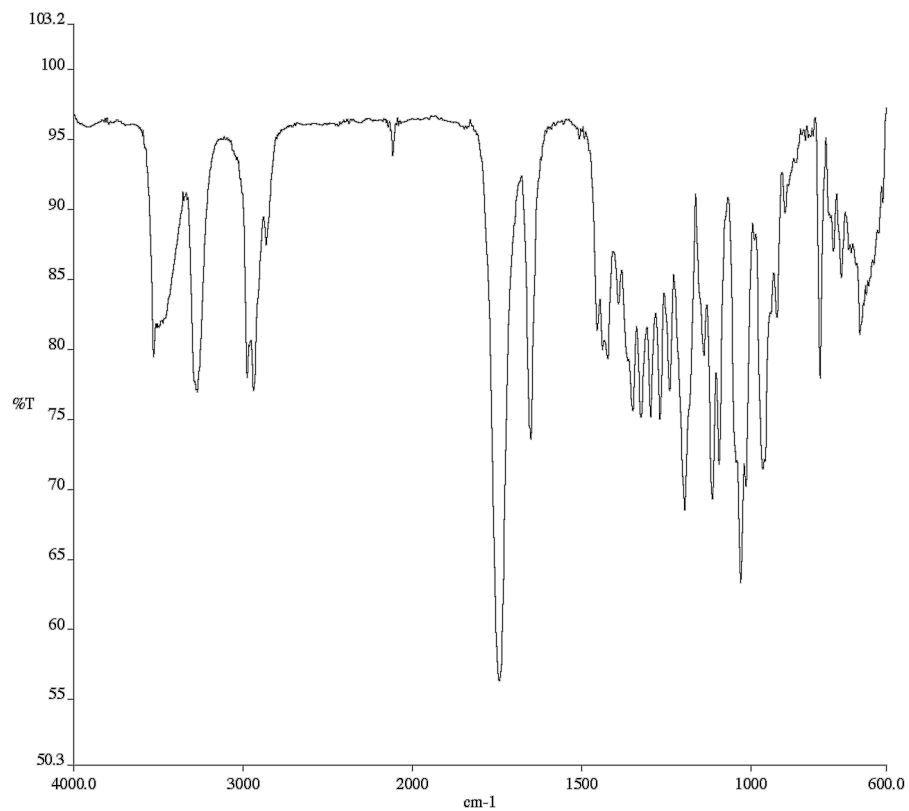
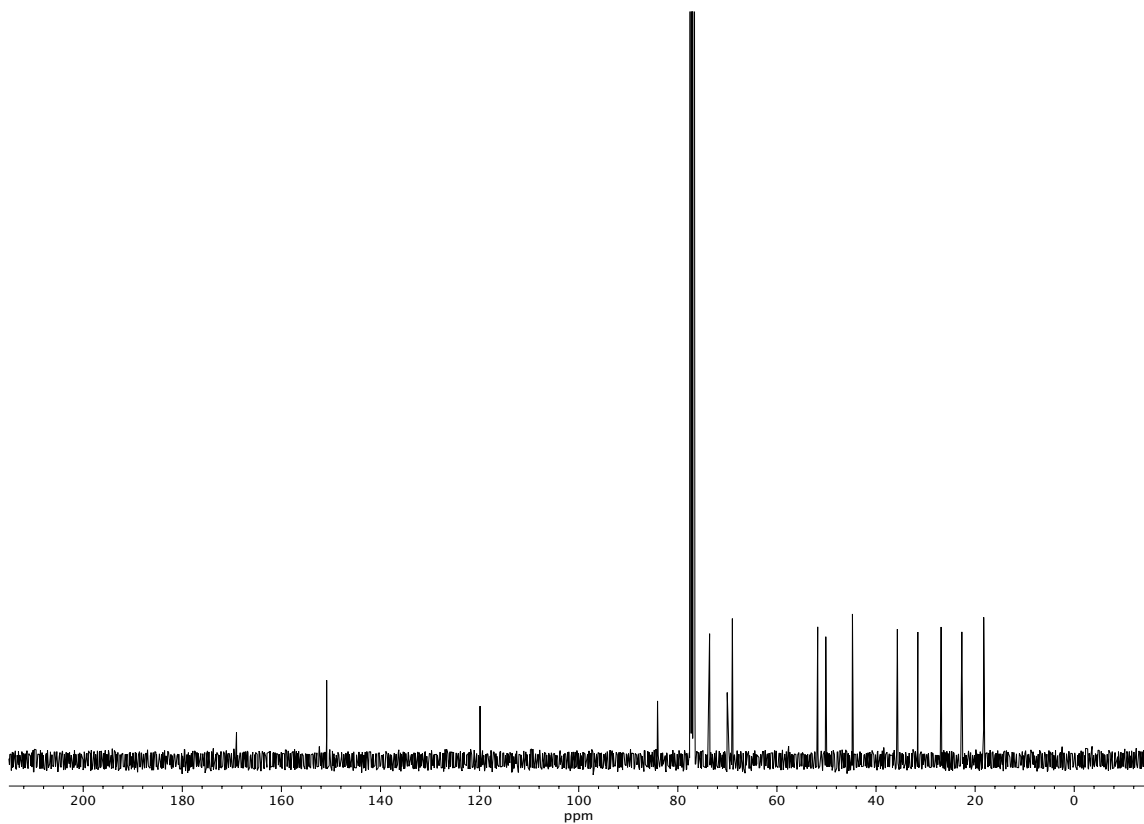


Figure A2.67 <sup>1</sup>H NMR (400 MHz, CDCl<sub>3</sub>) of compound **101**.



**Figure A2.68** Infrared spectrum (Thin Film, NaCl) of compound **101**.



**Figure A2.69** <sup>13</sup>C NMR (100 MHz, CDCl<sub>3</sub>) of compound **101**.

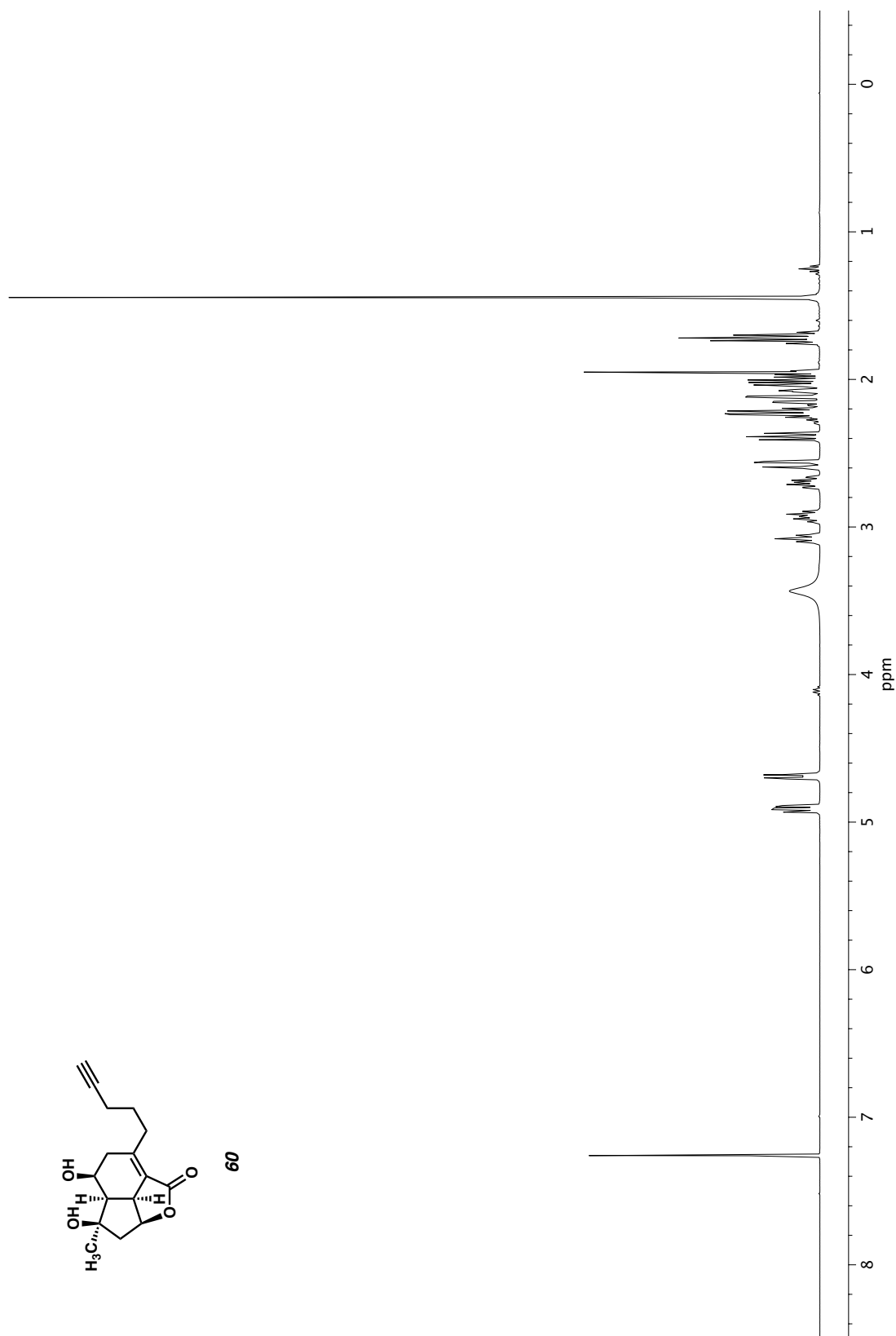
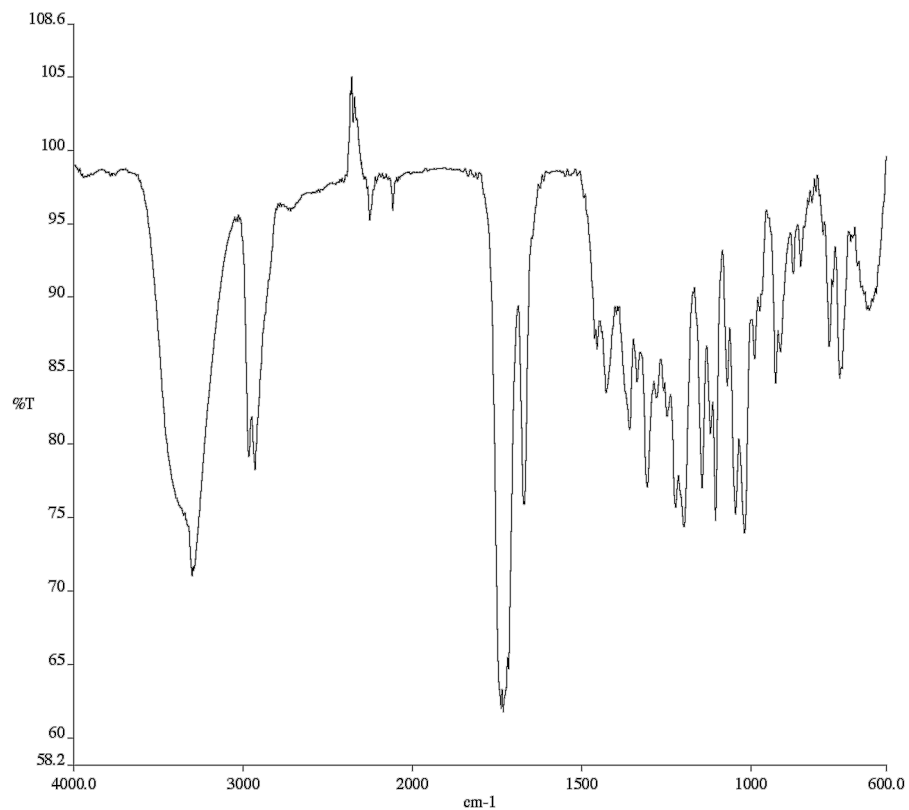
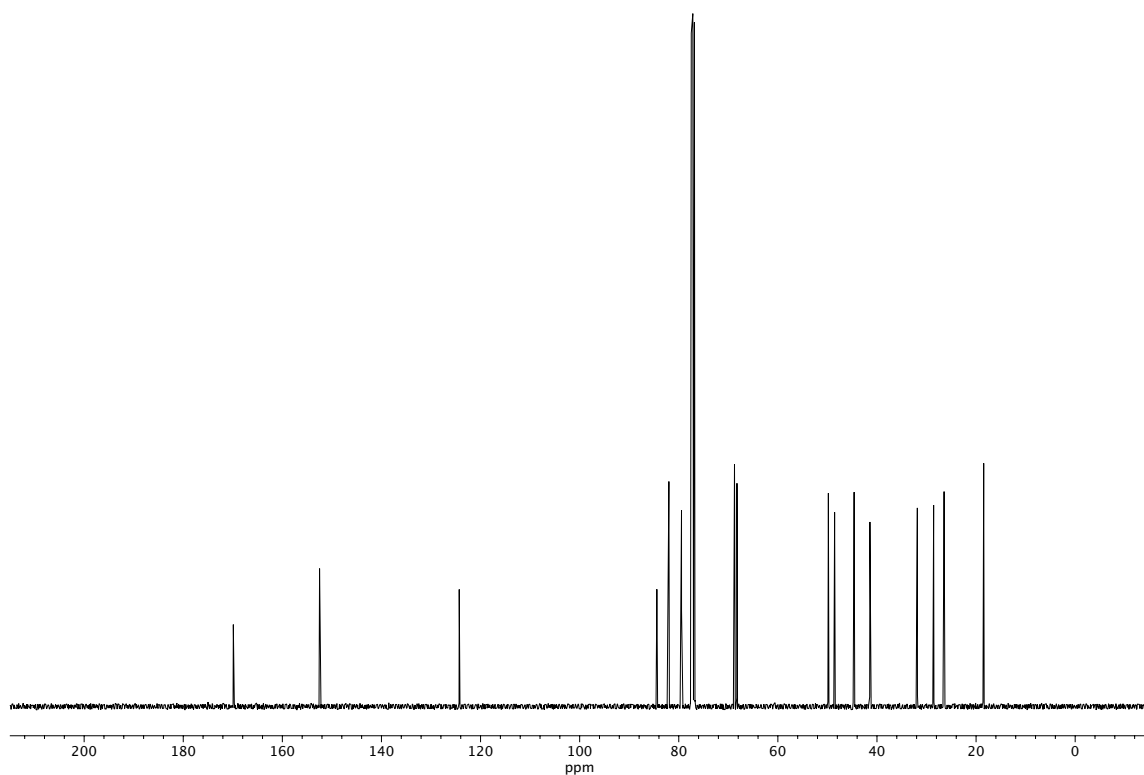


Figure A2.70 <sup>1</sup>H NMR (400 MHz, CDCl<sub>3</sub>) of compound **60**.



**Figure A2.71** Infrared spectrum (Thin Film, NaCl) of compound **60**.



**Figure A2.72** <sup>13</sup>C NMR (100 MHz, CDCl<sub>3</sub>) of compound **60**.

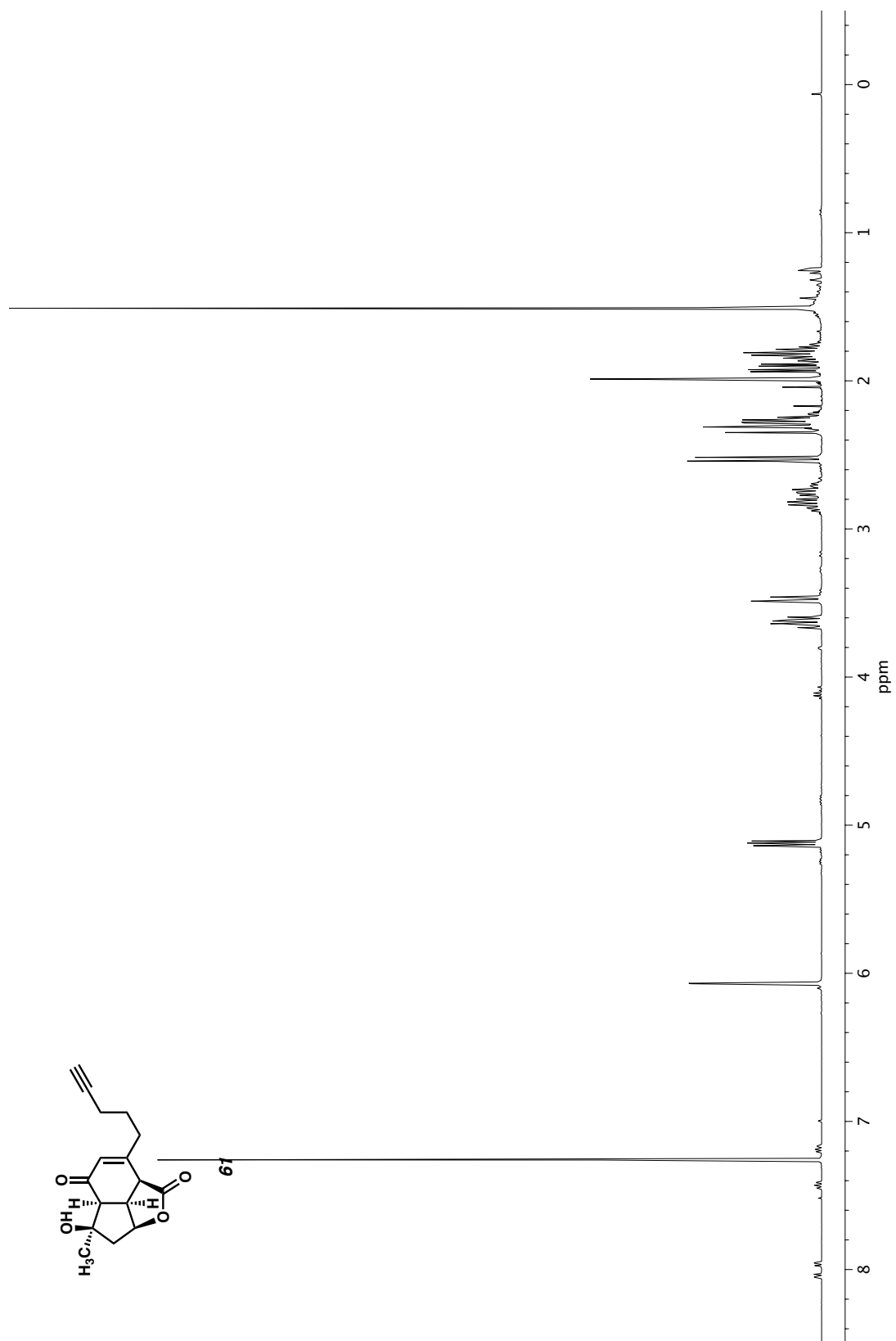


**Figure A2.73**  $^1\text{H NMR}$  (400 MHz,  $\text{CDCl}_3$ ) of compound **61**.



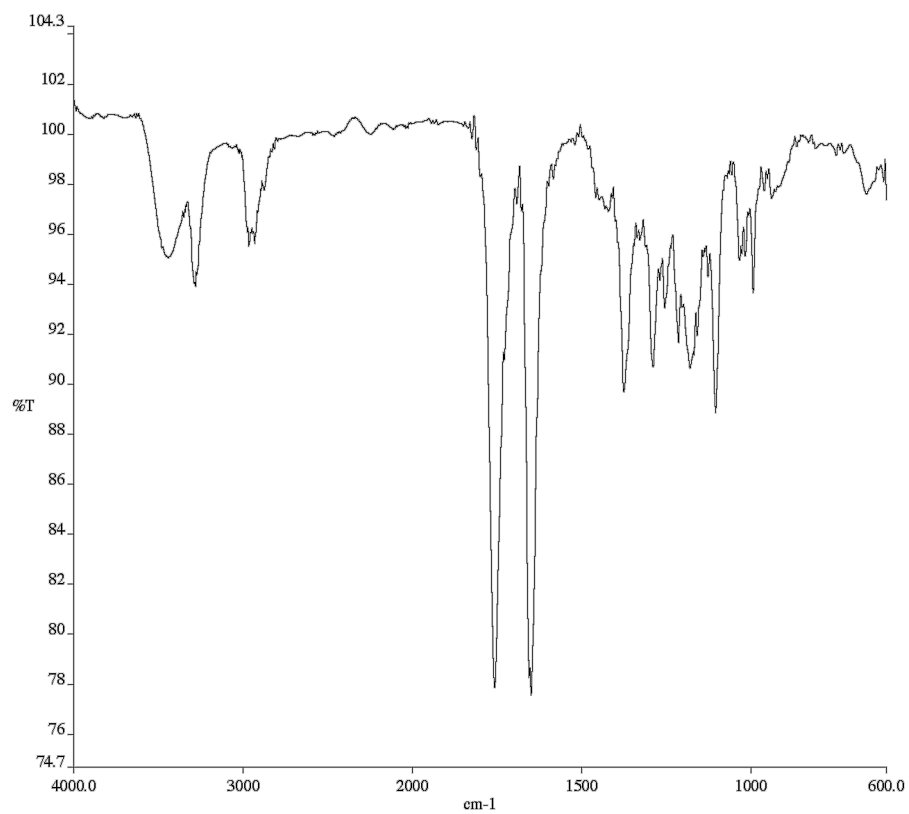


**Figure A2.74** Infrared spectrum (Thin Film, NaCl) of compound **61**.

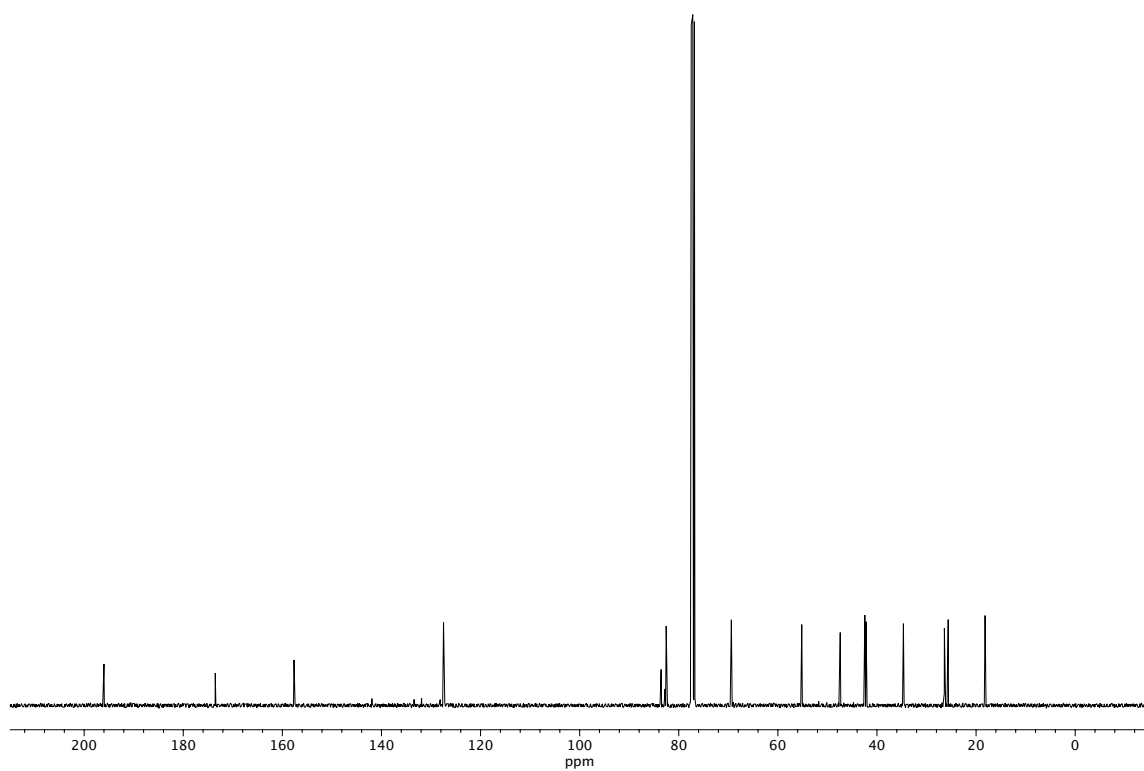


**Figure A2.75** <sup>13</sup>C NMR (100 MHz, CDCl<sub>3</sub>) of compound **61**.

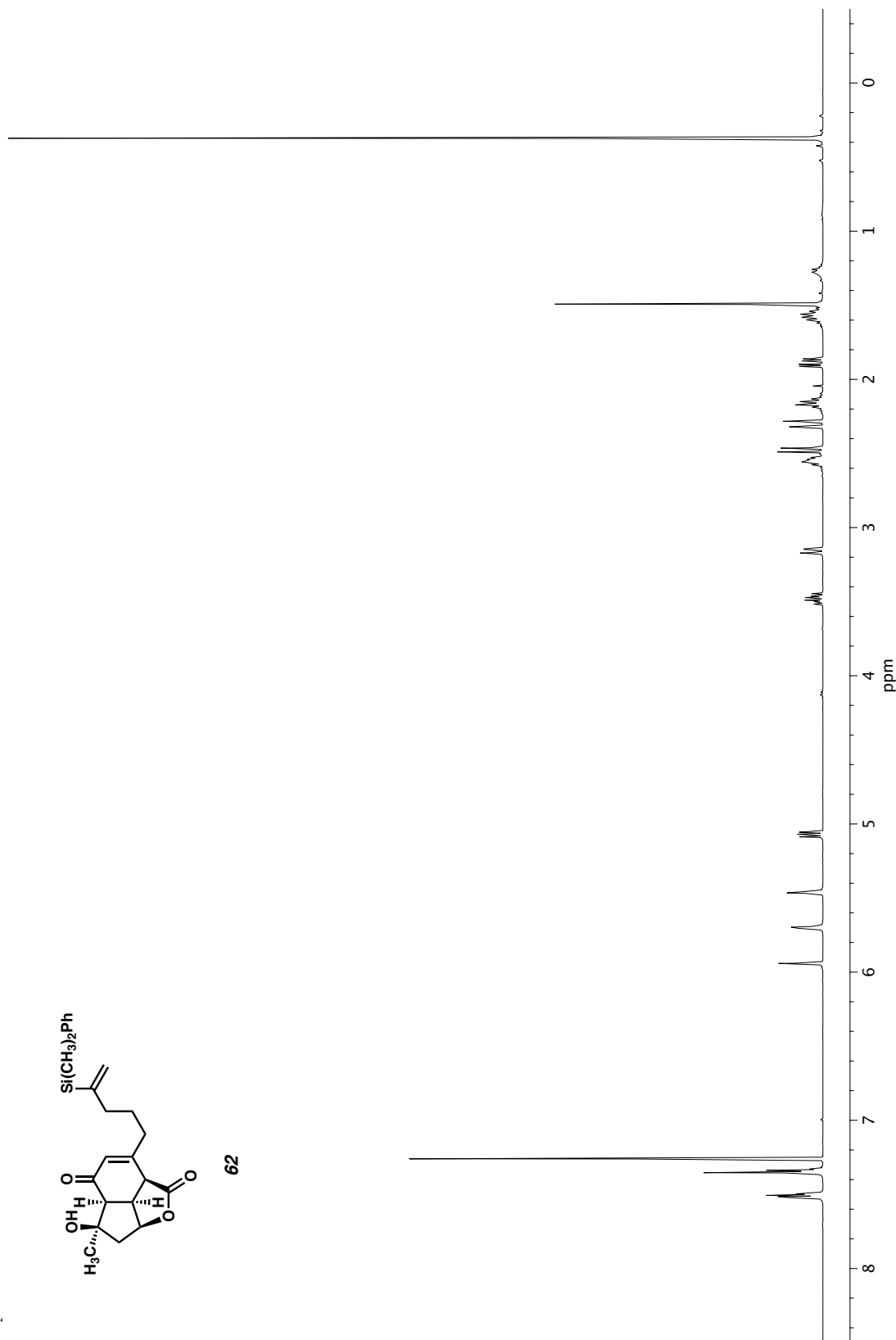
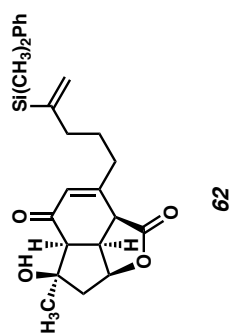
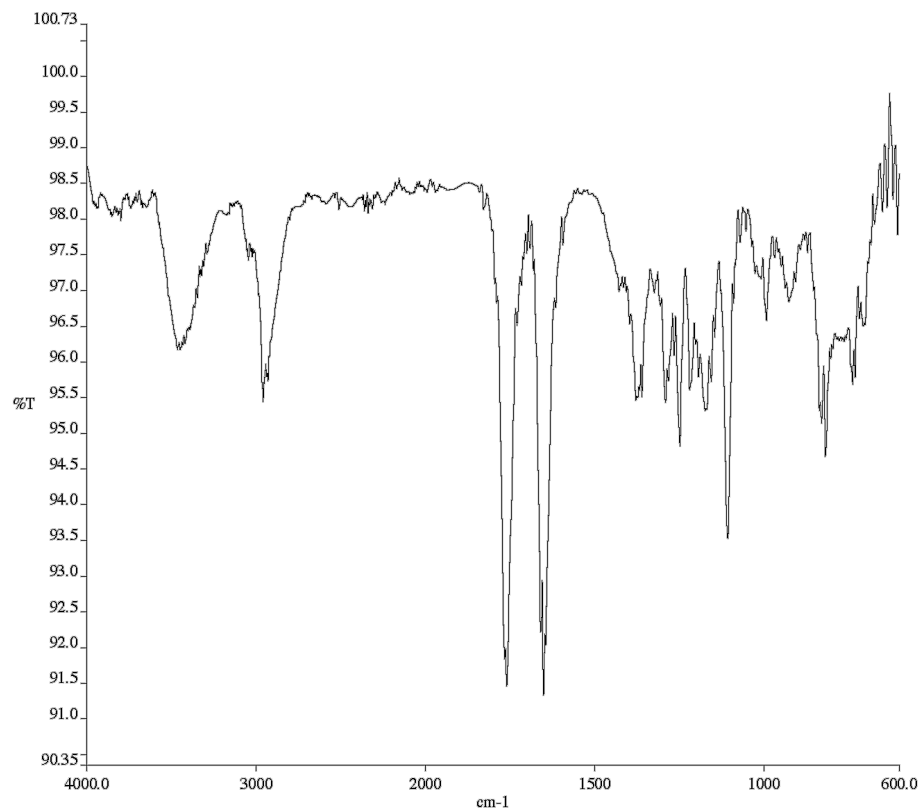
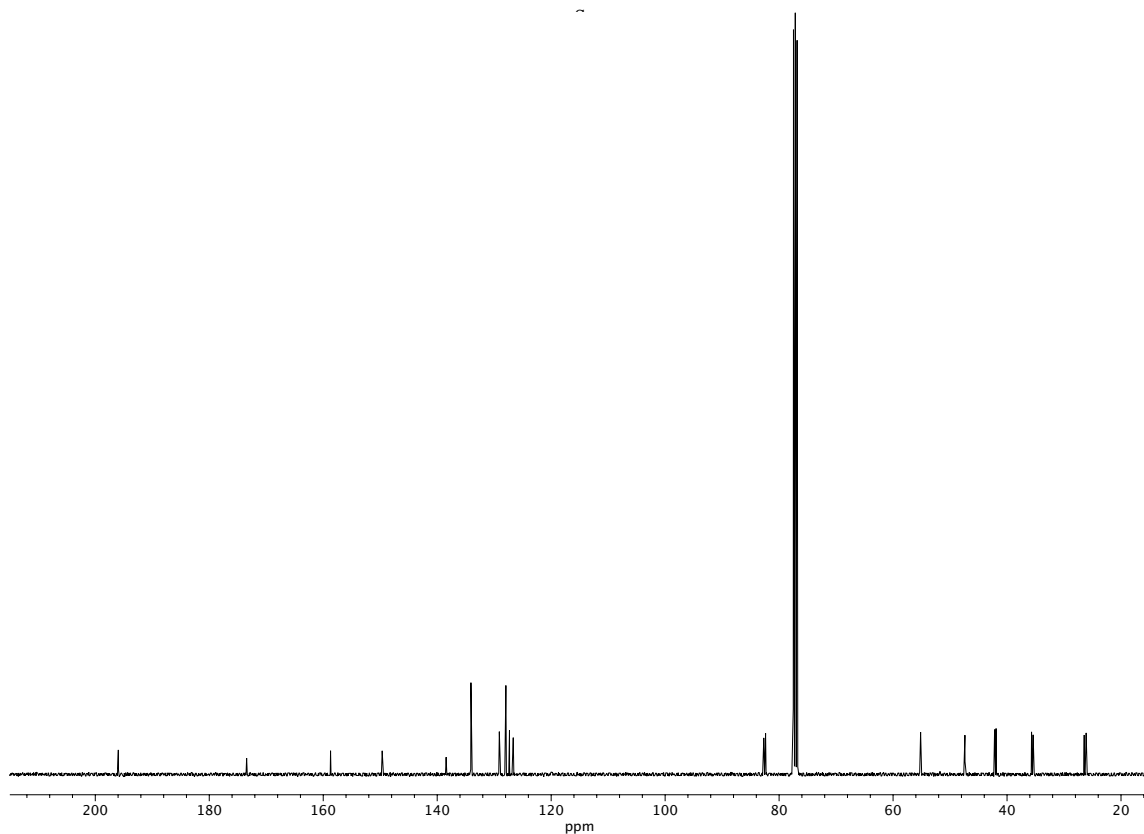


Figure A2.76 <sup>1</sup>H NMR (400 MHz, CDCl<sub>3</sub>) of compound 62.



**Figure A2.77** Infrared spectrum (Thin Film, NaCl) of compound **62**.



**Figure A2.78** <sup>13</sup>C NMR (100 MHz, CDCl<sub>3</sub>) of compound **62**.

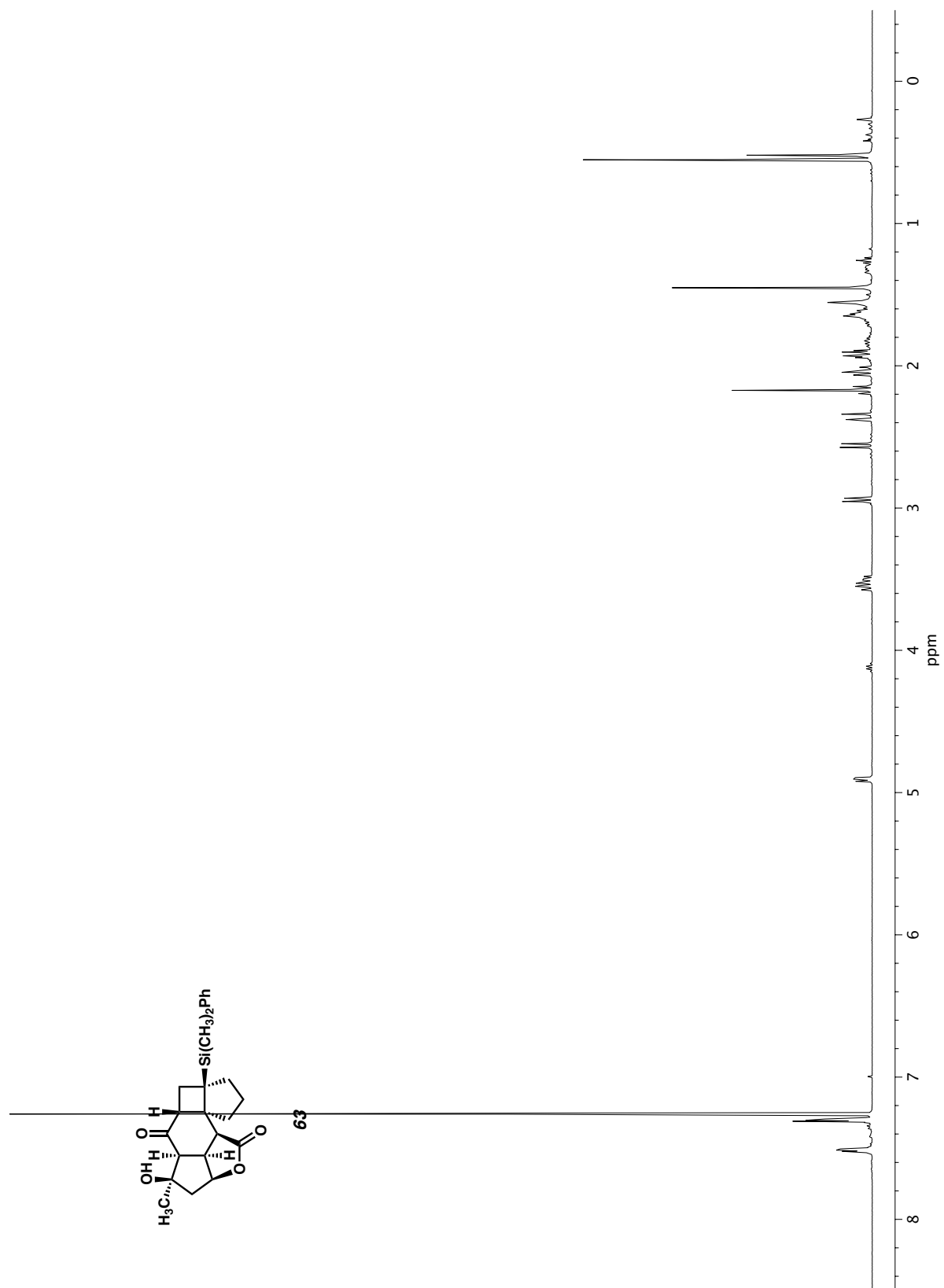
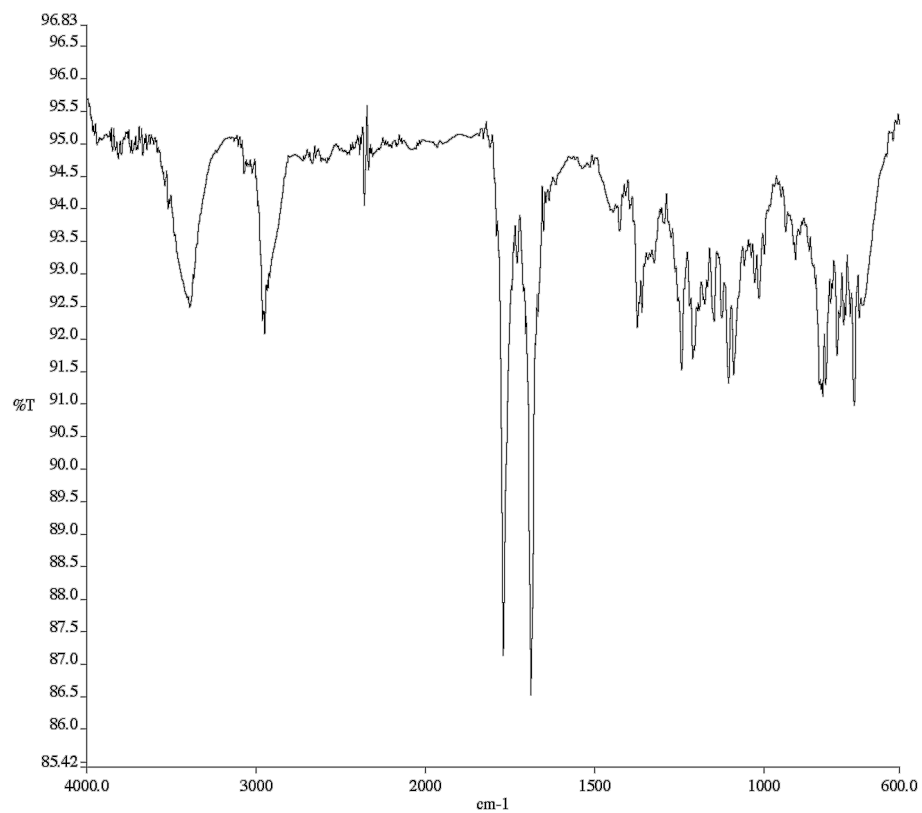
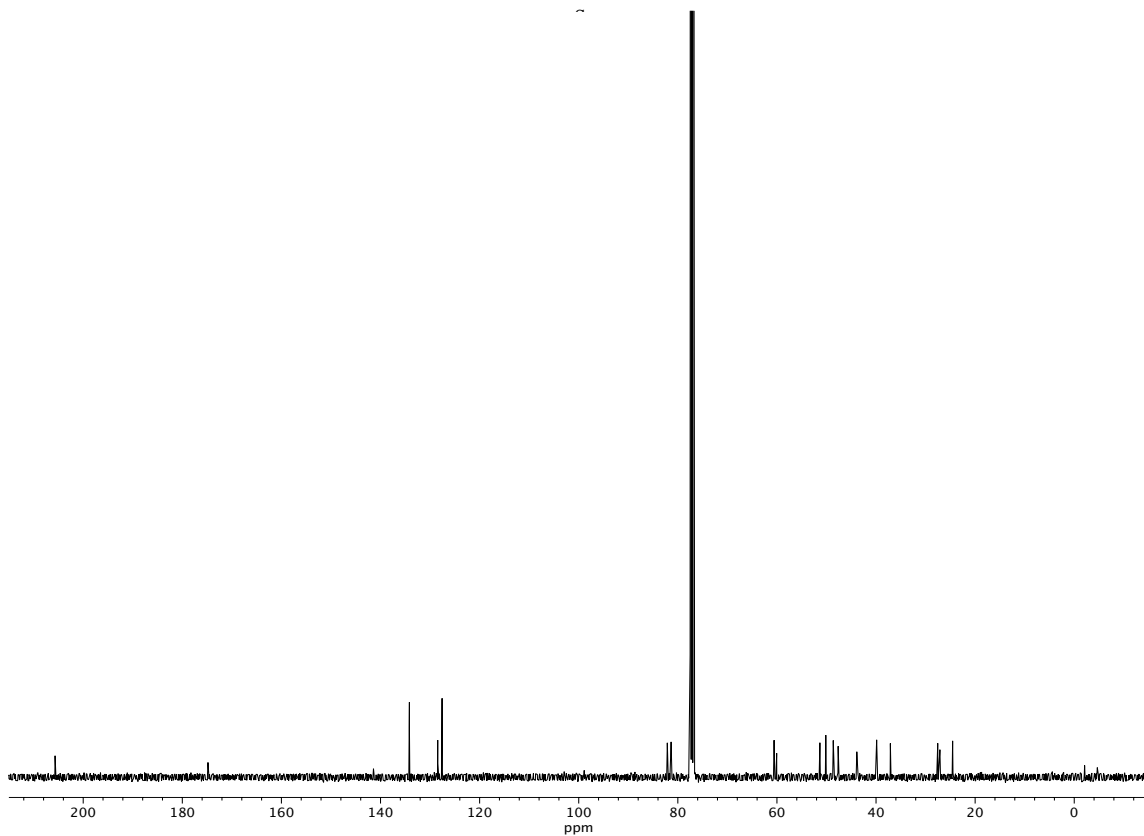


Figure A2.79  $^1\text{H}$  NMR (400 MHz,  $\text{CDCl}_3$ ) of compound **63**.



**Figure A2.80** Infrared spectrum (Thin Film, NaCl) of compound **63**.



**Figure A2.81** <sup>13</sup>C NMR (100 MHz, CDCl<sub>3</sub>) of compound **63**.

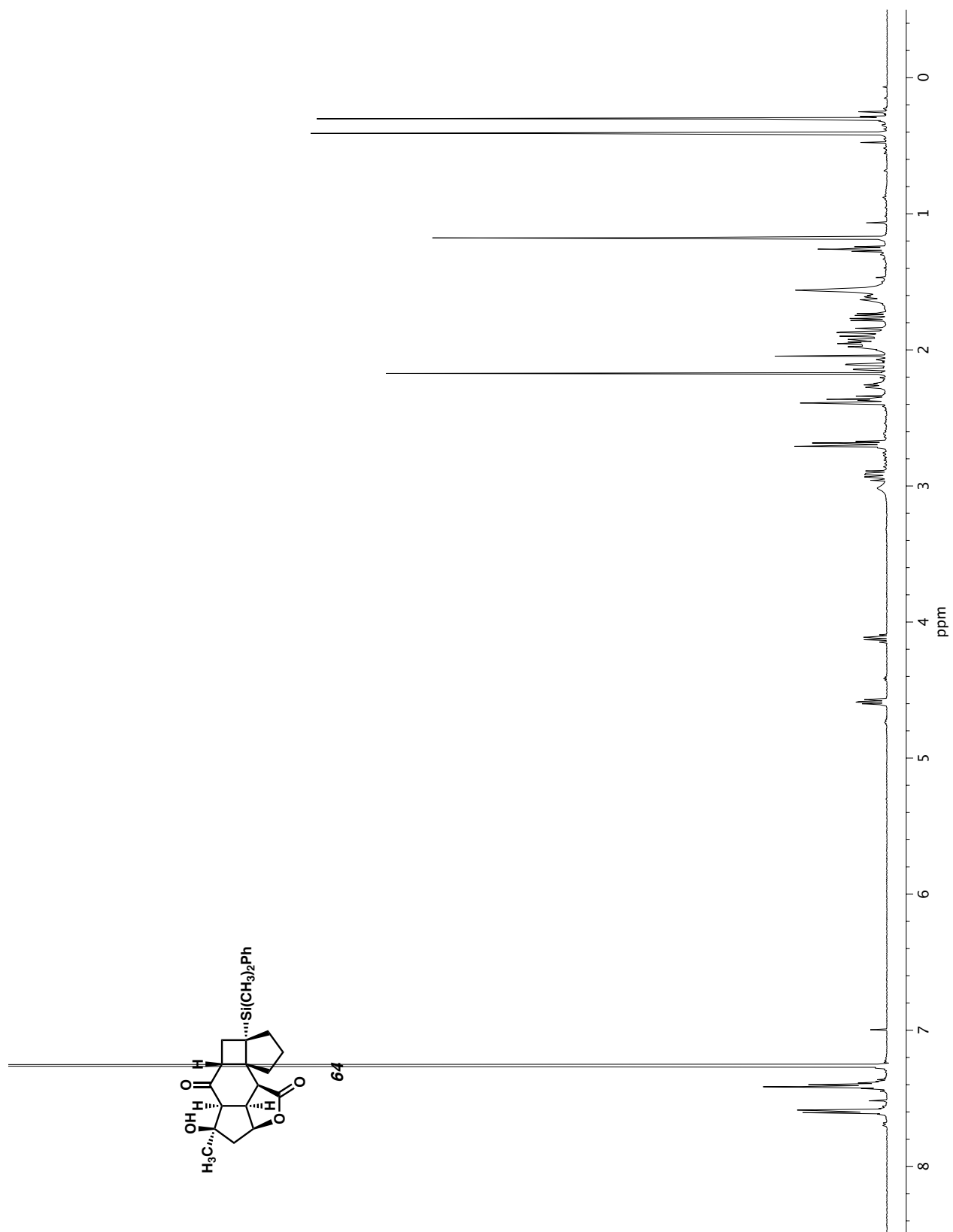


**Figure A2.82**  $^1\text{H NMR}$  (400 MHz,  $\text{CDCl}_3$ ) of compound **64**.

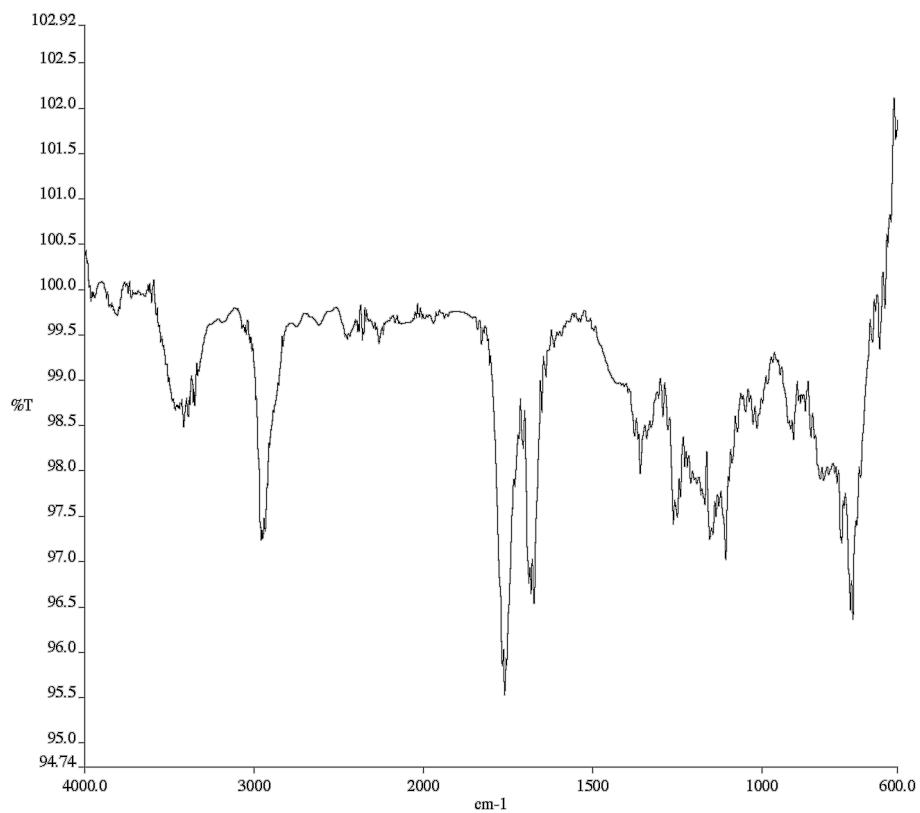


**Figure A2.83** Infrared spectrum (Thin Film, NaCl) of compound **64**.

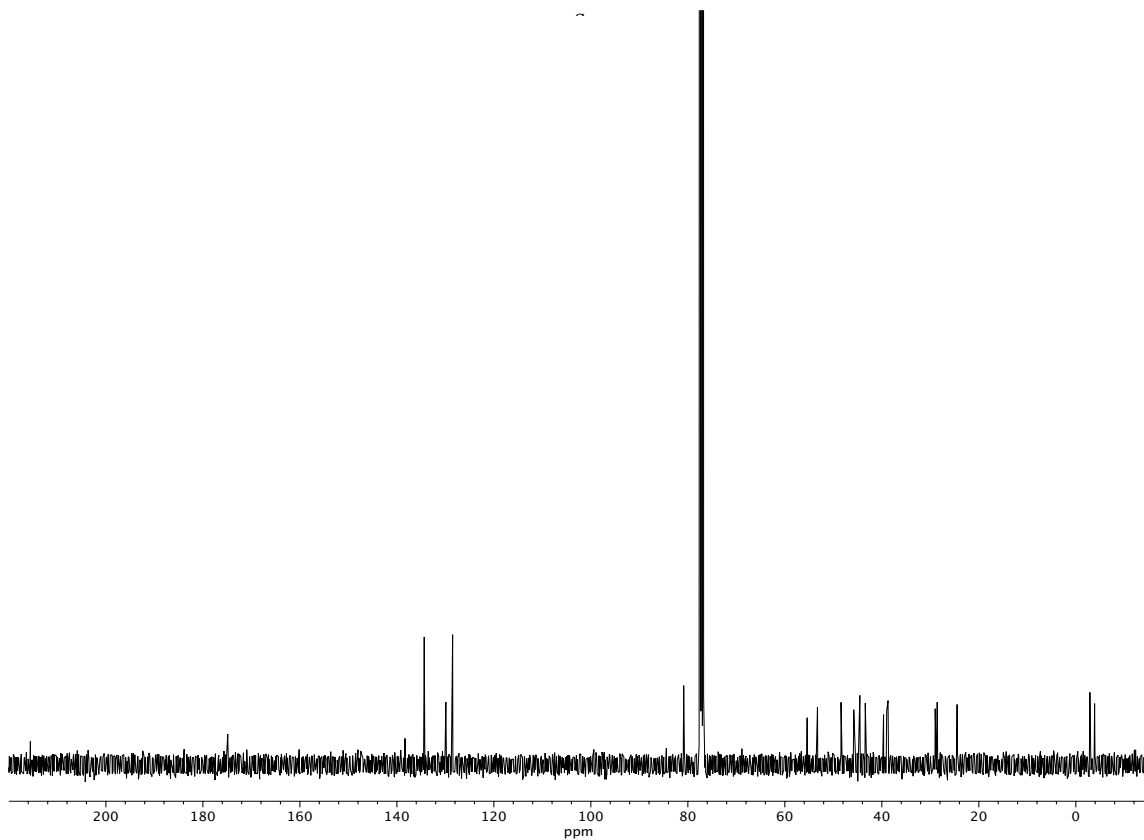


**Figure A2.84** <sup>13</sup>C NMR (100 MHz, CDCl<sub>3</sub>) of compound **64**.

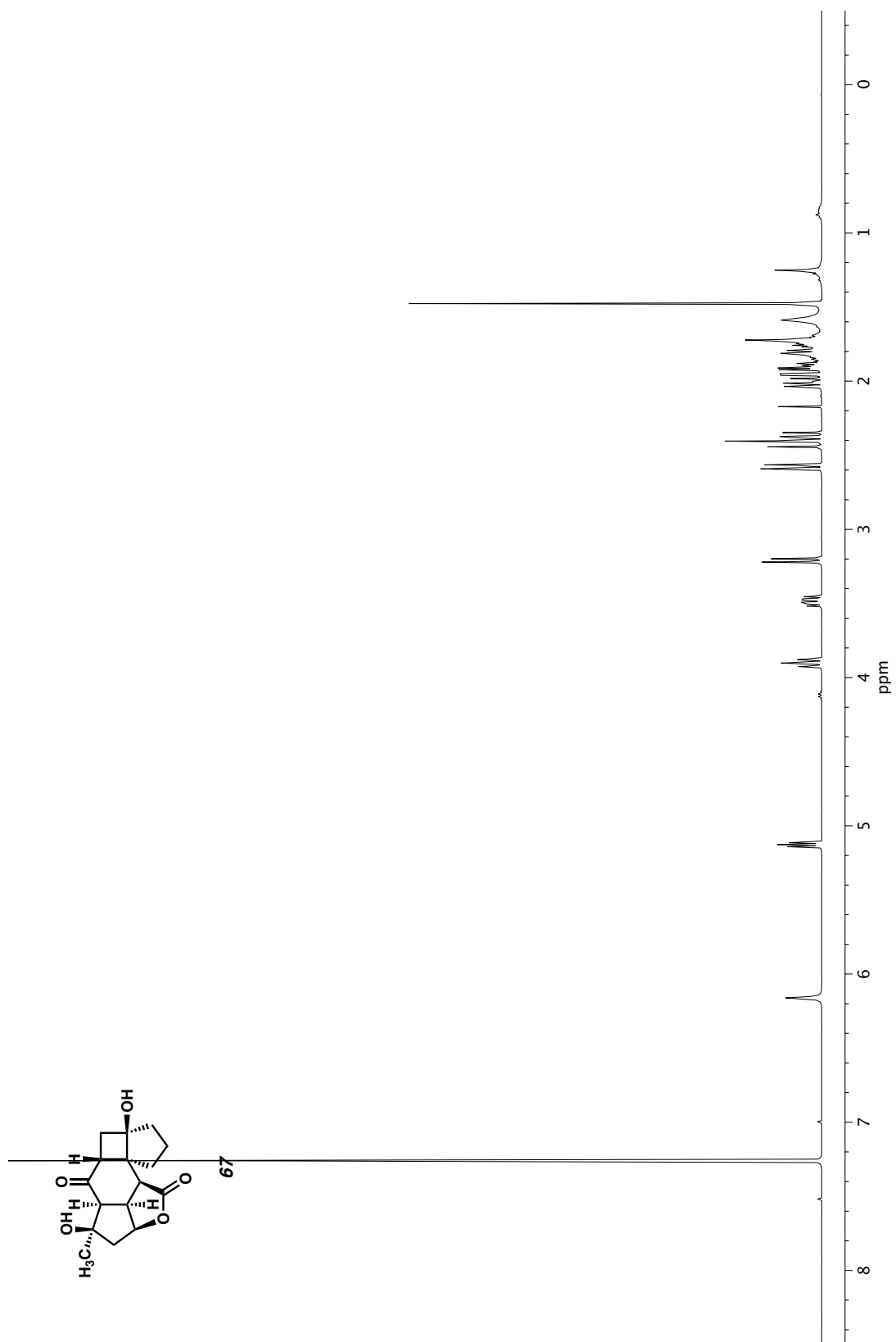
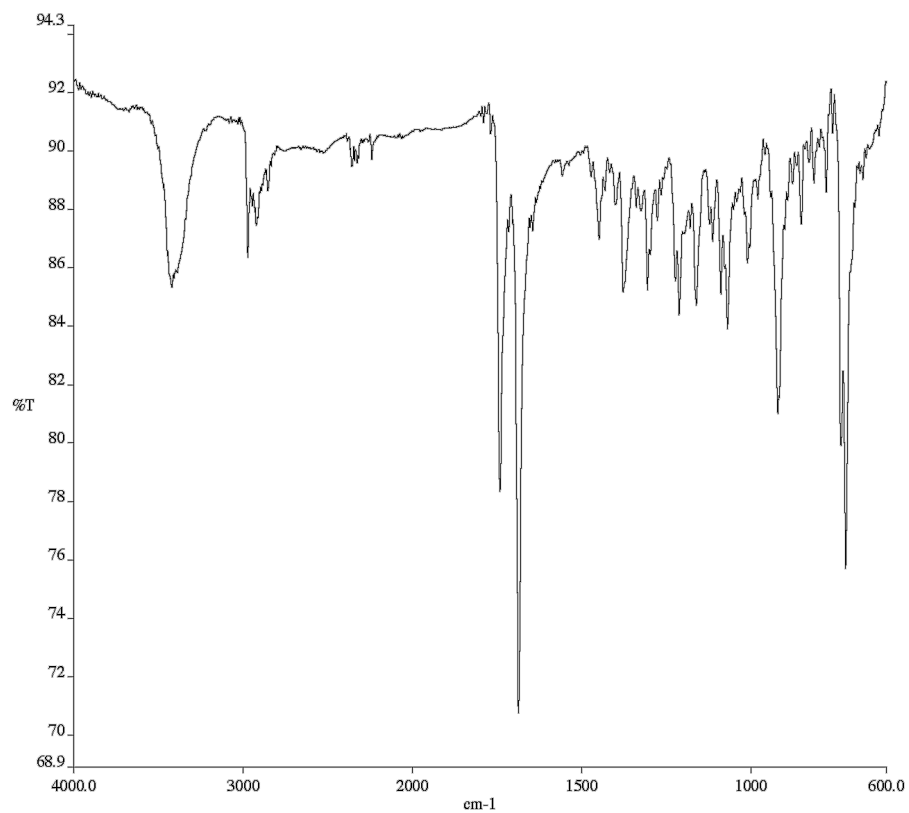
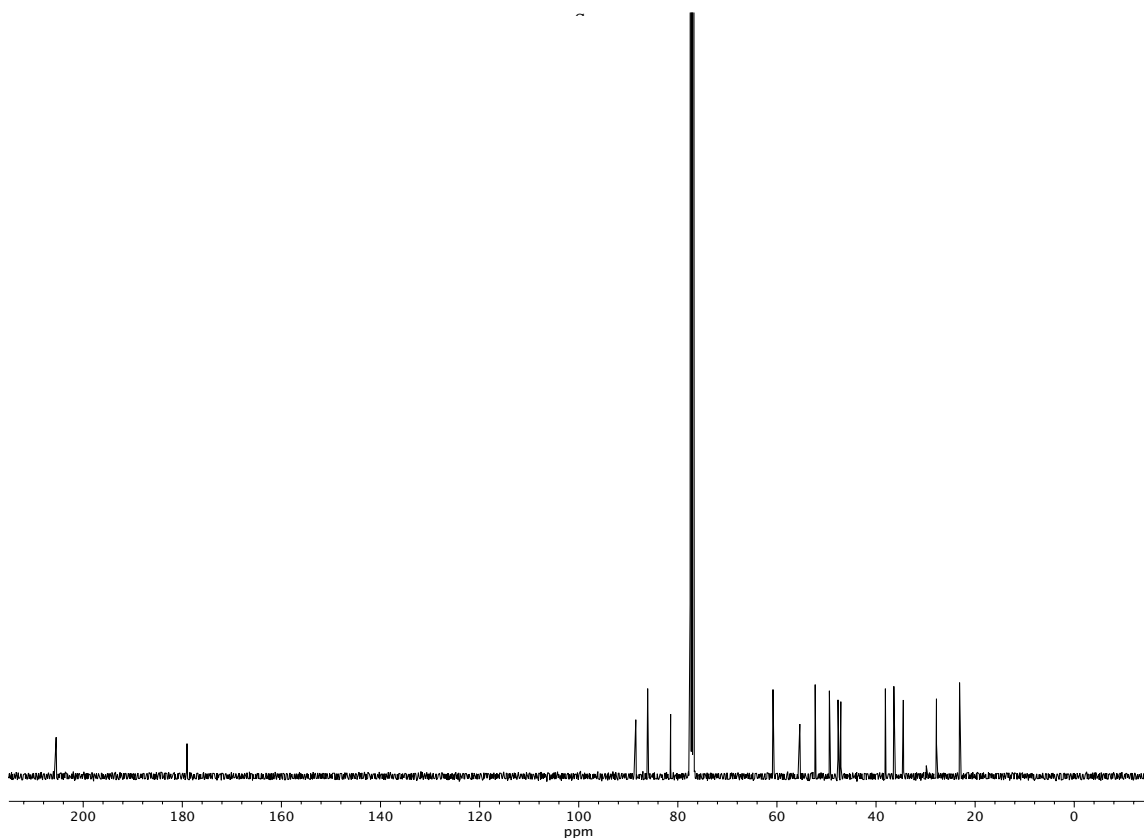


Figure A2.85  $^1\text{H}$  NMR (400 MHz,  $\text{CDCl}_3$ ) of compound **67**.





**Figure A2.86** Infrared spectrum (Thin Film, NaCl) of compound **67**.



**Figure A2.87** <sup>13</sup>C NMR (100 MHz, CDCl<sub>3</sub>) of compound **67**.

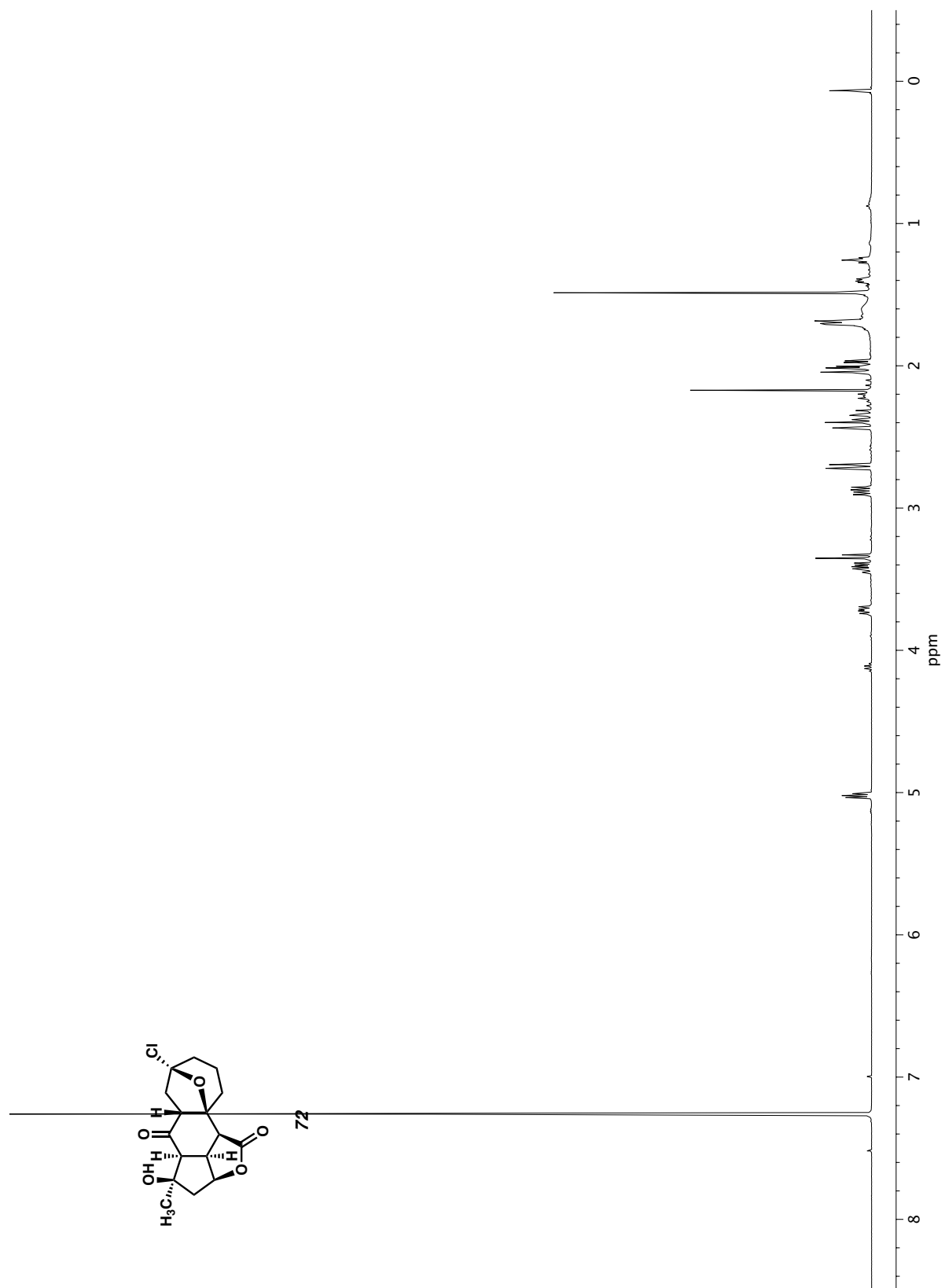
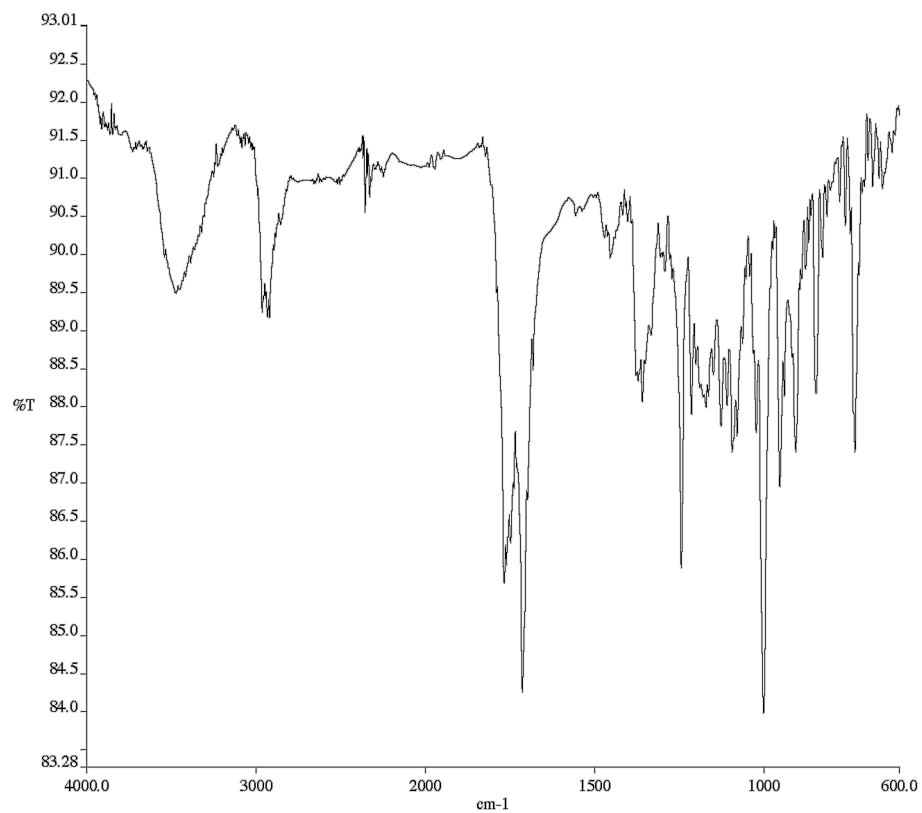
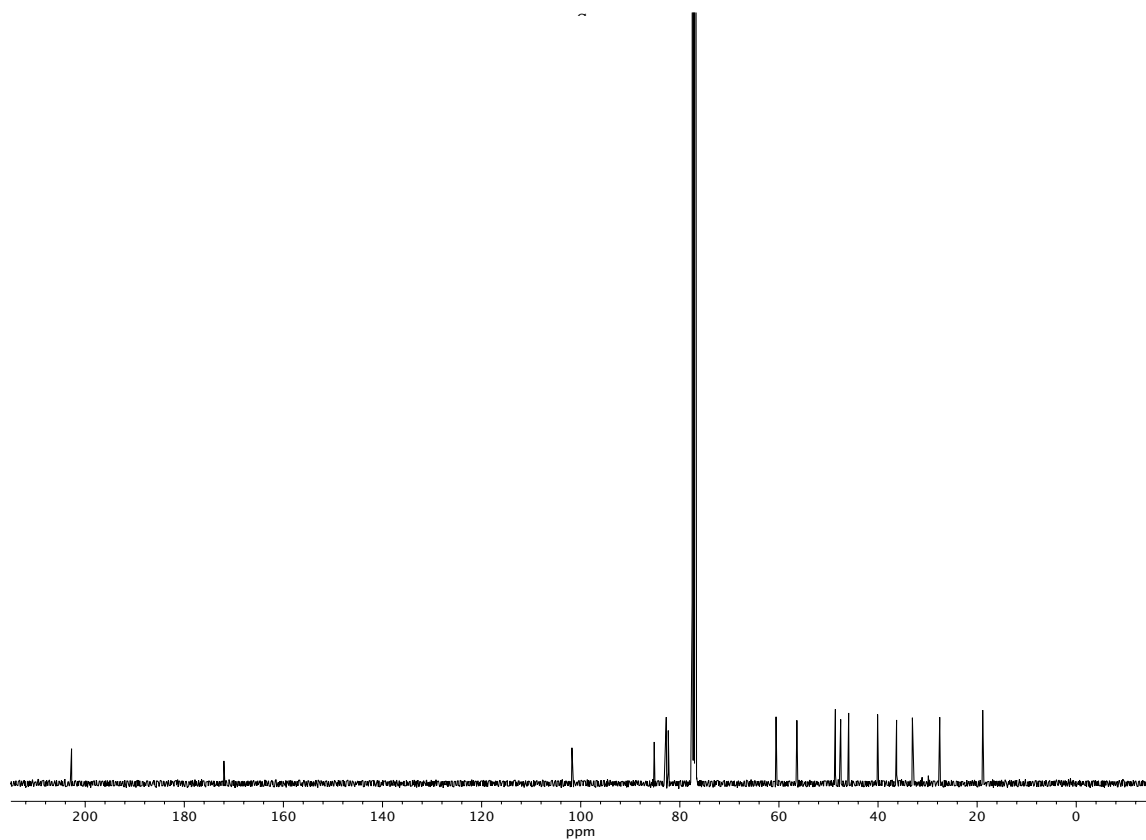


Figure A2.88 <sup>1</sup>H NMR (400 MHz, CDCl<sub>3</sub>) of compound 72.



**Figure A2.89** Infrared spectrum (Thin Film, NaCl) of compound 72.



**Figure A2.90** <sup>13</sup>C NMR (100 MHz, CDCl<sub>3</sub>) of compound 72.

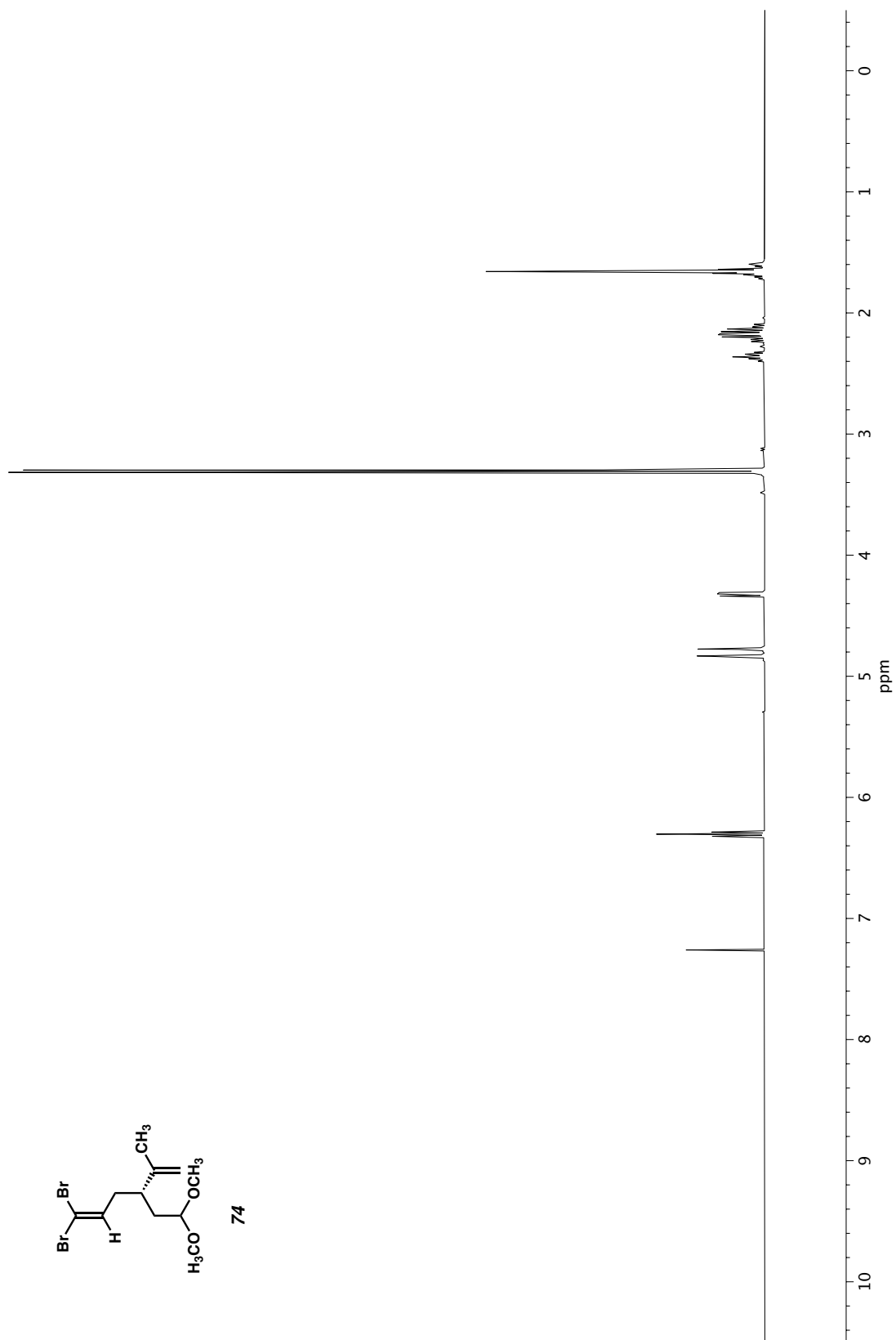
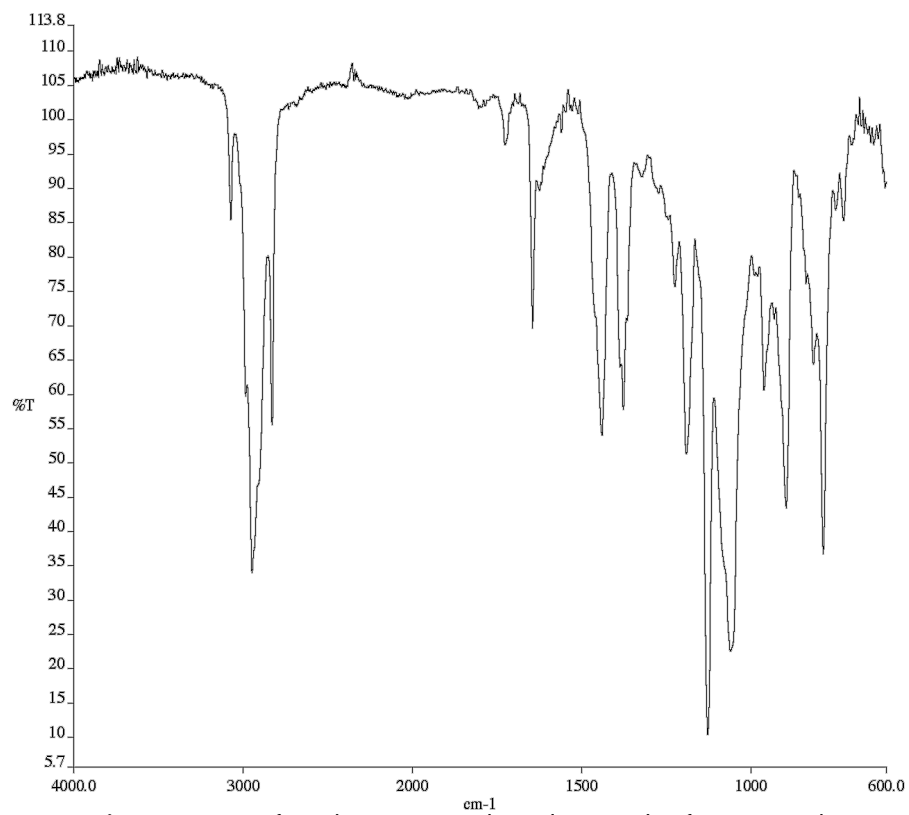
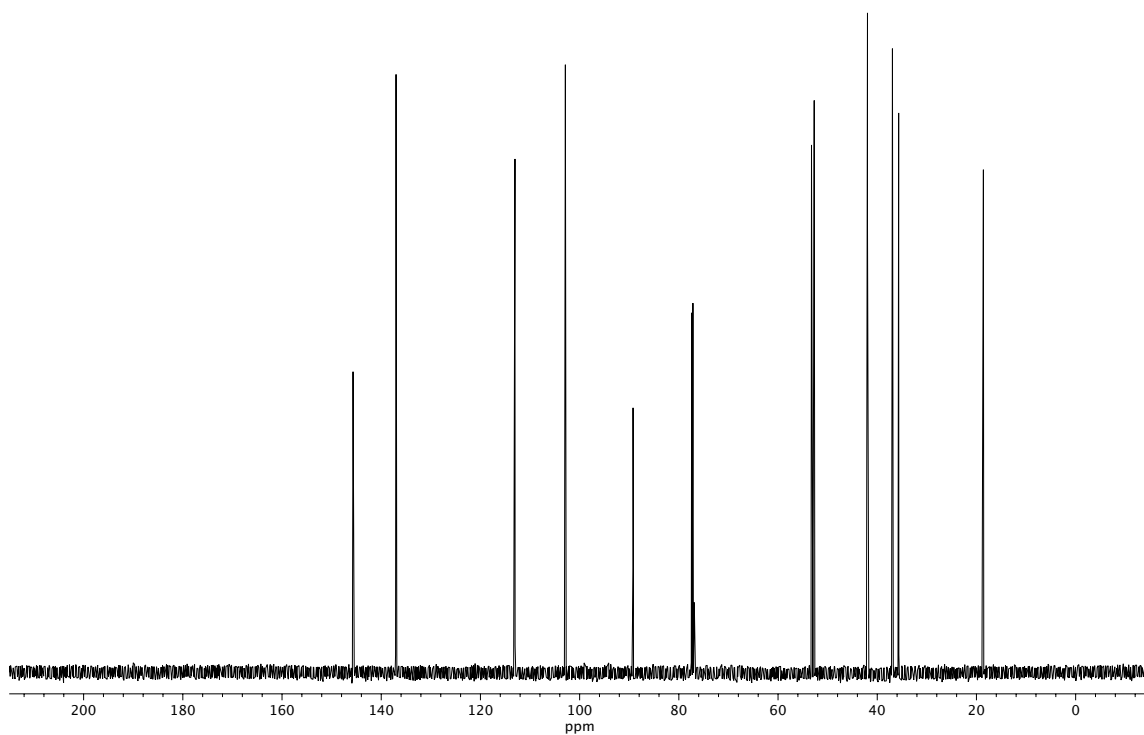


Figure A2.91 <sup>1</sup>H NMR (400 MHz, CDCl<sub>3</sub>) of compound 74.



**Figure A2.92** Infrared spectrum (Thin Film, NaCl) of compound **74**.



**Figure A2.93** <sup>13</sup>C NMR (100 MHz, CDCl<sub>3</sub>) of compound **74**.

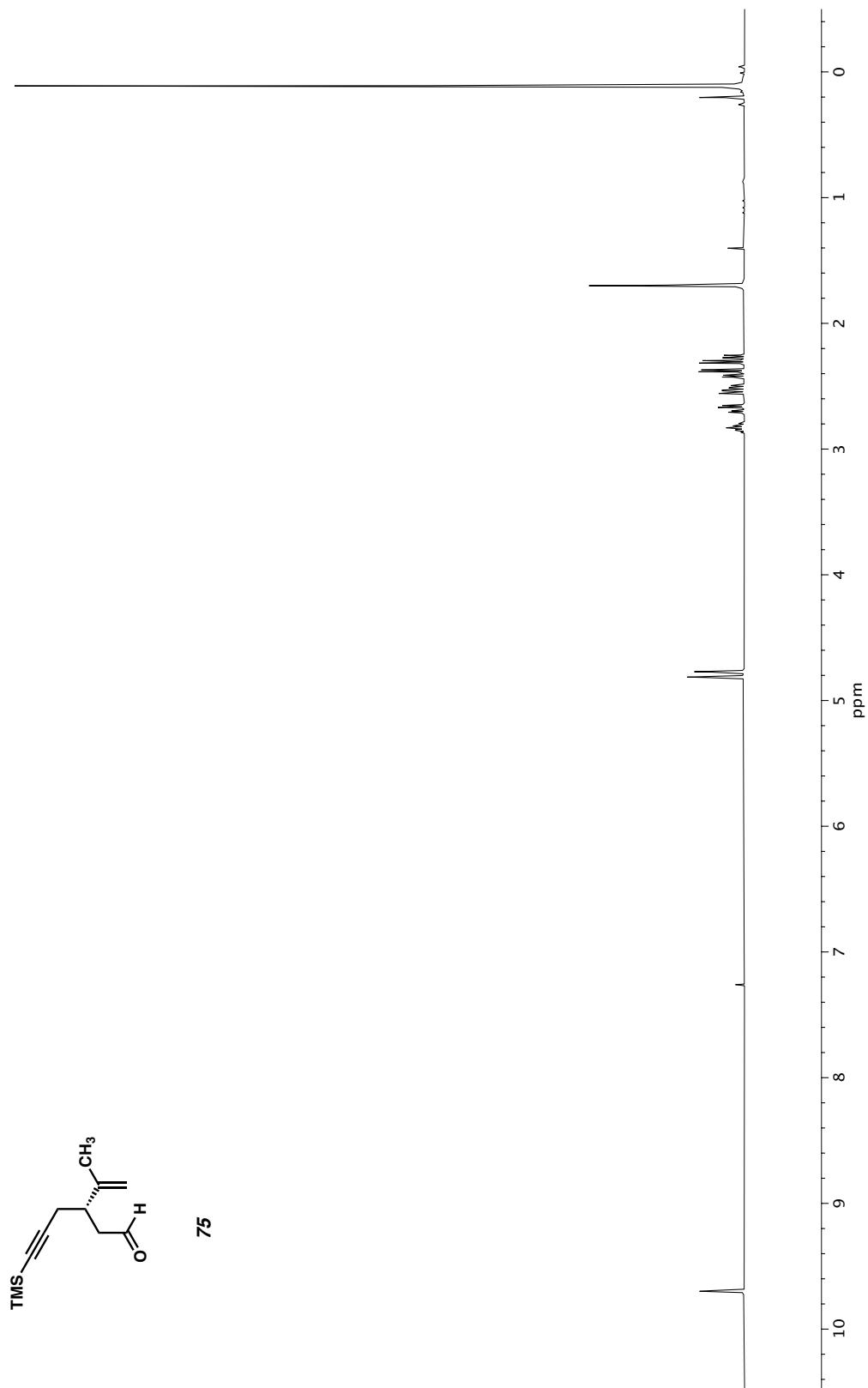
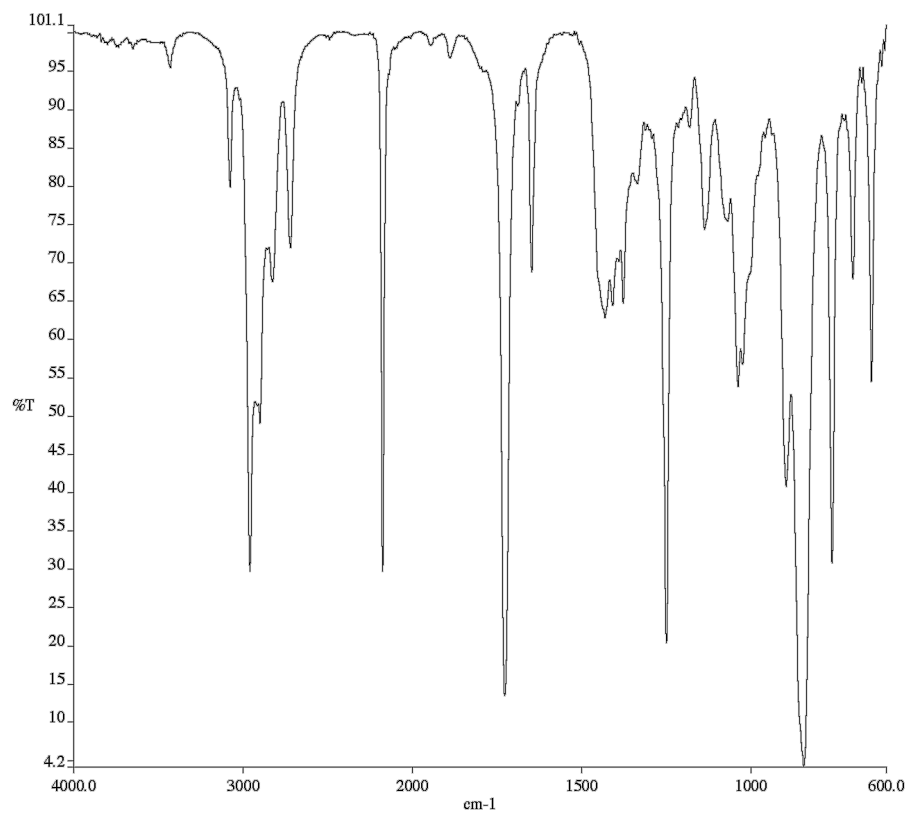
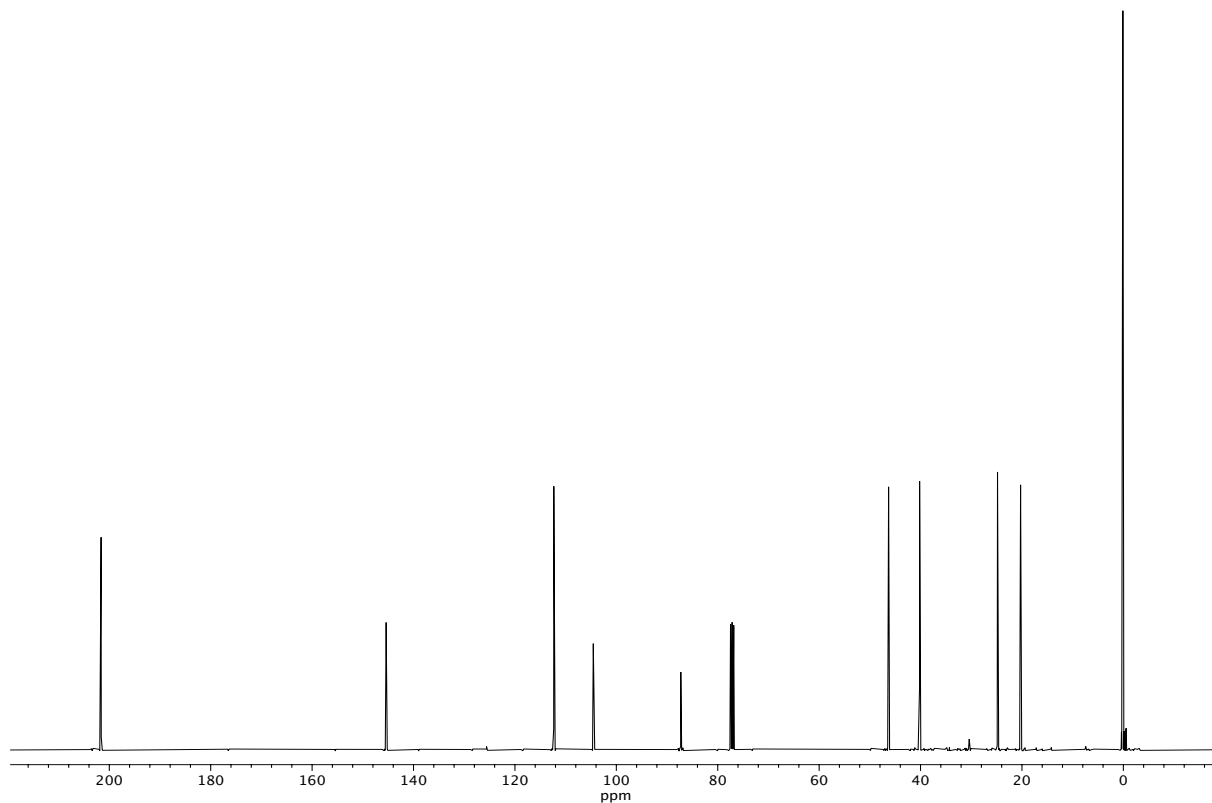


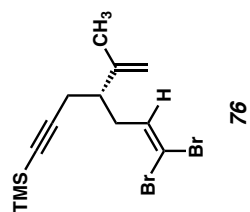
Figure A2.94  $^1\text{H}$  NMR (400 MHz,  $\text{CDCl}_3$ ) of compound 75.



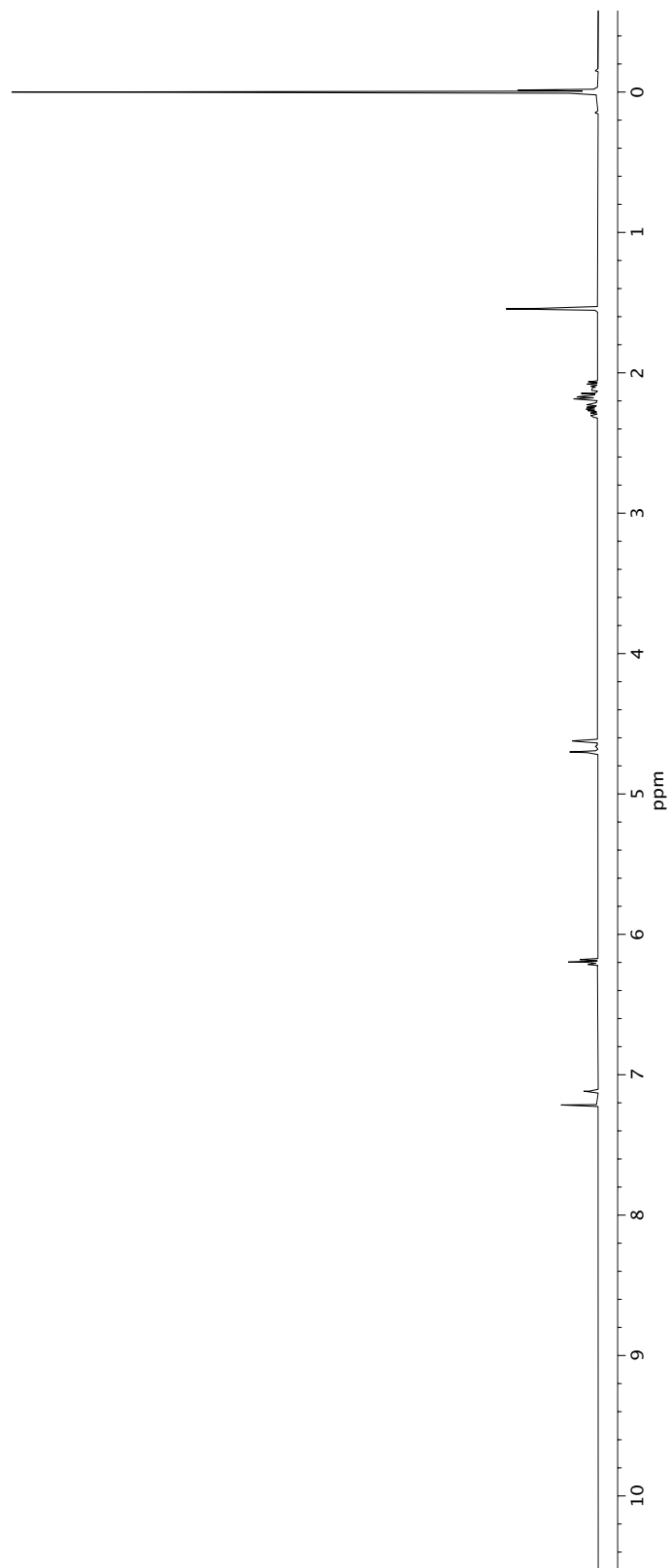
**Figure A2.95** Infrared spectrum (Thin Film, NaCl) of compound 75.



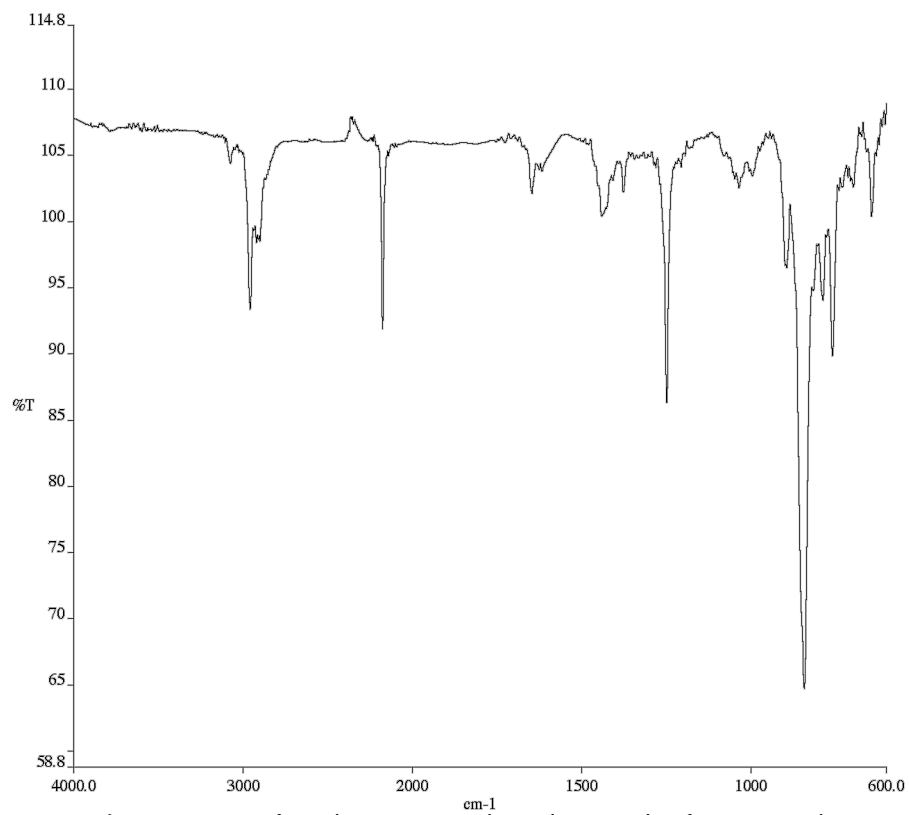
**Figure A2.96** <sup>13</sup>C NMR (100 MHz, CDCl<sub>3</sub>) of compound 75.



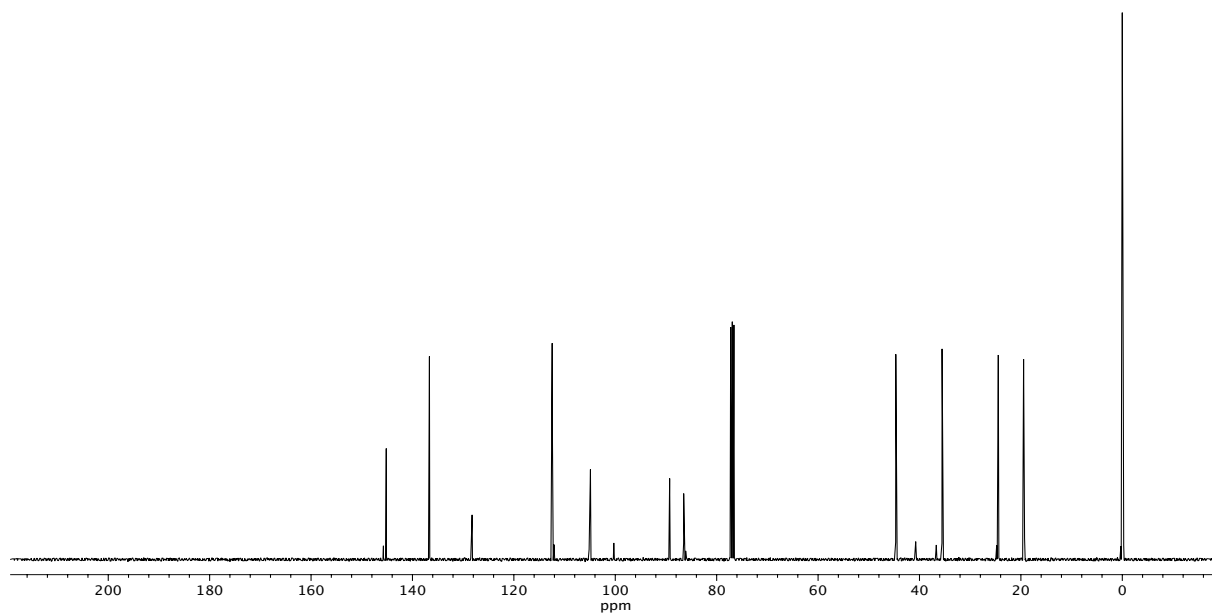
76

Figure A2.97 <sup>1</sup>H NMR (400 MHz, CDCl<sub>3</sub>) of compound 76.





**Figure A2.98** Infrared spectrum (Thin Film, NaCl) of compound **76**.



**Figure A2.99** <sup>13</sup>C NMR (100 MHz, CDCl<sub>3</sub>) of compound **76**.

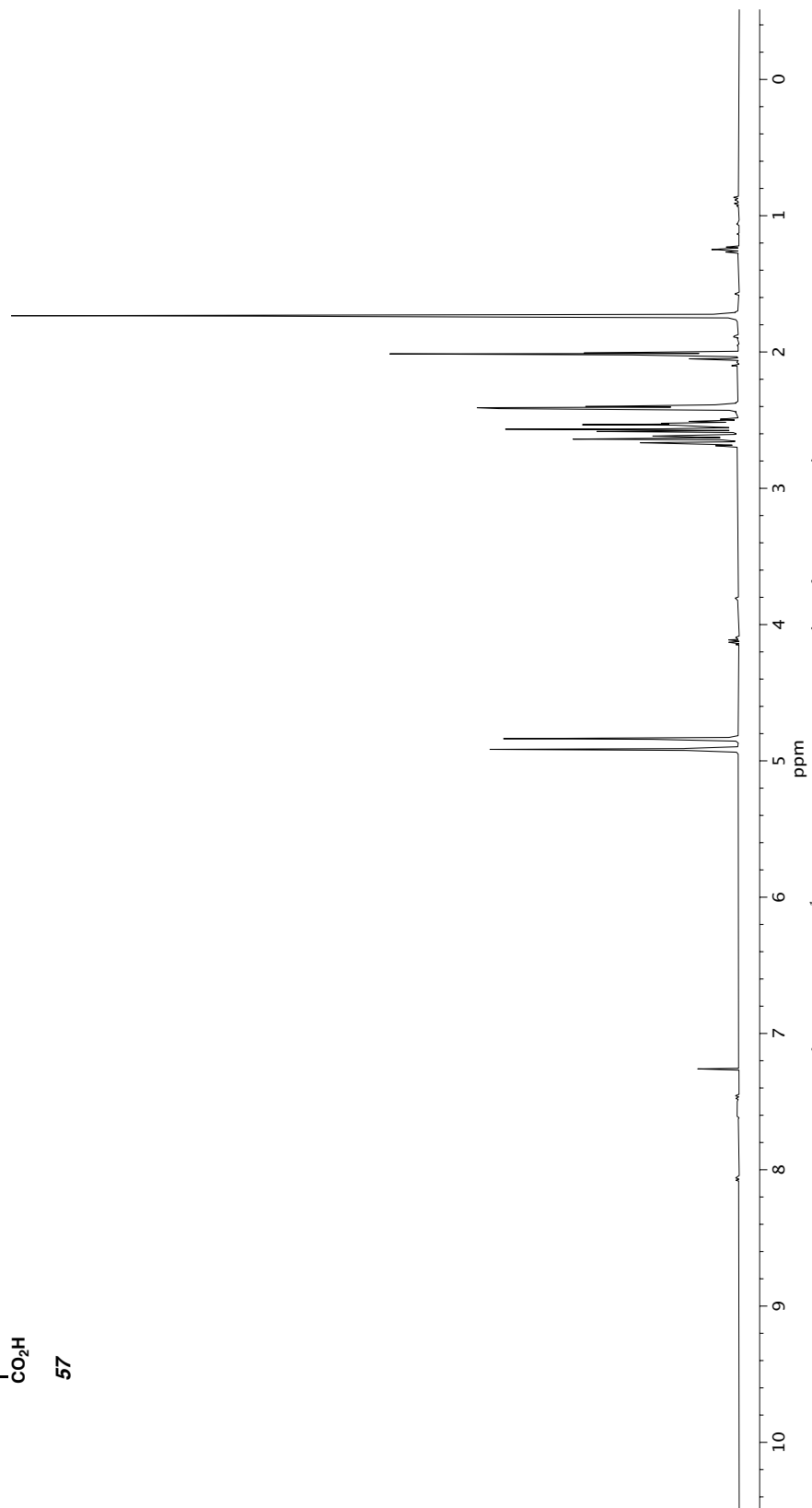
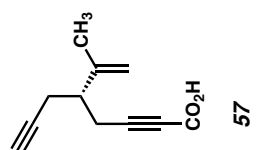
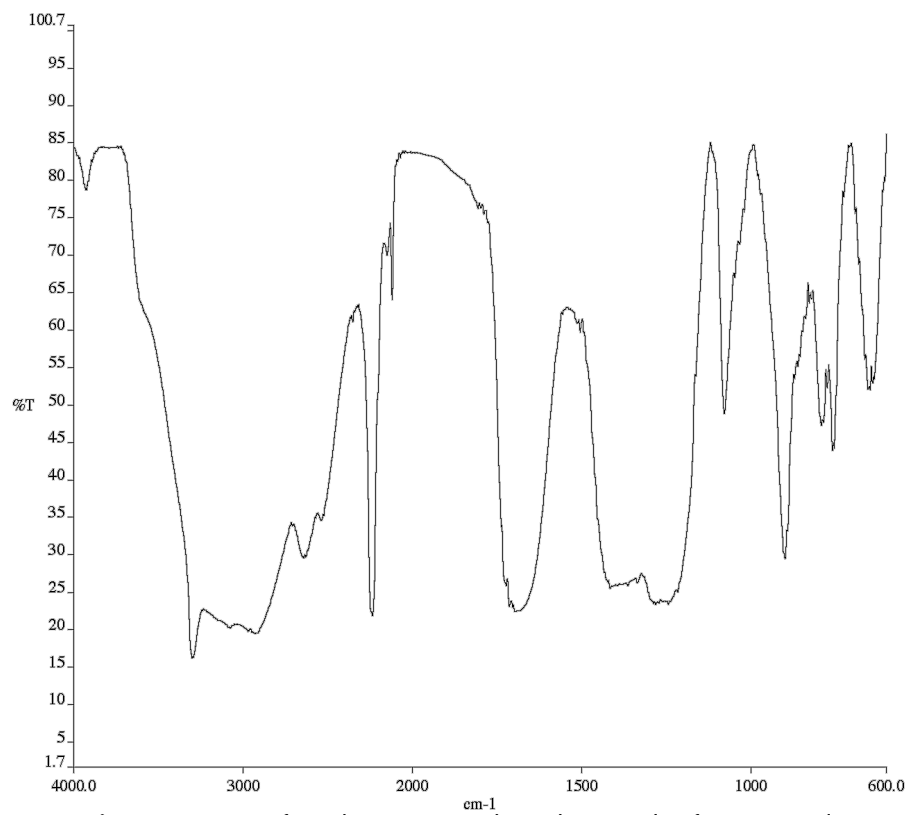
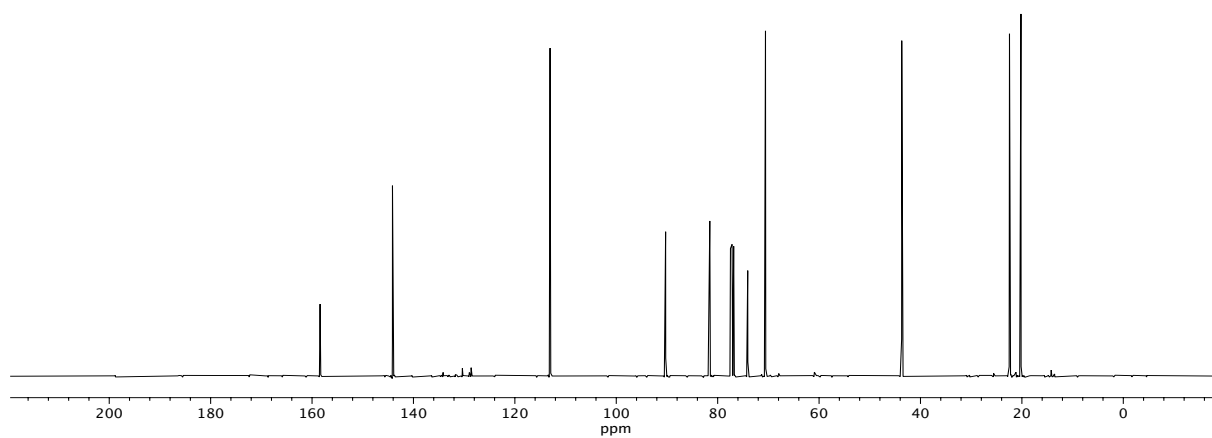


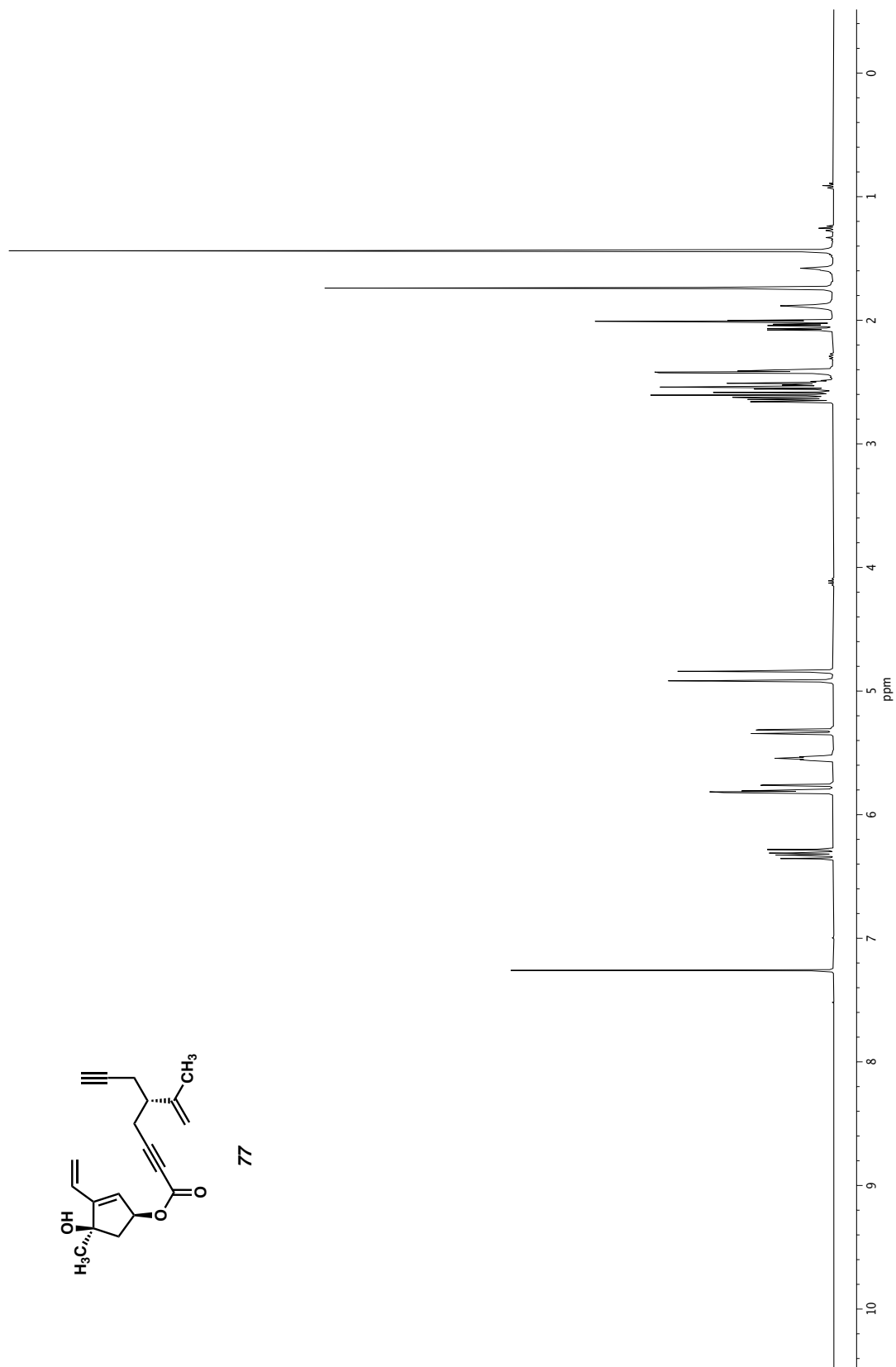
Figure A2.100 <sup>1</sup>H NMR (400 MHz, CDCl<sub>3</sub>) of compound 57.



**Figure A2.101** Infrared spectrum (Thin Film, NaCl) of compound 57.



**Figure A2.102** <sup>13</sup>C NMR (100 MHz, CDCl<sub>3</sub>) of compound 57.

Figure A2.103  $^1\text{H}$  NMR (400 MHz,  $\text{CDCl}_3$ ) of compound 77.

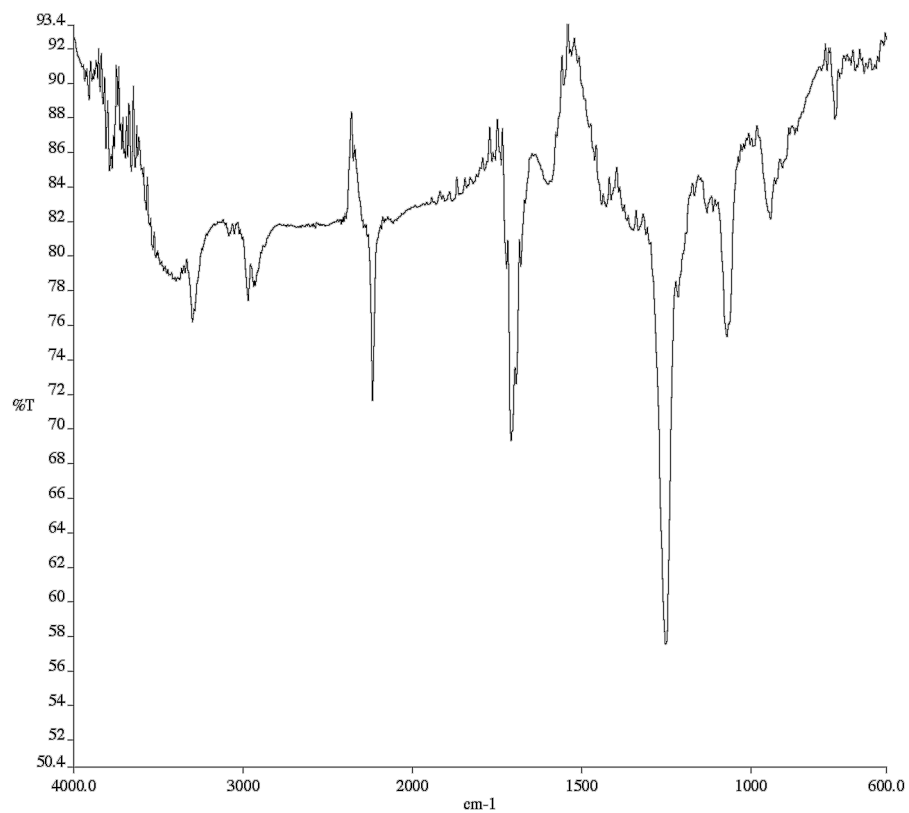


**Figure A2.104** Infrared spectrum (Thin Film, NaCl) of compound 77.

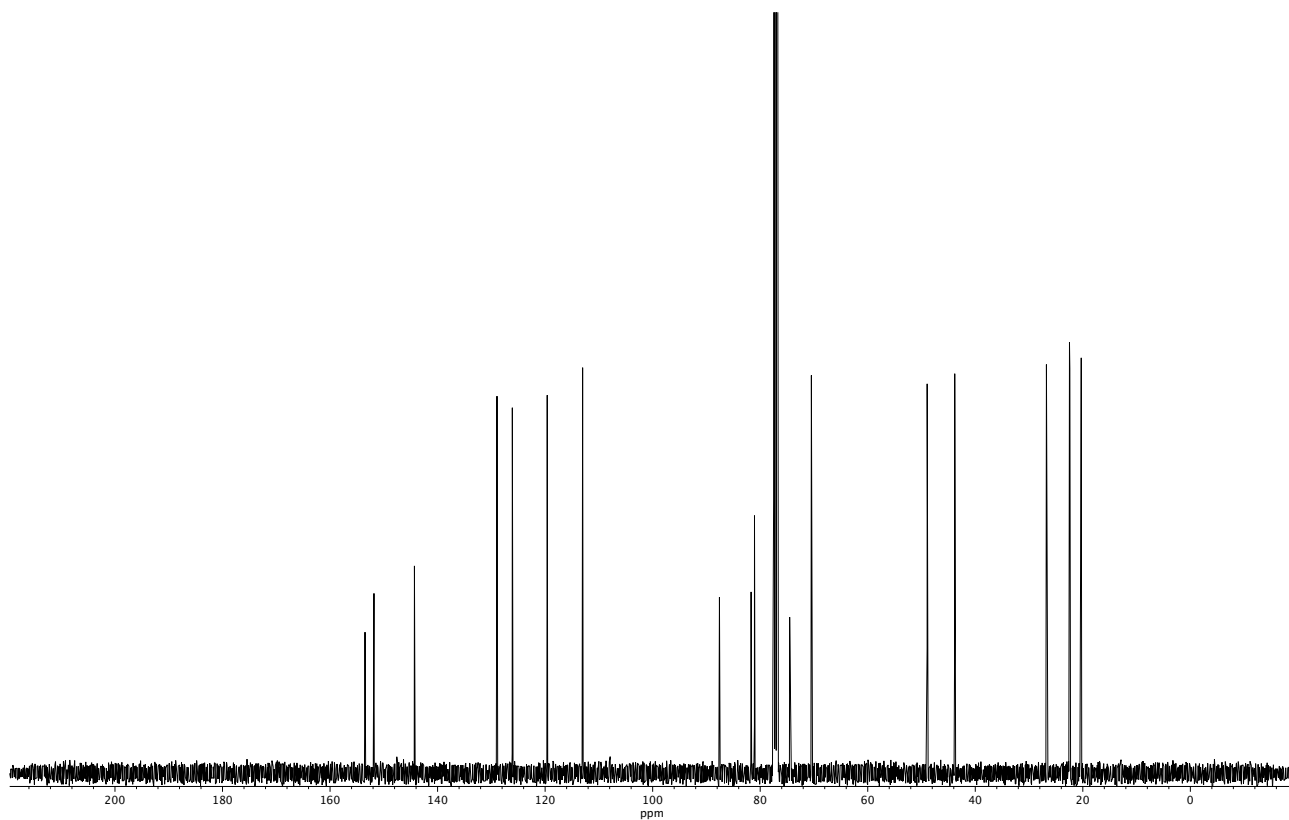


**Figure A2.105** <sup>13</sup>C NMR (100 MHz, CDCl<sub>3</sub>) of compound 77.

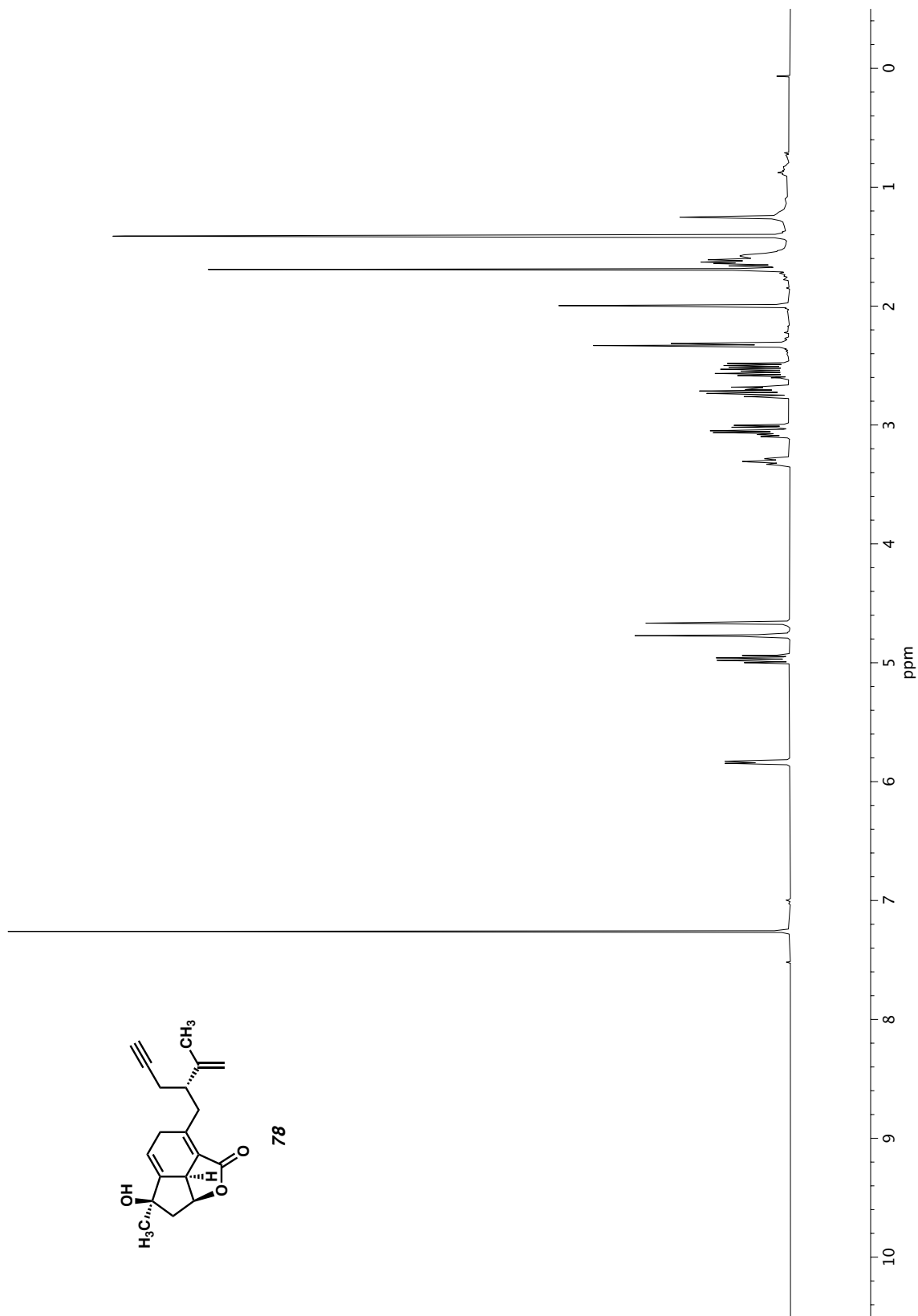
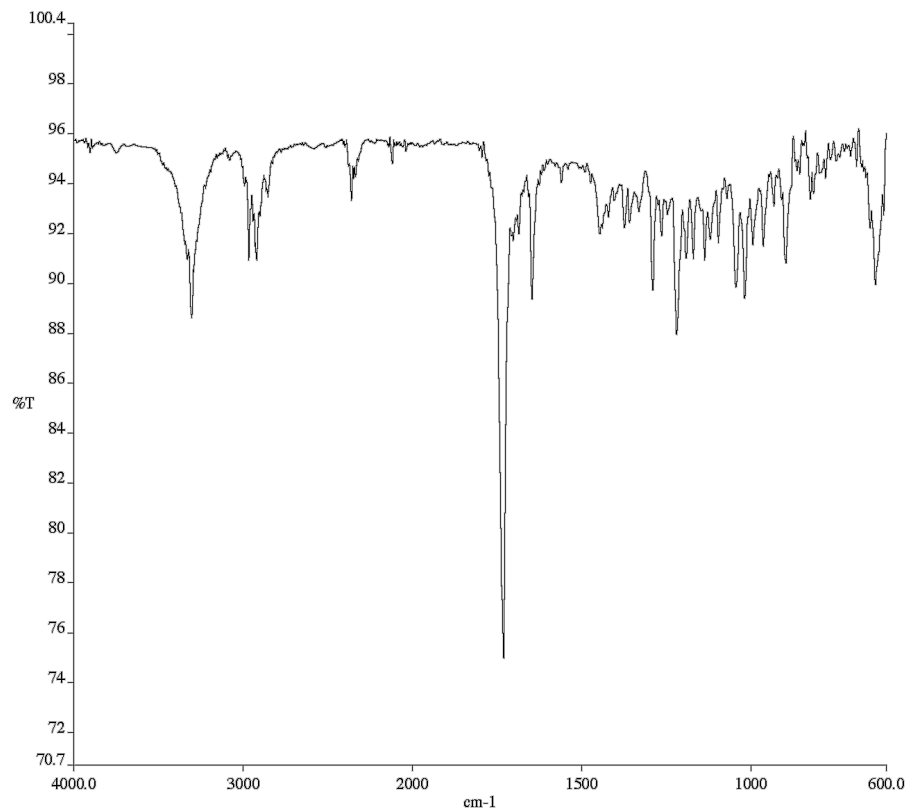
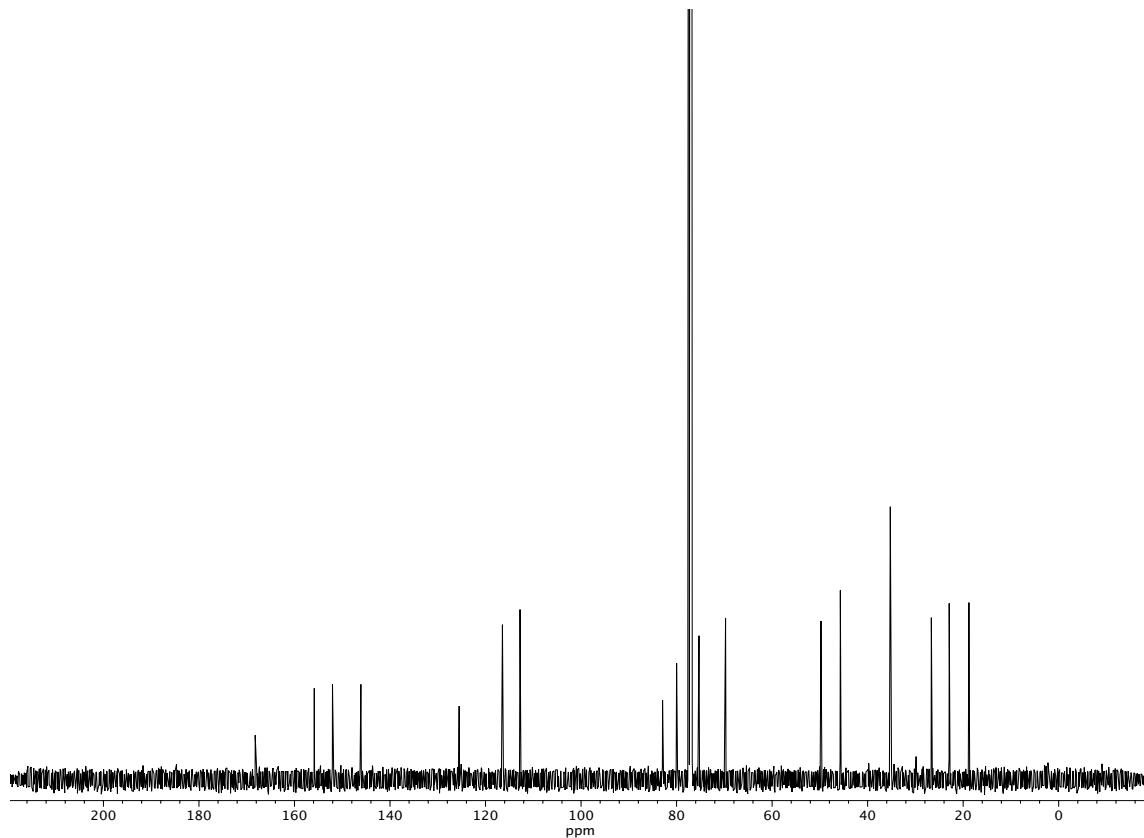


Figure A2.106 <sup>1</sup>H NMR (400 MHz, CDCl<sub>3</sub>) of compound 78.



**Figure A2.107** Infrared spectrum (Thin Film, NaCl) of compound **78**.



**Figure A2.108** <sup>13</sup>C NMR (100 MHz, CDCl<sub>3</sub>) of compound **78**.

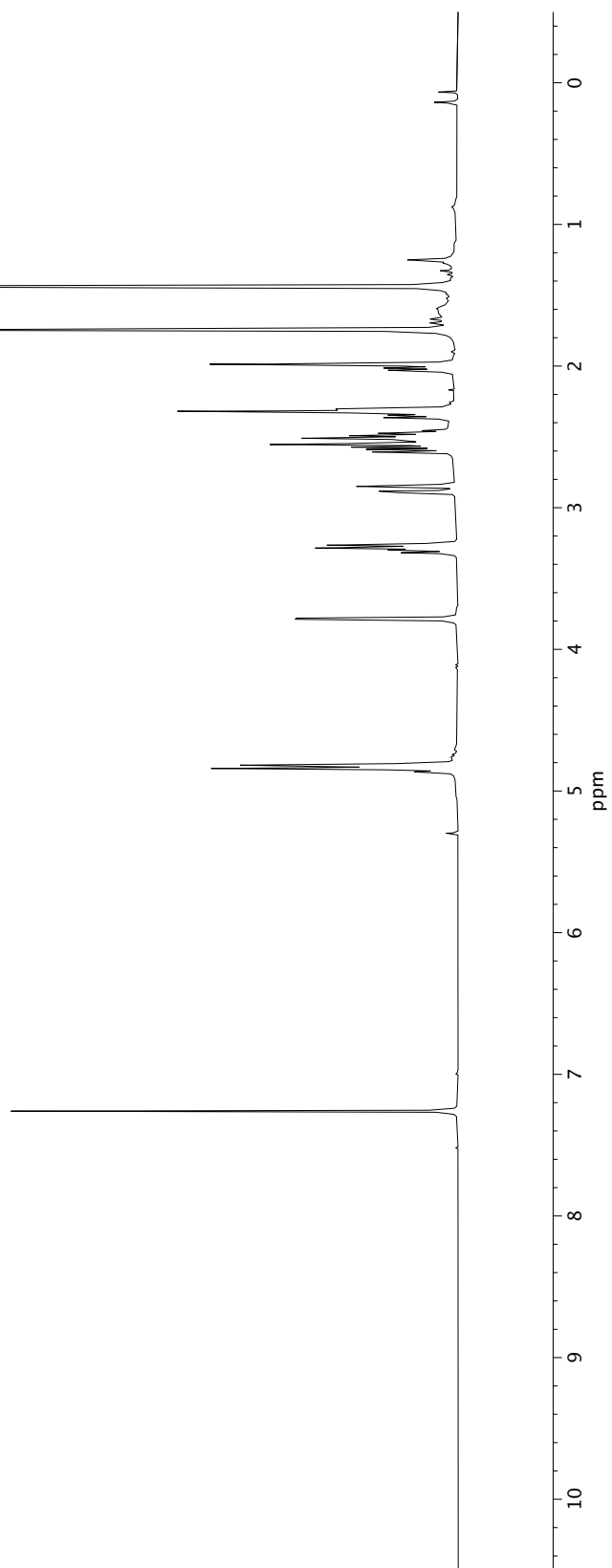
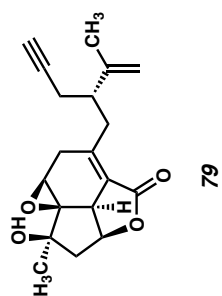
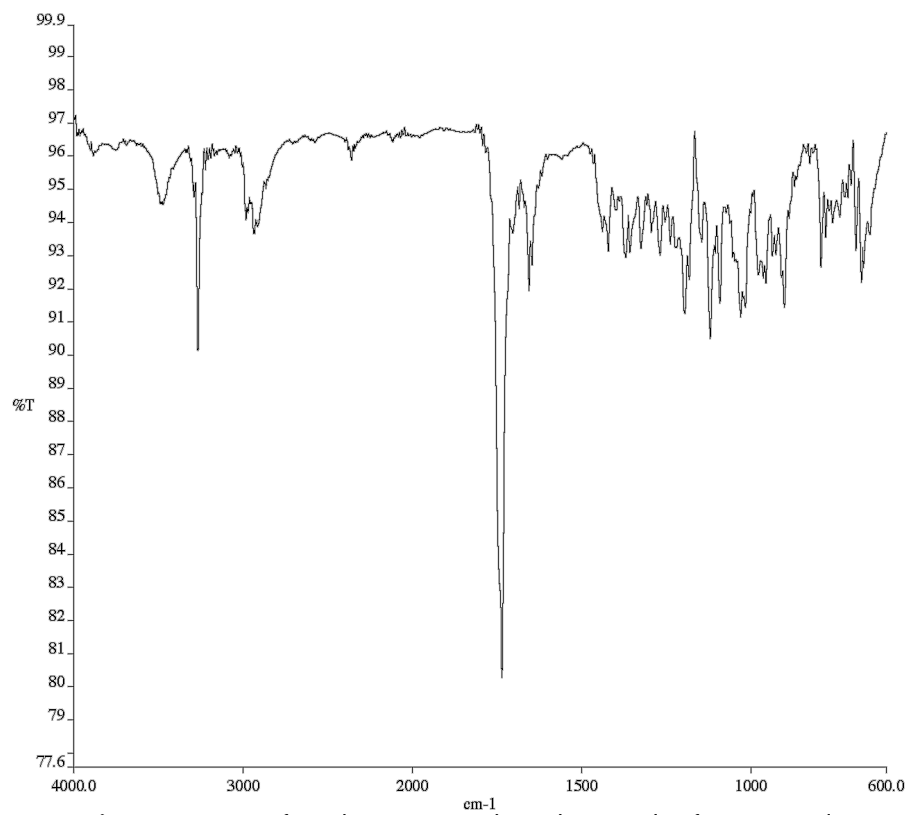
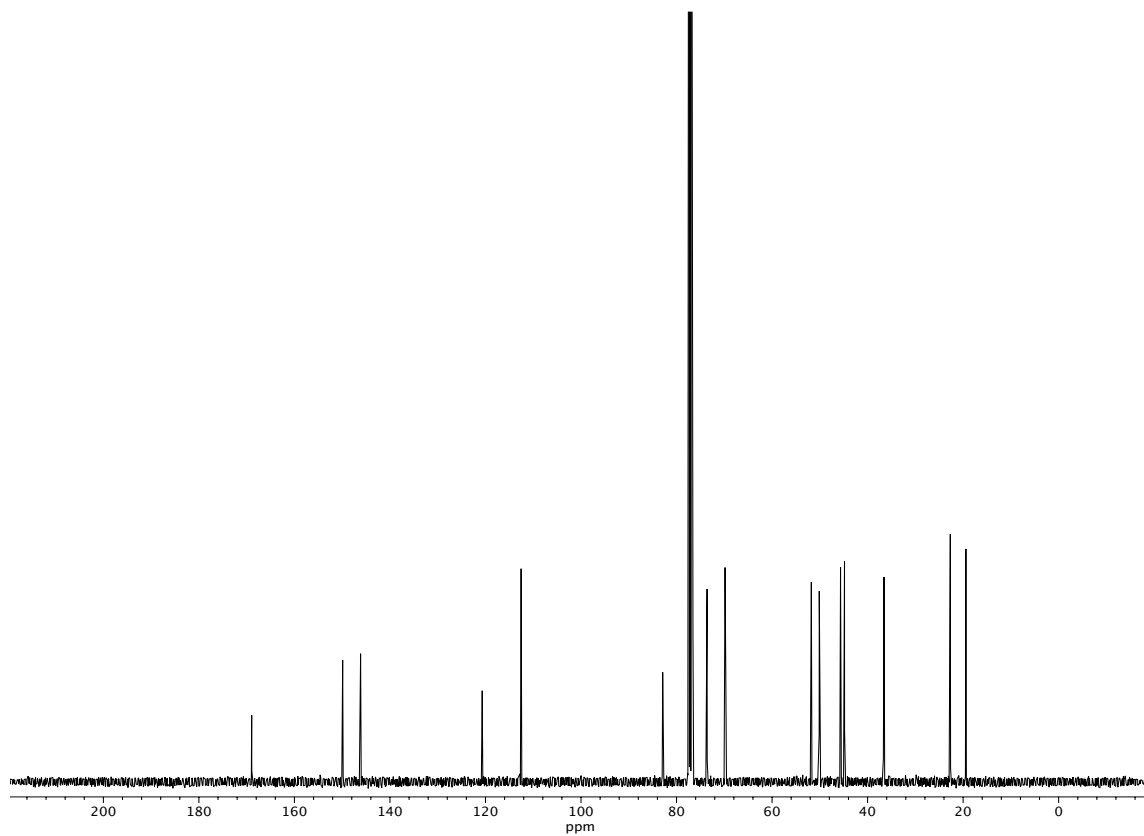


Figure A2.109 <sup>1</sup>H NMR (400 MHz, CDCl<sub>3</sub>) of compound 79.





**Figure A2.110** Infrared spectrum (Thin Film, NaCl) of compound **79**.



**Figure A2.111** <sup>13</sup>C NMR (100 MHz, CDCl<sub>3</sub>) of compound **79**.

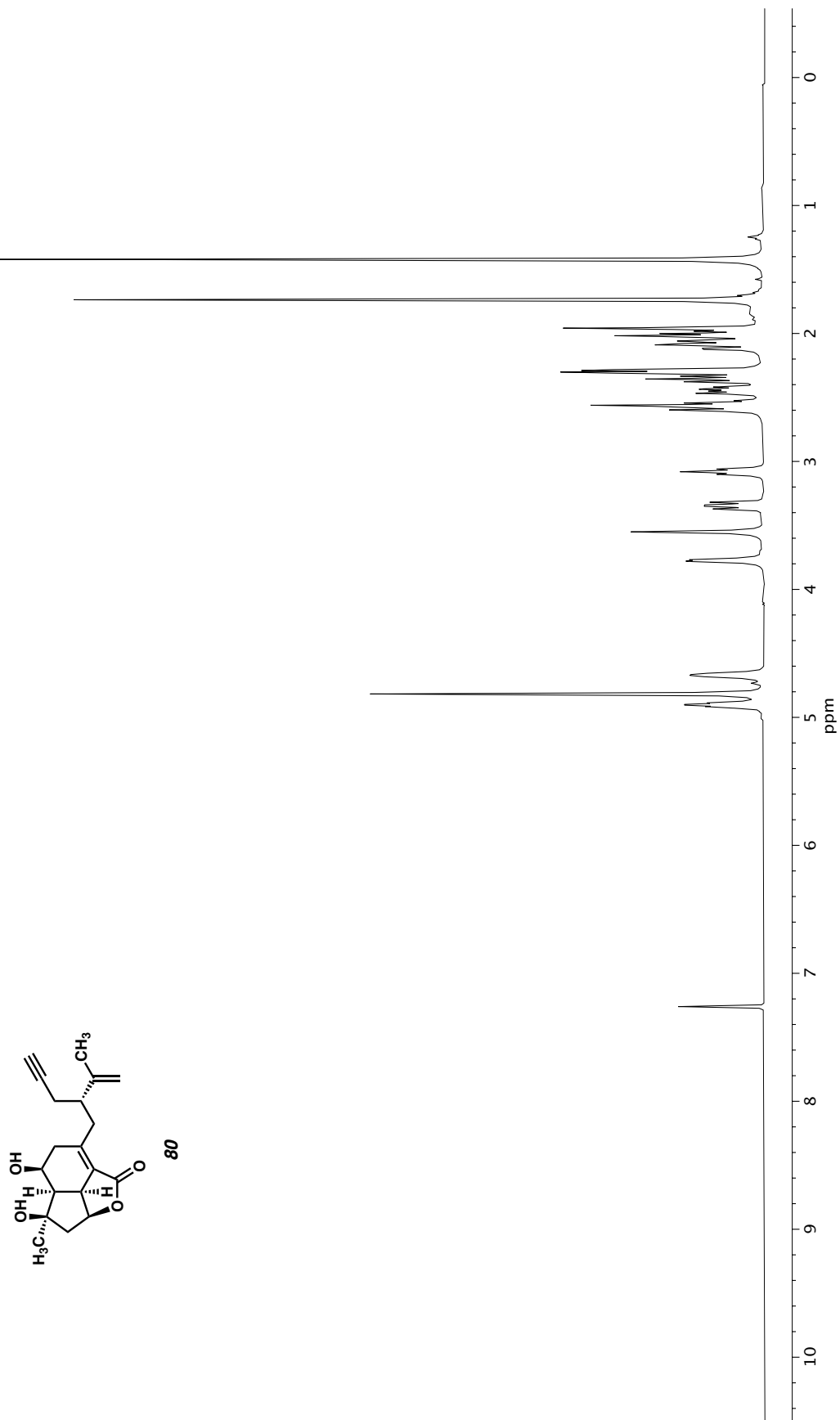
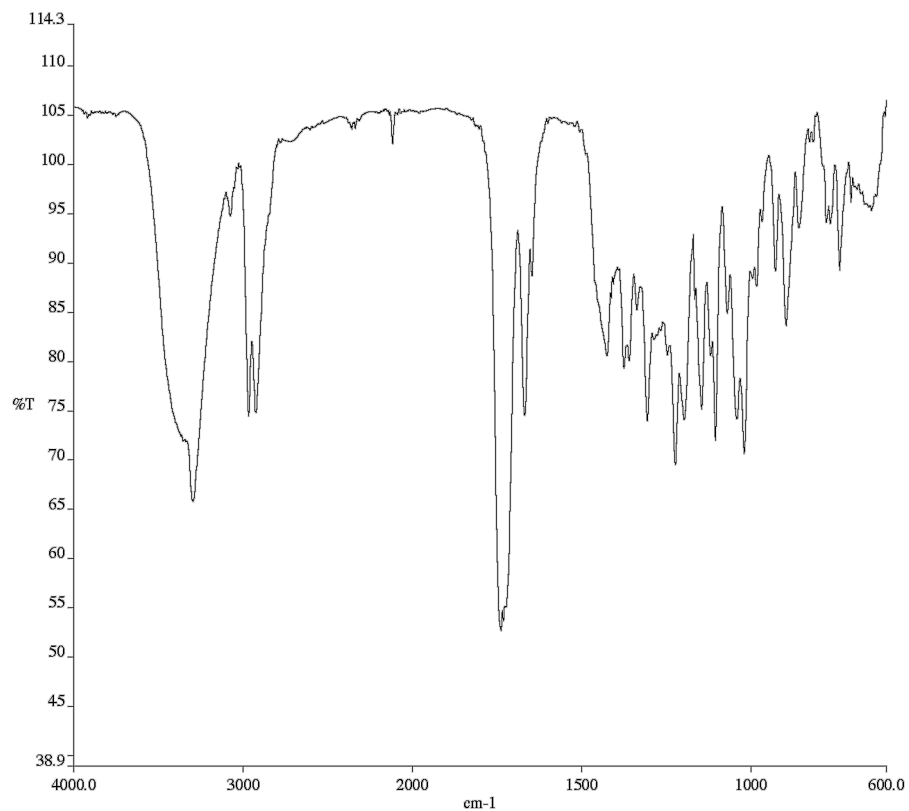
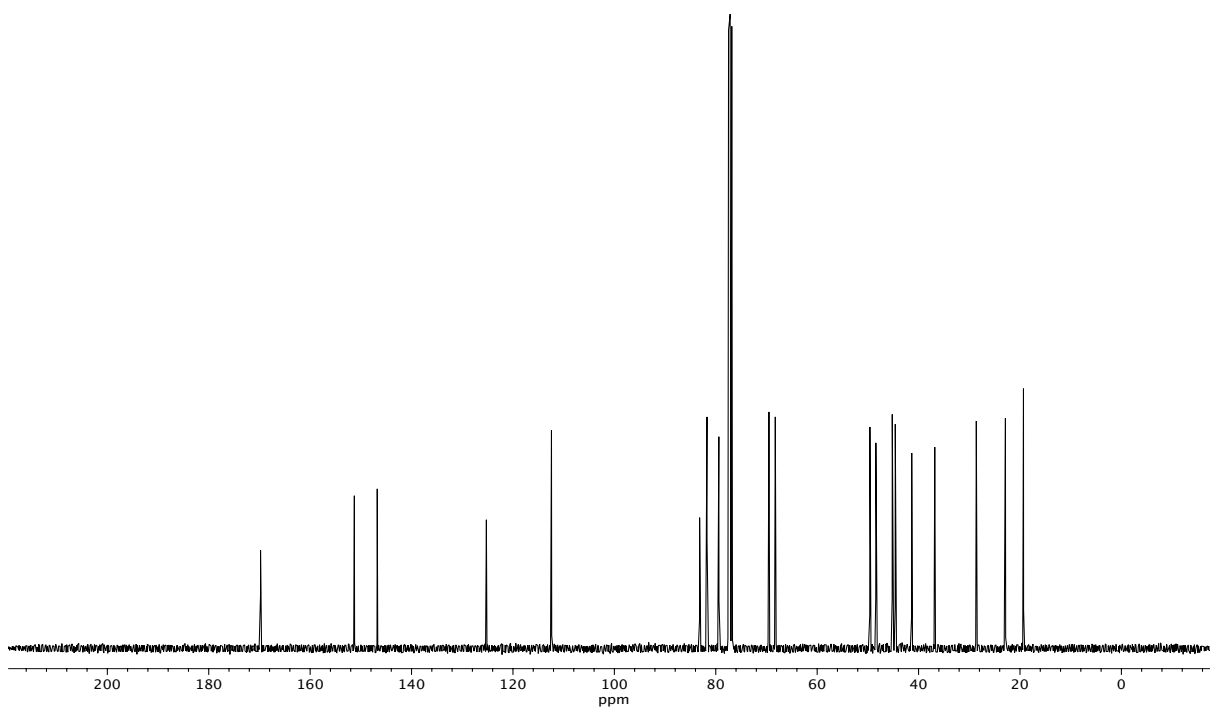


Figure A2.112  $^1\text{H}$  NMR (400 MHz,  $\text{CDCl}_3$ ) of compound **80**.



**Figure A2.113** Infrared spectrum (Thin Film, NaCl) of compound **80**.



**Figure A2.114** <sup>13</sup>C NMR (100 MHz, CDCl<sub>3</sub>) of compound **80**.

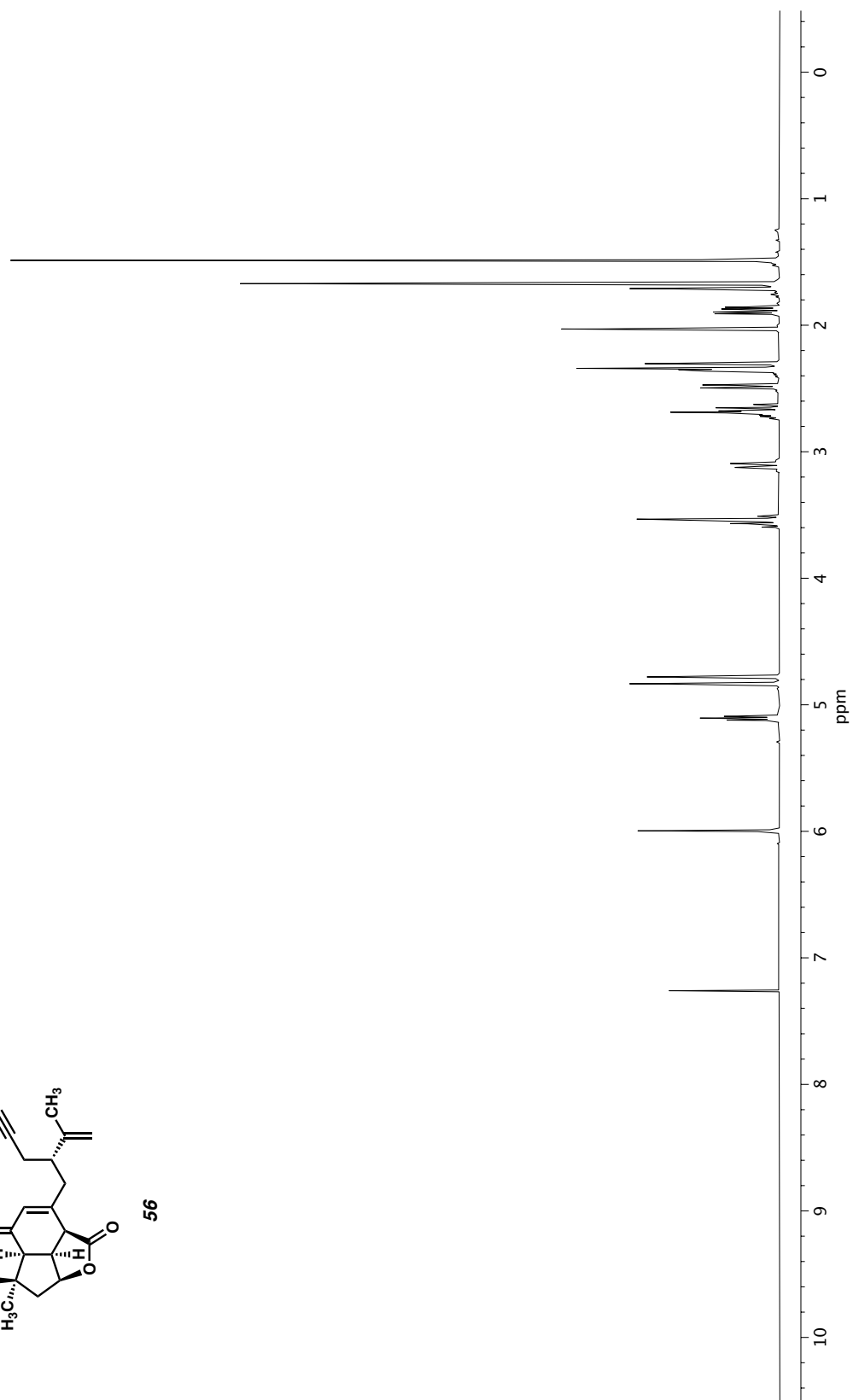
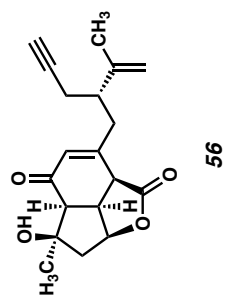
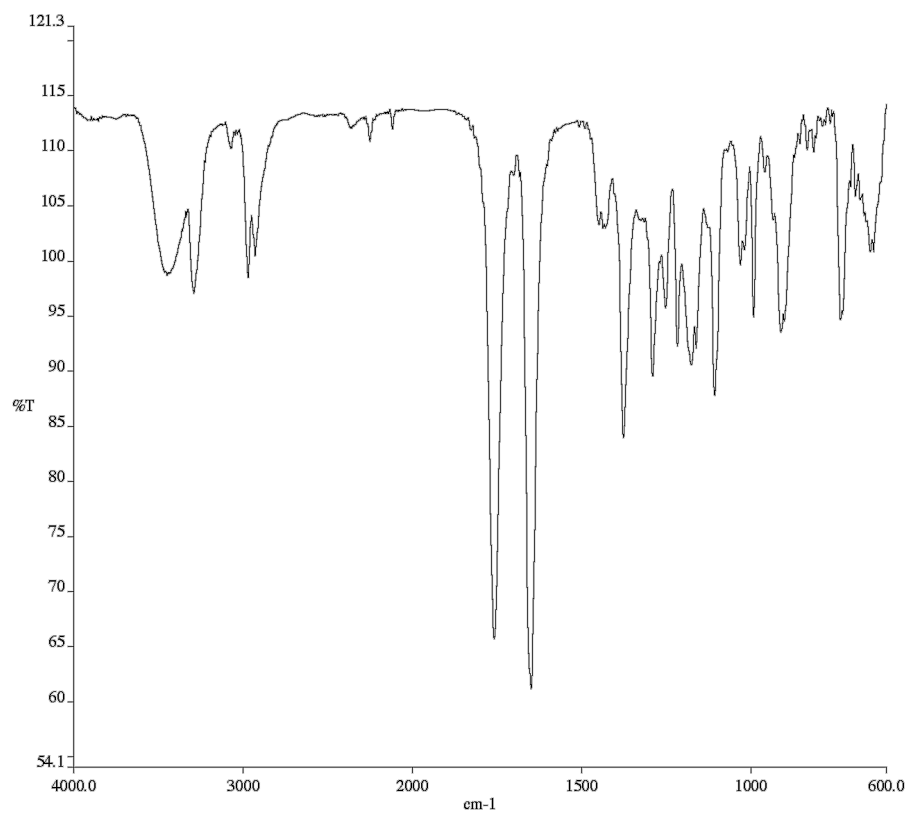
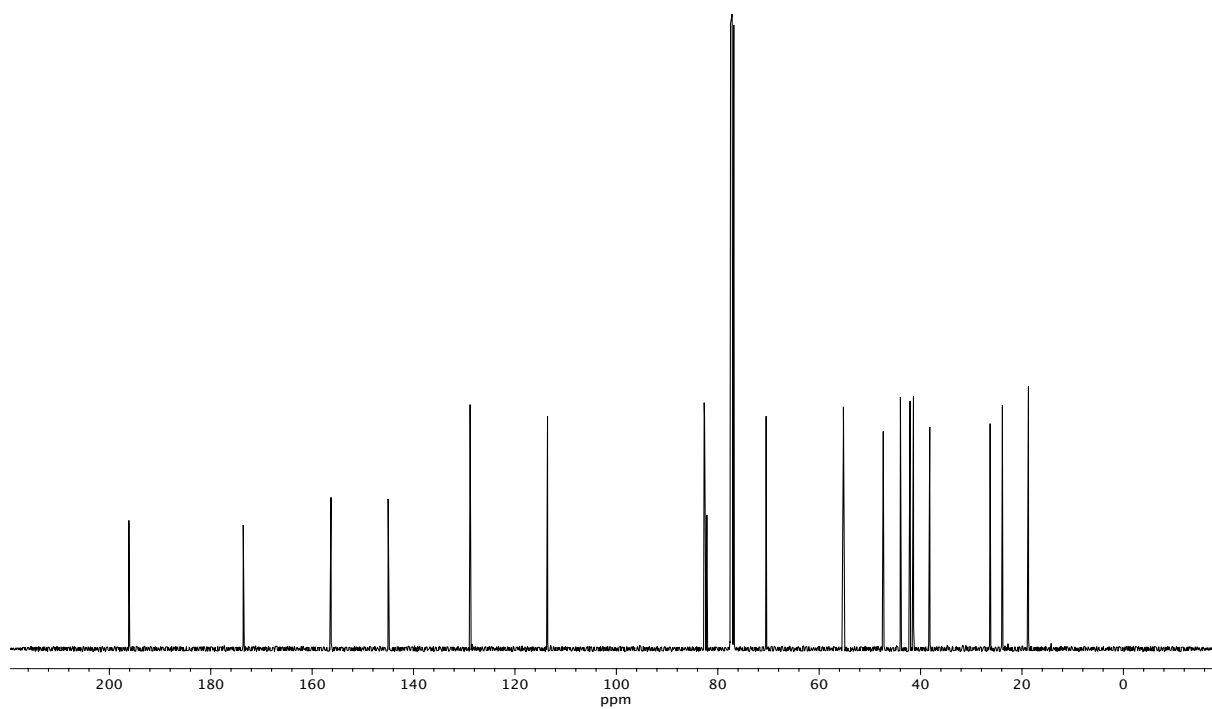


Figure A2.115  $^1\text{H}$  NMR (400 MHz,  $\text{CDCl}_3$ ) of compound 56.



**Figure A2.116** Infrared spectrum (Thin Film, NaCl) of compound 56.



**Figure A2.117** <sup>13</sup>C NMR (100 MHz, CDCl<sub>3</sub>) of compound 56.

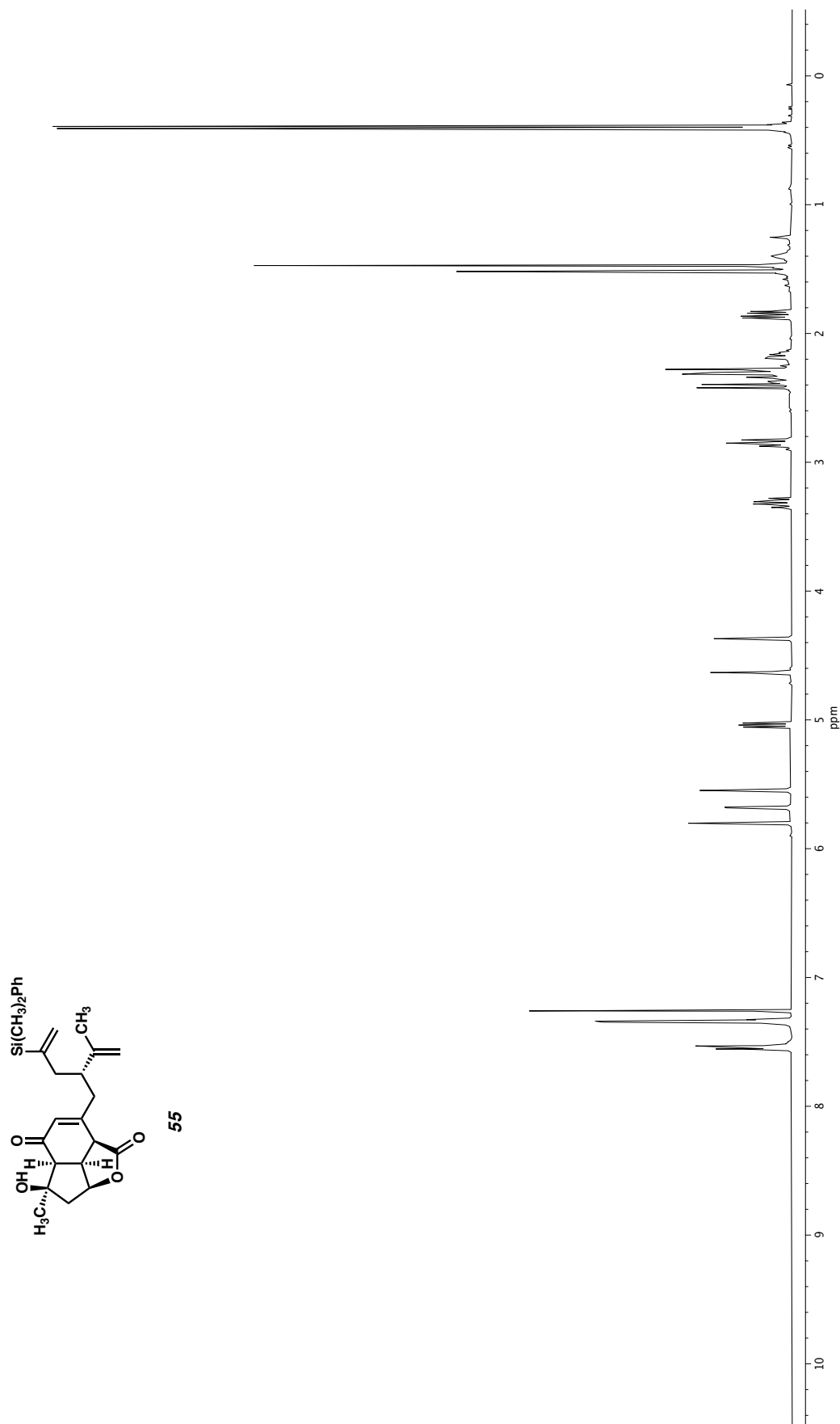
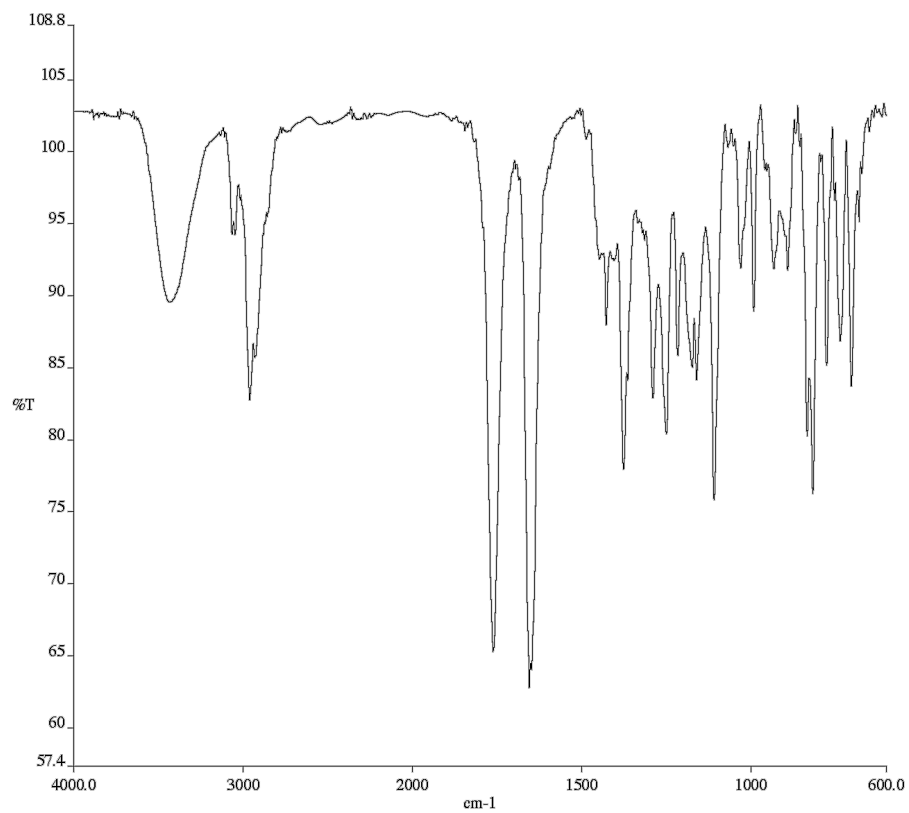
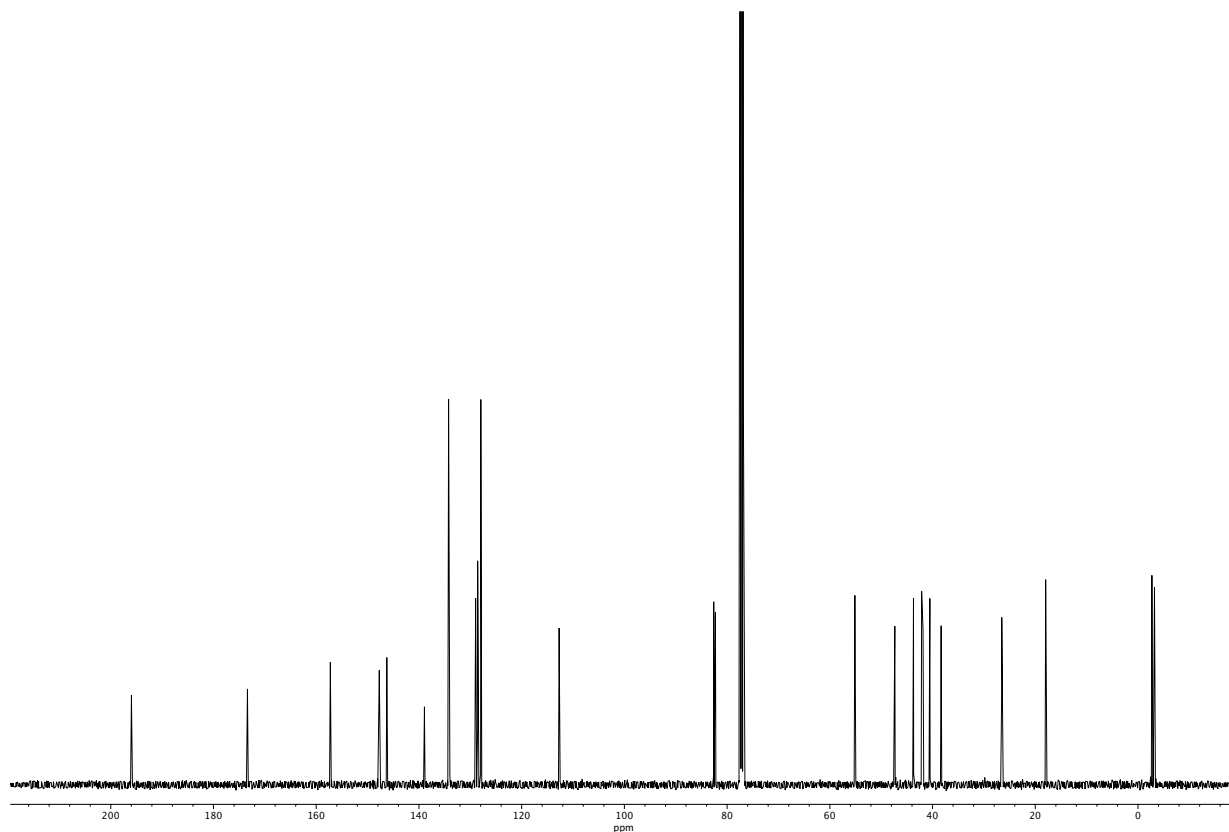


Figure A2.118  $^1\text{H}$  NMR (400 MHz,  $\text{CDCl}_3$ ) of compound 55.



**Figure A2.119** Infrared spectrum (Thin Film, NaCl) of compound 55.



**Figure A2.120** <sup>13</sup>C NMR (100 MHz, CDCl<sub>3</sub>) of compound 55.

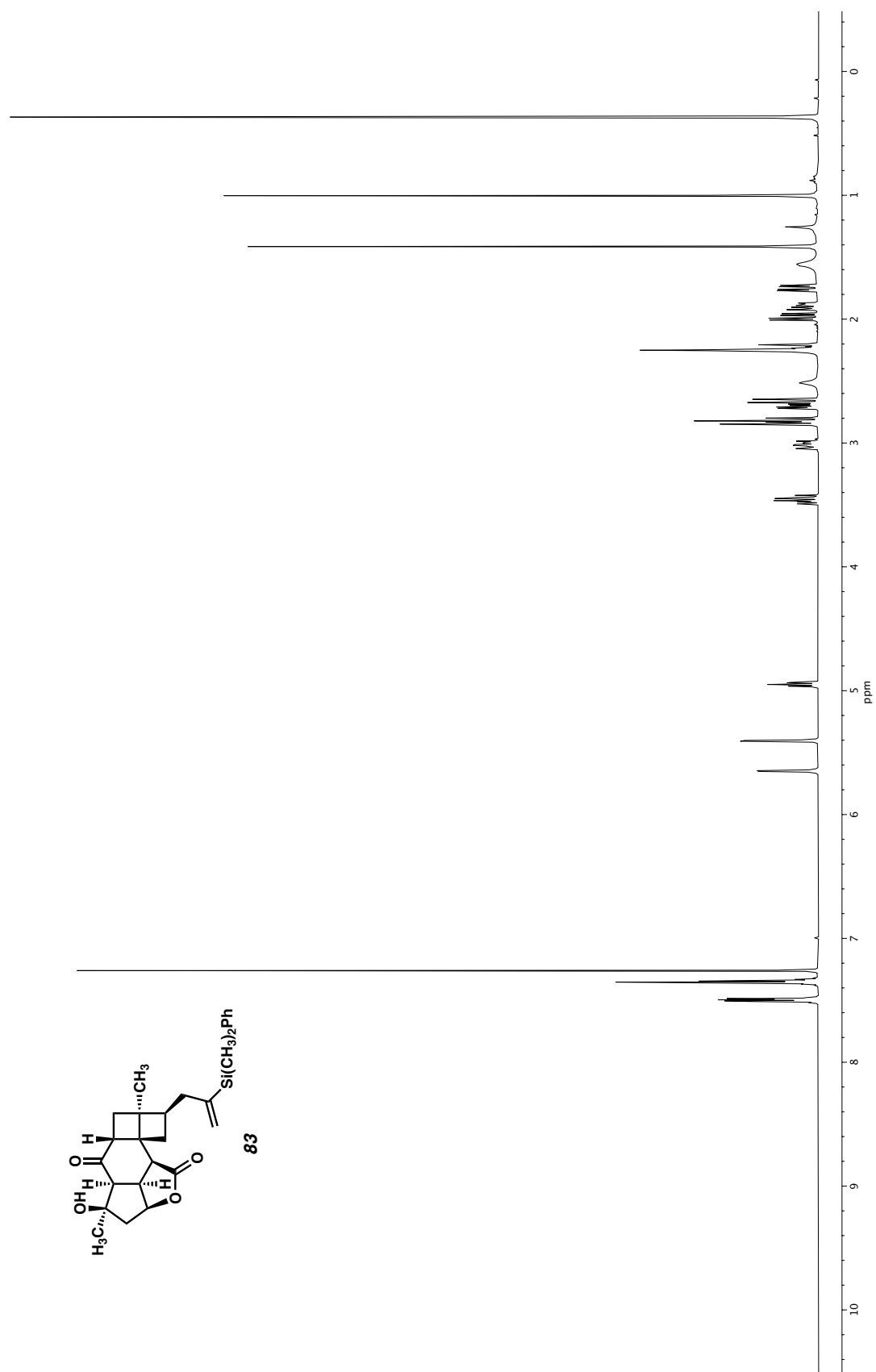
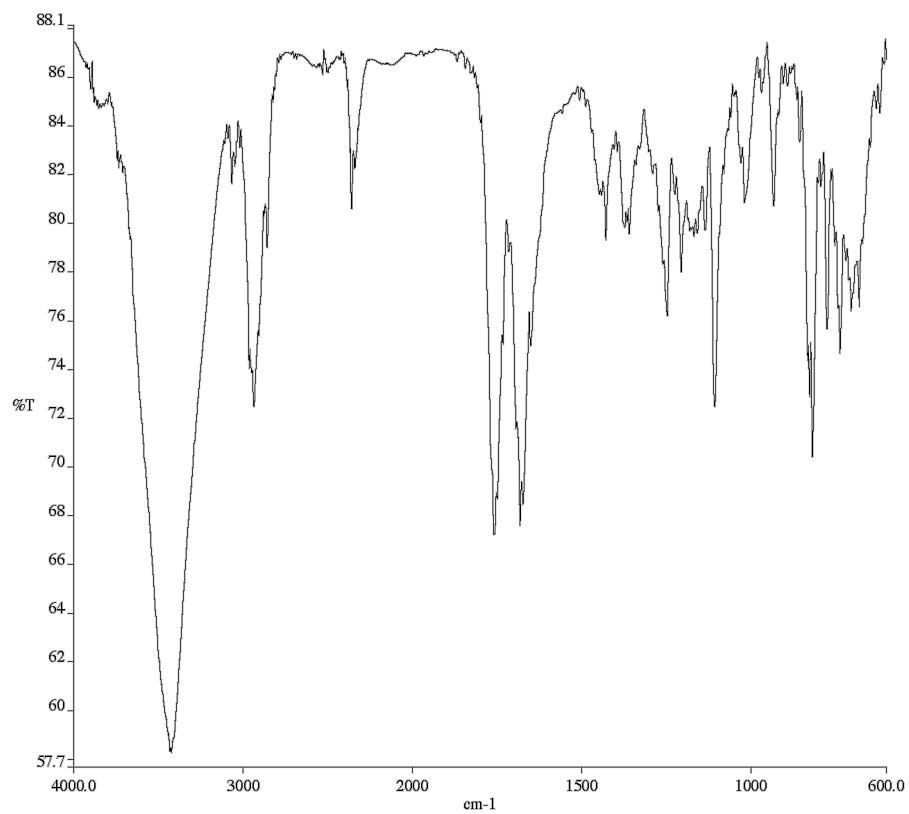
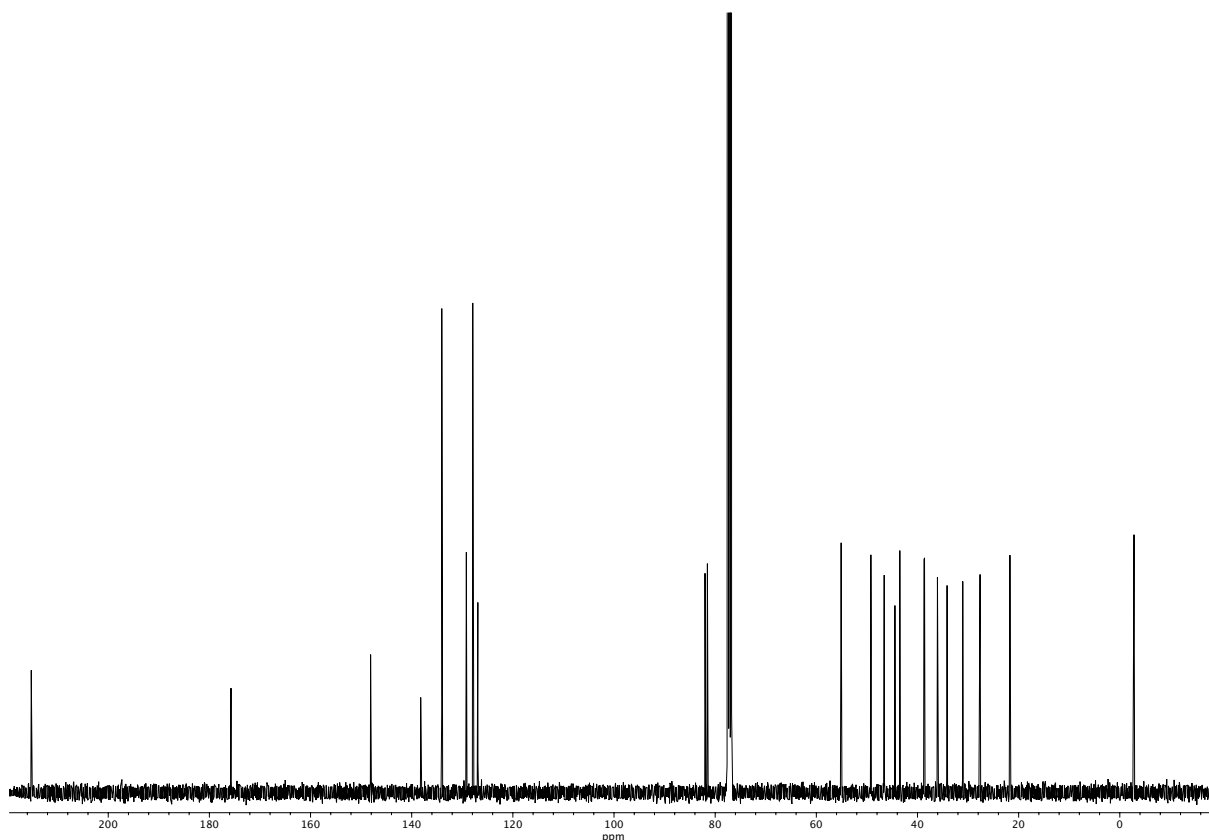


Figure A2.121 <sup>1</sup>H NMR (400 MHz, CDCl<sub>3</sub>) of compound 83.





**Figure A2.122** Infrared spectrum (Thin Film, NaCl) of compound **83**.



**Figure A2.123** <sup>13</sup>C NMR (100 MHz, CDCl<sub>3</sub>) of compound **83**.

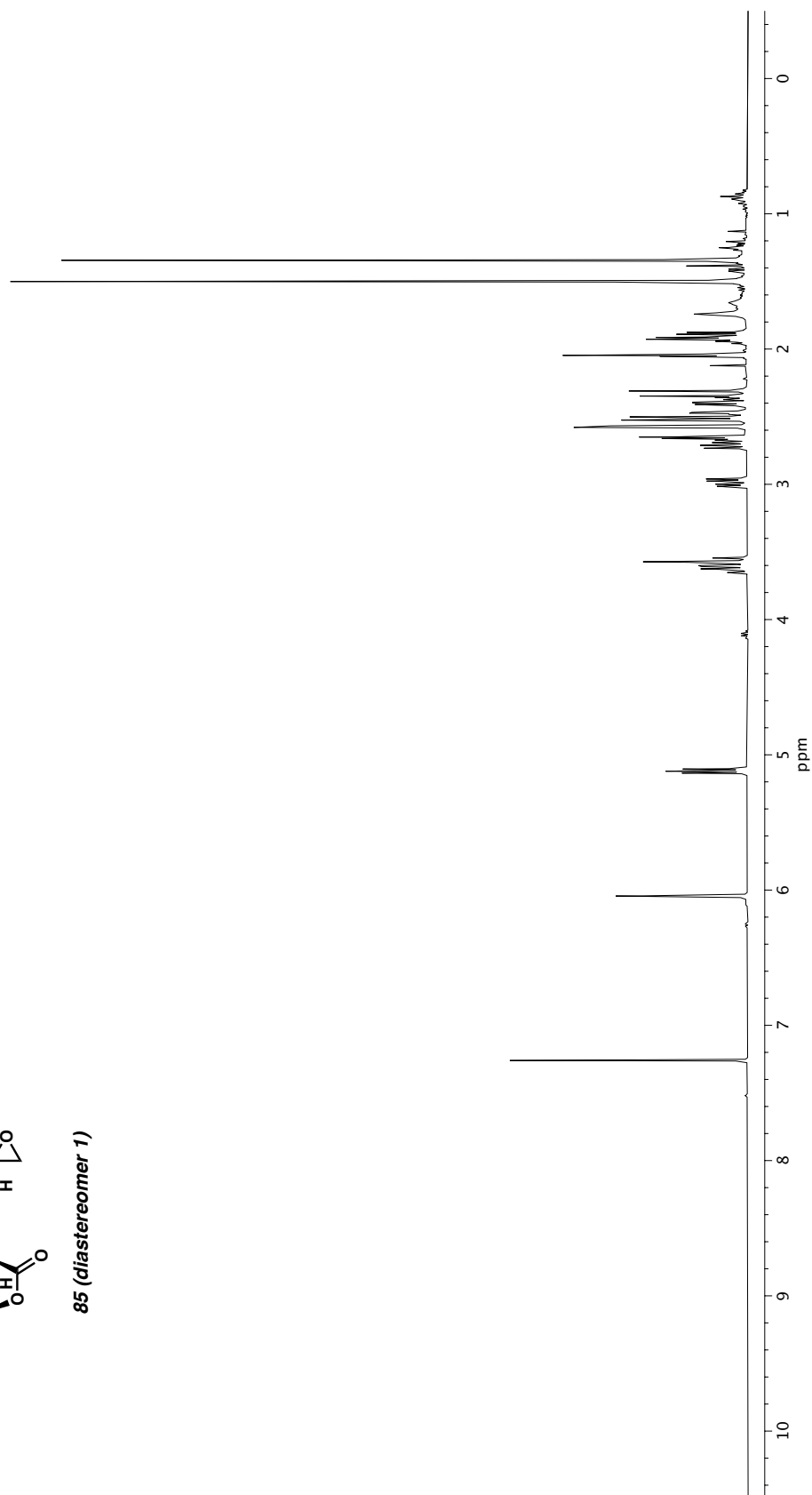
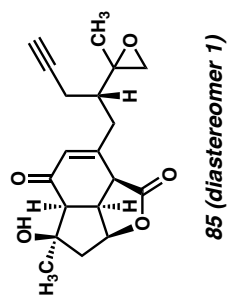


**Figure A2.124**  $^1\text{H}$  NMR (400 MHz,  $\text{CDCl}_3$ ) of compound **85** (diastereomer 1).

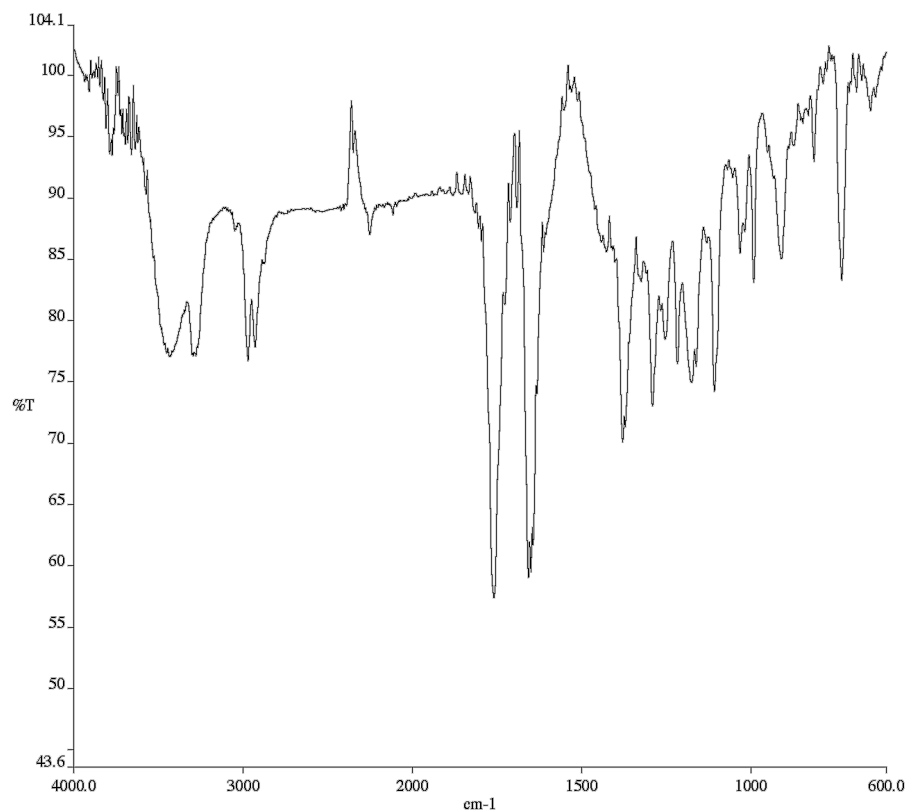


**Figure A2.125** Infrared spectrum (Thin Film, NaCl) of compound **85** (diastereomer 1).

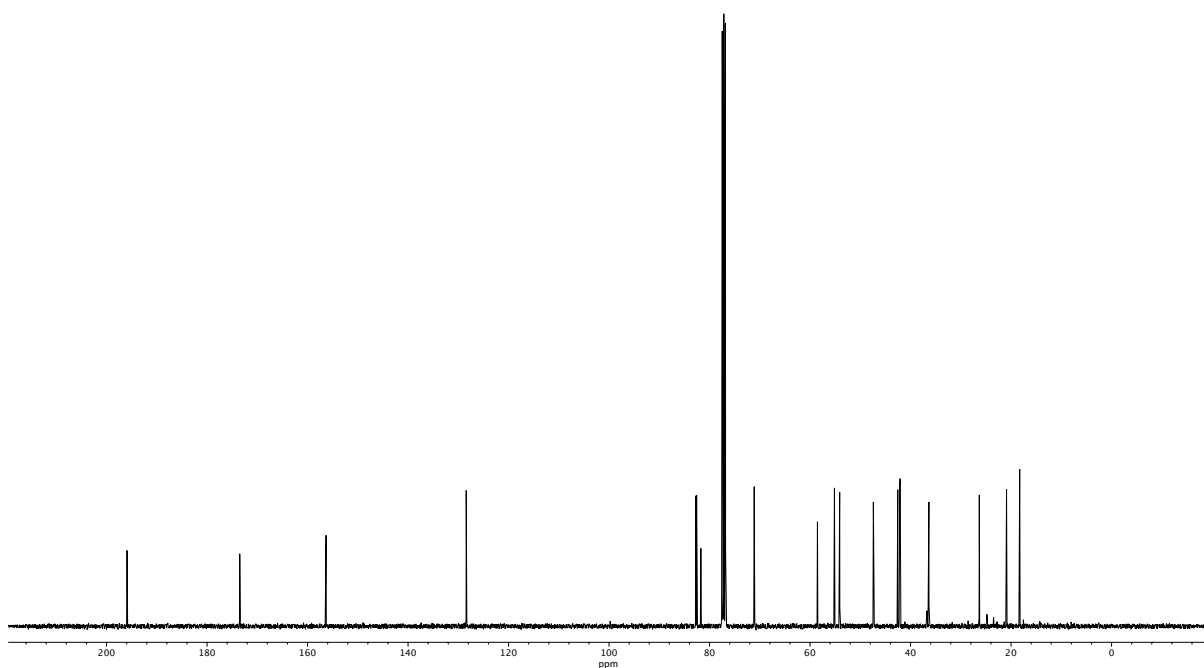


**Figure A2.126** <sup>13</sup>C NMR (100 MHz, CDCl<sub>3</sub>) of compound **85** (diastereomer 1).

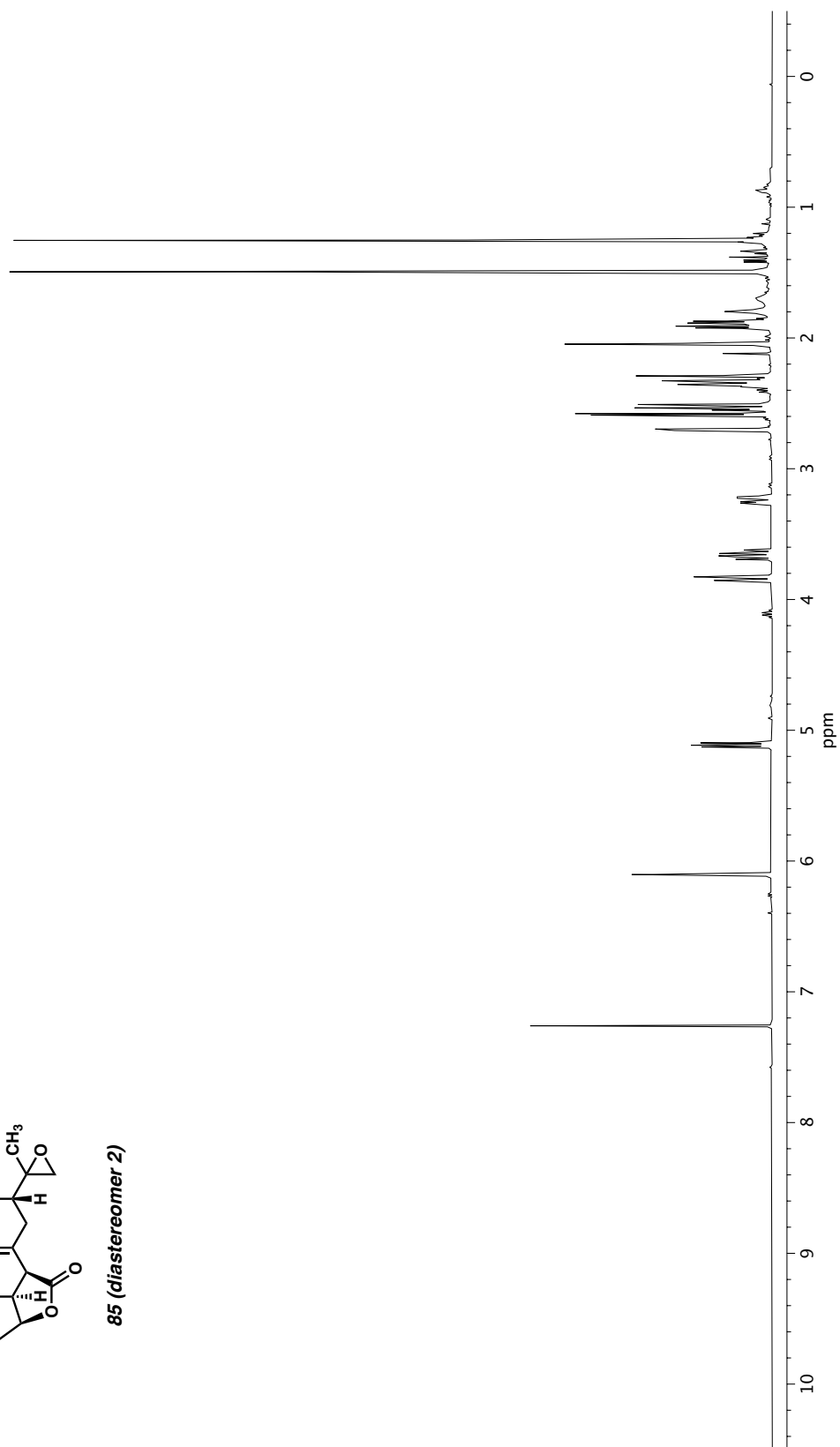
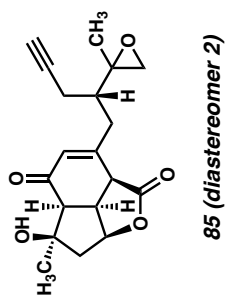


**Figure A2.127**  $^1\text{H}$  NMR (400 MHz,  $\text{CDCl}_3$ ) of compound **85** (diastereomer 2).

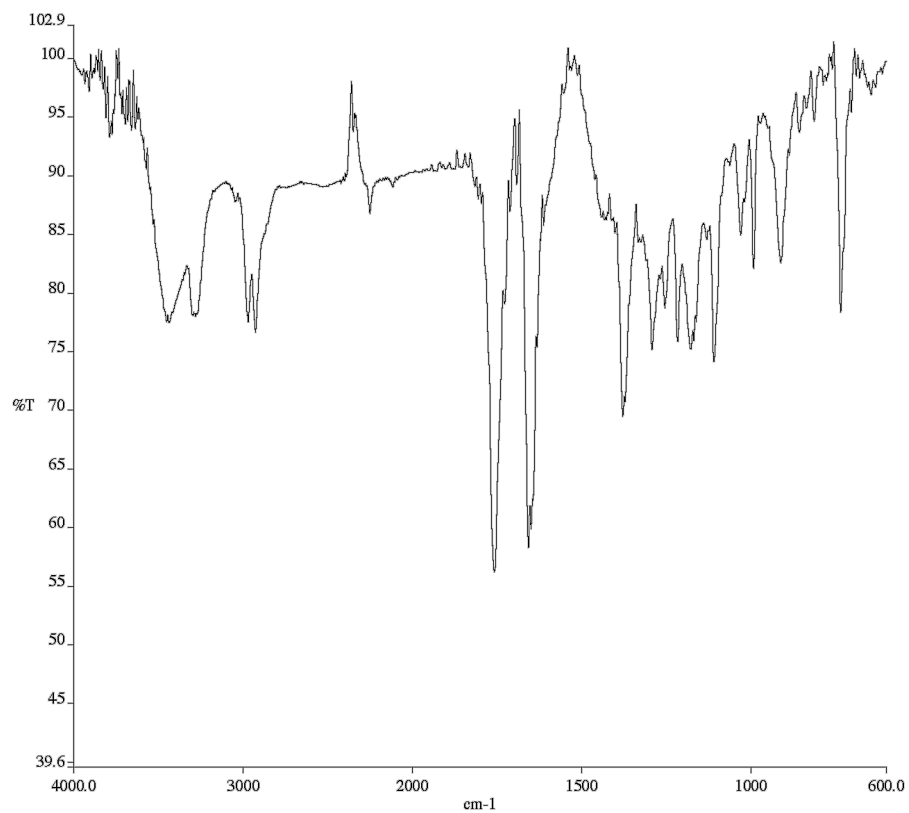


**Figure A2.128** Infrared spectrum (Thin Film, NaCl) of compound **85** (diastereomer 2).

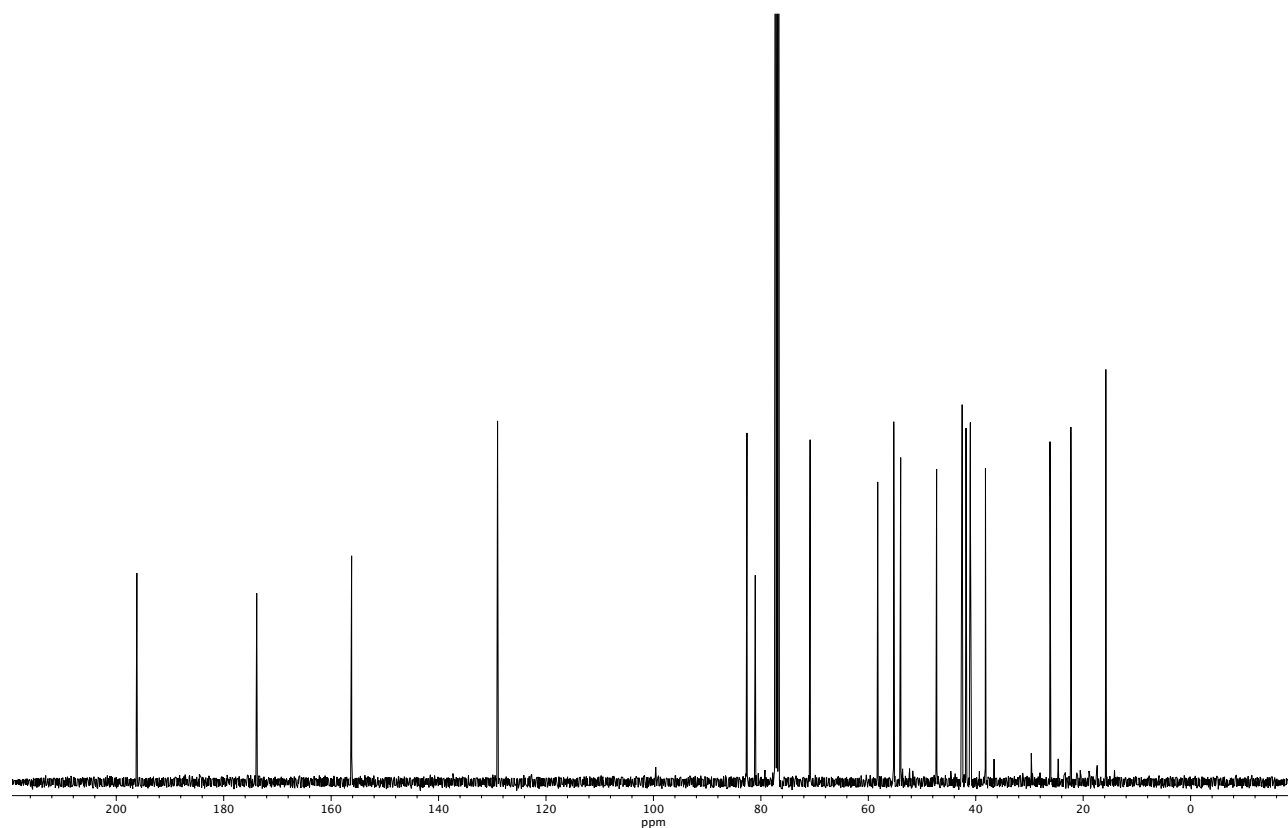


**Figure A2.129** <sup>13</sup>C NMR (100 MHz, CDCl<sub>3</sub>) of compound **85** (diastereomer 2).

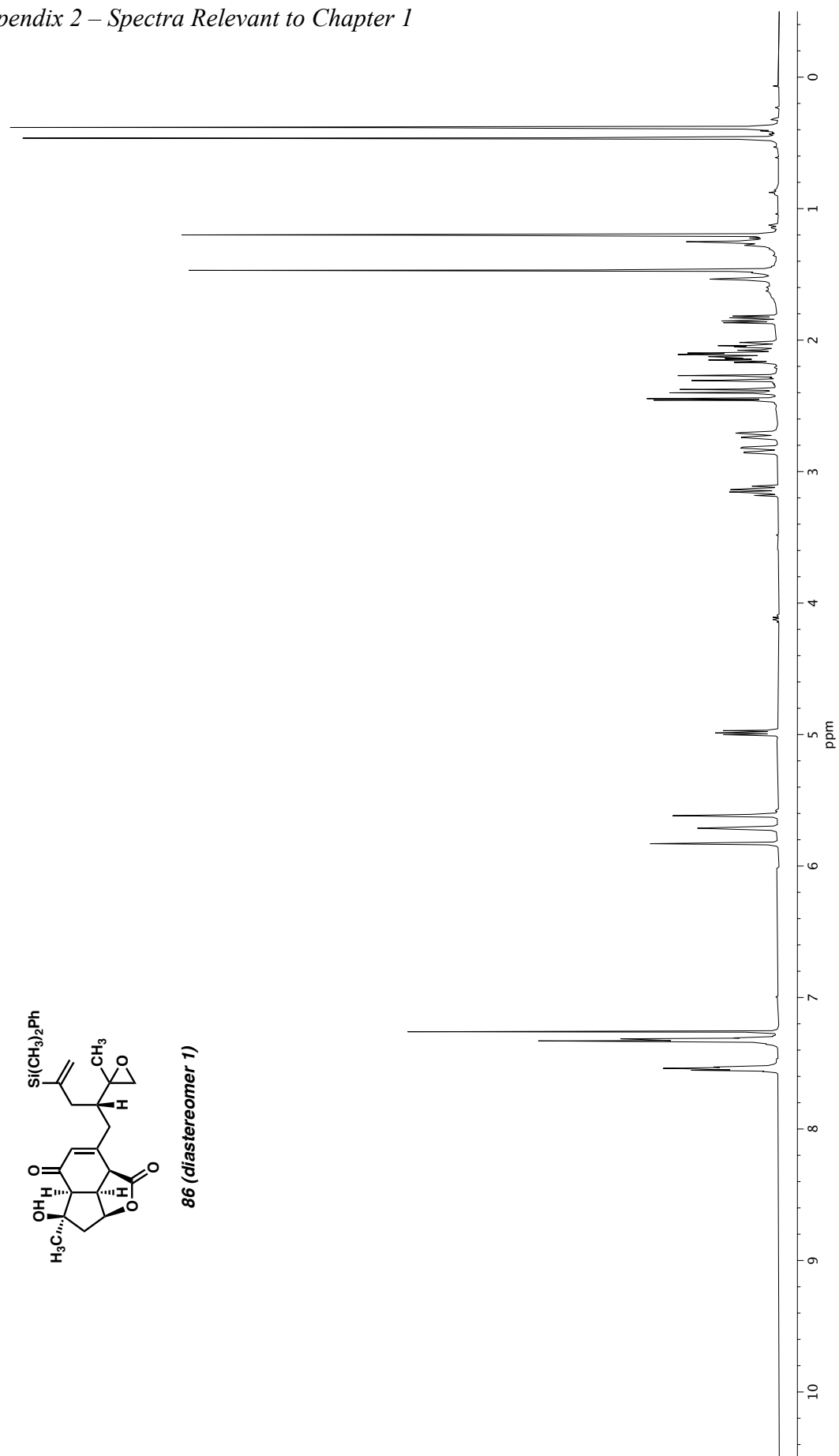
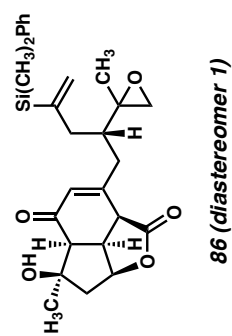


**Figure A2.130**  $^1\text{H}$  NMR (400 MHz,  $\text{CDCl}_3$ ) of compound **86** (diastereomer 1).

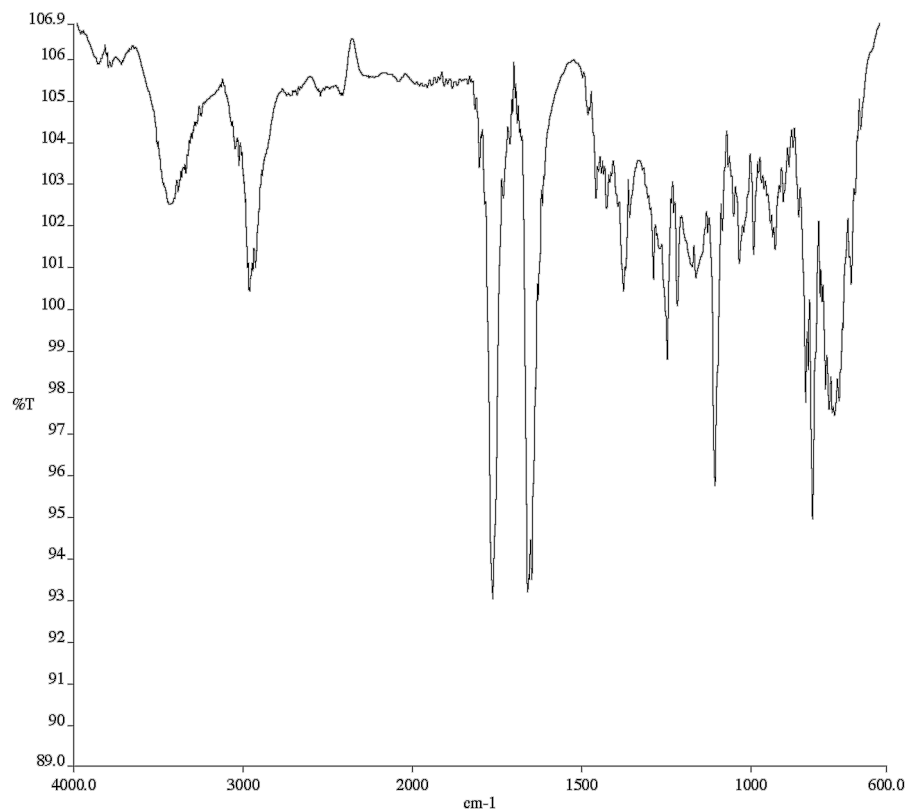


Figure A2.131 Infrared spectrum (Thin Film, NaCl) of compound **86** (diastereomer 1).

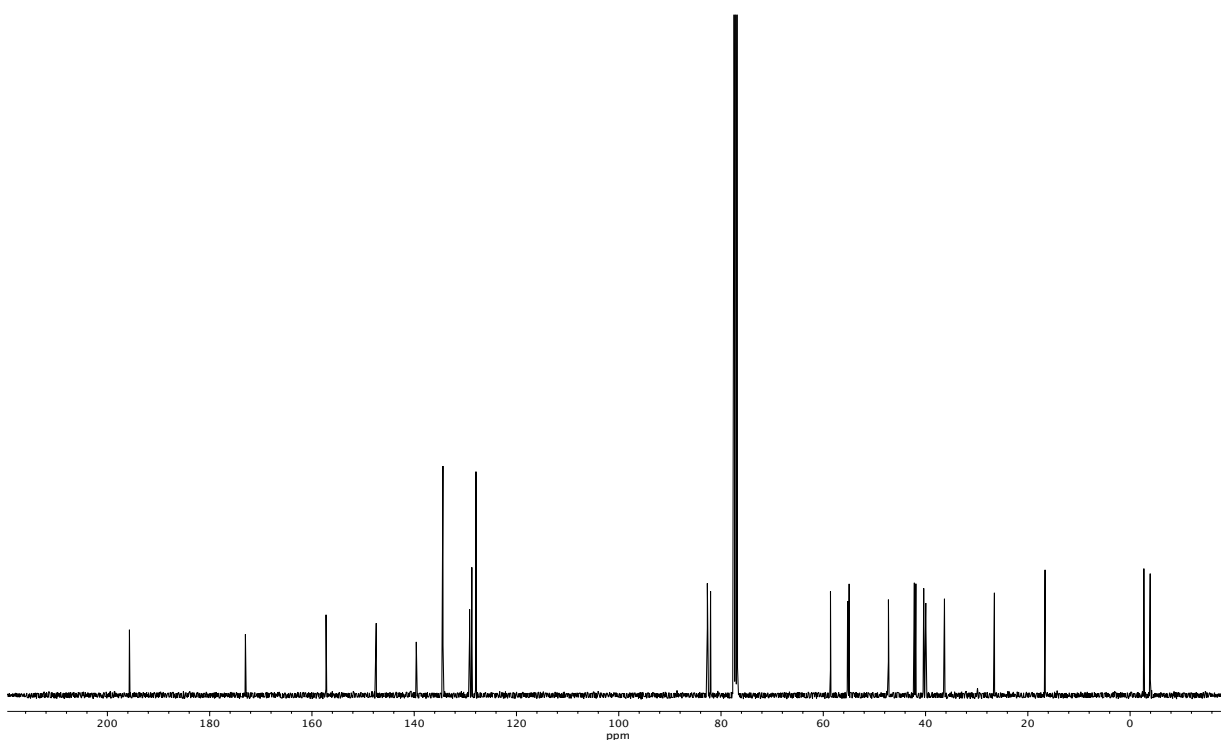


Figure A2.132  $^{13}\text{C}$  NMR (100 MHz,  $\text{CDCl}_3$ ) of compound **86** (diastereomer 1).

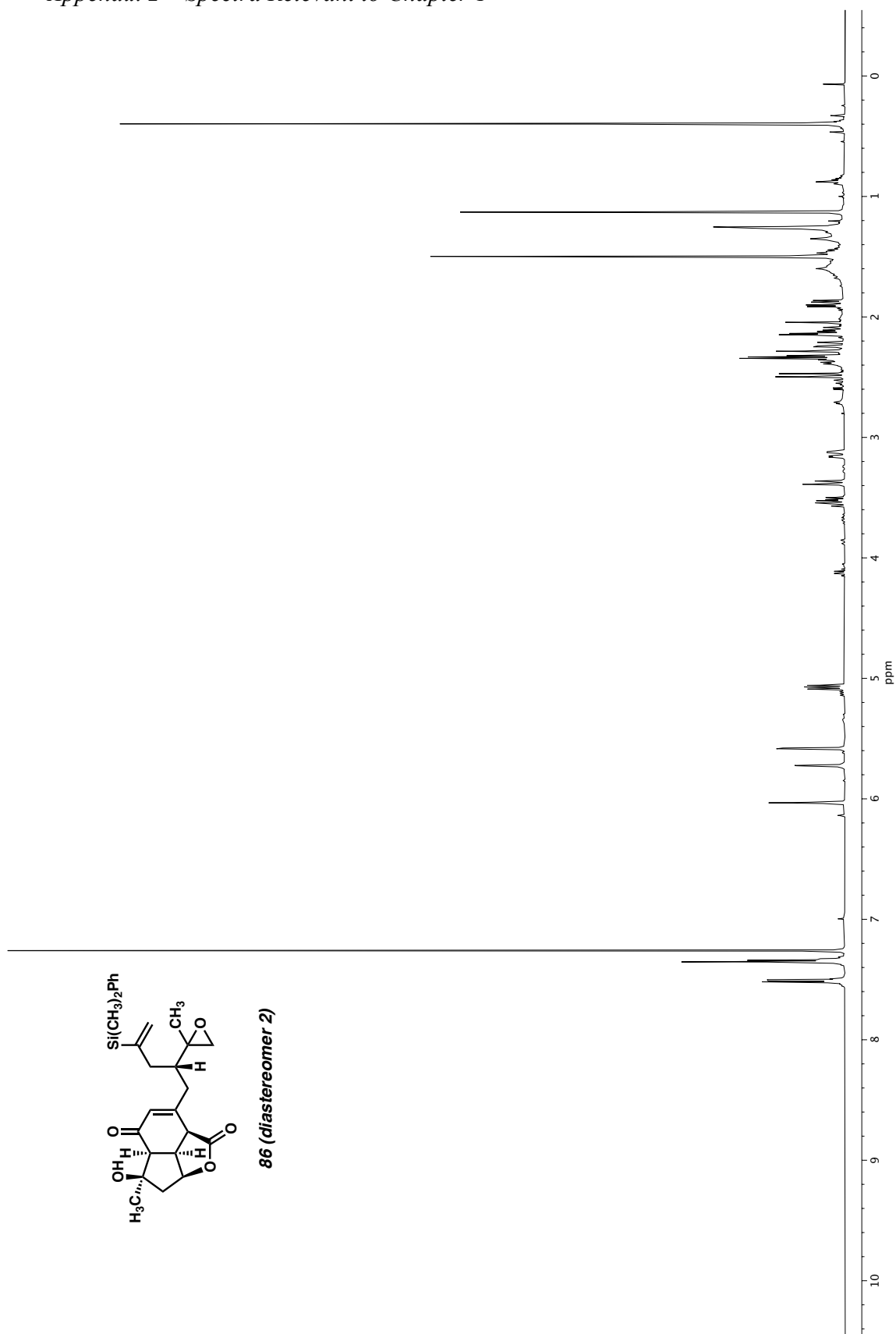
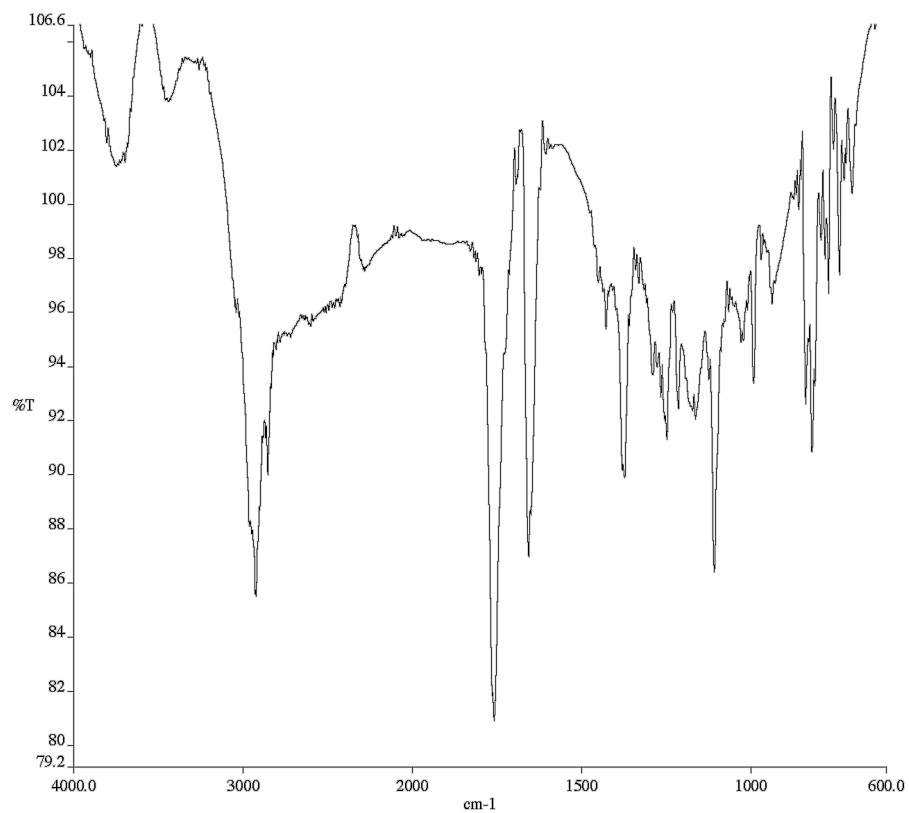
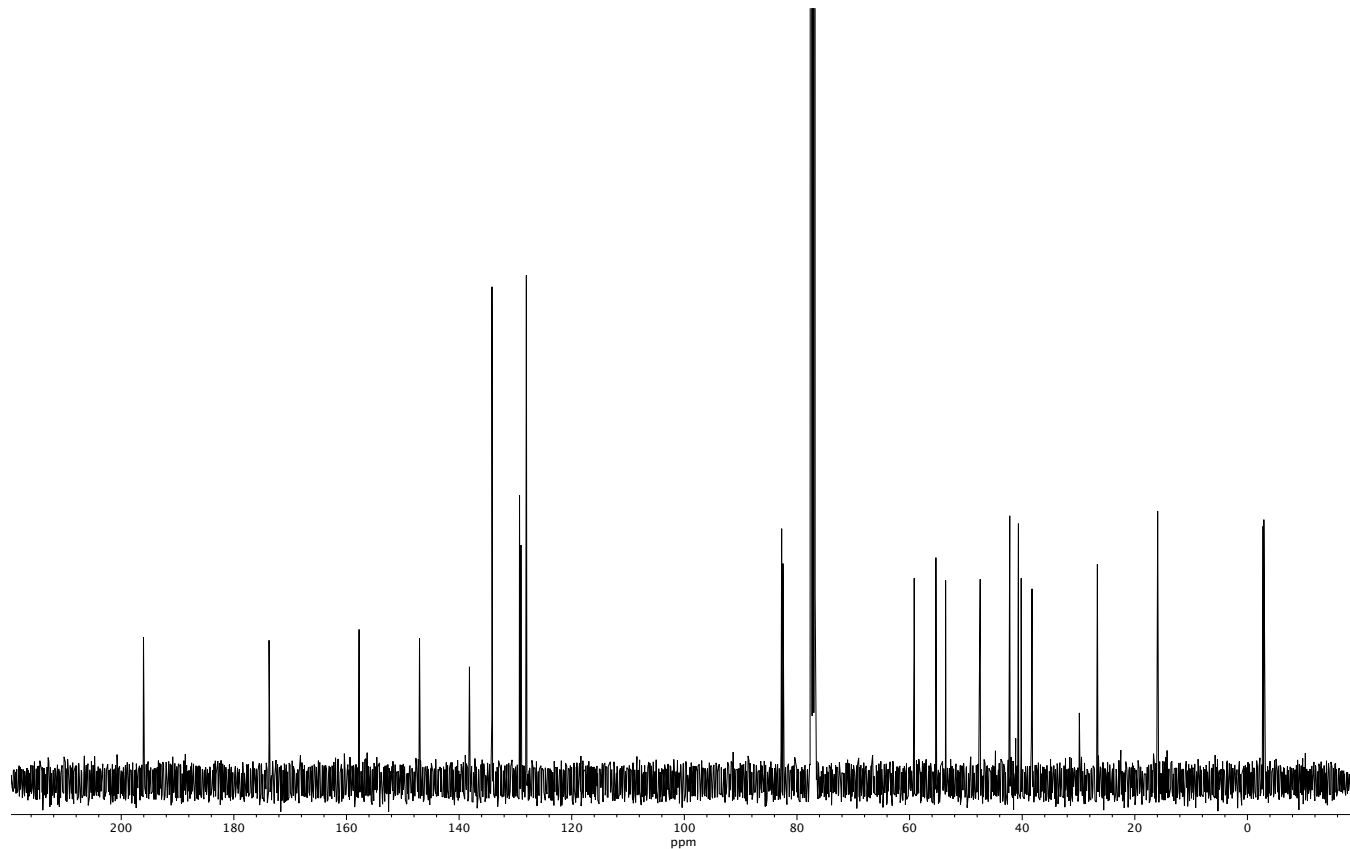


Figure A2.133  $^1\text{H}$  NMR (400 MHz,  $\text{CDCl}_3$ ) of compound **86** (diastereomer 2).





**Figure A2.134** Infrared spectrum (Thin Film, NaCl) of compound **86** (diastereomer 2).



**Figure A2.135** <sup>13</sup>C NMR (100 MHz, CDCl<sub>3</sub>) of compound **86** (diastereomer 2).

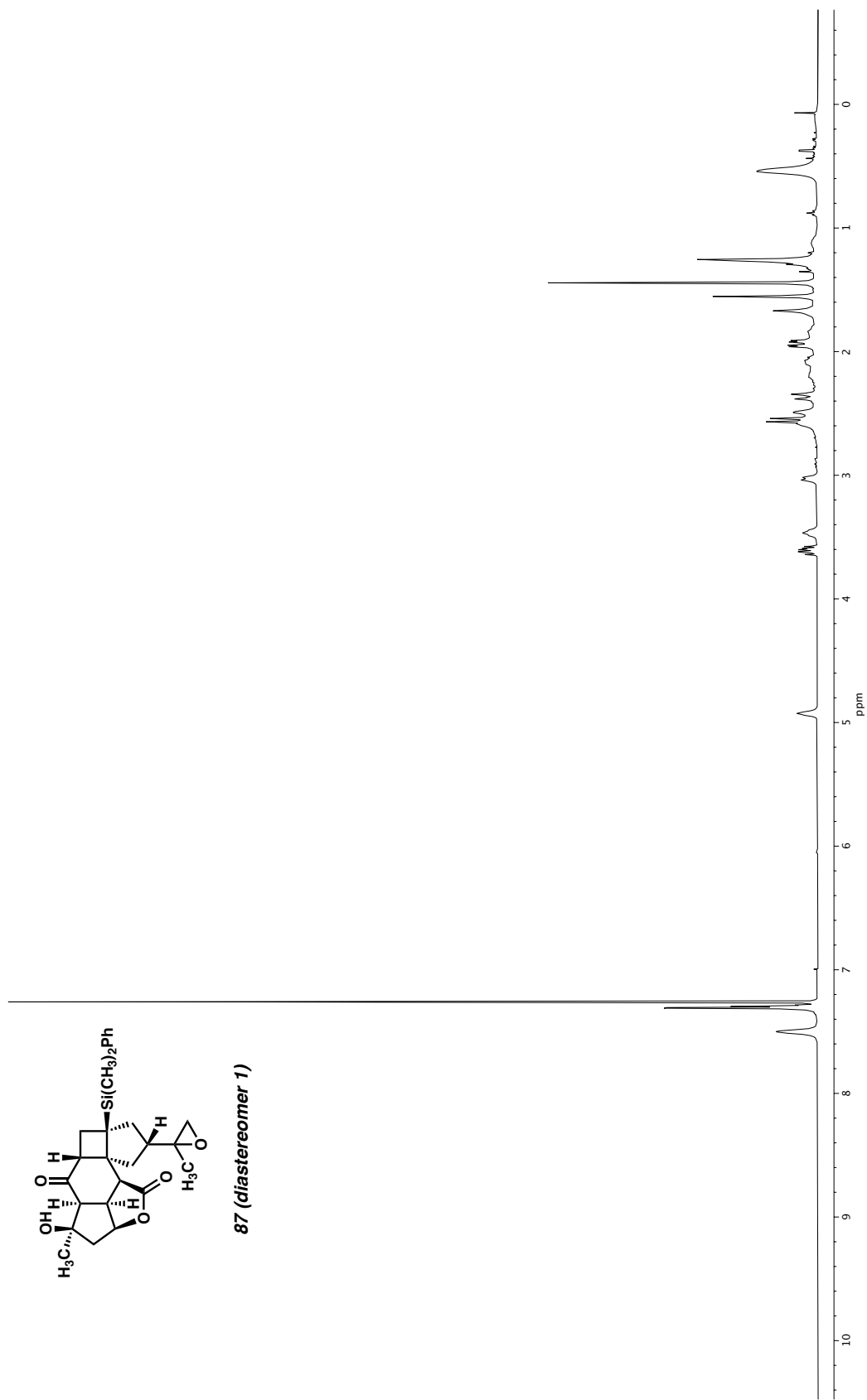
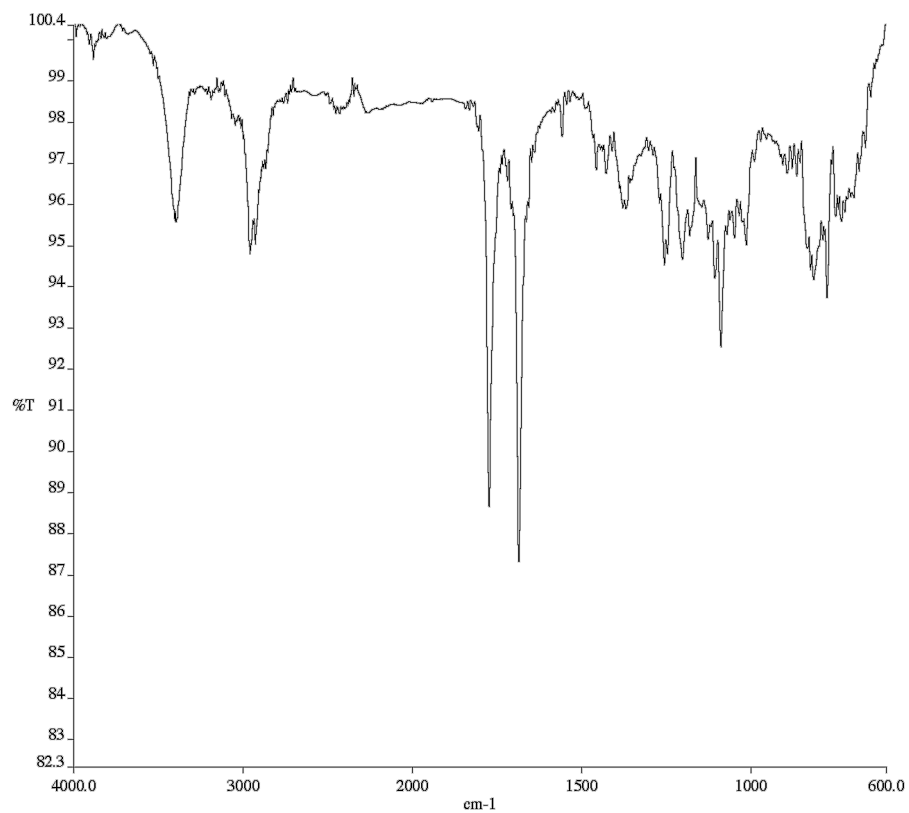
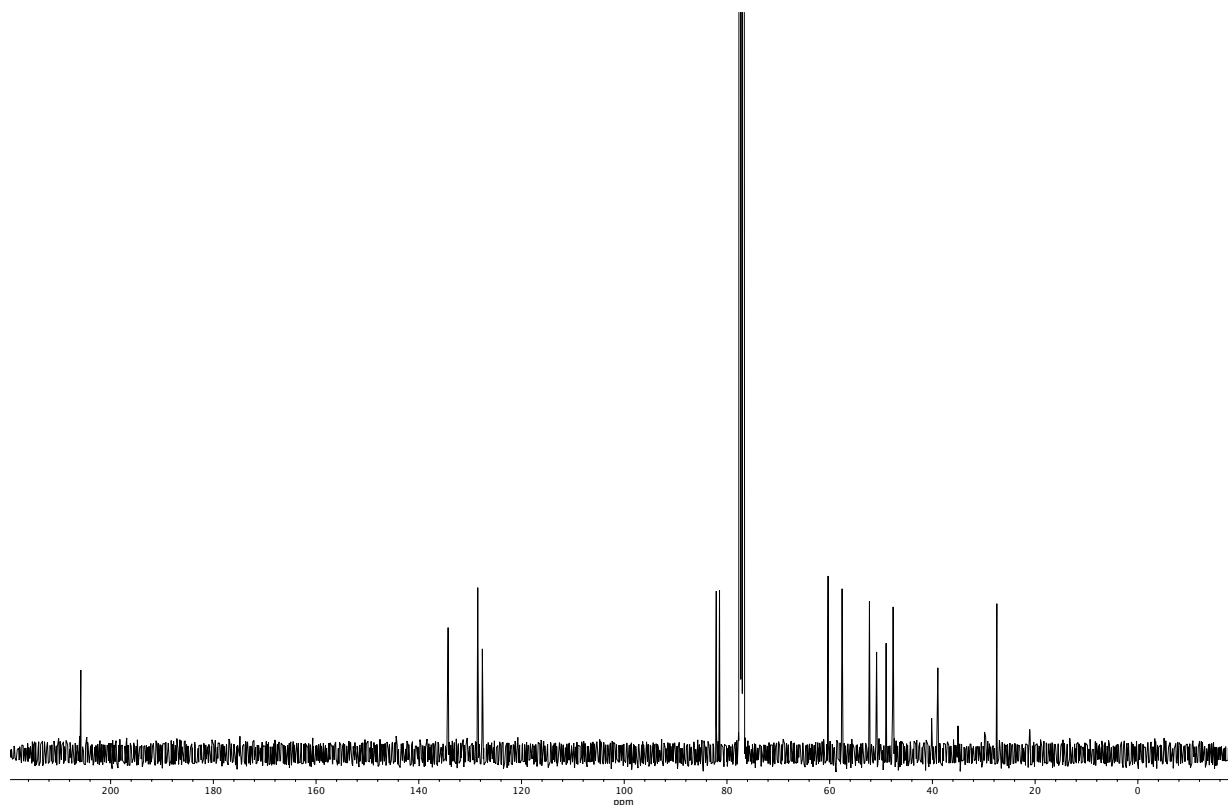


Figure A2.136  $^1\text{H}$  NMR (400 MHz,  $\text{CDCl}_3$ ) of compound **87** (diastereomer 1).



**Figure A2.137** Infrared spectrum (Thin Film, NaCl) of compound **87** (diastereomer 1).



**Figure A2.138** <sup>13</sup>C NMR (100 MHz, CDCl<sub>3</sub>) of compound **87** (diastereomer 1).

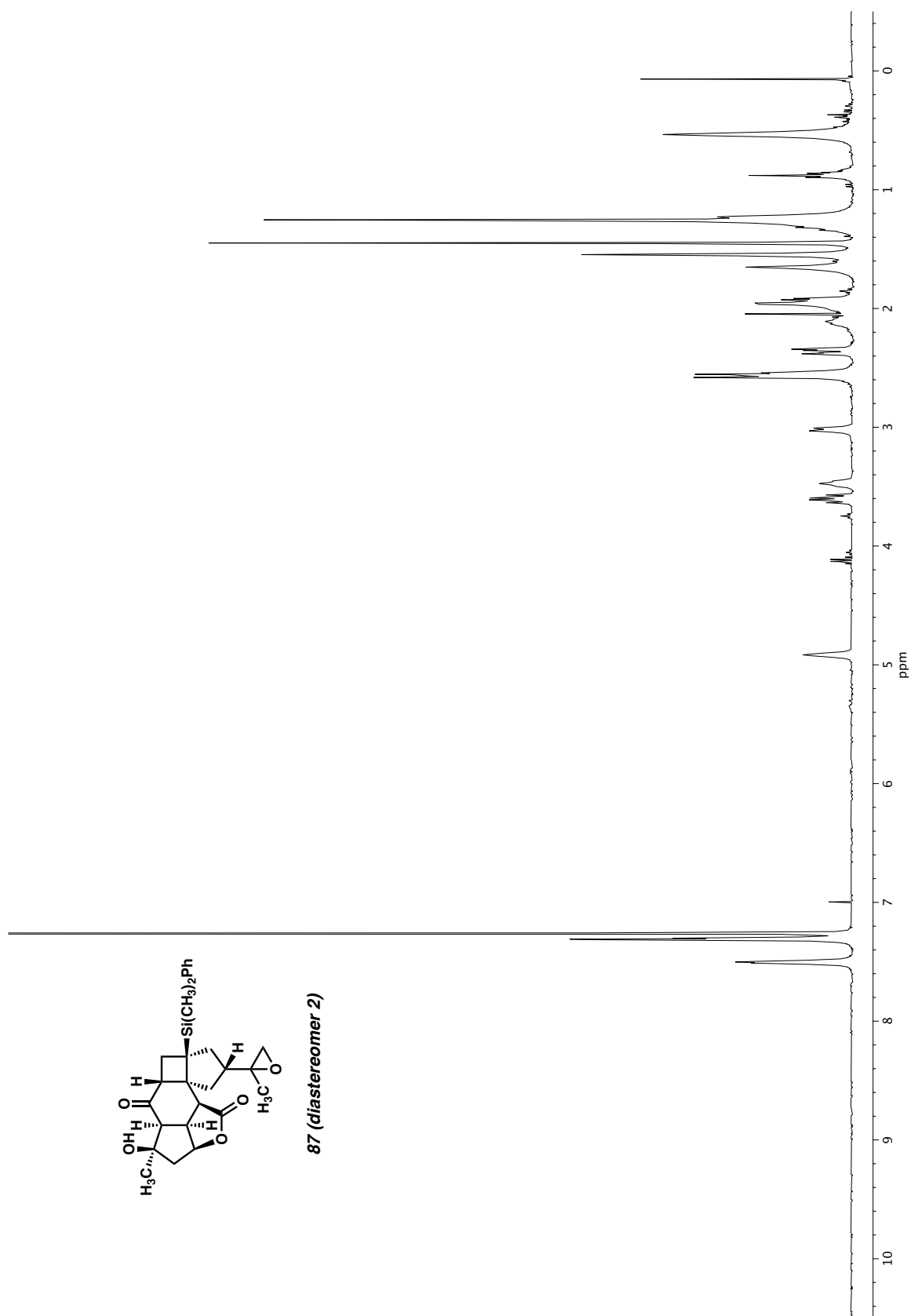
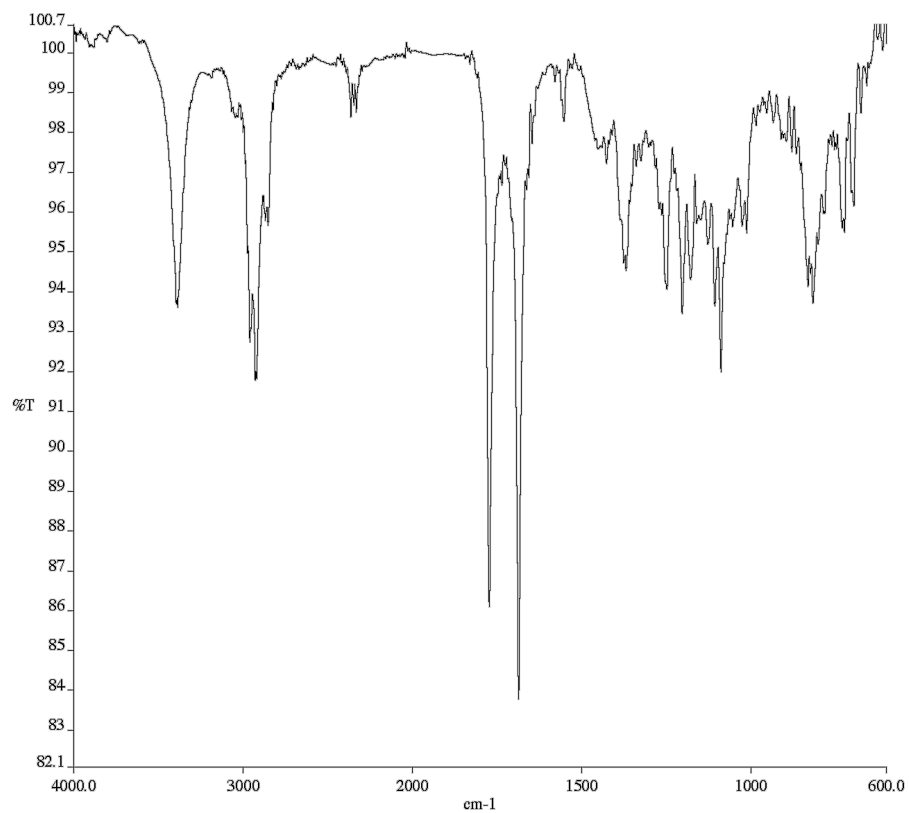
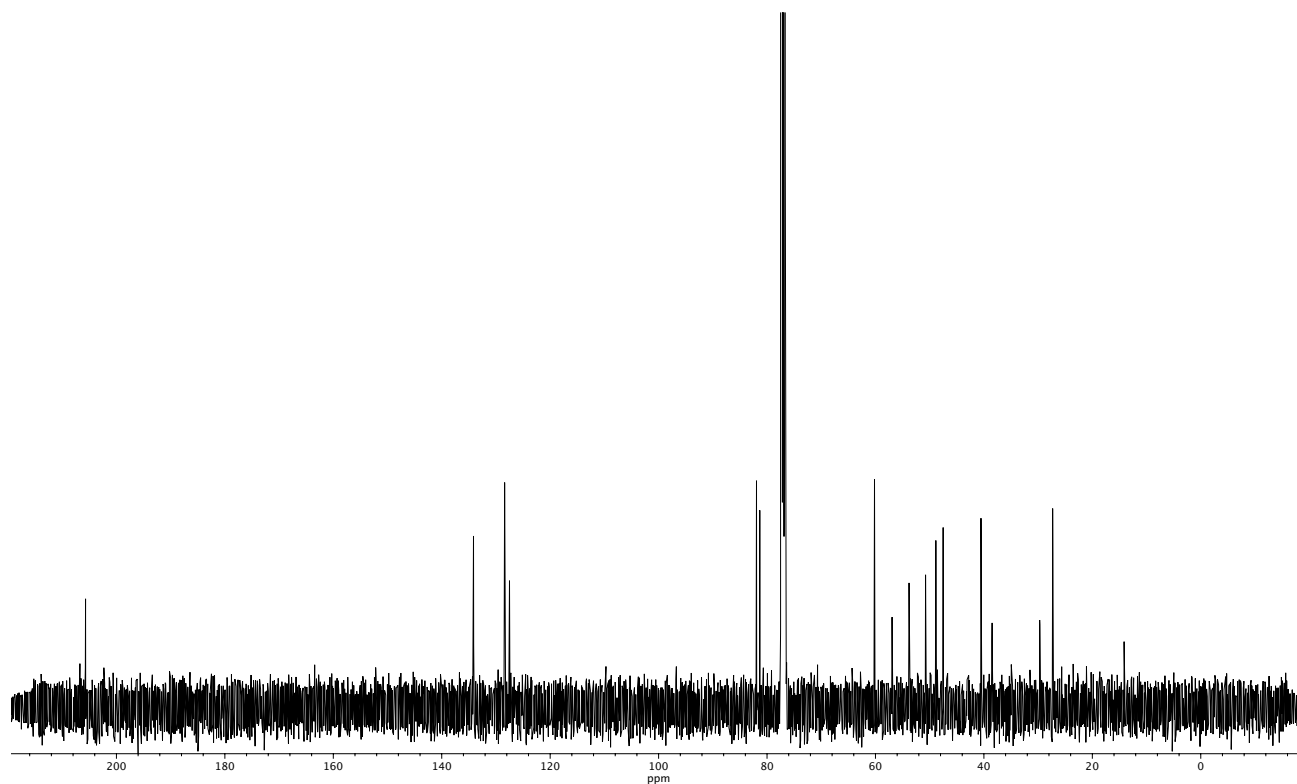


Figure A2.139  $^1\text{H}$  NMR (400 MHz,  $\text{CDCl}_3$ ) of compound **87** (diastereomer 2).



**Figure A2.140** Infrared spectrum (Thin Film, NaCl) of compound **87** (diastereomer 2).



**Figure A2.141** <sup>13</sup>C NMR (100 MHz, CDCl<sub>3</sub>) of compound **87** (diastereomer 2).

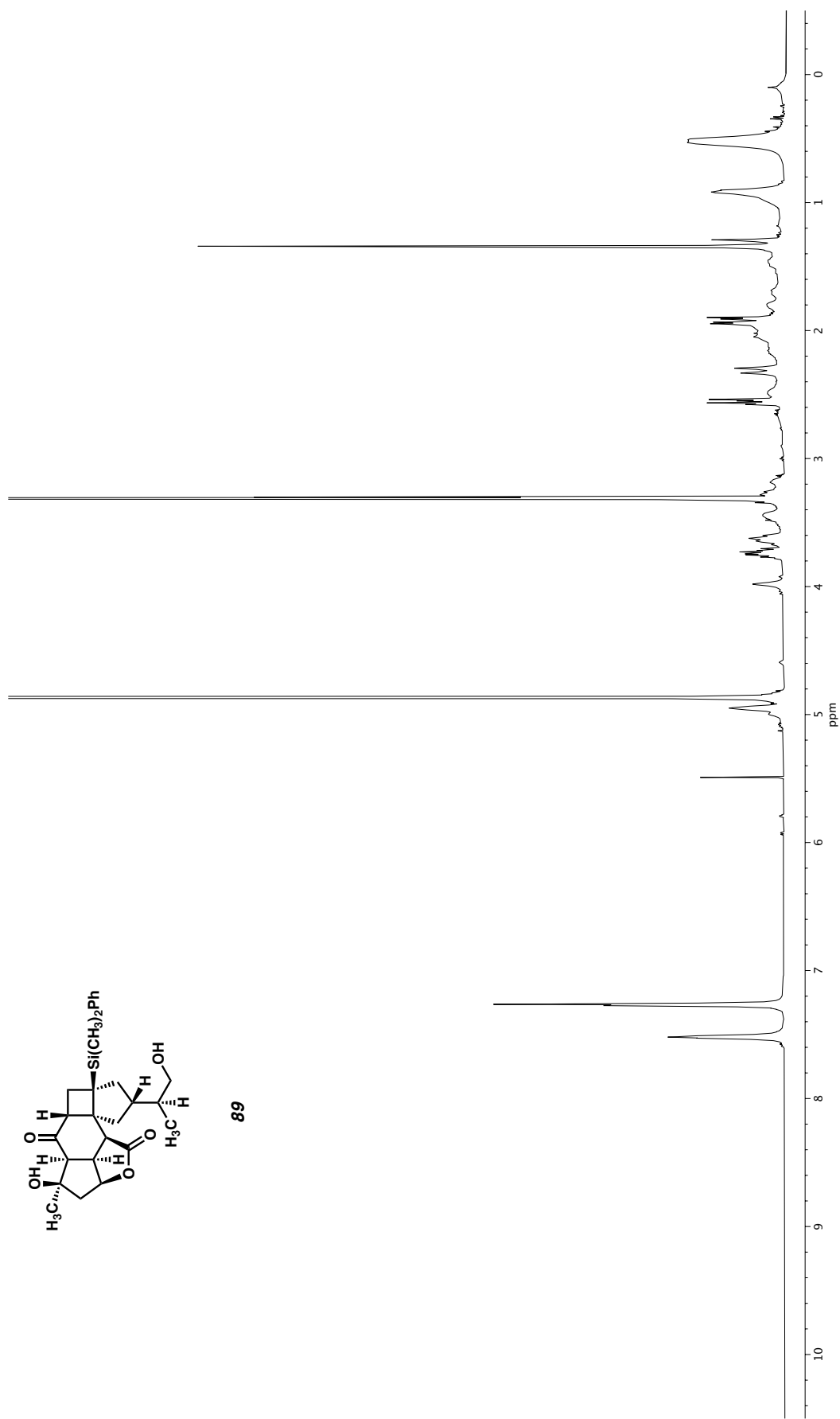
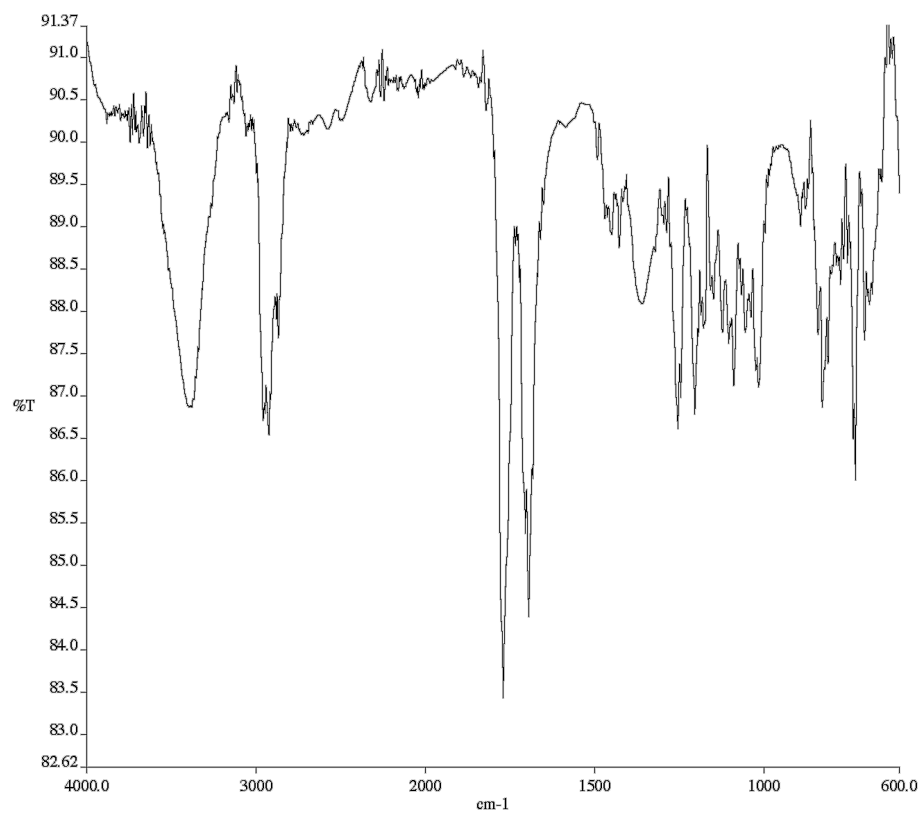
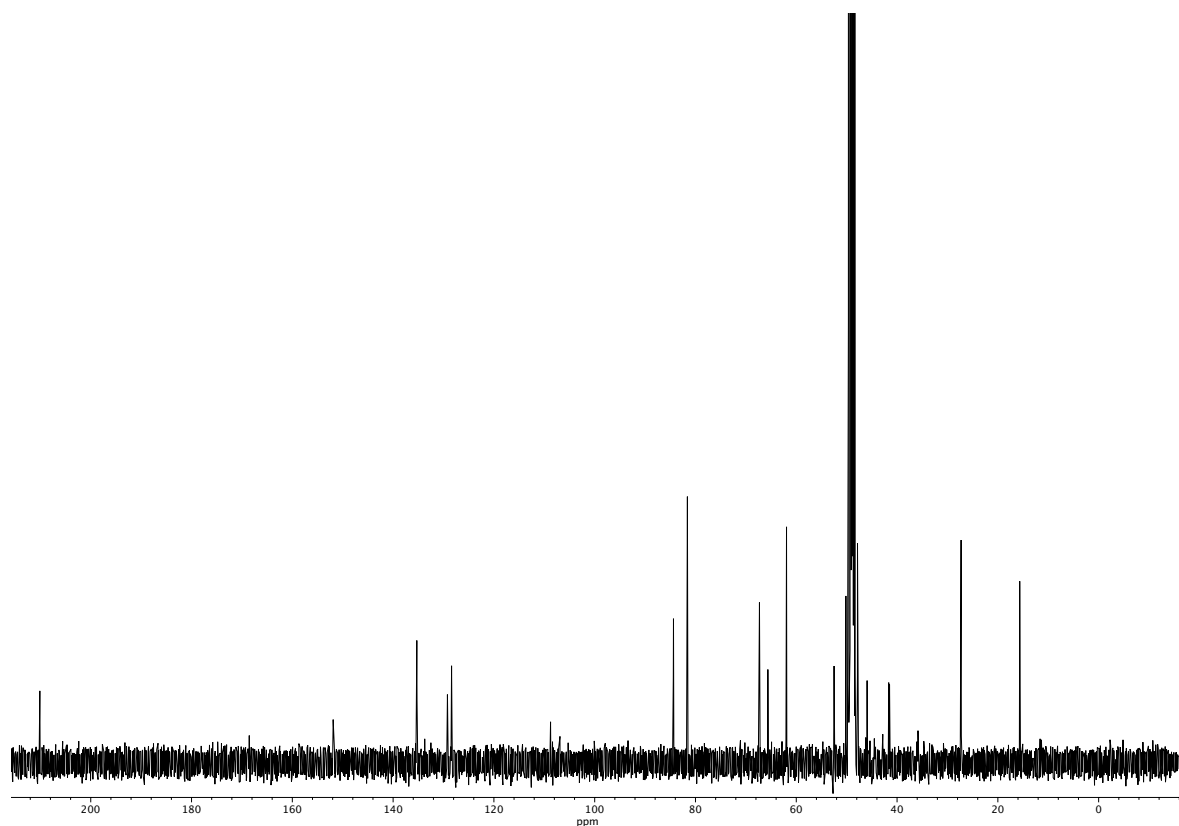


Figure A2.142  $^1\text{H}$  NMR (400 MHz,  $\text{CD}_3\text{OD}$ ) of compound **89**.



**Figure A2.143** Infrared spectrum (Thin Film, NaCl) of compound **89**.



**Figure A2.144**  $^{13}\text{C}$  NMR (100 MHz,  $\text{CD}_3\text{OD}$ ) of compound **89**.

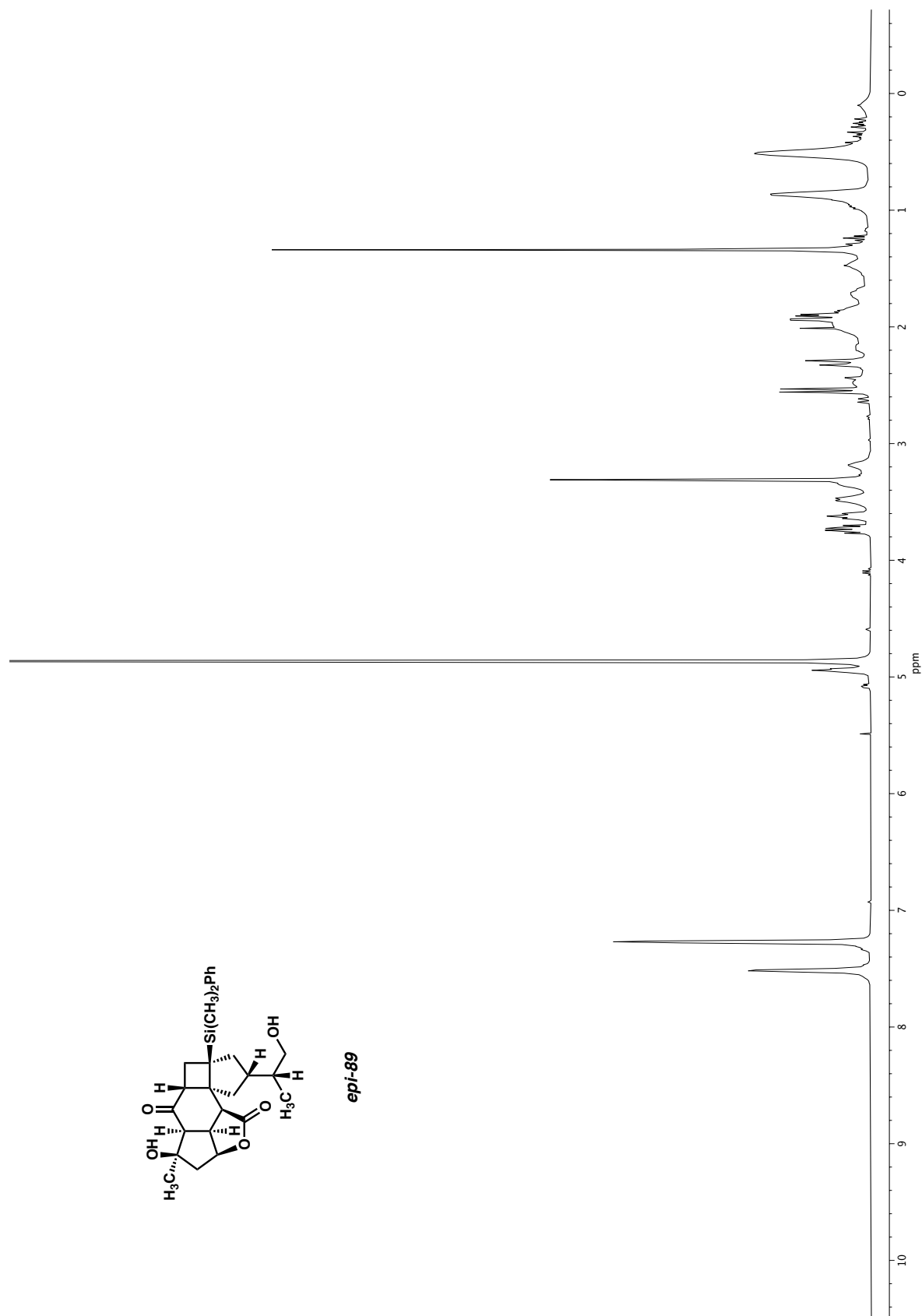
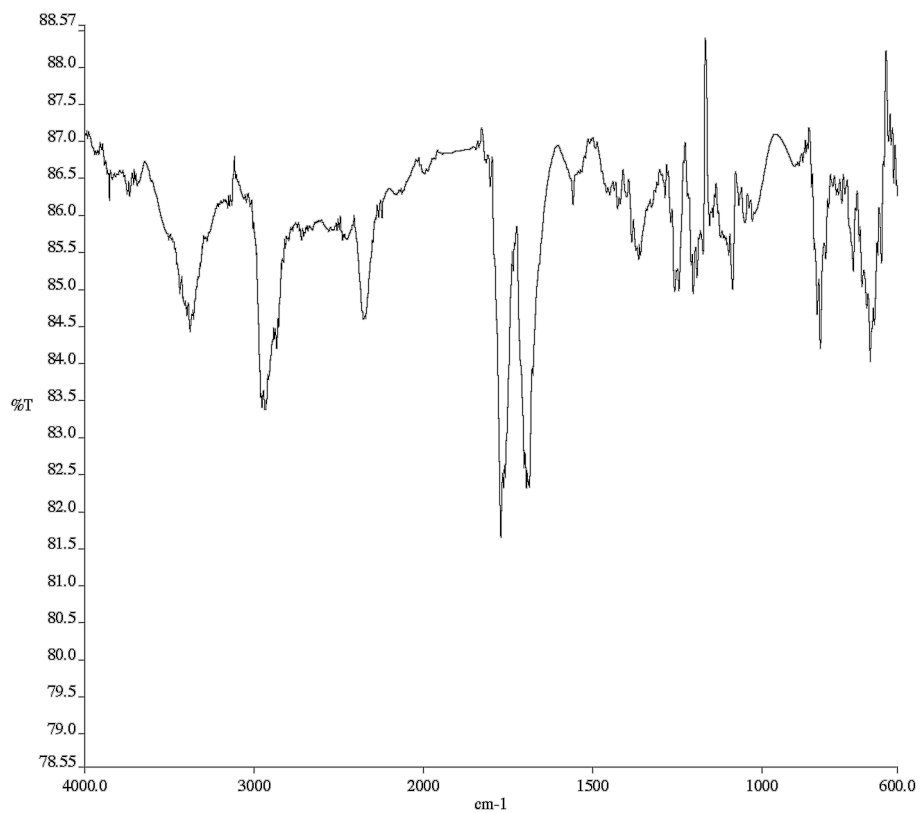
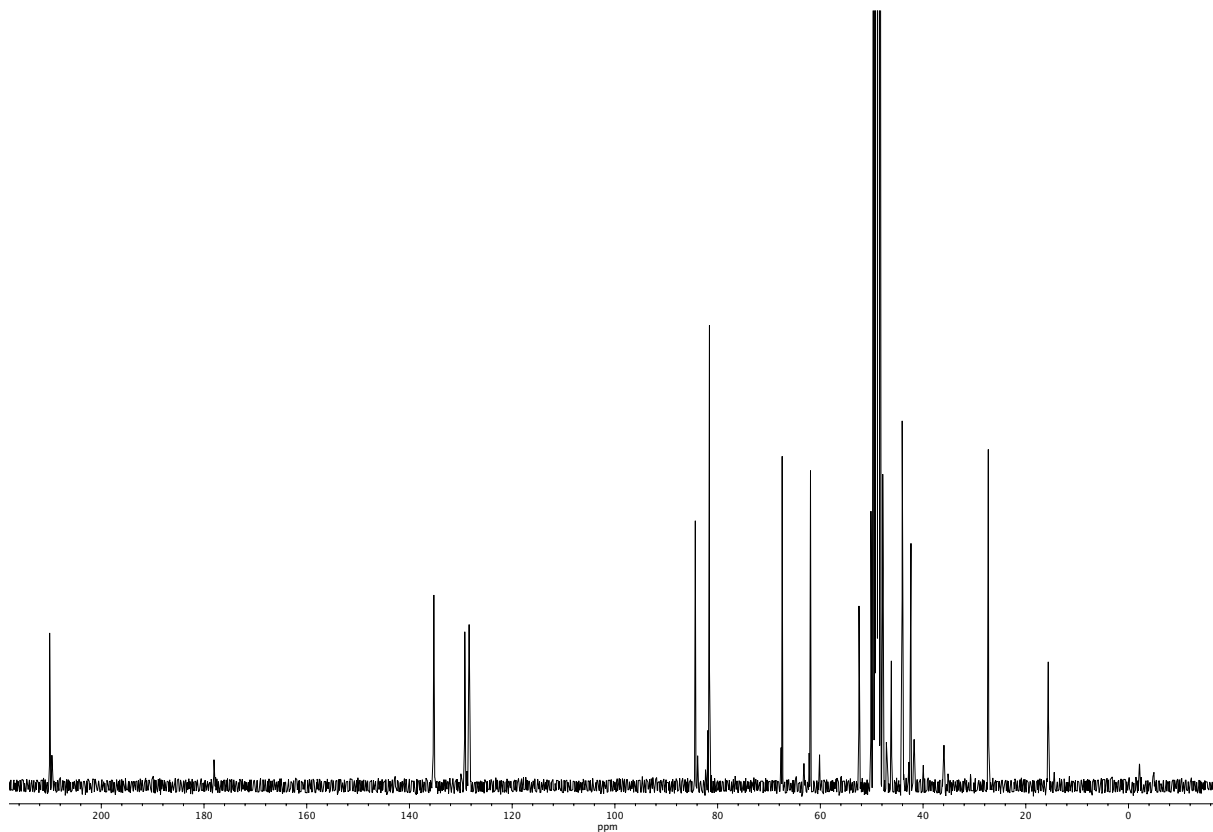


Figure A2.145 <sup>1</sup>H NMR (400 MHz, CD<sub>3</sub>OD) of compound *epi-89*.





**Figure A2.146** Infrared spectrum (Thin Film, NaCl) of compound epi-89.



**Figure A2.147** <sup>13</sup>C NMR (100 MHz, CD<sub>3</sub>OD) of compound epi-89.

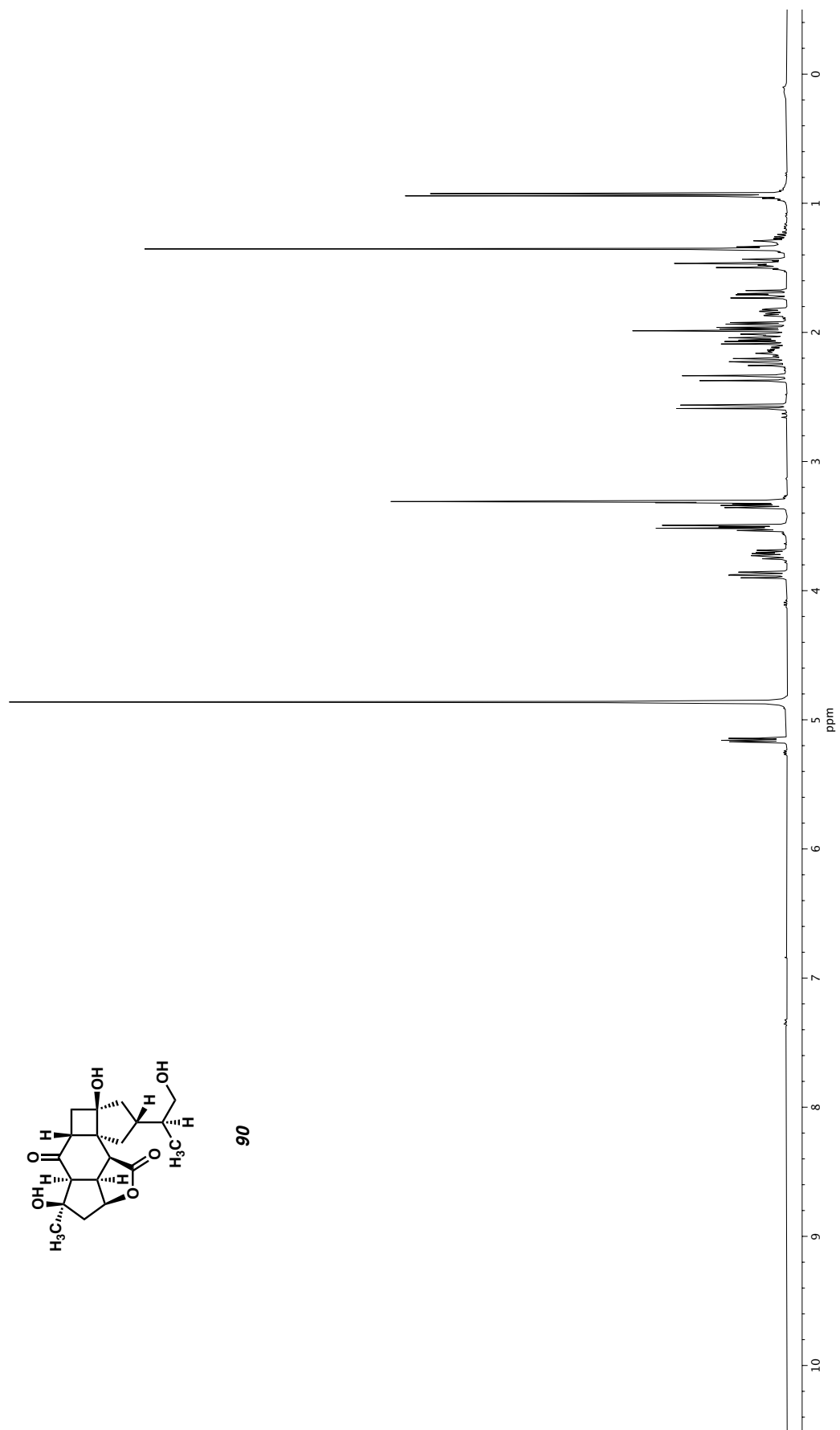
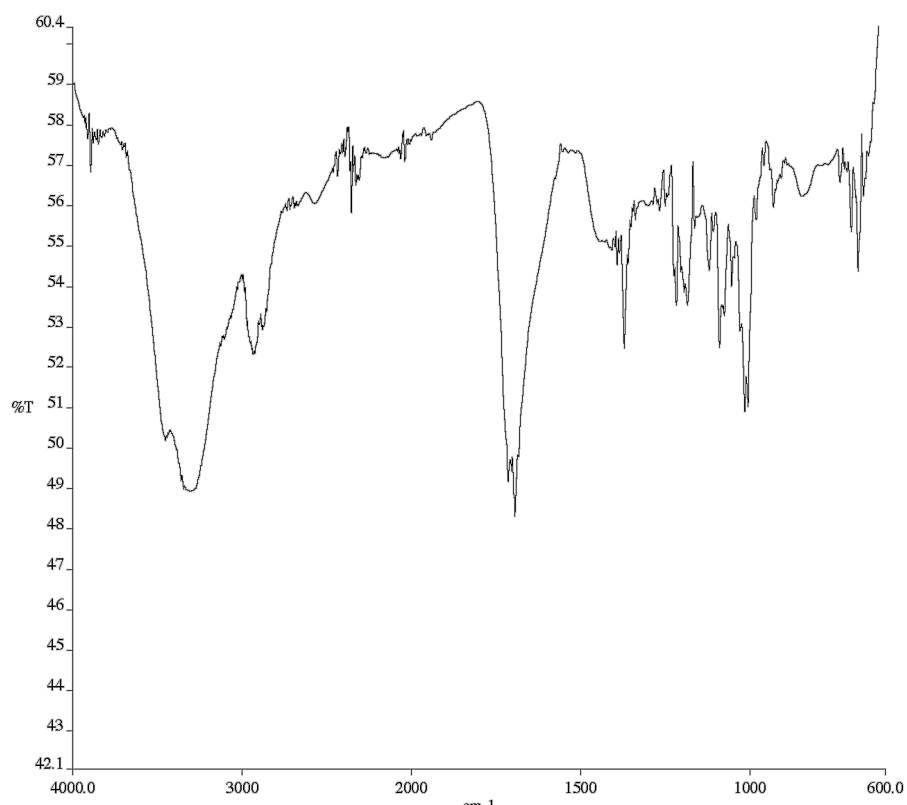
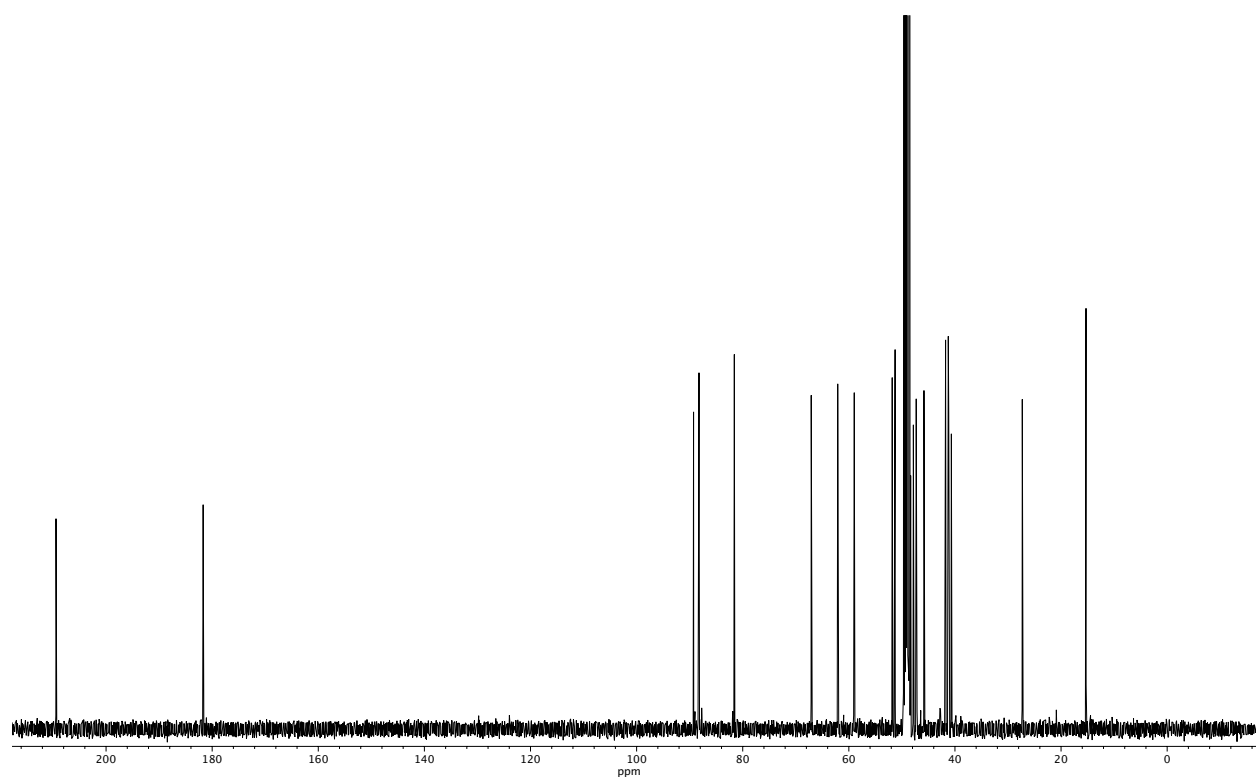


Figure A2.148  $^1\text{H}$  NMR (400 MHz,  $\text{CD}_3\text{OD}$ ) of compound **90**.



**Figure A2.149** Infrared spectrum (Thin Film, NaCl) of compound **90**.



**Figure A2.150** <sup>13</sup>C NMR (100 MHz, CD<sub>3</sub>OD) of compound **90**.

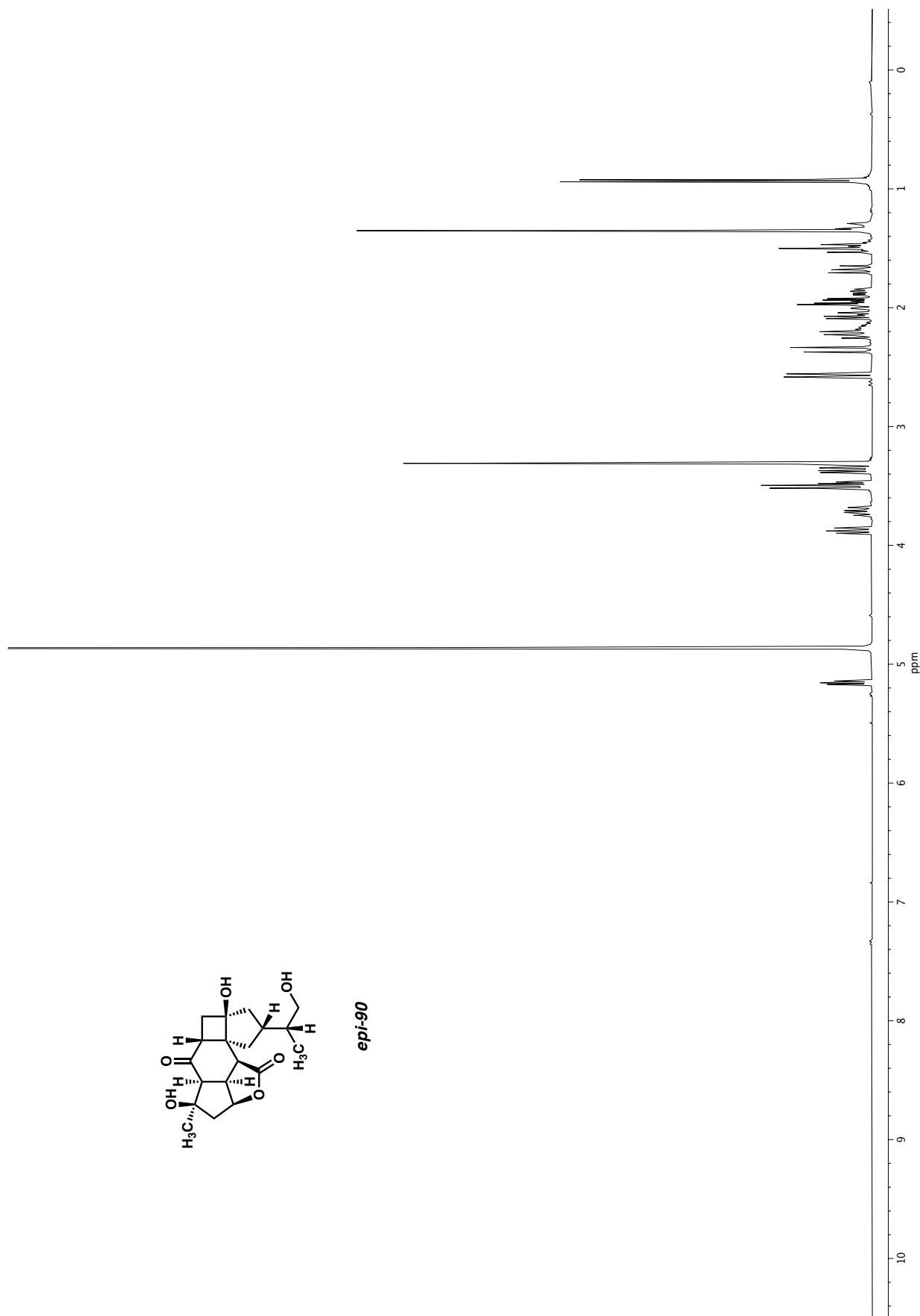
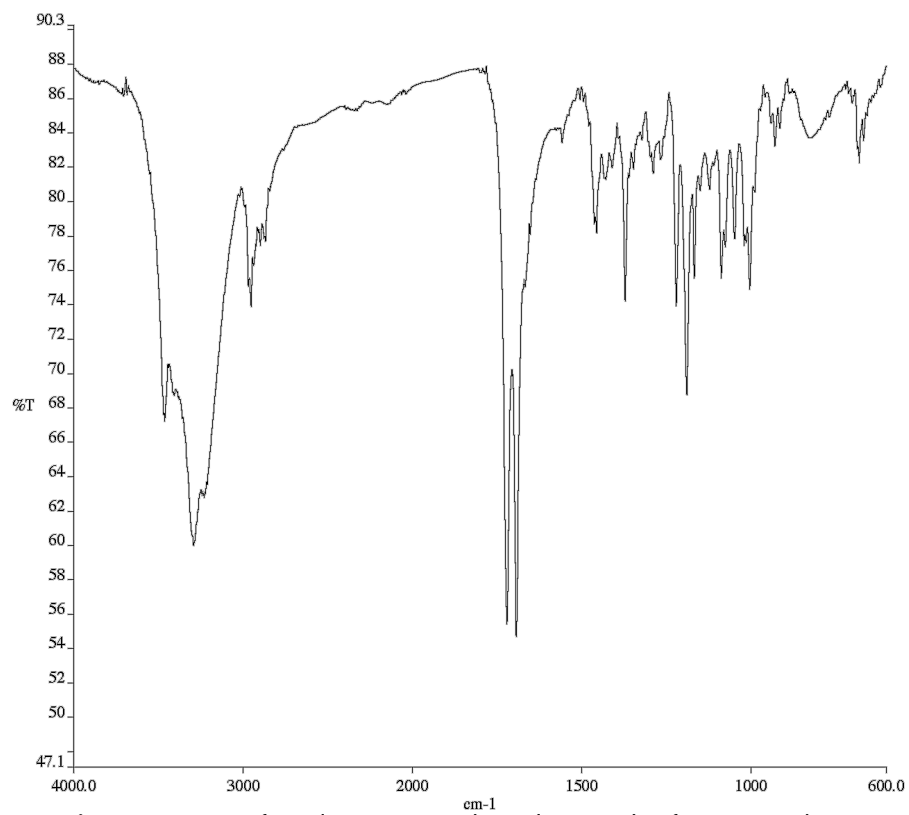
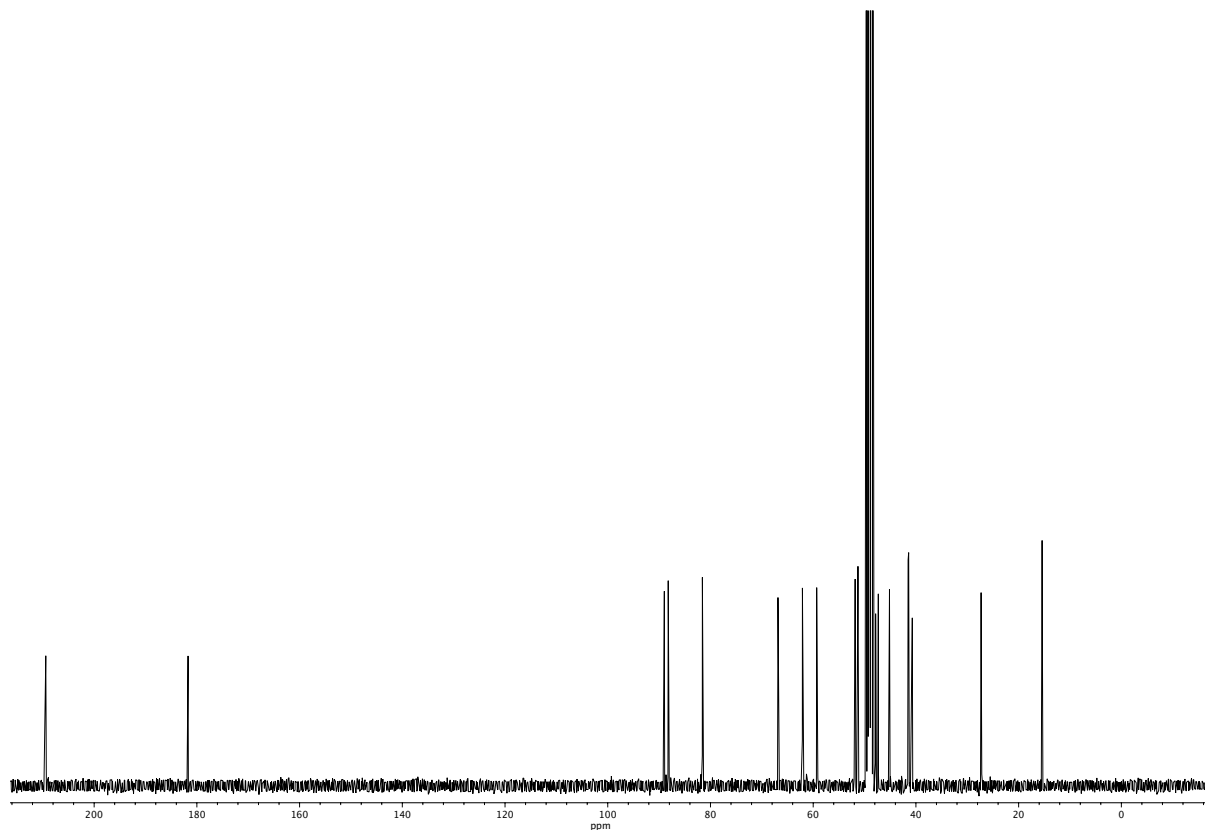


Figure A2.151 <sup>1</sup>H NMR (400 MHz, CD<sub>3</sub>OD) of compound epi-90.



**Figure A2.152** Infrared spectrum (Thin Film, NaCl) of compound epi-90.



**Figure A2.153** <sup>13</sup>C NMR (100 MHz, CD<sub>3</sub>OD) of compound epi-90.

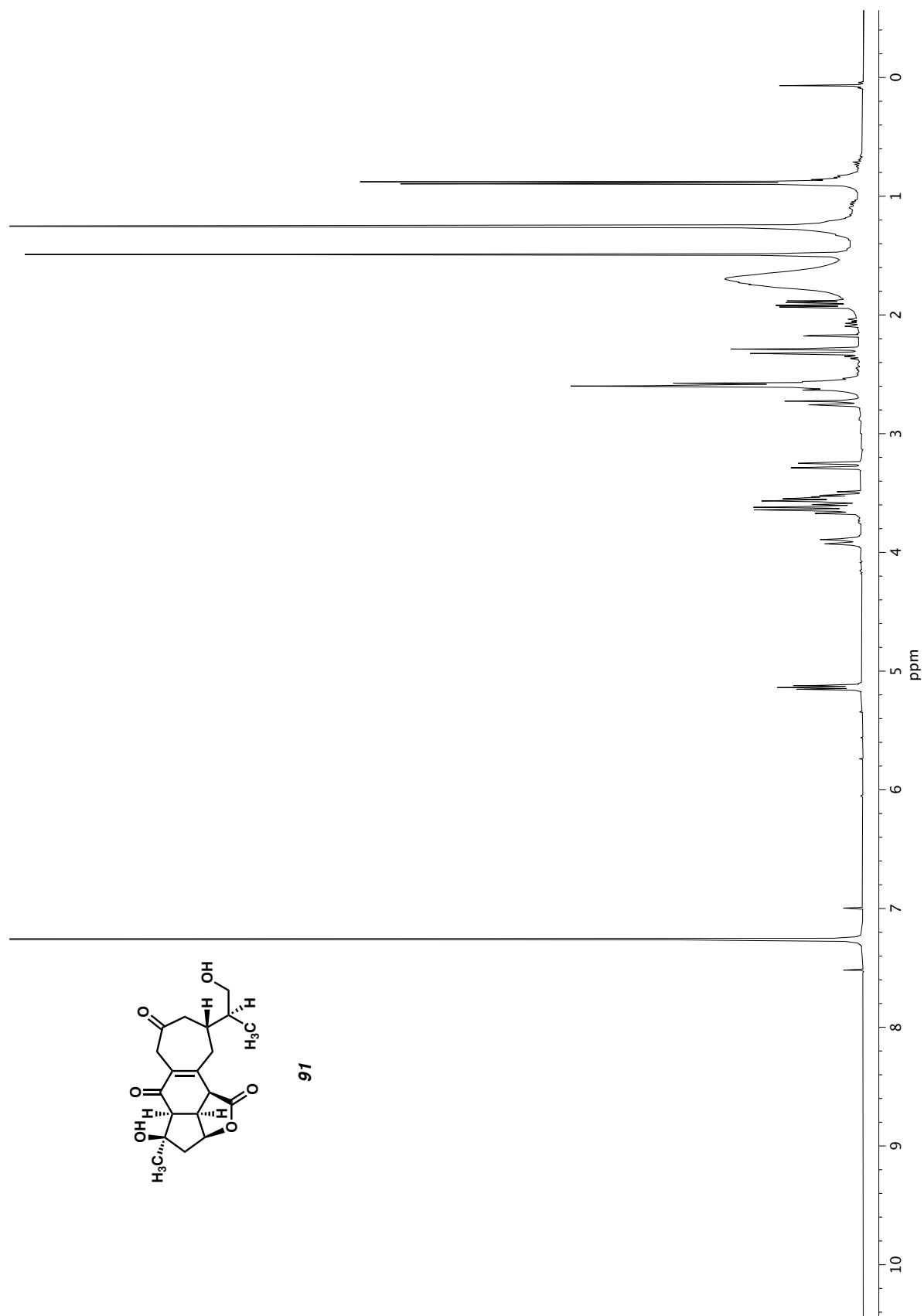
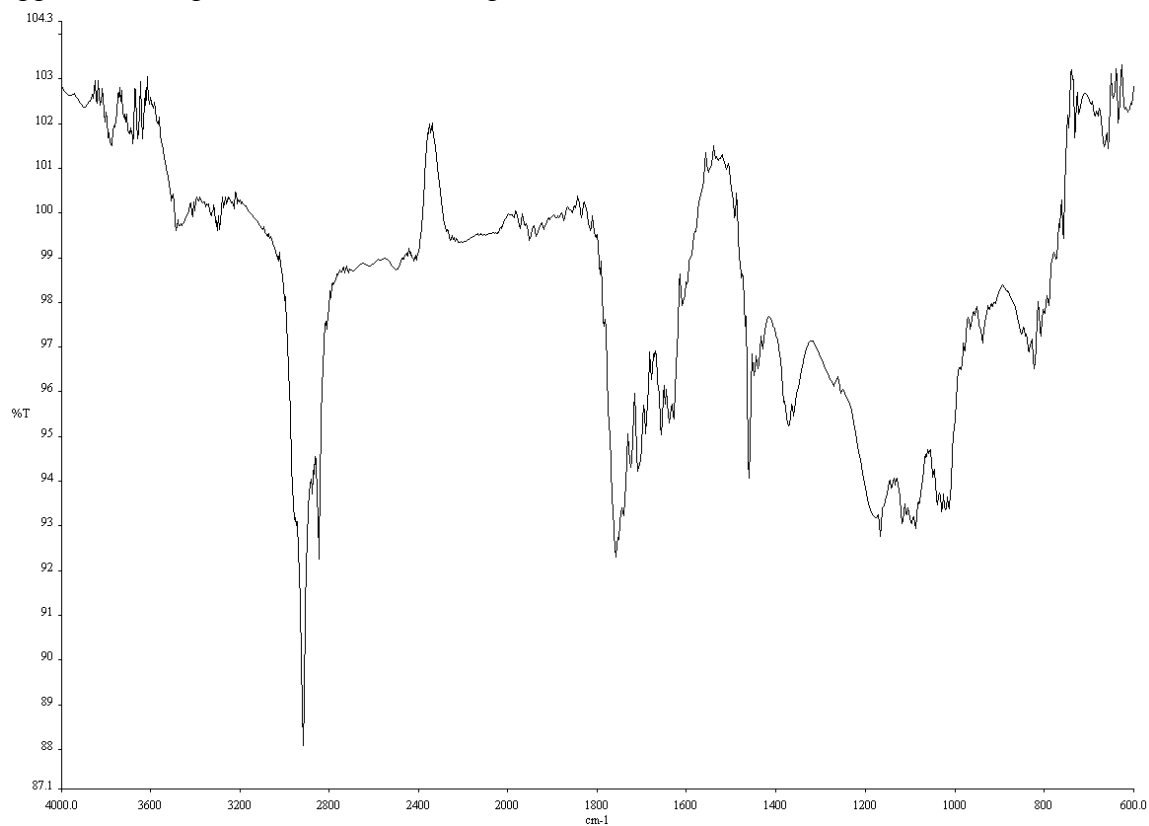
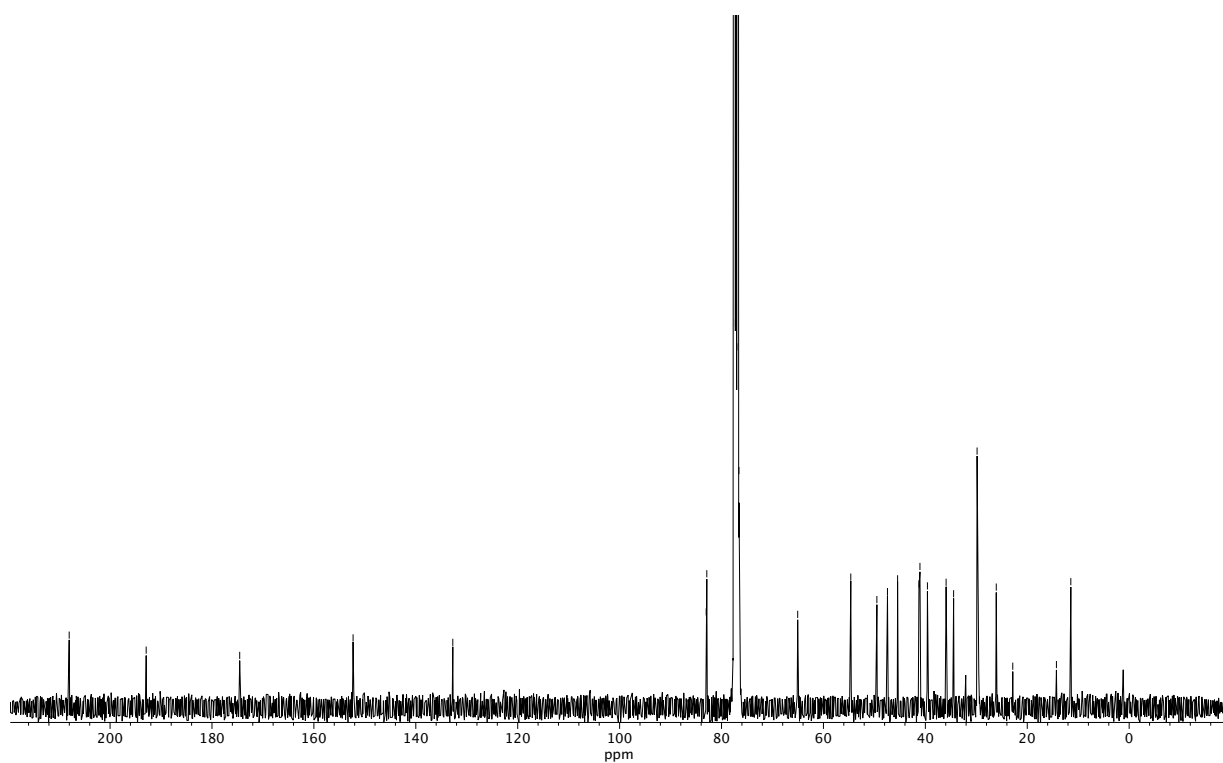


Figure A2.154  $^1\text{H}$  NMR (400 MHz,  $\text{CDCl}_3$ ) of compound **91**.



**Figure A2.155** Infrared spectrum (Thin Film, NaCl) of compound **91**.



**Figure A2.156** <sup>13</sup>C NMR (100 MHz, CDCl<sub>3</sub>) of compound **91**.

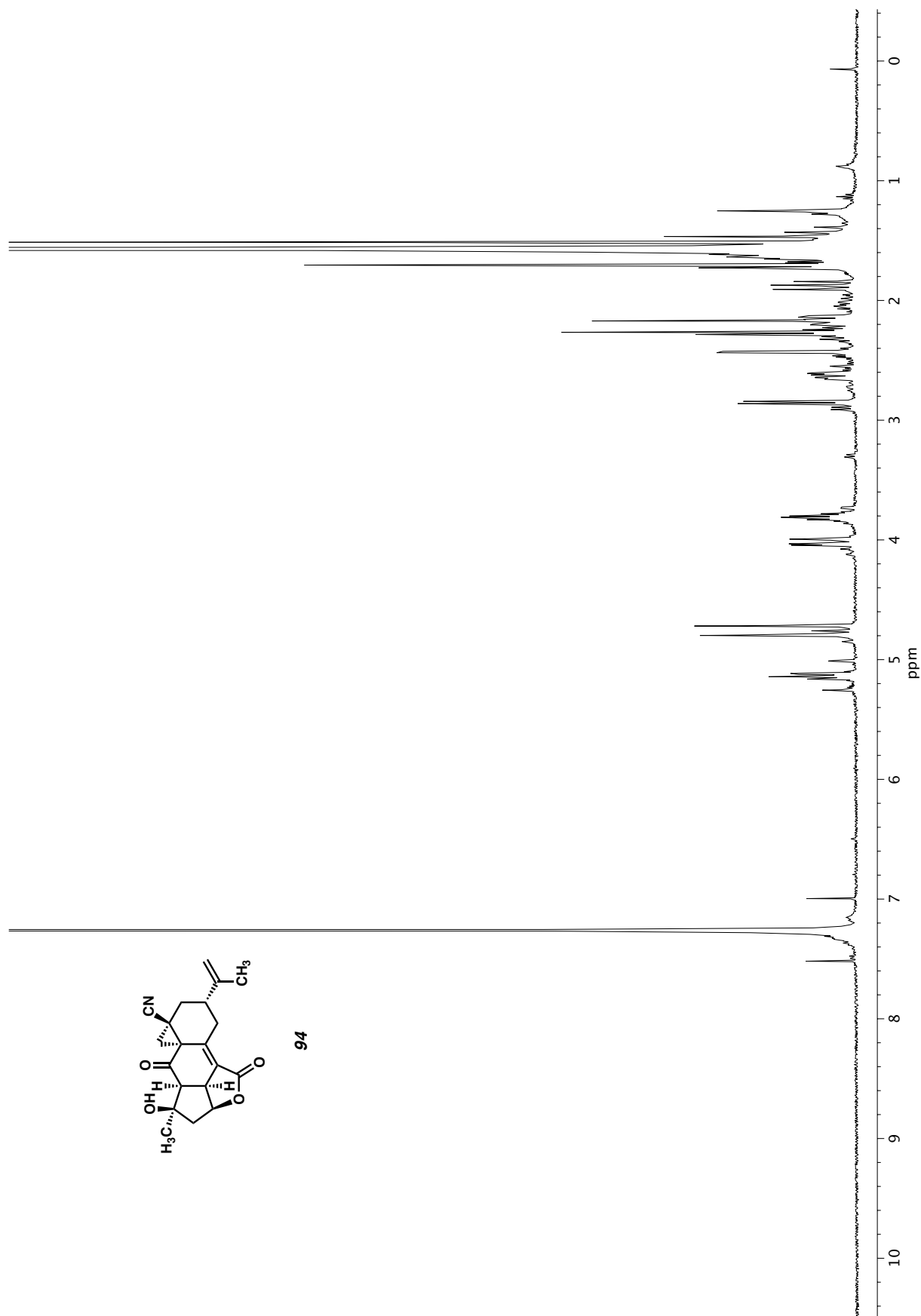
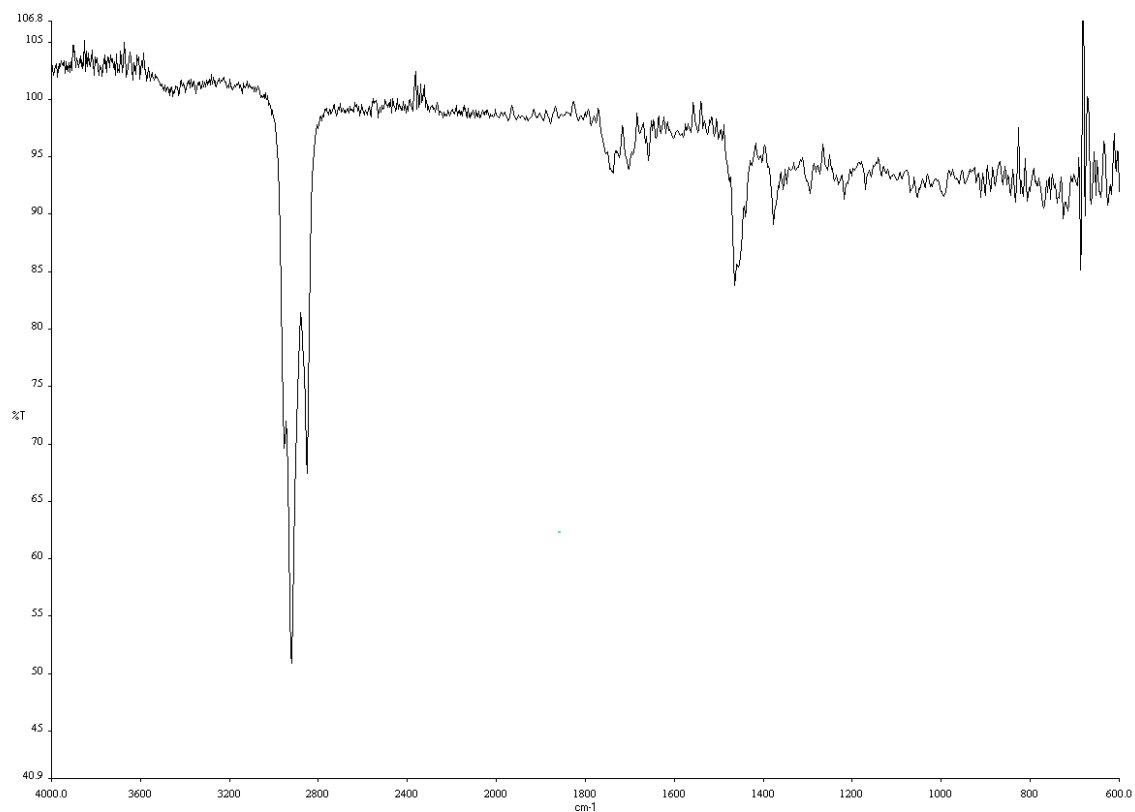
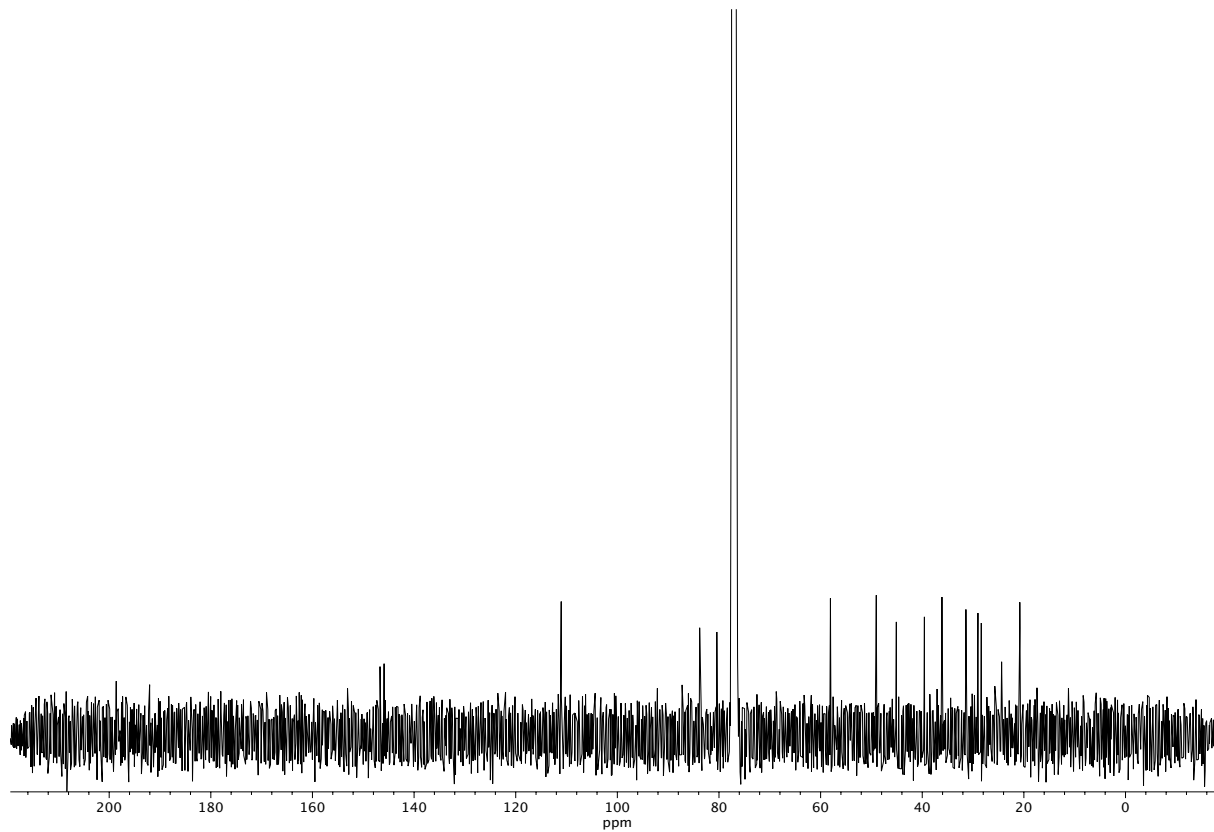


Figure A2.157  $^1\text{H}$  NMR (400 MHz,  $\text{CDCl}_3$ ) of compound **94**.





**Figure A2.158** Infrared spectrum (Thin Film, NaCl) of compound **94**.



**Figure A2.159** <sup>13</sup>C NMR (100 MHz, CDCl<sub>3</sub>) of compound **94**.

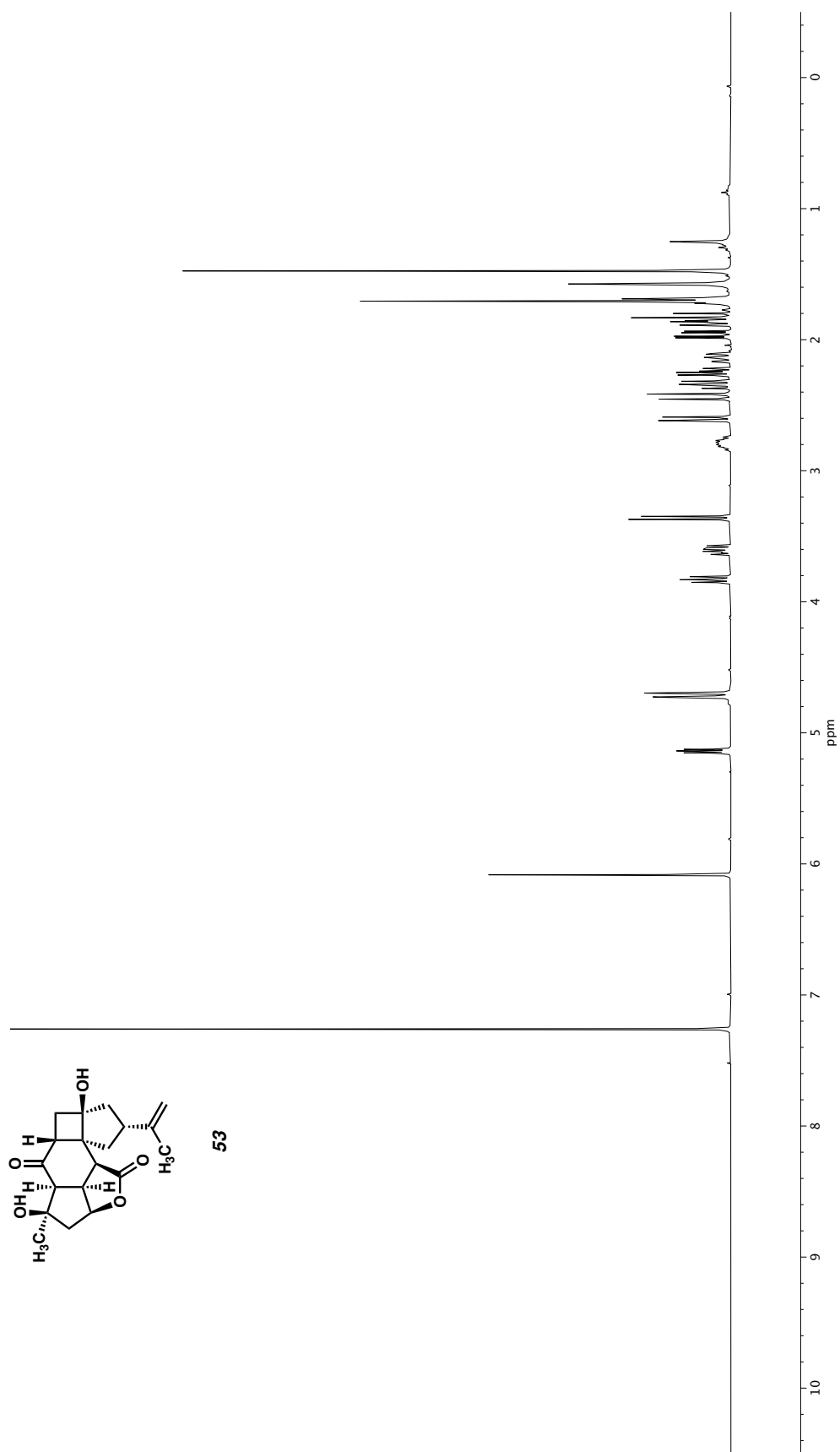
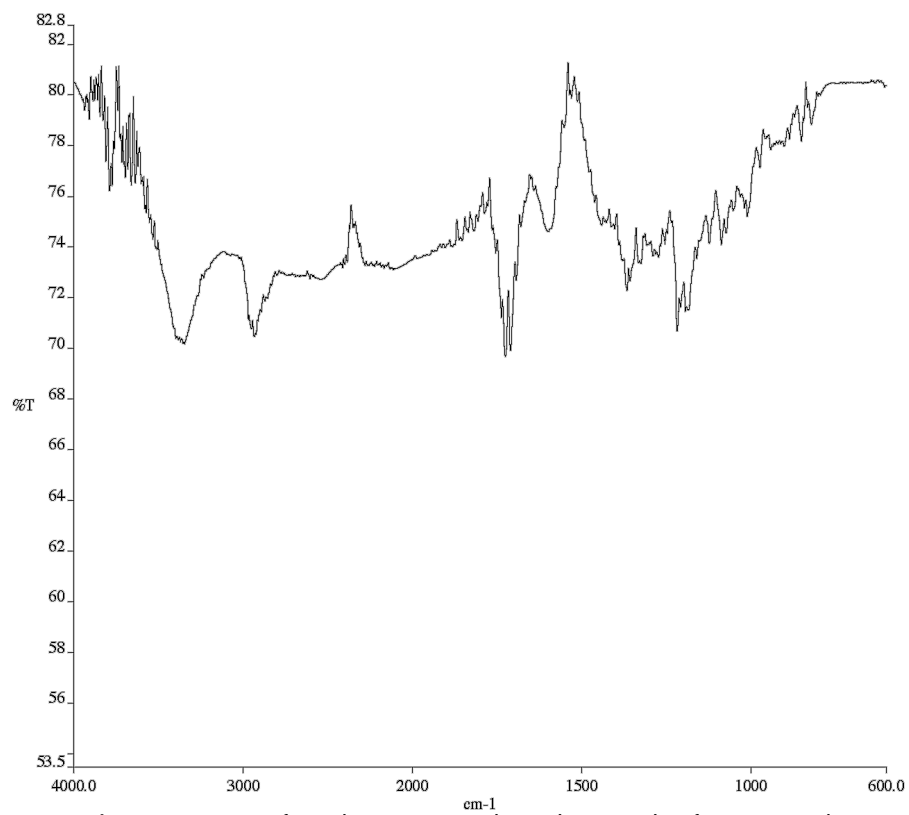
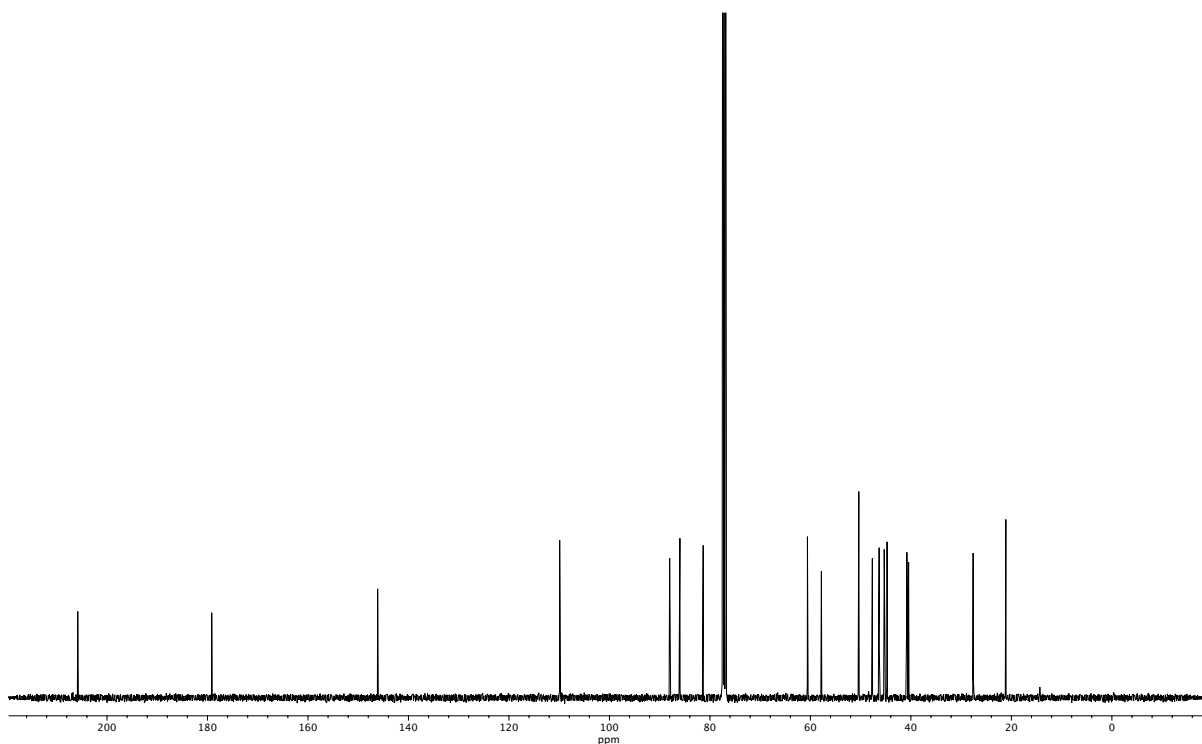


Figure A2.160  $^1\text{H}$  NMR (400 MHz,  $\text{CDCl}_3$ ) of compound 53.



**Figure A2.161** Infrared spectrum (Thin Film, NaCl) of compound 53.



**Figure A2.162** <sup>13</sup>C NMR (100 MHz, CDCl<sub>3</sub>) of compound 53.

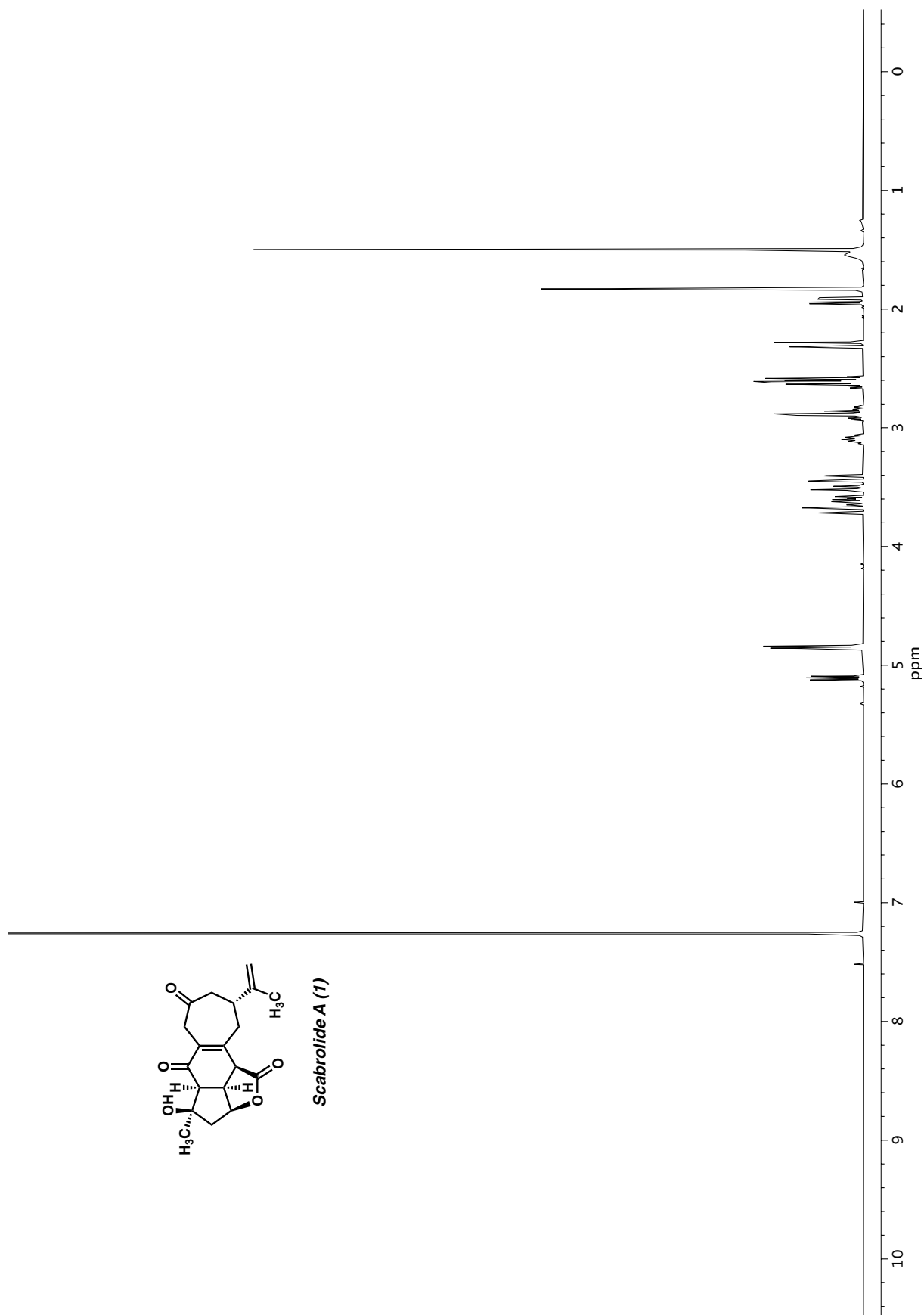
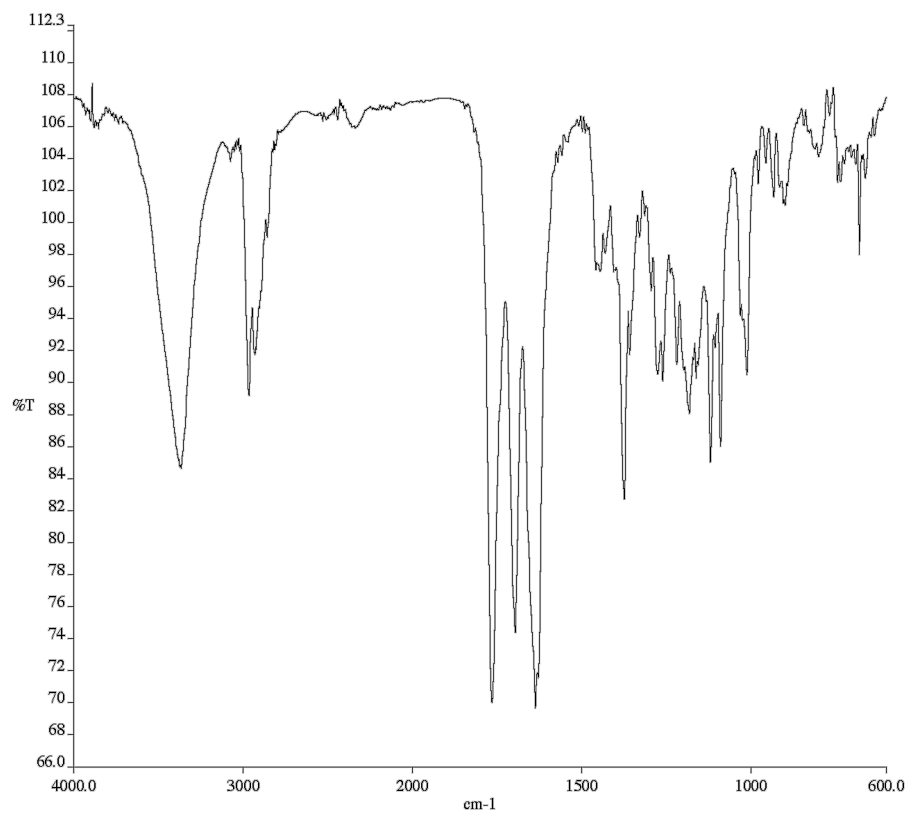
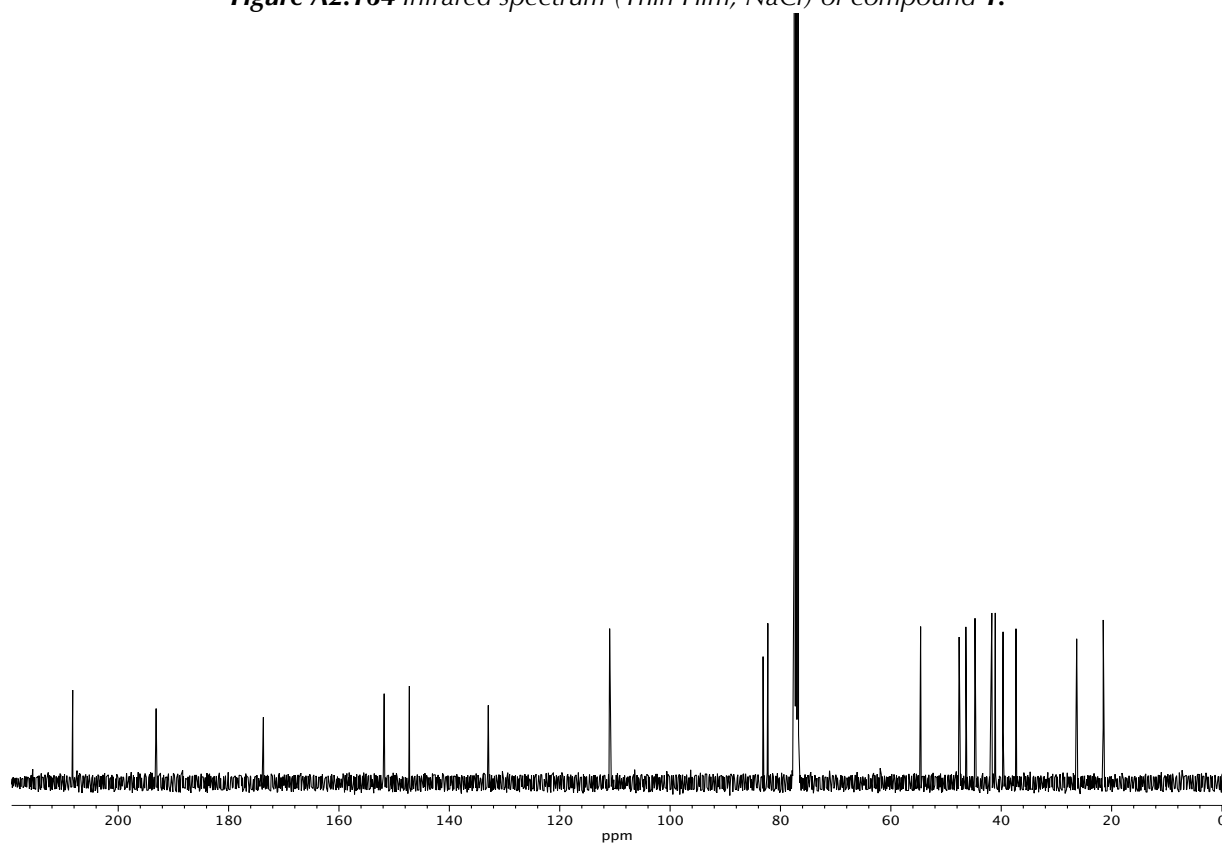


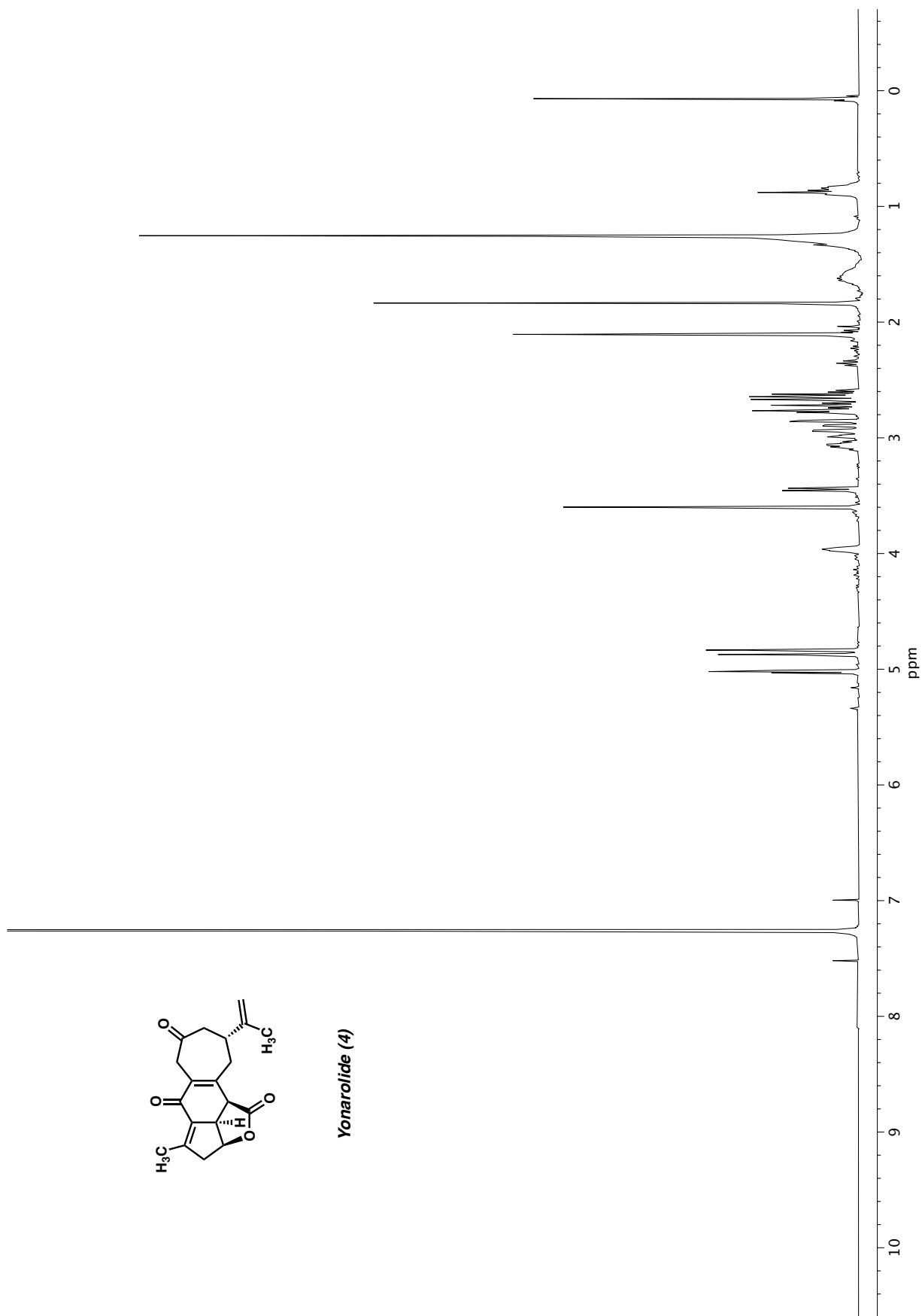
Figure A2.163  $^1\text{H}$  NMR (400 MHz,  $\text{CDCl}_3$ ) of compound **1**.



**Figure A2.164** Infrared spectrum (Thin Film, NaCl) of compound **1**.



**Figure A2.165** <sup>13</sup>C NMR (100 MHz, CDCl<sub>3</sub>) of compound **1**.



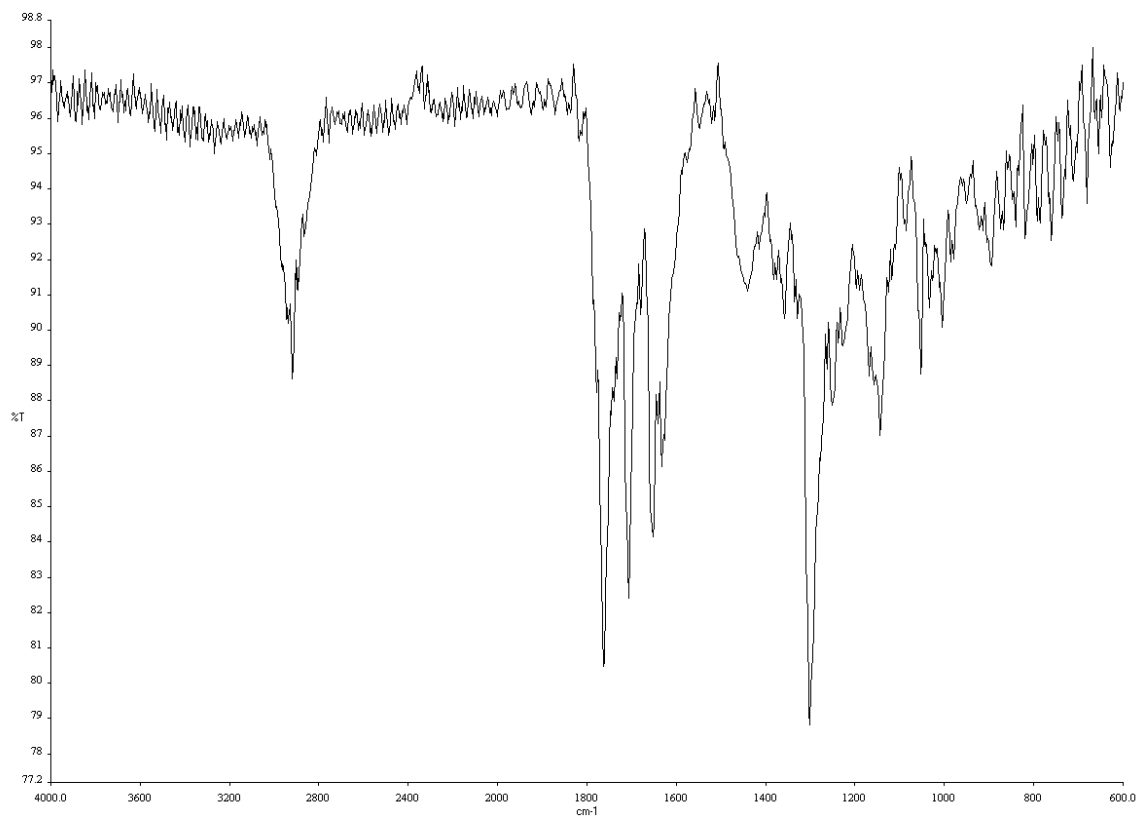


**Figure A2.167** Infrared spectrum (Thin Film, NaCl) of compound **4**.

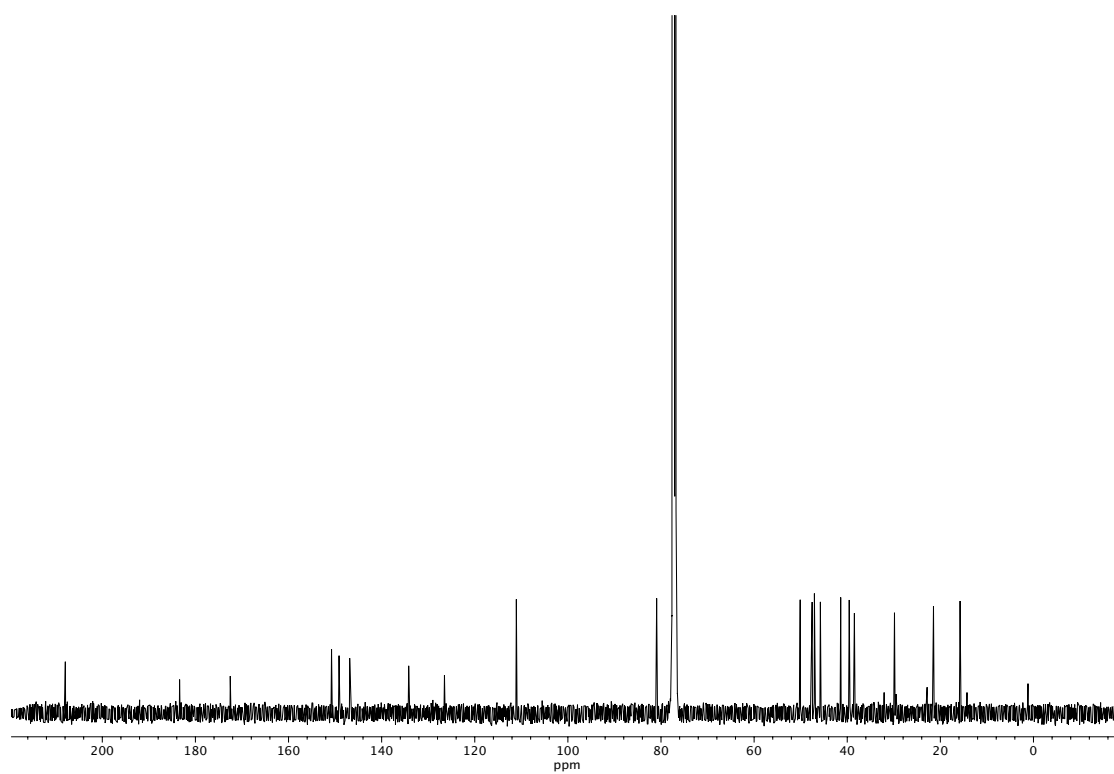


**Figure A2.168** <sup>13</sup>C NMR (100 MHz, CDCl<sub>3</sub>) of compound **4**.

## **APPENDIX 3**

*X-Ray Crystallography Reports Relevant to Chapter 1:*

*The Total Synthesis of (–)-Scabrolide A*



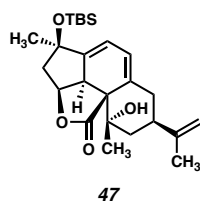
**A3.1 X-RAY CRYSTAL STRUCTURE ANALYSIS OF TETRACYCLE 47**Contents

Table A3.1.1. Experimental Details

Table A3.1.2. Crystal Data

Table A3.1.3. Atomic Coordinates

Table A3.1.4. Full Bond Distances and Angles

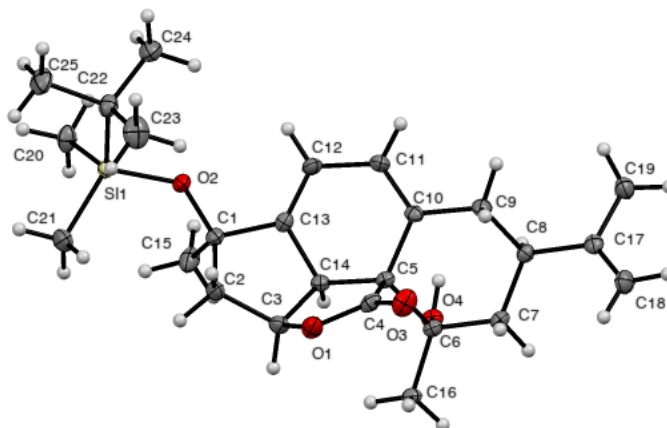
Table A3.1.5. Anisotropic Displacement Parameters

Table A3.1.6. Hydrogen Atomic Coordinates

Table A3.1.7. Torsion Angles

Table A3.1.8. Hydrogen Bond Distances and Angles

**Figure A3.1.1** X-Ray Crystal Structure of Tetracycline 47.



**Table A3.1.1** Experimental Details for X-Ray Structure Determination of Tetracycle **47**.

Low-temperature diffraction data ( $\phi$ - and  $\omega$ -scans) were collected on a Bruker AXS D8 VENTURE KAPPA diffractometer coupled to a PHOTON II CPAD detector with Cu  $K_{\alpha}$  radiation ( $\lambda = 1.54178 \text{ \AA}$ ) from an I $\mu$ S micro-source for the structure of compound **47**. The structure was solved by direct methods using SHELXS and refined against  $F^2$  on all data by full-matrix least squares with SHELXL-2016 using established refinement techniques. All non-hydrogen atoms were refined anisotropically. All hydrogen atoms were included into the model at geometrically calculated positions and refined using a riding model. The isotropic displacement parameters of all hydrogen atoms were fixed to 1.2 times the  $U$  value of the atoms they are linked to (1.5 times for methyl groups).

Compound **47** crystallizes in the orthorhombic space group  $P2_12_12_1$  with one molecule in the asymmetric unit. The coordinates for the hydrogen atom bound to O4 were located in the difference Fourier synthesis and refined semi-freely with the help of a restraint on the O-H distance (0.84(4)  $\text{\AA}$ ).

**Table A3.1.2** Crystal Data and Structure Refinement for Tetracycline 47

Empirical formula	C <sub>25</sub> H <sub>38</sub> O <sub>4</sub> Si	
Formula weight	430.64	
Temperature	100(2) K	
Wavelength	1.54178 Å	
Crystal system	Orthorhombic	
Space group	P2 <sub>1</sub> 2 <sub>1</sub> 2 <sub>1</sub>	
Unit cell dimensions	a = 6.3347(3) Å	a = 90°.
	b = 12.3768(5) Å	b = 90°.
	c = 30.9537(13) Å	g = 90°.
Volume	2426.87(18) Å <sup>3</sup>	
Z	4	
Density (calculated)	1.179 Mg/m <sup>3</sup>	
Absorption coefficient	1.064 mm <sup>-1</sup>	
F(000)	936	
Crystal size	0.300 x 0.150 x 0.100 mm <sup>3</sup>	
Theta range for data collection	2.855 to 74.566°.	
Index ranges	-7 ≤ h ≤ 7, -15 ≤ k ≤ 14, -38 ≤ l ≤ 38	
Reflections collected	25153	
Independent reflections	4954 [R(int) = 0.0480]	
Completeness to theta = 67.679°	99.9 %	
Absorption correction	Semi-empirical from equivalents	
Max. and min. transmission	0.7538 and 0.6036	
Refinement method	Full-matrix least-squares on F <sup>2</sup>	
Data / restraints / parameters	4954 / 1 / 282	
Goodness-of-fit on F <sup>2</sup>	1.045	
Final R indices [I > 2σ(I)]	R1 = 0.0315, wR2 = 0.0776	
R indices (all data)	R1 = 0.0341, wR2 = 0.0795	
Absolute structure parameter	0.001(10)	
Extinction coefficient	n/a	
Largest diff. peak and hole	0.271 and -0.190 e.Å <sup>-3</sup>	

**Table A3.1.3** Atomic Coordinates ( $\times 10^4$ ) and Equivalent Isotropic Displacement Parameters ( $\text{\AA}^2 \times 10^3$ ) for Tetracycline **47**.  $U(\text{eq})$  is Defined as One Third of the Orthogonalized  $U^{ij}$  Tensor.

	x	y	z	U(eq)
C(1)	2853(3)	1349(2)	3662(1)	17(1)
C(15)	4285(4)	511(2)	3878(1)	27(1)
O(2)	2611(2)	1129(1)	3218(1)	19(1)
Si(1)	1788(1)	60(1)	2947(1)	16(1)
C(20)	4027(3)	-872(2)	2822(1)	24(1)
C(21)	-250(4)	-722(2)	3251(1)	27(1)
C(22)	679(3)	665(2)	2435(1)	22(1)
C(23)	-1264(4)	1358(2)	2539(1)	34(1)
C(24)	2358(4)	1396(2)	2225(1)	27(1)
C(25)	61(4)	-241(2)	2120(1)	31(1)
C(2)	716(3)	1448(2)	3904(1)	23(1)
C(3)	1072(3)	2289(2)	4263(1)	21(1)
O(1)	-488(2)	3141(1)	4231(1)	24(1)
C(4)	390(3)	4128(2)	4204(1)	18(1)
O(3)	-697(2)	4922(1)	4186(1)	26(1)
C(5)	2811(3)	4065(2)	4224(1)	14(1)
C(6)	3546(3)	4471(2)	4685(1)	15(1)
O(4)	5671(2)	4121(1)	4755(1)	17(1)
C(16)	2269(3)	3954(2)	5047(1)	18(1)
C(7)	3408(3)	5707(1)	4721(1)	16(1)
C(8)	4719(3)	6285(2)	4379(1)	16(1)
C(17)	4820(3)	7503(2)	4426(1)	18(1)
C(18)	3432(4)	8079(2)	4649(1)	24(1)
C(19)	6667(4)	8017(2)	4198(1)	24(1)
C(9)	3849(3)	5956(2)	3933(1)	20(1)
C(10)	3843(3)	4750(2)	3871(1)	16(1)
C(11)	4656(3)	4292(2)	3517(1)	20(1)
C(12)	4409(3)	3144(2)	3418(1)	18(1)

**Table A3.1.3** Cont'd

C(13)	3699(3)	2478(2)	3720(1)	15(1)
C(14)	3205(3)	2845(1)	4173(1)	15(1)

---

**Table A3.1.4** Bond Lengths [ $\text{\AA}$ ] and angles [ $^\circ$ ] for Tetracycline **47**

---

C(1)-O(2)	1.412(2)
C(1)-C(13)	1.507(3)
C(1)-C(15)	1.530(3)
C(1)-C(2)	1.551(3)
C(15)-H(15A)	0.9800
C(15)-H(15B)	0.9800
C(15)-H(15C)	0.9800
O(2)-Si(1)	1.6507(14)
Si(1)-C(21)	1.868(2)
Si(1)-C(20)	1.869(2)
Si(1)-C(22)	1.887(2)
C(20)-H(20A)	0.9800
C(20)-H(20B)	0.9800
C(20)-H(20C)	0.9800
C(21)-H(21A)	0.9800
C(21)-H(21B)	0.9800
C(21)-H(21C)	0.9800
C(22)-C(23)	1.534(3)
C(22)-C(25)	1.537(3)
C(22)-C(24)	1.540(3)
C(23)-H(23A)	0.9800
C(23)-H(23B)	0.9800
C(23)-H(23C)	0.9800
C(24)-H(24A)	0.9800
C(24)-H(24B)	0.9800
C(24)-H(24C)	0.9800
C(25)-H(25A)	0.9800
C(25)-H(25B)	0.9800
C(25)-H(25C)	0.9800
C(2)-C(3)	1.541(3)
C(2)-H(2A)	0.9900
C(2)-H(2B)	0.9900

**Table A.3.1.4** *Cont'd*

C(3)-O(1)	1.448(3)
C(3)-C(14)	1.542(3)
C(3)-H(3)	1.0000
O(1)-C(4)	1.345(3)
C(4)-O(3)	1.201(3)
C(4)-C(5)	1.537(2)
C(5)-C(10)	1.529(2)
C(5)-C(14)	1.538(2)
C(5)-C(6)	1.585(2)
C(6)-O(4)	1.430(2)
C(6)-C(16)	1.522(3)
C(6)-C(7)	1.535(2)
O(4)-H(4O)	0.84(2)
C(16)-H(16A)	0.9800
C(16)-H(16B)	0.9800
C(16)-H(16C)	0.9800
C(7)-C(8)	1.524(3)
C(7)-H(7A)	0.9900
C(7)-H(7B)	0.9900
C(8)-C(17)	1.515(3)
C(8)-C(9)	1.540(3)
C(8)-H(8)	1.0000
C(17)-C(18)	1.326(3)
C(17)-C(19)	1.506(3)
C(18)-H(18A)	0.9500
C(18)-H(18B)	0.9500
C(19)-H(19A)	0.9800
C(19)-H(19B)	0.9800
C(19)-H(19C)	0.9800
C(9)-C(10)	1.505(3)
C(9)-H(9A)	0.9900
C(9)-H(9B)	0.9900
C(10)-C(11)	1.336(3)
C(11)-C(12)	1.462(3)

**Table A.3.1.4** *Cont'd*

C(11)-H(11)	0.9500
C(12)-C(13)	1.325(3)
C(12)-H(12)	0.9500
C(13)-C(14)	1.505(2)
C(14)-H(14)	1.0000
O(2)-C(1)-C(13)	109.48(15)
O(2)-C(1)-C(15)	111.00(16)
C(13)-C(1)-C(15)	111.47(16)
O(2)-C(1)-C(2)	112.91(16)
C(13)-C(1)-C(2)	100.35(15)
C(15)-C(1)-C(2)	111.20(17)
C(1)-C(15)-H(15A)	109.5
C(1)-C(15)-H(15B)	109.5
H(15A)-C(15)-H(15B)	109.5
C(1)-C(15)-H(15C)	109.5
H(15A)-C(15)-H(15C)	109.5
H(15B)-C(15)-H(15C)	109.5
C(1)-O(2)-Si(1)	133.20(12)
O(2)-Si(1)-C(21)	112.17(9)
O(2)-Si(1)-C(20)	111.08(9)
C(21)-Si(1)-C(20)	107.95(10)
O(2)-Si(1)-C(22)	103.08(8)
C(21)-Si(1)-C(22)	111.81(10)
C(20)-Si(1)-C(22)	110.76(10)
Si(1)-C(20)-H(20A)	109.5
Si(1)-C(20)-H(20B)	109.5
H(20A)-C(20)-H(20B)	109.5
Si(1)-C(20)-H(20C)	109.5
H(20A)-C(20)-H(20C)	109.5
H(20B)-C(20)-H(20C)	109.5
Si(1)-C(21)-H(21A)	109.5
Si(1)-C(21)-H(21B)	109.5
H(21A)-C(21)-H(21B)	109.5
Si(1)-C(21)-H(21C)	109.5
H(21A)-C(21)-H(21C)	109.5



**Table A.7.1.4** *Cont'd*

H(21B)-C(21)-H(21C)	109.5
C(23)-C(22)-C(25)	109.66(19)
C(23)-C(22)-C(24)	108.29(18)
C(25)-C(22)-C(24)	109.73(18)
C(23)-C(22)-Si(1)	110.17(15)
C(25)-C(22)-Si(1)	109.73(14)
C(24)-C(22)-Si(1)	109.24(14)
C(22)-C(23)-H(23A)	109.5
C(22)-C(23)-H(23B)	109.5
H(23A)-C(23)-H(23B)	109.5
C(22)-C(23)-H(23C)	109.5
H(23A)-C(23)-H(23C)	109.5
H(23B)-C(23)-H(23C)	109.5
C(22)-C(24)-H(24A)	109.5
C(22)-C(24)-H(24B)	109.5
H(24A)-C(24)-H(24B)	109.5
C(22)-C(24)-H(24C)	109.5
H(24A)-C(24)-H(24C)	109.5
H(24B)-C(24)-H(24C)	109.5
C(22)-C(25)-H(25A)	109.5
C(22)-C(25)-H(25B)	109.5
H(25A)-C(25)-H(25B)	109.5
C(22)-C(25)-H(25C)	109.5
H(25A)-C(25)-H(25C)	109.5
H(25B)-C(25)-H(25C)	109.5
C(3)-C(2)-C(1)	105.86(16)
C(3)-C(2)-H(2A)	110.6
C(1)-C(2)-H(2A)	110.6
C(3)-C(2)-H(2B)	110.6
C(1)-C(2)-H(2B)	110.6
H(2A)-C(2)-H(2B)	108.7
O(1)-C(3)-C(2)	110.00(17)

**Table A.3.1.4** *Cont'd*

O(1)-C(3)-C(14)	105.10(15)
C(2)-C(3)-C(14)	107.37(15)
O(1)-C(3)-H(3)	111.4
C(2)-C(3)-H(3)	111.4
C(14)-C(3)-H(3)	111.4
C(4)-O(1)-C(3)	112.56(15)
O(3)-C(4)-O(1)	120.61(18)
O(3)-C(4)-C(5)	128.00(19)
O(1)-C(4)-C(5)	111.32(17)
C(10)-C(5)-C(4)	111.75(15)
C(10)-C(5)-C(14)	113.68(15)
C(4)-C(5)-C(14)	102.01(15)
C(10)-C(5)-C(6)	109.99(15)
C(4)-C(5)-C(6)	108.18(15)
C(14)-C(5)-C(6)	110.88(14)
O(4)-C(6)-C(16)	105.17(15)
O(4)-C(6)-C(7)	110.16(16)
C(16)-C(6)-C(7)	109.63(15)
O(4)-C(6)-C(5)	108.43(14)
C(16)-C(6)-C(5)	111.94(15)
C(7)-C(6)-C(5)	111.31(15)
C(6)-O(4)-H(4O)	112.7(19)
C(6)-C(16)-H(16A)	109.5
C(6)-C(16)-H(16B)	109.5
H(16A)-C(16)-H(16B)	109.5
C(6)-C(16)-H(16C)	109.5
H(16A)-C(16)-H(16C)	109.5
H(16B)-C(16)-H(16C)	109.5
C(8)-C(7)-C(6)	112.79(15)
C(8)-C(7)-H(7A)	109.0
C(6)-C(7)-H(7A)	109.0
C(8)-C(7)-H(7B)	109.0
C(6)-C(7)-H(7B)	109.0
H(7A)-C(7)-H(7B)	107.8

**Table A3.1.4** Cont'd

C(17)-C(8)-C(7)	115.09(16)
C(17)-C(8)-C(9)	111.31(15)
C(7)-C(8)-C(9)	107.63(15)
C(17)-C(8)-H(8)	107.5
C(7)-C(8)-H(8)	107.5
C(9)-C(8)-H(8)	107.5
C(18)-C(17)-C(19)	122.07(19)
C(18)-C(17)-C(8)	123.84(19)
C(19)-C(17)-C(8)	114.09(17)
C(17)-C(18)-H(18A)	120.0
C(17)-C(18)-H(18B)	120.0
H(18A)-C(18)-H(18B)	120.0
C(17)-C(19)-H(19A)	109.5
C(17)-C(19)-H(19B)	109.5
H(19A)-C(19)-H(19B)	109.5
C(17)-C(19)-H(19C)	109.5
H(19A)-C(19)-H(19C)	109.5
H(19B)-C(19)-H(19C)	109.5
C(10)-C(9)-C(8)	112.16(15)
C(10)-C(9)-H(9A)	109.2
C(8)-C(9)-H(9A)	109.2
C(10)-C(9)-H(9B)	109.2
C(8)-C(9)-H(9B)	109.2
H(9A)-C(9)-H(9B)	107.9
C(11)-C(10)-C(9)	121.61(17)
C(11)-C(10)-C(5)	120.96(17)
C(9)-C(10)-C(5)	117.41(16)
C(10)-C(11)-C(12)	122.87(18)
C(10)-C(11)-H(11)	118.6
C(12)-C(11)-H(11)	118.6
C(13)-C(12)-C(11)	119.56(17)
C(13)-C(12)-H(12)	120.2
C(11)-C(12)-H(12)	120.2
C(12)-C(13)-C(14)	122.60(17)

**Table A3.1.4** *Cont'd*

C(12)-C(13)-C(1)	127.85(17)
C(14)-C(13)-C(1)	108.49(15)
C(13)-C(14)-C(5)	115.21(15)
C(13)-C(14)-C(3)	102.49(15)
C(5)-C(14)-C(3)	106.08(15)
C(13)-C(14)-H(14)	110.9
C(5)-C(14)-H(14)	110.9
C(3)-C(14)-H(14)	110.9

---

Symmetry transformations used to generate equivalent atoms:

**Table A3.1.5** Anisotropic Displacement Parameters ( $\text{\AA}^2 \times 10^3$ ) for Tetracycline **47**. The

Anisotropic Displacement Factor Exponent Takes the Form:  $-2p^2[h^2a^*2U^{11} + \dots + 2hka^*b^*U^{12}]$ .

	U <sup>11</sup>	U <sup>22</sup>	U <sup>33</sup>	U <sup>23</sup>	U <sup>13</sup>	U <sup>12</sup>
C(1)	20(1)	18(1)	13(1)	-1(1)	0(1)	-3(1)
C(15)	38(1)	19(1)	24(1)	-3(1)	-8(1)	4(1)
O(2)	25(1)	18(1)	14(1)	-2(1)	0(1)	-4(1)
Si(1)	16(1)	15(1)	17(1)	-2(1)	0(1)	-1(1)
C(20)	20(1)	19(1)	34(1)	-5(1)	-2(1)	3(1)
C(21)	28(1)	25(1)	28(1)	-2(1)	4(1)	-10(1)
C(22)	24(1)	21(1)	21(1)	-2(1)	-5(1)	0(1)
C(23)	28(1)	29(1)	47(1)	0(1)	-10(1)	7(1)
C(24)	35(1)	26(1)	20(1)	-1(1)	0(1)	-2(1)
C(25)	38(1)	31(1)	25(1)	-5(1)	-11(1)	-6(1)
C(2)	25(1)	23(1)	22(1)	-4(1)	6(1)	-9(1)
C(3)	22(1)	23(1)	18(1)	-1(1)	5(1)	-6(1)
O(1)	16(1)	28(1)	27(1)	-7(1)	5(1)	-5(1)
C(4)	13(1)	26(1)	15(1)	-5(1)	-1(1)	1(1)
O(3)	16(1)	31(1)	32(1)	-6(1)	-4(1)	6(1)
C(5)	13(1)	17(1)	12(1)	-1(1)	0(1)	1(1)
C(6)	15(1)	19(1)	13(1)	-1(1)	1(1)	1(1)
O(4)	14(1)	21(1)	15(1)	1(1)	-2(1)	2(1)
C(16)	20(1)	21(1)	13(1)	1(1)	3(1)	-1(1)
C(7)	16(1)	18(1)	13(1)	-2(1)	0(1)	2(1)
C(8)	16(1)	16(1)	16(1)	-1(1)	0(1)	2(1)
C(17)	21(1)	18(1)	16(1)	1(1)	-4(1)	0(1)
C(18)	28(1)	17(1)	28(1)	-1(1)	1(1)	2(1)
C(19)	27(1)	18(1)	28(1)	0(1)	3(1)	-3(1)
C(9)	27(1)	18(1)	15(1)	2(1)	0(1)	0(1)
C(10)	16(1)	18(1)	13(1)	2(1)	-2(1)	-1(1)
C(11)	25(1)	20(1)	16(1)	1(1)	5(1)	-5(1)

**Table A3.1.5** *Cont'd*

C(12)	19(1)	22(1)	15(1)	-4(1)	5(1)	-2(1)
C(13)	13(1)	17(1)	16(1)	-3(1)	-1(1)	2(1)
C(14)	15(1)	16(1)	13(1)	1(1)	1(1)	0(1)

---

**Table A3.1.6** Hydrogen Coordinates ( $\times 10^4$ ) and Isotropic Displacement Parameters ( $\text{\AA}^2 \times 10^3$ ) for Tetracycline **47**.

	x	y	z	U(eq)
H(15A)	3655	-209	3848	41
H(15B)	4443	685	4185	41
H(15C)	5674	519	3738	41
H(20A)	5104	-483	2656	37
H(20B)	3507	-1485	2653	37
H(20C)	4646	-1136	3092	37
H(21A)	372	-1007	3517	41
H(21B)	-752	-1323	3072	41
H(21C)	-1437	-247	3322	41
H(23A)	-1856	1647	2270	52
H(23B)	-850	1957	2728	52
H(23C)	-2326	914	2685	52
H(24A)	1858	1638	1942	40
H(24B)	3675	990	2190	40
H(24C)	2611	2026	2410	40
H(25A)	-1010	-704	2254	47
H(25B)	1310	-674	2050	47
H(25C)	-513	76	1855	47
H(2A)	-408	1691	3704	28
H(2B)	300	743	4029	28
H(3)	1053	1945	4555	25
H(4O)	6480(40)	4290(20)	4552(8)	20
H(16A)	2464	3169	5040	27
H(16B)	771	4125	5008	27
H(16C)	2751	4236	5326	27
H(7A)	1914	5930	4691	19
H(7B)	3899	5931	5011	19
H(8)	6195	6004	4400	19

**Table A3.1.6** *Cont'd*

H(18A)	3586	8841	4669	29
H(18B)	2284	7730	4788	29
H(19A)	6682	8794	4258	36
H(19B)	6537	7900	3886	36
H(19C)	7982	7690	4302	36
H(9A)	2391	6233	3902	24
H(9B)	4723	6293	3705	24
H(11)	5428	4732	3322	24
H(12)	4756	2877	3140	22
H(14)	4310	2591	4380	18

---



**Table A3.1.7** Torsion Angles [°] for Tetracycle 47.

---

C(13)-C(1)-O(2)-Si(1)	179.54(13)
C(15)-C(1)-O(2)-Si(1)	56.1(2)
C(2)-C(1)-O(2)-Si(1)	-69.6(2)
C(1)-O(2)-Si(1)-C(21)	31.7(2)
C(1)-O(2)-Si(1)-C(20)	-89.25(19)
C(1)-O(2)-Si(1)-C(22)	152.10(17)
O(2)-Si(1)-C(22)-C(23)	-65.50(17)
C(21)-Si(1)-C(22)-C(23)	55.18(18)
C(20)-Si(1)-C(22)-C(23)	175.62(15)
O(2)-Si(1)-C(22)-C(25)	173.66(15)
C(21)-Si(1)-C(22)-C(25)	-65.66(18)
C(20)-Si(1)-C(22)-C(25)	54.79(18)
O(2)-Si(1)-C(22)-C(24)	53.33(15)
C(21)-Si(1)-C(22)-C(24)	174.01(14)
C(20)-Si(1)-C(22)-C(24)	-65.55(16)
O(2)-C(1)-C(2)-C(3)	-147.14(16)
C(13)-C(1)-C(2)-C(3)	-30.70(19)
C(15)-C(1)-C(2)-C(3)	87.3(2)
C(1)-C(2)-C(3)-O(1)	125.61(17)
C(1)-C(2)-C(3)-C(14)	11.8(2)
C(2)-C(3)-O(1)-C(4)	-125.15(17)
C(14)-C(3)-O(1)-C(4)	-9.8(2)
C(3)-O(1)-C(4)-O(3)	-178.16(17)
C(3)-O(1)-C(4)-C(5)	-0.9(2)
O(3)-C(4)-C(5)-C(10)	-50.1(3)
O(1)-C(4)-C(5)-C(10)	132.92(16)
O(3)-C(4)-C(5)-C(14)	-171.86(19)
O(1)-C(4)-C(5)-C(14)	11.1(2)
O(3)-C(4)-C(5)-C(6)	71.2(2)
O(1)-C(4)-C(5)-C(6)	-105.85(17)
C(10)-C(5)-C(6)-O(4)	-74.73(17)
C(4)-C(5)-C(6)-O(4)	162.96(15)

**Table A3.1.7** Cont'd

C(14)-C(5)-C(6)-O(4)	51.88(19)
C(10)-C(5)-C(6)-C(16)	169.70(15)
C(4)-C(5)-C(6)-C(16)	47.4(2)
C(14)-C(5)-C(6)-C(16)	-63.7(2)
C(10)-C(5)-C(6)-C(7)	46.6(2)
C(4)-C(5)-C(6)-C(7)	-75.7(2)
C(14)-C(5)-C(6)-C(7)	173.21(15)
O(4)-C(6)-C(7)-C(8)	62.5(2)
C(16)-C(6)-C(7)-C(8)	177.78(15)
C(5)-C(6)-C(7)-C(8)	-57.8(2)
C(6)-C(7)-C(8)-C(17)	-174.09(17)
C(6)-C(7)-C(8)-C(9)	61.2(2)
C(7)-C(8)-C(17)-C(18)	-20.2(3)
C(9)-C(8)-C(17)-C(18)	102.6(2)
C(7)-C(8)-C(17)-C(19)	159.28(17)
C(9)-C(8)-C(17)-C(19)	-77.9(2)
C(17)-C(8)-C(9)-C(10)	177.00(17)
C(7)-C(8)-C(9)-C(10)	-56.0(2)
C(8)-C(9)-C(10)-C(11)	-130.3(2)
C(8)-C(9)-C(10)-C(5)	51.3(2)
C(4)-C(5)-C(10)-C(11)	-103.3(2)
C(14)-C(5)-C(10)-C(11)	11.5(3)
C(6)-C(5)-C(10)-C(11)	136.48(19)
C(4)-C(5)-C(10)-C(9)	75.0(2)
C(14)-C(5)-C(10)-C(9)	-170.19(16)
C(6)-C(5)-C(10)-C(9)	-45.2(2)
C(9)-C(10)-C(11)-C(12)	-171.04(19)
C(5)-C(10)-C(11)-C(12)	7.2(3)
C(10)-C(11)-C(12)-C(13)	-12.7(3)
C(11)-C(12)-C(13)-C(14)	-2.5(3)
C(11)-C(12)-C(13)-C(1)	164.33(19)
O(2)-C(1)-C(13)-C(12)	-8.9(3)
C(15)-C(1)-C(13)-C(12)	114.3(2)
C(2)-C(1)-C(13)-C(12)	-127.8(2)

**Table A3.1.7** Cont'd

O(2)-C(1)-C(13)-C(14)	159.42(15)
C(15)-C(1)-C(13)-C(14)	-77.38(19)
C(2)-C(1)-C(13)-C(14)	40.45(18)
C(12)-C(13)-C(14)-C(5)	20.8(3)
C(1)-C(13)-C(14)-C(5)	-148.21(16)
C(12)-C(13)-C(14)-C(3)	135.51(19)
C(1)-C(13)-C(14)-C(3)	-33.52(19)
C(10)-C(5)-C(14)-C(13)	-24.1(2)
C(4)-C(5)-C(14)-C(13)	96.36(18)
C(6)-C(5)-C(14)-C(13)	-148.65(16)
C(10)-C(5)-C(14)-C(3)	-136.71(15)
C(4)-C(5)-C(14)-C(3)	-16.25(18)
C(6)-C(5)-C(14)-C(3)	98.75(17)
O(1)-C(3)-C(14)-C(13)	-104.81(16)
C(2)-C(3)-C(14)-C(13)	12.3(2)
O(1)-C(3)-C(14)-C(5)	16.37(18)
C(2)-C(3)-C(14)-C(5)	133.48(17)

---

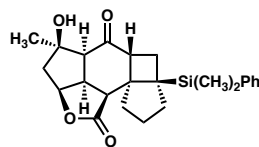
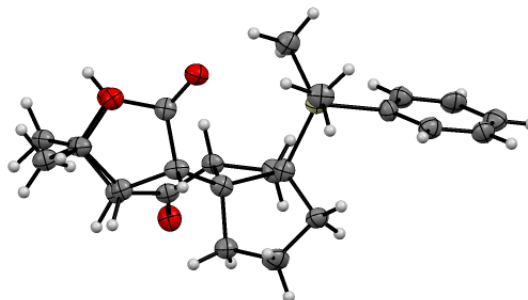
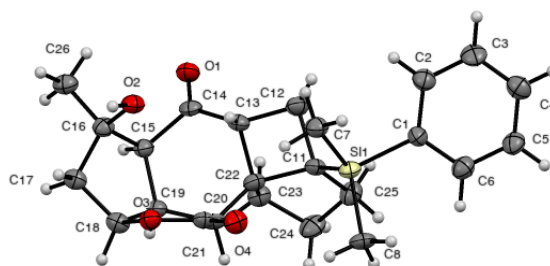
Symmetry transformations used to generate equivalent atoms:

**Table A3.1.8** Hydrogen Bonds for Tetracycline **47** [ $\text{\AA}$  and  $^\circ$ ].

D-H...A	d(D-H)	d(H...A)	d(D...A)	$\angle$ (DHA)
C(3)-H(3)...O(4)#1	1.00	2.52	3.514(2)	171.9
O(4)-H(4O)...O(1)#2	0.84(2)	2.59(3)	3.167(2)	127(2)
O(4)-H(4O)...O(3)#2	0.84(2)	2.25(2)	3.062(2)	162(3)
C(7)-H(7A)...O(3)	0.99	2.59	3.231(2)	122.0

Symmetry transformations used to generate equivalent atoms:

#1  $x-1/2, -y+1/2, -z+1$  #2  $x+1, y, z$

**A3.2 X-RAY CRYSTAL STRUCTURE ANALYSIS OF CYCLOBUTANE 63****63**Contents*Table A3.2.1. Experimental Details**Table A3.2.2. Crystal Data**Table A3.2.3. Atomic Coordinates**Table A3.2.4. Full Bond Distances and Angles**Table A3.2.5. Anisotropic Displacement Parameters**Table A3.2.6. Hydrogen Atomic Coordinates**Table A3.2.7. Torsion Angles**Table A3.2.8. Hydrogen Bond Distances and Angles***Figure A3.2.1 X-Ray Crystal Structure of Cyclobutane 63.**

**Table A3.2.1** Experimental Details for X-Ray Structure Determination of Cyclobutane**63.**

Low-temperature diffraction data ( $\phi$ - and  $\omega$ -scans) were collected on a Bruker AXS D8 VENTURE KAPPA diffractometer coupled to a PHOTON II CPAD detector with Cu  $K_{\alpha}$  radiation ( $\lambda = 1.54178 \text{ \AA}$ ) from an I $\mu$ S micro-source for the structure of compound **63**. The structure was solved by direct methods using SHELXS and refined against  $F^2$  on all data by full-matrix least squares with SHELXL-2017 using established refinement techniques. All non-hydrogen atoms were refined anisotropically. Unless otherwise noted, all hydrogen atoms were included into the model at geometrically calculated positions and refined using a riding model. The isotropic displacement parameters of all hydrogen atoms were fixed to 1.2 times the  $U$  value of the atoms they are linked to (1.5 times for methyl groups).

Compound **63** crystallizes in the monoclinic space group  $P2_1$  with one molecule in the asymmetric unit. The coordinates for the hydrogen atom bound to O2 were located in the difference Fourier synthesis and refined semi-freely with the help of a restraint on the O-H distance (0.84(4)  $\text{\AA}$ ). The structure was refined as a twin  $[-1 \ 0 \ 0 \ 0 \ -1 \ 0 \ 1 \ 0 \ 1]$ .

**Table A3.2.2** Crystal Data and Structure Refinement for Cyclobutane **63**.

Empirical formula	C <sub>24</sub> H <sub>30</sub> O <sub>4</sub> Si
Formula weight	410.57
Temperature	100(2) K
Wavelength	1.54178 Å
Crystal system	Monoclinic
Space group	P2 <sub>1</sub>
Unit cell dimensions	a = 6.7649(5) Å      a = 90°. b = 10.9273(9) Å      b = 103.394(5)°. c = 14.4629(14) Å      c = 90°.
Volume	1040.05(15) Å <sup>3</sup>
Z	2
Density (calculated)	1.311 Mg/m <sup>3</sup>
Absorption coefficient	1.224 mm <sup>-1</sup>
F(000)	440
Crystal size	0.200 x 0.150 x 0.050 mm <sup>3</sup>
Theta range for data collection	3.141 to 74.630°.
Index ranges	-7<=h<=8, -13<=k<=13, -18<=l<=17
Reflections collected	17179
Independent reflections	4172 [R(int) = 0.0797]
Completeness to theta = 67.679°	99.7 %
Absorption correction	Semi-empirical from equivalents
Max. and min. transmission	0.7504 and 0.5626
Refinement method	Full-matrix least-squares on F <sup>2</sup>
Data / restraints / parameters	4172 / 2 / 269
Goodness-of-fit on F <sup>2</sup>	1.071
Final R indices [I>2sigma(I)]	R1 = 0.0880, wR2 = 0.2288
R indices (all data)	R1 = 0.0893, wR2 = 0.2312
Absolute structure parameter	0.03(6)
Extinction coefficient	n/a
Largest diff. peak and hole	0.686 and -0.364 e.Å <sup>-3</sup>

**Table A3.2.3** Atomic Coordinates ( $\times 10^4$ ) and Equivalent Isotropic Displacement Parameters ( $\text{\AA}^2 \times 10^3$ ) for Cyclobutane **63**.  $U(\text{eq})$  is Defined as One Third of the Trace of the Orthogonalized  $U^{ij}$  Tensor.

	x	y	z	U(eq)
Si(1)	5500(3)	3644(2)	3733(2)	26(1)
C(1)	5454(13)	4028(8)	5009(6)	28(2)
C(2)	3622(15)	4276(9)	5275(7)	34(2)
C(3)	3582(16)	4570(10)	6208(8)	38(2)
C(4)	5409(17)	4598(10)	6909(8)	37(2)
C(5)	7217(15)	4334(10)	6668(7)	35(2)
C(6)	7249(16)	4064(9)	5719(7)	34(2)
C(7)	3130(15)	2738(10)	3256(7)	34(2)
C(8)	7879(13)	2754(9)	3754(8)	33(2)
C(11)	5539(13)	5208(8)	3156(6)	26(2)
C(12)	3363(14)	5841(9)	3012(7)	32(2)
C(13)	2992(13)	5596(8)	1937(6)	26(2)
C(14)	2128(13)	6460(8)	1150(6)	26(2)
O(1)	1187(12)	7376(6)	1210(5)	34(2)
C(15)	2743(13)	6116(8)	223(6)	27(2)
C(16)	1075(14)	5330(8)	-431(6)	28(2)
C(26)	-690(15)	6100(9)	-971(7)	34(2)
O(2)	321(10)	4436(6)	135(5)	31(1)
C(17)	2279(15)	4700(8)	-1074(6)	28(2)
C(18)	4326(15)	4391(8)	-447(6)	29(2)
C(19)	4824(13)	5439(8)	283(6)	26(2)
C(20)	5848(13)	4788(8)	1237(6)	27(2)
C(21)	5101(13)	3456(8)	1047(6)	27(2)
O(3)	4251(10)	3301(6)	116(5)	30(1)
O(4)	5290(12)	2622(6)	1593(5)	34(2)
C(22)	5312(13)	5490(8)	2053(6)	27(2)
C(23)	6384(15)	6755(8)	2115(7)	30(2)



**Table A3.2.3** *Cont'd*

C(24)	8208(15)	6643(10)	2960(8)	39(2)
C(25)	7315(15)	5980(9)	3715(7)	34(2)

---

**Table A3.2.4** Bond Lengths [ $\text{\AA}$ ] and angles [ $^\circ$ ] for Cyclobutane **63**.

Si(1)-C(8)	1.874(9)
Si(1)-C(7)	1.875(10)
Si(1)-C(1)	1.900(9)
Si(1)-C(11)	1.905(9)
C(1)-C(6)	1.397(13)
C(1)-C(2)	1.406(13)
C(2)-C(3)	1.393(14)
C(2)-H(2)	0.9500
C(3)-C(4)	1.406(15)
C(3)-H(3)	0.9500
C(4)-C(5)	1.378(15)
C(4)-H(4)	0.9500
C(5)-C(6)	1.409(14)
C(5)-H(5)	0.9500
C(6)-H(6)	0.9500
C(7)-H(7A)	0.9800
C(7)-H(7B)	0.9800
C(7)-H(7C)	0.9800
C(8)-H(8A)	0.9800
C(8)-H(8B)	0.9800
C(8)-H(8C)	0.9800
C(11)-C(25)	1.535(12)
C(11)-C(12)	1.596(12)
C(11)-C(22)	1.598(12)
C(12)-C(13)	1.541(13)
C(12)-H(12A)	0.9900
C(12)-H(12B)	0.9900
C(13)-C(14)	1.489(12)
C(13)-C(22)	1.544(12)
C(13)-H(13)	1.0000
C(14)-O(1)	1.201(12)
C(14)-C(15)	1.541(12)
C(15)-C(16)	1.552(12)

**Table A3.2.4** Cont'd

C(15)-C(19)	1.574(12)
C(15)-H(15)	1.0000
C(16)-O(2)	1.441(11)
C(16)-C(26)	1.521(13)
C(16)-C(17)	1.534(12)
C(26)-H(26A)	0.9800
C(26)-H(26B)	0.9800
C(26)-H(26C)	0.9800
O(2)-H(2A)	0.83(3)
C(17)-C(18)	1.508(13)
C(17)-H(17A)	0.9900
C(17)-H(17B)	0.9900
C(18)-O(3)	1.450(11)
C(18)-C(19)	1.541(12)
C(18)-H(18)	1.0000
C(19)-C(20)	1.565(12)
C(19)-H(19)	1.0000
C(20)-C(22)	1.520(12)
C(20)-C(21)	1.544(12)
C(20)-H(20)	1.0000
C(21)-O(4)	1.193(11)
C(21)-O(3)	1.347(11)
C(22)-C(23)	1.554(13)
C(23)-C(24)	1.527(13)
C(23)-H(23A)	0.9900
C(23)-H(23B)	0.9900
C(24)-C(25)	1.545(14)
C(24)-H(24A)	0.9900
C(24)-H(24B)	0.9900
C(25)-H(25A)	0.9900
C(25)-H(25B)	0.9900
C(8)-Si(1)-C(7)	112.9(5)
C(8)-Si(1)-C(1)	107.8(4)

**Table A3.2.4** Cont'd

C(7)-Si(1)-C(1)	105.7(4)
C(8)-Si(1)-C(11)	111.9(4)
C(7)-Si(1)-C(11)	114.2(4)
C(1)-Si(1)-C(11)	103.4(4)
C(6)-C(1)-C(2)	117.7(9)
C(6)-C(1)-Si(1)	120.9(7)
C(2)-C(1)-Si(1)	121.4(7)
C(3)-C(2)-C(1)	121.7(9)
C(3)-C(2)-H(2)	119.2
C(1)-C(2)-H(2)	119.2
C(2)-C(3)-C(4)	119.5(10)
C(2)-C(3)-H(3)	120.2
C(4)-C(3)-H(3)	120.2
C(5)-C(4)-C(3)	119.7(10)
C(5)-C(4)-H(4)	120.1
C(3)-C(4)-H(4)	120.1
C(4)-C(5)-C(6)	120.4(9)
C(4)-C(5)-H(5)	119.8
C(6)-C(5)-H(5)	119.8
C(1)-C(6)-C(5)	121.0(9)
C(1)-C(6)-H(6)	119.5
C(5)-C(6)-H(6)	119.5
Si(1)-C(7)-H(7A)	109.5
Si(1)-C(7)-H(7B)	109.5
H(7A)-C(7)-H(7B)	109.5
Si(1)-C(7)-H(7C)	109.5
H(7A)-C(7)-H(7C)	109.5
H(7B)-C(7)-H(7C)	109.5
Si(1)-C(8)-H(8A)	109.5
Si(1)-C(8)-H(8B)	109.5
H(8A)-C(8)-H(8B)	109.5
Si(1)-C(8)-H(8C)	109.5
H(8A)-C(8)-H(8C)	109.5
H(8B)-C(8)-H(8C)	109.5

**Table A3.2.4** Cont'd

C(25)-C(11)-C(12)	114.6(7)
C(25)-C(11)-C(22)	107.6(7)
C(12)-C(11)-C(22)	85.0(6)
C(25)-C(11)-Si(1)	110.5(6)
C(12)-C(11)-Si(1)	109.9(6)
C(22)-C(11)-Si(1)	127.1(6)
C(13)-C(12)-C(11)	89.2(7)
C(13)-C(12)-H(12A)	113.8
C(11)-C(12)-H(12A)	113.8
C(13)-C(12)-H(12B)	113.8
C(11)-C(12)-H(12B)	113.8
H(12A)-C(12)-H(12B)	111.0
C(14)-C(13)-C(12)	127.2(8)
C(14)-C(13)-C(22)	109.9(7)
C(12)-C(13)-C(22)	88.8(7)
C(14)-C(13)-H(13)	109.5
C(12)-C(13)-H(13)	109.5
C(22)-C(13)-H(13)	109.5
O(1)-C(14)-C(13)	126.4(8)
O(1)-C(14)-C(15)	121.4(8)
C(13)-C(14)-C(15)	111.9(7)
C(14)-C(15)-C(16)	111.1(7)
C(14)-C(15)-C(19)	119.0(7)
C(16)-C(15)-C(19)	106.8(7)
C(14)-C(15)-H(15)	106.4
C(16)-C(15)-H(15)	106.4
C(19)-C(15)-H(15)	106.4
O(2)-C(16)-C(26)	109.1(8)
O(2)-C(16)-C(17)	110.3(7)
C(26)-C(16)-C(17)	113.6(7)
O(2)-C(16)-C(15)	109.4(7)
C(26)-C(16)-C(15)	112.3(7)
C(17)-C(16)-C(15)	101.8(7)
C(16)-C(26)-H(26A)	109.5

**Table A3.2.4** Cont'd

C(16)-C(26)-H(26B)	109.5
H(26A)-C(26)-H(26B)	109.5
C(16)-C(26)-H(26C)	109.5
H(26A)-C(26)-H(26C)	109.5
H(26B)-C(26)-H(26C)	109.5
C(16)-O(2)-H(2A)	106(10)
C(18)-C(17)-C(16)	106.2(7)
C(18)-C(17)-H(17A)	110.5
C(16)-C(17)-H(17A)	110.5
C(18)-C(17)-H(17B)	110.5
C(16)-C(17)-H(17B)	110.5
H(17A)-C(17)-H(17B)	108.7
O(3)-C(18)-C(17)	112.0(7)
O(3)-C(18)-C(19)	104.9(7)
C(17)-C(18)-C(19)	105.7(7)
O(3)-C(18)-H(18)	111.3
C(17)-C(18)-H(18)	111.3
C(19)-C(18)-H(18)	111.3
C(18)-C(19)-C(20)	104.4(7)
C(18)-C(19)-C(15)	105.1(7)
C(20)-C(19)-C(15)	118.0(7)
C(18)-C(19)-H(19)	109.7
C(20)-C(19)-H(19)	109.7
C(15)-C(19)-H(19)	109.7
C(22)-C(20)-C(21)	119.2(7)
C(22)-C(20)-C(19)	108.6(6)
C(21)-C(20)-C(19)	102.2(7)
C(22)-C(20)-H(20)	108.8
C(21)-C(20)-H(20)	108.8
C(19)-C(20)-H(20)	108.8
O(4)-C(21)-O(3)	121.4(8)
O(4)-C(21)-C(20)	128.5(8)
O(3)-C(21)-C(20)	110.1(7)
C(21)-O(3)-C(18)	113.3(7)

**Table A3.2.4** *Cont'd*

C(20)-C(22)-C(13)	111.9(7)
C(20)-C(22)-C(23)	107.6(7)
C(13)-C(22)-C(23)	112.9(8)
C(20)-C(22)-C(11)	133.8(7)
C(13)-C(22)-C(11)	89.0(6)
C(23)-C(22)-C(11)	100.2(7)
C(24)-C(23)-C(22)	104.8(8)
C(24)-C(23)-H(23A)	110.8
C(22)-C(23)-H(23A)	110.8
C(24)-C(23)-H(23B)	110.8
C(22)-C(23)-H(23B)	110.8
H(23A)-C(23)-H(23B)	108.9
C(23)-C(24)-C(25)	103.1(8)
C(23)-C(24)-H(24A)	111.1
C(25)-C(24)-H(24A)	111.1
C(23)-C(24)-H(24B)	111.1
C(25)-C(24)-H(24B)	111.1
H(24A)-C(24)-H(24B)	109.1
C(11)-C(25)-C(24)	105.8(8)
C(11)-C(25)-H(25A)	110.6
C(24)-C(25)-H(25A)	110.6
C(11)-C(25)-H(25B)	110.6
C(24)-C(25)-H(25B)	110.6
H(25A)-C(25)-H(25B)	108.7

---

Symmetry transformations used to generate equivalent atoms:

**Table A3.2.5** Anisotropic Displacement Parameters ( $\text{\AA}^2 \times 10^3$ ) for Cyclobutane **63**. The

Anisotropic Displacement Factor Exponent Takes the Form:  $-2p^2[h^2a^{*2}U^{11} + \dots + 2hka^*b^*U^{12}]$ .

	U <sup>11</sup>	U <sup>22</sup>	U <sup>33</sup>	U <sup>23</sup>	U <sup>13</sup>	U <sup>12</sup>
Si(1)	19(1)	29(1)	32(1)	0(1)	7(1)	-1(1)
C(1)	26(4)	33(4)	24(4)	2(3)	7(3)	0(3)
C(2)	31(5)	36(5)	35(4)	3(4)	11(4)	-4(4)
C(3)	26(4)	44(5)	44(5)	-1(4)	10(4)	-13(4)
C(4)	42(6)	32(4)	39(5)	-4(4)	15(4)	-2(4)
C(5)	27(4)	41(5)	34(5)	2(4)	4(4)	-8(4)
C(6)	30(4)	34(5)	37(5)	2(3)	5(4)	-2(4)
C(7)	27(4)	41(5)	37(5)	-3(4)	10(4)	-1(4)
C(8)	20(4)	34(5)	47(5)	1(4)	11(4)	7(3)
C(11)	21(4)	31(4)	30(4)	-2(3)	10(3)	4(3)
C(12)	26(4)	32(4)	37(5)	3(4)	10(4)	7(4)
C(13)	21(4)	29(4)	31(4)	-1(3)	11(3)	0(3)
C(14)	15(3)	30(4)	34(4)	-1(3)	7(3)	-2(3)
O(1)	32(3)	38(4)	36(3)	0(3)	12(3)	9(3)
C(15)	22(4)	31(4)	28(4)	2(3)	7(3)	2(3)
C(16)	24(4)	28(4)	31(4)	2(3)	7(3)	-3(4)
C(26)	26(4)	35(5)	42(5)	-2(4)	9(4)	-1(4)
O(2)	25(3)	34(3)	35(3)	1(2)	12(3)	0(3)
C(17)	30(4)	24(4)	34(4)	-1(3)	12(3)	-1(3)
C(18)	30(4)	26(4)	33(4)	-2(3)	13(3)	-2(4)
C(19)	21(4)	29(4)	29(4)	0(3)	8(3)	2(3)
C(20)	20(4)	22(4)	40(4)	-2(3)	10(3)	5(3)
C(21)	22(4)	29(4)	31(4)	-1(3)	9(3)	6(3)
O(3)	27(3)	29(3)	32(3)	-1(2)	7(2)	2(2)
O(4)	35(4)	31(3)	37(3)	3(3)	9(3)	-1(3)
C(22)	20(4)	28(4)	33(4)	3(3)	6(3)	5(3)
C(23)	29(4)	28(4)	34(4)	0(3)	7(4)	0(4)
C(24)	26(5)	41(5)	48(6)	2(4)	4(4)	-9(4)
C(25)	32(4)	31(4)	35(4)	1(4)	3(4)	-6(4)



**Table A3.2.6** Hydrogen Coordinates ( $\times 10^4$ ) and Isotropic Displacement Parameters ( $\text{\AA}^2 \times 10^3$ ) for Cyclobutane **63**.

	x	y	z	U(eq)
H(2)	2380	4242	4806	40
H(3)	2330	4751	6369	45
H(4)	5397	4799	7547	44
H(5)	8449	4333	7144	42
H(6)	8510	3903	5559	41
H(7A)	1946	3280	3161	52
H(7B)	3004	2092	3709	52
H(7C)	3201	2367	2647	52
H(8A)	8045	2119	4244	50
H(8B)	9051	3307	3897	50
H(8C)	7785	2371	3133	50
H(12A)	2417	5398	3324	38
H(12B)	3426	6721	3180	38
H(13)	2354	4772	1789	31
H(15)	2817	6900	-124	32
H(26A)	-1691	5569	-1381	51
H(26B)	-188	6704	-1362	51
H(26C)	-1329	6524	-518	51
H(2A)	-100(200)	3860(90)	-230(80)	46
H(17A)	1573	3948	-1357	34
H(17B)	2433	5255	-1594	34
H(18)	5385	4317	-825	35
H(19)	5814	6014	96	31
H(20)	7355	4806	1316	32
H(23A)	6832	6932	1524	36
H(23B)	5462	7416	2222	36
H(24A)	8746	7459	3189	47
H(24B)	9308	6156	2792	47

**Table A3.2.6** *Cont'd*

H(25A)	8353	5450	4119	40
H(25B)	6829	6579	4125	40

---

**Table A3.2.7** Torsion Angles [°] for Cyclobutane **63**.

---

C(8)-Si(1)-C(1)-C(6)	23.2(9)
C(7)-Si(1)-C(1)-C(6)	144.2(8)
C(11)-Si(1)-C(1)-C(6)	-95.5(8)
C(8)-Si(1)-C(1)-C(2)	-156.3(8)
C(7)-Si(1)-C(1)-C(2)	-35.2(9)
C(11)-Si(1)-C(1)-C(2)	85.1(8)
C(6)-C(1)-C(2)-C(3)	1.2(15)
Si(1)-C(1)-C(2)-C(3)	-179.4(8)
C(1)-C(2)-C(3)-C(4)	-1.3(15)
C(2)-C(3)-C(4)-C(5)	-0.1(16)
C(3)-C(4)-C(5)-C(6)	1.5(16)
C(2)-C(1)-C(6)-C(5)	0.3(15)
Si(1)-C(1)-C(6)-C(5)	-179.2(8)
C(4)-C(5)-C(6)-C(1)	-1.6(16)
C(25)-C(11)-C(12)-C(13)	127.8(8)
C(22)-C(11)-C(12)-C(13)	20.7(6)
Si(1)-C(11)-C(12)-C(13)	-107.0(6)
C(11)-C(12)-C(13)-C(14)	-135.6(8)
C(11)-C(12)-C(13)-C(22)	-21.4(7)
C(12)-C(13)-C(14)-O(1)	-17.2(15)
C(22)-C(13)-C(14)-O(1)	-121.5(10)
C(12)-C(13)-C(14)-C(15)	157.4(8)
C(22)-C(13)-C(14)-C(15)	53.1(10)
O(1)-C(14)-C(15)-C(16)	-89.6(11)
C(13)-C(14)-C(15)-C(16)	95.4(8)
O(1)-C(14)-C(15)-C(19)	145.8(9)
C(13)-C(14)-C(15)-C(19)	-29.2(11)
C(14)-C(15)-C(16)-O(2)	-42.2(10)
C(19)-C(15)-C(16)-O(2)	89.0(8)
C(14)-C(15)-C(16)-C(26)	79.1(9)
C(19)-C(15)-C(16)-C(26)	-149.6(8)
C(14)-C(15)-C(16)-C(17)	-159.0(7)

**Table A3.2.7** *Cont'd*

C(19)-C(15)-C(16)-C(17)	-27.8(8)
O(2)-C(16)-C(17)-C(18)	-77.6(9)
C(26)-C(16)-C(17)-C(18)	159.5(7)
C(15)-C(16)-C(17)-C(18)	38.5(8)
C(16)-C(17)-C(18)-O(3)	79.1(8)
C(16)-C(17)-C(18)-C(19)	-34.6(9)
O(3)-C(18)-C(19)-C(20)	22.3(8)
C(17)-C(18)-C(19)-C(20)	140.8(7)
O(3)-C(18)-C(19)-C(15)	-102.6(7)
C(17)-C(18)-C(19)-C(15)	16.0(9)
C(14)-C(15)-C(19)-C(18)	134.4(8)
C(16)-C(15)-C(19)-C(18)	7.8(9)
C(14)-C(15)-C(19)-C(20)	18.7(11)
C(16)-C(15)-C(19)-C(20)	-107.9(8)
C(18)-C(19)-C(20)-C(22)	-147.5(7)
C(15)-C(19)-C(20)-C(22)	-31.4(10)
C(18)-C(19)-C(20)-C(21)	-20.7(8)
C(15)-C(19)-C(20)-C(21)	95.4(8)
C(22)-C(20)-C(21)-O(4)	-51.9(12)
C(19)-C(20)-C(21)-O(4)	-171.5(9)
C(22)-C(20)-C(21)-O(3)	132.0(8)
C(19)-C(20)-C(21)-O(3)	12.4(8)
O(4)-C(21)-O(3)-C(18)	-174.6(8)
C(20)-C(21)-O(3)-C(18)	1.9(9)
C(17)-C(18)-O(3)-C(21)	-129.8(7)
C(19)-C(18)-O(3)-C(21)	-15.7(9)
C(21)-C(20)-C(22)-C(13)	-59.4(10)
C(19)-C(20)-C(22)-C(13)	57.0(9)
C(21)-C(20)-C(22)-C(23)	176.1(7)
C(19)-C(20)-C(22)-C(23)	-67.6(8)
C(21)-C(20)-C(22)-C(11)	51.8(13)
C(19)-C(20)-C(22)-C(11)	168.1(9)
C(14)-C(13)-C(22)-C(20)	-71.5(10)
C(12)-C(13)-C(22)-C(20)	159.0(7)

**Table A3.2.7** Cont'd

C(14)-C(13)-C(22)-C(23)	50.1(10)
C(12)-C(13)-C(22)-C(23)	-79.4(8)
C(14)-C(13)-C(22)-C(11)	150.8(7)
C(12)-C(13)-C(22)-C(11)	21.3(7)
C(25)-C(11)-C(22)-C(20)	105.0(10)
C(12)-C(11)-C(22)-C(20)	-140.7(10)
Si(1)-C(11)-C(22)-C(20)	-29.5(13)
C(25)-C(11)-C(22)-C(13)	-134.9(7)
C(12)-C(11)-C(22)-C(13)	-20.6(7)
Si(1)-C(11)-C(22)-C(13)	90.6(8)
C(25)-C(11)-C(22)-C(23)	-21.8(8)
C(12)-C(11)-C(22)-C(23)	92.4(7)
Si(1)-C(11)-C(22)-C(23)	-156.3(7)
C(20)-C(22)-C(23)-C(24)	-103.1(8)
C(13)-C(22)-C(23)-C(24)	132.9(8)
C(11)-C(22)-C(23)-C(24)	39.6(9)
C(22)-C(23)-C(24)-C(25)	-43.1(10)
C(12)-C(11)-C(25)-C(24)	-96.0(9)
C(22)-C(11)-C(25)-C(24)	-3.4(10)
Si(1)-C(11)-C(25)-C(24)	139.2(7)
C(23)-C(24)-C(25)-C(11)	28.0(10)

---

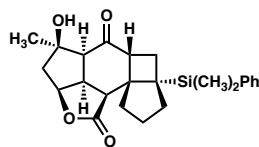
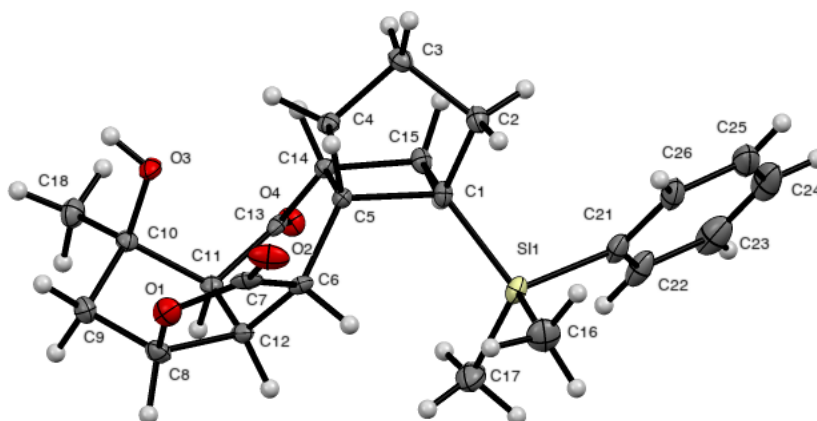
Symmetry transformations used to generate equivalent atoms:

**Table A3.2.8** Hydrogen Bonds for Cyclobutane **63** [ $\text{\AA}$  and  $^\circ$ ].

D-H...A	d(D-H)	d(H...A)	d(D...A)	$\angle$ (DHA)
C(13)-H(13)...O(2)	1.00	2.49	3.079(11)	116.9
C(15)-H(15)...O(3)#1	1.00	2.50	3.246(11)	130.8
O(2)-H(2A)...O(1)#2	0.83(3)	2.16(3)	2.996(10)	178(15)
C(17)-H(17A)...O(1)#2	0.99	2.58	3.430(11)	143.8
C(19)-H(19)...O(3)#1	1.00	2.52	3.267(11)	131.5

Symmetry transformations used to generate equivalent atoms:

#1  $-x+1, y+1/2, -z$  #2  $-x, y-1/2, -z$

**A3.3 X-RAY CRYSTAL STRUCTURE ANALYSIS OF CYCLOBUTANE 64****64**Contents*Table A3.3.1. Experimental Details**Table A3.3.2. Crystal Data**Table A3.3.3. Atomic Coordinates**Table A3.3.4. Full Bond Distances and Angles**Table A3.3.5. Anisotropic Displacement Parameters**Table A3.3.6. Hydrogen Atomic Coordinates**Table A3.3.7. Torsion Angles**Table A3.3.8. Hydrogen Bond Distances and Angles***Figure A3.3.1** X-Ray Crystal Structure of Cyclobutane **64**.

**Table A3.3.1** Experimental Details for X-Ray Structure Determination of Cyclobutane**64.**

Low-temperature diffraction data ( $\phi$ - and  $\omega$ -scans) were collected on a Bruker AXS KAPPA APEX II diffractometer coupled to an PHOTON 100 CMOS detector with graphite monochromated Mo  $K_{\alpha}$  radiation ( $\lambda = 0.71073 \text{ \AA}$ ) for the structure of compound **64**. The structure was solved by direct methods using SHELXS and refined against  $F^2$  on all data by full-matrix least squares with SHELXL-2017 using established refinement techniques. All non-hydrogen atoms were refined anisotropically. All hydrogen atoms were included into the model at geometrically calculated positions and refined using a riding model. The isotropic displacement parameters of all hydrogen atoms were fixed to 1.2 times the  $U$  value of the atoms they are linked to (1.5 times for methyl groups).

Compound **64** crystallizes in the monoclinic space group  $P2_1$  with one molecule in the asymmetric unit. The molecule was refined with a disordered hydroxide.



**Table A3.3.2** Crystal Data and Structure Refinement for Cyclobutane **64**.

Empirical formula	C <sub>24</sub> H <sub>30</sub> O <sub>4</sub> .16 Si
Formula weight	413.21
Temperature	100(2) K
Wavelength	0.71073 Å
Crystal system	Monoclinic
Space group	P2 <sub>1</sub>
Unit cell dimensions	a = 7.267(3) Å                      a = 90°. b = 9.667(3) Å                      b = 99.237(16)°. c = 15.436(4) Å                      g = 90°.
Volume	1070.3(7) Å <sup>3</sup>
Z	2
Density (calculated)	1.282 Mg/m <sup>3</sup>
Absorption coefficient	0.138 mm <sup>-1</sup>
F(000)	443
Crystal size	0.300 x 0.100 x 0.050 mm <sup>3</sup>
Theta range for data collection	2.495 to 30.501°.
Index ranges	-10<=h<=9, -13<=k<=13, -22<=l<=22
Reflections collected	16781
Independent reflections	5995 [R(int) = 0.0322]
Completeness to theta = 25.242°	99.7 %
Absorption correction	Semi-empirical from equivalents
Max. and min. transmission	0.7466 and 0.6535
Refinement method	Full-matrix least-squares on F <sup>2</sup>
Data / restraints / parameters	5995 / 2 / 280
Goodness-of-fit on F <sup>2</sup>	1.024
Final R indices [I>2sigma(I)]	R1 = 0.0392, wR2 = 0.0861
R indices (all data)	R1 = 0.0494, wR2 = 0.0897
Absolute structure parameter	0.04(4)
Extinction coefficient	n/a
Largest diff. peak and hole	0.316 and -0.247 e.Å <sup>-3</sup>

**Table A3.3.3** Atomic Coordinates ( $\times 10^4$ ) and Equivalent Isotropic Displacement Parameters ( $\text{\AA}^2 \times 10^3$ ) for Cyclobutane **64**.  $U(\text{eq})$  is Defined as One Third of the Trace of the Orthogonalized  $U^{ij}$  Tensor.

	x	y	z	U(eq)
Si(1)	4386(1)	6279(1)	8522(1)	15(1)
C(1)	3245(3)	4685(2)	7973(1)	12(1)
C(2)	3535(3)	3370(2)	8547(1)	17(1)
C(3)	2928(3)	2185(2)	7909(1)	16(1)
C(4)	3789(3)	2600(2)	7113(1)	12(1)
C(5)	3459(3)	4173(2)	7001(1)	10(1)
C(6)	4859(3)	4923(2)	6488(1)	12(1)
O(6B)	6250(11)	5648(9)	7055(5)	9(3)
C(7)	6204(3)	3975(2)	6103(2)	17(1)
O(1)	6138(2)	4182(2)	5238(1)	20(1)
O(2)	7296(2)	3157(2)	6489(1)	24(1)
C(8)	5001(3)	5372(2)	4925(1)	17(1)
C(9)	3445(3)	4958(2)	4187(1)	18(1)
C(10)	1752(3)	4665(2)	4626(1)	13(1)
C(18)	-89(3)	4728(2)	4002(1)	19(1)
O(3)	1978(2)	3371(2)	5078(1)	15(1)
C(11)	1954(3)	5803(2)	5343(1)	12(1)
C(12)	4054(3)	5873(2)	5706(1)	13(1)
C(13)	749(3)	5568(2)	6031(1)	12(1)
O(4)	-691(2)	6223(2)	6041(1)	17(1)
C(14)	1345(3)	4496(2)	6715(1)	11(1)
C(15)	1116(3)	4936(2)	7652(1)	14(1)
C(16)	6926(3)	6088(3)	8901(2)	27(1)
C(17)	3947(4)	7835(3)	7791(2)	26(1)
C(21)	3208(3)	6548(2)	9508(1)	19(1)
C(22)	1903(3)	7607(3)	9547(2)	25(1)
C(23)	1014(4)	7768(3)	10273(2)	35(1)

**Table A3.3.3** *Cont'd*

C(24)	1401(4)	6871(3)	10974(2)	37(1)
C(25)	2668(4)	5819(3)	10955(2)	30(1)
C(26)	3574(3)	5662(3)	10235(1)	23(1)

---

**Table A3.3.4** Bond Lengths [ $\text{\AA}$ ] and angles [ $^\circ$ ] for Cyclobutane **64**.

---

Si(1)-C(16)	1.853(2)
Si(1)-C(17)	1.877(3)
Si(1)-C(21)	1.881(2)
Si(1)-C(1)	1.886(2)
C(1)-C(2)	1.545(3)
C(1)-C(15)	1.566(3)
C(1)-C(5)	1.611(3)
C(2)-C(3)	1.529(3)
C(2)-H(2A)	0.9900
C(2)-H(2B)	0.9900
C(3)-C(4)	1.520(3)
C(3)-H(3A)	0.9900
C(3)-H(3B)	0.9900
C(4)-C(5)	1.545(3)
C(4)-H(4A)	0.9900
C(4)-H(4B)	0.9900
C(5)-C(14)	1.561(3)
C(5)-C(6)	1.564(3)
C(6)-O(6B)	1.412(8)
C(6)-C(7)	1.529(3)
C(6)-C(12)	1.554(3)
C(6)-H(6)	1.0000
O(6B)-H(6OB)	0.8400
C(7)-O(2)	1.207(3)
C(7)-O(1)	1.343(3)
O(1)-C(8)	1.452(3)
C(8)-C(9)	1.525(3)
C(8)-C(12)	1.558(3)
C(8)-H(8)	1.0000
C(9)-C(10)	1.524(3)
C(9)-H(9A)	0.9900
C(9)-H(9B)	0.9900

**Table A3.3.4** *Cont'd*

C(10)-O(3)	1.430(2)
C(10)-C(18)	1.519(3)
C(10)-C(11)	1.551(3)
C(18)-H(18A)	0.9800
C(18)-H(18B)	0.9800
C(18)-H(18C)	0.9800
O(3)-H(3O)	0.81(2)
C(11)-C(13)	1.499(3)
C(11)-C(12)	1.541(3)
C(11)-H(11)	1.0000
C(12)-H(12)	1.0000
C(13)-O(4)	1.225(2)
C(13)-C(14)	1.492(3)
C(14)-C(15)	1.542(3)
C(14)-H(14)	1.0000
C(15)-H(15A)	0.9900
C(15)-H(15B)	0.9900
C(16)-H(16A)	0.9800
C(16)-H(16B)	0.9800
C(16)-H(16C)	0.9800
C(17)-H(17A)	0.9800
C(17)-H(17B)	0.9800
C(17)-H(17C)	0.9800
C(21)-C(26)	1.403(3)
C(21)-C(22)	1.403(3)
C(22)-C(23)	1.390(3)
C(22)-H(22)	0.9500
C(23)-C(24)	1.380(5)
C(23)-H(23)	0.9500
C(24)-C(25)	1.375(4)
C(24)-H(24)	0.9500
C(25)-C(26)	1.387(3)
C(25)-H(25)	0.9500
C(26)-H(26)	0.9500

**Table A3.3.4** *Cont'd*

C(16)-Si(1)-C(17)	109.50(13)
C(16)-Si(1)-C(21)	108.58(11)
C(17)-Si(1)-C(21)	108.67(11)
C(16)-Si(1)-C(1)	113.85(11)
C(17)-Si(1)-C(1)	111.37(10)
C(21)-Si(1)-C(1)	104.63(10)
C(2)-C(1)-C(15)	110.28(17)
C(2)-C(1)-C(5)	104.92(16)
C(15)-C(1)-C(5)	89.47(14)
C(2)-C(1)-Si(1)	113.87(14)
C(15)-C(1)-Si(1)	110.89(13)
C(5)-C(1)-Si(1)	124.62(14)
C(3)-C(2)-C(1)	104.36(16)
C(3)-C(2)-H(2A)	110.9
C(1)-C(2)-H(2A)	110.9
C(3)-C(2)-H(2B)	110.9
C(1)-C(2)-H(2B)	110.9
H(2A)-C(2)-H(2B)	108.9
C(4)-C(3)-C(2)	102.09(17)
C(4)-C(3)-H(3A)	111.4
C(2)-C(3)-H(3A)	111.4
C(4)-C(3)-H(3B)	111.4
C(2)-C(3)-H(3B)	111.4
H(3A)-C(3)-H(3B)	109.2
C(3)-C(4)-C(5)	105.86(16)
C(3)-C(4)-H(4A)	110.6
C(5)-C(4)-H(4A)	110.6
C(3)-C(4)-H(4B)	110.6
C(5)-C(4)-H(4B)	110.6
H(4A)-C(4)-H(4B)	108.7
C(4)-C(5)-C(14)	110.87(16)
C(4)-C(5)-C(6)	114.26(16)
C(14)-C(5)-C(6)	117.03(16)

**Table A3.3.4** Cont'd

C(4)-C(5)-C(1)	103.58(15)
C(14)-C(5)-C(1)	87.97(14)
C(6)-C(5)-C(1)	119.85(16)
O(6B)-C(6)-C(7)	95.7(4)
O(6B)-C(6)-C(12)	109.3(4)
C(7)-C(6)-C(12)	103.69(16)
O(6B)-C(6)-C(5)	112.1(4)
C(7)-C(6)-C(5)	115.31(17)
C(12)-C(6)-C(5)	118.24(16)
C(7)-C(6)-H(6)	106.2
C(12)-C(6)-H(6)	106.2
C(5)-C(6)-H(6)	106.2
C(6)-O(6B)-H(6OB)	109.5
O(2)-C(7)-O(1)	120.3(2)
O(2)-C(7)-C(6)	127.7(2)
O(1)-C(7)-C(6)	111.93(18)
C(7)-O(1)-C(8)	112.11(17)
O(1)-C(8)-C(9)	110.79(18)
O(1)-C(8)-C(12)	106.70(16)
C(9)-C(8)-C(12)	107.08(18)
O(1)-C(8)-H(8)	110.7
C(9)-C(8)-H(8)	110.7
C(12)-C(8)-H(8)	110.7
C(10)-C(9)-C(8)	105.72(17)
C(10)-C(9)-H(9A)	110.6
C(8)-C(9)-H(9A)	110.6
C(10)-C(9)-H(9B)	110.6
C(8)-C(9)-H(9B)	110.6
H(9A)-C(9)-H(9B)	108.7
O(3)-C(10)-C(18)	111.44(17)
O(3)-C(10)-C(9)	110.04(17)
C(18)-C(10)-C(9)	113.72(17)
O(3)-C(10)-C(11)	106.37(15)
C(18)-C(10)-C(11)	113.38(17)

**Table A3.3.4** *Cont'd*

C(9)-C(10)-C(11)	101.23(16)
C(10)-C(18)-H(18A)	109.5
C(10)-C(18)-H(18B)	109.5
H(18A)-C(18)-H(18B)	109.5
C(10)-C(18)-H(18C)	109.5
H(18A)-C(18)-H(18C)	109.5
H(18B)-C(18)-H(18C)	109.5
C(10)-O(3)-H(3O)	110.9(19)
C(13)-C(11)-C(12)	113.93(16)
C(13)-C(11)-C(10)	113.52(17)
C(12)-C(11)-C(10)	105.39(16)
C(13)-C(11)-H(11)	107.9
C(12)-C(11)-H(11)	107.9
C(10)-C(11)-H(11)	107.9
C(11)-C(12)-C(6)	118.97(16)
C(11)-C(12)-C(8)	103.86(16)
C(6)-C(12)-C(8)	105.05(16)
C(11)-C(12)-H(12)	109.5
C(6)-C(12)-H(12)	109.5
C(8)-C(12)-H(12)	109.5
O(4)-C(13)-C(14)	120.14(18)
O(4)-C(13)-C(11)	121.80(18)
C(14)-C(13)-C(11)	118.06(17)
C(13)-C(14)-C(15)	114.11(17)
C(13)-C(14)-C(5)	119.99(17)
C(15)-C(14)-C(5)	92.24(14)
C(13)-C(14)-H(14)	109.7
C(15)-C(14)-H(14)	109.7
C(5)-C(14)-H(14)	109.7
C(14)-C(15)-C(1)	90.25(15)
C(14)-C(15)-H(15A)	113.6
C(1)-C(15)-H(15A)	113.6
C(14)-C(15)-H(15B)	113.6
C(1)-C(15)-H(15B)	113.6



**Table A3.3.4** Cont'd

H(15A)-C(15)-H(15B)	110.9
Si(1)-C(16)-H(16A)	109.5
Si(1)-C(16)-H(16B)	109.5
H(16A)-C(16)-H(16B)	109.5
Si(1)-C(16)-H(16C)	109.5
H(16A)-C(16)-H(16C)	109.5
H(16B)-C(16)-H(16C)	109.5
Si(1)-C(17)-H(17A)	109.5
Si(1)-C(17)-H(17B)	109.5
H(17A)-C(17)-H(17B)	109.5
Si(1)-C(17)-H(17C)	109.5
H(17A)-C(17)-H(17C)	109.5
H(17B)-C(17)-H(17C)	109.5
C(26)-C(21)-C(22)	117.0(2)
C(26)-C(21)-Si(1)	120.69(17)
C(22)-C(21)-Si(1)	122.26(19)
C(23)-C(22)-C(21)	121.4(3)
C(23)-C(22)-H(22)	119.3
C(21)-C(22)-H(22)	119.3
C(24)-C(23)-C(22)	120.0(3)
C(24)-C(23)-H(23)	120.0
C(22)-C(23)-H(23)	120.0
C(25)-C(24)-C(23)	120.0(2)
C(25)-C(24)-H(24)	120.0
C(23)-C(24)-H(24)	120.0
C(24)-C(25)-C(26)	120.3(3)
C(24)-C(25)-H(25)	119.9
C(26)-C(25)-H(25)	119.9
C(25)-C(26)-C(21)	121.4(2)
C(25)-C(26)-H(26)	119.3
C(21)-C(26)-H(26)	119.3

---

Symmetry transformations used to generate equivalent atoms:

**Table A3.3.5** Anisotropic Displacement Parameters ( $\text{\AA}^2 \times 10^3$ ) for Cyclobutane **64**. The

Anisotropic Displacement Factor Exponent Takes the Form:  $-2p^2[h^2a^*2U^{11} + \dots + 2hka^*b^*U^{12}]$ .

	$U^{11}$	$U^{22}$	$U^{33}$	$U^{23}$	$U^{13}$	$U^{12}$
Si(1)	15(1)	15(1)	14(1)	-4(1)	1(1)	1(1)
C(1)	13(1)	14(1)	10(1)	-1(1)	1(1)	3(1)
C(2)	20(1)	17(1)	13(1)	1(1)	3(1)	2(1)
C(3)	18(1)	14(1)	16(1)	2(1)	5(1)	1(1)
C(4)	14(1)	10(1)	14(1)	-1(1)	3(1)	1(1)
C(5)	11(1)	10(1)	10(1)	-1(1)	1(1)	-1(1)
C(6)	10(1)	10(1)	16(1)	-1(1)	1(1)	-3(1)
O(6B)	4(4)	15(5)	9(4)	-3(3)	2(3)	-1(3)
C(7)	11(1)	14(1)	28(1)	0(1)	7(1)	-5(1)
O(1)	16(1)	22(1)	24(1)	-4(1)	8(1)	1(1)
O(2)	12(1)	21(1)	42(1)	7(1)	8(1)	1(1)
C(8)	17(1)	18(1)	18(1)	1(1)	8(1)	-3(1)
C(9)	22(1)	19(1)	14(1)	-1(1)	6(1)	-2(1)
C(10)	15(1)	11(1)	12(1)	1(1)	2(1)	1(1)
C(18)	21(1)	21(1)	16(1)	0(1)	-1(1)	1(1)
O(3)	21(1)	10(1)	13(1)	-1(1)	1(1)	-1(1)
C(11)	14(1)	9(1)	13(1)	1(1)	2(1)	0(1)
C(12)	14(1)	11(1)	15(1)	-1(1)	5(1)	-2(1)
C(13)	14(1)	8(1)	13(1)	-3(1)	-1(1)	0(1)
O(4)	14(1)	18(1)	18(1)	2(1)	3(1)	5(1)
C(14)	10(1)	11(1)	11(1)	-1(1)	2(1)	0(1)
C(15)	16(1)	15(1)	12(1)	0(1)	3(1)	2(1)
C(16)	16(1)	35(2)	29(1)	-1(1)	2(1)	-2(1)
C(17)	37(2)	18(1)	24(1)	-2(1)	3(1)	-1(1)
C(21)	14(1)	23(1)	18(1)	-10(1)	2(1)	-2(1)
C(22)	16(1)	29(1)	29(1)	-14(1)	0(1)	-1(1)
C(23)	18(1)	41(2)	47(2)	-23(1)	11(1)	-4(1)

**Table A3.3.5** *Cont'd*

C(24)	26(1)	51(2)	38(1)	-24(1)	21(1)	-12(1)
C(25)	32(1)	38(2)	23(1)	-10(1)	11(1)	-13(1)
C(26)	21(1)	29(1)	19(1)	-9(1)	5(1)	-4(1)

---

**Table A3.3.6** Hydrogen Coordinates ( $\times 10^4$ ) and Isotropic Displacement Parameters ( $\text{\AA}^2 \times 10^3$ ) for Cyclobutane **64**.

	x	y	z	U(eq)
H(2A)	4860	3268	8816	20
H(2B)	2760	3400	9019	20
H(3A)	3424	1287	8151	19
H(3B)	1553	2127	7765	19
H(4A)	3185	2097	6584	15
H(4B)	5140	2390	7209	15
H(6)	5647	5529	6924	15
H(6OB)	6985	6026	6759	90(90)
H(8)	5785	6123	4729	20
H(9A)	3177	5718	3754	21
H(9B)	3801	4124	3881	21
H(18A)	-81	4048	3531	29
H(18B)	-260	5657	3747	29
H(18C)	-1113	4520	4324	29
H(3O)	1630(40)	2740(20)	4749(16)	22
H(11)	1581	6705	5049	15
H(12)	4418	6853	5851	15
H(14)	646	3617	6555	13
H(15A)	297	4314	7928	17
H(15B)	733	5913	7695	17
H(16A)	7531	5787	8409	40
H(16B)	7141	5397	9371	40
H(16C)	7449	6978	9122	40
H(17A)	4148	8677	8147	40
H(17B)	2659	7815	7483	40
H(17C)	4805	7824	7362	40
H(22)	1622	8227	9066	30
H(23)	140	8495	10287	42

**Table A3.3.6** *Cont'd*

H(24)	792	6979	11471	44
H(25)	2924	5197	11436	36
H(26)	4461	4941	10235	27

---

**Table A3.3.7** Torsion Angles [°] for Cyclobutane **64**.

---

C(16)-Si(1)-C(1)-C(2)	56.33(18)
C(17)-Si(1)-C(1)-C(2)	-179.28(15)
C(21)-Si(1)-C(1)-C(2)	-62.05(17)
C(16)-Si(1)-C(1)-C(15)	-178.59(14)
C(17)-Si(1)-C(1)-C(15)	-54.20(17)
C(21)-Si(1)-C(1)-C(15)	63.02(15)
C(16)-Si(1)-C(1)-C(5)	-74.03(18)
C(17)-Si(1)-C(1)-C(5)	50.4(2)
C(21)-Si(1)-C(1)-C(5)	167.59(16)
C(15)-C(1)-C(2)-C(3)	67.9(2)
C(5)-C(1)-C(2)-C(3)	-27.2(2)
Si(1)-C(1)-C(2)-C(3)	-166.73(14)
C(1)-C(2)-C(3)-C(4)	42.6(2)
C(2)-C(3)-C(4)-C(5)	-42.0(2)
C(3)-C(4)-C(5)-C(14)	-68.47(19)
C(3)-C(4)-C(5)-C(6)	156.67(16)
C(3)-C(4)-C(5)-C(1)	24.6(2)
C(2)-C(1)-C(5)-C(4)	1.8(2)
C(15)-C(1)-C(5)-C(4)	-109.09(16)
Si(1)-C(1)-C(5)-C(4)	135.63(15)
C(2)-C(1)-C(5)-C(14)	112.77(17)
C(15)-C(1)-C(5)-C(14)	1.90(15)
Si(1)-C(1)-C(5)-C(14)	-113.38(16)
C(2)-C(1)-C(5)-C(6)	-126.96(19)
C(15)-C(1)-C(5)-C(6)	122.16(18)
Si(1)-C(1)-C(5)-C(6)	6.9(2)
C(4)-C(5)-C(6)-O(6B)	-102.5(4)
C(14)-C(5)-C(6)-O(6B)	125.6(4)
C(1)-C(5)-C(6)-O(6B)	21.3(4)
C(4)-C(5)-C(6)-C(7)	5.6(2)
C(14)-C(5)-C(6)-C(7)	-126.37(19)
C(1)-C(5)-C(6)-C(7)	129.33(19)

**Table A3.3.7** Cont'd

C(4)-C(5)-C(6)-C(12)	129.03(18)
C(14)-C(5)-C(6)-C(12)	-2.9(2)
C(1)-C(5)-C(6)-C(12)	-107.2(2)
O(6B)-C(6)-C(7)-O(2)	60.3(4)
C(12)-C(6)-C(7)-O(2)	171.8(2)
C(5)-C(6)-C(7)-O(2)	-57.4(3)
O(6B)-C(6)-C(7)-O(1)	-116.5(4)
C(12)-C(6)-C(7)-O(1)	-5.0(2)
C(5)-C(6)-C(7)-O(1)	125.80(18)
O(2)-C(7)-O(1)-C(8)	-169.35(19)
C(6)-C(7)-O(1)-C(8)	7.8(2)
C(7)-O(1)-C(8)-C(9)	-123.23(18)
C(7)-O(1)-C(8)-C(12)	-7.0(2)
O(1)-C(8)-C(9)-C(10)	94.2(2)
C(12)-C(8)-C(9)-C(10)	-21.8(2)
C(8)-C(9)-C(10)-O(3)	-74.5(2)
C(8)-C(9)-C(10)-C(18)	159.71(18)
C(8)-C(9)-C(10)-C(11)	37.8(2)
O(3)-C(10)-C(11)-C(13)	-50.7(2)
C(18)-C(10)-C(11)-C(13)	72.2(2)
C(9)-C(10)-C(11)-C(13)	-165.64(17)
O(3)-C(10)-C(11)-C(12)	74.70(19)
C(18)-C(10)-C(11)-C(12)	-162.48(17)
C(9)-C(10)-C(11)-C(12)	-40.28(19)
C(13)-C(11)-C(12)-C(6)	36.0(2)
C(10)-C(11)-C(12)-C(6)	-89.1(2)
C(13)-C(11)-C(12)-C(8)	152.21(17)
C(10)-C(11)-C(12)-C(8)	27.10(19)
O(6B)-C(6)-C(12)-C(11)	-142.6(4)
C(7)-C(6)-C(12)-C(11)	116.25(18)
C(5)-C(6)-C(12)-C(11)	-12.8(3)
O(6B)-C(6)-C(12)-C(8)	101.8(4)
C(7)-C(6)-C(12)-C(8)	0.6(2)
C(5)-C(6)-C(12)-C(8)	-128.44(18)

**Table A7.3.3** *Cont'd*

O(1)-C(8)-C(12)-C(11)	-122.18(17)
C(9)-C(8)-C(12)-C(11)	-3.5(2)
O(1)-C(8)-C(12)-C(6)	3.5(2)
C(9)-C(8)-C(12)-C(6)	122.15(18)
C(12)-C(11)-C(13)-O(4)	135.85(19)
C(10)-C(11)-C(13)-O(4)	-103.5(2)
C(12)-C(11)-C(13)-C(14)	-44.4(2)
C(10)-C(11)-C(13)-C(14)	76.2(2)
O(4)-C(13)-C(14)-C(15)	-42.7(3)
C(11)-C(13)-C(14)-C(15)	137.55(18)
O(4)-C(13)-C(14)-C(5)	-150.63(19)
C(11)-C(13)-C(14)-C(5)	29.6(3)
C(4)-C(5)-C(14)-C(13)	-138.52(18)
C(6)-C(5)-C(14)-C(13)	-5.0(3)
C(1)-C(5)-C(14)-C(13)	117.72(18)
C(4)-C(5)-C(14)-C(15)	101.83(17)
C(6)-C(5)-C(14)-C(15)	-124.68(17)
C(1)-C(5)-C(14)-C(15)	-1.93(15)
C(13)-C(14)-C(15)-C(1)	-122.46(17)
C(5)-C(14)-C(15)-C(1)	1.98(16)
C(2)-C(1)-C(15)-C(14)	-107.64(17)
C(5)-C(1)-C(15)-C(14)	-1.92(15)
Si(1)-C(1)-C(15)-C(14)	125.28(14)
C(16)-Si(1)-C(21)-C(26)	-49.7(2)
C(17)-Si(1)-C(21)-C(26)	-168.77(18)
C(1)-Si(1)-C(21)-C(26)	72.18(19)
C(16)-Si(1)-C(21)-C(22)	131.85(19)
C(17)-Si(1)-C(21)-C(22)	12.8(2)
C(1)-Si(1)-C(21)-C(22)	-106.24(19)
C(26)-C(21)-C(22)-C(23)	-0.1(3)
Si(1)-C(21)-C(22)-C(23)	178.40(18)
C(21)-C(22)-C(23)-C(24)	-0.3(4)
C(22)-C(23)-C(24)-C(25)	0.1(4)
C(23)-C(24)-C(25)-C(26)	0.6(4)



**Table A7.3.3** *Cont'd*

C(24)-C(25)-C(26)-C(21)	-1.0(4)
C(22)-C(21)-C(26)-C(25)	0.8(3)
Si(1)-C(21)-C(26)-C(25)	-177.75(18)

---

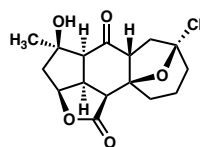
Symmetry transformations used to generate equivalent atoms:

**Table A3.3.8** Hydrogen Bonds for Cyclobutane **64** [ $\text{\AA}$  and  $^\circ$ ].

D-H...A	d(D-H)	d(H...A)	d(D...A)	$\angle$ (DHA)
C(9)-H(9A)...O(2)#1	0.99	2.40	3.280(3)	147.2
C(18)-H(18C)...O(1)#2	0.98	2.64	3.622(3)	175.1
O(3)-H(3O)...O(4)#3	0.81(2)	1.96(2)	2.766(2)	177(3)
C(14)-H(14)...O(2)#2	1.00	2.46	3.182(3)	128.6

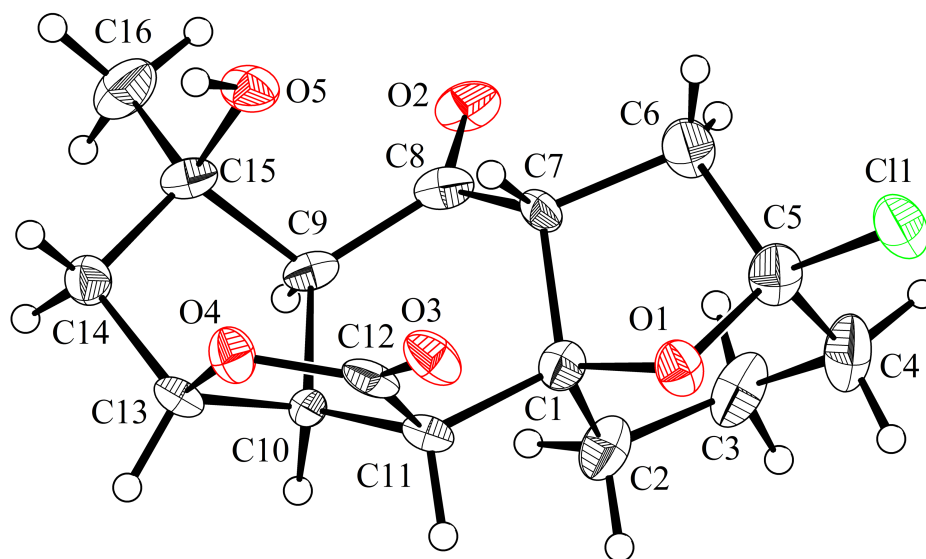
Symmetry transformations used to generate equivalent atoms:

#1  $-x+1, y+1/2, -z+1$  #2  $x-1, y, z$  #3  $-x, y-1/2, -z+1$

**A7.4 X-RAY CRYSTAL STRUCTURE ANALYSIS OF CYCLOHEPTANE 72**

72

Contents*Table A3.4.1. Experimental Details**Table A3.4.2. Crystal Data**Table A3.4.3. Atomic Coordinates**Table A3.4.4. Full Bond Distances and Angles**Table A3.4.5. Anisotropic Displacement Parameters**Table A3.4.6. Hydrogen Atomic Coordinates**Table A3.4.7. Torsion Angles**Table A3.4.8. Hydrogen Bond Distances and Angles*

**Figure A3.4.1** X-Ray Crystal Structure of Cycloheptane **72**.**Table A3.4.1** Experimental Details for X-Ray Structure Determination of Cycloheptane **72***Refinement details*

A crystal was mounted on a polyimide MiTeGen loop with STP Oil Treatment and placed under a nitrogen stream. Low temperature (100K) X-ray data were collected with a Bruker AXS D8 VENTURE KAPPA diffractometer running at 50 kV and 1mA (Cu  $K_{\alpha}$  = 1.54178 Å; PHOTON II CPAD detector and Helios focusing multilayer mirror optics). All diffractometer manipulations, including data collection, integration, and scaling were carried out using the Bruker APEX3 software. An absorption correction was applied using SADABS. The space group was determined and the structure solved by intrinsic phasing using XT. Refinement was full-matrix least squares on  $F^2$  using XL. All non-hydrogen atoms (except the carbon of a disordered chloroform) were refined using anisotropic displacement parameters. Hydrogen atoms were placed in idealized positions and refined

using a riding model. The isotropic displacement parameters of all hydrogen atoms were fixed at 1.2 times (1.5 times for methyl groups) the  $U_{eq}$  value of the bonded atom.

*Special refinement details*

Compound **72** crystallizes in the monoclinic space group  $C2$  with two molecules, one water molecule, and 38% of a chloroform in the asymmetric unit. The structure was refined as a two-component twin (refined ratio of 85:15) on an HKLF 5 file generated by PLATON.

**Table A3.4.2** Crystal Data and Structure Refinement for Cycloheptane 72

Empirical formula	C16.19 H20.19 Cl1.59 O5.50
Formula weight	359.09
Temperature	100 K
Wavelength	1.54178 Å
Crystal system	Monoclinic
Space group	C 1 2 1
Unit cell dimensions	a = 34.102(5) Å                      a = 90° b = 14.485(2) Å                      b = 94.960(10)° c = 6.6087(11) Å                      g = 90°
Volume	3252.2(9) Å <sup>3</sup>
Z	8
Density (calculated)	1.467 g/cm <sup>3</sup>
Absorption coefficient	3.208 mm <sup>-1</sup>
F(000)	1507
Crystal size	0.11 x 0.04 x 0.03 mm <sup>3</sup>
Theta range for data collection	3.317 to 76.122°.
Index ranges	-41 ≤ h ≤ 40, -17 ≤ k ≤ 17, 0 ≤ l ≤ 8
Reflections collected	6144
Independent reflections	6144 [R(int) = ?]
Completeness to theta = 67.679°	98.9 %
Absorption correction	Semi-empirical from equivalents
Max. and min. transmission	0.9904 and 0.7072
Refinement method	Full-matrix least-squares on F <sup>2</sup>
Data / restraints / parameters	6144 / 4 / 434
Goodness-of-fit on F <sup>2</sup>	1.065
Final R indices [I > 2σ(I)]	R1 = 0.0840, wR2 = 0.2207
R indices (all data)	R1 = 0.0969, wR2 = 0.2291
Absolute structure parameter [Flack]	0.163(12)
Extinction coefficient	n/a
Largest diff. peak and hole	0.708 and -0.538 e.Å <sup>-3</sup>

**Table A3.4.3** Atomic Coordinates ( $\times 10^4$ ) and Equivalent Isotropic Displacement Parameters ( $\text{\AA}^2 \times 10^3$ ) for Cycloheptane **72**.  $U(\text{eq})$  is Defined as One Third of the Trace of the Orthogonalized  $U^{ij}$  Tensor.

	x	y	z	U(eq)
Cl(1)	6462(1)	349(2)	11229(4)	36(1)
O(1)	6294(2)	1950(4)	12668(10)	25(1)
O(2)	5281(2)	2980(5)	8327(10)	29(2)
O(3)	6853(2)	3559(5)	11901(10)	28(1)
O(4)	6508(2)	4844(4)	11323(10)	25(1)
O(5)	6000(2)	4396(5)	7538(10)	27(1)
C(1)	6013(2)	2698(6)	12313(13)	23(2)
C(2)	5664(3)	2506(7)	13588(15)	31(2)
C(3)	5480(3)	1561(8)	13098(18)	38(2)
C(4)	5790(3)	823(7)	12868(19)	40(3)
C(5)	6094(3)	1208(7)	11574(16)	30(2)
C(6)	5924(3)	1617(7)	9532(16)	32(2)
C(7)	5919(3)	2650(6)	10038(12)	21(2)
C(8)	5562(3)	3240(7)	9446(13)	25(2)
C(9)	5591(2)	4203(6)	10287(12)	21(2)
C(10)	5876(3)	4396(6)	12246(13)	19(2)
C(11)	6178(2)	3656(6)	12938(13)	20(2)
C(12)	6543(3)	3974(7)	12019(13)	23(2)
C(13)	6124(2)	5226(6)	11765(12)	20(2)
C(14)	5911(3)	5671(6)	9851(14)	24(2)
C(15)	5723(2)	4889(7)	8647(13)	23(2)
C(16)	5371(3)	5187(8)	7186(16)	37(2)
Cl(1B)	5600(1)	7225(2)	14099(5)	54(1)
O(1B)	6287(2)	7010(5)	16090(11)	35(2)
O(2B)	7121(2)	8559(5)	12394(11)	41(2)
O(3B)	6650(2)	5146(5)	15897(10)	31(2)
O(4B)	7290(2)	5266(6)	15553(12)	43(2)

**Table A3.4.3** Cont'd

O(5B)	7372(2)	6411(5)	11759(11)	33(2)
C(1B)	6692(4)	7307(8)	16092(16)	42(3)
C(2B)	6754(5)	8185(9)	17260(18)	64(4)
C(3B)	6466(5)	8945(9)	16450(19)	65(4)
C(4B)	6047(5)	8570(9)	15850(20)	63(4)
C(5B)	6081(3)	7679(8)	14762(17)	42(3)
C(6B)	6326(3)	7773(7)	12972(15)	33(2)
C(7B)	6725(3)	7396(7)	13782(13)	30(2)
C(8B)	7108(3)	7877(7)	13444(13)	32(2)
C(9B)	7466(3)	7454(8)	14569(15)	40(3)
C(10B)	7409(3)	6845(10)	16518(15)	46(3)
C(11B)	6992(3)	6573(9)	16972(16)	42(3)
C(12B)	6950(3)	5610(8)	16141(16)	36(2)
C(13B)	7614(3)	5924(10)	16200(20)	55(4)
C(14B)	7873(3)	6067(10)	14504(19)	51(3)
C(15B)	7675(3)	6800(8)	13096(15)	35(2)
C(16B)	7962(3)	7313(9)	11897(15)	44(3)
O(6)	7478(2)	4630(5)	10479(12)	41(2)
Cl(2)	5193(2)	-332(5)	7527(14)	100(5)
Cl(3)	4852(3)	-647(9)	11220(19)	169(12)
Cl(4)	5237(3)	-2147(5)	9390(20)	147(9)
C(17)	4947(2)	-1158(6)	8908(16)	130(30)

---



**Table A3.4.4** Bond Lengths [ $\text{\AA}$ ] and angles [ $^\circ$ ] for Cycloheptane **72**

---

Cl(1)-C(5)	1.796(10)
O(1)-C(1)	1.452(10)
O(1)-C(5)	1.435(11)
O(2)-C(8)	1.217(11)
O(3)-C(12)	1.224(11)
O(4)-C(12)	1.343(11)
O(4)-C(13)	1.473(10)
O(5)-H(5)	0.8400
O(5)-C(15)	1.434(10)
C(1)-C(2)	1.542(12)
C(1)-C(7)	1.512(12)
C(1)-C(11)	1.541(12)
C(2)-H(2A)	0.9900
C(2)-H(2B)	0.9900
C(2)-C(3)	1.528(15)
C(3)-H(3A)	0.9900
C(3)-H(3B)	0.9900
C(3)-C(4)	1.521(15)
C(4)-H(4A)	0.9900
C(4)-H(4B)	0.9900
C(4)-C(5)	1.505(15)
C(5)-C(6)	1.540(13)
C(6)-H(6A)	0.9900
C(6)-H(6B)	0.9900
C(6)-C(7)	1.533(13)
C(7)-H(7)	1.0000
C(7)-C(8)	1.511(13)
C(8)-C(9)	1.501(13)
C(9)-H(9)	1.0000
C(9)-C(10)	1.576(12)
C(9)-C(15)	1.564(12)
C(10)-H(10)	1.0000

**Table A3.4.4** Cont'd

C(10)-C(11)	1.528(12)
C(10)-C(13)	1.520(12)
C(11)-H(11)	1.0000
C(11)-C(12)	1.504(12)
C(13)-H(13)	1.0000
C(13)-C(14)	1.544(12)
C(14)-H(14A)	0.9900
C(14)-H(14B)	0.9900
C(14)-C(15)	1.497(13)
C(15)-C(16)	1.534(13)
C(16)-H(16A)	0.9800
C(16)-H(16B)	0.9800
C(16)-H(16C)	0.9800
Cl(1B)-C(5B)	1.788(13)
O(1B)-C(1B)	1.447(13)
O(1B)-C(5B)	1.448(13)
O(2B)-C(8B)	1.210(12)
O(3B)-C(12B)	1.223(12)
O(4B)-C(12B)	1.350(14)
O(4B)-C(13B)	1.495(14)
O(5B)-H(5B)	0.8400
O(5B)-C(15B)	1.416(12)
C(1B)-C(2B)	1.494(16)
C(1B)-C(7B)	1.546(13)
C(1B)-C(11B)	1.553(18)
C(2B)-H(2C)	0.9900
C(2B)-H(2D)	0.9900
C(2B)-C(3B)	1.54(2)
C(3B)-H(3C)	0.9900
C(3B)-H(3D)	0.9900
C(3B)-C(4B)	1.55(2)
C(4B)-H(4D)	0.9900
C(4B)-H(4C)	0.9900
C(4B)-C(5B)	1.487(18)

**Table A3.4.4** Cont'd

C(5B)-C(6B)	1.513(15)
C(6B)-H(6C)	0.9900
C(6B)-H(6D)	0.9900
C(6B)-C(7B)	1.519(15)
C(7B)-H(7B)	1.0000
C(7B)-C(8B)	1.514(13)
C(8B)-C(9B)	1.504(16)
C(9B)-H(9B)	1.0000
C(9B)-C(10B)	1.586(14)
C(9B)-C(15B)	1.572(16)
C(10B)-H(10B)	1.0000
C(10B)-C(11B)	1.531(15)
C(10B)-C(13B)	1.53(2)
C(11B)-H(11B)	1.0000
C(11B)-C(12B)	1.502(17)
C(13B)-H(13B)	1.0000
C(13B)-C(14B)	1.503(18)
C(14B)-H(14C)	0.9900
C(14B)-H(14D)	0.9900
C(14B)-C(15B)	1.531(16)
C(15B)-C(16B)	1.510(13)
C(16B)-H(16D)	0.9800
C(16B)-H(16E)	0.9800
C(16B)-H(16F)	0.9800
O(6)-H(6E)	0.8689
O(6)-H(6F)	0.9962
Cl(2)-Cl(3)#1	0.969(17)
Cl(2)-C(17)	1.7602
Cl(3)-Cl(4)#1	2.227(5)
Cl(3)-C(17)	1.7534
Cl(4)-C(17)	1.7546
C(17)-H(17)	0.9198
C(5)-O(1)-C(1)	101.4(6)

**Table A3.4.4** Cont'd

C(12)-O(4)-C(13)	109.9(7)
C(15)-O(5)-H(5)	109.5
O(1)-C(1)-C(2)	107.9(7)
O(1)-C(1)-C(7)	102.0(7)
O(1)-C(1)-C(11)	114.1(7)
C(7)-C(1)-C(2)	115.3(8)
C(7)-C(1)-C(11)	110.5(7)
C(11)-C(1)-C(2)	107.3(7)
C(1)-C(2)-H(2A)	109.3
C(1)-C(2)-H(2B)	109.3
H(2A)-C(2)-H(2B)	108.0
C(3)-C(2)-C(1)	111.5(8)
C(3)-C(2)-H(2A)	109.3
C(3)-C(2)-H(2B)	109.3
C(2)-C(3)-H(3A)	109.2
C(2)-C(3)-H(3B)	109.2
H(3A)-C(3)-H(3B)	107.9
C(4)-C(3)-C(2)	112.1(8)
C(4)-C(3)-H(3A)	109.2
C(4)-C(3)-H(3B)	109.2
C(3)-C(4)-H(4A)	110.0
C(3)-C(4)-H(4B)	110.0
H(4A)-C(4)-H(4B)	108.4
C(5)-C(4)-C(3)	108.3(8)
C(5)-C(4)-H(4A)	110.0
C(5)-C(4)-H(4B)	110.0
O(1)-C(5)-Cl(1)	105.9(6)
O(1)-C(5)-C(4)	108.2(9)
O(1)-C(5)-C(6)	106.3(8)
C(4)-C(5)-Cl(1)	109.7(7)
C(4)-C(5)-C(6)	114.6(8)
C(6)-C(5)-Cl(1)	111.7(7)
C(5)-C(6)-H(6A)	111.5
C(5)-C(6)-H(6B)	111.5

**Table A3.4.4** *Cont'd*

H(6A)-C(6)-H(6B)	109.3
C(7)-C(6)-C(5)	101.2(8)
C(7)-C(6)-H(6A)	111.5
C(7)-C(6)-H(6B)	111.5
C(1)-C(7)-C(6)	104.9(7)
C(1)-C(7)-H(7)	106.9
C(1)-C(7)-C(8)	109.2(7)
C(6)-C(7)-H(7)	106.9
C(8)-C(7)-C(6)	121.3(7)
C(8)-C(7)-H(7)	106.9
O(2)-C(8)-C(7)	123.7(9)
O(2)-C(8)-C(9)	122.4(9)
C(9)-C(8)-C(7)	113.8(7)
C(8)-C(9)-H(9)	107.2
C(8)-C(9)-C(10)	119.0(7)
C(8)-C(9)-C(15)	110.3(7)
C(10)-C(9)-H(9)	107.2
C(15)-C(9)-H(9)	107.2
C(15)-C(9)-C(10)	105.3(7)
C(9)-C(10)-H(10)	109.2
C(11)-C(10)-C(9)	118.3(7)
C(11)-C(10)-H(10)	109.2
C(13)-C(10)-C(9)	106.4(7)
C(13)-C(10)-H(10)	109.2
C(13)-C(10)-C(11)	104.2(7)
C(1)-C(11)-H(11)	108.9
C(10)-C(11)-C(1)	109.3(7)
C(10)-C(11)-H(11)	108.9
C(12)-C(11)-C(1)	117.6(7)
C(12)-C(11)-C(10)	103.0(7)
C(12)-C(11)-H(11)	108.9
O(3)-C(12)-O(4)	119.4(8)
O(3)-C(12)-C(11)	128.7(9)
O(4)-C(12)-C(11)	111.8(7)

**Table A3.4.4** Cont'd

O(4)-C(13)-C(10)	105.3(7)
O(4)-C(13)-H(13)	111.5
O(4)-C(13)-C(14)	110.9(7)
C(10)-C(13)-H(13)	111.5
C(10)-C(13)-C(14)	105.8(7)
C(14)-C(13)-H(13)	111.5
C(13)-C(14)-H(14A)	110.6
C(13)-C(14)-H(14B)	110.6
H(14A)-C(14)-H(14B)	108.7
C(15)-C(14)-C(13)	105.7(7)
C(15)-C(14)-H(14A)	110.6
C(15)-C(14)-H(14B)	110.6
O(5)-C(15)-C(9)	106.2(7)
O(5)-C(15)-C(14)	112.1(7)
O(5)-C(15)-C(16)	109.3(7)
C(14)-C(15)-C(9)	104.4(7)
C(14)-C(15)-C(16)	113.5(8)
C(16)-C(15)-C(9)	111.1(7)
C(15)-C(16)-H(16A)	109.5
C(15)-C(16)-H(16B)	109.5
C(15)-C(16)-H(16C)	109.5
H(16A)-C(16)-H(16B)	109.5
H(16A)-C(16)-H(16C)	109.5
H(16B)-C(16)-H(16C)	109.5
C(1B)-O(1B)-C(5B)	102.4(8)
C(12B)-O(4B)-C(13B)	108.3(10)
C(15B)-O(5B)-H(5B)	109.5
O(1B)-C(1B)-C(2B)	110.3(11)
O(1B)-C(1B)-C(7B)	100.1(8)
O(1B)-C(1B)-C(11B)	113.2(8)
C(2B)-C(1B)-C(7B)	114.9(9)
C(2B)-C(1B)-C(11B)	109.3(11)
C(7B)-C(1B)-C(11B)	109.0(9)
C(1B)-C(2B)-H(2C)	109.3

**Table A3.4.4** *Cont'd*

C(1B)-C(2B)-H(2D)	109.3
C(1B)-C(2B)-C(3B)	111.7(12)
H(2C)-C(2B)-H(2D)	107.9
C(3B)-C(2B)-H(2C)	109.3
C(3B)-C(2B)-H(2D)	109.3
C(2B)-C(3B)-H(3C)	109.1
C(2B)-C(3B)-H(3D)	109.1
C(2B)-C(3B)-C(4B)	112.7(11)
H(3C)-C(3B)-H(3D)	107.8
C(4B)-C(3B)-H(3C)	109.1
C(4B)-C(3B)-H(3D)	109.1
C(3B)-C(4B)-H(4D)	110.0
C(3B)-C(4B)-H(4C)	110.0
H(4D)-C(4B)-H(4C)	108.3
C(5B)-C(4B)-C(3B)	108.7(11)
C(5B)-C(4B)-H(4D)	110.0
C(5B)-C(4B)-H(4C)	110.0
O(1B)-C(5B)-Cl(1B)	106.8(7)
O(1B)-C(5B)-C(4B)	110.0(10)
O(1B)-C(5B)-C(6B)	105.2(9)
C(4B)-C(5B)-Cl(1B)	109.2(10)
C(4B)-C(5B)-C(6B)	111.8(10)
C(6B)-C(5B)-Cl(1B)	113.5(8)
C(5B)-C(6B)-H(6C)	111.1
C(5B)-C(6B)-H(6D)	111.1
C(5B)-C(6B)-C(7B)	103.3(8)
H(6C)-C(6B)-H(6D)	109.1
C(7B)-C(6B)-H(6C)	111.1
C(7B)-C(6B)-H(6D)	111.1
C(1B)-C(7B)-H(7B)	106.9
C(6B)-C(7B)-C(1B)	103.8(8)
C(6B)-C(7B)-H(7B)	106.9
C(8B)-C(7B)-C(1B)	108.8(8)
C(8B)-C(7B)-C(6B)	122.6(8)

**Table A3.4.4** *Cont'd*

C(8B)-C(7B)-H(7B)	106.9
O(2B)-C(8B)-C(7B)	122.5(10)
O(2B)-C(8B)-C(9B)	123.2(9)
C(9B)-C(8B)-C(7B)	114.3(8)
C(8B)-C(9B)-H(9B)	107.8
C(8B)-C(9B)-C(10B)	118.5(9)
C(8B)-C(9B)-C(15B)	109.3(8)
C(10B)-C(9B)-H(9B)	107.8
C(15B)-C(9B)-H(9B)	107.8
C(15B)-C(9B)-C(10B)	105.1(9)
C(9B)-C(10B)-H(10B)	108.9
C(11B)-C(10B)-C(9B)	118.9(9)
C(11B)-C(10B)-H(10B)	108.9
C(13B)-C(10B)-C(9B)	106.6(9)
C(13B)-C(10B)-H(10B)	108.9
C(13B)-C(10B)-C(11B)	104.2(10)
C(1B)-C(11B)-H(11B)	108.6
C(10B)-C(11B)-C(1B)	110.1(9)
C(10B)-C(11B)-H(11B)	108.6
C(12B)-C(11B)-C(1B)	117.4(9)
C(12B)-C(11B)-C(10B)	103.2(10)
C(12B)-C(11B)-H(11B)	108.6
O(3B)-C(12B)-O(4B)	119.2(10)
O(3B)-C(12B)-C(11B)	127.7(10)
O(4B)-C(12B)-C(11B)	113.0(9)
O(4B)-C(13B)-C(10B)	105.1(9)
O(4B)-C(13B)-H(13B)	111.6
O(4B)-C(13B)-C(14B)	109.9(11)
C(10B)-C(13B)-H(13B)	111.6
C(14B)-C(13B)-C(10B)	106.6(10)
C(14B)-C(13B)-H(13B)	111.6
C(13B)-C(14B)-H(14C)	110.3
C(13B)-C(14B)-H(14D)	110.3
C(13B)-C(14B)-C(15B)	107.0(11)



**Table A3.4.4** Cont'd

H(14C)-C(14B)-H(14D)	108.6
C(15B)-C(14B)-H(14C)	110.3
C(15B)-C(14B)-H(14D)	110.3
O(5B)-C(15B)-C(9B)	106.4(8)
O(5B)-C(15B)-C(14B)	111.3(9)
O(5B)-C(15B)-C(16B)	109.8(8)
C(14B)-C(15B)-C(9B)	104.0(9)
C(16B)-C(15B)-C(9B)	112.2(9)
C(16B)-C(15B)-C(14B)	112.8(9)
C(15B)-C(16B)-H(16D)	109.5
C(15B)-C(16B)-H(16E)	109.5
C(15B)-C(16B)-H(16F)	109.5
H(16D)-C(16B)-H(16E)	109.5
H(16D)-C(16B)-H(16F)	109.5
H(16E)-C(16B)-H(16F)	109.5
H(6E)-O(6)-H(6F)	111.1
Cl(3)#1-Cl(2)-C(17)	28.3(8)
Cl(2)#1-Cl(3)-Cl(4)#1	125.8(10)
Cl(2)#1-Cl(3)-C(17)	176.6(7)
C(17)-Cl(3)-Cl(4)#1	57.4(6)
Cl(2)-C(17)-Cl(4)#1	170.4(6)
Cl(2)-C(17)-H(17)	109.8
Cl(3)-C(17)-Cl(2)	107.2
Cl(3)#1-C(17)-Cl(2)	26.9(11)
Cl(3)#1-C(17)-Cl(3)	86.6(10)
Cl(3)#1-C(17)-Cl(4)#1	146.3(17)
Cl(3)#1-C(17)-Cl(4)	103.7(6)
Cl(3)-C(17)-Cl(4)#1	73.5(5)
Cl(3)-C(17)-Cl(4)	109.3
Cl(3)#1-C(17)-H(17)	134.5
Cl(3)-C(17)-H(17)	109.0
Cl(4)-C(17)-Cl(2)	111.4
Cl(4)-C(17)-Cl(4)#1	60.1(6)
Cl(4)#1-C(17)-H(17)	78.5

**Table A3.4.4** Cont'd

Cl(4)-C(17)-H(17)                      110.1

---

Symmetry transformations used to generate equivalent atoms:

#1 -x+1,y,-z+2

**Table A3.4.5** Anisotropic Displacement Parameters ( $\text{\AA}^2 \times 10^3$ ) for Cycloheptane 72.

The Anisotropic Displacement Factor Exponent Takes the Form:  $-2p^2[h^2a^{*2}U^{11} + \dots + 2hka^*b^*U^{12}]$ .

	U <sup>11</sup>	U <sup>22</sup>	U <sup>33</sup>	U <sup>23</sup>	U <sup>13</sup>	U <sup>12</sup>
Cl(1)	36(1)	26(1)	42(1)	-7(1)	-7(1)	4(1)
O(1)	21(3)	22(3)	31(3)	-2(3)	-3(3)	3(2)
O(2)	21(3)	42(4)	22(3)	2(3)	-10(2)	-9(3)
O(3)	24(3)	28(3)	33(4)	-11(3)	1(3)	6(3)
O(4)	24(3)	20(3)	32(3)	-2(3)	2(3)	3(3)
O(5)	28(3)	32(4)	22(3)	-4(3)	10(3)	-6(3)
C(1)	22(4)	22(4)	23(4)	2(4)	3(3)	1(4)
C(2)	27(5)	30(5)	36(5)	11(4)	8(4)	3(4)
C(3)	30(5)	38(6)	47(6)	20(5)	5(4)	4(4)
C(4)	41(6)	24(5)	56(7)	10(5)	-2(5)	-5(4)
C(5)	25(5)	28(5)	36(5)	3(4)	-9(4)	-1(4)
C(6)	32(5)	26(5)	34(5)	-2(4)	-16(4)	2(4)
C(7)	27(4)	15(4)	19(4)	-5(3)	-4(3)	-2(4)
C(8)	24(5)	35(5)	17(4)	0(4)	1(3)	-2(4)
C(9)	18(4)	31(5)	14(4)	2(4)	0(3)	1(4)
C(10)	28(4)	14(4)	14(4)	1(3)	-1(3)	4(3)
C(11)	20(4)	24(4)	16(4)	-7(3)	2(3)	-1(3)
C(12)	23(4)	28(5)	18(4)	-12(4)	-4(3)	1(4)
C(13)	21(4)	21(4)	18(4)	-8(3)	1(3)	0(3)
C(14)	26(4)	21(4)	24(5)	0(4)	-2(4)	1(3)
C(15)	22(4)	32(5)	15(4)	1(4)	3(3)	-1(4)
C(16)	37(5)	42(6)	30(5)	12(5)	-6(4)	-1(5)
Cl(1B)	45(2)	40(2)	77(2)	16(2)	14(1)	11(1)
O(1B)	44(4)	32(4)	31(4)	9(3)	9(3)	-5(3)
O(2B)	65(5)	26(4)	34(4)	-2(3)	13(4)	-15(3)
O(3B)	27(3)	37(4)	27(3)	5(3)	-3(3)	-5(3)
O(4B)	20(3)	52(5)	55(5)	28(4)	-6(3)	-6(3)

**Table A3.4.5** *Cont'd*

O(5B)	35(4)	26(4)	37(4)	0(3)	-9(3)	-1(3)
C(1B)	58(7)	38(6)	29(5)	-10(5)	4(5)	-19(5)
C(2B)	122(13)	46(7)	27(6)	-11(6)	20(7)	-34(8)
C(3B)	129(14)	37(7)	32(6)	-17(5)	28(8)	-16(8)
C(4B)	97(11)	37(7)	59(8)	7(6)	39(8)	10(7)
C(5B)	50(6)	35(6)	42(6)	5(5)	8(5)	1(5)
C(6B)	50(6)	19(5)	28(5)	2(4)	3(4)	-6(4)
C(7B)	42(5)	32(6)	17(4)	-6(4)	7(4)	-12(4)
C(8B)	50(6)	32(5)	12(4)	2(4)	2(4)	-15(5)
C(9B)	50(6)	45(7)	23(5)	-2(5)	-2(4)	-32(5)
C(10B)	43(6)	75(9)	19(5)	4(5)	-8(4)	-38(6)
C(11B)	45(6)	59(8)	23(5)	2(5)	5(4)	-29(6)
C(12B)	29(5)	47(7)	31(5)	14(4)	-7(4)	-13(4)
C(13B)	34(6)	79(10)	50(7)	32(7)	-12(5)	-24(6)
C(14B)	30(6)	75(9)	46(7)	27(6)	-10(5)	-20(6)
C(15B)	36(5)	43(6)	25(5)	13(4)	-4(4)	-14(5)
C(16B)	53(7)	59(8)	20(5)	5(5)	6(4)	-22(6)
O(6)	39(4)	37(4)	49(5)	-11(4)	14(3)	-6(3)
Cl(2)	78(8)	64(7)	162(16)	5(8)	34(9)	31(6)
Cl(3)	74(10)	310(40)	120(15)	28(19)	16(10)	-12(15)
Cl(4)	100(10)	200(20)	148(15)	93(14)	27(10)	74(12)

---

**Table A3.4.6** Hydrogen Coordinates ( $\times 10^4$ ) and Isotropic Displacement Parameters ( $\text{\AA}^2 \times 10^3$ ) for Cycloheptane **468**.

	x	y	z	U(eq)
H(5)	6187	4747	7314	40
H(2A)	5756	2532	15049	37
H(2B)	5462	2991	13313	37
H(3A)	5316	1380	14197	46
H(3B)	5307	1603	11821	46
H(4A)	5916	646	14219	49
H(4B)	5667	266	12218	49
H(6A)	6096	1485	8433	38
H(6B)	5656	1381	9136	38
H(7)	6145	2937	9406	25
H(9)	5321	4391	10601	25
H(10)	5717	4553	13399	23
H(11)	6226	3680	14452	24
H(13)	6152	5671	12926	24
H(14A)	5710	6117	10229	29
H(14B)	6101	5999	9056	29
H(16A)	5464	5588	6130	56
H(16B)	5182	5525	7941	56
H(16C)	5244	4640	6555	56
H(5B)	7454	5921	11262	49
H(2C)	7028	8401	17168	77
H(2D)	6719	8068	18709	77
H(3C)	6568	9239	15249	78
H(3D)	6451	9426	17506	78
H(4D)	5906	8475	17082	75
H(4C)	5896	9019	14961	75
H(6C)	6347	8427	12557	39
H(6D)	6213	7408	11798	39

**Table A3.4.6** *Cont'd*

H(7B)	6744	6755	13237	36
H(9B)	7653	7965	14989	48
H(10B)	7542	7158	17739	55
H(11B)	6981	6547	18479	51
H(13B)	7768	5712	17474	66
H(14C)	7903	5483	13754	61
H(14D)	8138	6279	15048	61
H(16D)	8113	6870	11152	66
H(16E)	8143	7671	12826	66
H(16F)	7818	7732	10933	66
H(6E)	7684	4303	10257	62
H(6F)	7299	4281	11315	62
H(17)	4712	-1315	8203	155

---

**Table A3.4.7** Torsion Angles [°] for Cycloheptane **72**.

Cl(1)-C(5)-C(6)-C(7)	-135.7(7)
O(1)-C(1)-C(2)-C(3)	-56.0(10)
O(1)-C(1)-C(7)-C(6)	36.0(9)
O(1)-C(1)-C(7)-C(8)	167.4(7)
O(1)-C(1)-C(11)-C(10)	172.7(7)
O(1)-C(1)-C(11)-C(12)	55.9(10)
O(1)-C(5)-C(6)-C(7)	-20.7(10)
O(2)-C(8)-C(9)-C(10)	159.3(8)
O(2)-C(8)-C(9)-C(15)	-78.9(10)
O(4)-C(13)-C(14)-C(15)	81.2(8)
C(1)-O(1)-C(5)-Cl(1)	162.9(6)
C(1)-O(1)-C(5)-C(4)	-79.5(8)
C(1)-O(1)-C(5)-C(6)	44.0(9)
C(1)-C(2)-C(3)-C(4)	41.8(12)
C(1)-C(7)-C(8)-O(2)	-131.9(9)
C(1)-C(7)-C(8)-C(9)	50.8(10)
C(1)-C(11)-C(12)-O(3)	-49.2(12)
C(1)-C(11)-C(12)-O(4)	133.0(8)
C(2)-C(1)-C(7)-C(6)	-80.7(10)
C(2)-C(1)-C(7)-C(8)	50.8(10)
C(2)-C(1)-C(11)-C(10)	-67.8(8)
C(2)-C(1)-C(11)-C(12)	175.4(8)
C(2)-C(3)-C(4)-C(5)	-45.3(12)
C(3)-C(4)-C(5)-Cl(1)	-179.1(8)
C(3)-C(4)-C(5)-O(1)	65.8(11)
C(3)-C(4)-C(5)-C(6)	-52.5(12)
C(4)-C(5)-C(6)-C(7)	98.7(10)
C(5)-O(1)-C(1)-C(2)	72.7(8)
C(5)-O(1)-C(1)-C(7)	-49.1(8)
C(5)-O(1)-C(1)-C(11)	-168.2(7)
C(5)-C(6)-C(7)-C(1)	-9.4(9)
C(5)-C(6)-C(7)-C(8)	-133.5(8)
C(6)-C(7)-C(8)-O(2)	-9.8(14)

**Table A3.4.7** Cont'd

C(6)-C(7)-C(8)-C(9)	172.9(8)
C(7)-C(1)-C(2)-C(3)	57.1(11)
C(7)-C(1)-C(11)-C(10)	58.6(9)
C(7)-C(1)-C(11)-C(12)	-58.2(10)
C(7)-C(8)-C(9)-C(10)	-23.3(11)
C(7)-C(8)-C(9)-C(15)	98.5(8)
C(8)-C(9)-C(10)-C(11)	13.5(11)
C(8)-C(9)-C(10)-C(13)	130.2(8)
C(8)-C(9)-C(15)-O(5)	-36.7(9)
C(8)-C(9)-C(15)-C(14)	-155.2(7)
C(8)-C(9)-C(15)-C(16)	82.1(9)
C(9)-C(10)-C(11)-C(1)	-29.8(10)
C(9)-C(10)-C(11)-C(12)	96.0(8)
C(9)-C(10)-C(13)-O(4)	-102.0(7)
C(9)-C(10)-C(13)-C(14)	15.5(8)
C(10)-C(9)-C(15)-O(5)	93.0(7)
C(10)-C(9)-C(15)-C(14)	-25.6(9)
C(10)-C(9)-C(15)-C(16)	-148.3(8)
C(10)-C(11)-C(12)-O(3)	-169.4(8)
C(10)-C(11)-C(12)-O(4)	12.8(9)
C(10)-C(13)-C(14)-C(15)	-32.4(9)
C(11)-C(1)-C(2)-C(3)	-179.4(7)
C(11)-C(1)-C(7)-C(6)	157.5(7)
C(11)-C(1)-C(7)-C(8)	-71.0(9)
C(11)-C(10)-C(13)-O(4)	23.8(8)
C(11)-C(10)-C(13)-C(14)	141.3(7)
C(12)-O(4)-C(13)-C(10)	-16.8(8)
C(12)-O(4)-C(13)-C(14)	-130.7(7)
C(13)-O(4)-C(12)-O(3)	-175.7(7)
C(13)-O(4)-C(12)-C(11)	2.4(9)
C(13)-C(10)-C(11)-C(1)	-147.6(7)
C(13)-C(10)-C(11)-C(12)	-21.9(8)
C(13)-C(14)-C(15)-O(5)	-78.7(9)
C(13)-C(14)-C(15)-C(9)	35.7(9)



**Table A3.4.7** *Cont'd*

C(13)-C(14)-C(15)-C(16)	156.8(7)
C(15)-C(9)-C(10)-C(11)	-110.8(8)
C(15)-C(9)-C(10)-C(13)	5.9(8)
Cl(1B)-C(5B)-C(6B)-C(7B)	-135.5(7)
O(1B)-C(1B)-C(2B)-C(3B)	-55.2(13)
O(1B)-C(1B)-C(7B)-C(6B)	37.4(10)
O(1B)-C(1B)-C(7B)-C(8B)	169.4(8)
O(1B)-C(1B)-C(11B)-C(10B)	168.1(9)
O(1B)-C(1B)-C(11B)-C(12B)	50.5(12)
O(1B)-C(5B)-C(6B)-C(7B)	-19.1(10)
O(2B)-C(8B)-C(9B)-C(10B)	155.9(10)
O(2B)-C(8B)-C(9B)-C(15B)	-83.8(11)
O(4B)-C(13B)-C(14B)-C(15B)	83.0(13)
C(1B)-O(1B)-C(5B)-Cl(1B)	165.3(7)
C(1B)-O(1B)-C(5B)-C(4B)	-76.3(11)
C(1B)-O(1B)-C(5B)-C(6B)	44.3(10)
C(1B)-C(2B)-C(3B)-C(4B)	39.5(14)
C(1B)-C(7B)-C(8B)-O(2B)	-126.1(11)
C(1B)-C(7B)-C(8B)-C(9B)	52.1(11)
C(1B)-C(11B)-C(12B)-O(3B)	-48.0(15)
C(1B)-C(11B)-C(12B)-O(4B)	129.5(9)
C(2B)-C(1B)-C(7B)-C(6B)	-80.8(13)
C(2B)-C(1B)-C(7B)-C(8B)	51.3(15)
C(2B)-C(1B)-C(11B)-C(10B)	-68.5(12)
C(2B)-C(1B)-C(11B)-C(12B)	173.9(9)
C(2B)-C(3B)-C(4B)-C(5B)	-42.0(14)
C(3B)-C(4B)-C(5B)-Cl(1B)	179.0(9)
C(3B)-C(4B)-C(5B)-O(1B)	62.0(12)
C(3B)-C(4B)-C(5B)-C(6B)	-54.5(14)
C(4B)-C(5B)-C(6B)-C(7B)	100.3(11)
C(5B)-O(1B)-C(1B)-C(2B)	71.4(11)
C(5B)-O(1B)-C(1B)-C(7B)	-50.0(10)
C(5B)-O(1B)-C(1B)-C(11B)	-165.8(9)
C(5B)-C(6B)-C(7B)-C(1B)	-11.2(10)

**Table A3.4.7** Cont'd

C(5B)-C(6B)-C(7B)-C(8B)	-134.6(9)
C(6B)-C(7B)-C(8B)-O(2B)	-5.0(14)
C(6B)-C(7B)-C(8B)-C(9B)	173.2(9)
C(7B)-C(1B)-C(2B)-C(3B)	57.0(15)
C(7B)-C(1B)-C(11B)-C(10B)	57.7(11)
C(7B)-C(1B)-C(11B)-C(12B)	-59.9(11)
C(7B)-C(8B)-C(9B)-C(10B)	-22.3(13)
C(7B)-C(8B)-C(9B)-C(15B)	98.0(9)
C(8B)-C(9B)-C(10B)-C(11B)	10.3(16)
C(8B)-C(9B)-C(10B)-C(13B)	127.5(10)
C(8B)-C(9B)-C(15B)-O(5B)	-33.4(10)
C(8B)-C(9B)-C(15B)-C(14B)	-151.0(8)
C(8B)-C(9B)-C(15B)-C(16B)	86.7(10)
C(9B)-C(10B)-C(11B)-C(1B)	-27.7(14)
C(9B)-C(10B)-C(11B)-C(12B)	98.3(12)
C(9B)-C(10B)-C(13B)-O(4B)	-101.6(9)
C(9B)-C(10B)-C(13B)-C(14B)	15.1(11)
C(10B)-C(9B)-C(15B)-O(5B)	94.9(9)
C(10B)-C(9B)-C(15B)-C(14B)	-22.7(10)
C(10B)-C(9B)-C(15B)-C(16B)	-145.0(9)
C(10B)-C(11B)-C(12B)-O(3B)	-169.2(10)
C(10B)-C(11B)-C(12B)-O(4B)	8.2(11)
C(10B)-C(13B)-C(14B)-C(15B)	-30.4(13)
C(11B)-C(1B)-C(2B)-C(3B)	179.8(10)
C(11B)-C(1B)-C(7B)-C(6B)	156.3(8)
C(11B)-C(1B)-C(7B)-C(8B)	-71.6(10)
C(11B)-C(10B)-C(13B)-O(4B)	25.0(11)
C(11B)-C(10B)-C(13B)-C(14B)	141.7(9)
C(12B)-O(4B)-C(13B)-C(10B)	-20.7(11)
C(12B)-O(4B)-C(13B)-C(14B)	-135.1(11)
C(13B)-O(4B)-C(12B)-O(3B)	-174.5(9)
C(13B)-O(4B)-C(12B)-C(11B)	7.8(11)
C(13B)-C(10B)-C(11B)-C(1B)	-146.2(9)
C(13B)-C(10B)-C(11B)-C(12B)	-20.1(11)

**Table A3.4.7** Cont'd

C(13B)-C(14B)-C(15B)-O(5B)	-81.1(12)
C(13B)-C(14B)-C(15B)-C(9B)	33.1(12)
C(13B)-C(14B)-C(15B)-C(16B)	154.9(10)
C(15B)-C(9B)-C(10B)-C(11B)	-112.2(12)
C(15B)-C(9B)-C(10B)-C(13B)	5.0(10)
Cl(3)#1-Cl(2)-C(17)-Cl(3)	41.5(13)
Cl(3)#1-Cl(2)-C(17)-Cl(4)	-78.0(13)
Cl(4)#1-Cl(3)-C(17)-Cl(2)	-170.0(7)
Cl(4)#1-Cl(3)-C(17)-Cl(3)#1	-152.5(14)
Cl(4)#1-Cl(3)-C(17)-Cl(4)	-49.2(7)

---

Symmetry transformations used to generate equivalent atoms:

#1  $-x+1, y, -z+2$

**Table A3.4.8** Hydrogen Bonds for Cycloheptane **72** [ $\text{\AA}$  and  $^\circ$ ].

D-H...A	d(D-H)	d(H...A)	d(D...A)	<(DHA)
O(5)-H(5)...O(3B)#2	0.84	1.99	2.772(9)	154.9
O(5B)-H(5B)...O(6)	0.84	1.94	2.749(10)	160.2
O(6)-H(6E)...O(2B)#3	0.87	2.21	2.886(10)	134.6
O(6)-H(6F)...O(3)	1.00	1.91	2.858(9)	157.8

Symmetry transformations used to generate equivalent atoms:

#1  $-x+1, y, -z+2$  #2  $x, y, z-1$  #3  $-x+3/2, y-1/2, -z+2$

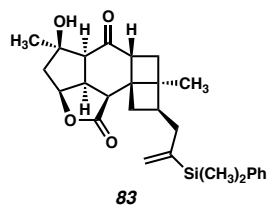
**A3.5 X-RAY CRYSTAL STRUCTURE ANALYSIS OF CYCLOBUTANE 83**Contents

Table A3.5.1. Experimental Details

Table A3.5.2. Crystal Data

Table A3.5.3. Atomic Coordinates

Table A3.5.4. Full Bond Distances and Angles

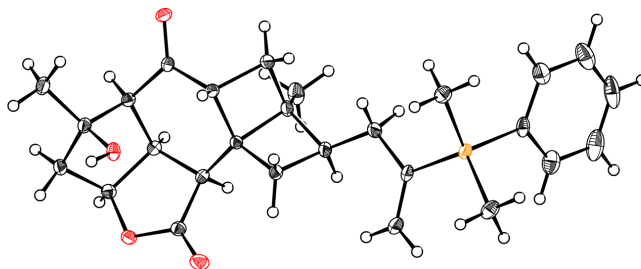
Table A3.5.5. Anisotropic Displacement Parameters

Table A3.5.6. Hydrogen Atomic Coordinates

Table A3.5.7. Torsion Angles

Table A3.5.8. Hydrogen Bond Distances and Angles

**Figure A3.5.1** X-Ray crystal structure of cyclobutane **83**.



**Table A3.5.1** Experimental details for X-ray structure determination of cyclobutane**83.***Refinement Details*

Two crystals were mounted on polyimide MiTeGen loops with STP Oil Treatment and placed under nitrogen streams. Low temperature (100K) X-ray data were collected with both a Bruker AXS D8 KAPPA diffractometer running at 50 kV and 30 mA (Mo  $K_{\alpha}$  = 0.71073 Å; PHOTON 100 CMOS detector with TRIUMPH graphite monochromator) (d20010) and a Bruker AXS D8 VENTURE KAPPA diffractometer running at 50 kV and 1mA (Cu  $K_{\alpha}$  = 1.54178 Å; PHOTON II CPAD detector and Helios focusing multilayer mirror optics). All diffractometer manipulations, including data collection, integration, and scaling were carried out using the Bruker APEX3 software. An absorption correction was applied using SADABS. The space group was determined and the structure solved by intrinsic phasing using XT. Refinement was full-matrix least squares on  $F^2$  using XL. All non-hydrogen atoms were refined using anisotropic displacement parameters. Hydrogen atoms were placed in idealized positions and the coordinates refined. The isotropic displacement parameters of all hydrogen atoms were fixed at 1.2 times the  $U_{eq}$  value of the bonded atom.

*Special Refinement Details*

Compound **83** crystallizes in the monoclinic space group  $P2_1$  (# 4) with one molecule in the asymmetric unit. Both crystals were composed of the same enantiomer. The structures are virtually identical with a barely noticeable difference in the position of the H atom of the OH group. The Mo dataset has a marginally better C-C bond precision of 0.0024 Å vs. 0.0026 Å for the Cu dataset.

**Table A3.5.2** Crystal Data and Structure Refinement for Cyclobutane **83**.

Empirical formula	C <sub>27</sub> H <sub>34</sub> O <sub>4</sub> Si	
Formula weight	450.63	
Temperature	100 K	
Wavelength	0.71073 $\approx$	
Crystal system	Monoclinic	
Space group	P 1 21 1 (# 4)	
Unit cell dimensions	a = 6.9085(14) $\approx$	$\alpha = 90^\circ$
	b = 10.3765(19) $\approx$	$\beta = 90.920(7)^\circ$
	c = 17.058(3) $\approx$	$\gamma = 90^\circ$
Volume	1222.7(4) $\approx^3$	
Z	2	
Density (calculated)	1.224 g/cm <sup>3</sup>	
Absorption coefficient	0.126 mm <sup>-1</sup>	
F(000)	484	
Crystal size	0.04 x 0.32 x 0.33 mm <sup>3</sup>	
Theta range for data collection	2.30 to 32.80 $^\circ$	
Index ranges	-10 $\leq$ h $\leq$ 10, -15 $\leq$ k $\leq$ 14, -25 $\leq$ l $\leq$ 25	
Reflections collected	76181	
Independent reflections	8271 [R(int) = 0.0400]	
Completeness to theta = 25.242 $^\circ$	99.9 %	
Absorption correction	Semi-empirical from equivalents	
Max. and min. transmission	1.0000 and 0.9658	
Refinement method	Full-matrix least-squares on F <sup>2</sup>	
Data / restraints / parameters	8271 / 1 / 294	
Goodness-of-fit on F <sup>2</sup>	1.035	
Final R indices [I > 2 $\sigma$ (I)]	R1 = 0.0401, wR2 = 0.0827	
R indices (all data)	R1 = 0.0511, wR2 = 0.0865	
Absolute structure parameter [Flack]	0.03(2)	
Absolute structure parameter [Hoofit]	0.03(2)	
Extinction coefficient	n/a	
Largest diff. peak and hole	0.38 and -0.28 e. $\approx^3$	

**Table A3.5.3** Atomic coordinates ( $\times 10^5$ ) and equivalent isotropic displacement parameters ( $\text{\AA}^2 10^{-2}$ ) for cyclobutane **83**.  $U(\text{eq})$  is defined as one third of the trace of the orthogonalized  $U^{ij}$  tensor.

	x	y	z	U(eq)
Si(1)	84284(6)	63687(4)	52641(3)	131(1)
O(1)	111852(17)	29694(12)	7683(7)	152(2)
O(2)	79881(18)	57572(12)	914(7)	147(2)
O(3)	38726(17)	51229(12)	1471(7)	144(2)
O(4)	38244(19)	62608(14)	12393(8)	225(3)
C(1)	82860(30)	50711(17)	60272(10)	171(3)
C(2)	99300(30)	44260(19)	63105(11)	232(4)
C(3)	98070(40)	34900(20)	68921(13)	321(5)
C(4)	80480(40)	31820(20)	72063(12)	351(6)
C(5)	63960(40)	38080(20)	69452(13)	352(5)
C(6)	65160(30)	47390(20)	63599(12)	262(4)
C(7)	110220(30)	66249(18)	50382(11)	186(4)
C(8)	73000(30)	78492(19)	56752(12)	216(4)
C(9)	70990(20)	58674(17)	43479(10)	146(3)
C(10)	54230(20)	64340(20)	41591(10)	198(3)
C(11)	79900(30)	48322(19)	38422(10)	187(4)
C(12)	69380(20)	45416(17)	30720(9)	143(3)
C(13)	78020(20)	35684(16)	24887(9)	141(3)
C(14)	71910(30)	21741(18)	25210(11)	229(4)
C(15)	99620(30)	38166(19)	22866(10)	171(3)
C(16)	93360(20)	44468(16)	14974(9)	125(3)
C(17)	96770(20)	35768(16)	8123(9)	112(3)
C(18)	81300(20)	34745(16)	1844(9)	119(3)
C(19)	80950(20)	46296(17)	-3905(9)	134(3)
C(20)	98020(20)	46930(20)	-9383(10)	186(3)
C(21)	61600(20)	43949(18)	-8193(10)	147(3)
C(22)	47800(20)	39861(16)	-1795(10)	131(3)



**Table A3.5.3** *Cont'd*

C(23)	43930(20)	53252(16)	8983(10)	136(3)
C(24)	60350(20)	33804(15)	4887(9)	115(3)
C(25)	55500(20)	41887(15)	12201(10)	116(3)
C(26)	72260(20)	44950(16)	17844(9)	109(3)
C(27)	69120(20)	55650(16)	24121(9)	129(3)

**Table A3.5.4** Bond Lengths [ $\text{\AA}$ ] and angles [ $^\circ$ ] for Cyclobutane **83**.

Si(1)-C(1)	1.8765(19)
Si(1)-C(7)	1.8576(18)
Si(1)-C(8)	1.8646(19)
Si(1)-C(9)	1.8736(17)
O(1)-C(17)	1.221(2)
O(2)-H(2)	0.8400
O(2)-C(19)	1.433(2)
O(3)-C(22)	1.451(2)
O(3)-C(23)	1.342(2)
O(4)-C(23)	1.201(2)
C(1)-C(2)	1.398(3)
C(1)-C(6)	1.399(3)
C(2)-H(2A)	0.9500
C(2)-C(3)	1.392(3)
C(3)-H(3)	0.9500
C(3)-C(4)	1.374(4)
C(4)-H(4)	0.9500
C(4)-C(5)	1.381(4)
C(5)-H(5)	0.9500
C(5)-C(6)	1.392(3)
C(6)-H(6)	0.9500
C(7)-H(7A)	0.9800
C(7)-H(7B)	0.9800
C(7)-H(7C)	0.9800
C(8)-H(8A)	0.9800
C(8)-H(8B)	0.9800
C(8)-H(8C)	0.9800
C(9)-C(10)	1.334(2)
C(9)-C(11)	1.514(2)
C(10)-H(10A)	0.9500
C(10)-H(10B)	0.9500
C(11)-H(11A)	0.9900
C(11)-H(11B)	0.9900
C(11)-C(12)	1.521(2)

**Table A3.5.4** Cont'd

C(12)-H(12)	1.0000
C(12)-C(13)	1.544(2)
C(12)-C(27)	1.547(2)
C(13)-C(14)	1.508(3)
C(13)-C(15)	1.558(2)
C(13)-C(26)	1.585(2)
C(14)-H(14A)	0.9800
C(14)-H(14B)	0.9800
C(14)-H(14C)	0.9800
C(15)-H(15A)	0.9900
C(15)-H(15B)	0.9900
C(15)-C(16)	1.552(2)
C(16)-H(16)	1.0000
C(16)-C(17)	1.498(2)
C(16)-C(26)	1.546(2)
C(17)-C(18)	1.505(2)
C(18)-H(18)	1.0000
C(18)-C(19)	1.549(2)
C(18)-C(24)	1.548(2)
C(19)-C(20)	1.518(2)
C(19)-C(21)	1.533(2)
C(20)-H(20A)	0.9800
C(20)-H(20B)	0.9800
C(20)-H(20C)	0.9800
C(21)-H(21A)	0.9900
C(21)-H(21B)	0.9900
C(21)-C(22)	1.521(2)
C(22)-H(22)	1.0000
C(22)-C(24)	1.554(2)
C(23)-C(25)	1.522(2)
C(24)-H(24)	1.0000
C(24)-C(25)	1.544(2)
C(25)-H(25)	1.0000
C(25)-C(26)	1.527(2)

**Table A3.5.4** Cont'd

C(26)-C(27)	1.560(2)
C(27)-H(27A)	0.9900
C(27)-H(27B)	0.9900
C(7)-Si(1)-C(1)	107.95(9)
C(7)-Si(1)-C(8)	111.74(9)
C(7)-Si(1)-C(9)	109.15(8)
C(8)-Si(1)-C(1)	107.66(9)
C(8)-Si(1)-C(9)	109.90(9)
C(9)-Si(1)-C(1)	110.42(8)
C(19)-O(2)-H(2)	109.5
C(23)-O(3)-C(22)	112.53(13)
C(2)-C(1)-Si(1)	122.14(14)
C(2)-C(1)-C(6)	116.87(18)
C(6)-C(1)-Si(1)	120.95(16)
C(1)-C(2)-H(2A)	119.3
C(3)-C(2)-C(1)	121.5(2)
C(3)-C(2)-H(2A)	119.3
C(2)-C(3)-H(3)	119.8
C(4)-C(3)-C(2)	120.3(2)
C(4)-C(3)-H(3)	119.8
C(3)-C(4)-H(4)	120.1
C(3)-C(4)-C(5)	119.8(2)
C(5)-C(4)-H(4)	120.1
C(4)-C(5)-H(5)	120.0
C(4)-C(5)-C(6)	120.0(2)
C(6)-C(5)-H(5)	120.0
C(1)-C(6)-H(6)	119.2
C(5)-C(6)-C(1)	121.6(2)
C(5)-C(6)-H(6)	119.2
Si(1)-C(7)-H(7A)	109.5
Si(1)-C(7)-H(7B)	109.5
Si(1)-C(7)-H(7C)	109.5
H(7A)-C(7)-H(7B)	109.5
H(7A)-C(7)-H(7C)	109.5

**Table A3.5.4** Cont'd

H(7B)-C(7)-H(7C)	109.5
Si(1)-C(8)-H(8A)	109.5
Si(1)-C(8)-H(8B)	109.5
Si(1)-C(8)-H(8C)	109.5
H(8A)-C(8)-H(8B)	109.5
H(8A)-C(8)-H(8C)	109.5
H(8B)-C(8)-H(8C)	109.5
C(10)-C(9)-Si(1)	119.42(13)
C(10)-C(9)-C(11)	122.28(16)
C(11)-C(9)-Si(1)	118.29(12)
C(9)-C(10)-H(10A)	120.0
C(9)-C(10)-H(10B)	120.0
H(10A)-C(10)-H(10B)	120.0
C(9)-C(11)-H(11A)	108.3
C(9)-C(11)-H(11B)	108.3
C(9)-C(11)-C(12)	116.09(15)
H(11A)-C(11)-H(11B)	107.4
C(12)-C(11)-H(11A)	108.3
C(12)-C(11)-H(11B)	108.3
C(11)-C(12)-H(12)	108.9
C(11)-C(12)-C(13)	120.12(14)
C(11)-C(12)-C(27)	119.48(15)
C(13)-C(12)-H(12)	108.9
C(13)-C(12)-C(27)	88.87(12)
C(27)-C(12)-H(12)	108.9
C(12)-C(13)-C(15)	114.57(14)
C(12)-C(13)-C(26)	89.81(12)
C(14)-C(13)-C(12)	119.49(14)
C(14)-C(13)-C(15)	115.87(15)
C(14)-C(13)-C(26)	122.86(15)
C(15)-C(13)-C(26)	87.81(12)
C(13)-C(14)-H(14A)	109.5
C(13)-C(14)-H(14B)	109.5
C(13)-C(14)-H(14C)	109.5

**Table A3.5.4** Cont'd

H(14A)-C(14)-H(14B)	109.5
H(14A)-C(14)-H(14C)	109.5
H(14B)-C(14)-H(14C)	109.5
C(13)-C(15)-H(15A)	113.6
C(13)-C(15)-H(15B)	113.6
H(15A)-C(15)-H(15B)	110.8
C(16)-C(15)-C(13)	90.41(12)
C(16)-C(15)-H(15A)	113.6
C(16)-C(15)-H(15B)	113.6
C(15)-C(16)-H(16)	112.6
C(17)-C(16)-C(15)	112.18(14)
C(17)-C(16)-H(16)	112.6
C(17)-C(16)-C(26)	115.32(13)
C(26)-C(16)-C(15)	89.42(12)
C(26)-C(16)-H(16)	112.6
O(1)-C(17)-C(16)	120.27(15)
O(1)-C(17)-C(18)	121.13(15)
C(16)-C(17)-C(18)	118.59(14)
C(17)-C(18)-H(18)	107.7
C(17)-C(18)-C(19)	113.56(13)
C(17)-C(18)-C(24)	115.02(13)
C(19)-C(18)-H(18)	107.7
C(24)-C(18)-H(18)	107.7
C(24)-C(18)-C(19)	104.83(13)
O(2)-C(19)-C(18)	105.62(13)
O(2)-C(19)-C(20)	111.44(14)
O(2)-C(19)-C(21)	110.55(13)
C(20)-C(19)-C(18)	114.76(14)
C(20)-C(19)-C(21)	113.17(14)
C(21)-C(19)-C(18)	100.60(13)
C(19)-C(20)-H(20A)	109.5
C(19)-C(20)-H(20B)	109.5
C(19)-C(20)-H(20C)	109.5
H(20A)-C(20)-H(20B)	109.5

**Table A3.5.4** Cont'd

H(20A)-C(20)-H(20C)	109.5
H(20B)-C(20)-H(20C)	109.5
C(19)-C(21)-H(21A)	110.8
C(19)-C(21)-H(21B)	110.8
H(21A)-C(21)-H(21B)	108.9
C(22)-C(21)-C(19)	104.71(13)
C(22)-C(21)-H(21A)	110.8
C(22)-C(21)-H(21B)	110.8
O(3)-C(22)-C(21)	109.16(14)
O(3)-C(22)-H(22)	111.3
O(3)-C(22)-C(24)	106.65(12)
C(21)-C(22)-H(22)	111.3
C(21)-C(22)-C(24)	106.87(13)
C(24)-C(22)-H(22)	111.3
O(3)-C(23)-C(25)	110.75(14)
O(4)-C(23)-O(3)	120.29(16)
O(4)-C(23)-C(25)	128.72(16)
C(18)-C(24)-C(22)	104.01(13)
C(18)-C(24)-H(24)	110.4
C(22)-C(24)-H(24)	110.4
C(25)-C(24)-C(18)	116.90(13)
C(25)-C(24)-C(22)	104.31(13)
C(25)-C(24)-H(24)	110.4
C(23)-C(25)-C(24)	104.41(13)
C(23)-C(25)-H(25)	105.9
C(23)-C(25)-C(26)	117.04(13)
C(24)-C(25)-H(25)	105.9
C(26)-C(25)-C(24)	116.77(13)
C(26)-C(25)-H(25)	105.9
C(16)-C(26)-C(13)	89.64(12)
C(16)-C(26)-C(27)	112.50(13)
C(25)-C(26)-C(13)	122.03(14)
C(25)-C(26)-C(16)	120.17(13)
C(25)-C(26)-C(27)	117.93(13)

**Table A3.5.4** Cont'd

C(27)-C(26)-C(13)	86.99(12)
C(12)-C(27)-C(26)	90.61(12)
C(12)-C(27)-H(27A)	113.5
C(12)-C(27)-H(27B)	113.5
C(26)-C(27)-H(27A)	113.5
C(26)-C(27)-H(27B)	113.5
H(27A)-C(27)-H(27B)	110.8

---

Symmetry transformations used to generate equivalent atoms:



**Table A3.5.5** Anisotropic displacement parameters ( $\text{\AA}^2 \times 10^4$ ) for cyclobutane **83**.

The anisotropic displacement factor exponent takes the form:  $-2\pi^2 [ h^2 a^{*2} U^{11} + \dots$

$+ 2 h k a^* b^* U^{12} ]$

	U <sup>11</sup>	U <sup>22</sup>	U <sup>33</sup>	U <sup>23</sup>	U <sup>13</sup>	U <sup>12</sup>
Si(1)	159(2)	129(2)	106(2)	-10(2)	21(2)	6(2)
O(1)	118(5)	178(6)	160(6)	-24(5)	17(4)	24(5)
O(2)	205(6)	121(5)	116(5)	10(4)	11(5)	-30(5)
O(3)	140(5)	149(6)	142(6)	-6(5)	-20(4)	22(4)
O(4)	247(6)	212(7)	214(6)	-56(6)	-47(5)	99(6)
C(1)	269(9)	143(8)	102(7)	-31(6)	9(6)	-29(7)
C(2)	332(10)	174(9)	190(9)	-5(7)	-24(7)	0(8)
C(3)	538(14)	193(10)	230(10)	32(8)	-100(9)	-2(9)
C(4)	682(17)	213(10)	157(9)	47(8)	-33(10)	-139(10)
C(5)	521(14)	326(12)	212(10)	7(9)	93(9)	-188(11)
C(6)	292(10)	287(11)	208(9)	1(8)	36(7)	-79(8)
C(7)	176(8)	190(9)	194(8)	0(7)	28(6)	-11(6)
C(8)	256(9)	181(9)	211(9)	-71(7)	48(7)	24(7)
C(9)	175(8)	169(8)	95(7)	-17(6)	25(6)	3(6)
C(10)	193(8)	259(9)	143(7)	-44(8)	24(6)	38(8)
C(11)	230(8)	212(9)	117(7)	-29(6)	-24(6)	88(7)
C(12)	176(7)	150(8)	103(7)	-8(6)	2(6)	21(6)
C(13)	200(8)	127(7)	94(7)	1(6)	-3(6)	25(6)
C(14)	380(11)	129(8)	177(9)	26(7)	11(8)	6(8)
C(15)	169(8)	224(9)	120(8)	-34(7)	-25(6)	64(7)
C(16)	117(7)	140(7)	117(7)	-24(6)	-9(5)	11(6)
C(17)	123(7)	106(7)	109(7)	10(6)	17(5)	-21(6)
C(18)	113(7)	126(7)	118(7)	-20(6)	0(5)	-2(6)
C(19)	133(7)	158(8)	110(7)	-11(6)	6(6)	-8(6)
C(20)	152(8)	286(9)	120(7)	-10(7)	19(6)	-22(7)
C(21)	147(7)	187(8)	108(7)	0(6)	-12(6)	-1(6)
C(22)	124(7)	138(7)	130(8)	-25(6)	-22(6)	-5(6)
C(23)	112(7)	145(8)	150(8)	2(6)	1(6)	-6(6)

**Table A3.5.5** *Cont'd*

C(24)	110(7)	110(7)	125(7)	-18(6)	4(6)	-24(5)
C(25)	113(7)	114(7)	121(7)	-7(6)	17(5)	-17(5)
C(26)	123(7)	104(7)	100(7)	-2(6)	-2(5)	9(6)
C(27)	162(8)	114(7)	110(7)	-23(6)	-5(6)	15(6)

---

**Table A3.5.6** Hydrogen coordinates ( $\times 10^2$ ) and isotropic displacement parameters $(\text{\AA}^2 \times 10^2)$  for cyclobutane **83**.

	x	y	z	U(eq)
H(2)	8157	6416	-185	22
H(2A)	11158	4631	6101	28
H(3)	10946	3063	7073	39
H(4)	7969	2541	7602	42
H(5)	5179	3604	7165	42
H(6)	5368	5158	6182	31
H(7A)	11550	5842	4802	28
H(7B)	11742	6823	5523	28
H(7C)	11141	7345	4670	28
H(8A)	7307	8535	5280	32
H(8B)	8038	8129	6140	32
H(8C)	5963	7662	5821	32
H(10A)	4744	6191	3693	24
H(10B)	4907	7080	4490	24
H(11A)	8064	4026	4152	22
H(11B)	9332	5093	3723	22
H(12)	5576	4284	3185	17
H(14A)	5777	2123	2544	34
H(14B)	7764	1767	2988	34
H(14C)	7635	1726	2051	34
H(15A)	10625	4419	2652	21
H(15B)	10726	3017	2223	21
H(16)	9907	5324	1425	15
H(18)	8391	2679	-127	14
H(20A)	9563	5356	-1337	28
H(20B)	9968	3855	-1194	28
H(20C)	10979	4908	-637	28

**Table A3.5.6** *Cont'd*

H(21A)	5698	5191	-1081	18
H(21B)	6288	3708	-1218	18
H(22)	3791	3362	-384	16
H(24)	5666	2459	570	14
H(25)	4617	3660	1526	14
H(27A)	7993	6189	2452	15
H(27B)	5656	6017	2353	15

**Table A3.5.7** Torsion angles [°] for cyclobutane **83**.

---

Si(1)-C(1)-C(2)-C(3)	178.21(15)
Si(1)-C(1)-C(6)-C(5)	-177.84(16)
Si(1)-C(9)-C(11)-C(12)	-175.06(13)
O(1)-C(17)-C(18)-C(19)	-101.67(18)
O(1)-C(17)-C(18)-C(24)	137.55(16)
O(2)-C(19)-C(21)-C(22)	-69.88(17)
O(3)-C(22)-C(24)-C(18)	-116.84(13)
O(3)-C(22)-C(24)-C(25)	6.18(16)
O(3)-C(23)-C(25)-C(24)	11.88(17)
O(3)-C(23)-C(25)-C(26)	142.66(14)
O(4)-C(23)-C(25)-C(24)	-173.87(17)
O(4)-C(23)-C(25)-C(26)	-43.1(2)
C(1)-Si(1)-C(9)-C(10)	108.36(16)
C(1)-Si(1)-C(9)-C(11)	-72.16(15)
C(1)-C(2)-C(3)-C(4)	-0.3(3)
C(2)-C(1)-C(6)-C(5)	-0.1(3)
C(2)-C(3)-C(4)-C(5)	-0.2(3)
C(3)-C(4)-C(5)-C(6)	0.6(3)
C(4)-C(5)-C(6)-C(1)	-0.5(3)
C(6)-C(1)-C(2)-C(3)	0.5(3)
C(7)-Si(1)-C(1)-C(2)	-2.71(18)
C(7)-Si(1)-C(1)-C(6)	174.94(15)
C(7)-Si(1)-C(9)-C(10)	-133.12(15)
C(7)-Si(1)-C(9)-C(11)	46.36(16)
C(8)-Si(1)-C(1)-C(2)	-123.49(16)
C(8)-Si(1)-C(1)-C(6)	54.16(17)
C(8)-Si(1)-C(9)-C(10)	-10.26(18)
C(8)-Si(1)-C(9)-C(11)	169.22(14)
C(9)-Si(1)-C(1)-C(2)	116.53(15)
C(9)-Si(1)-C(1)-C(6)	-65.82(17)
C(9)-C(11)-C(12)-C(13)	175.87(15)
C(9)-C(11)-C(12)-C(27)	68.3(2)
C(10)-C(9)-C(11)-C(12)	4.4(3)

**Table A3.5.7** *Cont'd*

C(11)-C(12)-C(13)-C(14)	93.2(2)
C(11)-C(12)-C(13)-C(15)	-50.9(2)
C(11)-C(12)-C(13)-C(26)	-138.41(16)
C(11)-C(12)-C(27)-C(26)	139.19(15)
C(12)-C(13)-C(15)-C(16)	-101.10(15)
C(12)-C(13)-C(26)-C(16)	126.97(12)
C(12)-C(13)-C(26)-C(25)	-106.95(16)
C(12)-C(13)-C(26)-C(27)	14.41(12)
C(13)-C(12)-C(27)-C(26)	14.75(12)
C(13)-C(15)-C(16)-C(17)	-104.61(14)
C(13)-C(15)-C(16)-C(26)	12.62(13)
C(13)-C(26)-C(27)-C(12)	-14.38(12)
C(14)-C(13)-C(15)-C(16)	113.47(16)
C(14)-C(13)-C(26)-C(16)	-107.31(17)
C(14)-C(13)-C(26)-C(25)	18.8(2)
C(14)-C(13)-C(26)-C(27)	140.14(16)
C(15)-C(13)-C(26)-C(16)	12.37(12)
C(15)-C(13)-C(26)-C(25)	138.45(15)
C(15)-C(13)-C(26)-C(27)	-100.19(12)
C(15)-C(16)-C(17)-O(1)	-43.4(2)
C(15)-C(16)-C(17)-C(18)	136.71(15)
C(15)-C(16)-C(26)-C(13)	-12.41(13)
C(15)-C(16)-C(26)-C(25)	-139.99(15)
C(15)-C(16)-C(26)-C(27)	74.19(15)
C(16)-C(17)-C(18)-C(19)	78.18(18)
C(16)-C(17)-C(18)-C(24)	-42.6(2)
C(16)-C(26)-C(27)-C(12)	-102.75(14)
C(17)-C(16)-C(26)-C(13)	101.98(15)
C(17)-C(16)-C(26)-C(25)	-25.6(2)
C(17)-C(16)-C(26)-C(27)	-171.42(13)
C(17)-C(18)-C(19)-O(2)	-53.01(17)
C(17)-C(18)-C(19)-C(20)	70.15(18)
C(17)-C(18)-C(19)-C(21)	-168.04(13)
C(17)-C(18)-C(24)-C(22)	151.53(14)
C(17)-C(18)-C(24)-C(25)	37.2(2)

**Table A3.5.7** *Cont'd*

C(18)-C(19)-C(21)-C(22)	41.39(16)
C(18)-C(24)-C(25)-C(23)	103.80(15)
C(18)-C(24)-C(25)-C(26)	-27.1(2)
C(19)-C(18)-C(24)-C(22)	26.08(16)
C(19)-C(18)-C(24)-C(25)	-88.27(16)
C(19)-C(21)-C(22)-O(3)	88.93(15)
C(19)-C(21)-C(22)-C(24)	-26.05(17)
C(20)-C(19)-C(21)-C(22)	164.31(15)
C(21)-C(22)-C(24)-C(18)	-0.18(17)
C(21)-C(22)-C(24)-C(25)	122.84(14)
C(22)-O(3)-C(23)-O(4)	176.83(15)
C(22)-O(3)-C(23)-C(25)	-8.36(18)
C(22)-C(24)-C(25)-C(23)	-10.38(15)
C(22)-C(24)-C(25)-C(26)	-141.32(14)
C(23)-O(3)-C(22)-C(21)	-113.97(15)
C(23)-O(3)-C(22)-C(24)	1.16(17)
C(23)-C(25)-C(26)-C(13)	146.06(15)
C(23)-C(25)-C(26)-C(16)	-103.13(17)
C(23)-C(25)-C(26)-C(27)	40.9(2)
C(24)-C(18)-C(19)-O(2)	73.35(14)
C(24)-C(18)-C(19)-C(20)	-163.50(14)
C(24)-C(18)-C(19)-C(21)	-41.68(15)
C(24)-C(25)-C(26)-C(13)	-89.16(18)
C(24)-C(25)-C(26)-C(16)	21.6(2)
C(24)-C(25)-C(26)-C(27)	165.67(13)
C(25)-C(26)-C(27)-C(12)	110.60(15)
C(26)-C(13)-C(15)-C(16)	-12.32(12)
C(26)-C(16)-C(17)-O(1)	-143.85(16)
C(26)-C(16)-C(17)-C(18)	36.3(2)
C(27)-C(12)-C(13)-C(14)	-142.94(16)
C(27)-C(12)-C(13)-C(15)	72.99(15)
C(27)-C(12)-C(13)-C(26)	-14.51(12)

---

Symmetry transformations used to generate equivalent atoms:

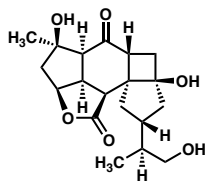
**Table A3.5.8** Hydrogen bonds for cyclobutane **83** [ $\text{\AA}$  and  $^\circ$ ].

D-H...A	d(D-H)	d(H...A)	d(D...A)	<(DHA)
C(13)-H(13)...O(2)	1.00	2.49	3.079(11)	116.9
C(15)-H(15)...O(3)#1	1.00	2.50	3.246(11)	130.8
O(2)-H(2A)...O(1)#2	0.83(3)	2.16(3)	2.996(10)	178(15)
C(17)-H(17A)...O(1)#2	0.99	2.58	3.430(11)	143.8
C(19)-H(19)...O(3)#1	1.00	2.52	3.267(11)	131.5

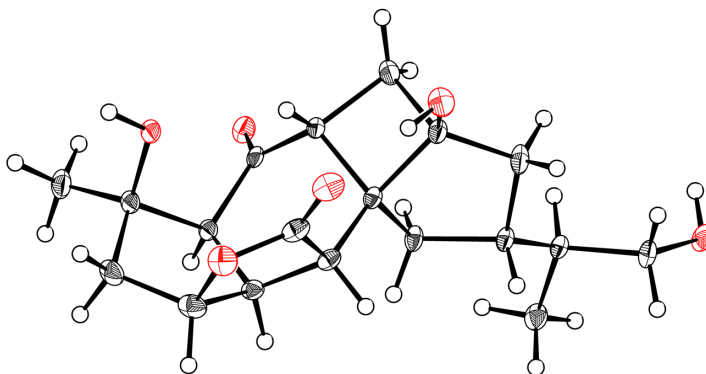
Symmetry transformations used to generate equivalent atoms:

#1  $-x+1, y+1/2, -z$  #2  $-x, y-1/2, -z$



**A3.6 X-RAY CRYSTAL STRUCTURE ANALYSIS OF CYCLOBUTANOL 90**

90

Contents*Table A3.6.1. Experimental Details**Table A3.6.2. Crystal Data**Table A3.6.3. Atomic Coordinates**Table A3.6.4. Full Bond Distances and Angles**Table A3.6.5. Anisotropic Displacement Parameters**Table A3.6.6. Hydrogen Atomic Coordinates**Table A3.6.7. Torsion Angles**Table A3.6.8. Hydrogen Bond Distances and Angles***Figure A3.6.1** X-Ray crystal structure of cyclobutanol 90

**Table A3.6.1.** Experimental details for X-Ray structure determination of cyclobutanol **90**.

*Refinement Details*

A crystal was mounted on a polyimide MiTeGen loop with STP Oil Treatment and placed under a nitrogen stream. Low temperature (100K) X-ray data were collected with a Bruker AXS KAPPA APEX II diffractometer diffractometer running at 50 kV and 30 mA (Mo  $K_{\alpha}$  = 0.71073 Å; PHOTON 100 CMOS detector with TRIUMPH graphite monochromator). All diffractometer manipulations, including data collection, integration, and scaling were carried out using the Bruker APEX3 software. An absorption correction was applied using SADABS. The space group was determined and the structure solved by intrinsic phasing using XT. Refinement was full-matrix least squares on  $F^2$  using XL. All non-hydrogen atoms were refined using anisotropic displacement parameters. Hydrogen atoms were placed in idealized positions and the coordinates refined. The isotropic displacement parameters of all hydrogen atoms were fixed at 1.2 times the  $U_{eq}$  value of the bonded atom.

*Special Refinement Details*

Compound **90** crystallizes in the orthorhombic space group  $P2_12_12_1$  (#19) with one molecule in the asymmetric unit.

**Table A3.6.2** Crystal data and structure refinement for cyclobutanol **90**.

Empirical formula	C <sub>19</sub> H <sub>26</sub> O <sub>6</sub>	
Formula weight	350.40	
Temperature	100 K	
Wavelength	0.71073 Å	
Crystal system	Orthorhombic	
Space group	P2 <sub>1</sub> 2 <sub>1</sub> 2 <sub>1</sub>	
Unit cell dimensions	a = 10.221(3) Å	a = 90°
	b = 12.581(3) Å	b = 90°
	c = 13.333(4) Å	g = 90°
Volume	1714.4(8) Å <sup>3</sup>	
Z	4	
Density (calculated)	1.358 g/cm <sup>3</sup>	
Absorption coefficient	0.100 mm <sup>-1</sup>	
F(000)	752	
Crystal size	0.31 x 0.19 x 0.18 mm <sup>3</sup>	
Theta range for data collection	2.226 to 36.285°.	
Index ranges	-16 ≤ h ≤ 16, -20 ≤ k ≤ 20, -22 ≤ l ≤ 22	
Reflections collected	73152	
Independent reflections	7997 [R(int) = 0.0477]	
Completeness to theta = 25.242°	100.0 %	
Absorption correction	Semi-empirical from equivalents	
Max. and min. transmission	1.0000 and 0.9208	
Refinement method	Full-matrix least-squares on F <sup>2</sup>	
Data / restraints / parameters	7997 / 0 / 231	
Goodness-of-fit on F <sup>2</sup>	1.069	
Final R indices [I > 2σ(I)]	R1 = 0.0424, wR2 = 0.0942	
R indices (all data)	R1 = 0.0592, wR2 = 0.1007	
Absolute structure parameter [Flack]	0.21(16)	
Absolute structure parameter [Hooft]	0.26(15)	
Extinction coefficient	n/a	
Largest diff. peak and hole	0.383 and -0.250 e.Å <sup>-3</sup>	

**Table A3.6.3** Atomic coordinates ( $\times 10^5$ ) and equivalent isotropic displacement parameters ( $\text{\AA}^2 \times 10^4$ ) for cyclobutanol **90**.  $U(\text{eq})$  is defined as one third of the trace of the orthogonalized  $U^{ij}$  tensor.

	x	y	z	U(eq)
O(1)	68042(10)	78131(7)	63641(8)	165(2)
O(2)	86227(11)	70321(8)	47229(8)	213(2)
O(3)	70632(11)	61684(9)	39054(7)	213(2)
O(4)	52317(11)	47286(8)	43910(8)	209(2)
O(5)	62828(10)	58461(8)	81516(7)	170(2)
O(6)	61450(11)	-568(7)	63049(8)	186(2)
C(1)	80656(12)	63996(9)	70998(9)	120(2)
C(2)	79658(13)	76259(9)	69319(10)	142(2)
C(3)	79192(15)	82417(10)	79130(11)	201(3)
C(4)	91843(14)	78776(11)	63116(11)	195(3)
C(5)	94105(14)	69305(11)	56324(11)	193(3)
C(6)	88652(12)	59459(10)	61866(9)	136(2)
C(7)	81180(12)	53340(10)	53598(9)	136(2)
C(8)	78429(13)	61948(11)	45872(10)	170(2)
C(9)	69363(12)	47732(9)	58110(9)	116(2)
C(10)	56514(13)	43122(10)	53164(10)	139(2)
C(11)	48826(13)	48194(11)	62174(10)	181(2)
C(12)	60524(12)	55734(9)	63681(9)	124(2)
C(13)	67102(12)	59314(9)	72997(9)	118(2)
C(14)	73647(13)	38142(9)	64645(9)	139(2)
C(15)	70260(13)	28115(9)	58468(9)	131(2)
C(16)	57444(15)	31051(10)	52945(11)	187(3)
C(17)	68816(13)	17984(9)	64757(9)	127(2)
C(18)	66587(14)	8454(10)	57824(10)	159(2)
C(19)	80353(15)	15980(10)	71809(10)	181(2)

**Table A3.6.4** Bond lengths [ $\text{\AA}$ ] and angles [ $^\circ$ ] for cyclobutanol **90**.

---

O(1)-H(1)	0.8400
O(1)-C(2)	1.4276(16)
O(2)-C(5)	1.4612(19)
O(2)-C(8)	1.3333(18)
O(3)-C(8)	1.2094(17)
O(4)-H(4)	0.8400
O(4)-C(10)	1.4075(16)
O(5)-C(13)	1.2217(15)
O(6)-H(6)	0.8400
O(6)-C(18)	1.4316(16)
C(1)-H(1A)	1.0000
C(1)-C(2)	1.5623(17)
C(1)-C(6)	1.5736(18)
C(1)-C(13)	1.5287(18)
C(2)-C(3)	1.5210(19)
C(2)-C(4)	1.528(2)
C(3)-H(3A)	0.9800
C(3)-H(3B)	0.9800
C(3)-H(3C)	0.9800
C(4)-H(4A)	0.9900
C(4)-H(4B)	0.9900
C(4)-C(5)	1.514(2)
C(5)-H(5)	1.0000
C(5)-C(6)	1.5463(18)
C(6)-H(6A)	1.0000
C(6)-C(7)	1.5464(18)
C(7)-H(7)	1.0000
C(7)-C(8)	1.5209(17)
C(7)-C(9)	1.5227(17)
C(9)-C(10)	1.5799(18)
C(9)-C(12)	1.5432(16)

**Table A3.6.4** *Cont'd*

C(9)-C(14)	1.5513(17)
C(10)-C(11)	1.5708(19)
C(10)-C(16)	1.5219(18)
C(11)-H(11A)	0.9900
C(11)-H(11B)	0.9900
C(11)-C(12)	1.5394(18)
C(12)-H(12)	1.0000
C(12)-C(13)	1.4825(17)
C(14)-H(14A)	0.9900
C(14)-H(14B)	0.9900
C(14)-C(15)	1.5459(17)
C(15)-H(15)	1.0000
C(15)-C(16)	1.5474(19)
C(15)-C(17)	1.5328(17)
C(16)-H(16A)	0.9900
C(16)-H(16B)	0.9900
C(17)-H(17)	1.0000
C(17)-C(18)	1.5310(17)
C(17)-C(19)	1.5290(19)
C(18)-H(18A)	0.9900
C(18)-H(18B)	0.9900
C(19)-H(19A)	0.9800
C(19)-H(19B)	0.9800
C(19)-H(19C)	0.9800
C(2)-O(1)-H(1)	109.5
C(8)-O(2)-C(5)	111.89(10)
C(10)-O(4)-H(4)	109.5
C(18)-O(6)-H(6)	109.5
C(2)-C(1)-H(1A)	107.3
C(2)-C(1)-C(6)	106.34(10)
C(6)-C(1)-H(1A)	107.3
C(13)-C(1)-H(1A)	107.3
C(13)-C(1)-C(2)	110.27(10)
C(13)-C(1)-C(6)	117.76(10)
O(1)-C(2)-C(1)	107.05(10)

**Table A3.6.4** *Cont'd*

O(1)-C(2)-C(3)	110.24(11)
O(1)-C(2)-C(4)	110.89(11)
C(3)-C(2)-C(1)	112.44(10)
C(3)-C(2)-C(4)	112.67(11)
C(4)-C(2)-C(1)	103.24(10)
C(2)-C(3)-H(3A)	109.5
C(2)-C(3)-H(3B)	109.5
C(2)-C(3)-H(3C)	109.5
H(3A)-C(3)-H(3B)	109.5
H(3A)-C(3)-H(3C)	109.5
H(3B)-C(3)-H(3C)	109.5
C(2)-C(4)-H(4A)	110.4
C(2)-C(4)-H(4B)	110.4
H(4A)-C(4)-H(4B)	108.6
C(5)-C(4)-C(2)	106.56(11)
C(5)-C(4)-H(4A)	110.4
C(5)-C(4)-H(4B)	110.4
O(2)-C(5)-C(4)	110.08(12)
O(2)-C(5)-H(5)	111.4
O(2)-C(5)-C(6)	105.55(11)
C(4)-C(5)-H(5)	111.4
C(4)-C(5)-C(6)	106.83(11)
C(6)-C(5)-H(5)	111.4
C(1)-C(6)-H(6A)	109.6
C(5)-C(6)-C(1)	105.44(10)
C(5)-C(6)-H(6A)	109.6
C(5)-C(6)-C(7)	103.66(10)
C(7)-C(6)-C(1)	118.41(10)
C(7)-C(6)-H(6A)	109.6
C(6)-C(7)-H(7)	109.0
C(8)-C(7)-C(6)	102.68(10)
C(8)-C(7)-H(7)	109.0
C(8)-C(7)-C(9)	116.80(11)
C(9)-C(7)-C(6)	109.92(10)
C(9)-C(7)-H(7)	109.0

**Table A3.6.4** Cont'd

O(2)-C(8)-C(7)	111.12(11)
O(3)-C(8)-O(2)	121.17(12)
O(3)-C(8)-C(7)	127.68(13)
C(7)-C(9)-C(10)	131.65(10)
C(7)-C(9)-C(12)	110.62(9)
C(7)-C(9)-C(14)	111.00(10)
C(12)-C(9)-C(10)	87.35(9)
C(12)-C(9)-C(14)	113.72(10)
C(14)-C(9)-C(10)	100.58(9)
O(4)-C(10)-C(9)	118.85(11)
O(4)-C(10)-C(11)	111.51(11)
O(4)-C(10)-C(16)	111.94(11)
C(11)-C(10)-C(9)	86.99(9)
C(16)-C(10)-C(9)	108.81(10)
C(16)-C(10)-C(11)	116.83(12)
C(10)-C(11)-H(11A)	114.0
C(10)-C(11)-H(11B)	114.0
H(11A)-C(11)-H(11B)	111.2
C(12)-C(11)-C(10)	87.80(10)
C(12)-C(11)-H(11A)	114.0
C(12)-C(11)-H(11B)	114.0
C(9)-C(12)-H(12)	108.2
C(11)-C(12)-C(9)	89.41(9)
C(11)-C(12)-H(12)	108.2
C(13)-C(12)-C(9)	109.63(10)
C(13)-C(12)-C(11)	130.45(11)
C(13)-C(12)-H(12)	108.2
O(5)-C(13)-C(1)	121.33(11)
O(5)-C(13)-C(12)	126.17(12)
C(12)-C(13)-C(1)	112.45(10)
C(9)-C(14)-H(14A)	110.6
C(9)-C(14)-H(14B)	110.6
H(14A)-C(14)-H(14B)	108.7
C(15)-C(14)-C(9)	105.80(9)
C(15)-C(14)-H(14A)	110.6



**Table A3.6.4** Cont'd

C(15)-C(14)-H(14B)	110.6
C(14)-C(15)-H(15)	108.7
C(14)-C(15)-C(16)	104.37(10)
C(16)-C(15)-H(15)	108.7
C(17)-C(15)-C(14)	114.12(10)
C(17)-C(15)-H(15)	108.7
C(17)-C(15)-C(16)	112.17(11)
C(10)-C(16)-C(15)	106.38(11)
C(10)-C(16)-H(16A)	110.5
C(10)-C(16)-H(16B)	110.5
C(15)-C(16)-H(16A)	110.5
C(15)-C(16)-H(16B)	110.5
H(16A)-C(16)-H(16B)	108.6
C(15)-C(17)-H(17)	107.5
C(18)-C(17)-C(15)	109.58(10)
C(18)-C(17)-H(17)	107.5
C(19)-C(17)-C(15)	113.53(11)
C(19)-C(17)-H(17)	107.5
C(19)-C(17)-C(18)	110.91(10)
O(6)-C(18)-C(17)	112.44(10)
O(6)-C(18)-H(18A)	109.1
O(6)-C(18)-H(18B)	109.1
C(17)-C(18)-H(18A)	109.1
C(17)-C(18)-H(18B)	109.1
H(18A)-C(18)-H(18B)	107.8
C(17)-C(19)-H(19A)	109.5
C(17)-C(19)-H(19B)	109.5
C(17)-C(19)-H(19C)	109.5
H(19A)-C(19)-H(19B)	109.5
H(19A)-C(19)-H(19C)	109.5
H(19B)-C(19)-H(19C)	109.5

---

Symmetry transformations used to generate equivalent atoms:

**Table A3.6.5** Anisotropic displacement parameters ( $\text{\AA}^2 \times 10^4$ ) for cyclobutanol **90**.

The anisotropic displacement factor exponent takes the form:  $-2p^2 [h^2 a^* 2U^{11} + \dots + 2hk a^* b^* U^{12}]$ .

	U <sup>11</sup>	U <sup>22</sup>	U <sup>33</sup>	U <sup>23</sup>	U <sup>13</sup>	U <sup>12</sup>
O(1)	160(4)	78(3)	256(4)	18(3)	-73(4)	14(3)
O(2)	247(5)	195(5)	197(4)	86(4)	30(4)	-22(4)
O(3)	248(5)	234(5)	155(4)	65(4)	9(4)	49(4)
O(4)	240(5)	171(5)	217(5)	47(4)	-100(4)	13(4)
O(5)	207(5)	140(4)	162(4)	-7(3)	37(3)	-6(3)
O(6)	220(5)	90(4)	246(5)	18(3)	38(4)	9(3)
C(1)	129(5)	80(4)	150(5)	16(4)	-14(4)	3(4)
C(2)	145(5)	78(4)	203(5)	26(4)	-39(4)	-7(4)
C(3)	249(7)	106(5)	248(6)	-17(4)	-65(5)	-1(5)
C(4)	164(6)	138(5)	281(7)	57(5)	-14(5)	-46(4)
C(5)	148(6)	190(6)	241(6)	75(5)	30(5)	-21(5)
C(6)	119(5)	118(5)	171(5)	28(4)	6(4)	15(4)
C(7)	150(5)	119(5)	137(5)	24(4)	14(4)	37(4)
C(8)	183(6)	165(5)	161(5)	45(4)	60(4)	45(5)
C(9)	146(5)	88(4)	113(4)	2(4)	-10(4)	13(4)
C(10)	175(5)	99(5)	144(5)	-7(4)	-40(4)	12(4)
C(11)	159(5)	160(6)	224(6)	-54(5)	21(5)	-41(5)
C(12)	124(5)	96(5)	150(5)	-16(4)	10(4)	-5(4)
C(13)	138(5)	61(4)	156(5)	-1(4)	9(4)	7(4)
C(14)	199(6)	82(4)	137(5)	6(4)	-40(4)	6(4)
C(15)	180(5)	83(4)	131(5)	-6(4)	-18(4)	9(4)
C(16)	260(7)	97(5)	205(6)	-18(4)	-106(5)	11(5)
C(17)	164(5)	83(4)	135(5)	-1(4)	-2(4)	8(4)
C(18)	225(6)	89(5)	164(5)	-17(4)	14(5)	-7(4)
C(19)	215(6)	127(5)	201(6)	14(4)	-43(5)	19(5)

**Table A3.6.6** Hydrogen coordinates ( $\times 10^4$ ) and isotropic displacement parameters ( $\text{\AA}^2 \times 10^3$ ) for cycloburanol **90**.

	x	y	z	U(eq)
H(1)	6684	8471	6306	25
H(4)	5784	5170	4181	31
H(6)	5423	103	6566	28
H(1A)	8603	6283	7717	14
H(3A)	7789	8999	7771	30
H(3B)	8745	8144	8275	30
H(3C)	7194	7979	8324	30
H(4A)	9046	8529	5909	23
H(4B)	9948	7989	6756	23
H(5)	10360	6843	5470	23
H(6A)	9606	5501	6439	16
H(7)	8714	4791	5058	16
H(11A)	4063	5183	6019	22
H(11B)	4732	4326	6784	22
H(12)	5924	6206	5925	15
H(14A)	8315	3845	6603	17
H(14B)	6887	3812	7111	17
H(15)	7729	2696	5337	16
H(16A)	5768	2845	4594	22
H(16B)	4982	2784	5637	22
H(17)	6081	1881	6899	15
H(18A)	6042	1052	5244	19
H(18B)	7499	647	5464	19
H(19A)	7913	917	7525	27
H(19B)	8084	2171	7677	27
H(19C)	8849	1578	6792	27

**Table A3.6.7** Torsion angles [°] for cyclobutanol **90**.

---

O(1)-C(2)-C(4)-C(5)	-79.58(13)
O(2)-C(5)-C(6)-C(1)	-105.80(11)
O(2)-C(5)-C(6)-C(7)	19.30(13)
O(4)-C(10)-C(11)-C(12)	-98.40(12)
O(4)-C(10)-C(16)-C(15)	137.74(11)
C(1)-C(2)-C(4)-C(5)	34.76(13)
C(1)-C(6)-C(7)-C(8)	94.36(12)
C(1)-C(6)-C(7)-C(9)	-30.62(14)
C(2)-C(1)-C(6)-C(5)	9.99(13)
C(2)-C(1)-C(6)-C(7)	-105.35(12)
C(2)-C(1)-C(13)-O(5)	-91.19(14)
C(2)-C(1)-C(13)-C(12)	91.19(12)
C(2)-C(4)-C(5)-O(2)	84.92(13)
C(2)-C(4)-C(5)-C(6)	-29.20(14)
C(3)-C(2)-C(4)-C(5)	156.31(11)
C(4)-C(5)-C(6)-C(1)	11.36(14)
C(4)-C(5)-C(6)-C(7)	136.46(11)
C(5)-O(2)-C(8)-O(3)	175.54(12)
C(5)-O(2)-C(8)-C(7)	-6.18(15)
C(5)-C(6)-C(7)-C(8)	-21.94(12)
C(5)-C(6)-C(7)-C(9)	-146.91(10)
C(6)-C(1)-C(2)-O(1)	89.94(12)
C(6)-C(1)-C(2)-C(3)	-148.85(11)
C(6)-C(1)-C(2)-C(4)	-27.15(13)
C(6)-C(1)-C(13)-O(5)	146.60(12)
C(6)-C(1)-C(13)-C(12)	-31.03(14)
C(6)-C(7)-C(8)-O(2)	18.23(13)
C(6)-C(7)-C(8)-O(3)	-163.63(13)
C(6)-C(7)-C(9)-C(10)	161.05(11)
C(6)-C(7)-C(9)-C(12)	55.47(12)
C(6)-C(7)-C(9)-C(14)	-71.76(12)
C(7)-C(9)-C(10)-O(4)	-24.01(18)
C(7)-C(9)-C(10)-C(11)	-136.98(13)

**Table A3.6.7** *Cont'd*

C(7)-C(9)-C(10)-C(16)	105.66(14)
C(7)-C(9)-C(12)-C(11)	155.80(10)
C(7)-C(9)-C(12)-C(13)	-70.95(12)
C(7)-C(9)-C(14)-C(15)	-106.00(11)
C(8)-O(2)-C(5)-C(4)	-123.70(12)
C(8)-O(2)-C(5)-C(6)	-8.76(15)
C(8)-C(7)-C(9)-C(10)	44.64(17)
C(8)-C(7)-C(9)-C(12)	-60.94(14)
C(8)-C(7)-C(9)-C(14)	171.83(10)
C(9)-C(7)-C(8)-O(2)	138.56(11)
C(9)-C(7)-C(8)-O(3)	-43.30(18)
C(9)-C(10)-C(11)-C(12)	21.52(9)
C(9)-C(10)-C(16)-C(15)	4.37(15)
C(9)-C(12)-C(13)-O(5)	-121.85(13)
C(9)-C(12)-C(13)-C(1)	55.64(13)
C(9)-C(14)-C(15)-C(16)	-35.43(13)
C(9)-C(14)-C(15)-C(17)	-158.22(11)
C(10)-C(9)-C(12)-C(11)	21.90(9)
C(10)-C(9)-C(12)-C(13)	155.15(10)
C(10)-C(9)-C(14)-C(15)	36.73(12)
C(10)-C(11)-C(12)-C(9)	-22.02(9)
C(10)-C(11)-C(12)-C(13)	-137.67(13)
C(11)-C(10)-C(16)-C(15)	-91.96(14)
C(11)-C(12)-C(13)-O(5)	-15.0(2)
C(11)-C(12)-C(13)-C(1)	162.49(12)
C(12)-C(9)-C(10)-O(4)	91.51(12)
C(12)-C(9)-C(10)-C(11)	-21.47(9)
C(12)-C(9)-C(10)-C(16)	-138.83(11)
C(12)-C(9)-C(14)-C(15)	128.49(11)
C(13)-C(1)-C(2)-O(1)	-38.79(13)
C(13)-C(1)-C(2)-C(3)	82.43(13)
C(13)-C(1)-C(2)-C(4)	-155.87(10)
C(13)-C(1)-C(6)-C(5)	134.19(11)
C(13)-C(1)-C(6)-C(7)	18.86(15)
C(14)-C(9)-C(10)-O(4)	-154.85(11)

**Table A3.6.7** *Cont'd*

C(14)-C(9)-C(10)-C(11)	92.17(10)
C(14)-C(9)-C(10)-C(16)	-25.19(13)
C(14)-C(9)-C(12)-C(11)	-78.49(12)
C(14)-C(9)-C(12)-C(13)	54.76(13)
C(14)-C(15)-C(16)-C(10)	18.65(14)
C(14)-C(15)-C(17)-C(18)	-175.42(11)
C(14)-C(15)-C(17)-C(19)	-50.80(15)
C(15)-C(17)-C(18)-O(6)	-163.03(11)
C(16)-C(10)-C(11)-C(12)	131.10(12)
C(16)-C(15)-C(17)-C(18)	66.15(14)
C(16)-C(15)-C(17)-C(19)	-169.23(11)
C(17)-C(15)-C(16)-C(10)	142.70(11)
C(19)-C(17)-C(18)-O(6)	70.85(15)

---

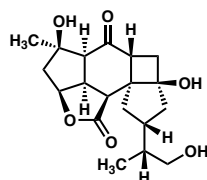
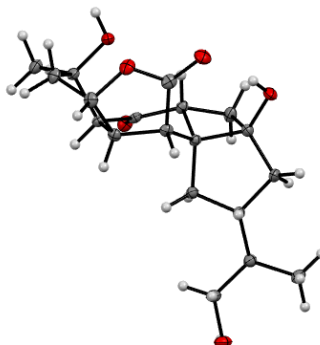
Symmetry transformations used to generate equivalent atoms:

**Table A3.6.8** Hydrogen bonds for cyclobutanol **90** [ $\text{\AA}$  and  $^\circ$ ].

D-H...A	d(D-H)	d(H...A)	d(D...A)	$\angle$ (DHA)
O(1)-H(1)...O(6)#1	0.84	1.93	2.7645(15)	170.3
O(4)-H(4)...O(3)	0.84	1.85	2.6841(17)	172.0
O(6)-H(6)...O(5)#2	0.84	2.01	2.8235(16)	161.6

Symmetry transformations used to generate equivalent atoms:

#1  $x, y+1, z$  #2  $-x+1, y-1/2, -z+3/2$

**A3.7 X-RAY CRYSTAL STRUCTURE ANALYSIS OF CYCLOBUTANOL *EPI-*****90*****epi-90***Contents*Table A3.7.1. Experimental Details**Table A3.7.2. Crystal Data**Table A3.7.3. Atomic Coordinates**Table A3.7.4. Full Bond Distances and Angles**Table A3.7.5. Anisotropic Displacement Parameters**Table A3.7.6. Hydrogen Atomic Coordinates**Table A3.7.7. Torsion Angles**Table A3.7.8. Hydrogen Bond Distances and Angles***Figure A3.7.1 X-ray Crystal Structure for Compound *epi-90***



**Table A3.7.1** Experimental Details for X-Ray Structure Determination of Cyclobutanol **epi-90**.

*Refinement Details*

Low-temperature diffraction data ( $\phi$ - and  $\omega$ -scans) were collected on a Bruker AXS D8 VENTURE KAPPA diffractometer coupled to a PHOTON II CPAD detector with Cu  $K_{\alpha}$  radiation ( $\lambda = 1.54178 \text{ \AA}$ ) from an I $\mu$ S micro-source for the structure of compound **epi-90**. The structure was solved by direct methods using SHELXS and refined against  $F^2$  on all data by full-matrix least squares with SHELXL-2017 using established refinement techniques. All non-hydrogen atoms were refined anisotropically. Unless otherwise noted, all hydrogen atoms were included into the model at geometrically calculated positions and refined using a riding model. The isotropic displacement parameters of all hydrogen atoms were fixed to 1.2 times the  $U$  value of the atoms they are linked to (1.5 times for methyl groups).

*Special Refinement Details*

Compound **epi-90** crystallizes in the orthorhombic space group  $P2_12_12_1$  with one molecule in the asymmetric unit along with three molecules of water. The coordinates for the hydrogen atoms bound to O3, O4, O6, O1W, O2W and O3W were located in the difference Fourier synthesis and refined semi-freely with the help of a restraint on the O-H distance (0.84(4)  $\text{\AA}$ ).

**Table A3.7.2** Crystal data and structure refinement for cyclobutanol **epi-90**.

Empirical formula	C <sub>19</sub> H <sub>32</sub> O <sub>9</sub>	
Formula weight	404.44	
Temperature	100(2) K	
Wavelength	1.54178 Å	
Crystal system	Orthorhombic	
Space group	P2 <sub>1</sub> 2 <sub>1</sub> 2 <sub>1</sub>	
Unit cell dimensions	a = 9.0245(13) Å	α = 90°
	b = 13.383(2) Å	β = 90°
	c = 16.329(3) Å	γ = 90°
Volume	1972.1(5) Å <sup>3</sup>	
Z	4	
Density (calculated)	1.362 Mg/m <sup>3</sup>	
Absorption coefficient	0.906 mm <sup>-1</sup>	
F(000)	872	
Crystal size	0.600 x 0.300 x 0.150 mm <sup>3</sup>	
Theta range for data collection	4.271 to 74.810°	
Index ranges	-11 ≤ h ≤ 10, -16 ≤ k ≤ 15, -19 ≤ l ≤ 20	
Reflections collected	20468	
Independent reflections	4017 [R(int) = 0.0461]	
Completeness to theta = 67.679°	99.7 %	
Absorption correction	Semi-empirical from equivalents	
Max. and min. transmission	0.7538 and 0.5503	
Refinement method	Full-matrix least-squares on F <sup>2</sup>	
Data / restraints / parameters	4017 / 9 / 282	
Goodness-of-fit on F <sup>2</sup>	1.087	
Final R indices [I > 2σ(I)]	R <sub>1</sub> = 0.0314, wR <sub>2</sub> = 0.0874	
R indices (all data)	R <sub>1</sub> = 0.0315, wR <sub>2</sub> = 0.0875	
Absolute structure parameter	0.06(4)	
Extinction coefficient	n/a	
Largest diff. peak and hole	0.342 and -0.300 e.Å <sup>-3</sup>	

**Table A3.7.3** Atomic coordinates ( $\times 10^4$ ) and equivalent isotropic displacement parameters ( $\text{\AA}^2 \times 10^2$ ) for **epi-90**.  $U(\text{eq})$  is defined as one third of the trace of the orthogonalized  $U^{ij}$  tensor.

	x	y	z	U(eq)
O(1)	7488(2)	5070(1)	8786(1)	20(1)
C(1)	6251(2)	5178(1)	8340(1)	17(1)
O(2)	5331(2)	5794(1)	8528(1)	23(1)
C(2)	6244(2)	4454(1)	7623(1)	14(1)
C(3)	4778(2)	3952(1)	7419(1)	12(1)
C(4)	4938(2)	3335(1)	6621(1)	14(1)
C(5)	4168(2)	3973(1)	5960(1)	14(1)
C(6)	2780(2)	4388(1)	6396(1)	16(1)
C(16)	3800(2)	3404(1)	5169(1)	16(1)
C(17)	5215(2)	3010(1)	4767(1)	19(1)
O(3)	4944(2)	2495(1)	4010(1)	22(1)
C(18)	2929(2)	4059(2)	4575(1)	22(1)
C(7)	3164(2)	4383(1)	7305(1)	14(1)
O(4)	2807(2)	5300(1)	7691(1)	21(1)
C(8)	2599(2)	3462(1)	7821(1)	18(1)
C(9)	4188(2)	3370(1)	8165(1)	14(1)
C(10)	5111(2)	2472(1)	8330(1)	13(1)
O(5)	4650(1)	1619(1)	8426(1)	18(1)
C(11)	6770(2)	2710(1)	8379(1)	13(1)
C(12)	7370(2)	3649(1)	7898(1)	14(1)
C(13)	8371(2)	4213(1)	8507(1)	18(1)
C(14)	8646(2)	3502(2)	9217(1)	18(1)
C(15)	7232(2)	2868(1)	9288(1)	14(1)
O(6)	6066(1)	3429(1)	9662(1)	17(1)
C(19)	7469(2)	1889(1)	9746(1)	19(1)
O(1W)	4785(2)	3561(1)	2568(1)	28(1)
O(2W)	6663(2)	3854(1)	1302(1)	21(1)

**Table A3.7.3** Cont'd

O(3W)	3494(2)	756(1)	4427(1)	36(1)
-------	---------	--------	---------	-------

---

**Table A3.7.4** Bond lengths [ $\text{\AA}$ ] and angles [ $^\circ$ ] for **epi-90**.

---

O(1)-C(1)	1.340(2)
O(1)-C(13)	1.469(2)
C(1)-O(2)	1.210(2)
C(1)-C(2)	1.520(2)
C(2)-C(3)	1.521(2)
C(2)-C(12)	1.549(2)
C(2)-H(2)	1.0000
C(3)-C(9)	1.541(2)
C(3)-C(4)	1.549(2)
C(3)-C(7)	1.578(2)
C(4)-C(5)	1.542(2)
C(4)-H(4A)	0.9900
C(4)-H(4B)	0.9900
C(5)-C(16)	1.536(2)
C(5)-C(6)	1.544(2)
C(5)-H(5)	1.0000
C(6)-C(7)	1.525(2)
C(6)-H(6A)	0.9900
C(6)-H(6B)	0.9900
C(16)-C(18)	1.525(3)
C(16)-C(17)	1.529(3)
C(16)-H(16)	1.0000
C(17)-O(3)	1.436(2)
C(17)-H(17A)	0.9900
C(17)-H(17B)	0.9900
O(3)-H(3O)	0.80(2)
C(18)-H(18A)	0.9800
C(18)-H(18B)	0.9800
C(18)-H(18C)	0.9800
C(7)-O(4)	1.417(2)
C(7)-C(8)	1.577(2)
O(4)-H(4O)	0.82(2)
C(8)-C(9)	1.545(2)
C(8)-H(8A)	0.9900

**Table A3.7.4** *Cont'd*

C(8)-H(8B)	0.9900
C(9)-C(10)	1.486(2)
C(9)-H(9)	1.0000
C(10)-O(5)	1.226(2)
C(10)-C(11)	1.533(2)
C(11)-C(15)	1.557(2)
C(11)-C(12)	1.577(2)
C(11)-H(11)	1.0000
C(12)-C(13)	1.541(2)
C(12)-H(12)	1.0000
C(13)-C(14)	1.520(3)
C(13)-H(13)	1.0000
C(14)-C(15)	1.536(2)
C(14)-H(14A)	0.9900
C(14)-H(14B)	0.9900
C(15)-O(6)	1.430(2)
C(15)-C(19)	1.523(2)
O(6)-H(6O)	0.85(2)
C(19)-H(19A)	0.9800
C(19)-H(19B)	0.9800
C(19)-H(19C)	0.9800
O(1W)-H(1W1)	0.85(2)
O(1W)-H(1W2)	0.85(2)
O(2W)-H(2W1)	0.84(2)
O(2W)-H(2W2)	0.86(2)
O(3W)-H(3W1)	0.84(2)
O(3W)-H(3W2)	0.87(2)
C(1)-O(1)-C(13)	111.53(14)
O(2)-C(1)-O(1)	120.48(17)
O(2)-C(1)-C(2)	128.76(17)
O(1)-C(1)-C(2)	110.76(15)
C(1)-C(2)-C(3)	117.03(14)
C(1)-C(2)-C(12)	102.49(14)
C(3)-C(2)-C(12)	109.07(14)
C(1)-C(2)-H(2)	109.3

**Table A3.7.4** *Cont'd*

C(3)-C(2)-H(2)	109.3
C(12)-C(2)-H(2)	109.3
C(2)-C(3)-C(9)	110.52(13)
C(2)-C(3)-C(4)	109.79(14)
C(9)-C(3)-C(4)	115.36(14)
C(2)-C(3)-C(7)	131.85(15)
C(9)-C(3)-C(7)	87.64(13)
C(4)-C(3)-C(7)	100.48(13)
C(5)-C(4)-C(3)	104.57(13)
C(5)-C(4)-H(4A)	110.8
C(3)-C(4)-H(4A)	110.8
C(5)-C(4)-H(4B)	110.8
C(3)-C(4)-H(4B)	110.8
H(4A)-C(4)-H(4B)	108.9
C(16)-C(5)-C(4)	114.32(15)
C(16)-C(5)-C(6)	113.02(15)
C(4)-C(5)-C(6)	103.99(13)
C(16)-C(5)-H(5)	108.4
C(4)-C(5)-H(5)	108.4
C(6)-C(5)-H(5)	108.4
C(7)-C(6)-C(5)	105.26(14)
C(7)-C(6)-H(6A)	110.7
C(5)-C(6)-H(6A)	110.7
C(7)-C(6)-H(6B)	110.7
C(5)-C(6)-H(6B)	110.7
H(6A)-C(6)-H(6B)	108.8
C(18)-C(16)-C(17)	110.89(15)
C(18)-C(16)-C(5)	111.16(15)
C(17)-C(16)-C(5)	110.59(15)
C(18)-C(16)-H(16)	108.0
C(17)-C(16)-H(16)	108.0
C(5)-C(16)-H(16)	108.0
O(3)-C(17)-C(16)	113.11(16)
O(3)-C(17)-H(17A)	109.0
C(16)-C(17)-H(17A)	109.0

**Table A3.7.4** *Cont'd*

O(3)-C(17)-H(17B)	109.0
C(16)-C(17)-H(17B)	109.0
H(17A)-C(17)-H(17B)	107.8
C(17)-O(3)-H(3O)	104(2)
C(16)-C(18)-H(18A)	109.5
C(16)-C(18)-H(18B)	109.5
H(18A)-C(18)-H(18B)	109.5
C(16)-C(18)-H(18C)	109.5
H(18A)-C(18)-H(18C)	109.5
H(18B)-C(18)-H(18C)	109.5
O(4)-C(7)-C(6)	112.16(15)
O(4)-C(7)-C(8)	111.50(14)
C(6)-C(7)-C(8)	116.74(15)
O(4)-C(7)-C(3)	118.31(15)
C(6)-C(7)-C(3)	109.03(14)
C(8)-C(7)-C(3)	87.12(13)
C(7)-O(4)-H(4O)	112(2)
C(9)-C(8)-C(7)	87.50(13)
C(9)-C(8)-H(8A)	114.1
C(7)-C(8)-H(8A)	114.1
C(9)-C(8)-H(8B)	114.1
C(7)-C(8)-H(8B)	114.1
H(8A)-C(8)-H(8B)	111.3
C(10)-C(9)-C(3)	110.97(14)
C(10)-C(9)-C(8)	130.51(16)
C(3)-C(9)-C(8)	89.58(12)
C(10)-C(9)-H(9)	107.7
C(3)-C(9)-H(9)	107.7
C(8)-C(9)-H(9)	107.7
O(5)-C(10)-C(9)	125.92(16)
O(5)-C(10)-C(11)	121.20(16)
C(9)-C(10)-C(11)	112.88(15)
C(10)-C(11)-C(15)	109.83(13)
C(10)-C(11)-C(12)	118.35(14)
C(15)-C(11)-C(12)	105.90(13)



**Table A3.7.4** *Cont'd*

C(10)-C(11)-H(11)	107.4
C(15)-C(11)-H(11)	107.4
C(12)-C(11)-H(11)	107.4
C(13)-C(12)-C(2)	103.35(14)
C(13)-C(12)-C(11)	105.74(13)
C(2)-C(12)-C(11)	118.28(14)
C(13)-C(12)-H(12)	109.7
C(2)-C(12)-H(12)	109.7
C(11)-C(12)-H(12)	109.7
O(1)-C(13)-C(14)	109.94(15)
O(1)-C(13)-C(12)	105.36(14)
C(14)-C(13)-C(12)	106.27(14)
O(1)-C(13)-H(13)	111.7
C(14)-C(13)-H(13)	111.7
C(12)-C(13)-H(13)	111.7
C(13)-C(14)-C(15)	105.55(14)
C(13)-C(14)-H(14A)	110.6
C(15)-C(14)-H(14A)	110.6
C(13)-C(14)-H(14B)	110.6
C(15)-C(14)-H(14B)	110.6
H(14A)-C(14)-H(14B)	108.8
O(6)-C(15)-C(19)	110.20(15)
O(6)-C(15)-C(14)	110.70(14)
C(19)-C(15)-C(14)	113.33(14)
O(6)-C(15)-C(11)	106.36(13)
C(19)-C(15)-C(11)	112.85(15)
C(14)-C(15)-C(11)	103.01(14)
C(15)-O(6)-H(6O)	109.5(19)
C(15)-C(19)-H(19A)	109.5
C(15)-C(19)-H(19B)	109.5
H(19A)-C(19)-H(19B)	109.5
C(15)-C(19)-H(19C)	109.5
H(19A)-C(19)-H(19C)	109.5
H(19B)-C(19)-H(19C)	109.5
H(1W1)-O(1W)-H(1W2)	103(3)

**Table A3.7.4** *Cont'd*

H(2W1)-O(2W)-H(2W2)	105(3)
H(3W1)-O(3W)-H(3W2)	111(3)

---

Symmetry transformations used to generate equivalent atoms:

**Table A3.7.5** Anisotropic displacement parameters ( $\text{\AA}^2 \times 10^3$ ) for **epi-90**. The anisotropic displacement factor exponent takes the form:  $-2\pi^2 [h^2 a^{*2} U^{11} + \dots + 2 h k a^* b^* U^{12}]$

	U <sup>11</sup>	U <sup>22</sup>	U <sup>33</sup>	U <sup>23</sup>	U <sup>13</sup>	U <sup>12</sup>
O(1)	22(1)	15(1)	22(1)	-2(1)	-5(1)	-4(1)
C(1)	22(1)	11(1)	18(1)	2(1)	-1(1)	-5(1)
O(2)	28(1)	16(1)	25(1)	-5(1)	0(1)	1(1)
C(2)	16(1)	12(1)	13(1)	2(1)	2(1)	-1(1)
C(3)	14(1)	12(1)	10(1)	2(1)	0(1)	0(1)
C(4)	17(1)	14(1)	12(1)	0(1)	0(1)	2(1)
C(5)	18(1)	13(1)	11(1)	1(1)	-1(1)	2(1)
C(6)	19(1)	18(1)	13(1)	2(1)	-1(1)	6(1)
C(16)	18(1)	16(1)	13(1)	0(1)	-1(1)	0(1)
C(17)	23(1)	21(1)	13(1)	-3(1)	0(1)	2(1)
O(3)	34(1)	19(1)	13(1)	-3(1)	2(1)	1(1)
C(18)	28(1)	25(1)	14(1)	0(1)	-4(1)	5(1)
C(7)	15(1)	15(1)	14(1)	0(1)	1(1)	2(1)
O(4)	21(1)	22(1)	21(1)	-8(1)	-2(1)	7(1)
C(8)	14(1)	23(1)	17(1)	5(1)	0(1)	-1(1)
C(9)	14(1)	15(1)	12(1)	3(1)	-1(1)	-2(1)
C(10)	16(1)	15(1)	8(1)	1(1)	-1(1)	-2(1)
O(5)	20(1)	15(1)	20(1)	4(1)	-1(1)	-4(1)
C(11)	14(1)	14(1)	11(1)	1(1)	0(1)	-1(1)
C(12)	13(1)	15(1)	15(1)	1(1)	2(1)	-2(1)
C(13)	15(1)	18(1)	21(1)	0(1)	-1(1)	-3(1)
C(14)	14(1)	21(1)	20(1)	0(1)	-5(1)	-2(1)
C(15)	15(1)	16(1)	13(1)	-1(1)	-3(1)	0(1)
O(6)	17(1)	20(1)	13(1)	-2(1)	-1(1)	4(1)
C(19)	21(1)	19(1)	16(1)	3(1)	-4(1)	1(1)
O(1W)	25(1)	39(1)	20(1)	9(1)	5(1)	12(1)
O(2W)	22(1)	26(1)	16(1)	0(1)	-1(1)	6(1)
O(3W)	61(1)	22(1)	25(1)	0(1)	8(1)	-2(1)

**Table A3.7.6** Hydrogen coordinates ( $\times 10^4$ ) and isotropic displacement parameters ( $\text{\AA}^2 \times 10^3$ ) for **epi-90**.

	x	y	z	U(eq)
H(2)	6630	4801	7124	16
H(4A)	5995	3229	6485	17
H(4B)	4448	2676	6677	17
H(5)	4831	4546	5819	17
H(6A)	2559	5075	6207	20
H(6B)	1908	3959	6287	20
H(16)	3168	2818	5316	19
H(17A)	5892	3578	4662	22
H(17B)	5717	2549	5152	22
H(3O)	4480(30)	2009(19)	4146(18)	33
H(18A)	2013	4285	4839	33
H(18B)	2685	3673	4084	33
H(18C)	3528	4640	4422	33
H(4O)	3520(30)	5530(20)	7947(16)	31
H(8A)	1843	3633	8237	22
H(8B)	2282	2884	7485	22
H(9)	4262	3819	8653	16
H(11)	7318	2112	8171	16
H(12)	7970	3424	7418	17
H(13)	9319	4431	8245	22
H(14A)	8825	3878	9729	22
H(14B)	9516	3073	9105	22
H(6O)	6270(30)	3525(19)	10162(13)	25
H(19A)	7686	2030	10322	28
H(19B)	8302	1527	9501	28
H(19C)	6570	1480	9708	28
H(1W1)	4840(40)	3250(20)	3020(15)	42
H(1W2)	4070(30)	3960(20)	2643(19)	42
H(2W1)	6130(30)	3730(20)	1714(15)	32
H(2W2)	7530(30)	3640(20)	1429(17)	32

**Table A3.7.6** *Cont'd*

H(3W1)	3680(40)	690(30)	4929(15)	54
H(3W2)	3500(40)	174(19)	4180(20)	54

---

---

**Table A3.7.7.** Torsion angles [°] for **epi-90**.

---

C(13)-O(1)-C(1)-O(2)	173.80(17)
C(13)-O(1)-C(1)-C(2)	-6.71(19)
O(2)-C(1)-C(2)-C(3)	-40.9(3)
O(1)-C(1)-C(2)-C(3)	139.63(15)
O(2)-C(1)-C(2)-C(12)	-160.19(19)
O(1)-C(1)-C(2)-C(12)	20.37(18)
C(1)-C(2)-C(3)-C(9)	-57.69(19)
C(12)-C(2)-C(3)-C(9)	57.98(18)
C(1)-C(2)-C(3)-C(4)	173.93(14)
C(12)-C(2)-C(3)-C(4)	-70.40(17)
C(1)-C(2)-C(3)-C(7)	48.3(2)
C(12)-C(2)-C(3)-C(7)	164.02(16)
C(2)-C(3)-C(4)-C(5)	-103.66(16)
C(9)-C(3)-C(4)-C(5)	130.68(15)
C(7)-C(3)-C(4)-C(5)	38.30(16)
C(3)-C(4)-C(5)-C(16)	-164.03(14)
C(3)-C(4)-C(5)-C(6)	-40.33(17)
C(16)-C(5)-C(6)-C(7)	149.27(15)
C(4)-C(5)-C(6)-C(7)	24.73(18)
C(4)-C(5)-C(16)-C(18)	175.24(16)
C(6)-C(5)-C(16)-C(18)	56.5(2)
C(4)-C(5)-C(16)-C(17)	-61.13(19)
C(6)-C(5)-C(16)-C(17)	-179.83(15)
C(18)-C(16)-C(17)-O(3)	-54.5(2)
C(5)-C(16)-C(17)-O(3)	-178.33(15)
C(5)-C(6)-C(7)-O(4)	132.31(15)
C(5)-C(6)-C(7)-C(8)	-97.27(17)
C(5)-C(6)-C(7)-C(3)	-0.71(19)
C(2)-C(3)-C(7)-O(4)	-24.0(3)
C(9)-C(3)-C(7)-O(4)	91.77(16)
C(4)-C(3)-C(7)-O(4)	-152.87(15)

**Table A3.7.7** *Cont'd*

C(2)-C(3)-C(7)-C(6)	105.8(2)
C(9)-C(3)-C(7)-C(6)	-138.51(15)
C(4)-C(3)-C(7)-C(6)	-23.14(17)
C(2)-C(3)-C(7)-C(8)	-136.90(18)
C(9)-C(3)-C(7)-C(8)	-21.17(12)
C(4)-C(3)-C(7)-C(8)	94.19(13)
O(4)-C(7)-C(8)-C(9)	-98.27(15)
C(6)-C(7)-C(8)-C(9)	131.00(15)
C(3)-C(7)-C(8)-C(9)	21.11(12)
C(2)-C(3)-C(9)-C(10)	-70.31(18)
C(4)-C(3)-C(9)-C(10)	54.98(19)
C(7)-C(3)-C(9)-C(10)	155.46(14)
C(2)-C(3)-C(9)-C(8)	155.83(15)
C(4)-C(3)-C(9)-C(8)	-78.88(16)
C(7)-C(3)-C(9)-C(8)	21.60(13)
C(7)-C(8)-C(9)-C(10)	-139.29(18)
C(7)-C(8)-C(9)-C(3)	-21.61(13)
C(3)-C(9)-C(10)-O(5)	-129.31(18)
C(8)-C(9)-C(10)-O(5)	-20.8(3)
C(3)-C(9)-C(10)-C(11)	51.09(19)
C(8)-C(9)-C(10)-C(11)	159.58(16)
O(5)-C(10)-C(11)-C(15)	-84.3(2)
C(9)-C(10)-C(11)-C(15)	95.36(17)
O(5)-C(10)-C(11)-C(12)	154.02(16)
C(9)-C(10)-C(11)-C(12)	-26.4(2)
C(1)-C(2)-C(12)-C(13)	-24.82(16)
C(3)-C(2)-C(12)-C(13)	-149.51(14)
C(1)-C(2)-C(12)-C(11)	91.56(17)
C(3)-C(2)-C(12)-C(11)	-33.1(2)
C(10)-C(11)-C(12)-C(13)	133.11(16)
C(15)-C(11)-C(12)-C(13)	9.42(18)
C(10)-C(11)-C(12)-C(2)	18.0(2)
C(15)-C(11)-C(12)-C(2)	-105.67(16)
C(1)-O(1)-C(13)-C(14)	-124.26(15)
C(1)-O(1)-C(13)-C(12)	-10.13(19)

**Table A3.7.7** *Cont'd*

C(2)-C(12)-C(13)-O(1)	21.90(17)
C(11)-C(12)-C(13)-O(1)	-103.05(15)
C(2)-C(12)-C(13)-C(14)	138.55(14)
C(11)-C(12)-C(13)-C(14)	13.60(18)
O(1)-C(13)-C(14)-C(15)	81.46(17)
C(12)-C(13)-C(14)-C(15)	-32.08(18)
C(13)-C(14)-C(15)-O(6)	-75.99(18)
C(13)-C(14)-C(15)-C(19)	159.61(15)
C(13)-C(14)-C(15)-C(11)	37.36(17)
C(10)-C(11)-C(15)-O(6)	-40.78(18)
C(12)-C(11)-C(15)-O(6)	88.10(15)
C(10)-C(11)-C(15)-C(19)	80.17(18)
C(12)-C(11)-C(15)-C(19)	-150.95(15)
C(10)-C(11)-C(15)-C(14)	-157.26(14)
C(12)-C(11)-C(15)-C(14)	-28.37(17)

---

Symmetry transformations used to generate equivalent atoms:



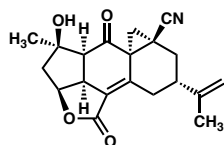
**Table A3.7.8** Hydrogen bonds for **epi-90** [ $\text{\AA}$  and  $^\circ$ ].

D-H...A	d(D-H)	d(H...A)	d(D...A)	$\angle$ (DHA)
O(3)-H(3O)...O(3W)	0.80(2)	1.95(2)	2.755(2)	175(3)
O(4)-H(4O)...O(2)	0.82(2)	1.93(2)	2.737(2)	168(3)
C(9)-H(9)...O(6)	1.00	2.37	2.976(2)	117.8
O(6)-H(6O)...O(2W)#1	0.85(2)	1.95(2)	2.790(2)	175(3)
O(1W)-H(1W1)...O(3)	0.85(2)	1.91(2)	2.758(2)	178(3)
O(1W)-H(1W2)...O(4)#2	0.85(2)	1.96(2)	2.799(2)	169(3)
O(2W)-H(2W1)...O(1W)	0.84(2)	1.86(2)	2.701(2)	173(3)
O(2W)-H(2W2)...O(5)#3	0.86(2)	1.96(2)	2.804(2)	168(3)
O(3W)-H(3W1)...O(1)#4	0.84(2)	2.49(3)	3.184(2)	141(3)
O(3W)-H(3W2)...O(2W)#5	0.87(2)	1.94(2)	2.814(2)	175(4)

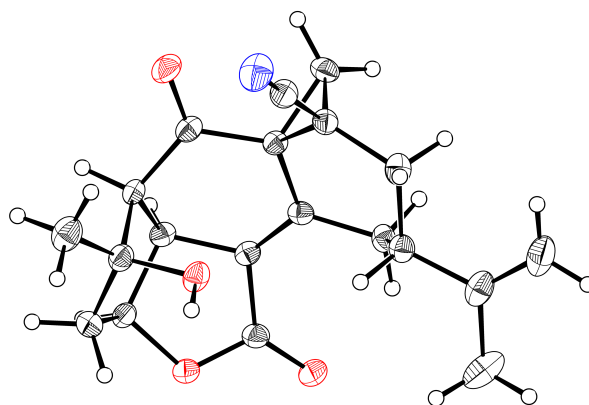
Symmetry transformations used to generate equivalent atoms:

#1  $x, y, z+1$  #2  $-x+1/2, -y+1, z-1/2$  #3  $x+1/2, -y+1/2, -z+1$

#4  $-x+1, y-1/2, -z+3/2$  #5  $-x+1, y-1/2, -z+1/2$

**A3.8 X-RAY CRYSTAL STRUCTURE ANALYSIS OF NITRILE 94**

94

Contents*Table A3.8.1. Experimental Details**Table A3.8.2. Crystal Data**Table A3.8.3. Atomic Coordinates**Table A3.8.4. Full Bond Distances and Angles**Table A3.8.5. Anisotropic Displacement Parameters**Table A3.8.6. Hydrogen Atomic Coordinates**Table A3.8.7. Torsion Angles**Table A3.8.8. Hydrogen Bond Distances and Angles***Figure A3.8.1** X-Ray Crystal Structure of Nitrile **94**.

**Table A3.8.1** *Experimental Details for X-Ray Structure Determination of Nitrile 94.**Refinement Details*

A crystal was mounted on a polyimide MiTeGen loop with STP Oil Treatment and placed under a nitrogen stream. Low temperature (100K) X-ray data were collected with a Bruker AXS D8 VENTURE KAPPA diffractometer running at 50 kV and 1mA (Cu  $K_{\alpha}$  = 1.54178 Å; PHOTON II CPAD detector and Helios focusing multilayer mirror optics). All diffractometer manipulations, including data collection, integration, and scaling were carried out using the Bruker APEX3 software. An absorption correction was applied using SADABS. The space group was determined and the structure solved by intrinsic phasing using XT. Refinement was full-matrix least squares on  $F^2$  using XL. All non-hydrogen atoms were refined using anisotropic displacement parameters. Hydrogen atoms were placed in idealized positions and refined using a riding model. The isotropic displacement parameters of all hydrogen atoms were fixed at 1.2 times (1.5 times for methyl groups) the  $U_{eq}$  value of the bonded atom.

*Special Refinement Details*

Compound **94** crystallizes in the monoclinic space group  $P2_1$  (#4) with one molecule in the asymmetric unit. The final difference map exhibits four small positive excursions near the isopropenyl group. These represent some disorder or impurity and were not interpreted.

**Table A3.8.2** Crystal data and structure refinement for nitrile **94**.

Empirical formula	C <sub>20</sub> H <sub>21</sub> N O <sub>4</sub>	
Formula weight	339.38	
Temperature	100 K	
Wavelength	1.54178 Å	
Crystal system	Monoclinic	
Space group	P 1 21 1 (# 4)	
Unit cell dimensions	a = 10.105(2) Å	a = 90°
	b = 8.9547(18) Å	b = 110.038(10)°
	c = 10.215(2) Å	g = 90°
Volume	868.4(3) Å <sup>3</sup>	
Z	2	
Density (calculated)	1.298 g/cm <sup>3</sup>	
Absorption coefficient	0.737 mm <sup>-1</sup>	
F(000)	360	
Crystal size	0.02 x 0.06 x 0.31 mm <sup>3</sup>	
Theta range for data collection	4.6 to 79.9°.	
Index ranges	-12 ≤ h ≤ 12, -11 ≤ k ≤ 11, -11 ≤ l ≤ 12	
Reflections collected	15034	
Independent reflections	3650 [R(int) = 0.0537]	
Completeness to theta = 67.679°	100.0 %	
Absorption correction	Semi-empirical from equivalents	
Max. and min. transmission	1.000 and 0.886	
Refinement method	Full-matrix least-squares on F <sup>2</sup>	
Data / restraints / parameters	3650 / 1 / 229	
Goodness-of-fit on F <sup>2</sup>	1.074	
Final R indices [I > 2σ(I)]	R1 = 0.0415, wR2 = 0.1027	
R indices (all data)	R1 = 0.0446, wR2 = 0.1048	
Absolute structure parameter [Flack]	0.08(10)	
Absolute structure parameter [Hooft]	0.14(10)	
Extinction coefficient	n/a	
Largest diff. peak and hole	0.70 and -0.20 e.Å <sup>-3</sup>	

**Table A3.8.3** Atomic coordinates ( $\times 10^4$ ) and equivalent isotropic displacement parameters ( $\text{\AA}^2 \times 10^2$ ) for nitrile **94**.  $U(\text{eq})$  is defined as one third of the trace of the orthogonalized  $U_{ij}$  tensor.

	x	y	z	U(eq)
O(1)	6691(2)	5925(2)	780(2)	32(1)
O(2)	5021(2)	5006(2)	3358(2)	25(1)
O(3)	5217(2)	1146(2)	3785(2)	26(1)
O(4)	7182(2)	1082(2)	5628(2)	29(1)
N(1)	6896(3)	8901(3)	2463(3)	37(1)
C(1)	7848(3)	4993(3)	3049(3)	18(1)
C(2)	6663(3)	5022(3)	1655(3)	20(1)
C(3)	5485(3)	3912(3)	1411(3)	18(1)
C(4)	4315(3)	4410(3)	1997(3)	22(1)
C(5)	3601(3)	2917(3)	2090(3)	26(1)
C(6)	4718(3)	1690(3)	2352(3)	22(1)
C(7)	6000(3)	2412(3)	2115(3)	19(1)
C(8)	7021(3)	2586(3)	3568(3)	18(1)
C(9)	6566(3)	1536(3)	4455(3)	22(1)
C(10)	7881(3)	3752(3)	4033(3)	18(1)
C(11)	8769(3)	3988(3)	5528(3)	20(1)
C(12)	8368(3)	5460(3)	6072(3)	22(1)
C(13)	8759(3)	6762(3)	5310(3)	24(1)
C(14)	8270(3)	6566(3)	3722(3)	21(1)
C(15)	3319(3)	5557(4)	1090(3)	32(1)
C(16)	9050(3)	5567(4)	7640(3)	29(1)
C(17)	8592(5)	4393(4)	8444(4)	44(1)
C(18)	9980(4)	6633(5)	8294(4)	40(1)
C(19)	7478(3)	7838(3)	2970(3)	25(1)
C(20)	9192(3)	5758(3)	3063(3)	24(1)

**Table A3.8.4** Bond lengths [ $\text{\AA}$ ] and angles [ $^\circ$ ] for nitrile **94**.

---

O(1)-C(2)	1.213(3)
O(2)-H(2)	0.8400
O(2)-C(4)	1.430(3)
O(3)-C(6)	1.459(3)
O(3)-C(9)	1.345(3)
O(4)-C(9)	1.215(3)
N(1)-C(19)	1.146(4)
C(1)-C(2)	1.514(4)
C(1)-C(10)	1.491(4)
C(1)-C(14)	1.562(4)
C(1)-C(20)	1.517(4)
C(2)-C(3)	1.505(4)
C(3)-H(3)	1.0000
C(3)-C(4)	1.562(4)
C(3)-C(7)	1.528(4)
C(4)-C(5)	1.537(4)
C(4)-C(15)	1.512(4)
C(5)-H(5A)	0.9900
C(5)-H(5B)	0.9900
C(5)-C(6)	1.531(4)
C(6)-H(6)	1.0000
C(6)-C(7)	1.539(4)
C(7)-H(7)	1.0000
C(7)-C(8)	1.498(4)
C(8)-C(9)	1.484(4)
C(8)-C(10)	1.338(4)
C(10)-C(11)	1.497(4)
C(11)-H(11A)	0.9900
C(11)-H(11B)	0.9900
C(11)-C(12)	1.538(4)
C(12)-H(12)	1.0000
C(12)-C(13)	1.527(4)
C(12)-C(16)	1.515(4)
C(13)-H(13A)	0.9900

**Table A3.8.4** *Cont'd*

C(13)-H(13B)	0.9900
C(13)-C(14)	1.535(4)
C(14)-C(19)	1.451(4)
C(14)-C(20)	1.508(4)
C(15)-H(15A)	0.9800
C(15)-H(15B)	0.9800
C(15)-H(15C)	0.9800
C(16)-C(17)	1.502(5)
C(16)-C(18)	1.345(5)
C(17)-H(17A)	0.9800
C(17)-H(17B)	0.9800
C(17)-H(17C)	0.9800
C(18)-H(18A)	0.9500
C(18)-H(18B)	0.9500
C(20)-H(20A)	0.9900
C(20)-H(20B)	0.9900
C(4)-O(2)-H(2)	109.5
C(9)-O(3)-C(6)	111.4(2)
C(2)-C(1)-C(14)	114.0(2)
C(2)-C(1)-C(20)	114.7(2)
C(10)-C(1)-C(2)	118.4(2)
C(10)-C(1)-C(14)	115.8(2)
C(10)-C(1)-C(20)	121.1(2)
C(20)-C(1)-C(14)	58.64(17)
O(1)-C(2)-C(1)	119.6(2)
O(1)-C(2)-C(3)	122.4(2)
C(3)-C(2)-C(1)	118.0(2)
C(2)-C(3)-H(3)	108.6
C(2)-C(3)-C(4)	114.1(2)
C(2)-C(3)-C(7)	112.3(2)
C(4)-C(3)-H(3)	108.6
C(7)-C(3)-H(3)	108.6
C(7)-C(3)-C(4)	104.5(2)
O(2)-C(4)-C(3)	106.7(2)
O(2)-C(4)-C(5)	110.7(2)

**Table A3.8.4** *Cont'd*

O(2)-C(4)-C(15)	110.4(2)
C(5)-C(4)-C(3)	102.0(2)
C(15)-C(4)-C(3)	113.0(2)
C(15)-C(4)-C(5)	113.6(2)
C(4)-C(5)-H(5A)	110.2
C(4)-C(5)-H(5B)	110.2
H(5A)-C(5)-H(5B)	108.5
C(6)-C(5)-C(4)	107.6(2)
C(6)-C(5)-H(5A)	110.2
C(6)-C(5)-H(5B)	110.2
O(3)-C(6)-C(5)	113.3(2)
O(3)-C(6)-H(6)	110.3
O(3)-C(6)-C(7)	106.2(2)
C(5)-C(6)-H(6)	110.3
C(5)-C(6)-C(7)	106.3(2)
C(7)-C(6)-H(6)	110.3
C(3)-C(7)-C(6)	105.9(2)
C(3)-C(7)-H(7)	111.8
C(6)-C(7)-H(7)	111.8
C(8)-C(7)-C(3)	112.5(2)
C(8)-C(7)-C(6)	102.6(2)
C(8)-C(7)-H(7)	111.8
C(9)-C(8)-C(7)	106.7(2)
C(10)-C(8)-C(7)	125.2(2)
C(10)-C(8)-C(9)	125.3(2)
O(3)-C(9)-C(8)	109.0(2)
O(4)-C(9)-O(3)	120.2(2)
O(4)-C(9)-C(8)	130.7(3)
C(1)-C(10)-C(11)	116.8(2)
C(8)-C(10)-C(1)	118.7(2)
C(8)-C(10)-C(11)	124.2(2)
C(10)-C(11)-H(11A)	109.6
C(10)-C(11)-H(11B)	109.6
C(10)-C(11)-C(12)	110.4(2)
H(11A)-C(11)-H(11B)	108.1



**Table A3.8.4** *Cont'd*

C(12)-C(11)-H(11A)	109.6
C(12)-C(11)-H(11B)	109.6
C(11)-C(12)-H(12)	108.1
C(13)-C(12)-C(11)	108.9(2)
C(13)-C(12)-H(12)	108.1
C(16)-C(12)-C(11)	110.8(2)
C(16)-C(12)-H(12)	108.1
C(16)-C(12)-C(13)	112.8(2)
C(12)-C(13)-H(13A)	108.8
C(12)-C(13)-H(13B)	108.8
C(12)-C(13)-C(14)	113.9(2)
H(13A)-C(13)-H(13B)	107.7
C(14)-C(13)-H(13A)	108.8
C(14)-C(13)-H(13B)	108.8
C(13)-C(14)-C(1)	120.6(2)
C(19)-C(14)-C(1)	117.2(2)
C(19)-C(14)-C(13)	112.9(2)
C(19)-C(14)-C(20)	116.9(2)
C(20)-C(14)-C(1)	59.19(17)
C(20)-C(14)-C(13)	120.1(2)
C(4)-C(15)-H(15A)	109.5
C(4)-C(15)-H(15B)	109.5
C(4)-C(15)-H(15C)	109.5
H(15A)-C(15)-H(15B)	109.5
H(15A)-C(15)-H(15C)	109.5
H(15B)-C(15)-H(15C)	109.5
C(17)-C(16)-C(12)	114.9(3)
C(18)-C(16)-C(12)	123.9(3)
C(18)-C(16)-C(17)	121.3(3)
C(16)-C(17)-H(17A)	109.5
C(16)-C(17)-H(17B)	109.5
C(16)-C(17)-H(17C)	109.5
H(17A)-C(17)-H(17B)	109.5
H(17A)-C(17)-H(17C)	109.5
H(17B)-C(17)-H(17C)	109.5

**Table A3.8.4** *Cont'd*

C(16)-C(18)-H(18A)	120.0
C(16)-C(18)-H(18B)	120.0
H(18A)-C(18)-H(18B)	120.0
N(1)-C(19)-C(14)	175.0(3)
C(1)-C(20)-H(20A)	117.5
C(1)-C(20)-H(20B)	117.5
C(14)-C(20)-C(1)	62.17(18)
C(14)-C(20)-H(20A)	117.5
C(14)-C(20)-H(20B)	117.5
H(20A)-C(20)-H(20B)	114.6

---

Symmetry transformations used to generate equivalent atoms:

**Table A3.8.5** Anisotropic displacement parameters ( $\text{\AA}^2 \times 10^3$ ) for nitrile **94**. The

anisotropic displacement factor exponent takes the form:  $-2p^2 [h^2 a^{*2} U^{11} + \dots + 2h$

$k a^* b^* U^{12}]$

	U <sup>11</sup>	U <sup>22</sup>	U <sup>33</sup>	U <sup>23</sup>	U <sup>13</sup>	U <sup>12</sup>
O(1)	42(1)	29(1)	21(1)	6(1)	6(1)	-9(1)
O(2)	25(1)	32(1)	18(1)	-5(1)	8(1)	5(1)
O(3)	27(1)	29(1)	21(1)	5(1)	6(1)	-8(1)
O(4)	30(1)	31(1)	23(1)	11(1)	5(1)	-4(1)
N(1)	47(2)	22(1)	35(2)	6(1)	6(1)	1(1)
C(1)	21(1)	15(1)	18(1)	0(1)	7(1)	-1(1)
C(2)	27(1)	17(1)	17(1)	0(1)	8(1)	1(1)
C(3)	20(1)	20(1)	14(1)	0(1)	4(1)	0(1)
C(4)	21(1)	28(1)	18(1)	-1(1)	6(1)	2(1)
C(5)	21(1)	34(2)	23(1)	0(1)	8(1)	-4(1)
C(6)	26(1)	24(1)	15(1)	1(1)	5(1)	-6(1)
C(7)	24(1)	16(1)	18(1)	-2(1)	9(1)	-1(1)
C(8)	20(1)	16(1)	18(1)	3(1)	7(1)	4(1)
C(9)	24(1)	20(1)	22(1)	1(1)	9(1)	-3(1)
C(10)	16(1)	18(1)	21(1)	2(1)	8(1)	3(1)
C(11)	17(1)	20(1)	21(1)	3(1)	2(1)	3(1)
C(12)	19(1)	22(1)	22(1)	0(1)	6(1)	3(1)
C(13)	25(1)	19(1)	24(1)	-2(1)	4(1)	1(1)
C(14)	22(1)	17(1)	22(1)	1(1)	6(1)	-2(1)
C(15)	30(2)	36(2)	28(2)	3(1)	7(1)	11(1)
C(16)	30(2)	32(2)	22(1)	-1(1)	6(1)	12(1)
C(17)	70(3)	38(2)	27(2)	6(1)	21(2)	11(2)
C(18)	36(2)	52(2)	25(2)	-1(2)	1(1)	8(2)
C(19)	30(2)	19(1)	24(1)	0(1)	7(1)	-4(1)
C(20)	22(1)	22(1)	28(1)	2(1)	10(1)	-4(1)

**Table A3.8.6** Hydrogen coordinates ( $\times 10^4$ ) and isotropic displacement parameters ( $\text{\AA}^2 \times 10^3$ ) for nitrile **94**.

	x	y	z	U(eq)
H(2)	4424	5339	3687	37
H(3)	5041	3744	385	22
H(5A)	3218	2946	2861	31
H(5B)	2816	2721	1209	31
H(6)	4353	843	1689	27
H(7)	6387	1763	1535	23
H(11A)	9776	4016	5617	25
H(11B)	8632	3145	6096	25
H(12)	7323	5470	5841	26
H(13A)	9795	6886	5670	28
H(13B)	8338	7689	5523	28
H(15A)	2559	5756	1458	48
H(15B)	2919	5175	136	48
H(15C)	3835	6484	1089	48
H(17A)	7567	4274	8052	66
H(17B)	8862	4696	9423	66
H(17C)	9047	3442	8383	66
H(18A)	10359	6653	9283	48
H(18B)	10257	7366	7767	48
H(20A)	10096	5347	3692	28
H(20B)	9223	6149	2168	28

**Table A3.8.7** Torsion angles [°] for **94**.

---

O(1)-C(2)-C(3)-C(4)	-96.4(3)
O(1)-C(2)-C(3)-C(7)	144.8(3)
O(2)-C(4)-C(5)-C(6)	-83.4(3)
O(3)-C(6)-C(7)-C(3)	-133.3(2)
O(3)-C(6)-C(7)-C(8)	-15.2(3)
C(1)-C(2)-C(3)-C(4)	83.7(3)
C(1)-C(2)-C(3)-C(7)	-35.1(3)
C(1)-C(10)-C(11)-C(12)	53.3(3)
C(2)-C(1)-C(10)-C(8)	11.3(4)
C(2)-C(1)-C(10)-C(11)	-161.9(2)
C(2)-C(1)-C(14)-C(13)	145.6(2)
C(2)-C(1)-C(14)-C(19)	1.3(4)
C(2)-C(1)-C(14)-C(20)	-105.3(3)
C(2)-C(1)-C(20)-C(14)	104.1(2)
C(2)-C(3)-C(4)-O(2)	-44.1(3)
C(2)-C(3)-C(4)-C(5)	-160.3(2)
C(2)-C(3)-C(4)-C(15)	77.4(3)
C(2)-C(3)-C(7)-C(6)	155.2(2)
C(2)-C(3)-C(7)-C(8)	43.9(3)
C(3)-C(4)-C(5)-C(6)	29.8(3)
C(3)-C(7)-C(8)-C(9)	133.3(2)
C(3)-C(7)-C(8)-C(10)	-28.3(4)
C(4)-C(3)-C(7)-C(6)	31.0(3)
C(4)-C(3)-C(7)-C(8)	-80.3(3)
C(4)-C(5)-C(6)-O(3)	104.8(3)
C(4)-C(5)-C(6)-C(7)	-11.4(3)
C(5)-C(6)-C(7)-C(3)	-12.4(3)
C(5)-C(6)-C(7)-C(8)	105.7(2)
C(6)-O(3)-C(9)-O(4)	-174.6(3)
C(6)-O(3)-C(9)-C(8)	8.5(3)
C(6)-C(7)-C(8)-C(9)	20.0(3)
C(6)-C(7)-C(8)-C(10)	-141.7(3)
C(7)-C(3)-C(4)-O(2)	79.0(3)

**Table A3.8.7** *Cont'd*

C(7)-C(3)-C(4)-C(5)	-37.2(3)
C(7)-C(3)-C(4)-C(15)	-159.6(2)
C(7)-C(8)-C(9)-O(3)	-18.6(3)
C(7)-C(8)-C(9)-O(4)	165.0(3)
C(7)-C(8)-C(10)-C(1)	-0.2(4)
C(7)-C(8)-C(10)-C(11)	172.5(2)
C(8)-C(10)-C(11)-C(12)	-119.5(3)
C(9)-O(3)-C(6)-C(5)	-111.7(3)
C(9)-O(3)-C(6)-C(7)	4.6(3)
C(9)-C(8)-C(10)-C(1)	-158.5(2)
C(9)-C(8)-C(10)-C(11)	14.1(4)
C(10)-C(1)-C(2)-O(1)	-172.3(3)
C(10)-C(1)-C(2)-C(3)	7.6(4)
C(10)-C(1)-C(14)-C(13)	3.1(4)
C(10)-C(1)-C(14)-C(19)	-141.2(2)
C(10)-C(1)-C(14)-C(20)	112.2(3)
C(10)-C(1)-C(20)-C(14)	-103.2(3)
C(10)-C(8)-C(9)-O(3)	143.1(3)
C(10)-C(8)-C(9)-O(4)	-33.3(5)
C(10)-C(11)-C(12)-C(13)	-66.3(3)
C(10)-C(11)-C(12)-C(16)	169.1(2)
C(11)-C(12)-C(13)-C(14)	47.7(3)
C(11)-C(12)-C(16)-C(17)	-63.1(3)
C(11)-C(12)-C(16)-C(18)	118.0(3)
C(12)-C(13)-C(14)-C(1)	-17.6(4)
C(12)-C(13)-C(14)-C(19)	128.1(3)
C(12)-C(13)-C(14)-C(20)	-87.5(3)
C(13)-C(12)-C(16)-C(17)	174.5(3)
C(13)-C(12)-C(16)-C(18)	-4.4(4)
C(13)-C(14)-C(20)-C(1)	109.8(3)
C(14)-C(1)-C(2)-O(1)	46.2(4)
C(14)-C(1)-C(2)-C(3)	-133.9(2)
C(14)-C(1)-C(10)-C(8)	152.1(2)
C(14)-C(1)-C(10)-C(11)	-21.1(3)
C(15)-C(4)-C(5)-C(6)	151.7(2)

**Table A3.8.7** *Cont'd*

C(16)-C(12)-C(13)-C(14)	171.2(2)
C(19)-C(14)-C(20)-C(1)	-107.1(3)
C(20)-C(1)-C(2)-O(1)	-18.8(4)
C(20)-C(1)-C(2)-C(3)	161.1(2)
C(20)-C(1)-C(10)-C(8)	-140.4(3)
C(20)-C(1)-C(10)-C(11)	46.4(3)
C(20)-C(1)-C(14)-C(13)	-109.1(3)
C(20)-C(1)-C(14)-C(19)	106.7(3)

---

Symmetry transformations used to generate equivalent atoms:

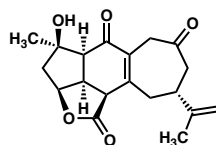
**Table A3.8.8** Hydrogen bonds for nitrile **94** [ $\text{\AA}$  and  $^\circ$ ].

D-H...A	d(D-H)	d(H...A)	d(D...A)	$\angle$ (DHA)
O(2)-H(2)...O(3)#1	0.84	2.58	3.178(3)	128.7
O(2)-H(2)...O(4)#1	0.84	2.08	2.923(3)	175.4
C(6)-H(6)...O(1)#2	1.00	2.38	3.100(3)	128.4
C(11)-H(11B)...O(4)	0.99	2.30	3.077(3)	134.1

Symmetry transformations used to generate equivalent atoms:

#1  $-x+1, y+1/2, -z+1$  #2  $-x+1, y-1/2, -z$



**A3.9 X-RAY CRYSTAL STRUCTURE ANALYSIS OF SCABROLIDE A (1)****Scabrolide A (1)**Contents

*Table A3.9.1. Experimental Details*

*Table A3.9.2. Crystal Data*

*Table A3.9.3. Atomic Coordinates*

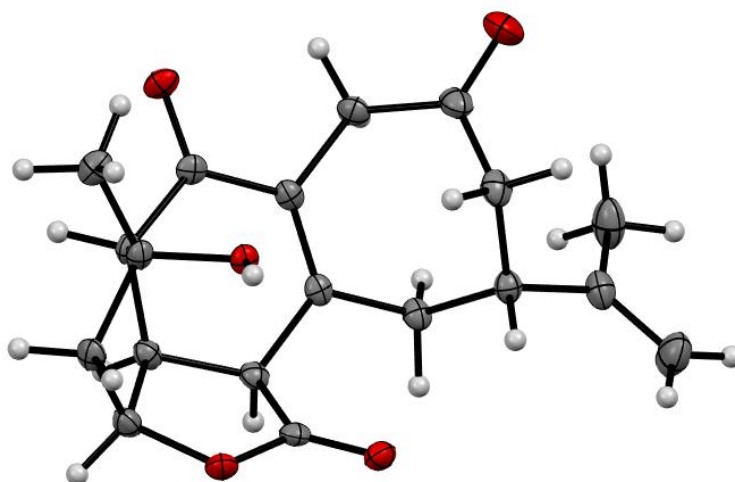
*Table A3.9.4. Full Bond Distances and Angles*

*Table A3.9.5. Anisotropic Displacement Parameters*

*Table A3.9.6. Hydrogen Atomic Coordinates*

*Table A3.9.7. Torsion Angles*

*Table A3.9.8. Hydrogen Bond Distances and Angles*

**Figure A3.9.1 X-ray Crystal Structure for scabrolide A (1)**

**Table A3.9.1** *Experimental Details for X-Ray Structure Determination of scabrolide A (1).*

*Refinement Details*

Low-temperature diffraction data ( $\phi$ - and  $\omega$ -scans) were collected on a Bruker AXS D8 VENTURE KAPPA diffractometer coupled to a PHOTON II CPAD detector with Cu  $K_{\alpha}$  radiation ( $\lambda = 1.54178 \text{ \AA}$ ) from an I $\mu$ S micro-source for the structure of compound **1**. The structure was solved by direct methods using SHELXS and refined against  $F^2$  on all data by full-matrix least squares with SHELXL-2017 using established refinement techniques. All non-hydrogen atoms were refined anisotropically. All hydrogen atoms were included into the model at geometrically calculated positions and refined using a riding model. The isotropic displacement parameters of all hydrogen atoms were fixed to 1.2 times the  $U$  value of the atoms they are linked to (1.5 times for methyl groups).

*Special Refinement Details*

Compound **1** crystallizes in the orthorhombic space group  $P2_12_12_1$  with one molecule in the asymmetric unit.

**Table A3.9.2** Crystal data and structure refinement for compound **1**.

Empirical formula	C <sub>19</sub> H <sub>22</sub> O <sub>5</sub>	
Formula weight	330.36	
Temperature	100(2) K	
Wavelength	1.54178 $\approx$	
Crystal system	Orthorhombic	
Space group	P2 <sub>1</sub> 2 <sub>1</sub> 2 <sub>1</sub>	
Unit cell dimensions	a = 6.1878(4) $\approx$	$\alpha = 90^\circ$ .
	b = 14.9676(14) $\approx$	$\beta = 90^\circ$ .
	c = 17.511(2) $\approx$	$\gamma = 90^\circ$ .
Volume	1621.8(3) $\approx^3$	
Z	4	
Density (calculated)	1.353 Mg/m <sup>3</sup>	
Absorption coefficient	0.800 mm <sup>-1</sup>	
F(000)	704	
Crystal size	0.450 x 0.200 x 0.150 mm <sup>3</sup>	
Theta range for data collection	3.885 to 74.514 $^\circ$ .	
Index ranges	-7 $\leq$ h $\leq$ 7, -18 $\leq$ k $\leq$ 18, -20 $\leq$ l $\leq$ 21	
Reflections collected	14706	
Independent reflections	3306 [R(int) = 0.0575]	
Completeness to theta = 67.679 $^\circ$	100.0 %	
Absorption correction	Semi-empirical from equivalents	
Max. and min. transmission	0.7538 and 0.6083	
Refinement method	Full-matrix least-squares on F <sup>2</sup>	
Data / restraints / parameters	3306 / 1 / 222	
Goodness-of-fit on F <sup>2</sup>	1.048	
Final R indices [I > 2 $\sigma$ (I)]	R1 = 0.0353, wR2 = 0.0889	
R indices (all data)	R1 = 0.0369, wR2 = 0.0906	
Absolute structure parameter	0.00(7)	
Extinction coefficient	n/a	
Largest diff. peak and hole	0.657 and -0.199 e. $\approx^3$	

**Table A3.9.3** Atomic coordinates ( $\times 10^4$ ) and equivalent isotropic displacement parameters ( $\text{\AA}^2 \times 10^3$ ) for compound **1**.  $U(\text{eq})$  is defined as one third of the trace of the orthogonalized  $U^{ij}$  tensor.

	x	y	z	U(eq)
O(1)	1620(2)	5711(1)	5387(1)	19(1)
C(1)	2687(3)	6235(1)	4894(1)	16(1)
O(2)	1762(2)	6741(1)	4470(1)	20(1)
C(2)	5129(3)	6135(1)	5002(1)	16(1)
C(3)	6351(3)	6183(1)	4262(1)	14(1)
C(4)	6411(3)	7080(1)	3873(1)	17(1)
C(5)	5192(3)	7133(1)	3101(1)	18(1)
C(16)	5851(4)	7974(2)	2674(1)	22(1)
C(17)	4347(5)	8604(2)	2509(2)	34(1)
C(18)	8117(4)	8092(2)	2448(2)	34(1)
C(6)	5415(4)	6278(2)	2609(1)	21(1)
C(7)	7669(4)	5905(1)	2542(1)	22(1)
O(3)	8577(4)	5848(1)	1932(1)	38(1)
C(8)	8816(3)	5587(2)	3257(1)	18(1)
C(9)	7470(3)	5491(1)	3974(1)	15(1)
C(10)	7522(3)	4620(1)	4364(1)	15(1)
O(4)	8720(2)	4016(1)	4141(1)	19(1)
C(11)	6084(3)	4457(1)	5040(1)	15(1)
C(12)	3939(3)	3993(1)	4811(1)	16(1)
O(5)	3102(2)	4518(1)	4189(1)	15(1)
C(19)	4176(3)	3021(1)	4572(1)	21(1)
C(13)	2585(3)	4137(1)	5535(1)	18(1)
C(14)	3075(3)	5093(1)	5780(1)	19(1)
C(15)	5399(3)	5298(1)	5486(1)	16(1)

**Table A3.9.4** Bond lengths [ $\text{\AA}$ ] and angles [ $^\circ$ ] for compound **1**.

---

O(1)-C(1)	1.341(3)
O(1)-C(14)	1.462(3)
C(1)-O(2)	1.206(3)
C(1)-C(2)	1.530(3)
C(2)-C(3)	1.502(3)
C(2)-C(15)	1.522(3)
C(2)-H(2)	1.0000
C(3)-C(9)	1.345(3)
C(3)-C(4)	1.506(3)
C(4)-C(5)	1.551(3)
C(4)-H(4A)	0.9900
C(4)-H(4B)	0.9900
C(5)-C(16)	1.519(3)
C(5)-C(6)	1.549(3)
C(5)-H(5)	1.0000
C(16)-C(17)	1.356(4)
C(16)-C(18)	1.468(4)
C(17)-H(17A)	0.9500
C(17)-H(17B)	0.9500
C(18)-H(18A)	0.9800
C(18)-H(18B)	0.9800
C(18)-H(18C)	0.9800
C(6)-C(7)	1.507(3)
C(6)-H(6A)	0.9900
C(6)-H(6B)	0.9900
C(7)-O(3)	1.210(3)
C(7)-C(8)	1.515(3)
C(8)-C(9)	1.514(3)
C(8)-H(8A)	0.9900
C(8)-H(8B)	0.9900
C(9)-C(10)	1.472(3)
C(10)-O(4)	1.232(3)
C(10)-C(11)	1.501(3)
C(11)-C(15)	1.540(3)

**Table A3.9.4** *Cont'd*

C(11)-C(12)	1.551(3)
C(11)-H(11)	1.0000
C(12)-O(5)	1.439(2)
C(12)-C(19)	1.522(3)
C(12)-C(13)	1.535(3)
O(5)-H(5O)	0.84(2)
C(19)-H(19A)	0.9800
C(19)-H(19B)	0.9800
C(19)-H(19C)	0.9800
C(13)-C(14)	1.524(3)
C(13)-H(13A)	0.9900
C(13)-H(13B)	0.9900
C(14)-C(15)	1.558(3)
C(14)-H(14)	1.0000
C(15)-H(15)	1.0000
C(1)-O(1)-C(14)	111.70(15)
O(2)-C(1)-O(1)	122.04(19)
O(2)-C(1)-C(2)	127.36(19)
O(1)-C(1)-C(2)	110.44(17)
C(3)-C(2)-C(15)	117.69(17)
C(3)-C(2)-C(1)	112.65(16)
C(15)-C(2)-C(1)	104.94(16)
C(3)-C(2)-H(2)	107.0
C(15)-C(2)-H(2)	107.0
C(1)-C(2)-H(2)	107.0
C(9)-C(3)-C(2)	123.12(18)
C(9)-C(3)-C(4)	120.27(18)
C(2)-C(3)-C(4)	116.46(17)
C(3)-C(4)-C(5)	115.37(16)
C(3)-C(4)-H(4A)	108.4
C(5)-C(4)-H(4A)	108.4
C(3)-C(4)-H(4B)	108.4
C(5)-C(4)-H(4B)	108.4
H(4A)-C(4)-H(4B)	107.5
C(16)-C(5)-C(6)	112.80(17)

**Table A3.9.4** *Cont'd*

C(16)-C(5)-C(4)	109.91(17)
C(6)-C(5)-C(4)	113.52(17)
C(16)-C(5)-H(5)	106.7
C(6)-C(5)-H(5)	106.7
C(4)-C(5)-H(5)	106.7
C(17)-C(16)-C(18)	121.0(2)
C(17)-C(16)-C(5)	119.8(2)
C(18)-C(16)-C(5)	119.3(2)
C(16)-C(17)-H(17A)	120.0
C(16)-C(17)-H(17B)	120.0
H(17A)-C(17)-H(17B)	120.0
C(16)-C(18)-H(18A)	109.5
C(16)-C(18)-H(18B)	109.5
H(18A)-C(18)-H(18B)	109.5
C(16)-C(18)-H(18C)	109.5
H(18A)-C(18)-H(18C)	109.5
H(18B)-C(18)-H(18C)	109.5
C(7)-C(6)-C(5)	115.61(17)
C(7)-C(6)-H(6A)	108.4
C(5)-C(6)-H(6A)	108.4
C(7)-C(6)-H(6B)	108.4
C(5)-C(6)-H(6B)	108.4
H(6A)-C(6)-H(6B)	107.4
O(3)-C(7)-C(6)	121.7(2)
O(3)-C(7)-C(8)	119.3(2)
C(6)-C(7)-C(8)	119.01(18)
C(9)-C(8)-C(7)	117.25(18)
C(9)-C(8)-H(8A)	108.0
C(7)-C(8)-H(8A)	108.0
C(9)-C(8)-H(8B)	108.0
C(7)-C(8)-H(8B)	108.0
H(8A)-C(8)-H(8B)	107.2
C(3)-C(9)-C(10)	121.31(18)
C(3)-C(9)-C(8)	121.41(18)
C(10)-C(9)-C(8)	117.22(17)

**Table A3.9.4** *Cont'd*

O(4)-C(10)-C(9)	121.05(18)
O(4)-C(10)-C(11)	119.20(18)
C(9)-C(10)-C(11)	119.75(17)
C(10)-C(11)-C(15)	115.54(17)
C(10)-C(11)-C(12)	112.03(16)
C(15)-C(11)-C(12)	105.17(16)
C(10)-C(11)-H(11)	107.9
C(15)-C(11)-H(11)	107.9
C(12)-C(11)-H(11)	107.9
O(5)-C(12)-C(19)	110.42(17)
O(5)-C(12)-C(13)	110.60(16)
C(19)-C(12)-C(13)	114.45(17)
O(5)-C(12)-C(11)	105.04(15)
C(19)-C(12)-C(11)	114.65(17)
C(13)-C(12)-C(11)	100.97(16)
C(12)-O(5)-H(5O)	107(2)
C(12)-C(19)-H(19A)	109.5
C(12)-C(19)-H(19B)	109.5
H(19A)-C(19)-H(19B)	109.5
C(12)-C(19)-H(19C)	109.5
H(19A)-C(19)-H(19C)	109.5
H(19B)-C(19)-H(19C)	109.5
C(14)-C(13)-C(12)	104.79(16)
C(14)-C(13)-H(13A)	110.8
C(12)-C(13)-H(13A)	110.8
C(14)-C(13)-H(13B)	110.8
C(12)-C(13)-H(13B)	110.8
H(13A)-C(13)-H(13B)	108.9
O(1)-C(14)-C(13)	109.84(16)
O(1)-C(14)-C(15)	106.79(15)
C(13)-C(14)-C(15)	106.01(17)
O(1)-C(14)-H(14)	111.3
C(13)-C(14)-H(14)	111.3
C(15)-C(14)-H(14)	111.3
C(2)-C(15)-C(11)	114.84(16)



**Table A3.9.4** *Cont'd*

C(2)-C(15)-C(14)	104.14(16)
C(11)-C(15)-C(14)	105.07(16)
C(2)-C(15)-H(15)	110.8
C(11)-C(15)-H(15)	110.8
C(14)-C(15)-H(15)	110.8

---

Symmetry transformations used to generate equivalent atoms:

**Table A3.9.5** Anisotropic displacement parameters ( $\text{\AA}^2 \times 10^3$ ) for compound **1**. Theanisotropic displacement factor exponent takes the form:  $-2\pi^2 [h^2 a^{*2} U^{11} + \dots + 2h$  $k a^* b^* U^{12}]$ 

	U <sup>11</sup>	U <sup>22</sup>	U <sup>33</sup>	U <sup>23</sup>	U <sup>13</sup>	U <sup>12</sup>
O(1)	17(1)	21(1)	20(1)	0(1)	4(1)	5(1)
C(1)	17(1)	18(1)	14(1)	-4(1)	2(1)	1(1)
O(2)	19(1)	20(1)	21(1)	-2(1)	-1(1)	6(1)
C(2)	16(1)	18(1)	13(1)	-2(1)	-2(1)	0(1)
C(3)	11(1)	18(1)	14(1)	0(1)	-3(1)	-4(1)
C(4)	19(1)	17(1)	16(1)	0(1)	-2(1)	-3(1)
C(5)	16(1)	20(1)	17(1)	2(1)	-2(1)	-1(1)
C(16)	26(1)	23(1)	18(1)	4(1)	-3(1)	-4(1)
C(17)	34(1)	27(1)	41(1)	13(1)	4(1)	4(1)
C(18)	27(1)	38(1)	35(1)	17(1)	-1(1)	-6(1)
C(6)	24(1)	23(1)	17(1)	-1(1)	-7(1)	-3(1)
C(7)	30(1)	19(1)	17(1)	-3(1)	2(1)	0(1)
O(3)	49(1)	45(1)	20(1)	-1(1)	10(1)	14(1)
C(8)	16(1)	21(1)	19(1)	0(1)	4(1)	-1(1)
C(9)	10(1)	21(1)	14(1)	1(1)	-1(1)	-2(1)
C(10)	8(1)	19(1)	17(1)	-2(1)	-3(1)	-1(1)
O(4)	11(1)	19(1)	27(1)	0(1)	1(1)	1(1)
C(11)	12(1)	17(1)	16(1)	4(1)	-2(1)	2(1)
C(12)	11(1)	18(1)	17(1)	3(1)	0(1)	1(1)
O(5)	10(1)	18(1)	17(1)	2(1)	-1(1)	-1(1)
C(19)	15(1)	17(1)	29(1)	2(1)	0(1)	-2(1)
C(13)	14(1)	22(1)	19(1)	5(1)	3(1)	-1(1)
C(14)	17(1)	24(1)	15(1)	2(1)	3(1)	2(1)
C(15)	14(1)	21(1)	14(1)	0(1)	-1(1)	-1(1)

**Table A3.9.6** Hydrogen coordinates ( $\times 10^4$ ) and isotropic displacement parameters ( $\text{\AA}^2 \times 10^3$ ) for compound **1**.

	x	y	z	U(eq)
H(2)	5617	6652	5321	19
H(4A)	7940	7245	3785	21
H(4B)	5787	7530	4224	21
H(5)	3622	7198	3225	21
H(17A)	4754	9131	2244	41
H(17B)	2887	8518	2659	41
H(18A)	8266	8645	2153	50
H(18B)	8575	7584	2135	50
H(18C)	9025	8127	2906	50
H(6A)	4469	5811	2829	26
H(6B)	4874	6411	2089	26
H(8A)	9481	5001	3144	22
H(8B)	10006	6010	3367	22
H(11)	6869	4053	5401	18
H(5O)	1810(40)	4353(19)	4117(16)	22
H(19A)	2797	2803	4369	31
H(19B)	4593	2660	5015	31
H(19C)	5292	2972	4176	31
H(13A)	1027	4062	5425	22
H(13B)	3009	3708	5939	22
H(14)	2975	5162	6347	22
H(15)	6404	5411	5923	20

**Table A3.9.7** Torsion angles [°] for compound **1**.

---

C(14)-O(1)-C(1)-O(2)	174.04(18)
C(14)-O(1)-C(1)-C(2)	-10.2(2)
O(2)-C(1)-C(2)-C(3)	-40.7(3)
O(1)-C(1)-C(2)-C(3)	143.75(16)
O(2)-C(1)-C(2)-C(15)	-169.96(19)
O(1)-C(1)-C(2)-C(15)	14.5(2)
C(15)-C(2)-C(3)-C(9)	7.3(3)
C(1)-C(2)-C(3)-C(9)	-115.0(2)
C(15)-C(2)-C(3)-C(4)	-168.25(17)
C(1)-C(2)-C(3)-C(4)	69.4(2)
C(9)-C(3)-C(4)-C(5)	71.1(3)
C(2)-C(3)-C(4)-C(5)	-113.2(2)
C(3)-C(4)-C(5)-C(16)	-165.26(18)
C(3)-C(4)-C(5)-C(6)	-37.9(3)
C(6)-C(5)-C(16)-C(17)	114.0(2)
C(4)-C(5)-C(16)-C(17)	-118.3(2)
C(6)-C(5)-C(16)-C(18)	-66.2(3)
C(4)-C(5)-C(16)-C(18)	61.6(3)
C(16)-C(5)-C(6)-C(7)	79.8(2)
C(4)-C(5)-C(6)-C(7)	-46.1(3)
C(5)-C(6)-C(7)-O(3)	-118.2(2)
C(5)-C(6)-C(7)-C(8)	62.2(3)
O(3)-C(7)-C(8)-C(9)	-167.6(2)
C(6)-C(7)-C(8)-C(9)	12.0(3)
C(2)-C(3)-C(9)-C(10)	1.6(3)
C(4)-C(3)-C(9)-C(10)	177.02(16)
C(2)-C(3)-C(9)-C(8)	-175.38(18)
C(4)-C(3)-C(9)-C(8)	0.0(3)
C(7)-C(8)-C(9)-C(3)	-57.2(3)
C(7)-C(8)-C(9)-C(10)	125.7(2)
C(3)-C(9)-C(10)-O(4)	-172.57(19)
C(8)-C(9)-C(10)-O(4)	4.6(3)
C(3)-C(9)-C(10)-C(11)	7.9(3)
C(8)-C(9)-C(10)-C(11)	-174.98(17)

**Table A3.9.7** *Cont'd*

O(4)-C(10)-C(11)-C(15)	155.15(18)
C(9)-C(10)-C(11)-C(15)	-25.3(2)
O(4)-C(10)-C(11)-C(12)	-84.4(2)
C(9)-C(10)-C(11)-C(12)	95.1(2)
C(10)-C(11)-C(12)-O(5)	-50.5(2)
C(15)-C(11)-C(12)-O(5)	75.75(18)
C(10)-C(11)-C(12)-C(19)	70.9(2)
C(15)-C(11)-C(12)-C(19)	-162.86(17)
C(10)-C(11)-C(12)-C(13)	-165.57(16)
C(15)-C(11)-C(12)-C(13)	-39.29(18)
O(5)-C(12)-C(13)-C(14)	-69.4(2)
C(19)-C(12)-C(13)-C(14)	165.12(17)
C(11)-C(12)-C(13)-C(14)	41.41(18)
C(1)-O(1)-C(14)-C(13)	-112.91(18)
C(1)-O(1)-C(14)-C(15)	1.6(2)
C(12)-C(13)-C(14)-O(1)	86.82(18)
C(12)-C(13)-C(14)-C(15)	-28.20(19)
C(3)-C(2)-C(15)-C(11)	-24.3(2)
C(1)-C(2)-C(15)-C(11)	101.83(19)
C(3)-C(2)-C(15)-C(14)	-138.68(17)
C(1)-C(2)-C(15)-C(14)	-12.52(19)
C(10)-C(11)-C(15)-C(2)	32.7(2)
C(12)-C(11)-C(15)-C(2)	-91.33(19)
C(10)-C(11)-C(15)-C(14)	146.55(16)
C(12)-C(11)-C(15)-C(14)	22.47(19)
O(1)-C(14)-C(15)-C(2)	7.3(2)
C(13)-C(14)-C(15)-C(2)	124.43(17)
O(1)-C(14)-C(15)-C(11)	-113.76(17)
C(13)-C(14)-C(15)-C(11)	3.33(19)

---

Symmetry transformations used to generate equivalent atoms:

**Table A3.9.8** Hydrogen bonds for compound **1** [ $\text{\AA}$  and  $^\circ$ ].

D-H...A	d(D-H)	d(H...A)	d(D...A)	$\angle$ (DHA)
C(2)-H(2)...O(2)#1	1.00	2.53	3.461(2)	154.0
C(8)-H(8B)...O(2)#2	0.99	2.47	3.289(3)	139.6
O(5)-H(5O)...O(4)#3	0.84(2)	1.98(2)	2.815(2)	170(3)
C(19)-H(19C)...O(4)	0.98	2.64	3.270(3)	122.7
C(15)-H(15)...O(3)#4	1.00	2.58	3.123(3)	113.7

Symmetry transformations used to generate equivalent atoms:

#1  $x+1/2, -y+3/2, -z+1$  #2  $x+1, y, z$  #3  $x-1, y, z$

#4  $-x+3/2, -y+1, z+1/2$

## **APPENDIX 4**

### *Synthesis of a Tricyclic Model System*

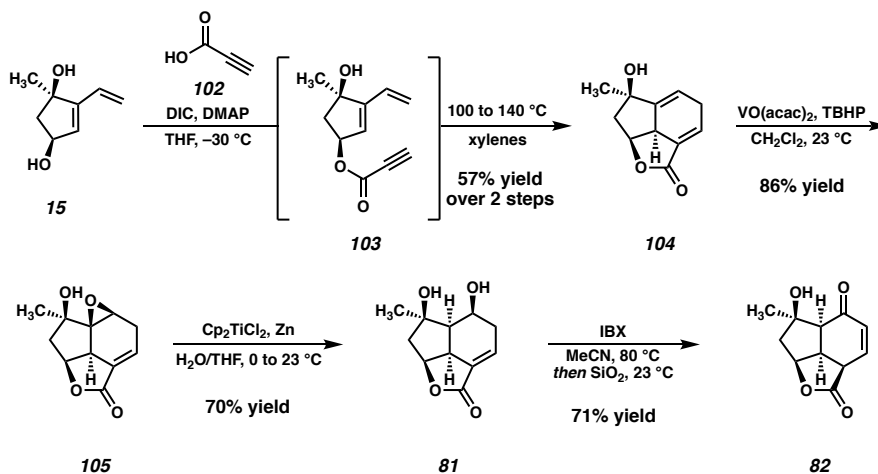
#### A4.1 INTRODUCTION

During the course of our studies toward scabrolide A (**1**) we explored alternative routes which involved the synthesis of the western tricyclic [5–5–6] ring system followed by annulation to form the 7-membered ring. As such, we developed the synthesis of a tricyclic enone intermediate (**82**) possessing 3 of the 4 rings of scabrolide A (**1**). The intermediate alcohol (**81**) was also employed as a model system for the optimization of the C(6) oxidation in the total synthesis (See table 1.7.1).

#### A4.2 SYNTHESIS

The synthesis of model enone **82**, shown in Scheme A4.2.1, employs essentially the same sequence as the scabrolide A (**1**) synthesis. Notably, instead of a substituted alkyne dienophile for the Diels–Alder reaction, an unsubstituted propiolate is required. It was found in practice that this propiolate ester (**103**) was unstable upon concentration for appreciable amounts of time (i.e. hours). As such, a solvent swap technique was employed to obviate the need to isolate this fragile intermediate. The same epoxidation/opening/oxidation sequence was then used to access enone **82**.

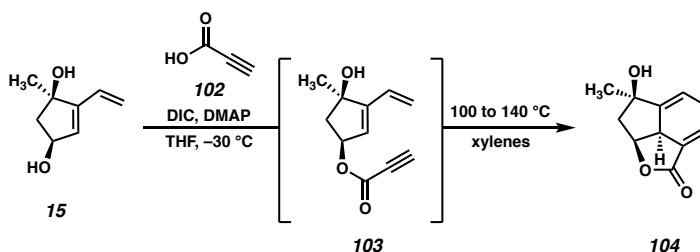


**Scheme A4.2.1** Synthesis of tricyclic enone **82**.**A4.3 EXPERIMENTAL SECTION****A4.3.1 MATERIALS AND METHODS**

Unless otherwise stated, reactions were performed in flame-dried glassware under a nitrogen atmosphere using dry, deoxygenated solvents. Solvents were dried by passage through an activated alumina column under argon. Reaction progress was monitored by thin-layer chromatography (TLC). TLC was performed using E. Merck silica gel 60 F254 precoated glass plates (0.25 mm) and visualized by UV fluorescence quenching, *p*-anisaldehyde, or  $\text{KMnO}_4$  staining. Silicycle SiliaFlash® P60 Academic Silica gel (particle size 40–63  $\mu\text{m}$ ) was used for flash chromatography.  $^1\text{H}$  NMR spectra were recorded on Varian Inova 500 MHz and 600 MHz and Bruker 400 MHz spectrometers and are reported relative to residual  $\text{CHCl}_3$  ( $\delta$  7.26 ppm),  $\text{C}_6\text{D}_6$  ( $\delta$  7.16 ppm) or  $\text{CD}_3\text{OD}$  ( $\delta$  3.31 ppm).  $^{13}\text{C}$  NMR spectra were recorded on a Varian Inova 500 MHz spectrometer (125 MHz) and Bruker 400 MHz spectrometers (100 MHz) and are reported relative to  $\text{CHCl}_3$  ( $\delta$  77.16 ppm),  $\text{C}_6\text{D}_6$  ( $\delta$  128.06 ppm) or  $\text{CD}_3\text{OD}$  ( $\delta$  49.01 ppm). Data for  $^1\text{H}$  NMR are reported as follows: chemical shift ( $\delta$  ppm) (multiplicity, coupling constant (Hz), integration).

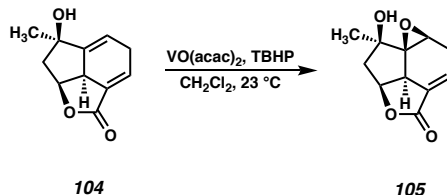
Multiplicities are reported as follows: s = singlet, d = doublet, t = triplet, q = quartet, p = pentet, sept = septuplet, m = multiplet, br s = broad singlet, br d = broad doublet. Data for  $^{13}\text{C}$  NMR are reported in terms of chemical shifts ( $\delta$  ppm). IR spectra were obtained by use of a Perkin Elmer Spectrum BXII spectrometer or Nicolet 6700 FTIR spectrometer using thin films deposited on NaCl plates and reported in frequency of absorption ( $\text{cm}^{-1}$ ). Optical rotations were measured with a Jasco P-2000 polarimeter operating on the sodium D-line (589 nm), using a 100 mm path-length cell. High resolution mass spectra (HRMS) were obtained from the Caltech Mass Spectral Facility using a JEOL JMS-600H High Resolution Mass Spectrometer in fast atom bombardment (FAB+) or electron ionization (EI+) mode, or using an Agilent 6200 Series TOF with an Agilent G1978A Multimode source in electrospray ionization (ESI+), atmospheric pressure chemical ionization (APCI+), or mixed ionization mode (MM: ESI-APCI+).

#### A4.3.2 EXPERIMENTAL PROCEDURES

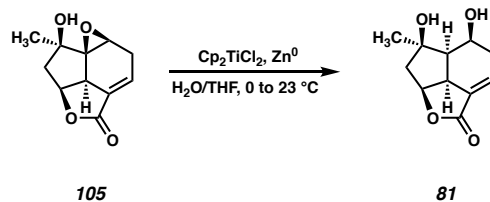


**Tricycle 104:** To a stirred solution of diol **15** (500 mg, 3.57 mmol, 1.0 eq) and DMAP (44 mg, 0.357 mmol, 0.10 eq) in THF (7.1 mL) was added propiolic acid (**102**, 663  $\mu\text{L}$ , 10.7 mmol, 3.0 eq) at room temperature. The flask was sealed and cooled to  $-30$  °C. DIC (1.68 mL, 10.70 mmol, 3.0 eq) was added dropwise and the resulting solution was stirred for 16 h at  $-30$  °C, until consumption of diol **15** as judged by TLC. The reaction mixture was then loaded directly onto a flash column ( $\text{SiO}_2$ , 10% EtOAc/Hexanes), and the flask rinsed with

a small amount (c.a. 1 mL) of CH<sub>2</sub>Cl<sub>2</sub> and eluted with a gradient of 10%–15%–20% EtOAc/Hexanes. The column fractions containing the product were pooled in a 1 L round bottom flask, and 83 mL xylenes was added. The EtOAc/Hexanes were removed by rotary evaporation, leaving a xylenes solution of ester **103**. This solution was transferred to a flame-dried 250 mL round bottom flask containing a stir bar, and sparged with N<sub>2</sub> for 10 min. The solution was heated to 100 °C and stirred for 5 h after which starting material remained as judged by TLC. The temperature was increased to 140 °C and the mixture was stirred for an additional 5 h. The mixture was cooled to 23 °C, and loaded directly onto a flash column (100% Hexanes). The xylenes were flushed off with hexanes, and the product was then eluted with 50%→60% EtOAc/Hexanes, affording tricycle **104** as an off-white solid (390 mg, 2.03 mmol, 57% yield over two steps); <sup>1</sup>H NMR (400 MHz, C<sub>6</sub>D<sub>6</sub>) δ 6.75 (ddd, *J* = 6.7, 3.4, 2.1 Hz, 1H), 5.39 (ddd, *J* = 6.2, 2.9, 1.7 Hz, 1H), 4.29 (dt, *J* = 8.8, 7.4 Hz, 1H), 2.53 – 2.31 (m, 2H), 2.08 (ddt, *J* = 19.3, 11.4, 1.9 Hz, 1H), 1.99 (dd, *J* = 12.7, 7.1 Hz, 1H), 1.18 (dd, *J* = 12.8, 7.9 Hz, 1H), 1.01 (s, 3H); <sup>13</sup>C NMR (100 MHz, C<sub>6</sub>D<sub>6</sub>) 167.9, 151.5, 138.2, 133.7, 116.1, 80.0, 75.6, 49.7, 44.2, 29.4, 26.1; IR (Neat Film, NaCl) 1003, 1208, 1639, 1754, 2967, 3434 cm<sup>-1</sup>; HRMS (MM:ESI-APCI+) *m/z* calc'd for C<sub>11</sub>H<sub>13</sub>O<sub>3</sub> [M+H]<sup>+</sup>: 193.0859, found 193.0856. [α]<sub>D</sub><sup>25</sup> –109.8 ° (*c* 1.0, CHCl<sub>3</sub>).



**Epoxide 105:** To a stirred solution of diene **104** (199 mg, 1.04 mmol, 1.0 eq) in  $\text{CH}_2\text{Cl}_2$  (35 mL) was added  $\text{VO}(\text{acac})_2$  (28 mg, 0.104 mmol, 0.10 eq) in one portion. The solution was allowed to stir for 15 min. at 23 °C until it was pale-green in color. TBHP (5.0 M/decane, 228  $\mu\text{L}$ , 1.4 mmol, 1.10 eq) was added dropwise, causing the reaction mixture to become deep red in color. The mixture was allowed to stir for 3 h at 23 °C, until the disappearance of starting material as judged by TLC. The mixture was then loaded directly onto a flash column ( $\text{SiO}_2$ , 100% EtOAc) and eluted with 100% EtOAc to afford epoxide **105** as a white solid (187 mg, 0.898 mmol, 86% yield);  $^1\text{H}$  NMR (400 MHz,  $(\text{CD}_3)_2\text{CO}$ )  $\delta$  6.41 (dtd,  $J = 7.4, 3.2, 1.0$  Hz, 1H), 4.97 (td,  $J = 7.8, 6.2$  Hz, 1H), 3.81 (d,  $J = 3.2$  Hz, 1H), 3.55 (dt,  $J = 8.2, 2.8$  Hz, 1H), 3.47 (s, 1H), 2.97 (ddd,  $J = 17.1, 7.4, 3.2$  Hz, 1H), 2.49 (ddd,  $J = 13.3, 5.0, 1.8$  Hz, 2H), 1.90 (dd,  $J = 13.2, 6.1$  Hz, 1H), 1.42 (s, 3H);  $^{13}\text{C}$  NMR (100 MHz,  $(\text{CD}_3)_2\text{CO}$ )  $\delta$  169.6, 133.0, 129.6, 77.6, 75.3, 69.6, 52.0, 50.1, 45.1, 30.8, 23.3; IR (Neat Film, NaCl) 780, 954, 1007, 12078, 1646, 1755, 2972, 3500  $\text{cm}^{-1}$ ; HRMS (MM:ESI-APCI+)  $m/z$  calc'd for  $\text{C}_{11}\text{H}_{14}\text{O}_5$   $[\text{M}+\text{H}_2\text{O}]^+$ : 226.0836, found 226.0838.  $[\alpha]_{\text{D}}^{25} -193.9^\circ$  ( $c$  1.0, EtOH).

**Diol 81:**

*Preparation of 0.5 M Cp<sub>2</sub>TiCl Solution:* A 25 mL round-bottom flask was charged with TiCp<sub>2</sub>Cl<sub>2</sub> (1.64 g, 6.60 mmol, 1.0 eq) and Zn dust (1.29 g, 19.8 mmol, 3.0 eq). The flask was evacuated and backfilled with N<sub>2</sub>, and THF (13.2 mL) was added. The red mixture was allowed to stir for 1h after which it became a deep green. Stirring was ceased and the solids were allowed to settle at the bottom of the flask before use of the supernatant.

*Epoxide Opening:* To a stirred solution of epoxide **105** (300 mg, 1.44 mmol, 1.0 eq) in THF (72 mL) was added H<sub>2</sub>O (2.00 mL, 110.74 mmol, 76.9 eq). The mixture was cooled to 0 ° and TiCp<sub>2</sub>Cl was added (11.5 mL, 0.5 M, 5.76 mmol, 4.0 eq) dropwise. The mixture was allowed to gradually warm to 23 °C and stirred for 12 h. The reaction was quenched with Na<sub>2</sub>HPO<sub>4</sub> (sat. aq., 10 mL) and brine (30 mL), and diluted with EtOAc (20 mL). The layers were separated, and the aqueous layer was filtered through a plug of celite, washing with brine and EtOAc. The aqueous layer was extracted with EtOAc until no product was detected by TLC in the subsequent extracts (c.a. 10x 25 mL). The organic extracts were pooled and dried over MgSO<sub>4</sub>, filtered, and concentrated *in vacuo*. The bright orange crude product was purified by flash chromatography on SiO<sub>2</sub> (20%→30%→40% Acetone/Hexanes) to afford diol **81** as a white foam (213 mg, 1.01 mmol, 70% yield); <sup>1</sup>H NMR (500 MHz, CDCl<sub>3</sub>) δ 6.97 – 6.83 (m, 1H), 4.99 (tdd, *J* = 6.6, 3.5, 1.3 Hz, 1H), 4.70 (dd, *J* = 7.2, 3.4 Hz, 1H), 3.17 – 3.03 (m, 1H), 2.80 – 2.69 (m, 1H), 2.43 (ddd, *J* = 9.3, 7.7,

1.2 Hz, 1H), 2.11 (ddd,  $J = 14.4, 3.6, 1.2$  Hz, 1H), 2.06 – 1.93 (m, 2H), 1.42 (s, 3H);  $^{13}\text{C}$  NMR (125 MHz,  $\text{CDCl}_3$ ) 170.6, 135.6, 133.0, 81.8, 80.9, 68.0, 49.7, 47.9, 43.7, 35.6, 28.5; IR (Neat Film, NaCl) 752, 1015, 1104, 1186, 1216, 1307, 1457, 1668, 1746, 2925, 1966, 3377  $\text{cm}^{-1}$ ; HRMS (MM:ESI-APCI+)  $m/z$  calc'd for  $\text{C}_{11}\text{H}_{15}\text{O}_4$   $[\text{M}+\text{H}]^+$ : 211.0965, found 211.0963.  $[\alpha]_{\text{D}}^{25} = +10.7^\circ$  ( $c$  1.0,  $\text{CHCl}_3$ ).



**Enone 82:** To a stirred solution of diol **81** (20 mg, 0.0951 mmol, 1.0 eq) in MeCN (1.9 mL) was added IBX (59 mg, 0.209 mmol, 2.2 eq) in one portion. The resulting suspension was heated to 80 °C and stirred for 1 h, until the disappearance of diol **81** as judged by TLC. The mixture was cooled to 23 °C, and  $\text{SiO}_2$  gel (50 mg) was added in one portion. The suspension was stirred for 10 min at 23 °C, then was diluted with EtOAc (1 mL), filtered over Celite, and the filtrate concentrated *in vacuo*. The crude residue was purified by flash chromatography ( $\text{SiO}_2$ , 60% EtOAc/Hexanes) affording enone **82** as a white solid (14 mg, 0.0720 mmol, 71% yield);  $^1\text{H}$  NMR (600 MHz,  $\text{CDCl}_3$ )  $\delta$  7.00 (dd,  $J = 10.2, 4.8$  Hz, 1H), 6.22 (d,  $J = 10.2$  Hz, 1H), 5.31 – 5.01 (m, 1H), 3.77 – 3.50 (m, 2H), 2.57 (d,  $J = 9.7$  Hz, 1H), 2.32 (d,  $J = 15.0$  Hz, 1H), 1.93 (dd,  $J = 15.0, 5.7$  Hz, 1H), 1.49 (s, 3H);  $^{13}\text{C}$  NMR (100 MHz,  $\text{CDCl}_3$ )  $\delta$  196.2, 174.3, 142.5, 131.0, 82.9, 55.8, 47.4, 41.1, 40.0, 26.1; IR (Neat Film, NaCl) 764, 1003, 1032, 1100, 1183, 1366, 1655, 1756, 2928, 3418  $\text{cm}^{-1}$ ; HRMS (MM:ESI-APCI+)  $m/z$  calc'd for  $\text{C}_{11}\text{H}_{16}\text{O}_4\text{N}$   $[\text{M}+\text{NH}_4]^+$ : 226.1074, found 226.1075.  $[\alpha]_{\text{D}}^{25} = -230.0^\circ$  ( $c$  1.0, EtOH).

## **APPENDIX 5**

*Spectra Relevant to Appendix 4:  
Synthesis of a Tricyclic Model System*

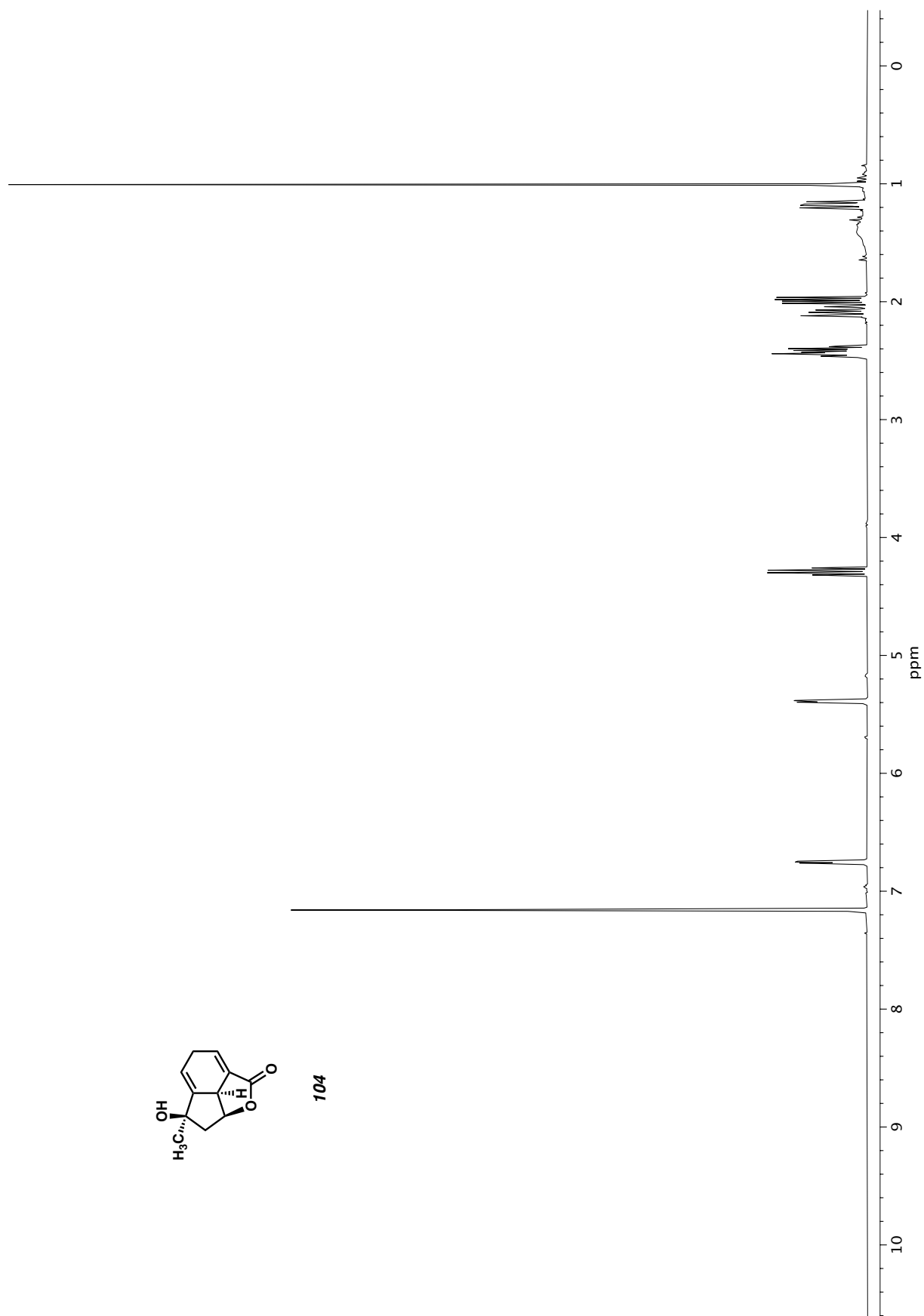


**Figure A5.1**  $^1\text{H}$  NMR (400 MHz,  $\text{C}_6\text{D}_6$ ) of compound **104**.



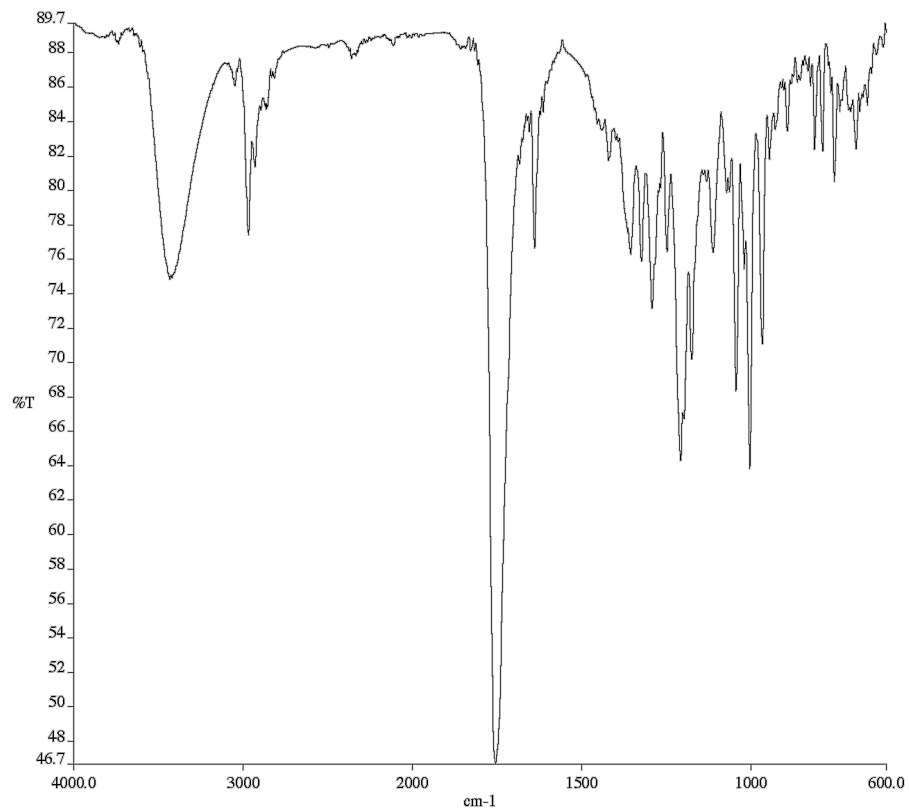


**Figure A5.2** Infrared spectrum (Thin Film, NaCl) of compound **104**.

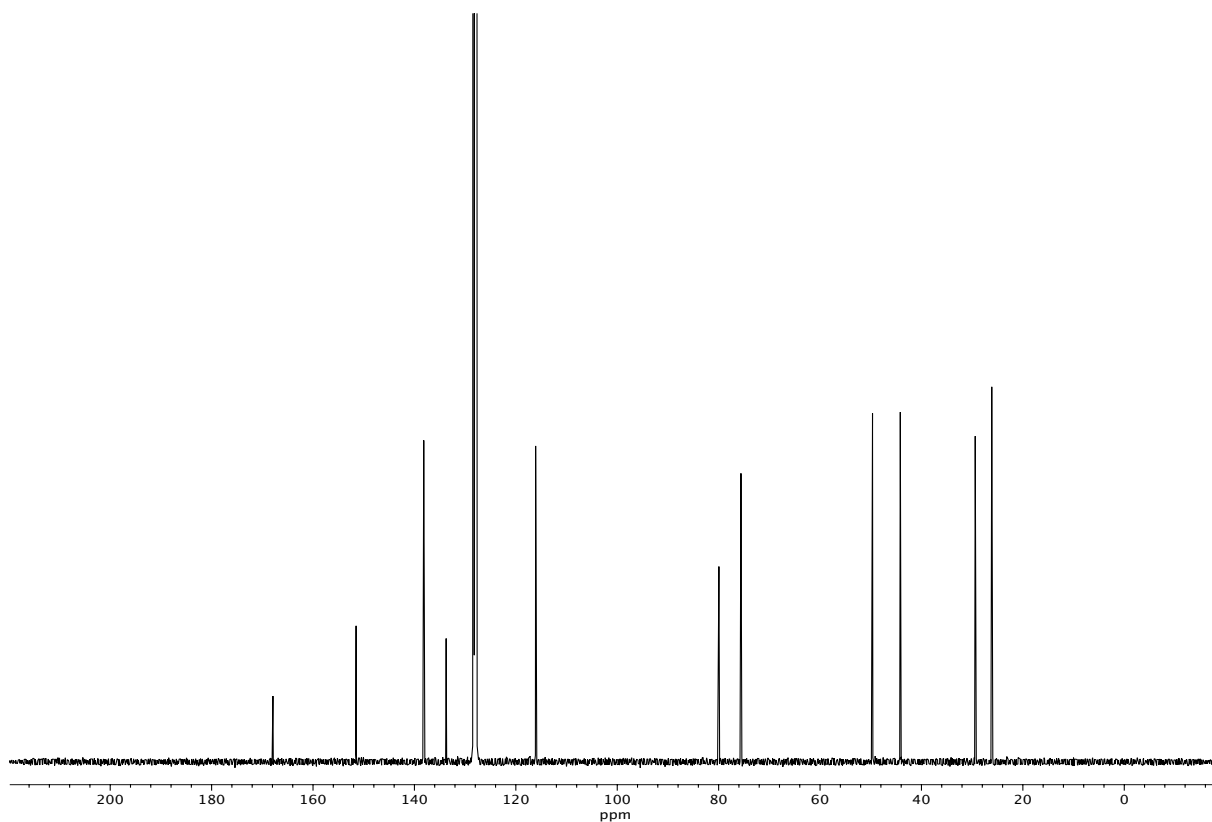


**Figure A5.3** <sup>13</sup>C NMR (100 MHz, C<sub>6</sub>D<sub>6</sub>) of compound **104**.

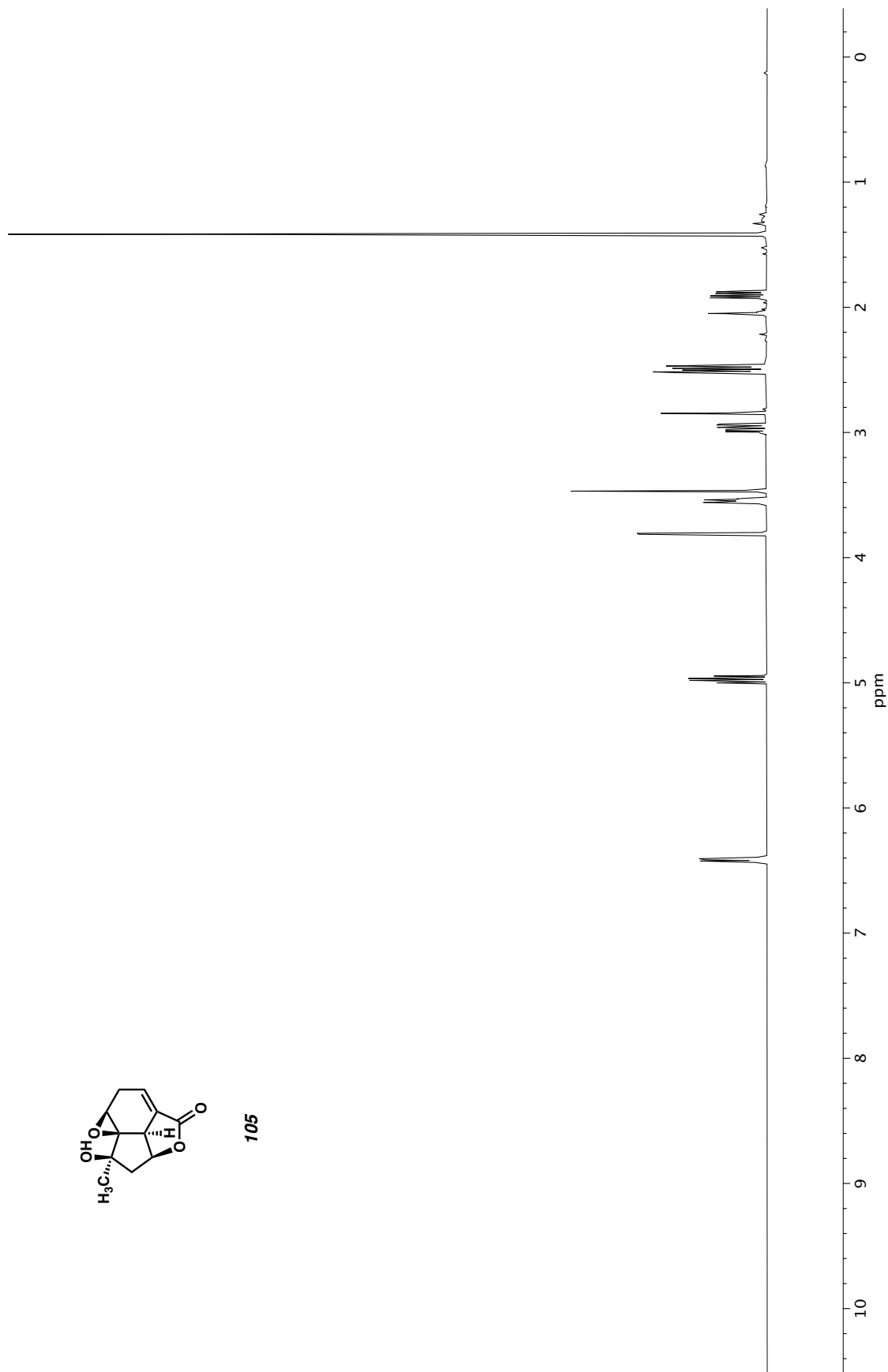
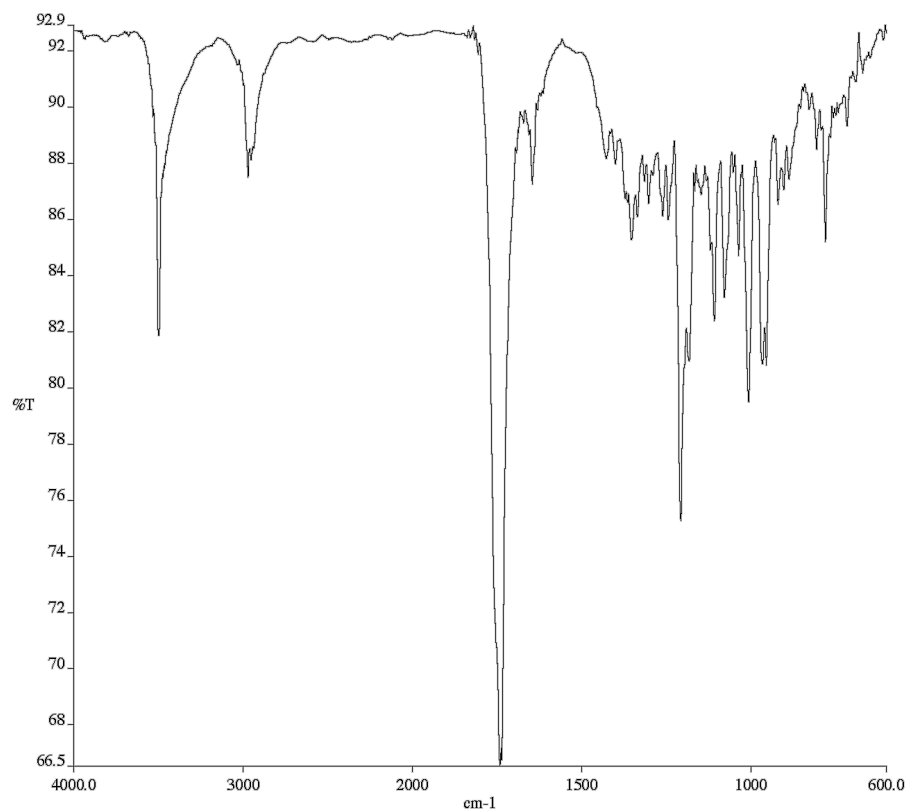
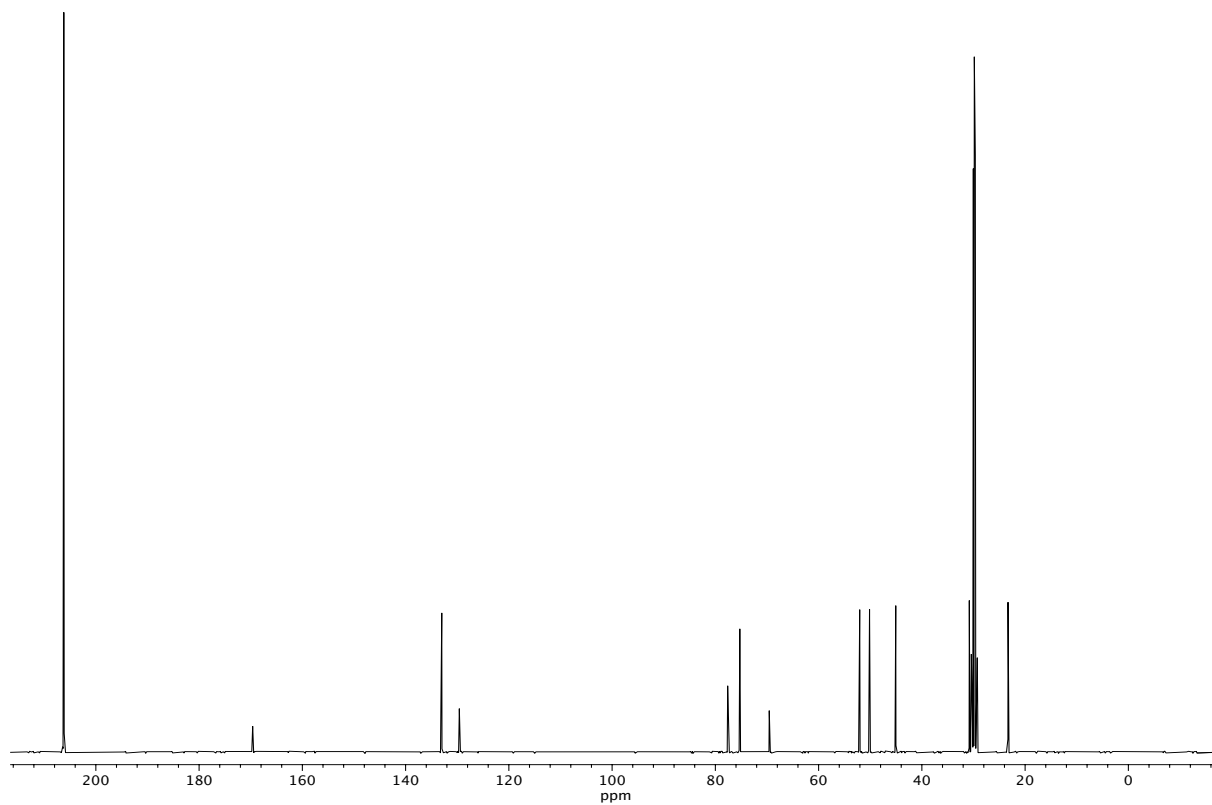


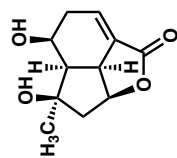
Figure A5.4  $^1\text{H}$  NMR (500 MHz,  $(\text{CD}_3)_2\text{CO}$ ) of compound **105**.



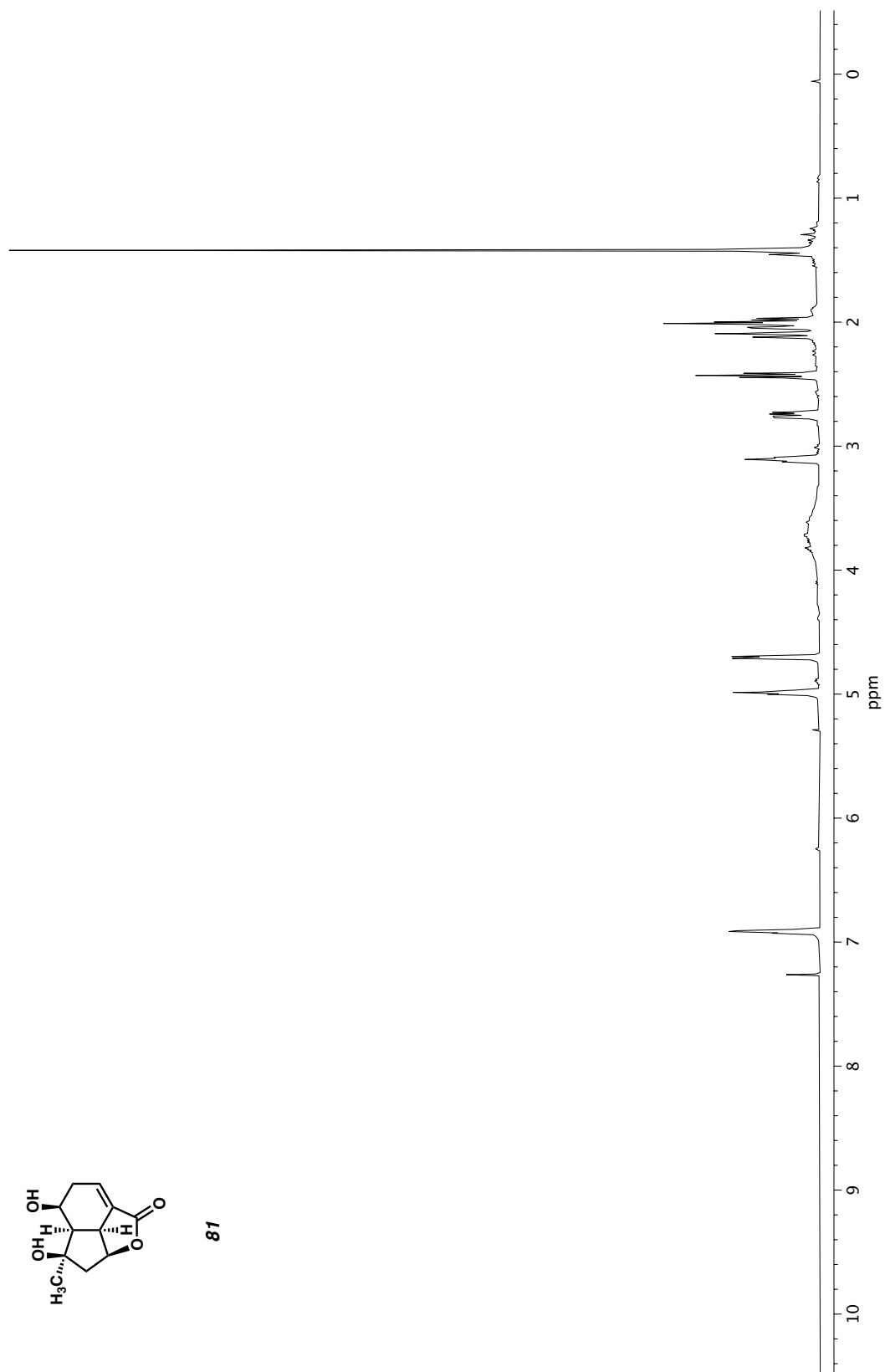
**Figure A5.5** Infrared spectrum (Thin Film, NaCl) of compound **105**.



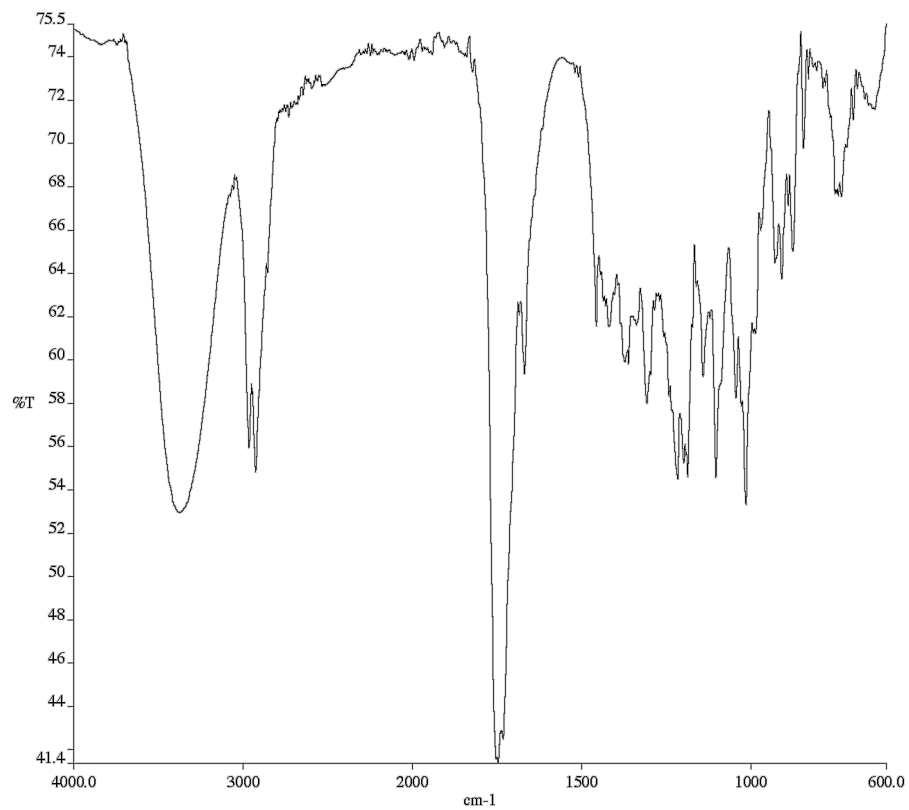
**Figure A5.6** <sup>13</sup>C NMR (100 MHz, (CD<sub>3</sub>)<sub>2</sub>CO) of compound **105**.



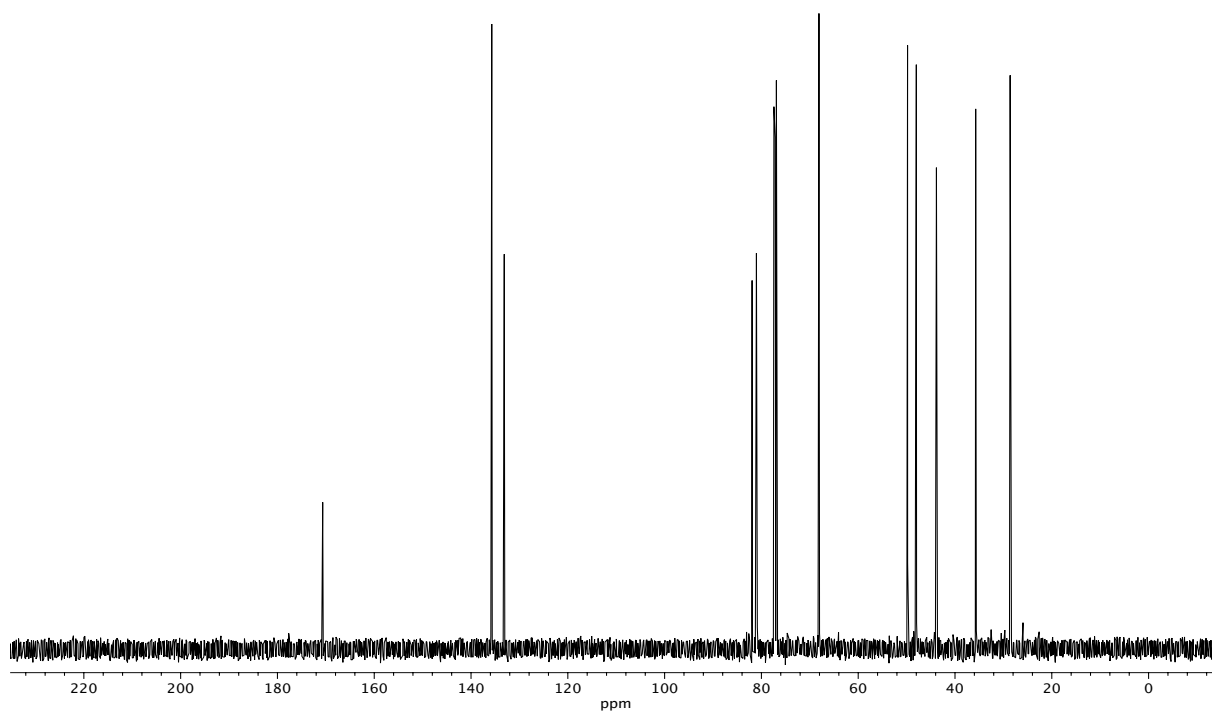
**81**



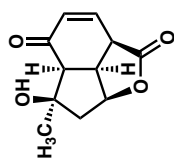
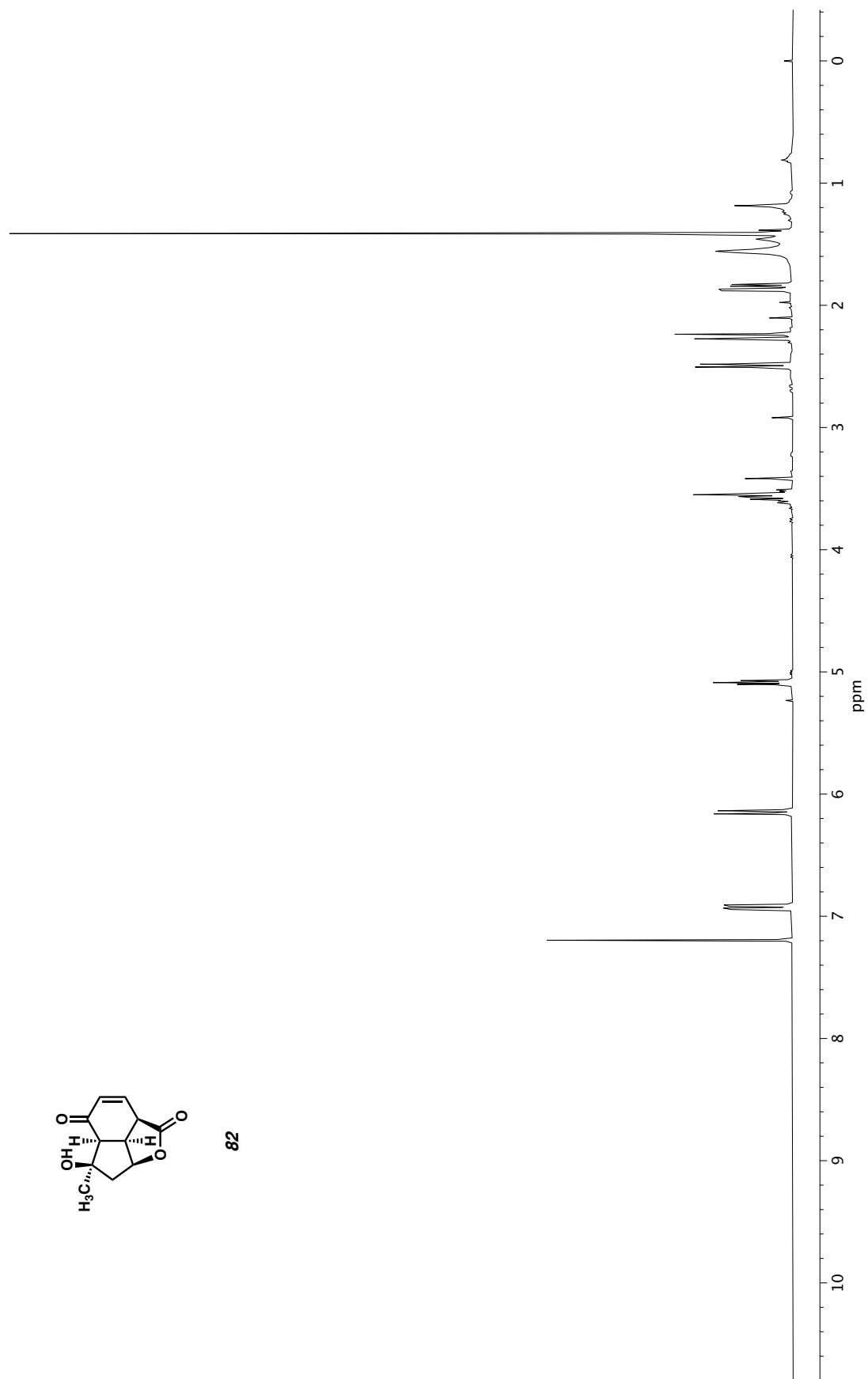
**Figure A5.7**  $^1\text{H}$  NMR (500 MHz,  $\text{CDCl}_3$ ) of compound **81**.



**Figure A5.8** Infrared spectrum (Thin Film, NaCl) of compound **81**.



**Figure A5.9** <sup>13</sup>C NMR (100 MHz, CDCl<sub>3</sub>) of compound **81**.

**82****Figure A5.10**  $^1\text{H}$  NMR (500 MHz,  $\text{CDCl}_3$ ) of compound **82**.

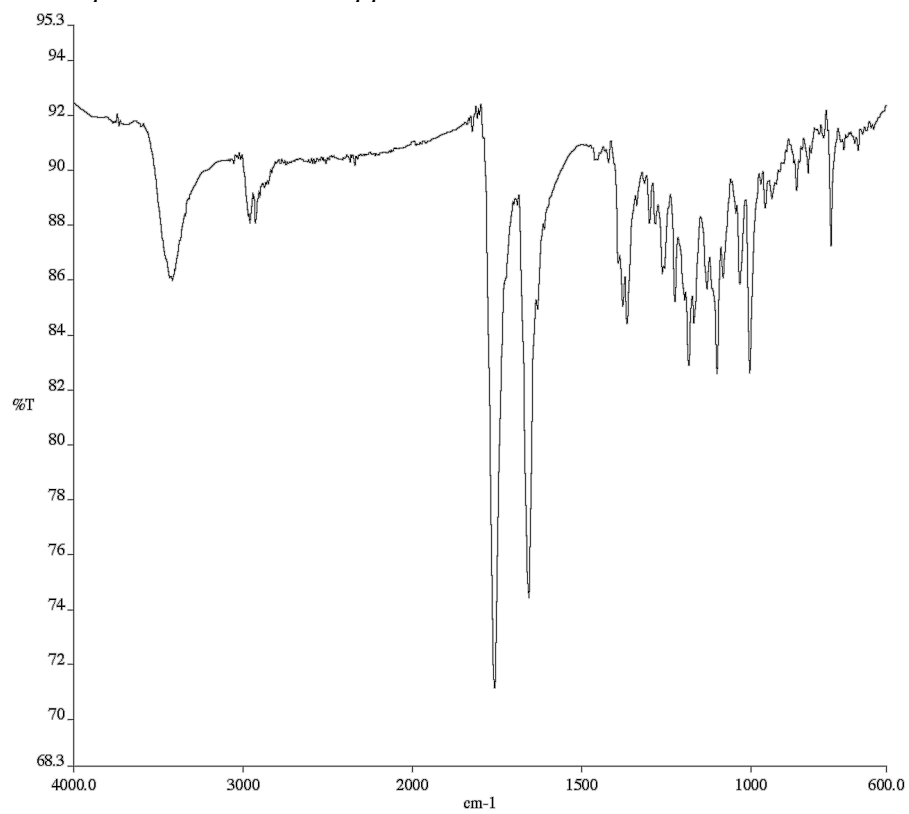


**Figure A5.11** Infrared spectrum (Thin Film, NaCl) of compound **82**.

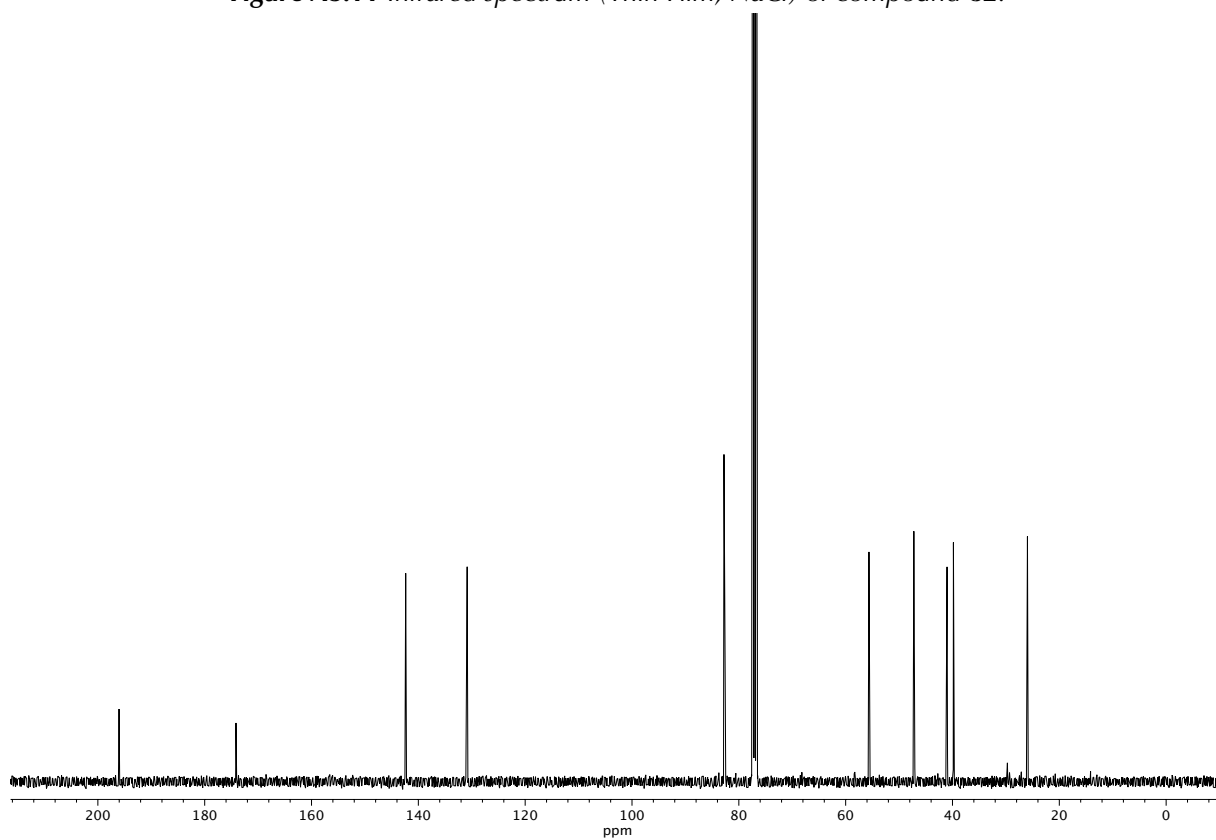


**Figure A5.12** <sup>13</sup>C NMR (100 MHz, CDCl<sub>3</sub>) of compound **82**.

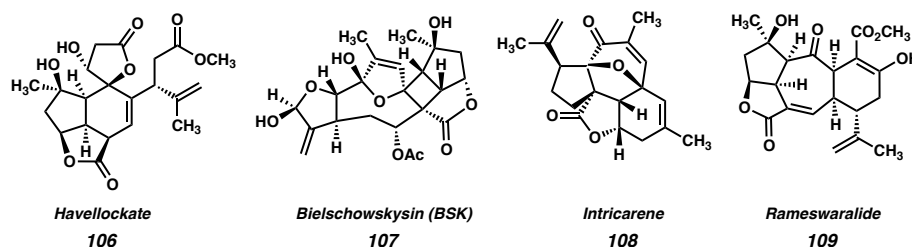
## CHAPTER 2

### *Asymmetric Total Synthesis of Havellockate<sup>†</sup>*

#### 2.1 INTRODUCTION

Marine organisms provide a seemingly endless supply of complex natural products that have captivated synthetic chemists for decades.<sup>1</sup> Soft corals of the genus *Simularia* are no exception, as dozens of macrocyclic and polycyclic molecules have been isolated from their extracts.<sup>2</sup> The polycyclic furanobutenolide-derived cembranoid diterpenoids (the C<sub>20</sub> congeners of the C<sub>19</sub> polycyclic furanobutenolide-derived norcembranoids) have long served as challenging and elusive synthetic targets,<sup>3</sup> with only one member, intricarene (**108**), having succumbed to total synthesis to date (Figure 2.1.1).<sup>4</sup> The structural complexity of this family of natural products, coupled with the bioactivity associated with several of its members, render these molecules challenging and exciting targets for total synthesis.<sup>5</sup>

**Figure 2.1.1** Examples of the polycyclic furanobutenolide-derived cembranoids.

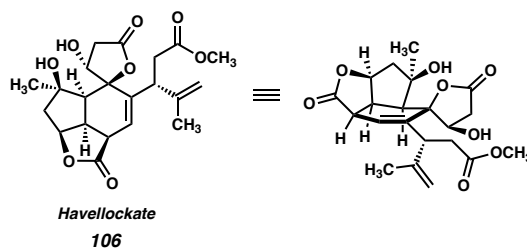


<sup>†</sup>This research was performed in collaboration with Melinda Chan, Tyler J. Fulton, Eric J. Alexy and Steven A. Loskot.



Havellockate (**106**) was first isolated in 1998 from *Sinularia granosa*, and is a prime example of the synthetic challenge posed by the polycyclic furanobutanolide-derived cembranoid family.<sup>6</sup> Havellockate (**106**) is characterized by a highly oxygenated *cis*-fused tricyclic core reminiscent of that of the yonarane-type norcembranoids (e.g. scabrolide A, **1**, chapter 1). A second characteristic feature of havellockate (**106**) is a spiro-fused  $\beta$ -hydroxybutanolide ring, a motif which is not seen in other members of the polycyclic furanobutanolide-derived cembranoid class. In addition, to these topological features, havellockate (**106**) possesses eight stereogenic centers, seven of which are contiguous around the highly substituted and densely functionalized core. Although no completed total syntheses of havellockate (**106**) have been reported, previous efforts by Mehta<sup>7</sup> and Barriault<sup>8</sup> highlight the difficult nature of this target from a synthetic perspective.

**Figure 2.1.2** Havellockate (**106**) in two- and three-dimensions.

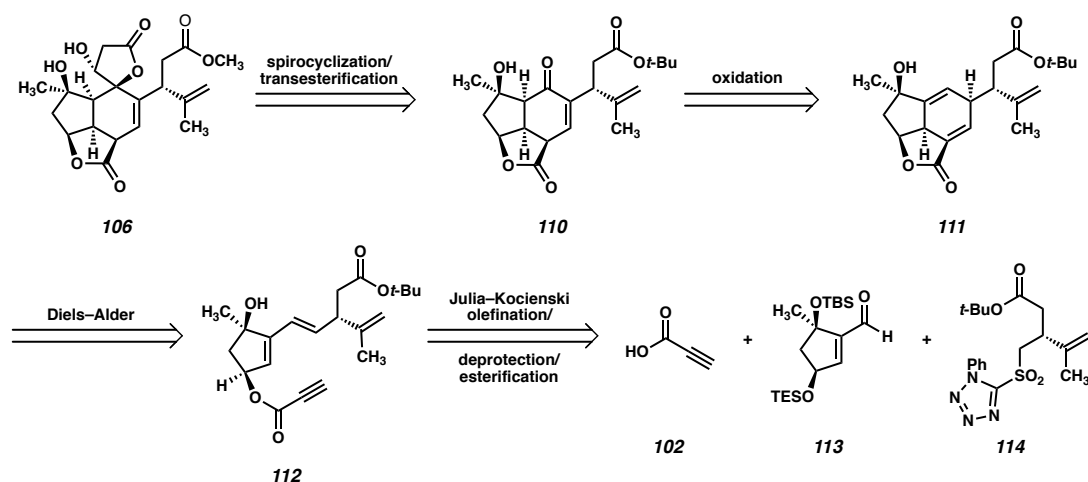


## 2.2 RETROSYNTHETIC ANALYSIS OF HAVELLOCKATE

When devising a retrosynthetic strategy targeting havellockate (**106**) we first focused on disconnecting the butanolide ring to reveal enone **110** (Figure 2.2.1). In the forward direction, it was envisioned that the lactone could be installed via 1,2-addition of a suitable nucleophile into enone **110**, followed by subsequent elaboration to the requisite lactone. Enone **110** bears a strong resemblance to enone **56** (Scheme 1.6.1), employed in our synthesis of scabrolide A (**1**),<sup>9</sup> and this fact informed the remainder of our

retrosynthetic analysis of havellockate (**106**). As such, enone **110**, was envisaged as arising from an intramolecular Diels–Alder reaction of propiolic ester **112** followed by redox manipulations, using the sequence that we successfully employed in our synthesis of scabrolide A (**1**). Ester **112** could be forged via a convergent Julia–Kocienski olefination between aldehyde **113** and sulfone **114** followed by alcohol deprotection and esterification with propiolic acid (**102**).

**Figure 2.2.1** Retrosynthetic analysis of havellockate (**106**).

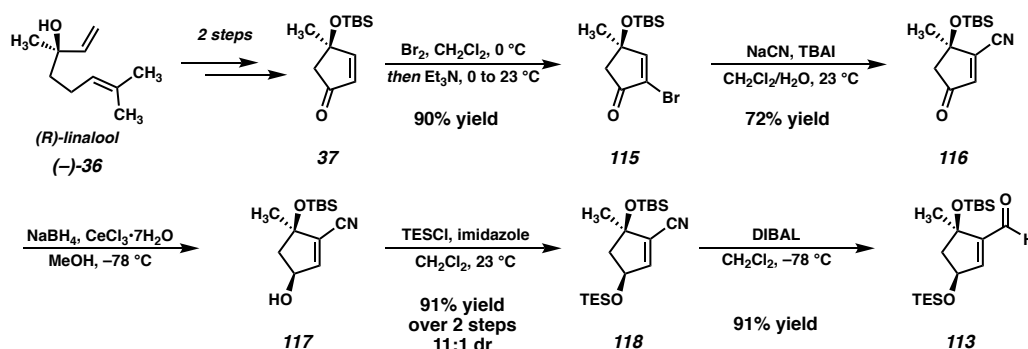


## 2.3 SYNTHESIS OF OLEFINATION BUILDING BLOCKS

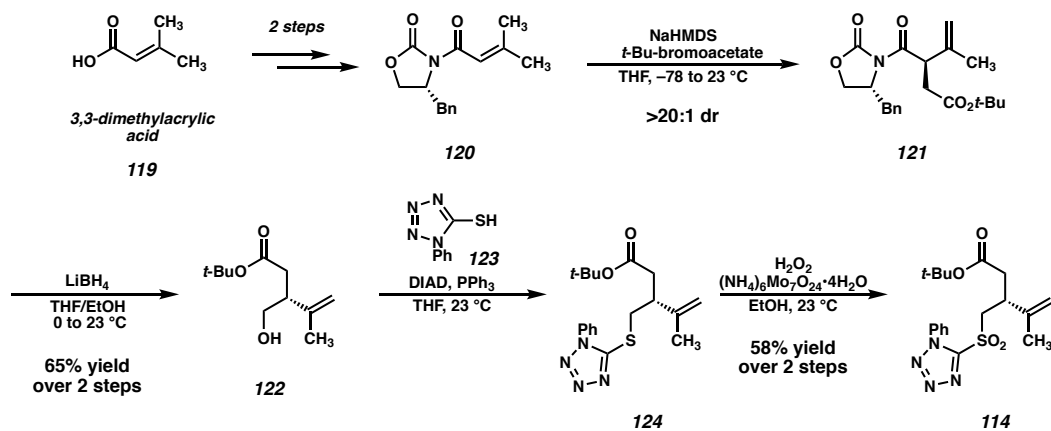
In anticipation of the convergent Julia–Kocienski olefination, we required access to the requisite coupling partners aldehyde **113** and sulfone **114**. The synthesis of aldehyde **113** commences with enone **37**, which is available in two steps from (*R*)-linalool ((–)-**36**) as reported by Maimone,<sup>10</sup> and was employed in our earlier synthesis of scabrolide A (**1**) (Scheme 2.3.1). Upon treatment with bromine, enone **37** undergoes  $\alpha$ -bromination to afford bromoenone **115**. Conjugate addition of cyanide with elimination of bromide proceeds smoothly under phase-transfer conditions to afford vinylogous acyl nitrile **116**.<sup>11</sup> This intermediate (**116**) can then undergo a diastereoselective Luche reduction to afford

alcohol **117**, which is then protected as the corresponding TES ether (**118**). DIBAL reduction of the nitrile to the requisite aldehyde then affords **113**, the first coupling partner for the key convergent olefination.

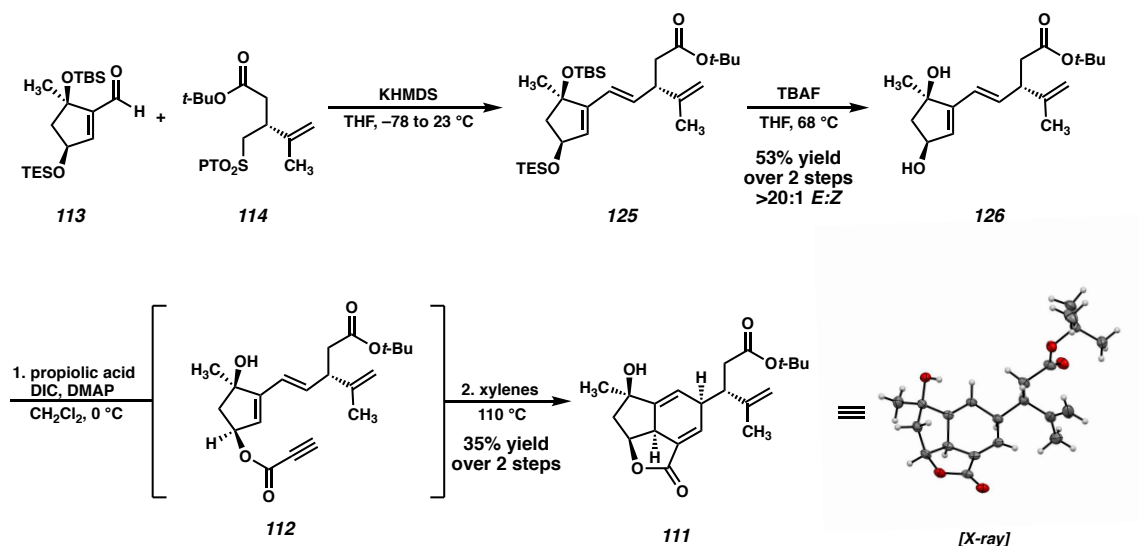
**Scheme 2.3.1** Synthesis of aldehyde **113**.



The second coupling partner, sulfone **114** is accessible in four steps from known oxazolidinone **120**,<sup>12</sup> which itself can be obtained in two steps from commercially available 3,3-dimethylacrylic (**119**) acid and benzyloxazolidinone. Deprotonation of **120** at the  $\gamma$ -position is followed by kinetic alkylation at the  $\alpha$ -position with *t*-Bu bromoacetate,<sup>13</sup> which occurs with excellent diastereoselectivity (>20:1) to provide alkylated oxazolidinone **121**. Subsequent reductive removal of the auxiliary furnishes alcohol **122** as a single enantiomer. A Mitsunobu reaction with 1-phenyltetrazol-5-thiol (**123**) then affords sulfide **124**, which then undergoes oxidation to the requisite sulfone (**114**).<sup>14</sup>

**Scheme 2.3.2** Synthesis of sulfone **114**.**2.4 JULIA–KOCIENSKI OLEFINATION AND DIELS–ALDER**

With **113** and **114** in hand, we next investigated the convergent union of these fragments. Pleasingly, upon addition of KHMDS to a mixture of aldehyde **113** and sulfone **114**, Julia–Kocienski olefination proceeds to forge the requisite C=C bond with excellent (>20:1) selectivity for the *E*-isomer of diene **125** (Scheme 2.4.1).<sup>15</sup> Following treatment of diene **125** with TBAF in THF at elevated temperature, diol **126** is isolated, setting the stage for the esterification and subsequent Diels–Alder reaction to forge the fused [5–5–6] tricyclic framework of havellockate (**106**).

**Scheme 2.4.1** Synthesis of tricycle **111**.

Upon treatment of diol **126** with propiolic acid, DIC and DMAP, conversion to ester **112** occurs, however, major difficulties are encountered when attempting to isolate and purify this key intermediate. We have observed that ester **112** decomposes after prolonged exposure to silica (i.e. flash chromatography) or upon concentration to the neat compound. Consequently, the esterification reaction mixture is crudely purified by filtering over a pad of silica, after which the filtrate is poured directly into xylenes to minimize decomposition of this sensitive intermediate. The lower boiling solvents ( $\text{CH}_2\text{Cl}_2$ , EtOAc, hexanes) are removed by rotary evaporation to leave a solution of ester **112** in xylenes, which is then heated to trigger the subsequent Diels–Alder reaction. This solvent-exchange protocol thus circumvents the need to concentrate sensitive ester **112**.

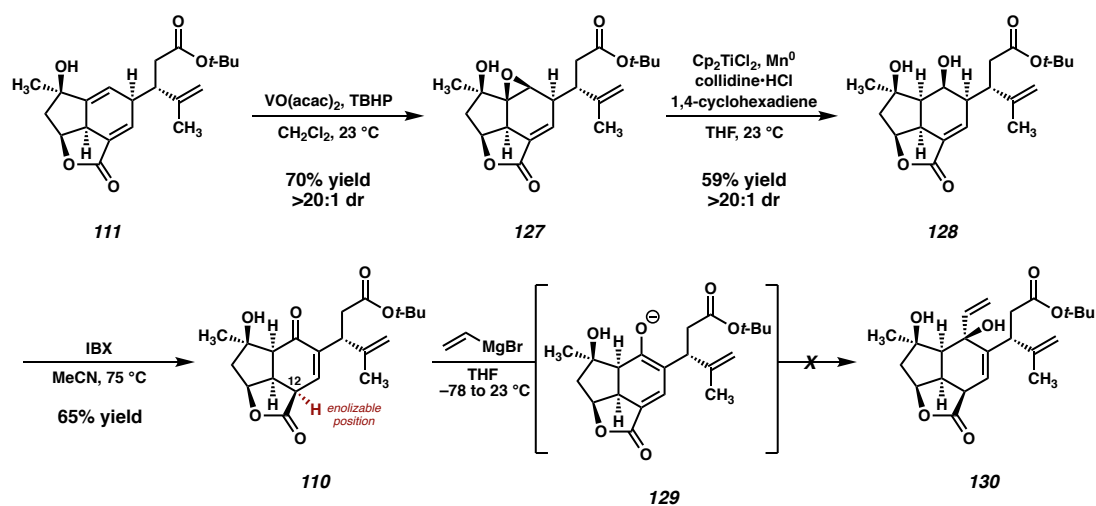
Due at least in part to the unstable nature of ester **112**, cyclohexadiene **113** is prepared in a modest 35% yield over the two steps. Despite extensive efforts to optimize this sequence, including exploring a variety of alternative propiolic acid surrogates,<sup>16,17</sup> we were never able to realize a higher-yielding alternative to this reaction. Despite this low

yield, we have been able to pass sufficient quantities of material through this sequence, which has allowed us to explore the late-stage chemistry, and ultimately, complete the total synthesis of havellockate (**106**).

## 2.5 SYNTHESIS OF THE ENONE

In order to access key enone **110**, we applied the same olefin oxidation sequence to Diels–Alder adduct **111** that we employed in the scabrolide A synthesis, which we anticipated would be successful given the similarity between the two substrates (Scheme 2.5.1). VO(acac)<sub>2</sub>-catalyzed directed epoxidation of **111** delivers epoxide **127** as a single diastereomer, followed by reductive opening of the epoxide to afford diol **128**. Subsequent oxidation with IBX in MeCN occurs with olefin migration at elevated temperature to generate the key enone **110**.

**Scheme 2.5.1** Synthesis of enone **110**, and failed Grignard addition.

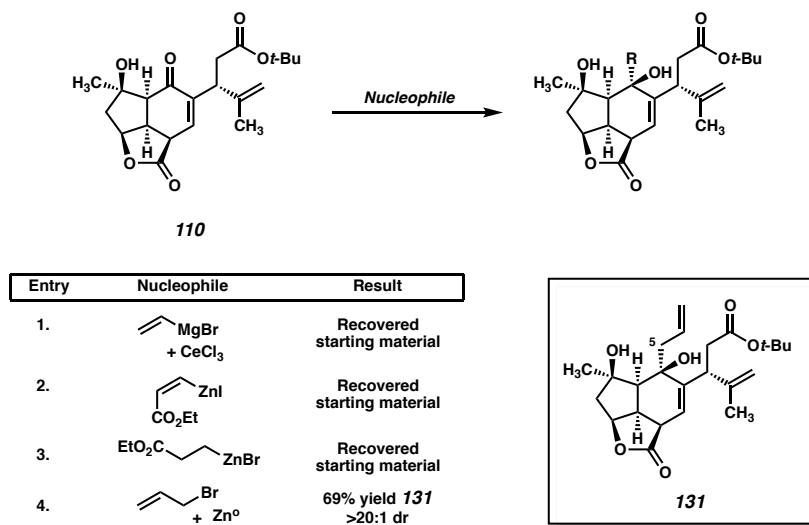


With enone **110** in hand, just one C–C bond remained in our plan for the completion of havellockate (**106**). We envisioned a diastereoselective 1,2-addition of an organometallic (e.g. Grignard reagent) into enone **110** to forge this key bond and begin the construction of the butanolide ring. First, to test the reactivity of enone **110**, it was treated

with vinylmagnesium bromide in THF, but we observed no reactivity whatsoever, recovering only starting material from the reaction. While initially surprised by this lack of reactivity, we realized that upon addition of the strongly basic Grignard reagent, instead of the desired addition into enone **110**, deprotonation of the acidic C(12) proton likely occurs, generating extended enolate **129**. Following this deprotonation, the enolate (**129**) is rendered completely non-electrophilic, thus thwarting our efforts at this key addition.

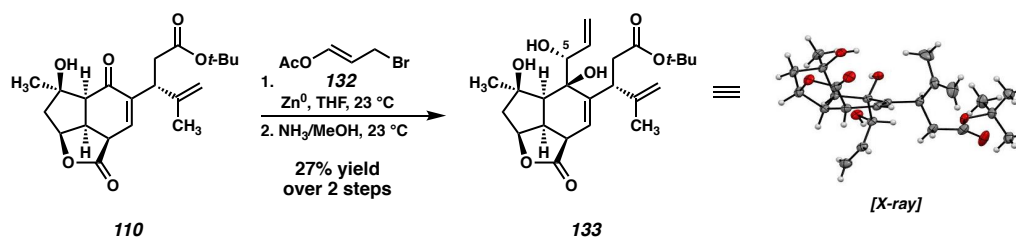
## 2.6 ALLYLATION

Given the failure of the Grignard addition, we turned our attention to less basic organometallics for the final C–C bond forming step of the synthesis (Table 2.6.1). We first investigated the less basic organocerium reagents, which are often employed in situations where enolization must be avoided.<sup>18</sup> Disappointingly, treatment of enone **110** with the organocerium nucleophile generated from vinylmagnesium bromide and anhydrous CeCl<sub>3</sub> yielded no product, again returning only starting material (entry 1). Likewise, employing less basic vinyl- or alkyl-zinc reagents (entries 2 and 3) led to no productive bond formation even after stirring for prolonged periods at elevated temperature. To our delight, addition of allylzinc bromide (generated in situ from allyl bromide and Zn dust) led to smooth 1,2-addition, generating tertiary alcohol **131** as a single diastereomer in 69% yield (entry 4).<sup>19</sup>

**Table 2.6.1** Initial investigation of the 1,2-addition to enone **110**.

At this stage we were gratified to have identified a suitable nucleophile to forge the final C–C bond of havellockate (**106**). However, when inspecting alcohol **131** it became obvious to us that the installation of the C(5) oxidation required for the natural product would likely prove extremely difficult from this intermediate. Searching for more elaborated allylzinc nucleophiles, we found a report detailing the use of 1-acetoxy-3-bromopropene (**132**) in Zn- and In-mediated allylation reactions of aldehydes.<sup>20</sup> Unsure whether this system would be suitable for ketone electrophiles, we were delighted to find that this nucleophile undergoes 1,2-addition into enone **110**, albeit with low (c.a. 1:1) branched-to-linear selectivity (Scheme 2.6.1). After deacetylation of the inseparable branched/linear mixture with methanolic ammonia, the branched triol **133** is isolated as a single diastereomer in 27% yield over the two steps. Critically, the X-ray structure of **133** shows that it possesses the same stereochemistry at the C(5) alcohol as havellockate (**106**). As such, this reaction represents a significant and powerful step in the synthesis, despite the modest yield.



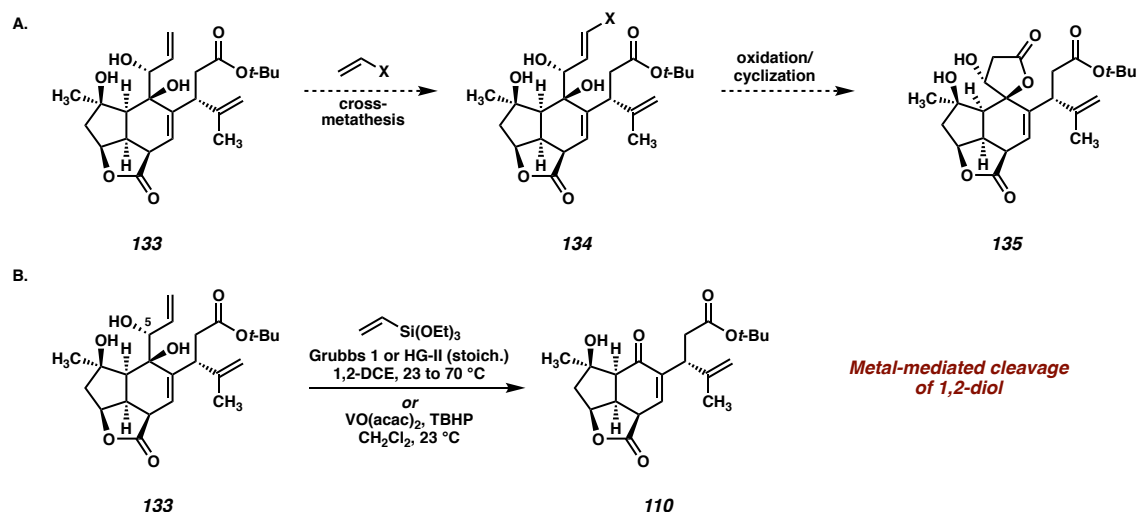
**Scheme 2.6.1.** Allylation of enone **110** with acetoxyallylzinc reagent.**2.7 ATTEMPTED TRANSFORMATIONS OF THE ALLYLIATION PRODUCT**

With triol **133** in hand two critical operations still remained for the completion of the total synthesis: the elaboration of the newly installed allyl fragment to the requisite butanolide ring, and the replacement of the *t*-butyl ester with the methyl ester present in the natural product. We first turned our attention to the formation of the spirocycle, the task that we anticipated would be the more difficult of the two. In our initial strategy, we imagined that an olefin cross-metathesis reaction could be employed to substitute the terminal allyl carbon with one in the aldehyde oxidation state, followed by further oxidation and cyclization to install the desired spirocycle (Scheme 2.7.1A). As enol ethers are not competent in Ru-catalyzed metathesis reactions, vinyl boronic esters or silanes are typically employed,<sup>21</sup> and the boronic ester or silane are oxidized to the aldehyde in a subsequent step.

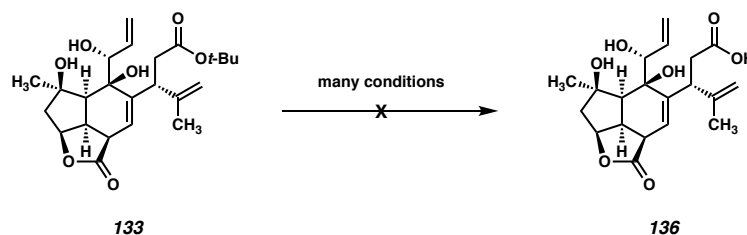
Surprisingly, upon exposure of diol **133** to metathesis conditions using either first-generation Grubbs catalyst or second generation Hoveyda-Grubbs catalyst (in stoichiometric quantities due to the small scale of the reactions), no desired product formation is observed (Scheme 2.7.1B). Instead, quantitative conversion to enone **110** occurs, effectively “undoing” the key allylation reaction. While initially puzzled by this

outcome, a search of the literature reveals that Ru metathesis catalysts have been shown to perform oxidative cleavage of allylic 1,2-diols.<sup>22</sup>

**Scheme 2.7.1** A. Planned cross-metathesis of triol **133**. B. Unexpected oxidative cleavage.



Given this unexpected result, we turned to alternative tactics for the oxidation of the terminal allyl olefin. We imagined that the secondary C(5) alcohol might be able to direct an epoxidation of the allyl olefin, and the epoxide could be reductively opened to provide the required oxidation handle at the terminal position of the chain. Exposure of triol **133** to standard V-catalyzed epoxidation conditions does result in quantitative consumption of the starting material, however, we were surprised to again isolate only enone **110** as the product of this reaction (Scheme 2.7.1B). Another literature search reveals that several transition metal complexes, including  $\text{VO}(\text{acac})_2$ , are capable of catalyzing the oxidative cleavage of 1,2-diols, rendering our planned epoxidation unfeasible.<sup>23</sup>

**Scheme 2.7.2** Failed removal of the *t*-Bu ester from enone **133**.

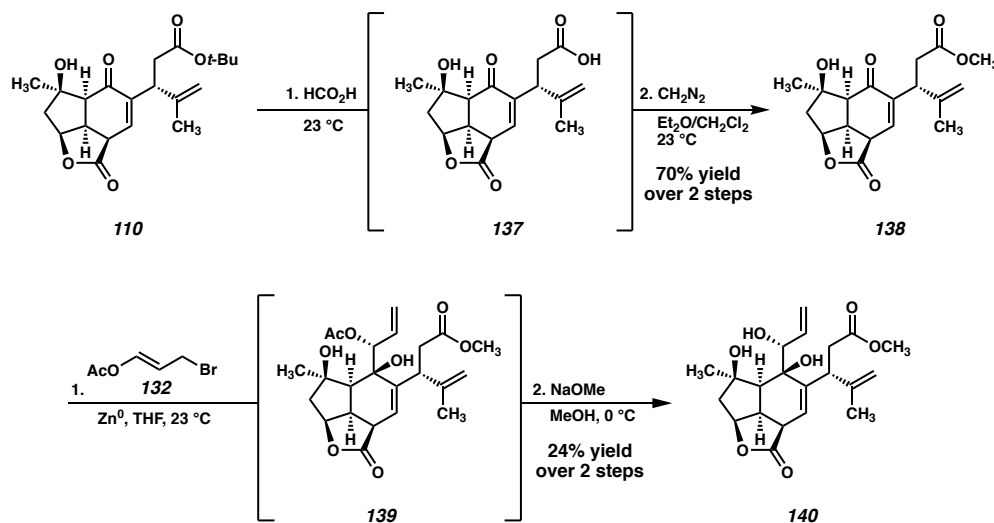
At this stage, we also investigated the removal of the *t*-Bu ester from triol **133** in attempts to convert it to the requisite methyl ester present in havellockate (**106**). Disappointingly, treatment of triol **133** with a variety of conditions commonly employed for the cleavage of *t*-Bu esters (e.g. TFA/Et<sub>3</sub>SiH) failed to effect this transformation, instead leading to the formation of unidentified byproducts (Scheme 2.7.2). Realizing that this key transesterification would likely only prove more difficult on a cyclized intermediate (should we be able to access it), we focused instead on identifying a suitable point earlier in the synthesis to perform this operation.

## 2.8 TRANSESTERIFICATION, ALLYLATION, AND COMPLETION OF THE SYNTHESIS

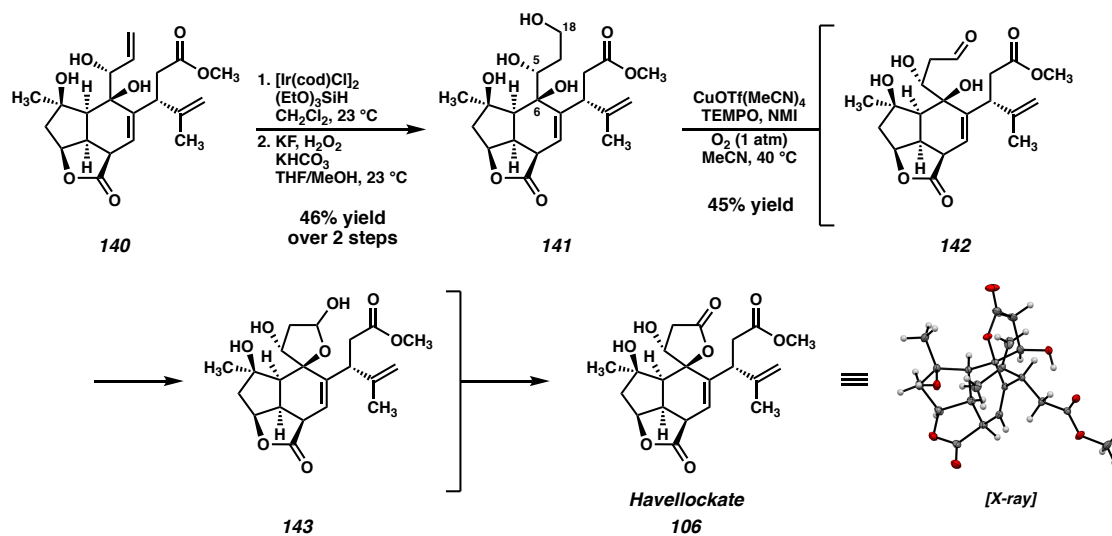
After extensive experimentation, we found that the *t*-Bu ester can be smoothly cleaved from enone **110** by stirring in formic acid,<sup>24</sup> to produce intermediate acid **137** (Scheme 2.8.1). Exposure of other intermediates (e.g. Diels–Alder adduct **111** or allylation product **133**) to these conditions results exclusively in deleterious side-reactivity, demonstrating that enone **110** is a uniquely suited point in the synthesis for this deprotection. Treatment of the intermediate acid with diazomethane then furnishes methyl ester-bearing enone **138** in 70% yield over the two-step sequence. Gratifyingly, enone **138**

is also a competent substrate for the key allylation, leading to triol **140** in 24% yield following deacetylation with NaOMe of the allylation product (**139**) with NaOMe.

**Scheme 2.8.1** Successful transesterification of enone **110** and allylation to generate triol **140**.



With triol **140** in hand, we were again faced with the problem of functionalizing the terminal olefin of the allyl group to forge the spirocycle and complete the synthesis. After exploring several methods for the catalytic hydrofunctionalization of the terminal olefin (e.g. Rh-catalyzed hydroboration or hydrosilylation)<sup>25,26</sup> we ultimately found success implementing an Ir-catalyzed hydrosilylation protocol reported by Ding (Scheme 2.8.2).<sup>27</sup> Treatment of triol **140** with  $[\text{Ir}(\text{cod})\text{Cl}]_2$  and  $(\text{EtO})_3\text{SiH}$  leads to rapid consumption of the starting material to furnish a putative silane, which is then oxidized by treatment with KF and  $\text{H}_2\text{O}_2$  to furnish tetraol **141**.<sup>28</sup>

**Scheme 2.8.2** Completion of the total synthesis of havellockate (**106**).

With tetraol **141** in hand, the final remaining task in the synthesis was the formation of the butanolide ring. This necessitated the selective oxidation of the C(18) primary alcohol to the carboxylic acid oxidation state, a potentially challenging operation in the presence of the C(5) secondary the C(6) tertiary allylic alcohols. We were drawn to the Cu-catalyzed aerobic oxidation conditions reported by Stahl and coworkers,<sup>29</sup> which have been shown to selectively oxidize primary alcohols when TEMPO is employed as a cocatalyst. Gratifyingly, exposure of tetraol **141** to these conditions results in the concomitant oxidation and cyclization to install the requisite butanolide to furnish havellockate (**106**) directly. As depicted in Scheme 2.8.2, this likely occurs via an initial oxidation of the C(18) alcohol to the corresponding aldehyde, which then cyclizes to form lactol **142**. Lactol **142** then undergoes a second oxidation to the lactone,<sup>30</sup> completing the total synthesis of havellockate (**106**). The product was isolated as a crystalline solid which was amenable to X-ray diffraction, allowing us to unambiguously determine the identity of our final compound.

## 2.9 CONCLUSION

We have completed the first total synthesis of the furanobutenolide-derived cembranoid diteperenoid havellockate (**106**). The synthetic route draws on strategies and lessons learned during our recent total synthesis of scabrolide A (**1**) (see chapter 1). Key elements include a convergent Julia–Kocienski olefination, a challenging esterification/Diels–Alder sequence, and a diastereoselective enone allylation. Finally, a hydrosilylation/Tamao–Fleming sequence followed by a Cu-catalyzed oxidative lactonization completes the stereoselective and enantiospecific total synthesis.

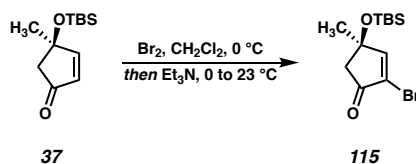
## 2.10 EXPERIMENTAL SECTION

### 2.10.1 MATERIALS AND METHODS

Unless otherwise stated, reactions were performed in flame-dried glassware under a nitrogen atmosphere using dry, deoxygenated solvents. Solvents were dried by passage through an activated alumina column under argon.<sup>31</sup> Reaction progress was monitored by thin-layer chromatography (TLC). TLC was performed using E. Merck silica gel 60 F254 precoated glass plates (0.25 mm) and visualized by UV fluorescence quenching, *p*-anisaldehyde, or KMnO<sub>4</sub> staining. Silicycle SiliaFlash® P60 Academic Silica gel (particle size 40–63 μm) was used for flash chromatography. <sup>1</sup>H NMR spectra were recorded on Varian Inova 500 MHz and 600 MHz and Bruker 400 MHz spectrometers and are reported relative to residual CHCl<sub>3</sub> (δ 7.26 ppm), C<sub>6</sub>D<sub>6</sub> (δ 7.16 ppm) or CD<sub>3</sub>OD (δ 3.31 ppm). <sup>13</sup>C NMR spectra were recorded on a Varian Inova 500 MHz spectrometer (125 MHz) and Bruker 400 MHz spectrometers (100 MHz) and are reported relative to CHCl<sub>3</sub> (δ 77.16 ppm), C<sub>6</sub>D<sub>6</sub> (δ 128.06 ppm) or CD<sub>3</sub>OD (δ 49.01 ppm). Data for <sup>1</sup>H NMR are reported as follows: chemical shift (δ ppm) (multiplicity, coupling constant (Hz), integration). Multiplicities are reported as follows: s = singlet, d = doublet, t = triplet, q = quartet, p = pentet, sept = septuplet, m = multiplet, br s = broad singlet, br d = broad doublet. Data for <sup>13</sup>C NMR are reported in terms of chemical shifts (δ ppm). IR spectra were obtained by use of a Perkin Elmer Spectrum BXII spectrometer or Nicolet 6700 FTIR spectrometer using thin films deposited on NaCl plates and reported in frequency of absorption (cm<sup>-1</sup>). Optical rotations were measured with a Jasco P-2000 polarimeter operating on the sodium D-line (589 nm), using a 100 mm path-length cell. High resolution mass spectra (HRMS) were obtained from the Caltech Mass Spectral Facility using a JEOL JMS-600H High

Resolution Mass Spectrometer in fast atom bombardment (FAB+) or electron ionization (EI+) mode, or using an Agilent 6200 Series TOF with an Agilent G1978A Multimode source in electrospray ionization (ESI+), atmospheric pressure chemical ionization (APCI+), or mixed ionization mode (MM: ESI-APCI+).

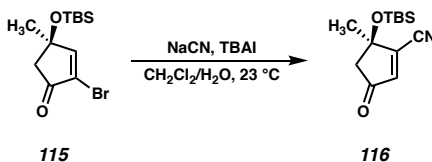
### 2.10.2 EXPERIMENTAL PROCEDURES



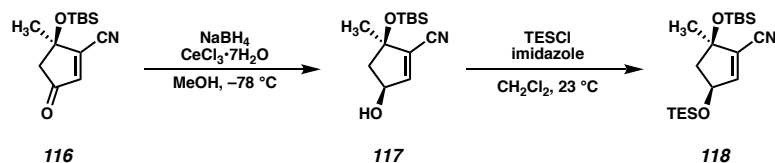
**Bromoenone 115:** A flame dried round-bottom flask was charged with enone **37** (2.76 g, 12.2 mmol, 1.0 equiv) in  $\text{CH}_2\text{Cl}_2$  (122 mL, 0.1 M). The solution was cooled to 0 °C and  $\text{Br}_2$  (0.687 mL, 13.4 mmol, 1.1 equiv) was added dropwise over 10 min. The resultant solution was stirred for 30 min at 0 °C. Upon complete consumption of starting material (as determined by TLC),  $\text{Et}_3\text{N}$  (2.5 mL, 18.3 mmol, 1.5 equiv) was added and the mixture was warmed to 23 °C and allowed to stir for 1 h. The reaction was diluted with a saturated solution of  $\text{Na}_2\text{S}_2\text{O}_3$  and the product was extracted with EtOAc (3 x 100 mL). The combined organic layers were washed with brine, dried over  $\text{MgSO}_4$ , filtered, and concentrated under reduced pressure. The crude product was purified by column chromatography ( $\text{SiO}_2$ , 10% EtOAc/Hexanes) to afford bromoenone **115** (3.3 g, 90% yield) as a colorless oil;  $^1\text{H}$  NMR (400 MHz,  $\text{CDCl}_3$ )  $\delta$  = 7.51 (s, 1H), 2.64 (d,  $J$  = 3.6 Hz, 2H), 1.51 (s, 3H), 0.85 (d,  $J$  = 0.5 Hz, 9H), 0.09 (s, 3H), 0.08 (s, 3H);  $^{13}\text{C}$  NMR (100 MHz,  $\text{CDCl}_3$ )  $\delta$  = 198.9, 165.0, 125.4, 50.4, 29.2, 25.7, 18.0, -2.3, -2.4; IR (thin film, NaCl) 2956, 2930, 2888, 2858, 1733, 1593, 1472, 1463, 1374, 1292, 1254, 1205, 1106, 1081,



1018, 922, 837, 776  $\text{cm}^{-1}$ ; HRMS (ESI)  $m/z$  calc'd  $\text{C}_{12}\text{H}_{22}\text{BrO}_2\text{Si}$   $[\text{M}+\text{H}]^+$ : 305.0567, found: 305.0567;  $[\alpha]_{\text{D}}^{25} + 2.3^\circ$  ( $c$  0.21,  $\text{CHCl}_3$ ).

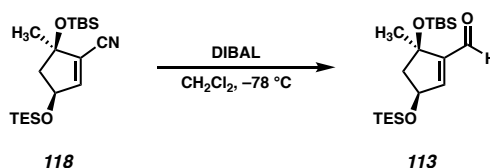


**Cyanoenone 116:** A round bottom flask was charged with NaCN (2.3 g, 47 mmol, 2.2 equiv) and TBAI (1.1 g, 3.6 mmol, 0.17 equiv) dissolved in  $\text{H}_2\text{O}$  (66 mL, 0.32 M). Upon complete dissolution, a solution of bromoenone **115** (6.5 g, 21.3 mmol, 1 equiv) in  $\text{CH}_2\text{Cl}_2$  (107 mL, 0.2 M) was added and the biphasic mixture was stirred vigorously for 16 h. Upon complete consumption of starting material (as determined by TLC) the reaction mixture was allowed to stand until complete separation of the biphasic mixture. The organic layer was drained into an Erlenmeyer flask, and the aqueous layer was extracted with EtOAc (5 x 100 mL). The combined organic layers were washed with brine, dried over  $\text{MgSO}_4$ , filtered, and concentrated under reduced pressure. The crude product was purified by column chromatography ( $\text{SiO}_2$ , 10% EtOAc/Hexanes) to afford cyanoenone **116** (3.8 g, 72% yield) as a pale yellow oil;  $^1\text{H}$  NMR (400 MHz,  $\text{CDCl}_3$ )  $\delta$  = 6.56 (s, 1H), 2.65 (d,  $J$  = 3.7 Hz, 2H), 1.64 (s, 3H), 0.88 (s, 9H), 0.17 (s, 3H), 0.13 (s, 3H);  $^{13}\text{C}$  NMR (100 MHz,  $\text{CDCl}_3$ )  $\delta$  = 203.0, 149.6, 139.6, 113.3, 78.8, 51.1, 28.1, 25.6, 18.1, -2.4, -2.7; IR (thin film, NaCl) 3449, 3087, 2957, 2932, 2888, 2859, 2231, 2736, 1606, 1473, 1378, 1290, 1254, 1217, 1170, 1093, 1006, 838, 778, 673  $\text{cm}^{-1}$ ; HRMS (FAB+)  $m/z$  calc'd  $\text{C}_{13}\text{H}_{22}\text{O}_2\text{NSi}$   $[\text{M}+\text{H}]^+$ : 252.1420, found: 252.1416;  $[\alpha]_{\text{D}}^{23} - 34.6^\circ$  ( $c$  0.34,  $\text{CHCl}_3$ ).



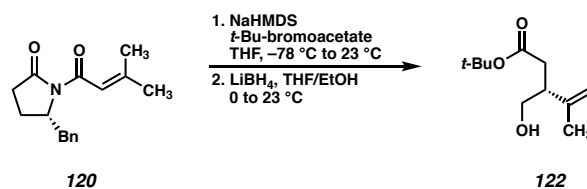
**Nitrile 118:** A round bottom flask was charged with enone **116** (9.4 g, 37.3 mmol, 1 equiv) in dissolved in methanol (373 mL, 0.1 M). The solution was stirred for 5 min followed by the addition of  $\text{CeCl}_3 \cdot 7\text{H}_2\text{O}$  (13.2 g, 41 mmol, 1.1 equiv). Once homogeneous, the solution was cooled to  $-78\text{ }^\circ\text{C}$  and allowed to stir for 1 h.  $\text{NaBH}_4$  (1.4 g, 37.3 mmol, 1 equiv) was added slowly in portions to the reaction and was allowed to stir until complete consumption of starting material (as determined by TLC). Upon complete consumption of starting material, the reaction was quenched with a saturated solution of  $\text{NH}_4\text{Cl}$  (300 mL) and the biphasic mixture was allowed to warm to room temperature. The biphasic mixture was extracted with 2:1  $\text{Et}_2\text{O}$ :hexanes (3 x 300 mL) and the combined organic layers were dried over  $\text{Na}_2\text{SO}_4$ , filtered, and concentrated under reduced pressure. The crude product was used directly into the next reaction without further purification (assuming quantitative yield). This product could be purified by column chromatography ( $\text{SiO}_2$ , 10%  $\text{EtOAc}$ /hexanes) to afford pure alcohol **117** as a white amorphous powder; (4:1 hexanes: $\text{EtOAc}$ );  $^1\text{H}$  NMR (400 MHz,  $\text{CDCl}_3$ )  $\delta$  = 6.40 (d,  $J$  = 2.1 Hz, 1H), 4.60 (dddd,  $J$  = 8.1, 7.1, 5.2, 2.2 Hz, 1H), 2.34 (dd,  $J$  = 13.3, 6.9 Hz, 1H), 1.80 (dd,  $J$  = 13.2, 5.2 Hz, 1H), 1.65 (d,  $J$  = 8.2 Hz, 1H), 1.29 (d,  $J$  = 0.6 Hz, 3H), 0.72 (s, 9H), 0.00 (s, 3H), -0.01 (s, 3H);  $^{13}\text{C}$  NMR (101 MHz,  $\text{CDCl}_3$ )  $\delta$  146.6, 127.2, 114.7, 83.0, 74.2, 50.8, 27.8, 25.7, 18.0, -2.2, -2.4; IR (thin film, NaCl) 3429, 2956, 2930, 2887, 2858, 2229, 1472, 1255, 1176, 1126, 1082, 1031, 868, 838, 777, 668  $\text{cm}^{-1}$ ; HRMS (ESI)  $m/z$  calc'd  $\text{C}_{13}\text{H}_{27}\text{N}_2\text{O}_2\text{Si}$   $[\text{M}+\text{NH}_4]^+$ : 271.1836; found: 271.1842;  $[\alpha]_{\text{D}}^{23}$  - 53.0 ( $c$  0.28,  $\text{CHCl}_3$ ).

Crude alcohol **117** (37.3 mmol, 1 equiv) was dissolved in CH<sub>2</sub>Cl<sub>2</sub> (266 mL, 0.14 M). Once homogeneous, imidazole (7.6 g, 111.9 mmol, 3 equiv) and TESC1 (7.1 mL, 55.9 mL, 1.5 equiv) were added. The reaction was allowed to stir until completion at 23 °C. Upon complete consumption of starting material (as determined by TLC), the reaction was quenched with H<sub>2</sub>O (200 mL) and the biphasic mixture was extracted with Et<sub>2</sub>O (3 x 400 mL). The combined organic layers were washed with brine, dried over MgSO<sub>4</sub>, filtered and concentrated under reduced pressure. The resultant crude product was purified by column chromatography (SiO<sub>2</sub>, 10% EtOAc/Hexanes) to afford nitrile **118** (12.5 g, 91% yield, 11:1 dr) as a pale yellow oil; <sup>1</sup>H NMR (400 MHz, CDCl<sub>3</sub>) δ = 6.41 (d, *J* = 2.0 Hz, 1H), 4.72 (ddd, *J* = 7.0, 6.2, 2.0 Hz, 1H), 2.49 (dd, *J* = 12.8, 7.0 Hz, 1H), 1.98 (ddd, *J* = 12.8, 6.3, 0.8 Hz, 1H), 1.40 (d, *J* = 0.8 Hz, 3H), 0.96 (t, *J* = 7.9 Hz, 9H), 0.89 (s, 9H), 0.61 (q, *J* = 7.8 Hz, 6H), 0.14 (s, 3H), 0.13 (s, 3H); <sup>13</sup>C NMR (100 MHz, CDCl<sub>3</sub>) δ = 147.3, 126.1, 114.9, 82.4, 73.8, 51.5, 28.7, 25.8, 18.1, 6.8, 4.8, -2.2, -2.6; IR (thin film, NaCl) 2957, 2879, 2858, 2224, 1463, 1414, 1360, 1308, 1254, 1198, 1177, 1132, 1099, 1047, 1006, 893, 869, 837, 809, 777 cm<sup>-1</sup>; HRMS (ESI) *m/z* calc'd C<sub>19</sub>H<sub>38</sub>NO<sub>2</sub>Si<sub>2</sub> [M+H]<sup>+</sup>: 268.2436; found: 368.2449; [α]<sub>D</sub><sup>25</sup> – 52.0 ° (*c* 0.40, CHCl<sub>3</sub>).



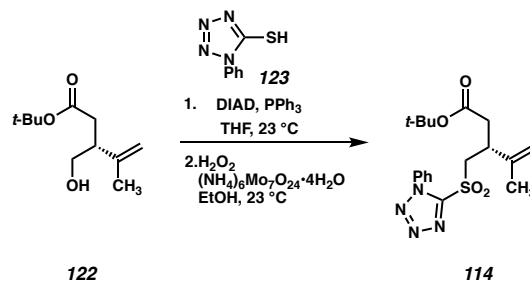
**Aldehyde 113:** A round bottom flask was charged with nitrile **118** (250 mg, 0.68 mmol, 1 equiv) in CH<sub>2</sub>Cl<sub>2</sub> (6.8 mL, 0.1M) and cooled to –78 °C. DIBAL (1.36 mL, 1 M in DCM, 2 equiv) was added dropwise and allowed to stir for 1 h at –78 °C. Upon complete consumption of starting material (as determined by TLC analysis, 19:1 hexanes:Et<sub>2</sub>O) the

reaction was quenched with EtOAc (0.5 mL), diluted with Et<sub>2</sub>O and warmed to room temperature. A 50% solution of Rochelle's salt (10 mL) was added and the biphasic mixture was allowed to stir for 0.5 h. If the biphasic mixture does not separate completely, another portion of Rochelle's salt is add and stirred for another 0.5 h. The biphasic mixture is separated and the aqueous layer is extracted with Et<sub>2</sub>O (3 x 10 mL). The combined organic layers are dried over MgSO<sub>4</sub>, filtered, and concentrated in vacuo. The resultant crude product was the purified by column chromatography (SiO<sub>2</sub>, 5% Et<sub>2</sub>O/Hexanes) to afford aldehyde **113** (252 mg, 91% yield, 17:1 dr) as a pale yellow oil; <sup>1</sup>H NMR (400 MHz, CDCl<sub>3</sub>) δ = 9.77 (s, 1H), 6.53 (d, *J* = 1.8 Hz, 1H), 4.70 (td, *J* = 6.9, 1.9 Hz, 1H), 2.49 (dd, *J* = 12.7, 7.1 Hz, 1H), 2.08 (dd, *J* = 12.6, 6.6 Hz, 1H), 1.45 (s, 3H), 0.97 (t, *J* = 7.9 Hz, 9H), 0.84 (d, *J* = 0.9 Hz, 9H), 0.63 (q, *J* = 7.9 Hz, 6H), 0.11 (s, 3H), 0.07 (s, 3H); <sup>13</sup>C NMR (100 MHz, CDCl<sub>3</sub>) δ = 189.7, 149.8, 147.8, 80.6, 72.9, 53.9, 28.6, 25.8, 18.1, 6.9, 4.9, -2.2, -2.4; IR (thin film, NaCl) 2956, 2936, 2879, 2857, 2805, 2708, 1698, 1627, 1472, 1462, 1414, 1359, 1253, 1203, 1172, 1103, 1058, 975, 897, 837, 806, 775, 746, 671; HRMS (FAB+) *m/z* calc'd C<sub>19</sub>H<sub>37</sub>O<sub>3</sub>Si<sub>2</sub> [M+H-H<sub>2</sub>]<sup>+</sup>: 369.2250, found: 369.2262; [α]<sub>D</sub><sup>25</sup> - 117.2 ° (*c* 0.20, CHCl<sub>3</sub>).



**Alcohol 122:** A 2L round bottom flask was charged with NaHMDS (1.0 M solution in THF, 100.0 mL, 100.0 mmol, 1.05 equiv) in THF (476 mL). The flask was cooled to -78 °C and oxazolidinone **121** (24.7 g, 95.2 mmol, 1.0 equiv) in THF (125 mL) was added dropwise. The mixture was stirred at -78 °C for 1 h, followed by the addition of *t*-Bu-

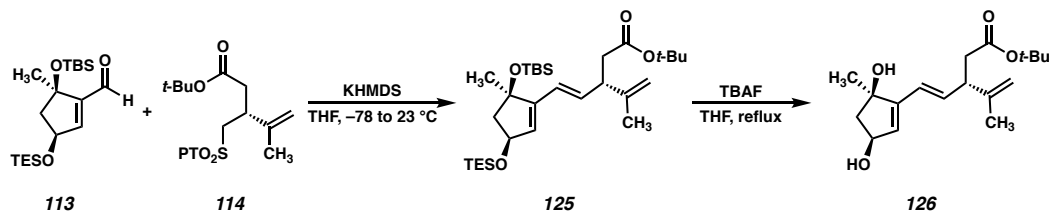
bromoacetate (35.1 mL, 238.0 mmol, 2.5 equiv). The reaction mixture was stirred for 1 h at  $-78\text{ }^{\circ}\text{C}$ , then warmed to  $-40\text{ }^{\circ}\text{C}$  and stirred an additional hour. The reaction was quenched with saturated aqueous  $\text{NaHCO}_3$ , then warmed to  $23\text{ }^{\circ}\text{C}$ . The reaction mixture was partitioned between water and  $\text{Et}_2\text{O}$  and the aqueous phase extracted with  $\text{Et}_2\text{O}$  (3x). The organic extracts were combined, washed with brine, dried over  $\text{MgSO}_4$ , filtered and concentrated to afford crude oxazolidinone **121** (>20:1 dr) as a flakey orange solid. This procedure was repeated, and the crude products were combined and used directly in the subsequent step. A 3 L round bottom flask was charged with the crude oxazolidinone (190.4 mmol assuming quantitative yield) in  $\text{Et}_2\text{O}$  (925 mL). The flask was cooled to  $0\text{ }^{\circ}\text{C}$ , and  $\text{LiBH}_4$  (5.0 g, 228.5 mmol, 1.2 equiv) was added in a single portion.  $\text{MeOH}$  (9.2 mL, 228.5 mmol, 1.2 equiv) was added slowly, and gas evolution was observed. The reaction was stirred 2 h at  $0\text{ }^{\circ}\text{C}$ , after which all starting material had been consumed (as judged by TLC). The reaction was quenched with saturated aqueous  $\text{NaHCO}_3$ , partitioned between water and  $\text{Et}_2\text{O}$  and extracted with  $\text{Et}_2\text{O}$  (3x). The organic extracts were combined, washed with brine, dried over  $\text{MgSO}_4$ , filtered, and concentrated under reduced pressure to afford a yellow oil that was purified by flash chromatography ( $\text{SiO}_2$ , 20%-30%-40%-50%  $\text{EtOAc}$ /hexanes) to afford alcohol **122** (24.6 g, 65% yield over 2 steps) as a colorless oil;  $^1\text{H}$  NMR (400 MHz,  $\text{CDCl}_3$ )  $\delta$  4.91 (dh,  $J = 3.1, 1.6$  Hz, 1H), 4.81 (pq,  $J = 1.8, 1.2$  Hz, 1H), 3.62 – 3.50 (m, 1H), 2.76 – 2.65 (m, 1H), 2.46 – 2.28 (m, 2H), 1.73 (dq,  $J = 2.3, 1.2$  Hz, 3H), 1.42 (d,  $J = 4.0$  Hz, 8H);  $^{13}\text{C}$  NMR (100 MHz,  $\text{CDCl}_3$ )  $\delta$  172.15, 144.4, 113.2 (d,  $J = 4.0$  Hz), 80.7 (d,  $J = 1.5$  Hz), 64.0, 45.9, 36.8, 28.2 (d,  $J = 2.6$  Hz), 20.4; IR (Neat film,  $\text{NaCl}$ ) 3434, 2977, 2932, 1729, 1454, 1367, 1354, 1049, 890, 844  $\text{cm}^{-1}$ ; HRMS (FD+)  $m/z$  calc'd  $\text{C}_{11}\text{H}_{20}\text{O}_3$  [ $\text{M}\cdot$ ] $^+$ : 200.1412, found: 200.1399;  $[\alpha]_{\text{D}}^{25} + 3.6\text{ }^{\circ}$  ( $c$  1.0,  $\text{CHCl}_3$ ).



**Sulfone 114:** To a flame-dried 2 L two-necked round-bottom flask with an addition funnel and large stirring bar was added 5-phenyl-1*H*-tetrazole (PTSH, 30.70 g, 172.0 mmol, 1.6 equiv), PPh<sub>3</sub> (45.10 g, 172.0 mmol, 1.6 equiv), THF (540 mL), and alcohol **122** (21.50 g, 107.3 mmol, 1.0 equiv). The addition funnel was charged with DIAD (33.9 mL, 172 mmol, 1.6 equiv). The resulting clear, colorless solution was immersed in an ice bath with stirring for 15 min, after which time DIAD was added dropwise over a period of 30 min, resulting in a yellow homogeneous solution. The reaction was then stirred an additional 30 min at 0 ° at which time consumption of alcohol **122** was observed by TLC analysis. The reaction was quenched at 0 °C with sat. NaHCO<sub>3</sub> and the crude mixture was transferred to a separatory funnel with EtOAc. The layers were separated, and the aqueous layer was extracted with EtOAc (2x). The combined organics were dried over MgSO<sub>4</sub>, filtered, and concentrated by rotary evaporation to yield a crude yellow oil. The crude product was dry loaded on 300 g of silica gel and purified by flash column chromatography (5 to 30% EtOAc/hexanes) to yield an intermediate sulfide as colorless oil (27.51 g, 76.31 mmol, 71% yield).

To a 2 L round-bottom flask with a large stirring bar was added the intermediate sulfide (27.51 g, 76.31 mmol, 1.0 equiv), and EtOH (200 proof, 380 mL). The resulting clear, colorless solution was immersed in an ice bath for 20 min, after which time (NH<sub>4</sub>)<sub>6</sub>MO<sub>7</sub>O<sub>24</sub>•4H<sub>2</sub>O (37.70 g, 30.52 mmol, 0.40 equiv) was added. The flask was then

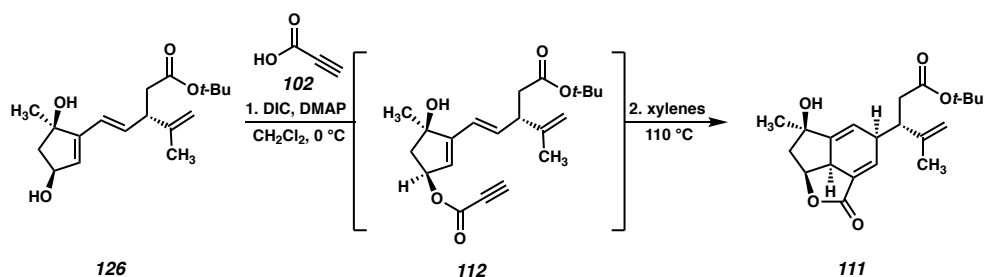
affixed with an addition funnel which was charged with 30% aq. H<sub>2</sub>O<sub>2</sub> (156 mL, 1.53 mmol, 20.0 equiv.). The H<sub>2</sub>O<sub>2</sub> was then slowly added to the reaction solution with vigorous stirring over ca. 1 h, resulting in the formation of a bright yellow suspension. The reaction was slowly allowed to warm to 20 °C over 4 h and maintained at 20 °C in a water bath for an additional 8 h, after which time LC/MS analysis indicated full conversion. *Caution: removal of the cooling bath results in an unpredictable exothermic reaction.* The reaction mixture was then transferred to a separatory funnel with Et<sub>2</sub>O and brine. The layers were separated, and the aqueous layer was extracted with Et<sub>2</sub>O (2x). The combined organic extracts were washed with 1:1 brine/sat. Na<sub>2</sub>S<sub>2</sub>O<sub>3</sub>. The organics were then dried over MgSO<sub>4</sub>, filtered, and concentrated by rotary evaporation to yield a crude yellow oil. The crude product was dry loaded on 300 g of silica gel and purified by flash column chromatography (5 to 25% EtOAc/hexanes) to yield sulfone **114** (24.25 g, 61.79 mmol, 81% yield) as a semi-crystalline white solid; <sup>1</sup>H NMR (500 MHz, CDCl<sub>3</sub>) δ 7.72 – 7.55 (m, 5H), 4.86 (d, *J* = 2.6 Hz, 2H), 3.99 (dd, *J* = 14.6, 7.5 Hz, 1H), 3.89 (dd, *J* = 14.6, 6.1 Hz, 1H), 3.33 (p, *J* = 7.0 Hz, 1H), 2.61 (dd, *J* = 15.6, 6.6 Hz, 1H), 2.49 (dd, *J* = 15.5, 8.0 Hz, 1H), 1.76 (s, 3H), 1.42 (s, 9H); <sup>13</sup>C NMR (100 MHz, CDCl<sub>3</sub>) δ 169.9, 153.8, 142.9, 133.0, 131.5, 129.7, 125.3, 114.5, 81.3, 58.1, 38.8, 37.7, 28.0, 19.3; IR (Neat film, NaCl) 2978, 2931, 2362, 2341, 1725, 1497, 1348, 1152, 900, 763, 688 cm<sup>-1</sup>; HRMS (MM: ESI-APCI+) *m/z* calc'd for C<sub>18</sub>H<sub>25</sub>N<sub>4</sub>O<sub>4</sub>S [M+H]<sup>+</sup> : 393.1597, found 393.1582; [α]<sub>D</sub><sup>25</sup> + 14.4 ° (*c* 1.0, CHCl<sub>3</sub>).



**Diol 126:** A 250 mL round bottom flask was charged with aldehyde **113** (2.4 g, 6.47 mmol, 1.0 equiv) and sulfone **114** (4.6 g, 11.65 mmol, 1.8 equiv) in THF (65 mL). The mixture was cooled to  $-78 \text{ }^\circ\text{C}$ , followed by the addition of KHMDS (0.5 M solution in THF, 23.3 mL, 11.65 mmol, 1.8 equiv) dropwise. The mixture was allowed to stir for 16 h while gradually warming to  $23 \text{ }^\circ\text{C}$ . TLC indicated a small amount of aldehyde **113** remained. The reaction was quenched with saturated aqueous  $\text{NH}_4\text{Cl}$ , partitioned between water and  $\text{Et}_2\text{O}$ , and extracted with  $\text{Et}_2\text{O}$  (3X). The organic extracts were combined, washed with brine, dried over  $\text{MgSO}_4$ , filtered and concentrated to afford a yellow oil which was subjected to flash chromatography ( $\text{SiO}_2$ , 0%-5%  $\text{Et}_2\text{O}$ /Hexanes) to afford the product (2.7 g, c.a. 5.03 mmol) as a c.a. 10:1 mixture with aldehyde **113**. This mixture was dissolved in THF (68 mL) in a 250 mL round bottom flask fitted with a reflux condenser, and TBAF (1.0 M solution in THF, 19.17 mmol, 3.9 equiv) was added. The brown solution was heated to reflux and stirred 5 h, after which no starting material remained, as judged by TLC. The mixture was cooled to  $23 \text{ }^\circ\text{C}$ , partitioned between  $\text{EtOAc}$  and water, and extracted with  $\text{EtOAc}$  (3x). The combined organic extracts were washed with brine, dried over  $\text{Na}_2\text{SO}_4$ , filtered and concentrated under reduced pressure to afford a dark brown oil which was purified by flash chromatography ( $\text{SiO}_2$ , 40%-50%-60%-70%  $\text{EtOAc}$ /hexanes) to afford diol **126** (1.06 g, 3.43 mmol, 53% yield over two steps) as an orange/white solid.  $^1\text{H}$  NMR (400 MHz,  $\text{CDCl}_3$ )  $\delta$  6.13 (dd,  $J = 16.1, 7.9 \text{ Hz}$ , 1H), 6.04 – 5.95 (m, 2H), 5.71 (d,  $J = 2.4 \text{ Hz}$ , 1H), 4.82 – 4.79 (m, 1H), 4.77 (dd,  $J = 1.7, 0.8 \text{ Hz}$ , 1H), 4.60 (td,  $J = 4.6, 2.3 \text{ Hz}$ , 1H),

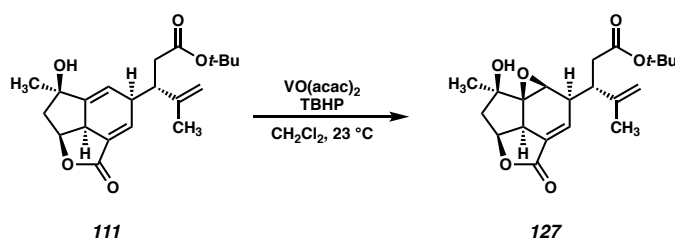


3.19 (q,  $J = 8.1$  Hz, 1H), 2.60 – 2.44 (m, 2H), 2.38 (dd,  $J = 14.5, 8.3$  Hz, 1H), 1.90 – 1.80 (m, 1H), 1.71 (d,  $J = 0.6$  Hz, 2H), 1.43 (s, 4H), 1.41 (s, 10H), 0.89 (d,  $J = 6.6$  Hz, 1H);  $^{13}\text{C}$  NMR (100 MHz,  $\text{CDCl}_3$ )  $\delta$  171.8, 148.9, 135.4, 130.2, 123.2, 111.3, 81.1, 80.7, 72.9, 52.6, 47.4, 39.6, 28.2, 26.9, 20.9; IR (Neat film, NaCl) 3288, 2975, 2932, 2357, 2106, 1758, 1727, 1636, 1539, 1506, 1457, 1368, 1290, 1167, 1147, 1026, 963, 847, 751  $\text{cm}^{-1}$ ;  $m/z$  calc'd for  $\text{C}_{18}\text{H}_{28}\text{O}_4\text{Na}$   $[\text{M}+\text{Na}]^+$  : 331.1855, found 331.1877;  $[\alpha]_{\text{D}}^{25} - 46.1^\circ$  ( $c$  1.0,  $\text{CHCl}_3$ ).



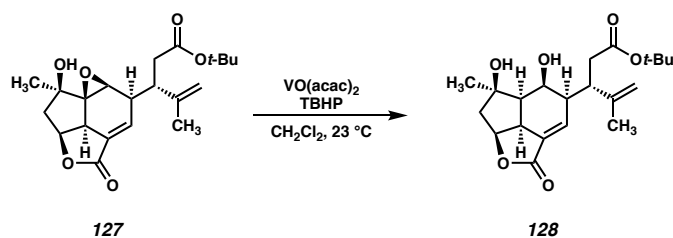
**Cyclohexadiene 112:** A 25 mL round bottom flask was charged with diol **126** (400 mg, 1.30 mmol, 1.0 equiv), DMAP (8.0 mg, 0.065 mmol, 0.05 equiv) and propiolic acid (119  $\mu\text{L}$ , 1.95 mmol, 1.5 equiv) in  $\text{CH}_2\text{Cl}_2$  (13 mL). The solution was cooled to  $0^\circ\text{C}$ , and DIC (305  $\mu\text{L}$ , 1.95 mmol, 1.5 equiv) was added dropwise. The reaction mixture was stirred at  $0^\circ\text{C}$  for 2 h, then the reaction mixture was filtered directly over a pad of  $\text{SiO}_2$ , rinsing with 50% EtOAc/hexanes. The eluent was collected in test tubes, and the fractions containing product were combined in a flame-dried 250 mL round bottom flask containing xylenes (130 mL). The lower-boiling solvents (EtOAc, hexanes,  $\text{CH}_2\text{Cl}_2$ ) were removed by rotary evaporation, leaving a solution of intermediate ester **112** in xylenes. This solution was sparged with  $\text{N}_2$  for 10 min, then heated to  $110^\circ\text{C}$  and stirred for 3 h. The reaction mixture was cooled to  $23^\circ\text{C}$ , and the xylenes removed by rotary evaporation leaving a yellow residue which was purified by flash chromatography ( $\text{SiO}_2$ , 20%–30% EtOAc/hexanes) to

afford tricycle **111** (165 mg, 0.458 mmol, 35% yield) as a white solid. Crystals suitable for X-ray diffraction were obtained by slow evaporation of a solution in CH<sub>2</sub>Cl<sub>2</sub>/hexanes (5:1); <sup>1</sup>H NMR (400 MHz, CDCl<sub>3</sub>) δ 7.06 (dd, *J* = 3.5, 1.6 Hz, 1H), 5.79 – 5.74 (m, 1H), 5.03 (dt, *J* = 9.0, 7.5 Hz, 1H), 4.97 (t, *J* = 1.5 Hz, 1H), 4.89 – 4.86 (m, 1H), 3.39 – 3.29 (m, 1H), 2.86 (dt, *J* = 8.4, 2.8 Hz, 2H), 2.57 – 2.37 (m, 3H), 1.75 – 1.69 (m, 3H), 1.42 (s, 11H); <sup>13</sup>C NMR (101 MHz, CDCl<sub>3</sub>) δ 171.4, 168.2, 152.3, 144.0, 143.1, 133.6, 120.3, 114.9, 80.9, 80.3, 76.0, 49.8, 45.8, 45.6, 37.8, 28.2, 26.7, 19.8.; IR (Neat film, NaCl); 3422, 2976, 1749, 1716, 1636, 1540, 1456, 1368, 1288, 1168, 1149, 758; *m/z* calc'd for C<sub>21</sub>H<sub>28</sub>O<sub>5</sub>Na [M+Na]<sup>+</sup>: 383.1834, found 383.1844; [α]<sub>D</sub><sup>25</sup> – 50.9 ° (*c* 1.0, CHCl<sub>3</sub>).



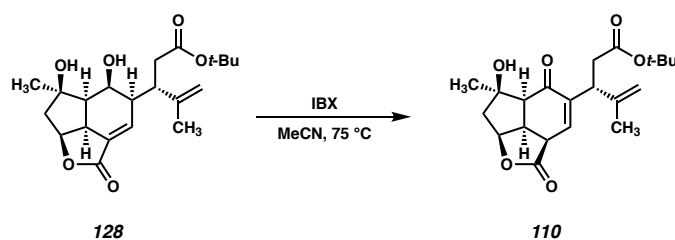
**Epoxide 127:** A 500 mL round-bottomed flask was charged with VO(acac)<sub>2</sub> (71.6 mg, 0.270 mmol, 0.10 equiv), tricycle **111** (981.1 mg, 2.72 mmol, 1.0 equiv), and CH<sub>2</sub>Cl<sub>2</sub> (136 mL). To the resulting green, homogenous reaction mixture was added *t*-BuOOH (990 μL, 5.5 M solution in decane, 5.44 mmol, 2.0 equiv) dropwise over 2 min, causing the reaction solution to turn dark red. The reaction was stirred at 20 °C for 3 h, after which time it turns from dark red to orange. The reaction solution was concentrated to approximately 10 mL and the resulting solution was purified directly by flash column chromatography (0-100% EtOAc/Hexanes) to provide epoxide **127** (720.2 mg, 1.91 mmol, 70% yield) as a white, semicrystalline solid. <sup>1</sup>H NMR (500 MHz, CDCl<sub>3</sub>) δ 6.46 (dd, *J* = 3.7, 2.3 Hz, 1H), 5.02 – 4.99 (m, 1H), 4.93 – 4.86 (m, 2H), 3.75 (s, 1H), 3.34 (dd, *J* = 8.3, 3.0 Hz, 1H), 2.97 (q, *J* =

7.0 Hz, 1H), 2.72 (dt,  $J = 6.2, 3.0$  Hz, 1H), 2.58 (dd,  $J = 13.6, 7.5$  Hz, 1H), 2.56 – 2.51 (m, 3H), 1.99 (dd,  $J = 13.7, 6.1$  Hz, 1H), 1.79 (s, 3H), 1.45 (s, 3H), 1.43 (s, 9H);  $^{13}\text{C}$  NMR (100 MHz,  $\text{CDCl}_3$ )  $\delta$  171.1, 169.0, 143.9, 137.1, 127.1, 114.3, 81.0, 77.0, 74.3, 69.0, 53.3, 49.9, 44.6, 44.4, 43.9, 37.0, 28.1, 22.6, 21.2; IR (Neat film, NaCl) 3478, 3076, 3057, 2977, 2035, 1760, 1727, 1648, 1448, 1431, 1392, 1368, 1355, 1312, 1291, 1262, 1196, 1158, 1150, 1100, 1051, 1020, 974, 953, 918, 900, 844, 817, 779, 737, 703, 676  $\text{cm}^{-1}$ ; HRMS (MM:ESI-APCI+)  $m/z$  calc'd for  $\text{C}_{21}\text{H}_{29}\text{O}_6$   $[\text{M}+\text{H}]^+$ : 377.1964, found 377.1952;  $[\alpha]_{\text{D}}^{25} - 96.1^\circ$  ( $c$  0.40,  $\text{CHCl}_3$ ).



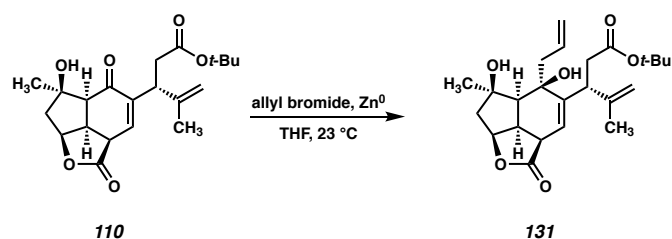
**Alcohol 128:** A 250 mL round-bottomed flask was charged with  $\text{Cp}_2\text{TiCl}_2$  (101.1 mg, 0.406 mmol, 0.20 equiv),  $\text{Mn}^0$  (245.6 mg, 4.47 mmol, 2.20 equiv), collidine $\cdot\text{HCl}$  (800.8 mg, 5.08 mmol, 2.5 equiv). The flask was then evacuated and back-filled with  $\text{N}_2$  gas. To the flask was then added epoxide **127** (765.7 mg, 2.03 mmol, 1.0 equiv) in THF (41 mL). The resulting heterogenous yellow/orange mixture was stirred rapidly and 1,4-cyclohexadiene (865  $\mu\text{L}$ , 9.14 mmol, 4.5 equiv) was added dropwise over 2 min. The reaction was stirred for 2 h at 20  $^\circ\text{C}$ , after which time it turned from yellow/orange to blue.  $\text{SiO}_2$  (20 g) was added to the reaction mixture, the solvent was removed by rotary evaporation, and the solid loaded onto a column and purified by flash chromatography (0–100% EtOAc/Hexanes) to provide diol **128** (454.8 mg, 1.20 mmol, 59% yield) as a white, semicrystalline solid.  $^1\text{H}$  NMR (500 MHz,  $\text{CDCl}_3$ )  $\delta$  6.67 (t,  $J = 3.9$  Hz, 1H), 4.95 (dt,  $J =$

7.8, 5.5 Hz, 1H), 4.90 (s, 2H), 4.43 – 4.37 (m, 1H), 4.33 – 4.29 (m, 1H), 4.24 (s, 1H), 3.20 – 3.10 (m, 1H), 2.91 (ddd,  $J = 12.1, 7.8, 4.5$  Hz, 1H), 2.52 (dd,  $J = 16.8, 7.8$  Hz, 1H), 2.48 – 2.40 (m, 2H), 2.09 (dd,  $J = 13.7, 4.7$  Hz, 1H), 1.98 (dd,  $J = 13.7, 6.6$  Hz, 1H), 1.94 – 1.88 (m, 1H), 1.64 (s, 3H), 1.46 (s, 9H), 1.38 (s, 3H);  $^{13}\text{C}$  NMR (100 MHz,  $\text{CDCl}_3$ )  $\delta$  174.2, 170.0, 144.9, 138.3, 132.6, 114.8, 82.2, 81.3, 80.0, 69.3, 51.1, 47.9, 47.6, 43.5, 41.9, 38.7, 28.6, 28.1, 19.1; IR (Neat film, NaCl) 3380, 2924, 2852, 1742, 1168  $\text{cm}^{-1}$ ; HRMS (MM:ESI-APCI+)  $m/z$  calc'd for  $\text{C}_{21}\text{H}_{31}\text{O}_6$   $[\text{M}+\text{H}]^+$ : 379.2121, found 379.2110.  $[\alpha]_{\text{D}}^{25} - 2.57^\circ$  ( $c$  0.67,  $\text{CHCl}_3$ ).



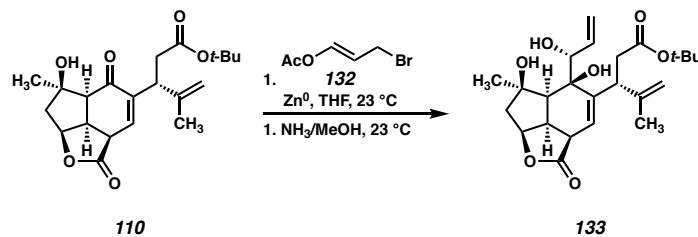
**Enone 110:** A 20 mL scintillation vial was charged with diol **128** (71.0 mg, 0.188 mmol, 1.0 equiv) in MeCN (7.5 mL). IBX (263 mg, 0.938 mmol, 5.0 equiv) was added, and the vial was sealed and placed in a preheated 75 °C aluminum block. The suspension was stirred for 2 h at 75 °C, after which no starting material remained (as judged by TLC). The reaction mixture was cooled to 23 °C, then filtered over a pad of  $\text{SiO}_2$ , rinsing with EtOAc. The filtrate was concentrated by rotary evaporation leaving a crude oil which was purified by flash chromatography ( $\text{SiO}_2$ , 30%-40%-50% EtOAc/hexanes) to afford enone **110** (46.0 mg, 0.122 mmol, 65% yield) as a white foam;  $^1\text{H}$  NMR (500 MHz,  $\text{CDCl}_3$ )  $\delta$  6.75 (d,  $J = 3.9$  Hz, 1H), 5.11 (t,  $J = 6.0$  Hz, 1H), 4.84 (d,  $J = 11.2$  Hz, 2H), 3.67 – 3.41 (m, 3H), 2.86 (dd,  $J = 14.7, 10.0$  Hz, 1H), 2.61 – 2.44 (m, 2H), 2.31 (d,  $J = 14.9$  Hz, 1H), 1.83 (dd,  $J = 14.8, 5.7$  Hz, 1H), 1.69 (s, 3H), 1.42 (s, 3H), 1.40 (d,  $J = 1.2$  Hz, 10H);  $^{13}\text{C}$  NMR (100

MHz, CDCl<sub>3</sub>) δ 174.4, 172.6, 145.4, 140.0, 139.5, 112.0, 82.8, 81.2, 57.3, 47.1, 44.2, 40.8, 40.2, 37.9, 28.2, 25.6, 21.6; IR (Neat film, NaCl) 3484, 2921, 1742, 1667, 1371, 1229, 1027, 681 cm<sup>-1</sup>; HRMS (MM:ESI-APCI+) *m/z* calc'd for C<sub>21</sub>H<sub>28</sub>O<sub>6</sub>Na [M+Na]<sup>+</sup>: 399.1778, found 399.1788; [α]<sub>D</sub><sup>25</sup> -22.0 ° (*c* 0.53, CHCl<sub>3</sub>).



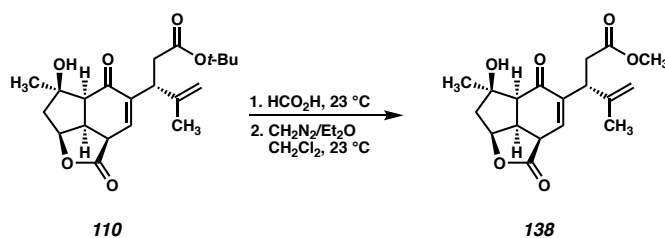
**Diol 131:** A 1-dram vial was charged with Zn dust (6 mg, 0.0956 mmol, 4.0 equiv) and allyl bromide (8 μL, 0.0956 mmol, 4.0 equiv) in THF (300 μL). The suspension was stirred at 23 °C and a solution of enone **110** (9.0 mg, 0.0239 mmol, 1.0 equiv) in THF (180 μL) was added. The mixture was stirred for 2 h at 23 °C, after which no conversion was observed. TMSCl (1 drop) was added, and the starting material was consumed instantaneously as judged by TLC. The reaction mixture was passed through a plug of SiO<sub>2</sub> and concentrated to afford a crude oil which was purified by flash chromatography (30%-40% EtOAc/hexanes) to afford alcohol **131** (6.2 mg, 0.0148 mmol, 62% yield) as an amorphous solid; <sup>1</sup>H NMR (400 MHz, C<sub>6</sub>D<sub>6</sub>) δ 5.92 (d, *J* = 3.9 Hz, 1H), 5.84 (ddt, *J* = 17.4, 10.2, 7.3 Hz, 1H), 5.12 – 5.07 (m, 1H), 5.08 – 4.96 (m, 2H), 4.77 (p, *J* = 1.5 Hz, 1H), 4.28 – 4.21 (m, 1H), 3.80 (dd, *J* = 9.2, 6.9 Hz, 1H), 2.69 (ddd, *J* = 11.8, 3.9, 1.4 Hz, 1H), 2.64 – 2.48 (m, 3H), 2.43 (dd, *J* = 15.3, 7.0 Hz, 1H), 2.14 (dd, *J* = 14.1, 7.6 Hz, 1H), 1.74 – 1.62 (m, 5H), 1.38 (s, 9H), 1.16 – 1.02 (m, 4H); <sup>13</sup>C NMR (100 MHz, C<sub>6</sub>D<sub>6</sub>) δ 175.5, 171.4, 148.7, 142.7, 134.6, 120.0, 118.2, 113.6, 81.6, 80.9, 79.9, 75.4, 51.7, 48.8, 47.0, 43.6, 40.1, 39.9, 39.6, 29.5, 28.2, 20.6. IR (Neat film, NaCl) 3415, 2927, 1729, 1369, 1168, 1148, 762

$\text{cm}^{-1}$ ; HRMS (MM:ESI-APCI+)  $m/z$  calc'd for  $\text{C}_{24}\text{H}_{38}\text{O}_6\text{N}$   $[\text{M}+\text{NH}_4]^+$ : 436.2694, found 436.2700;  $[\alpha]_{\text{D}}^{25} -12.2^\circ$  ( $c$  0.33,  $\text{CHCl}_3$ ).



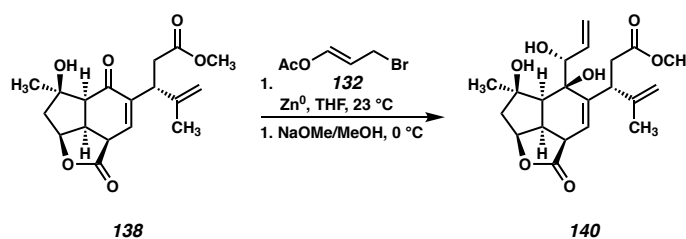
**Triol 133:** A 1-dram vial was charged with activated Zn dust (36 mg, 0.548 mmol, 6.25 equiv) in THF (890  $\mu\text{L}$ ). The suspension was stirred at 23  $^\circ\text{C}$  while a solution of allyl bromide **132** (98.0 mg, 0.548 mmol, 6.25 equiv) in THF (250  $\mu\text{L}$ ) was added. This suspension was stirred for 10 min at 23  $^\circ\text{C}$ , followed by the addition of a solution of enone **110** (33.0 mg, 0.0877 mmol, 1.0 equiv) in THF (1.60 mL). The reaction mixture quickly changed from colorless to yellow/green. This solution was stirred for 30 min at 23  $^\circ\text{C}$ , after which no starting material remained (as judged by TLC). The reaction was quenched with saturated aqueous  $\text{NaHCO}_3$ , and extracted with  $\text{EtOAc}$  (3x). The combined organic extracts were washed with brine, dried over  $\text{Na}_2\text{SO}_4$ , filtered and concentrated to afford a crude oil which was purified by flash chromatography (0%-30%-40%-50%  $\text{EtOAc}$ /hexanes) to afford a mixture of branched and linear allylation products which was used directly in the next reaction. The mixture of allylation products was dissolved in methanolic ammonia (2.0 mL) and stirred 30 min at 23  $^\circ\text{C}$  after which no starting material remained (as judged by TLC). The reaction mixture was concentrated and loaded directly onto a column and purified by flash chromatography (0%-5%-10%  $\text{EtOAc}/\text{CH}_2\text{Cl}_2$ ) to afford triol **133** (10.4 mg, 0.0239 mmol, 27% yield) as an amorphous white solid. X-ray quality crystals were obtained by slow diffusion of hexanes into a  $\text{CH}_2\text{Cl}_2$  solution;  $^1\text{H}$  NMR (400 MHz,  $\text{CDCl}_3$ )

$\delta$  5.98 – 5.76 (m, 2H), 5.50 – 5.34 (m, 1H), 5.26 (dt,  $J$  = 10.6, 1.5 Hz, 1H), 5.01 – 4.93 (m, 2H), 4.90 (q,  $J$  = 1.5 Hz, 1H), 4.50 (d,  $J$  = 3.5 Hz, 1H), 4.16 (ddd,  $J$  = 6.3, 3.6, 1.6 Hz, 1H), 3.56 (dd,  $J$  = 11.6, 4.9 Hz, 1H), 3.33 – 3.19 (m, 2H), 2.73 (dd,  $J$  = 17.2, 11.7 Hz, 1H), 2.53 (dd,  $J$  = 17.2, 5.0 Hz, 1H), 2.19 – 2.01 (m, 3H), 1.88 – 1.75 (m, 4H), 1.74 (d,  $J$  = 1.9 Hz, 1H), 1.43 (s, 12H);  $^{13}\text{C}$  NMR (100 MHz,  $\text{CDCl}_3$ )  $\delta$  176.7, 173.4, 148.3, 142.2, 135.6, 120.7, 117.4, 113.5, 82.2, 81.9, 81.8, 79.2, 48.8, 48.1, 42.9, 39.9, 39.6, 39.6, 29.1, 28.2, 21.5; IR; HRMS (MM:ESI-APCI+)  $m/z$  calc'd for  $\text{C}_{21}\text{H}_{32}\text{O}_7\text{N}$   $[\text{M}+\text{NH}_4]^+$ : 452.2643, found 452.2632;  $[\alpha]_{\text{D}}^{25}$   $-35.2^\circ$  ( $c$  0.20,  $\text{CHCl}_3$ ).



**Methyl Ester 138:** A solution of enone **110** (63.0 mg, 0.167 mmol, 1.0 equiv) in  $\text{HCO}_2\text{H}$  (3.3 mL) was stirred for 4 h in a 20 mL scintillation vial, after which no starting material remained (as judged by LCMS). The solvent was removed by rotary evaporation, and then the resulting crude oil was dissolved in  $\text{CH}_2\text{Cl}_2$  (3.3 mL). This solution was stirred at  $23^\circ\text{C}$  while diazomethane (c.a. 0.5 M solution in  $\text{Et}_2\text{O}$ ) was added until the yellow color of the reagent persisted (c.a. 2 mL). At this point, excess diazomethane was quenched by the addition of  $\text{AcOH}$  (100  $\mu\text{L}$ ). The solvent was removed by rotary evaporation, leaving a crude oil which was purified by flash chromatography ( $\text{SiO}_2$ , 50%-60%-70%  $\text{EtOAc}$ /Hexanes) to afford methyl ester **138** (39.0 mg, 0.117, 70% yield over 2 steps) as a white foam;  $^1\text{H}$  NMR (400 MHz,  $\text{CDCl}_3$ )  $\delta$  6.74 (d,  $J$  = 4.3 Hz, 1H), 5.15 – 5.07 (m, 1H), 4.89 – 4.83 (m, 1H), 4.82 (s, 1H), 3.73 – 3.66 (m, 1H), 3.66 – 3.53 (m, 6H), 2.85 (dd,  $J$  =

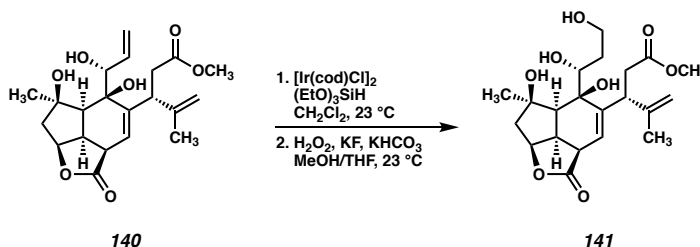
15.0, 9.4 Hz, 1H), 2.65 – 2.52 (m, 2H), 2.29 (d,  $J = 14.9$  Hz, 1H), 2.04 (s, 1H), 1.90 – 1.78 (m, 1H), 1.67 (s, 4H), 1.41 (s, 3H);  $^{13}\text{C}$  NMR (100 MHz,  $\text{CDCl}_3$ )  $\delta$  195.5, 174.5, 173.4, 145.3, 140.1, 139.4, 112.1, 82.8, 82.8, 57.0, 52.0, 47.2, 43.3, 40.8, 40.2, 36.8, 25.7, 21.7; IR (Neat film, NaCl) 3486, 2964, 1732, 1661, 1435, 1376, 1256, 1168, 1120, 1107, 652  $\text{cm}^{-1}$ , HRMS (MM:ESI-APCI+)  $m/z$  calc'd for  $\text{C}_{18}\text{H}_{32}\text{O}_6$   $[\text{M}+\text{H}]^+$ : 335.1489, found 335.1495;  $[\alpha]_{\text{D}}^{25} -119.5^\circ$  ( $c$  0.40,  $\text{CHCl}_3$ ).



**Triol 140:** A 1-dram vial was charged with Zn dust (37.0 mg, 0.561 mmol, 6.25 equiv) in THF (840  $\mu\text{L}$ ). The suspension was stirred vigorously at 23  $^\circ\text{C}$  while a solution of allyl bromide **132** (100 mg, 0.561 mmol, 6.25 equiv) was added. The reaction mixture was stirred for 5 min at 23  $^\circ\text{C}$  after which the initially heterogenous suspension had changed to a near-homogeneous solution. At this point, a solution of enone **138** (30 mg, 0.0897 mmol, 1.0 equiv) in THF (1.70 mL) was added dropwise at 23  $^\circ\text{C}$ . The mixture was stirred for 30 min at 23  $^\circ\text{C}$  at which point the starting material had been completely consumed (as judged by TLC). The reaction mixture was quenched with saturated aqueous  $\text{NaHCO}_3$  and extracted with EtOAc (3x). The organic extracts were combined, washed with brine, dried over  $\text{Na}_2\text{SO}_4$ , filtered and concentrated to afford a crude oil which was purified by preparative TLC ( $\text{SiO}_2$ , 80% EtOAc/hexanes) to afford a mixture of branched and linear allylation products which was used directly in the next reaction. The mixture of allylation products was dissolved in dry MeOH (8.9 mL) in a 20 mL scintillation vial and cooled to 0  $^\circ\text{C}$ . A solution of NaOMe/MeOH (c.a. 2.5 M, 57  $\mu\text{L}$ , 0.144 mmol, 1.6 equiv based on

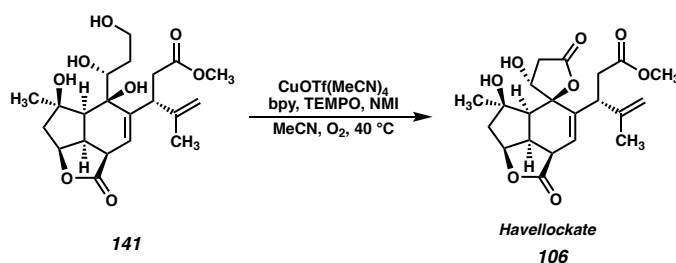


starting enone) was added dropwise. The solution was stirred at 0 °C with careful monitoring by TLC. Once the starting material had been consumed (c.a. 1 h), the reaction was quenched with saturated aqueous NH<sub>4</sub>Cl. The mixture was extracted with EtOAc (3x), and the organic extracts were combined, washed with brine, filtered and concentrated to afford a crude oil which was purified by preparative TLC (SiO<sub>2</sub>, 100% EtOAc) to afford triol **140** (8.4 mg, 0.0214 mmol, 24% yield over 2 steps) as an amorphous white solid; *The <sup>1</sup>H NMR spectrum shows a minor impurity which was not characterized. Shifts are reported for the major product only:* <sup>1</sup>H NMR (400 MHz, C<sub>6</sub>D<sub>6</sub>) δ 6.03 (d, *J* = 3.4 Hz, 1H), 5.76 (ddd, *J* = 17.2, 10.6, 4.6 Hz, 1H), 5.47 (dt, *J* = 17.2, 2.1 Hz, 1H), 5.11 (dt, *J* = 10.8, 2.0 Hz, 1H), 5.06 (d, *J* = 1.2 Hz, 1H), 4.79 – 4.76 (m, 1H), 4.29 (dd, *J* = 4.5, 2.3 Hz, 1H), 4.24 – 4.16 (m, 1H), 3.65 (dd, *J* = 11.2, 5.2 Hz, 1H), 3.27 (s, 3H), 3.10 (s, 1H), 2.67 – 2.53 (m, 3H), 2.34 – 2.25 (m, 1H), 1.94 (d, *J* = 9.8 Hz, 1H), 1.76 (d, *J* = 15.2 Hz, 1H), 1.69 – 1.63 (m, 3H), 1.16 (s, 3H), 1.02 (dd, *J* = 15.3, 6.3 Hz, 1H); <sup>13</sup>C NMR (100 MHz, C<sub>6</sub>D<sub>6</sub>) δ 175.33, 173.16, 148.10, 140.40, 136.31, 122.44, 115.86, 113.34, 81.90, 81.53, 77.50, 76.75, 51.37, 48.12, 47.31, 43.18, 40.29, 39.64, 38.33, 30.48, 29.30, 20.99; IR (Neat film, NaCl) 3455, 2920, 2852, 2359, 1732, 1458, 1370, 1258, 1117, 1013, 805 cm<sup>-1</sup>; HRMS (MM:ESI-APCI+) *m/z* calc'd for C<sub>21</sub>H<sub>32</sub>O<sub>7</sub>N [M+NH<sub>4</sub>]<sup>+</sup>: 410.2173, found 410.2191; [α]<sub>D</sub><sup>25</sup> –130.3 ° (c 0.083, CHCl<sub>3</sub>).



**Tetrol 141:** In a nitrogen-filled glovebox, a 1-dram vial was charged with triol **140** (4.2 mg, 0.0107 mmol, 1.0 equiv) and  $[\text{Ir}(\text{cod})\text{Cl}]_2$  (2.8 mg, 0.00428 mmol, 0.4 equiv) in  $\text{CH}_2\text{Cl}_2$  (1.10 mL). Triethoxysilane (8  $\mu\text{L}$ , 0.0535 mmol, 5.0 equiv) was added, and the orange solution was allowed to stir 1 h at 23  $^\circ\text{C}$ , after which time it had changed to bright yellow in color. LCMS and TLC analysis indicated that no starting material remained. The vial was removed from the glovebox and concentrated under vacuum. The remaining orange residue was reconstituted in THF/MeOH (1:1, 2.7 mL). To this solution was added  $\text{KHCO}_3$  (21.0 mg, 0.214 mmol, 20.0 equiv) followed by KF (12.0 mg, 0.214 mmol, 20.0 equiv). To this dark orange suspension was added  $\text{H}_2\text{O}_2$  (30% aqueous, 60  $\mu\text{L}$ , 0.0535 mmol, 50.0 equiv) after which the reaction mixture became deep blue in color. The reaction was stirred 2 h at 23  $^\circ\text{C}$ , then quenched with saturated aqueous  $\text{Na}_2\text{S}_2\text{O}_3$ , and the MeOH and THF were removed by rotary evaporation. The remaining residue was partitioned between EtOAc and water and extracted with EtOAc (5x). The combined organic extracts were combined, washed with brine, and dried over  $\text{Na}_2\text{SO}_4$ , filtered and concentrated, leaving a crude solid that was purified by flash chromatography (0%-100% acetone/EtOAc) to afford tetrol **141** (2.0 mg, 0.00487 mmol, 46% yield over 2 steps) as a white solid. *Tetrol 141* was found to be insoluble in most conventional NMR solvents, but sparingly soluble in  $d_6$ -acetone. Difficulty was encountered when attempting to prepare an NMR sample of sufficient concentration for a  $^{13}\text{C}$  NMR spectrum, and thus, many signals are missing. Additionally,

the  $^1\text{H}$  NMR spectrum shows a mixture of two compounds, making shift assignment challenging. The spectra are reported as observed:  $^1\text{H}$  NMR (400 MHz, Acetone)  $\delta$  5.73 (d,  $J = 3.8$  Hz, 1H), 4.86 (dd,  $J = 7.5, 5.8$  Hz, 1H), 4.76 – 4.73 (m, 1H), 4.63 – 4.59 (m, 1H), 3.64 – 3.48 (m, 2H), 3.47 (d,  $J = 1.0$  Hz, 3H), 3.34 – 3.21 (m, 1H), 3.21 – 3.14 (m, 2H), 2.37 (d,  $J = 10.1$  Hz, 1H), 2.12 – 2.05 (m, 1H), 1.84 – 1.80 (m, 1H), 1.79 – 1.74 (m, 1H), 1.62 (s, 3H), 1.32 (d,  $J = 0.7$  Hz, 4H);  $^{13}\text{C}$  NMR (100 MHz, Acetone)  $\delta$  173.4, 123.4, 113.4, 111.5, 83.3, 61.8, 60.9, 51.9, 43.0, 41.5, 40.3, 39.6, 22.2. IR (Neat film, NaCl) 3448, 2921, 2852, 1730, 1361, 1168, 681  $\text{cm}^{-1}$ ; HRMS (MM:ESI-APCI+)  $m/z$  calc'd for  $\text{C}_{21}\text{H}_{30}\text{O}_8\text{Na}$   $[\text{M}+\text{Na}]^+$ : 433.1833, found 433.1840;  $[\alpha]_{\text{D}}^{25}$  165.5  $^\circ$  ( $c$  0.53, EtOH).



**Havellockate (106):** A stock solution was prepared which included  $\text{CuOTf}(\text{MeCN})_4$  (19.0 mg, 0.050 mmol), bipyridine (9.0 mg, 0.050 mmol), TEMPO (9.0 mg, 0.05 mmol), and *N*-methylimidazole (8.0  $\mu\text{L}$ , 0.10 mmol) in MeCN (5.0 mL, 0.01 M with respect to Cu). 487  $\mu\text{L}$  (0.00487 mmol, 1.00 equiv) of this solution was added to a 1-dram vial containing tetrol **141** (2.0 mg, 0.00487 mmol, 1.0 equiv). The solution was sparged with  $\text{O}_2$  (balloon) for 5 min during which time the solution changed from dark red to green. The vial was affixed with an  $\text{O}_2$  balloon and placed in a preheated 40  $^\circ\text{C}$  aluminum block. The solution was stirred rapidly at 40  $^\circ\text{C}$  for 5 h, after which no starting material remained (as judged by LCMS). The vial was cooled to 23  $^\circ\text{C}$ , and the contents purified directly by preparative HPLC to afford havellockate (**161**) (0.9 mg, 0.00221 mmol, 45% yield) as a white solid.

The natural product was obtained as a 9:1 mixture of epimers at C(5) as judged by  $^1\text{H}$  NMR and X-ray diffraction. Presumably this mixture is formed during the allylation of **138** to form **140**. Crystals suitable for X-ray diffraction were obtained by layer diffusion of hexanes into  $\text{CH}_2\text{Cl}_2$ ;  $^1\text{H}$  NMR (400 MHz,  $d_5$ -Pyr)  $\delta$  6.39 (d,  $J = 3.5$  Hz, 1H), 5.31 (s, 1H), 4.88 – 4.87 (m, 1H), 4.84 (s, 1H), 4.72 (t,  $J = 4.8$  Hz, 1H), 4.18 (dd,  $J = 10.2, 5.4$  Hz, 1H), 3.53 (s, 3H), 3.53 – 3.49 (m, 1H), 3.47 (dd,  $J = 3.6, 1.2$  Hz, 1H), 3.41 (dd,  $J = 18.0, 6.1$  Hz, 1H), 3.20 (dd,  $J = 14.9, 5.4$  Hz, 1H), 3.04 (dd,  $J = 14.9, 10.6$  Hz, 1H), 2.93 (dd,  $J = 18.1, 1.3$  Hz, 1H), 2.24 (d,  $J = 14.9$  Hz, 1H), 2.11 (d,  $J = 8.9$  Hz, 1H), 2.05 (s, 3H), 1.77 (dd,  $J = 14.9, 6.2$  Hz, 1H), 1.56 (s, 3H);  $^{13}\text{C}$  NMR (100 MHz,  $d_5$ -Pyr)  $\delta$  176.6, 176.1, 173.2, 147.9, 138.4, 113.0, 91.8, 81.6, 80.1, 76.0, 51.5, 51.4, 49.1, 44.8, 40.5, 40.4, 39.1, 38.2, 28.1, 20.7; IR (Neat film, NaCl) 3347, 2919, 2849, 1762, 1632, 1551, 1460, 1374, 1171, 1102, 1032, 809, 687, 615  $\text{cm}^{-1}$ ; HRMS (MM:ESI-APCI+)  $m/z$  calc'd for  $\text{C}_{21}\text{H}_{26}\text{O}_8\text{Na}$   $[\text{M}+\text{Na}]^+$ : 429.1520, found 429.1528;  $[\alpha]_{\text{D}}^{25} -34.0^\circ$  ( $c$  0.075, pyridine).<sup>32</sup>

## 2.10.3 COMPARISON OF SYNTHETIC HAVELLOCKATE TO PUBLISHED DATA

**Table 2.10.1** Comparison of  $^1\text{H}$  NMR shifts of synthetic and natural havellockate (106).

Synthetic Havellockate	Natural Havellockate (Anjaneyulu, 1997)
$^1\text{H}$ NMR, 600 MHz, $d_5$ -pyridine (referenced to 7.18 ppm)	$^1\text{H}$ NMR, 400 MHz, $d_5$ -pyridine
7.34 (1H, d, $J = 4.5$ )	7.48 (1H, br, -OH)
6.35 (1H, d, $J = 3.7$ )	6.34 (1H, d, $J = 3.0$ )
5.27 (1H, s)	5.27 (1H, brs)
4.98 (1H, dd, $J = 7.6, 6.0$ )	5.02 (1H, m)
4.84 (1H, m)	4.86 (1H, brs)
4.78 (1H, s)	4.72 (1H, brs, -OH)
4.68 (1H, t, $J = 4.9$ )	4.70 (1H, d, $J = 6.0$ )
4.14 (1H, dd, $J = 10.9, 5.5$ )	4.15 (1H, dd, $J = 8.3$ )
3.49 (3H, s)	3.50 (3H, s)
3.47 (1H, m)	3.48 (1H, m)
3.41 (1H, dd, $J = 12.0, 3.5$ )	3.46 (1H, d, $J = 3.0$ )
3.36 (1H, dd, $J = 18.1, 6.4$ )	3.36 (1H, dd, $J = 19.5, 6.5$ )
3.15 (1H, dd, $J = 14.8, 5.4$ )	3.16 (1H, dd, $J = 13.4$ )
3.00 (1H, dd, $J = 14.9, 10.5$ )	3.02 (1H, dd, $J = 13.8$ )
2.89 (1H, dd, $J = 18.1, 1.4$ )	2.90 (1H, d, $J = 16.3$ )
2.20 (1H, d, $J = 14.9$ )	2.20 (1H, d, $J = 13.3$ )
2.07 (1H, d, $J = 9.2$ )	2.08 (1H, d, $J = 8.2$ )
2.01 (3H, s)	2.02 (3H, s)
1.73 (dd, $J = 15.2, 5.9$ )	1.73 (1H, dd, $J = 13.3, 6.5$ )
1.52 (3H, s)	1.53 (3H, s)

**Table 2.10.2** Comparison of  $^{13}\text{C}$  NMR shifts of synthetic and natural havellockate (106).

Synthetic Havellockate	Natural Havellockate (Anjaneyulu, 1997)
$^{13}\text{C}$ NMR, 100 MHz, $d_5$ -pyridine (referenced to 123.57 ppm)	$^{13}\text{C}$ NMR, 22.5 MHz, $d_5$ -pyridine
173.2	173.1
147.9	147.9
138.4	138.3
---	123.1
113.0	112.9
91.8	91.7
81.6	81.8
80.1	80.2
76.0	76.0
51.5	51.3
51.4	“5.10”
49.1	49.0
44.8	44.8
40.5	40.4
40.3	40.3
39.1	39.1
38.2	38.2
28.1	28.1
20.7	20.7

## 2.11 NOTES AND REFERENCES

<sup>1</sup> Carroll, A. R.; Copp, B. R.; Davis, R. A.; Keyzers, R. A.; Prinsep, M. R. Marine Natural Products. *Nat. Prod. Rep.* **2022**, (Advance Article) and previous articles in this series.

<sup>2</sup> Li, Y.; Pattenden, G. Perspectives on the Structural and Biosynthetic Interrelationships Between Oxygenated Furanocembranoids and Their Polycyclic Congeners Found in Corals. *Nat. Prod. Rep.* **2011**, *28*, 1269–1310.

<sup>3</sup> For efforts toward the polycyclic furanobutenolide cembranoids see: Craig, R. A., II; Stoltz, B. M. Polycyclic Furanobutenolide-Derived Cembranoid and Norcembranoid Natural Products: Biosynthetic Connections and Synthetic Efforts. *Chem. Rev.* **2017**, *117*, 7878–7909.

<sup>4</sup> Total syntheses of intricarene were reported independently by Pattenden and Trauner. See: (a) Tang, B.; Bray, C. D.; Pattenden, G. A Biomimetic Total Synthesis of (+)-Intricarene. *Tetrahedron Lett.* **2006**, *47*, 6401–6404. (b) Roethle, P. A.; Hernandez, P. T.; Trauner, D. Exploring Biosynthetic Relationships Among Furanocembranoids: Synthesis of (–)-Bipinnatin J, (+)-Intricarene, (+)-Rubifolide, and (+)-Isoepilophodione B. *Org. Lett.* **2006**, *8*, 5901–5904. (c) Stichnoth, D.; Kölle, P.; Kimbrough, T. J.; Riedle, E.; de Vivie-Riedle, R.; Trauner, D. Photochemical Formation of Intricarene. *Nat. Commun.* **2014**, *5*, 5597.

<sup>5</sup> For examples of bioactivity in the polycyclic furanobutenolide-derived cembranoid family, see: (a) Marrero, J.; Rodríguez, A. D.; Baran, P.; Raptis, R. G.; Sánchez, E. O.; Capson, T. L. Bielschowskysin, a Gorgonian-Derived Biologically Active Diterpene with an Unprecedented Carbon Skeleton. *Org. Lett.* **2004**, *6*, 1661–1664. (b) Marrero, J.; Rodríguez, A. D.; Barnes, C. L. Intricarene, an Unprecedented Trispiropentacyclic

Diterpene from the Caribbean Sea Plume *Pseudopterogorgia kallos*. *Org. Lett.* **2005**, *7*, 1877–1880. (c) Faulkner, D. J.; Venkateswarlu, Y.; Raghavan, K. V.; Yadav, J. S. Rameswaralide and Rameswaralide Derivatives. U.S. Patent 6,300,371, Oct 9, 2001.

<sup>6</sup> Anjaneyulu, A. S. R.; Venugopal, M. J. R. V.; Sarada, P.; Clardy, J.; Lobkovsky, E. Havellockate, A Novel Seco and Spiro Lactone Diterpenoid from the Indian Ocean Soft Coral *Sinularia granosa*. *Tetrahedron Lett.* **1998**, *39*, 139–142.

<sup>7</sup> Mehta, G.; Kumaran, R. S. Studies Towards the Total Synthesis of Novel Marine Diterpene Havellockate. Construction of the Tetracyclic Core. *Tetrahedron Lett.* **2001**, *42*, 8097–8100.

<sup>8</sup> Beingessner, R. L.; Farand, J. A.; Barriault, L. Progress toward the Total Synthesis of (±)-Havellockate. *J. Org. Chem.* **2010**, *75*, 6337–6346.

<sup>9</sup> Hafeman, N. J.; Loskot, S. A.; Reimann, C. E.; Pritchett, B. P.; Virgil, S. C.; Stoltz, B. M. The Total Synthesis of (–)-Scabrolide A. *J. Am. Chem. Soc.* **2020**, *142*, 8585–8590.

<sup>10</sup> (a) Brill, Z. G.; Gover, H. K.; Maimone, T. J. Enantioselective Synthesis of an Ophiobolin Sesterpene via a Programmed Radical Cascade. *Science* **2016**, *352*, 1078–1082. (b) Thach, D. Q.; Brill, Z. G.; Grover, H. K.; Esguerra, K. V.; Thompson, J. K.; Maimone, T. J. Total Synthesis of (+)-6-*epi*-Ophiobolin A. *Angew. Chem., Int. Ed.* **2020**, *59*, 1532–1536.

<sup>11</sup> Bauta, W.; Booth, J.; Bos, M. E.; DeLuca, M.; Diorazio, L.; Donohoe, T.; Magnus, N.; Magnus, P.; Mendoza, J.; Pye, P.; Tarrant, J.; Thom, S.; Ujjainwalla, F. New Strategy for the Synthesis of the Taxane Diterpenes: Formation of the BC-Rings of Taxol via a [5+2]-Pyrilium Ylide-Alkene Cyclization, Ring Expansion Strategy. *Tetrahedron Lett.* **1995**, 5327–5330.



<sup>12</sup> Prashad, M.; Kim, H.-Y.; Har, D.; Repic, O.; Blacklock, T. J. A Convenient and Practical Method for N-Acylation of 2-Oxazolidinone Chiral Auxiliaries with Acids. *Tetrahedron Lett.* **1998**, *39*, 9369–9372.

<sup>13</sup> Attempts to perform this alkylation with methyl bromoacetate resulted in low dr. Also, subsequent steps (e.g. the Julia–Kocienski olefination) fail in the presence of a methyl ester.

<sup>14</sup> Saito, T.; Fuwa, J.; Sasaki, M. Synthetic Studies on Goniodomin A: Convergent Assembly of the C15–C36 Segment via Palladium-Catalyzed Organostannane–Thioester Coupling. *Tetrahedron* **2011**, *67*, 429–445.

<sup>15</sup> Blakemore, P. R.; Sephton, S. M.; Ciganek, E. The Julia–Kocienski Olefination. In *Organic Reactions*, Vol. 95, Wiley, 2018, pp 1–422.

<sup>16</sup> For examples, see: (a) Corey, E. J.; Danheiser, R. L.; Chandrasekaran, S.; Siret, P.; Keck, G. E.; Gras, J.-L. Stereospecific Total Synthesis of Gibberellic Acid. *J. Am. Chem. Soc.* **1978**, *100*, 8034–8036. (b) Shen, M.; Schultz, A. G. Preparation and Diels–Alder Reactivity of Ethyl- $\beta$ -Phenylsulfonylpropionate. *Tetrahedron Lett.* **1981**, 3347–3350.

<sup>17</sup> The corresponding propargyl ether is readily prepared, and interestingly undergoes smooth a Diels–Alder reaction. However, C–H oxidation of the product or any subsequent intermediates was never realized.

<sup>18</sup> Immoto, T.; Sugiura, Y.; Takiyama, N. Organocerium Reagents. Nucleophilic Addition to Easily Enolizable Ketones. *Tetrahedron Lett.* **1984**, *25*, 4233–4236.

<sup>19</sup> Ranu, B. C.; Majee, A.; Das, A. R. Facile and Efficient Synthesis of Homoallylic Alcohols Using Allyl Bromide and Commercial Zinc Dust. *Tetrahedron Lett.* **1995**, *36*, 4885–4888.

- <sup>20</sup> Lombardo, M.; Morganti, S.; Trombini, C. 3-Bromopropenyl Esters in Organic Synthesis: Indium- and Zinc-Mediated Entries to Alk-1-ene-3,4-diols. *J. Org. Chem.* **2003**, *68*, 997–1006.
- <sup>21</sup> (a) Blackwell, H. E.; O’Leary, D. J.; Chatterjee, A. K.; Washenfelder, R. A.; Busmann, D. A.; Grubbs, R. H. New Approaches to Olefin Cross-Metathesis. *J. Am. Chem. Soc.* **2000**, *122*, 58–71. (b) Pietraszuk, C.; Marciniak, B.; Fischer, H. Cross-Metathesis of Vinylsilanes with Styrene Catalyzed by Ruthenium-Carbene Complexes. *Organometallics* **2000**, *19*, 913–917.
- <sup>22</sup> Han, C.; Uemura, D. Novel Cleavage of (*E*)-allyl *vic*-Diols to Aldehydes Using the 2<sup>nd</sup>-Generation Grubbs Catalyst. *Tetrahedron Lett.* **2008**, *49*, 6988–6990.
- <sup>23</sup> Zviely, M.; Goldman, A.; Kirson, I.; Glotter, E. Selective Cleavage of Ditertiary Glycols under Mild Conditions, with Bisacetylacetonato-oxovanadium. *J. Chem. Soc., Perkin Trans. I* **1986**, 229–231.
- <sup>24</sup> Chandrasekaran, S.; Kluge, A. F.; Edwards, J. A. Synthesis of Substituted  $\beta$ -Lactams by Addition of Nitromethane to 6-Oxopenicillanates and 7-Oxocephalosporanates. *J. Org. Chem.* **1977**, 3972–3974.
- <sup>25</sup> Evans, D. A.; Fu, G. C.; Hoveyda, A. H. Rhodium(I)- and Iridium(I)-Catalyzed Hydroboration Reactions: Scope and Synthetic Applications. *J. Am. Chem. Soc.* **1992**, *114*, 6671–6679.
- <sup>26</sup> Crudden, C. M.; Hleba, Y. B.; Chen, A. C. Regio- and Enantiocontrol in the Room-Temperature Hydroboration of Vinyl Arenes with Pinacol Borane. *J. Am. Chem. Soc.* **2004**, *126*, 9200–9201.

<sup>27</sup> Xie, X.; Zhang, X.; Yang, H.; Ji, X.; Li, J.; Ding, S. Iridium-Catalyzed Hydrosilylation of Unactivated Alkenes: Scope and Application to Late-Stage Functionalization. *J. Org. Chem.* **2019**, *84*, 1085–1093.

<sup>28</sup> Itami, K.; Nokami, T.; Yoshida, J. 2-Pyridyldimethylsilyl as a Removable Hydrophilic Group in Aqueous Diels–Alder Reactions. *Angew. Chem., Int. Ed.* **2001**, *40*, 1074–1076.

<sup>29</sup> Hoover, J. M.; Stahl, S. S. Highly Practical Copper(I)/TEMPO Catalyst System for Chemoselective Aerobic Oxidation of Primary Alcohols. *J. Am. Chem. Soc.* **2011**, *133*, 16901–16910.

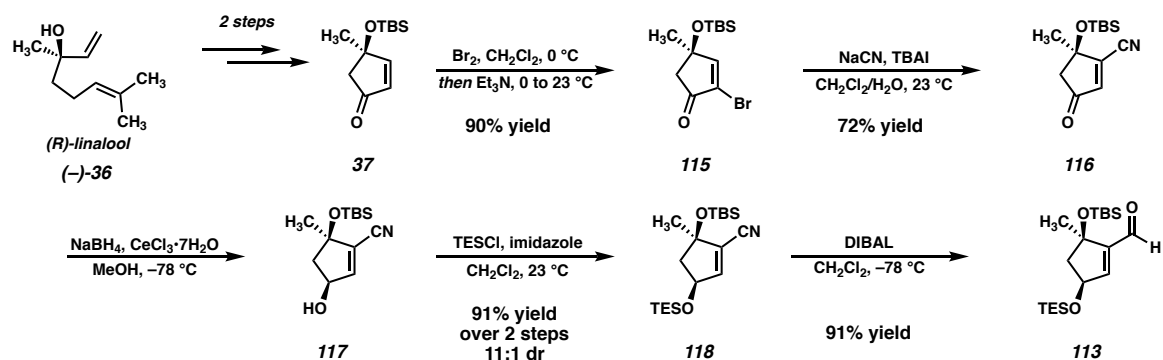
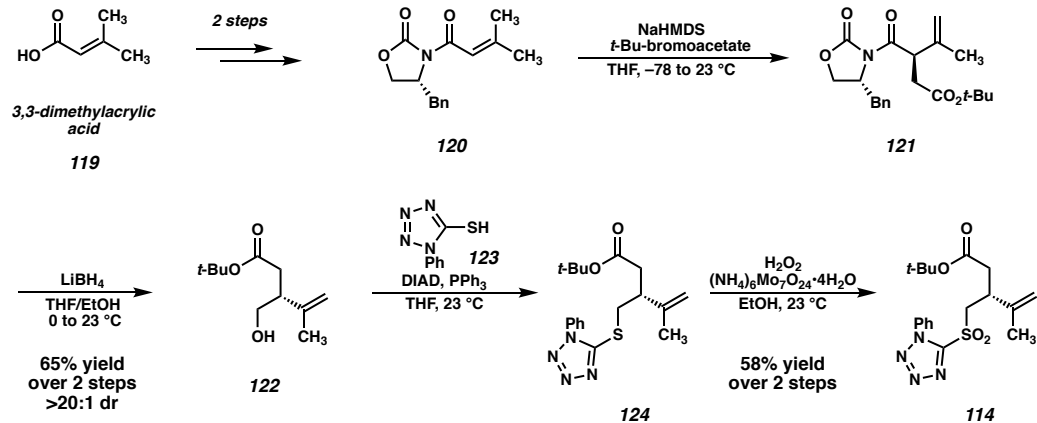
<sup>30</sup> Xie, X.; Stahl, S. S. Efficient and Selective Cu/Nitroxyl-Catalyzed Methods for Aerobic Oxidative Lactonization of Diols. *J. Am. Chem. Soc.* **2015**, *137*, 3767–3770.

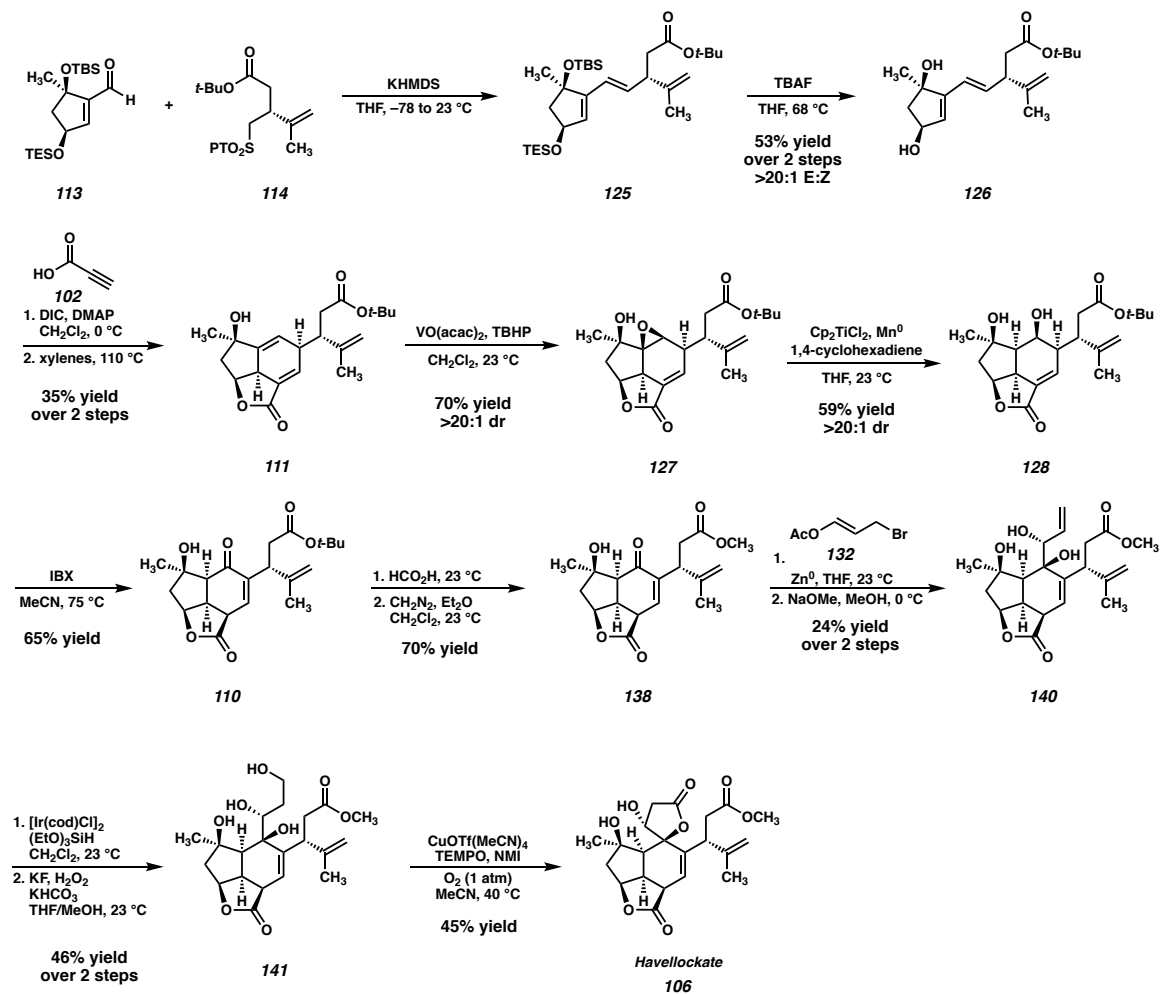
<sup>31</sup> A. M. Pangborn, M. A. Giardello, R. H. Grubbs, R. K. Rosen, F. J. Timmers, F. J. Safe and Convenient Method for Solvent Purification. *Organometallics* **1996**, *15*, 1518–1520.

<sup>32</sup> Natural havellockate displays a specific rotation of +23.70 ° (c 0.43, pyridine), which is nearly equal and opposite to that of our synthetic sample. However, due to the low concentration the sample used for our measurement (which generates an optical rotation lower in magnitude than the blank measurement of pyridine on our instrument), we believe that this may be an erroneous observation, and that a more concentrated sample will be required to definitively determine the specific rotation of the synthetic material.

## **APPENDIX 6**

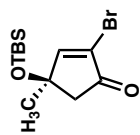
*Synthetic Summary for Chapter 2:  
Asymmetric Total Synthesis of Havellockate*

**Scheme A6.1** Synthesis of aldehyde **113**.**Scheme A6.2** Synthesis of sulfone **114**.

**Scheme A6.3** Completion of the synthesis of havellockate (**106**).

## **APPENDIX 7**

*Spectra Relevant to Chapter 2:  
Asymmetric Synthesis of Havellockate*



115

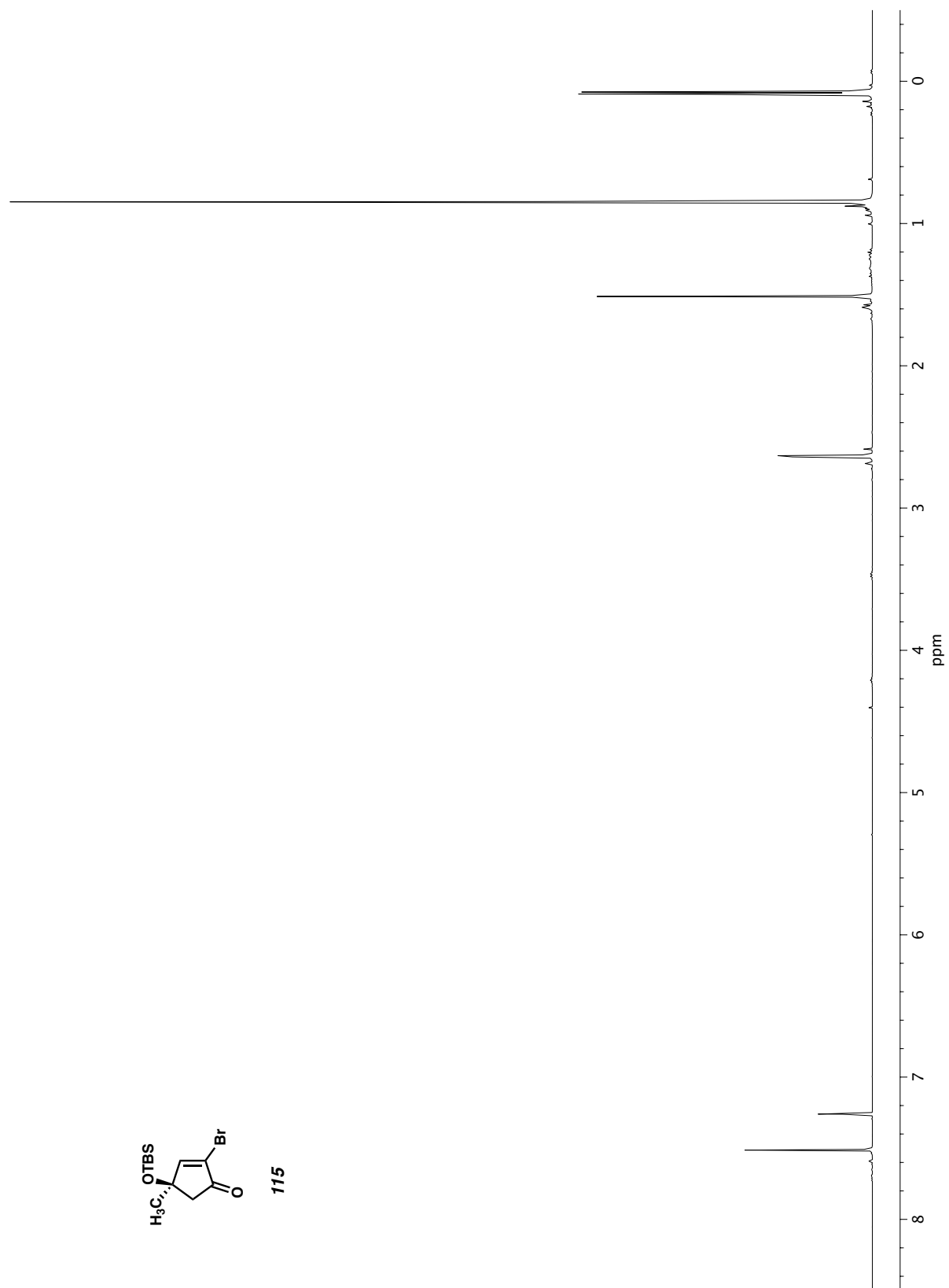
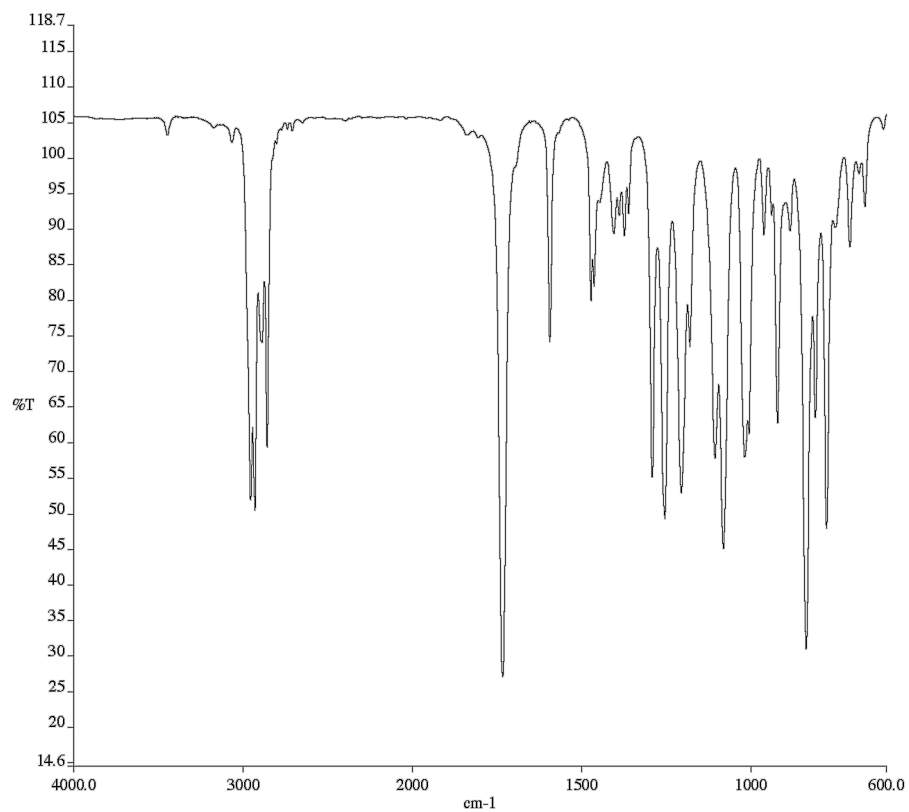
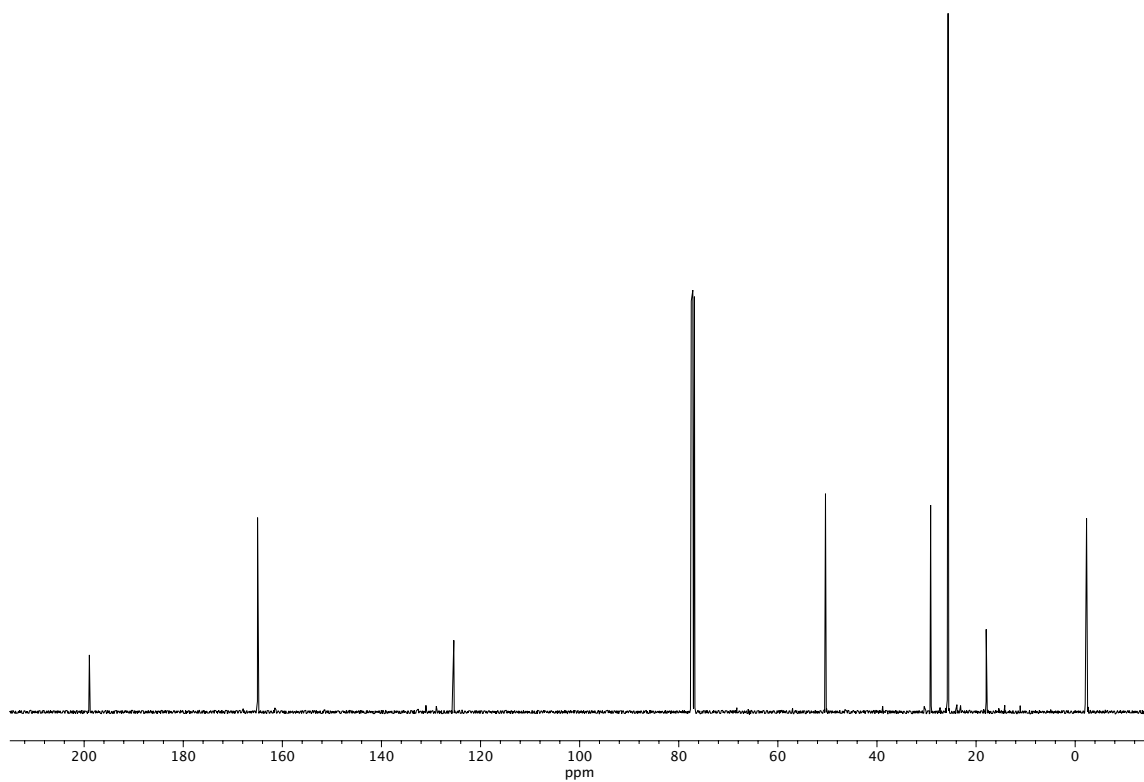


Figure A7.1  $^1\text{H}$  NMR (400 MHz,  $\text{CDCl}_3$ ) of compound **115**.





**Figure A7.2** Infrared spectrum (Thin Film, NaCl) of compound **115**.



**Figure A7.3** <sup>13</sup>C NMR (100 MHz, CDCl<sub>3</sub>) of compound **115**.

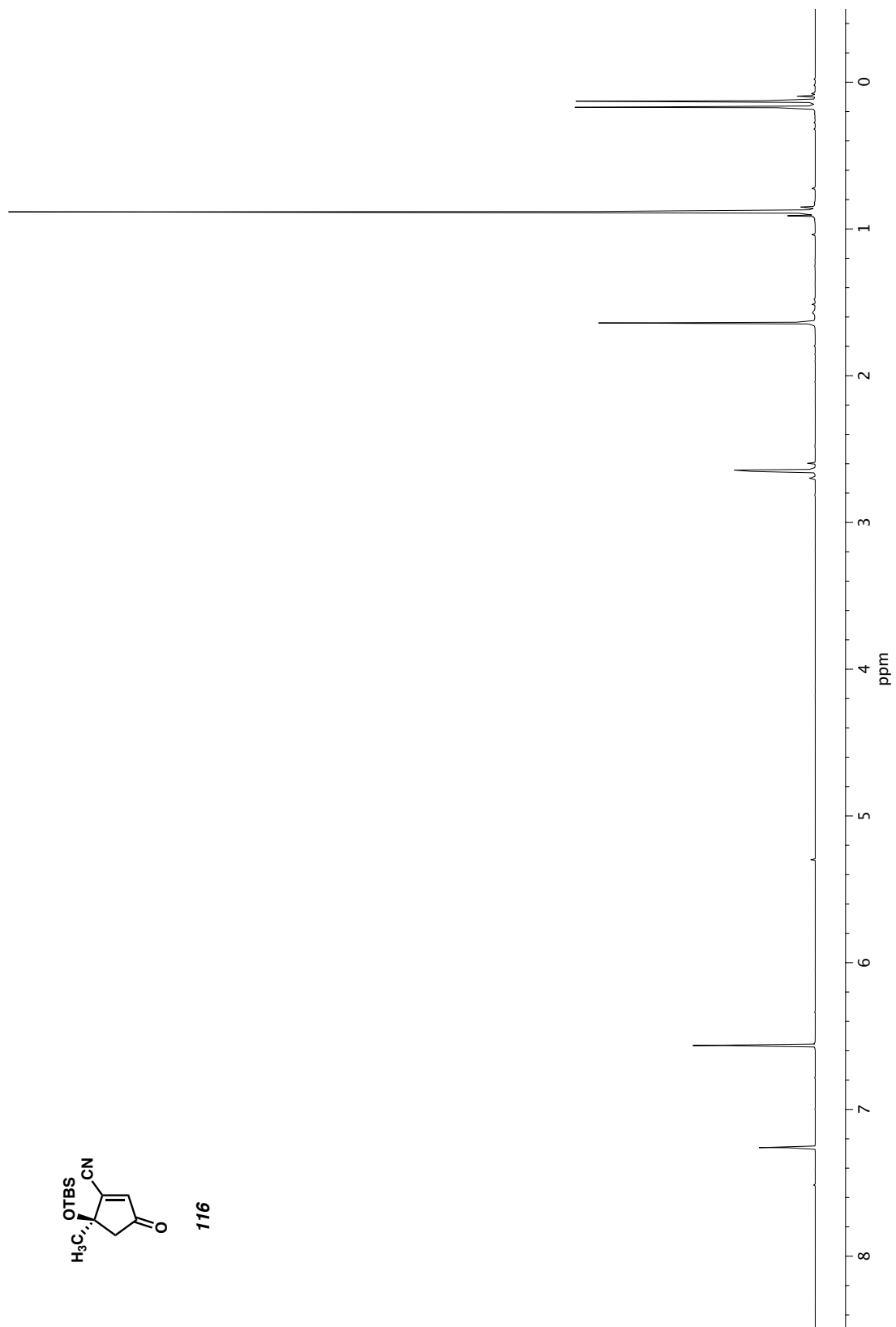
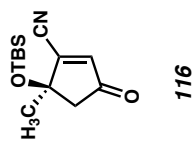
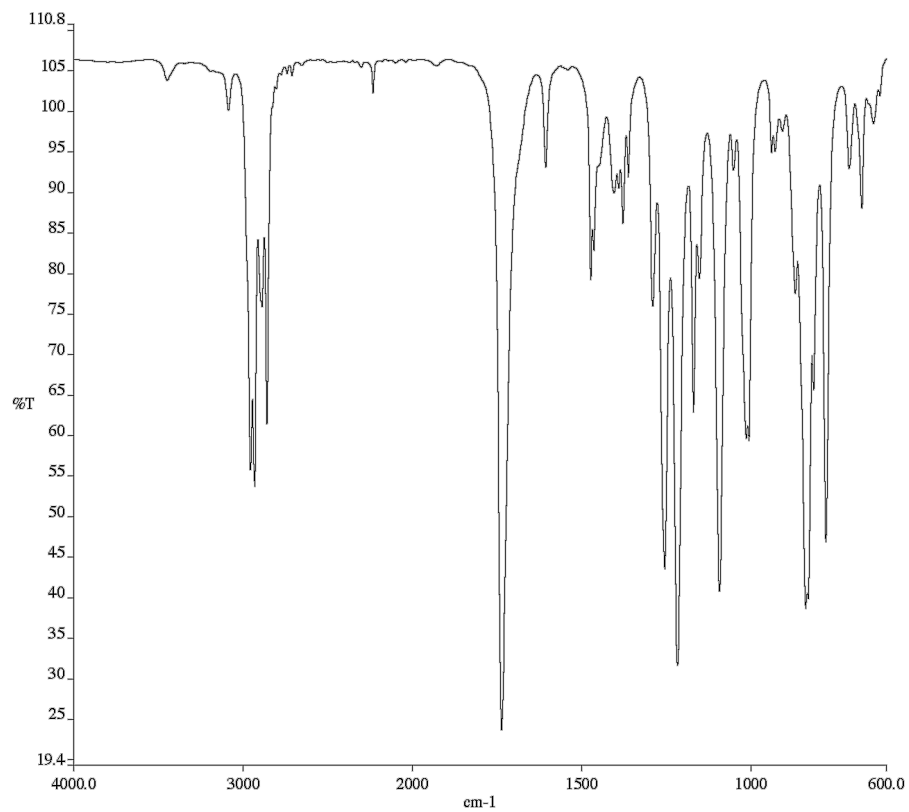
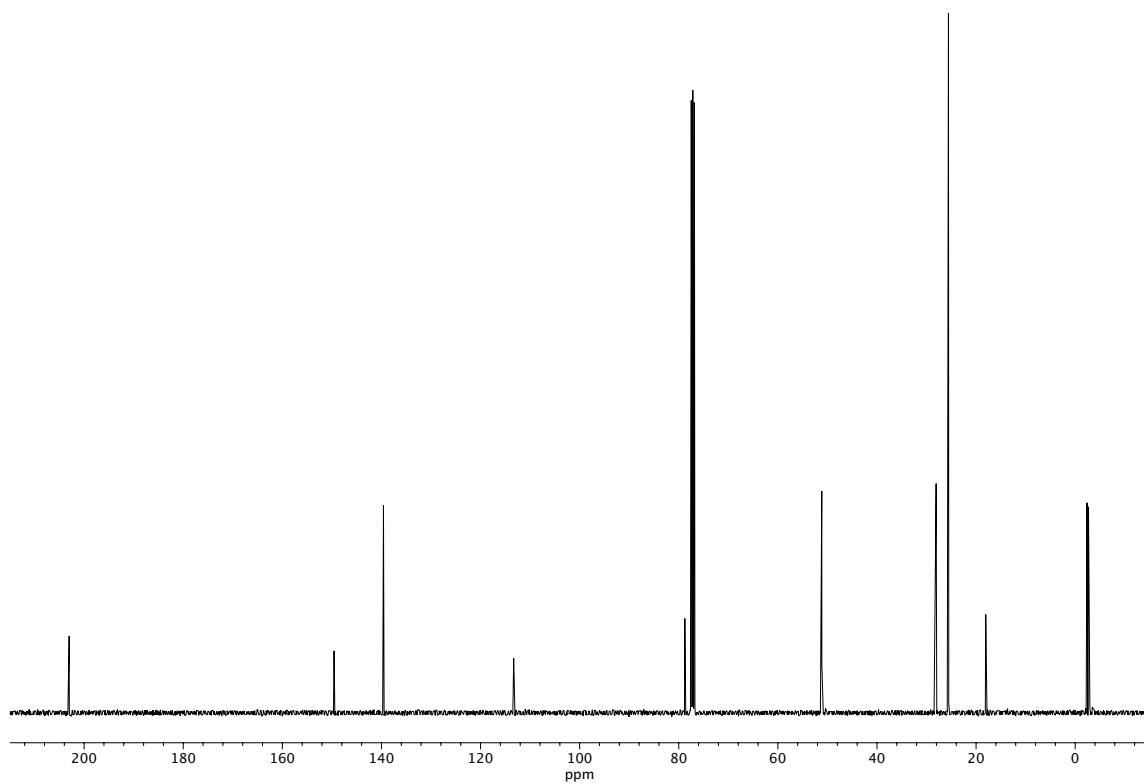


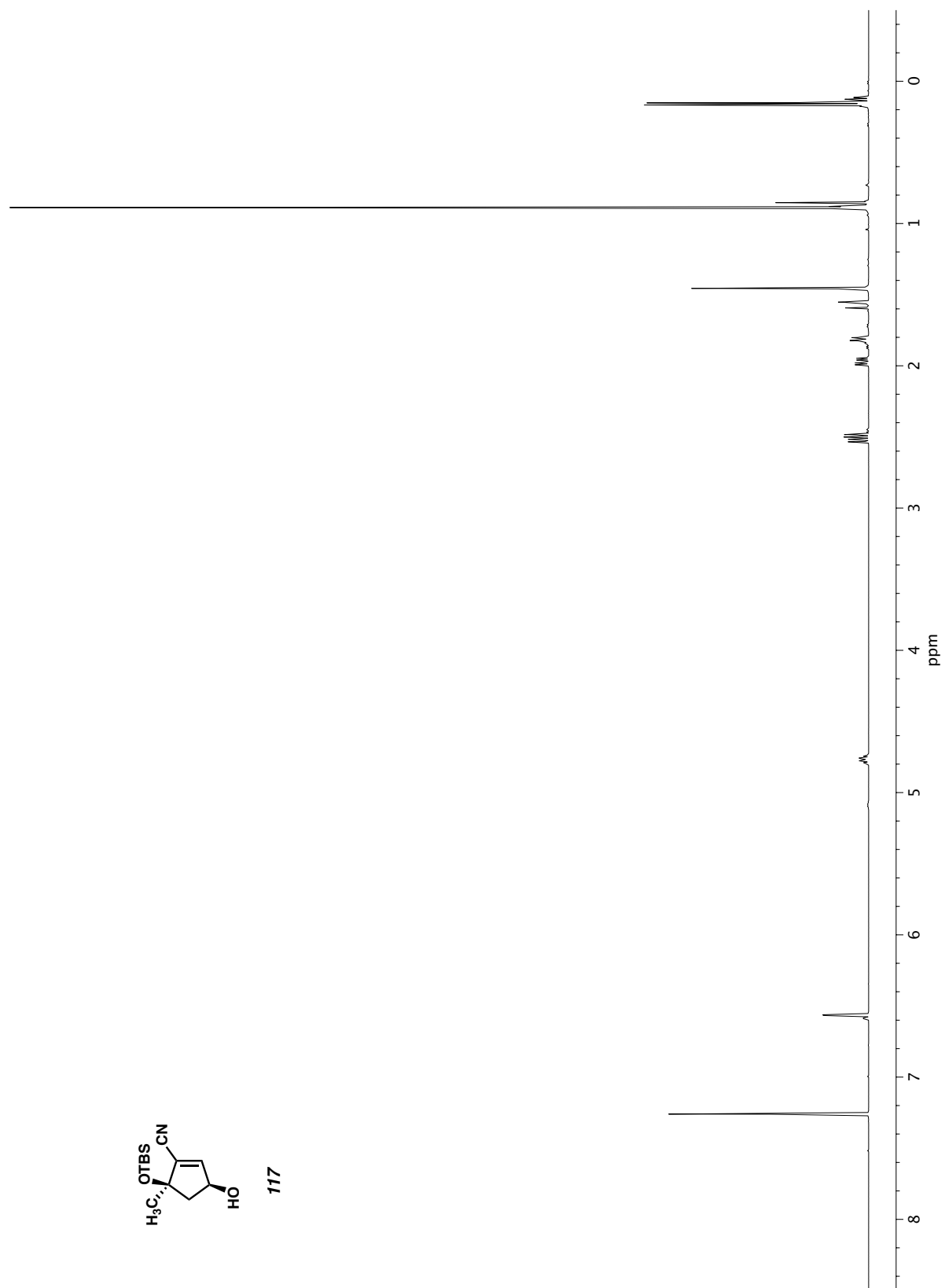
Figure A7.4 <sup>1</sup>H NMR (400 MHz, CDCl<sub>3</sub>) of compound **116**.



**Figure A7.5** Infrared spectrum (Thin Film, NaCl) of compound **116**.



**Figure A7.6** <sup>13</sup>C NMR (100 MHz, CDCl<sub>3</sub>) of compound **116**.

Figure A7.7  $^1\text{H}$  NMR (400 MHz,  $\text{CDCl}_3$ ) of compound **117**.

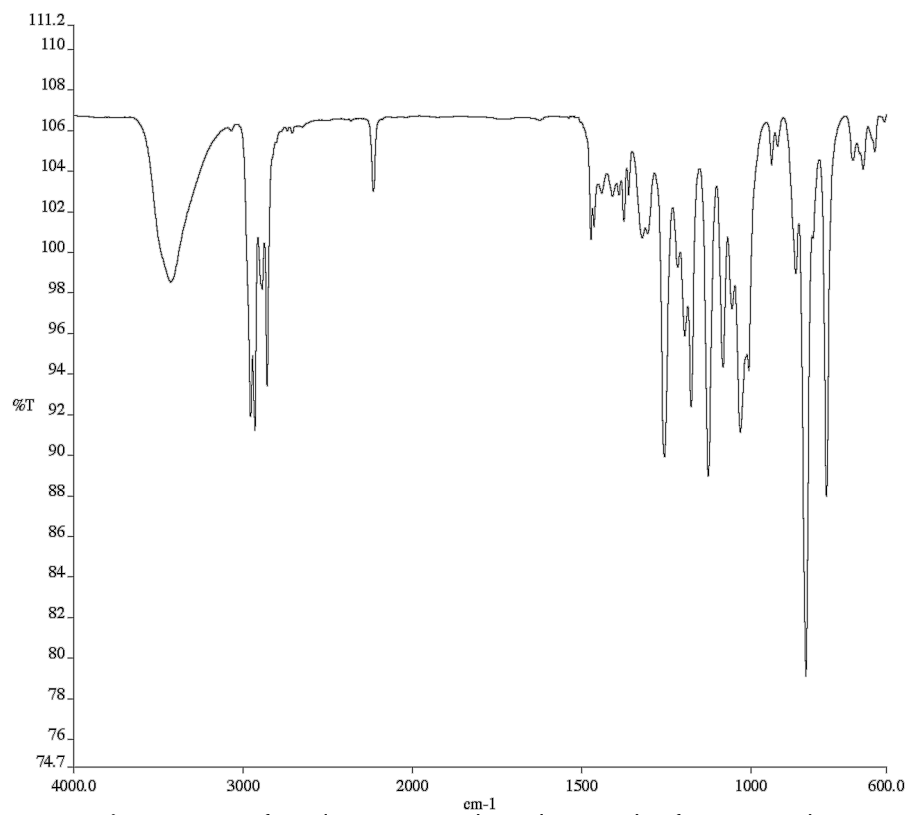


**Figure A7.8** Infrared spectrum (Thin Film, NaCl) of compound **117**.

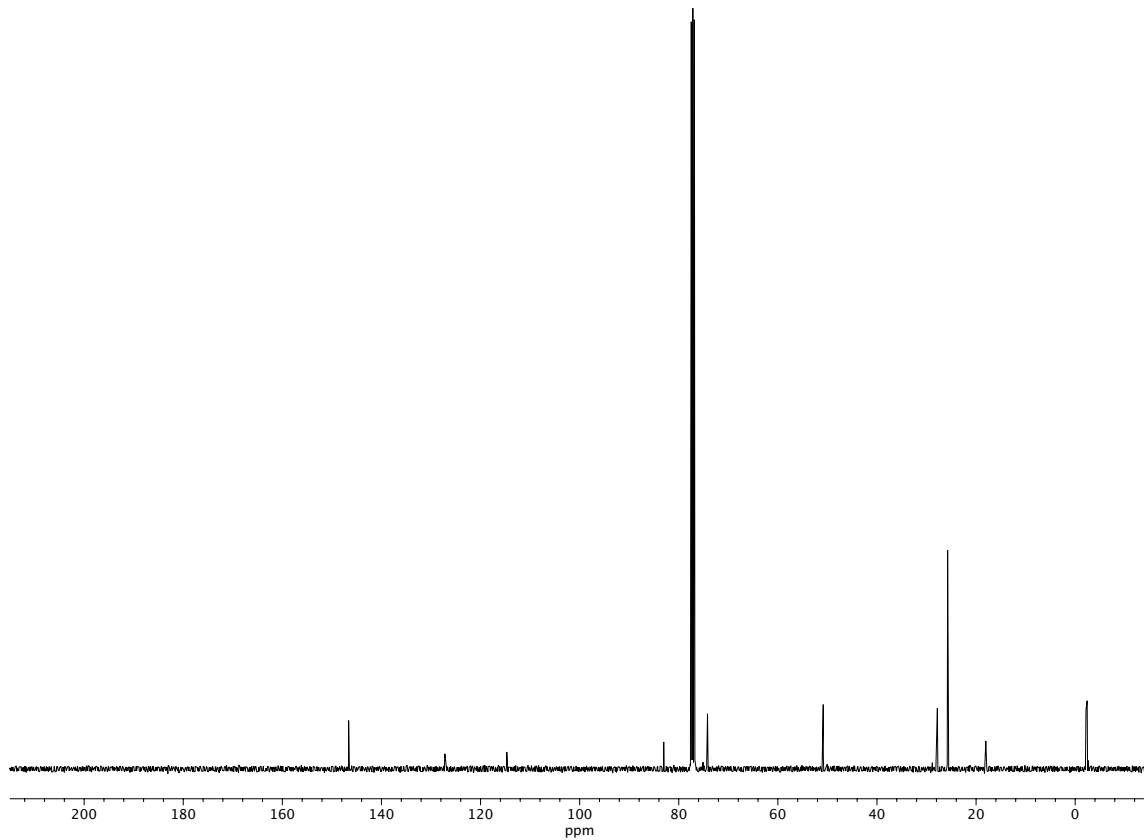


**Figure A7.9** <sup>13</sup>C NMR (100 MHz, CDCl<sub>3</sub>) of compound **117**.

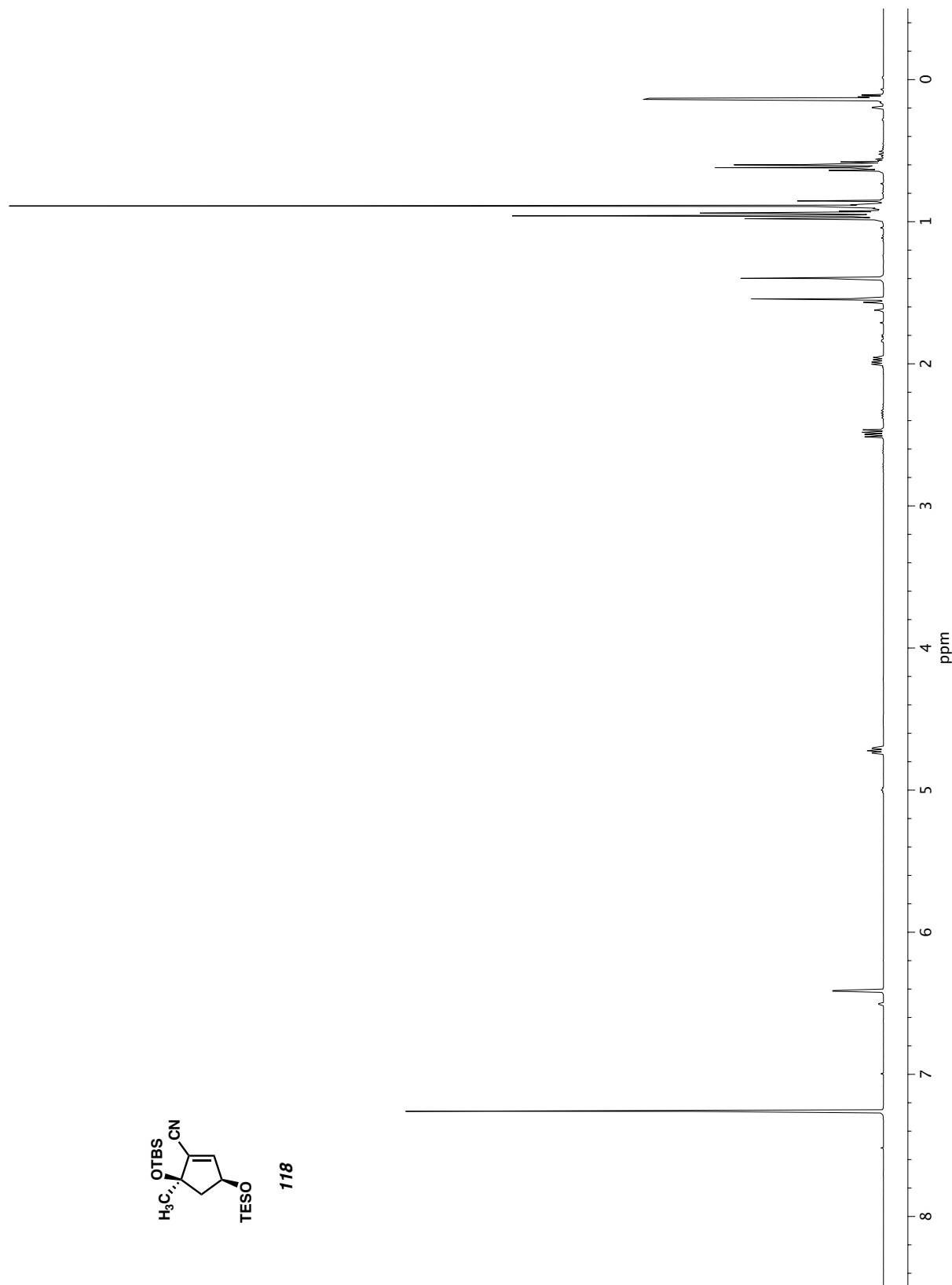


**Figure A7.10**  $^1\text{H}$  NMR (400 MHz,  $\text{CDCl}_3$ ) of compound **118**.

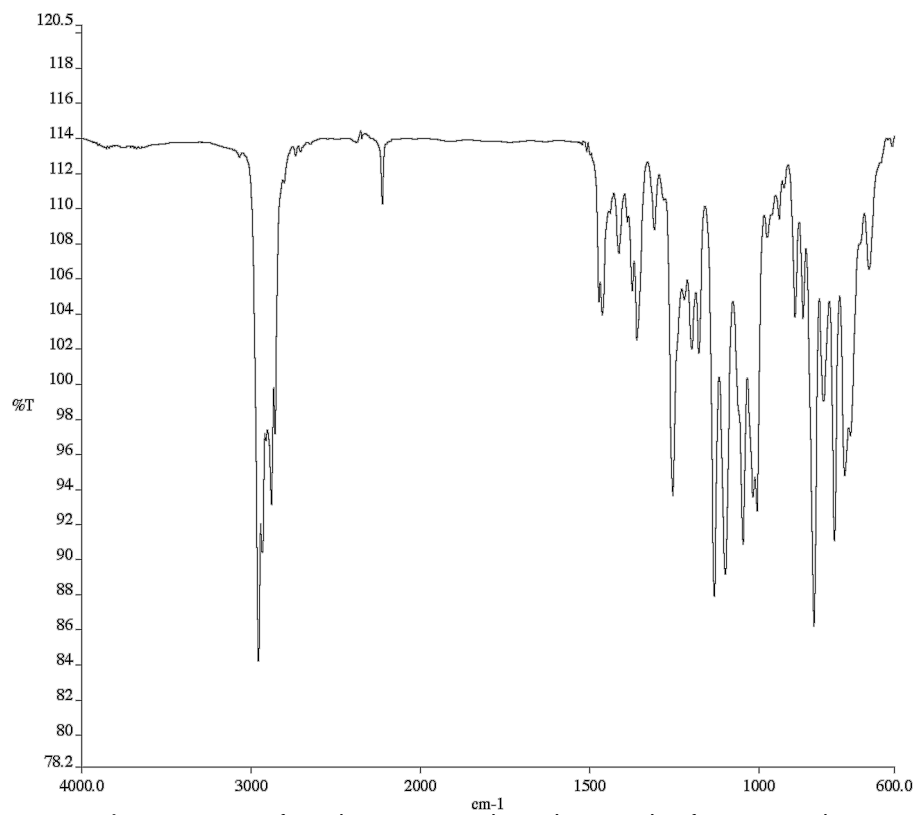


**Figure A7.11** Infrared spectrum (Thin Film, NaCl) of compound **118**.

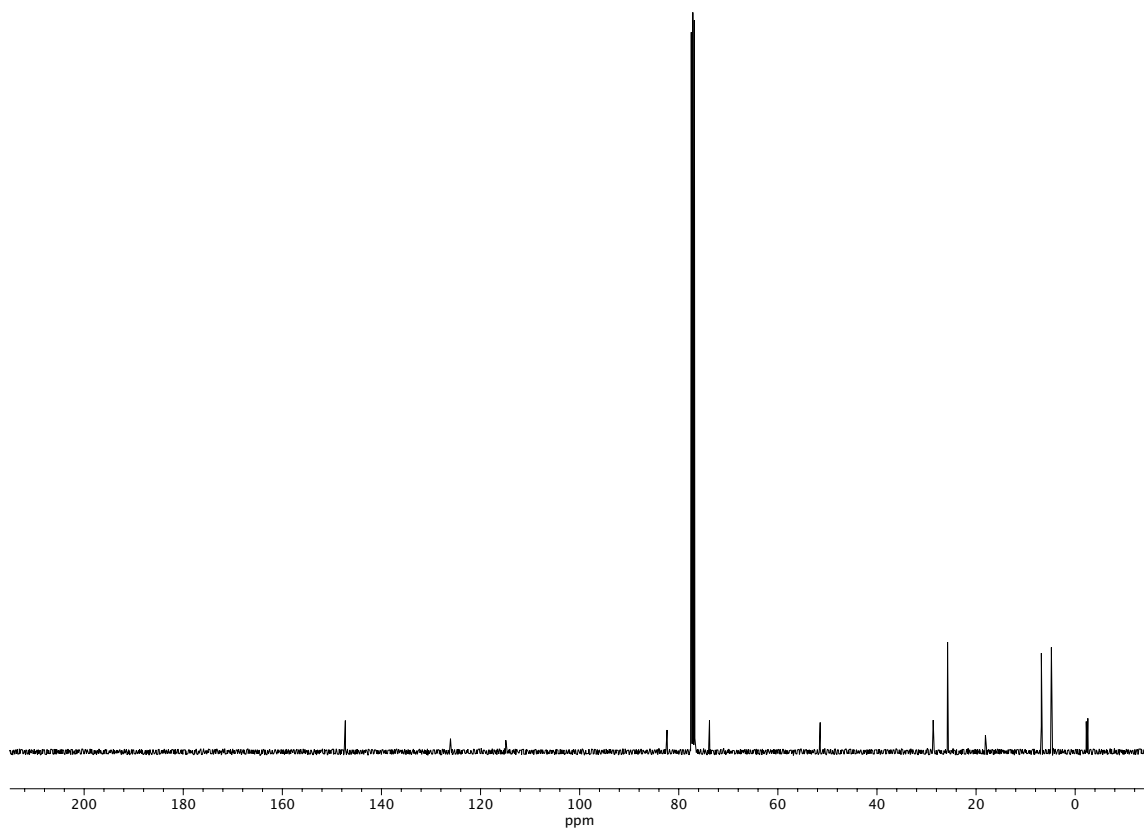


**Figure A7.12** <sup>13</sup>C NMR (100 MHz, CDCl<sub>3</sub>) of compound **118**.

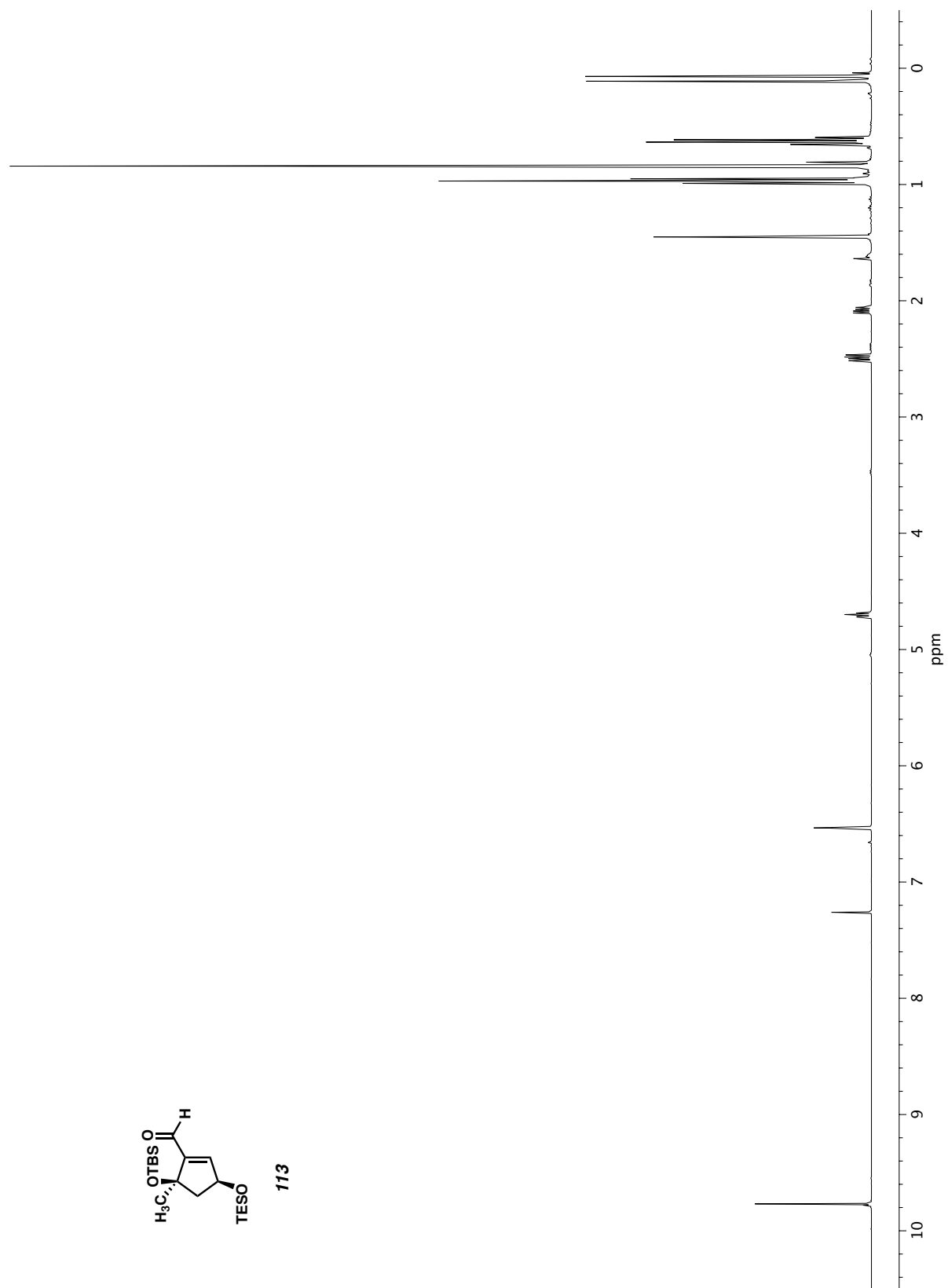
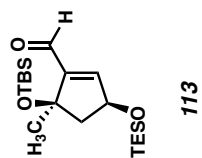


**Figure A7.13**  $^1\text{H}$  NMR (400 MHz,  $\text{CDCl}_3$ ) of compound **113**.



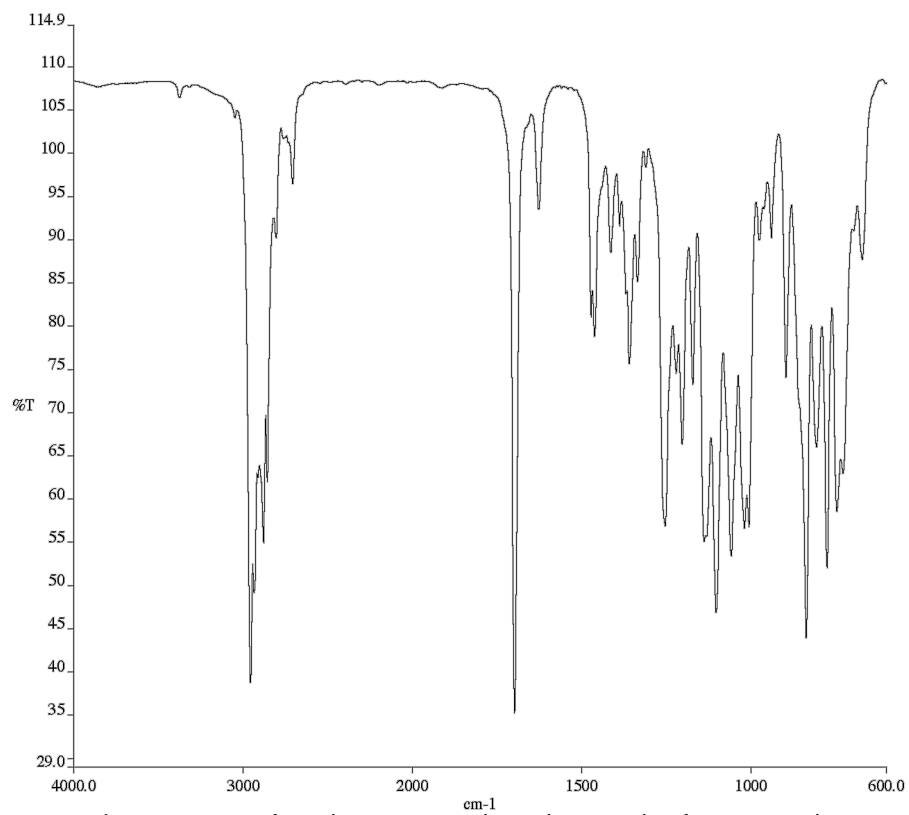


**Figure A7.14** Infrared spectrum (Thin Film, NaCl) of compound **113**.

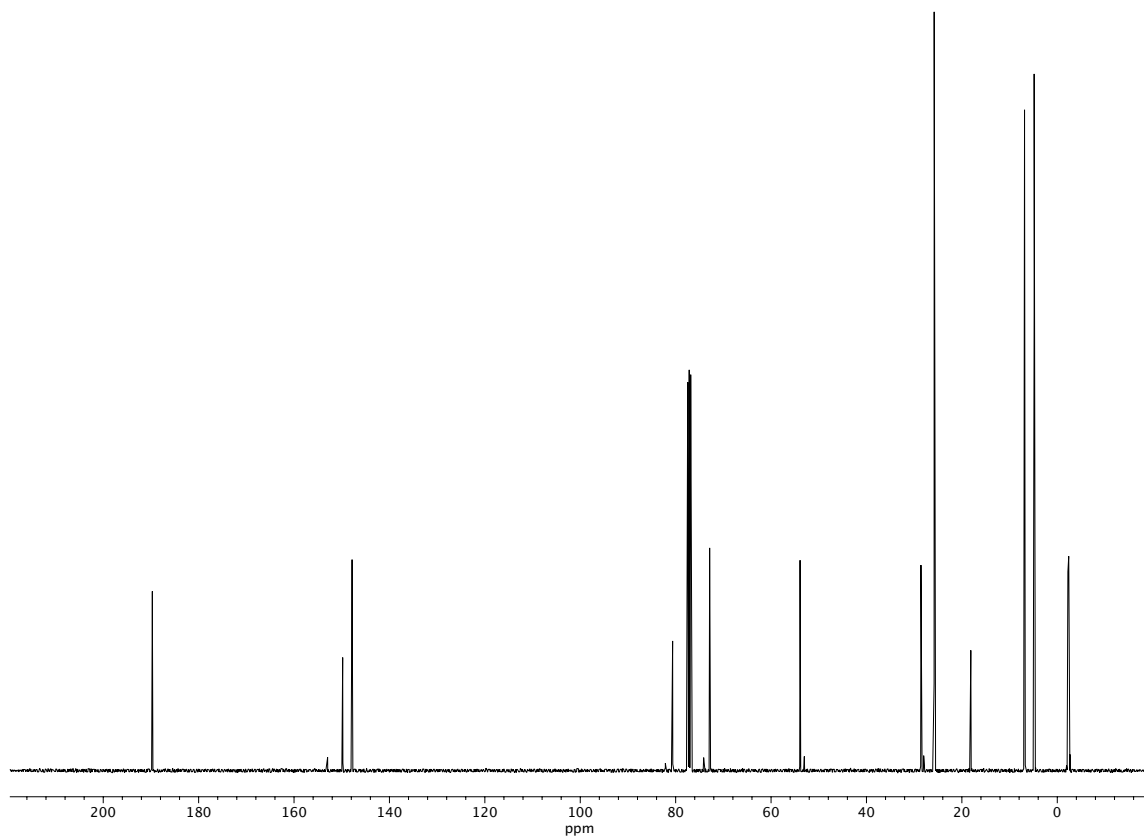


**Figure A7.15** <sup>13</sup>C NMR (100 MHz, CDCl<sub>3</sub>) of compound **113**.

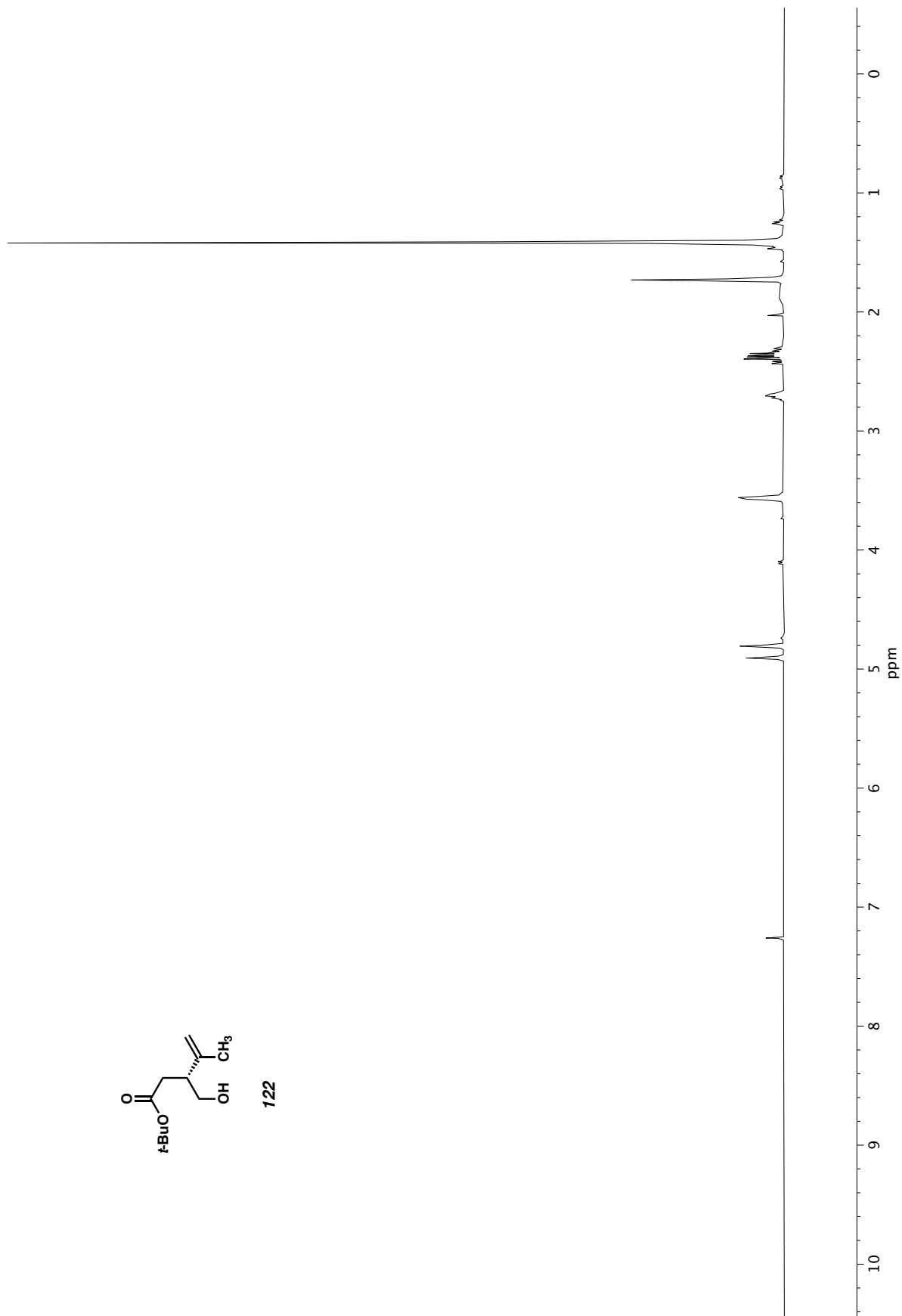


**Figure A7.16**  $^1\text{H}$  NMR (400 MHz,  $\text{CDCl}_3$ ) of compound **122**.

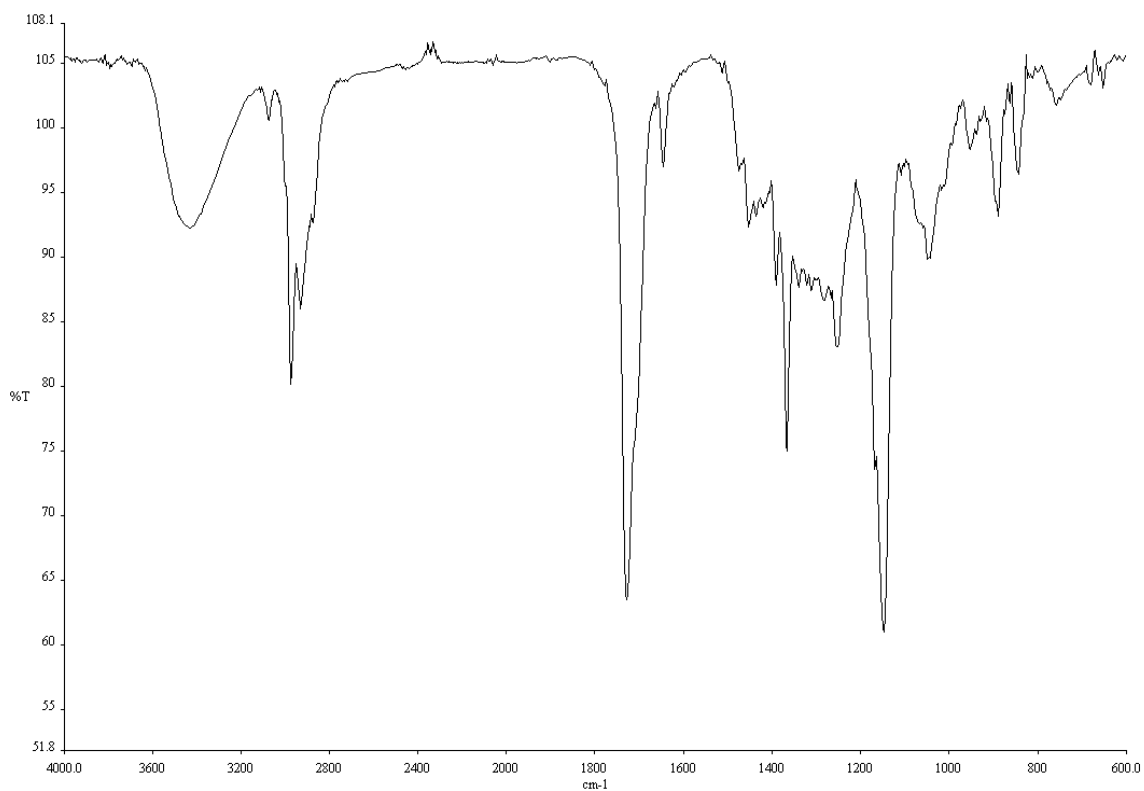


**Figure A7.17** Infrared spectrum (Thin Film, NaCl) of compound **122**.

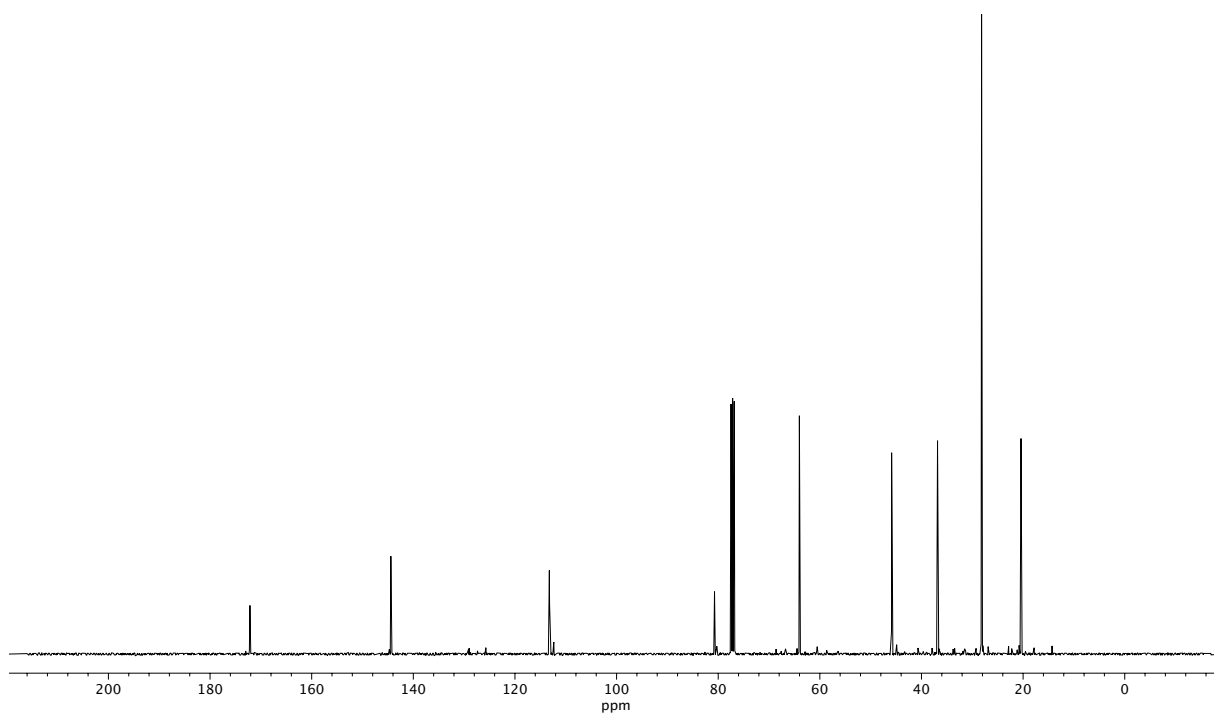
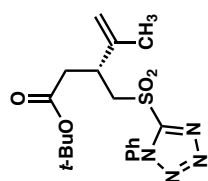


**Figure A7.18** <sup>13</sup>C NMR (100 MHz, CDCl<sub>3</sub>) of compound **122**.



114

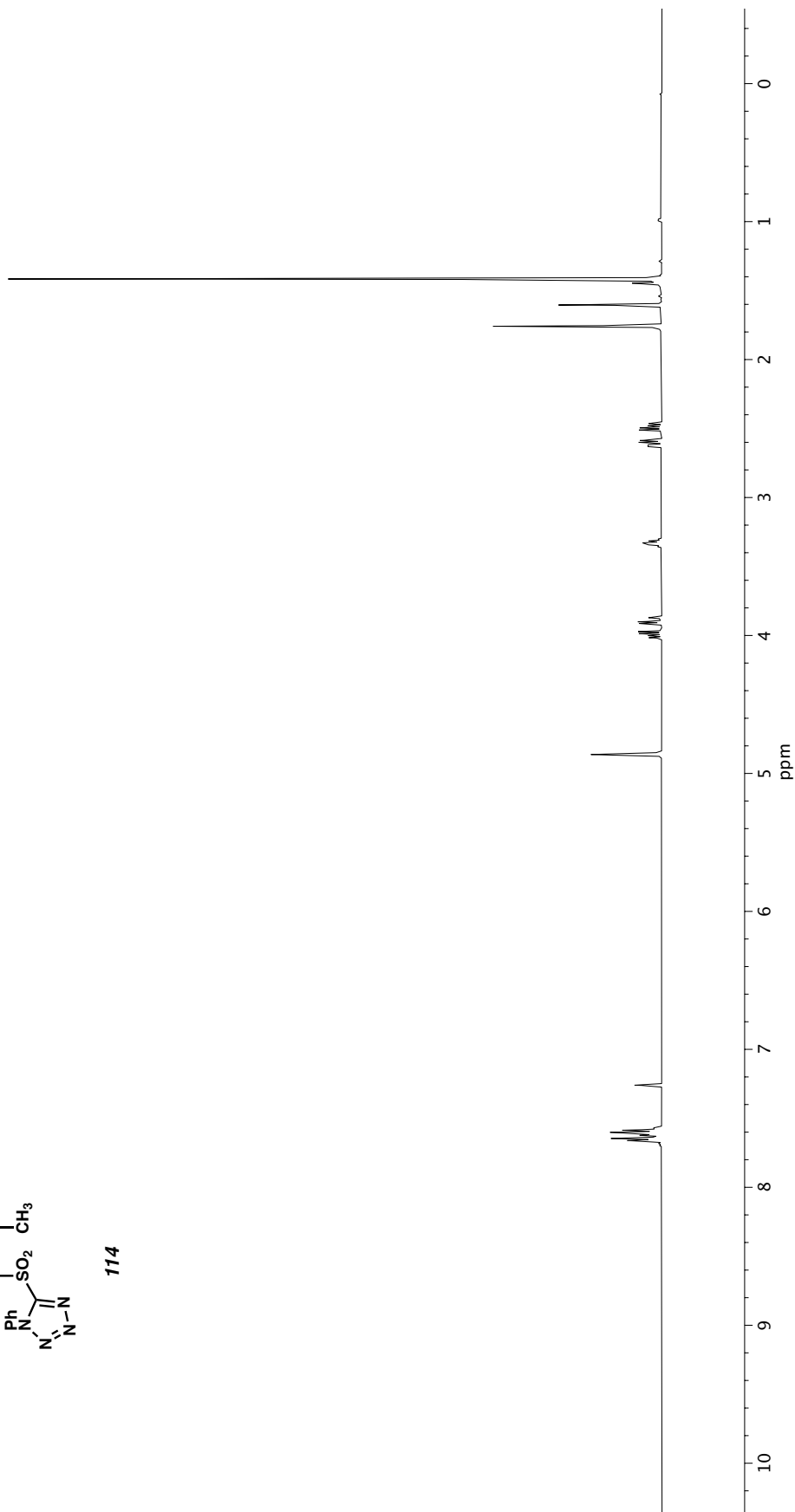
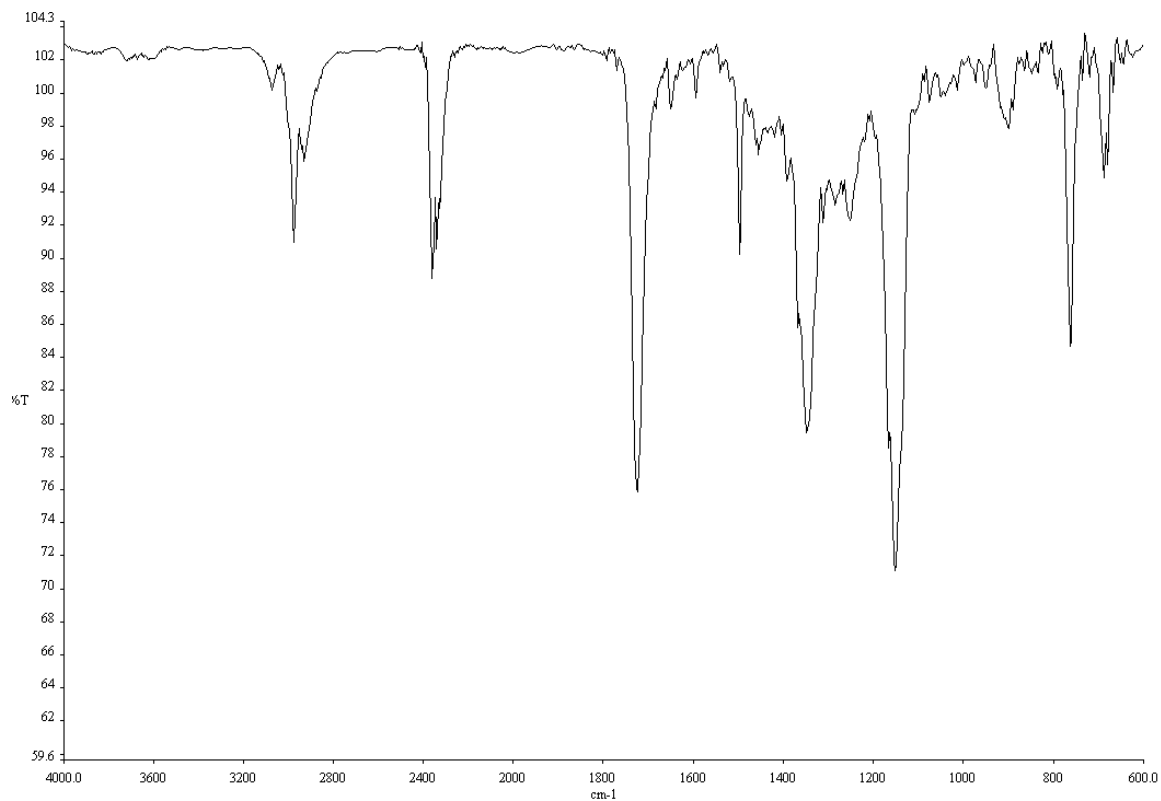
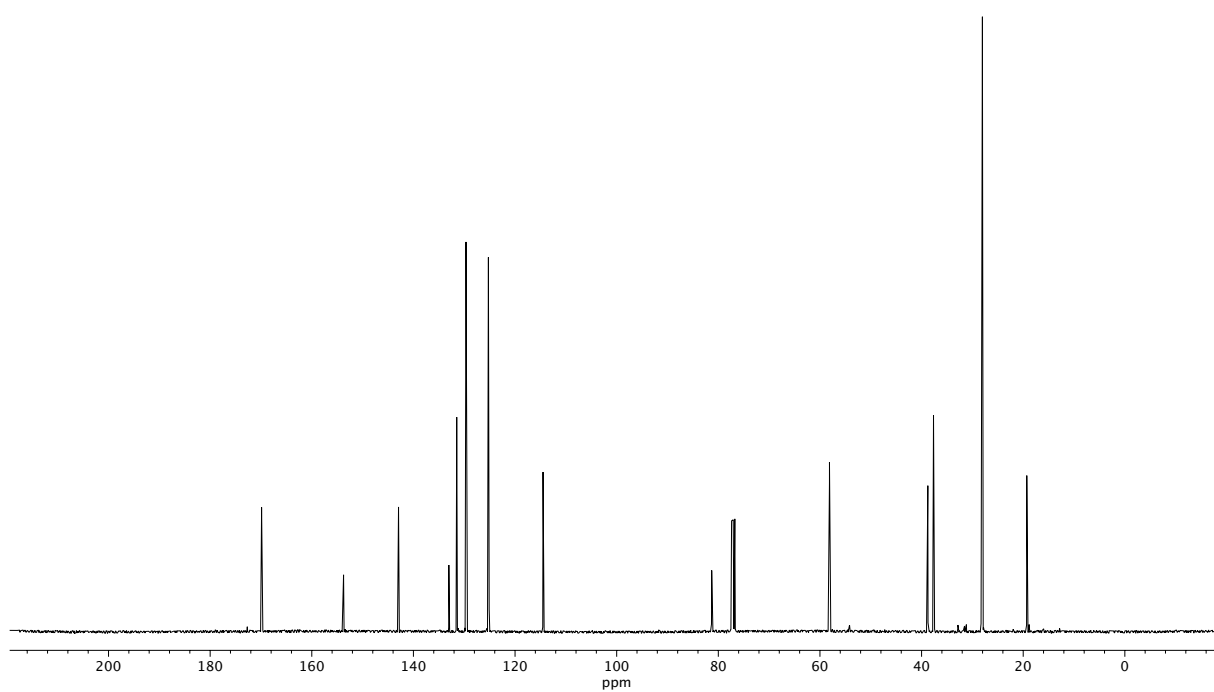


Figure A7.19 <sup>1</sup>H NMR (500 MHz, CDCl<sub>3</sub>) of compound 114.



**Figure A7.20** Infrared spectrum (Thin Film, NaCl) of compound **114**.



**Figure A7.21** <sup>13</sup>C NMR (100 MHz, CDCl<sub>3</sub>) of compound **114**.

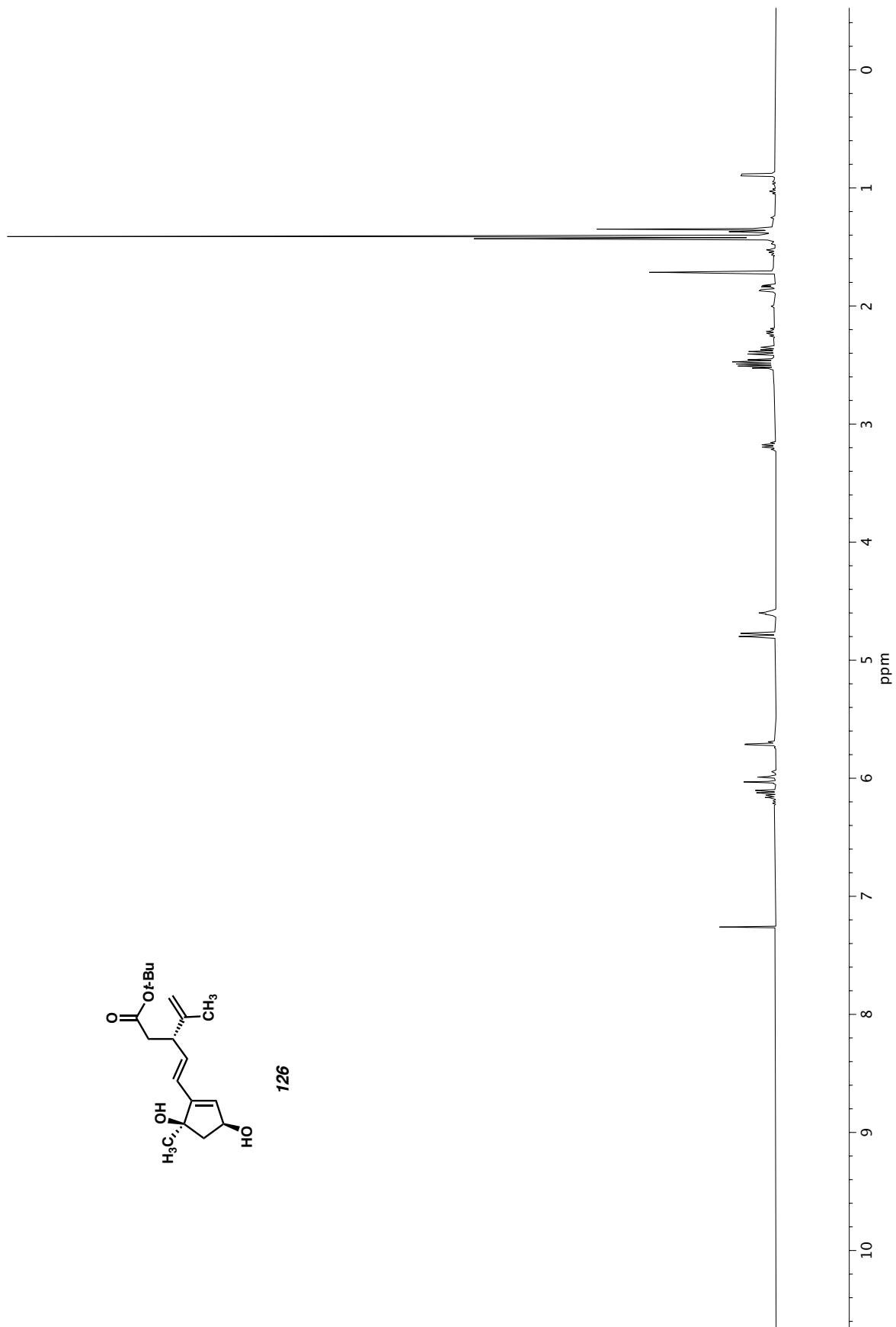
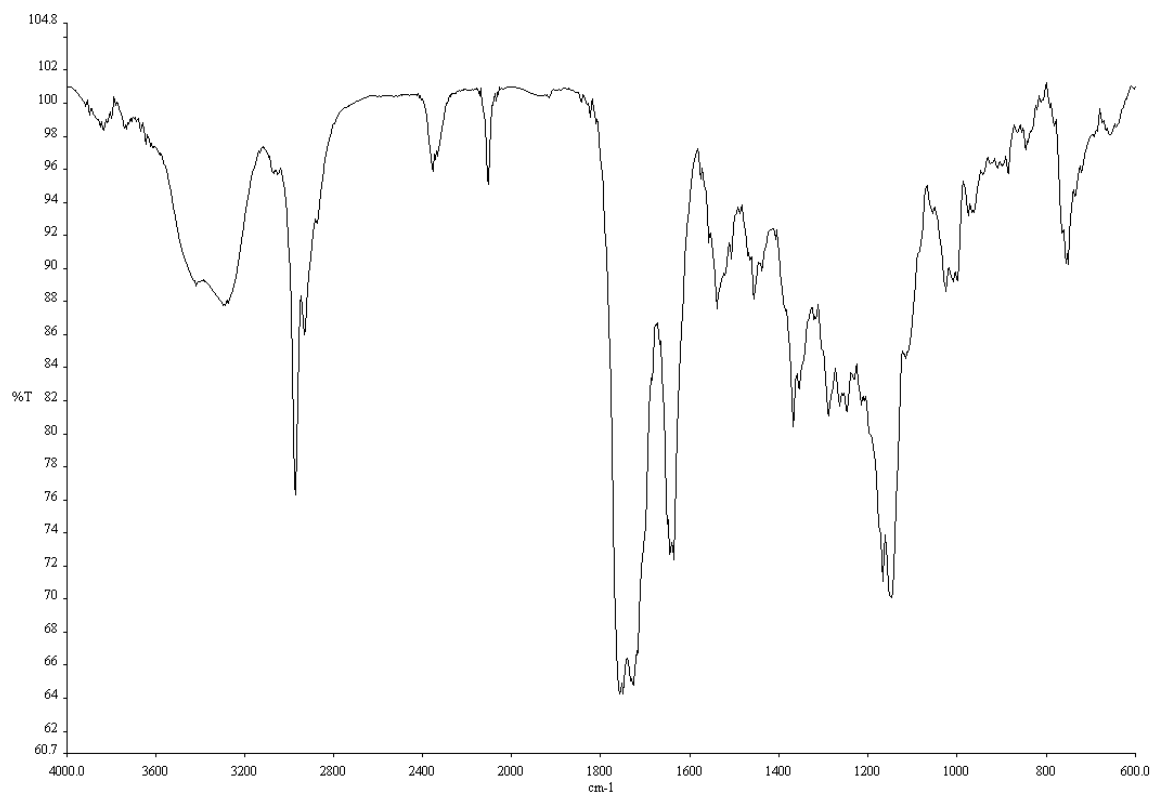
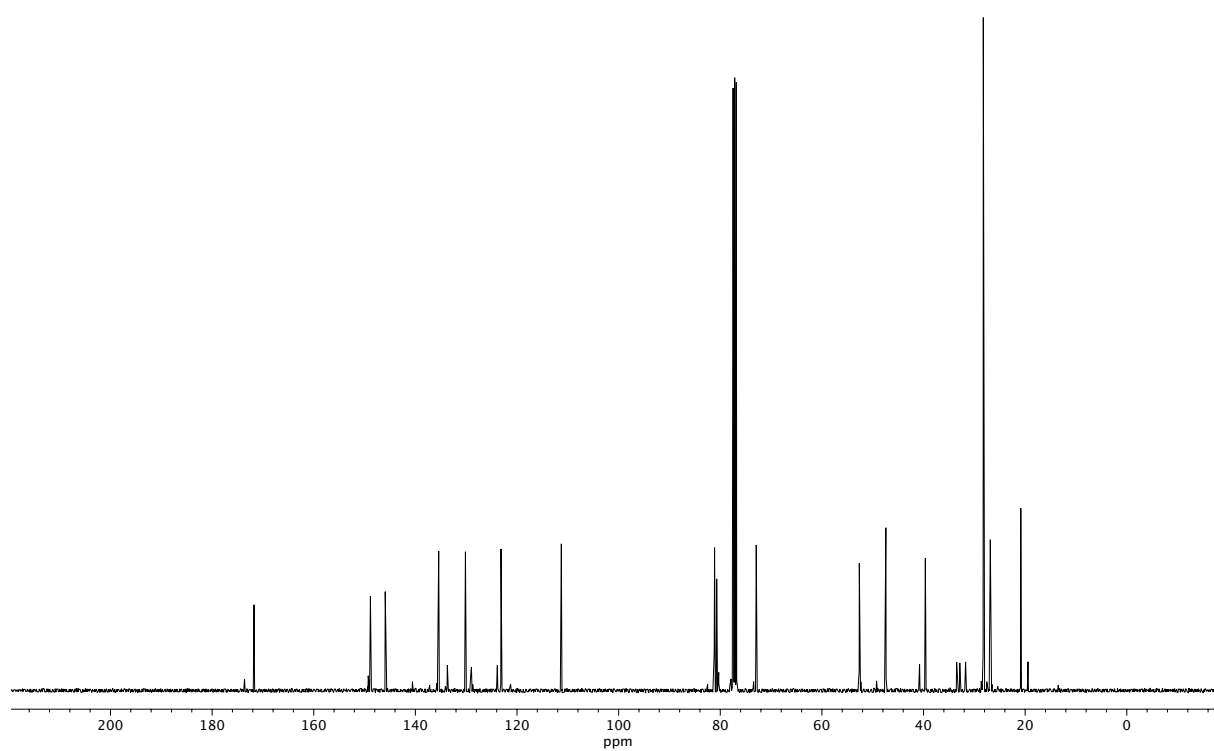


Figure A7.22  $^1\text{H}$  NMR (400 MHz,  $\text{CDCl}_3$ ) of compound **126**.



**Figure A7.23** Infrared spectrum (Thin Film, NaCl) of compound **126**.



**Figure A7.24** <sup>13</sup>C NMR (100 MHz, CDCl<sub>3</sub>) of compound **126**.

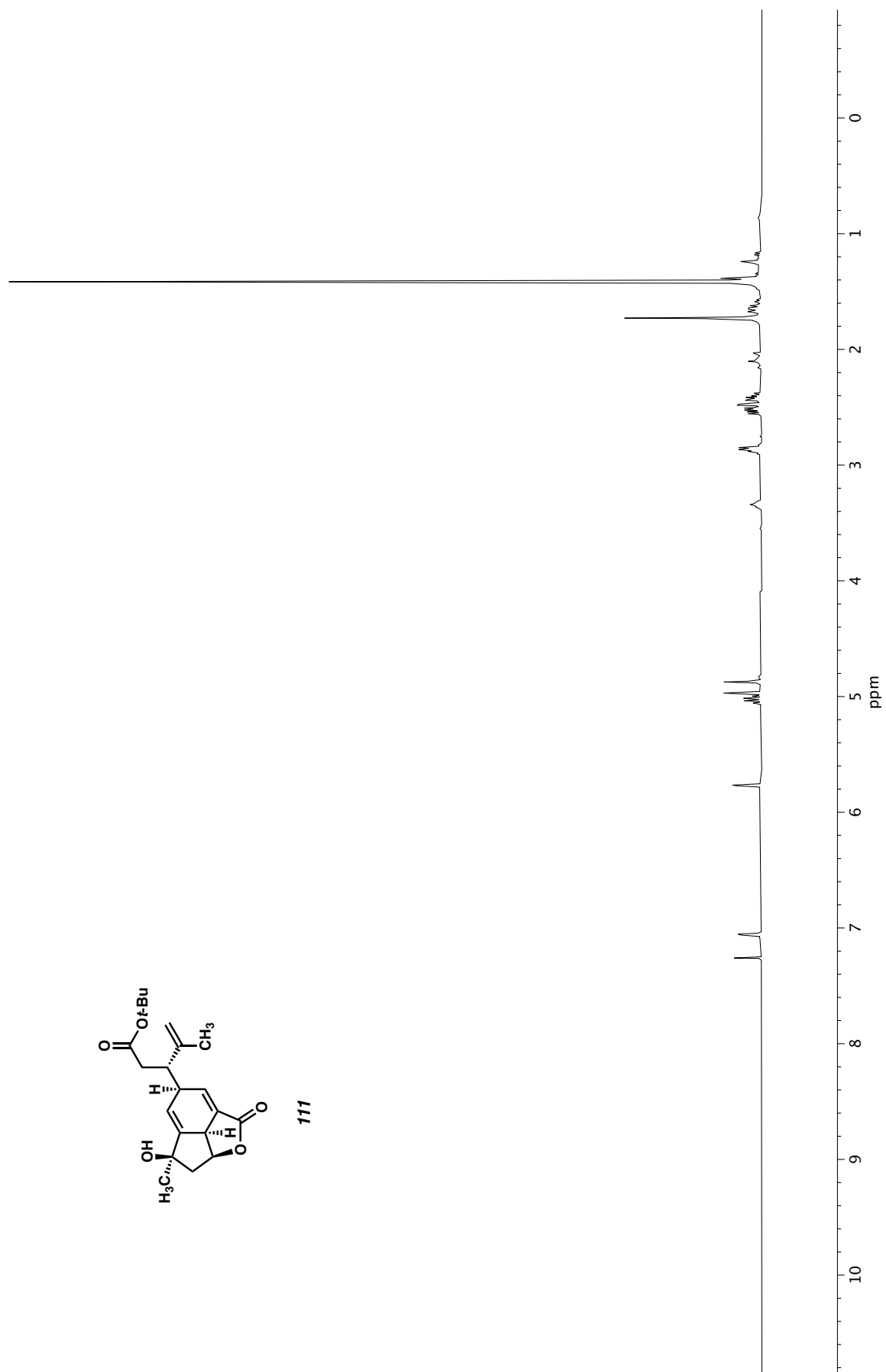
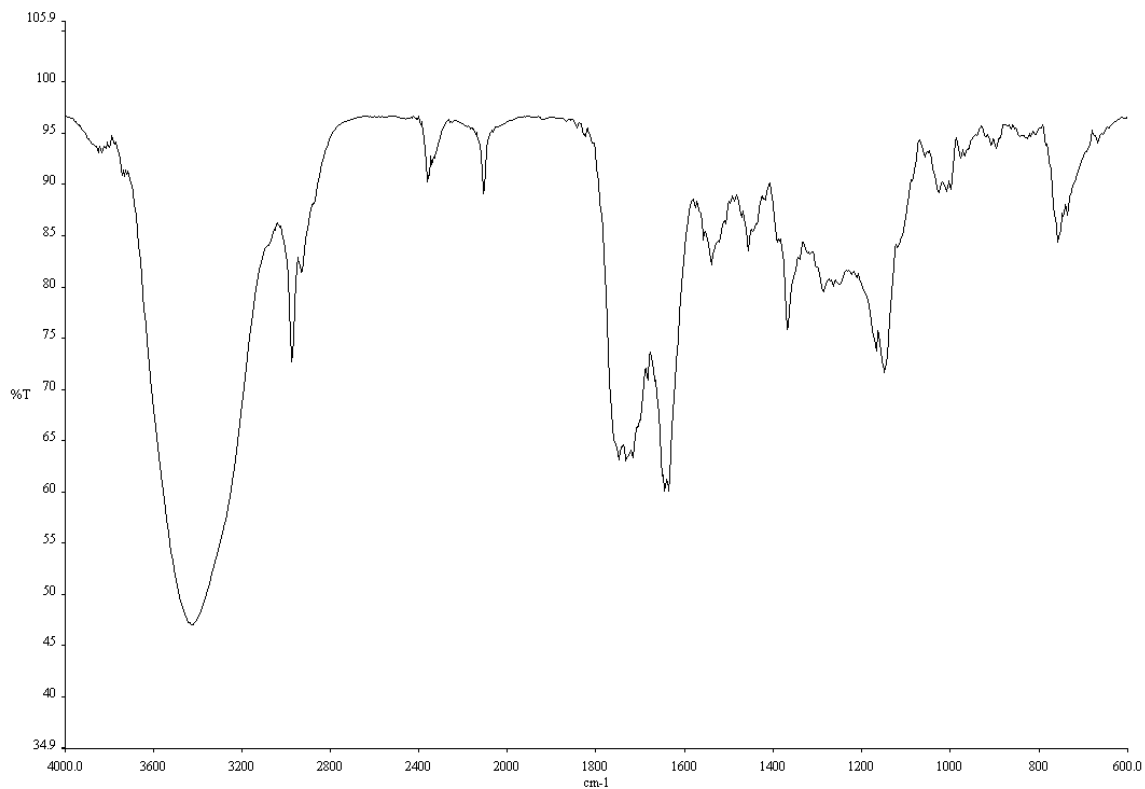
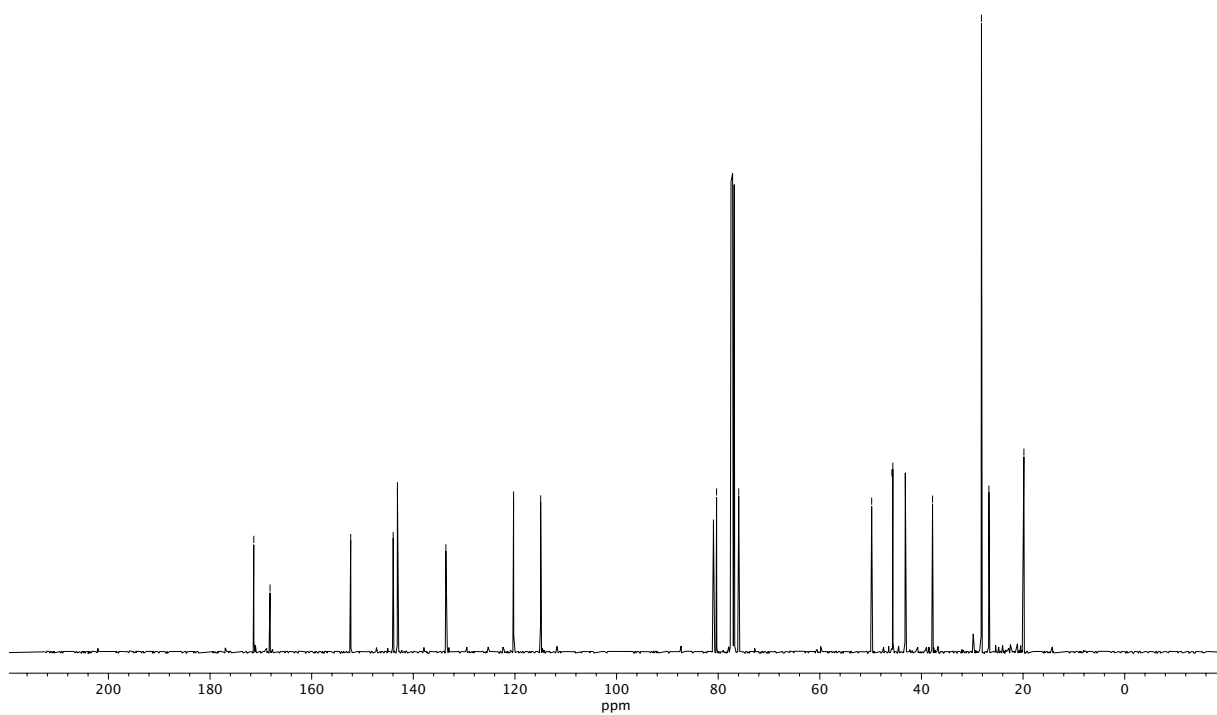


Figure A7.25  $^1\text{H}$  NMR (400 MHz,  $\text{CDCl}_3$ ) of compound **111**.





**Figure A7.26** Infrared spectrum (Thin Film, NaCl) of compound **111**.



**Figure A7.27** <sup>13</sup>C NMR (100 MHz, CDCl<sub>3</sub>) of compound **111**.

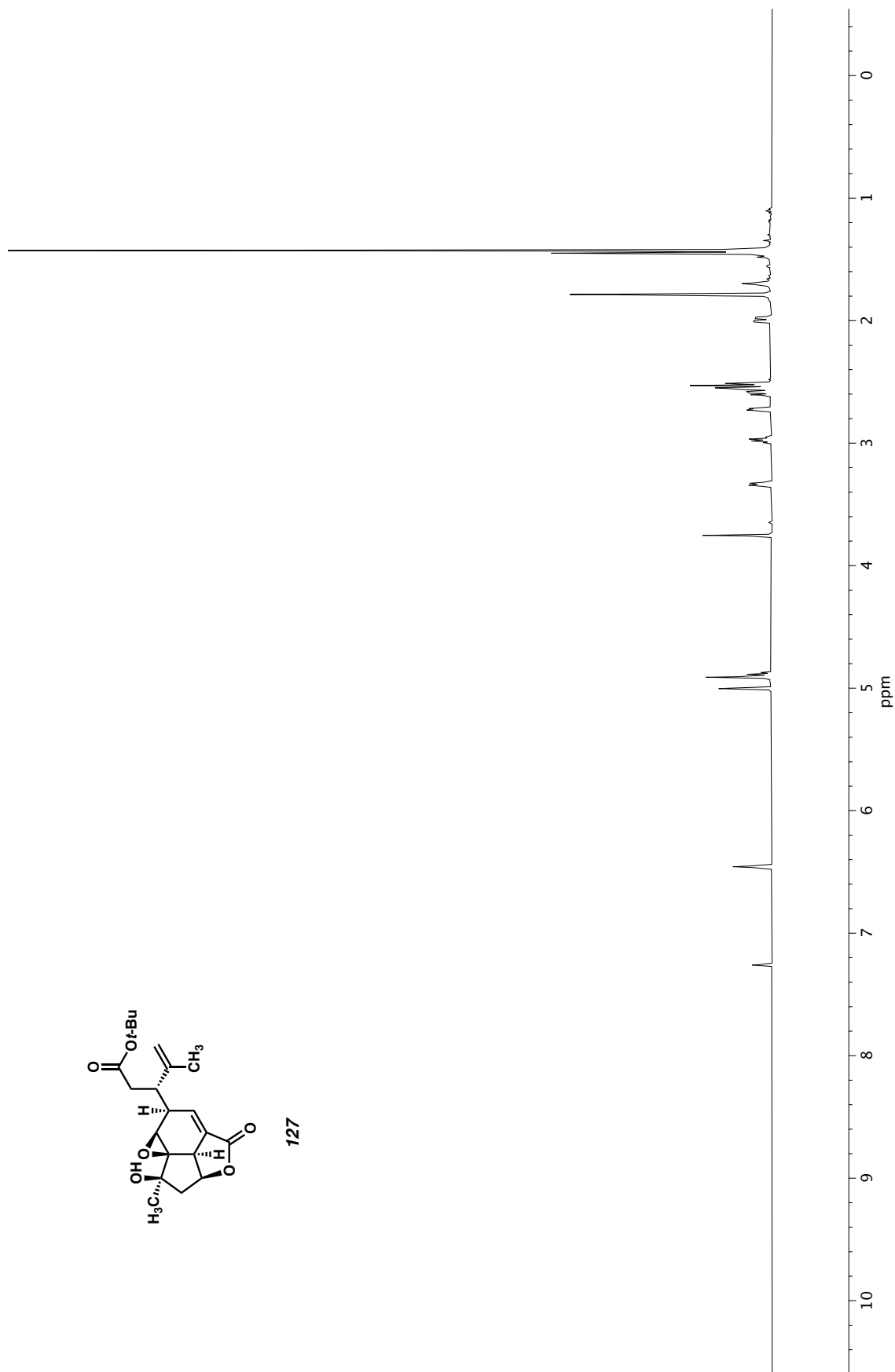
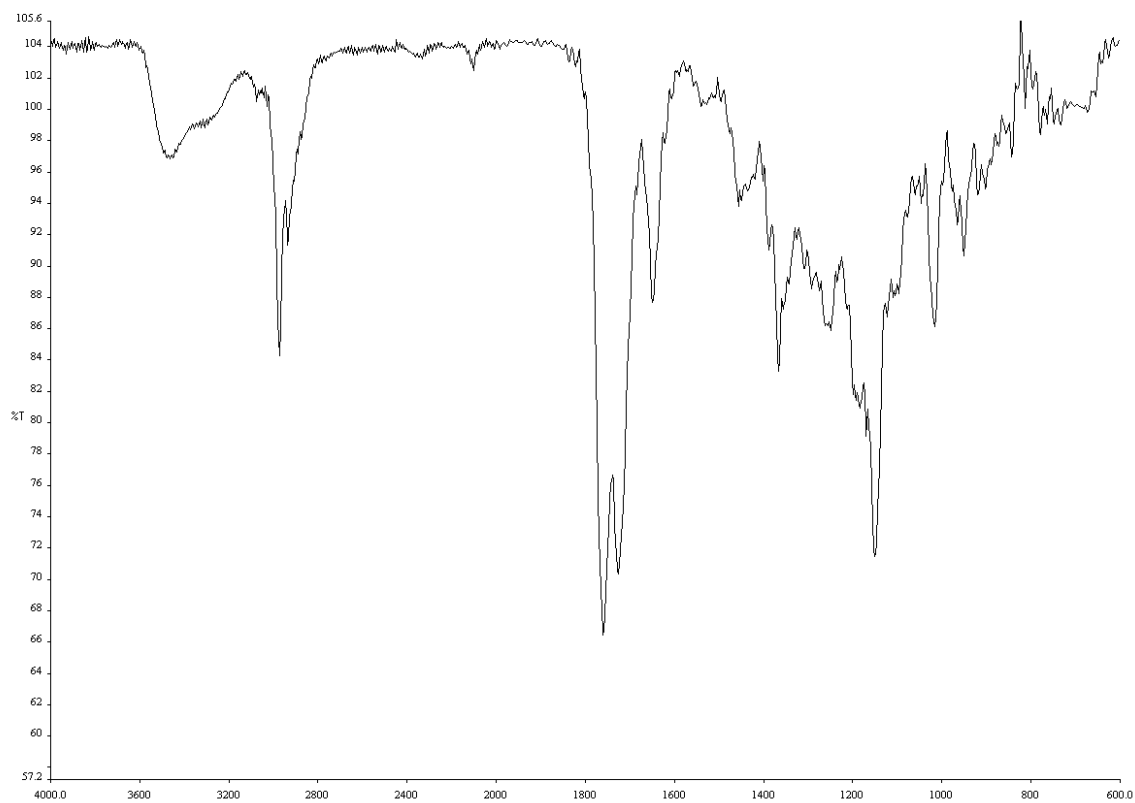
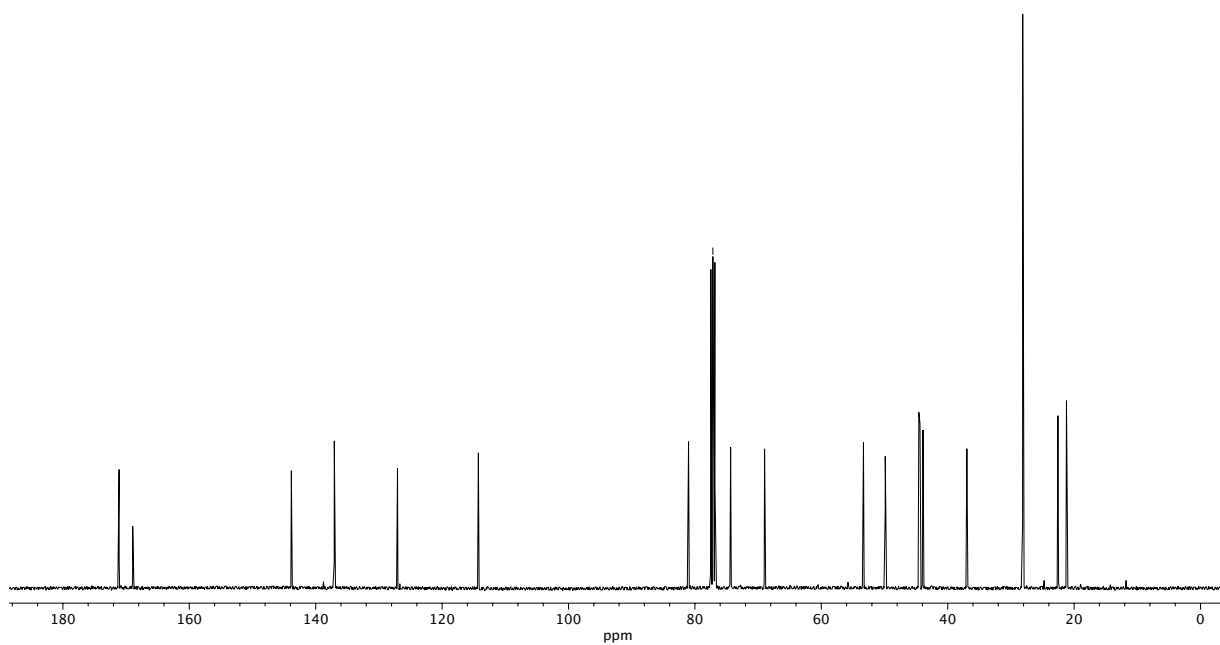


Figure A7.28  $^1\text{H}$  NMR (500 MHz,  $\text{CDCl}_3$ ) of compound **127**.



**Figure A7.29** Infrared spectrum (Thin Film, NaCl) of compound **127**.



**Figure A7.30** <sup>13</sup>C NMR (100 MHz, CDCl<sub>3</sub>) of compound **127**.

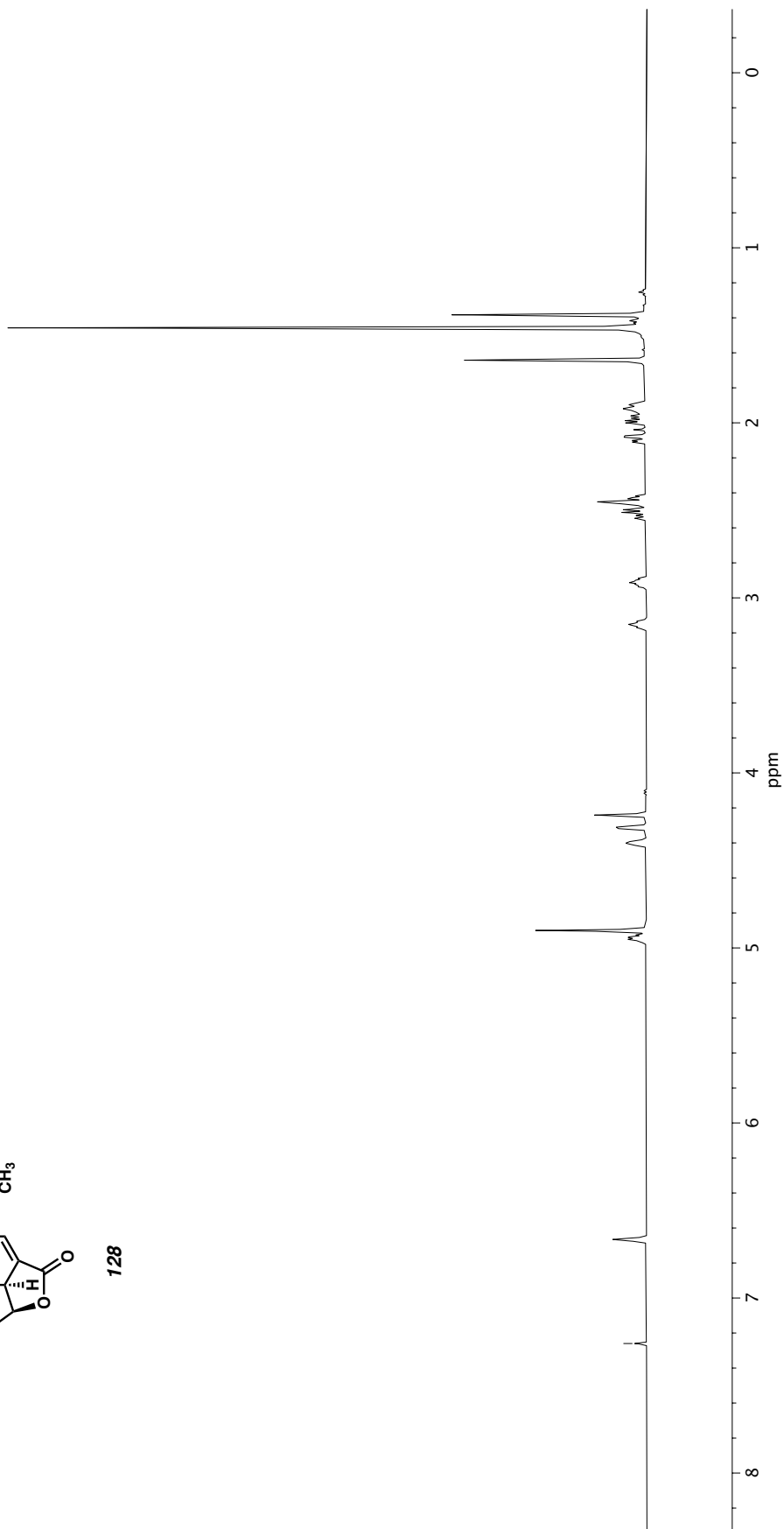
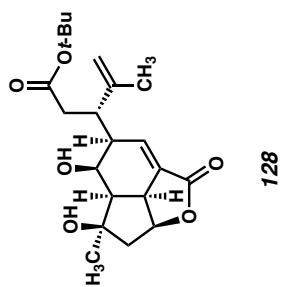
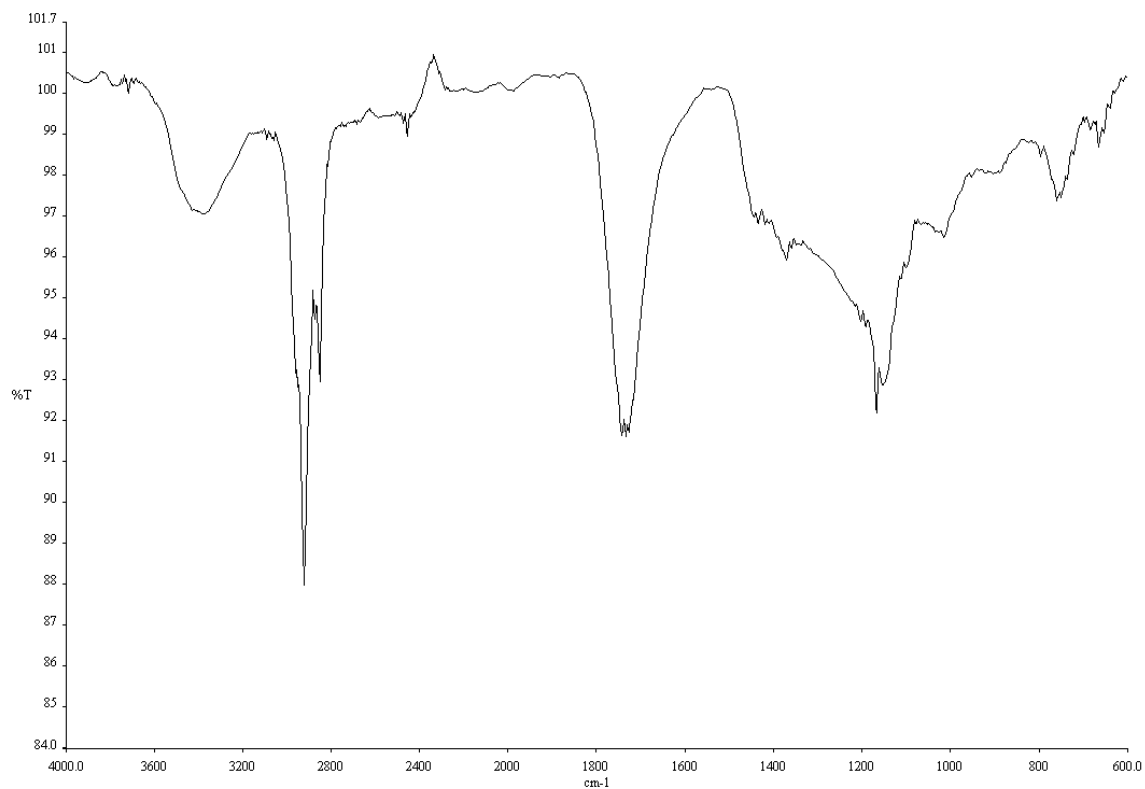
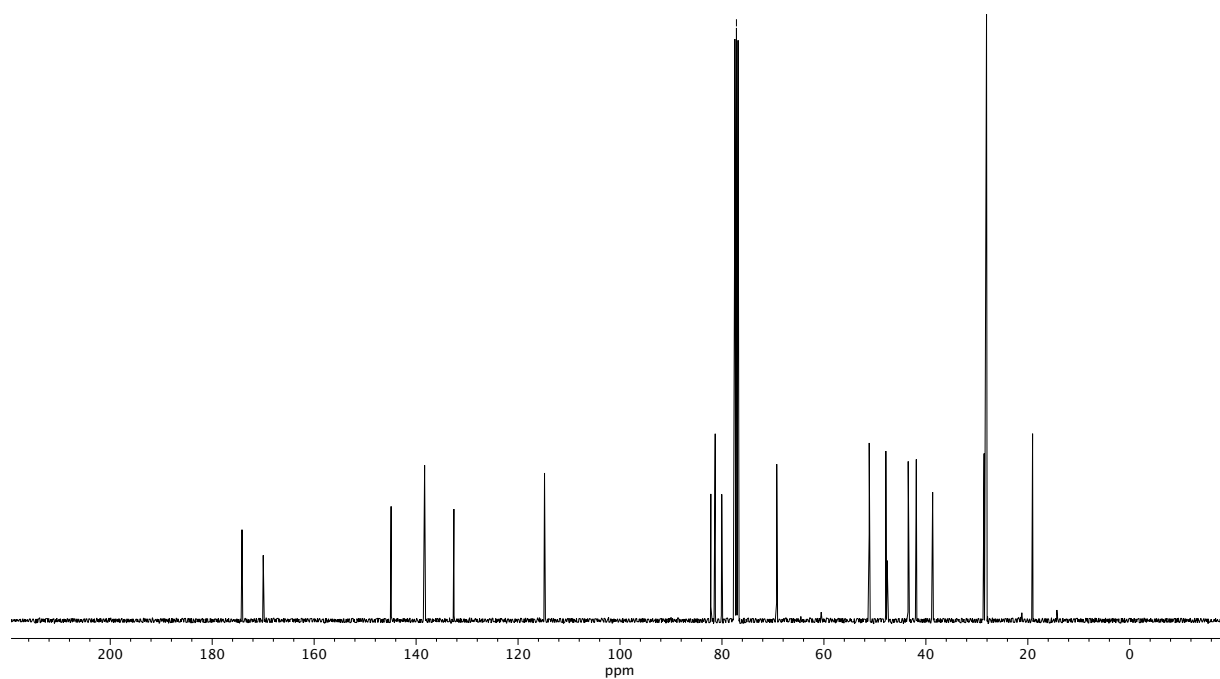


Figure A7.31 <sup>1</sup>H NMR (500 MHz, CDCl<sub>3</sub>) of compound 128.



**Figure A7.32** Infrared spectrum (Thin Film, NaCl) of compound **128**.



**Figure A7.33** <sup>13</sup>C NMR (100 MHz, CDCl<sub>3</sub>) of compound **128**.

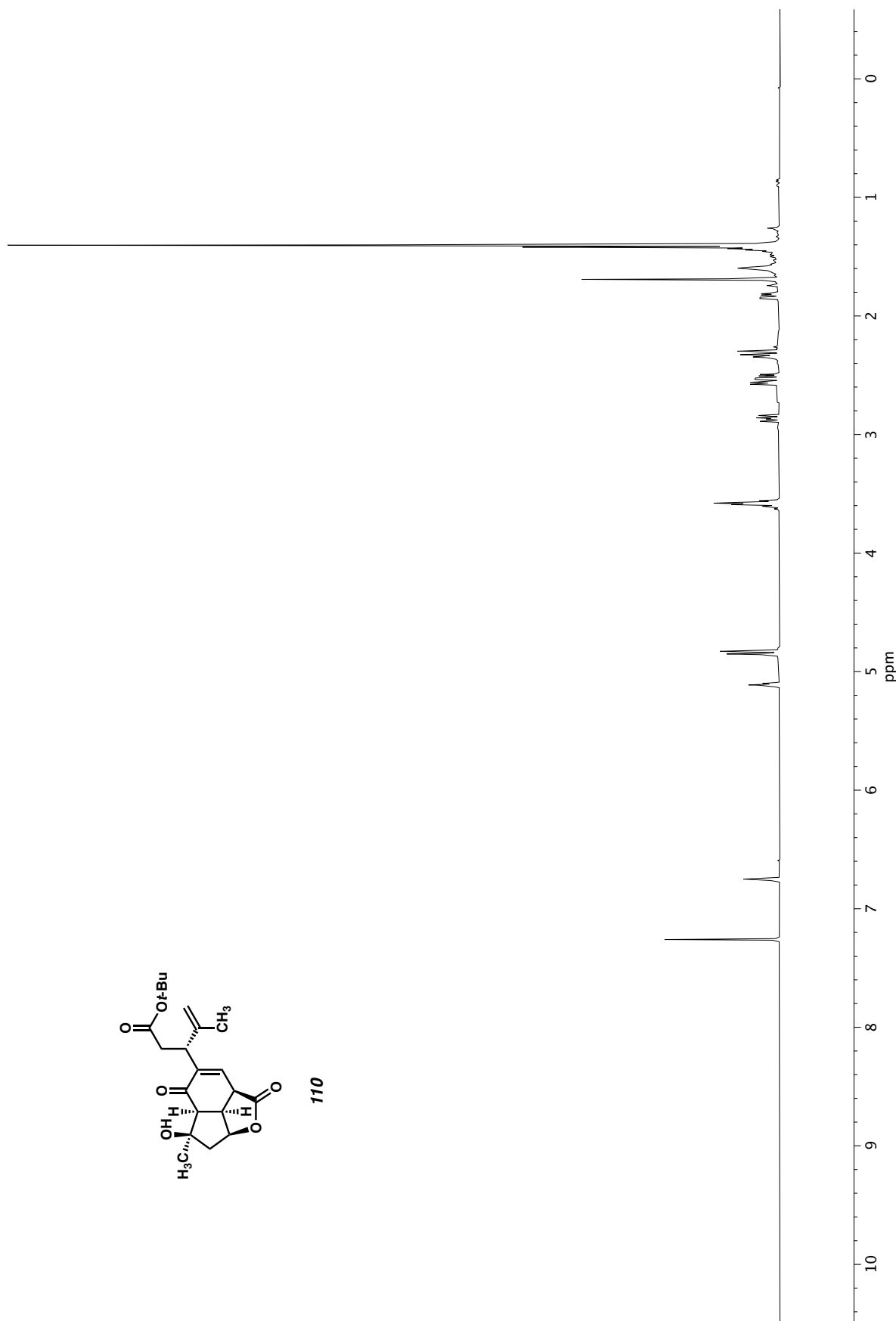
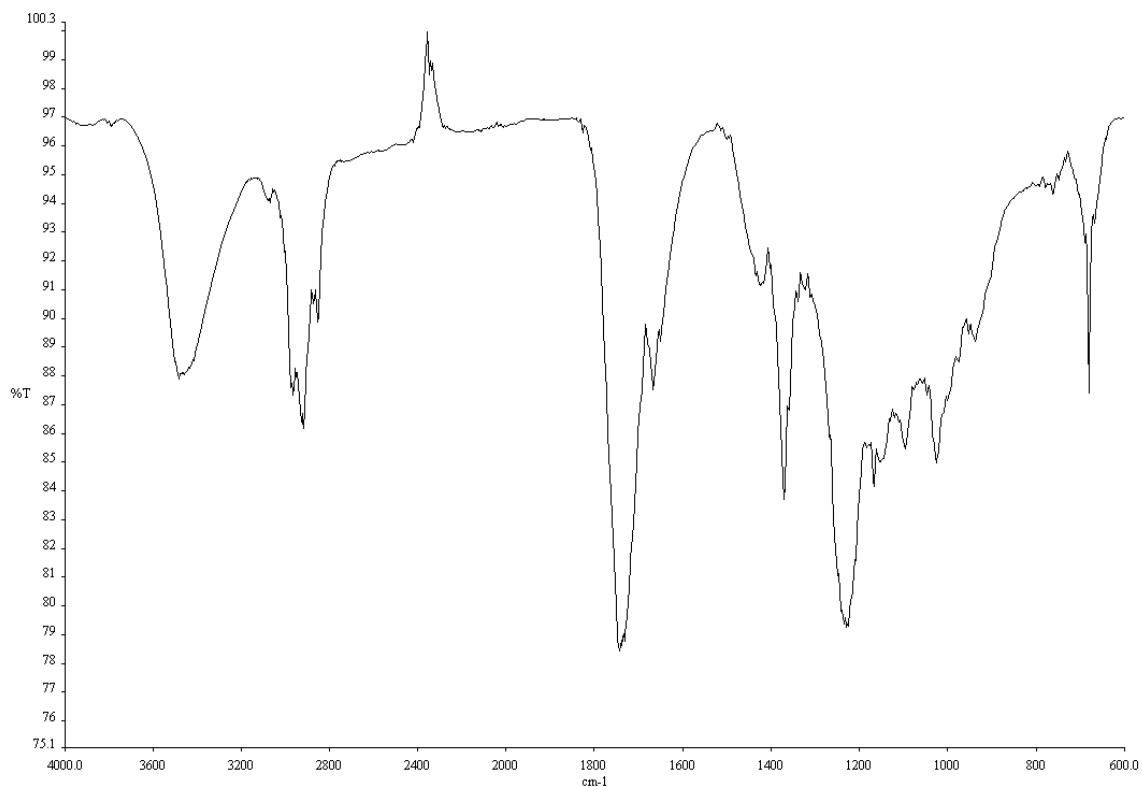
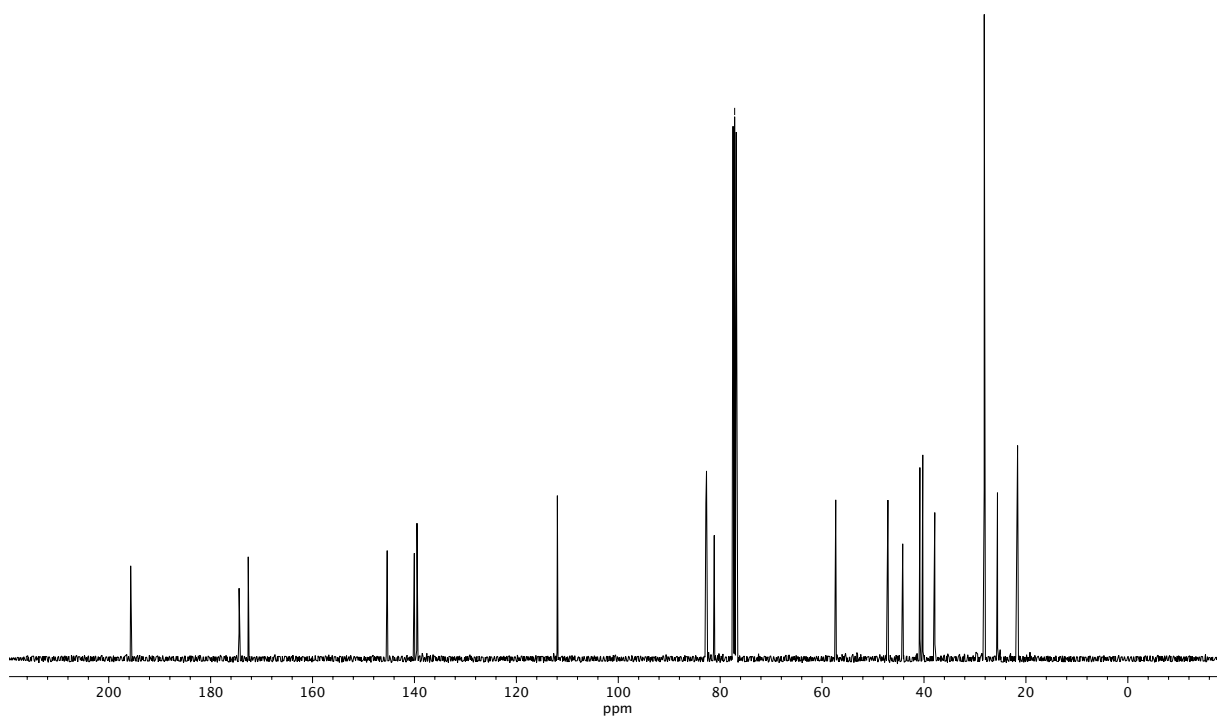


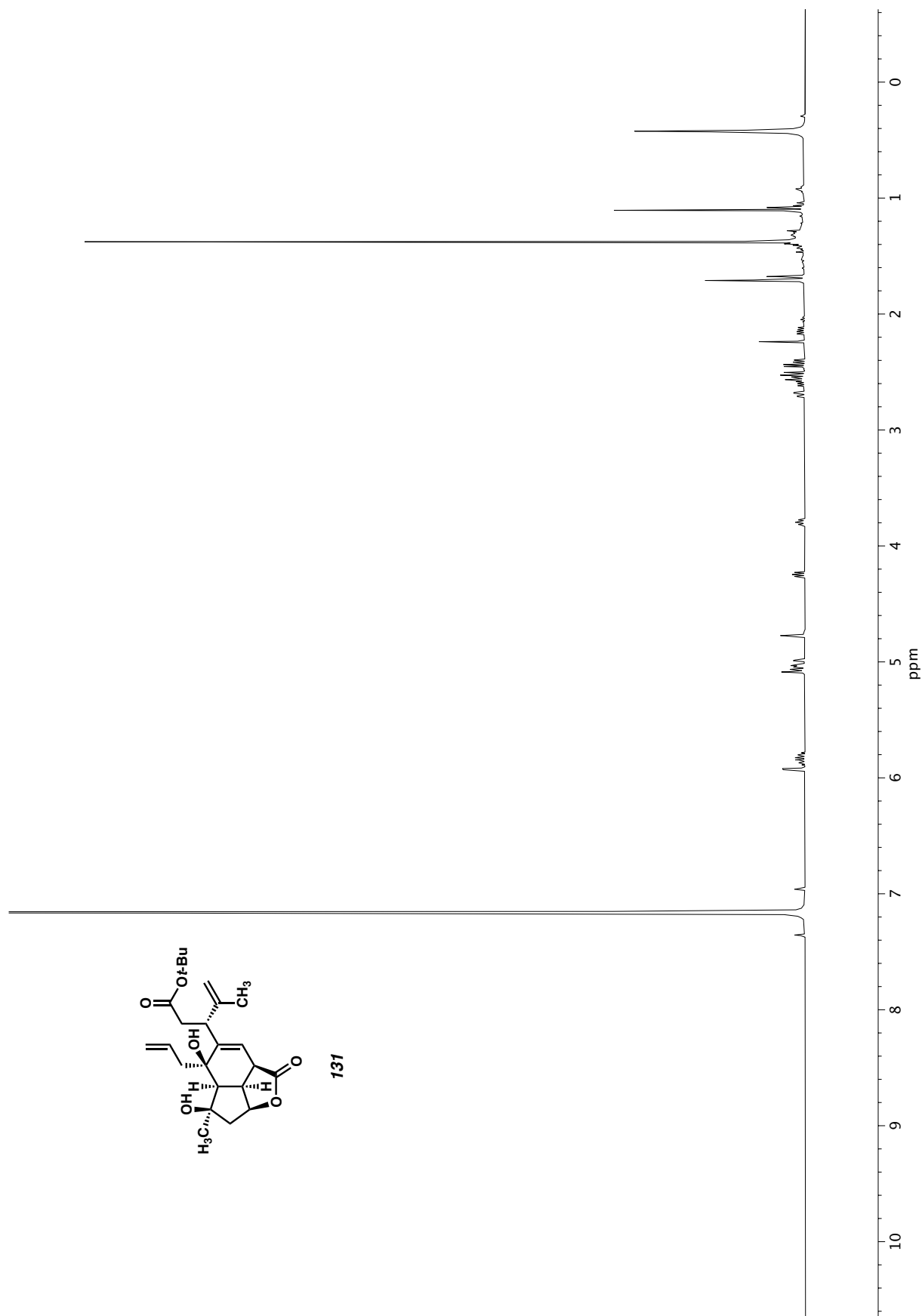
Figure A7.34 <sup>1</sup>H NMR (500 MHz, CDCl<sub>3</sub>) of compound **110**.



**Figure A7.35** Infrared spectrum (Thin Film, NaCl) of compound **110**.



**Figure A7.36** <sup>13</sup>C NMR (100 MHz, CDCl<sub>3</sub>) of compound **110**.





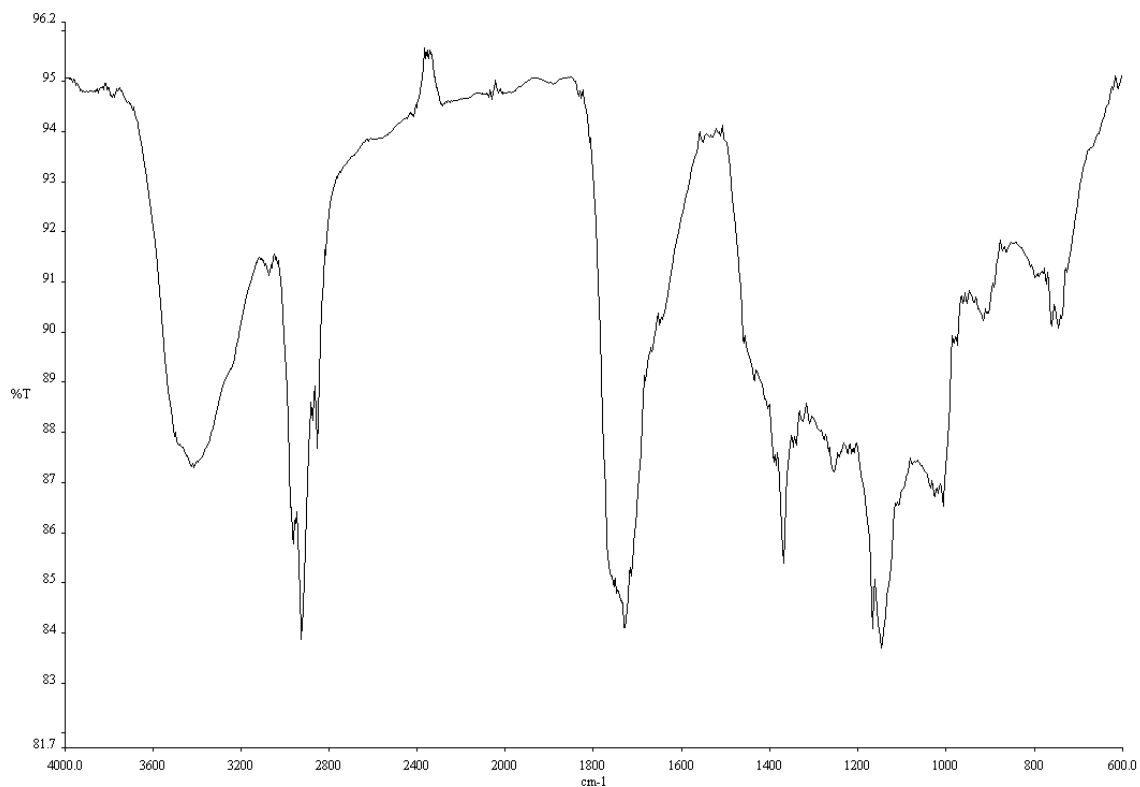


**Figure A7.38** Infrared spectrum (Thin Film, NaCl) of compound **131**.

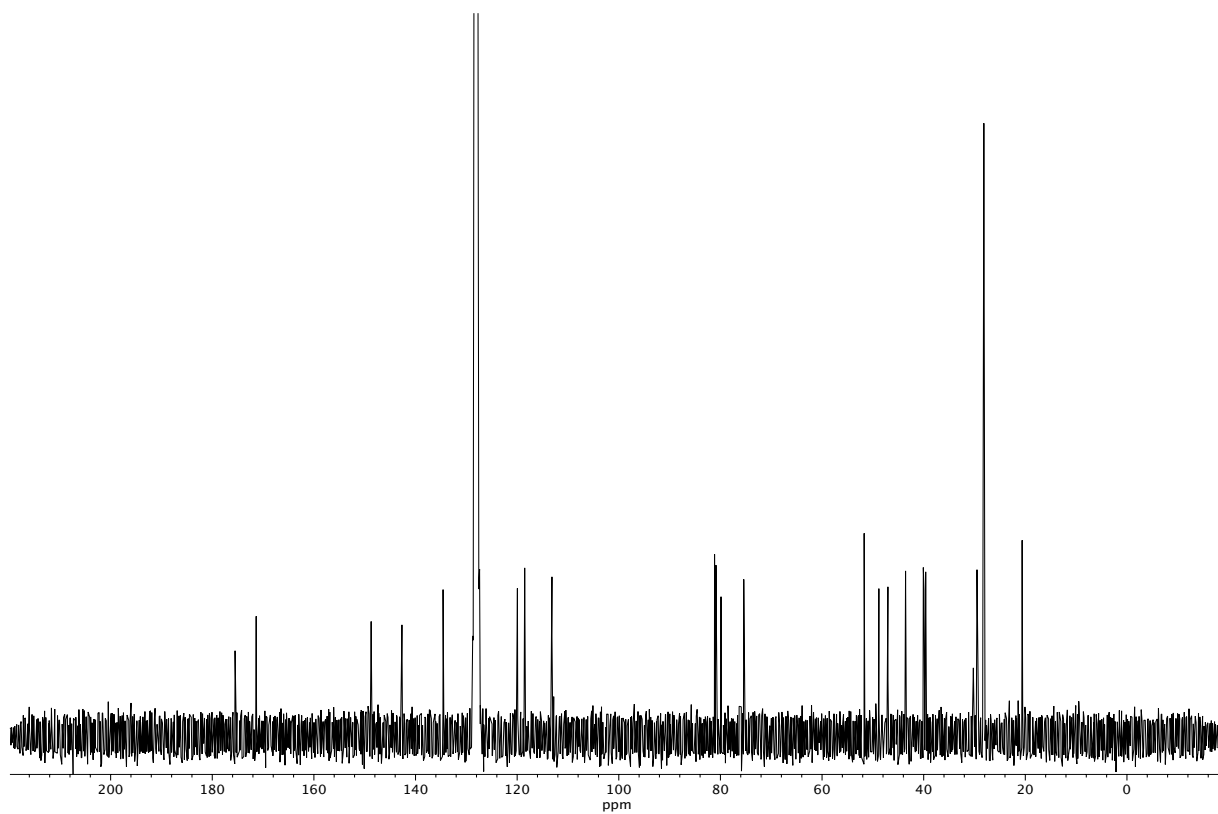


**Figure A7.39** <sup>13</sup>C NMR (100 MHz, CDCl<sub>3</sub>) of compound **131**.

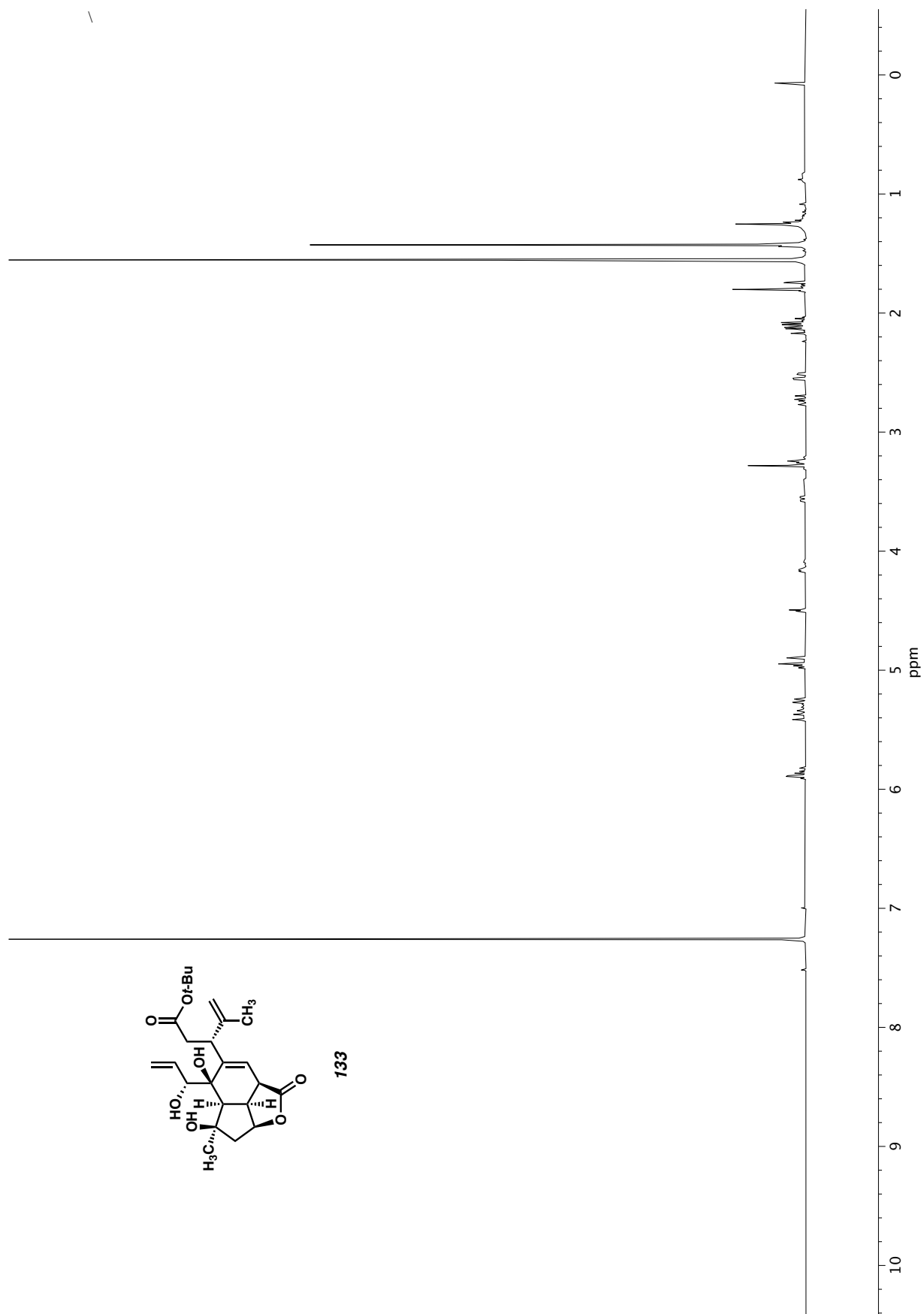
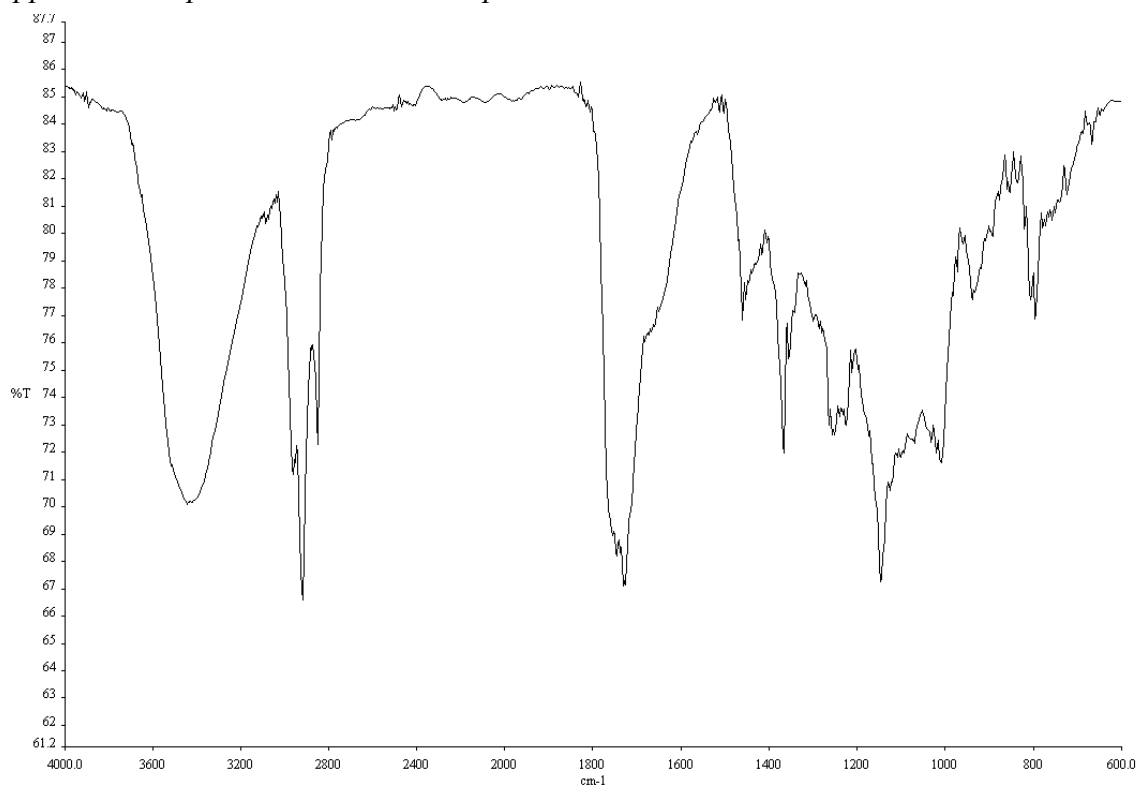
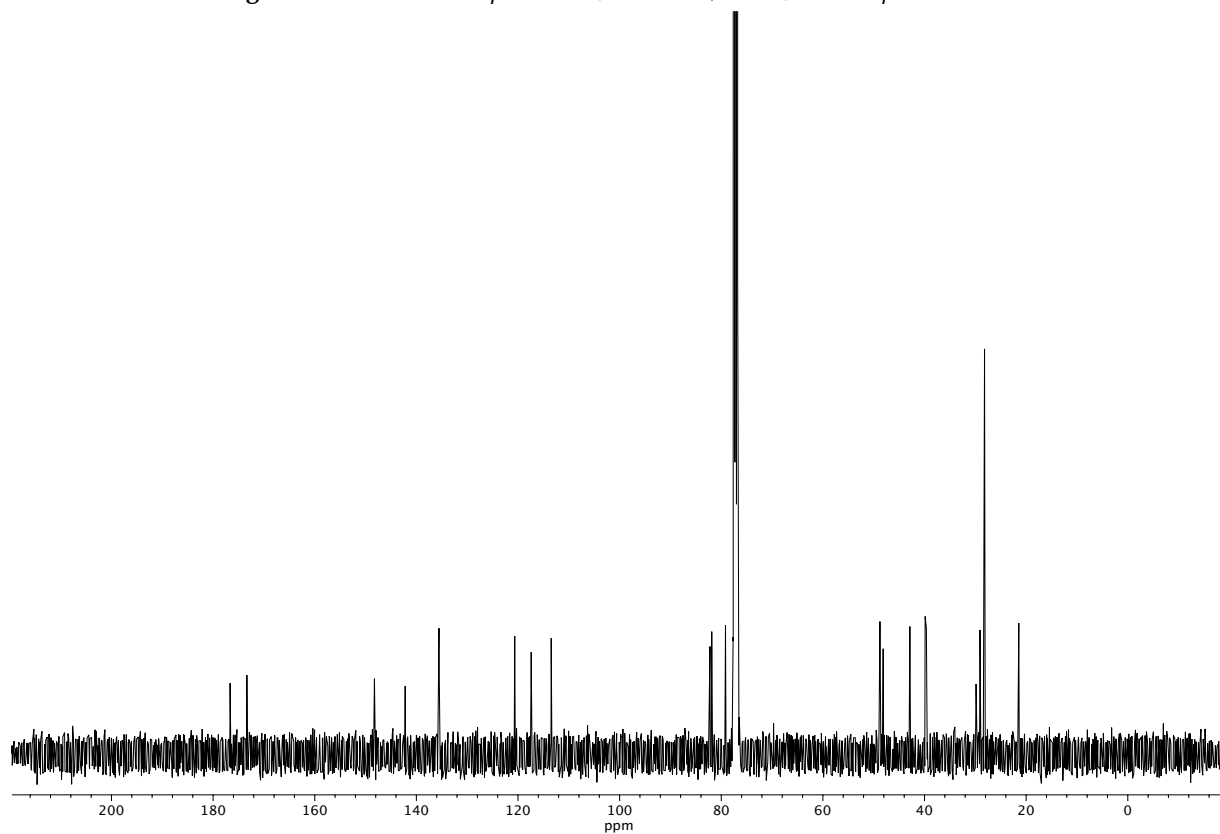


Figure A7.40  $^1\text{H}$  NMR (400 MHz,  $\text{CDCl}_3$ ) of compound **133**.



**Figure A7.41** Infrared spectrum (Thin Film, NaCl) of compound **133**.



**Figure A7.42** <sup>13</sup>C NMR (100 MHz, CDCl<sub>3</sub>) of compound **133**.

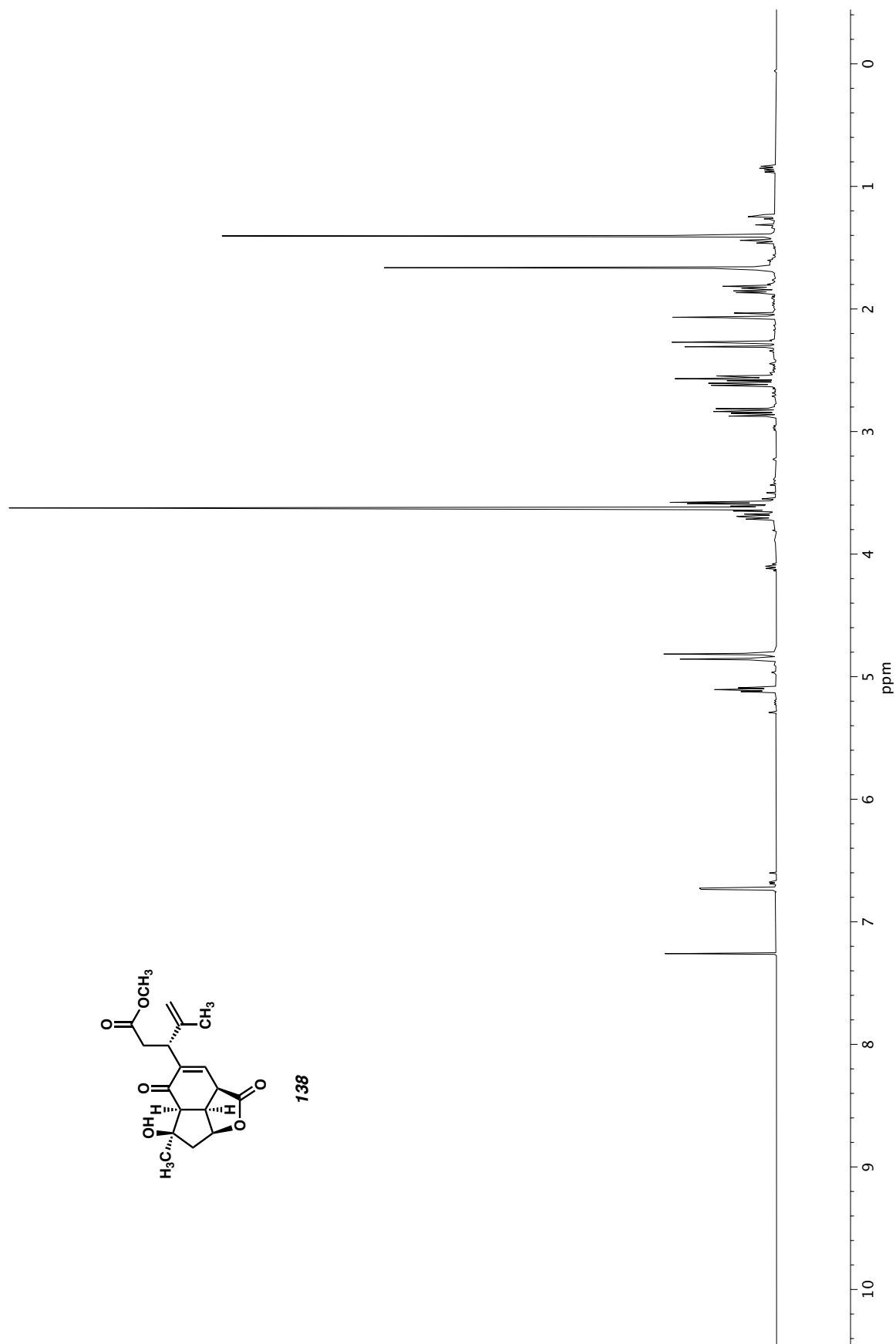


**Figure A7.43**  $^1\text{H}$  NMR (400 MHz,  $\text{CDCl}_3$ ) of compound **138**.

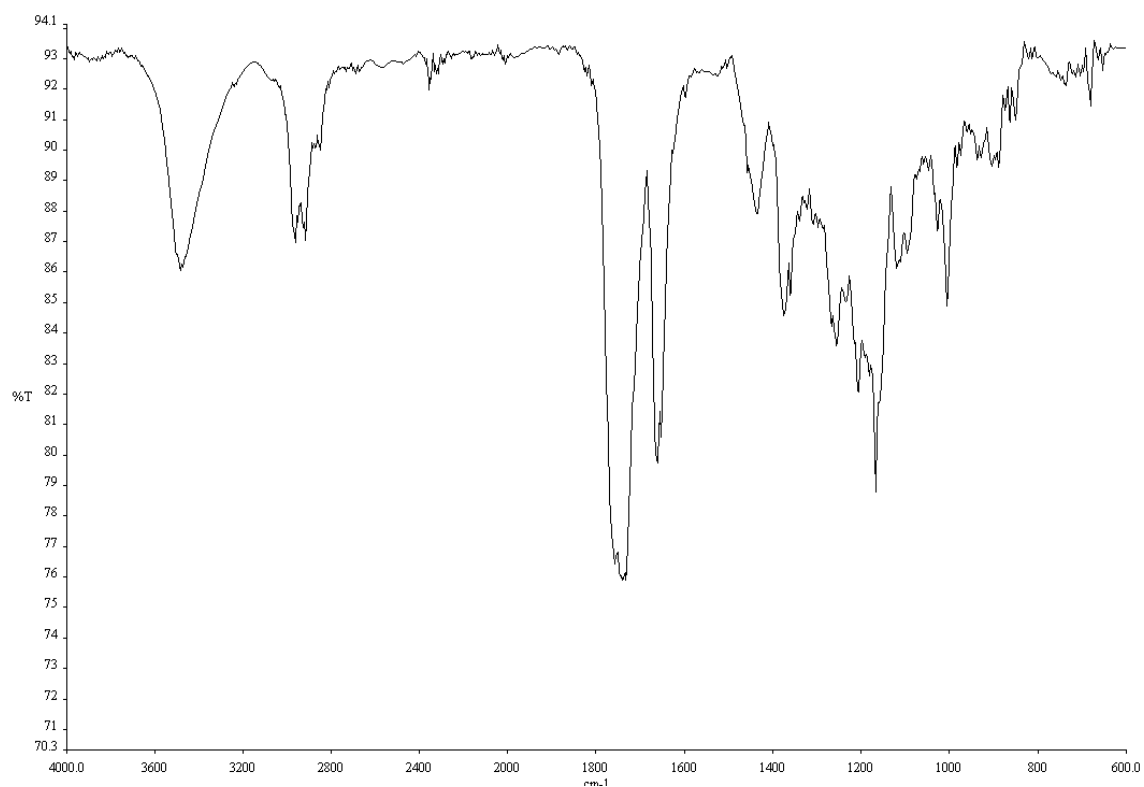


**Figure A7.44** Infrared spectrum (Thin Film, NaCl) of compound **138**.

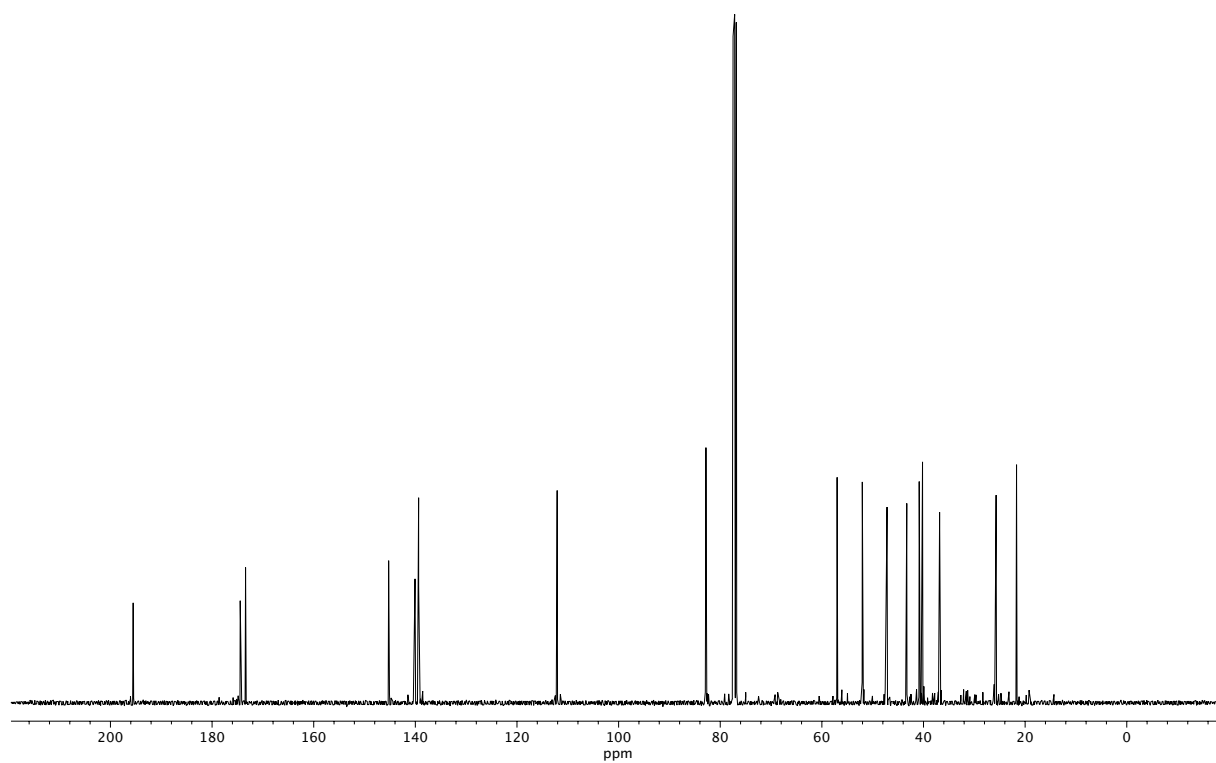


**Figure A7.45** <sup>13</sup>C NMR (100 MHz, CDCl<sub>3</sub>) of compound **133**.

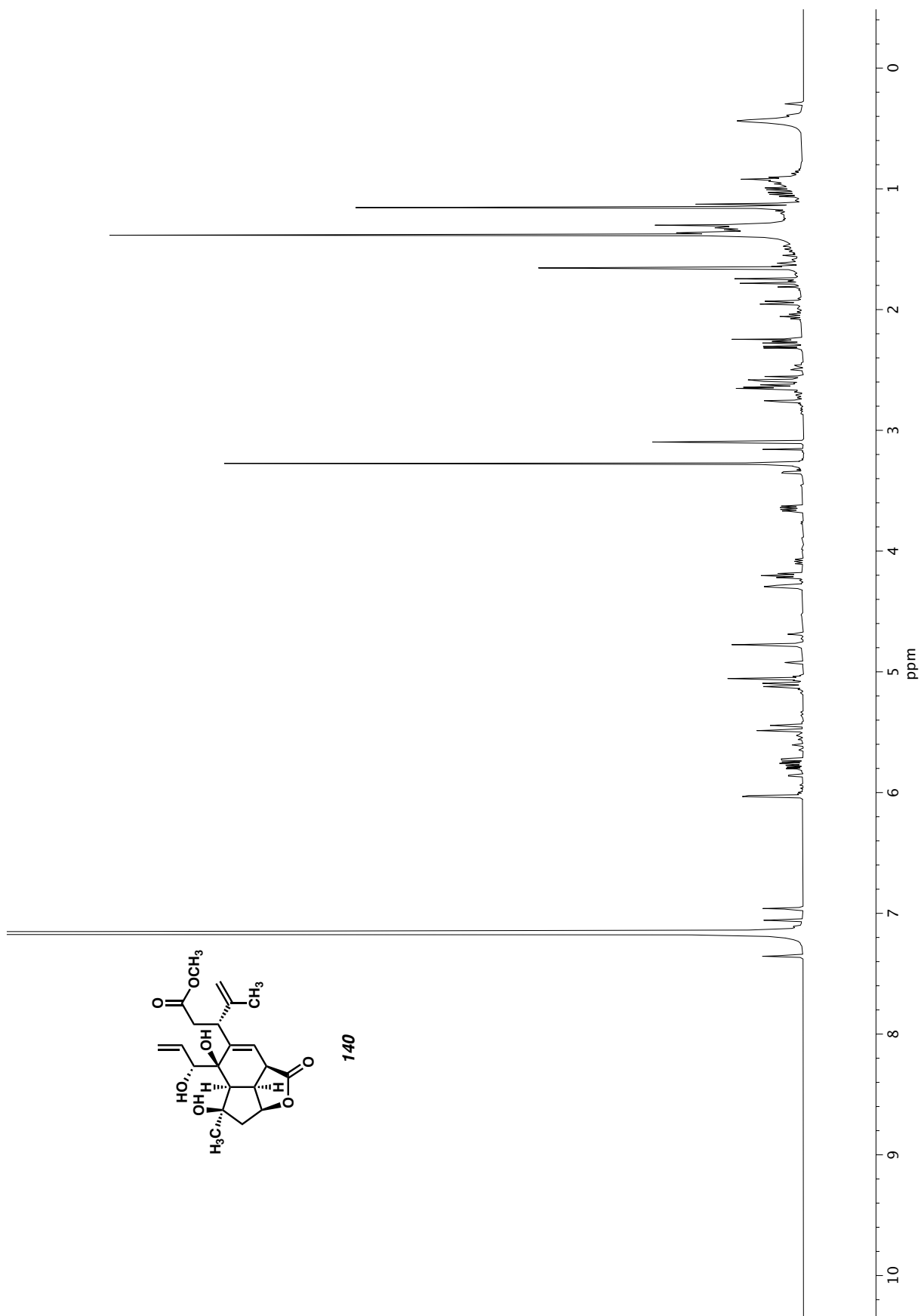
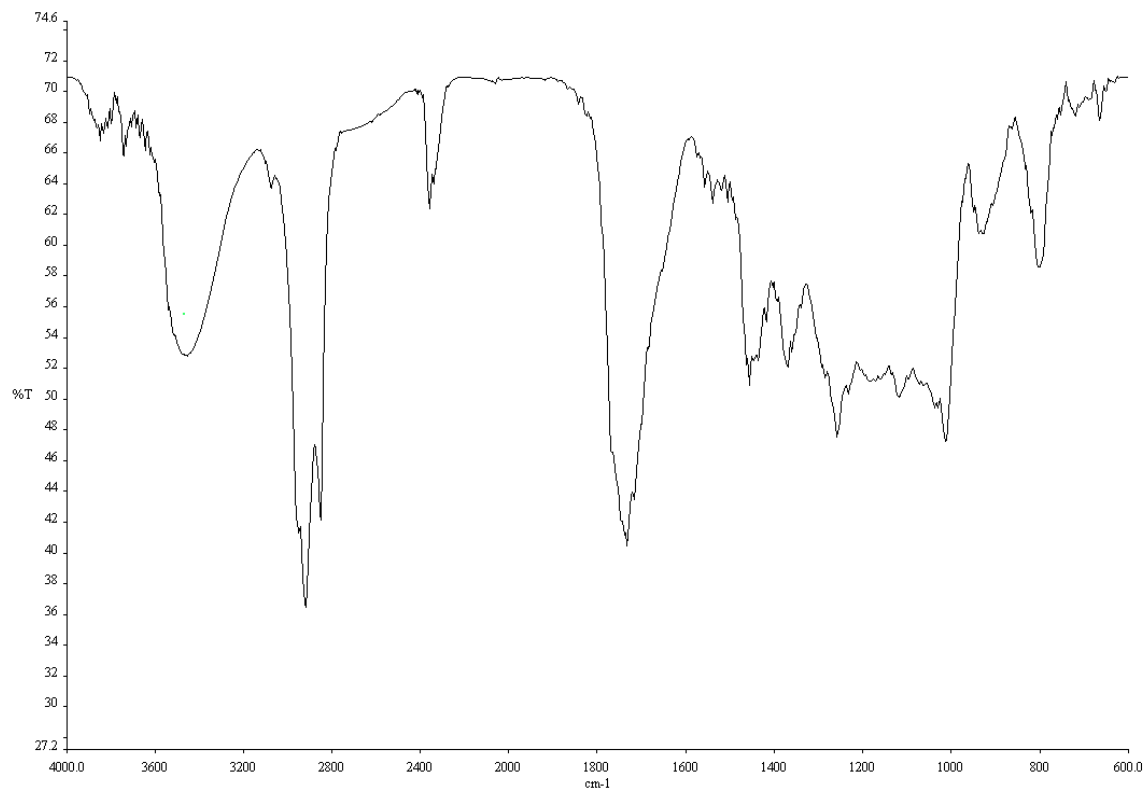
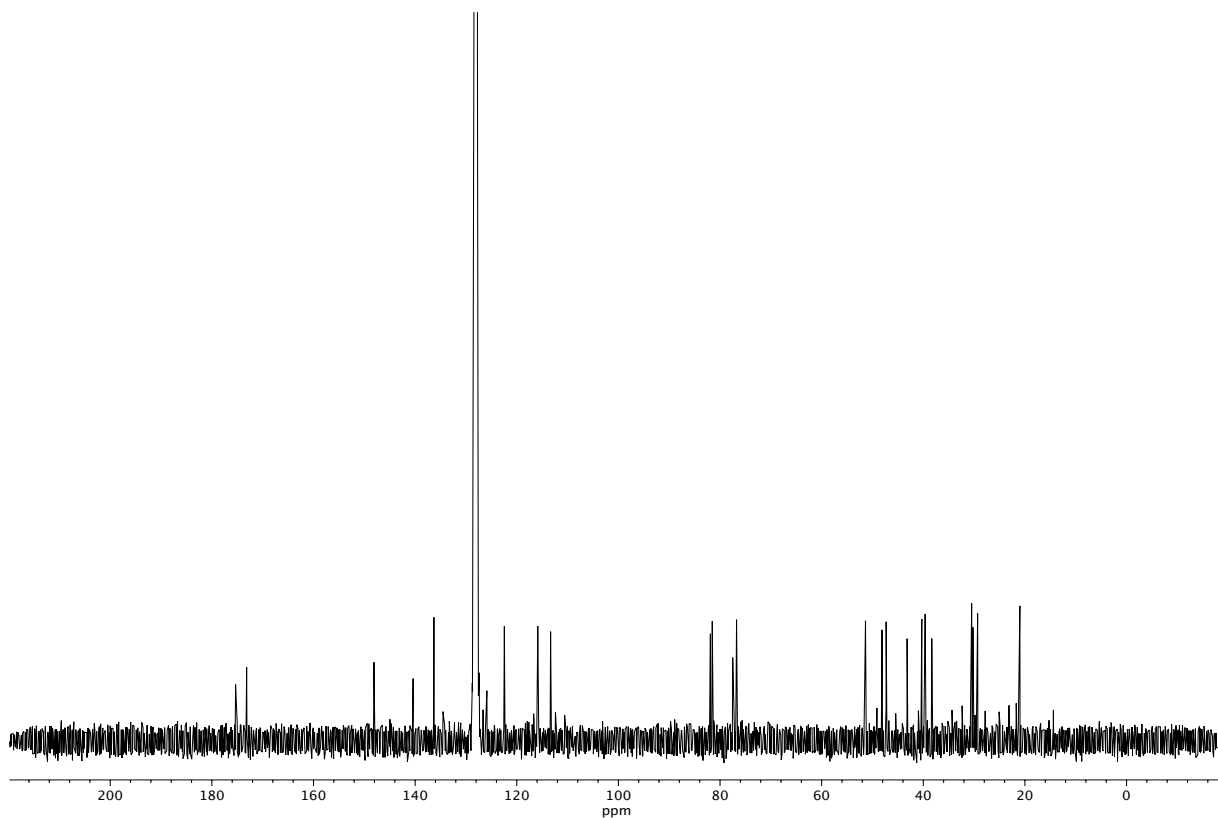


Figure A7.46  $^1\text{H}$  NMR (400 MHz,  $\text{C}_6\text{D}_6$ ) of compound **140**.



**Figure A7.47** Infrared spectrum (Thin Film, NaCl) of compound **140**.



**Figure A7.48**  $^{13}\text{C}$  NMR (100 MHz,  $\text{CDCl}_3$ ) of compound **140**.

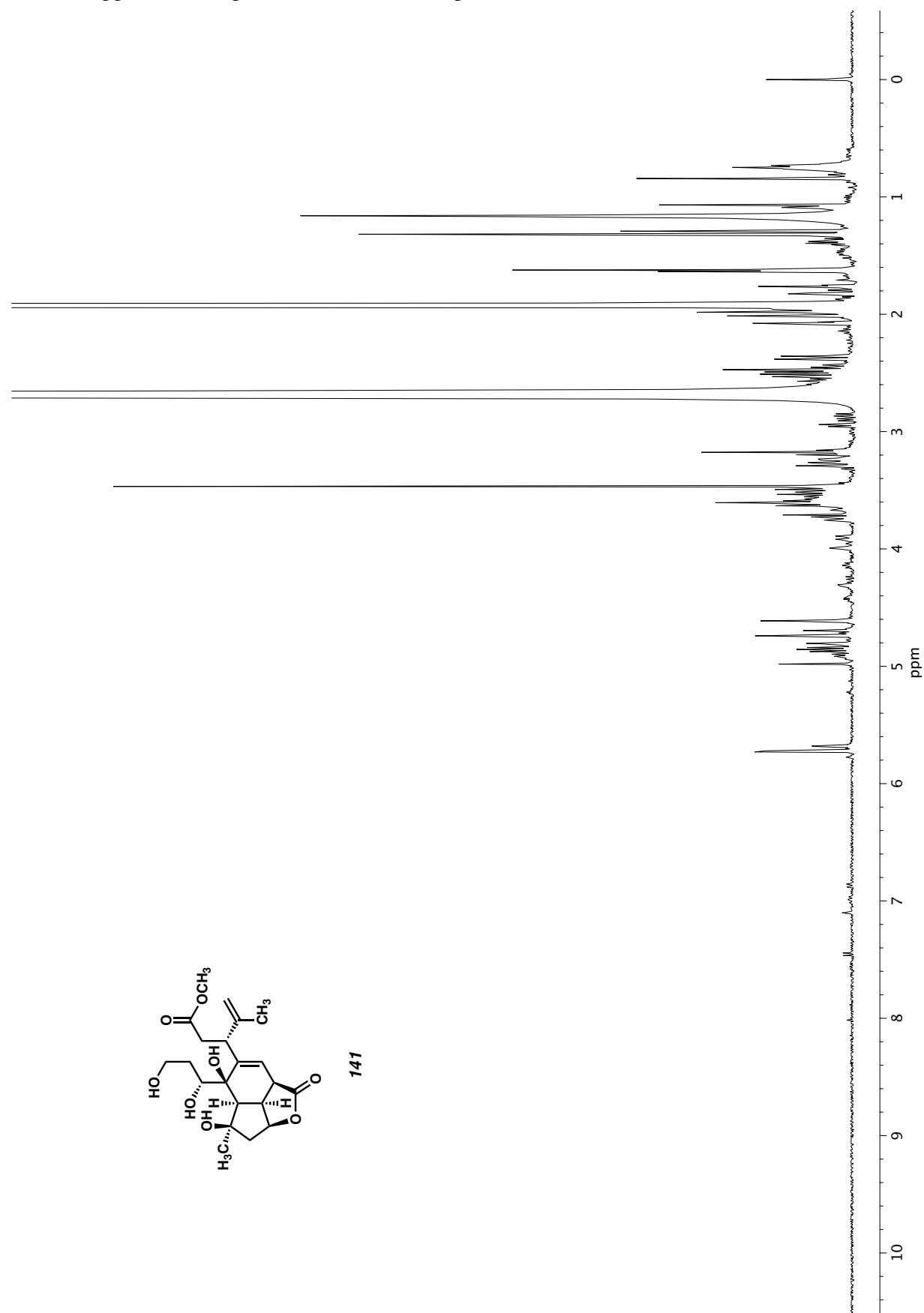
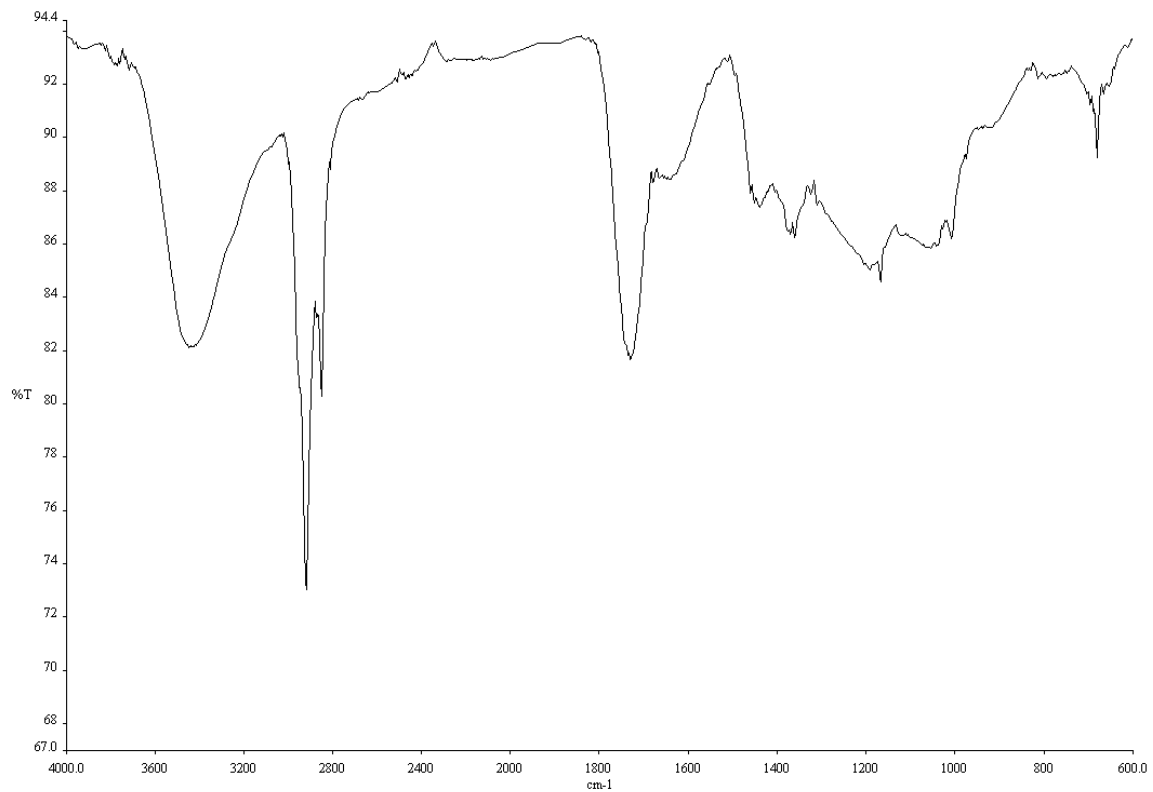
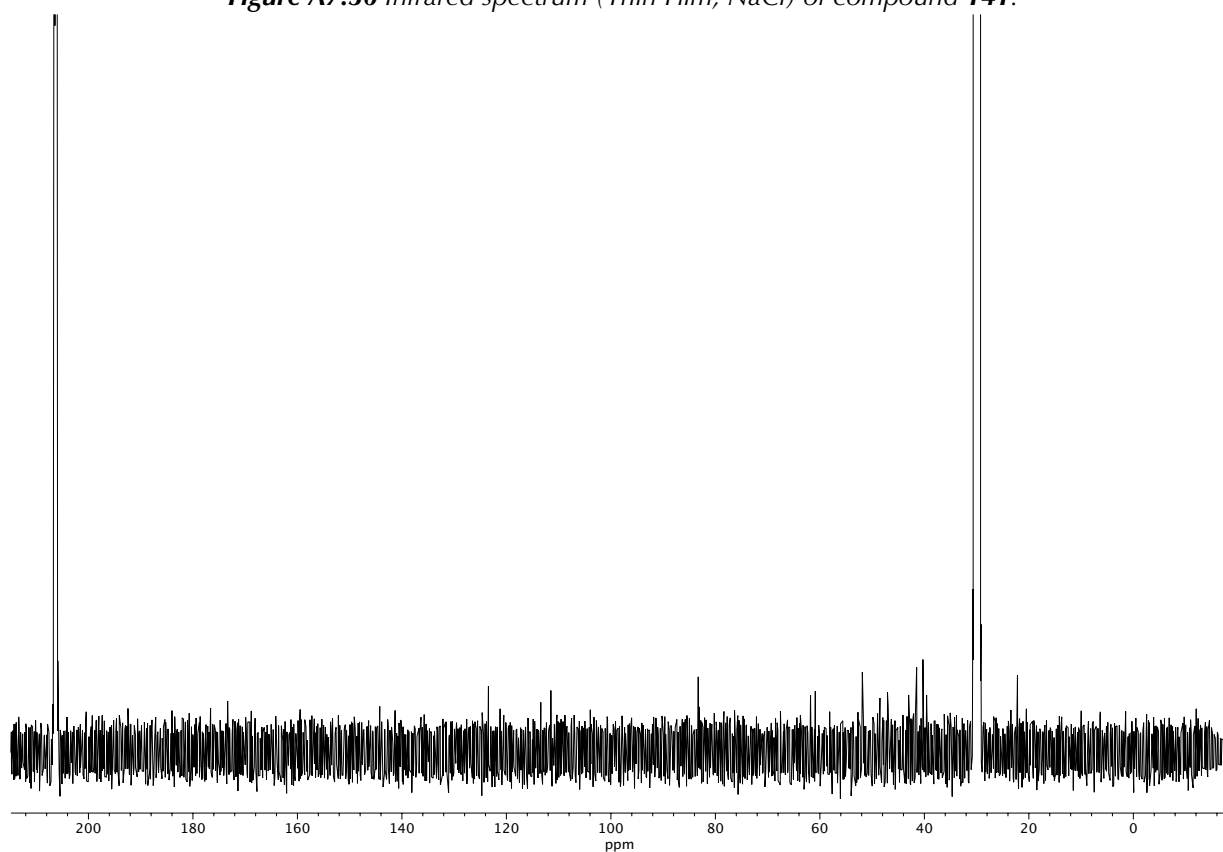


Figure A7.49 <sup>1</sup>H NMR (400 MHz, d<sub>6</sub>-acetone) of compound 141.

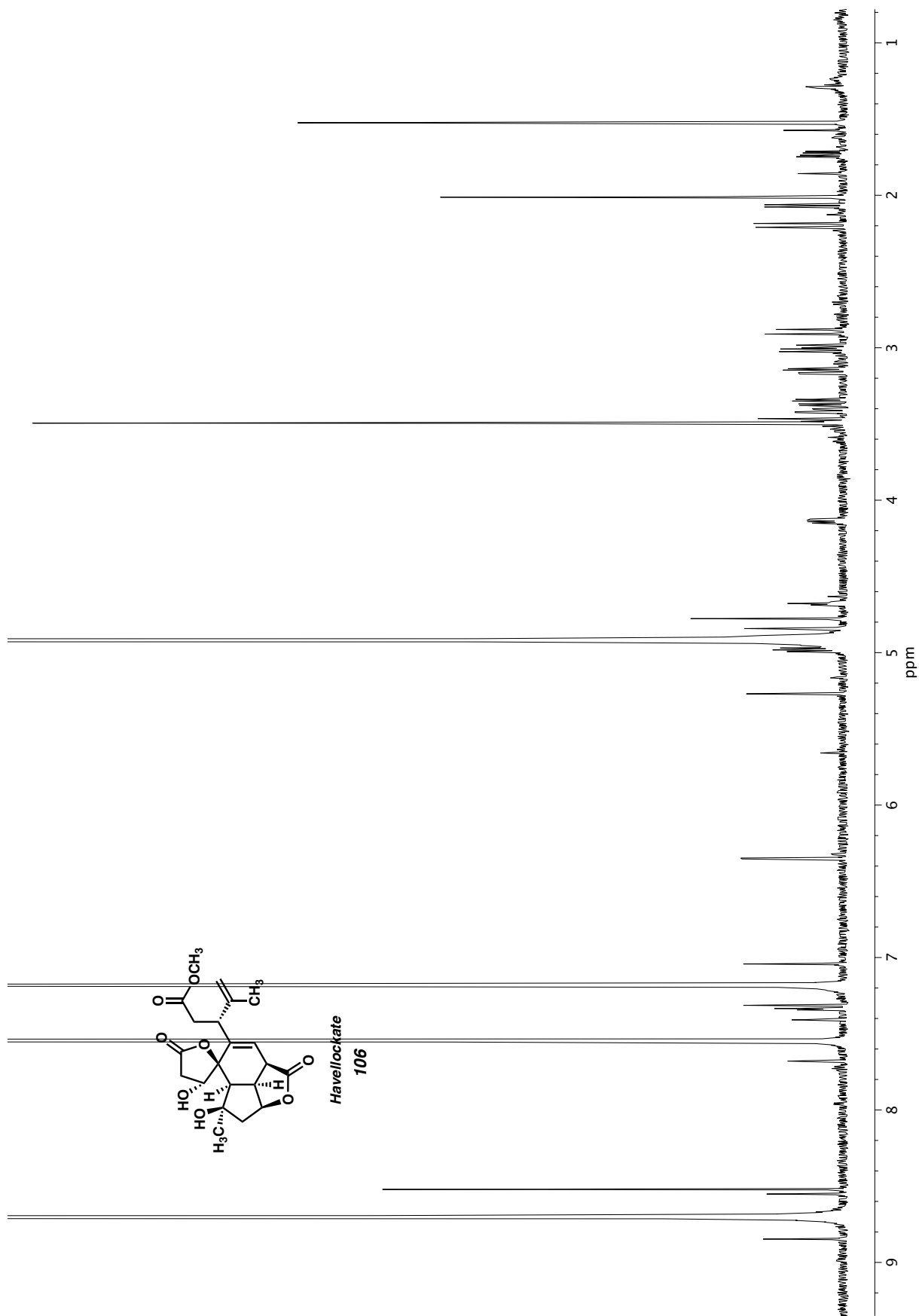


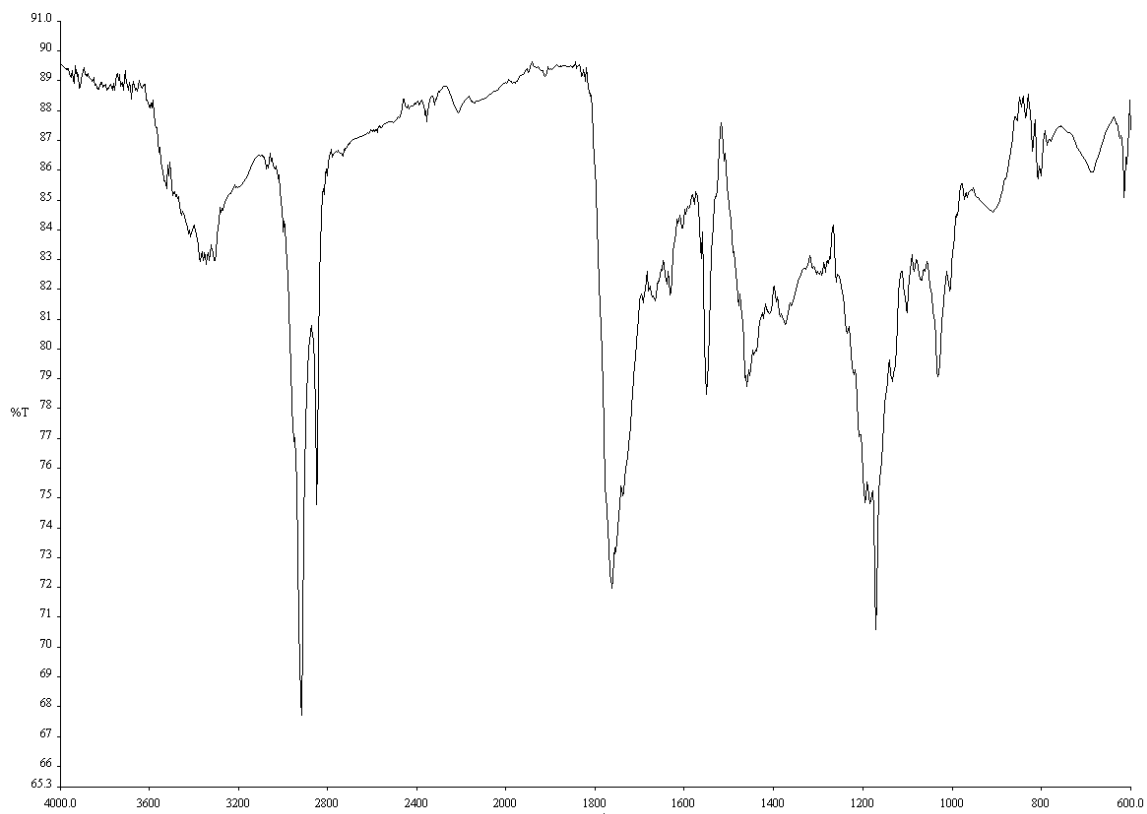


**Figure A7.50** Infrared spectrum (Thin Film, NaCl) of compound **141**.

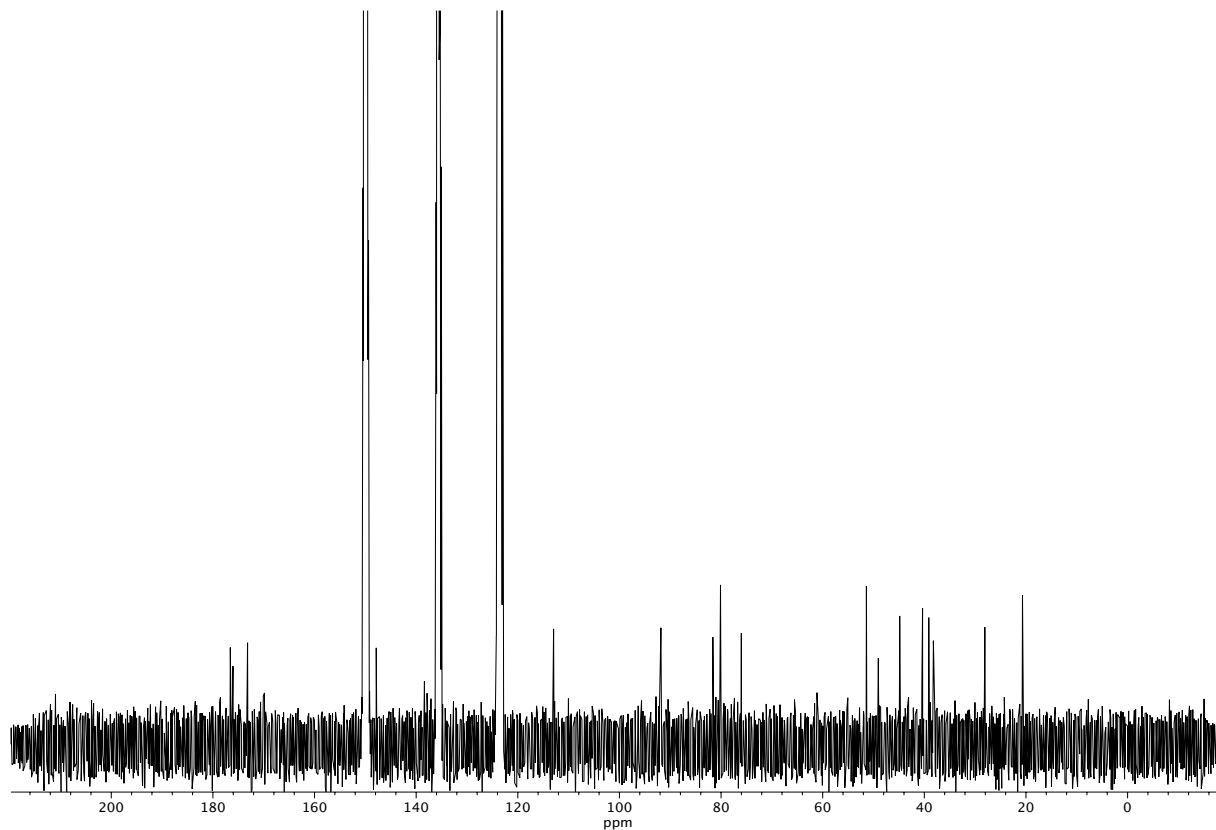


**Figure A7.51** <sup>13</sup>C NMR (100 MHz, d<sub>6</sub>-acetone) of compound **141**.

Figure A7.52  $^1\text{H}$  NMR (600 MHz,  $\text{pyridine-d}_5$ ) of havellockate (106).



**Figure A7.53** Infrared spectrum (Thin Film, NaCl) of havellockate (**106**).

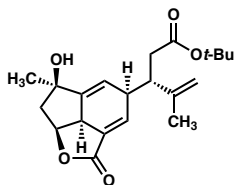


**Figure A7.54** <sup>13</sup>C NMR (100 MHz, pyridine-d<sub>5</sub>) of havellockate (**106**).

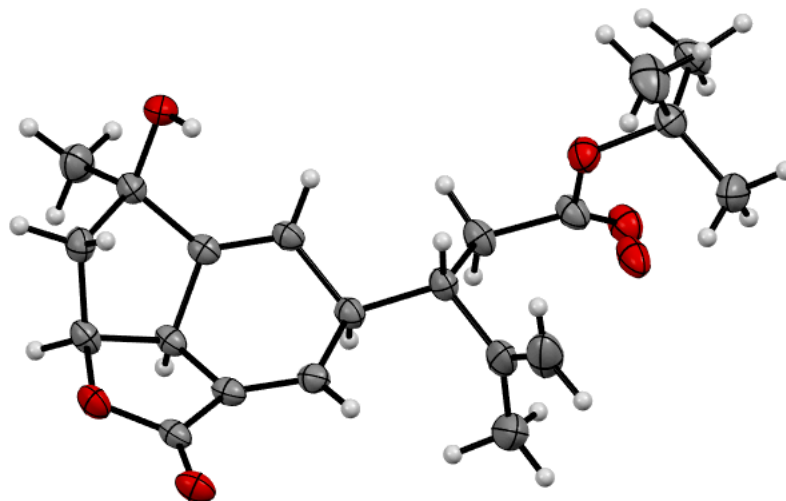
## **APPENDIX 8**

*X-Ray Crystallography Reports Relevant to Chapter 2:*

*Asymmetric Total Synthesis of Havellockate*

**A8.1 X-RAY CRYSTAL STRUCTURE ANALYSIS OF TRICYCLE 111**

111

Contents*Table A8.1.1. Experimental Details**Table A8.1.2. Crystal Data**Table A8.1.3. Atomic Coordinates**Table A8.1.4. Full Bond Distances and Angles**Table A8.1.5. Anisotropic Displacement Parameters**Table A8.1.6. Hydrogen Atomic Coordinates**Table A8.1.7. Torsion Angles**Table A8.1.8. Hydrogen Bond Distances and Angles***Figure A8.1.1** X-Ray Coordinate of compound **111**.

**Table A8.1.1** Experimental Details for X-Ray Structure Determination of Tetracycle **111**.

Low-temperature diffraction data ( $\phi$ - and  $\omega$ -scans) were collected on a Bruker AXS D8 VENTURE KAPPA diffractometer coupled to a PHOTON II CPAD detector with Cu  $K_{\alpha}$  radiation ( $\lambda = 1.54178 \text{ \AA}$ ) from an  $I\mu\text{S}$  micro-source for the structure of compound V21171. The structure was solved by direct methods using SHELXS and refined against  $F^2$  on all data by full-matrix least squares with SHELXL-2017 using established refinement techniques. All non-hydrogen atoms were refined anisotropically. All hydrogen atoms were included into the model at geometrically calculated positions and refined using a riding model. The isotropic displacement parameters of all hydrogen atoms were fixed to 1.2 times the  $U$  value of the atoms they are linked to (1.5 times for methyl groups).

Compound **111** crystallizes in the orthorhombic space group  $P2_12_12_1$  with one molecule in the asymmetric unit. The coordinates for the hydrogen atom bound to O3 was located in the difference Fourier synthesis and refined semi-freely with the help of a restraint on the O–H distance (0.84(4)  $\text{\AA}$ ).

**Table A8.1.2** Crystal data and structure refinement for compound **111**.

Empirical formula	C <sub>21</sub> H <sub>28</sub> O <sub>5</sub>
Formula weight	360.43
Temperature	100(2) K
Wavelength	1.54178 Å
Crystal system	Orthorhombic
Space group	P2 <sub>1</sub> 2 <sub>1</sub> 2 <sub>1</sub>
Unit cell dimensions	a = 7.7405(8) Å      a = 90°. b = 10.0404(15) Å      b = 90°. c = 24.768(3) Å      g = 90°.
Volume	1924.9(4) Å <sup>3</sup>
Z	4
Density (calculated)	1.244 Mg/m <sup>3</sup>
Absorption coefficient	0.712 mm <sup>-1</sup>
F(000)	776
Crystal size	0.300 x 0.150 x 0.100 mm <sup>3</sup>
Theta range for data collection	3.569 to 74.388°.
Index ranges	-9<=h<=9, -12<=k<=12, -29<=l<=30
Reflections collected	22865
Independent reflections	3937 [R(int) = 0.0391]
Completeness to theta = 67.679°	100.0 %
Absorption correction	Semi-empirical from equivalents
Max. and min. transmission	0.7538 and 0.6303
Refinement method	Full-matrix least-squares on F <sup>2</sup>
Data / restraints / parameters	3937 / 33 / 285
Goodness-of-fit on F <sup>2</sup>	1.042
Final R indices [I>2sigma(I)]	R1 = 0.0338, wR2 = 0.0874
R indices (all data)	R1 = 0.0362, wR2 = 0.0896
Absolute structure parameter	0.02(7)
Extinction coefficient	n/a
Largest diff. peak and hole	0.242 and -0.188 e.Å <sup>-3</sup>

**Table A8.1.3** Atomic coordinates ( $\times 10^4$ ) and equivalent isotropic displacement parameters ( $\text{\AA}^2 \times 10^3$ ) for compound **111**.  $U(\text{eq})$  is defined as one third of the trace of the orthogonalized  $U^{ij}$  tensor.

	x	y	z	U(eq)
O(1)	5155(2)	6438(2)	5690(1)	30(1)
O(2)	5084(2)	8662(2)	5619(1)	32(1)
C(1)	5247(2)	7587(2)	5404(1)	26(1)
C(2)	5489(2)	7261(2)	4827(1)	25(1)
C(3)	5033(2)	7972(2)	4396(1)	26(1)
C(4)	4992(3)	7263(2)	3853(1)	26(1)
C(12)	4031(3)	8031(2)	3402(1)	28(1)
C(13)	4432(4)	9506(2)	3400(1)	38(1)
C(14)	6278(4)	9909(3)	3344(1)	56(1)
C(15)	3152(5)	10397(3)	3434(1)	51(1)
C(16)	4496(3)	7394(2)	2851(1)	31(1)
C(17)	3723(3)	8128(2)	2377(1)	31(1)
O(4)	2019(2)	8083(2)	2384(1)	32(1)
O(5)	4553(7)	8387(18)	1975(4)	35(2)
O(5A)	4549(7)	8970(20)	2109(6)	40(3)
C(18)	957(3)	8749(2)	1964(1)	31(1)
C(19)	-818(8)	8707(10)	2246(3)	51(2)
C(20)	1023(9)	7899(7)	1484(3)	40(2)
C(21)	1513(11)	10164(7)	1893(4)	41(2)
C(19A)	-794(11)	8136(12)	2002(5)	66(3)
C(20A)	1707(12)	8509(10)	1371(2)	45(2)
C(21A)	897(15)	10213(8)	2055(4)	44(2)
C(5)	4207(3)	5885(2)	3944(1)	25(1)
C(6)	4606(2)	5212(2)	4386(1)	23(1)
C(7)	3693(3)	4046(2)	4650(1)	26(1)
C(11)	4687(3)	2750(2)	4589(1)	37(1)
O(3)	2024(2)	3812(2)	4438(1)	31(1)
C(8)	3644(3)	4524(2)	5249(1)	29(1)



**Table A8.1.3** *Cont'd*

C(9)	5347(3)	5260(2)	5342(1)	27(1)
C(10)	5858(2)	5805(2)	4783(1)	24(1)

---

**Table A8.1.4** Bond lengths [ $\text{\AA}$ ] and angles [ $^\circ$ ] for compound **111**.

---

O(1)-C(1)	1.356(3)
O(1)-C(9)	1.471(2)
O(2)-C(1)	1.209(3)
C(1)-C(2)	1.477(3)
C(2)-C(3)	1.332(3)
C(2)-C(10)	1.494(3)
C(3)-C(4)	1.521(3)
C(3)-H(3)	0.9500
C(4)-C(5)	1.528(3)
C(4)-C(12)	1.549(3)
C(4)-H(4)	1.0000
C(12)-C(13)	1.513(3)
C(12)-C(16)	1.549(3)
C(12)-H(12)	1.0000
C(13)-C(15)	1.338(4)
C(13)-C(14)	1.491(4)
C(14)-H(14A)	0.9800
C(14)-H(14B)	0.9800
C(14)-H(14C)	0.9800
C(15)-H(15A)	0.9500
C(15)-H(15B)	0.9500
C(16)-C(17)	1.509(3)
C(16)-H(16A)	0.9900
C(16)-H(16B)	0.9900
C(17)-O(5)	1.213(6)
C(17)-O(5A)	1.248(9)
C(17)-O(4)	1.320(3)
O(4)-C(18)	1.485(2)
C(18)-C(20)	1.465(5)
C(18)-C(21A)	1.489(8)
C(18)-C(19A)	1.491(7)
C(18)-C(21)	1.495(7)
C(18)-C(19)	1.542(6)
C(18)-C(20A)	1.598(6)

**Table A8.1.4** *Cont'd*

C(19)-H(19A)	0.9800
C(19)-H(19B)	0.9800
C(19)-H(19C)	0.9800
C(20)-H(20A)	0.9800
C(20)-H(20B)	0.9800
C(20)-H(20C)	0.9800
C(21)-H(21A)	0.9800
C(21)-H(21B)	0.9800
C(21)-H(21C)	0.9800
C(19A)-H(19D)	0.9800
C(19A)-H(19E)	0.9800
C(19A)-H(19F)	0.9800
C(20A)-H(20D)	0.9800
C(20A)-H(20E)	0.9800
C(20A)-H(20F)	0.9800
C(21A)-H(21D)	0.9800
C(21A)-H(21E)	0.9800
C(21A)-H(21F)	0.9800
C(5)-C(6)	1.323(3)
C(5)-H(5)	0.9500
C(6)-C(10)	1.505(3)
C(6)-C(7)	1.516(3)
C(7)-O(3)	1.414(2)
C(7)-C(11)	1.519(3)
C(7)-C(8)	1.561(3)
C(11)-H(11A)	0.9800
C(11)-H(11B)	0.9800
C(11)-H(11C)	0.9800
O(3)-H(3O)	0.83(2)
C(8)-C(9)	1.528(3)
C(8)-H(8A)	0.9900
C(8)-H(8B)	0.9900
C(9)-C(10)	1.539(3)
C(9)-H(9)	1.0000
C(10)-H(10)	1.0000

**Table A8.1.4** Cont'd

C(1)-O(1)-C(9)	111.94(14)
O(2)-C(1)-O(1)	121.63(17)
O(2)-C(1)-C(2)	129.52(19)
O(1)-C(1)-C(2)	108.80(17)
C(3)-C(2)-C(1)	128.57(19)
C(3)-C(2)-C(10)	121.03(18)
C(1)-C(2)-C(10)	108.20(17)
C(2)-C(3)-C(4)	117.65(18)
C(2)-C(3)-H(3)	121.2
C(4)-C(3)-H(3)	121.2
C(3)-C(4)-C(5)	107.59(15)
C(3)-C(4)-C(12)	114.54(17)
C(5)-C(4)-C(12)	111.43(16)
C(3)-C(4)-H(4)	107.7
C(5)-C(4)-H(4)	107.7
C(12)-C(4)-H(4)	107.7
C(13)-C(12)-C(4)	112.98(17)
C(13)-C(12)-C(16)	110.77(18)
C(4)-C(12)-C(16)	108.59(17)
C(13)-C(12)-H(12)	108.1
C(4)-C(12)-H(12)	108.1
C(16)-C(12)-H(12)	108.1
C(15)-C(13)-C(14)	122.3(3)
C(15)-C(13)-C(12)	120.2(3)
C(14)-C(13)-C(12)	117.5(2)
C(13)-C(14)-H(14A)	109.5
C(13)-C(14)-H(14B)	109.5
H(14A)-C(14)-H(14B)	109.5
C(13)-C(14)-H(14C)	109.5
H(14A)-C(14)-H(14C)	109.5
H(14B)-C(14)-H(14C)	109.5
C(13)-C(15)-H(15A)	120.0
C(13)-C(15)-H(15B)	120.0
H(15A)-C(15)-H(15B)	120.0
C(17)-C(16)-C(12)	113.03(18)

**Table A8.1.4** *Cont'd*

C(17)-C(16)-H(16A)	109.0
C(12)-C(16)-H(16A)	109.0
C(17)-C(16)-H(16B)	109.0
C(12)-C(16)-H(16B)	109.0
H(16A)-C(16)-H(16B)	107.8
O(5)-C(17)-O(4)	123.2(4)
O(5A)-C(17)-O(4)	122.8(4)
O(5)-C(17)-C(16)	122.2(3)
O(5A)-C(17)-C(16)	122.7(3)
O(4)-C(17)-C(16)	111.60(18)
C(17)-O(4)-C(18)	121.86(17)
C(20)-C(18)-O(4)	106.7(3)
O(4)-C(18)-C(21A)	110.9(4)
O(4)-C(18)-C(19A)	105.9(4)
C(21A)-C(18)-C(19A)	111.7(6)
C(20)-C(18)-C(21)	116.5(4)
O(4)-C(18)-C(21)	110.6(3)
C(20)-C(18)-C(19)	112.5(4)
O(4)-C(18)-C(19)	99.5(3)
C(21)-C(18)-C(19)	109.6(4)
O(4)-C(18)-C(20A)	112.0(2)
C(21A)-C(18)-C(20A)	107.4(4)
C(19A)-C(18)-C(20A)	109.0(5)
C(18)-C(19)-H(19A)	109.5
C(18)-C(19)-H(19B)	109.5
H(19A)-C(19)-H(19B)	109.5
C(18)-C(19)-H(19C)	109.5
H(19A)-C(19)-H(19C)	109.5
H(19B)-C(19)-H(19C)	109.5
C(18)-C(20)-H(20A)	109.5
C(18)-C(20)-H(20B)	109.5
H(20A)-C(20)-H(20B)	109.5
C(18)-C(20)-H(20C)	109.5
H(20A)-C(20)-H(20C)	109.5
H(20B)-C(20)-H(20C)	109.5

**Table A8.1.4** *Cont'd*

C(18)-C(21)-H(21A)	109.5
C(18)-C(21)-H(21B)	109.5
H(21A)-C(21)-H(21B)	109.5
C(18)-C(21)-H(21C)	109.5
H(21A)-C(21)-H(21C)	109.5
H(21B)-C(21)-H(21C)	109.5
C(18)-C(19A)-H(19D)	109.5
C(18)-C(19A)-H(19E)	109.5
H(19D)-C(19A)-H(19E)	109.5
C(18)-C(19A)-H(19F)	109.5
H(19D)-C(19A)-H(19F)	109.5
H(19E)-C(19A)-H(19F)	109.5
C(18)-C(20A)-H(20D)	109.5
C(18)-C(20A)-H(20E)	109.5
H(20D)-C(20A)-H(20E)	109.5
C(18)-C(20A)-H(20F)	109.5
H(20D)-C(20A)-H(20F)	109.5
H(20E)-C(20A)-H(20F)	109.5
C(18)-C(21A)-H(21D)	109.5
C(18)-C(21A)-H(21E)	109.5
H(21D)-C(21A)-H(21E)	109.5
C(18)-C(21A)-H(21F)	109.5
H(21D)-C(21A)-H(21F)	109.5
H(21E)-C(21A)-H(21F)	109.5
C(6)-C(5)-C(4)	119.39(18)
C(6)-C(5)-H(5)	120.3
C(4)-C(5)-H(5)	120.3
C(5)-C(6)-C(10)	119.33(18)
C(5)-C(6)-C(7)	129.99(18)
C(10)-C(6)-C(7)	108.88(16)
O(3)-C(7)-C(6)	113.19(16)
O(3)-C(7)-C(11)	106.47(17)
C(6)-C(7)-C(11)	112.47(17)
O(3)-C(7)-C(8)	112.49(16)
C(6)-C(7)-C(8)	100.60(16)

**Table A8.1.4** Cont'd

C(11)-C(7)-C(8)	111.75(17)
C(7)-C(11)-H(11A)	109.5
C(7)-C(11)-H(11B)	109.5
H(11A)-C(11)-H(11B)	109.5
C(7)-C(11)-H(11C)	109.5
H(11A)-C(11)-H(11C)	109.5
H(11B)-C(11)-H(11C)	109.5
C(7)-O(3)-H(3O)	102(2)
C(9)-C(8)-C(7)	105.70(16)
C(9)-C(8)-H(8A)	110.6
C(7)-C(8)-H(8A)	110.6
C(9)-C(8)-H(8B)	110.6
C(7)-C(8)-H(8B)	110.6
H(8A)-C(8)-H(8B)	108.7
O(1)-C(9)-C(8)	112.92(17)
O(1)-C(9)-C(10)	105.45(16)
C(8)-C(9)-C(10)	105.02(15)
O(1)-C(9)-H(9)	111.1
C(8)-C(9)-H(9)	111.1
C(10)-C(9)-H(9)	111.1
C(2)-C(10)-C(6)	108.18(16)
C(2)-C(10)-C(9)	103.45(16)
C(6)-C(10)-C(9)	106.35(16)
C(2)-C(10)-H(10)	112.7
C(6)-C(10)-H(10)	112.7
C(9)-C(10)-H(10)	112.7

---

Symmetry transformations used to generate equivalent atoms:

**Table A8.1.5** Anisotropic displacement parameters ( $\text{\AA}^2 \times 10^3$ ) for compound **111**.  
The anisotropic displacement factor exponent takes the form:  $-2p^2[h^2 a^*{}^2 U^{11} + \dots + 2 h k a^* b^* U^{12}]$

	U11	U22	U33	U23	U13	U12
O(1)	34(1)	38(1)	19(1)	-2(1)	-3(1)	0(1)
O(2)	29(1)	40(1)	26(1)	-10(1)	-2(1)	0(1)
C(1)	20(1)	35(1)	21(1)	-2(1)	-4(1)	-2(1)
C(2)	20(1)	32(1)	22(1)	-4(1)	-1(1)	-4(1)
C(3)	26(1)	29(1)	23(1)	-2(1)	0(1)	-5(1)
C(4)	27(1)	31(1)	19(1)	0(1)	-1(1)	-2(1)
C(12)	31(1)	32(1)	20(1)	2(1)	-3(1)	-2(1)
C(13)	59(2)	35(1)	20(1)	2(1)	-8(1)	-7(1)
C(14)	71(2)	54(2)	42(1)	14(1)	-18(1)	-27(2)
C(15)	85(2)	33(1)	34(1)	-3(1)	-12(1)	6(1)
C(16)	33(1)	38(1)	21(1)	0(1)	-2(1)	3(1)
C(17)	27(1)	44(1)	21(1)	1(1)	-1(1)	-2(1)
O(4)	27(1)	35(1)	34(1)	7(1)	-2(1)	0(1)
O(5)	30(2)	49(5)	26(2)	4(3)	3(2)	-1(2)
O(5A)	29(2)	64(8)	27(3)	14(4)	-1(2)	-7(3)
C(18)	26(1)	32(1)	35(1)	4(1)	-6(1)	2(1)
C(19)	29(2)	71(5)	53(4)	16(3)	-2(2)	7(3)
C(20)	43(3)	38(3)	38(3)	-4(2)	-19(2)	9(2)
C(21)	42(4)	33(3)	47(4)	10(3)	-11(3)	-1(3)
C(19A)	39(4)	81(6)	79(7)	32(5)	-24(4)	-28(4)
C(20A)	62(5)	53(5)	21(2)	-2(3)	-15(3)	27(4)
C(21A)	49(5)	39(3)	45(5)	-2(3)	-7(3)	2(4)
C(5)	25(1)	29(1)	20(1)	-3(1)	-1(1)	-1(1)
C(6)	20(1)	28(1)	22(1)	-2(1)	0(1)	1(1)
C(7)	26(1)	28(1)	24(1)	3(1)	-4(1)	-1(1)
C(11)	43(1)	30(1)	39(1)	0(1)	-7(1)	5(1)
O(3)	29(1)	31(1)	33(1)	3(1)	-7(1)	-6(1)
C(8)	32(1)	32(1)	22(1)	5(1)	-1(1)	-1(1)
C(9)	29(1)	33(1)	20(1)	-1(1)	-5(1)	3(1)
C(10)	19(1)	33(1)	20(1)	-2(1)	-2(1)	0(1)



**Table A8.1.6** Hydrogen coordinates ( $\times 10^4$ ) and isotropic displacement parameters ( $\text{\AA}^2 \times 10^3$ ) for compound **111**.

	x	y	z	U(eq)
H(3)	4744	8888	4426	31
H(4)	6215	7135	3733	31
H(12)	2762	7920	3461	33
H(14A)	6375	10877	3381	84
H(14B)	6705	9639	2988	84
H(14C)	6967	9474	3625	84
H(15A)	3404	11323	3422	61
H(15B)	1991	10105	3470	61
H(16A)	5769	7378	2811	37
H(16B)	4082	6461	2846	37
H(19A)	-1689	9114	2011	76
H(19B)	-758	9201	2587	76
H(19C)	-1137	7780	2319	76
H(20A)	2168	7967	1317	60
H(20B)	141	8189	1225	60
H(20C)	804	6972	1588	60
H(21A)	2616	10189	1698	61
H(21B)	1652	10584	2247	61
H(21C)	636	10647	1685	61
H(19D)	-723	7191	1907	99
H(19E)	-1580	8590	1752	99
H(19F)	-1230	8226	2371	99
H(20D)	2760	9038	1323	68
H(20E)	844	8779	1103	68
H(20F)	1978	7562	1324	68
H(21D)	546	10393	2428	66
H(21E)	61	10616	1807	66
H(21F)	2043	10595	1990	66
H(5)	3438	5515	3685	29
H(11A)	4095	2043	4789	56
H(11B)	5858	2863	4732	56

**Table A8.1.6** *Cont'd*

H(11C)	4749	2508	4206	56
H(3O)	1560(40)	4560(20)	4471(12)	41(8)
H(8A)	2651	5127	5310	35
H(8B)	3544	3755	5497	35
H(9)	6252	4644	5485	33
H(10)	7090	5615	4689	29

---

**Table A8.1.7** Torsion angles [°] for compound **111**.

---

C(9)-O(1)-C(1)-O(2)	178.52(18)
C(9)-O(1)-C(1)-C(2)	0.8(2)
O(2)-C(1)-C(2)-C(3)	-24.5(3)
O(1)-C(1)-C(2)-C(3)	153.0(2)
O(2)-C(1)-C(2)-C(10)	172.54(19)
O(1)-C(1)-C(2)-C(10)	-10.0(2)
C(1)-C(2)-C(3)-C(4)	-164.13(18)
C(10)-C(2)-C(3)-C(4)	-3.0(3)
C(2)-C(3)-C(4)-C(5)	41.0(2)
C(2)-C(3)-C(4)-C(12)	165.50(18)
C(3)-C(4)-C(12)-C(13)	42.0(2)
C(5)-C(4)-C(12)-C(13)	164.46(18)
C(3)-C(4)-C(12)-C(16)	165.34(17)
C(5)-C(4)-C(12)-C(16)	-72.2(2)
C(4)-C(12)-C(13)-C(15)	-124.2(2)
C(16)-C(12)-C(13)-C(15)	113.7(2)
C(4)-C(12)-C(13)-C(14)	57.6(3)
C(16)-C(12)-C(13)-C(14)	-64.5(3)
C(13)-C(12)-C(16)-C(17)	-51.4(2)
C(4)-C(12)-C(16)-C(17)	-176.01(17)
C(12)-C(16)-C(17)-O(5)	134.8(11)
C(12)-C(16)-C(17)-O(5A)	97.3(14)
C(12)-C(16)-C(17)-O(4)	-64.1(3)
O(5)-C(17)-O(4)-C(18)	-20.0(11)
O(5A)-C(17)-O(4)-C(18)	17.8(14)
C(16)-C(17)-O(4)-C(18)	179.11(17)
C(17)-O(4)-C(18)-C(20)	77.4(4)
C(17)-O(4)-C(18)-C(21A)	-76.2(6)
C(17)-O(4)-C(18)-C(19A)	162.4(7)
C(17)-O(4)-C(18)-C(21)	-50.3(5)
C(17)-O(4)-C(18)-C(19)	-165.6(5)
C(17)-O(4)-C(18)-C(20A)	43.8(5)
C(3)-C(4)-C(5)-C(6)	-39.0(2)
C(12)-C(4)-C(5)-C(6)	-165.34(18)

**Table A8.1.7** *Cont'd*

C(4)-C(5)-C(6)-C(10)	-1.4(3)
C(4)-C(5)-C(6)-C(7)	161.42(19)
C(5)-C(6)-C(7)-O(3)	-12.0(3)
C(10)-C(6)-C(7)-O(3)	152.28(17)
C(5)-C(6)-C(7)-C(11)	108.8(2)
C(10)-C(6)-C(7)-C(11)	-87.0(2)
C(5)-C(6)-C(7)-C(8)	-132.2(2)
C(10)-C(6)-C(7)-C(8)	32.05(19)
O(3)-C(7)-C(8)-C(9)	-157.26(17)
C(6)-C(7)-C(8)-C(9)	-36.53(19)
C(11)-C(7)-C(8)-C(9)	83.0(2)
C(1)-O(1)-C(9)-C(8)	-105.85(18)
C(1)-O(1)-C(9)-C(10)	8.3(2)
C(7)-C(8)-C(9)-O(1)	142.33(16)
C(7)-C(8)-C(9)-C(10)	27.9(2)
C(3)-C(2)-C(10)-C(6)	-37.6(2)
C(1)-C(2)-C(10)-C(6)	126.88(17)
C(3)-C(2)-C(10)-C(9)	-150.18(18)
C(1)-C(2)-C(10)-C(9)	14.3(2)
C(5)-C(6)-C(10)-C(2)	39.8(2)
C(7)-C(6)-C(10)-C(2)	-126.43(17)
C(5)-C(6)-C(10)-C(9)	150.34(18)
C(7)-C(6)-C(10)-C(9)	-15.8(2)
O(1)-C(9)-C(10)-C(2)	-13.53(19)
C(8)-C(9)-C(10)-C(2)	105.98(17)
O(1)-C(9)-C(10)-C(6)	-127.39(16)
C(8)-C(9)-C(10)-C(6)	-7.9(2)

---

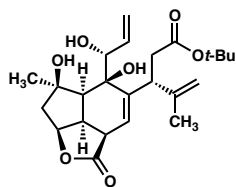
Symmetry transformations used to generate equivalent atoms:

**Table A8.1.8** Hydrogen bonds for compound **111** [ $\text{\AA}$  and  $^\circ$ ].

D-H...A	d(D-H)	d(H...A)	d(D...A)	$\angle(\text{DHA})$	
C(20 <sup>a</sup> )-H(20A <sup>a</sup> )...O(5 <sup>a</sup> )	0.98	2.50	3.030(12)	113.9	
C(20 <sup>a</sup> )-H(20B <sup>a</sup> )...O(3)#10	0.98	2.43	3.407(5)	177.3	
C(21 <sup>a</sup> )-H(21A <sup>a</sup> )...O(5 <sup>a</sup> )	0.98	2.45	2.960(12)	112.2	
C(20A <sup>b</sup> )-H(20D <sup>b</sup> )...O(5A <sup>b</sup> )	0.98	0.98	2.39	2.896(14)	111.4
C(20A <sup>b</sup> )-H(20E <sup>b</sup> )...O(3)#1	0.98	0.98	2.59	3.528(7)	159.6
C(21A <sup>b</sup> )-H(21F <sup>b</sup> )...O(5A <sup>b</sup> )	0.98	0.98	2.55	3.095(16)	114.7
O(3)-H(3O)...O(2)#2	0.83(2)	2.13(2)	2.951(2)	166(3)	
C(10)-H(10)...O(2)#3	1.00	2.55	3.460(2)	152.1	

Symmetry transformations used to generate equivalent atoms:

#1  $-x, y+1/2, -z+1/2$  #2  $x-1/2, -y+3/2, -z+1$  #3  $x+1/2, -y+3/2, -z+1$

**A8.2 X-RAY CRYSTAL STRUCTURE ANALYSIS OF COMPOUND 133****133**Contents

*Table A8.2.1. Experimental Details*

*Table A8.2.2. Crystal Data*

*Table A8.2.3. Atomic Coordinates*

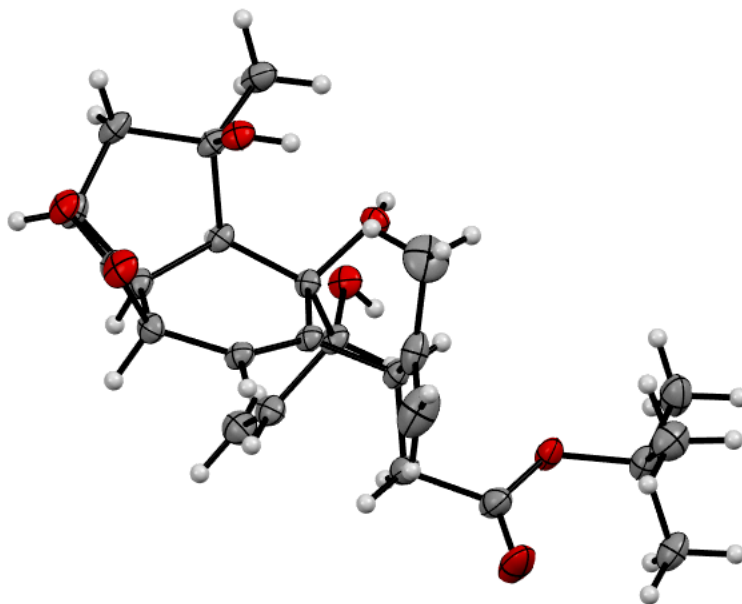
*Table A8.2.4. Full Bond Distances and Angles*

*Table A8.2.5. Anisotropic Displacement Parameters*

*Table A8.2.6. Hydrogen Atomic Coordinates*

*Table A8.2.7. Torsion Angles*

*Table A8.2.8. Hydrogen Bond Distances and Angles*

**Figure A8.2.1** X-Ray Coordinate of Allylation Product **133**.

**Table A8.2.1** Experimental Details for X-Ray Structure Determination of Compound **133**.

Low-temperature diffraction data ( $\phi$ - and  $\omega$ -scans) were collected on a Bruker AXS D8 VENTURE KAPPA diffractometer coupled to a PHOTON II CPAD detector with Cu  $K_{\alpha}$  radiation ( $\lambda = 1.54178 \text{ \AA}$ ) from an I $\mu$ S micro-source for the structure of compound **133**. The structure was solved by direct methods using SHELXS and refined against  $F^2$  on all data by full-matrix least squares with SHELXL-2017 using established refinement techniques. All non-hydrogen atoms were refined anisotropically. All hydrogen atoms were included into the model at geometrically calculated positions and refined using a riding model. The isotropic displacement parameters of all hydrogen atoms were fixed to 1.2 times the  $U$  value of the atoms they are linked to (1.5 times for methyl groups).

Compound **133** crystallizes in the monoclinic space group  $P2_1$  with two molecules in the asymmetric unit. The coordinates for the hydrogen atom bound to O5, O6, O7, O105, O106, and O107 were located in the difference Fourier synthesis and refined semi-freely with the help of a restraint on the O–H distance (0.84(4)  $\text{\AA}$ ).

**Table A8.2.2** Crystal data and structure refinement for compound **133**.

Empirical formula	C48 H68 O14
Formula weight	869.02
Temperature	100(2) K
Wavelength	1.54178 Å
Crystal system	Monoclinic
Space group	P2 <sub>1</sub>
Unit cell dimensions	a = 10.7573(12) Å      a = 90°. b = 9.3693(8) Å      b = 99.208(8)°. c = 23.419(2) Å      g = 90°.
Volume	2329.9(4) Å <sup>3</sup>
Z	2
Density (calculated)	1.239 Mg/m <sup>3</sup>
Absorption coefficient	0.740 mm <sup>-1</sup>
F(000)	936
Crystal size	0.200 x 0.100 x 0.100 mm <sup>3</sup>
Theta range for data collection	3.824 to 74.727°.
Index ranges	-13 ≤ h ≤ 13, -11 ≤ k ≤ 11, -29 ≤ l ≤ 28
Reflections collected	26279
Independent reflections	9108 [R(int) = 0.0405]
Completeness to theta = 67.679°	99.9 %
Absorption correction	Semi-empirical from equivalents
Max. and min. transmission	0.7538 and 0.6055
Refinement method	Full-matrix least-squares on F <sup>2</sup>
Data / restraints / parameters	9108 / 7 / 587
Goodness-of-fit on F <sup>2</sup>	1.054
Final R indices [I > 2σ(I)]	R1 = 0.0417, wR2 = 0.1124
R indices (all data)	R1 = 0.0427, wR2 = 0.1132
Absolute structure parameter	-0.02(6)
Extinction coefficient	n/a
Largest diff. peak and hole	0.433 and -0.242 e.Å <sup>-3</sup>



**Table A8.2.3** Atomic coordinates ( $\times 10^4$ ) and equivalent isotropic displacement parameters ( $\text{\AA}^2 \times 10^3$ ) for compound **133**.  $U(\text{eq})$  is defined as one third of the trace of the orthogonalized  $U_{ij}$  tensor.

	x	y	z	U(eq)
O(1)	15897(2)	8181(2)	8684(1)	42(1)
O(2)	13949(3)	9056(2)	8525(1)	44(1)
C(1)	14658(3)	8066(3)	8503(1)	35(1)
C(2)	14324(3)	6582(3)	8267(1)	29(1)
C(3)	13108(3)	6048(3)	8412(1)	28(1)
C(4)	12981(3)	4901(3)	8731(1)	27(1)
C(11)	11679(3)	4389(3)	8827(1)	30(1)
C(14)	11225(3)	5025(4)	9355(1)	44(1)
C(15)	10660(4)	4152(5)	9699(2)	60(1)
C(16)	11391(5)	6530(5)	9466(2)	68(1)
C(12)	10654(3)	4656(3)	8291(1)	37(1)
C(13)	9504(3)	3714(3)	8260(1)	37(1)
O(3)	8444(2)	4143(3)	8205(1)	58(1)
O(4)	9834(2)	2335(2)	8278(1)	43(1)
C(17)	8913(4)	1160(4)	8255(2)	49(1)
C(18)	8217(5)	1285(5)	8761(2)	70(1)
C(19)	9770(5)	-158(5)	8345(4)	93(2)
C(20)	8090(6)	1143(7)	7679(2)	95(2)
C(5)	14100(3)	4008(3)	9009(1)	29(1)
O(5)	13905(2)	3801(2)	9594(1)	36(1)
C(21)	14025(3)	2501(3)	8722(1)	34(1)
O(6)	15041(3)	1683(2)	9018(1)	43(1)
C(22)	14057(3)	2522(3)	8086(1)	39(1)
C(23)	13147(4)	1940(4)	7715(2)	48(1)
C(6)	15420(3)	4678(3)	8987(1)	30(1)
C(7)	16031(3)	5535(3)	9526(1)	36(1)
O(7)	15123(2)	6540(2)	9680(1)	40(1)
C(24)	16601(4)	4643(4)	10048(1)	47(1)

**Table A8.2.3** *Cont'd*

C(8)	17060(3)	6378(4)	9294(2)	45(1)
C(9)	16530(3)	6801(3)	8682(1)	40(1)
C(10)	15495(3)	5687(3)	8465(1)	31(1)
O(101)	11991(2)	2076(2)	6185(1)	27(1)
O(102)	10195(2)	1236(2)	6408(1)	30(1)
C(101)	10938(2)	2199(3)	6421(1)	23(1)
C(102)	10905(2)	3635(2)	6716(1)	22(1)
C(103)	9607(2)	4226(2)	6656(1)	21(1)
C(104)	9237(2)	5425(2)	6373(1)	18(1)
C(111)	7897(2)	5963(3)	6361(1)	22(1)
C(114)	6948(3)	4787(3)	6179(1)	30(1)
C(115)	6235(3)	4196(4)	6523(2)	47(1)
C(116)	6894(3)	4309(4)	5563(2)	48(1)
C(112)	7754(3)	6666(3)	6946(1)	28(1)
C(113)	6529(3)	7470(3)	6911(1)	29(1)
O(103)	5770(2)	7299(3)	7230(1)	44(1)
O(104)	6420(2)	8405(2)	6475(1)	25(1)
C(117)	5239(2)	9194(3)	6284(1)	26(1)
C(118)	4205(3)	8130(3)	6069(1)	36(1)
C(119)	5564(3)	10096(3)	5791(1)	37(1)
C(120)	4923(3)	10153(3)	6764(1)	32(1)
C(105)	10080(2)	6312(2)	6046(1)	18(1)
O(105)	9342(2)	6525(2)	5483(1)	20(1)
C(121)	10292(2)	7802(2)	6334(1)	21(1)
O(106)	10904(2)	8647(2)	5962(1)	26(1)
C(122)	11027(3)	7738(3)	6943(1)	25(1)
C(123)	11991(3)	8552(3)	7138(1)	31(1)
C(106)	11365(2)	5617(2)	5992(1)	19(1)
C(107)	11451(2)	4823(2)	5420(1)	21(1)
O(107)	10420(2)	3830(2)	5297(1)	24(1)
C(124)	11544(3)	5760(3)	4900(1)	29(1)
C(108)	12654(2)	3939(3)	5580(1)	26(1)
C(109)	12663(2)	3437(3)	6194(1)	26(1)
C(110)	11885(2)	4543(3)	6480(1)	22(1)

---

**Table A8.2.4** Bond lengths [ $\text{\AA}$ ] and angles [ $^\circ$ ] for compound **133**.

---

O(1)-C(1)	1.336(4)
O(1)-C(9)	1.462(4)
O(2)-C(1)	1.208(4)
C(1)-C(2)	1.518(4)
C(2)-C(3)	1.490(4)
C(2)-C(10)	1.523(4)
C(2)-H(2)	1.0000
C(3)-C(4)	1.329(4)
C(3)-H(3)	0.9500
C(4)-C(5)	1.524(4)
C(4)-C(11)	1.531(4)
C(11)-C(14)	1.523(4)
C(11)-C(12)	1.552(4)
C(11)-H(11)	1.0000
C(14)-C(15)	1.358(5)
C(14)-C(16)	1.439(6)
C(15)-H(15A)	0.9500
C(15)-H(15B)	0.9500
C(16)-H(16A)	0.9800
C(16)-H(16B)	0.9800
C(16)-H(16C)	0.9800
C(12)-C(13)	1.512(5)
C(12)-H(12A)	0.9900
C(12)-H(12B)	0.9900
C(13)-O(3)	1.197(4)
C(13)-O(4)	1.338(4)
O(4)-C(17)	1.477(4)
C(17)-C(20)	1.491(6)
C(17)-C(18)	1.504(6)
C(17)-C(19)	1.535(6)
C(18)-H(18A)	0.9800
C(18)-H(18B)	0.9800
C(18)-H(18C)	0.9800
C(19)-H(19A)	0.9800

**Table A8.2.4** *Cont'd*

C(19)-H(19B)	0.9800
C(19)-H(19C)	0.9800
C(20)-H(20A)	0.9800
C(20)-H(20B)	0.9800
C(20)-H(20C)	0.9800
C(5)-O(5)	1.433(3)
C(5)-C(21)	1.559(4)
C(5)-C(6)	1.560(4)
O(5)-H(5O)	0.83(2)
C(21)-O(6)	1.421(4)
C(21)-C(22)	1.496(4)
C(21)-H(21)	1.0000
O(6)-H(6O)	0.83(3)
C(22)-C(23)	1.319(5)
C(22)-H(22)	0.9500
C(23)-H(23A)	0.9500
C(23)-H(23B)	0.9500
C(6)-C(7)	1.550(4)
C(6)-C(10)	1.559(4)
C(6)-H(6)	1.0000
C(7)-O(7)	1.443(4)
C(7)-C(24)	1.526(4)
C(7)-C(8)	1.528(5)
O(7)-H(7O)	0.83(3)
C(24)-H(24A)	0.9800
C(24)-H(24B)	0.9800
C(24)-H(24C)	0.9800
C(8)-C(9)	1.509(5)
C(8)-H(8A)	0.9900
C(8)-H(8B)	0.9900
C(9)-C(10)	1.550(4)
C(9)-H(9)	1.0000
C(10)-H(10)	1.0000
O(101)-C(101)	1.342(3)
O(101)-C(109)	1.464(3)

**Table A8.2.4** *Cont'd*

O(102)-C(101)	1.203(3)
C(101)-C(102)	1.514(3)
C(102)-C(103)	1.488(3)
C(102)-C(110)	1.525(3)
C(102)-H(102)	1.0000
C(103)-C(104)	1.331(3)
C(103)-H(103)	0.9500
C(104)-C(105)	1.523(3)
C(104)-C(111)	1.523(3)
C(111)-C(114)	1.516(4)
C(111)-C(112)	1.549(3)
C(111)-H(111)	1.0000
C(114)-C(115)	1.319(5)
C(114)-C(116)	1.504(5)
C(115)-H(11A)	0.9500
C(115)-H(11B)	0.9500
C(116)-H(11C)	0.9800
C(116)-H(11D)	0.9800
C(116)-H(11E)	0.9800
C(112)-C(113)	1.508(4)
C(112)-H(11F)	0.9900
C(112)-H(11G)	0.9900
C(113)-O(103)	1.202(3)
C(113)-O(104)	1.336(3)
O(104)-C(117)	1.475(3)
C(117)-C(119)	1.515(4)
C(117)-C(120)	1.518(4)
C(117)-C(118)	1.519(4)
C(118)-H(11H)	0.9800
C(118)-H(11I)	0.9800
C(118)-H(11J)	0.9800
C(119)-H(11K)	0.9800
C(119)-H(11L)	0.9800
C(119)-H(11M)	0.9800
C(120)-H(12C)	0.9800

**Table A8.2.4** Cont'd

C(120)-H(12D)	0.9800
C(120)-H(12E)	0.9800
C(105)-O(105)	1.440(3)
C(105)-C(121)	1.551(3)
C(105)-C(106)	1.551(3)
O(105)-H(05O)	0.83(2)
C(121)-O(106)	1.415(3)
C(121)-C(122)	1.517(3)
C(121)-H(121)	1.0000
O(106)-H(06O)	0.84(2)
C(122)-C(123)	1.309(4)
C(122)-H(122)	0.9500
C(123)-H(12F)	0.9500
C(123)-H(12G)	0.9500
C(106)-C(107)	1.549(3)
C(106)-C(110)	1.558(3)
C(106)-H(106)	1.0000
C(107)-O(107)	1.441(3)
C(107)-C(124)	1.517(3)
C(107)-C(108)	1.532(3)
O(107)-H(07O)	0.82(2)
C(124)-H(12H)	0.9800
C(124)-H(12I)	0.9800
C(124)-H(12J)	0.9800
C(108)-C(109)	1.512(4)
C(108)-H(10A)	0.9900
C(108)-H(10B)	0.9900
C(109)-C(110)	1.550(3)
C(109)-H(109)	1.0000
C(110)-H(110)	1.0000
C(1)-O(1)-C(9)	111.6(2)
O(2)-C(1)-O(1)	122.0(3)
O(2)-C(1)-C(2)	127.2(3)
O(1)-C(1)-C(2)	110.8(3)
C(3)-C(2)-C(1)	113.0(2)

**Table A8.2.4** *Cont'd*

C(3)-C(2)-C(10)	117.3(2)
C(1)-C(2)-C(10)	104.9(2)
C(3)-C(2)-H(2)	107.0
C(1)-C(2)-H(2)	107.0
C(10)-C(2)-H(2)	107.0
C(4)-C(3)-C(2)	125.0(3)
C(4)-C(3)-H(3)	117.5
C(2)-C(3)-H(3)	117.5
C(3)-C(4)-C(5)	122.6(3)
C(3)-C(4)-C(11)	121.0(3)
C(5)-C(4)-C(11)	116.4(2)
C(14)-C(11)-C(4)	114.6(2)
C(14)-C(11)-C(12)	108.4(3)
C(4)-C(11)-C(12)	112.3(2)
C(14)-C(11)-H(11)	107.0
C(4)-C(11)-H(11)	107.0
C(12)-C(11)-H(11)	107.0
C(15)-C(14)-C(16)	122.5(3)
C(15)-C(14)-C(11)	118.6(3)
C(16)-C(14)-C(11)	118.9(3)
C(14)-C(15)-H(15A)	120.0
C(14)-C(15)-H(15B)	120.0
H(15A)-C(15)-H(15B)	120.0
C(14)-C(16)-H(16A)	109.5
C(14)-C(16)-H(16B)	109.5
H(16A)-C(16)-H(16B)	109.5
C(14)-C(16)-H(16C)	109.5
H(16A)-C(16)-H(16C)	109.5
H(16B)-C(16)-H(16C)	109.5
C(13)-C(12)-C(11)	114.5(2)
C(13)-C(12)-H(12A)	108.6
C(11)-C(12)-H(12A)	108.6
C(13)-C(12)-H(12B)	108.6
C(11)-C(12)-H(12B)	108.6
H(12A)-C(12)-H(12B)	107.6

**Table A8.2.4** *Cont'd*

O(3)-C(13)-O(4)	124.9(3)
O(3)-C(13)-C(12)	124.6(3)
O(4)-C(13)-C(12)	110.5(3)
C(13)-O(4)-C(17)	123.1(3)
O(4)-C(17)-C(20)	109.8(3)
O(4)-C(17)-C(18)	109.2(3)
C(20)-C(17)-C(18)	114.5(4)
O(4)-C(17)-C(19)	102.2(3)
C(20)-C(17)-C(19)	111.8(5)
C(18)-C(17)-C(19)	108.6(4)
C(17)-C(18)-H(18A)	109.5
C(17)-C(18)-H(18B)	109.5
H(18A)-C(18)-H(18B)	109.5
C(17)-C(18)-H(18C)	109.5
H(18A)-C(18)-H(18C)	109.5
H(18B)-C(18)-H(18C)	109.5
C(17)-C(19)-H(19A)	109.5
C(17)-C(19)-H(19B)	109.5
H(19A)-C(19)-H(19B)	109.5
C(17)-C(19)-H(19C)	109.5
H(19A)-C(19)-H(19C)	109.5
H(19B)-C(19)-H(19C)	109.5
C(17)-C(20)-H(20A)	109.5
C(17)-C(20)-H(20B)	109.5
H(20A)-C(20)-H(20B)	109.5
C(17)-C(20)-H(20C)	109.5
H(20A)-C(20)-H(20C)	109.5
H(20B)-C(20)-H(20C)	109.5
O(5)-C(5)-C(4)	104.8(2)
O(5)-C(5)-C(21)	106.4(2)
C(4)-C(5)-C(21)	109.3(2)
O(5)-C(5)-C(6)	111.0(2)
C(4)-C(5)-C(6)	115.2(2)
C(21)-C(5)-C(6)	109.6(2)
C(5)-O(5)-H(5O)	108(3)



**Table A8.2.4** *Cont'd*

O(6)-C(21)-C(22)	110.7(3)
O(6)-C(21)-C(5)	107.2(2)
C(22)-C(21)-C(5)	114.1(2)
O(6)-C(21)-H(21)	108.2
C(22)-C(21)-H(21)	108.2
C(5)-C(21)-H(21)	108.2
C(21)-O(6)-H(6O)	110(3)
C(23)-C(22)-C(21)	121.3(3)
C(23)-C(22)-H(22)	119.4
C(21)-C(22)-H(22)	119.4
C(22)-C(23)-H(23A)	120.0
C(22)-C(23)-H(23B)	120.0
H(23A)-C(23)-H(23B)	120.0
C(7)-C(6)-C(10)	104.8(2)
C(7)-C(6)-C(5)	116.9(2)
C(10)-C(6)-C(5)	115.5(2)
C(7)-C(6)-H(6)	106.3
C(10)-C(6)-H(6)	106.3
C(5)-C(6)-H(6)	106.3
O(7)-C(7)-C(24)	111.0(3)
O(7)-C(7)-C(8)	108.0(2)
C(24)-C(7)-C(8)	110.3(3)
O(7)-C(7)-C(6)	109.0(2)
C(24)-C(7)-C(6)	115.6(2)
C(8)-C(7)-C(6)	102.5(2)
C(7)-O(7)-H(7O)	109(4)
C(7)-C(24)-H(24A)	109.5
C(7)-C(24)-H(24B)	109.5
H(24A)-C(24)-H(24B)	109.5
C(7)-C(24)-H(24C)	109.5
H(24A)-C(24)-H(24C)	109.5
H(24B)-C(24)-H(24C)	109.5
C(9)-C(8)-C(7)	106.7(3)
C(9)-C(8)-H(8A)	110.4
C(7)-C(8)-H(8A)	110.4

**Table A8.2.4** *Cont'd*

C(9)-C(8)-H(8B)	110.4
C(7)-C(8)-H(8B)	110.4
H(8A)-C(8)-H(8B)	108.6
O(1)-C(9)-C(8)	109.5(3)
O(1)-C(9)-C(10)	106.6(3)
C(8)-C(9)-C(10)	106.1(3)
O(1)-C(9)-H(9)	111.5
C(8)-C(9)-H(9)	111.5
C(10)-C(9)-H(9)	111.5
C(2)-C(10)-C(9)	104.2(2)
C(2)-C(10)-C(6)	115.4(2)
C(9)-C(10)-C(6)	106.0(2)
C(2)-C(10)-H(10)	110.3
C(9)-C(10)-H(10)	110.3
C(6)-C(10)-H(10)	110.3
C(101)-O(101)-C(109)	111.50(18)
O(102)-C(101)-O(101)	121.7(2)
O(102)-C(101)-C(102)	127.9(2)
O(101)-C(101)-C(102)	110.3(2)
C(103)-C(102)-C(101)	112.2(2)
C(103)-C(102)-C(110)	116.8(2)
C(101)-C(102)-C(110)	105.2(2)
C(103)-C(102)-H(102)	107.4
C(101)-C(102)-H(102)	107.4
C(110)-C(102)-H(102)	107.4
C(104)-C(103)-C(102)	124.2(2)
C(104)-C(103)-H(103)	117.9
C(102)-C(103)-H(103)	117.9
C(103)-C(104)-C(105)	123.7(2)
C(103)-C(104)-C(111)	119.7(2)
C(105)-C(104)-C(111)	116.62(19)
C(114)-C(111)-C(104)	110.9(2)
C(114)-C(111)-C(112)	113.6(2)
C(104)-C(111)-C(112)	110.6(2)
C(114)-C(111)-H(111)	107.1

**Table A8.2.4** *Cont'd*

C(104)-C(111)-H(111)	107.1
C(112)-C(111)-H(111)	107.1
C(115)-C(114)-C(116)	121.6(3)
C(115)-C(114)-C(111)	124.4(3)
C(116)-C(114)-C(111)	114.0(2)
C(114)-C(115)-H(11A)	120.0
C(114)-C(115)-H(11B)	120.0
H(11A)-C(115)-H(11B)	120.0
C(114)-C(116)-H(11C)	109.5
C(114)-C(116)-H(11D)	109.5
H(11C)-C(116)-H(11D)	109.5
C(114)-C(116)-H(11E)	109.5
H(11C)-C(116)-H(11E)	109.5
H(11D)-C(116)-H(11E)	109.5
C(113)-C(112)-C(111)	111.9(2)
C(113)-C(112)-H(11F)	109.2
C(111)-C(112)-H(11F)	109.2
C(113)-C(112)-H(11G)	109.2
C(111)-C(112)-H(11G)	109.2
H(11F)-C(112)-H(11G)	107.9
O(103)-C(113)-O(104)	125.2(3)
O(103)-C(113)-C(112)	125.0(3)
O(104)-C(113)-C(112)	109.8(2)
C(113)-O(104)-C(117)	121.7(2)
O(104)-C(117)-C(119)	102.6(2)
O(104)-C(117)-C(120)	110.9(2)
C(119)-C(117)-C(120)	109.8(2)
O(104)-C(117)-C(118)	108.7(2)
C(119)-C(117)-C(118)	111.1(2)
C(120)-C(117)-C(118)	113.2(2)
C(117)-C(118)-H(11H)	109.5
C(117)-C(118)-H(11I)	109.5
H(11H)-C(118)-H(11I)	109.5
C(117)-C(118)-H(11J)	109.5
H(11H)-C(118)-H(11J)	109.5

**Table A8.2.4** *Cont'd*

H(11I)-C(118)-H(11J)	109.5
C(117)-C(119)-H(11K)	109.5
C(117)-C(119)-H(11L)	109.5
H(11K)-C(119)-H(11L)	109.5
C(117)-C(119)-H(11M)	109.5
H(11K)-C(119)-H(11M)	109.5
H(11L)-C(119)-H(11M)	109.5
C(117)-C(120)-H(12C)	109.5
C(117)-C(120)-H(12D)	109.5
H(12C)-C(120)-H(12D)	109.5
C(117)-C(120)-H(12E)	109.5
H(12C)-C(120)-H(12E)	109.5
H(12D)-C(120)-H(12E)	109.5
O(105)-C(105)-C(104)	104.50(18)
O(105)-C(105)-C(121)	107.07(17)
C(104)-C(105)-C(121)	109.34(18)
O(105)-C(105)-C(106)	110.54(18)
C(104)-C(105)-C(106)	114.97(18)
C(121)-C(105)-C(106)	110.01(18)
C(105)-O(105)-H(05O)	105(2)
O(106)-C(121)-C(122)	112.1(2)
O(106)-C(121)-C(105)	106.69(18)
C(122)-C(121)-C(105)	113.00(18)
O(106)-C(121)-H(121)	108.3
C(122)-C(121)-H(121)	108.3
C(105)-C(121)-H(121)	108.3
C(121)-O(106)-H(06O)	107(3)
C(123)-C(122)-C(121)	124.7(2)
C(123)-C(122)-H(122)	117.6
C(121)-C(122)-H(122)	117.6
C(122)-C(123)-H(12F)	120.0
C(122)-C(123)-H(12G)	120.0
H(12F)-C(123)-H(12G)	120.0
C(107)-C(106)-C(105)	116.74(19)
C(107)-C(106)-C(110)	105.14(18)

**Table A8.2.4** *Cont'd*

C(105)-C(106)-C(110)	115.52(19)
C(107)-C(106)-H(106)	106.2
C(105)-C(106)-H(106)	106.2
C(110)-C(106)-H(106)	106.2
O(107)-C(107)-C(124)	111.2(2)
O(107)-C(107)-C(108)	107.00(19)
C(124)-C(107)-C(108)	110.4(2)
O(107)-C(107)-C(106)	109.34(18)
C(124)-C(107)-C(106)	116.0(2)
C(108)-C(107)-C(106)	102.3(2)
C(107)-O(107)-H(07O)	105(3)
C(107)-C(124)-H(12H)	109.5
C(107)-C(124)-H(12I)	109.5
H(12H)-C(124)-H(12I)	109.5
C(107)-C(124)-H(12J)	109.5
H(12H)-C(124)-H(12J)	109.5
H(12I)-C(124)-H(12J)	109.5
C(109)-C(108)-C(107)	106.2(2)
C(109)-C(108)-H(10A)	110.5
C(107)-C(108)-H(10A)	110.5
C(109)-C(108)-H(10B)	110.5
C(107)-C(108)-H(10B)	110.5
H(10A)-C(108)-H(10B)	108.7
O(101)-C(109)-C(108)	109.2(2)
O(101)-C(109)-C(110)	106.8(2)
C(108)-C(109)-C(110)	106.3(2)
O(101)-C(109)-H(109)	111.4
C(108)-C(109)-H(109)	111.4
C(110)-C(109)-H(109)	111.4
C(102)-C(110)-C(109)	103.61(19)
C(102)-C(110)-C(106)	115.9(2)
C(109)-C(110)-C(106)	105.68(19)
C(102)-C(110)-H(110)	110.4
C(109)-C(110)-H(110)	110.4
C(106)-C(110)-H(110)	110.4

---

Symmetry transformations used to generate equivalent atoms:

**Table A8.2.5** Anisotropic displacement parameters ( $\text{\AA}^2 \times 10^3$ ) for compound **133**.

The anisotropic displacement factor exponent takes the form:  $-2p^2[h^2 a^*2U^{11} + \dots + 2 h k a^* b^* U^{12}]$

	U <sup>11</sup>	U <sup>22</sup>	U <sup>33</sup>	U <sup>23</sup>	U <sup>13</sup>	U <sup>12</sup>
O(1)	55(1)	23(1)	43(1)	2(1)	-1(1)	-8(1)
O(2)	64(2)	22(1)	45(1)	2(1)	4(1)	0(1)
C(1)	53(2)	21(1)	29(1)	4(1)	4(1)	-5(1)
C(2)	44(2)	23(1)	22(1)	2(1)	9(1)	-3(1)
C(3)	39(2)	22(1)	25(1)	1(1)	9(1)	1(1)
C(4)	44(2)	19(1)	19(1)	-3(1)	10(1)	-2(1)
C(11)	42(2)	25(1)	23(1)	2(1)	8(1)	-1(1)
C(14)	47(2)	60(2)	28(1)	-10(1)	12(1)	-6(2)
C(15)	73(3)	77(3)	32(2)	-4(2)	16(2)	-25(2)
C(16)	98(3)	48(2)	70(3)	-25(2)	51(3)	-13(2)
C(12)	48(2)	36(2)	26(1)	5(1)	5(1)	-2(1)
C(13)	46(2)	37(2)	27(1)	3(1)	3(1)	1(1)
O(3)	41(1)	48(2)	82(2)	14(1)	0(1)	5(1)
O(4)	41(1)	34(1)	55(1)	-11(1)	9(1)	-7(1)
C(17)	48(2)	38(2)	60(2)	-6(2)	4(2)	-14(2)
C(18)	84(3)	52(2)	76(3)	3(2)	24(2)	-17(2)
C(19)	72(3)	36(2)	172(6)	-15(3)	19(4)	-4(2)
C(20)	120(5)	79(4)	72(3)	4(3)	-33(3)	-55(4)
C(5)	50(2)	18(1)	21(1)	0(1)	8(1)	-1(1)
O(5)	57(1)	29(1)	23(1)	7(1)	9(1)	6(1)
C(21)	45(2)	22(1)	37(1)	-6(1)	9(1)	-2(1)
O(6)	62(2)	20(1)	46(1)	-2(1)	4(1)	4(1)
C(22)	48(2)	35(2)	36(1)	-9(1)	9(1)	4(1)
C(23)	65(2)	37(2)	40(2)	-8(1)	1(2)	16(2)
C(6)	44(2)	21(1)	25(1)	-3(1)	2(1)	4(1)
C(7)	52(2)	22(1)	31(1)	-2(1)	-4(1)	0(1)
O(7)	67(2)	23(1)	27(1)	-6(1)	3(1)	2(1)

**Table A8.2.5** *Cont'd*

C(24)	67(2)	33(2)	35(2)	1(1)	-12(2)	0(2)
C(8)	48(2)	32(2)	48(2)	-2(1)	-9(1)	-5(1)
C(9)	44(2)	31(2)	42(2)	-1(1)	4(1)	-5(1)
C(10)	39(2)	27(1)	28(1)	-2(1)	8(1)	-5(1)
O(101)	32(1)	14(1)	36(1)	-1(1)	9(1)	5(1)
O(102)	39(1)	13(1)	40(1)	1(1)	10(1)	1(1)
C(101)	29(1)	15(1)	26(1)	2(1)	4(1)	6(1)
C(102)	28(1)	15(1)	23(1)	1(1)	2(1)	3(1)
C(103)	26(1)	15(1)	23(1)	-1(1)	7(1)	2(1)
C(104)	22(1)	14(1)	20(1)	-2(1)	5(1)	1(1)
C(111)	23(1)	16(1)	26(1)	1(1)	6(1)	4(1)
C(114)	22(1)	20(1)	49(2)	1(1)	5(1)	2(1)
C(115)	37(2)	28(2)	80(2)	2(2)	22(2)	-3(1)
C(116)	43(2)	40(2)	56(2)	-15(2)	-6(2)	-13(2)
C(112)	32(1)	28(1)	25(1)	4(1)	11(1)	9(1)
C(113)	36(1)	25(1)	30(1)	2(1)	13(1)	7(1)
O(103)	46(1)	46(1)	47(1)	18(1)	31(1)	19(1)
O(104)	24(1)	21(1)	32(1)	5(1)	11(1)	6(1)
C(117)	22(1)	22(1)	34(1)	2(1)	7(1)	6(1)
C(118)	31(1)	35(2)	43(2)	-7(1)	7(1)	-3(1)
C(119)	35(2)	34(2)	45(2)	13(1)	10(1)	9(1)
C(120)	30(1)	25(1)	43(2)	-4(1)	9(1)	6(1)
C(105)	23(1)	11(1)	20(1)	0(1)	4(1)	2(1)
O(105)	25(1)	17(1)	19(1)	3(1)	4(1)	0(1)
C(121)	26(1)	12(1)	25(1)	-1(1)	6(1)	1(1)
O(106)	35(1)	12(1)	30(1)	1(1)	8(1)	-1(1)
C(122)	32(1)	17(1)	26(1)	-2(1)	5(1)	4(1)
C(123)	37(1)	25(1)	31(1)	-3(1)	4(1)	1(1)
C(106)	20(1)	12(1)	24(1)	-2(1)	5(1)	-1(1)
C(107)	24(1)	14(1)	28(1)	-3(1)	9(1)	1(1)
O(107)	29(1)	17(1)	27(1)	-5(1)	6(1)	-2(1)
C(124)	36(1)	24(1)	29(1)	0(1)	15(1)	2(1)
C(108)	27(1)	19(1)	37(1)	-2(1)	14(1)	4(1)
C(109)	25(1)	18(1)	36(1)	-2(1)	7(1)	4(1)
C(110)	24(1)	16(1)	26(1)	-2(1)	2(1)	3(1)





**Table A8.2.6** Hydrogen coordinates ( $\times 10^4$ ) and isotropic displacement parameters ( $\text{\AA}^2 \times 10^3$ ) for compound **133**.

	x	y	z	U(eq)
H(2)	14223	6648	7835	35
H(3)	12366	6566	8264	34
H(11)	11736	3333	8887	36
H(15A)	10356	4530	10027	72
H(15B)	10568	3164	9611	72
H(16A)	11012	6790	9805	102
H(16B)	10983	7070	9129	102
H(16C)	12293	6755	9539	102
H(12A)	10385	5666	8293	44
H(12B)	11033	4504	7937	44
H(18A)	8821	1425	9117	104
H(18B)	7734	410	8794	104
H(18C)	7641	2101	8702	104
H(19A)	10316	-94	8721	140
H(19B)	10288	-202	8037	140
H(19C)	9251	-1021	8333	140
H(20A)	7540	304	7651	143
H(20B)	8615	1102	7374	143
H(20C)	7576	2011	7633	143
H(5O)	14370(40)	3130(40)	9735(19)	54
H(21)	13219	2041	8786	41
H(6O)	15020(50)	870(30)	8880(20)	65
H(22)	14745	2962	7947	47
H(23A)	12454	1497	7850	58
H(23B)	13184	1964	7312	58
H(6)	16000	3863	8949	36
H(7O)	14610(40)	6110(50)	9844(19)	59
H(24A)	17172	5238	10316	71
H(24B)	17070	3841	9918	71
H(24C)	15927	4278	10244	71

**Table A8.2.6** *Cont'd*

H(8A)	17290	7238	9534	53
H(8B)	17822	5782	9300	53
H(9)	17199	6819	8430	48
H(10)	15728	5133	8133	37
H(102)	11209	3487	7138	27
H(103)	9003	3716	6830	25
H(111)	7746	6725	6059	26
H(11A)	5671	3450	6382	57
H(11B)	6287	4517	6911	57
H(11C)	6215	3610	5466	72
H(11D)	7699	3871	5516	72
H(11E)	6733	5134	5304	72
H(11F)	7793	5918	7247	33
H(11G)	8464	7332	7062	33
H(11H)	4479	7512	5776	54
H(11I)	3441	8644	5900	54
H(11J)	4027	7546	6394	54
H(11K)	6299	10690	5932	56
H(11L)	4846	10708	5643	56
H(11M)	5756	9472	5481	56
H(12C)	4751	9565	7088	48
H(12D)	4177	10725	6617	48
H(12E)	5636	10787	6894	48
H(05O)	9680(30)	7210(30)	5342(14)	31
H(121)	9450	8235	6353	25
H(06O)	10810(30)	9500(30)	6052(16)	38
H(122)	10770	7058	7201	30
H(12F)	12275	9244	6892	38
H(12G)	12405	8451	7526	38
H(106)	11989	6415	6018	23
H(07O)	9790(30)	4330(40)	5208(15)	36
H(12H)	11723	5165	4579	43
H(12I)	12223	6456	5001	43
H(12J)	10744	6263	4784	43
H(10A)	12650	3113	5316	32

**Table A8.2.6** *Cont'd*

H(10B)	13407	4529	5555	32
H(109)	13542	3355	6410	31
H(110)	12433	5048	6803	26

---

---

**Table A8.2.7** Torsion angles [°] for compound **133**.

---

C(9)-O(1)-C(1)-O(2)	172.8(3)
C(9)-O(1)-C(1)-C(2)	-8.5(3)
O(2)-C(1)-C(2)-C(3)	-38.8(4)
O(1)-C(1)-C(2)-C(3)	142.6(2)
O(2)-C(1)-C(2)-C(10)	-167.8(3)
O(1)-C(1)-C(2)-C(10)	13.6(3)
C(1)-C(2)-C(3)-C(4)	-117.7(3)
C(10)-C(2)-C(3)-C(4)	4.5(4)
C(2)-C(3)-C(4)-C(5)	2.0(4)
C(2)-C(3)-C(4)-C(11)	-176.5(2)
C(3)-C(4)-C(11)-C(14)	-90.2(3)
C(5)-C(4)-C(11)-C(14)	91.2(3)
C(3)-C(4)-C(11)-C(12)	34.1(3)
C(5)-C(4)-C(11)-C(12)	-144.5(2)
C(4)-C(11)-C(14)-C(15)	-137.0(3)
C(12)-C(11)-C(14)-C(15)	96.7(4)
C(4)-C(11)-C(14)-C(16)	44.1(5)
C(12)-C(11)-C(14)-C(16)	-82.2(4)
C(14)-C(11)-C(12)-C(13)	-74.6(3)
C(4)-C(11)-C(12)-C(13)	157.8(3)
C(11)-C(12)-C(13)-O(3)	126.6(3)
C(11)-C(12)-C(13)-O(4)	-56.0(3)
O(3)-C(13)-O(4)-C(17)	-2.6(5)
C(12)-C(13)-O(4)-C(17)	-180.0(3)
C(13)-O(4)-C(17)-C(20)	66.1(5)
C(13)-O(4)-C(17)-C(18)	-60.2(4)
C(13)-O(4)-C(17)-C(19)	-175.1(4)
C(3)-C(4)-C(5)-O(5)	133.0(3)
C(11)-C(4)-C(5)-O(5)	-48.5(3)
C(3)-C(4)-C(5)-C(21)	-113.3(3)
C(11)-C(4)-C(5)-C(21)	65.2(3)
C(3)-C(4)-C(5)-C(6)	10.7(3)
C(11)-C(4)-C(5)-C(6)	-170.8(2)
O(5)-C(5)-C(21)-O(6)	-63.9(3)

**Table A8.2.7** *Cont'd*

C(4)-C(5)-C(21)-O(6)	-176.6(2)
C(6)-C(5)-C(21)-O(6)	56.2(3)
O(5)-C(5)-C(21)-C(22)	173.2(3)
C(4)-C(5)-C(21)-C(22)	60.5(3)
C(6)-C(5)-C(21)-C(22)	-66.7(3)
O(6)-C(21)-C(22)-C(23)	115.7(3)
C(5)-C(21)-C(22)-C(23)	-123.3(3)
O(5)-C(5)-C(6)-C(7)	-23.8(3)
C(4)-C(5)-C(6)-C(7)	95.1(3)
C(21)-C(5)-C(6)-C(7)	-141.0(2)
O(5)-C(5)-C(6)-C(10)	-147.8(2)
C(4)-C(5)-C(6)-C(10)	-28.9(3)
C(21)-C(5)-C(6)-C(10)	94.9(3)
C(10)-C(6)-C(7)-O(7)	79.9(3)
C(5)-C(6)-C(7)-O(7)	-49.4(3)
C(10)-C(6)-C(7)-C(24)	-154.3(3)
C(5)-C(6)-C(7)-C(24)	76.4(4)
C(10)-C(6)-C(7)-C(8)	-34.4(3)
C(5)-C(6)-C(7)-C(8)	-163.7(2)
O(7)-C(7)-C(8)-C(9)	-78.0(3)
C(24)-C(7)-C(8)-C(9)	160.6(3)
C(6)-C(7)-C(8)-C(9)	37.1(3)
C(1)-O(1)-C(9)-C(8)	-114.5(3)
C(1)-O(1)-C(9)-C(10)	-0.2(3)
C(7)-C(8)-C(9)-O(1)	89.7(3)
C(7)-C(8)-C(9)-C(10)	-25.0(3)
C(3)-C(2)-C(10)-C(9)	-139.0(3)
C(1)-C(2)-C(10)-C(9)	-12.7(3)
C(3)-C(2)-C(10)-C(6)	-23.2(3)
C(1)-C(2)-C(10)-C(6)	103.1(3)
O(1)-C(9)-C(10)-C(2)	8.4(3)
C(8)-C(9)-C(10)-C(2)	125.0(3)
O(1)-C(9)-C(10)-C(6)	-113.8(3)
C(8)-C(9)-C(10)-C(6)	2.8(3)
C(7)-C(6)-C(10)-C(2)	-95.0(3)

**Table A8.2.7** *Cont'd*

C(5)-C(6)-C(10)-C(2)	35.2(3)
C(7)-C(6)-C(10)-C(9)	19.8(3)
C(5)-C(6)-C(10)-C(9)	149.9(2)
C(109)-O(101)-C(101)-O(102)	173.1(2)
C(109)-O(101)-C(101)-C(102)	-10.0(3)
O(102)-C(101)-C(102)-C(103)	-39.4(4)
O(101)-C(101)-C(102)-C(103)	144.0(2)
O(102)-C(101)-C(102)-C(110)	-167.4(2)
O(101)-C(101)-C(102)-C(110)	16.0(3)
C(101)-C(102)-C(103)-C(104)	-116.1(3)
C(110)-C(102)-C(103)-C(104)	5.5(3)
C(102)-C(103)-C(104)-C(105)	3.3(4)
C(102)-C(103)-C(104)-C(111)	-177.4(2)
C(103)-C(104)-C(111)-C(114)	-50.5(3)
C(105)-C(104)-C(111)-C(114)	128.8(2)
C(103)-C(104)-C(111)-C(112)	76.4(3)
C(105)-C(104)-C(111)-C(112)	-104.2(2)
C(104)-C(111)-C(114)-C(115)	112.0(3)
C(112)-C(111)-C(114)-C(115)	-13.3(4)
C(104)-C(111)-C(114)-C(116)	-66.8(3)
C(112)-C(111)-C(114)-C(116)	167.8(2)
C(114)-C(111)-C(112)-C(113)	-66.1(3)
C(104)-C(111)-C(112)-C(113)	168.5(2)
C(111)-C(112)-C(113)-O(103)	126.5(3)
C(111)-C(112)-C(113)-O(104)	-54.0(3)
O(103)-C(113)-O(104)-C(117)	-9.4(4)
C(112)-C(113)-O(104)-C(117)	171.1(2)
C(113)-O(104)-C(117)-C(119)	-179.9(2)
C(113)-O(104)-C(117)-C(120)	62.9(3)
C(113)-O(104)-C(117)-C(118)	-62.2(3)
C(103)-C(104)-C(105)-O(105)	129.3(2)
C(111)-C(104)-C(105)-O(105)	-50.0(2)
C(103)-C(104)-C(105)-C(121)	-116.3(2)
C(111)-C(104)-C(105)-C(121)	64.3(2)
C(103)-C(104)-C(105)-C(106)	8.0(3)

**Table A8.2.7** *Cont'd*

C(111)-C(104)-C(105)-C(106)	-171.36(19)
O(105)-C(105)-C(121)-O(106)	-58.1(2)
C(104)-C(105)-C(121)-O(106)	-170.82(19)
C(106)-C(105)-C(121)-O(106)	62.0(2)
O(105)-C(105)-C(121)-C(122)	178.17(19)
C(104)-C(105)-C(121)-C(122)	65.5(3)
C(106)-C(105)-C(121)-C(122)	-61.7(3)
O(106)-C(121)-C(122)-C(123)	11.4(3)
C(105)-C(121)-C(122)-C(123)	132.1(3)
O(105)-C(105)-C(106)-C(107)	-20.5(3)
C(104)-C(105)-C(106)-C(107)	97.5(2)
C(121)-C(105)-C(106)-C(107)	-138.53(19)
O(105)-C(105)-C(106)-C(110)	-144.87(19)
C(104)-C(105)-C(106)-C(110)	-26.9(3)
C(121)-C(105)-C(106)-C(110)	97.1(2)
C(105)-C(106)-C(107)-O(107)	-51.1(3)
C(110)-C(106)-C(107)-O(107)	78.4(2)
C(105)-C(106)-C(107)-C(124)	75.5(3)
C(110)-C(106)-C(107)-C(124)	-155.0(2)
C(105)-C(106)-C(107)-C(108)	-164.25(19)
C(110)-C(106)-C(107)-C(108)	-34.7(2)
O(107)-C(107)-C(108)-C(109)	-77.1(2)
C(124)-C(107)-C(108)-C(109)	161.8(2)
C(106)-C(107)-C(108)-C(109)	37.8(2)
C(101)-O(101)-C(109)-C(108)	-114.7(2)
C(101)-O(101)-C(109)-C(110)	-0.1(3)
C(107)-C(108)-C(109)-O(101)	88.7(2)
C(107)-C(108)-C(109)-C(110)	-26.1(3)
C(103)-C(102)-C(110)-C(109)	-140.1(2)
C(101)-C(102)-C(110)-C(109)	-14.9(2)
C(103)-C(102)-C(110)-C(106)	-24.8(3)
C(101)-C(102)-C(110)-C(106)	100.4(2)
O(101)-C(109)-C(110)-C(102)	9.7(2)
C(108)-C(109)-C(110)-C(102)	126.2(2)
O(101)-C(109)-C(110)-C(106)	-112.6(2)



**Table A8.2.7** *Cont'd*

C(108)-C(109)-C(110)-C(106)	3.9(3)
C(107)-C(106)-C(110)-C(102)	-94.7(2)
C(105)-C(106)-C(110)-C(102)	35.5(3)
C(107)-C(106)-C(110)-C(109)	19.4(2)
C(105)-C(106)-C(110)-C(109)	149.6(2)

---

Symmetry transformations used to generate equivalent atoms:

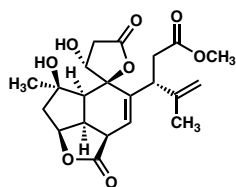
**Table A8.2.8** Hydrogen bonds for compound **133**[Å and °].

D-H...A	d(D-H)	d(H...A)	d(D...A)	<(DHA)
C(2)-H(2)...O(103)#1	1.00	2.43	3.159(3)	129.1
C(18)-H(18C)...O(3)	0.98	2.47	3.006(5)	114.3
C(20)-H(20C)...O(3)	0.98	2.50	3.068(7)	116.6
O(5)-H(5O)...O(6)	0.83(2)	2.36(4)	2.790(3)	112(4)
O(5)-H(5O)...O(7)#2	0.83(2)	2.04(3)	2.810(3)	154(4)
O(6)-H(6O)...O(2)#3	0.83(3)	2.14(3)	2.887(3)	150(5)
C(6)-H(6)...O(6)	1.00	2.31	2.838(4)	112.2
O(7)-H(7O)...O(5)	0.83(3)	2.34(5)	2.874(3)	123(4)
C(24)-H(24C)...O(5)	0.98	2.49	3.029(5)	114.6
C(118)-H(11J)...O(103)	0.98	2.50	3.059(4)	116.4
C(120)-H(12C)...O(103)	0.98	2.39	2.975(4)	117.9
O(105)-H(05O)...O(106)	0.83(2)	2.24(3)	2.725(3)	117(3)
O(105)-H(05O)...O(107)#4	0.83(2)	2.12(3)	2.867(2)	149(3)
O(106)-H(06O)...O(102)#5	0.84(2)	1.99(3)	2.795(3)	162(4)
O(107)-H(07O)...O(105)	0.82(2)	2.23(3)	2.841(2)	131(3)
C(124)-H(12J)...O(105)	0.98	2.41	3.004(3)	118.5

Symmetry transformations used to generate equivalent atoms:

#1  $x+1, y, z$  #2  $-x+3, y-1/2, -z+2$  #3  $x, y-1, z$

#4  $-x+2, y+1/2, -z+1$  #5  $x, y+1, z$

**A8.3 X-RAY CRYSTAL STRUCTURE ANALYSIS OF HAVELLOCKATE (106)**

*Havellockate*  
106

Contents

*Table A8.3.1. Experimental Details*

*Table A8.3.2. Crystal Data*

*Table A8.3.3. Atomic Coordinates*

*Table A8.3.4. Full Bond Distances and Angles*

*Table A8.3.5. Anisotropic Displacement Parameters*

*Table A8.3.6. Hydrogen Atomic Coordinates*

*Table A8.3.7. Torsion Angles*

*Table A8.3.8. Hydrogen Bond Distances and Angles*

**Figure A8.3.1** X-Ray Coordinate of Havellockate (106).

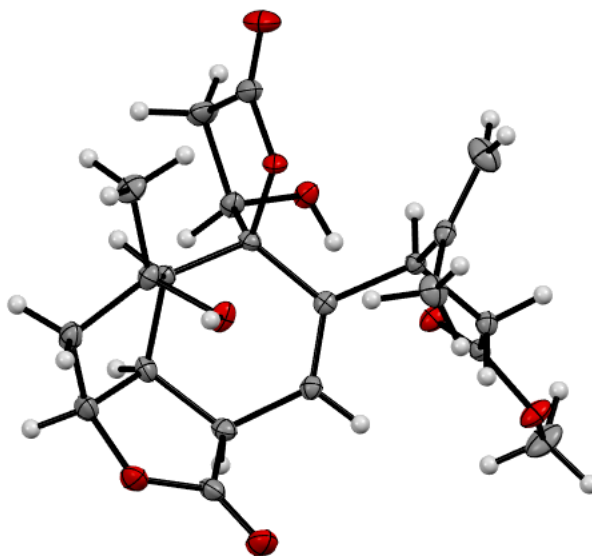


**Table A8.3.1** Experimental Details for X-Ray Structure Determination of Havellockate (**106**).

Low-temperature diffraction data ( $\phi$ - and  $\omega$ -scans) were collected on a Bruker AXS D8 VENTURE KAPPA diffractometer coupled to a PHOTON II CPAD detector with Cu  $K_{\alpha}$  radiation ( $\lambda = 1.54178 \text{ \AA}$ ) from an  $I\mu\text{S}$  micro-source for the structure of compound V21175. The structure was solved by direct methods using SHELXS and refined against  $F^2$  on all data by full-matrix least squares with SHELXL-2017 using established refinement techniques. All non-hydrogen atoms were refined anisotropically. All hydrogen atoms were included into the model at geometrically calculated positions and refined using a riding model. The isotropic displacement parameters of all hydrogen atoms were fixed to 1.2 times the  $U$  value of the atoms they are linked to (1.5 times for methyl groups).

Compound **106** crystallizes in the orthorhombic space group  $P2_12_12_1$  with one molecule in the asymmetric unit. The coordinates for the hydrogen atom bound to O5 and O8 were located in the difference Fourier synthesis and refined semi-freely with the help of a restraint on the O–H distance (0.84(4)  $\text{\AA}$ ).

**Table A8.3.2** Crystal data and structure refinement for havellockate (**106**).

Empirical formula	C21 H26 O8	
Formula weight	406.42	
Temperature	100(2) K	
Wavelength	1.54178 Å	
Crystal system	Triclinic	
Space group	P1	
Unit cell dimensions	a = 7.4661(9) Å	a = 72.913(5)°.
	b = 8.5740(7) Å	b = 66.009(6)°.
	c = 8.9144(5) Å	g = 68.527(5)°.
Volume	478.06(8) Å <sup>3</sup>	
Z	1	
Density (calculated)	1.412 Mg/m <sup>3</sup>	
Absorption coefficient	0.907 mm <sup>-1</sup>	
F(000)	216	
Crystal size	0.200 x 0.150 x 0.100 mm <sup>3</sup>	
Theta range for data collection	5.512 to 74.507°.	
Index ranges	-9<=h<=8, -10<=k<=10, -11<=l<=11	
Reflections collected	15864	
Independent reflections	3781 [R(int) = 0.0334]	
Completeness to theta = 67.679°	100.0 %	
Absorption correction	Semi-empirical from equivalents	
Max. and min. transmission	0.7538 and 0.6853	
Refinement method	Full-matrix least-squares on F <sup>2</sup>	
Data / restraints / parameters	3781 / 5 / 279	
Goodness-of-fit on F <sup>2</sup>	1.050	
Final R indices [I>2sigma(I)]	R1 = 0.0260, wR2 = 0.0653	
R indices (all data)	R1 = 0.0265, wR2 = 0.0655	
Absolute structure parameter	0.05(6)	
Extinction coefficient	n/a	
Largest diff. peak and hole	0.164 and -0.154 e.Å <sup>-3</sup>	

**Table A8.3.3** Atomic coordinates ( $\times 10^4$ ) and equivalent isotropic displacement parameters ( $\text{\AA}^2 \times 10^3$ ) for havellockate (**106**).  $U(\text{eq})$  is defined as one third of the trace of the orthogonalized  $U_{ij}$  tensor.

	x	y	z	U(eq)
O(1)	5084(2)	5344(2)	9846(2)	22(1)
O(2)	4929(2)	7935(2)	8334(2)	25(1)
C(1)	5407(3)	6424(2)	8393(2)	18(1)
C(2)	6501(3)	5451(2)	6939(2)	15(1)
C(3)	5563(3)	6259(2)	5594(2)	13(1)
C(4)	4856(3)	5466(2)	4973(2)	12(1)
C(11)	3939(3)	6344(2)	3579(2)	12(1)
C(12)	4656(3)	7902(2)	2482(2)	14(1)
C(13)	6898(3)	7567(2)	1487(2)	14(1)
O(3)	8120(2)	6192(2)	1250(2)	17(1)
O(4)	7382(2)	9035(2)	826(2)	21(1)
C(14)	9442(3)	8956(3)	-320(3)	27(1)
C(15)	1604(3)	6941(2)	4209(2)	16(1)
C(16)	602(3)	6645(3)	3383(3)	26(1)
C(17)	582(3)	7866(3)	5591(3)	22(1)
C(5)	4962(3)	3596(2)	5620(2)	12(1)
C(18)	6789(3)	2373(2)	4469(2)	16(1)
O(5)	7333(2)	3050(2)	2751(2)	17(1)
O(5A)	8460(30)	1770(20)	4850(20)	42(6)
C(19)	5864(3)	980(2)	4678(2)	21(1)
C(20)	3620(3)	1884(2)	5022(2)	20(1)
O(6)	3160(2)	3353(2)	5549(2)	15(1)
O(7)	2328(3)	1445(2)	4920(2)	32(1)
C(6)	5028(3)	2966(2)	7408(2)	13(1)
C(7)	3022(3)	3314(2)	8907(2)	15(1)
O(8)	2012(2)	5096(2)	8634(2)	18(1)
C(21)	1620(3)	2254(3)	9234(2)	20(1)
C(8)	3876(3)	2887(2)	10329(2)	19(1)

**Table A8.3.3** *Cont'd*

C(9)	5710(3)	3583(2)	9618(2)	19(1)
C(10)	6522(3)	3599(2)	7711(2)	15(1)

---

**Table A8.3.4** Bond lengths [ $\text{\AA}$ ] and angles [ $^\circ$ ] for havellockate (**106**).

---

O(1)-C(1)	1.340(2)
O(1)-C(9)	1.458(2)
O(2)-C(1)	1.202(2)
C(1)-C(2)	1.523(2)
C(2)-C(3)	1.499(2)
C(2)-C(10)	1.531(3)
C(2)-H(2)	1.0000
C(3)-C(4)	1.330(3)
C(3)-H(3)	0.9500
C(4)-C(5)	1.520(2)
C(4)-C(11)	1.531(2)
C(11)-C(15)	1.528(2)
C(11)-C(12)	1.536(2)
C(11)-H(11)	1.0000
C(12)-C(13)	1.504(2)
C(12)-H(12A)	0.9900
C(12)-H(12B)	0.9900
C(13)-O(3)	1.212(2)
C(13)-O(4)	1.337(2)
O(4)-C(14)	1.449(2)
C(14)-H(14A)	0.9800
C(14)-H(14B)	0.9800
C(14)-H(14C)	0.9800
C(15)-C(16)	1.365(3)
C(15)-C(17)	1.447(3)
C(16)-H(16A)	0.9500
C(16)-H(16B)	0.9500
C(17)-H(17A)	0.9800
C(17)-H(17B)	0.9800
C(17)-H(17C)	0.9800
C(5)-O(6)	1.463(2)
C(5)-C(6)	1.540(2)
C(5)-C(18)	1.568(2)



**Table A8.3.4** *Cont'd*

C(18)-O(5A)	1.30(2)
C(18)-O(5)	1.411(2)
C(18)-C(19)	1.519(3)
C(18)-H(18)	1.0000
C(18)-H(18A)	1.0000
O(5)-H(5O)	0.85(2)
O(5A)-H(5A)	0.8400
C(19)-C(20)	1.508(3)
C(19)-H(19A)	0.9900
C(19)-H(19B)	0.9900
C(20)-O(7)	1.200(3)
C(20)-O(6)	1.350(2)
C(6)-C(10)	1.545(3)
C(6)-C(7)	1.548(2)
C(6)-H(6)	1.0000
C(7)-O(8)	1.431(2)
C(7)-C(21)	1.516(3)
C(7)-C(8)	1.536(3)
O(8)-H(8O)	0.85(2)
C(21)-H(21A)	0.9800
C(21)-H(21B)	0.9800
C(21)-H(21C)	0.9800
C(8)-C(9)	1.518(3)
C(8)-H(8A)	0.9900
C(8)-H(8B)	0.9900
C(9)-C(10)	1.552(3)
C(9)-H(9)	1.0000
C(10)-H(10)	1.0000
C(1)-O(1)-C(9)	112.36(14)
O(2)-C(1)-O(1)	121.88(16)
O(2)-C(1)-C(2)	127.58(17)
O(1)-C(1)-C(2)	110.48(15)
C(3)-C(2)-C(1)	111.23(15)
C(3)-C(2)-C(10)	116.69(15)
C(1)-C(2)-C(10)	105.44(15)

**Table A8.3.4** *Cont'd*

C(3)-C(2)-H(2)	107.7
C(1)-C(2)-H(2)	107.7
C(10)-C(2)-H(2)	107.7
C(4)-C(3)-C(2)	125.03(16)
C(4)-C(3)-H(3)	117.5
C(2)-C(3)-H(3)	117.5
C(3)-C(4)-C(5)	120.38(16)
C(3)-C(4)-C(11)	123.03(16)
C(5)-C(4)-C(11)	116.59(15)
C(15)-C(11)-C(4)	113.51(14)
C(15)-C(11)-C(12)	106.40(14)
C(4)-C(11)-C(12)	114.19(14)
C(15)-C(11)-H(11)	107.5
C(4)-C(11)-H(11)	107.5
C(12)-C(11)-H(11)	107.5
C(13)-C(12)-C(11)	116.15(14)
C(13)-C(12)-H(12A)	108.2
C(11)-C(12)-H(12A)	108.2
C(13)-C(12)-H(12B)	108.2
C(11)-C(12)-H(12B)	108.2
H(12A)-C(12)-H(12B)	107.4
O(3)-C(13)-O(4)	123.27(17)
O(3)-C(13)-C(12)	126.63(16)
O(4)-C(13)-C(12)	110.06(15)
C(13)-O(4)-C(14)	117.26(15)
O(4)-C(14)-H(14A)	109.5
O(4)-C(14)-H(14B)	109.5
H(14A)-C(14)-H(14B)	109.5
O(4)-C(14)-H(14C)	109.5
H(14A)-C(14)-H(14C)	109.5
H(14B)-C(14)-H(14C)	109.5
C(16)-C(15)-C(17)	123.58(18)
C(16)-C(15)-C(11)	118.04(17)
C(17)-C(15)-C(11)	118.30(16)
C(15)-C(16)-H(16A)	120.0

**Table A8.3.4** *Cont'd*

C(15)-C(16)-H(16B)	120.0
H(16A)-C(16)-H(16B)	120.0
C(15)-C(17)-H(17A)	109.5
C(15)-C(17)-H(17B)	109.5
H(17A)-C(17)-H(17B)	109.5
C(15)-C(17)-H(17C)	109.5
H(17A)-C(17)-H(17C)	109.5
H(17B)-C(17)-H(17C)	109.5
O(6)-C(5)-C(4)	107.04(13)
O(6)-C(5)-C(6)	109.49(14)
C(4)-C(5)-C(6)	114.38(14)
O(6)-C(5)-C(18)	103.36(14)
C(4)-C(5)-C(18)	113.70(14)
C(6)-C(5)-C(18)	108.24(14)
O(5A)-C(18)-C(19)	112.0(9)
O(5)-C(18)-C(19)	104.97(15)
O(5A)-C(18)-C(5)	115.3(9)
O(5)-C(18)-C(5)	114.84(15)
C(19)-C(18)-C(5)	101.68(15)
O(5)-C(18)-H(18)	111.6
C(19)-C(18)-H(18)	111.6
C(5)-C(18)-H(18)	111.6
O(5A)-C(18)-H(18A)	109.2
C(19)-C(18)-H(18A)	109.2
C(5)-C(18)-H(18A)	109.2
C(18)-O(5)-H(5O)	112(2)
C(18)-O(5A)-H(5A)	109.5
C(20)-C(19)-C(18)	103.80(15)
C(20)-C(19)-H(19A)	111.0
C(18)-C(19)-H(19A)	111.0
C(20)-C(19)-H(19B)	111.0
C(18)-C(19)-H(19B)	111.0
H(19A)-C(19)-H(19B)	109.0
O(7)-C(20)-O(6)	121.25(19)
O(7)-C(20)-C(19)	129.09(19)

**Table A8.3.4** *Cont'd*

O(6)-C(20)-C(19)	109.64(16)
C(20)-O(6)-C(5)	111.50(14)
C(5)-C(6)-C(10)	112.76(14)
C(5)-C(6)-C(7)	119.68(14)
C(10)-C(6)-C(7)	105.62(14)
C(5)-C(6)-H(6)	105.9
C(10)-C(6)-H(6)	105.9
C(7)-C(6)-H(6)	105.9
O(8)-C(7)-C(21)	111.45(15)
O(8)-C(7)-C(8)	109.87(15)
C(21)-C(7)-C(8)	111.95(15)
O(8)-C(7)-C(6)	107.25(14)
C(21)-C(7)-C(6)	114.99(15)
C(8)-C(7)-C(6)	100.73(14)
C(7)-O(8)-H(8O)	106(2)
C(7)-C(21)-H(21A)	109.5
C(7)-C(21)-H(21B)	109.5
H(21A)-C(21)-H(21B)	109.5
C(7)-C(21)-H(21C)	109.5
H(21A)-C(21)-H(21C)	109.5
H(21B)-C(21)-H(21C)	109.5
C(9)-C(8)-C(7)	105.88(14)
C(9)-C(8)-H(8A)	110.6
C(7)-C(8)-H(8A)	110.6
C(9)-C(8)-H(8B)	110.6
C(7)-C(8)-H(8B)	110.6
H(8A)-C(8)-H(8B)	108.7
O(1)-C(9)-C(8)	110.49(16)
O(1)-C(9)-C(10)	106.84(14)
C(8)-C(9)-C(10)	106.08(15)
O(1)-C(9)-H(9)	111.1
C(8)-C(9)-H(9)	111.1
C(10)-C(9)-H(9)	111.1
C(2)-C(10)-C(6)	115.16(15)
C(2)-C(10)-C(9)	104.14(15)

**Table A8.3.4** *Cont'd*

C(6)-C(10)-C(9)	105.07(15)
C(2)-C(10)-H(10)	110.7
C(6)-C(10)-H(10)	110.7
C(9)-C(10)-H(10)	110.7

---

Symmetry transformations used to generate equivalent atoms:

**Table A8.3.5** Anisotropic displacement parameters ( $\text{\AA}^2 \times 10^3$ ) for havellockate (106). The anisotropic displacement factor exponent takes the form:  $-2p^2[h^2 a^{*2}U^{11} + \dots + 2hk a^* b^* U^{12}]$

	U11	U22	U33	U23	U13	U12
O(1)	32(1)	22(1)	15(1)	-4(1)	-9(1)	-11(1)
O(2)	38(1)	22(1)	21(1)	-5(1)	-10(1)	-12(1)
C(1)	20(1)	23(1)	15(1)	-3(1)	-8(1)	-9(1)
C(2)	15(1)	18(1)	15(1)	-3(1)	-6(1)	-7(1)
C(3)	13(1)	14(1)	12(1)	-1(1)	-3(1)	-5(1)
C(4)	9(1)	12(1)	11(1)	-3(1)	-1(1)	-3(1)
C(11)	14(1)	13(1)	11(1)	-2(1)	-4(1)	-5(1)
C(12)	14(1)	14(1)	13(1)	0(1)	-5(1)	-4(1)
C(13)	17(1)	16(1)	11(1)	-1(1)	-6(1)	-7(1)
O(3)	15(1)	14(1)	18(1)	-3(1)	-2(1)	-5(1)
O(4)	17(1)	15(1)	26(1)	-2(1)	-1(1)	-8(1)
C(14)	20(1)	22(1)	32(1)	-3(1)	4(1)	-12(1)
C(15)	15(1)	14(1)	17(1)	2(1)	-5(1)	-5(1)
C(16)	16(1)	39(1)	22(1)	-4(1)	-6(1)	-8(1)
C(17)	14(1)	24(1)	25(1)	-4(1)	-7(1)	-2(1)
C(5)	11(1)	14(1)	12(1)	-2(1)	-4(1)	-5(1)
C(18)	18(1)	14(1)	13(1)	-3(1)	-4(1)	-3(1)
O(5)	22(1)	15(1)	12(1)	-3(1)	-2(1)	-6(1)
C(19)	28(1)	16(1)	22(1)	-7(1)	-7(1)	-8(1)
C(20)	29(1)	18(1)	18(1)	-1(1)	-10(1)	-12(1)
O(6)	16(1)	15(1)	19(1)	-1(1)	-8(1)	-7(1)
O(7)	40(1)	29(1)	44(1)	-6(1)	-23(1)	-18(1)
C(6)	14(1)	12(1)	12(1)	-2(1)	-4(1)	-3(1)
C(7)	15(1)	14(1)	13(1)	-2(1)	-3(1)	-4(1)
O(8)	16(1)	14(1)	16(1)	-3(1)	-1(1)	-1(1)
C(21)	19(1)	20(1)	19(1)	-2(1)	-1(1)	-10(1)
C(8)	24(1)	17(1)	13(1)	0(1)	-5(1)	-6(1)
C(9)	25(1)	18(1)	14(1)	-2(1)	-10(1)	-5(1)
C(10)	15(1)	18(1)	14(1)	-1(1)	-8(1)	-4(1)

**Table A8.3.6** Hydrogen coordinates ( $\times 10^4$ ) and isotropic displacement parameters ( $\text{\AA}^2 \times 10^3$ ) for havellockate (**106**).

	x	y	z	U(eq)
H(2)	7948	5501	6457	18
H(3)	5466	7428	5152	16
H(11)	4371	5497	2842	15
H(12A)	3881	8448	1699	17
H(12B)	4297	8728	3207	17
H(14A)	10418	8316	272	41
H(14B)	9577	10111	-777	41
H(14C)	9723	8386	-1231	41
H(16A)	-846	7055	3708	31
H(16B)	1352	6029	2484	31
H(17A)	-892	8265	5788	33
H(17B)	1106	8843	5326	33
H(17C)	839	7115	6593	33
H(18)	8001	1917	4850	19
H(18A)	7105	2976	3287	19
H(5O)	7620(50)	3980(30)	2550(40)	22(7)
H(5A)	8966	2565	4662	63
H(19A)	6457	480	3651	25
H(19B)	6090	66	5621	25
H(6)	5593	1700	7527	15
H(8O)	970(40)	5270(40)	9510(30)	32(7)
H(21A)	565	2356	10333	31
H(21B)	2417	1060	9204	31
H(21C)	972	2662	8376	31
H(8A)	2834	3428	11289	23
H(8B)	4292	1642	10704	23
H(9)	6784	2861	10127	22
H(10)	7942	2825	7357	18

**Table A8.3.7** Torsion angles [°] for havellockate (**106**).

---

C(9)-O(1)-C(1)-O(2)	177.76(18)
C(9)-O(1)-C(1)-C(2)	-4.7(2)
O(2)-C(1)-C(2)-C(3)	-47.0(3)
O(1)-C(1)-C(2)-C(3)	135.68(16)
O(2)-C(1)-C(2)-C(10)	-174.3(2)
O(1)-C(1)-C(2)-C(10)	8.3(2)
C(1)-C(2)-C(3)-C(4)	-124.70(19)
C(10)-C(2)-C(3)-C(4)	-3.7(3)
C(2)-C(3)-C(4)-C(5)	0.0(3)
C(2)-C(3)-C(4)-C(11)	-179.07(16)
C(3)-C(4)-C(11)-C(15)	-98.46(19)
C(5)-C(4)-C(11)-C(15)	82.47(18)
C(3)-C(4)-C(11)-C(12)	23.8(2)
C(5)-C(4)-C(11)-C(12)	-155.32(14)
C(15)-C(11)-C(12)-C(13)	-170.21(15)
C(4)-C(11)-C(12)-C(13)	63.8(2)
C(11)-C(12)-C(13)-O(3)	12.9(3)
C(11)-C(12)-C(13)-O(4)	-169.19(15)
O(3)-C(13)-O(4)-C(14)	4.4(3)
C(12)-C(13)-O(4)-C(14)	-173.53(16)
C(4)-C(11)-C(15)-C(16)	-135.91(18)
C(12)-C(11)-C(15)-C(16)	97.66(19)
C(4)-C(11)-C(15)-C(17)	47.3(2)
C(12)-C(11)-C(15)-C(17)	-79.14(19)
C(3)-C(4)-C(5)-O(6)	146.39(16)
C(11)-C(4)-C(5)-O(6)	-34.51(18)
C(3)-C(4)-C(5)-C(6)	24.9(2)
C(11)-C(4)-C(5)-C(6)	-155.98(14)
C(3)-C(4)-C(5)-C(18)	-100.12(19)
C(11)-C(4)-C(5)-C(18)	78.98(19)
O(6)-C(5)-C(18)-O(5A)	-151.2(10)
C(4)-C(5)-C(18)-O(5A)	93.2(10)
C(6)-C(5)-C(18)-O(5A)	-35.1(10)



**Table A8.3.7** *Cont'd*

O(6)-C(5)-C(18)-O(5)	82.97(18)
C(4)-C(5)-C(18)-O(5)	-32.7(2)
C(6)-C(5)-C(18)-O(5)	-160.96(15)
O(6)-C(5)-C(18)-C(19)	-29.75(17)
C(4)-C(5)-C(18)-C(19)	-145.43(15)
C(6)-C(5)-C(18)-C(19)	86.31(17)
O(5A)-C(18)-C(19)-C(20)	153.2(9)
O(5)-C(18)-C(19)-C(20)	-90.37(17)
C(5)-C(18)-C(19)-C(20)	29.58(18)
C(18)-C(19)-C(20)-O(7)	162.1(2)
C(18)-C(19)-C(20)-O(6)	-19.8(2)
O(7)-C(20)-O(6)-C(5)	178.26(18)
C(19)-C(20)-O(6)-C(5)	-0.1(2)
C(4)-C(5)-O(6)-C(20)	139.53(14)
C(6)-C(5)-O(6)-C(20)	-95.97(16)
C(18)-C(5)-O(6)-C(20)	19.21(18)
O(6)-C(5)-C(6)-C(10)	-164.70(13)
C(4)-C(5)-C(6)-C(10)	-44.6(2)
C(18)-C(5)-C(6)-C(10)	83.29(18)
O(6)-C(5)-C(6)-C(7)	-39.6(2)
C(4)-C(5)-C(6)-C(7)	80.53(19)
C(18)-C(5)-C(6)-C(7)	-151.60(16)
C(5)-C(6)-C(7)-O(8)	-51.6(2)
C(10)-C(6)-C(7)-O(8)	76.87(17)
C(5)-C(6)-C(7)-C(21)	73.0(2)
C(10)-C(6)-C(7)-C(21)	-158.57(15)
C(5)-C(6)-C(7)-C(8)	-166.46(15)
C(10)-C(6)-C(7)-C(8)	-38.03(17)
O(8)-C(7)-C(8)-C(9)	-73.21(18)
C(21)-C(7)-C(8)-C(9)	162.39(15)
C(6)-C(7)-C(8)-C(9)	39.71(18)
C(1)-O(1)-C(9)-C(8)	-115.82(17)
C(1)-O(1)-C(9)-C(10)	-0.9(2)
C(7)-C(8)-C(9)-O(1)	88.88(17)
C(7)-C(8)-C(9)-C(10)	-26.57(19)

**Table A8.3.7** *Cont'd*

C(3)-C(2)-C(10)-C(6)	-17.7(2)
C(1)-C(2)-C(10)-C(6)	106.30(17)
C(3)-C(2)-C(10)-C(9)	-132.21(16)
C(1)-C(2)-C(10)-C(9)	-8.20(18)
C(5)-C(6)-C(10)-C(2)	41.1(2)
C(7)-C(6)-C(10)-C(2)	-91.38(17)
C(5)-C(6)-C(10)-C(9)	155.01(14)
C(7)-C(6)-C(10)-C(9)	22.58(18)
O(1)-C(9)-C(10)-C(2)	5.83(18)
C(8)-C(9)-C(10)-C(2)	123.72(16)
O(1)-C(9)-C(10)-C(6)	-115.63(16)
C(8)-C(9)-C(10)-C(6)	2.26(19)

---

Symmetry transformations used to generate equivalent atoms:

**Table A8.3.8** Hydrogen bonds for havellockate (**106**) [ $\text{\AA}$  and  $^\circ$ ].

D-H...A	d(D-H)	d(H...A)	d(D...A)	$\angle(\text{DHA})$
O(5 <sup>a</sup> )-H(5O <sup>a</sup> )...O(3)	0.85(2)	1.99(2)	2.792(2)	157(3)
O(5A <sup>b</sup> )-H(5A <sup>b</sup> )...O(7)#10.84		2.42	2.82(2)	110.5
C(19)-H(19B)...O(2)#2	0.99	2.61	3.523(2)	153.8
O(8)-H(8O)...O(3)#3	0.85(2)	2.09(2)	2.9229(18)	166(3)
C(21)-H(21A)...O(5 <sup>a</sup> )#3	0.98	2.51	3.470(2)	166.5
C(21)-H(21C)...O(6)	0.98	2.42	2.983(2)	116.1
C(8)-H(8B)...O(4)#4	0.99	2.57	3.422(2)	143.9
C(9)-H(9)...O(5 <sup>a</sup> )#5	1.00	2.59	3.328(2)	130.4

Symmetry transformations used to generate equivalent atoms:

#1  $x+1,y,z$  #2  $x,y-1,z$  #3  $x-1,y,z+1$  #4  $x,y-1,z+1$

#5  $x,y,z+1$

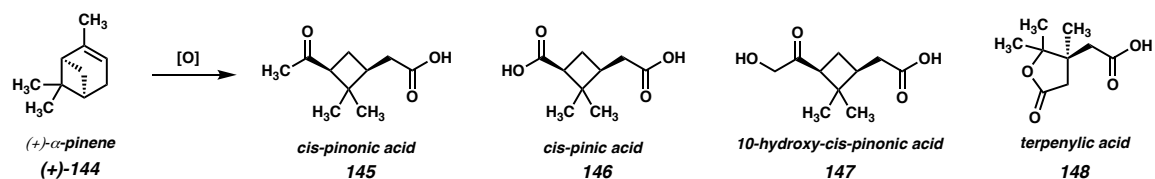
## CHAPTER 3

### Synthesis of Carboxylic Acids and Dimer Esters from Pinene-Derived Secondary Organic Aerosol†

#### 3.1 INTRODUCTION

Secondary organic aerosol (SOA) is formed in the atmosphere when volatile organic compounds (VOCs) undergo gas-phase chemical reactions forming lower-volatility products that condense to form aerosol particles.<sup>1</sup> SOA is understood to represent 15–80% (by mass) of atmospheric fine particulate matter (PM<sub>2.5</sub>),<sup>2</sup> which has a major impact on climate, air quality, and human health. Consequently, fundamental study of both the formation and composition of SOA is crucial to assessing its environmental and health impacts.

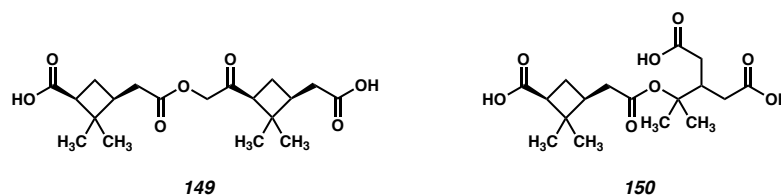
**Figure 3.1.1** Examples of SOA components derived from  $\alpha$ -pinene (**144**).



†This research was performed in collaboration with Christopher M. Kenseth, Samir P. Rezgui, Yuanlong Huang, Nathan F. Dalleska, and John H. Seinfeld. Portions of this chapter have been reproduced with permission from Kenseth, C. M.; Hafeman, N. J.; Huang, Y.; Dalleska, N. F.; Stoltz, B. M.; and Seinfeld, J. H. *Environ. Sci. Technol.* **2020**, *54*, 12829–12893. © 2020 American Chemical Society.

One of the many VOCs that has been implicated in the formation of SOA is pinene, both the  $\alpha$  and  $\beta$  isomers. It has been demonstrated that gas-phase oxidation of  $\alpha$ -pinene and  $\beta$ -pinene gives rise to a variety of SOA-forming products (Figure 3.1.1), notably carboxylic acids, which have been characterized extensively in the literature.<sup>3</sup> Furthermore, these oxidation products have been shown to undergo accretion reactions in laboratory experiments, yielding even higher-molecular-weight products that have been implicated as key drivers of both nucleation and the initial growth of SOA. Specifically, dimeric oxidation products proposed to contain ester linkages, such as **149** and **150** (Figure 3.1.2), have been detected in both laboratory-derived and ambient pinene SOA.<sup>4,5,6,7,8,9</sup>

**Figure 3.1.2** Examples of pinene-derived dimer esters detected in SOA mixtures.



Due to the complex and dynamic nature of SOA, identifying and quantifying their molecular constituents remains an immense challenge. Electrospray ionization mass spectrometry (ESI-MS), typically coupled with liquid chromatographic (LC) separation is commonly employed to analyze the molecular composition of SOA.<sup>10,11</sup> However, in many cases authentic standards are lacking, and product structures are inferred from MS fragmentation data, which prevents accurate identification and quantification of SOA constituents, as well as mechanistic understanding of their formation. In the case of pinene-derived SOA, commercially available monomeric terpenoic acids (e.g. *cis*-pinonic acid) are often used as surrogates to quantify both monomeric and dimeric SOA constituents,

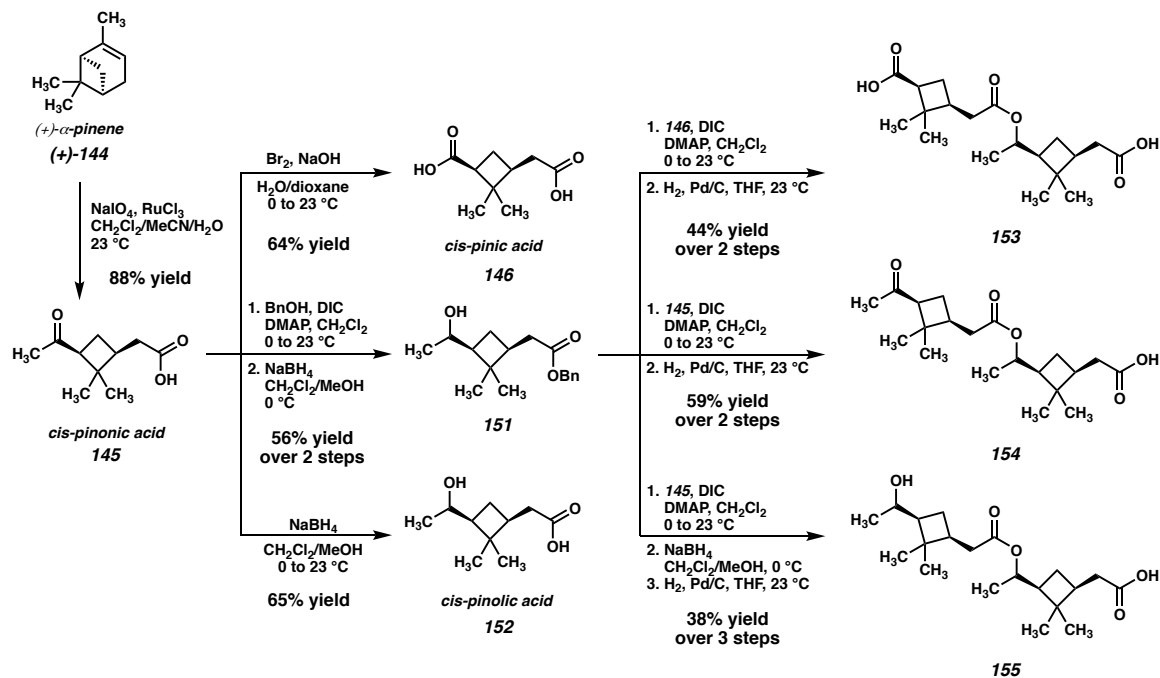
despite the dependence of ESI efficiency on molecular structure.<sup>12,13</sup> As such, access to authentic samples of pinene-derived SOA constituents is of great interest.

In this study, we report the synthesis of a series of pinene-derived carboxylic acids and dimer ester homologues for analysis by LC/ESI-MS. These experiments reveal a significant difference in ESI efficiency between the monomeric acids and the synthetic dimer esters. Additionally, we report the first synthesis of authentic standards of several major dimer esters identified in SOA from ozonolysis of  $\alpha$ - and  $\beta$ -pinene. This research led to structural reassignment of four previously observed dimer esters, highlighting the importance of obtaining authentic standards for structure determination and resolving a decades-long debate within the atmospheric community.<sup>14,15</sup>

### 3.2 SYNTHESIS AND CHARACTERIZATION OF MONOMERS **145**, **146**, AND **152**, AND DIMER ESTER HOMOLOGUES **153**–**155**

Our first task was the synthesis of the three pinene oxidation products *cis*-pinonic acid (**145**), *cis*-pinic acid (**146**), and *cis*-pinolic acid (**152**). Starting with readily available (+)- $\alpha$ -pinene, an oxidative cleavage of the C=C bond using a known procedure<sup>16</sup> furnishes *cis*-pinonic acid (**145**).<sup>17</sup> Exposure of *cis*-pinonic acid (**145**) to NaBrO then effects a haloform reaction, which generates *cis*-pinic acid (**146**), the second of the desired monomeric pinene oxidation products. Finally, treatment of *cis*-pinonic acid (**145**) with sodium borohydride provides *cis*-pinolic acid (**152**).<sup>18</sup>

**Scheme 3.2.1** Synthesis of pinonic acid (**145**), pinic acid (**146**), and pinolic acid (**148**), pinolic acid benzyl ester (**147**), and dimers **153–155**.



With the three monomeric oxidation products in hand, we next turned our attention to the preparation of the three dimer ester homologues **153–155**. In the target structures, *cis*-pinolic acid (**152**) serves as the alcohol component of the dimeric ester linkage. However, as a hydroxyl-bearing acid, **152** has the potential to dimerize or cyclize under esterification conditions. To avoid these potential issues, we prepared pinolic acid benzyl ester (**151**) by esterification of *cis*-pinonic acid (**145**) with benzyl alcohol, followed by reduction of the ketone with sodium borohydride to the requisite alcohol. The benzyl ester was chosen as the protecting group because it could be removed by hydrogenolysis after the dimerization, which would not cleave the newly formed ester linkage.

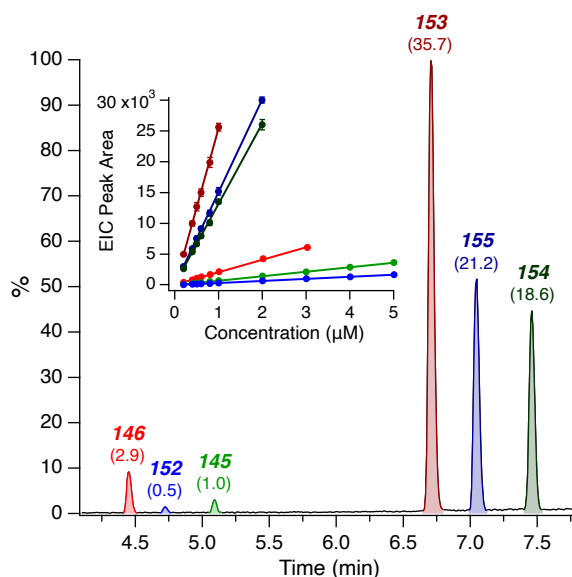
In the event, *cis*-pinolic acid benzyl ester (**151**) undergoes DIC-mediated coupling with *cis*-pinic acid (**146**), to afford a mixture of two esters (of the primary and secondary

carboxylates) which are separated by flash chromatography. Hydrogenolytic removal of the benzyl ester then affords pinolic/pinic dimer **153**. The pinolic/pinonic dimer (**154**) is prepared by esterification of **151** with *cis*-pinonic acid (**145**), followed by hydrogenolysis. Finally, esterification of *cis*-pinolic acid benzyl ester (**151**) with *cis*-pinonic acid (**145**), followed by sodium borohydride reduction and hydrogenolysis furnishes the pinolic/pinolic dimer (**155**).

With the monomers and dimer ester homologues in hand, we turned our attention to characterizing their ESI-MS behavior. To this end, equimolar aqueous solutions of carboxylic acids **145**, **146**, and **152**, and dimer esters **153–155** were analyzed by UPLC/(–)ESI-Q-TOF-MS. Contrary to the assumptions of previous LC/(–)ESI-MS studies that monoterpene oxidation products exhibit comparable (–)ESI efficiencies due to the presence of similar structures/functional groups, the (–)ESI efficiencies of the monomeric carboxylic acids (i.e. **145**, **146**, and **148**) varied by almost a factor of six despite differing only in identity of the terminal functional group (i.e. ketone vs. carboxylic acid vs. alcohol). More strikingly, the (–)ESI efficiencies of dimer esters **153–155** were found to be 19–36 times higher than that of commercially available *cis*-pinonic acid (**145**). These findings conclusively demonstrate that, as a result of fundamental differences in ionizing behavior, the mass contribution of dimers (and to a lesser extent of dicarboxylic acids) to monoterpene SOA has been significantly overestimated in past studies.



**Figure 3.2.1** UPLC/(-)ESI-Q-TOF-MS BPI chromatogram of an equimolar (1.00  $\mu\text{M}$ ) aqueous solution of carboxylic acids **145**, **146**, and **152** and dimer esters **153–155**. (-)ESI efficiencies, normalized to that of *cis*-pinonic acid (**145**), are given in parentheses. (Inset) Weighted (1/X), linear ( $R^2 > 0.998$ ) calibration curves, generated from triplicate measurements (1 $\sigma$ ) of equimolar aqueous solutions of carboxylic acids **145**, **146**, and **152** and dimer esters **153–155** spanning a concentration range from 0.200 to 5.00  $\mu\text{M}$ .

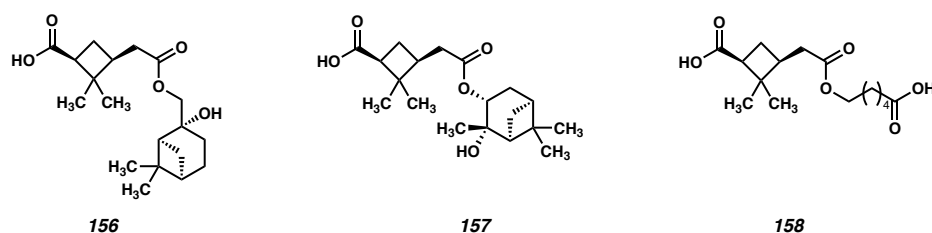


### 3.3 SYNTHESIS AND CHARACTERIZATION OF DIMER ESTERS 156–158

Next, we sought to synthesize and characterize a series of dimer esters of *cis*-pinic acid that have been observed in pinene derived SOA (i.e. **156–158**, Figure 3.3.1). For this purpose, we considered a modular synthetic strategy in which a suitably mono protected *cis*-pinic acid derivative could be coupled with a variety of alcohols, followed by deprotection. This would avoid selectivity issues between the two carboxylic acids that could potentially complicate purification and characterization. It was envisioned that a

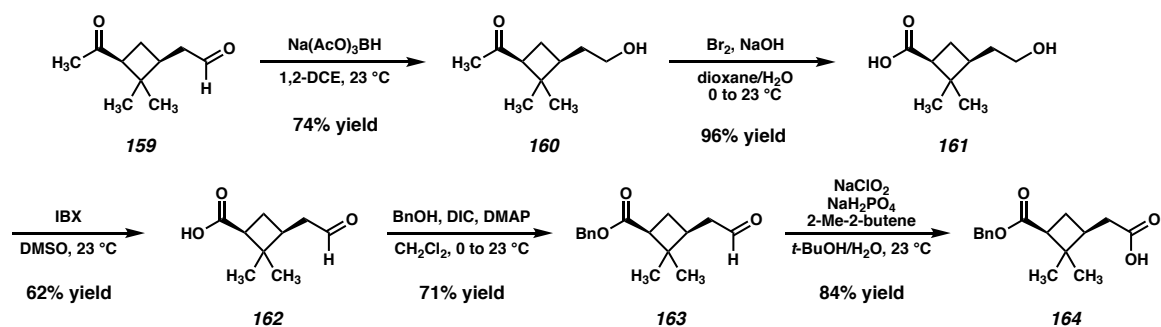
precursor such as pinic acid monobenzyl ester (**164**, Scheme 3.3.1) could serve as an ideal intermediate for this strategy. With the secondary carboxylate suitably protected, esterification would occur exclusively at the primary carboxylic acid to afford the desired dimer esters after deprotection by hydrogenolysis.

**Figure 3.3.1** Pinic acid dimer ester targets **156–158**.



The synthesis of the monobenzyl ester of pinic acid is shown in Scheme 3.3.1. Aldehyde-selective monoreduction of ketoaldehyde **159**, accessible in two steps from (+)- $\alpha$ -pinene (**144**),<sup>19</sup> furnishes ketoalcohol **160**. A haloform reaction then converts the methyl ketone to the corresponding acid, furnishing hydroxy acid **161**. Oxidation of the alcohol to the aldehyde with IBX, followed by esterification with benzyl alcohol furnishes aldehyde **163**. A final Pinnick oxidation then affords the desired acid (**164**) monomer.

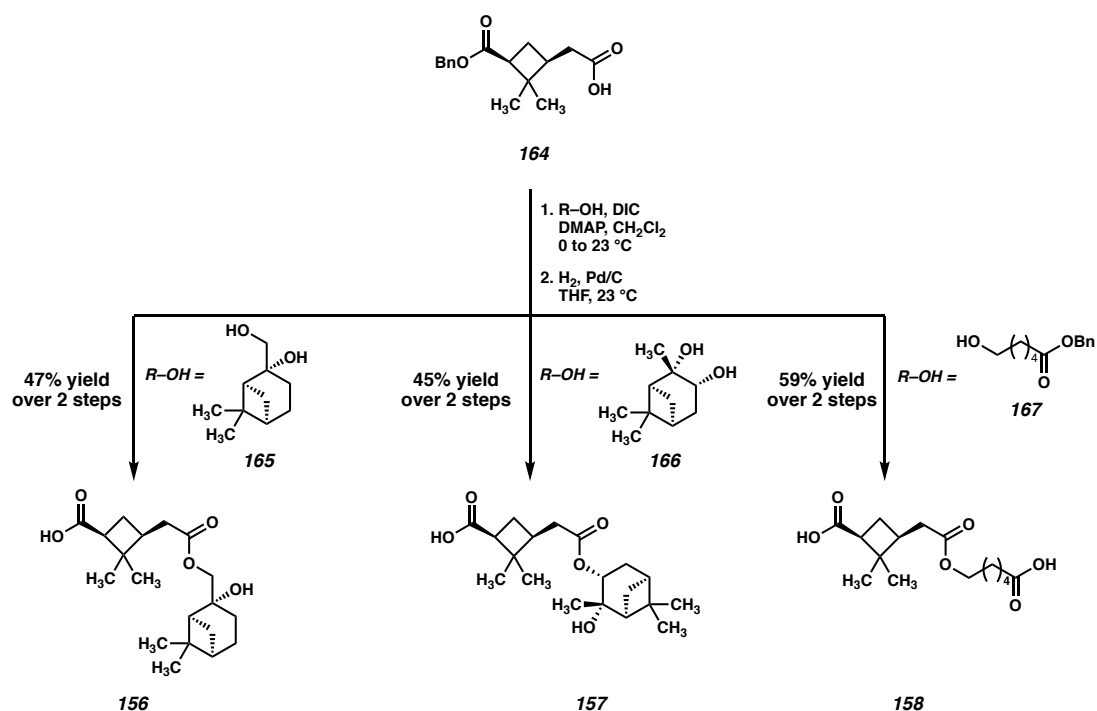
**Scheme 3.3.1** Synthesis of pinic acid monobenzyl ester (**164**).



Acid **164** undergoes esterification with  $\beta$ -pinene diol (**165**), followed by hydrogenation of the intermediate diester to afford dimer ester **156**, the first target in this

series (Scheme 3.3.1). The same sequence can be employed to using  $\alpha$ -pinene diol (**166**) or 6-hydroxy benzylhexanoate (**167**) as the coupling partners to afford dimer esters **157** and **158** respectively. All three of these dimer esters have been tentatively observed SOA mixtures generated by  $\alpha$ -pinene ozonolysis, but this represents the first preparative-scale synthesis of these putative oxidation products.

**Scheme 3.3.2** Synthesis of pinic acid dimer esters **156–158**.

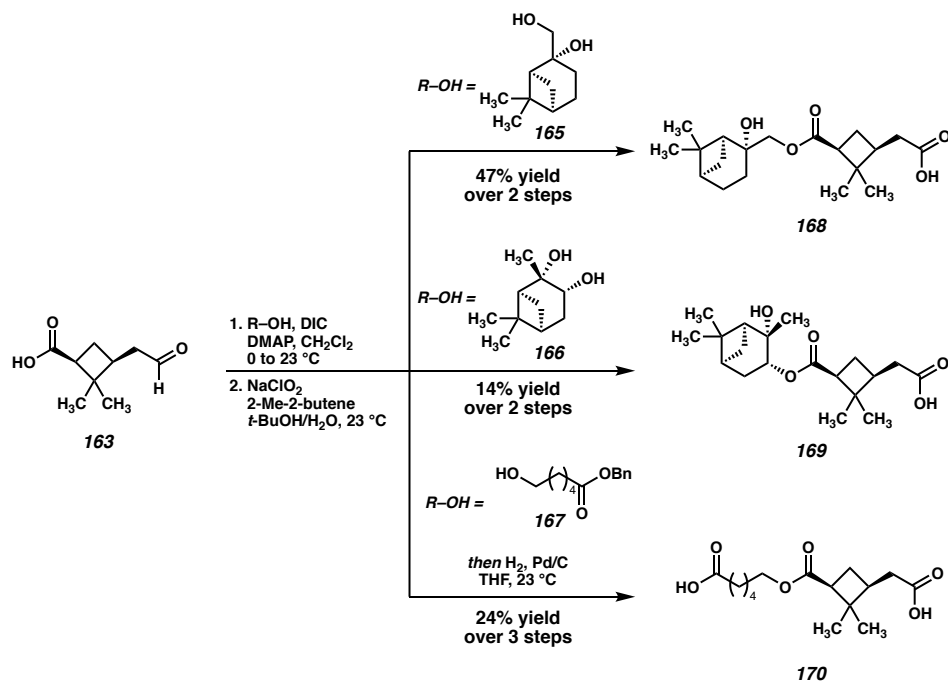


With ready access to the dimer ester standards, we compared their LC/ESI-MS profiles to those of dimer esters observed in laboratory-generated pinene SOA. Surprisingly, slight discrepancies in LC retention times and distinct differences in MS/MS fragmentation patterns were observed between the standards and the SOA molecular products (see figure 3.4.1). These inconsistencies called into question the previously reported structural assignments of these dimer esters, which were based solely on MS data.

### 3.4 SYNTHESIS AND CHARACTERIZATION OF ISOMERIC DIMER ESTERS 168–170

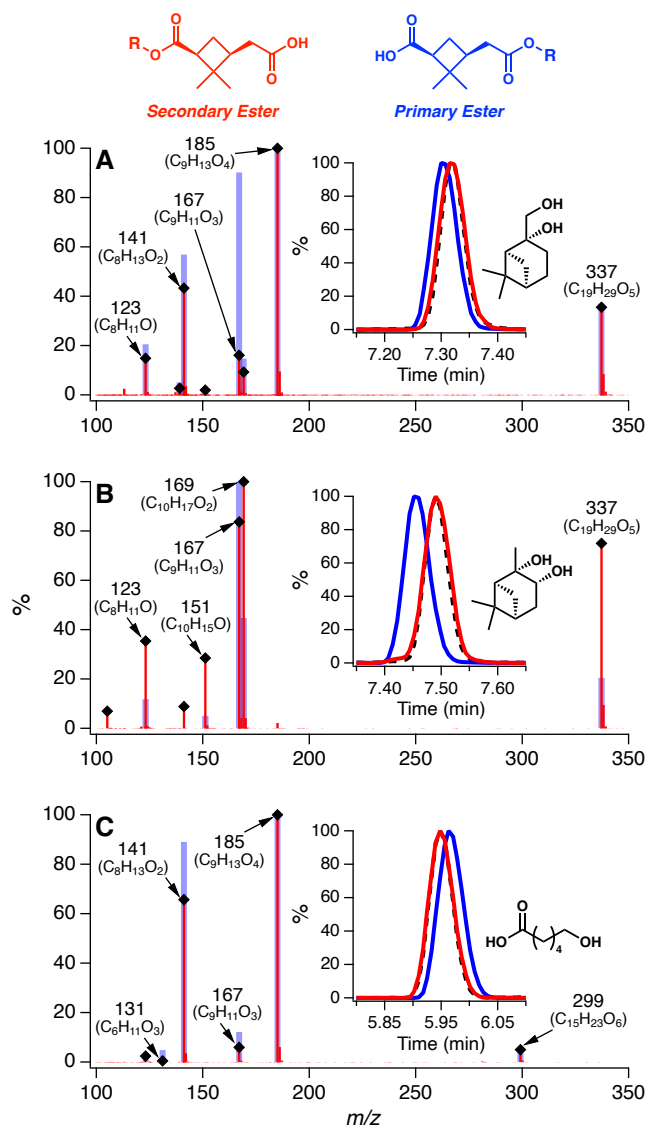
Given the discrepancy in the LCMS data for dimer esters **156–158**, we hypothesized that the correct structures might be esters of the primary (rather than secondary) carboxylic acid of *cis*-pinic acid (**146**). The synthesis of these targets would again necessitate a differentiated pinic acid monomer. Fortunately, acid **163** (an intermediate in the route toward pinic acid monobenzyl ester **164**) meets the requirements of the desired monomeric coupling partner. As such it was employed for the synthesis of second series of dimer esters (**156–158**) shown in scheme 3.4.1. Esterification of acid **163** with  $\alpha$ - and  $\beta$ - pinene diol (**165** and **166**) as well 6-hydroxy benzylhexanoate (**167**), followed by Pinnick oxidation of the intermediate aldehyde, furnishes the desired isomeric dimer esters **168–170**.

**Scheme 3.4.1** Synthesis of isomeric dimer esters **168–170**.



Gratifyingly, the LC retention times and MS/MS fragmentation patterns of dimer esters **168–170** are in good accordance with those of the dimer esters generated in SOA experiments. As such, we propose a structural reassignment of putative structures **156–158** to structures **168–170** and report the first synthesis of authentic standards of dimer esters in pinene SOA.

**Figure 3.4.1.** Extracted ion chromatograms (EIC) and MS/MS spectra of synthesized secondary (red) and primary (blue) dimer esters of *cis*-pinic acid and (A)  $\beta$ -pinene diol, (B)  $\alpha$ -pinene diol, and (C) 6-hydroxyhexanoic acid, as well as of dimer esters identified in SOA (black diamonds, dashed lines).



**3.5 CONCLUSION**

We have reported the synthesis of several atmospherically-relevant pinene oxidation products, and their use in studies of pinene-derived SOAs. Notably, several erroneous structural assignments based solely upon MS data were corrected by preparing authentic standards and comparing their LC/ESI-MS behavior to the SOA-derived samples. These results highlight the power of chemical synthesis in the context of atmospheric chemistry for the elucidation of structural information about SOA constituents.

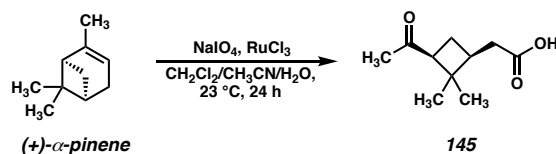
### 3.6 EXPERIMENTAL

#### 3.6.1 MATERIALS AND METHODS

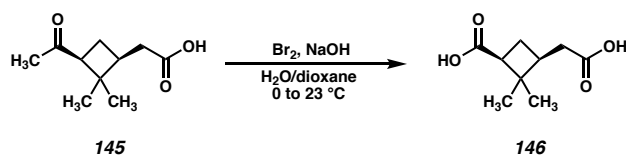
Unless otherwise stated, reactions were performed in flame-dried glassware under ambient conditions using dry, deoxygenated solvents. Solvents were dried by passage through an activated alumina column under argon. Reagents were purchased from commercial sources and used as received. Reaction temperatures were controlled by an IKAmag temperature modulator. Thin-layer chromatography (TLC) was performed using E. Merck silica gel 60 F254 pre-coated plates (250  $\mu\text{m}$ ) and visualized by UV fluorescence quenching, potassium permanganate staining, or *p*-anisaldehyde staining. Silicycle SiliaFlash P60 Academic Silica gel (particle size 40–63  $\mu\text{m}$ ) was used for flash chromatography. Preparative HPLC was performed using an Agilent 1200 HPLC system equipped with an ACE C<sub>18</sub> column (5  $\mu\text{m}$ , 21.2 mm  $\times$  250 mm). H and C NMR spectra were recorded on a Varian Inova 500 (500 and 125 MHz, respectively) spectrometer and are reported in terms of chemical shift relative to CHCl<sub>3</sub> ( $\delta$  7.26 and 77.16 ppm, respectively). Data for <sup>1</sup>H NMR are reported as follows: chemical shift ( $\delta$  ppm) (multiplicity, coupling constant, integration). Abbreviations are used as follows: s = singlet, d = doublet, t = triplet, q = quartet, m = multiplet. IR spectra were obtained from thin films deposited on NaCl plates using a Perkin Elmer Spectrum BXII spectrometer and are reported in frequency of absorption (cm<sup>-1</sup>). Optical rotations were measured with a Jasco P-2000 polarimeter operating on the sodium D-line (589 nm) using a 100 mm path-length cell. High resolution mass spectra (HRMS) were acquired using a Waters ACQUITY UPLC I-Class system coupled to a Xevo G2-S ESI-Q-TOF-MS (see Experimental).



### 3.6.2 SYNTHETIC PROCEDURES

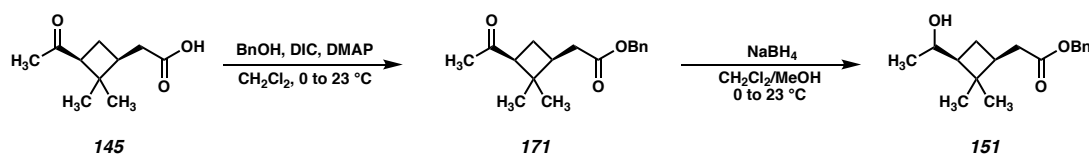


**(+)-*cis*-pinonic acid (145):** Prepared according to a modified literature procedure.<sup>16</sup> To a stirred solution of (+)- $\alpha$ -pinene (5.0 mL, 32.0 mmol, 1.0 eq) in  $\text{CH}_2\text{Cl}_2$ :MeCN:H<sub>2</sub>O (2:2:3, 260 mL) at room temperature was added NaIO<sub>4</sub> (26.8 g, 125.3 mmol, 3.9 eq) followed by RuCl<sub>3</sub> hydrate (240 mg, 1.15 mmol, 0.036 eq). The mixture was allowed to stir at ambient temperature for 24 h. The mixture was then diluted with Et<sub>2</sub>O (100 mL) and H<sub>2</sub>O (100 mL). The layers were separated and the aqueous layer was extracted with Et<sub>2</sub>O (3x 100 mL). The organic extracts were filtered over celite and concentrated *in vacuo*. The crude residue was dissolved in Et<sub>2</sub>O (100 mL) and extracted with 10% aqueous Na<sub>2</sub>CO<sub>3</sub> (3x 150 mL). The aqueous extracts were combined, acidified to pH 1 with conc. H<sub>2</sub>SO<sub>4</sub>, and extracted with Et<sub>2</sub>O (3x 100 mL). The combined organic extracts were washed with brine (100 mL), dried over MgSO<sub>4</sub>, and concentrated. The crude residue was purified by flash chromatography on SiO<sub>2</sub> (40% EtOAc/Hexanes) to afford (+)-*cis*-pinonic acid (**145**) as a white solid (5.2 g, 28.2 mmol, 88% yield). All physical and spectral data were in good accordance with previously reported values.



**(-)-*cis*-pinonic acid (146):** Prepared according to literature procedure.<sup>16</sup> A 1 L round bottom flask was charged with (+)-*cis*-pinonic acid (**145**) (2.50 g, 13.55 mmol, 1.0 equiv) in

dioxane:H<sub>2</sub>O (5:1, 200 mL) and cooled to 0 °C. In a separate, 500 mL round bottom flask, Br<sub>2</sub> (2.29 mL, 44.72 mmol, 3.3 equiv) was added dropwise to a solution of NaOH (7.05 g, 176.2 mmol, 13.0 equiv) in H<sub>2</sub>O (68 mL) at 0 °C. This mixture was allowed to stir for 10 min, after which dioxane (17 mL) was added. The contents of this flask was transferred to an pressure-equalized addition funnel and added to the dioxane:water solution of **145** dropwise at 0 °C. Upon completion of the addition, the reaction mixture was allowed to stir for 16 h while gradually warming to 23 °C. The mixture was then washed with CH<sub>2</sub>Cl<sub>2</sub> (3x) and the aqueous phase was quenched with NaHSO<sub>3</sub> (40% aqueous). The aqueous phase was acidified to pH ~ 1 with HCl (conc.) then extracted with Et<sub>2</sub>O (3x). The combined organic extracts were washed with brine, dried over MgSO<sub>4</sub>, filtered and concentrated leaving a crude oil which was purified by flash chromatography (SiO<sub>2</sub>, 40% EtOAc/hexanes) then preparative HPLC (C-18, 0-18% MeCN/H<sub>2</sub>O over 12 min) to afford (-)-*cis*-pinic acid (**146**) (1.60 g, 8.60 mmol, 64% yield) as a white solid. All physical and spectral data were in good accordance with previously reported values.



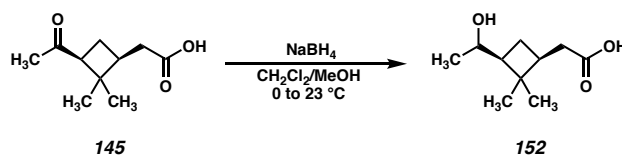
**benzyl *cis*-pinonic acid (**151**):** To a stirred solution of (-)-*cis*-pinonic acid (**145**) (3.00 g, 16.28 mmol, 1.0 eq), benzyl alcohol (5.08 mL, 48.84 mmol, 3.0 eq) and DMAP (199 mg, 1.63 mmol, 0.10 eq) in CH<sub>2</sub>Cl<sub>2</sub> (33.0 mL) at 0 °C was added DIC (2.55 mL, 16.28 mmol, 1.0 eq) dropwise. The solution was stirred for 16 h and gradually allowed to warm to 23 °C. Upon disappearance of the starting material as judged by TLC, the solution was diluted with Et<sub>2</sub>O (100 mL) and H<sub>2</sub>O (100 mL). The layers were separated and the aqueous layer was extracted with Et<sub>2</sub>O (3x, 100 mL). The combined organic extracts were washed with

brine (100 mL), dried over  $\text{MgSO}_4$ , and concentrated. The crude product was purified by flash chromatography on  $\text{SiO}_2$  (30%  $\text{Et}_2\text{O}$ /Hexanes) to afford intermediate ketoester **171** (3.89 g, 14.18 mmol, 87% yield) as a colorless oil;  $^1\text{H}$  NMR (500 MHz,  $\text{CDCl}_3$ )  $\delta$  7.55 – 7.06 (m, 5H), 5.08 (s, 2H), 2.85 (dd,  $J = 10.1, 7.5$  Hz, 1H), 2.54 – 2.18 (m, 3H), 2.02 (s, 3H), 2.01 – 1.93 (m, 1H), 1.93 – 1.83 (m, 1H), 1.28 (s, 3H), 0.84 (s, 3H).  $^{13}\text{C}$  NMR (125 MHz,  $\text{CDCl}_3$ )  $\delta$  207.5, 172.6, 135.9, 128.6, 128.3, 128.3, 66.2, 43.3, 38.0, 35.2, 30.2, 30.2, 17.3; IR (Neat Film, NaCl) 699, 751, 1164, 1704, 1733, 2954  $\text{cm}^{-1}$ ; HRMS (MM:ESI-APCI+)  $m/z$  calc'd for  $\text{C}_{17}\text{H}_{22}\text{O}_3\text{Na}$   $[\text{M}+\text{Na}]^+$ : 297.1467, found 297.1476;  $[\alpha]_{\text{D}}^{25} + 44.8^\circ$  ( $c$  1.0,  $\text{CHCl}_3$ );

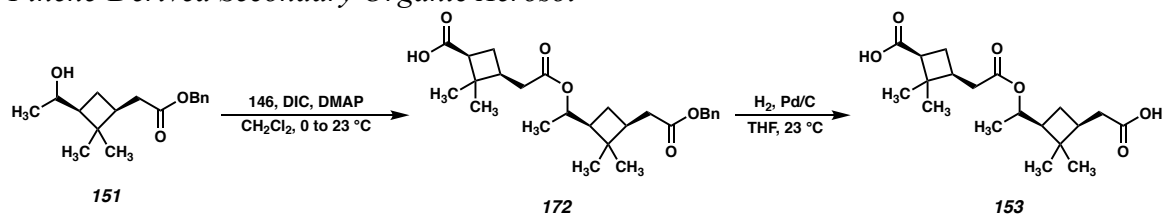
To a stirred solution of the intermediate ketoester **171** (2.00 g, 7.29 mmol, 1.0 eq) in MeOH (73 mL) at 0 °C was added  $\text{NaBH}_4$  (827 mg, 21.87 mmol, 3.0 eq) in one portion. The resulting suspension was stirred at 0 °C for 10 min, until disappearance of starting material as judged by TLC. The mixture was quenched by slow addition of  $\text{NH}_4\text{Cl}$  (sat. aq., 20 mL) until gas evolution ceased. The resulting mixture was diluted with  $\text{Et}_2\text{O}$  (100 mL) and  $\text{H}_2\text{O}$  (100 mL). The layers were separated and the aqueous layer was extracted with  $\text{Et}_2\text{O}$  (3x, 100 mL). The combined organic extracts were washed with brine (100 mL), dried over  $\text{MgSO}_4$ , and concentrated. The crude product was purified by flash chromatography on  $\text{SiO}_2$  (40%  $\text{Et}_2\text{O}$ /Hexanes) to afford benzyl *cis*-pinolic acid (**151**) (1.28 g mg, 4.63 mmol, 64% yield) as a colorless oil;  $^1\text{H}$  NMR (500 MHz,  $\text{CDCl}_3$ )  $\delta$  7.39 – 7.29 (m, 5H), 5.09 (s, 2H), 3.69 (dq,  $J = 9.9, 6.2$  Hz, 1H), 2.49 – 2.31 (m, 1H), 2.31 – 2.12 (m, 2H), 1.97 (dt,  $J = 10.9, 7.7$  Hz, 1H), 1.75 (td,  $J = 10.2, 8.0$  Hz, 1H), 1.45 (s, 1H), 1.18 (q,  $J = 10.4$  Hz, 1H), 1.12 (s, 3H), 1.04 (d,  $J = 6.1$  Hz, 3H), 1.01 (s, 3H);  $^{13}\text{C}$  NMR (125 MHz,  $\text{CDCl}_3$ )  $\delta$  173.0, 136.1, 128.6, 128.3, 128.3, 69.2, 66.2, 50.3, 39.9, 38.0, 35.3, 31.0, 26.6, 21.3, 16.8;

IR (Neat Film, NaCl) 698, 1164, 1456, 1734, 2959, 3425  $\text{cm}^{-1}$ ; HRMS (MM:ESI-APCI+)

$m/z$  calc'd for  $\text{C}_{17}\text{H}_{24}\text{O}_3\text{Na}$   $[\text{M}+\text{Na}]^+$ : 299.1623, found 299.1616;  $[\alpha]_{\text{D}}^{25} = -23.8^\circ$  ( $c$  1.0,  $\text{CHCl}_3$ ).



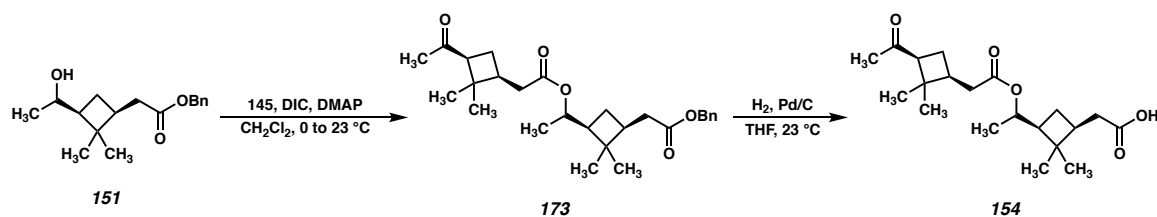
**(-)-*cis*-pinolic acid (152):** To a stirred solution of (+)-*cis*-pinonic acid (**145**) (2.00 g, 10.86 mmol, 1.0 eq) in  $\text{MeOH}/\text{CH}_2\text{Cl}_2$  (1:4, 108 mL) was added  $\text{NaBH}_4$  (2.46 g, 65.03 mmol, 6.0 eq) at 0 °C in one portion. The solution was allowed to warm to room temperature gradually, and was stirred for 10 h. The reaction mixture was cooled to 0 °C and quenched by slow addition of saturated aqueous  $\text{NH}_4\text{Cl}$ . The mixture was diluted with  $\text{Et}_2\text{O}$  (100 mL) and  $\text{H}_2\text{O}$  (100 mL). The layers were separated, and the aqueous layer was extracted with  $\text{Et}_2\text{O}$  (3x 100 mL). The combined organic extracts were washed with brine (50 mL), dried over  $\text{MgSO}_4$ , and concentrated. The crude product was purified by flash chromatography on  $\text{SiO}_2$  (40%  $\text{EtOAc}$ /hexanes) to afford (-)-*cis*-pinolic acid (**152**) (1.32 g, 7.09 mmol, 65% yield) as a white solid;  $\delta$  3.78 (dq,  $J = 9.9, 6.2$  Hz, 1H), 2.50 – 2.35 (m, 1H), 2.33 – 2.18 (m, 2H), 2.13 – 1.98 (m, 1H), 1.83 (td,  $J = 10.3, 8.0$  Hz, 1H), 1.30 – 1.22 (m, 1H), 1.21 (s, 3H), 1.11 (d,  $J = 6.2$  Hz, 3H), 1.09 (s, 3H);  $^{13}\text{C}$  NMR (125 MHz,  $\text{CDCl}_3$ )  $\delta$  178.9, 69.3, 50.3, 37.7, 34.9, 30.9, 26.5, 21.2, 16.8; IR (Neat Film, NaCl) 668, 1169, 1255, 1683, 2962, 3304  $\text{cm}^{-1}$ ; HRMS (MM:ESI-APCI-)  $m/z$  calc'd for  $\text{C}_{10}\text{H}_{17}\text{O}_3$   $[\text{M}-\text{H}]^-$ : 185.1178, found 185.1179;  $[\alpha]_{\text{D}}^{25} = -28.7^\circ$  ( $c$  1.0,  $\text{CHCl}_3$ ).



**Dimer Ester 153:** To a stirred solution of alcohol **151** (99 mg, 0.358 mmol, 1.00 eq), (-)-*cis*-pinic acid (**146**) (100 mg, 0.537 mmol, 1.5 eq), and DMAP (4 mg, 0.0358 mmol, 0.10 eq) in CH<sub>2</sub>Cl<sub>2</sub> (3.6 mL) was added DIC (84  $\mu$ L, 0.537 mmol, 1.5 eq) dropwise. The solution was stirred for 24 h and gradually allowed to warm to 23 °C. Upon disappearance of the starting material as judged by TLC, the solution was diluted with EtOAc (20 mL) and H<sub>2</sub>O (20 mL). The layers were separated and the aqueous layer was extracted with Et<sub>2</sub>O (3x, 20 mL). The combined organic extracts were washed with brine (20 mL), dried over MgSO<sub>4</sub>, and concentrated. The crude product was purified by flash chromatography on SiO<sub>2</sub> (30% to 40% Et<sub>2</sub>O/Hexanes) to afford intermediate diester **172** (83 mg, 0.187 mmol, 52% yield) as a colorless oil; <sup>1</sup>H NMR (500 MHz, CDCl<sub>3</sub>)  $\delta$  7.38 – 7.28 (m, 5H), 5.08 (s, 2H), 4.76 (dq, *J* = 10.1, 6.1 Hz, 1H), 2.78 (dd, *J* = 10.3, 7.8 Hz, 1H), 2.41 – 2.29 (m, 3H), 2.29 – 2.18 (m, 3H), 2.11 (dt, *J* = 11.3, 7.8 Hz, 1H), 2.06 – 1.95 (m, 2H), 1.90 (dt, *J* = 11.4, 10.3 Hz, 1H), 1.25 (s, 3H), 1.06 (s, 4H), 1.05 (d, *J* = 6.2 Hz, 3H), 1.00 (s, 3H), 0.86 (s, 3H); <sup>13</sup>C NMR (125 MHz, CDCl<sub>3</sub>)  $\delta$  178.8, 172.9, 172.2, 136.0, 77.4, 77.2, 76.9, 71.8, 66.3, 47.0, 46.1, 38.4, 38.1, 35.9, 35.2, 30.5, 30.4, 30.1, 26.5, 24.5, 17.7, 17.7, 16.9; IR (Neat Film, NaCl) 697, 750, 1067, 1170, 1456, 1731, 2657, 2958, 3033 cm<sup>-1</sup>; HRMS (MM:ESI-APCI-) *m/z* calc'd for C<sub>26</sub>H<sub>35</sub>O<sub>6</sub> [M-H]<sup>-</sup>: 443.2434, found 443.2442; ; [ $\alpha$ ]<sub>D</sub><sup>25</sup> = -11.3° (*c* 1.0, CHCl<sub>3</sub>).

In a 2-necked round bottom flask equipped with a 3-way valve, diester **172** (100 mg, 0.225 mmol, 1.0 eq) was dissolved in THF (2.3 mL), and to this solution was added

Pd/C (10% w/w, 25 mg). The flask was evacuated and backfilled with N<sub>2</sub> (3x), then purged and backfilled with H<sub>2</sub> (3x). The suspension was allowed to stir for 1h under H<sub>2</sub> (1 atm, balloon), until disappearance of starting material as judged by TLC. The flask was evacuated and backfilled with N<sub>2</sub> (3x), and the suspension was filtered over a plug of celite with EtOAc (20 mL). The filtrate was concentrated and purified by flash chromatography on SiO<sub>2</sub> (50% EtOAc/Hexanes) to afford dimer ester **153** (67 mg, 0.189 mmol, 84% yield) as a white solid; <sup>1</sup>H NMR (500 MHz, CDCl<sub>3</sub>) δ 4.76 (dt, *J* = 10.1, 6.0 Hz, 1H), 2.77 (dd, *J* = 10.3, 7.7 Hz, 1H), 2.43 – 2.17 (m, 7H), 2.15 – 1.94 (m, 3H), 1.89 (q, *J* = 10.6 Hz, 1H), 1.24 (s, 3H), 1.09 (s, 3H), 1.04 (d, *J* = 6.1 Hz, 3H), 0.99 (s, 3H), 0.87 (s, 3H); <sup>13</sup>C NMR (125 MHz, CDCl<sub>3</sub>) δ 179.8, 179.2, 172.3, 71.8, 47.1, 46.2, 43.1, 39.9, 38.5, 37.8, 35.9, 35.1, 30.5, 30.1, 26.5, 24.5, 17.7, 17.7, 16.9; IR (Neat Film, NaCl) 739, 958, 1211, 1247, 1704, 2957 cm<sup>-1</sup>; HRMS (MM:ESI-APCI-) *m/z* calc'd for C<sub>19</sub>H<sub>29</sub>O<sub>6</sub> [M-H]<sup>-</sup>: 353.1964, found 353.1967; [α]<sub>D</sub><sup>25</sup> = -11.4° (*c* 1.0, CHCl<sub>3</sub>).

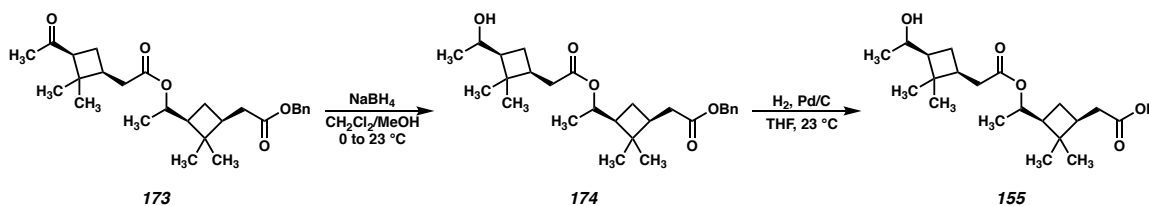


**Dimer Ester 154:** To a stirred solution of alcohol **151** (500 mg, 1.81 mmol, 1.0 eq), (+)-*cis*-pinonic acid (665 mg, 3.61 mmol, 2.0 eq), and DMAP (22 mg, 0.181 mmol, 0.10 eq) in CH<sub>2</sub>Cl<sub>2</sub> was added DIC (565 μL, 3.61 mmol, 2.0 eq) dropwise. The solution was stirred for 24 h and gradually allowed to warm to 23 °C. Upon disappearance of the starting material as judged by TLC, the solution was diluted with Et<sub>2</sub>O (100 mL) and H<sub>2</sub>O (100 mL). The layers were separated and the aqueous layer was extracted with Et<sub>2</sub>O (3x, 100 mL). The combined organic extracts were washed with brine (100 mL), dried over MgSO<sub>4</sub>,

and concentrated. The crude product was purified by flash chromatography on SiO<sub>2</sub> (30% Et<sub>2</sub>O/Hexanes) to afford intermediate diester **173** (726 mg, 1.64 mmol, 91% yield) as a colorless oil; <sup>1</sup>H NMR (500 MHz, CDCl<sub>3</sub>) δ 7.31 (qd, *J* = 7.2, 3.5 Hz, 5H), 5.06 (s, 2H), 4.74 (dd, *J* = 10.2, 6.0 Hz, 1H), 2.85 (dd, *J* = 10.0, 7.6 Hz, 1H), 2.38 – 2.29 (m, 2H), 2.28 – 2.19 (m, 3H), 2.15 (dd, *J* = 15.4, 7.6 Hz, 1H), 2.02 (s, 3H), 2.00 – 1.87 (m, 4H), 1.30 (s, 3H), 1.21 (q, *J* = 9.7, 9.0 Hz, 1H), 1.04 (s, 3H), 1.02 (d, *J* = 6.1 Hz, 3H), 0.84 (s, 6H). <sup>13</sup>C NMR (125 MHz, CDCl<sub>3</sub>) δ 207.4, 172.7, 172.1, 136.0, 128.5, 128.3, 128.2, 71.6, 66.1, 54.1, 46.9, 43.2, 39.8, 38.0, 38.0, 35.5, 35.1, 30.4, 30.2, 30.2, 26.4, 23.1, 17.6, 17.3, 16.8; IR (Neat Film, NaCl) 698, 1166, 1369, 1455, 1706, 1730, 2871, 2955 cm<sup>-1</sup>; HRMS (MM:ESI-APCI+) *m/z* calc'd for C<sub>27</sub>H<sub>38</sub>O<sub>5</sub>Na [M+Na]<sup>+</sup>: 465.2617, found 465.2611; [α]<sub>D</sub><sup>25</sup> + 22.4° (*c* 1.0, CHCl<sub>3</sub>)

In a 2-necked round bottom flask equipped with a 3-way valve, the intermediate diester (100 mg, 0.226 mmol, 1.0 eq) was dissolved in THF (2.3 mL), and to this solution was added Pd/C (10%, 100 mg). The flask was evacuated and backfilled with N<sub>2</sub> (3x), then purged and backfilled with H<sub>2</sub> (3x). The suspension was allowed to stir for 1h under H<sub>2</sub> (1 atm, balloon), until disappearance of starting material as judged by TLC. The flask was evacuated and backfilled with N<sub>2</sub> (3x), and the suspension was filtered over a plug of celite with EtOAc. The filtrate was concentrated and purified by flash chromatography on SiO<sub>2</sub> (40% EtOAc/Hexanes) to afford dimer ester **154** (52 mg, 0.148 mmol, 65% yield) as a white solid; <sup>1</sup>H NMR (500 MHz, CDCl<sub>3</sub>) δ (ddd, *J* = 12.2, 8.1, 5.1 Hz, 1H), 2.85 (dd, *J* = 10.0, 7.6 Hz, 1H), 2.37 – 2.09 (m, 6H), 2.08 – 1.83 (m, 7H), 1.29 (s, 3H), 1.21 (q, *J* = 9.9 Hz, 1H), 1.06 (s, 3H), 1.01 (d, *J* = 6.1 Hz, 3H), 0.83 (d, *J* = 8.4 Hz, 6H). <sup>13</sup>C NMR (125 MHz, CDCl<sub>3</sub>) δ 207.9, 179.0, 172.3, 71.7, 54.2, 47.0, 43.3, 39.8, 38.0, 37.7, 35.5, 34.9,

30.4, 30.2, 30.2, 26.4, 23.1, 17.6, 17.3, 16.7; IR (Neat Film, NaCl) 867, 959, 1179, 1369, 1706, 1727, 2871, 2956  $\text{cm}^{-1}$ ; HRMS (MM:ESI-APCI-)  $m/z$  calc'd for  $\text{C}_{20}\text{H}_{31}\text{O}_5$   $[\text{M}-\text{H}]^-$ : 351.2171, found 351.2178.  $[\alpha]_{\text{D}}^{25} +22.4^\circ$  ( $c$  1.0,  $\text{CHCl}_3$ ).

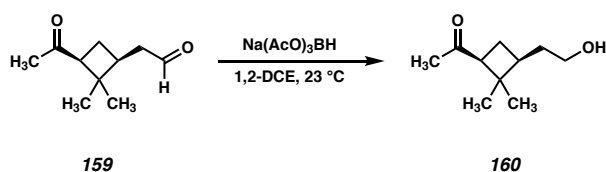


**Dimer Ester 155:** To a stirred solution of benzyl ester **173** (400 mg, 0.904 mmol, 1.0 eq) in  $\text{CH}_2\text{Cl}_2/\text{MeOH}$  (4:1, 9.0 mL) at  $0^\circ\text{C}$  was added  $\text{NaBH}_4$  (103 mg, 2.71 mmol, 3.0 eq) in one portion. The resulting suspension was allowed to warm to room temperature and stirred until disappearance of starting material as judged by TLC. The mixture was quenched by slow addition of  $\text{NH}_4\text{Cl}$  (sat. aq., 5.0 mL) until gas evolution ceased. The resulting mixture was diluted with  $\text{Et}_2\text{O}$  (100 mL) and  $\text{H}_2\text{O}$  (100 mL). The layers were separated and the aqueous layer was extracted with  $\text{Et}_2\text{O}$  (3x, 100 mL). The combined organic extracts were washed with brine (50 mL), dried over  $\text{MgSO}_4$ , and concentrated. The crude product was purified by flash chromatography on  $\text{SiO}_2$  (40%  $\text{Et}_2\text{O}/\text{Hexanes}$ ) to afford intermediate hydroxy ester **174** (245 mg, 0.551 mmol, 61% yield) as a colorless oil;  $^1\text{H}$  NMR (500 MHz,  $\text{CDCl}_3$ )  $\delta$  7.62 – 7.11 (m, 5H), 5.07 (s, 2H), 4.74 (dq,  $J = 9.9, 6.1$  Hz, 1H), 3.68 (dq,  $J = 9.9, 6.2$  Hz, 1H), 2.41 – 2.05 (m, 6H), 2.04 – 1.91 (m, 3H), 1.74 (td,  $J = 10.3, 8.0$  Hz, 1H), 1.22 (d,  $J = 9.6$  Hz, 1H), 1.13 (s, 4H), 1.05 (s, 3H), 1.03 (dd,  $J = 6.1, 3.3$  Hz, 6H), 1.00 (s, 3H), 0.85 (s, 3H);  $^{13}\text{C}$  NMR (125 MHz,  $\text{CDCl}_3$ )  $\delta$  172.9, 172.6, 136.0, 128.6, 128.3, 128.3, 71.5, 69.2, 66.2, 50.3, 47.0, 39.9, 39.9, 38.1, 35.8, 35.2, 31.1, 30.4, 26.7, 26.5, 21.3, 17.7, 16.9, 16.8; IR (Neat Film, NaCl) 697, 1166, 1187, 1267, 1366, 1455, 1731, 2870, 2958,



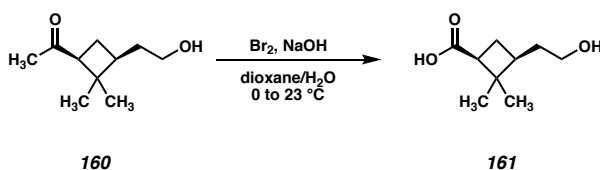
3504  $\text{cm}^{-1}$ ; HRMS (MM:ESI-APCI+)  $m/z$  calc'd for  $\text{C}_{27}\text{H}_{40}\text{O}_5\text{Na}$   $[\text{M}+\text{Na}]^+$ : 467.2773, found 467.2773;  $[\alpha]_{\text{D}}^{25} -22.1^\circ$  ( $c$  1.0,  $\text{CHCl}_3$ ).

In a 2-necked round bottom flask equipped with a 3-way valve, hydroxy ester **174** (60 mg, 0.226 mmol, 1.0 eq) was dissolved in THF (1.4 mL), and to this solution was added Pd/C (10%, 60 mg). The flask was evacuated and backfilled with  $\text{N}_2$  (3x), then purged and backfilled with  $\text{H}_2$  (3x). The suspension was allowed to stir for 1h under  $\text{H}_2$  (1 atm, balloon), until disappearance of starting material as judged by TLC. The flask was evacuated and backfilled with  $\text{N}_2$  (3x), and the suspension was filtered over a plug of celite with EtOAc. The filtrate was concentrated and purified by flash chromatography on  $\text{SiO}_2$  (50% EtOAc/Hexanes) to afford dimer ester **155** (33 mg, 0.093 mmol, 69% yield) as a white solid;  $^1\text{H}$  NMR (500 MHz,  $\text{CDCl}_3$ )  $\delta$  4.75 (dq,  $J = 10.0, 6.1$  Hz, 1H), 3.70 (dq,  $J = 9.9, 6.2$  Hz, 1H), 2.39 – 1.92 (m, 10H), 1.74 (td,  $J = 10.2, 8.0$  Hz, 1H), 1.22 (q,  $J = 9.5, 9.1$  Hz, 1H), 1.12 (s, 4H), 1.08 (s, 3H), 1.05 – 1.02 (m, 6H), 0.99 (s, 3H), 0.86 (s, 3H);  $^{13}\text{C}$  NMR (125 MHz,  $\text{CDCl}_3$ )  $\delta$  178.6, 172.7, 71.6, 69.4, 50.2, 47.1, 39.9, 38.1, 37.9, 35.8, 35.0, 31.0, 30.5, 26.71, 26.5, 21.2, 17.7, 16.9, 16.8; IR (Neat Film, NaCl) 873, 873, 1190, 1367, 1709, 2871, 2959, 3441  $\text{cm}^{-1}$ ; HRMS (MM:ESI-APCI-)  $m/z$  calc'd for  $\text{C}_{20}\text{H}_{33}\text{O}_5$   $[\text{M}-\text{H}]^-$ : 353.2328, found 353.2332;  $[\alpha]_{\text{D}}^{25} -17.8^\circ$  ( $c$  1.0,  $\text{CHCl}_3$ ).



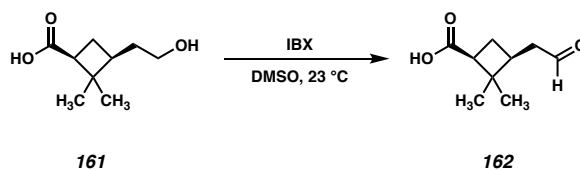
**Alcohol 160:** A 100 mL round bottom flask was charged with pinonaldehyde<sup>19</sup> (**159**, 2.5 g, 14.9 mmol, 1.0 equiv) in 1,2-dichloroethane (25 mL). To this stirred solution was added  $\text{Na}(\text{OAc})_3\text{BH}$  (7.2 g, 34.2 mmol, 2.3 equiv) in a single portion at 23 °C. The thick slurry

was stirred at 23 °C for 24 h, then quenched with water and partitioned between water and Et<sub>2</sub>O and extracted with Et<sub>2</sub>O (3x). The organic extracts were combined, washed with brine, dried over MgSO<sub>4</sub>, filtered, and concentrated to afford an oil which was purified by flash chromatography (SiO<sub>2</sub>, 30%-60% EtOAc/hexanes) to afford alcohol **160** (1.9 g, 11.0 mmol, 74% yield) as a colorless liquid; <sup>1</sup>H NMR (400 MHz, CDCl<sub>3</sub>) δ 3.70 – 3.52 (m, 2H), 2.75 (dd, *J* = 10.4, 7.5 Hz, 1H), 2.12 – 1.98 (m, 2H), 1.93 – 1.81 (m, 1H), 1.73 – 1.59 (m, 1H), 1.58 – 1.45 (m, 1H), 1.22 (s, 4H), 1.01 (s, 4H); <sup>13</sup>C NMR (100 MHz, CDCl<sub>3</sub>) δ 178.6, 61.3, 46.2, 43.1, 39.1, 33.4, 30.3, 24.5, 17.6; IR (thin film, NaCl) 3413, 2948, 2872, 1702, 1461, 1384, 1367, 1357, 1224, 1181, 1157, 1181, 1053 cm<sup>-1</sup>; HRMS (MM:ESI-APCI+) *m/z* calc'd for C<sub>10</sub>H<sub>18</sub>O<sub>2</sub>Na [M+Na]<sup>+</sup>: 193.1204, found 193.1205; [α]<sub>D</sub><sup>25</sup> + 65.5 ° (*c* 1.0, CHCl<sub>3</sub>).



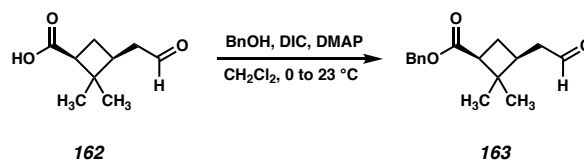
**Acid 161:** A 500 mL round bottom flask was charged with alcohol **160** (750 mg, 4.40 mmol, 1.0 equiv) in dioxane/H<sub>2</sub>O (5:1, 65 mL). This solution was cooled to 0 °C in an ice/water bath. In a separate Erlenmeyer flask, NaOH (2.3 g, 57.2 mmol, 13.0 equiv) was dissolved in H<sub>2</sub>O (22 mL). This solution was cooled to 0 °C, followed by the addition of bromine (745 μL, 14.5 mmol, 3.3 equiv). The contents of the Erlenmeyer flask was then added to the initial reaction vessel dropwise via addition funnel at 0 °C, and the resulting solution was allowed to stir for 2h while gradually warming to 23 °C. The reaction mixture was diluted with water, and washed with Et<sub>2</sub>O (1x). The aqueous phase was then acidified by addition of conc HCl to pH ~ 2. The acidified aqueous phase was then extracted with

EtOAc (3x). These organic extracts were combined, washed with brine, dried over Na<sub>2</sub>SO<sub>4</sub>, filtered and concentrated to afford acid **161** (729 mg, 4.23 mmol, 96% yield) which was found to be sufficiently pure by NMR and was used in the subsequent reaction; <sup>1</sup>H NMR (400 MHz, CDCl<sub>3</sub>) δ 3.56 (ddt, *J* = 10.5, 7.6, 3.6 Hz, 2H), 2.78 – 2.66 (m, 1H), 2.08 – 1.95 (m, 2H), 1.93 – 1.78 (m, 1H), 1.63 (dt, *J* = 13.1, 7.0 Hz, 1H), 1.56 – 1.43 (m, 1H), 1.20 (s, 3H), 0.98 (s, 4H); <sup>13</sup>C NMR (100 MHz, CDCl<sub>3</sub>) δ 178.5, 61.2, 46.2, 43.0, 39.0, 33.3, 30.3, 24.5, 17.6; IR (thin film, NaCl) 3373, 2952, 2885, 2730, 1699, 1460, 1417, 1369, 1332, 1244, 1203, 1050, 1029 cm<sup>-1</sup>; HRMS (MM:ESI-APCI-) *m/z* calc'd for C<sub>9</sub>H<sub>15</sub>O<sub>3</sub> [M-H]<sup>-</sup>: 171.1021, found 171.1021; [α]<sub>D</sub><sup>25</sup> – 9.4 ° (*c* 1.0, CHCl<sub>3</sub>).

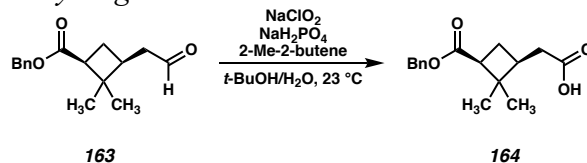


**Aldehyde 162:** A 100 mL round bottom flask was charged with alcohol **161** (729 mg, 4.23 mmol, 1.0 equiv) in DMSO (42 mL). IBX (1.8 g, 6.35 mmol, 1.5 equiv) was added at 23 °C and the reaction was allowed to stir at 23 °C for 16 h. The reaction was then diluted with H<sub>2</sub>O and extracted with EtOAc (3x). The combined organic extracts were washed with brine, dried over Na<sub>2</sub>SO<sub>4</sub>, filtered and concentrated to leave an oil which was purified by flash chromatography (SiO<sub>2</sub>, 20%-50% EtOAc/hexanes) to afford aldehyde **162** (443 mg, 2.60 mmol, 62% yield) as a colorless oil; <sup>1</sup>H NMR (600 MHz, CDCl<sub>3</sub>) δ 9.72 (t, *J* = 1.6 Hz, 1H), 2.81 (dd, *J* = 10.2, 7.9 Hz, 1H), 2.56 – 2.49 (m, 1H), 2.48 – 2.40 (m, 2H), 2.13 (dt, *J* = 11.4, 7.8 Hz, 1H), 1.91 (dt, *J* = 11.3, 10.0 Hz, 1H), 1.24 (s, 3H), 0.97 (s, 3H); <sup>13</sup>C NMR (100 MHz, CDCl<sub>3</sub>) δ 201.6, 179.0, 46.4, 45.4, 43.1, 36.1, 30.2, 24.2, 18.0; IR (thin

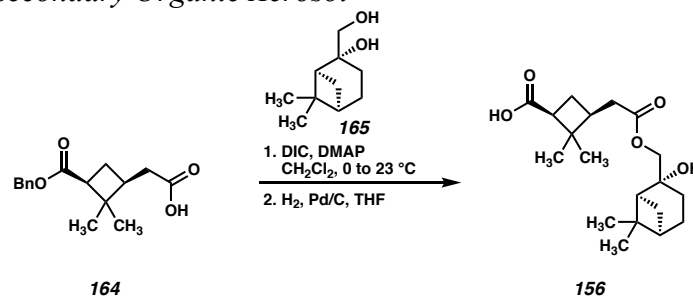
film, NaCl) 2960, 1873, 1733, 1705, 1698, 1650, 1425, 1247, 1216, 1161, 935;  $m/z$  calc'd for  $C_9H_{13}O_3$   $[M-H]^-$ : 169.0865, found 169.0864;  $[\alpha]_D^{25} - 0.80^\circ$  ( $c$  1.0,  $CHCl_3$ ).



**Benzyl Ester 163:** A 50 mL round bottom flask was charged with acid **162** (200 mg, 1.18 mmol, 1.0 equiv), benzyl alcohol (245  $\mu$ L, 2.36 mmol, 2.0 equiv) and DMAP (7.0 mg, 0.059 mmol, 0.05 equiv) in  $CH_2Cl_2$  (12 mL). The solution was cooled to 0  $^\circ C$ , and DIC (370  $\mu$ L, 2.36 mmol, 2.0 equiv) was added slowly. The reaction was allowed to stir for 2 h while gradually warming to 23  $^\circ C$ . The mixture was diluted with water and extracted with  $Et_2O$  (3x). The combined organic extracts were washed with brine, dried over  $MgSO_4$ , filtered and concentrated leaving a colorless oil which was purified by flash chromatography ( $SiO_2$ , 10%-20%  $EtOAc/Hexanes$ ) to afford ester **163** (219 mg, 0.841 mmol, 71% yield) as a colorless oil;  $^1H$  NMR (400 MHz,  $CDCl_3$ )  $\delta$  9.72 (t,  $J = 1.5$  Hz, 1H), 7.42 – 7.28 (m, 5H), 5.13 (d,  $J = 12.3$  Hz, 1H), 5.09 (d,  $J = 12.3$  Hz, 1H), 2.83 (dd,  $J = 10.2, 7.9$  Hz, 1H), 2.61 – 2.31 (m, 3H), 2.21 – 2.06 (m, 1H), 2.04 – 1.88 (m, 1H), 1.23 (s, 3H), 0.87 (s, 3H);  $^{13}C$  NMR (100 MHz,  $CDCl_3$ )  $\delta$  201.43, 172.59 (d,  $J = 1.8$  Hz), 136.18 (d,  $J = 2.9$  Hz), 128.5, 128.3, 128.2, 66.0 (d,  $J = 3.3$  Hz), 46.4, 45.3, 42.9, 36.1, 30.2, 24.3, 18.0; IR (thin film, NaCl) 2954, 2880, 2718, 1726, 1455, 1383, 1336, 1231, 1173, 1130, 1023, 749, 735, 696  $cm^{-1}$ ; HRMS (MM:ESI-APCI-)  $m/z$  calc'd for  $C_{16}H_{20}O_3Na$   $[M+Na]^+$ : 283.1310, found 283.1307;  $[\alpha]_D^{25} - 5.1^\circ$  ( $c$  0.833,  $CHCl_3$ ).

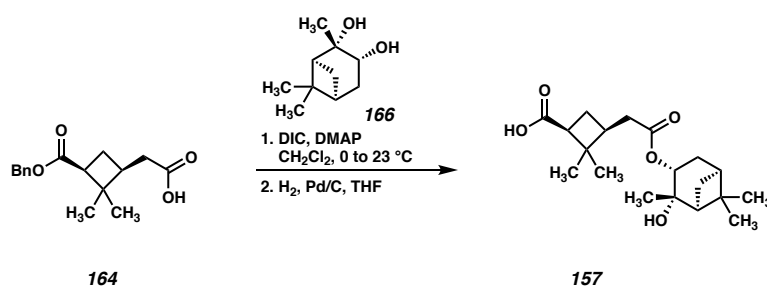


**Acid 164:** A 500 mL round bottom flask was charged with aldehyde **163** (397 mg, 1.52 mmol, 1.0 equiv), NaH<sub>2</sub>PO<sub>4</sub> (1.1 g, 9.12 mmol, 6.0 equiv), and 2-methyl-2-butene (12.8 mL, 121.6 mmol, 80.0 equiv) in *t*-BuOH (152 mL) and H<sub>2</sub>O (30 mL). NaClO<sub>2</sub> (413 mg, 4.57 mmol, 3.0 equiv) was added in one portion at 23 °C, and the reaction was allowed to stir 2 h at 23 °C. The *t*-BuOH was removed by rotary evaporation, and the remaining solution was partitioned between EtOAc and H<sub>2</sub>O and extracted with EtOAc (3x). The combined organic extracts were washed with brine, dried over Na<sub>2</sub>SO<sub>4</sub>, filtered and concentrated leaving a crude residue which was purified by column chromatography (SiO<sub>2</sub>, 50%-60% EtOAc/hexanes) to afford acid **164** (353 mg, 1.27 mmol, 84% yield) as a colorless oil; <sup>1</sup>H NMR (400 MHz, CDCl<sub>3</sub>) δ 7.38 – 7.29 (m, 5H), 5.13 (d, *J* = 12.3 Hz, 1H), 5.09 (d, *J* = 12.3 Hz, 1H), 2.80 (dd, *J* = 10.4, 7.8 Hz, 1H), 2.46 – 2.28 (m, 2H), 2.21 – 2.07 (m, 1H), 2.07 – 1.90 (m, 1H), 1.23 (s, 4H), 0.90 (s, 3H); <sup>13</sup>C NMR (100 MHz, CDCl<sub>3</sub>) δ 179.0, 172.7, 136.3, 128.6, 128.4, 128.3, 66.1, 46.3, 43.0, 38.2, 35.2, 30.1, 24.6, 17.8; IR (thin film, NaCl) 3064, 3032, 2956, 1731, 1705, 1455, 1385, 1234, 1170, 747, 697 cm<sup>-1</sup>; HRMS (MM:ESI-APCI-) *m/z* calc'd for C<sub>16</sub>H<sub>20</sub>O<sub>4</sub> [M-H]<sup>-</sup>: 275.1283, found 275.1290; [α]<sub>D</sub><sup>25</sup> – 9.4 ° (*c* 1.0, CHCl<sub>3</sub>).



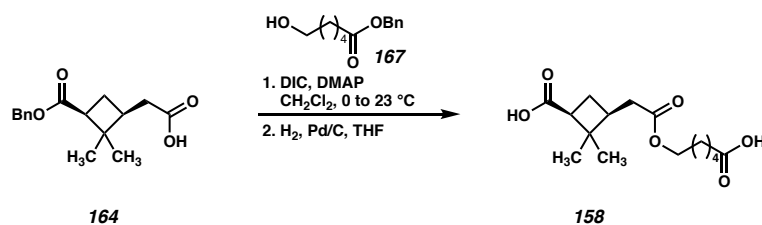
**Dimer Ester 156:** A 20 mL round bottom flask was charged with acid **164** (40.0 mg, 0.145 mmol, 1.0 equiv),  $\beta$ -pinenediol (**165**) (25.0 mg, 0.145 mmol, 1.0 mmol) and DMAP (1.0 mg, 0.00725 mmol, 0.05 equiv) in CH<sub>2</sub>Cl<sub>2</sub>. This solution was cooled to 0 °C, and DIC (23  $\mu$ L, 0.145 mmol, 1.0 equiv) was added dropwise. The reaction was stirred 16 h while gradually warming to 23 °C. The reaction was diluted with H<sub>2</sub>O, and extracted with EtOAc (3x). The combined organic extracts were washed with brine, dried over Na<sub>2</sub>SO<sub>4</sub>, filtered and concentrated leaving a crude oil which was purified by flash chromatography (SiO<sub>2</sub>, 20%-40% EtOAc/hexanes) to afford an intermediate diester (30.0 mg, 0.070 mmol, 49% yield). The intermediate ester (30.0 mg, 0.070 mmol, 1.0 equiv) was dissolved in THF (3.5 mL), and charged into a 25 mL 2-necked round bottom flask containing Pd/C (c.a. 10% Pd, 15 mg). The flask was subjected to evacuation/refill with N<sub>2</sub> (3x), followed by evacuation/refill with H<sub>2</sub> (3x). The black suspension was stirred at 23 °C under an atmosphere of H<sub>2</sub> for 3 h. The flask was then subjected to evacuation/refill with N<sub>2</sub> (3x) and the suspension was filtered over Celite®, rinsing with ethyl acetate. The filtrate was concentrated by rotary evaporation, and the remaining residue was purified by flash chromatography (SiO<sub>2</sub>, 50%-60% EtOAc/hexanes) to afford dimer ester **156** (23.0 mg, 0.0680 mmol, 97% yield, 47% yield over the two steps) as a colorless oil; <sup>1</sup>H NMR (400 MHz, CDCl<sub>3</sub>)  $\delta$  4.11 (d,  $J$  = 11.2 Hz, 1H), 4.04 (d,  $J$  = 11.4 Hz, 1H), 2.79 (dd,  $J$  = 10.3, 7.8

Hz, 1H), 2.48 – 2.29 (m, 2H), 2.28 – 2.18 (m, 1H), 2.18 – 2.08 (m, 1H), 2.04 – 1.87 (m, 3H), 1.87 – 1.71 (m, 2H), 1.54 (d,  $J = 10.3$  Hz, 1H), 1.25 (s, 3H), 1.24 (s, 3H), 1.01 (s, 2H), 0.94 (s, 3H);  $^{13}\text{C}$  NMR (100 MHz,  $\text{CDCl}_3$ )  $\delta$  178.0, 173.0, 75.7, 71.4, 49.0, 46.1, 43.0, 41.0, 38.5, 38.3, 35.4, 30.1, 27.6, 27.4, 26.9, 24.7, 24.6, 23.3, 17.8; IR (thin film, NaCl) 2922, 2872, 1711, 1233, 1204, 757  $\text{cm}^{-1}$ ; ; HRMS (MM:ESI-APCI+)  $m/z$  calc'd for  $\text{C}_{19}\text{H}_{30}\text{O}_5$   $[\text{M}-\text{H}]^-$ : 337.2015, found 337.2013;  $[\alpha]_{\text{D}}^{25} + 6.2^\circ$  (c 1.0  $\text{CHCl}_3$ ).



**Dimer Ester 157:** A 20 mL round bottom flask was charged with acid **164** (40.0 mg, 0.145 mmol, 1.0 equiv), alcohol  $\alpha$ -pinandiol (25.0 mg, 0.145 mmol, 1.0 mmol) and DMAP (1.0 mg, 0.00725 mmol, 0.05 equiv) in  $\text{CH}_2\text{Cl}_2$ . This solution was cooled to  $0^\circ\text{C}$ , and DIC (23  $\mu\text{L}$ , 0.145 mmol, 1.0 equiv) was added dropwise. The reaction was stirred 16 h while gradually warming to  $23^\circ\text{C}$ . The reaction was diluted with  $\text{H}_2\text{O}$ , and extracted with EtOAc (3x). The combined organic extracts were washed with brine, dried over  $\text{Na}_2\text{SO}_4$ , filtered and concentrated leaving a crude oil which was purified by flash chromatography ( $\text{SiO}_2$ , 50%-60% EtOAc/hexanes) to afford an intermediate diester (41.0 mg, 0.103 mmol, 71% yield). The intermediate ester (22.0 mg, 0.051 mmol, 1.0 equiv) was dissolved in THF (2.6 mL), and charged into a 25 mL 2-necked round bottom flask containing Pd/C (c.a. 10% Pd, 22 mg). The flask was subjected to evacuation/refill with  $\text{N}_2$  (3x), followed by evacuation/refill with  $\text{H}_2$  (3x). The black suspension was stirred at  $23^\circ\text{C}$  under an

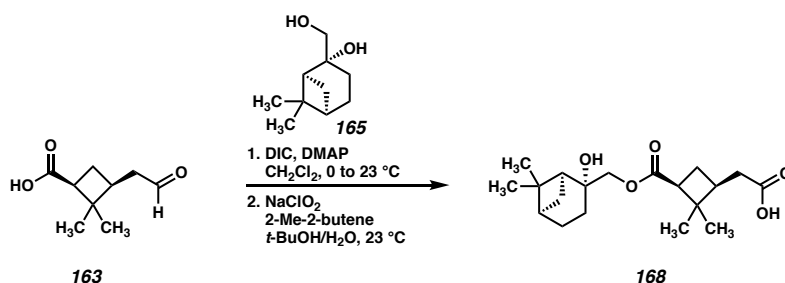
atmosphere of H<sub>2</sub> for 3 h. The flask was then subjected to evacuation/refill with N<sub>2</sub> (3x) and the suspension was filtered over Celite®, rinsing with ethyl acetate. The filtrate was concentrated by rotary evaporation, and the remaining residue was purified by flash chromatography (SiO<sub>2</sub>, 50%-60% EtOAc/hexanes) to afford dimer ester **157** (11.0 mg, 0.0325 mmol, 97% yield, 45% yield over the two steps) as a colorless oil; <sup>1</sup>H NMR (400 MHz, CDCl<sub>3</sub>) δ 5.12 (dd, *J* = 9.6, 5.4 Hz, 1H), 2.80 (dd, *J* = 10.3, 7.8 Hz, 1H), 2.55 – 2.32 (m, 3H), 2.24 (dtd, *J* = 10.6, 6.1, 2.5 Hz, 1H), 2.19 – 2.11 (m, 1H), 2.06 – 1.89 (m, 2H), 1.62 (ddd, *J* = 14.1, 5.5, 2.5 Hz, 1H), 1.46 (d, *J* = 10.5 Hz, 1H), 1.30 (s, 3H), 1.28 (s, 3H), 1.27 (s, 3H), 1.02 (s, 3H), 0.99 (s, 3H); <sup>13</sup>C NMR (100 MHz, CDCl<sub>3</sub>) δ 172.1, 74.0, 72.0, 54.3, 46.1, 43.0, 40.5, 38.8, 38.6, 35.7, 34.9, 30.2, 30.0, 28.4, 28.0, 24.5, 24.4, 17.9; IR (thin film, NaCl) 3794, 2953, 2924, 2873, 1726, 1705, 1234, 1217, 1187, 1157, 1010, 931, 828, 758 cm<sup>-1</sup>; HRMS (MM:ESI-APCI+) *m/z* calc'd for C<sub>19</sub>H<sub>30</sub>O<sub>5</sub> [M-H]<sup>-</sup>: 337.2015, found 337.2016; [α]<sub>D</sub><sup>25</sup> – 2.6 ° (c 1.0 CHCl<sub>3</sub>).



**Dimer Ester 158:** A 20 mL round bottom flask was charged with acid **164** (25.0 mg, 0.0900 mmol, 1.0 equiv), alcohol **167**<sup>20</sup> (20.0 mg, 0.0900 mmol, 1.0 mmol) and DMAP (0.5 mg, 0.00455 mmol, 0.05 equiv) in CH<sub>2</sub>Cl<sub>2</sub>. This solution was cooled to 0 °C, and DIC (14 μL, 0.0900 mmol, 1.0 equiv) was added dropwise. The reaction was stirred 16 h while gradually warming to 23 °C. The reaction was diluted with H<sub>2</sub>O, and extracted with Et<sub>2</sub>O (3x). The combined organic extracts were washed with brine, dried over MgSO<sub>4</sub>, filtered

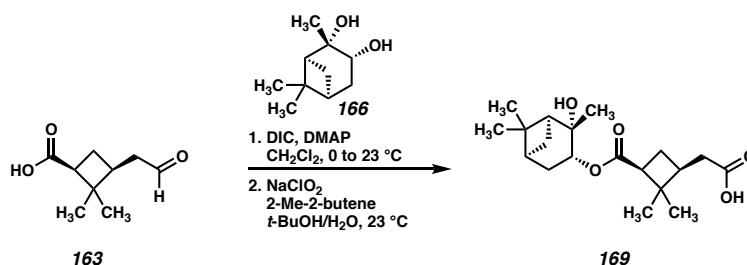


and concentrated leaving a crude oil which was purified by flash chromatography (SiO<sub>2</sub>, 40%-50% EtOAc/hexanes) to afford an intermediate diester (29.0 mg, 0.0603 mmol, 67% yield). The intermediate ester (20.0 mg, 0.0416 mmol, 1.0 equiv) was dissolved in THF (4.2 mL), and charged into a 25 mL 2-necked round bottom flask containing Pd/C (c.a. 10% Pd, 10 mg). The flask was subjected to evacuation/refill with N<sub>2</sub> (3x), followed by evacuation/refill with H<sub>2</sub> (3x). The black suspension was stirred at 23 °C under an atmosphere of H<sub>2</sub> for 3 h. The flask was then subjected to evacuation/refill with N<sub>2</sub> (3x) and the suspension was filtered over Celite®, rinsing with ethyl acetate. The filtrate was concentrated by rotary evaporation, and the remaining residue was purified by flash chromatography (SiO<sub>2</sub>, 50%-80% EtOAc/hexanes) to afford dimer ester **158** (11.0 mg, 0.0366 mmol, 88% yield, 59% yield over the two steps) as a colorless oil; <sup>1</sup>H NMR (400 MHz, CDCl<sub>3</sub>) δ 4.07 (t, *J* = 6.4 Hz, 2H), 2.79 (dd, *J* = 10.3, 7.8 Hz, 1H), 2.42 – 2.22 (m, 5H), 2.16 – 2.00 (m, 1H), 1.99 – 1.86 (m, 1H), 1.75 – 1.57 (m, 3H), 1.48 – 1.38 (m, 2H), 1.24 (s, 4H), 1.00 (s, 4H); <sup>13</sup>C NMR (100 MHz, CDCl<sub>3</sub>) δ 172.9, 64.3, 46.2, 43.1, 38.5, 35.6, 33.9, 30.0, 29.9, 28.4, 25.7, 24.5, 24.4, 17.7; IR (thin film, NaCl) 3801, 2352, 1725, 1704, 1416, 1255, 1234, 1219, 1204, 1187, 817, 682 cm<sup>-1</sup>; HRMS (MM:ESI-APCI+) *m/z* calc'd for C<sub>15</sub>H<sub>24</sub>O<sub>6</sub> [M-H]<sup>-</sup>: 299.1495, found 299.1493; [α]<sub>D</sub><sup>25</sup> – 1.3 ° (c 1.0 CHCl<sub>3</sub>).



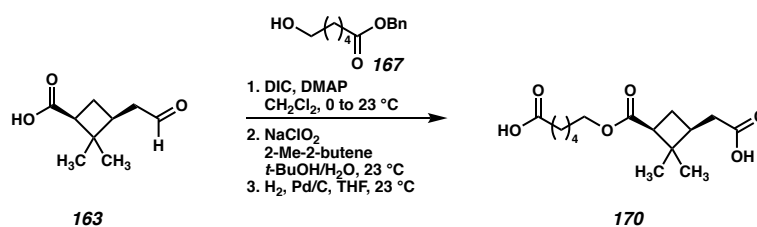
**Dimer Ester 168:** A 25 mL round bottom flask was charged with acid **183** (50.0 mg, 0.294 mmol, 1.0 equiv),  $\beta$ -pinanediol (**165**) (50.0 mg, 0.294 mmol, 1.0 equiv), and DMAP (2.0 mg, 0.0147 mmol, 0.05 equiv) in  $\text{CH}_2\text{Cl}_2$  (5.9 mL). The solution was cooled 0 °C and DIC (46  $\mu\text{L}$ , 0.294 mmol, 1.0 equiv) was added dropwise. The reaction was allowed to stir for 16 h while gradually warming to 23 °C. The reaction mixture was diluted with  $\text{H}_2\text{O}$  then extracted with EtOAc (3x). The combined organic extracts were washed with brine, dried over  $\text{Na}_2\text{SO}_4$ , filtered, and concentrated leaving a crude oil which was purified by flash chromatography (30%-50% EtOAc/hexanes) to afford an intermediate ester (83.0 mg, 0.257 mmol, 85% yield). A 50 mL round bottom flask was charged with the intermediate ester (30.0 mg, 0.0902 mmol, 1.0 equiv),  $\text{NaH}_2\text{PO}_4$  (65.0 mg, 0.541 mmol, 6.0 equiv), and 2-methyl-2-butene (765  $\mu\text{L}$ , 7.22 mmol, 80.0 equiv) in *t*-BuOH (9.0 mL) and  $\text{H}_2\text{O}$  (1.8 mL).  $\text{NaClO}_2$  (25.0 mg, 0.271 mmol, 3.0 equiv) was added in a single portion at 23 °C, and the reaction was allowed to stir at 23 °C for 2 h. The reaction was diluted with  $\text{H}_2\text{O}$  and extracted with EtOAc (3x). The combined organic extracts were washed with brine, dried over  $\text{Na}_2\text{SO}_4$ , filtered, and concentrated by rotary evaporation leaving a crude oil which was purified by flash chromatography ( $\text{SiO}_2$ , 20%-50% EtOAc/hexanes) to afford dimer ester **168** (17.0 mg, 0.0502 mmol, 56% yield, 47% yield over the two steps) as a colorless oil;  $^1\text{H}$  NMR (400 MHz,  $\text{CDCl}_3$ )  $\delta$  4.11 (d,  $J = 11.2$  Hz, 1H), 4.03 (d,  $J = 11.2$  Hz, 1H), 2.79 (dd,  $J = 10.4, 7.8$  Hz, 1H), 2.45 – 2.27 (m, 3H), 2.28 – 2.18 (m, 1H), 2.18 – 2.10 (m, 1H), 2.03 – 1.90 (m, 4H), 1.88 – 1.72 (m, 3H), 1.54 (d,  $J = 10.1$  Hz, 1H), 1.24 (s, 6H), 0.96 (s, 3H), 0.95 (s, 3H);  $^{13}\text{C}$  NMR (100 MHz,  $\text{CDCl}_3$ )  $\delta$  173.0, 75.7, 71.4, 49.1, 46.4, 43.0, 41.0, 38.4, 38.2, 30.2, 27.6, 27.5, 26.9, 24.7, 24.7, 18.1; IR (thin film, NaCl) 3793, 2953, 2923, 2869, 1725, 1710, 1386, 1233, 1219, 1187, 1175, 918, 828, 759  $\text{cm}^{-1}$ ; HRMS

(MM:ESI-APCI+)  $m/z$  calc'd for  $C_{19}H_{30}O_5$   $[M-H]^-$ : 337.2015, found 337.2018;  $[\alpha]_D^{25} + 11.2^\circ$  (c 1.0  $CHCl_3$ ).



**Dimer Ester 169:** A 25 mL round bottom flask was charged with acid **163** (50.0 mg, 0.294 mmol, 1.0 equiv),  $\alpha$ -pinandiol (**166**) (50.0 mg, 0.294 mmol, 1.0 equiv), and DMAP (2.0 mg, 0.0147 mmol, 0.05 equiv) in  $CH_2Cl_2$  (5.9 mL). The solution was cooled  $0^\circ C$  and DIC (46  $\mu L$ , 0.294 mmol, 1.0 equiv) was added dropwise. The reaction was allowed to stir for 16 h while gradually warming to  $23^\circ C$ . The reaction mixture was diluted with  $H_2O$  then extracted with EtOAc (3x). The combined organic extracts were washed with brine, dried over  $Na_2SO_4$ , filtered, and concentrated leaving a crude oil which was purified by flash chromatography (20%-40% EtOAc/hexanes) to afford an intermediate ester (44.0 mg, 0.136 mmol, 46% yield). A 50 mL round bottom flask was charged with the intermediate ester (20.0 mg, 0.0602 mmol, 1.0 equiv),  $NaH_2PO_4$  (43.0 mg, 0.361 mmol, 6.0 equiv), and 2-methyl-2-butene (510  $\mu L$ , 4.82 mmol, 80.0 equiv) in *t*-BuOH (6.0 mL) and  $H_2O$  (1.2 mL).  $NaClO_2$  (16.0 mg, 0.180 mmol, 3.0 equiv) was added in a single portion at  $23^\circ C$ , and the reaction was allowed to stir at  $23^\circ C$  for 2 h. The reaction was diluted with  $H_2O$  and extracted with EtOAc (3x). The combined organic extracts were washed with brine, dried over  $Na_2SO_4$ , filtered, and concentrated by rotary evaporation leaving a crude oil which was purified by flash chromatography ( $SiO_2$ , 20%-50% EtOAc/hexanes) to afford dimer

ester **169** (6.0 mg, 0.0177 mmol, 29% yield, 14% yield over the two steps) as a colorless oil;  $^1\text{H}$  NMR (400 MHz,  $\text{CDCl}_3$ )  $\delta$  5.14 (dd,  $J = 9.5, 5.5$  Hz, 1H), 2.83 (dd,  $J = 10.3, 7.8$  Hz, 1H), 2.56 – 2.30 (m, 4H), 2.24 (ddt,  $J = 10.4, 5.9, 2.9$  Hz, 1H), 2.17 (dt,  $J = 11.2, 7.7$  Hz, 1H), 2.07 – 1.90 (m, 3H), 1.63 (ddd,  $J = 14.1, 5.5, 2.5$  Hz, 1H), 1.47 (dd,  $J = 10.5, 2.3$  Hz, 1H), 1.30 (s, 3H), 1.29 (s, 3H), 1.27 (s, 3H), 0.99 (s, 3H), 0.98 (s, 3H);  $^{13}\text{C}$  NMR (100 MHz,  $\text{CDCl}_3$ )  $\delta$  172.1, 74.0, 71.8, 54.2 (d,  $J = 2.2$  Hz), 46.2, 43.0 (d,  $J = 5.5$  Hz), 40.5, 38.8 (d,  $J = 2.2$  Hz), 38.3, 35.3, 30.3, 29.9, 28.5, 28.0, 24.7, 24.4, 17.9; IR (thin film, NaCl) 3812, 2952, 2352, 2339, 1712, 1254, 1238, 1219, 1187, 829, 668  $\text{cm}^{-1}$ ; HRMS (MM:ESI-APCI+)  $m/z$  calc'd for  $\text{C}_{19}\text{H}_{30}\text{O}_5$   $[\text{M}-\text{H}]^-$ : 337.2015, found 337.2016;  $[\alpha]_{\text{D}}^{25} - 0.68^\circ$  (c 0.83  $\text{CHCl}_3$ ).



**Dimer Ester 170:** A 25 mL round bottom flask was charged with acid **163** (28.0 mg, 0.166 mmol, 1.0 equiv), alcohol **167** (37.0 mg, 0.166 mmol, 1.0 equiv), and DMAP (1.0 mg, 0.0083 mmol, 0.05 equiv) in  $\text{CH}_2\text{Cl}_2$  (3.3 mL). The solution was cooled 0 °C and DIC (26  $\mu\text{L}$ , 0.166 mmol, 1.0 equiv) was added dropwise. The reaction was allowed to stir for 16 h while gradually warming to 23 °C. The reaction mixture was diluted with  $\text{H}_2\text{O}$  then extracted with EtOAc (3x). The combined organic extracts were washed with brine, dried over  $\text{Na}_2\text{SO}_4$ , filtered, and concentrated leaving a crude oil which was purified by flash chromatography (20%-50% EtOAc/hexanes) to afford an intermediate diester (32.0 mg, 0.085 mmol, 51% yield). A 50 mL round bottom flask was charged with the intermediate ester (16.0 mg, 0.0427 mmol, 1.0 equiv),  $\text{NaH}_2\text{PO}_4$  (31.0 mg, 0.256 mmol, 6.0 equiv), and

2-methyl-2-butene (362  $\mu$ L, 3.42 mmol, 80.0 equiv) in *t*-BuOH (4.3 mL) and H<sub>2</sub>O (859  $\mu$ L). NaClO<sub>2</sub> (12.0 mg, 0.128 mmol, 3.0 equiv) was added in a single portion at 23 °C, and the reaction was allowed to stir at 23 °C for 2 h. The reaction was diluted with H<sub>2</sub>O and extracted with EtOAc (3x). The combined organic extracts were washed with brine, dried over Na<sub>2</sub>SO<sub>4</sub>, filtered, and concentrated by rotary evaporation leaving a crude oil which was purified by flash chromatography (SiO<sub>2</sub>, 30%-60% EtOAc/hexanes) to afford an intermediate half-acid (8.0 mg, 0.0204 mmol, 48% yield) as a colorless oil. The intermediate half acid (8.0 mg, 0.0204 mmol, 1.0 equiv) was dissolved in THF (2.1 mL), and charged into a 25 mL 2-necked round bottom flask containing Pd/C (c.a. 10% Pd, 10 mg). The flask was subjected to evacuation/refill with N<sub>2</sub> (3x), followed by evacuation/refill with H<sub>2</sub> (3x). The black suspension was stirred at 23 °C under an atmosphere of H<sub>2</sub> for 3 h. The flask was then subjected to evacuation/refill with N<sub>2</sub> (3x) and the suspension was filtered over Celite®, rinsing with ethyl acetate. The filtrate was concentrated to afford dimer ester **170** (6.0 mg, 0.0200 mmol, 98% yield, 24% yield over the three steps) as a colorless oil; <sup>1</sup>H NMR (400 MHz, CDCl<sub>3</sub>)  $\delta$  4.01 (qt, *J* = 11.0, 6.2 Hz, 2H), 2.67 (dd, *J* = 10.3, 7.8 Hz, 1H), 2.38 – 2.22 (m, 5H), 2.10 – 1.99 (m, 1H), 1.95 – 1.83 (m, 1H), 1.70 – 1.48 (m, 4H), 1.43 – 1.31 (m, 2H), 1.16 (s, 3H), 0.87 (s, 3H); <sup>13</sup>C NMR (100 MHz, CDCl<sub>3</sub>)  $\delta$  178.3, 177.5, 171.8, 62.9, 45.2, 41.7, 37.0, 34.1, 32.8, 29.0, 27.4, 24.6, 23.4, 23.2, 16.7; IR (thin film, NaCl) 3550, 3278, 2957, 2925, 1729, 1707, 1687, 1638, 1233, 1179; HRMS (MM:ESI-APCI+) *m/z* calc'd for C<sub>15</sub>H<sub>24</sub>O<sub>6</sub> [M-H]<sup>-</sup>: 299.1495, found 299.1495;  $[\alpha]_D^{25} + 6.1^\circ$  (c 0.5 CHCl<sub>3</sub>).

### 3.7 NOTES AND REFERENCES

<sup>1</sup> Seinfeld, J. H.; Pandis, S. N. *Atmospheric Chemistry and Physics: From Air Pollution to Climate Change*, 2nd ed.; John Wiley & Sons, Inc.: New York, 2006.

<sup>2</sup> Jimenez, J. L.; Canagaratna, M. R.; Donahue, N. M.; Prevot, A. S. H.; Zhang, Q.; Kroll, J. H.; DeCarlo, P. F.; Allan, J. D.; Coe, H.; Ng, N. L.; Aiken, A. C.; Docherty, K. S.; Ulbrich, I. M.; Grieshop, A. P.; Robinson, A. L.; Duplissy, J.; Smith, J. D.; Wilson, K. R.; Lanz, V. A.; Hueglin, C.; Sun, Y. L.; Tian, J.; Duplissy, J.; Smith, J. D.; Wilson, K. R.; Lanz, V. A.; Hueglin, C.; Sun, Y. L.; Tian, J.; Laaksonen, A.; Raatikainen, T.; Rautiainen, J.; Vaatovaara, P.; Ehn, M.; Kulmala, M.; Tomlinson, J. M.; Colins, D. R.; Cubison, M. J.; Dunlea, E. J.; Huffman, J. A.; Onasch, T. B.; Alfarra, M. R.; Williams, P. I.; Bower, K.; Kondo, Y.; Schneider, J.; Drewnick, F.; Borrmann, S.; Weimer, S.; Demerjian, K.; Salcedo, D.; Cottrell, L.; Griffin, R.; Takami, A.; Miyoshi, T.; Hatakeyama, S.; Shimono, A.; Sun, J. Y.; Zhang, Y. M.; Dzepina, K.; Kimmel, J. R.; Sueper, D.; Jayne, J. T.; Herndon, S. C.; Trimborn, A. M.; Williams, L. R.; Wood, E. C.; Middlebrook, A. M.; Kolb, C. E.; Baltensperger, U.; Worsnop, D. R. *Evolution of Organic Aerosols in the Atmosphere. Science* **2009**, *326*, 1525–1529.

<sup>3</sup> (a) Hoffman, T.; Bandur, R.; Marggraf, U.; Linscheid, M. *Molecular Composition of Organic Aerosols Formed in the  $\alpha$ -Pinene/O<sub>3</sub> Reaction: Implications for New Particle Formation Processes. J. Geophys. Res.* **1998**, *103*, 25569–25578. (b) Yu, J.; Cocker, D. R., III; Griffin, R. J.; Flagan, R. C.; Seinfeld, J. H. *Gas-Phase Ozone Oxidation of Monoterpenes: Gaseous and Particulate Products. J. Atmos. Chem.* **1999**, *34*, 207–258. (c) Glasius, M.; Lahaniati, M.; Calogirou, A.; Di Bella, D.; Jensen, N. R.; Hjorth, J.; Kotzias,

D.; Larsen, B. R. Carboxylic Acids in Secondary Aerosols from Oxidation of Cyclic Monoterpenes by Ozone. *Environ. Sci. Technol.* **2000**, *34*, 1001–1010.

<sup>4</sup> Müller, L.; Reinnig, M.-C.; Warnke, J.; Hoffmann, Th. Unambiguous Identification of Esters as Oligomers in Secondary Organic Aerosol Formed from Cyclohexene and Cyclohexene/ $\alpha$ -Pinene Ozonolysis. *Atmos. Chem. Phys.* **2008**, *8*, 1423–1433.

<sup>5</sup> Yasmineen, F.; Vermeylen, R.; Szmigielski, R.; Iinuma, Y.; Böge, O.; Herrmann, H.; Maenhaut, W.; Claeys, M. Terpenylic Acid and Related Compounds: Precursors for Dimers in Secondary Organic Aerosol from the Ozonolysis of  $\alpha$ - and  $\beta$ -Pinene. *Atmos. Chem. Phys.* **2010**, *10*, 9383–9392.

<sup>6</sup> Kristensen, K.; Watne, Å. K.; Hammes, J.; Lutz, A.; Petäjä, T.; Hallquist, M.; Bilde, M.; Glasius, M. High-Molecular Weight Dimer Esters Are Major Products in Aerosols from  $\alpha$ -Pinene Ozonolysis and the Boreal Forest. *Environ. Sci. Technol. Lett.* **2016**, *3*, 280–285.

<sup>7</sup> Zhang, X.; McVay, R. C.; Huang, D. D.; Dalleska, N. F.; Aumont, B.; Flagan, R. C.; Seinfeld, J. H. Formation and Evolution of Molecular Products in  $\alpha$ -Pinene Secondary Organic Aerosol. *Proc. Natl. Acad. Sci. U.S.A.* **2015**, *112* (46), 14168–14173.

<sup>8</sup> Kenseth, C. M.; Huang, Y.; Zhao, R.; Dalleska, N. F.; Hethcox, J. C.; Stoltz, B. M.; Seinfeld, J. H. Synergistic O<sub>3</sub> + OH Oxidation Pathway to Extremely Low-Volatility Dimers Revealed in  $\beta$ -Pinene Secondary Organic Aerosol. *Proc. Natl. Acad. Sci. U.S.A.* **2018**, *115*, 8301–8306.

<sup>9</sup> Kahnt, A.; Vermeylen, R.; Iinuma, Y.; Safi Shalamzari, M.; Maenhaut, W.; Claeys, M. High-Molecular-Weight Esters in  $\alpha$ -Pinene Ozonolysis Secondary Organic Aerosol: Structural Characterization and Mechanistic Proposal for Their Formation from Highly Oxygenated Molecules. *Atmos. Chem. Phys.* **2018**, *18*, 8453–8467.

- <sup>10</sup> Nozière, B.; Kalberer, M.; Claeys, M.; Allan, J.; D'Anna, B.; Decesari, S.; Finessi, E.; Glasius, M.; Grgić, I.; Hamilton, J. F.; Hoffmann, T.; Iinuma, Y.; Jaoui, M.; Kahnt, A.; Kampf, C. J.; Kourtchev, I.; Maenhaut, W.; Marsden, N.; Saarikoski, S.; Schnelle-Kreis, J.; Surratt, J. D.; Szidat, S.; Szmigielski, R.; Wisthaler, A. The Molecular Identification of Organic Compounds in the Atmosphere: State of the Art and Challenges. *Chem. Rev.* **2015**, *115*, 3919–3983.
- <sup>11</sup> Laskin, J.; Laskin, A.; Nizkorodov, S. A. Mass Spectrometry Analysis in Atmospheric Chemistry. *Anal. Chem.* **2018**, *90*, 166–189.
- <sup>12</sup> Konermann, L.; Ahadi, E.; Rodriguez, A. D.; Vahidi, S. Unraveling the Mechanism of Electrospray Ionization. *Anal. Chem.* **2013**, *85*, 2–9.
- <sup>13</sup> Kruve, A.; Kaupmees, K.; Liigand, J.; Leito, I. Negative Electrospray Ionization via Deprotonation: Predicting the Ionization Efficiency. *Anal. Chem.* **2014**, *86*, 4822–4830.
- <sup>14</sup> Beck, M.; Hoffmann, T. A Detailed MS<sub>n</sub> Study for the Molecular Identification of a Dimer Formed from Oxidation of Pinene. *Atmos. Environ.* **2016**, *130*, 120–126.
- <sup>15</sup> Iinuma, Y.; Ramasamy, S.; Sato, K.; Kołodziejczyk, A.; Szmigielski, R. Structural Characterisation of Dimeric Esters in  $\alpha$ -Pinene Secondary Organic Aerosol Using N<sub>2</sub> and CO<sub>2</sub> Ion Mobility Mass Spectrometry. *Atmosphere* **2020**, *12*, 17.
- <sup>16</sup> Moglioni, A. G.; García-Expósito, E.; Aguado, G. P.; Parella, T.; Branchadell, V.; Moltrasio, G. Y.; Ortuño, R. M. Divergent Routes to Chiral Cyclobutane Synthons from (–)- $\alpha$ -Pinene and Their Use in the Stereoselective Synthesis of Dehydro Amino Acids. *J. Org. Chem.* **2000**, *65*, 3934–3940.



- <sup>17</sup> Moglioni, A. G.; García-Expósito, E.; Moltrasio, G. Y.; Ortuño, R. M. Stereoselective Synthesis of Novel Cyclobutane Dehydro Amino Acids from  $\alpha$ -Pinene. *Tetrahedron Lett.* **1998**, 3593–3596.
- <sup>18</sup> Hergueta, A. R.; López, C.; Fernández, F.; Caamaño, O.; Blanco, J. Synthesis of Two Enantiomerically Pure Precursors of Cyclobutane Carbocyclic Nucleosides. *Tetrahedron Asymmetry* **1998**, 39, 3593–3596.
- <sup>19</sup> Zhao, Z.; Zhang, W.; Alexander, T.; Zhang, X.; Martin, D. B. C.; Zhang, H. Isolating  $\alpha$ -Pinene Ozonolysis Pathways Reveals New Insights into Peroxy Radical Chemistry and Secondary Organic Aerosol Formation. *Environ. Sci. Technol.* **2021**, 55, 6700–6709.
- <sup>20</sup> Nicolaou, K. C.; Hwang, C.-K.; Marron, B. E.; DeFrees, S. A.; Couladouros, E. A.; Abe, Y.; Carroll, P. J.; Snyder, J. P. Bridging of Macrodithionolactones to Bicyclic Systems. Synthesis and Modeling of Oxapolycyclic Frameworks. *J. Am. Chem. Soc.* **1990**, 112, 3040–3054.

## **APPENDIX 9**

*Spectra Relevant to Chapter 3:*

*Synthesis of Carboxylic Acid and Dimer Esters  
from Pinene-Derived Secondary Organic Aerosol*

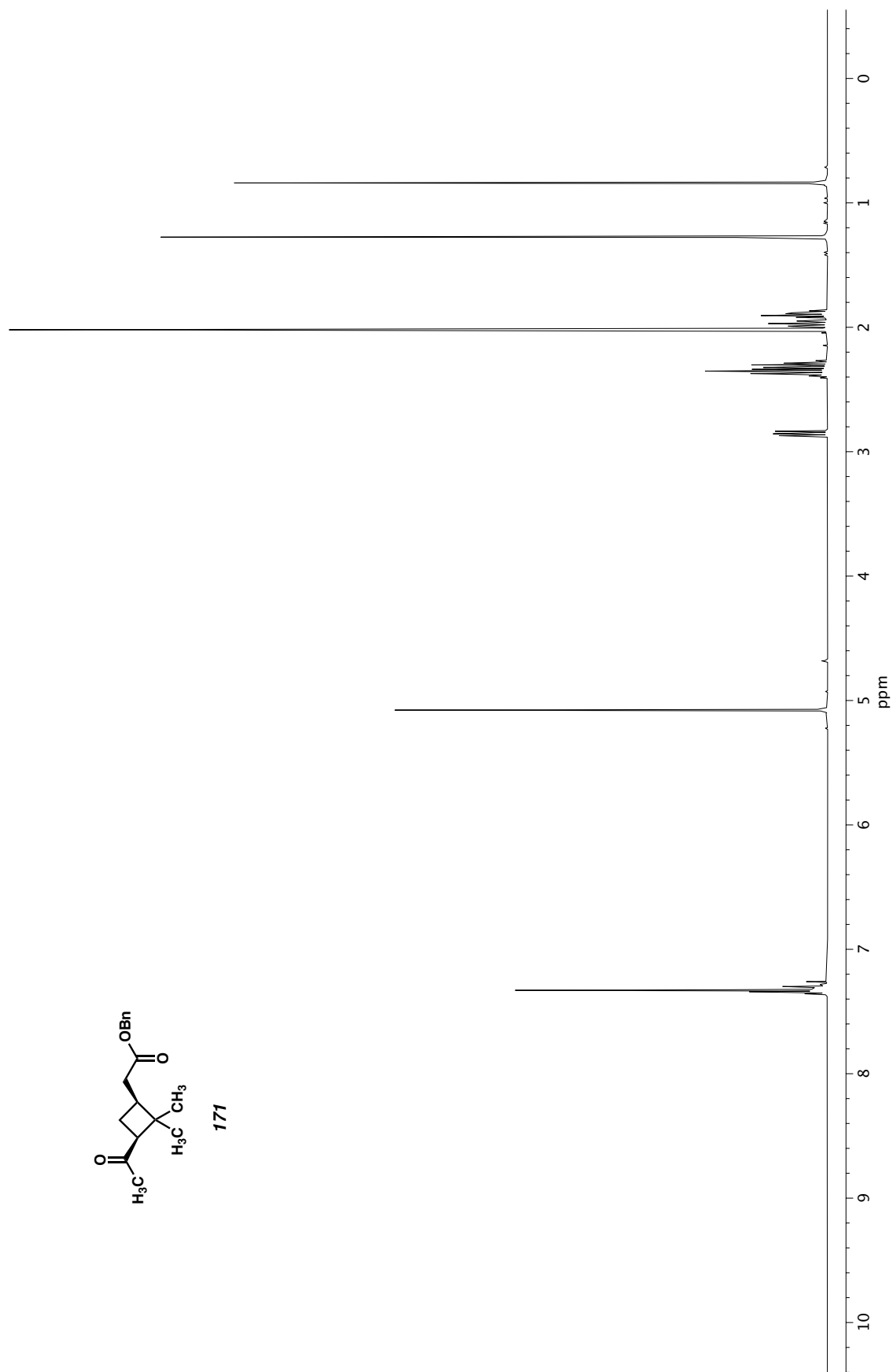


**Figure A8.1**  $^1\text{H}$  NMR (500 MHz,  $\text{CDCl}_3$ ) of compound **171**.

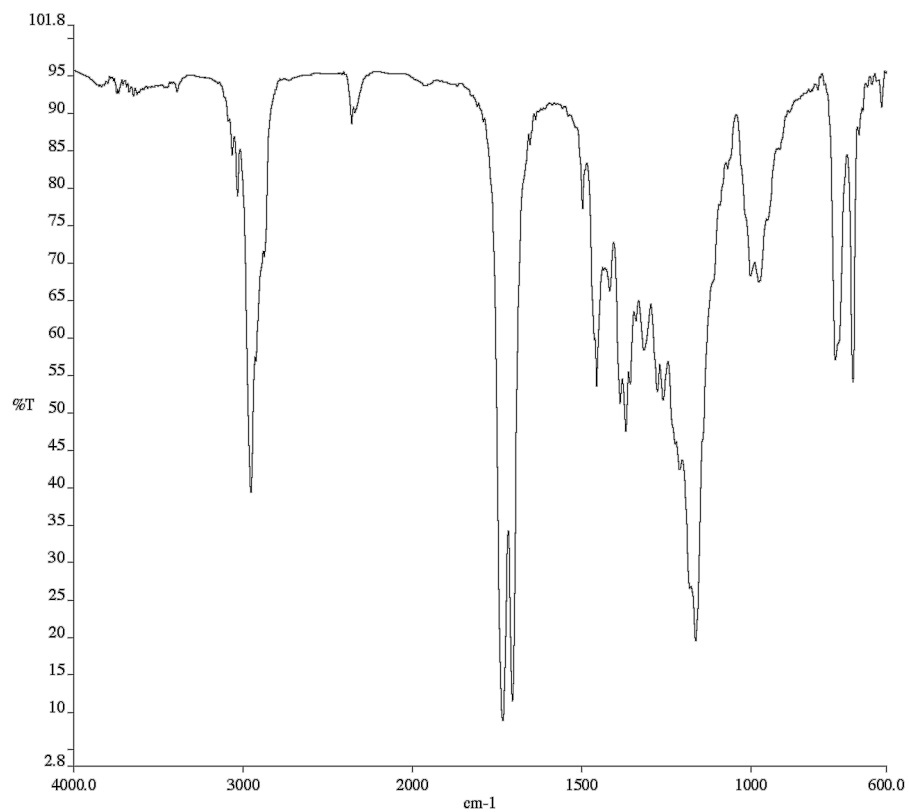


**Figure A8.2** Infrared spectrum (Thin Film, NaCl) of compound **171**.

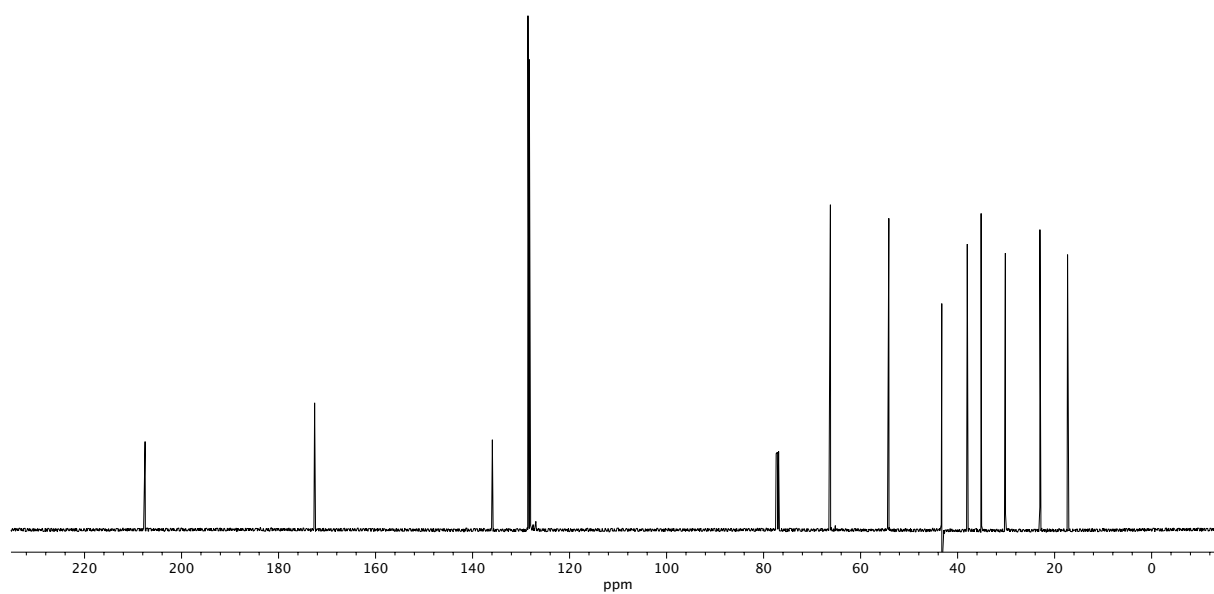


**Figure A8.3** <sup>13</sup>C NMR (100 MHz, CDCl<sub>3</sub>) of compound **171**.

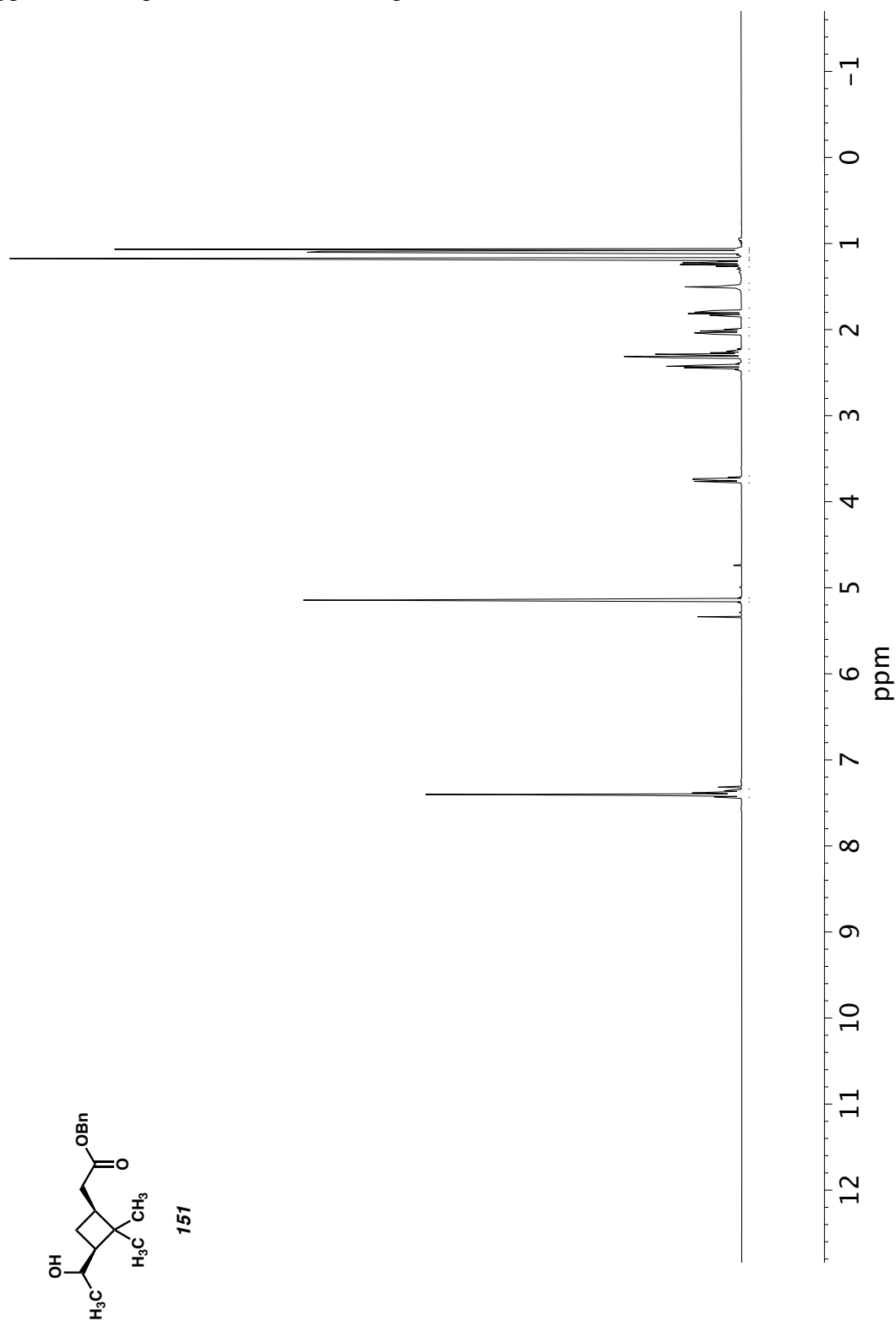
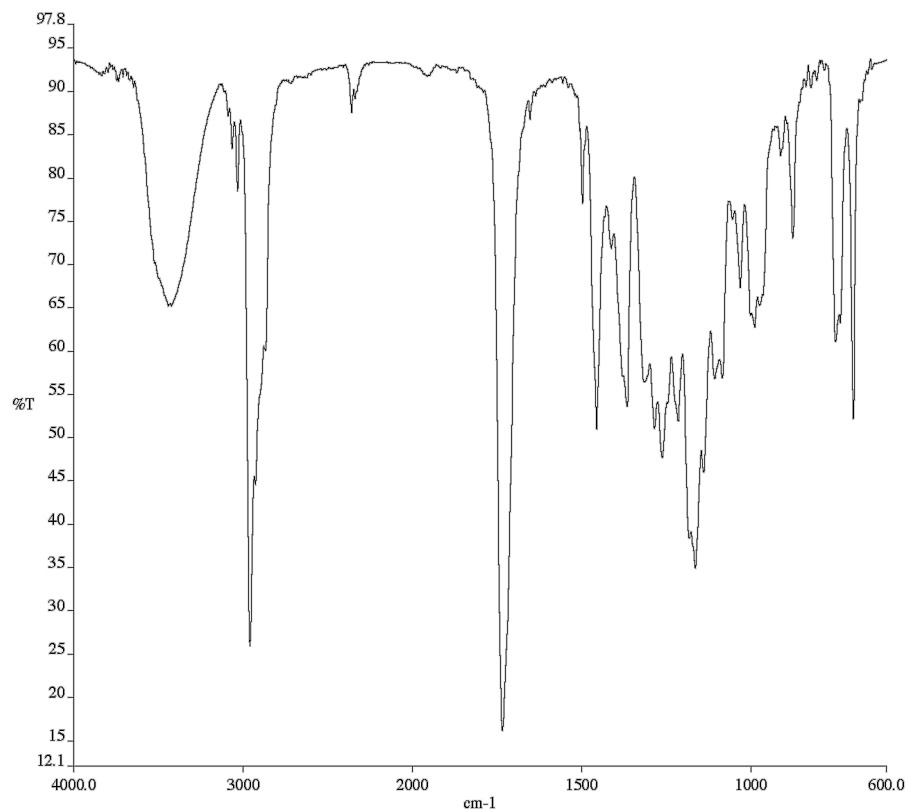
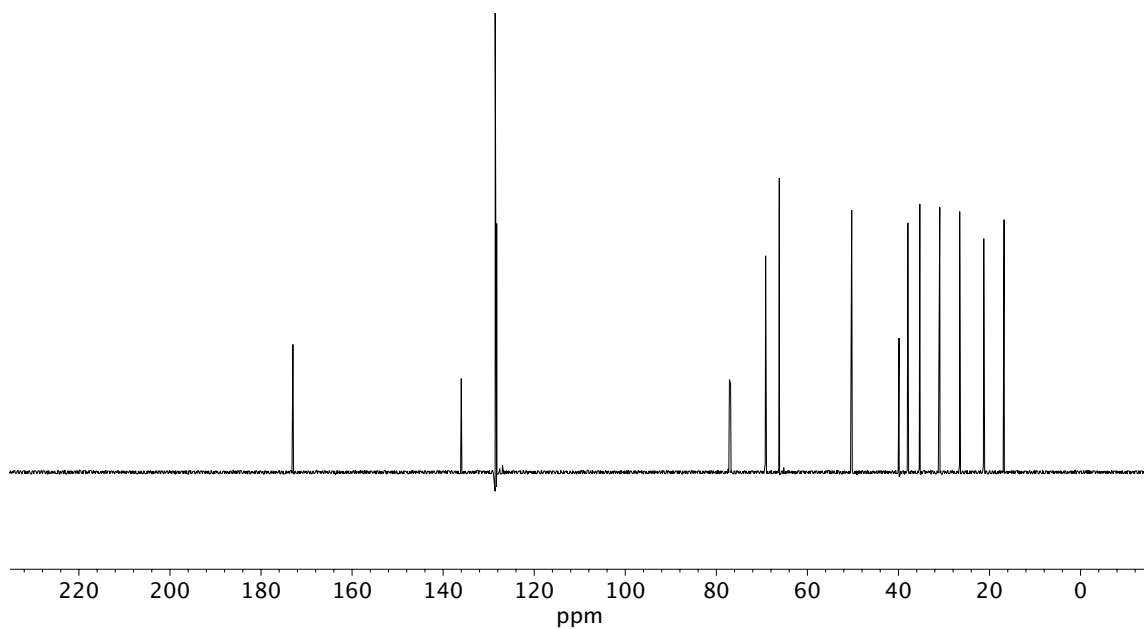


Figure A8.4 <sup>1</sup>H NMR (500 MHz, CDCl<sub>3</sub>) of compound **151**.



**Figure A8.5** Infrared spectrum (Thin Film, NaCl) of compound **151**.



**Figure A8.6** <sup>13</sup>C NMR (125 MHz, CDCl<sub>3</sub>) of compound **151**.

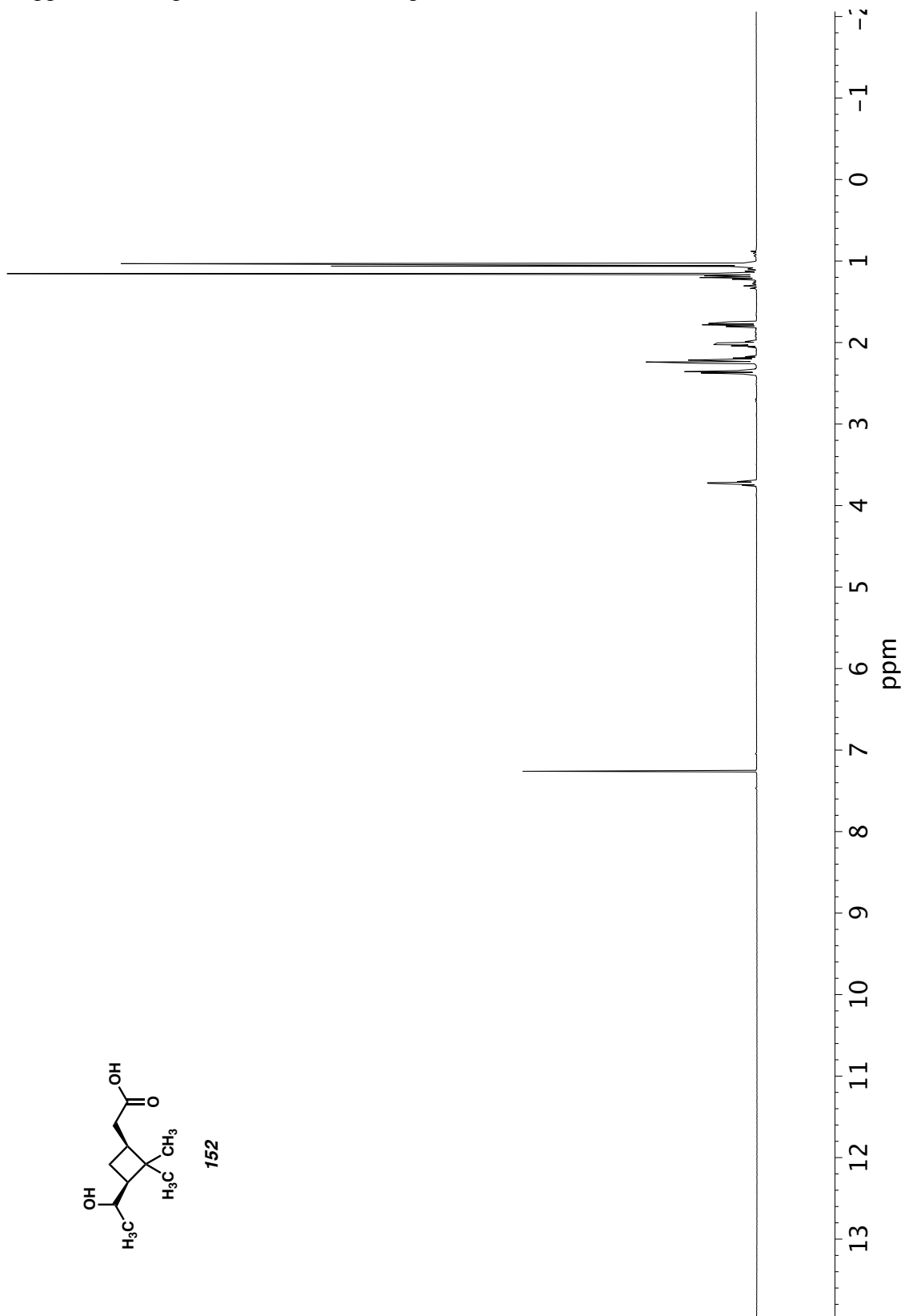
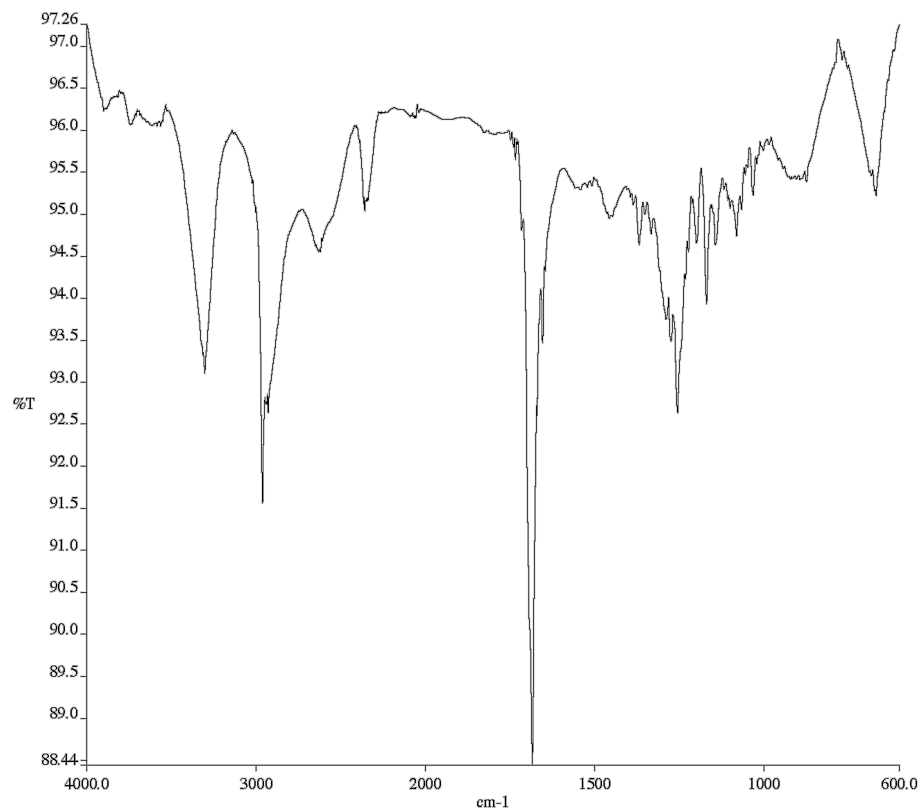
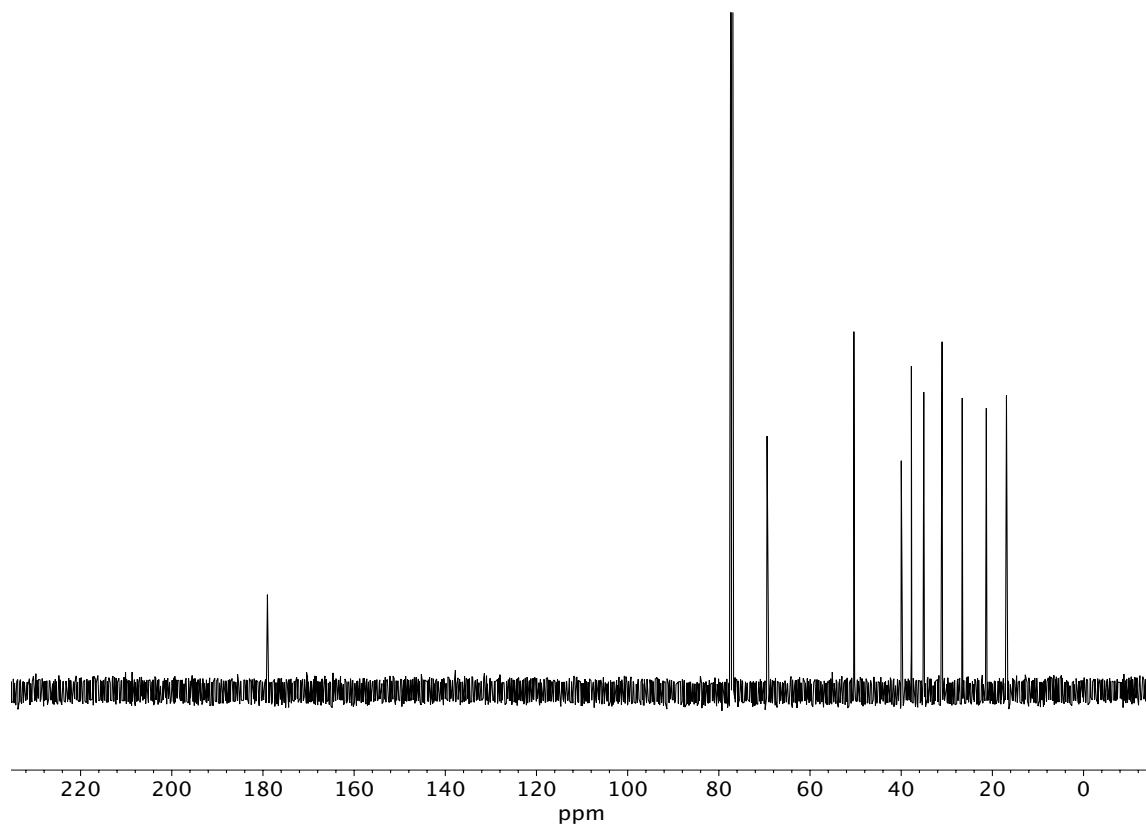


Figure A8.7  $^1\text{H}$  NMR (500 MHz,  $\text{CDCl}_3$ ) of compound 152.



**Figure A8.8** Infrared spectrum (Thin Film, NaCl) of compound **152**.



**Figure A8.9** <sup>13</sup>C NMR (125 MHz, CDCl<sub>3</sub>) of compound **152**.



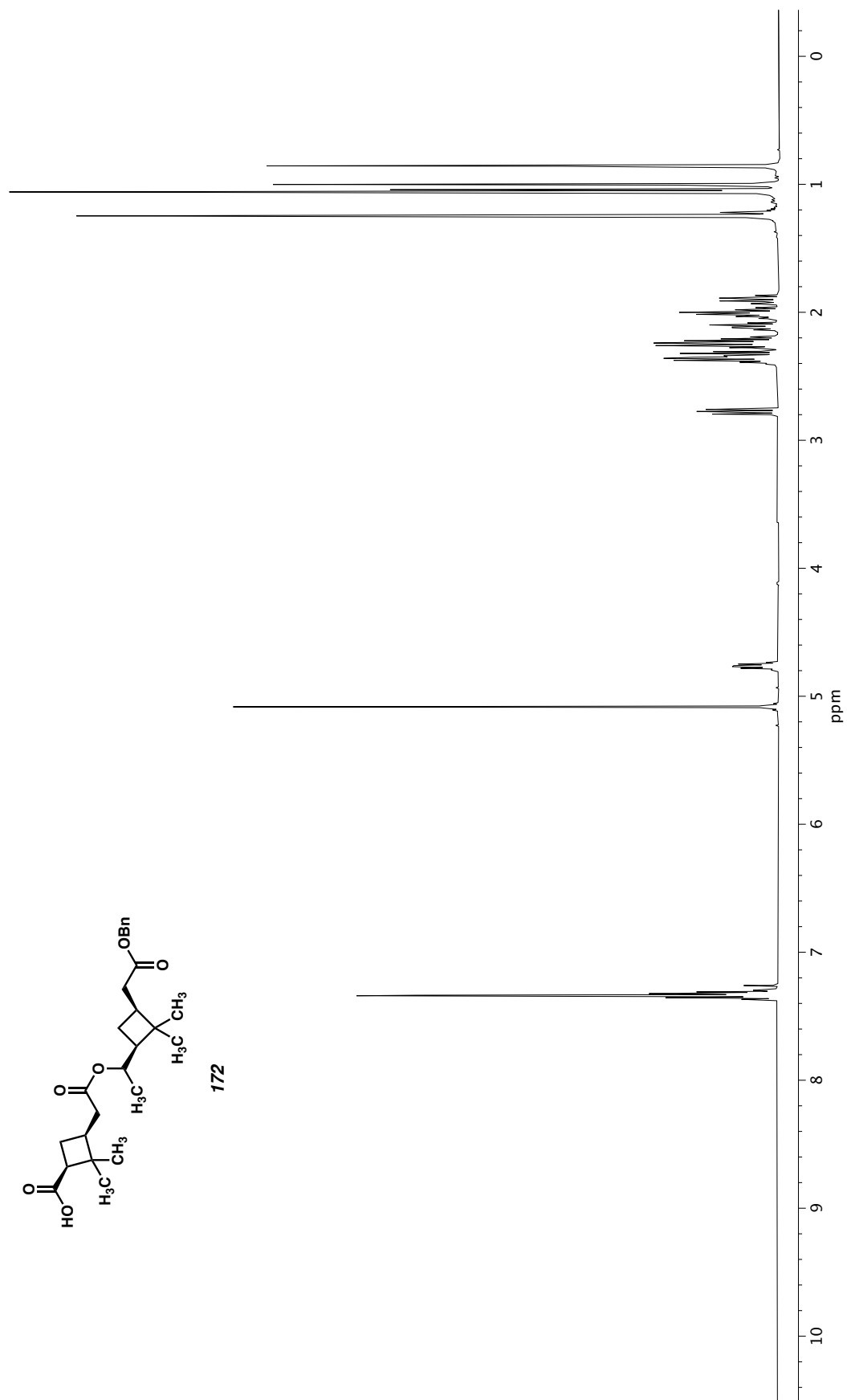
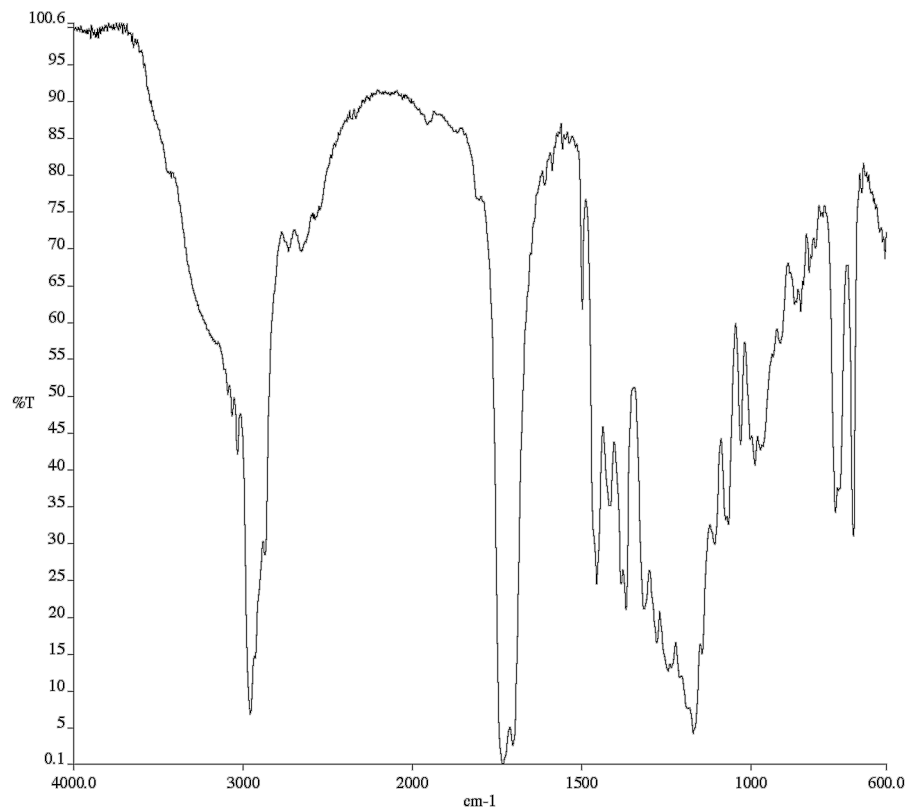
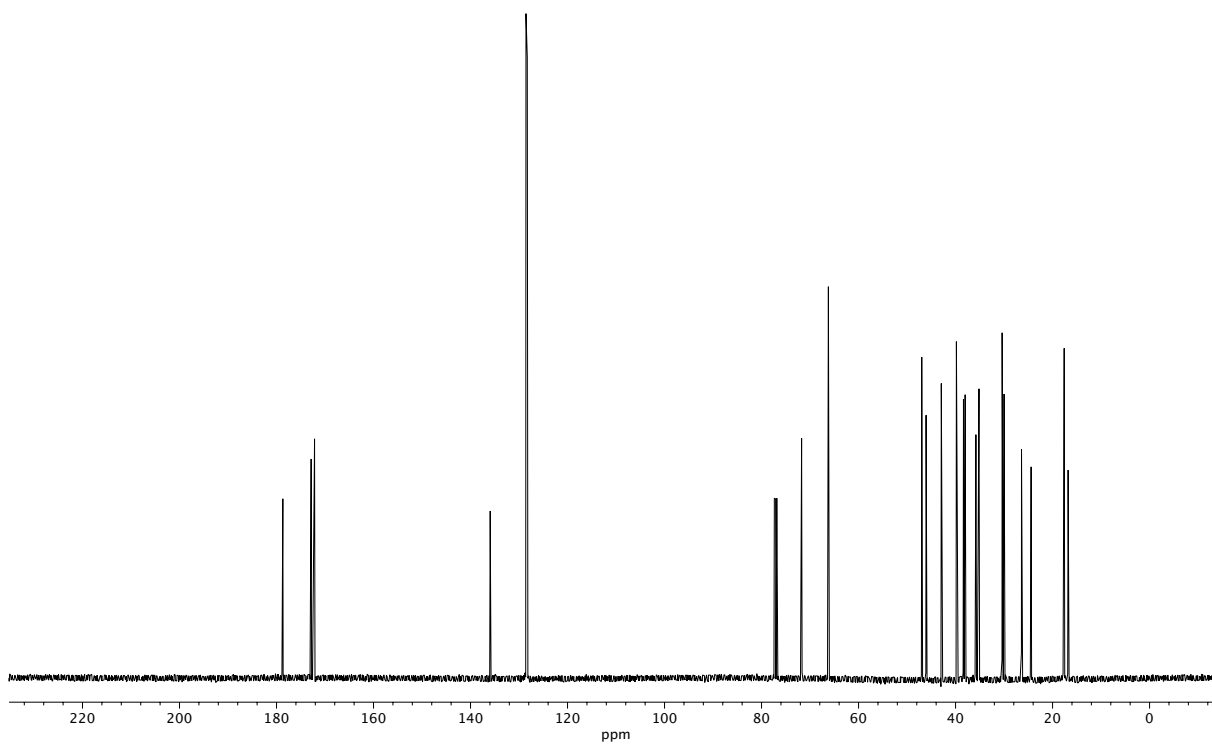


Figure A8.10  $^1\text{H}$  NMR (500 MHz,  $\text{CDCl}_3$ ) of compound 172.



**Figure A8.11** Infrared spectrum (Thin Film, NaCl) of compound **172**.



**Figure A8.12** <sup>13</sup>C NMR (125 MHz, CDCl<sub>3</sub>) of compound **172**.

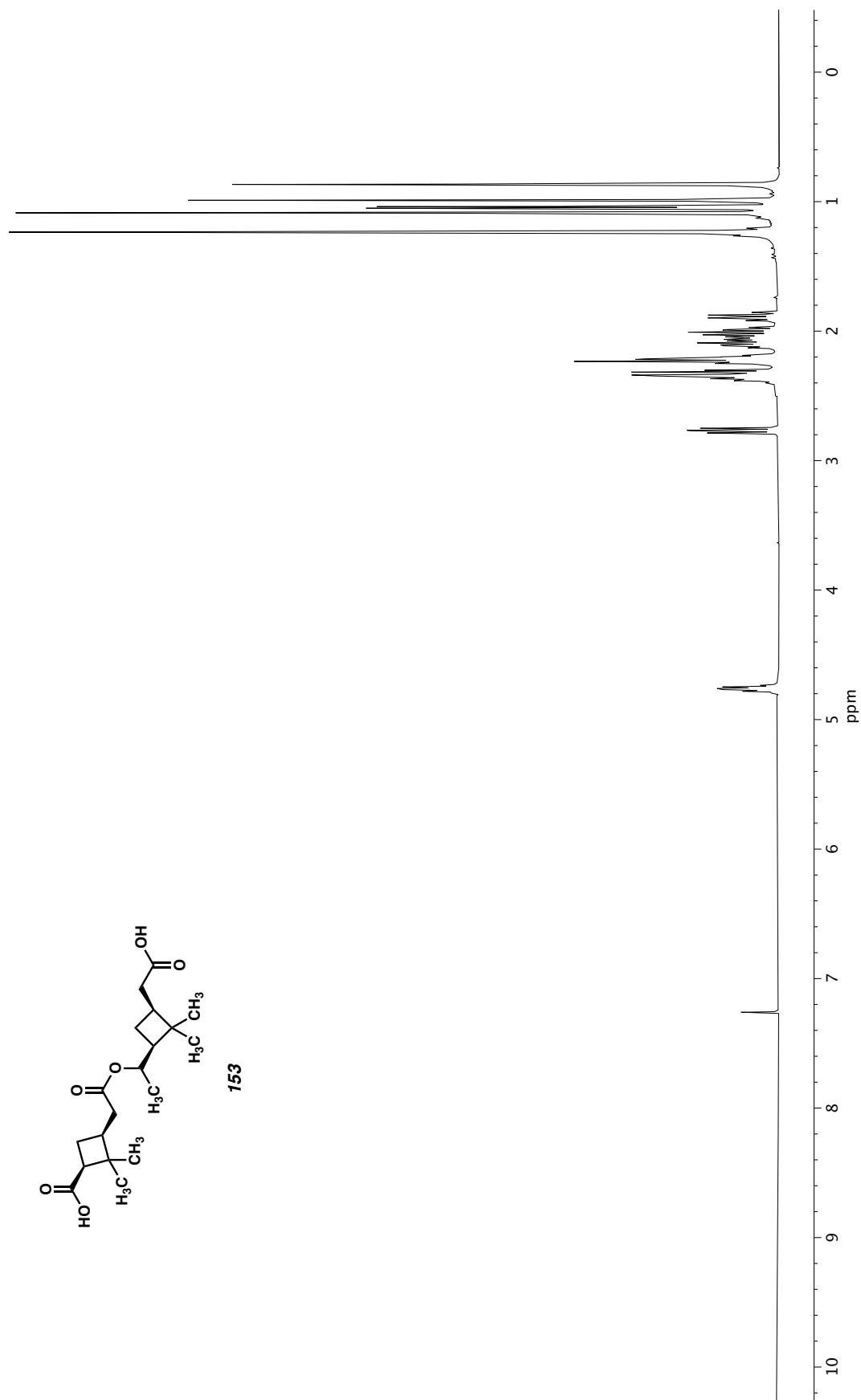


**Figure A8.13**  $^1\text{H}$  NMR (500 MHz,  $\text{CDCl}_3$ ) of compound **153**.

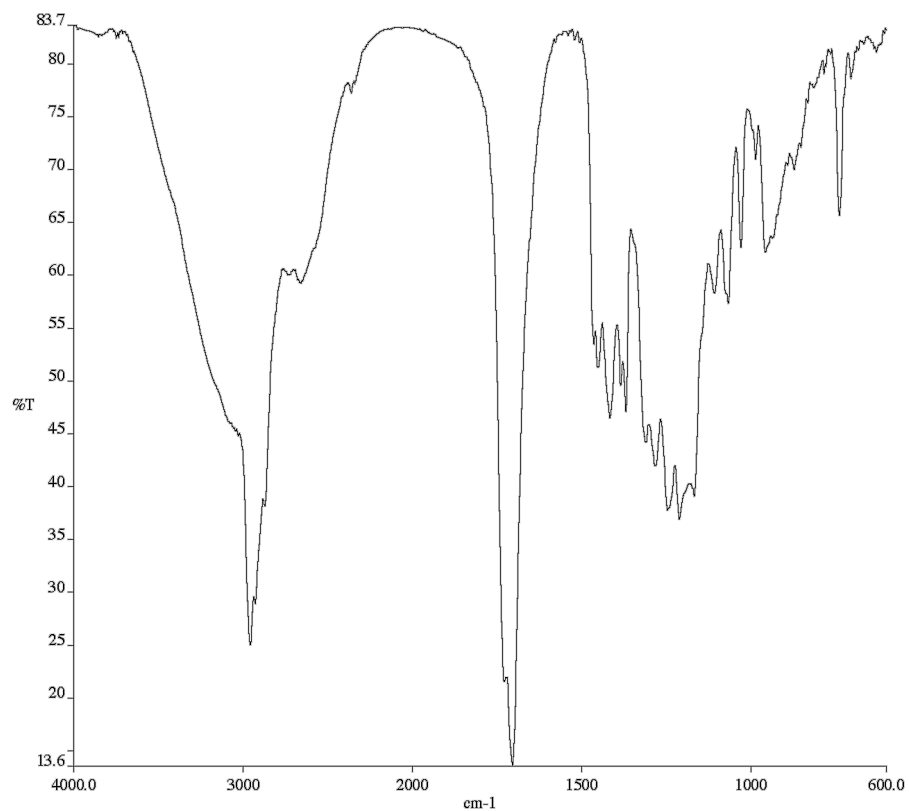


**Figure A8.14** Infrared spectrum (Thin Film, NaCl) of compound **153**.

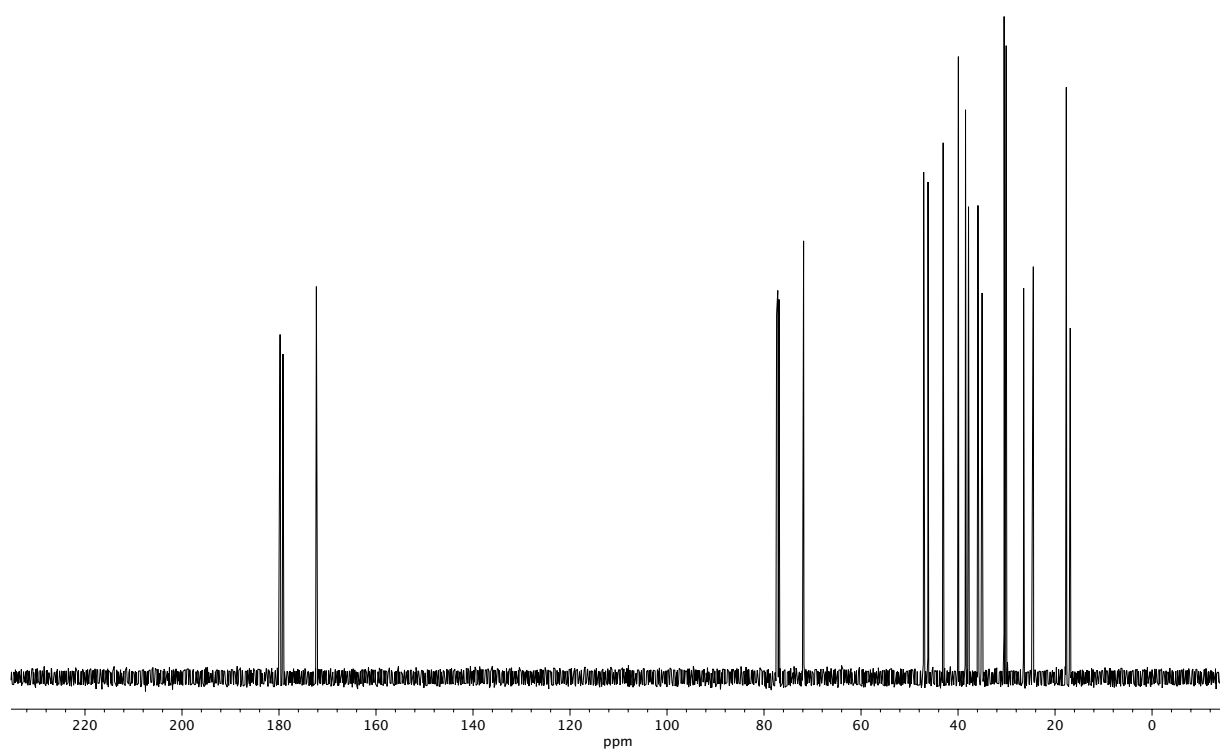


**Figure A8.15** <sup>13</sup>C NMR (125 MHz, CDCl<sub>3</sub>) of compound **153**.

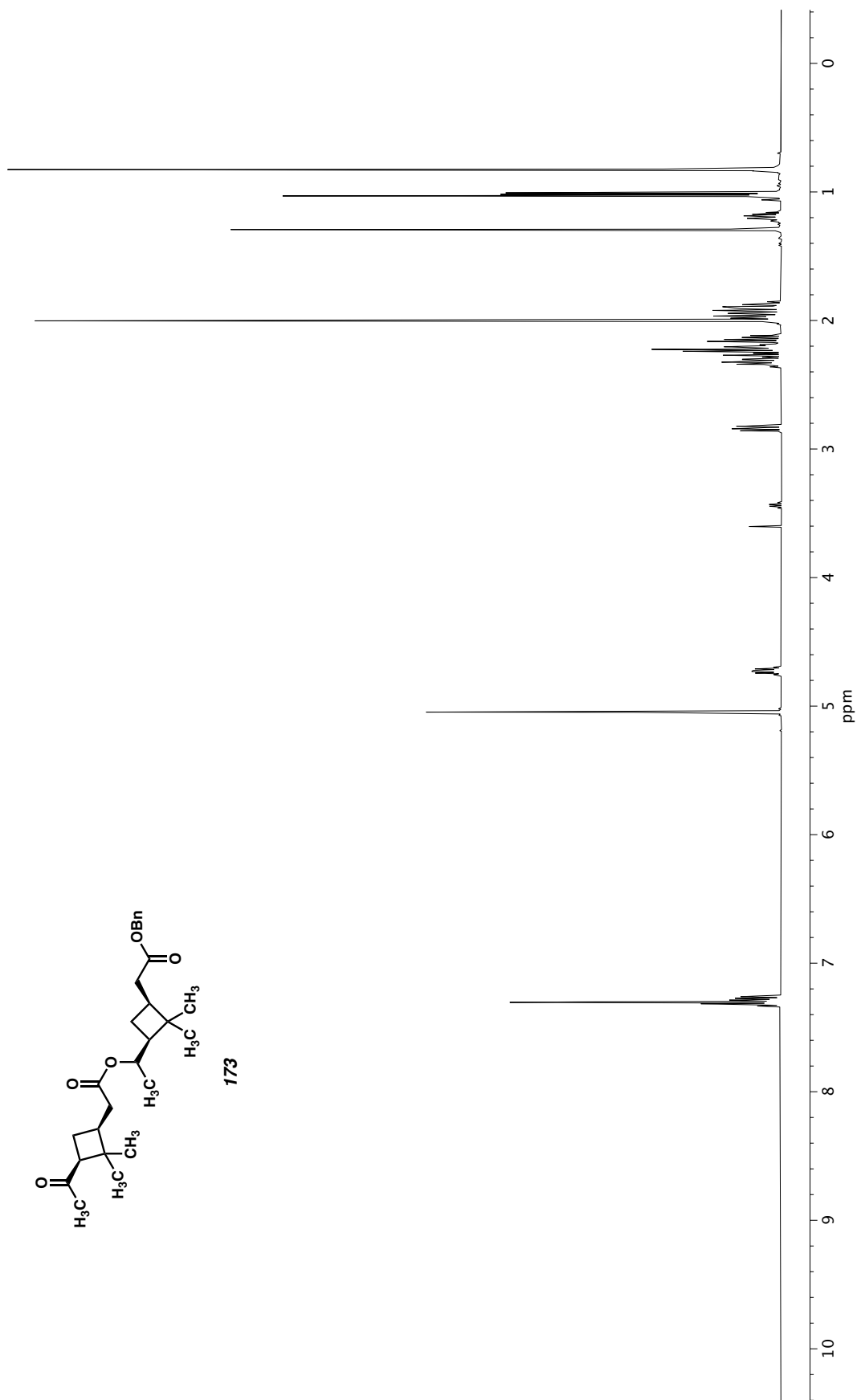


**Figure A8.16**  $^1\text{H}$  NMR (500 MHz,  $\text{CDCl}_3$ ) of compound **173**.

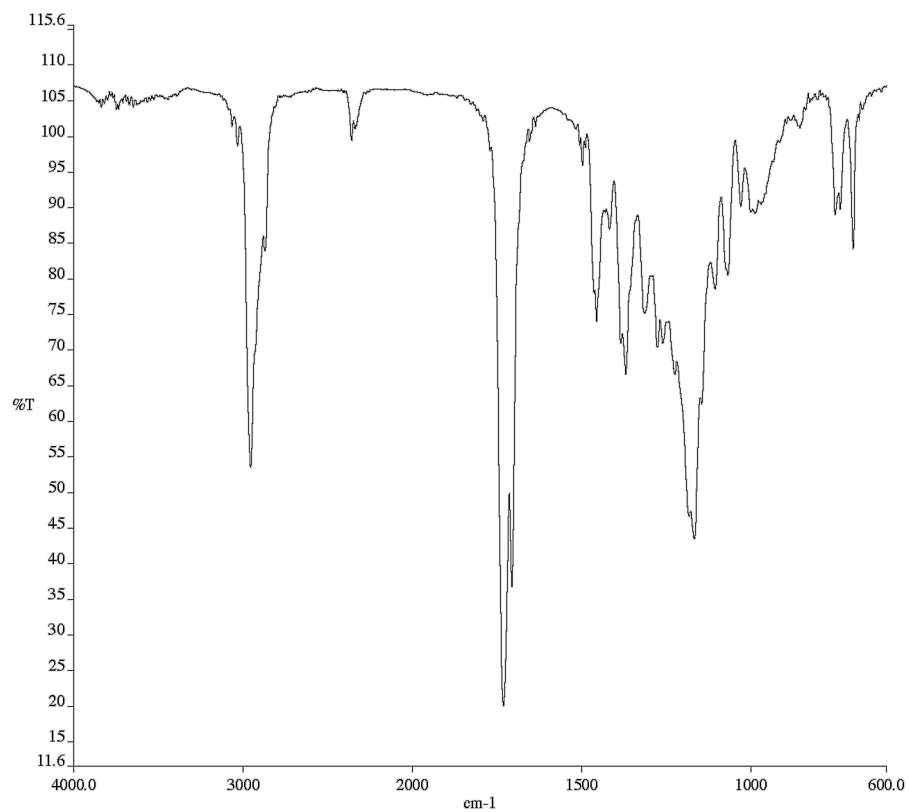


**Figure A8.17** Infrared spectrum (Thin Film, NaCl) of compound **173**.

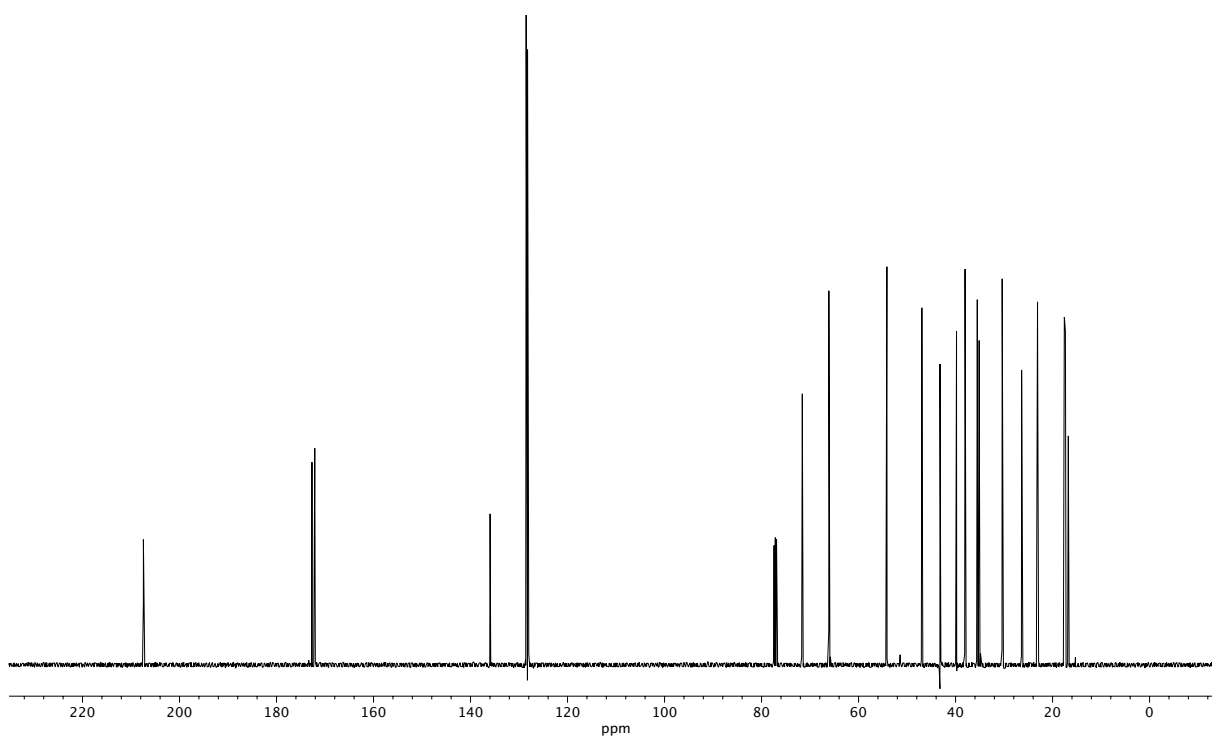


**Figure A8.18** <sup>13</sup>C NMR (125 MHz, CDCl<sub>3</sub>) of compound **173**.

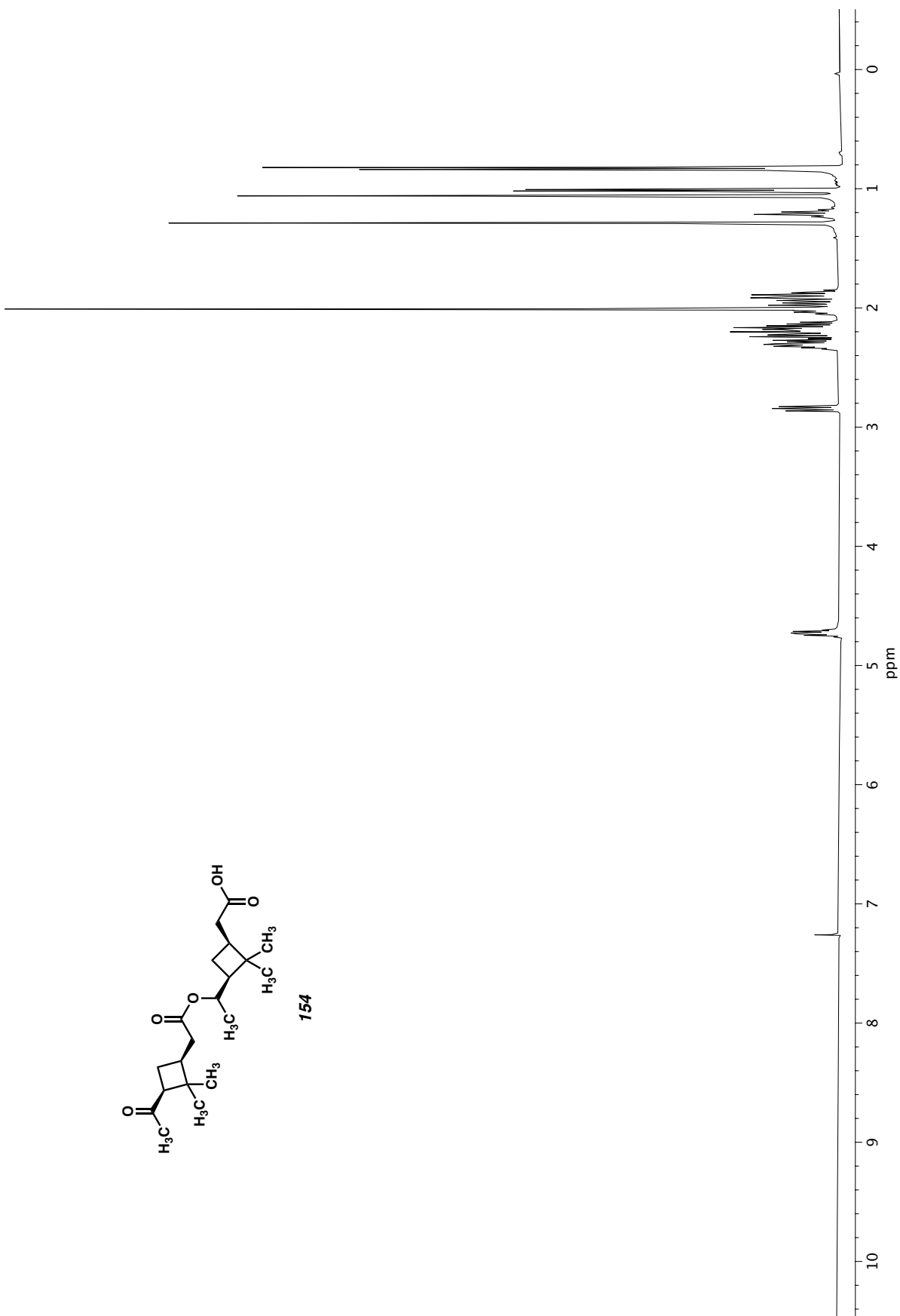
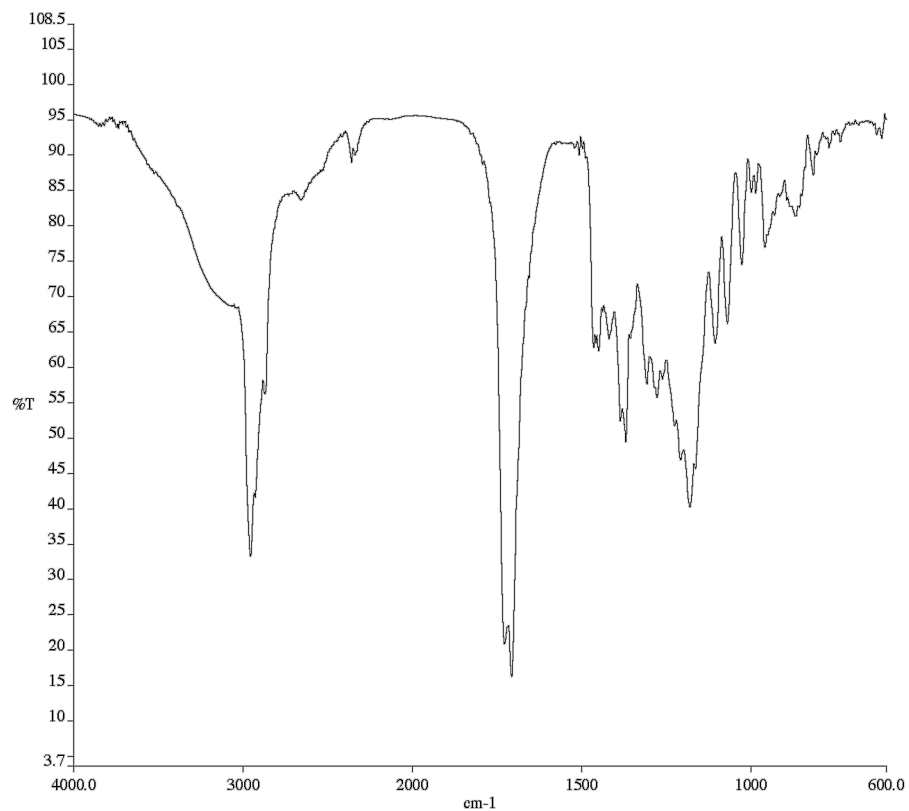
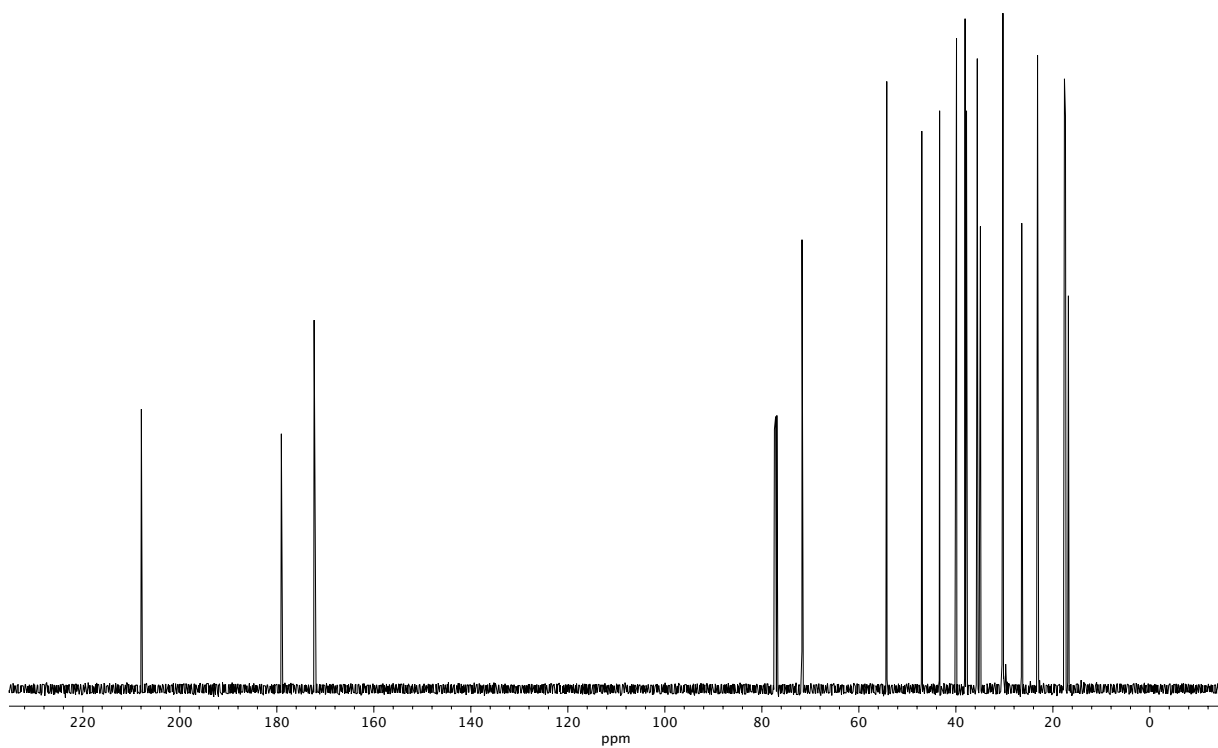


Figure A8.19  $^1\text{H}$  NMR (500 MHz,  $\text{CDCl}_3$ ) of compound 154.



**Figure A8.20** Infrared spectrum (Thin Film, NaCl) of compound **154**.



**Figure A8.21** <sup>13</sup>C NMR (125 MHz, CDCl<sub>3</sub>) of compound **154**.



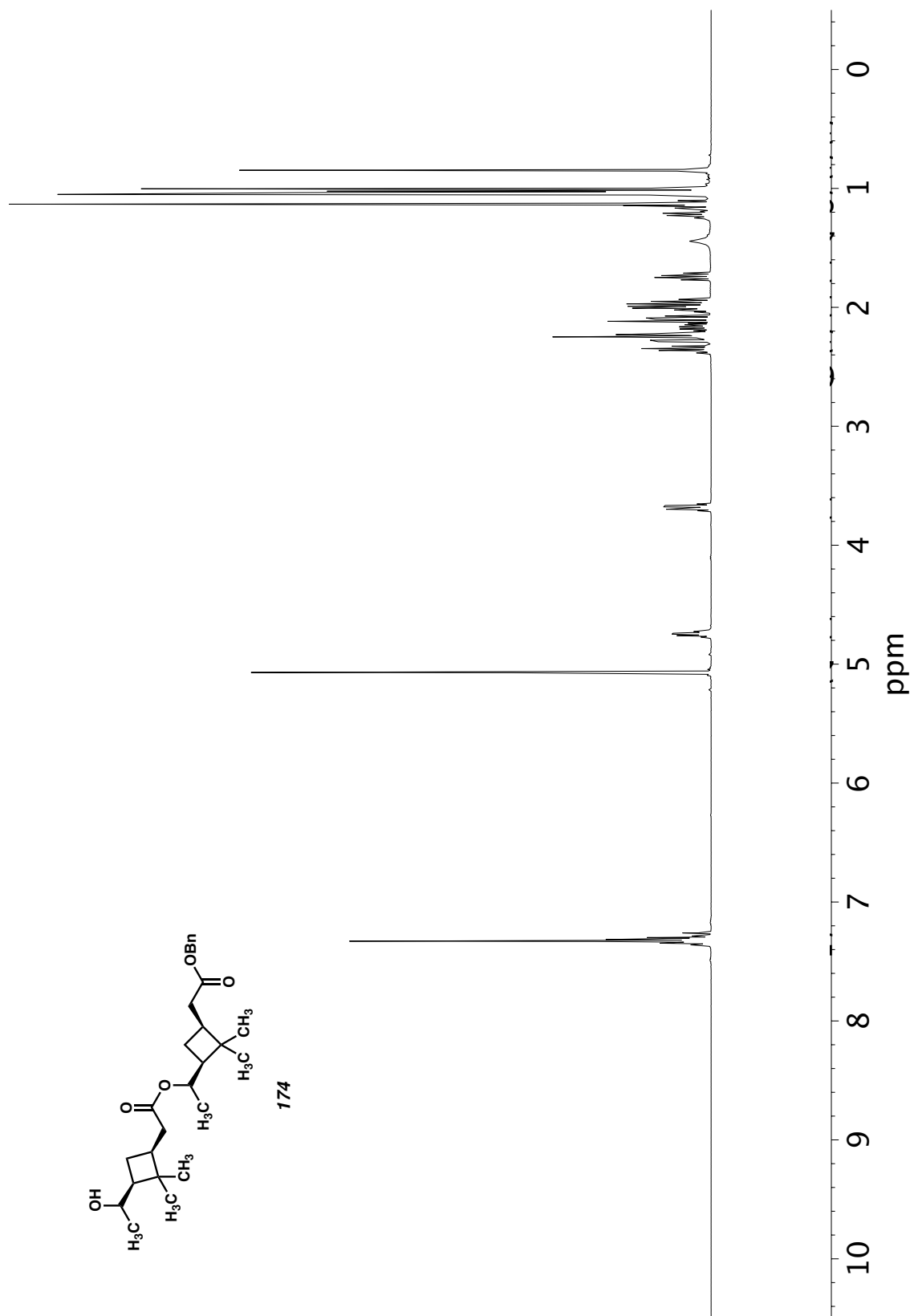
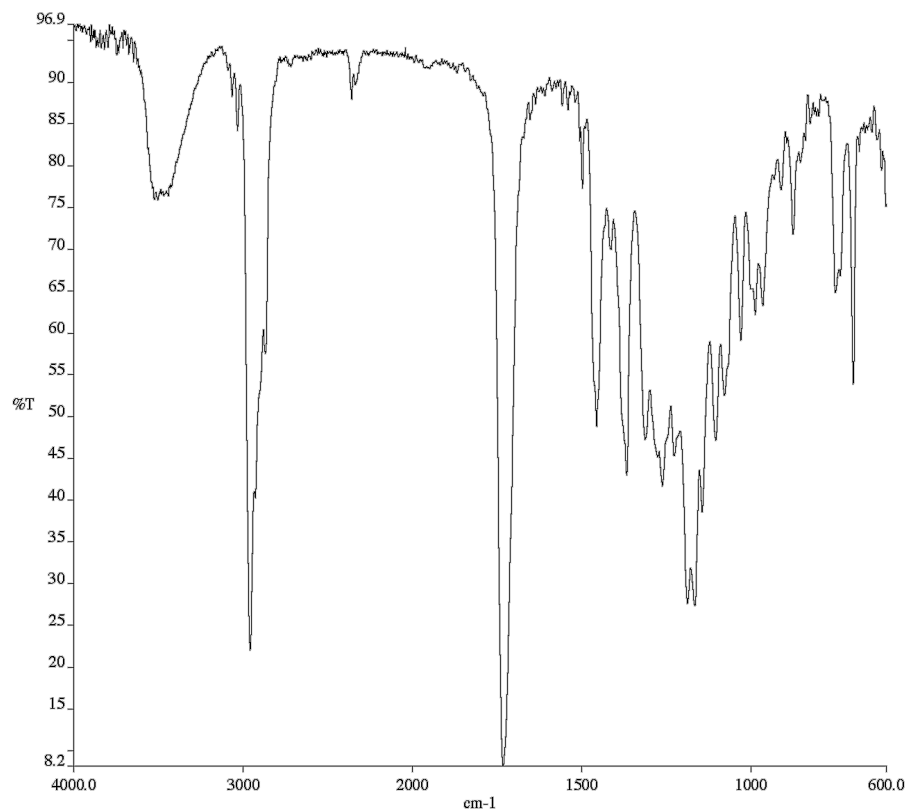
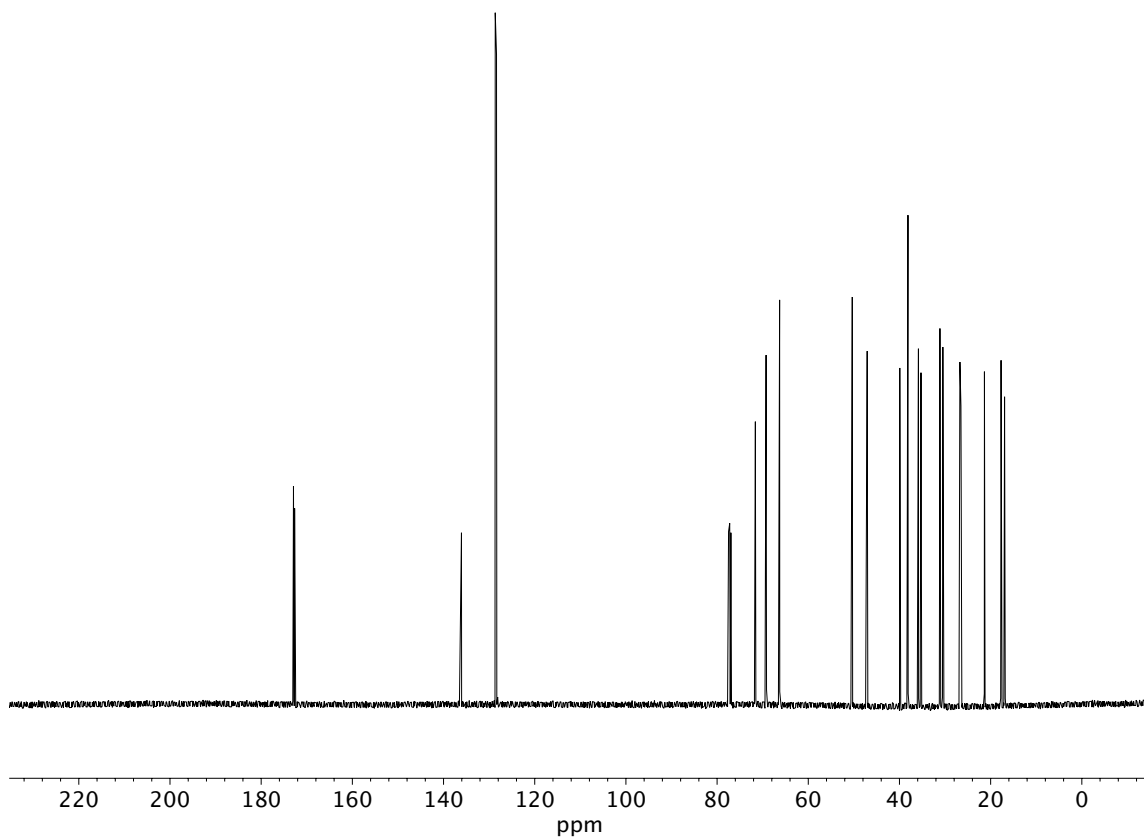


Figure A8.22 <sup>1</sup>H NMR (500 MHz, CDCl<sub>3</sub>) of compound 174.



**Figure A8.23** Infrared spectrum (Thin Film, NaCl) of compound **174**.



**Figure A8.24** <sup>13</sup>C NMR (125 MHz, CDCl<sub>3</sub>) of compound **174**.

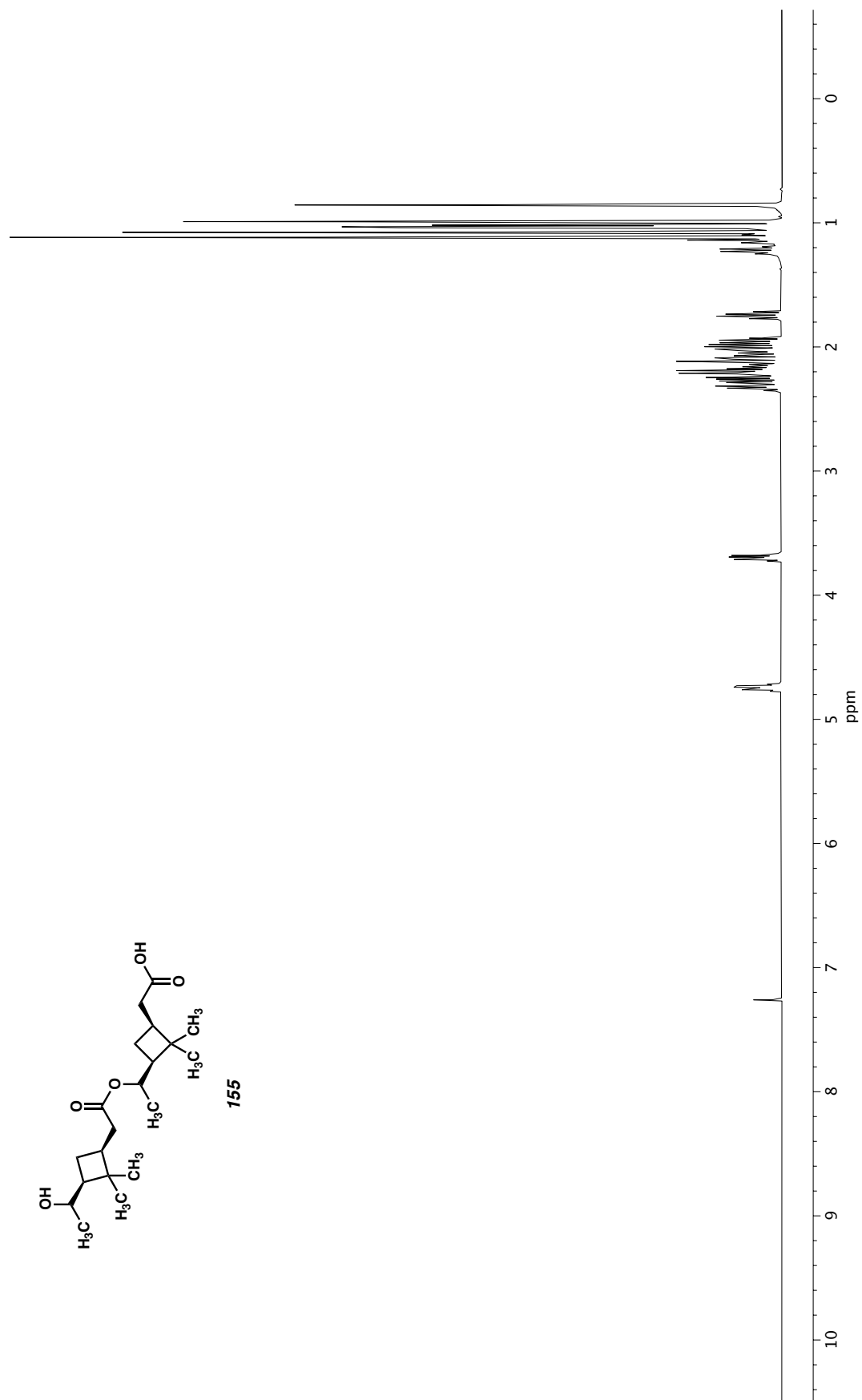
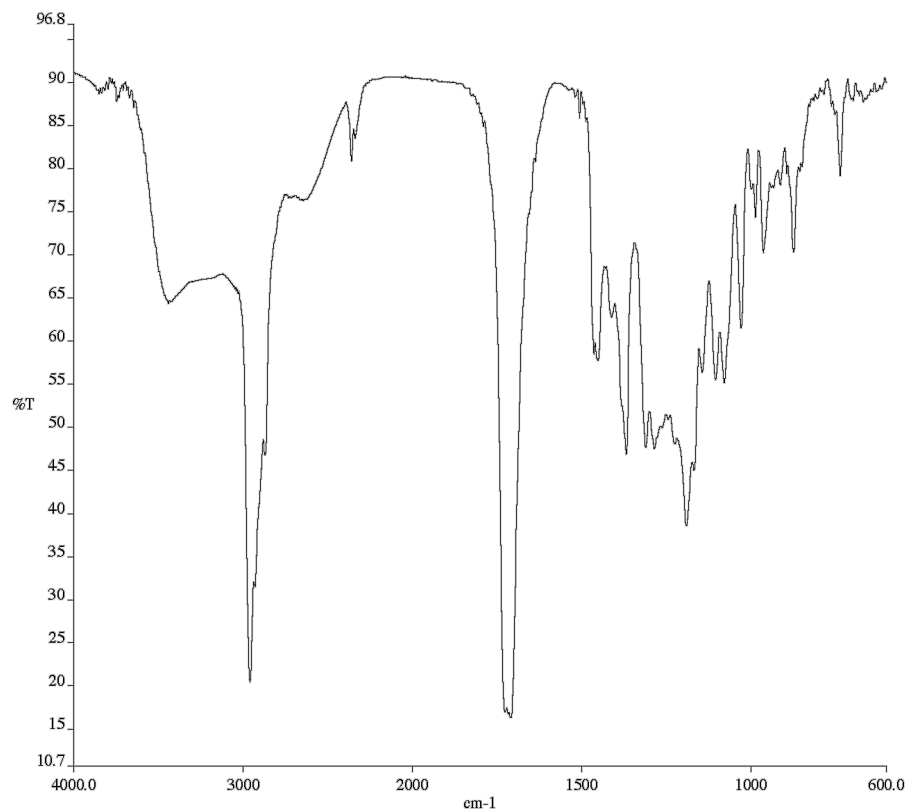
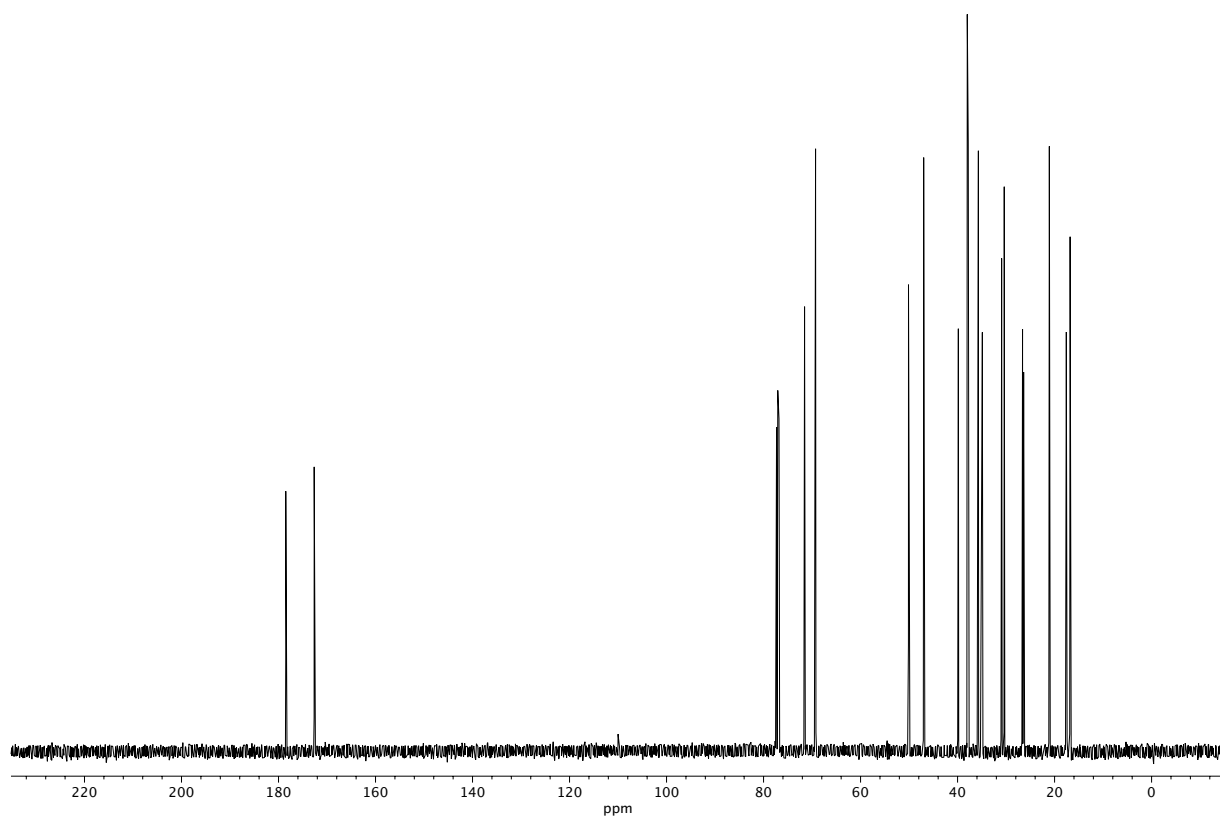


Figure A8.25 <sup>1</sup>H NMR (500 MHz, CDCl<sub>3</sub>) of compound 155.



**Figure A8.26** Infrared spectrum (Thin Film, NaCl) of compound **155**.



**Figure A8.27** <sup>13</sup>C NMR (125 MHz, CDCl<sub>3</sub>) of compound **155**.

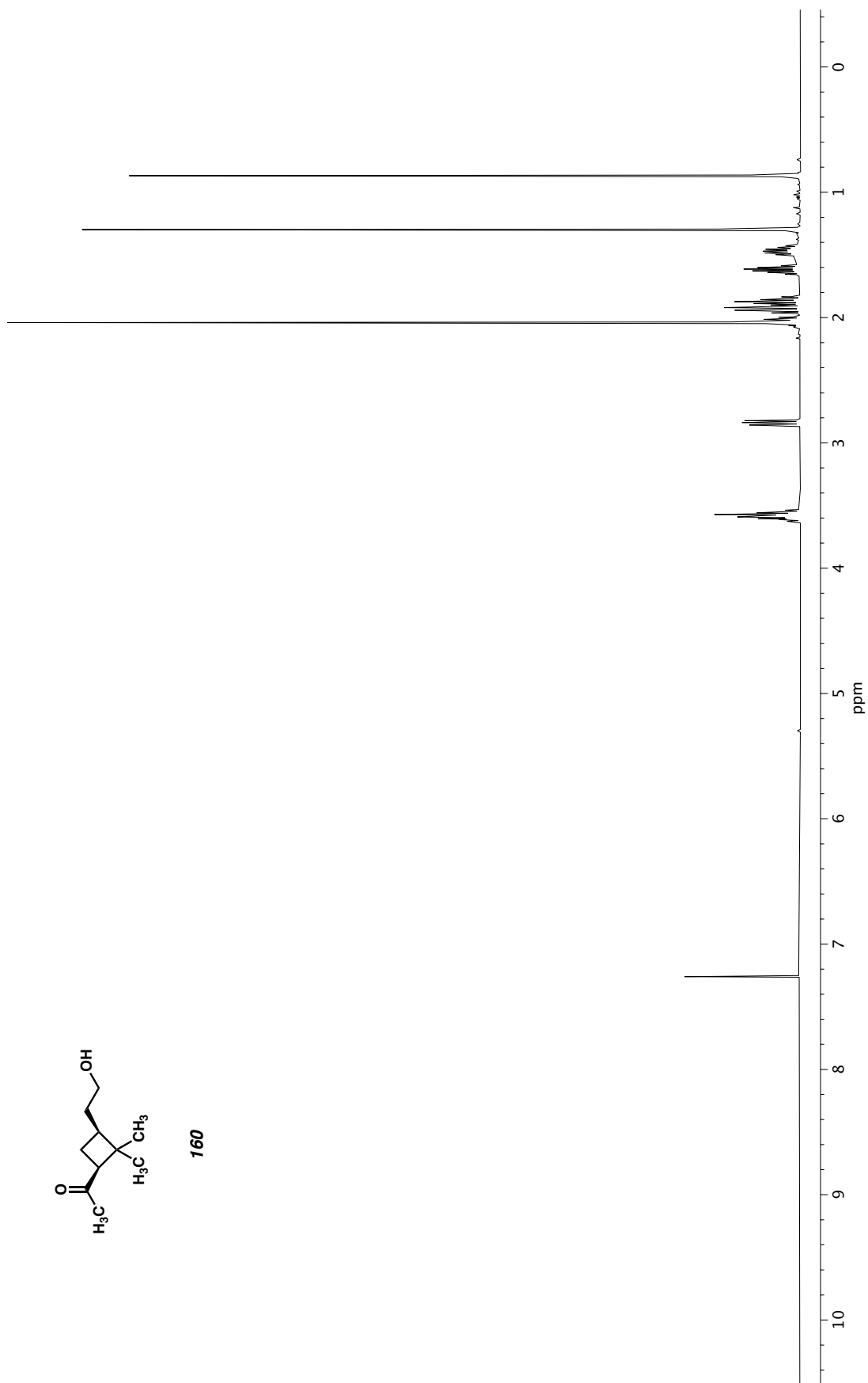


**Figure A8.28** <sup>1</sup>H NMR (500 MHz, CDCl<sub>3</sub>) of compound **160**.

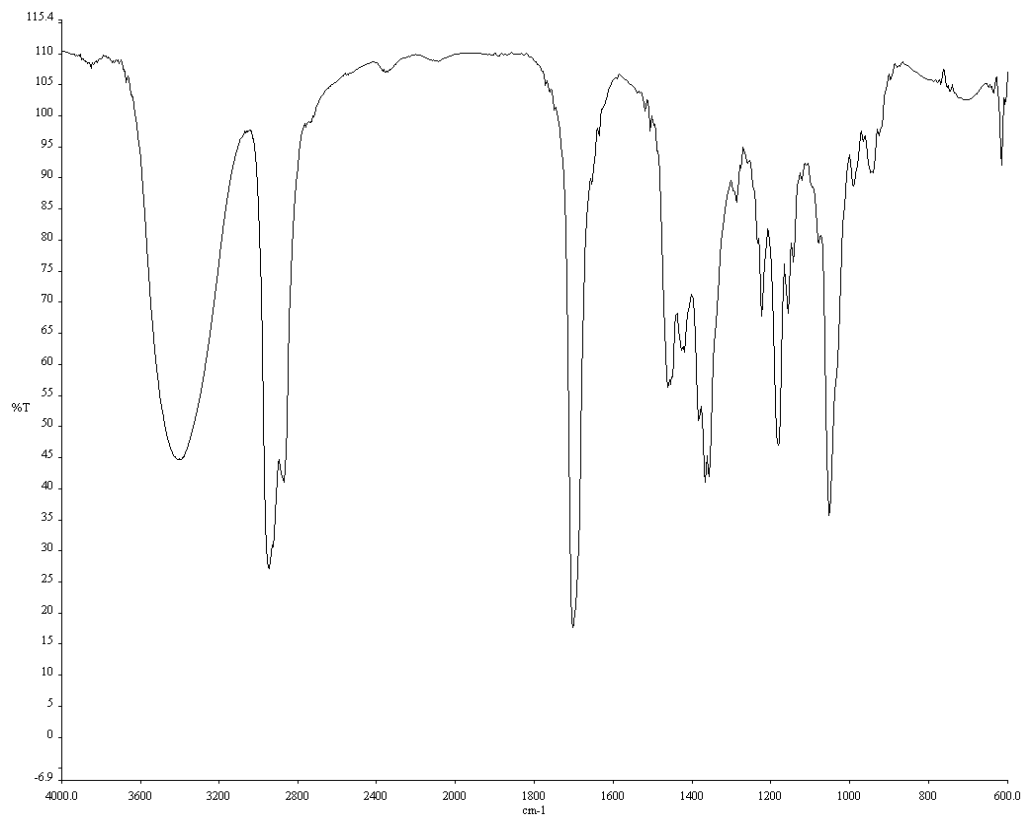


**Figure A8.29** Infrared spectrum (Thin Film, NaCl) of compound **160**.

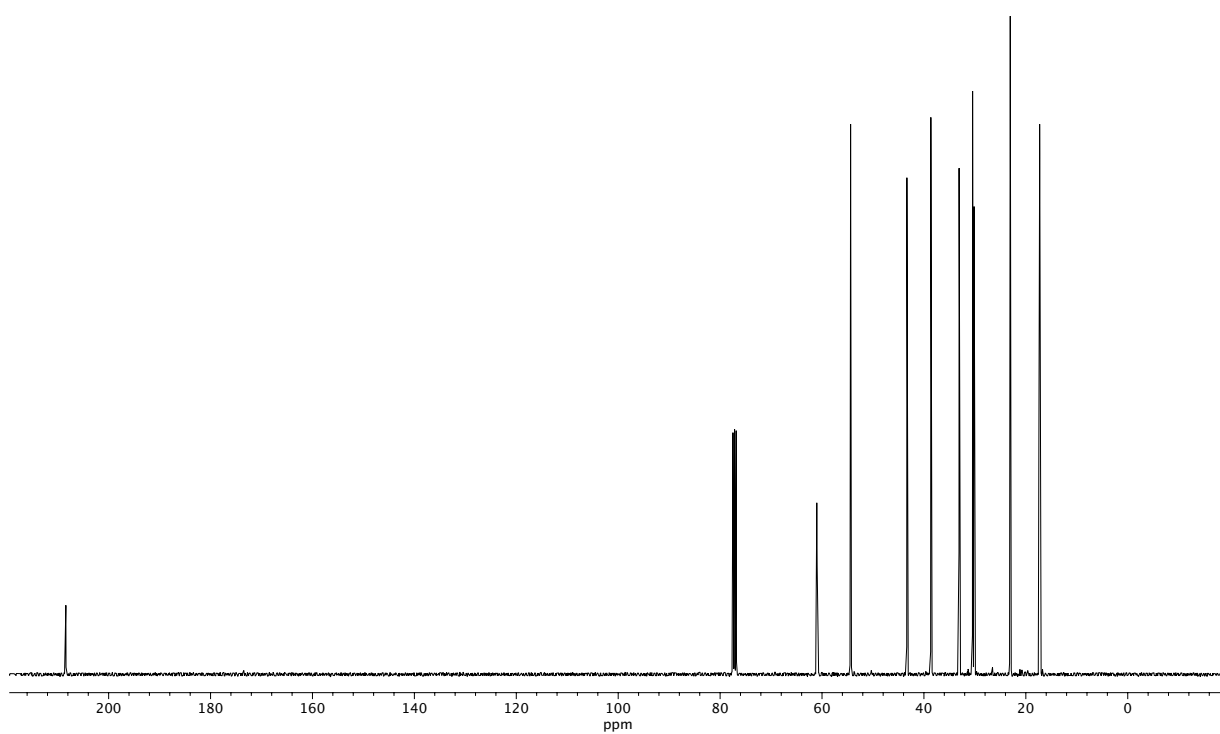


**Figure A8.30** <sup>13</sup>C NMR (125 MHz, CDCl<sub>3</sub>) of compound **160**.

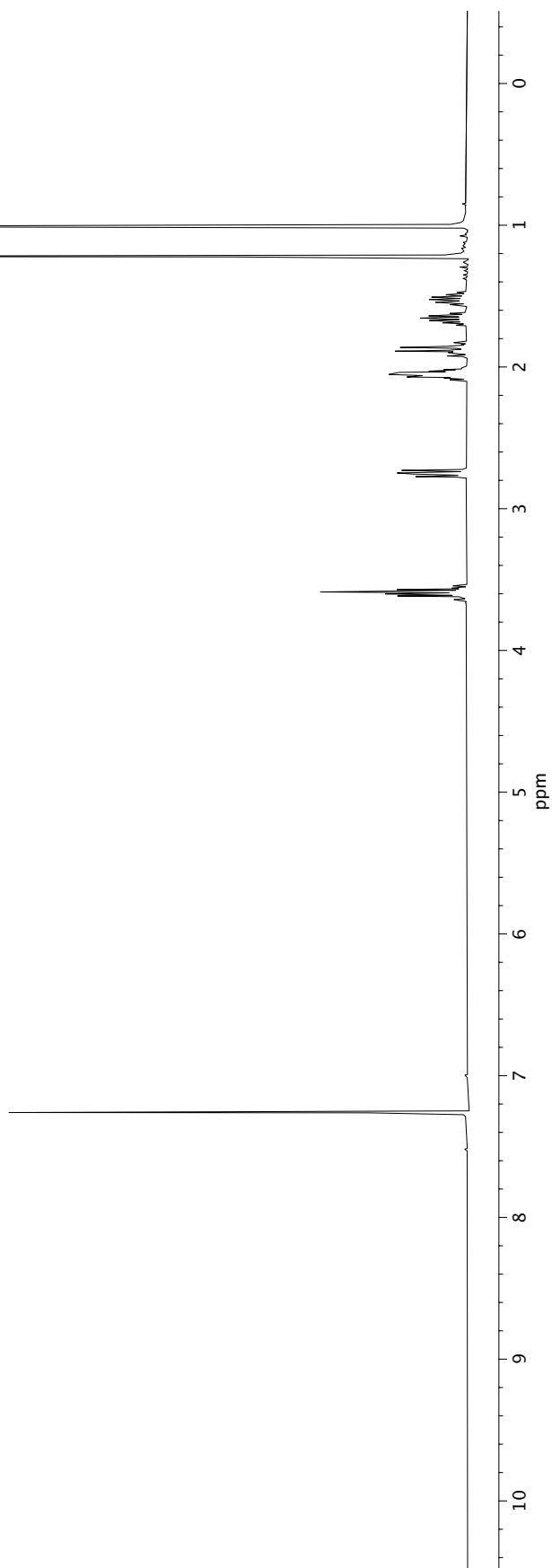
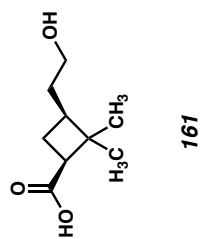
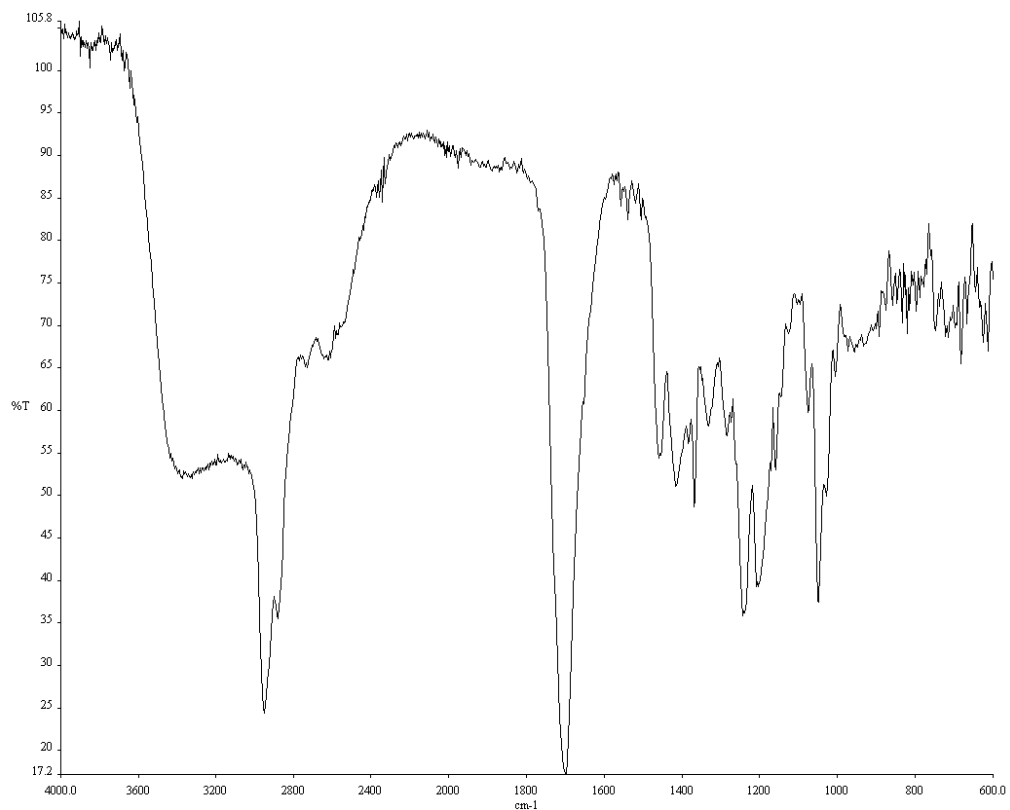
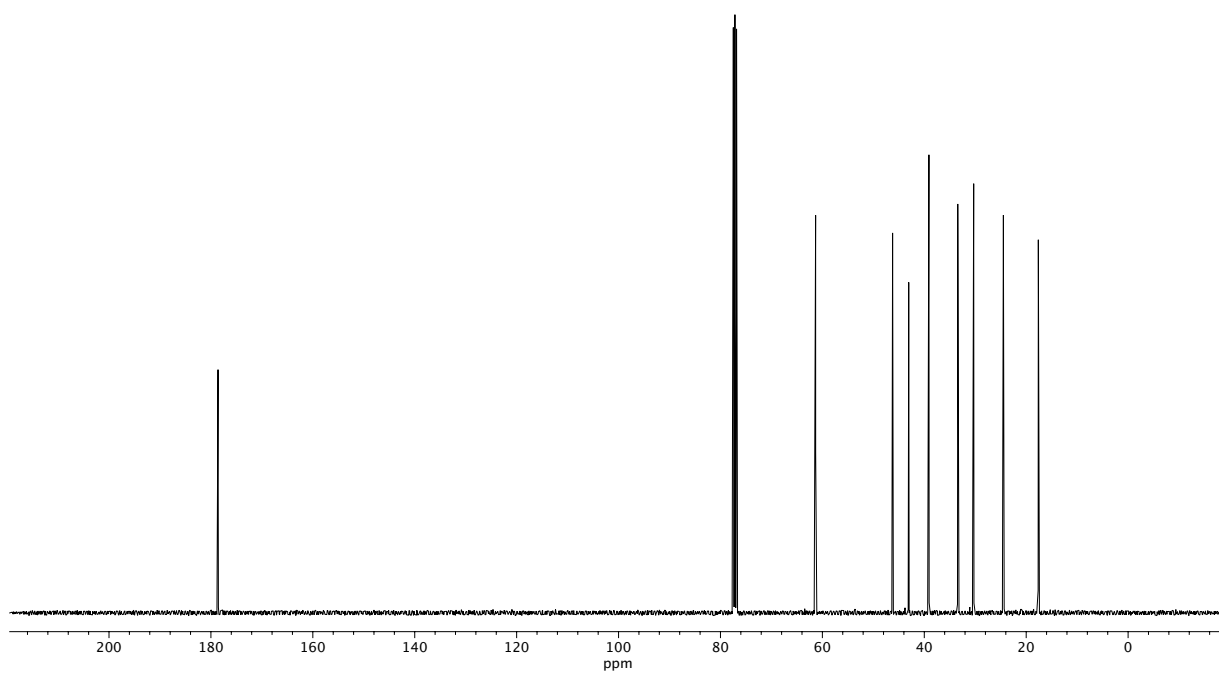


Figure A8.31 <sup>1</sup>H NMR (400 MHz, CDCl<sub>3</sub>) of compound **161**.

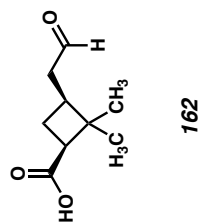
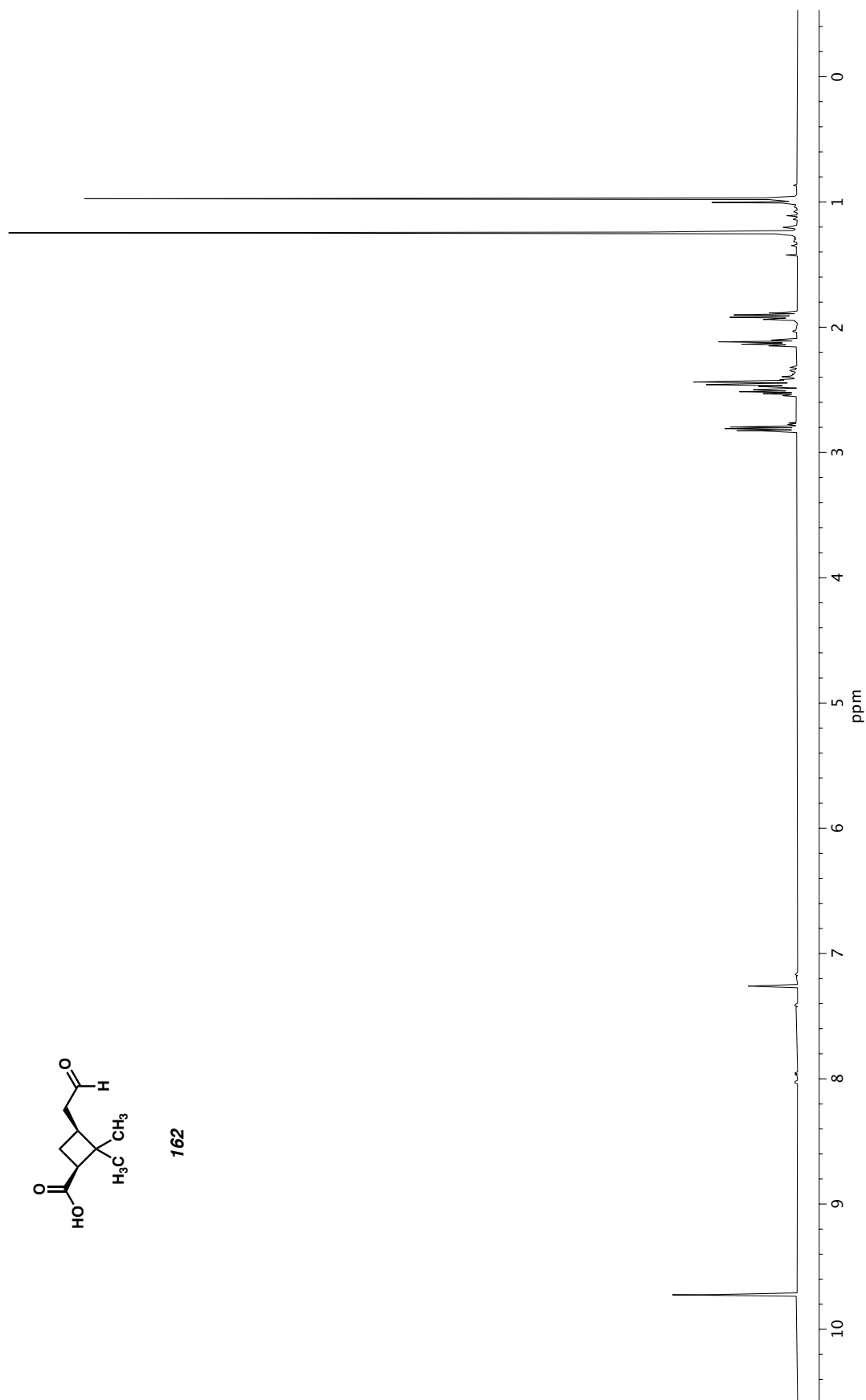


**Figure A8.32** Infrared spectrum (Thin Film, NaCl) of compound **161**.



**Figure A8.33** <sup>13</sup>C NMR (100 MHz, CDCl<sub>3</sub>) of compound **161**.



**162****Figure A8.34**  $^1\text{H}$  NMR (400 MHz,  $\text{CDCl}_3$ ) of compound **162**.

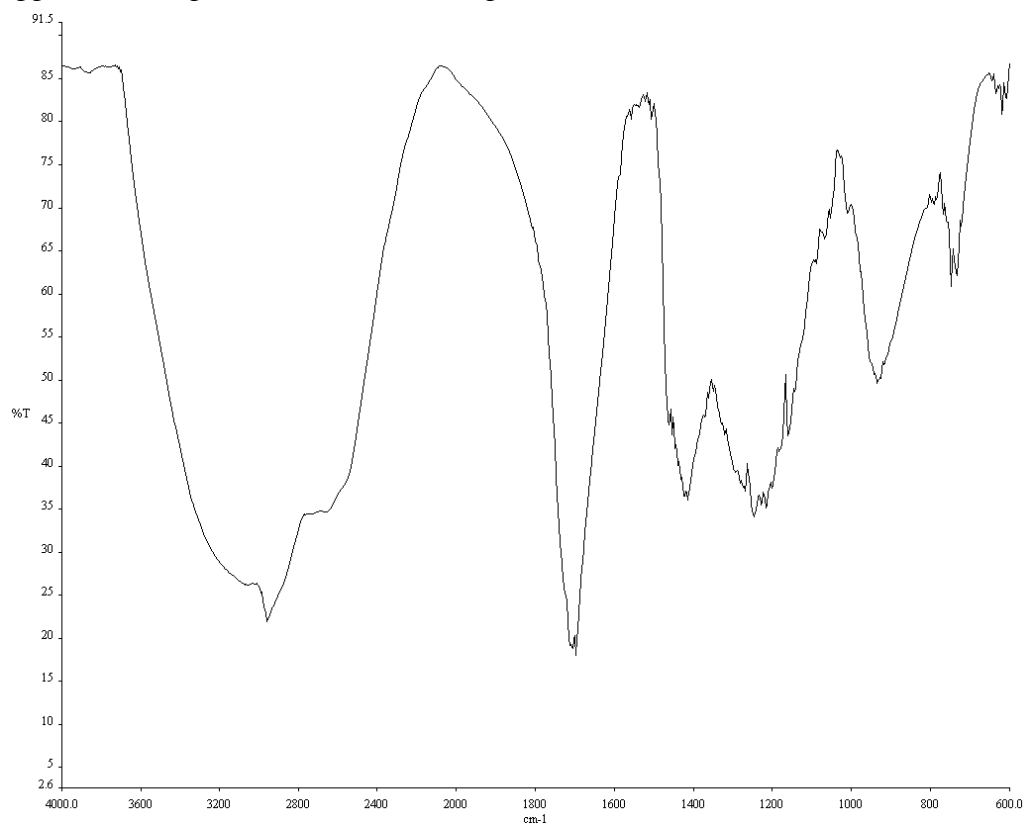


**Figure A8.35** Infrared spectrum (Thin Film, NaCl) of compound **162**.

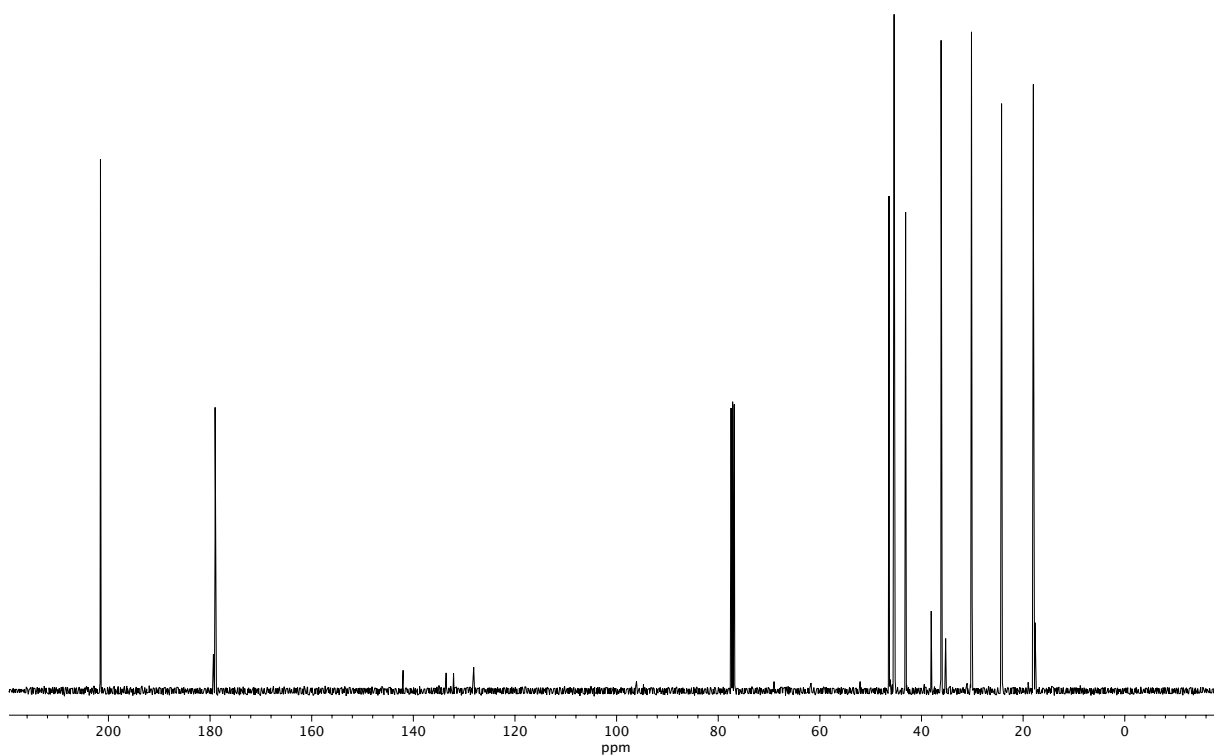


**Figure A8.36** <sup>13</sup>C NMR (100 MHz, CDCl<sub>3</sub>) of compound **162**.

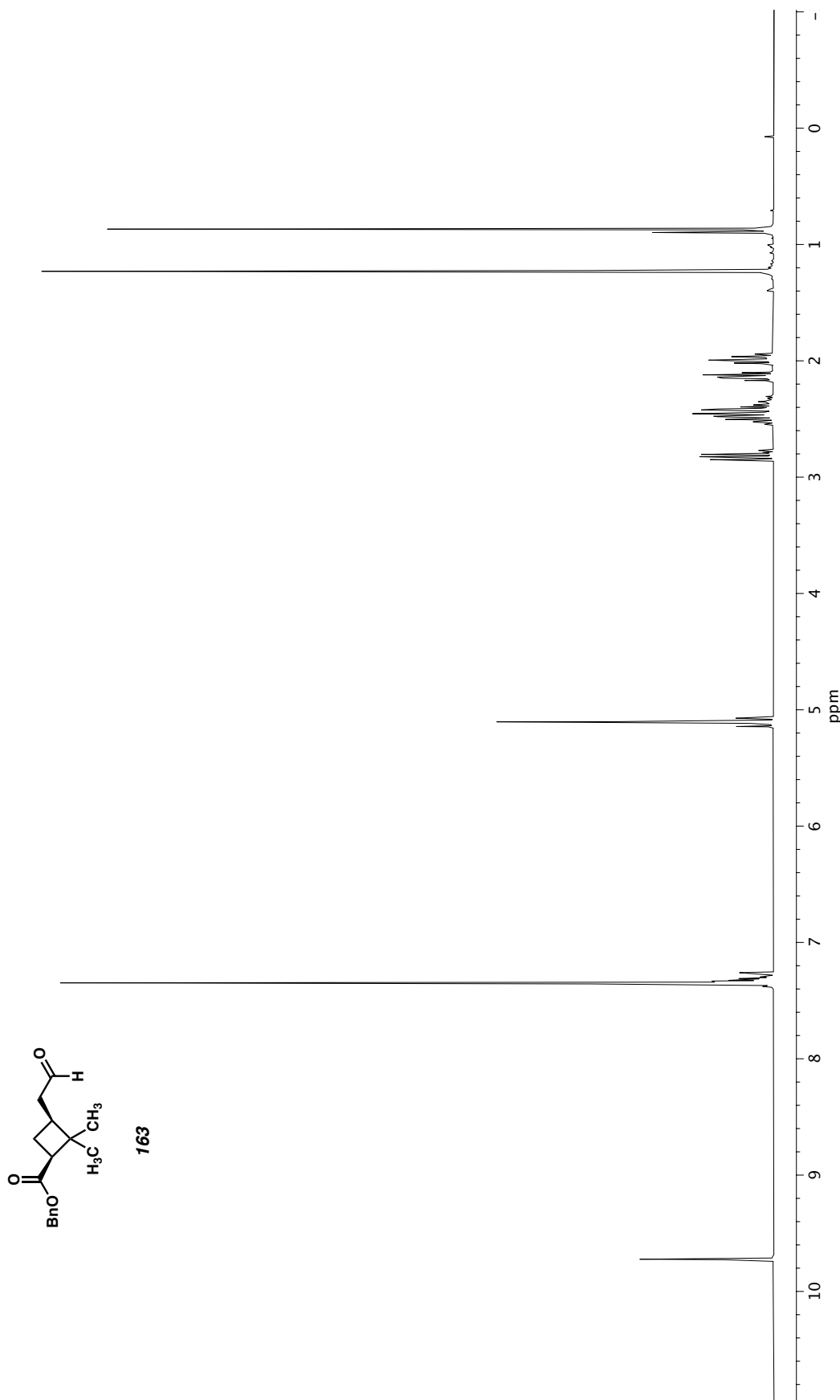
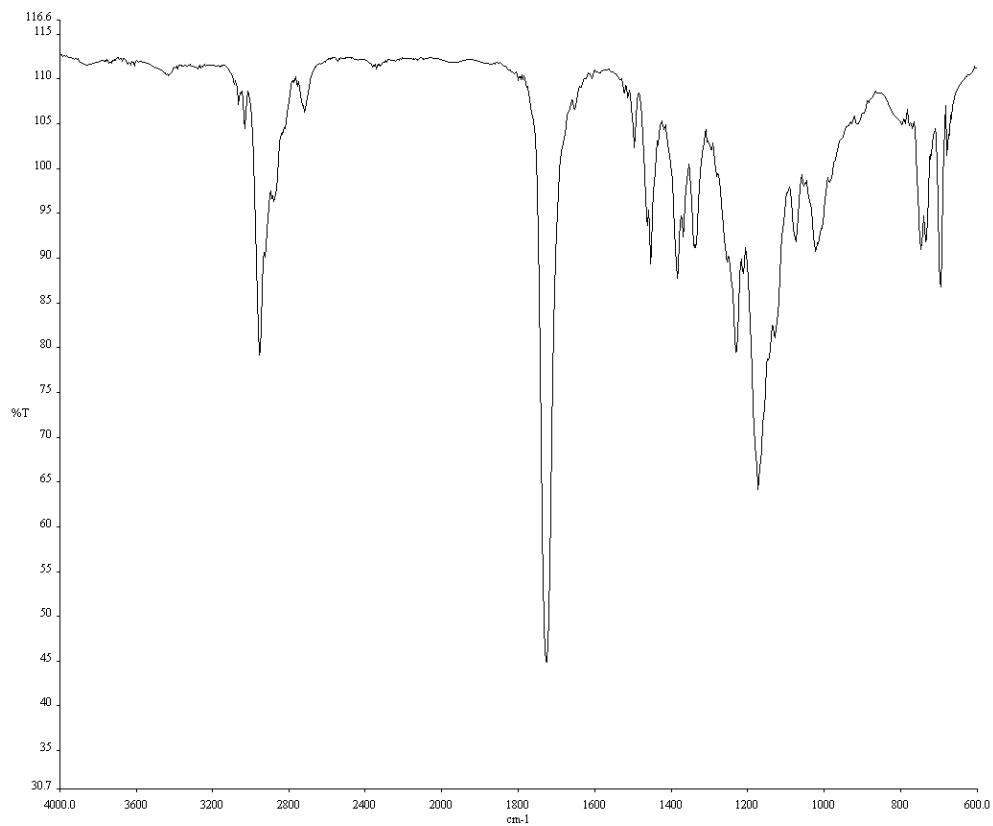
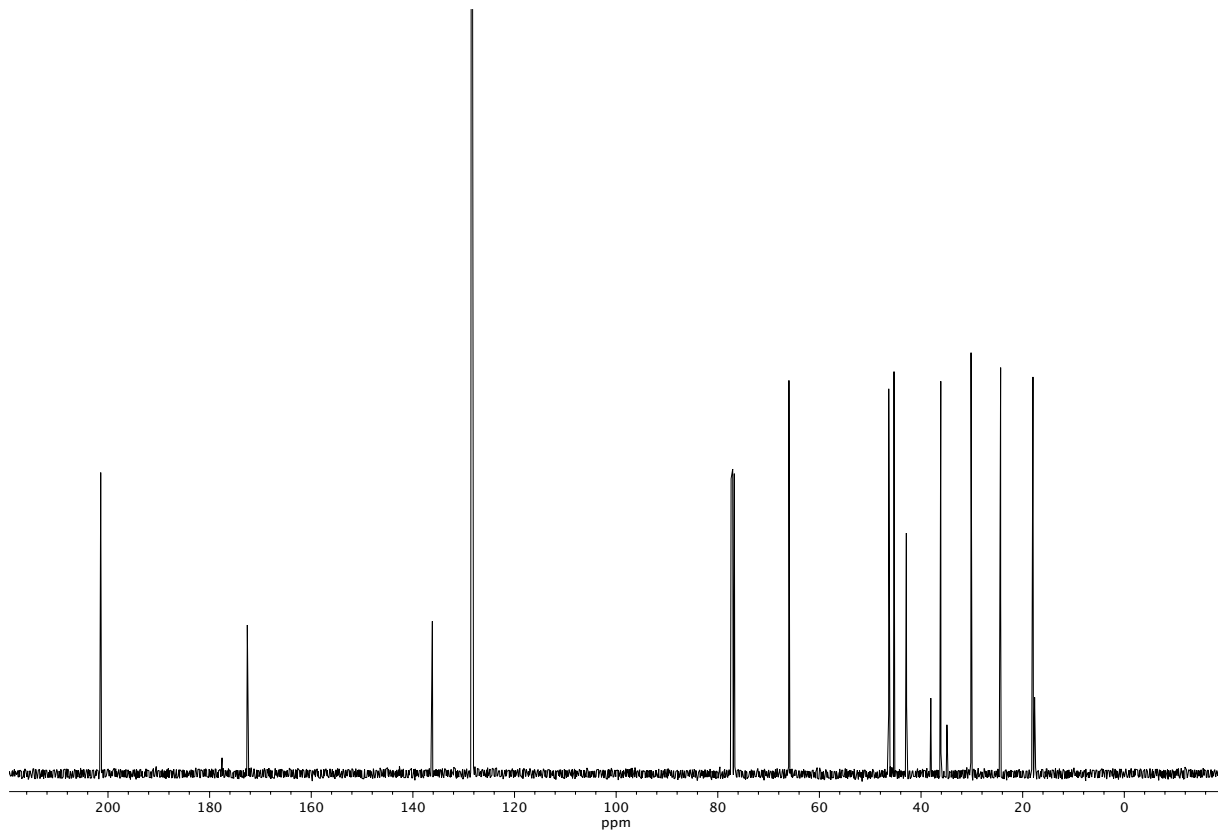


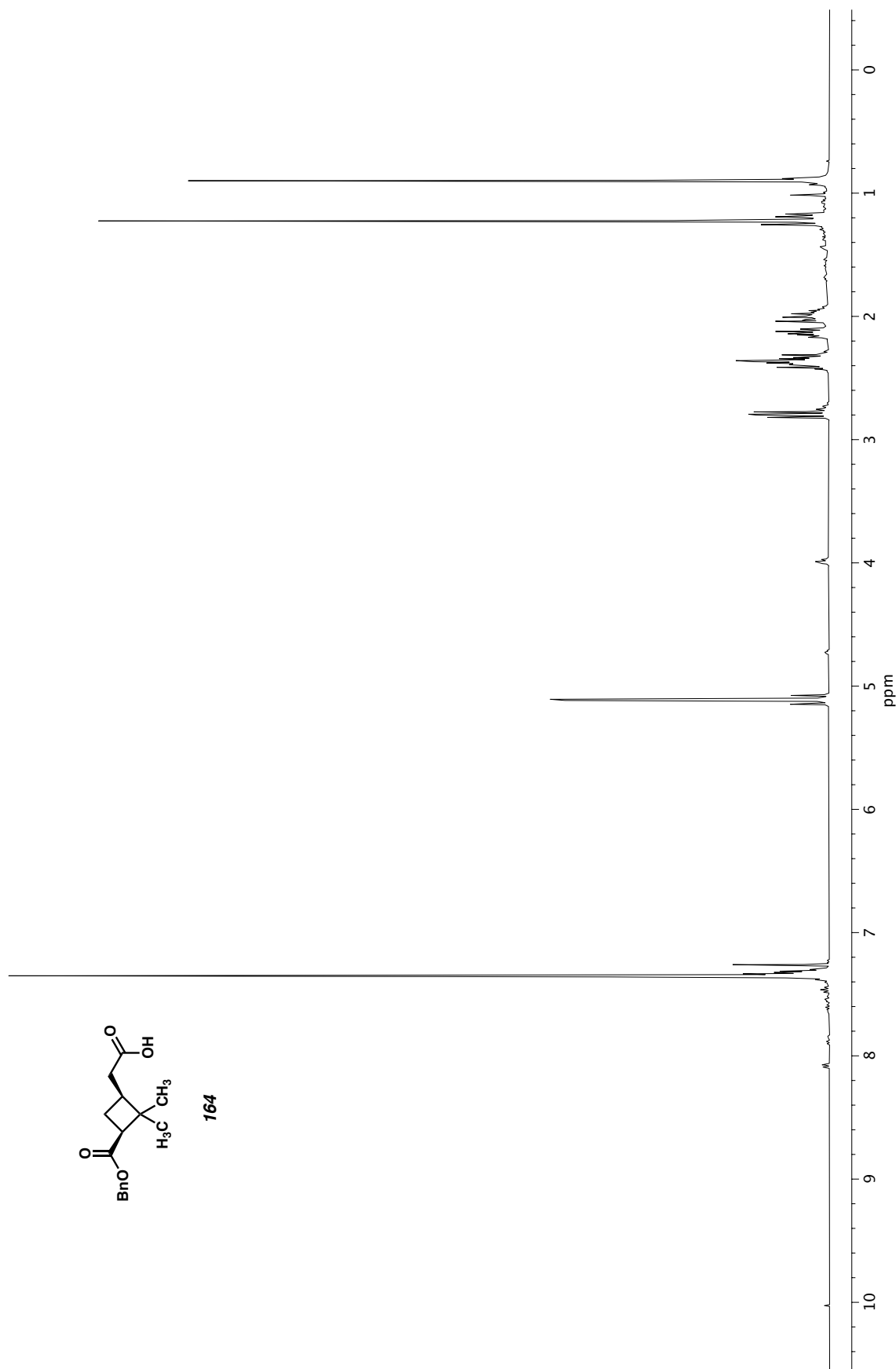
Figure A8.37  $^1\text{H}$  NMR (400 MHz,  $\text{CDCl}_3$ ) of compound **163**.

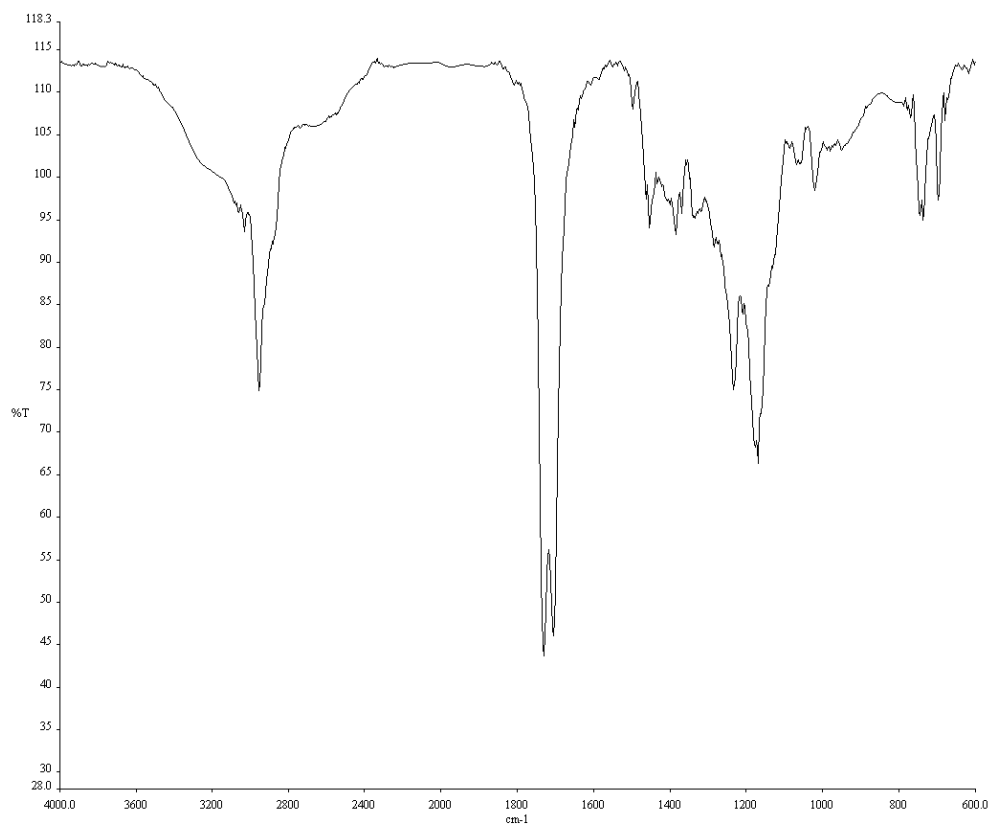


**Figure A8.38** Infrared spectrum (Thin Film, NaCl) of compound **163**.

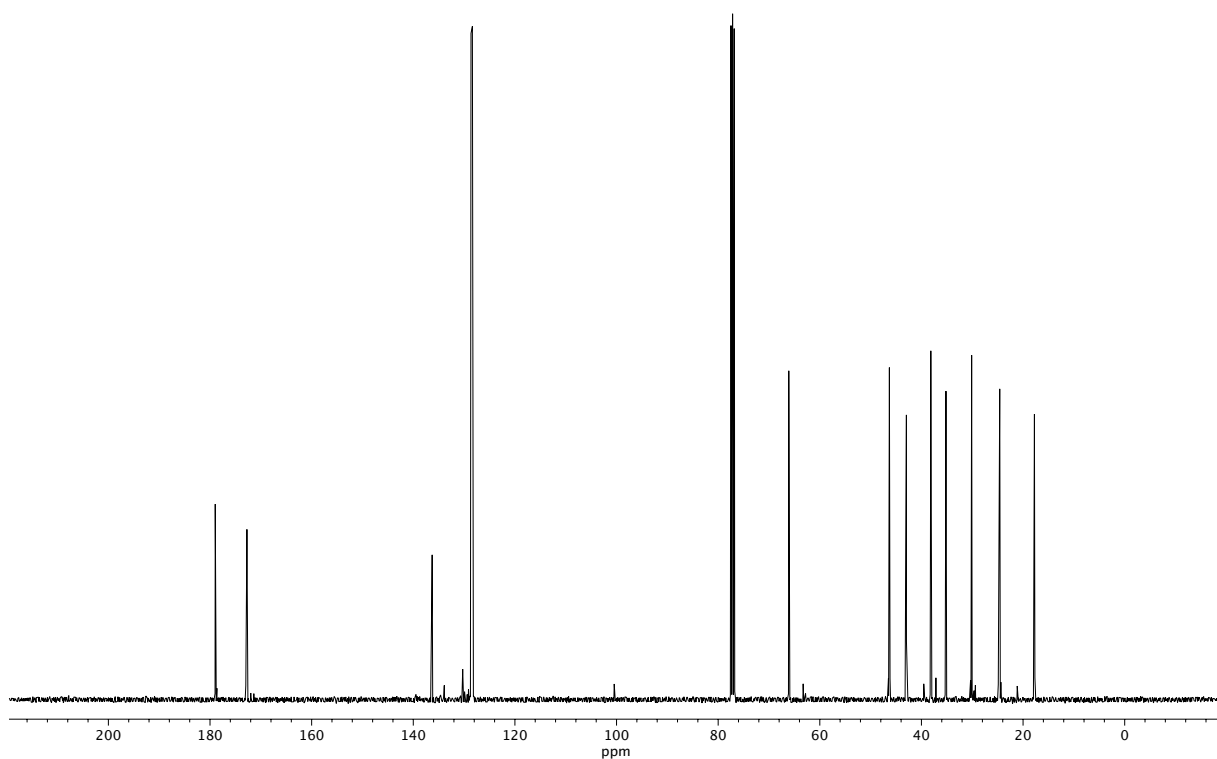


**Figure A8.39** <sup>13</sup>C NMR (100 MHz, CDCl<sub>3</sub>) of compound **163**.

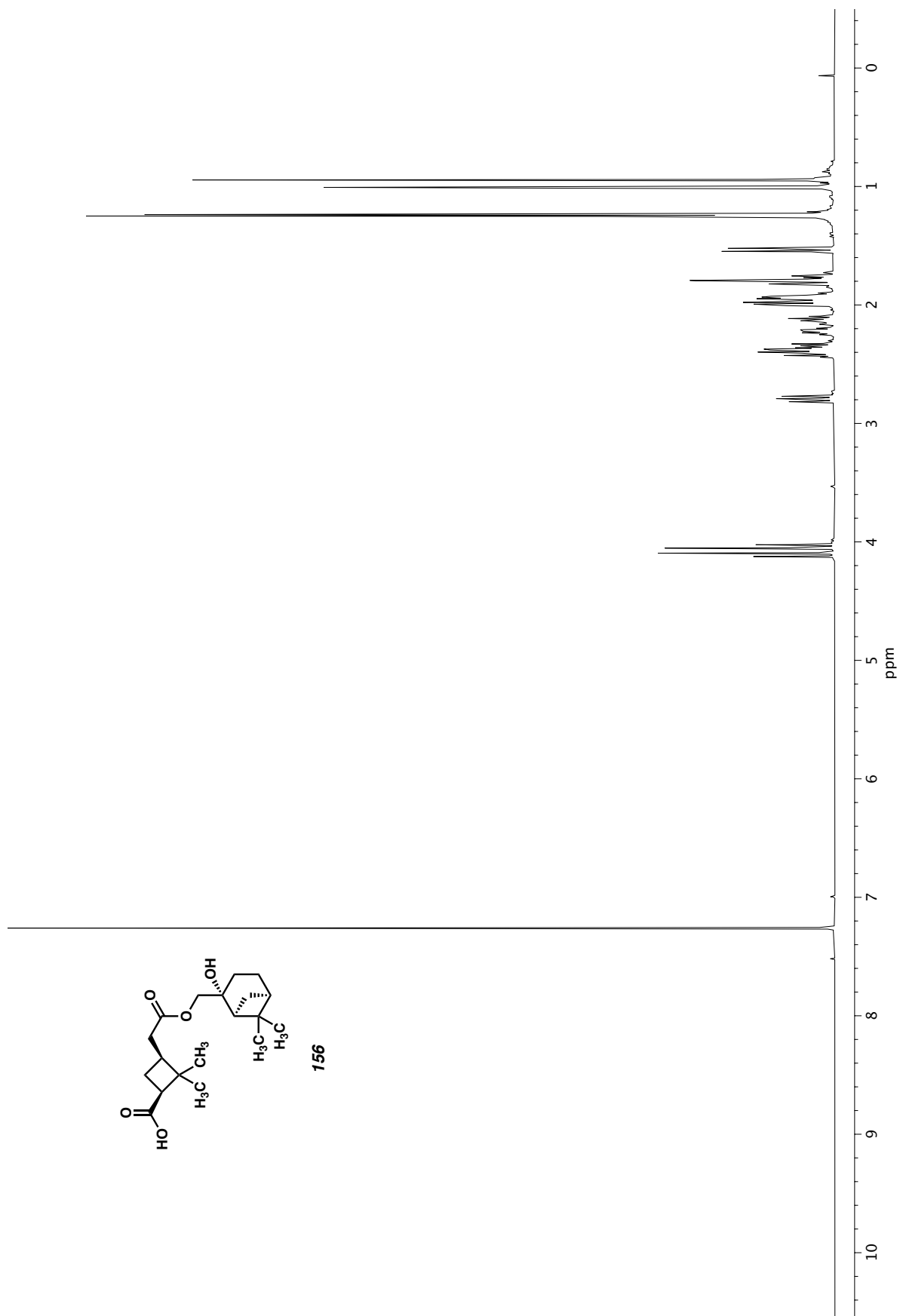


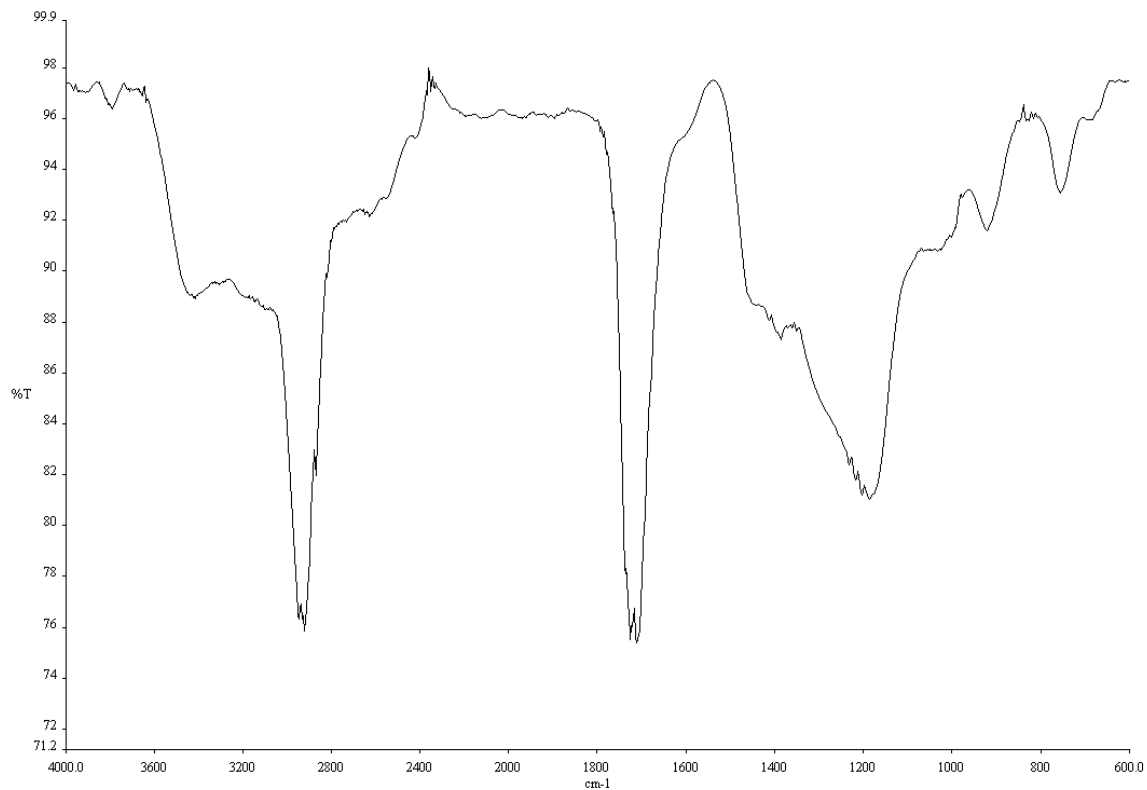


**Figure A8.41** Infrared spectrum (Thin Film, NaCl) of compound **164**.

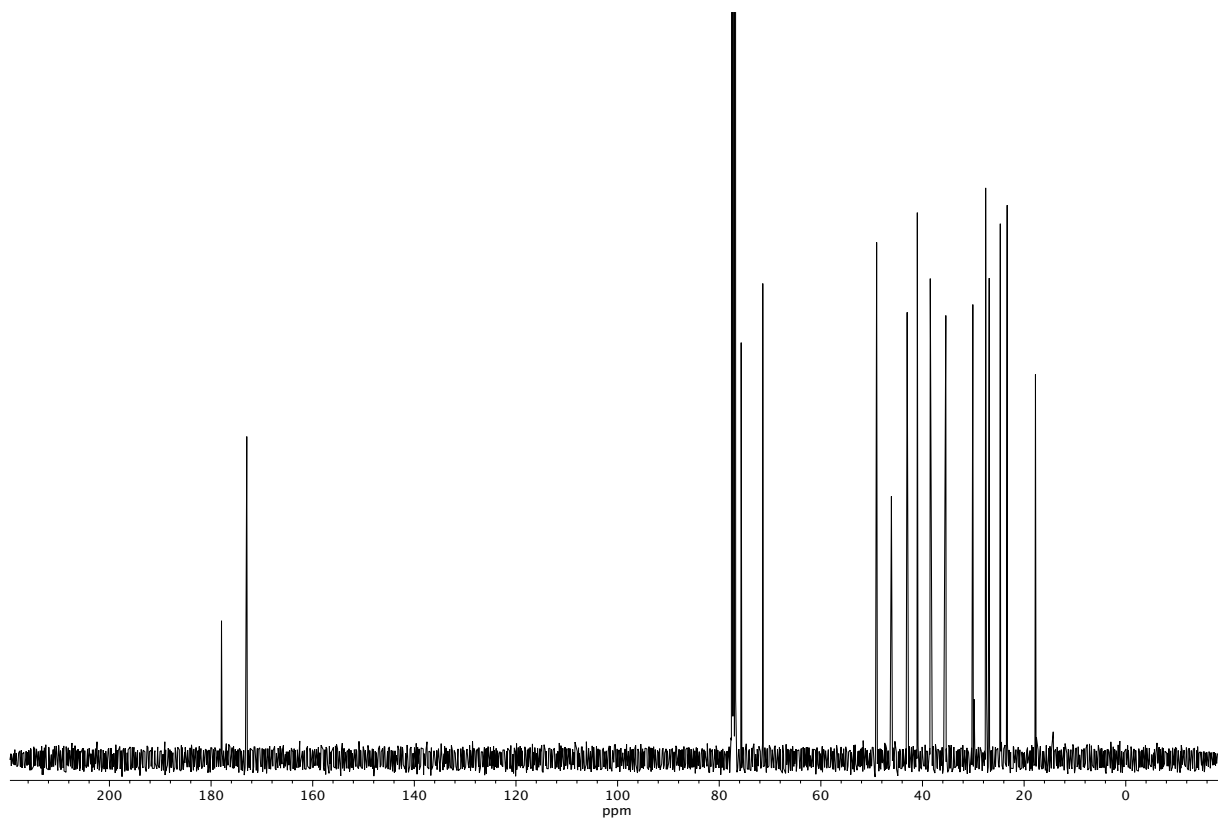


**Figure A8.42** <sup>13</sup>C NMR (100 MHz, CDCl<sub>3</sub>) of compound **164**.

Figure A8.43  $^1\text{H}$  NMR (400 MHz,  $\text{CDCl}_3$ ) of compound **156**.

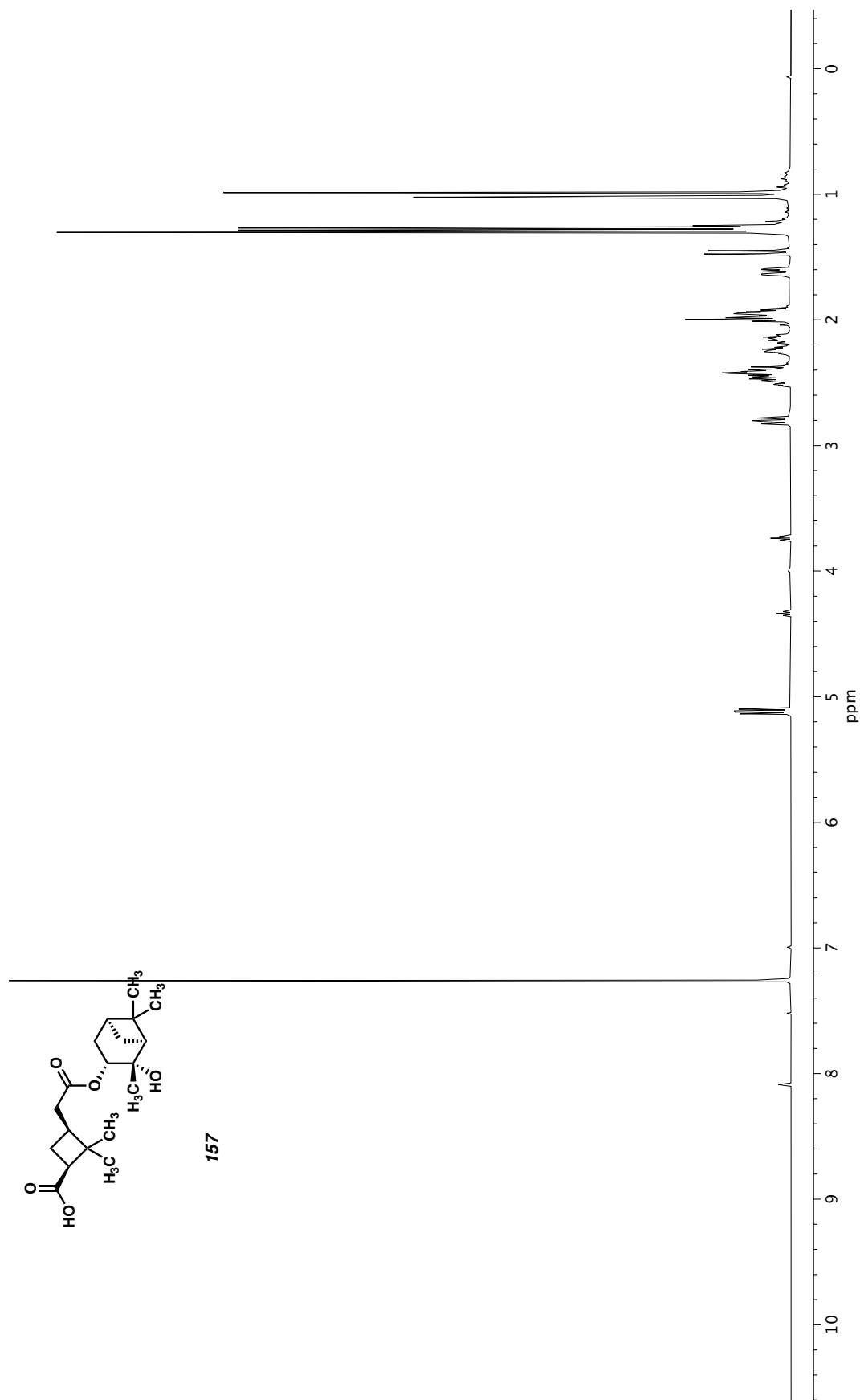


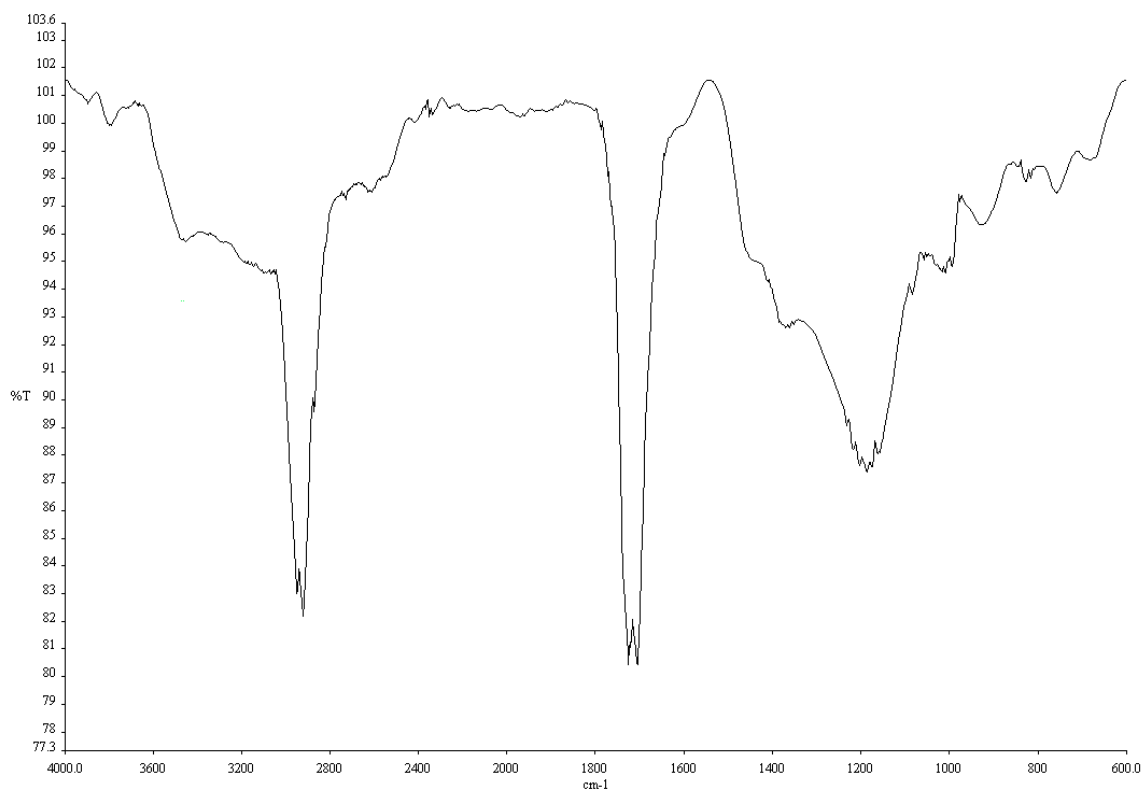
**Figure A8.44** Infrared spectrum (Thin Film, NaCl) of compound **156**.



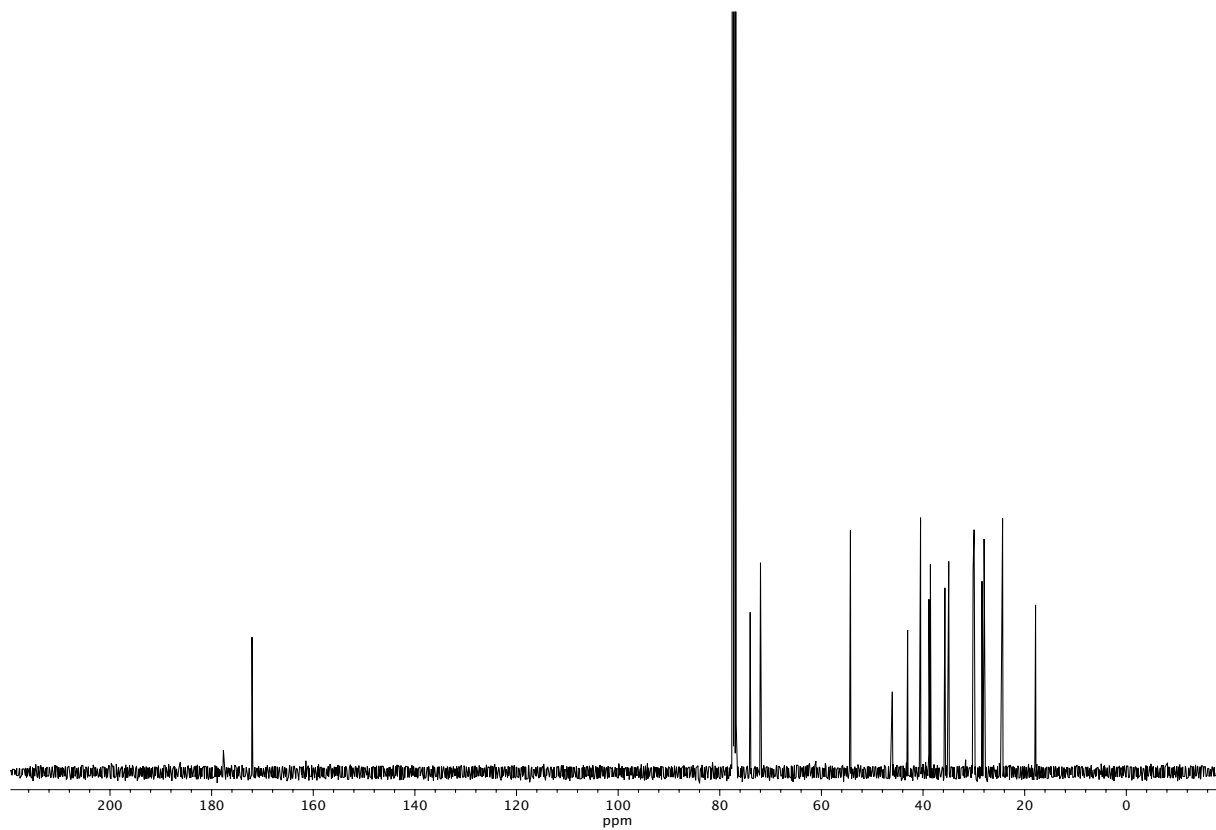
**Figure A8.45** <sup>13</sup>C NMR (100 MHz, CDCl<sub>3</sub>) of compound **156**.



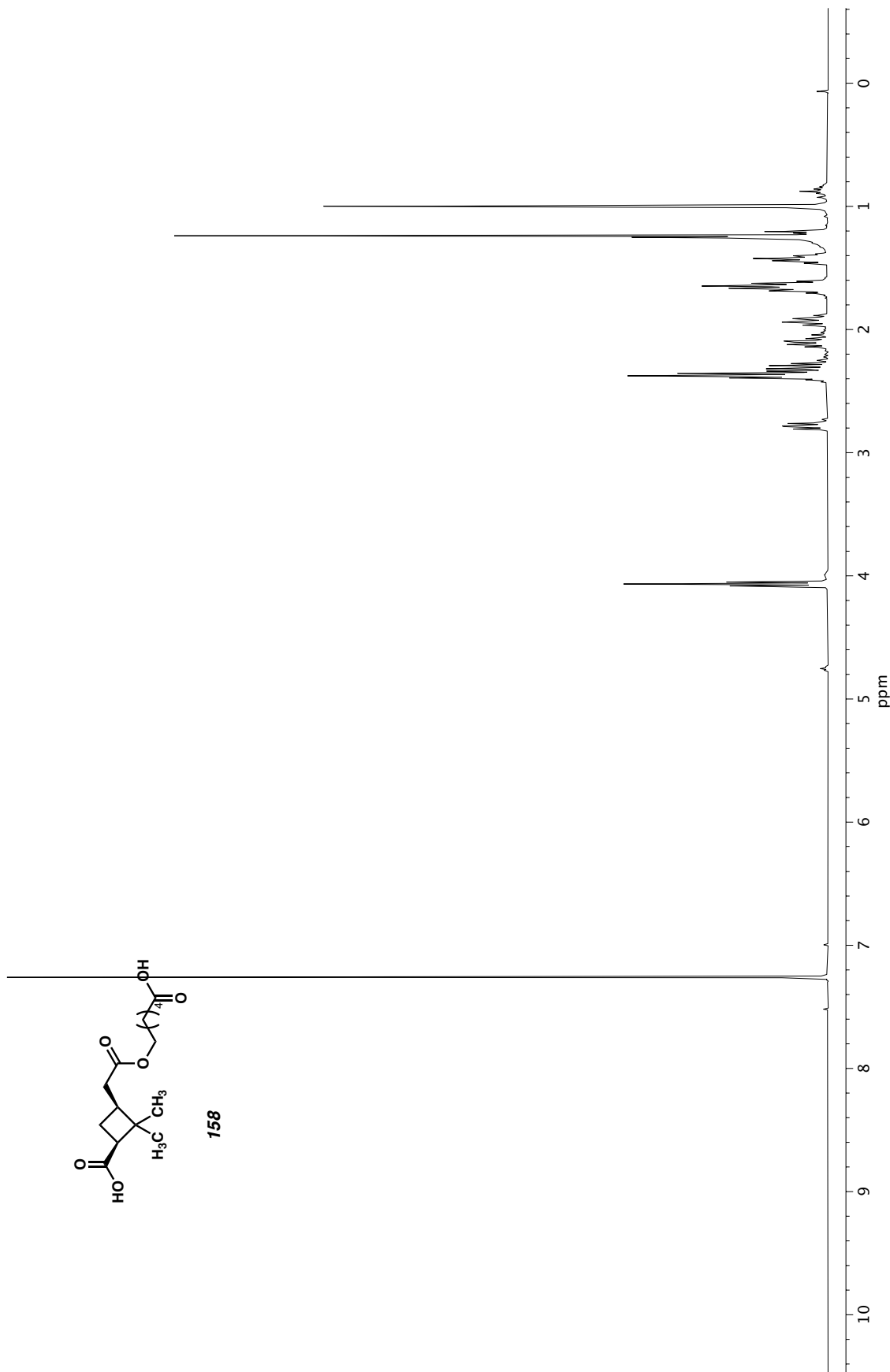




**Figure A8.47** Infrared spectrum (Thin Film, NaCl) of compound **157**.



**Figure A8.48** <sup>13</sup>C NMR (100 MHz, CDCl<sub>3</sub>) of compound **157**.

Figure A8.49  $^1\text{H}$  NMR (400 MHz,  $\text{CDCl}_3$ ) of compound 158.

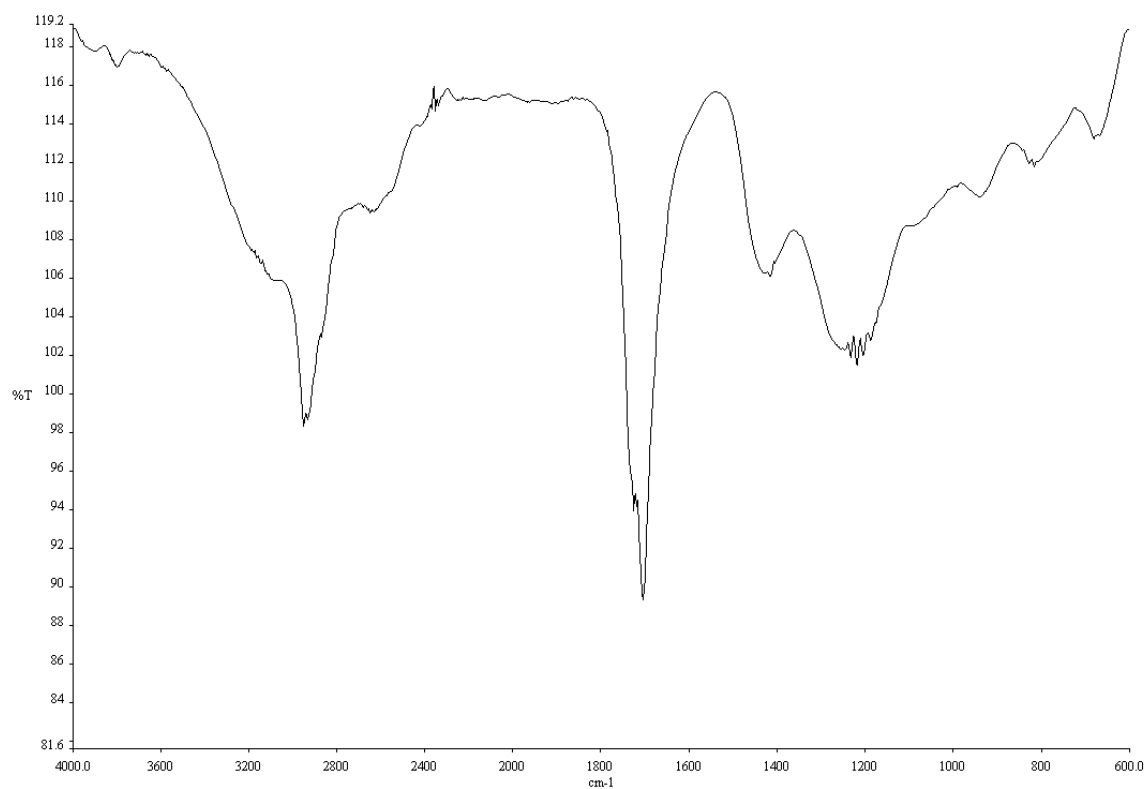


**Figure A8.50** Infrared spectrum (Thin Film, NaCl) of compound **158**.

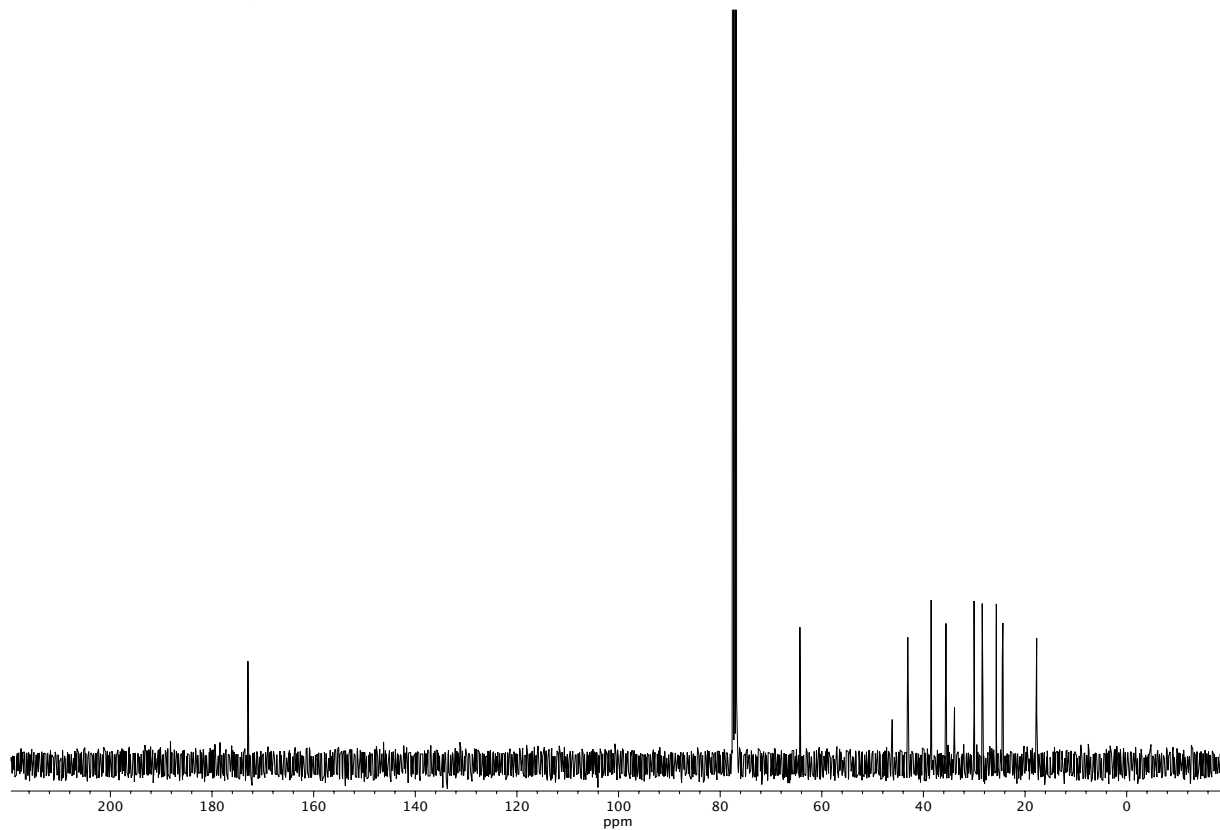


**Figure A8.51** <sup>13</sup>C NMR (100 MHz, CDCl<sub>3</sub>) of compound **158**.

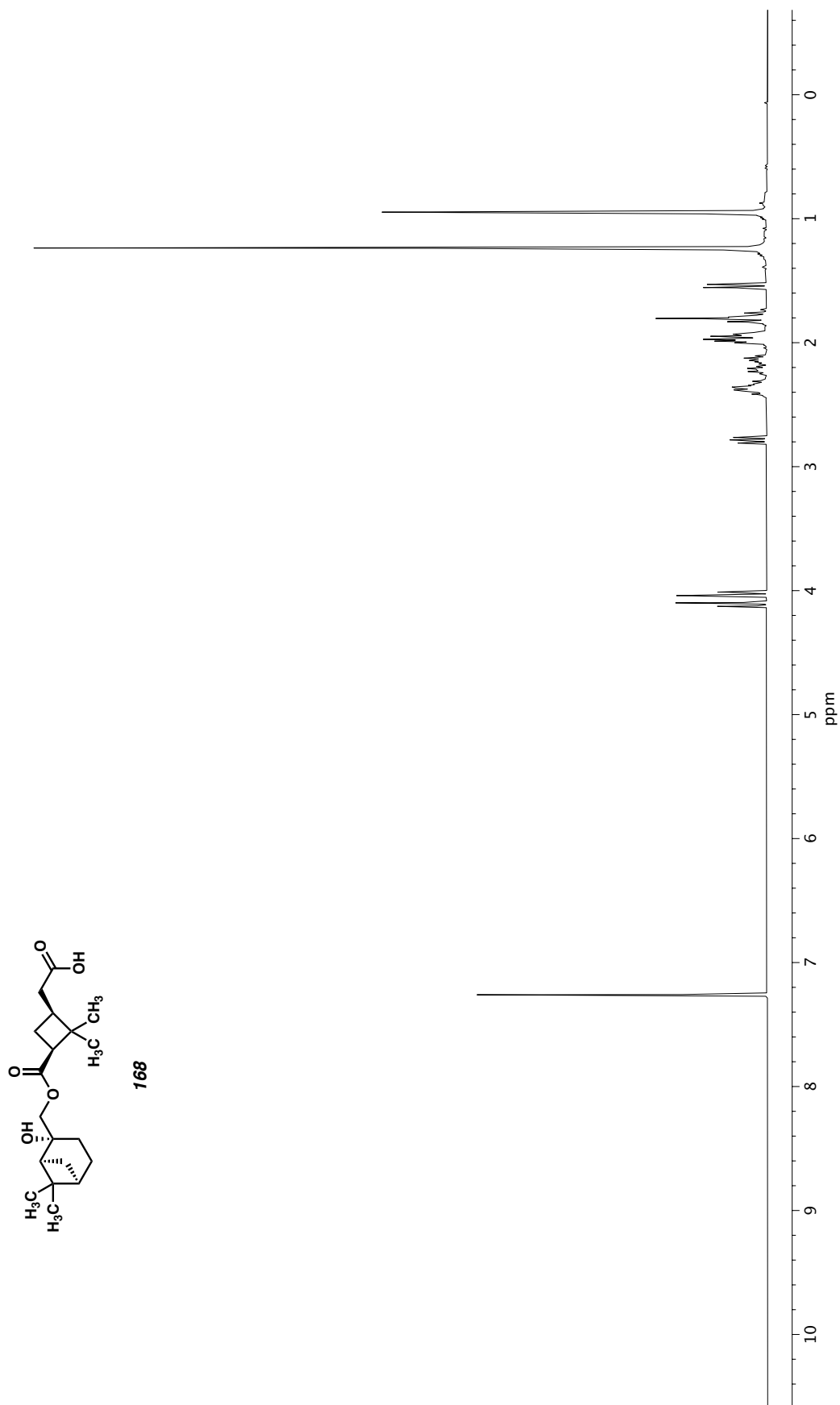
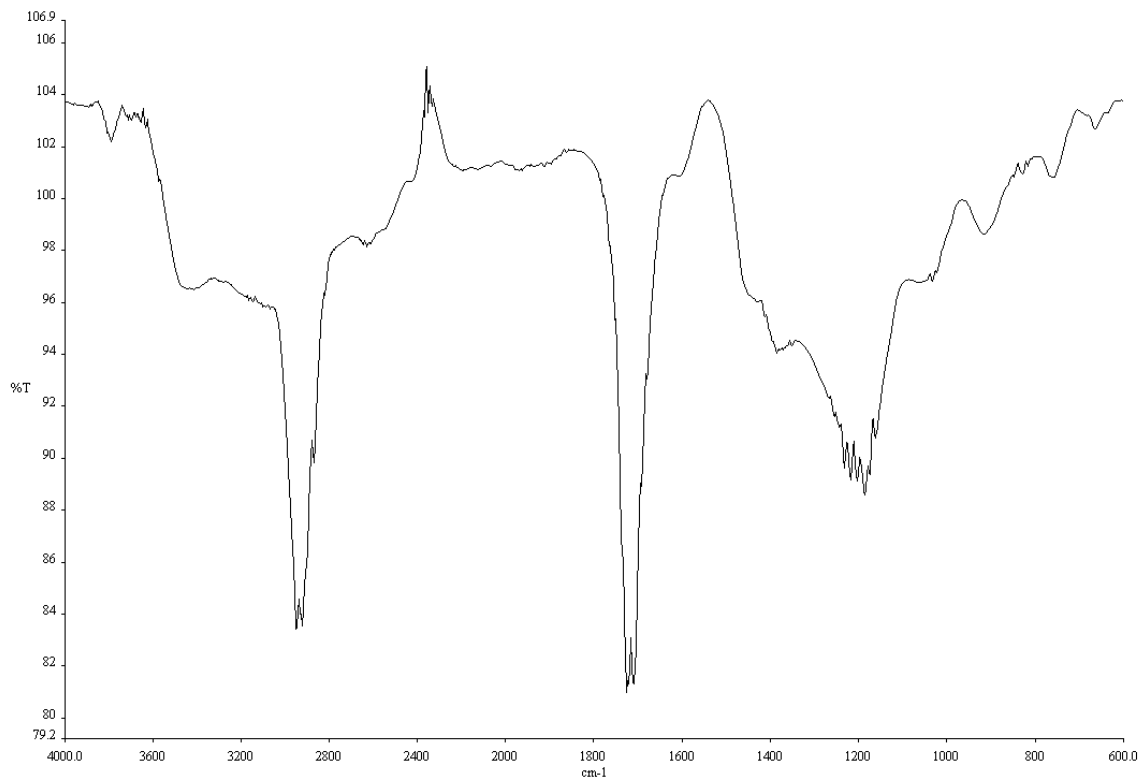
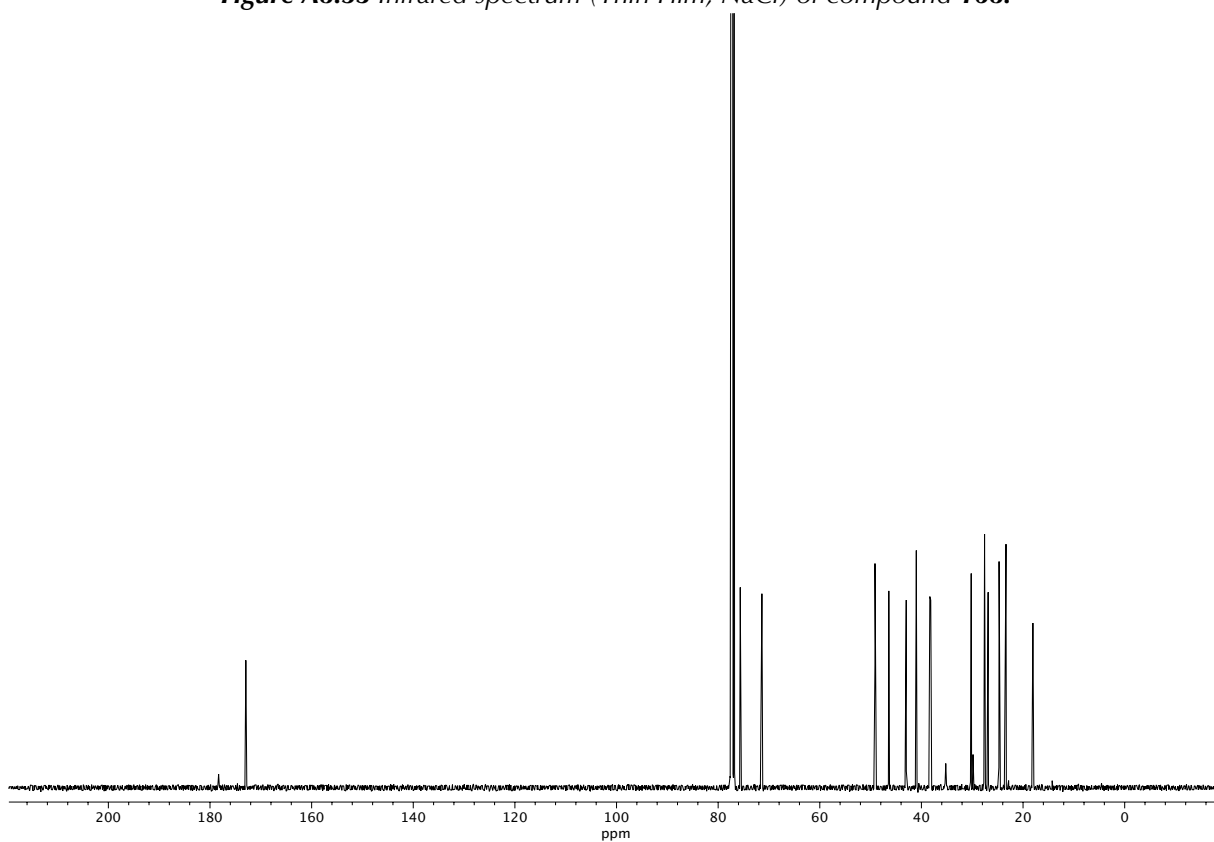


Figure A8.52  $^1\text{H}$  NMR (400 MHz,  $\text{CDCl}_3$ ) of compound **168**.



**Figure A8.53** Infrared spectrum (Thin Film, NaCl) of compound **168**.



**Figure A8.54** <sup>13</sup>C NMR (100 MHz, CDCl<sub>3</sub>) of compound **168**.

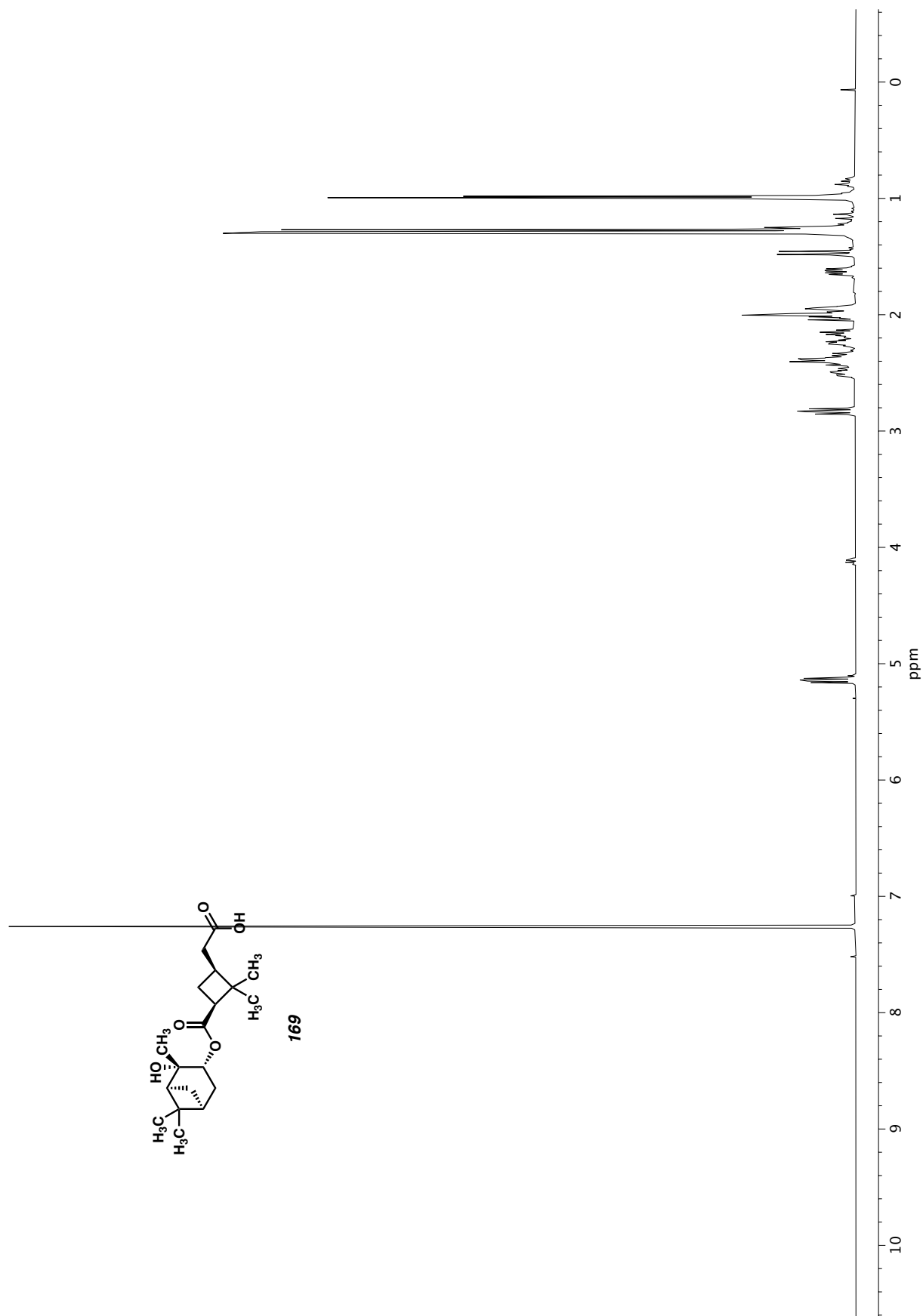


**Figure A8.55**  $^1\text{H}$  NMR (400 MHz,  $\text{CDCl}_3$ ) of compound **169**.

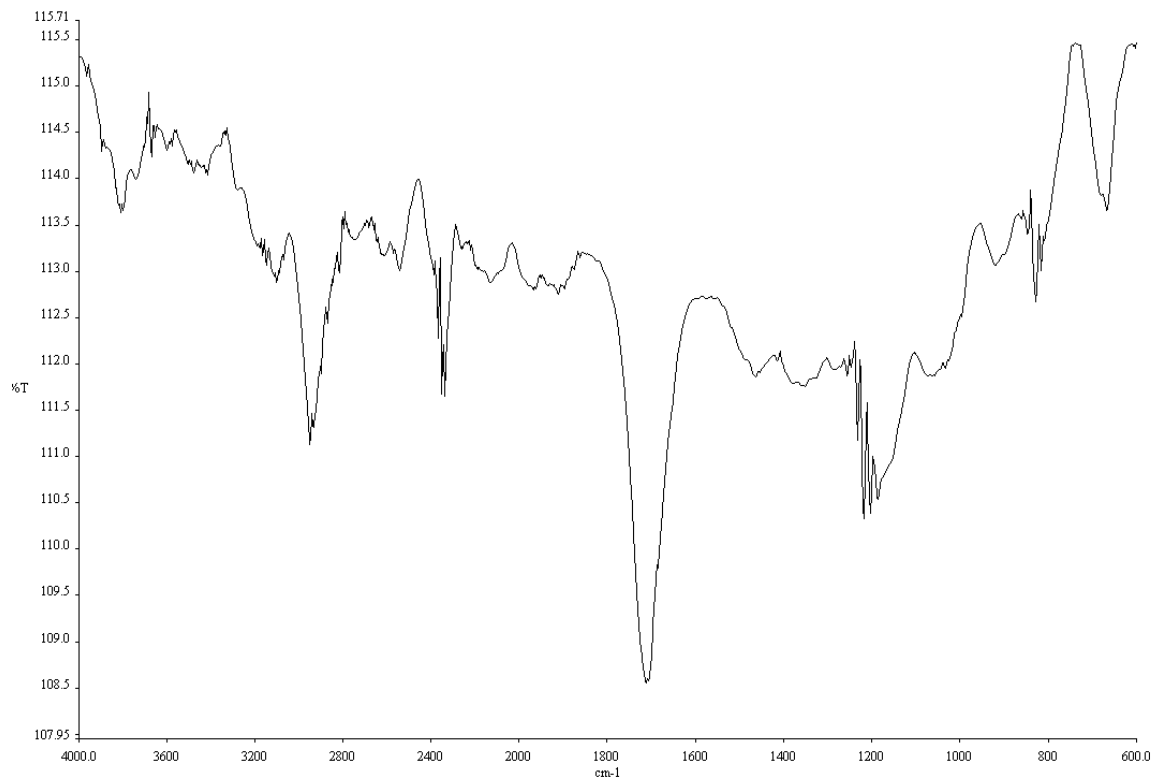


**Figure A8.56** Infrared spectrum (Thin Film, NaCl) of compound **169**.

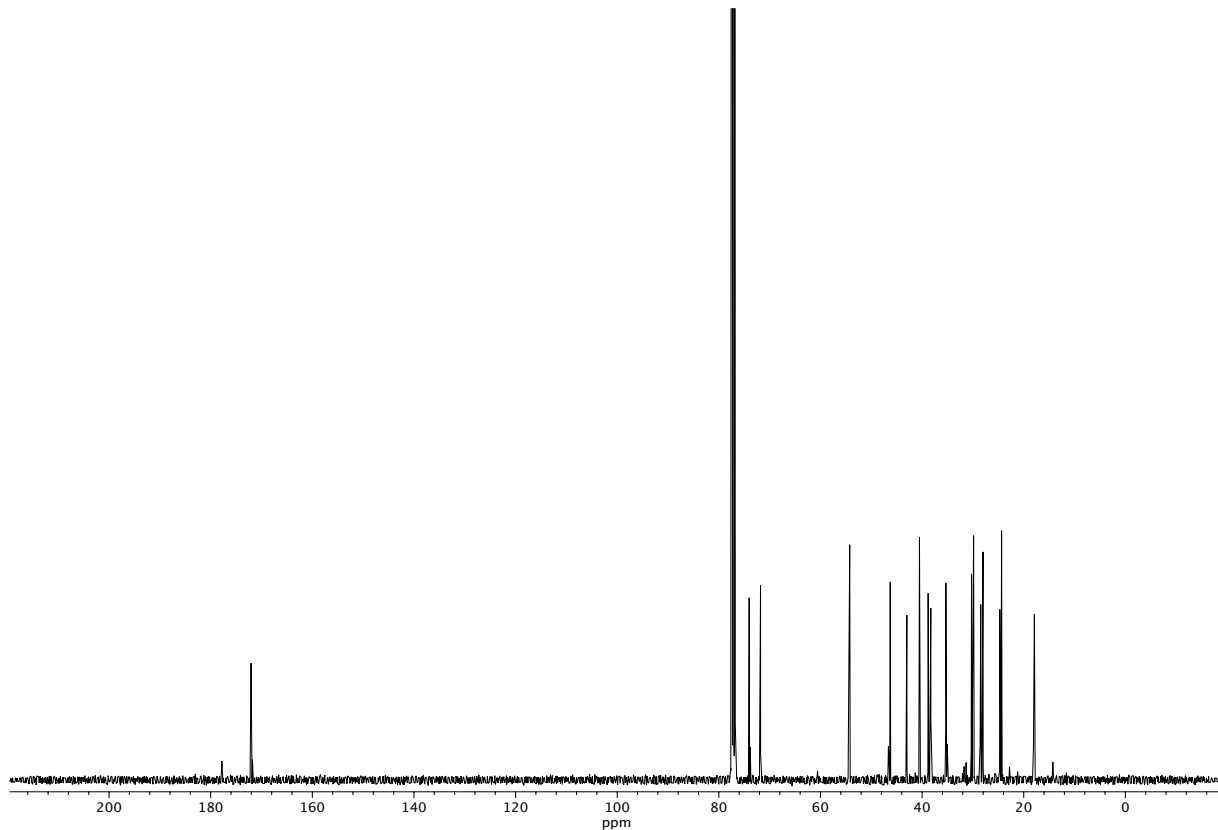


**Figure A8.57** <sup>13</sup>C NMR (100 MHz, CDCl<sub>3</sub>) of compound **169**.



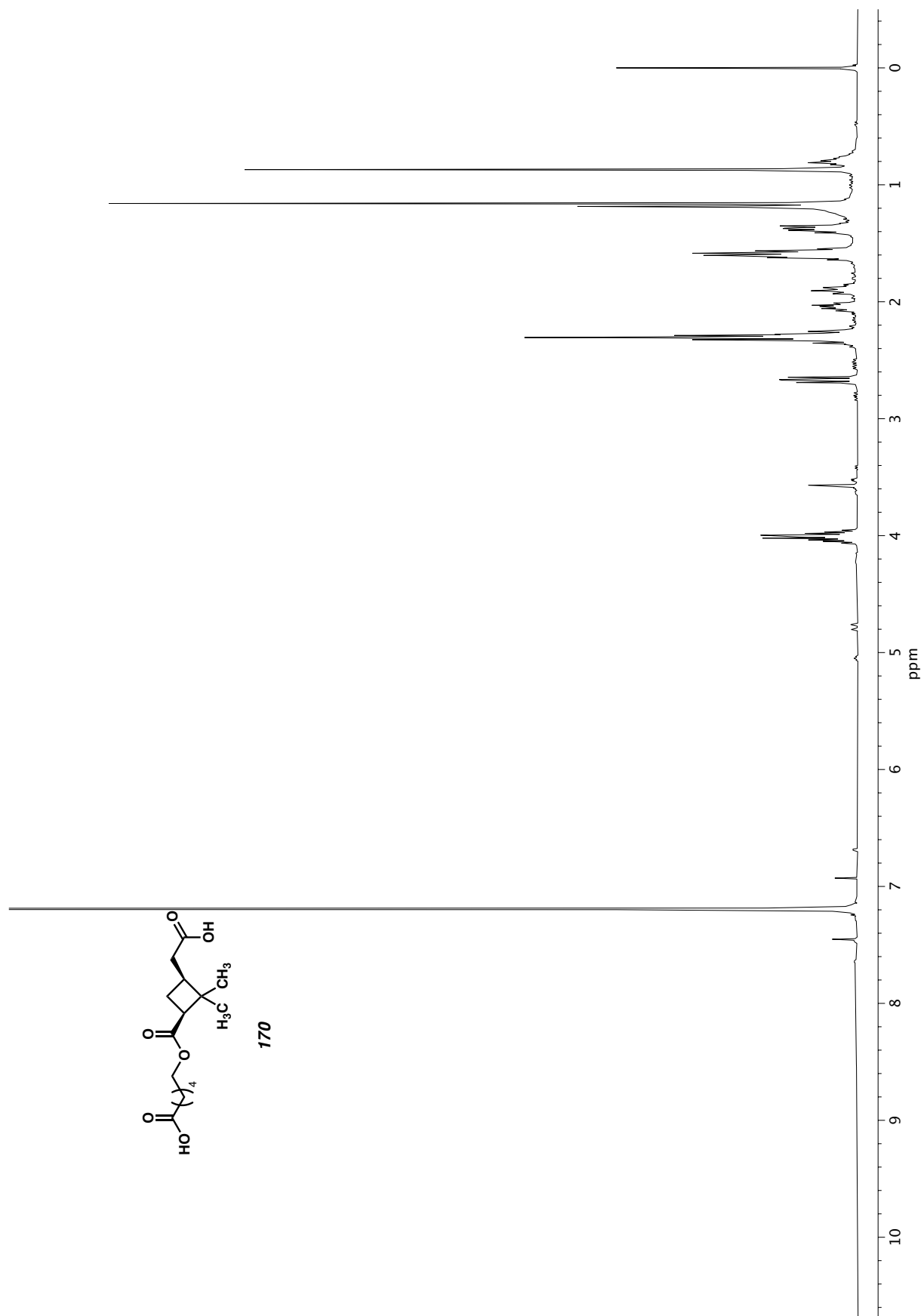


**Figure A8.58**  $^1\text{H}$  NMR (400 MHz,  $\text{CDCl}_3$ ) of compound **170**.

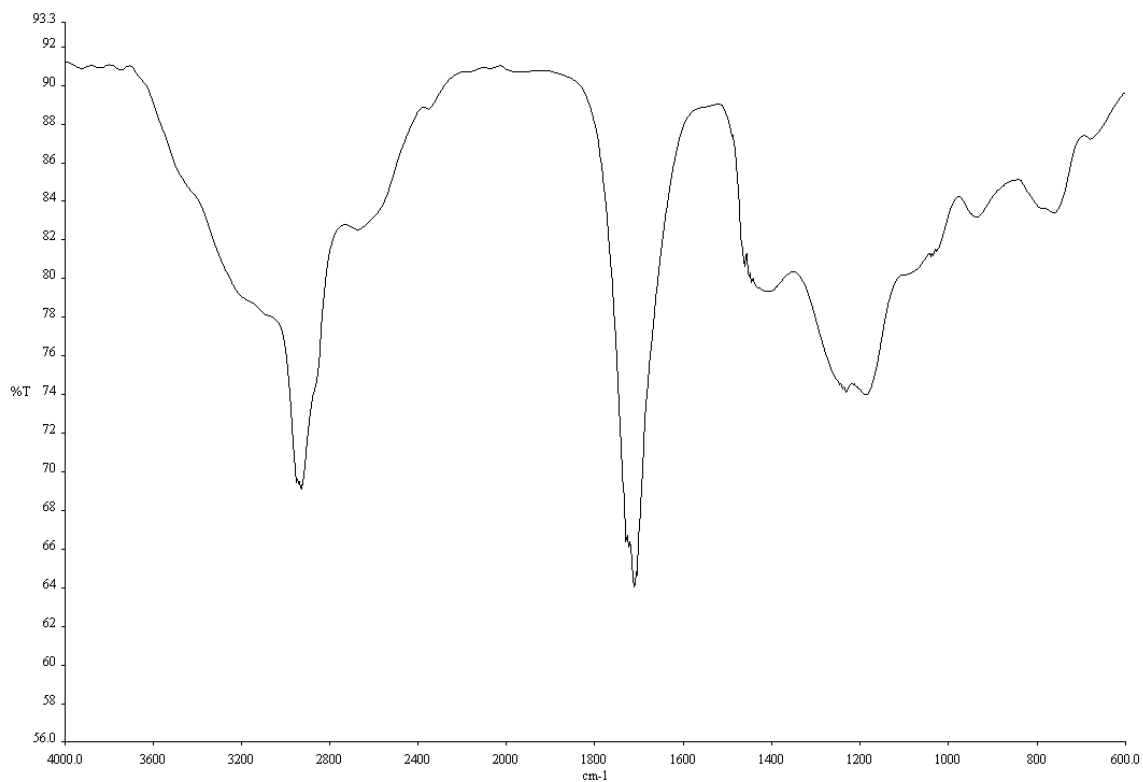


**Figure A8.59** Infrared spectrum (Thin Film, NaCl) of compound **170**.

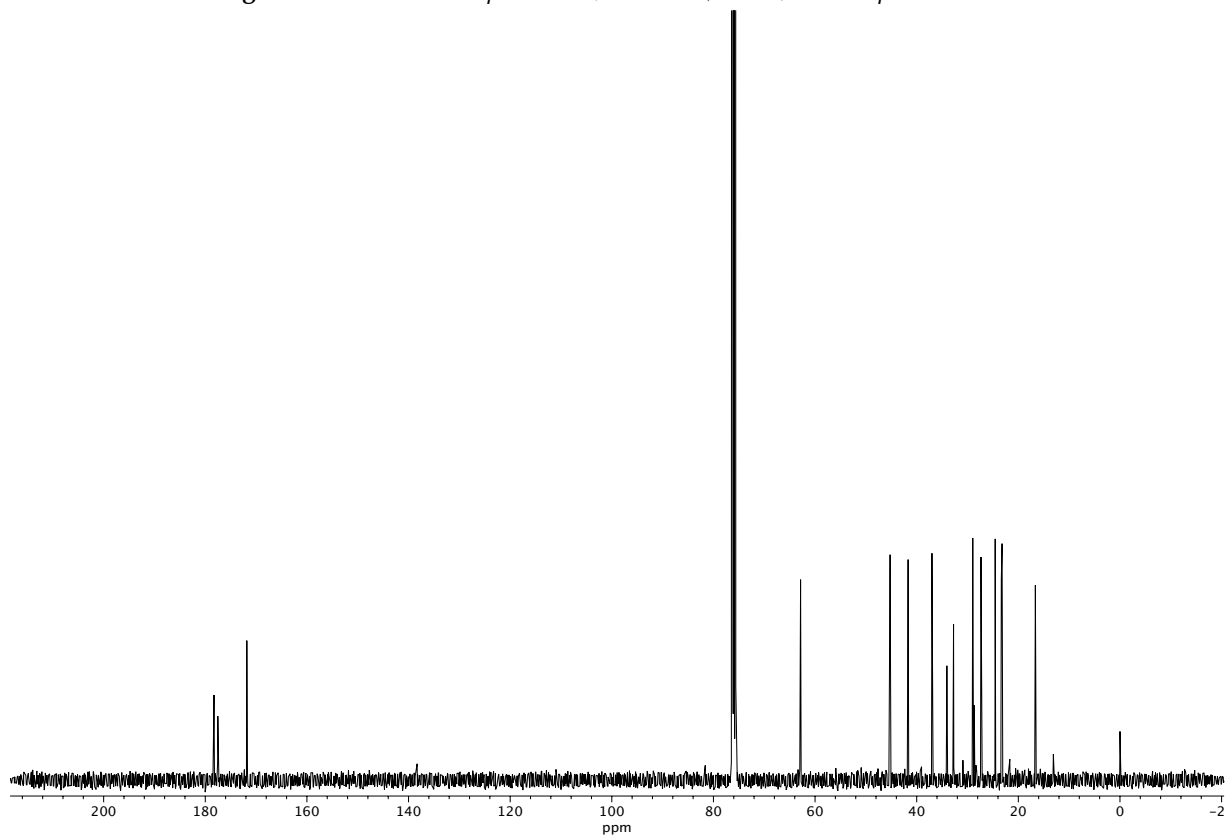


**Figure A8.60** <sup>13</sup>C NMR (100 MHz, CDCl<sub>3</sub>) of compound **170**.

## ABOUT THE AUTHOR

Nick Hafeman was born in Chicago, Illinois in 1990 to Bill Hafeman and Virginia McDonald. He was raised in the nearby suburb of River Forest, and attended Oak Park and River Forest High School as well as the Chicago Academy for the Arts, from which he graduated in 2008.

He then spent two years as a music major at Northern Illinois University in DeKalb, Illinois. After changing his focus, he started at Oakton Community College in 2011, where he quickly found an interest in science. Courses with Dr. Chad Landrie and Dr. Gary Mines instilled a strong passion for chemistry, and it was while at Oakton that he had his first exposure to laboratory research.

After earning his Associate's degree in 2014, he transferred to the University of Illinois at Chicago (UIC) to complete his undergraduate education. At UIC, Nick joined the lab of Dr. Duncan Wardrop, where he worked on the synthesis of influenza hemagglutinin inhibitors as well as nitrogen ion-mediated cyclization reactions. Mentorship from Prof. Wardrop, as well as from Prof. J. T. Mohr motivated him to continue the study of organic synthesis in graduate school after completing his bachelor's degree in 2016.

In the summer of 2017, Nick moved to Pasadena to pursue graduate studies at the California Institute of Technology under the guidance of Prof. Brian Stoltz. In the Stoltz group, he has focused on natural product total synthesis, particularly the total synthesis of the polycyclic furanobutenolide-derived cembranoid and norcembranoid diterpenoids. In July of 2022, Nick will begin his professional career as a process chemist at Abbvie in North Chicago, IL.